

Complexes of Divalent and Trivalent Ruthenium Incorporating Tethered Arenes

A thesis presented for the degree of
Doctor of Philosophy

in the

Research School of Chemistry

by

Joanne Rebecca Adams
B.Sc. (Hons) *Flinders*



The Australian National University

August 2003

“If we value the pursuit of knowledge, we must first be free to follow wherever that search may lead us. The free mind is not a barking dog, to be tethered on a ten-foot chain.”

Adlai E. Stevenson, Jr

Declaration

The work described in this thesis is the original work of the candidate, except where due reference is made in the text.



Joanne R. Adams

Publications

Some of the work described in this thesis has been reported in the following publications:

Bennett, M. A.; Edwards, A. J.; Harper[†], J. R.; Khimyak, T.; Willis, A. C. *J. Organomet. Chem.* **2001**, 629, 7-18.

Bond, A. D.; Brown, D. B.; Harper[†], J. R.; Johnson, B. F. G. *Acta Cryst.* **2001**, E57, o615-o616.

Bennett, M. A.; Harper[†], J. R. "Tethered Arene Complexes of Ruthenium", in: *Modern Coordination Chemistry: The Legacy of Joseph Chatt*; Leigh, G. J.; Winterton, N. Ed.: The Royal Society of Chemistry, Cambridge, 2002, pp. 163-168.

[†]Previous name.

Acknowledgements

I would like to thank:

my supervisor, Emeritus Professor Martin A. Bennett, for accepting me as his last Ph.D. student, for the guidance, enthusiasm and support he has readily supplied during the course of my studies, and for his support of my decision to study at the University of Cambridge for part of my Ph.D.;

Professor Brian F. G. Johnson for accepting me within his research group in Cambridge;

Dr Eric Wenger (ANU) for his assistance with and continued interest in my Ph.D. project;

the crystallographers who have solved the structures described in this thesis; Drs Alison J. Edwards, David C. R. Hockless, A. David Rae and Anthony C. Willis from the ANU, as well as Drs Andrew D. Bond, John E. Davies and Tetyana Khimyak from Cambridge, and Dr Michaele J. Hardie (Monash University) who collected the data for one of the structures;

Dr Richard D. Webster (ANU) for his assistance with some of the electrochemical, spectroelectrochemical and the ESR measurements;

Dr Graham A. Heath (ANU) for providing the instruments that I carried out some electrochemical experiments on;

Dr Lesley J. Yellowlees (University of Edinburgh) for allowing me to visit her group to carry out some spectroelectrochemical, controlled potential electrolysis and ESR experiments;

Dr Lorna A. Jack (Edinburgh) for her assistance during my visit;

Dr John E. McGrady (University of York) for the theoretical calculations described in this Thesis;

the technical and service staff at ANU, in particular Messrs. Paul A. Gugger, Horst Neumann and Lee L. Welling, as well as Mrs Joan E. Smith for her outstanding librarian skills;

the technical and service staff at the Universities of Cambridge and Edinburgh;

Drs Alison J. Edwards, Fiona H. Fry, Liz R. Humphrey and Madeleine Schultz for proofreading various Chapters of this Thesis.

the people I have had the pleasure of sharing a laboratory with, including Richard Baldwin, Matthew Byrnes, Maria Contel-Fernandez, Matthew Richmond, Rhodri Thomas (Bennett group), as well as David Brown, Colin Butcher, Vincent Ferrand, Sophie Hermans, Matthew Jones, Catherine Judkins, Tetyana Khimyak (Johnson group), and other previous members of these group;

the current members of the Hill group (ANU) whose laboratory space I occupied upon my return from Cambridge;

My friends, in Canberra and in various corners of the globe, including Alicia, Andrew, Anne-Marie, Colin, Erica, Felicity, Jan, Jenny, Kent, Lisa, Lynn, Matt F., Matt G., Marie and Stuart;

Alison Cameron for providing a place for me to stay on my return from Cambridge;

my parents and my brother Craig, for always believing in me and for their unconditional love and support.

Abstract

A series of tethered arene-ruthenium(II) complexes $[\text{RuCl}_2(\eta^1:\eta^6\text{-R}_2\text{P}(\text{CH}_2)_3\text{Ph})]$ ($\text{R} = \text{Me}, \text{Ph}, i\text{-Pr}, \text{Cy}, t\text{-Bu}$), $[\text{RuCl}_2(\eta^1:\eta^6\text{-R}_2\text{P}(\text{CH}_2)_3\text{-2,4,6-C}_6\text{R}_2\text{Me}_3)]$ ($\text{R} = \text{H}, \text{Me}$) and $[\text{RuCl}_2(\eta^1:\eta^6\text{-Ph}_2\text{PCH}_2\text{SiMe}_2\text{Ph})]$ has been prepared by thermal displacement of methyl *o*-toluate from the appropriate non-tethered complexes of the type $[\text{RuCl}_2(\eta^6\text{-1,2-MeC}_6\text{H}_4\text{CO}_2\text{Me})(\eta^1\text{-R}_2\text{PCH}_2\sim\text{aryl})]$ ($\sim = (\text{CH}_2)_2$ or SiMe_2). The three-atom strapped complexes carrying bulky substituents on the phosphorus, namely $[\text{RuCl}_2(\eta^1:\eta^6\text{-R}_2\text{P}(\text{CH}_2)_3\text{Ph})]$ ($\text{R} = i\text{-Pr}, \text{Cy}, t\text{-Bu}$), can also be obtained from the corresponding *p*-cymene complexes $[\text{RuCl}_2(\eta^6\text{-1,4-MeC}_6\text{H}_4\text{CHMe}_2)(\eta^1\text{-R}_2\text{P}(\text{CH}_2)_3\text{Ph})]$ ($\text{R} = i\text{-Pr}, \text{Cy}, t\text{-Bu}$). Similarly, the two-atom strapped complex $[\text{RuCl}_2(\eta^1:\eta^6\text{-R}_2\text{PCH}_2\text{SiMe}_2\text{Ph})]$ is accessible from its *p*-cymene precursor $[\text{RuCl}_2(\eta^6\text{-1,4-MeC}_6\text{H}_4\text{CHMe}_2)(\eta^1\text{-Ph}_2\text{PCH}_2\text{SiMe}_2\text{Ph})]$. These reactions, however, are much slower than those from the corresponding ester complexes. In some cases the tethered complexes can be prepared directly from the di- μ -chloro dimers $[\text{RuCl}_2(\eta^6\text{-arene})]_2$ (arene = 1,2-MeC₆H₄CO₂Me, 1,4-MeC₆H₄CHMe₂) and the corresponding phosphine.

The favourable influence of bulky substituents on the formation of the three-atom strapped complexes probably arises from conformational effects in the tether. It can be compared with the Thorpe-Ingold effect in organic chemistry and with the observation that cyclometallation of tertiary phosphines is favoured by bulky substituents for a similar reason.

The coordinated arene in the non-tethered methyl *o*-toluate complex $[\text{RuCl}_2(\eta^6\text{-1,2-MeC}_6\text{H}_4\text{CO}_2\text{Me})(\eta^1\text{-}t\text{-Bu}_2\text{P}(\text{CH}_2)_3\text{Ph})]$ seems to be particularly easily displaced. One product isolated serendipitously from a CD₂Cl₂ solution heated at 50°C is the tetranuclear compound

$[\text{Ru}_4(\mu_4\text{-O})(\mu_2\text{-Cl})_8(\eta^1\text{-}t\text{-Bu}_2\text{P}(\text{CH}_2)_3\text{Ph})_4]$, the oxygen atom presumably being derived from traces of water.

The presence of the tether enhances the stability of the η^6 -arene with respect to ligand displacement. The thermal displacement by acetonitrile of the η^6 -arene from the three-atom strapped complexes $[\text{RuCl}_2(\eta^1:\eta^6\text{-R}_2\text{P}(\text{CH}_2)_3\text{Ph})]$ ($\text{R} = \text{Ph}, i\text{-Pr}, \text{Cy}$), to form a *cis-trans* isomeric mixture of compounds of the type $[\text{RuCl}(\text{NCMe})_4(\eta^1\text{-R}_2\text{P}(\text{CH}_2)_3\text{Ph})]\text{Cl}$ ($\text{R} = \text{Ph}, i\text{-Pr}, \text{Cy}$), occurs much more slowly than the corresponding reaction from the non-tethered η^6 -benzene complexes $[\text{RuCl}_2(\eta^6\text{-C}_6\text{H}_6)(\eta^1\text{-R}_2\text{P}(\text{CH}_2)_3\text{Ph})]$ ($\text{R} = \text{Ph}, i\text{-Pr}, \text{Cy}$). In contrast, the η^6 -arene is displaced from the two-atom strapped complex $[\text{RuCl}_2(\eta^1:\eta^6\text{-Ph}_2\text{PCH}_2\text{SiMe}_2\text{Ph})]$ as easily as η^6 -benzene is from $[\text{RuCl}_2(\eta^6\text{-C}_6\text{H}_6)(\eta^1\text{-Ph}_2\text{PCH}_2\text{SiMe}_2\text{Ph})]$. Displacement of the η^6 -arene from $[\text{RuCl}_2(\eta^6\text{-arene})(\eta^1\text{-}i\text{-Pr}_2\text{P}(\text{CH}_2)_3\text{Ph})]$ by acetonitrile occurs more readily for η^6 -methyl *o*-toluate than for η^6 -benzene. The *cis*-isomers of each of the complexes of the type $[\text{RuCl}(\text{NCMe})_4(\eta^1\text{-R}_2\text{P}(\text{CH}_2)_3\text{Ph})]\text{Cl}$ are slowly converted, though not completely, into the thermodynamically more stable *trans*-isomers on heating.

The greater lability of η^6 -methyl *o*-toluate over both η^6 -*p*-cymene and η^6 -benzene in their Ru(II) complexes, which has been demonstrated in this work, may be due to a weaker metal-arene bond in the ground state. This behaviour has been correlated with enthalpies of formation of $[\text{Cr}(\eta^6\text{-arene})(\text{CO})_3]$ complexes and justified by theoretical calculations.

The tris-complexes $[\text{RuCl}_2(\text{nitrile})_3(\eta^1\text{-Ph}_2\text{P}(\text{CH}_2)_3\text{Ph})]$ (nitrile = MeCN or Me(CH₂)₂CN) are formed by potentiostat electrolysis experiments on complex $[\text{RuCl}_2(\eta^1:\eta^6\text{-Ph}_2\text{P}(\text{CH}_2)_3\text{Ph})]$, though they have not been isolated in a pure state. The tris-complexes were rapidly converted into the thermodynamically favoured tetrakis-compounds $[\text{RuCl}(\text{nitrile})_4(\eta^1\text{-}$

$\text{Ph}_2\text{P}(\text{CH}_2)_3\text{Ph})\text{Cl}$ (nitrile = MeCN or $\text{Me}(\text{CH}_2)_2\text{CN}$) by reaction with the appropriate N-donor.

The tethered complexes $[\text{RuCl}_2(\eta^1:\eta^6\text{-R}_2\text{P}(\text{CH}_2)_3\text{Ph})]$ ($\text{R} = \text{Me}, \text{Ph}, i\text{-Pr}, \text{Cy}$), $[\text{RuCl}_2(\eta^1:\eta^6\text{-R}_2\text{P}(\text{CH}_2)_3\text{-2,4,6-C}_6\text{R}_2\text{Me}_3)]$ ($\text{R} = \text{H}, \text{Me}$) and $[\text{RuCl}_2(\eta^1:\eta^6\text{-Ph}_2\text{PCH}_2\text{SiMe}_2\text{Ph})]$ generally display reversible redox behaviour by cyclic voltammetry, $E_{1/2} = + 0.55\text{-}0.82 \text{ V vs Fc}^{0/1}$ in CH_2Cl_2 . The tethered complexes generally show fully reversible spectroelectrochemical behaviour at *ca* 228K. Most of the electrogenerated arene-ruthenium(III) species show some stability above this temperature, and those containing alkyl-substituted cations are stable even at room temperature. The electronic spectra of those cations that do not decompose irreversibly revert towards those of the parent Ru(II) compounds. In contrast, the spectroelectrochemical behaviour of the non-tethered compounds $[\text{RuCl}_2(\eta^6\text{-C}_6\text{R}_6)(\text{PMe}_3)]$ ($\text{R} = \text{H}, \text{Me}$) is not reversible. Further, none of the electrogenerated arene-Ru(III) species of non-tethered complexes studied, namely $[\text{RuCl}_2(\eta^6\text{-C}_6\text{R}_6)(\text{PR}'_3)]^+$ ($\text{R} = \text{H}, \text{Me}; \text{R}' = \text{Me}, \text{Ph}$), are stable above *ca* 228K in solution; they undergo irreversible decomposition, presumably with loss of the η^6 -arene. The electrogenerated arene-Ru(III) species $[\text{RuCl}_2(\eta^6\text{-C}_6\text{Me}_6)(\text{PPh}_3)]^+$, $[\text{RuCl}_2(\eta^1:\eta^6\text{-}i\text{-Pr}_2\text{P}(\text{CH}_2)_3\text{Ph})]^+$ and $[\text{RuCl}_2(\eta^1:\eta^6\text{-Ph}_2\text{P}(\text{CH}_2)_3\text{C}_6\text{Me}_5)]^+$ show ESR spectra at *ca* 5K that are typical of octahedral Ru(III) complexes.

Chemical oxidation of the permethylated complexes $[\text{RuCl}_2(\eta^6\text{-C}_6\text{Me}_6)(\text{PPh}_3)]$ and $[\text{RuCl}_2(\eta^1:\eta^6\text{-Ph}_2\text{P}(\text{CH}_2)_3\text{C}_6\text{Me}_5)]$ with $[\text{N}(\text{C}_6\text{H}_4\text{Br-4})_3]\text{SbCl}_6$ generates the arene-ruthenium(III) complexes $[\text{RuCl}_2(\eta^6\text{-C}_6\text{Me}_6)(\text{PPh}_3)][\text{SbCl}_6]$ and $[\text{RuCl}_2(\eta^1:\eta^6\text{-Ph}_2\text{P}(\text{CH}_2)_3\text{C}_6\text{Me}_5)][\text{SbCl}_6]$ as isolable solids, which are the first structurally characterised arene-ruthenium(III) complexes. Although the structures of the cations are similar to those of their neutral precursors, oxidation causes a lengthening (*ca* 0.1 Å) of the Ru-C(arene) bonds and a shortening of the Ru-Cl bonds by about 0.1 Å.

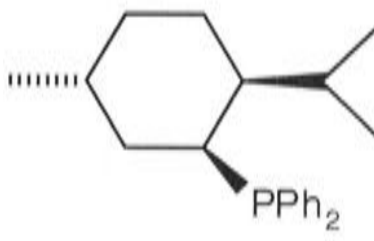
Thus the η^6 -arene is more weakly bound at the Ru(III) level. These trends are reproduced in theoretical calculations, which showed that the electron is removed from a HOMO which is Ru-Cl antibonding. The DFT calculations also indicate that the unpaired electron is located in a Ru-Cl-based orbital, in agreement with the ESR data. Decomposition of a CH_2Cl_2 solution of the non-tethered complex $[\text{RuCl}_2(\eta^6\text{-C}_6\text{Me}_6)(\text{PPh}_3)][\text{SbCl}_6]$ at *ca* -10°C forms the structurally characterised 1:1 charge transfer adduct of its Ru(II) precursor $[\text{RuCl}_2(\eta^6\text{-C}_6\text{Me}_6)(\text{PPh}_3)]\cdot\text{SbCl}_3$. The tethered compound $[\text{RuCl}_2(\eta^1:\eta^6\text{-Ph}_2\text{P}(\text{CH}_2)_3\text{C}_6\text{Me}_5)][\text{SbCl}_6]$ does not appear to decompose in the same way under these conditions. Thus the Ru(III) oxidation state in the $[\text{RuCl}_2(\eta^6\text{-C}_6\text{Me}_6)(\text{PPh}_3)]^+$ cation is stabilised by the presence of the tether, but is also dependent on the nature of the anion.

Abbreviations

acac	acetylacetonato, [MeC(O)CHC(O)Me] ⁻
ACV	Alternating Current Voltammetry
AIBN	2,2'-azobis(isobutyronitrile)
app. t	apparent triplet
a.u.	arbitrary units
av.	average
[Bar ^F ₄] ⁻	tetrakis[3,5-bis(trifluoromethyl)phenyl]borate, [B(3,5-C ₆ H ₃ (CF ₃) ₂) ₄] ⁻
ben	benzene, C ₆ H ₆
b.p.	boiling point
Binap	2,2'-bis(diphenylphosphino)-1,1'-binaphthyl, 1,1'-(C ₁₀ H ₆) ₂ -2,2-(PPh ₂) ₂
br.	broad signal
Bz	benzyl
Chem3D	CS Chem3D Pro
COD	1,5-cyclooctadiene, 1,5-C ₈ H ₁₂
Cp	cyclopentadienyl, η ⁵ -C ₅ H ₅
Cp*	pentamethylcyclopentadienyl, η ⁵ -C ₅ Me ₅
CPE	Controlled Potential Electrolysis
CSD	Cambridge Structural Database
CV	Cyclic Voltammetry or Cyclic Voltammogram
cym	<i>p</i> -cymene, 1,4-MeC ₆ H ₄ CHMe ₂
d	doublet
D	donor atom or deuterium where appropriate
DAM	1,1-bis(diphenylarsino)methane, Ph ₂ AsCH ₂ AsPh ₂
def.	deformation
DFT	Density Functional Theory
DIPP	2,6-diisopropylphenoxide, [<i>i</i> -Pr ₂ C ₆ H ₃ O-2,6] ⁻
DMF	dimethylformamide, Me ₂ NCHO

DMMP	2,6-dimethoxy-4-ethylphenoxide, [4-Et-2,6-(MeO) ₂ C ₆ H ₂ O] ⁻
dmpe	1,2-bis(dimethylphosphino)ethane, Me ₂ PCH ₂ CH ₂ PMe ₂
DMSO	dimethylsulfoxide, Me ₂ SO
DOMP	2,6-dimethoxyphenoxide, [2,6-(MeO) ₂ C ₆ H ₃ O] ⁻
dppe	1,2-bis(diphenylphosphino)ethane, Ph ₂ PCH ₂ CH ₂ PPh ₂
DPPH	diphenylpicrylhydrazyl, [Ph ₂ N-NC ₆ H ₂ (NO) ₃ -2,4,6]
dppm	1,1-bis(diphenylphosphino)methane, Ph ₂ PCH ₂ PPh ₂
dppmO	1,1-bis(diphenylphosphino)methane monoxide, Ph ₂ PCH ₂ P(O)Ph ₂
E°	formal electrode potential
$E_{1/2}$	electrode potential
E_{appl}	applied potential
edt	ethane-1,2-dithiolate, [SCH ₂ CH ₂ S] ²⁻
EI	Electron Impact
en	ethylenediamine, H ₂ NCH ₂ CH ₂ NH ₂
E_{pa}	anodic peak potential
EPA	2:5:5 mixture of ethanol/isopentane/ether
E_{pc}	cathodic peak potential
ΔE_{p}	$ E_{\text{pa}} - E_{\text{pc}} $
eq.	equivalents
EPR	Electron Paramagnetic Resonance
ESD	estimated standard deviation
ESI	Electrospray Ionisation
ESR	Electron Spin Resonance
GC	Gas Chromatography
FAB	Fast Atom Bombardment
facial	OC-6-22
Fc	ferrocene, [Fe(η^5 -C ₅ H ₅) ₂] [†]

[†]This is the standard abbreviation used in electrochemistry, although, strictly speaking, the correct abbreviation for ferrocene is FcH.

hmb	hexamethylbenzene, C_6Me_6	
HMPA	hexamethylphosphoric triamide, $(Me_2N)_3PO$	
HOMO	highest occupied molecular orbital	
Im	imidazole, $C_3H_4N_2$	
i_{pa}	Anodic Peak Current	
i_{pc}	Cathodic Peak Current	
IUPAC	International Union of Pure and Applied Chemistry	
lit.	literature	
m	multiplet (NMR)/medium intensity (IR)	
M	Transition Metal atom	
MALDI	Matrix-Assisted Laser Desorption/Ionisation	
MeIm	<i>N</i> -methylimidazole, $C_3H_3N_2Me$	
<i>mer</i>	meridional, OC-6-21	
mes	mesitylene, 1,3,5- $C_6H_3Me_3$	
MLCT	metal-to-ligand charge transfer	
m.p.	melting point	
mt	methyl <i>o</i> -toluate, 1,2- $MeC_6H_4CO_2Me$	
<i>n</i>	number of electrons or magnitude of charge on a metal complex where appropriate	
N/A	Not Applicable	
Naph	naphthyl, $C_{10}H_7$	
NIR	Near Infra-Red	
NMDPP	(+)-neomenthyldiphenylphosphine,	
NN'N	2,6-bis[(dimethylamino)methyl]pyridine, [$C_5H_3N(CH_2NMe_2)_2$ -2,6]	
OTf	triflate, $CF_3SO_3^-$	
OTTLE	Optically Transparent Thin-Layer Electrode	
pdf	portable document format	

(R)-PROPHOS	(R)-(+)-1,2-bis(diphenylphosphino)propane, (R)-(+)-1,2-Ph ₂ PCH ₂ CH(PPh ₂)Me
py	pyridine
q	quartet
r.t.	room temperature
s	singlet (NMR)/strong intensity (IR)
S	spin quantum number
SCE	Saturated Calomel Electrode
sept	septet
SOMO	singly occupied molecular orbital
SSCE	Saturated Sodium Chloride Electrode
<i>str.</i>	stretch
t	triplet
TCNE	tetracyanoethylene, (NC) ₂ C=C(CN) ₂
<i>tert</i>	tertiary
TFAB	tetrakis(perfluorophenyl)borate anion, B[(C ₆ F ₅) ₄] ⁻
THF	tetrahydrofuran, C ₄ H ₈ O
T. M.	Transition Metal
TMP	tetramethylpiperidide, [2,2,6,6-Me ₄ C ₅ H ₆ N] ⁻
TMS	tetramethylsilane, Me ₄ Si
TP* = TP ^{Me2}	hydro-tris(3,5-dimethylpyrazolyl)borate, [HB(N ₂ C ₃ HMe ₂ -3,5) ₃]
tren	tris(2-aminoethyl)amine, (NH ₂ CH ₂ CH ₂) ₃ N
TROMP	2,4,6-trimethoxyphenoxide, [C ₆ H ₂ O(OMe) ₃ -2,4,6]
Trpy	2,2':6',2''-terpyridine, 2,2''-(C ₅ H ₄ N) ₂ -2',6'-C ₅ H ₃ N
UV	Ultra-violet
Vis	Visible
w	weak
δ	chemical shift (ppm)
ε	molar absorptivity (L mol ⁻¹ cm ⁻¹)
Λ _m	molar conductivity (S cm ² mol ⁻¹)

Throughout this thesis, bidentate coordination of the arene-phosphines has been indicated with the prefix $\eta^1:\eta^6$, and monodentate P-coordination with the prefix η^1 . Strictly, these abbreviations are incorrect and should be replaced by $\kappa\text{-P-}\eta^6$ and $\kappa\text{-P}$, respectively. Similarly, monodentate or bidentate coordination of ligands such as DAM, dmpe, dppe, dppm, (*R*)-PROPHOS and dppmO, has been indicated with the symbols η^1 or η^2 , respectively.

Atom labelling employed in Chem3D representations:









	Antimony
	Carbon
	Chlorine
	Nitrogen
	Oxygen
	Phosphorus
	Silicon
	Ruthenium

Table of Contents

<i>Declaration</i>	<i>i</i>
<i>Publications</i>	<i>ii</i>
<i>Acknowledgements</i>	<i>iii</i>
<i>Abstract</i>	<i>v</i>
<i>Abbreviations</i>	<i>ix</i>
<i>Table of Contents</i>	<i>xiv</i>
Chapter 1: Introduction	1
1.1 <i>Paramagnetic Organometallic Complexes</i>	1
1.1.1 <i>Techniques for Detecting Paramagnetic Species</i>	3
1.1.2 <i>Reactivity of Paramagnetic Organometallic Complexes</i>	14
1.1.3 <i>Chemical Oxidants</i>	21
1.2 <i>Tethered Aromatic Complexes</i>	29
1.2.1 <i>Syntheses Proceeding by Initial Arene Coordination</i>	37
1.2.2 <i>Syntheses Proceeding by Initial Donor Atom Coordination</i> ..	43
1.2.3 <i>Intramolecular Construction of the Strap</i>	57
1.2.4 <i>Other Methods</i>	59
1.3 <i>Objectives of this Work</i>	60
<i>References</i>	61
Chapter 2: Preparation of Ligands	75
2.1 <i>Preparation of Ligands</i>	76
2.2 <i>Summary</i>	85
<i>References</i>	87
Chapter 3: Preparation of Tethered Arene Complexes and their Precursors	89
3.1 <i>Strategies to be Adopted</i>	89
3.2 <i>Strategy One; Initial Coordination of Donor Atom</i>	90
3.2.1 <i>Preparation of the Non-Tethered Complexes</i>	93
3.2.2 <i>Characterisation Data</i>	95
3.2.3 <i>Preparation of the Tethered Complexes</i>	100
3.2.4 <i>Characterisation Data</i>	104
3.2.5 <i>Structural Data</i>	115

3.2.6	Formation of Tethered Complexes from η^6 -Benzene and η^6 - <i>p</i> -Cymene Precursor Complexes.....	117
3.2.7	Reactions of Complexes Incorporating $t\text{-Bu}_2\text{P}(\text{CH}_2)_3\text{Ph}$	122
3.3	Strategy Two; Intramolecular Construction of the Tether.....	139
3.3.1	Preparation of Non-Tethered Compounds.....	139
3.3.2	Attempted Preparation of the Tethered Complexes.....	140
3.4	Preparation of Derivatives of Tethered Arene Complexes.....	145
3.4.1	Preparation of Complexes of the Type [Ru(X)(Y)($\eta^1:\eta^6\text{-R}_2\text{P}(\text{CH}_2)_3\text{Ph}$)].....	145
3.5	Discussion of Structural Data.....	154
3.6	Summary.....	181
	References.....	182
	Chapter 4: Arene Displacement Reactions of Tethered Arene Complexes and their Precursors.....	187
4.1	Reaction of Non-Tethered and Tethered Complexes with Acetonitrile.....	192
4.2	Summary.....	215
	References.....	216
	Chapter 5: Redox Properties of Tethered Arene and Non-Tethered Arene Ruthenium(II) Complexes.....	218
5.1	Cyclic Voltammetry, Spectroelectrochemistry and ESR Spectroscopy of Non-Tethered and Tethered Complexes.....	218
5.2	Controlled Potential Electrolysis of [RuCl ₂ ($\eta^1:\eta^6\text{-Ph}_2\text{P}(\text{CH}_2)_3\text{Ph}$)] in Nitriles.....	243
5.3	Summary.....	267
	References.....	268
	Chapter 6: Chemical Oxidation Reactions of Tethered and Non-Tethered Arene Complexes.....	270
6.1	Chemical Oxidation Reactions of Arene-Ruthenium(II) Complexes	271
6.2	Theoretical Calculations.....	295
6.3	Summary.....	298
	References.....	298

Chapter 7: Discussion of the Results of the Work Described in this Thesis	300
7.1 Arene-Ruthenium(III).....	300
7.2 Formation and Stability of the Arene-Ruthenium(II) Tethered Complexes	307
References.....	324
Chapter 8: Experimental Section	330
8.1 General Information.....	330
8.1.1 Cyclic Voltammetry and Controlled Potential Electrolysis: General Conditions	334
8.1.2 Spectroelectrochemistry: General Conditions.....	337
8.1.3 Electron Spin Resonance: General Conditions.....	338
8.2 Successful and Attempted Preparation of Compounds	341
Notes and References.....	413
Appendix of Structural Data	416
A.1 $\text{Ph}_2\text{P}(\text{CH}_2)_3\text{Ph}$	416
A.2 $[\text{RuCl}_2(\eta^6\text{-1,4-MeC}_6\text{H}_4\text{CHMe}_2)(\eta^1\text{-Me}_2\text{P}(\text{CH}_2)_3\text{Ph})]$	417
A.3 $[\text{RuCl}_2(\eta^6\text{-C}_6\text{H}_6)(\eta^1\text{-Ph}_2\text{P}(\text{CH}_2)_3\text{Ph})]$	418
A.4 $[\text{RuCl}_2(\eta^6\text{-1,4-MeC}_6\text{H}_4\text{CHMe}_2)(\eta^1\text{-i-Pr}_2\text{P}(\text{CH}_2)_3\text{Ph})]$	420
A.5 $[\text{RuCl}_2(\eta^6\text{-1,2-MeC}_6\text{H}_4\text{CO}_2\text{Me})(\eta^1\text{-Cy}_2\text{P}(\text{CH}_2)_3\text{Ph})]$	423
A.6 $[\text{RuCl}_2(\eta^6\text{-1,4-MeC}_6\text{H}_4\text{CHMe}_2)(\eta^1\text{-Ph}_2\text{P}(\text{CH}_2)_3\text{-2,4,6-C}_6\text{H}_2\text{Me}_3)]$...	427
A.7 $[\text{RuCl}_2(\eta^6\text{-1,4-MeC}_6\text{H}_4\text{CHMe}_2)(\eta^1\text{-Ph}_2\text{P}(\text{CH}_2)_3\text{C}_6\text{Me}_5)]$	428
A.8 $[\text{RuCl}_2(\eta^6\text{-1,4-MeC}_6\text{H}_4\text{CHMe}_2)(\eta^1\text{-Ph}_2\text{PCH}_2\text{SiMe}_2\text{Ph})]$	430
A.9 $[\text{RuCl}_2(\eta^6\text{-1,4-MeC}_6\text{H}_4\text{CHMe}_2)(\text{Ph}_2\text{PCH}=\text{CH}_2)]$	431
A.10 $[\text{RuCl}_2(\eta^1:\eta^6\text{-Me}_2\text{P}(\text{CH}_2)_3\text{Ph})]$	435
A.11 $[\text{RuCl}_2(\eta^1:\eta^6\text{-i-Pr}_2\text{P}(\text{CH}_2)_3\text{Ph})]$	437
A.12 $[\text{RuCl}_2(\eta^1:\eta^6\text{-t-Bu}_2\text{P}(\text{CH}_2)_3\text{Ph})]$	438
A.13 $[\text{RuCl}_2(\eta^1:\eta^6\text{-Ph}_2\text{P}(\text{CH}_2)_3\text{-2,4,6-C}_6\text{H}_2\text{Me}_3)]$	439
A.14 $[\text{RuCl}_2(\eta^1:\eta^6\text{-Ph}_2\text{P}(\text{CH}_2)_3\text{C}_6\text{Me}_5)]$	441
A.15 $[\text{RuCl}_2(\eta^1:\eta^6\text{-Ph}_2\text{PCH}_2\text{SiMe}_2\text{Ph})]$	442
A.16 $[\text{Ru}_4(\mu_4\text{-O})(\mu_2\text{-Cl})_8(\eta^1\text{-t-Bu}_2\text{P}(\text{CH}_2)_3\text{Ph})_4]$	444

A.17	$[\text{RuCl}(\text{NCMe})_4(\eta^1\text{-Ph}_2\text{P}(\text{CH}_2)_3\text{Ph})]\text{Cl}$	445
A.18	$[\text{RuCl}_2(\eta^1:\eta^6\text{-Ph}_2\text{P}(\text{CH}_2)_3\text{C}_6\text{Me}_5)][\text{SbCl}_6]$	446
A.19	$[\text{RuCl}_2(\eta^6\text{-C}_6\text{Me}_6)(\text{PPh}_3)][\text{SbCl}_6]$	447
A.20	$[\text{RuCl}_2(\eta^6\text{-C}_6\text{Me}_6)(\text{PPh}_3)].\text{SbCl}_3$	449
A.21	<i>Crystal Data and Details of Data Structure Collection and Refinement</i>	451
	<i>References</i>	466

Chapter 1: Introduction

This thesis is concerned with attempts to isolate and characterise an unusual class of organometallic compound in which an arene is η^6 -bound to a metal atom in a relatively high oxidation state, namely, trivalent ruthenium (electron configuration $4d^5$), derived by one-electron oxidation from the well-established arene-ruthenium(II) ($4d^6$) system. Since it was expected that the metal-arene binding would be weakened as a consequence of the oxidation, an effort has been made to stabilise the oxidised form of the complex by tethering or strapping the arene to another donor group (in this case, a tertiary phosphine), thus forming a potentially chelate ligand. A similar approach, using a nitrogen donor in place of phosphorus, has been employed to provide the first example of η^2 -alkene and η^2 -alkyne complexes of trivalent ruthenium.^{1,2} It is therefore necessary to provide some background to the two aspects of the work to be described, namely paramagnetic organo-transition metal complexes and tethered chelate complexes.

1.1 Paramagnetic Organometallic Complexes

There is no rigid distinction between organic and organometallic free radicals, on the one hand, and the traditional paramagnetic transition metal (T. M.) complexes on the other.³ Even for carbon donor ligands such as η^1 -alkyls, η^1 -aryls, η^5 -cyclopentadienyl and η^6 -arene, numerous stable paramagnetic T. M. complexes are known, particularly, but not exclusively, for the 3d-elements. The organometallic radicals considered in this Chapter are those that are generated either by one-electron reduction or oxidation of their parent 18-electron complexes.

Organometallic radicals have an important role in both materials science and certain molecular activation processes.³ All mononuclear T. M. complexes containing an odd number of valence electrons are paramagnetic,⁴ ($S \neq \text{integer}$) with one unpaired electron in the HOMO (highest occupied molecular orbital).³ The unpaired electron results in the

organometallic radicals displaying extensive redox chemistry as well as ligand lability.³ The geometry and size of the ligand (molecular structure), and the orientation, localisation and symmetry of the SOMO [singly occupied molecular orbital] (electronic structure), influence the behaviour of the complex towards ligand substitution and redox reactions.³

Organometallic and organic radicals may be short-lived, whereas T. M. radicals tend to be very stable and long-lived. In this Chapter examples of radicals involving Group 8 atoms, such as ruthenium, will be discussed, as well as isoelectronic Group 6 complexes. For example, the carbonyl complexes $[\text{M}(\text{CO})_6]^+$ ($\text{M} = \text{Cr}, \text{Mo}, \text{W}$),⁵⁻¹¹ $[\text{M}(\text{CO})_5]^-$, ($\text{M} = \text{Cr}, \text{Mo}, \text{W}$),¹²⁻¹⁶ $[\text{M}(\text{CO})_5]^+$ ($\text{M} = \text{Fe}, \text{Os}$)^{17,18} and $[\text{Fe}(\text{CO})_4]^-$,^{12,13,19} are all transient 17-electron species, whereas $[\text{V}(\text{CO})_6]$ is a stable 17-electron organometallic radical.²⁰ There are also transient 19-electron radicals, such as $[\text{Mo}(\text{CO})_6]^-$,²¹ and $[\text{Fe}(\text{CO})_5]^-$.^{19,22}

The transient 17-electron radicals can be stabilised by replacing one or more of the carbon monoxide moieties by larger and more strongly σ -donating ligands, such as tertiary phosphines.³ For example, the transient radical $[\text{Fe}(\text{CO})_5]^{+17}$ can be stabilised by replacing two of the carbon monoxide moieties to form $[\text{Fe}(\text{CO})_3(\text{PPh}_3)_2]^+$.²³⁻²⁷ Further, bidentate ligands have also been shown to stabilise highly reactive paramagnetic complexes.²⁸ The complex $[\text{Fe}(\eta^5\text{-C}_5\text{H}_5)(\text{Me})(\text{CO})_2]^+$ can only be detected on an electrochemical time-scale,²⁹ whereas, if the two carbon monoxide ligands are replaced by a chelating phosphine, the 17-electron complex $[\text{Fe}(\eta^5\text{-C}_5\text{H}_5)(\text{Me})(\eta^2\text{-dppe})]^+$ (dppe = 1,2-bis(dimethylphosphino)ethane) is thermally stable and can be isolated.²⁸

There are many examples of Group 6 and 8 metal complexes that contain either Cp (cyclopentadienyl), Cp* (pentamethylcyclopentadienyl) or η^6 -arene ligands, or a combination of arene and Cp or Cp* ligands. Some examples of chromium, molybdenum, tungsten, iron and ruthenium radicals, containing the ligands mentioned above, are listed in Table 1.

There are also many examples of paramagnetic metallocenes, such as the ferrocenium ion^{30,31}, and the decamethylcyclopentadienyl analogue of ferrocenium, $[\text{Fe}(\eta^5\text{-C}_5\text{Me}_5)_2]^+$,³² as well as $[\text{Ru}(\eta^5\text{-C}_5\text{Me}_5)_2]^+$,³³ and $[\text{Os}(\eta^5\text{-C}_5\text{Me}_5)_2]^+$.³⁴

1.1.1 Techniques for Detecting Paramagnetic Species

One of the most useful electrochemical techniques, for UV-active metal complexes, is undoubtedly spectroelectrochemistry.⁸⁸⁻⁹¹ The absorbance of the species present during the electrode process can be monitored at the electrode surface by UV/Vis spectroscopy, providing information which cannot be obtained from purely electrochemical experiments.⁹² This *in situ* technique allows simultaneous measurement of both spectroscopic and electrochemical information.⁹³ Optically Transparent Thin-Layer Electrodes (OTTLEs) are routinely used, due to both the ease in recording the spectra and the fact that the electroactive species can be totally electrolysed rapidly, since there are only short distances for the ions to traverse.^{93,94} Spectroelectrochemistry is therefore dependent upon diffusion rates and, for completely reversible systems, the whole solution reaches equilibrium.⁹² It allows detection of complexes that may be difficult to isolate, since they are often highly unstable. This technique is particularly useful for low spin d^6 systems which display relatively low energy metal-to-ligand charge transfer (MLCT) transitions.⁹⁵ For example, the electronic spectra of the Ru(II) complex $[\text{Ru}(\text{acac})_2(\eta^2\text{-C}_2\text{H}_4)(\text{SbPh}_3)]$ and its one-electron oxidation product showed charge transfer transitions at both the Ru(II) and Ru(III) level.⁹⁶

Table 1. Selected examples of paramagnetic organometallic transition metal complexes.

Complex	Variables	Oxidation State of the Metal	Number of Electrons	g-Values	References
$[\text{Cr}(\eta^5\text{-C}_5\text{H}_5)(\text{CO})_2]^+$	-	+1	15	-	35
$[\text{Cr}(\eta^5\text{-C}_5\text{H}_5)(\text{CO})_2\text{L}]$	L = PPh ₃ L = P(OMe) ₃ ^a	+1	17	L = PPh ₃ 1.96, 2.02, 2.13	36-41
$[\text{CrCl}(\eta^5\text{-C}_5\text{H}_5)(\text{R})\text{L}]$	R = Me, Ph; L = PPh ₃ , py	+3	15	-	42
$[\text{Cr}(\eta^5\text{-C}_5\text{R}_5)(\text{CO})_3]$	R = H, ^b Me, ^a Ph	+1	17	R = H monomer: 2.0353, 1.9969, 2.1339 dimer: 2.025 ^c R = Me: 2.1215, 2.0192, 1.9973 R = Ph: 2.1387, 2.0225, 1.9952	39,41,43-47
$[\text{CrCl}(\eta^5\text{-C}_5\text{Me}_5)(\text{py})\text{L}]$	L = Me, Et	+3	15	-	48
$[\text{Cr}(\eta^5\text{-C}_5\text{Me}_5)(\eta^6\text{-C}_6\text{Me}_6)]$	-	+1	17	-	48

Complex	Variables	Oxidation State of the Metal	Number of Electrons	<i>g</i> -Values	References
$[\text{Cr}(\text{CO})_3(\eta^6\text{-arene})]^+$	arene = C_6H_6 (1), 1,3,5- $\text{C}_6\text{H}_3\text{Me}_3$, C_6Me_6 ([2] ⁺)	+1	17	-	35,49-53
$[\text{Cr}(\text{CO})_2(\eta^6\text{-arene})(\text{PR}_3)]^+$	arene = 1,3,5- $\text{C}_6\text{H}_3\text{Me}_3$; R = <i>n</i> -Bu, O(<i>n</i> -Bu) arene = C_6Me_6 ; R = Ph (3)	+1	17	3 2.102, 2.026, 1.992	52,54-56
$[\text{Cr}(\text{CO})_2(\eta^6\text{-C}_6\text{Me}_6)\text{L}]^+$	L = PMe_2Ph , PMePh_2	+1	17	Similar to 3 ^d	55
$[\text{M}(\eta^5\text{-C}_5\text{R}_5)(\text{CO})_3]$	M = Mo, W; R = H M = Mo, W; R = Me	+1	17	-	49,57,58 52,59
$[\text{Mo}(\eta^5\text{-C}_5\text{Me}_5)(\text{Me})_3(\text{OR})]^+$	OR = DIPP, DOMP, DMMP, TROMP	+5	15	DIPP: 1.997 DOMP: 1.994 DMMP: 1.995 TROMP: 1.995	60
$[\text{W}(\eta^5\text{-C}_5\text{Me}_5)(\text{Me})_4]^+$	-	+5	15	-	61
$[\text{W}(\text{CO})_3(\eta^6\text{-C}_6\text{Me}_6)\text{.L}]^{+,e}$	L = PPh_3 , P(OPh)_3 , $\text{P}(n\text{-Bu})_3$, $\text{P}(O(n\text{-Bu}))_3$, CH_3CN , DMF	+1	17	-	49
$[\text{Fe}(\eta^5\text{-C}_5\text{H}_5)(\text{CO})_2]^f$	-	+1	17	-	62-65

Complex	Variables	Oxidation State of the Metal	Number of Electrons	g-Values	References
$[\text{Fe}(\eta^5\text{-C}_5\text{H}_5)(\text{PR}_3)_2]$	R = Me, Ph	+1	17	R = Ph: 2.30, 2.08	66,67
$[\text{Fe}(\eta^5\text{-C}_5\text{H}_5)(\text{PMe}_3)_3]$	-	+1	19	-	66,68,69
$[\text{Fe}(\eta^5\text{-C}_5\text{H}_5)(\text{Me})(\text{CO})(\eta^1\text{-dppe})]^+$	-	+3	17	-	28
$[\text{Fe}(\eta^5\text{-C}_5\text{H}_5)(\text{Me})(\eta^2\text{-dppe})]^+$	-	+3	17	-	28,70
$[\text{Fe}(\eta^5\text{-C}_5\text{H}_5)(\text{Me})(\text{P}(\text{OMe})_3)_2]^+$	-	+3	17	-	28
$[\text{Fe}(\eta^5\text{-C}_5\text{H}_5)(\eta^2\text{-dppe})\text{L}]^+$	L = Cl, Br, I, H, SnMe ₃ , CN, SCN, SPh	+	17	-	70,71
$[\text{Fe}(\eta^5\text{-C}_5\text{H}_5)\text{-}$ $(\eta^6\text{-9,10-dihydroanthracene})]$	-	+1	19	-	72
$[\text{Fe}(\eta^5\text{-C}_5\text{H}_5)(\eta^6\text{-arene})]$	arene = C ₆ H ₆ , C ₆ H ₅ Me, C ₆ H ₅ F, C ₆ HMe ₅ , C ₆ Me ₆ , C ₆ Et ₆	+1	19	arene = C ₆ H ₆ ^g : 2.096, 2.002 arene = C ₆ H ₅ F: 2.0045, 1.9385, 1.7707 arene = C ₆ Me ₆ ^g : 2.000, 2.063, 1.864 arene = C ₆ Et ₆ : 2.059, 2.003, 1.896	73-81
$[\text{Fe}(\eta^5\text{-C}_5\text{Me}_5)(\text{CO})_2]$	-	+1	17	-	59

Complex	Variables	Oxidation State of the Metal	Number of Electrons	g-Values	References
$[\text{Fe}(\eta^5\text{-C}_5\text{Me}_5)(\text{Me})(\text{PR}_3)_2]^+$	R = Me, OMe	+3	17	R = OMe: 2.352, 2.045, 1.997	28,82,83
$[\text{Fe}(\eta^5\text{-C}_5\text{Me}_5)(\text{Me})(\eta^2\text{-dppe})]^+$	-	+3	17	2.453, 2.045, 1.993	28,82
$[\text{Fe}(\eta^5\text{-C}_5\text{Me}_5)(\eta^2\text{-dppe})\text{L}]^+$	L = F, Cl, Br, I, H, Me	+3	17	L = F: 2.149, 2.018, 1.998	84
$[\text{Fe}(\eta^5\text{-C}_5\text{Me}_5)(\text{CO})(\eta^1\text{-dppe})]$	-	+1	17	2.05, 2.43, 1.98	85
$[\text{Fe}(\eta^5\text{-C}_5\text{Me}_5)(\text{Me})(\text{CO})(\eta^1\text{-dppe})]^+$	-	+3	17	-	28
$[\text{Fe}(\eta^5\text{-C}_5\text{Me}_5)(\text{Me})(\text{CO})(\eta^1\text{-dppe})]^+$	-	+3	17	-	28
$[\text{Fe}(\eta^5\text{-C}_5\text{Me}_5)(\text{CO})(\eta^2\text{-dppe})]$	-	+1	19	-	85
$[\text{Fe}(\eta^5\text{-C}_5\text{Me}_5)(\eta^2\text{-S}_2\text{CNMe}_2)\text{X}]^+$	X = CO, Me ₂ CO, MeCN, THF, CH ₂ Cl ₂	+3	17	X = CO: 2.237, 2.071, 2.071 X = Me ₂ CO: 2.453, 2.035, 1.995 X = MeCN: 2.611, 2.184, 2.001 X = CH ₂ Cl ₂ : 2.571, 2.135, 1.990	86

Complex	Variables	Oxidation State of the Metal	Number of Electrons	g-Values	References
$[\text{Fe}(\eta^5\text{-C}_5\text{R}_5)(\eta^2\text{-S}_2\text{CNMe}_2)(\text{PPh}_3)]^+$	R = H, Me	+3	17	-	69,86
$[\text{Fe}(\eta^5\text{-C}_5\text{Me}_5)(\eta^2\text{-S}_2\text{CNMe}_2)\text{X}]$	X = CN, SCN, $\eta^1\text{-S}_2\text{CNMe}_2$	+3	17	-	69
$[\text{Fe}(\eta^5\text{-C}_5\text{Me}_5)(\eta^2\text{-S}_2\text{CNMe}_2)\text{X}]^+$	X = MeCN, Me_2CO , CH_2Cl_2	+3	17	-	69
$[\text{Fe}(\eta^5\text{-C}_5\text{Me}_5)(\eta^2\text{-S}_2\text{CNMe}_2)_2]$	-	+3	19	-	86
$[\text{Fe}(\eta^5\text{-C}_5\text{Me}_5)(\eta^6\text{-arene})]$	arene = C_6H_6 , C_6Me_6	+1	19	arene = C_6Me_6 : 2.062, 2.002, 1.912	78
$[\text{Fe}(\eta^5\text{-C}_5\text{Ph}_4\text{Ar})(\text{CO})_2]$	Ar = Ph, $\text{C}_6\text{H}_5\text{Me}$	+1	17	-	65
$[\text{Fe}(\eta^6\text{-C}_6\text{Me}_6)(\text{CO})(\eta^1\text{-dppe})]^+$	-	+1	15	-	83
$[\text{Fe}(\eta^6\text{-C}_6\text{Me}_6)_2]^+$	-	+1	19	1.865, 1.996, 2.086	81,87
$[\text{Ru}(\eta^5\text{-C}_5\text{H}_5)(\text{CO})_2]$	-	+1	17	-	62

Note: for simplicity, neither the temperature nor the solvent (if applicable) have been specified.

^aExist as monomers in solution and dimers in the solid state; ^bexists in equilibrium with the dimeric form in solution; ^conly one broad signal observed; ^dexact values were not reported in reference(55); ^eligated cation, L, is not coordinated to the W(I); ^ftransient, dimerises at diffusion-controlled rate; ^gother values have also been reported.

DIPP = 2,6-diisopropylphenoxide; DMF = dimethylformamide; DMMP = 2,6-dimethoxy-4-ethylphenoxide; DOMP = 2,6-dimethoxyphenoxide; TROMP = 2,4,6-trimethoxyphenoxide.

The $4d^5$ configuration of the ruthenium(III) ion has one unpaired electron, resulting in most of its monomeric complexes being paramagnetic. Different techniques from those that characterise diamagnetic complexes are required to characterise paramagnetic species. Electron spin resonance (ESR) spectroscopy, also known as electron paramagnetic resonance (EPR), which is a technique applicable to these systems, or to those that can be placed in an excited state (for example, through irradiation⁹⁷), is probably the most widely employed since it is so useful for unstable paramagnetic species.⁹⁸ It can be used to detect free radicals and molecules or ions containing unpaired electrons, such as the 17- and 19-electron species mentioned above. ESR spectroscopy investigates the interaction between electromagnetic radiation and magnetic moments that arises from electrons,⁹⁹ rather than from nuclei, as is the case for NMR. Hence the ESR signal reflects the interactions between the unpaired electron and its environment.

A single electron ($S = 1/2$) can exist in two possible spin states, which are degenerate in the absence of a magnetic field.⁹⁸ The degeneracy is removed when a magnetic field, of strength B_0 , is applied, allowing transitions between the two levels. It is only unpaired electrons which are active in an applied magnetic field since, at absolute zero, the electrons (n) occupy $n/2$ most stable levels in pairs (Pauli exclusion principle) such that the spin magnetic moments of these electrons are not available for orientation in such an applied magnetic field.¹⁰⁰ Thus any ESR signal detected for d^5 Ru(III) is due only to the unpaired electron. The differences in energy between the two levels (see Figure 1) for the magnetic spin quantum number ($m_s = \pm 1/2$) is related to the spectroscopic splitting factor g by the equation⁹⁸:

$$\Delta E = g_e \mu_B B_0 \quad (1)$$

g_e = g -factor of the free electron (2.00232)⁹⁸

μ_B = Bohr magneton

B_0 = strength of applied magnetic field

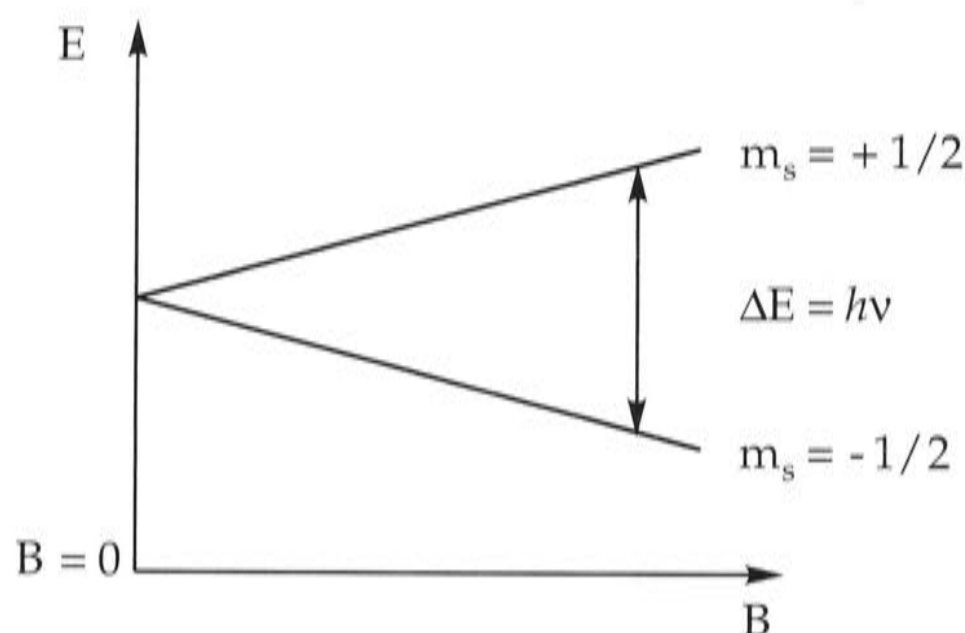


Figure 1. The splitting of the two degenerate spin states of an unpaired electron in a magnetic field.

The g -factor is a symmetric tensor which is diagonalised, giving rise to three principal values, g_{xx} , g_{yy} and g_{zz} .¹⁰¹ These terms are equal in systems with spherical or cubic symmetry, but systems of lower (at least axial) symmetry, such as ruthenium(III), have non-equivalent components along the x , y and z axes in a single crystal, giving rise to three different g -values.¹⁰¹ Thus measurements are recorded at various angles to obtain an ESR spectrum from which the g -values can usually be determined.¹⁰¹ A typical spectrum of a ruthenium(III) complex *mer*-[RuCl₃(PBU₂Ph)₃] (**4**) [*mer* = meridional (OC-6-21)¹⁰²], which shows three distinct g -values, is shown in Figure 2.¹⁰³ The g -values of **4**, and of other typical ruthenium(III) complexes, are listed in Table 2.

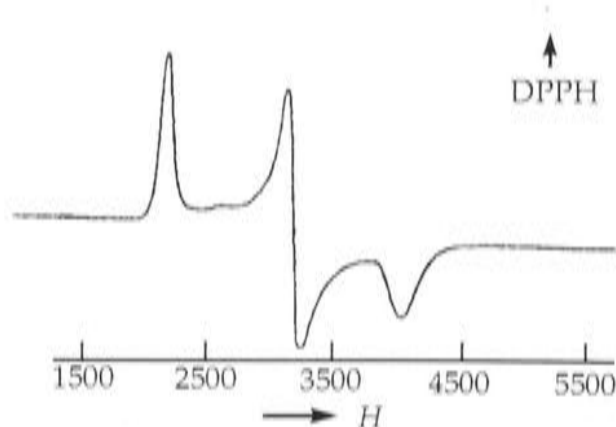


Figure 2. The ESR spectrum of *mer*-[RuCl₃(PBU₂Ph)₃] (**4**) at 77K in EPA (2:5:5 mixture of ethanol/isopentane/ether)¹⁰⁴ relative to diphenylpicrylhydrazyl (DPPH).¹⁰³

The ESR spectra of organometallic radicals are usually different from those of organic radicals, usually having a broader line width, and occurring over a wider field width. For example, the ESR spectrum of DPPH (Figure 3) has only one g -value (2.00) and, in comparison to the ESR spectrum in Figure 2, it spans a much smaller range.¹⁰⁵

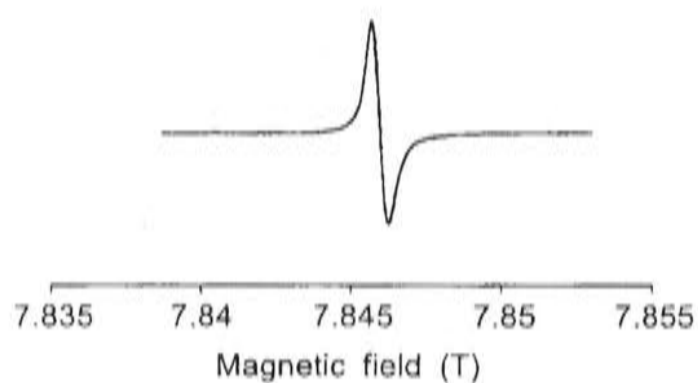


Figure 3. ESR spectrum of finely ground crystals of DPPH (recrystallised several times from CS_2) in the solid state at room temperature.¹⁰⁵

Table 2. g -Values obtained from ESR spectra of various reported ruthenium(III) complexes.

Complex	g_1	g_2	g_3	Temperature (K)	Reference
Ru^{3+} in $[\text{Co}(\text{NH}_3)_6]\text{Cl}_3$	2.02	2.06	1.72	20	106
$[\text{Ru}(\text{H}_2\text{O})_6]^{3+}$	2.517	2.517	1.494	3	107
$[\text{Ru}(\text{acac})_3]$	2.45	2.16	1.45	77	108
<i>trans</i> - $[\text{RuCl}_2(\text{NH}_3)_4]^+$	3.33	2.54	1.18	73	109
<i>trans</i> - $[\text{RuBr}_2(\text{en})_2]^+$	3.02	2.36	0.99	77	110
<i>mer</i> - $[\text{RuCl}_3(\text{PEt}_2\text{Ph})_3]$	2.96	2.01	1.59	77	103
<i>mer</i> - $[\text{RuCl}_3(\text{P}^i\text{Bu}_2\text{Ph})_3]$ (4) ^a	2.94	2.02	1.60	77	103
$[\text{Ru}(\eta^5\text{-C}_5\text{H}_5)(\text{Me})(\text{PPh}_3)_2]^+$	2.23	2.15	1.98	100	111
$[\text{Ru}(\eta^5\text{-C}_5\text{Me}_5)(\text{Me})(\text{PMe}_2\text{Ph})_2]^+$	2.26	2.11	1.98	100	111
$[\text{Ru}(\text{Me})_2(\eta^6\text{-C}_6\text{Me}_6)(\text{PPh}_3)]^+$ (5) ⁺	2.21	2.22	2.01	100	112
$[\text{Ru}(\text{Me})(\text{Ph})(\eta^6\text{-C}_6\text{Me}_6)(\text{PMePh}_2)]^+$ (6) ⁺	2.22	2.19	2.01	100	112

Note: the solvent (where applicable) used to record ESR spectra is not specified.

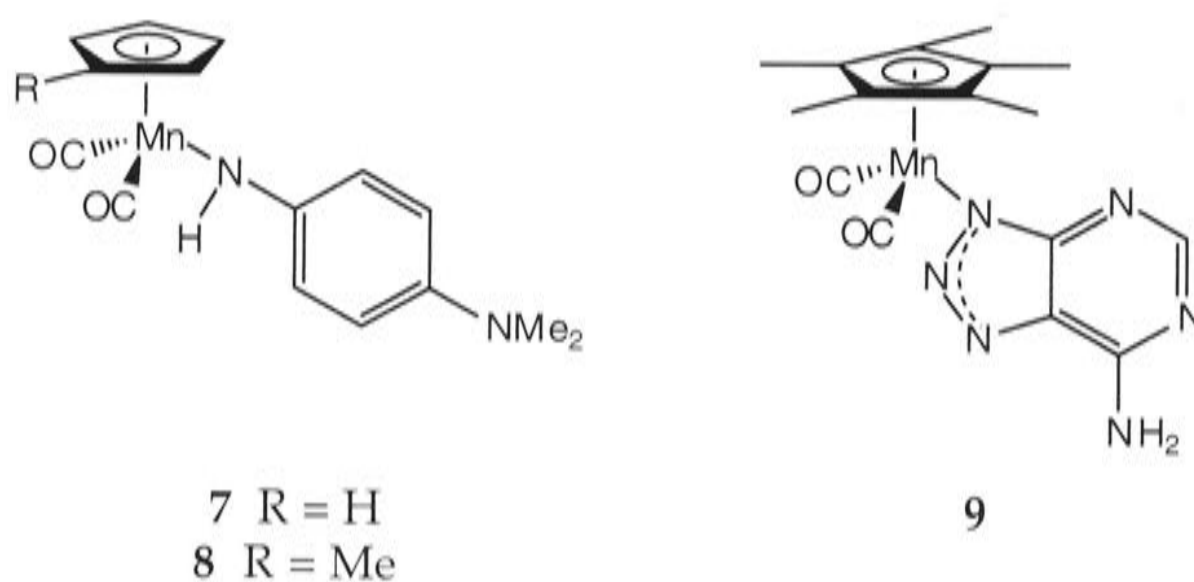
^aESR spectrum recorded in ether, not EPA as shown in Figure 2.¹⁰³

acac = acetylacetonato, $[\text{MeC}(\text{O})\text{CHC}(\text{O})\text{Me}]^-$

en = ethylenediamine

The g -values of mer -[RuCl₃(PBUⁿ₂Ph)₃] lie over a large range and are also significantly different from that of the free electron (2.00232).⁹⁸ Transition metal complexes can have significant variations between their g -values,⁹⁸ a phenomenon that is described as anisotropy. This is due to both the spin-orbit coupling (coupling of the spin angular momentum and the smaller effects due to the orbital angular momentum)^{98,113} and the fact that the d -orbitals of T. M. complexes do not interact equally with all of the ligands of the complex.¹¹⁴ The latter influence results in the splitting of levels into two or more groups, giving rise to more than one g -value. Thus the g -values are diagnostic features of the species responsible for the ESR spectrum, and can often provide specific information about the electronic structure of the complex.¹¹⁵

ESR spectroscopy can distinguish between a ligand centred radical, a metal-centred radical and radicals with mixed metal-ligand character,¹¹⁶ due to difference in the spectra that arise from coupling with spin-active nuclei, either with atoms in a ligand or within the metal itself. For example, the ESR spectra of the dicarbonylmanganese 17-electron complexes **7-9** were investigated.¹¹⁷⁻¹²⁰ The unpaired electron of complexes **7** and **8** is located in an orbital of mixed metal/ligand character,¹¹⁷⁻¹¹⁹ whilst the unpaired electron of the manganese(II) complex **9** resides on the metal itself.¹²⁰ This technique can also be extremely useful for monitoring a reaction, particularly for highly unstable complexes. For example, the thermally unstable 19-electron species [Fe(η^5 -C₅H₄CO₂H)(η^6 -C₆Me₆)] (arene also = C₆H₆, 1,3,5-C₆H₃Me₃, naphthalene) was prepared *via* Na/Hg reduction of [Fe(η^5 -C₅H₄CO₂H)(η^6 -C₆Me₆)]⁺, and the reaction was probed by ESR spectroscopy.^{121,122} The reduction of the zwitterion [Fe(η^5 -C₅H₄CO₂⁻)(η^6 -C₆Me₆)]⁺, generated by deprotonation of [Fe(η^5 -C₅H₄CO₂H)(η^6 -C₆Me₆)]⁺, gave rise to the very air-sensitive redox catalyst [Fe(η^5 -C₅H₄CO₂H)(η^6 -C₆Me₆)], which was also monitored by ESR spectroscopy.



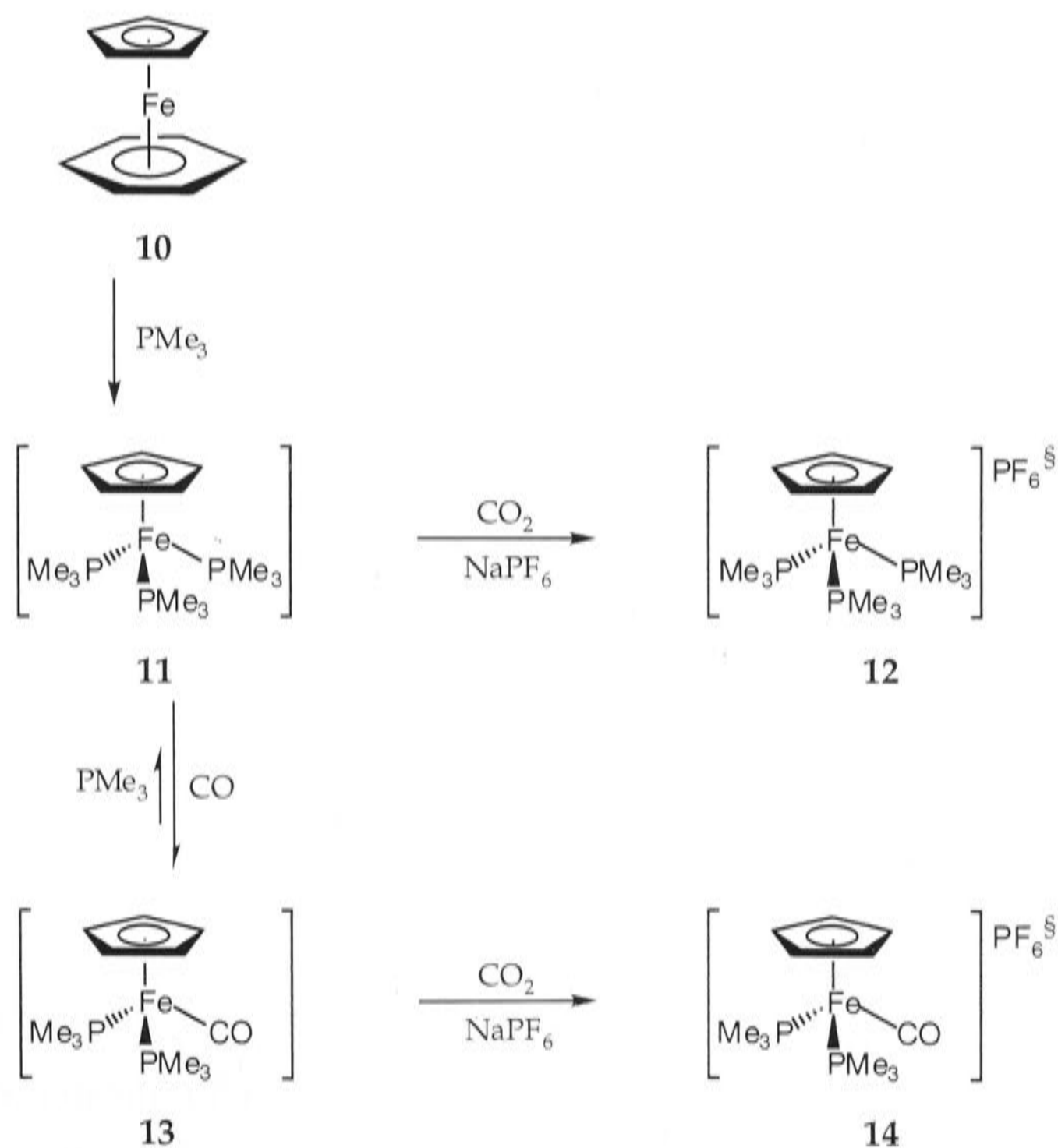
Although the presence of unpaired electrons would normally be expected to cause rapid relaxation of the nuclear excited state in the NMR experiment, causing broad NMR lines (short T_1), it is possible to study the solution $^1\text{H-NMR}$ spectra of certain paramagnetic T. M. complexes.¹²³ Rapid electron relaxation can decrease the efficiency of the nuclear relaxation mechanism, lengthening T_1 for the proton nucleus and causing the line to sharpen. Ruthenium(III) ($4d^5$) is among the T. M. ions for whose complexes $^1\text{H-NMR}$ spectra can be measured at room temperature, for example tris(β -diketonato)ruthenium(III).^{124,125} The magnetic field generated by the unpaired electron in such cases causes large isotropic shifts. The technique is complimentary to ESR spectroscopy, since systems that give "sharp" NMR spectra usually give broad ESR spectra at room temperature, and *vice versa*.

1.1.2 Reactivity of Paramagnetic Organometallic Complexes

As paramagnetic species are highly reactive, they have the ability to catalyse various reactions. The facile interconversion between 17- and 19-electron radicals^{69,126,127} results in enhanced ligand lability and allows many different types of reactions to occur, such as catalysis of ligand substitution and carbon monoxide insertion. There are numerous examples,^{128,129} and only selected ones will be described here.

The ligands of odd-electron species, generated by oxidation or reduction of the 18-electron parent complex, are generally much more labile towards displacement than those of the diamagnetic parent complexes.^{130,131} The

substitution of η^6 -arenes of 19-electron paramagnetic iron is extremely facile.^{67,68,72} The resulting 19-electron complex formed is not stable,^{68,132} and is immediately converted by an external reagent into a more stable 18-electron complex. For example, the complex $[\text{Fe}(\eta^5\text{-C}_5\text{H}_5)(\eta^6\text{-C}_6\text{H}_6)]$ (**10**) reacts with trimethylphosphine to give the 19-electron intermediate $[\text{Fe}(\eta^5\text{-C}_5\text{H}_5)(\text{PMe}_3)_3]$ (**11**), which catalytically reduces carbon dioxide to carbon monoxide and carbonate ion. In the presence of sodium hexafluorophosphate, **11** reacts with CO_2 to afford the Fe(II) complex $[\text{Fe}(\eta^5\text{-C}_5\text{H}_5)(\text{PMe}_3)_3]\text{PF}_6$ (**12**), Na_2CO_3 and CO (Scheme 1). Alternatively, one of the phosphines of the 19-electron intermediate **11** can be replaced by carbon monoxide to give the 19-electron species **13**, which also reacts with carbon dioxide and NaPF_6 to give the Fe(II) compound **14**.

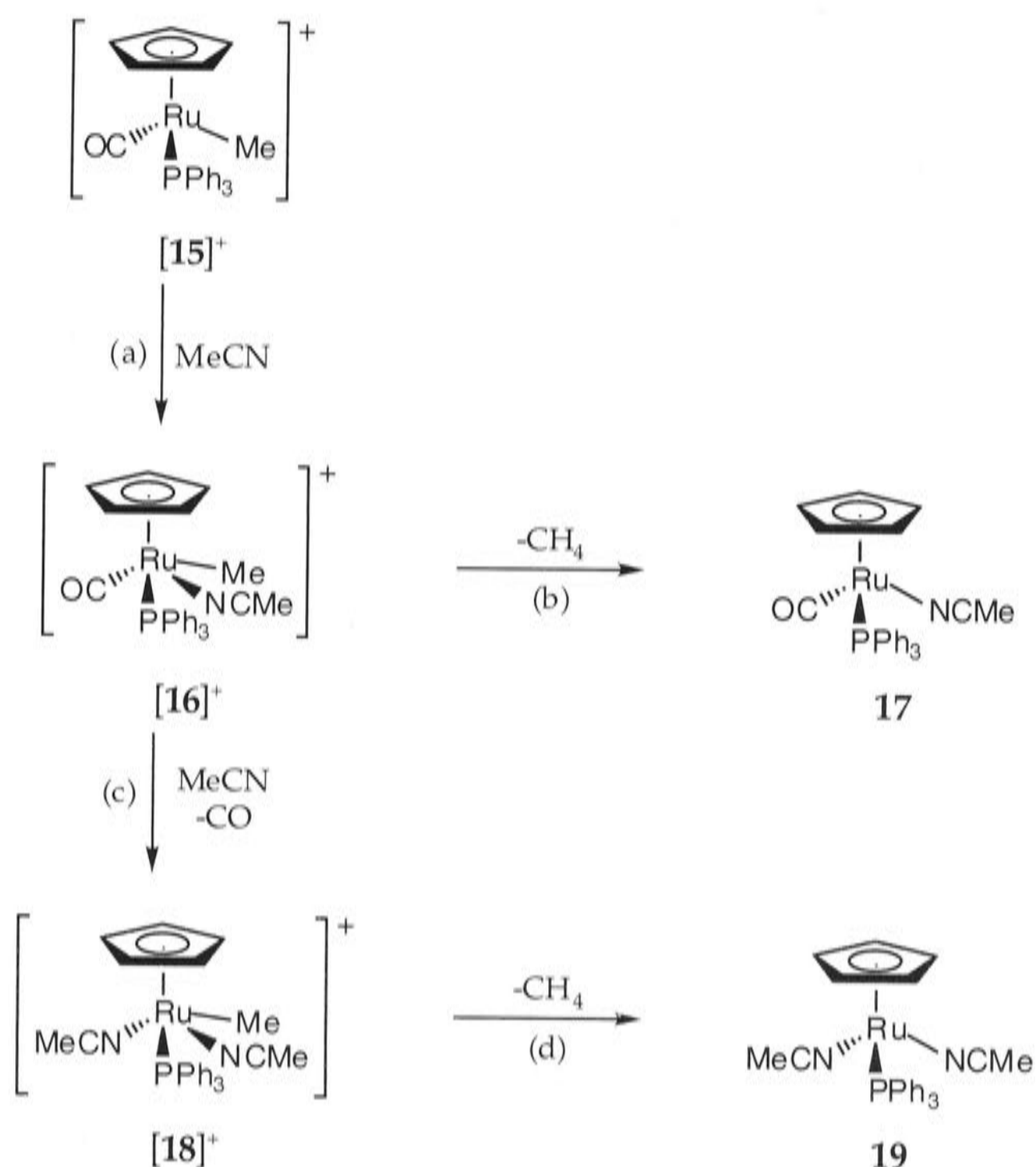


Scheme 1. Preparation of the Fe(II) complexes **12** and **14** from the 19-electron parent species **10**.⁶⁸ [§]Plus $1/2(\text{Na}_2\text{CO}_3)$ and $1/2(\text{CO})$.

The η^6 -arene of 18-electron iron complexes of the type $[\text{Fe}(\eta^5\text{-C}_5\text{H}_5)(\eta^6\text{-C}_6\text{R}_6)]\text{PF}_6$ ($\text{R} = \text{H}, \text{D}, \text{Me}$) is susceptible to nucleophilic attack.⁷⁹ Astruc and Michaud⁷⁹ have shown that attack by H^- (from LiAlH_4) proceeded by an electron transfer mechanism *via* the 19-electron intermediates $[\text{Fe}(\eta^5\text{-C}_5\text{H}_5)(\eta^6\text{-C}_6\text{R}_6)]$ ($\text{R} = \text{H}, \text{D}, \text{Me}$), which then abstract a hydrogen atom to form the 18-electron complexes $[\text{Fe}(\eta^5\text{-C}_5\text{H}_5)(\eta^5\text{-C}_6\text{R}_6\text{H})]$ ($\text{R} = \text{H}, \text{D}, \text{Me}$).

Because they are potentially related to the target arene-ruthenium(III) complexes, some reactions of paramagnetic cyclopentadienyl ruthenium complexes will now be discussed. Electrochemical oxidation of $[\text{RuMe}(\eta^5\text{-C}_5\text{Me}_5)(\text{CO})(\text{PPh}_3)]$ (**15**) in acetonitrile affords the 17-electron species $[\mathbf{15}]^+$.^{133,134} It reacts with acetonitrile to give the 19-electron intermediate $[\mathbf{16}]^+$ (Scheme 2a), which can react in two different ways: the Ru-Me bond can be cleaved to give the 18-electron product **17** and methane (Scheme 2b), or the carbon monoxide ligand of $[\mathbf{16}]^+$ can be replaced by another acetonitrile ligand, to give the 19-electron transient species $[\mathbf{18}]^+$ (Scheme 2c). Cleavage of the Ru-Me bond of $[\mathbf{18}]^+$ affords the stable compound **19** (Scheme 2d). These reactions illustrate the fact that Ru(III) complexes containing carbocyclic ligands are highly unstable and can sometimes only be studied by electrochemical techniques.

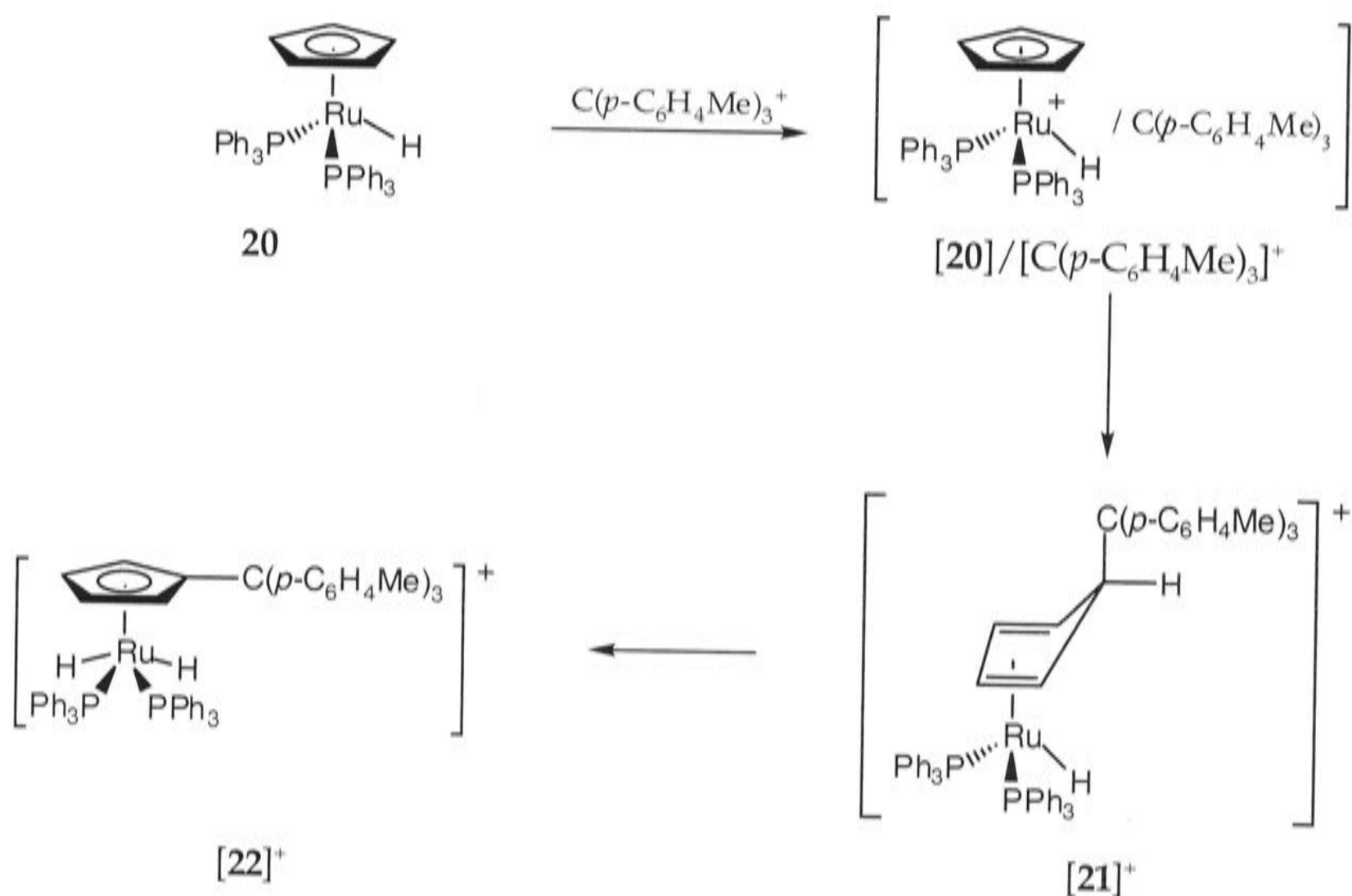
Ligand exchange reactions are not the only type of reactions to occur with paramagnetic complexes; the ligands themselves are also susceptible to reaction. For example, in an attempt to abstract the hydride ligand of the 18-electron complex $[\text{Ru}(\text{H})(\eta^5\text{-C}_5\text{H}_5)(\text{PPh}_3)_2]$ (**20**) with the substituted trityl reagent $[\text{C}(p\text{-C}_6\text{H}_4\text{Me})_3]\text{PF}_6$, the latter was found to add to the cyclopentadienyl ring to form, possibly within a 17-electron cage associated species $[\mathbf{20}]/[\text{C}(p\text{-C}_6\text{H}_4\text{Me})_3]^+$, the species $[\mathbf{21}]^+$ (Scheme 3).¹³⁵ Proton migration finally affords the η^5 -cyclopentadienyl complex $[\mathbf{22}]^+$.



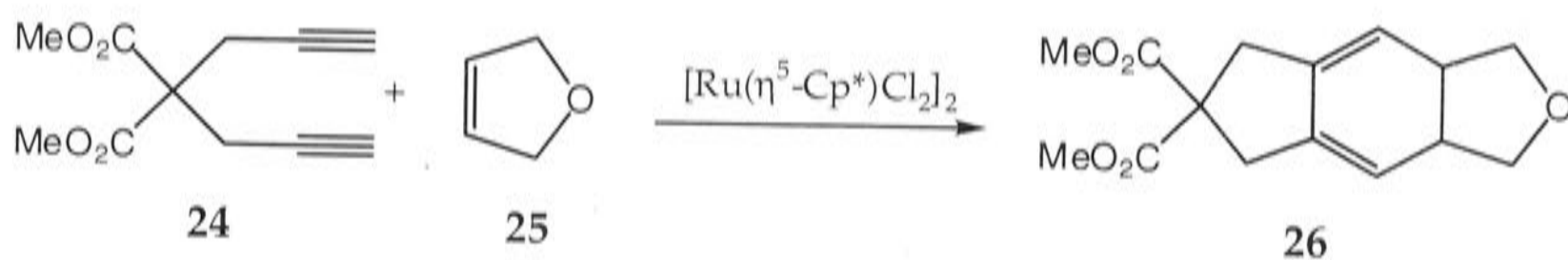
Scheme 2. Reaction of the 17-electron complex $[15]^+$ with acetonitrile to give the two 18-electron compounds **17** and **19** via the 19-electron complexes $[16]^+$ and $[18]^+$, respectively.¹³³

It is significant to note that for most organic reactions which are catalysed by organometallic complexes, paramagnetic species are not considered as intermediates.¹³⁶ The one-electron reduction of $[\text{Fe}(\eta^5\text{-C}_5\text{H}_4\text{R})(\eta^6\text{-C}_6\text{Me}_n\text{H}_{6-n})]^+$ ($\text{R} = \text{H}, \text{CO}_2\text{H}; 0 \leq n \leq 6$) gives rise to the 19-electron species $[\text{Fe}(\eta^5\text{-C}_5\text{H}_4\text{R})(\eta^6\text{-C}_6\text{Me}_n\text{H}_{6-n})]$, which induces the electroreduction of nitrate ion to ammonia in aqueous solutions.¹³⁷ There is also an example of a paramagnetic Ru(III) complex which catalyses cycloaddition reactions.¹³⁸ The dimer $[\text{RuCl}_2(\eta^5\text{-C}_5\text{Me}_5)]_2$ (**23**) catalyses the reaction of various diynes and heterocycles to give cycloaddition products. For example, the diyne (**24**) and 2,5-dihydrofuran (**25**) gave the product **26** (Scheme 4). The dimer **23** was found to be a far superior catalyst to the

mononuclear Ru(II) complex $[\text{RuCl}(\eta^5\text{-C}_5\text{Me}_5)(\eta^4\text{-1,5-COD})]$
(COD = 1,5-cyclooctadiene).



Scheme 3. Preparation of the 18-electron complex $[\text{22}]^+$ from the parent compound **20**.¹³⁵

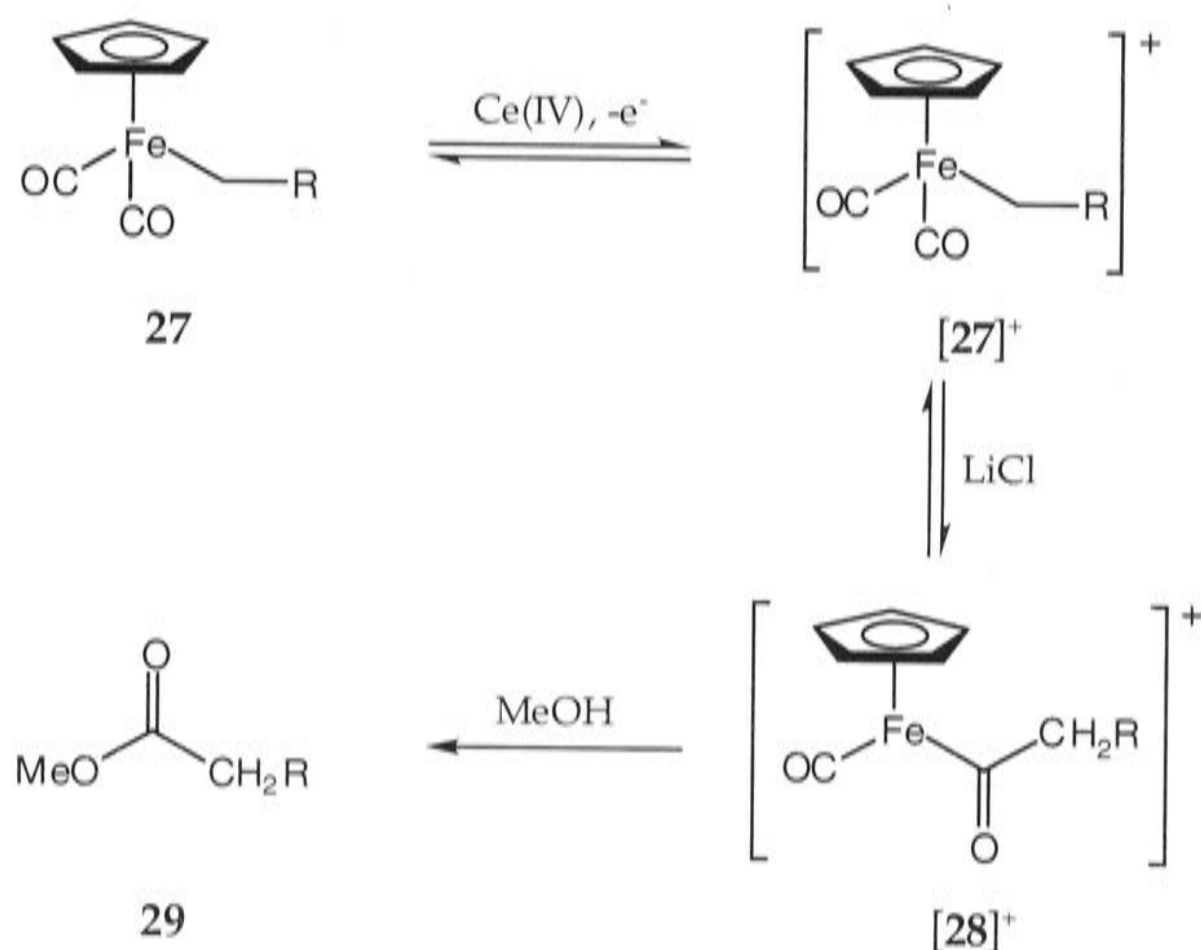


Scheme 4. $[\text{RuCl}_2(\eta^5\text{-C}_5\text{Me}_5)]_2$ (**23**) catalysed cyclotrimerisation reaction to afford the compound **26**.¹³⁸

There are some interesting examples of carbonyl migratory insertion reactions that occur *via* paramagnetic intermediates.^{139,140} These reactions are clearly distinct from the standard CO migratory insertion reaction that occurs *via* a coordinatively unsaturated 16-electron intermediate.¹⁴¹

The complexes $[\text{Mo}(\eta^5\text{-C}_5\text{H}_5)(\text{CH}_2\text{C}_6\text{H}_4\text{F-}p)(\text{CO})_3]$, $[\text{W}(\eta^5\text{-C}_5\text{H}_5)(\text{CH}_2\text{C}_6\text{H}_4\text{F-}p)(\text{CO})_3]$ and $[\text{Fe}(\eta^5\text{-C}_5\text{H}_5)(\text{CH}_2\text{-4-C}_6\text{H}_4\text{F})(\text{CO})_2]$ (**27**) can be oxidised with an excess of cerium(IV), and subsequent treatment with

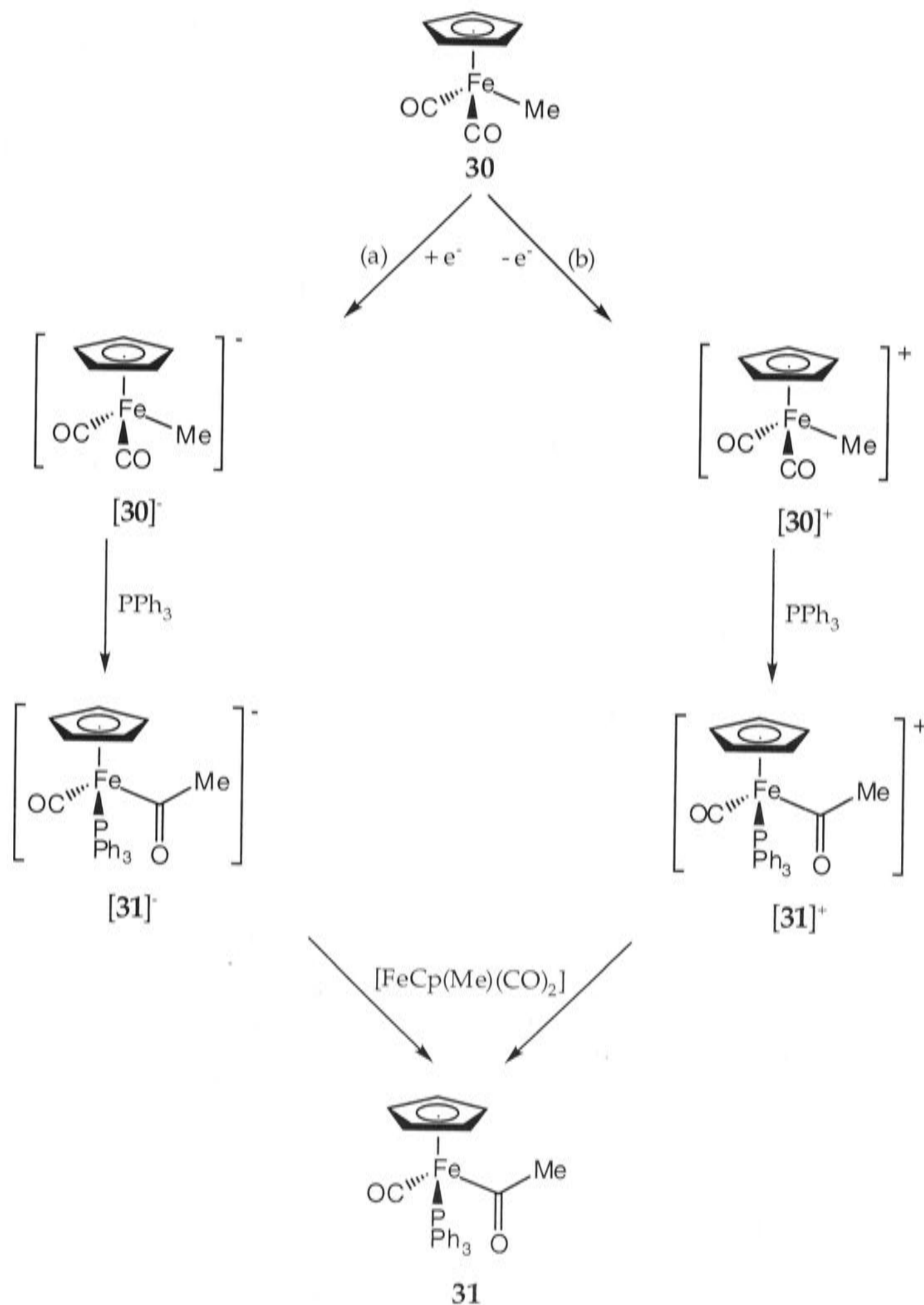
lithium chloride in methanol gives the ester methyl-4-fluorophenylacetate. In the case of tungsten and iron, both 4-fluorobenzylchloride and 4-fluorobenzylmethyl ether were obtained as by-products. The general reaction to give the main ester product is shown for the iron complex (Scheme 5). Oxidation of the complex **27** gives the 17-electron species $[27]^+$ which reacts with lithium chloride to give the 15-electron species **28**, formed as a result of CO migration, which eliminates the ester **29** upon reaction with methanol.



Scheme 5. Formation of the ester **29** *via* CO migratory insertion from the complex **27** ($\text{R} = 4\text{-C}_6\text{H}_4\text{F}$).¹³⁹

The organometallic iron complex $[\text{Fe}(\eta^5\text{-C}_5\text{H}_5)(\text{Me})(\text{CO})_2]$ (**30**) undergoes a CO migratory insertion reaction which is catalysed by paramagnetic species and can be induced either by reduction¹⁴⁰ or oxidation.¹⁴² The cathodic reduction of complex **30** produces the 19-electron species $[30]^-$, which reacts with triphenylphosphine to form the 19-electron CO migration product $[31]^-$ (Scheme 6a). The anion $[31]^-$ is then oxidized by the parent compound **30** and is itself reduced to the 19-electron radical $[30]^\cdot$, thus $[31]^-$ is oxidised to the 18-electron product **31**. The reduction of the parent complex **30** completes the catalytic cycle. Oxidation of the complex **30** gives rise to the 17-electron species $[30]^+$, which also reacts with phosphines, such as

triphenylphosphine, to form the CO migratory insertion product $[31]^+$ (Scheme 6b). This is then reduced by the parent complex **30** which itself is oxidised to form the radical $[30]^+$, affording the neutral compound **31**.



Scheme 6. Catalytic CO migratory insertion by (a) reductive and (b) oxidative pathways to form the complex **31** from the parent species **30**.^{140,142}

1.1.3 Chemical Oxidants

A number of different oxidants can be used to generate a paramagnetic complex from the diamagnetic parent species. Reagents such as the cations $[\text{NO}]^+$, Ag^+ , $[\text{Fe}(\text{C}_5\text{H}_5)_2]^+$, $[\text{p-FC}_6\text{H}_4\text{N}_2]^+$, and the neutral species TCNE (TCNE = tetracyanoethylene), SbCl_5 , chlorine and iodine, have all been employed as oxidants for η^6 -arene complexes of the Group 6 and 8 elements.^{55,56,111,112,143-149} The choice of oxidant is very much dependent on the compatibility of the electrode potentials of the two species, *i.e.* the potential of the oxidant needs to be sufficiently greater than that of the complex to be oxidised. The electrode potentials of some chemical oxidants are listed in Table 3. Further, not all chemical oxidants are inert towards coordination, so this must also be considered when choosing a reagent. This behaviour will be illustrated in some of the examples discussed below.

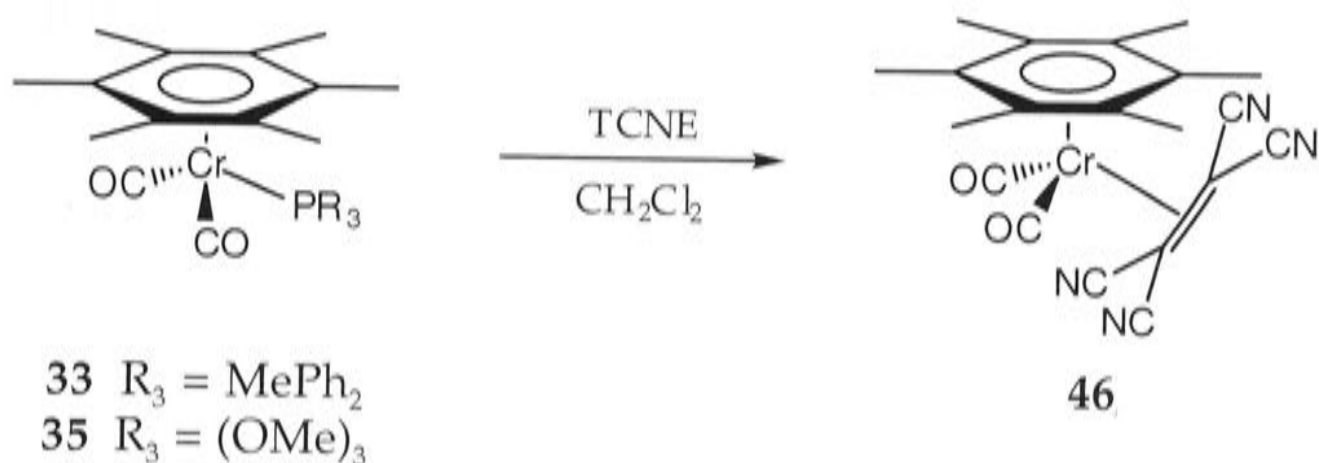
Table 3. Formal Electrode Potentials (E°') of some oxidising agents in acetonitrile (*vs* $\text{Fc}^{0/1}$) [Fc = ferrocene].¹⁵⁰

Oxidant	E°' (Volts)	Conversion Factor (Volts)	References
SbCl_5^\S	+ 1.2 ^a	-	151
$[\text{NO}]^{+,Y}$	+ 0.87	-	152
$[\text{N}(\text{C}_6\text{H}_4\text{Br-4})_3]^{+,Y}$	+ 0.67	- 0.38 [‡]	153
Cl_2^\S	+ 0.18	- 0.40 [‡]	154
$[\text{N}_2\text{C}_6\text{H}_4\text{NO}_2\text{-4}]^{+,Y}$	<i>ca</i> + 0.05 ^b	- 0.40 [‡]	155
$\text{Ag}^{+,Y}$	<i>ca</i> + 0.04	-0.40 ^{‡,c}	156
$[\text{Fe}(\eta^5\text{-C}_5\text{H}_5)_2]^{+,Y}$	0.00	-	-
TCNE ^Y	- 0.22 ^{d,e}	- 0.40 [‡]	157
$[\text{Fe}(\eta^5\text{-C}_5\text{Me}_5)_2]^{+,Y}$	- 0.59	-	150

[§]Two-electron oxidant; ^Yone-electron oxidant. ^aIn nitromethane; ^bin tetramethylene sulfone; ^can intermediate conversion factor of + 0.64 V was required to convert - 0.20 V *vs* Ag/AgNO_3 ¹⁵⁶ to + 0.44 V *vs* SCE (Saturated Calomel Electrode), which was not stated in reference(150); ^din DMF; ^equoted as - 0.27 V (*vs* $\text{Fc}^{0/1}$) in reference(150), but reference(157) quotes E°' as + 0.18 V *vs* aqueous SCE. [‡]Electrode potential converted to $\text{Fc}^{0/1}$ according to reference(150).

The reactions of $[\text{Cr}(\eta^6\text{-C}_6\text{Me}_6)(\text{CO})_2(\text{PR}_3)]$ ($\text{R}_3 = \text{Ph}_3$ (**32**), MePh_2 (**33**), Me_2Ph (**34**), $(\text{OMe})_3$ (**35**) and $(\text{OPh})_3$ (**36**)) with either $[\text{NO}]\text{PF}_6$ or $[\text{PhN}_2]\text{PF}_6$ have been investigated.^{55,56} Reaction with $[\text{NO}]\text{PF}_6$ yields either the complexes $[\text{Cr}(\eta^6\text{-C}_6\text{Me}_6)(\text{CO})(\text{PR}_3)(\text{NO})]\text{PF}_6$ ($\text{R}_3 = \text{Ph}_3$ (**37**), MePh_2 (**38**), Me_2Ph (**39**), $(\text{OMe})_3$ (**40**) and $(\text{OPh})_3$ (**41**)), arising from loss of carbon monoxide, or $[\text{Cr}(\eta^6\text{-C}_6\text{Me}_6)(\text{CO})_2(\text{NO})]\text{PF}_6$ (**42**), formed due to loss of PR_3 . The type of product formed with the reaction of **32-36** with the oxidant $[\text{PhN}_2]\text{PF}_6$ is dependent upon the nature of the substituents on the phosphorus atom. Compounds **32-34**, with tertiary phosphines, gave rise to the compounds $[\text{Cr}(\eta^6\text{-C}_6\text{Me}_6)(\text{CO})_2(\text{PR}_3)]\text{PF}_6$ ($\text{R}_3 = \text{Ph}_3$ ($[\text{32}]\text{PF}_6$), MePh_2 ($[\text{33}]\text{PF}_6$), Me_2Ph ($[\text{34}]\text{PF}_6$)). This oxidant, however, also coordinated to the chromium when tertiary phosphite ligands were present; complexes **35** and **36** gave rise to the species $[\text{Cr}(\eta^6\text{-C}_6\text{Me}_6)\{\text{P}(\text{OR})_3\}(\text{CO})(\text{PhN}_2)]\text{PF}_6$ ($\text{R} = \text{Me}$ (**43**), Ph (**44**)) formed due to loss of carbon monoxide, or $[\text{Cr}(\eta^6\text{-C}_6\text{Me}_6)(\text{CO})_2(\text{PhN}_2)]\text{PF}_6$ (**45**) formed as a result of phosphite ligand displacement.

Neutral chemical oxidants that form stable anions by reduction can also convert $\text{Cr}(0)$ to $\text{Cr}(\text{I})$. Tetracyanoethylene reacted with $[\text{Cr}(\eta^6\text{-C}_6\text{Me}_6)(\text{CO})_2(\text{PR}_3)]$ ($\text{R}_3 = \text{MePh}_2$ (**33**) or $(\text{OMe})_3$ (**35**)) to give the $\text{Cr}(0)$ complex $[\text{Cr}(\eta^6\text{-C}_6\text{Me}_6)(\text{CO})_2(\eta^2\text{-(NC)}_2\text{C}=\text{C}(\text{CN})_2)]$ (**46**) (Scheme 7).¹⁴³ Whilst the net reaction is not redox, it occurs *via* a redox process through an intermediate 19-electron cation, $[\text{33}]^+$ or $[\text{35}]^+$, which reacts with TCNE^- to give **46**.¹⁴³ The enhanced lability of the phosphine or phosphite ligands of $[\text{33}]^+$ or $[\text{35}]^+$ is reflected in the analogous reaction with $[\text{Cr}(\eta^6\text{-C}_6\text{Me}_6)(\text{CO})_3]$ (**2**); ligand replacement does not occur, and a 1:1 charge transfer adduct $[\text{Cr}(\eta^6\text{-C}_6\text{Me}_6)(\text{CO})_3][\text{TCNE}]$ ($[\text{2}][\text{TCNE}]$) was formed.¹⁵⁸



Scheme 7. Reaction of complexes of the type $[\text{Cr}(\eta^6\text{-C}_6\text{Me}_6)(\text{CO})_2(\text{PR}_3)]$ ($\text{R}_3 = \text{MePh}_2$ (33) or $(\text{OMe})_3$ (35)) with the neutral chemical oxidant TCNE.¹⁴³

Antimony pentachloride can also oxidise Group 6 metals. For example, complexes of the type $[\text{M}(\eta^6\text{-C}_6\text{Me}_6)(\text{CO})_3]$ ($\text{M} = \text{Mo}, \text{W}$) were converted into their two-electron oxidation products, $[\text{MCl}(\eta^6\text{-C}_6\text{Me}_6)(\text{CO})_3]\text{SbCl}_6$ ($\text{M} = \text{Mo}, \text{W}$), by reaction with SbCl_5 .¹⁴⁴ The two-electron oxidation products from the reactions of either the corresponding chromium analogue, or complexes of the type $[\text{M}(\eta^6\text{-arene})(\text{CO})_3]$ ($\text{M} = \text{Mo}, \text{W}$; arene = mesitylene, durene or *p*-cymene) could not be purified. Thus, only η^6 -peralkylarenes such as C_6Me_6 , gave rise to pure one-electron oxidation products. However, SbCl_5 can also act as a Lewis acid and may appear in the coordination sphere of the final product. For example, the reaction of SbCl_5 with *trans*- $[\text{Mn}(\text{CN})(\text{CO})_2\{\text{P}(\text{OEt})_3\}(\eta^2\text{-dppm})]$ (dppm = 1,1-bis(diphenylphosphine)methane) gave rise to *trans*- $[\text{Mn}(\text{CNSbCl}_5)(\text{CO})_2\{\text{P}(\text{OEt})_3\}(\eta^2\text{-dppm})]\text{SbCl}_6$.¹⁵⁹

Most of the Cr(I) complexes discussed incorporate both alkyl-substituted η^6 -arenes and tertiary phosphine or phosphite ligands, which help to stabilise the paramagnetic species. In contrast, due to the nature of the ligands, the 17-electron cation, $[\text{Cr}(\eta^6\text{-C}_6\text{H}_6)(\text{CO})_3]^+$ ($[\mathbf{1}]^+$) containing η^6 -benzene and only three carbon monoxide ligands is very unstable.³⁵ The nature of the anion has been shown to influence the stability $[\mathbf{1}]^+$; it decomposes by loss of benzene in the presence of anions such as $[\text{ClO}_4]^-$, $[\text{BF}_4]^-$, $[\text{PF}_6]^-$ and $[\text{CF}_3\text{SO}_3]^-$.^{51,52} However, the large (pentafluorophenyl)borate

anion, $[\text{B}(\text{C}_6\text{F}_5)_4]^-$ (TFAB), actually stabilises $[\mathbf{1}]^+$, allowing the electrochemistry of the $\mathbf{1}/[\mathbf{1}]^+$ couple to be investigated.³⁵ In fact, the TFAB anion stabilises complex $[\mathbf{1}]^+$ to the extent that it is inert to η^6 -arene displacement by triphenylphosphine. One of the carbon monoxide ligands is displaced when $[\mathbf{1}]^+$ was treated with triphenylphosphine, to give $[\text{Cr}(\eta^6\text{-C}_6\text{H}_6)(\text{CO})_2(\text{PPh}_3)]^+$, which was subsequently reduced to the 18-electron complex $[\text{Cr}(\eta^6\text{-C}_6\text{H}_6)(\text{CO})_2(\text{PPh}_3)]$.³⁵

The importance of the relative inertness of chemical oxidants is also illustrated in the reaction of $[\text{Fe}(\text{CO})_3(\text{PPh}_3)_2]$ (**47**) with various cationic oxidising agents in attempts to form $[\text{Fe}(\text{CO})_3(\text{PPh}_3)_2]\text{PF}_6$ ($[\mathbf{47}]\text{PF}_6$).²³ Reaction of **47** with AgPF_6 gave the Ag-Fe bonded adduct $[\text{Ag}\{\text{Fe}(\text{CO})_3(\text{PPh}_3)_2\}]\text{PF}_6$, whereas $[\text{NO}]\text{PF}_6$ and $[\text{N}_2\text{C}_6\text{H}_5]\text{PF}_6$ gave rise to the carbonyl substitution products $[\text{Fe}(\text{CO})_2(\text{X})(\text{PPh}_3)_2]\text{PF}_6$ ($\text{X} = \text{NO}, \text{N}_2\text{C}_6\text{H}_5$). Only the triarylamminium salt $[\text{N}(\text{C}_6\text{H}_4\text{Br-4})_3]\text{SbCl}_6$ ($[\mathbf{48}]\text{SbCl}_6$) afforded the desired product $[\mathbf{47}]\text{PF}_6$.

The SbCl_6^- anion, however, is not always innocent.¹⁵⁰ It can act as a source of chloride ion, both in organic¹⁶⁰ and inorganic¹⁴⁵ systems. Complex $[\text{MnCl}(\eta^5\text{-C}_5\text{H}_4\text{Me})(\text{CO})(\eta^2\text{-dppe})]^+$ formed when $[\text{Mn}(\eta^5\text{-C}_5\text{H}_4\text{Me})(\text{CO})(\eta^2\text{-dppe})]$ was treated with $[\mathbf{48}]\text{SbCl}_6$, though it was too unstable to be isolated.¹⁴⁵ Further, SbCl_6^- can be converted into other counter ions, such as SbCl_4^- or $\text{Sb}_2\text{Cl}_8^{2-}$, arising from reduction of SbCl_6^- , as it itself is an oxidising agent,¹⁵⁰ capable of oxidising aromatic amines.¹⁶¹ For example, reaction of the dimeric species $[\text{Mo}_2(\eta^5\text{-C}_5\text{H}_5)_2(\mu\text{-C}_8\text{H}_8)]$ with $[\text{N-}i\text{-Pr}_4]\text{SbCl}_6$ gave rise to $[\text{Mo}_2(\mu\text{-Cl})(\eta^5\text{-C}_5\text{H}_5)_2(\mu\text{-C}_8\text{H}_8)]_2\text{Sb}_2\text{Cl}_8$.¹⁴⁶

Similarly, $[\text{N}(\text{C}_6\text{H}_4\text{Br-4})_3]^+$ ($[\mathbf{48}]^+$) can react with metal complexes in ways other than as an oxidising agent, since it can undergo nucleophilic reactions with chloride and cyanide ions.¹⁵⁰ The stability of $[\mathbf{48}]^+$ is largely influenced by the nature of the anion.¹⁶² Smaller anions, such as BF_4^- and ClO_4^- , allow two radical cations to dimerise, whereas ion-pairing occurs between $[\mathbf{48}]^+$ and large anions, such as PF_6^- , WCl_6^- and SbCl_6^- , thus

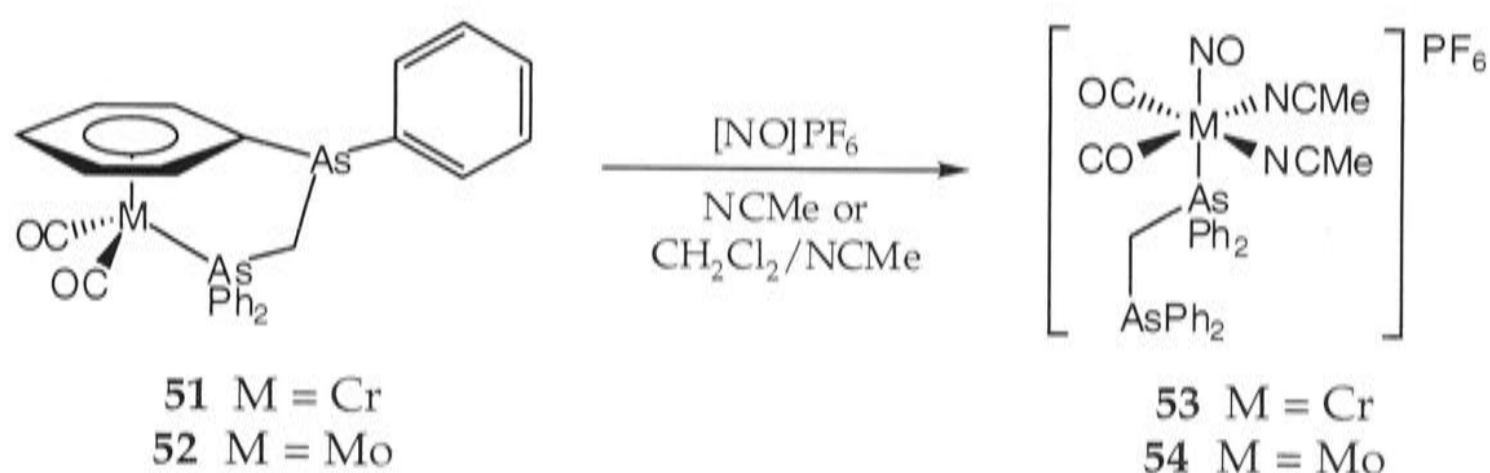
inhibiting dimerisation and enhancing the stability of the aminium salt.¹⁶² For example, [48]SbCl₆ is more stable, and easier to prepare, than the perchlorate salt.¹⁶³ The degradation of triarylamminium salts can be monitored by both UV/Vis spectroscopy^{162,164} and cyclic voltammetry (CV).¹⁵⁰ For example, Ebersson and Larsson^{162,164} have shown that acetonitrile solutions of [48]BF₄ degrade to give coupled products,¹⁶⁴ but that [48]SbCl₆ only undergoes slow reduction to the amine N(C₆H₄Br-4)₃ (49).¹⁶² Thus the stability of these triarylamminium salts is also influenced by the aryl substitution.¹⁵⁰ Increasing the degree of bromine substitution increases the oxidizing power, as shown by the electrode potentials.¹⁵⁰

The reaction of complexes [Mo(η⁶-arene)(CO)₃] (arene = C₆H₅Me, 1,4-C₆H₄Me₂, 1,3,5-C₆H₃Me₃, C₆Me₆) with iodine afforded the cations [MoI(η⁶-arene)(CO)₃]⁺ (arene = 1,3,5-C₆H₃Me₃, C₆Me₆); the nature of the anion (I₃⁻, [MoI₃(CO)₄]⁻ or [Mo₂I₅(CO)₆]⁻) varied depending on the stoichiometry of reagents and the reaction time.¹⁴⁷ The tungsten analogue, [W(η⁶-1,3,5-C₆H₃Me₃)(CO)₃], also reacts with I₂ to afford [WI(η⁶-1,3,5-C₆H₃Me₃)(CO)₃][W₂I₅(CO)₆].

The ruthenium(II) σ-alkyl complexes [Ru(Me)(η⁵-C₅Me₅)(PR₃)₂] (R₃ = Me₃, Me₂Ph), [Ru(CH₂CMe₃)(η⁵-C₅Me₅)(PMe₃)₂] and [Ru(Me)(η⁵-C₅H₅)(PPh₃)₂] (50) can undergo electrochemical one-electron oxidation to the corresponding paramagnetic Ru(III) cations, but these species could not be isolated using [Fe(η⁵-C₅H₅)₂]⁺ as a chemical oxidant.¹¹¹ Although reaction of either the σ-alkyl complex 50 or the chloro compounds [RuCl(η⁵-C₅Me₅)(PR₃)₂] (R₃ = Me₃, Me₂Ph, Me₃) with [NO]BF₄ proceeded *via* 17-electron intermediate species, the isolated products contained NO in the coordination sphere.

There are also some examples of the oxidation of tethered arene complexes (their preparation will be described in Section 1.2.2) and subsequent reaction with [NO]⁺.¹⁴⁸ Complexes [M(η¹:η⁶-Ph₂AsCH₂As(Ph)C₆H₅)(CO)₂]

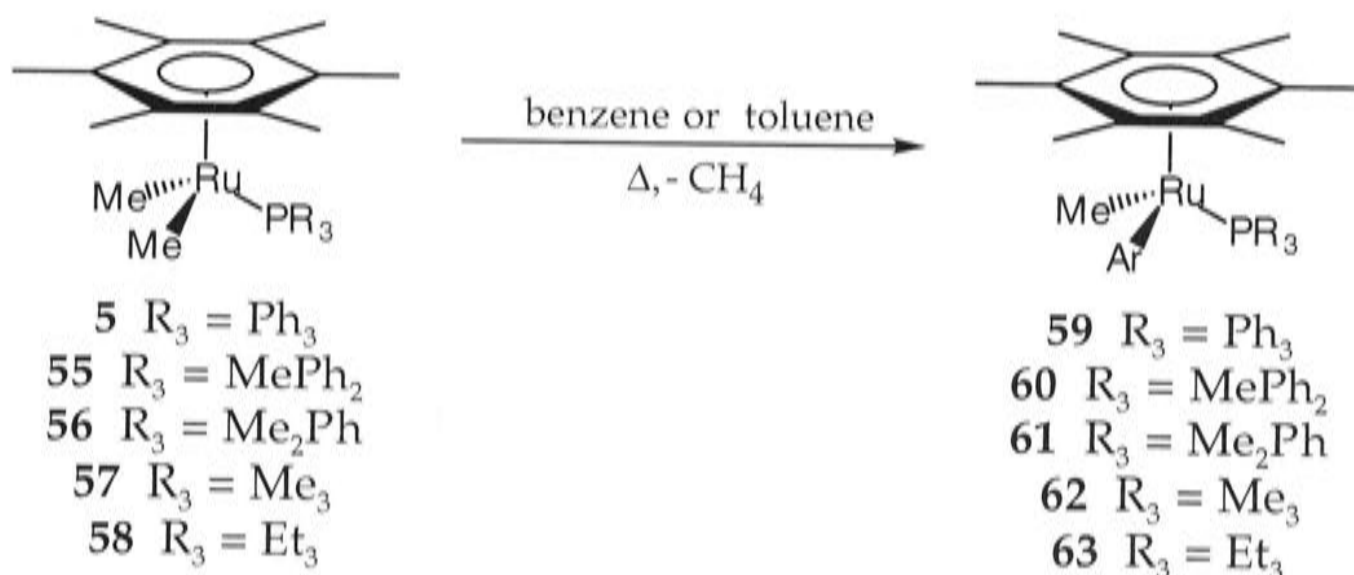
(M = Cr (**51**) or Mo (**52**)) were treated with $[\text{NO}]\text{PF}_6$ in either neat acetonitrile or dichloromethane (containing 10% acetonitrile), generating initially the corresponding Cr(I) or Mo(I) cations. However, displacement of the η^6 -arene by NO and two acetonitrile ligands, to form the 18-electron species $[\text{M}(\text{Ph}_2\text{AsCH}_2\text{AsPh}_2)(\text{CO})_2(\text{NCMe})_2(\text{NO})]\text{PF}_6$ (M = Cr (**53**) or Mo (**54**)), also occurred (Scheme 8). These results clearly indicate that the η^6 -arene of both **51** and **52** was not inert to displacement at the higher oxidation states of the metals. The reaction of **51** and **52** with AgClO_4 in a variety of solvents led to loss of both carbonyl ligands and decomposition. The use of iodine as the chemical oxidant converted the Cr(0) to Cr(III), which was detected by ESR, though loss of CO also occurred and the products were not characterised.



Scheme 8. Chemical oxidation of the tethered complexes **51** and **52** with $[\text{NO}]\text{PF}_6$.¹⁴⁸

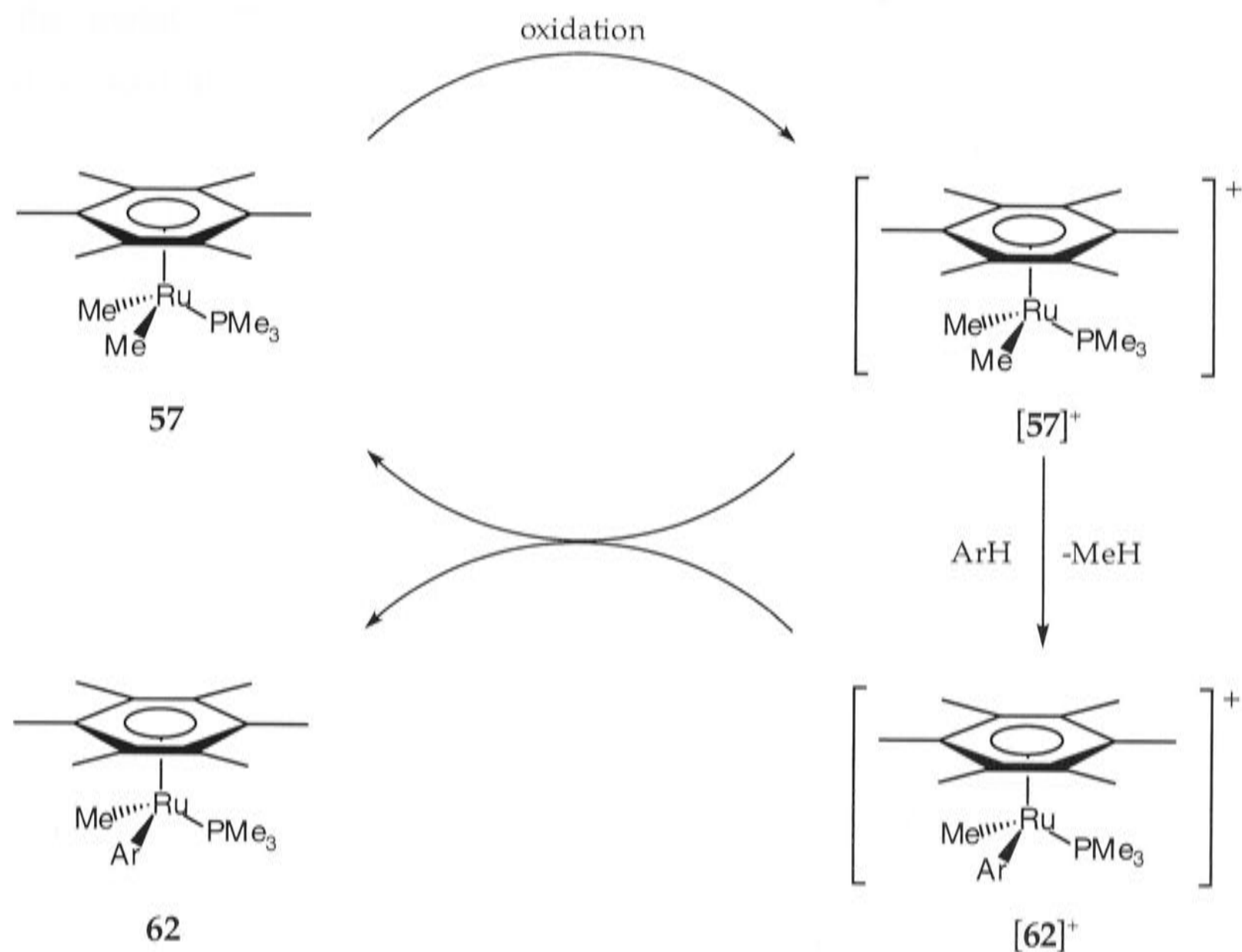
An interesting example of the involvement of paramagnetic arene-ruthenium complexes in the catalysis of C-H bond activation processes has been reported.¹¹² The complexes $[\text{RuMe}_2(\eta^6\text{-C}_6\text{Me}_6)(\text{PR}_3)]$ ($\text{R}_3 = \text{Ph}_3$ (**5**), MePh_2 (**55**), Me_2Ph (**56**), Me_3 (**57**), Et_3 (**58**)) react with either benzene or toluene on heating to give the methyl-aryl derivatives $[\text{Ru}(\text{Me})(\text{Ar})(\eta^6\text{-C}_6\text{Me}_6)(\text{PR}_3)]$ ($\text{R}_3 = \text{Ph}_3$ (**59**), MePh_2 (**60**), Me_2Ph (**61**), Me_3 (**62**), Et_3 (**63**); $\text{Ar} = \text{C}_6\text{H}_5$ or $\text{CH}_3\text{C}_6\text{H}_4$) (Scheme 9). The nature of the substituents on the phosphorus atom was found to influence the products formed from the reaction of the complexes **5** and **55-58** with benzene and toluene. Either both the methyl-aryl derivatives **59-63** and the intramolecular C-H bond activation products

$[\text{Ru}(\text{Me})(\text{C}_6\text{H}_4\text{PR}_2)(\eta^6\text{-C}_6\text{Me}_6)]$ ($\text{R}_2 = \text{Ph}_2$ (**64**), MePh (**65**)) were formed, or, when R contained a phenyl moiety, the cyclometallated complexes **64** and **65** were formed exclusively.



Scheme 9. Reaction of complexes $[\text{Ru}(\text{Me})_2(\eta^6\text{-C}_6\text{Me}_6)(\text{PR}_3)]$ ($\text{R} = \text{Ph}_3$ (**5**), MePh_2 (**55**), Me_2Ph (**56**), Me_3 (**57**) and Et_3 (**58**)) with either benzene or toluene to form the corresponding methyl-aryl derivatives $[\text{Ru}(\text{Me})(\text{Ar})(\eta^6\text{-C}_6\text{Me}_6)(\text{PR}_3)]$ ($\text{R} = \text{Ph}_3$ (**59**), MePh_2 (**60**), Me_2Ph (**61**), Me_3 (**62**) and Et_3 (**63**); $\text{Ar} = \text{C}_6\text{H}_5$ or $\text{CH}_3\text{C}_6\text{H}_4$).¹¹²

In contrast, the reaction of complexes **5** and **55-58** with either benzene or toluene in the presence of $[\text{Fe}(\eta^5\text{-C}_5\text{H}_5)_2]^+$ occurred at room temperature. Both electrochemical and ESR spectroscopic studies showed that a one-electron oxidation process took place to form a transient Ru(III) 17-electron species. The X-band ESR spectrum of $[\text{Ru}(\text{Me})(\text{Ph})(\eta^6\text{-C}_6\text{Me}_6)(\text{PMePh}_2)]^+$ (**[6]**⁺) is shown in Figure 4; the *g*-values are listed in Table 2. This implies that the catalytic reaction was triggered by ferrocenium ions and occurred by a redox pathway. The proposed mechanism of reaction of $[\text{Ru}(\text{Me})_2(\eta^6\text{-C}_6\text{Me}_6)(\text{PMe}_3)]$ (**57**) with either benzene or toluene is depicted in Scheme 10. The $[\text{Fe}(\eta^5\text{-C}_5\text{H}_5)_2]^+$ oxidises the parent Ru(II) species **57** to form the arene-Ru(III) derivative **[57]**⁺, which reacts with benzene, even at room temperature, to afford the cationic Ru(III) species of the type **[62]**⁺. This species then oxidises the parent Ru(II) complex **57**, itself being reduced to the final methyl aryl products of the type **62**.



Scheme 10. Catalytic cycle of C-H bond activation of benzene by the 17-electron intermediate species $[\text{Ru}(\text{Me})_2(\eta^6\text{-C}_6\text{Me}_6)(\text{PMe}_3)]^+$ ($[57]^+$).¹¹²

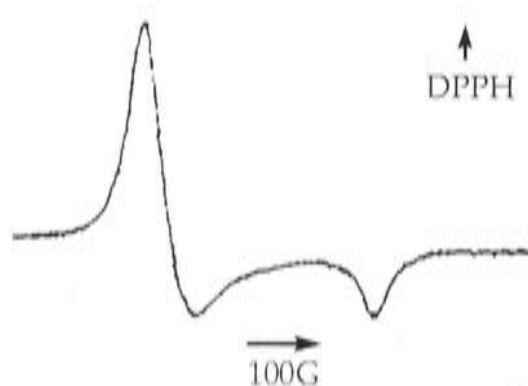
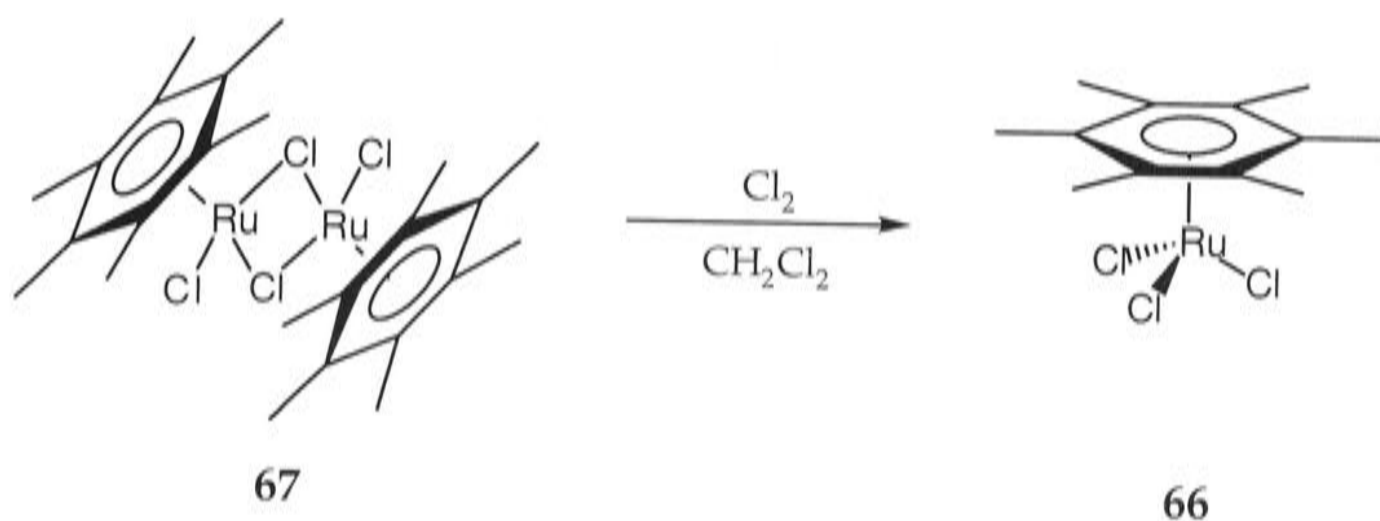


Figure 4. ESR spectrum recorded at 100K (relative to DPPH) on a CH_2Cl_2 sample solution of $[6]^+$ presumed to be formed in the first stages of controlled potential electrolysis of $[\text{Ru}(\text{Me})(\text{Ph})(\eta^6\text{-C}_6\text{Me}_6)(\text{PMePh}_2)]$ (**6**).¹¹²

The transient 17-electron species could only be detected by electrochemical and ESR techniques. Nothing is known about the solid state structure of the complex, and how it differs from that of the parent Ru(II) compounds. These arene-Ru(III) complexes are very unstable due to the lability of the η^6 -arene.¹⁶⁵ The stability of such species might be improved by incorporating the arene into part of a bidentate ligand, thus anchoring it to

the metal. These complexes, called tethered arene complexes, will be discussed in more detail below (see Section 1.2).

To date, there is only one example of an arene-ruthenium(III) complex which has been isolated: $[\text{RuCl}_3(\eta^6\text{-C}_6\text{Me}_6)]$ (**66**) was prepared from the reaction of $[\text{RuCl}_2(\eta^6\text{-C}_6\text{Me}_6)]_2$ (**67**) with chlorine. It has been isolated as a solid and detected by ESR spectroscopy, though it was not structurally characterised (Scheme 11).¹⁴⁹ In the presence of an excess of $[\text{Et}_3\text{BzN}]\text{Cl}$ (Bz = benzyl) it showed a reversible $\text{Ru}^{\text{III/II}}$ couple, with $E_{1/2} = + 0.25 \text{ V}$ (*vs* $\text{Fc}^{0/1}$ in CH_2Cl_2 [based on the conversion factor of $- 0.31 \text{ V}$ stated in reference(166)]. Complex **66** was unstable both as a solid and in solution; the solid reverted to the parent Ru(II) complex **67**, and the arene-Ru(III) species **66** decomposed in dichloromethane.

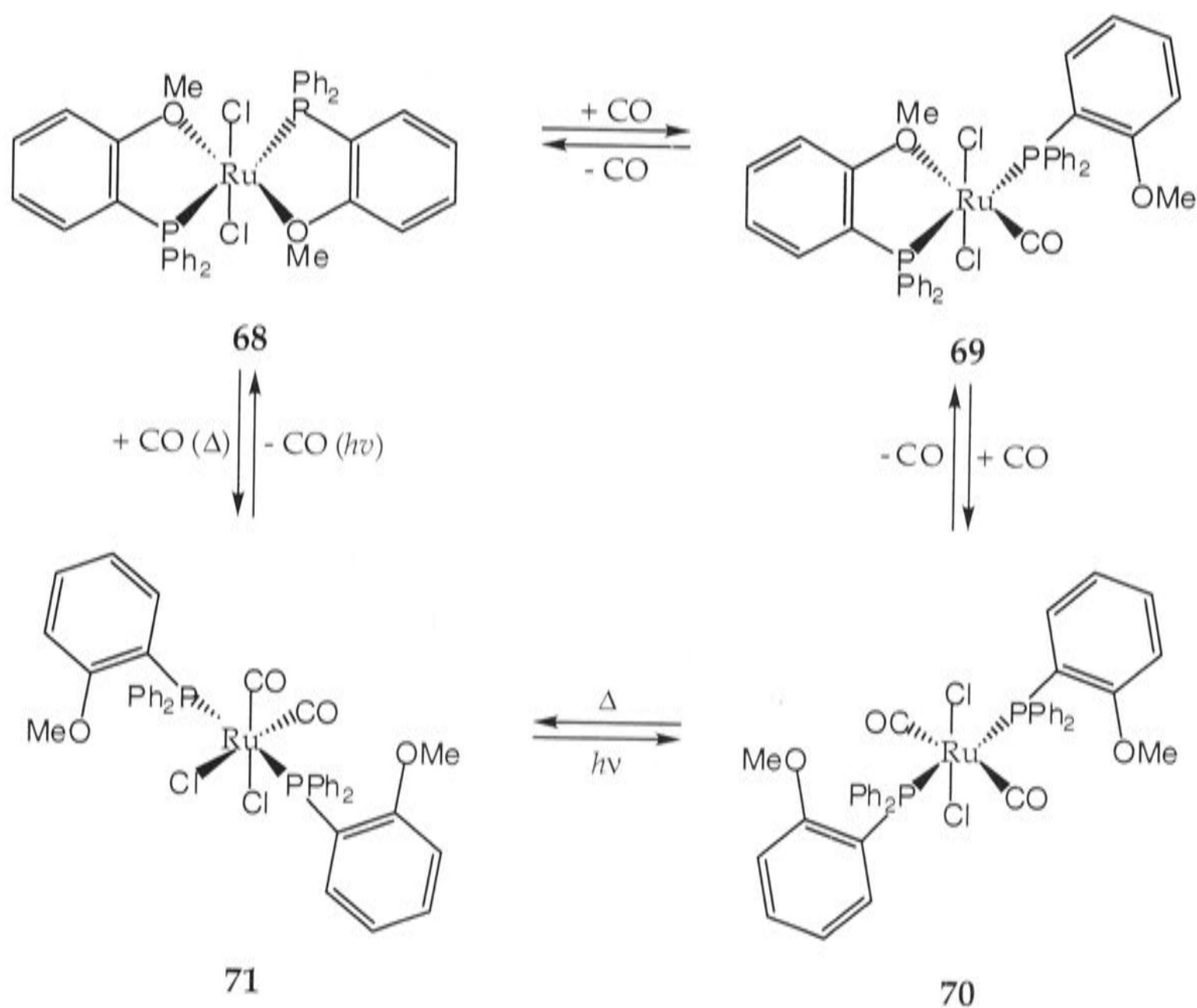


Scheme 11. Preparation of the arene-ruthenium(III) complex **66**.¹⁴⁹

1.2 Tethered Aromatic Complexes

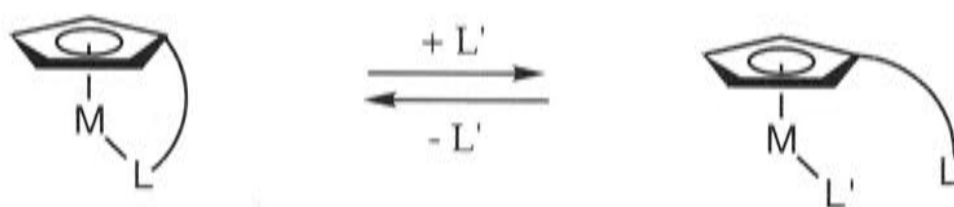
The chelating ligand of a tethered complex can be regarded as a special type of heterobidentate ligand, in which each end contains a different donor atom, which differ in both their binding ability and lability. For example, phosphino-ether ligands have been employed to form hemilabile ruthenium(II) complexes.¹⁶⁷ Carbon monoxide displaces the more labile oxygen atom of one of the bidentate ligands of $[\text{RuCl}_2(o\text{-Ph}_2\text{PC}_6\text{H}_4\text{OMe})_2]$ (**68**), whilst the phosphorus donor atom remains coordinated, to give the mono-substituted CO adduct

$[\text{RuCl}_2(\text{CO})(o\text{-Ph}_2\text{PC}_6\text{H}_4\text{OMe})(o\text{-Ph}_2\text{PC}_6\text{H}_4\text{OMe})]$ (**68**) (Scheme 12). This reacts with another molecule of CO, forming $[\text{RuCl}_2(\text{CO})_2(o\text{-Ph}_2\text{PC}_6\text{H}_4\text{OMe})_2]$ (**70**), where only the phosphorus atoms of the hemilabile ligands are coordinated to the Ru(II), and the chloride and CO ligands are coordinated *trans* with respect to one another. This species **70** converts to the respective *cis*-complex **71**, which can then revert to the starting bis-bidentate complex **68** by loss of CO. The use of tridentate phosphine-ether ligand systems can also assist in the stabilisation of mononuclear d^7 complexes. For example, the six-coordinate complex $[\text{Rh}(\eta^3\text{-tris}(2,4,6\text{-trimethoxyphenyl})\text{phosphine})_2][\text{BF}_4]_2$ was the first Rh(II) complex without a metal-metal bond to be structurally characterised.¹⁶⁸



Scheme 12. The reaction of complex **68** with carbon monoxide to form **70**.¹⁶⁷

The study of cyclopentadienyl transition metal complexes, many of which have a direct application as catalysts¹⁶⁹ and as reagents for stereoselective syntheses,^{170,171} has led to the investigation of cyclopentadienyl tethered complexes in order to improve their range of applications.¹⁷²⁻¹⁷⁶ The chelate effect of such ligands provides a route towards designing the coordination sphere to enable the stabilisation of reactive metal centres. Further, it can also introduce chirality at the metal centre. These types of transition metal complexes consist of a heterobidentate ligand which coordinates to the metal centre by the cyclopentadienyl moiety and an additional donor atom (L) attached by a tether to the five-membered ring. The donor atom anchors the cyclopentadienyl moiety to the metal, which serves to inhibit reactions where the cyclopentadienyl ring dissociates from the metal, resulting in decomposition. Alternatively, if the metal-donor bond of the donor atom is sufficiently weak, it can protect a vacant site at the metal centre until it may be required by an incoming ligand (L') (Scheme 13). Manipulation of the functional groups on the cyclopentadienyl ring, the nature of the donor atom as well as the number and type of atoms in the strap, generates a group of related tethered complexes.

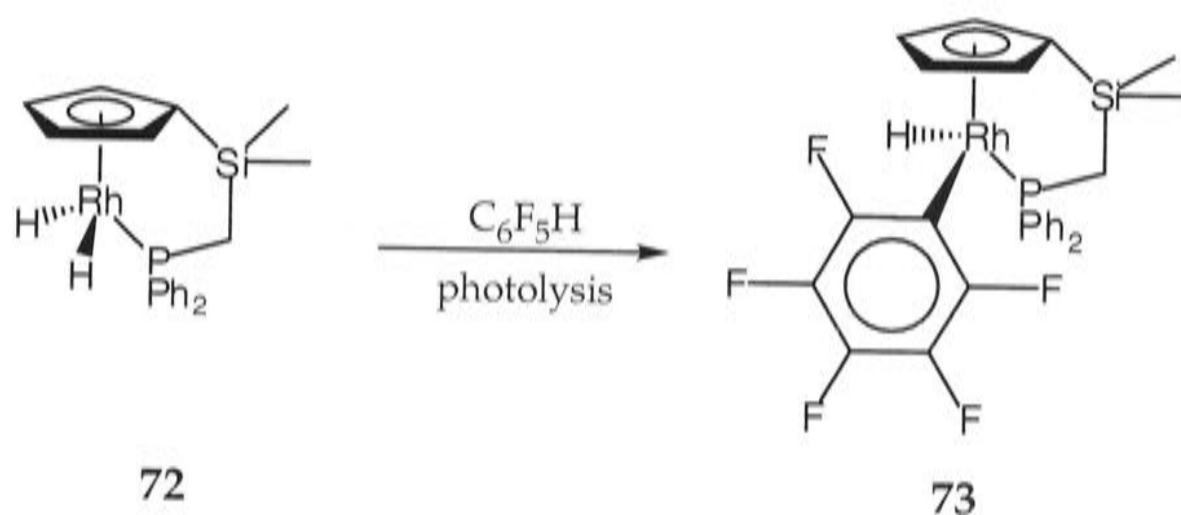


Scheme 13. Interaction of the incoming ligand (L') with tethered cyclopentadienyl complexes.

A recent example of a tethered cyclopentadienyl compound that displays catalytic behaviour is the zirconium(III) complex $[\text{ZrCl}_2(\eta^5\text{-MeS}(\text{CH}_2)_2\text{NSiMe}_2\text{C}_5\text{Me}_4)]$, which, when activated with methylaluminoxane, catalyses the polymerisation of ethylene to high-molecular weight polyethylene.¹⁷⁷

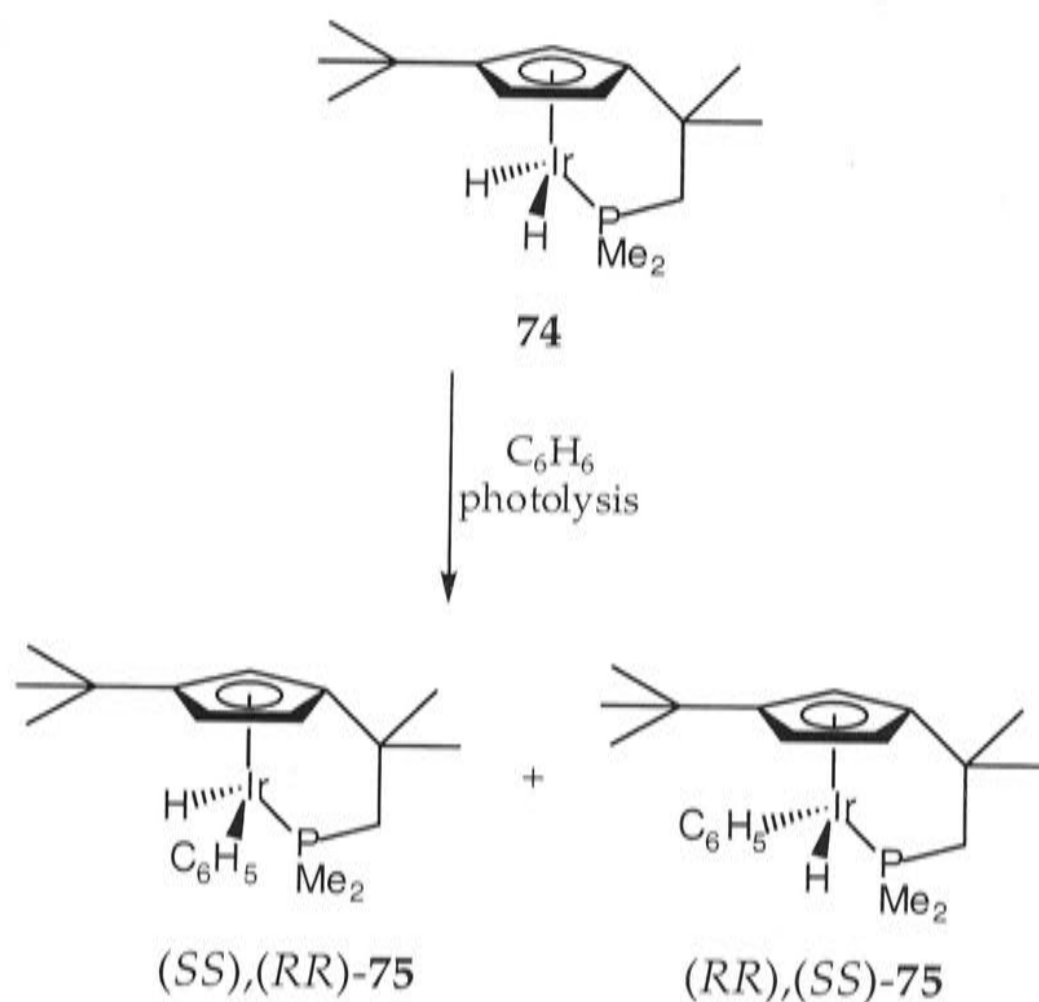
There are also some examples of tethered cyclopentadienyl iridium(III) and rhodium(III) complexes that exhibit carbon-hydrogen bond activation.¹⁷⁸⁻¹⁸⁰

Photolysis of the tethered complex $[\text{Rh}(\text{H})_2(\eta^1:\eta^5\text{-Ph}_2\text{PCH}_2\text{SiMe}_2\text{C}_5\text{H}_4)]$ (**72**) in the presence of pentafluorobenzene affords the hydride species $[\text{Rh}(\text{H})(\text{C}_6\text{F}_5)(\eta^1:\eta^5\text{-Ph}_2\text{PCH}_2\text{SiMe}_2\text{C}_5\text{H}_4)]$ (**73**) (Scheme 14).¹⁷⁸



Scheme 14. Photolysis of the tethered cyclopentadienyl complex **72** to form **73**.¹⁷⁸

A related iridium complex $[\text{Ir}(\text{H})_2(\eta^1:\eta^5\text{-Me}_2\text{PCH}_2\text{CMe}_2\text{-1,3-C}_5\text{H}_3\text{-}t\text{-Bu})]$ (**74**) also exhibits C-H bond activation with both benzene and cyclohexane (Scheme 15).¹⁷⁹ The substituents on the cyclopentadienyl group and the tether were selected to add steric bulk and rigidity to the complex, as well as introducing planar chirality. Photolysis of the dihydride species **74** in the presence of benzene produced the diastereomeric phenyl hydrides (*SS*),(*RR*)-**75** and (*RR*),(*SS*)-**75**. In order to avoid eclipsing interactions between the bulky *tert*-butyl group and the hydride or phenyl ligands, the tether twists, resulting in rotation of the cyclopentadienyl moiety, and the formation of diastereomers **75** in a 1:1 ratio. In contrast, the reaction of **74** with cyclohexane has a different stereochemical outcome: only the (*RR*),(*SS*) diastereomer of the cyclohexyliridium hydride complex $[\text{Ir}(\text{H})(\text{C}_6\text{H}_{11})(\eta^1:\eta^5\text{-Me}_2\text{PCH}_2\text{CMe}_2\text{-1,3-C}_5\text{H}_3\text{-}t\text{-Bu})]$ formed, which could not be converted into the other diastereoisomer.



Scheme 15. Activation of benzene by 74 to form the diastereomers (SS),(RR)-75 and (RR),(SS)-75.¹⁷⁹

A solution of the non-tethered complex $[IrCl_2(\eta^5-C_5Me_5)(PMe_3)]$ (76) in D_2O reacted with organic substrates, such as diethyl ether, and gave rise to extensive hydrogen-deuterium exchange (36% average; exchange occurred on both carbon atoms), although complex decomposition also occurred.¹⁸¹ Bergman and co-workers have continued their investigation into tethered cyclopentadienyl iridium(III) complexes which exhibit C-H bond activation.¹⁸⁰ It was envisaged that the chelate effect of the tethered complexes $[Ir(OTf)_2(\eta^1:\eta^5-Me_2PCH_2SiMe_2C_5Me_4)]$ (77) and $[Ir(OH_2)_2(\eta^1:\eta^5-Me_2PCH_2SiMe_2C_5Me_4)]SO_4$ (78) would inhibit the decomposition observed for 76.¹⁸⁰ In the presence of diethyl ether, compounds 77 and 78 catalysed partial hydrogen-deuterium exchange (33 and 40%, respectively), but they decomposed to materials that could not be characterised. Thus, similar results were obtained for both the non-tethered complex 76 and the tethered complexes 77 and 78.

Tethered complexes, containing an arene in place of the cyclopentadienyl ring, are less numerous and have not attracted as much attention. There are currently many examples of ruthenium(II) complexes containing

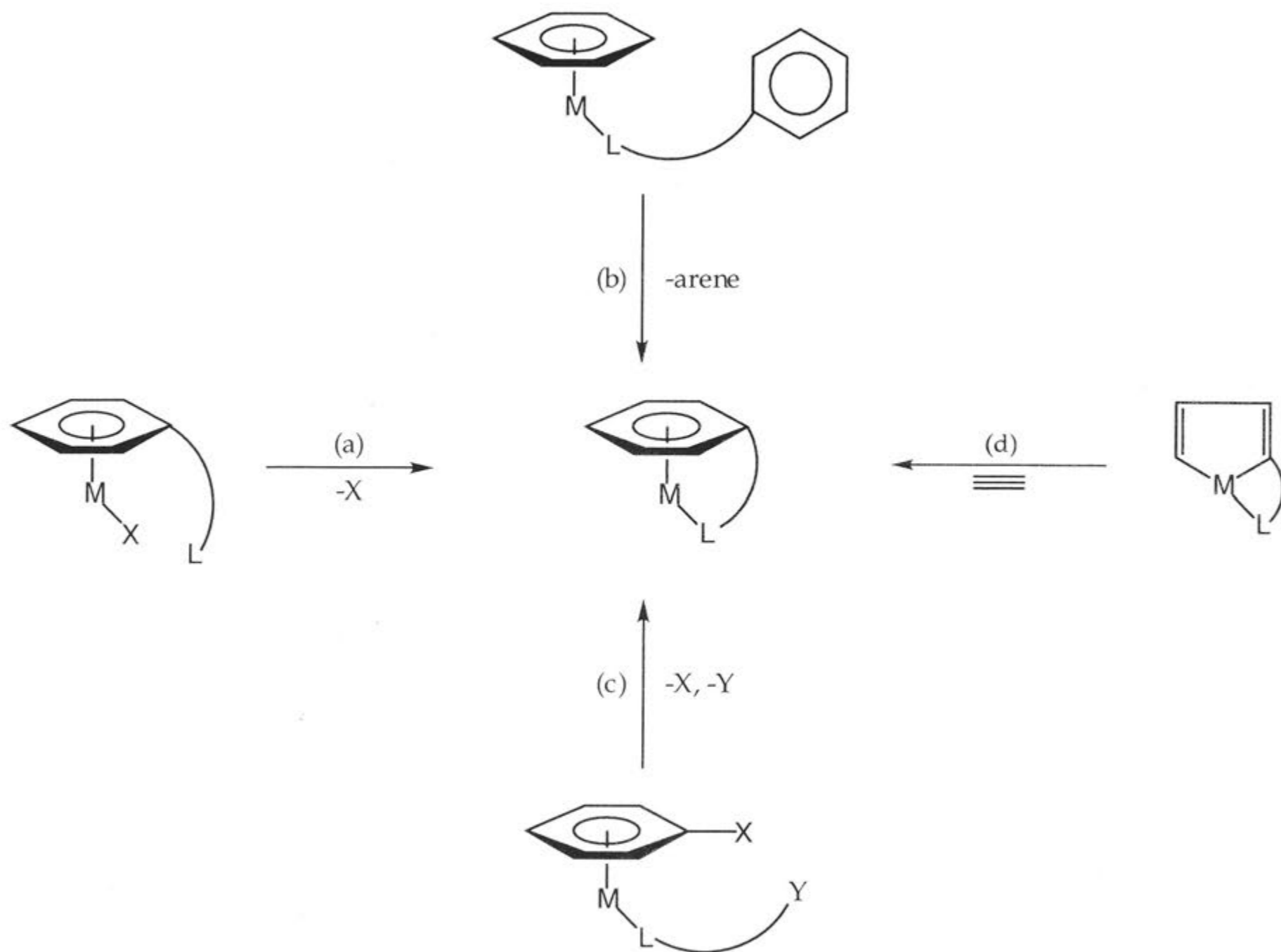
arene-phosphine ligands of this type, although few had been reported in March 1998 at the commencement of the work described in this Thesis.

Benzene complexes are generally less stable and less numerous than cyclopentadienyl complexes, in part because benzene, as a neutral molecule, is more readily lost or displaced by other ligands than the Cp anion. For example, $[\text{Ru}(\text{Me})_2(\eta^6\text{-C}_6\text{H}_6)(\text{PMe}_2\text{Ph})]$ (**79**) decomposes, presumably through loss of benzene, in the solid state above -40°C .¹⁸² In contrast, the isoelectronic rhodium complex $[\text{Rh}(\text{Me})_2(\eta^5\text{-C}_5\text{H}_5)(\text{PPh}_3)]$ is stable.¹⁸³ This difference in stability is also observed for iron(II) complexes: for example, the η^6 -arene of $[\text{Fe}(\eta^6\text{-C}_6\text{H}_6)_2]^{2+}$ is easily displaced by other ligands¹⁸⁴ making it is much less stable than ferrocene. In contrast, the η^6 -coordinated arene of a tethered complex should be more effectively anchored to the metal centre. This feature may serve to inhibit decomposition by loss of the η^6 -coordinated arene, resulting in the stabilisation of η^6 -arene coordination for a variety of metals and oxidation states.

In principle, the preparative procedures for tethered arene complexes fall into four distinct classes, which are represented in over-simplified form in Scheme 16. The first involves η^6 -coordination to the metal centre of a functionalised arene connected by a group of atoms to a potential donor and subsequent formation of the tether by displacement of a ligand (X) and coordination of the donor atom to the metal centre (Scheme 16a). In the second, a labile ligand, which may itself be an arene, is displaced by a second arene which is attached by a tether to the already coordinated donor atom (Scheme 16b). Routes (a) and (b) depicted in Scheme 16 thus differ according to whether the donor atom L is coordinated after or before the arene. The third procedure involves an intramolecular condensation reaction between a substituent on the η^6 -arene and a functional group on the donor atom (L) (Scheme 16c). The final method involves construction of the arene by an alkyne condensation reaction in the coordination sphere

(Scheme 16d). The metal atom is already coordinated to the donor atom (L) that is connected to a metalla-1,3-diene. The alkyne reacts with the diene to construct the six-membered ring, thus giving rise to the tethered species.

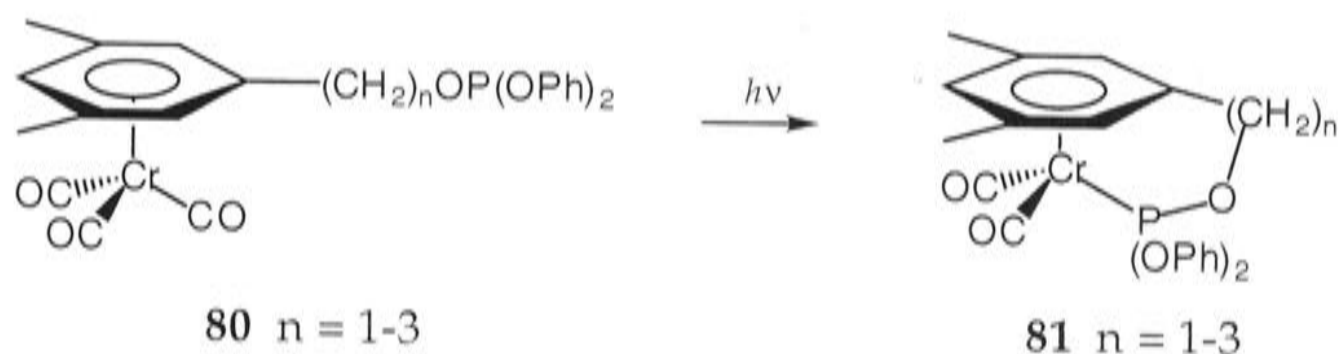
Some examples of these procedures will now be described. The majority of reported tethered arene complexes contain metals that have the stable electronic configurations $3d^6$ or $4d^6$, such as Cr(0) or Ru(II), respectively, or $4d^8$ or $5d^8$, such as Rh(I) and Ir(I), respectively. This is partly due to the fact that η^6 -arenes are weak bases, and require back-donation from the metal, which is less favourable for metals in high oxidation states. The tripodal arrangement of these half-sandwich complexes is a highly favourable geometry for Cr(0) and Ru(II) compounds.¹⁸⁵ As the exact mechanism for the formation of tethered arene complexes is not always clear, it may not be possible to categorise the preparation of each tethered complex into one of the four general approaches described in Scheme 16.

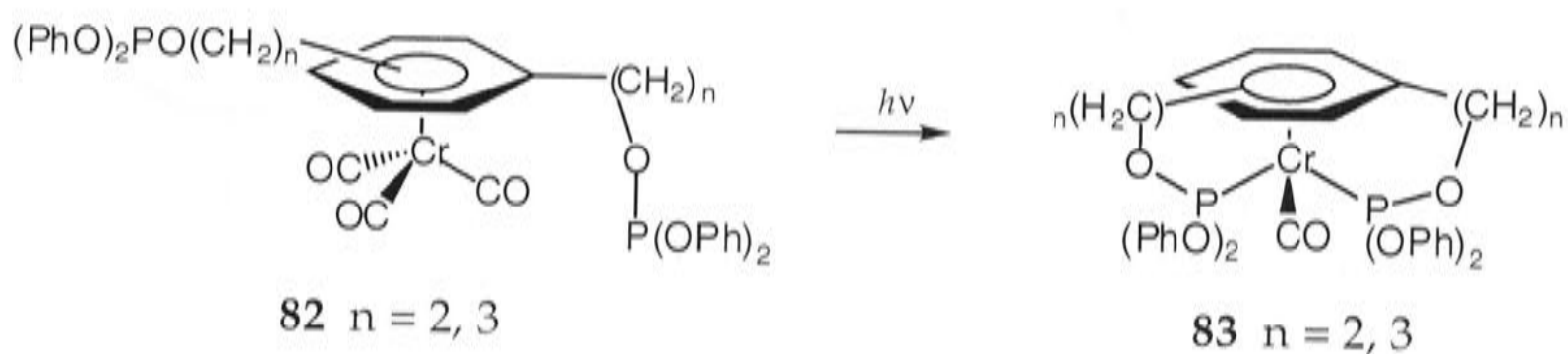


Scheme 16. Schematic representation of the four over-simplified, general approaches for the preparation of tethered arene complexes.

1.2.1 Syntheses Proceeding by Initial Arene Coordination (Scheme 16a)

There are several examples of tethered arene complexes containing chromium(0) and ruthenium(II) which have been prepared *via* the general approach depicted in Scheme 16a. The complexes $[\text{Cr}(\text{CO})_2(\eta^1:\eta^6\text{-CH}_2=\text{CHXC}_6\text{H}_5)]$ ($X = \text{CH}_2, \text{OCH}_2, (\text{CH}_2)_2, (\text{CH}_2)_3$ or $(\text{CH}_2)_4$), which were prepared by photolysis of $[\text{Cr}(\text{CO})_3(\eta^6\text{-C}_6\text{H}_5\text{XCH}=\text{CH}_2)]$, were some of the earliest reported examples of tethered arene complexes.¹⁸⁶ Attention was then directed towards tethered complexes that contained donor groups such as phosphite¹⁸⁷ which were expected to form more stable metal-ligand bonds. Photolysis of $[\text{Cr}(\text{CO})_3(\eta^6\text{-1,3,5-Me}_2\text{C}_6\text{H}_4(\text{CH}_2)_n\text{OP}(\text{OPh})_2)]$ (**80**) gave rise to $[\text{Cr}(\text{CO})_2(\eta^1:\eta^6\text{-(PhO)}_2\text{PO}(\text{CH}_2)_n\text{-3,5-C}_6\text{H}_3\text{Me}_2)]$ (**81**) ($n = 1-3$) (Scheme 17). A second strap could be formed by coordinating functionalised arenes of the type $1,4\text{-C}_6\text{H}_4\text{-}\{(\text{CH}_2)_n\text{OP}(\text{OPh})_2\}_2$ ($n = 2$ or 3) to the metal centre.¹⁸⁸ Photolysis of complex **82** containing two or three methylene units in the strap caused consecutive eliminations of two carbon monoxide ligands, followed by intramolecular cyclisation to generate the desired two-bridge chelate complexes **83** (Scheme 18). No chelate complex was formed when the strap contained only one methylene unit, and prolonged irradiation resulted in decomposition.

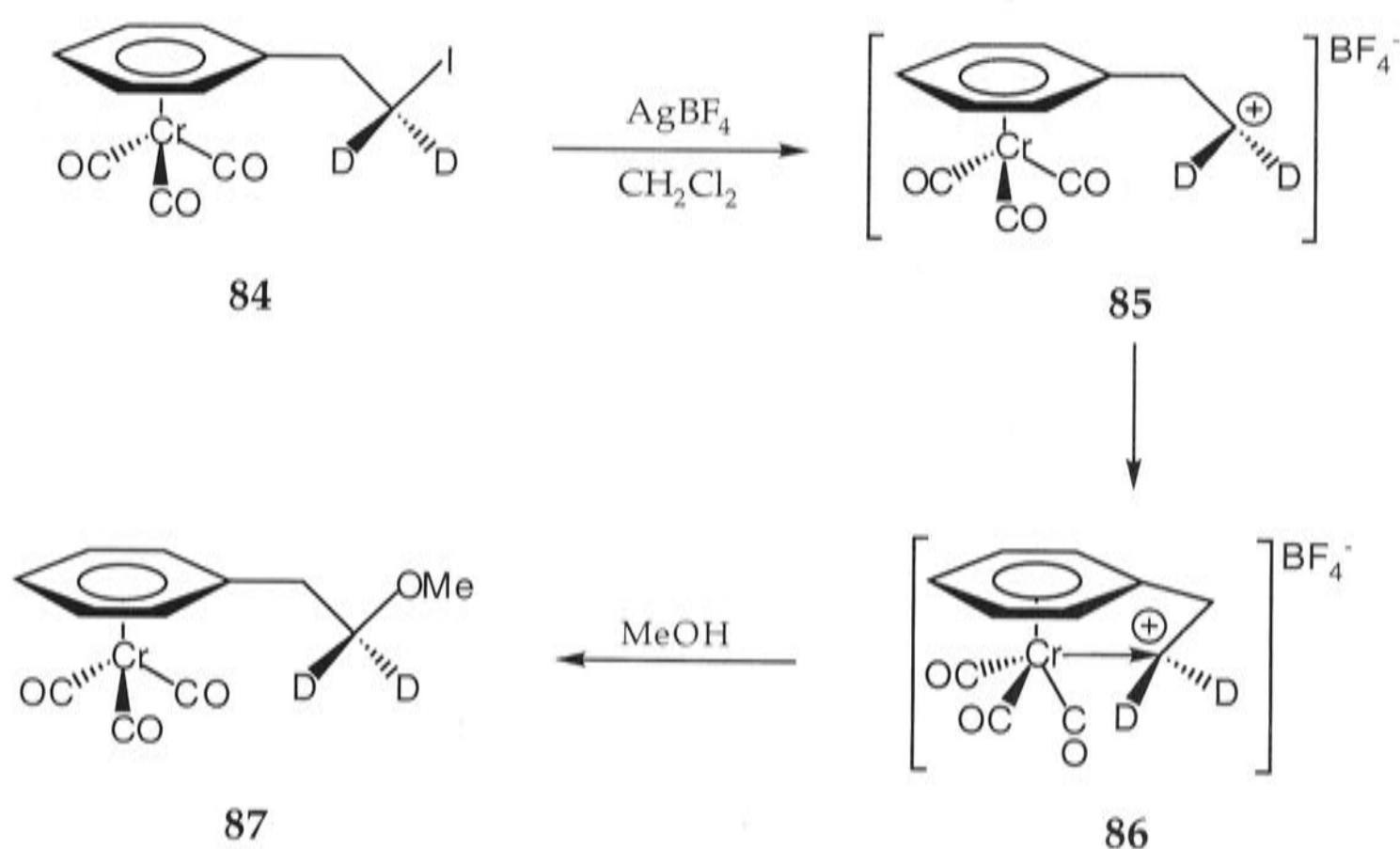
Scheme 17. Formation of tethered complexes of the type **81** ($n = 1-3$).¹⁸⁷



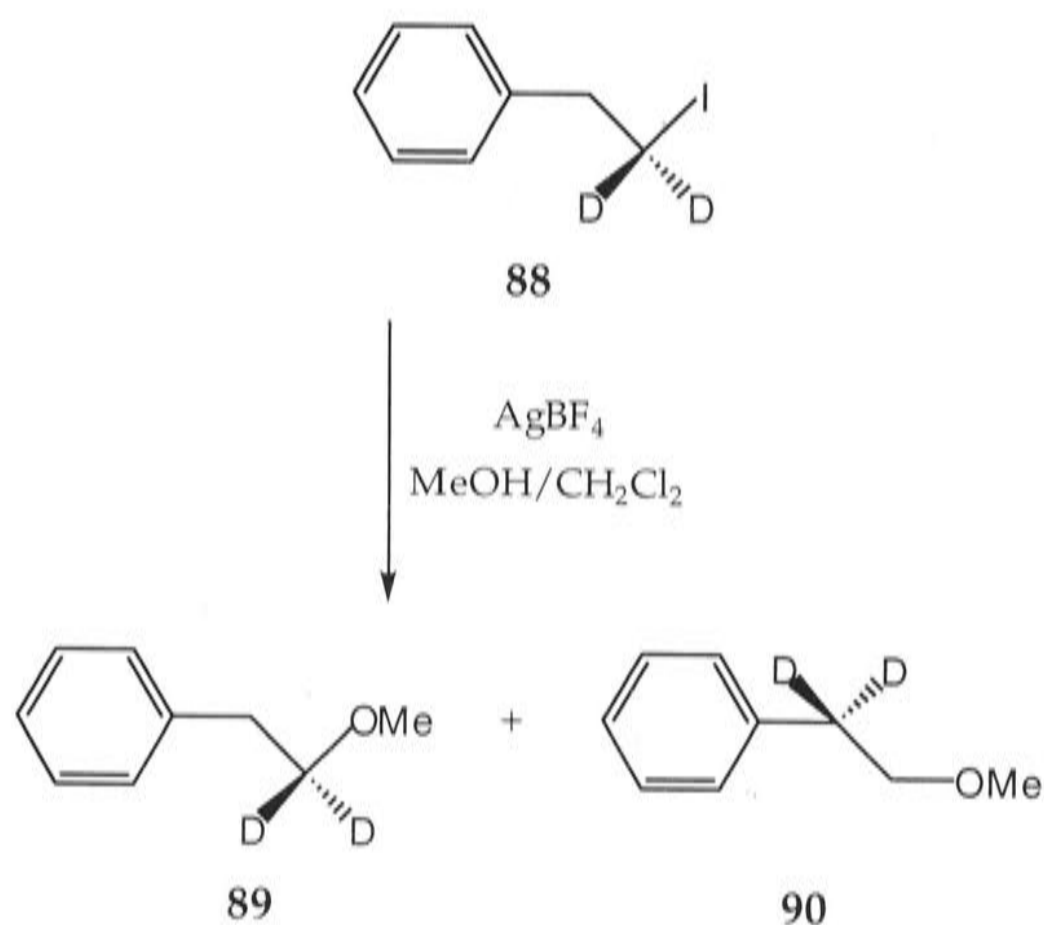
Scheme 18. Formation of multi-strapped complexes of the type **83** ($n = 2$ or 3).¹⁸⁸

Tethered arene complexes can also form as intermediates in reactions. The $\text{Cr}(\text{CO})_3$ derivative of $\text{C}_6\text{H}_5\text{CH}_2\text{CD}_2\text{I}$ (**84**), was treated with AgBF_4 to generate the carbocation $[\text{Cr}(\text{CO})_3(\eta^6\text{-C}_6\text{H}_5\text{CH}_2\text{CD}_2)]^+\text{BF}_4^-$ (**85**).¹⁸⁹ The chromium then donates electrons to the coordinatively and electronically unsaturated carbon atom, to form the tethered intermediate **86**, which is presumably stabilised by the tetrafluoroborate anion. This is similar to an oxidative addition reaction, as the $\text{Cr}(0)$ is oxidised to $\text{Cr}(\text{II})$. This intermediate **86** immediately undergoes nucleophilic attack by methanol to give a single methoxy-substituted product $[\text{Cr}(\text{CO})_3(\eta^6\text{-C}_6\text{H}_5\text{CH}_2\text{CD}_2\text{OMe})]$ (**87**) (Scheme 19). Additional experiments with substrates that contain two chiral centres in the side-chain indicated that the nucleophile enters exclusively from the remote side of the metal centre.

In contrast, the outcome of this reaction is significantly different in the absence of the $\text{Cr}(\text{CO})_3$ group. The reaction of the isotopically labelled halide $\text{C}_6\text{H}_5\text{CH}_2\text{CD}_2\text{I}$ (**88**) with AgBF_4 generates a phenonium ion intermediate that yielded a 1:1 ratio of the diastereomers $\text{C}_6\text{H}_5\text{CH}_2\text{CD}_2\text{OMe}$ (**89**) and $\text{C}_6\text{H}_5\text{CD}_2\text{CH}_2\text{OMe}$ (**90**) upon treatment with methanol (Scheme 20).¹⁸⁹ The formation of two products arises from the rearrangement of the phenonium ion, resulting in scrambling of the carbon side-chain, producing to two different carbocations susceptible to nucleophilic attack.



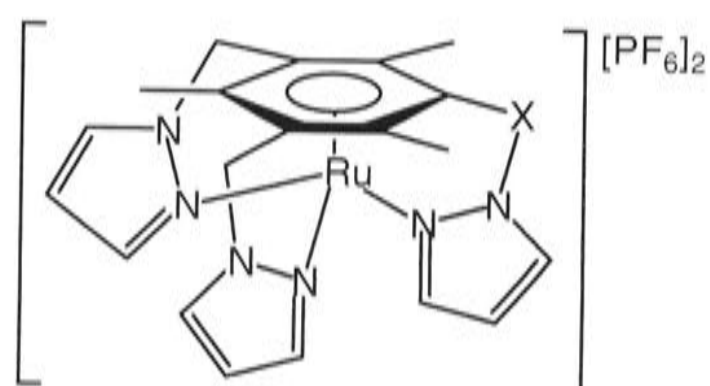
Scheme 19. Formation of the chromium complex **87** via the tethered complex **86**.¹⁸⁹



Scheme 20. Formation of the two diastereomers **89** and **90** in 1:1 ratio from the reaction of **88** and methanol in the absence of $\text{Cr}(\text{CO})_3$.¹⁸⁹

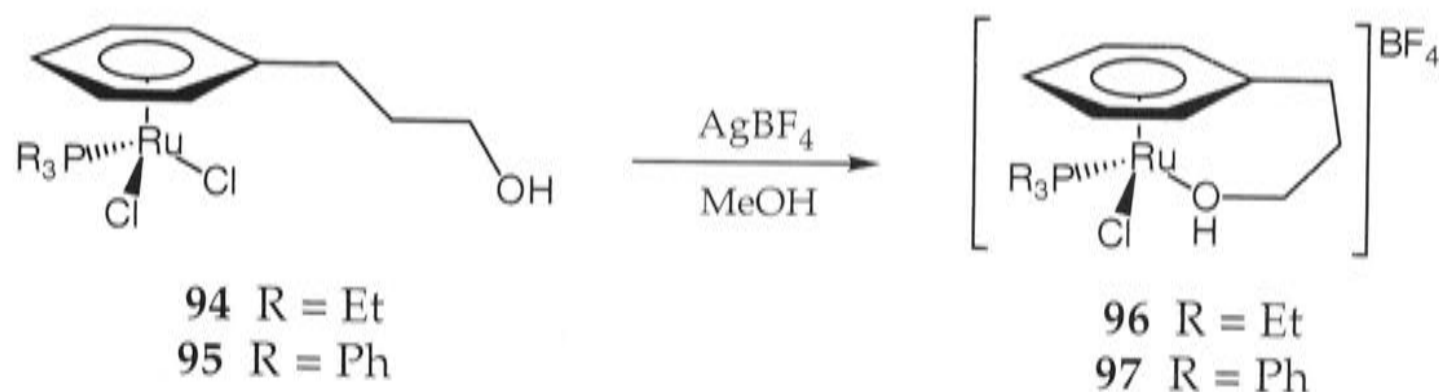
Tethered arene complexes incorporating a tripodal ligand with nitrogen donor atoms have also been prepared.¹⁹⁰ The appropriate heterocyclic tripodal ligands reacted with $[\text{RuCl}_2(\text{DMSO})_4]$ (DMSO = dimethylsulfoxide) in the presence of NH_4PF_6 to afford the complexes **91** and **92**. It is not

known if the η^6 -arene is coordinated before or after the nitrogen atoms, although the second possibility seems more likely.

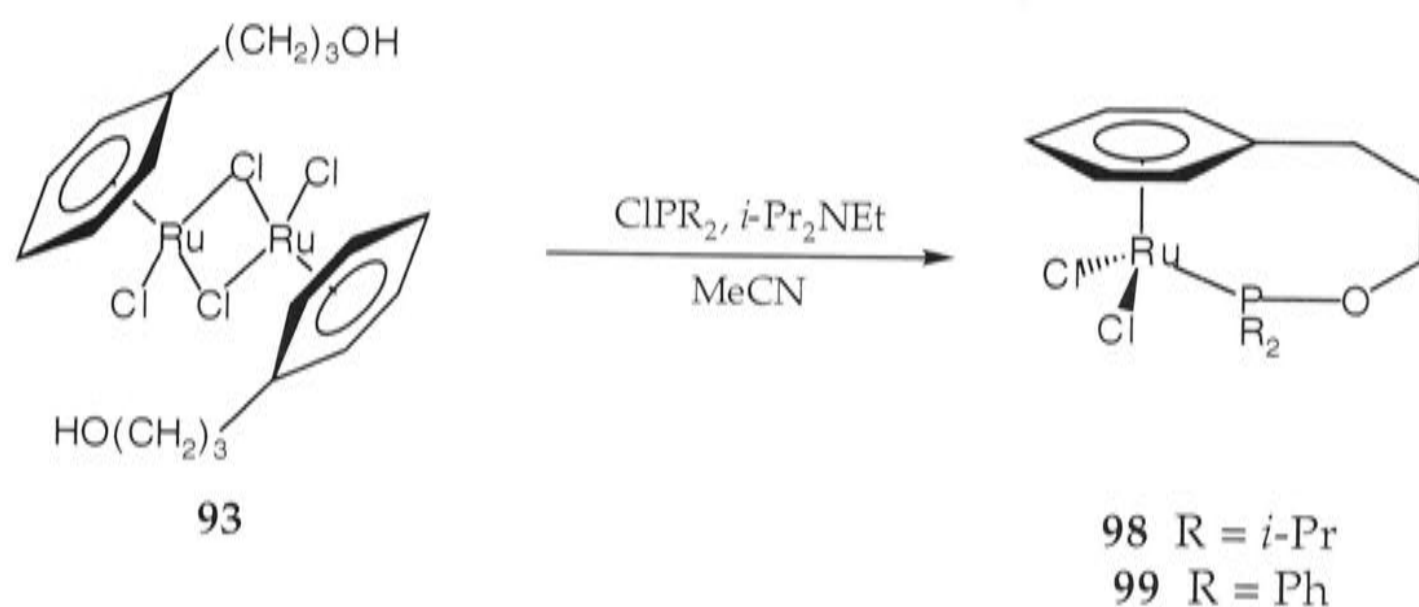


91 X = O
92 X = CH₂

Tethered arene-ruthenium complexes with oxygen as the second donor atom, derived from the 3-phenylpropanol complex $[\text{RuCl}_2(\eta^6\text{-C}_6\text{H}_4(\text{CH}_2)_3\text{OH})]_2$ (**93**), have been reported.¹⁹¹⁻¹⁹⁴ The phosphine derivatives $[\text{RuCl}_2(\eta^6\text{-C}_6\text{H}_5(\text{CH}_2)_3\text{OH})(\text{PR}_3)]$ (R = Et (**94**), Ph (**95**)), on treatment with silver ion, lost one of the chloride ions, giving the tethered complexes $[\text{RuCl}(\eta^1:\eta^6\text{-O(H)(CH}_2)_3\text{Ph})(\text{PR}_3)]\text{BF}_4$ (R = Et (**96**), Ph (**97**)) (Scheme 21). The bulky phosphine derivative $[\text{RuCl}(\eta^1:\eta^6\text{-O(H)(CH}_2)_3\text{C}_6\text{H}_5)(\text{PCy}_3)]\text{BF}_4$ was shown to act as a catalyst for ring closing metathesis reactions.¹⁹³ Alternatively, if **93** was treated with Ph_2PCL in the presence of a suitable base, neutral tethered phosphite complexes such as $[\text{RuCl}_2(\eta^1:\eta^6\text{-R}_2\text{PO(CH}_2)_3\text{Ph})]$ (R = *i*-Pr (**98**), Ph (**99**)) were formed (Scheme 22).¹⁹²

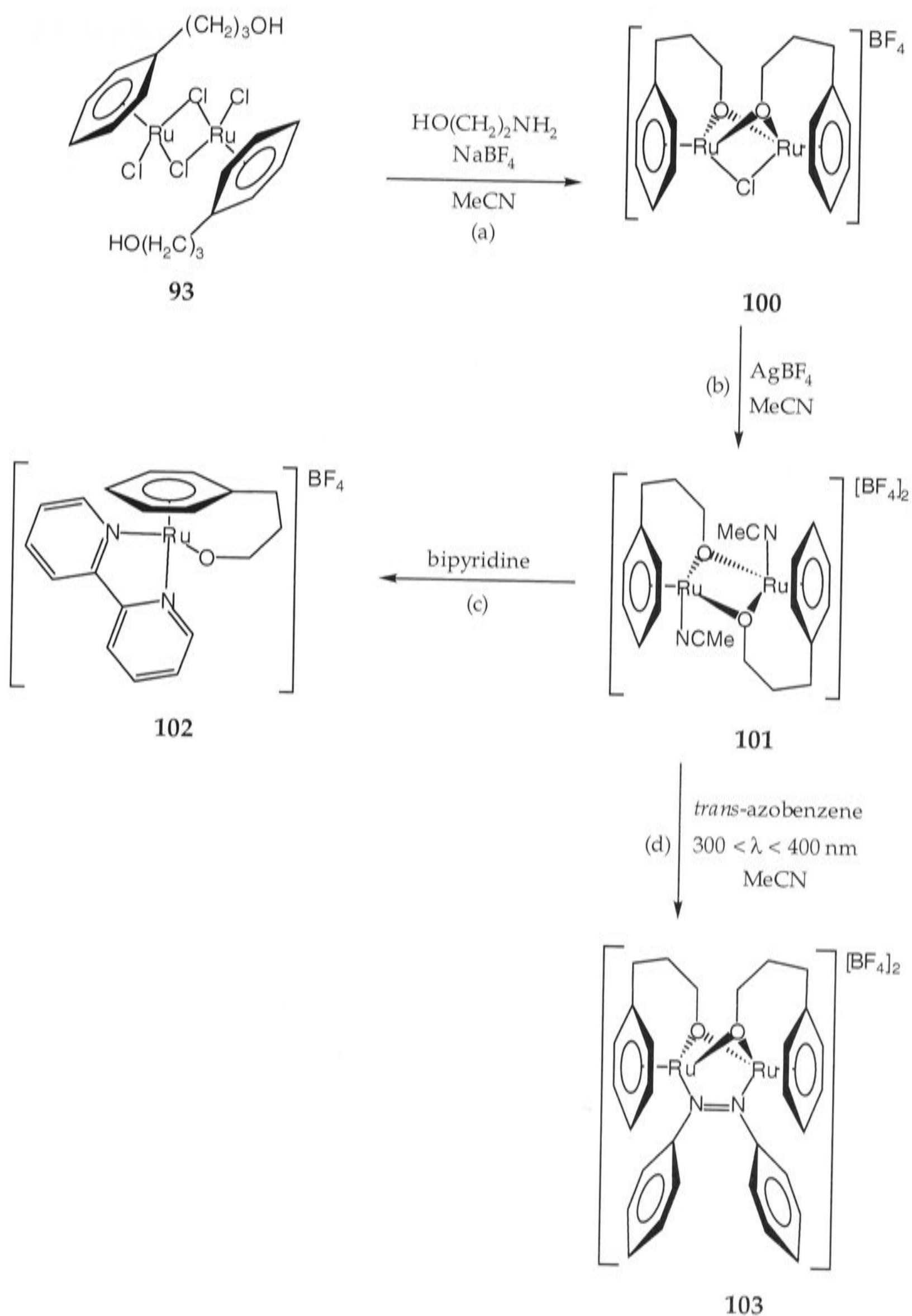


Scheme 21. Formation of the tethered complexes **96** (R = Et) and **97** (R = Ph).^{191,192}



Scheme 22. Formation of the tethered complexes **98** (R = *i*-Pr) and **99** (R = Ph).¹⁹²

Dinuclear tethered arene-ruthenium species were also prepared from the dimer **93**. Treatment with 2-aminoethanol in the presence of NaBF_4 in acetonitrile afforded the dimeric, tri-bridged species **100** (Scheme 23a).¹⁹⁴ The bridging chloride ligand was then abstracted with AgBF_4 , followed by coordination of two acetonitrile ligands to give complex **101**, where one of the oxygen atoms now lies below the two metal centres (Scheme 23b). This was then converted into a mononuclear tethered complex by treatment with 2,2'-bipyridine to afford **102** (Scheme 23c). The acetonitrile ligands on the dinuclear species **101** could also be exchanged for various bidentate ligands that bridge the two metal centres, without inverting one of the bridging oxygen donor atoms. For example, **101** reacts with *trans*-azobenzene under orange light to afford the *cis*-azobenzene complex **103** (Scheme 23d). A similar reaction occurs with disulfides and pyridazine.

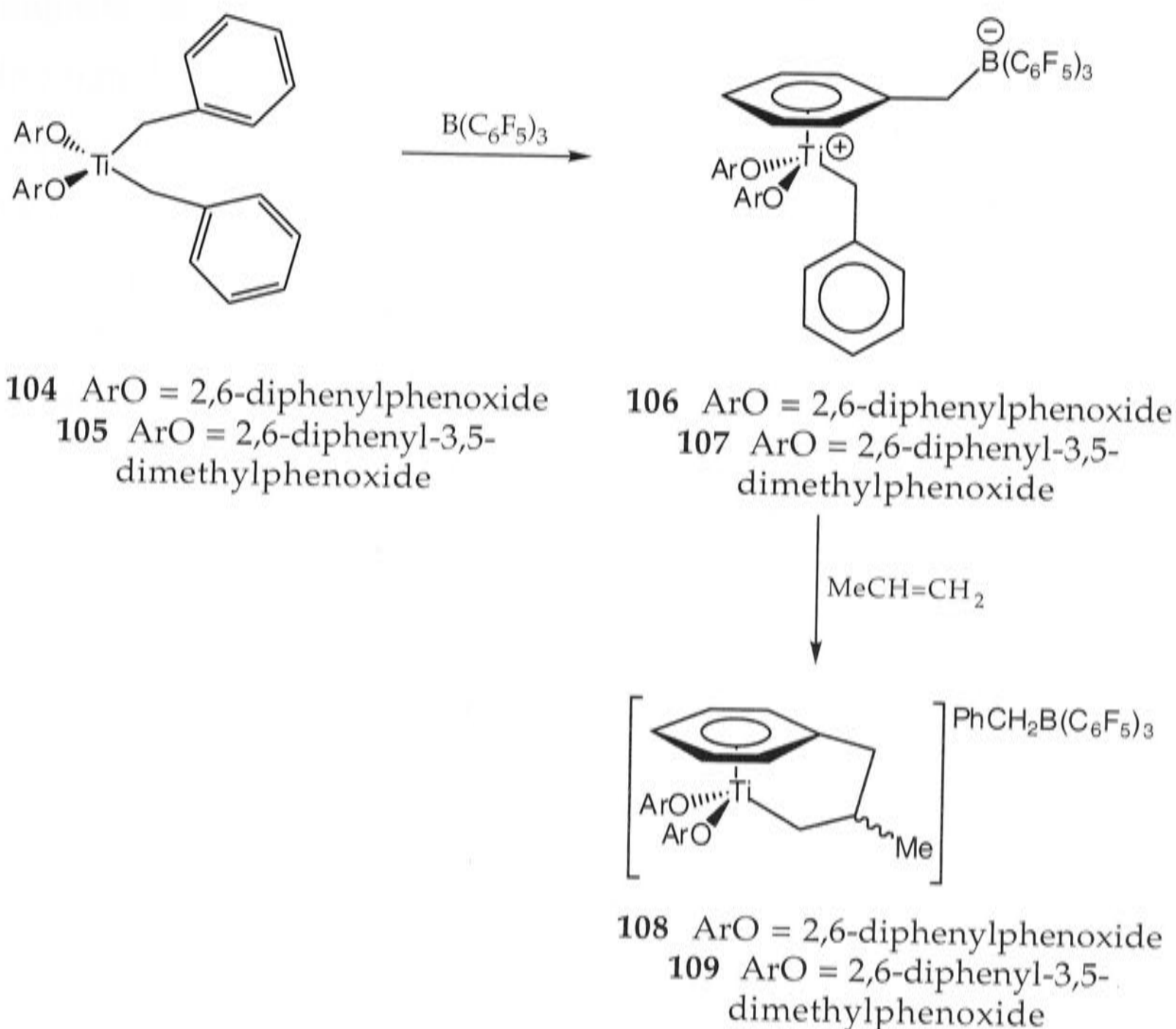


Scheme 23. Formation of the mono- and dinuclear tethered complexes **100-103**.¹⁹⁴

1.2.2 Syntheses Proceeding by Initial Donor Atom Coordination (Scheme 16b)

Intermolecular exchange between a free arene and arene-transition metal complexes of the type $[M(\text{CO})_3(\eta^6\text{-arene})]$ ($M = \text{Cr}, \text{Mo}$)¹⁹⁵⁻¹⁹⁷ or $[\text{Ir}(\eta^6\text{-arene})(\eta^4\text{-1,5-COD})]\text{BF}_4$ ¹⁹⁷ and $[\text{Ru}(\eta^6\text{-arene})(\eta^4\text{-1,5-COD})]$ ¹⁹⁷ has been studied extensively.

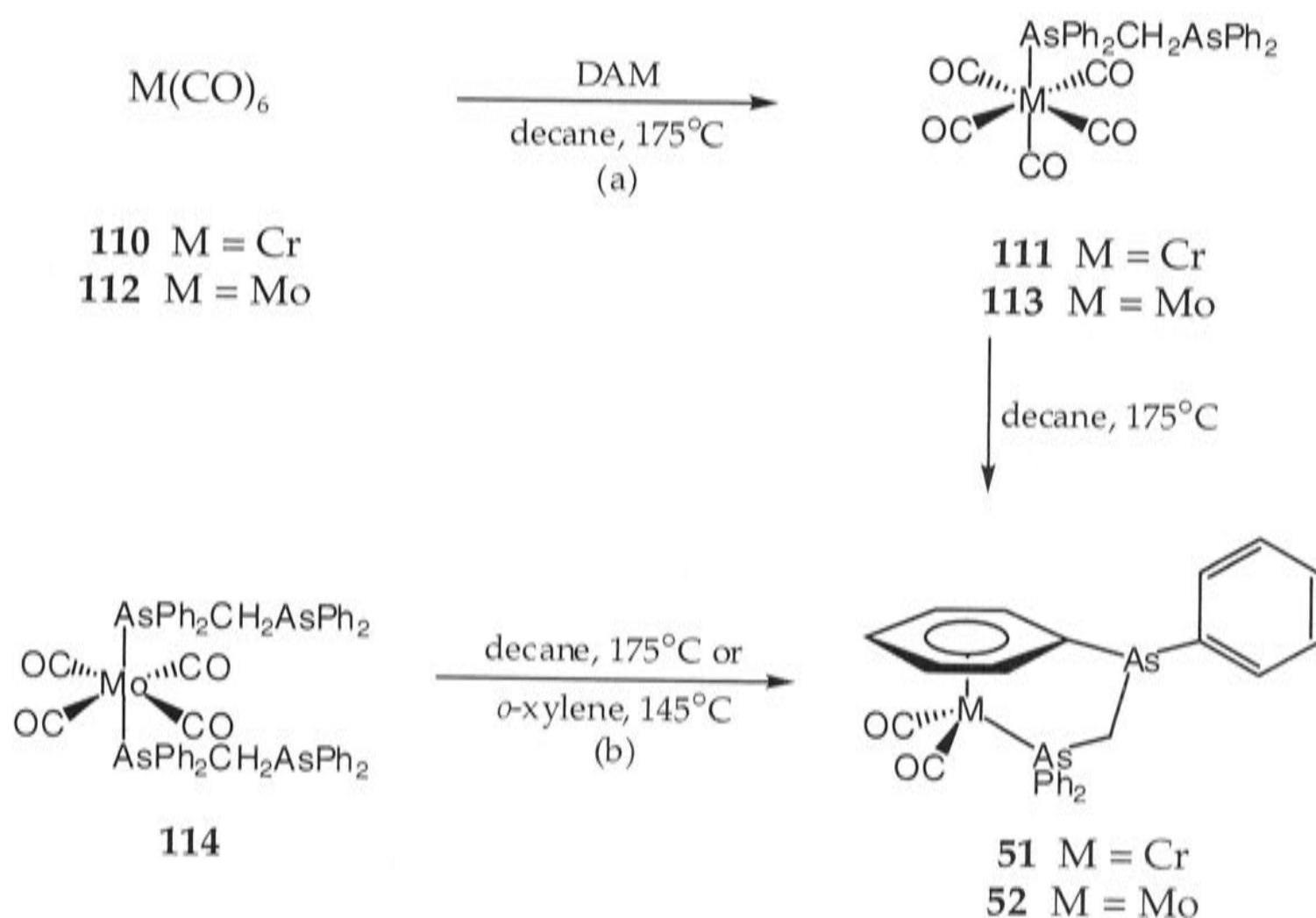
The intramolecular version of this exchange, depicted in Scheme 16b, has been used to prepare tethered arene compounds of titanium(IV), chromium(0), molybdenum(0) and (II), ruthenium(II), rhodium(I), iridium(I), and tungsten(0), (II) and (VI). The only examples of tethered arene complexes containing titanium have been prepared by coordination of the donor atom prior to the η^6 -arene, though it was necessary to complete construction of the tether between these two steps.^{198,199} Addition of tris(pentafluorophenyl)borane to the titanium bis(benzyl) complexes $[\text{Ti}(\text{OAr})_2(\text{CH}_2\text{Ph})_2]$ ($\text{ArO} = 2,6\text{-diphenylphenoxide}$ (**104**) or $2,6\text{-diphenyl-3,5-dimethylphenoxide}$ (**105**)) gave rise to the zwitterionic species $[\text{Ti}^+(\text{OAr})_2(\text{CH}_2\text{Ph})(\text{C}_6\text{H}_5\text{CH}_2\text{B}^-(\text{C}_6\text{F}_5)_3)]$ ($\text{ArO} = 2,6\text{-diphenylphenoxide}$ (**106**) or $2,6\text{-diphenyl-3,5-dimethylphenoxide}$ (**107**)), which then reacted with a variety of primary alkenes, such as propene, to afford the tethered arene complexes $[\text{Ti}(\text{OAr})_2(\eta^1:\eta^6\text{-CH}_2\text{CH}(\text{Me})\text{CH}_2\text{Ph})]\text{PhCH}_2\text{B}(\text{C}_6\text{F}_5)_3$ ($\text{ArO} = 2,6\text{-diphenylphenoxide}$ (**108**) or $2,6\text{-diphenyl-3,5-dimethylphenoxide}$ (**109**)) (Scheme 24). Spectroscopic data showed that these were formed by insertion of the alkene into the Ti-benzyl bond, and subsequent displacement of the coordinated arene, followed by η^6 -coordination of the dangling arene moiety to the metal centre. The zwitterionic species **106** also reacted with alkynes.



Scheme 24. Formation of tethered arene titanium complexes of the type **108** (ArO = 2,6-diphenylphenoxide) and **109** (ArO = 2,6-diphenyl-3,5-dimethylphenoxide).^{198,199}

Two of the first reported examples of tethered arene complexes involved chromium and molybdenum, $[\text{M}(\text{CO})_2(\eta^1:\eta^6\text{-Ph}_2\text{AsCH}_2\text{As}(\text{Ph})\text{C}_6\text{H}_5)]$ (M = Cr (**51**), Mo (**52**)).^{200,201} The chromium analogue **51** was prepared by heating either $\text{Cr}(\text{CO})_6$ (**110**) with 1,1-bis(diphenylarsino)methane (DAM) in decane (Scheme 25a), the compound $[\text{Cr}(\text{CO})_5(\eta^1\text{-Ph}_2\text{AsCH}_2\text{AsPh}_2)]$ (**111**) being the first formed intermediate.^{200,201} These reactions are somewhat reminiscent of the intermolecular formation of complexes of the type $[\text{Cr}(\text{CO})_3(\eta^6\text{-arene})]$ from **110**.²⁰² The molybdenum derivative **52** was prepared by similar methods (from $\text{Mo}(\text{CO})_6$ (**112**) and DAM, or from $[\text{Mo}(\text{CO})_5(\eta^1\text{-Ph}_2\text{AsCH}_2\text{AsPh}_2)]$ (**113**)), and also by heating $[\text{Mo}(\text{CO})_4(\eta^1\text{-DAM})_2]$ (**114**) (Scheme 25b) in either decane or *o*-xylene.²⁰¹ This is an interesting result, since the other arsenic atom does not

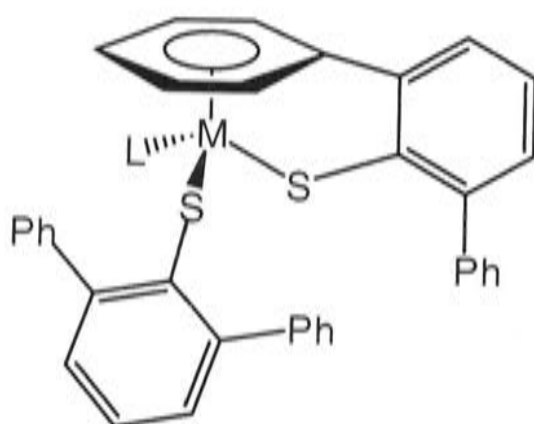
coordinate to the metal and form bidentate complexes of the type $[M(CO)_4(\eta^2\text{-Ph}_2\text{AsCH}_2\text{AsPh}_2)]$ ($M = \text{Cr, Mo}$), as has been observed with the phosphorus analogue. For example, compounds of the type $[M(CO)_4(\eta^2\text{-Ph}_2\text{PCH}_2\text{PPh}_2)]$ ($M = \text{Cr, Mo}$) were prepared by heating dppm with a slight excess of the metal carbonyl.²⁰³ Tethered complexes similar to **51** and **52** cannot be made with dppm, which acts preferentially as a bidentate ligand, in complexes of the type $[\text{Cr}(\text{CO})(\eta^6\text{-biphenyl})(\eta^2\text{-dppm})]$.²⁰⁴



Scheme 25. Preparation of the chromium and molybdenum tethered complexes **51** ($M = \text{Cr}$) and **52** ($X = \text{Mo}$).^{200,201}

The preparation of tethered arene-molybdenum(II) and arene-ruthenium(II) complexes incorporating sulfur donor atoms has been reported by Dilworth and co-workers.²⁰⁵⁻²⁰⁷ Reaction of sodium 2,6-diphenylbenzenethiolate with either $[\text{MoBr}_2(\text{CO})_4]$ or $[\text{RuCl}_2(\text{PPh}_3)_3]$ gave rise to either $[\text{Mo}(\eta^1:\eta^6\text{-SC}_6\text{H}_3\text{-2-Ph-6-C}_6\text{H}_5\text{)}-(2,6\text{-Ph}_2\text{C}_6\text{H}_3\text{S})(\text{CO})]$ ^{205,206} (**115**) or $[\text{Ru}(\eta^1:\eta^6\text{-SC}_6\text{H}_3\text{-2-Ph-6-C}_6\text{H}_5\text{)}-(2,6\text{-Ph}_2\text{C}_6\text{H}_3\text{S})(\text{PPh}_3)]$ ²⁰⁷ (**116**), respectively. Although not proved, it was thought that η^6 -coordination of

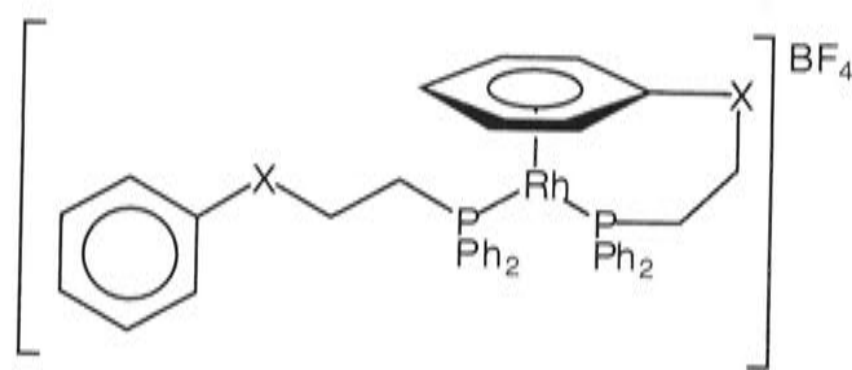
one of the phenyl groups of the 2,6-diphenylthiophenol to the metal centre was preceded by coordination of the sulfur atom.



115 M = Mo, L = CO

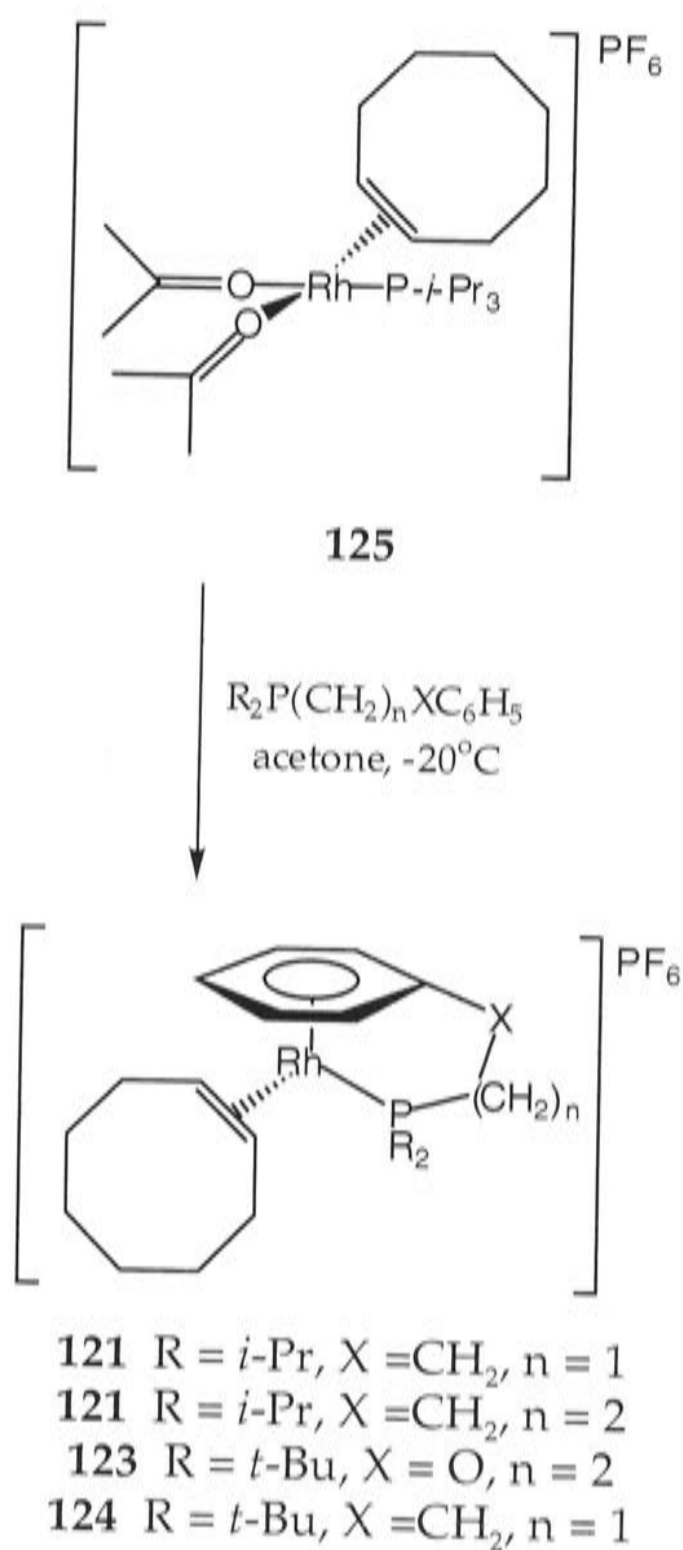
116 M = Ru, L = PPh₃

Mirkin *et al.* were the first to synthesise potentially chelating ligands containing both phosphine and arene moieties, Ph₂P(CH₂)₂XC₆H₅ (X = O (**117**), X = CH₂ (**118**)).^{208,209} These ligands react with [Rh(THF)₂(η²-C₈H₁₄)₂]BF₄ (C₈H₁₂ = cyclooctene) to form rhodium(I) complexes of the type [(η¹-Ph₂P(CH₂)₂XPh)Rh(η¹:η⁶-Ph₂P(CH₂)₂XC₆H₅)]BF₄ (X = O (**119**), X = CH₂ (**120**)).²⁰⁸⁻²¹⁰ No comment was given on the mechanism of this reaction, though it is likely that coordination of the η⁶-arene is preceded by η¹-coordination of the phosphorus donor atom. It has been shown that the η⁶-arene is moderately labile when bound to a (PPh₃)₂Rh(I) metal core in non-tethered species.²¹¹ Thus, the coordinated arene of **119** underwent rapid intramolecular exchange with the non-coordinated phenyl group. Compounds **119** and **120** also undergo electrochemically reversible one-electron oxidation. The study of this system has been extended by replacing the ligand containing the free arene moiety with (η⁵-C₅H₅)Fe(η⁵-C₅H₄)O(CH₂)₂PPh₂.^{212,213}



119 X = O
120 X = CH₂

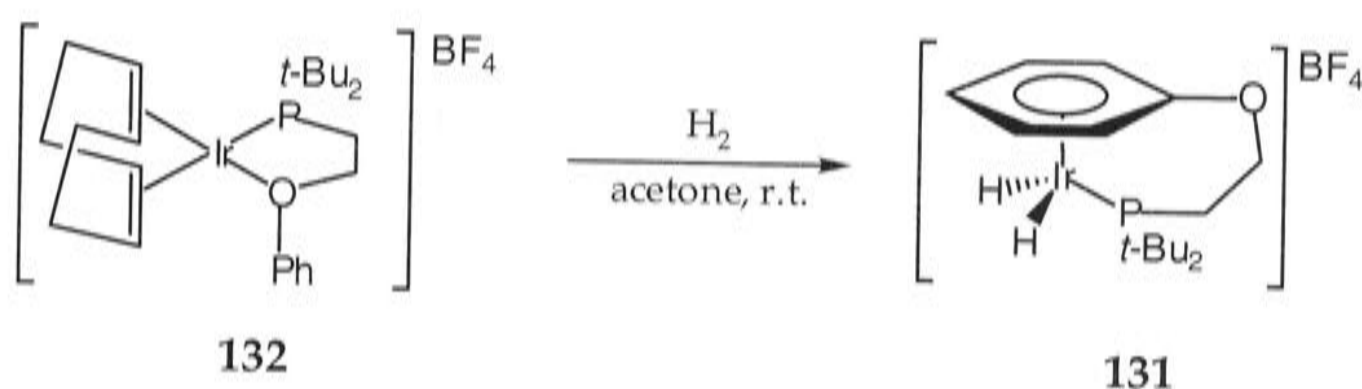
Several more examples of tethered arene-rhodium(I) complexes have been reported recently.²¹⁴ Although the mechanism for the formation of the complexes $[\text{Rh}(\eta^2\text{-C}_8\text{H}_{14})(\eta^1:\eta^6\text{-R}_2\text{P}(\text{CH}_2)_n\text{XC}_6\text{H}_5)]$ ($\text{R} = i\text{-Pr}_2$, $\text{X} = \text{CH}_2$, $n = 1$ (**121**); $\text{R} = i\text{-Pr}_2$, $\text{X} = \text{CH}_2$, $n = 2$ (**122**); $\text{R} = t\text{-Bu}$, $\text{X} = \text{O}$, $n = 2$ (**123**); $\text{R} = t\text{-Bu}$, $\text{X} = \text{CH}_2$, $n = 1$ (**124**)) is not known, it is thought that one of the acetone moieties of the precursor $[\text{Rh}(\text{OCMe}_2)_2(\eta^2\text{-C}_8\text{H}_{14})(\text{P-}i\text{-Pr}_3)]$ (**125**) was displaced to allow η^1 -coordination of the incoming phosphine ligand, presumably followed by displacement of the second acetone ligand and the triisopropylphosphine (Scheme 26). Careful control of the reaction conditions is required, otherwise the bis(phosphine) complexes $[(\eta^1\text{-}i\text{-Pr}_2\text{PCH}_2(\text{CH}_2)_n\text{Ph})\text{Rh}(\eta^1:\eta^6\text{-}i\text{-Pr}_2\text{PCH}_2(\text{CH}_2)_n\text{Ph})]$ ($n = 1$ (**126**); $n = 2$ (**127**)) are formed. It is interesting to note that there is no fluxional behaviour in solution, that is, neither **126** nor **127** show exchange of the η^6 -coordinated and free phenyl groups in the temperature range investigated. This is in agreement with **120**, which does not exhibit fluxionality, but is in contrast to $[(\eta^1\text{-Ph}_2\text{P}(\text{CH}_2)_2\text{OPh})\text{Rh}(\eta^1:\eta^6\text{-Ph}_2\text{P}(\text{CH}_2)_2\text{OPh})]\text{BF}_4$ (**119**), which does.²⁰⁹ Evidently the ether linkage in **119** facilitates the arene-arene exchange, possibly by initiating coordination to the metal centre.



Scheme 26. Formation of the tethered complexes **121** ($R = i\text{-Pr}_2, X = CH_2, n = 1$), **122** ($R = i\text{-Pr}_2, X = CH_2, n = 2$), **123** ($R = t\text{-Bu}_2, X = O, n = 2$) and **124** ($R = t\text{-Bu}_2, X = CH_2, n = 1$).²¹⁴

This methodology has recently been extended to iridium. Complex $[Ir(\eta^2\text{-C}_8\text{H}_{14})(\eta^1:\eta^6\text{-}i\text{-Pr}_2\text{P}(\text{CH}_2)_2\text{Ph})]PF_6$ (**128**) was prepared by treatment of $[Ir(\text{OCMe}_2)_2(\eta^2\text{-C}_8\text{H}_{14})_2]$ in acetone at room temperature.²¹⁵ The iridium(III) derivative $[Ir(\text{H})_2(\eta^1:\eta^6\text{-}i\text{-Pr}_2\text{P}(\text{CH}_2)_2\text{Ph})]BF_4$ (**129**) was isolated from the reaction of $[Ir(\text{OCMe}_2)(\eta^4\text{-C}_8\text{H}_{12})(\eta^1\text{-}i\text{-Pr}_2\text{P}(\text{CH}_2)_2\text{Ph})]BF_4$ (**130**) with hydrogen in acetone. Complex $[Ir(\text{H})_2(\eta^1:\eta^6\text{-}t\text{-Bu}_2\text{P}(\text{CH}_2)_2\text{OPh})]BF_4$ (**131**) was formed by treatment with hydrogen of the bidentate P-O bonded iridium(I) compound **132** (Scheme 27). The iridium(I) η^2 -alkene adduct $[Ir(\eta^1:\eta^6\text{-}i\text{-Pr}_2\text{P}(\text{CH}_2)_2\text{Ph})(\eta^2\text{-H}_2\text{C}=\text{CHMe})]BF_4$ (**133**), prepared from the reaction of **129** with propene in acetone, reacted with an excess of

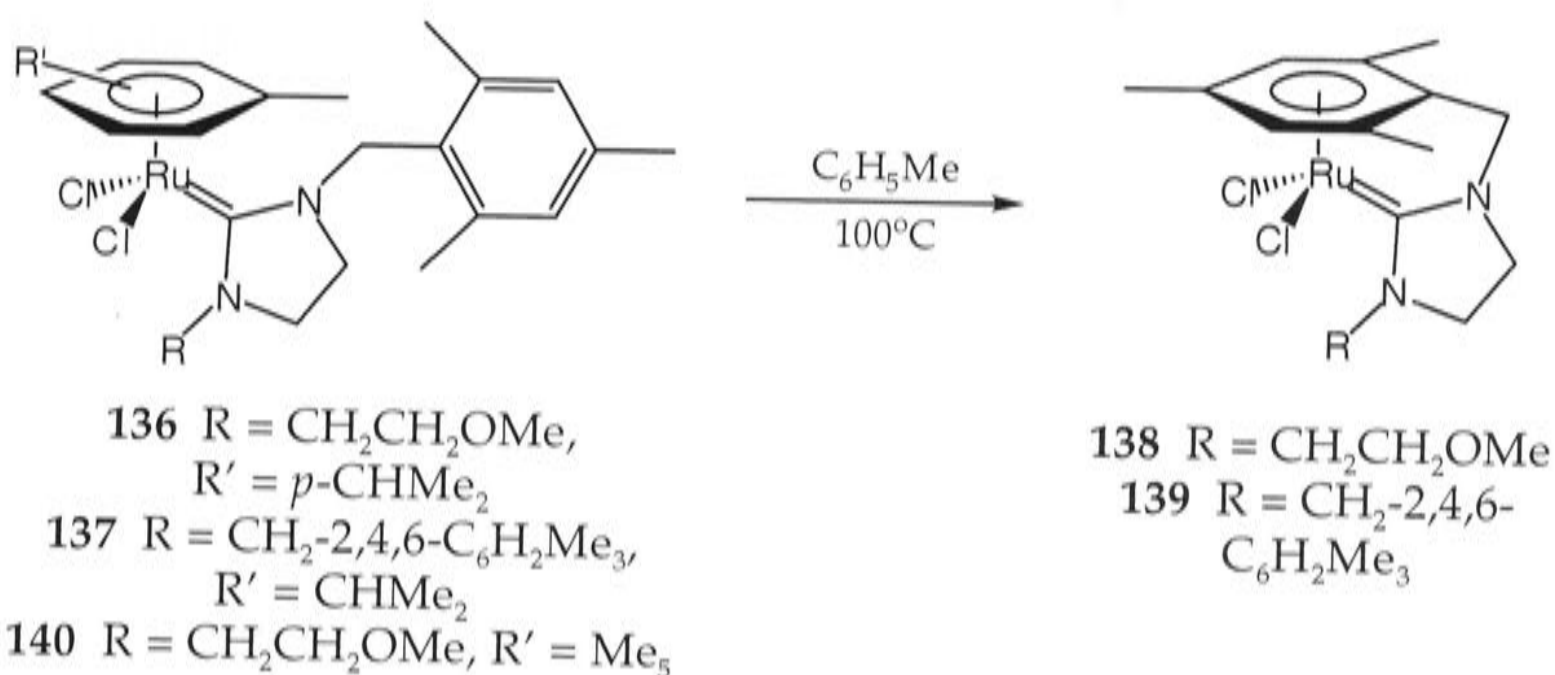
acetonitrile at room temperature, in the presence of acetone, to afford the arylhydrido product $[\text{Ir}(\text{H})(\eta^1\text{-}i\text{-Pr}_2\text{P}(\text{CH}_2)_2\text{C}_6\text{H}_4)(\text{NCMe})_3]\text{BF}_4$ (**134**). It was also formed from the reaction of the η^2 -alkyne complex $[\text{Ir}(\eta^1:\eta^6\text{-}i\text{-Pr}_2\text{P}(\text{CH}_2)_2\text{Ph})(\eta^2\text{-PhC}\equiv\text{CPh})]\text{BF}_4$ (**135**) with an excess of acetonitrile in acetone. Thus the tethered-arene iridium(I) complexes **133** and **135** undergo C-H bond activation.



Scheme 27. Synthesis of the iridium(III) tethered-arene complex **131**.²¹⁵

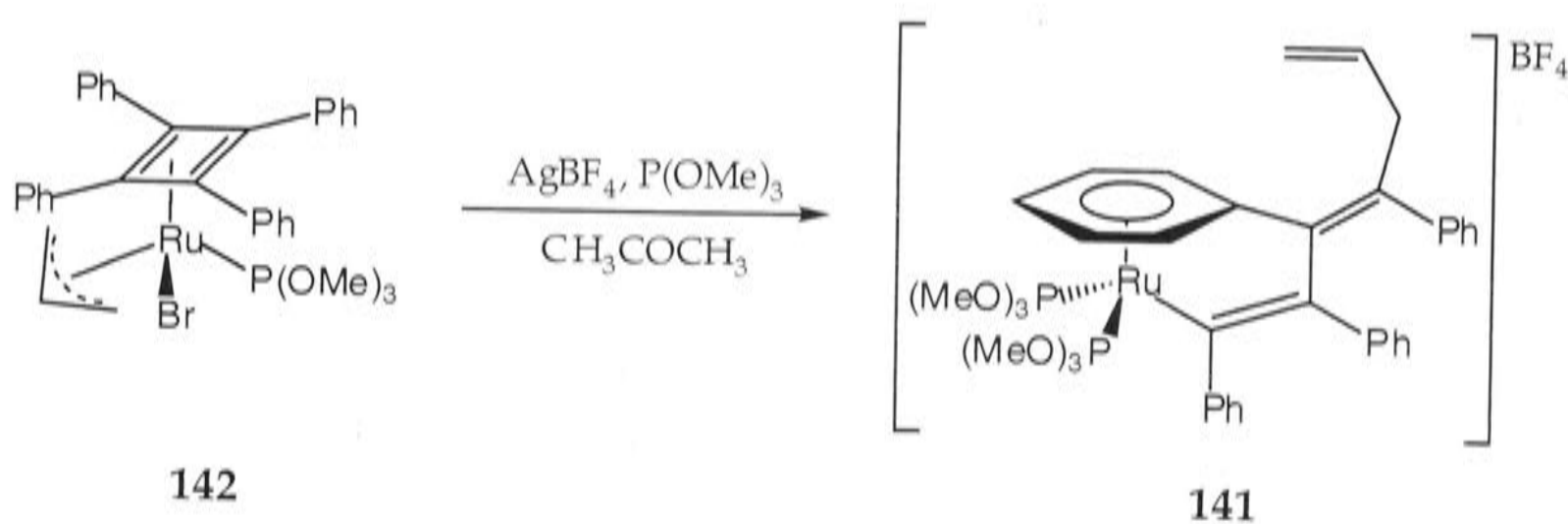
There are some examples of tethered ruthenium(II) complexes, containing carbon and sulfur (mentioned earlier) donor atoms, prepared *via* the general approach as shown in Scheme 16b. There are also many examples incorporating phosphorus donor atoms, and the study of these types of complexes forms the basis of this thesis; hence the discussion of most of the literature examples will be deferred to Chapter 7 (see Section 7.2).

The displacement of *p*-cymene and hexamethylbenzene from suitable precursor complexes has been employed to afford tethered complexes that contain a chelating carbene ligand.²¹⁶ The imidazolidin-2-ylidene complexes **136** and **137**, when heated in toluene, gave rise to the tethered complexes **138** and **139** in high yield (Scheme 28). Complex **138** was also prepared by heating the hexamethylbenzene precursor complex **140** in xylenes at 140°C, and was formed in 82% yield. These complexes were converted to unstable allenylidene intermediates which were active as catalysts for either alkene metathesis or cycloisomerisation.



Scheme 28. Preparation of the tethered complexes **138** ($R = \text{CH}_2\text{CH}_2\text{OMe}$) and **139** ($R = \text{CH}_2\text{-2,4,6-C}_6\text{H}_2\text{Me}_3$).²¹⁶

Complex $[\text{Ru}\{\text{C}(\text{Ph})=\text{C}(\text{Ph})\text{C}(\eta^6\text{-C}_6\text{H}_5)=\text{C}(\text{Ph})\text{CH}_2\text{CH}=\text{CH}_2\}\{\text{P}(\text{OMe})_3\}_2]\text{BF}_4$ (**141**), containing a σ -carbon donor atom tethered to a η^6 -arene, was formed by treatment of the η^4 -tetraphenylcyclobutadiene complex $[\text{RuBr}(\text{P}(\text{OMe})_3)(\eta^3\text{-C}_3\text{H}_5)(\eta^4\text{-C}_4\text{Ph}_4)]$ (**142**) with AgBF_4 and a slight excess of trimethylphosphite in acetone (Scheme 29).²¹⁷ The proposed mechanism requires ring-opening of the tetraphenylcyclobutadiene ring to form a butadienyl chain, to which the allyl ligand coordinates. The carbon donor atom of **141** was formerly part of the four-membered ring, and is thus already coordinated to the metal atom before the η^6 -arene, which is one of the C_4Ph_4 substituents, becomes coordinated.

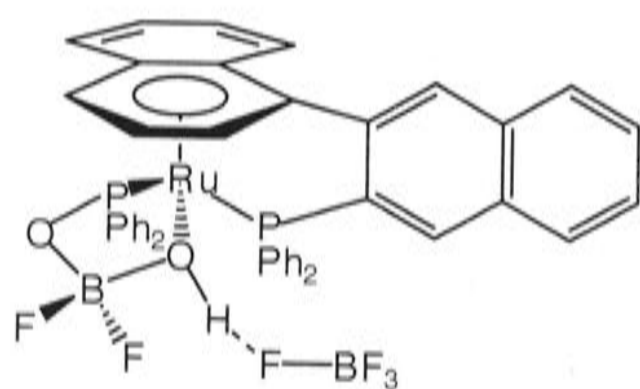


Scheme 29. Preparation of the tethered compound **141**.²¹⁷

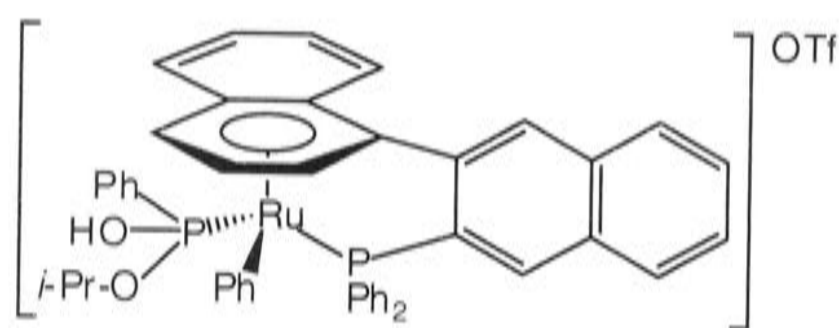
There are many examples of the formation of tethered ruthenium(II) complexes *via* P-C bond cleavage reactions of coordinated

2,2'-bis(methoxy)-6,6'-bis(diarylphosphino) ligands,²¹⁸⁻²²⁰ which have been discussed in a recent microreview.²²¹ Treatment of the complex **143** with three equivalents of an alkyl lithium reagent gave rise to the tethered complexes **144** and **145** (Scheme 30a).²¹⁸ The complexes **146-148** were formed by the reaction of the precursor complexes **149**, **150** and **143**, respectively, with HBF_4 by very slow hydrolysis of the tetrafluoroborate anion in the presence of water (Scheme 30b).²¹⁹ The slow hydrolysis process could be eliminated by heating the precursor **149** in the presence of wet triflic acid to afford the tethered complex **151** (Scheme 30c).²²⁰ The mechanism of these reactions proceeds *via* protonation of one acetate moiety and subsequent addition of water across the one of the P-C bonds of the bidentate ligand. Hence the donor atom is coordinated prior to the η^6 -arene, but P-C bond cleavage must occur to form the tethered species.

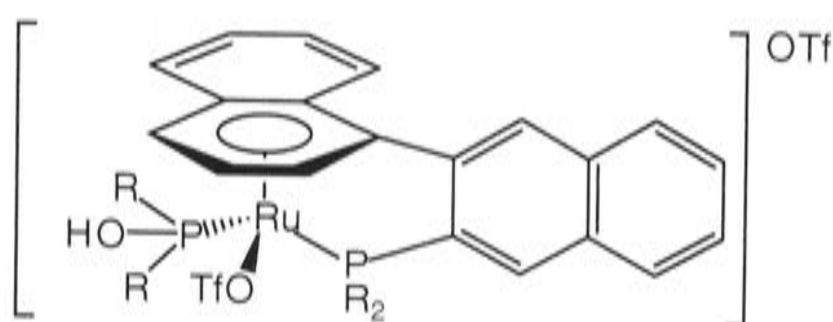
Similar methodology has been applied to the binaphthyl system 2,2'-bis(diphenylphosphino)-1,1'-binaphthyl (Binap), which gave rise to the mononuclear tethered complexes **152-156**.^{220,222-224}



152

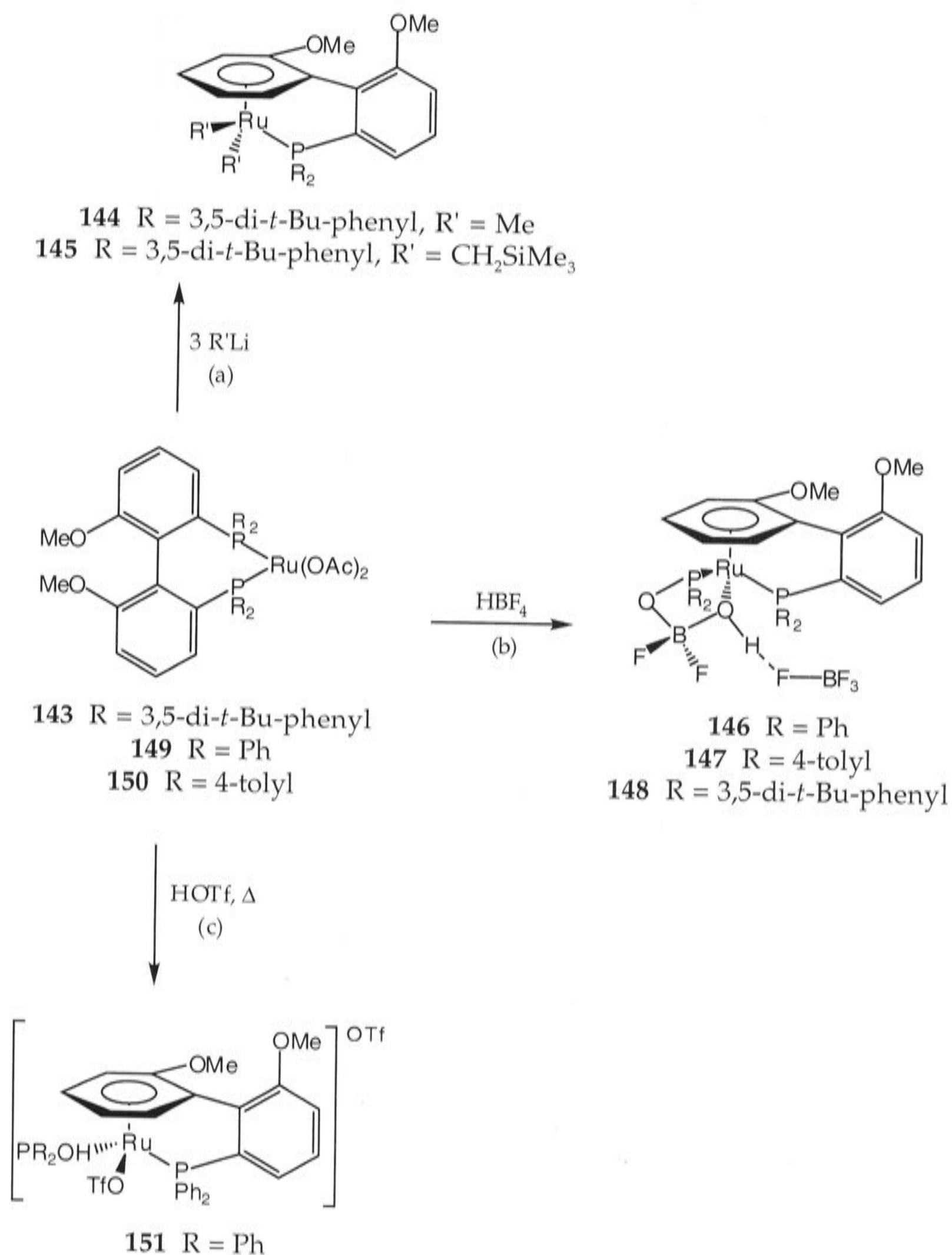


153

154 R = *i*-Pr

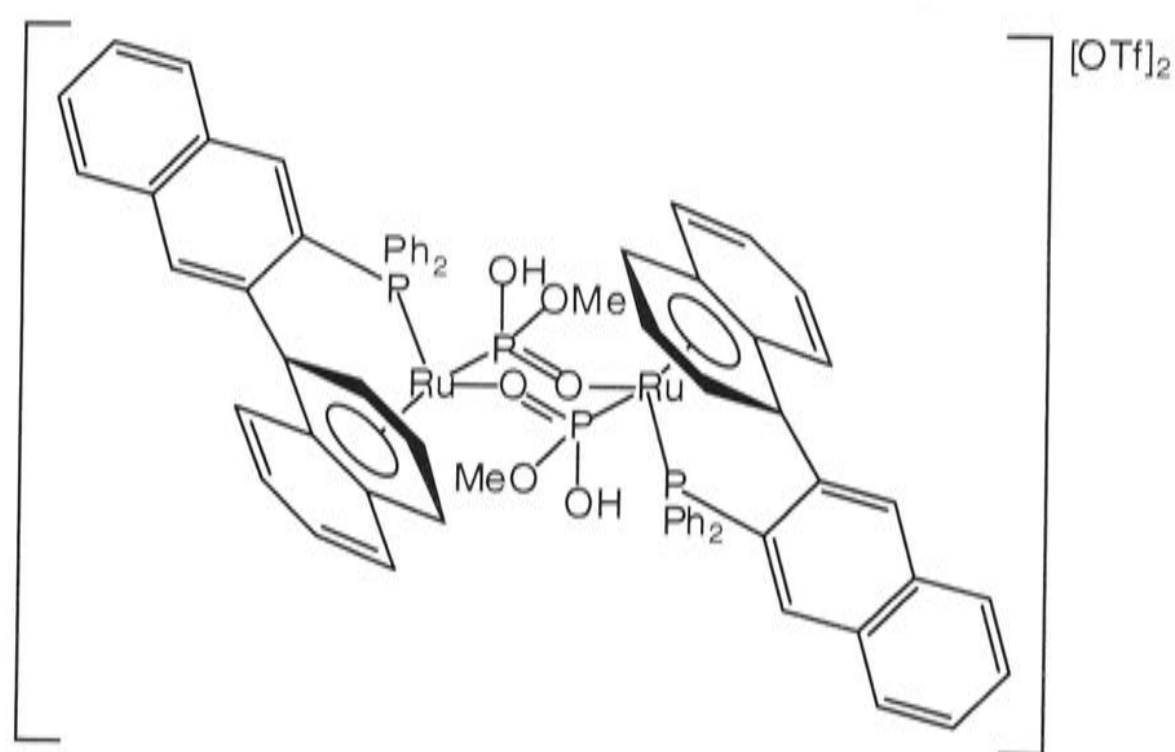
155 R = Ph

156 R = Cy



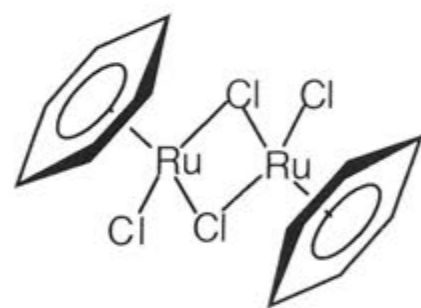
Scheme 30. Preparation of the tethered arene-ruthenium complexes **144** (R = 3,5-di-*t*-Bu-phenyl, R' = Me), **145** (R = 3,5-di-*t*-Bu-phenyl, R' = CH₂SiMe₃), **146** (R = Ph), **147** (R = 4-tolyl), **148** (R = 3,5-di-*t*-Bu-phenyl), and **151** (R = Ph).²¹⁸⁻²²⁰

The dinuclear complex **157** was formed during attempts to crystallise the an analogue of **153** (with a methyl group in place of the *iso*-propyl moiety) in THF that contained traces of water.²²³



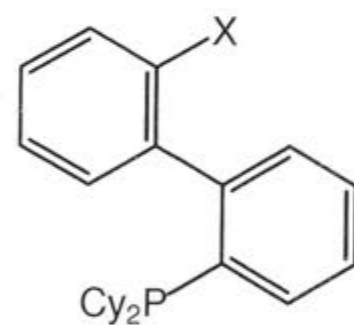
157

Compounds similar to those described by Pregosin *et al.*, incorporating bulky cyclohexyl substituents on the phosphorus, have recently been reported.²²⁵ The reaction of various biphenyl ligands 2-(dicyclohexylphosphino)biphenyl (**158**), 2-(dicyclohexylphosphino)-2'-methylbiphenyl (**159**) and 2-dicyclohexylphosphino-2'-(*N,N*-dimethylamino)biphenyl (**160**) with $[\text{RuCl}_2(\eta^6\text{-C}_6\text{H}_6)]_2$ (**161**) in DMF at 100°C gave rise to the tethered complexes **162-164**, respectively, in yields ranging from 31-96% (Scheme 31a). One of the chloride ligands of compounds **162-164** was replaced by various phosphines, including chiral phosphines, by treatment with AgSbF_6 in the presence of the desired phosphine, to afford the cationic complexes **165-172** (Scheme 31b). The remaining chloride ligand of complexes **167** and **169** was also removed by treatment with another equivalent of AgSbF_6 to afford complexes **173** and **174** (Scheme 31c). Bidentate phosphines were also coordinated to the ruthenium(II) center in place of the chloride ligands; reaction of **164** with either (*R*)-(+)-1,2-bis(diphenylphosphino)propane ((*R*)-PROPHOS) or 1,1-bis(diphenylphosphino)methane monoxide (dppmO) gave rise to the complexes **175** and **176** (Scheme 31d).



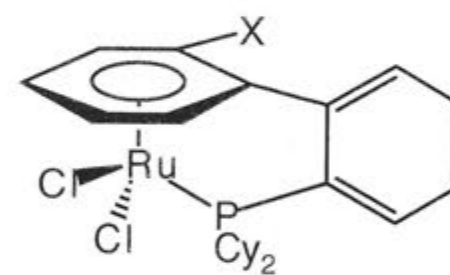
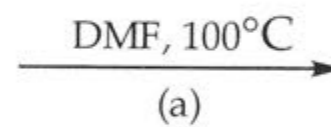
161

+



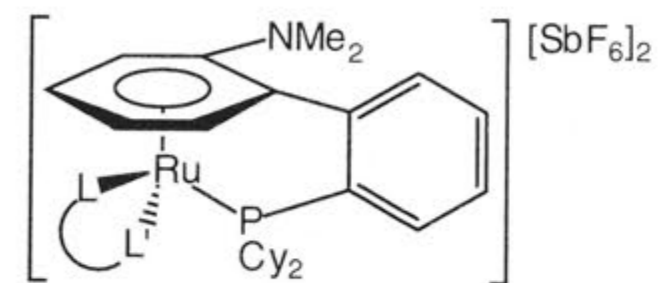
158 X = H

159 X = Me

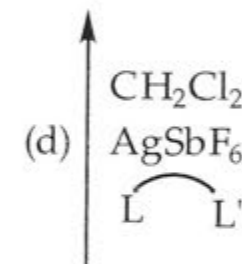
160 X = NMe₂

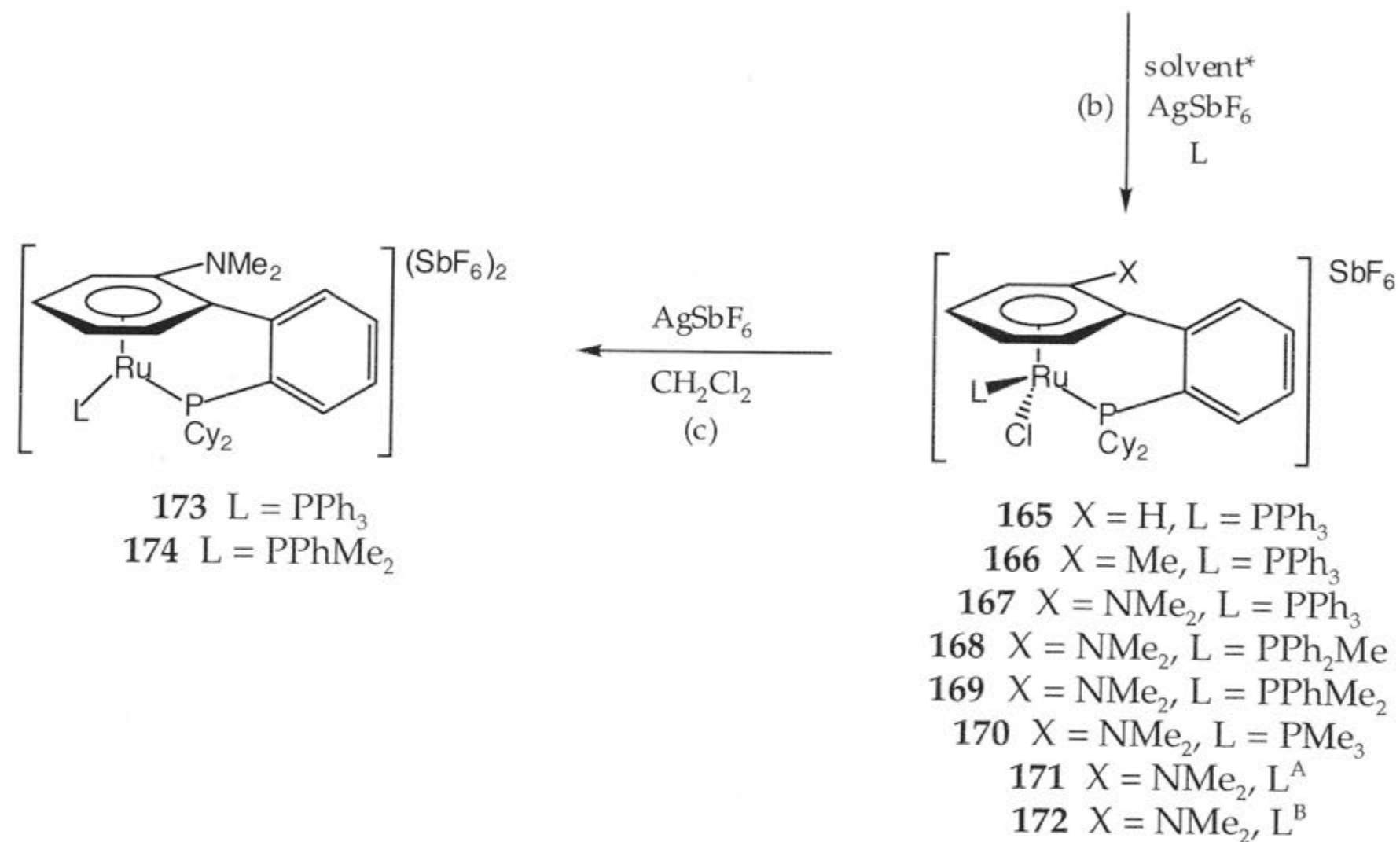
162 X = H

163 X = Me

164 X = NMe₂175 L L' = (R)-PROPHOS
(L = L')

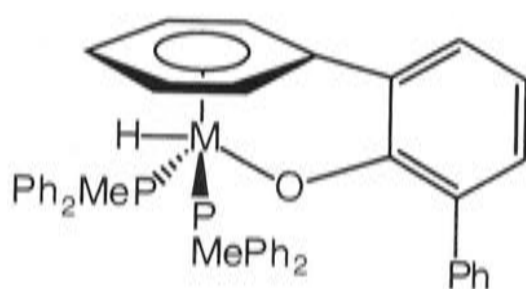
176 L L' = dppmO





Scheme 31. Preparation of various tethered complexes incorporating biphenyl tethered ligands.²²⁵
 * = CH₂Cl₂, CD₂Cl₂ or C₆H₅Cl; L^A = (S)-(-)-diphenyl(1-phenylethylamino)phosphine,
 L^B = (1R,7R)-9,9-dimethyl-2,2,4,6,6-pentaphenyl-3,5,8,10-tetroxa-4-phospha-bicyclo[5.3.0]decane.

Some examples of tethered molybdenum(II) and tungsten(0), (II) and (VI) complexes which incorporate oxygen as the donor atoms have been reported.²²⁶⁻²²⁹ Reaction of 2,6-diphenylphenol with $[\text{MH}_4(\text{PMePh}_2)_4]$ ($\text{M} = \text{Mo}, \text{W}$) at 150°C in the absence of solvent gave rise to either $[\text{MH}(\eta^1:\eta^6\text{-OC}_6\text{H}_3\text{-2-Ph-6-C}_6\text{H}_5)(\text{PMePh}_2)_2]$ ($\text{M} = \text{Mo}$ (**177**) and W (**178**)).²²⁶ Although not stated, the donor atom probably coordinated before η^6 -coordination of one of the phenyl groups occurs.

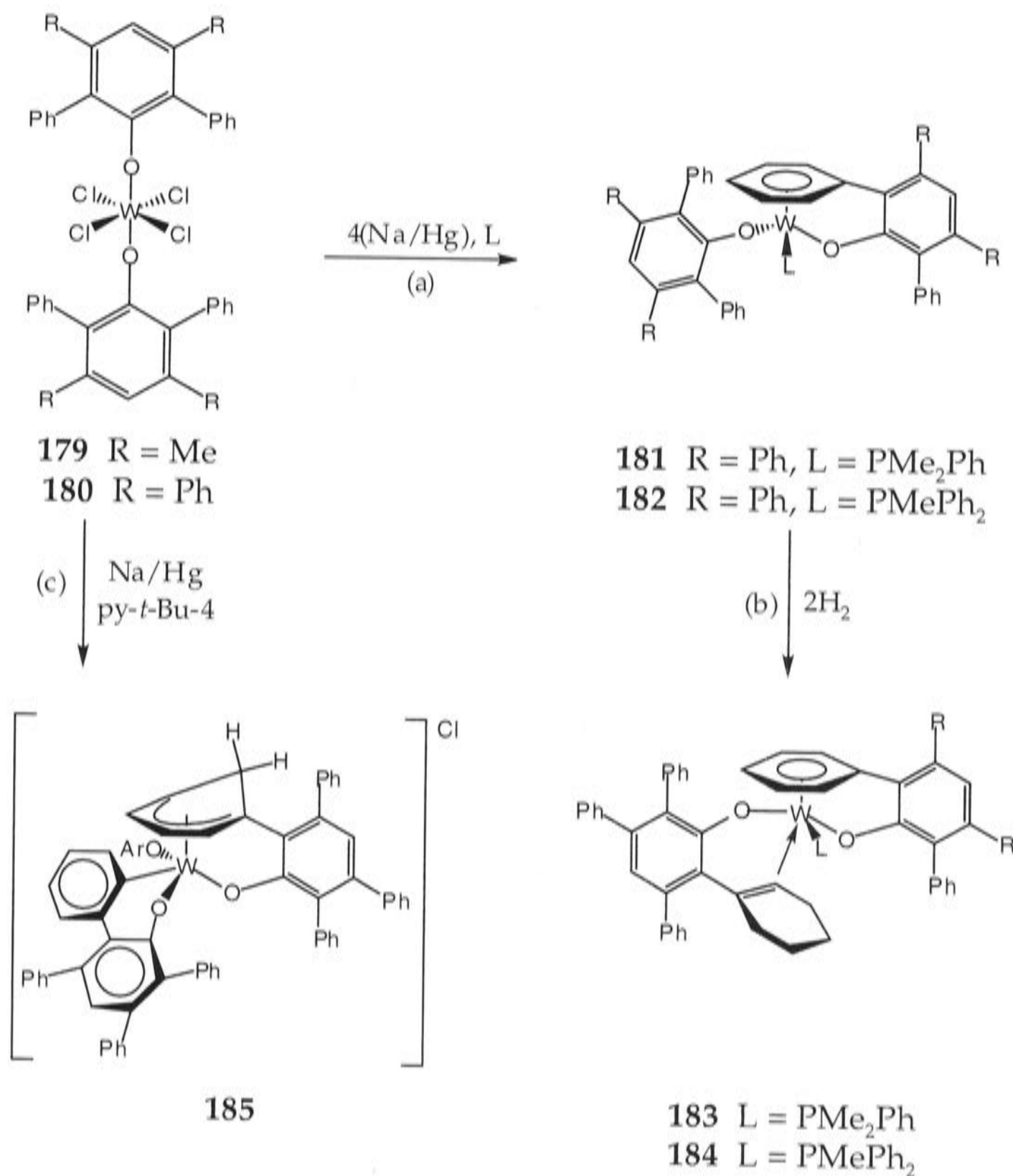


177 $\text{M} = \text{Mo}$

178 $\text{M} = \text{W}$

The methodology was then extended to aryl alcohols containing more substituents.²²⁷ Reaction of WCl_6 with the appropriate aryl alcohol afforded complexes of the type $[\text{WCl}_4(\text{OC}_6\text{H}_2\text{-2,6-Ph}_2\text{-3,5-R}_2)_2]$ ($\text{R} = \text{Me}$ (**179**), Ph (**180**)) which were reduced using sodium, in the presence of a phosphine, resulting in one of the phenyl groups of the aryl ether becoming π -bonded to the metal, thus forming the tethered complexes **181** ($\text{R} = \text{Ph}, \text{L} = \text{PMe}_2\text{Ph}$) and **182** ($\text{R} = \text{Ph}, \text{L} = \text{PMePh}_2$) (Scheme 32a). The hydrogenation of two of the double bonds of the *ortho*-phenyl group of the non-tethered aryl ether slowly gave rise to a cyclohexene ring when either **181** or **182** were placed under an atmosphere of hydrogen, resulting in the formation of the η^2 -cyclohexene complexes **183** ($\text{L} = \text{PMe}_2\text{Ph}$) and **184** ($\text{L} = \text{PMePh}_2$) (Scheme 32b). An additional product **185** was isolated, along with the tungsten(II) complex $[\text{W}(\eta^1:\eta^6\text{-OC}_6\text{H}_4\text{Ph}_3\text{-3,5,6-C}_6\text{H}_5)(\text{OC}_4\text{HPh}_4\text{-2,3,5,6})(\text{py-}t\text{-Bu-4})]$ (**186**), when the reduction of **180** was carried out in the presence of 4-*tert*-butylpyridine (Scheme 32c).²²⁹ The reaction is thought to proceed *via* a cyclometallated complex of the type $[\text{W}(\text{Cl})(\text{H})(\text{OC}_6\text{H}_4\text{Ph}_3\text{-2,3,5-C}_6\text{H}_4)(\text{OC}_6\text{HPh}_4\text{-2,3,5,6})]$

which undergoes hydride transfer to one of the *ortho*-phenyl rings afford **185**.

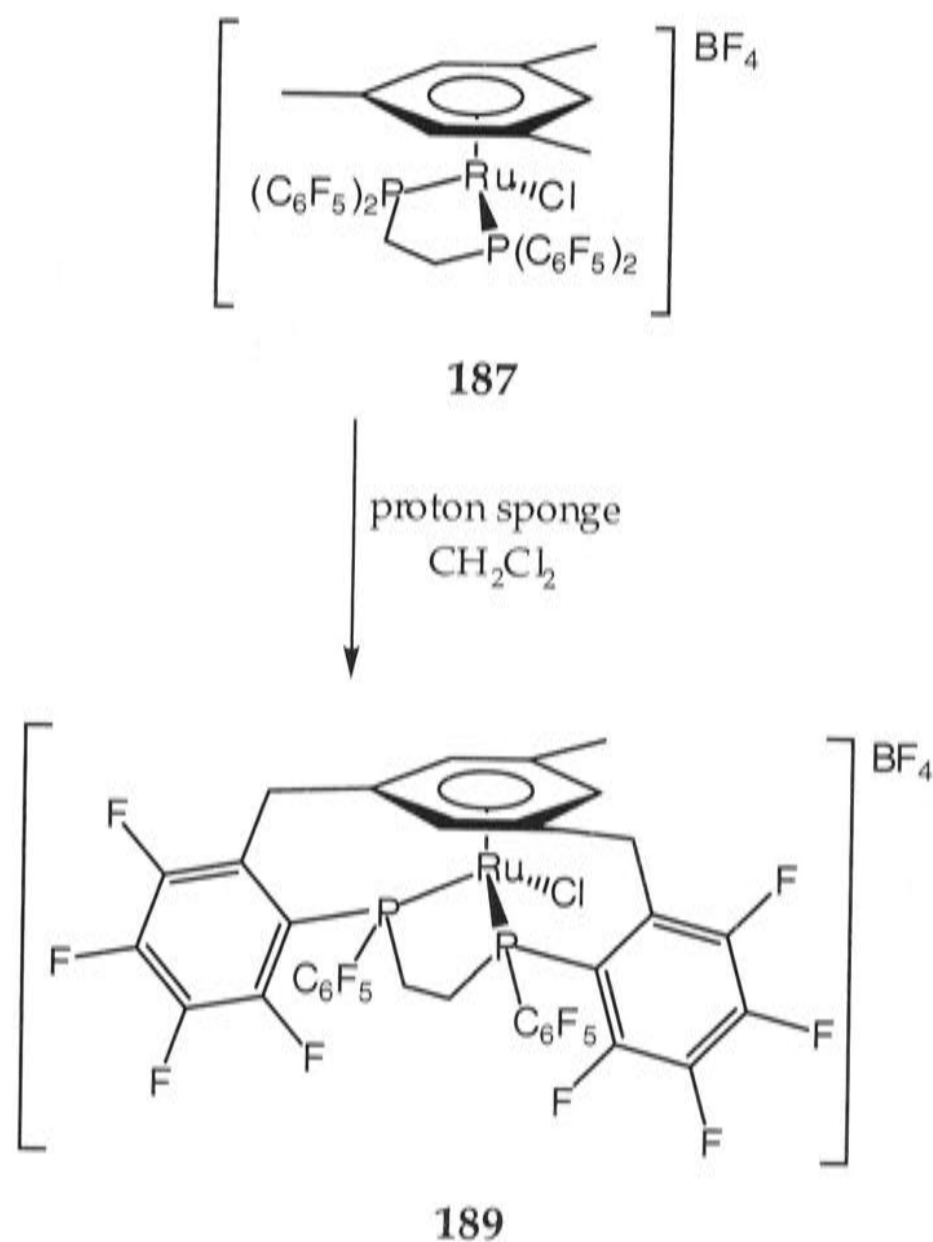


Scheme 32. Preparation of the tethered-arene tungsten compounds **181** (R = Ph, L = PMe₂Ph), **182** (R = Ph, L = PMePh₂), **183** (L = PMe₂Ph) and **184** (L = PMePh₂).^{227,229}

1.2.3 Intramolecular Construction of the Strap (Scheme 16c)

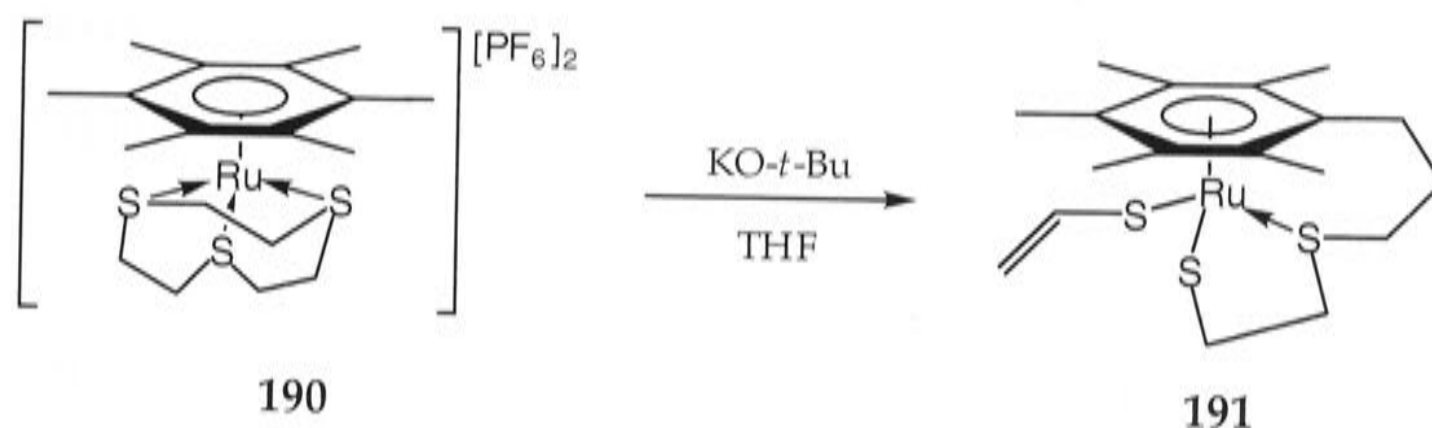
There are some examples of tethered ruthenium(II) complexes prepared *via* the general approach depicted in Scheme 16c that incorporate phosphorus and sulfur as donor atoms. An example of a bidentate phosphine which gave rise to a tethered arene-ruthenium complex was reported recently.²³⁰ Complex **187** was prepared from

$[\text{RuCl}_2(\eta^6\text{-1,3,5-C}_6\text{H}_3\text{Me}_3)]_2$ (**188**) and $(\text{C}_6\text{F}_5)_2\text{PCH}_2\text{CH}_2\text{P}(\text{C}_6\text{F}_5)_2$ with NaBF_4 . Stepwise intramolecular dehydrofluorinative carbon-carbon coupling then occurs when the complex **187** is treated with proton sponge, to give rise to the multi-strapped complex **189** (Scheme 33).



Scheme 33. Preparation of the multi-strapped complex **189**.²³⁰

Tridentate ligands can also give rise to a tethered arene complex, and an example of a η^6 -arene-thioether-thiolate chelating ligand has been reported.^{231,232} The reaction of $[\text{RuCl}_2(\eta^6\text{-C}_6\text{Me}_6)]_2$ with AgPF_6 , acetone and the macrocyclic tridentate sulfur donor 1,4,7-trithiacyclononane affords **190**. Treatment with potassium *tert*-butoxide results in deprotonation of one of the methylene units of the tridentate ligand, inducing carbon-sulfur bond cleavage. A second deprotonation then occurs, giving rise to two vinyl thioether moieties. One of the methyl groups of the hexamethylbenzene is also deprotonated, and reacts with one of the vinyl thioether moieties *via* an intramolecular Michael addition to afford the complex **191** (Scheme 34).

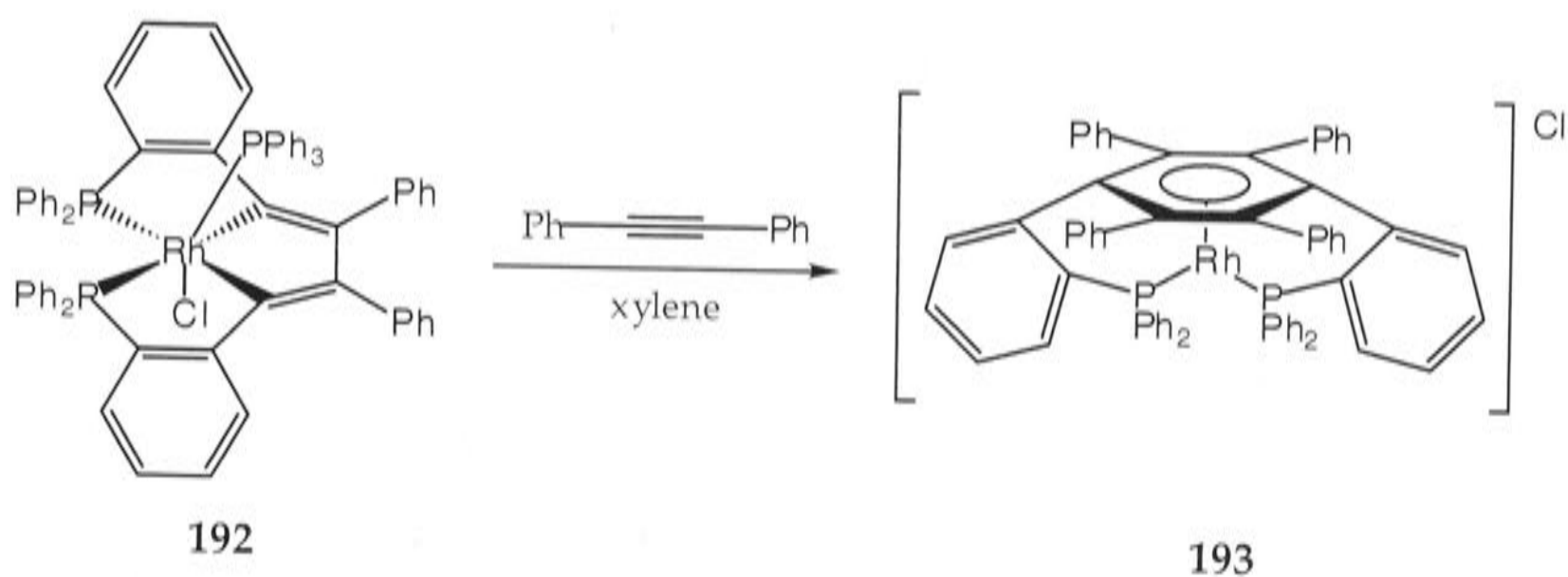


Scheme 34. Formation of the tethered complex **191**.^{231,232}

A similar approach has been applied by Nelson and co-workers to construct arene-phosphine and arene-arsine based tethered complexes,^{233,234} the nature of which will be discussed in Chapter 3 (see Section 3.3.4).

1.2.4 Other Methods (Scheme 16d)

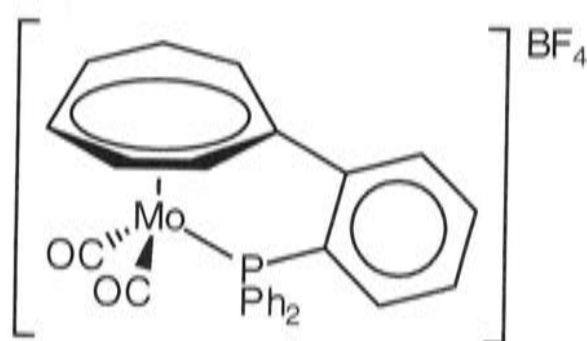
To date, there is one example of a tethered rhodium(I) complex which was prepared by the general approach represented in Scheme 16d. The rhodium complex $[\text{Rh}(\text{P}(\text{C}_6\text{H}_5)_3)_3\text{Cl}]$ was treated with two equivalents of (*o*-phenylethynyl)diphenylphosphane to afford the octahedral chelate rhodiacyclopentadiene complex **192**.²³⁵ This was converted to the bi-strapped species **193** through the reaction with diphenylacetylene in xylene (Scheme 35).



Scheme 35. Preparation of the multi-strapped complex **193**.²³⁵

The initial focus of tethered aromatic compounds was placed on cyclopentadienyl tethered complexes, and has shifted to tethered arene

complexes. More recently attention has been paid to tethered cycloheptatrienyl complexes, such as $[\text{Mo}(\text{CO})_2(\eta^1:\eta^7\text{-Ph}_2\text{P-}o\text{-C}_6\text{H}_4\text{-C}_7\text{H}_6)]$ (**194**).²³⁶⁻²³⁸ Many different metals are capable of forming tethered arene complexes. In the period beginning March 1998, when I started my Ph.D., until the submission date, thirty papers dealing with tethered arene-ruthenium complexes have appeared, most of which deal with arene-phosphine ligands. A cut off date of papers available to me at the time of writing of 27/6/03 has been adopted.

**194**

1.3 Objectives of this Work

There are many examples of monomeric half-sandwich Ru(II) complexes.²³⁹⁻²⁴¹ The objectives of the work in this thesis were to employ arene-phosphine ligands to prepare tethered arene-ruthenium(II) complexes and, if possible, to characterise, by structural, spectroscopic and electrochemical analysis, their one-electron oxidation products. Apart from the potential involvement of arene-ruthenium(III) complexes in C-H bond activation¹¹² (see Scheme 9 and Scheme 10), there is only one reported example of an isolated arene-ruthenium(III) complex, $[\text{Ru}^{\text{III}}\text{Cl}_3(\eta^6\text{-C}_6\text{Me}_6)]$ (**66**) which has been characterised by ESR spectroscopy and electrochemistry.³³ To do this it was necessary to prepare appropriate ligands (Chapter 2), to develop synthetic methods for the strapped arene-ruthenium(II) precursors (Chapter 3), to investigate their stability (Chapter 4) and to investigate the formation and reactivity of the oxidation products (Chapters 5 and 6). An overall discussion of the results is given in Chapter 7.

References

- (1) Bennett, M. A.; Heath, G. A.; Hockless, D. C. R.; Kováčik, I.; Willis, A. C. *J. Am. Chem. Soc.* **1998**, *120*, 932-941.
- (2) Bennett, M. A.; Heath, G. A.; Hockless, D. C. R.; Kováčik, I.; Willis, A. C. *Organometallics* **1998**, *17*, 5867-5873.
- (3) Astruc, D. *Electron Transfer and Radical Processes in Transition-Metal Chemistry*; VCH Publishers, Inc.: New York, 1995, pp. 197-200.
- (4) Collman, J. P.; Hegedus, L. S.; Norton, J. R.; Finke, R. G. *Principles and Applications of Organotransition Metal Chemistry*; University Science Books: Mill Valley, California, 1987, p. 36.
- (5) Pickett, C. J.; Pletcher, D. J. *Chem. Soc., Dalton Trans*, **1975**, 879-886.
- (6) Qi, F.; Yang, S.; Sheng, L.; Ye, W.; Gao, H.; Zhang, Y.; Yu, S. *J. Phys. Chem. A* **1997**, *101*, 7194-7199.
- (7) Horning, S. R.; Vincenti, M.; Cooks, R. G. *J. Am. Chem. Soc.* **1990**, *112*, 119-126.
- (8) Winters, R. E.; Kiser, R. W. *Inorg. Chem.* **1965**, *4*, 157-161.
- (9) Michels, G. D.; Flesch, G. D.; Svec, H. J. *Inorg. Chem.* **1980**, *19*, 479-485.
- (10) Milosavljević, E. B.; Solujić, L.; Affandi, S.; Nelson, J. H. *Organometallics* **1988**, *7*, 1735-1740.
- (11) Chen, Y.-J.; Liao, C.-L.; Ng, C. Y. *J. Chem. Phys.* **1997**, *107*, 4527-4536.
- (12) Breeze, P. A.; Burdett, J. K.; Turner, J. J. *Inorg. Chem.* **1981**, *20*, 3369-3378.
- (13) Lane, K.; Sallans, L.; Squires, R. R. *J. Am. Chem. Soc.* **1984**, *106*, 2719-2721.
- (14) Morton, J. R.; Preston, K. F.; Darensbourg, M. Y. *Mag. Res. Chem.* **1988**, *26*, 787-792.
- (15) Glezen, M. M.; Jonah, C. D. *J. Phys. Chem.* **1991**, *95*, 4736-4741.
- (16) Hop, C. E. C. A.; McMahon, T. B. *J. Am. Chem. Soc.* **1992**, *114*, 1237-1243.

- (17) Lionel, T.; Morton, J. R.; Preston, K. F. *J. Chem. Phys.* **1982**, *76*, 234-239.
- (18) Lionel, T.; Morton, J. R.; Preston, K. F. *J. Magn. Res* **1982**, *49*, 225-232.
- (19) Peake, B. M.; Symons, M. C. R.; Wyatt, J. L. *J. Chem. Soc., Dalton Trans.* **1983**, 1171-1174.
- (20) ref. 4, p. 244.
- (21) Dziegielewski, J. O. *Polyhedron* **1984**, *3*, 1131-1134.
- (22) Krusic, P. J. *J. Am. Chem. Soc.* **1981**, *103*, 2129-2131.
- (23) Baker, P. K.; Connelly, N. G.; Jones, B. M. R.; Maher, J. P.; Somers, K. R. *J. Chem. Soc., Dalton Trans.* **1980**, 579-585.
- (24) Blanch, S. W.; Bond, A. M.; Colton, R. *Inorg. Chem.* **1981**, *20*, 755-761.
- (25) Bagchi, R. N.; Bond, A. M.; Heggie, C. L.; Henderson, T. L.; Mocellin, E.; Seikel, R. A. *Inorg. Chem.* **1983**, *22*, 3007-3012.
- (26) Therien, M. J.; Trogler, W. C. *J. Am. Chem. Soc.* **1986**, *108*, 3697-3702.
- (27) Therien, M. J.; Ni, C.-L.; Anson, F. C.; Osteryoung, J. G.; Trogler, W. C. *J. Am. Chem. Soc.* **1986**, *108*, 4037-4042.
- (28) Morrow, J.; Catheline, D.; Desbois, M.-H.; Manriquez, J.-M.; Ruiz, J.; Astruc, D. *Organometallics* **1987**, *6*, 2605-2607.
- (29) Rogers, W. N.; Page, J. A.; Baird, M. C. *Inorg. Chem.* **1981**, *20*, 3521-3528.
- (30) Wilkinson, G.; Rosenblum, M.; Whiting, M. C.; Woodward, R. B. *J. Am. Chem. Soc.* **1952**, *74*, 2125-2126.
- (31) Fischer, E. O.; Pfab, W. Z. *Naturforsch.* **1952**, *7B*, 377-379.
- (32) Robbins, J. L.; Edelstein, N.; Spencer, B.; Smart, J. C. *J. Am. Chem. Soc.* **1982**, *104*, 1882-1893.
- (33) Koelle, U.; Salzer, A. *J. Organomet. Chem.* **1983**, *243*, C27-C30.
- (34) O'Hare, D.; Green, J. C.; Chadwick, T. P.; Miller, J. S. *Organometallics* **1988**, *7*, 1335-1342.
- (35) Camire, N.; Nafady, A.; Geiger, W. E. *J. Am. Chem. Soc.* **2002**, *124*, 7260-7261.

- (36) Hackett, P.; O'Neill, P. S.; Manning, A. R. *J. Chem. Soc., Dalton Trans.* **1974**, 1625-1627.
- (37) Goh, L.-Y.; D'Aniello, Jr, M. J.; Slater, S.; Muetterties, E. L.; Tavanaiepour, I.; Chang, M. I.; Fredrich, M. F.; Day, V. W. *Inorg. Chem.* **1979**, *18*, 192-197.
- (38) Cooley, N. A.; Watson, K. A.; Fortier, S.; Baird, M. C. *Organometallics* **1986**, *5*, 2563-2565.
- (39) Morton, J. R.; Preston, K. F.; Cooley, N. A.; Baird, M. C.; Krusic, P. J.; McLain, S. J. *J. Chem. Soc., Faraday Trans. 1* **1987**, *83*, 3535-3540.
- (40) Cooley, N. A.; Baird, M. C.; Morton, J. R.; Preston, K. F.; Le Page, Y. *J. Magn. Res* **1988**, *76*, 325-330.
- (41) Hoobler, R. J.; Hutton, M. A.; Dillard, M. M.; Castellani, M. P.; Rheingold, A. L.; Rieger, A. L.; Rieger, P. H.; Richards, T. C.; Geiger, W. E. *Organometallics* **1993**, *12*, 116-123.
- (42) Richeson, D. S.; Hsu, S.-W.; Fredd, N. H.; Van Duyne, G.; Theopold, K. H. *J. Am. Chem. Soc.* **1986**, *108*, 8273-8274.
- (43) Keller, H. J. *Z. Naturforsch.* **1968**, *23B*, 133-136.
- (44) Madach, T.; Vahrenkamp, H. *Z. Naturforsch.* **1978**, *33B*, 1301-1303.
- (45) Jaeger, T. J.; Baird, M. C. *Organometallics* **1988**, *7*, 2074-2076.
- (46) McLain, S. J. *J. Am. Chem. Soc.* **1988**, *110*, 643-644.
- (47) Fortier, S.; Baird, M. C.; Preston, K. F.; Morton, J. R.; Zeigler, T.; Jaeger, T. J.; Watkins, W. C.; MacNeil, J. H.; Watson, K. A.; Hensel, K.; Le Page, Y.; Charland, J.-P.; Williams, A. J. *J. Am. Chem. Soc.* **1991**, *113*, 542-551.
- (48) Richeson, D. S.; Mitchell, J. F.; Theopold, K. H. *Organometallics* **1989**, *8*, 2570-2577.
- (49) Doxsee, K. M.; Grubbs, R. H.; Anson, F. C. *J. Am. Chem. Soc.* **1984**, *106*, 7819-7824.
- (50) Howell, J. O.; Goncalves, J. M.; Amatore, C.; Klasinc, L.; Whightman, R. M.; Kochi, J. K. *J. Am. Chem. Soc.* **1984**, *106*, 3968-3976.
- (51) Stone, N. J.; Sweigart, D. A.; Bond, A. M. *Organometallics* **1986**, *5*, 2553-2555.

- (52) Zoski, C. G.; Sweigart, D. A.; Stone, N. J.; Rieger, P. H.; Mocellin, E.; Mann, T. F.; Mann, D. R.; Gosser, D. K.; Doeff, M. M.; Bond, A. M. *J. Am. Chem. Soc.* **1988**, *110*, 2109-2116.
- (53) Hunter, A. D.; Mozol, V.; Tsai, S. D. *Organometallics* **1992**, *11*, 2251-2262.
- (54) Connelly, N. G.; Demidowicz, Z. *J. Organomet. Chem.* **1974**, *73*, C31-C32.
- (55) Connelly, N. G.; Demidowicz, Z.; Kelly, R. L. *J. Chem. Soc., Dalton Trans.* **1975**, 2335-2340.
- (56) Connelly, N. G.; Geiger, W. E. *Adv. Organomet. Chem.* **1984**, *23*, 1-93.
- (57) Mahmoud, K. A.; Rest, A. J.; Alt, H. G. *J. Organomet. Chem.* **1983**, *246*, C37-C41.
- (58) Kadish, K. M.; Lacombe, D. A.; Anderson, J. E. *Inorg. Chem.* **1986**, *25*, 2246-2250.
- (59) Sun, X. Z.; Nikiforov, S. M.; Dedieu, A.; George, M. W. *Organometallics* **2001**, *20*, 1515-1520.
- (60) Schrock, R. R.; Kolodziej, R. M.; Liu, A. H.; Davis, W. M.; Vale, M. G. *J. Am. Chem. Soc.* **1990**, *112*, 4338-4345.
- (61) Liu, A. H.; Murray, R. C.; Dewan, J. C.; Santarsiero, B. D.; Schrock, R. R. *J. Am. Chem. Soc.* **1987**, *109*, 4282-4291.
- (62) Abrahamson, H. B.; Palazzotto, M. C.; Reichel, C. L.; Wrighton, M. S. *J. Am. Chem. Soc.* **1979**, *101*, 4123-4127.
- (63) Caspar, J. V.; Meyer, T. J. *J. Am. Chem. Soc.* **1980**, *102*, 7794-7795.
- (64) Tyler, D. R.; Schmidt, M. A.; Gray, H. B. *J. Am. Chem. Soc.* **1983**, *105*, 6018-6021.
- (65) Kuksis, I.; Baird, M. C. *Organometallics* **1994**, *13*, 1551-1553.
- (66) Ruiz, J.; Astruc, D. *J. Chem. Soc., Chem. Commun.* **1989**, 815-816.
- (67) Ruiz, J.; Lacoste, M.; Astruc, D. *J. Am. Chem. Soc.* **1990**, *112*, 5471-5483.
- (68) Ruiz, J.; Guerchais, V.; Astruc, D. *J. Chem. Soc., Chem. Commun.* **1989**, 812-813.

- (69) Astruc, D. *Acc. Chem. Res.* **1991**, *24*, 36-42.
- (70) Treichel, P. M.; Molzahn, D. C.; Wagner, K. P. *J. Organomet. Chem.* **1979**, *174*, 191-197.
- (71) Roger, C.; Hamon, P.; Toupet, L.; Rabaâ, H.; Saillard, J.-Y.; Hamon, J.-R.; Lapinte, C. *Organometallics* **1991**, *10*, 1045-1054.
- (72) Darchen, A. *J. Chem. Soc., Chem. Commun.* **1983**, 768-769.
- (73) Nesmeyanov, A. N.; Vol'kenau, N. A.; Bolesova, I. N. *Dokl. Akad. Nauk SSSR* **1963**, *149*, 615-618.
- (74) Nesmeyanov, A. N.; Vol'kenau, N. A.; Bolesova, I. N. *Tetrahedron Lett.* **1963**, 1725-1729.
- (75) Nesmeyanov, A. N.; Vol'kenau, N. A.; Shilovtseva, L. S.; Petrakova, V. A. *J. Organomet. Chem.* **1973**, *61*, 329-335.
- (76) Nesmeyanov, A. N.; Solodovnikov, S. P.; Vol'kenau, N. A.; Kotova, L. S.; Sinitsyna, N. A. *J. Organomet. Chem.* **1978**, *148*, C5-C8.
- (77) Solodovnikov, S. P.; Nesmeyanov, A. N.; Vol'kenau, N. A.; Sinitsyna, N. A.; Kotova, L. S. *J. Organomet. Chem.* **1979**, *182*, 239-243.
- (78) Hamon, J.-R.; Astruc, D.; Michaud, P. *J. Am. Chem. Soc.* **1981**, *103*, 758-766.
- (79) Michaud, P.; Astruc, D.; Ammeter, J. H. *J. Am. Chem. Soc.* **1982**, *104*, 3755-3757.
- (80) Rajasekharan, M. V.; Giezyński, S.; Ammeter, J. H.; Oswald, N.; Michaud, P.; Hamon, J. R.; Astruc, D. *J. Am. Chem. Soc.* **1982**, *104*, 2400-2407.
- (81) Astruc, D.; Hamon, J.-R.; Lacoste, M.; Desbois, M.-H.; Madonik, A.; Román, E. *Organometallic Syntheses*; King, R. B.; Eisch, J. J., Ed., Elsevier Science Publishers B. V.: Amsterdam, 1988; Vol. IV, pp. 172-187.
- (82) Morrow, J. R.; Astruc, D. *Bull. Soc. Chim. Fr.* **1992**, *129*, 319-328.
- (83) ref. 3, p. 203.
- (84) Tilset, M.; Fjeldahl, I.; Hamon, J.-R.; Hamon, P.; Toupet, L.; Saillard, J.-Y.; Costuas, K.; Haynes, A. *J. Am. Chem. Soc.* **2001**, *123*, 9984-10000.

- (85) Lapinte, C.; Catheline, D.; Astruc, D. *Organometallics* **1984**, *3*, 817-819.
- (86) Desbois, M.-H.; Astruc, D. *Angew. Chem. Int. Ed. Engl.* **1989**, *28*, 460-461.
- (87) Brintzinger, H.; Palmer, G.; Sands, R. H. *J. Am. Chem. Soc.* **1966**, *88*, 623.
- (88) Ryan, M. D.; Chambers, J. Q. *Anal. Chem.* **1992**, *64*, 79R-116R.
- (89) Ryan, M. D.; Bowden, E. F.; Chambers, J. Q. *Anal. Chem.* **1994**, *66*, 360R-427R.
- (90) Anderson, J. L.; Bowden, E. F.; Pickup, P. G. *Anal. Chem.* **1996**, *68*, 379R-444R.
- (91) Anderson, J. L.; L. A. Coury, Jr, J.; Leddy, J. *Anal. Chem.* **1998**, *70*, 519R-589R.
- (92) Bard, A. J.; Faulkner, L. R. *Electrochemical Methods: Fundamentals and Applications*; 2nd ed.; John Wiley & Sons, Inc.: New York, 2001, pp. 680-683.
- (93) Speiser, B. *Curr. Org. Chem.* **1999**, *3*, 171-191.
- (94) Robinson, J. *Electrochem.* **1984**, *9*, 101-161.
- (95) Lever, A. B. P. *Inorganic Electronic Spectroscopy*; Elsevier Publishing Company, Inc.: Amsterdam, 1984, p. 334.
- (96) Bennett, M. A.; Byrnes, M. J.; Willis, A. C. *Organometallics* **2003**, *22*, 1018-1028.
- (97) Weil, J. A.; Bolton, J. R.; Wertz, J. E. *Electron Paramagnetic Resonance: Elementary Theory and Practical Applications*; John Wiley & Sons, Inc.: New York, 1994, p. 8.
- (98) Ebsworth, E. A. V.; Rankin, D. W. H.; Craddock, S. *Structural Methods in Inorganic Chemistry*; Blackwell Scientific Publications: Oxford, 1987, pp. 105-106.
- (99) ref. 97, p. 1.
- (100) Pauling, L. C. *The Nature of the Chemical Bond and the Structure of Molecules and Crystals: an Introduction to Modern Structural Chemistry*; 3rd ed.; Cornell University Press: New York, 1960, pp. 393-394.
- (101) ref. 98, p. 111

- (102) Huheey, J. E.; Keiter, E. A.; Keiter, R. L. *Inorganic Chemistry: Principles of Structure and Reactivity*; 4th ed.; HarperCollins College Publishers: New York, 1993, p. A-75.
- (103) Hudson, A.; Kennedy, M. J. *J. Chem. Soc. A* **1969**, 1116-1120.
- (104) Drago, R. S. *Physical Methods in Chemistry*; Saunders College Publishing: Philadelphia, 1977, pp. 317-318.
- (105) Kolaczowski, S. V.; Cardin, J. T.; Budil, D. E. *Appl. Magn. Reson.* **1999**, *16*, 293-298.
- (106) Griffiths, J. H. E.; Owen, J.; Ward, I. M. *Proc. R. Soc. A* **1953**, *219*, 526-542.
- (107) Bernhard, P.; Stebler, A.; Ludi, A. *Inorg. Chem.* **1984**, *23*, 2151-2155.
- (108) DeSimone, R. E. *J. Am. Chem. Soc.* **1973**, *95*, 6238-6244.
- (109) Sakaki, S.; Yanase, Y.; Hagiwara, N.; Takeshita, T.; Naganuma, H.; Ohyoshi, A.; Ohkubo, K. *J. Phys. Chem.* **1982**, *86*, 1038-1043.
- (110) Raynor, J. B.; Jeliaskowa, B. G. *J. Chem. Soc., Dalton Trans.* **1982**, 1185-1189.
- (111) Diversi, P.; Fontani, M.; Fuligni, M.; Laschi, F.; Matteoni, S.; Pinzino, C.; Zanello, P. *J. Organomet. Chem.* **2001**, *626*, 145-156.
- (112) Ceccanti, A.; Diversi, P.; Ingrosso, G.; Laschi, F.; Lucherini, A.; Magagna, S.; Zanello, P. *J. Organomet. Chem.* **1996**, *526*, 251-262.
- (113) ref. 104, 334.
- (114) ref. 98, p. 114.
- (115) ref. 104, p. 467.
- (116) Kaim, W.; Gross, R. *Comments Inorg. Chem.* **1988**, *7*, 269-285.
- (117) Sellmann, D.; Müller, J. *J. Organomet. Chem.* **1985**, *281*, 249-262.
- (118) Gross, R.; Kaim, W. *Angew. Chem. Int. Ed. Engl.* **1985**, *24*, 856-858.
- (119) Gross, R.; Kaim, W. *Inorg. Chem.* **1987**, *26*, 3596-3600.
- (120) Gross, R.; Kaim, W. *J. Chem. Soc., Faraday Trans. 1* **1987**, *83*, 3549-3564.
- (121) Guerchais, V.; Astruc, D. *J. Chem. Soc., Chem. Commun.* **1984**, 881-882.

- (122) Guerchais, V.; Román, E.; Astruc, D. *Organometallics* **1986**, *5*, 2505-2511.
- (123) ref. 104, pp. 435-453.
- (124) Eaton, D. R. *J. Am. Chem. Soc.* **1965**, *87*, 3097-3102.
- (125) Gordon, II, J. G.; O'Connor, M. J.; Holm, R. H. *Inorg. Chim. Acta* **1971**, *5*, 381-391.
- (126) Astruc, D. *Chem. Rev.* **1988**, *88*, 1189-1216.
- (127) Astruc, D. *New. J. Chem.* **1992**, *16*, 305-328.
- (128) Kochi, J. K. *Organometallic Mechanisms and Catalysis*; Academic Press, Inc.: New York, 1978.
- (129) Astruc, D. *Electron Transfer and Radical Processes in Transition-Metal Chemistry*; VCH Publishers, Inc.: New York, 1995.
- (130) ref. 128, pp. 184-212
- (131) ref. 3, pp. 197-281.
- (132) Tyler, D. R. *Progress in Inorganic Chemistry*; Lippard, S. J. Ed., John Wiley & Sons: New York, 1988; Vol. 36, pp. 125-194.
- (133) Aase, T.; Tilset, M.; Parker, V. D. *J. Am. Chem. Soc.* **1990**, *112*, 4974-4975.
- (134) Tilset, M.; Aase, T. *Studies in Surface Science and Catalysis*; Holmen, A.; Jens, K.-J.; Kolboe, S. Ed., Elsevier: Amsterdam, 1991; Vol. 61, pp. 197-200.
- (135) Ryan, O. B.; Smith, K.-T.; Tilset, M. *J. Organomet. Chem.* **1991**, *421*, 315-322.
- (136) ref. 128, p. 4.
- (137) Buet, A.; Darchen, A.; Moinet, C. *J. Chem. Soc., Chem. Commun.* **1979**, 447-448.
- (138) Yamamoto, Y.; Kitahara, H.; Ogawa, R.; Kawaguchi, H.; Tatsumi, K.; Itoh, K. *J. Am. Chem. Soc.* **2000**, *122*, 4310-4319.
- (139) Anderson, S. N.; Fong, C.; Johnson, M. D. *J. Chem. Soc., Chem. Commun.* **1973**, 163.
- (140) Miholová, D.; Vlček, A. A. *J. Organomet. Chem.* **1982**, *240*, 413-419.
- (141) ref. 4, p. 362.

- (142) Magnuson, R. H.; Meirowitz, R.; Zulu, S.; Giering, W. P. *J. Am. Chem. Soc.* **1982**, *104*, 5790-5791.
- (143) Amos, K. L.; Connelly, N. G. *J. Organomet. Chem.* **1980**, *94*, C57-C59.
- (144) Stiddard, M. H. B.; Townsend, R. E. *J. Chem. Soc. A* **1969**, 2355-2357.
- (145) Connelly, N. G.; Kitchen, M. D. *J. Chem. Soc. Dalton Trans.* **1977**, 931-937.
- (146) Bott, S. G.; Brammer, L.; Connelly, N. G.; Green, M.; Orpen, A. G.; Paxton, J. F.; Schaverien, C. J.; Bristow, S.; Norman, N. C. *J. Chem. Soc. Dalton Trans.* **1990**, 1957-1969.
- (147) Barbati, A.; Calderazzo, F.; Poli, R.; Zanazzi, P. F. *J. Chem. Soc., Dalton Trans.* **1986**, 2569-2579.
- (148) Bond, A. M.; Colton, R.; Jackowski, J. J. *Inorg. Chem.* **1979**, *18*, 1977-1985.
- (149) Kölle, U.; Görissen, R.; Hörnig, A. *Inorg. Chim. Acta* **1994**, *218*, 33-39.
- (150) Connelly, N. G.; Geiger, W. G. *Chem. Rev.* **1996**, *96*, 877-910.
- (151) Bauer, D.; Foucault, A. *J. Electroanal. Chem. Interfacial Electrochem.* **1976**, *67*, 33-43.
- (152) Kochi, J. K. *Acc. Chem. Res.* **1992**, *25*, 39-47.
- (153) Reynolds, R.; Line, L. L.; Nelson, R. F. *J. Am. Chem. Soc.* **1974**, *96*, 1087-1092.
- (154) Parsons, R. *Handbook of Electrochemical Constants*; Butterworths Publications Limited: London, 1959, p. 73.
- (155) Eloffson, R. M.; Gadallah, F. F. *J. Org. Chem.* **1969**, *34*, 854-857.
- (156) Song, L.; Trogler, W. C. *Angew. Chem. Int. Ed. Engl.* **1992**, *31*, 770-772.
- (157) Gross-Lannert, R.; Kaim, W.; Olbrich-Deussner, B. *Inorg. Chem.* **1990**, *29*, 5046-5053.
- (158) Sennikov, P. G.; Kuznetsov, V. A.; Egorochkin, A. N.; Sirotkin, N. I.; Nazarova, R. G.; Razuvaev, G. A. *J. Organomet. Chem.* **1980**, *190*, 167-176.

- (159) Bellamy, D.; Brown, N. C.; Connelly, N. G.; Orpen, G. *J. Chem. Soc., Dalton Trans.* **1999**, 3191-3195.
- (160) Eberson, L.; Olofsson, B. *Acta Chem. Scand.* **1991**, 45, 316-326.
- (161) Cowell, G. W.; Ledwith, A.; White, A. C.; Woods, H. J. *J. Chem. Soc. B* **1970**, 227-231.
- (162) Eberson, L.; Larsson, B. *Acta Chem. Scand.* **1987**, B41, 367-378.
- (163) Bell, F. A.; Ledwith, A.; Sherrington, D. C. *J. Chem. Soc. C* **1969**, 2719-2720.
- (164) Eberson, L.; Larsson, B. *Acta Chem. Scand.* **1986**, B40, 210-225.
- (165) Crabtree, R. H. *Chem. Rev.* **1985**, 85, 245-269.
- (166) ref. 92, p. 811
- (167) Jeffrey, J. C.; Rauchfuss, T. B. *Inorg. Chem.* **1979**, 18, 2658-2666.
- (168) Dunbar, K. R. *Comments Inorg. Chem.* **1992**, 13, 313-357.
- (169) Collman, J. P.; Hegedus, L. S.; Norton, J. R.; Finke, R. G. *Principles and Applications of Organotransition Metal Chemistry*; University Science Books: Mill Valley, California, 1987.
- (170) Okuda, J. *Top. Curr. Chem.* **1991**, 160, 97-145.
- (171) Halterman, R. L. *Chem. Rev.* **1992**, 92, 965-994.
- (172) Fryzuk, M. D.; Mao, S. S. H.; Zaworotko, M. J.; MacGillivray, L. R. *J. Am. Chem. Soc.* **1993**, 115, 5336-5337.
- (173) Okuda, J. *Comments Inorg. Chem.* **1994**, 16, 185-205.
- (174) Antelmann, B.; Winterhalter, U.; Huttner, G.; Janssen, B. C.; Vogelgesang, J. *J. Organomet. Chem.* **1997**, 545-546, 407-420.
- (175) Siemeling, U. *Chem. Rev.* **2000**, 100, 1495-1526.
- (176) Butenschön, H. *Chem. Rev.* **2000**, 100, 1527-1564.
- (177) Okuda, J.; Eberle, T.; Spaniol, T. P.; Picquet-Fauré, V. *J. Organomet. Chem.* **1999**, 591, 127-1307.
- (178) Lefort, L.; Crane, T. W.; Farwell, M. D.; Baruch, D. M.; Kaeuper, J. A.; Lachiotte, R. J.; Jones, W. D. *Organometallics* **1998**, 17, 3889-3899.
- (179) Mobley, T. A.; Bergman, R. G. *J. Am. Chem. Soc.* **1998**, 120, 3523-3524.
- (180) Klei, S. R.; Tilley, T. D.; Bergman, R. G. *Organometallics* **2002**, 21, 4905-4911.

- (181) Klei, S. R.; Golden, J. T.; Tilley, T. D.; Bergman, R. G. *J. Am. Chem. Soc.* **2002**, *124*, 2092-2093.
- (182) Bennett, M. A.; Smith, A. K. *J. Chem. Soc., Dalton Trans.* **1974**, 233-241.
- (183) Kasahara, A.; Izumi, T.; Tanaka, K. *Bull. Chem. Soc. Jpn.* **1967**, *40*, 699.
- (184) Abdul-Rahman, S.; Houlton, A.; Roberts, R. M. G.; Silver, J. J. *Organomet. Chem.* **1989**, *359*, 331-341.
- (185) Muetterties, E. L.; Bleeke, J. R.; Wucherer, E. J.; Albright, T. A. *Chem. Rev.* **1982**, *82*, 499-525.
- (186) Nesmeyanov, A. N.; Rybinskaya, M. I.; Krivykh, V. V.; Kaganovich, V. S. *J. Organomet. Chem.* **1975**, *93*, C8-C10.
- (187) Nesmeyanov, A. N.; Krivykh, V. V.; Petrovskii, P. V.; Rybinskaya, M. I. *Dokl. Akad. Nauk SSSR* **1976**, *231*, 110-113.
- (188) Nesmeyanov, A. N.; Krivykh, V. V.; Rybinskaya, M. I. *J. Organomet. Chem.* **1979**, *164*, 159-165.
- (189) Merlic, C. A.; Miller, M. M. *Organometallics* **2001**, *20*, 373-375.
- (190) Hartshorn, C. M.; Steel, P. J. *Angew. Chem., Int. Ed. Engl.* **1996**, *35*, 2655-2657.
- (191) Ohnishi, T.; Miyaki, Y.; Asano, H.; Kurosawa, H. *Chem. Lett.* **1999**, 809-810.
- (192) Miyaki, Y.; Onishi, T.; Kurosawa, H. *Inorg. Chim. Acta* **2000**, *300-302*, 369-377.
- (193) Miyaki, Y.; Onishi, T.; Ogoshi, S.; Kurosawa, H. *J. Organomet. Chem.* **2000**, *616*, 135-139.
- (194) Kitaura, R.; Miyaki, Y.; Onishi, T.; Kurosawa, H. *Inorg. Chim. Acta* **2002**, *334*, 142-148.
- (195) Mahaffy, C. A.; Pauson, P. L. *J. Chem. Res., Synop.* **1979**, 126-127; *J. Chem. Res., Miniprint*, **1979**, 1752-1775.
- (196) Zimmerman, C. L.; Shaner, S. L.; Roth, S. A.; Willeford, B. R. *J. Chem. Res., Synop.* **1980**, 108; *J. Chem. Res., Miniprint*, **1980**, 197-216.
- (197) Muetterties, E. L.; Bleeke, J. R.; Sievert, A. C. *J. Organomet. Chem.* **1979**, *178*, 197-216.

- (198) Thorn, M. G.; Etheridge, Z. C.; Fanwick, P. E.; Rothwell, I. P. *Organometallics* **1998**, *17*, 3636-3638.
- (199) Thorn, M. G.; Etheridge, Z. C.; Fanwick, P. P.; Rothwell, I. P. *J. Organomet. Chem.* **1999**, *591*, 148-162.
- (200) Robertson, G. B.; Whimp, P. O.; Colton, R.; Rix, C. J. *Chem. Commun.* **1971**, 573-574.
- (201) Colton, R.; Rix, C. J. *Aust. J. Chem.* **1971**, *24*, 2461-2469.
- (202) Slawisch, A. *Gmelins Handbuch der Anorganischen Chemie*; Supplement to 8th ed.; Verlag Chemie: Weinheim, 1971; Vol. 3, pp. 181-289.
- (203) Chatt, J.; Watson, H. R. *J. Chem. Soc.* **1961**, 4980-4988.
- (204) Bitterwolf, T. E. *J. Organomet. Chem.* **1983**, *252*, 305-316.
- (205) Bishop, P. T.; Dilworth, J. R.; Zubieta, J. A. *J. Chem. Soc., Chem. Commun.* **1985**, 257-259.
- (206) Bishop, P. T.; Dilworth, J. R.; Nicholson, T.; Zubieta, J. *J. Chem. Soc., Dalton Trans.* **1991**, 385-392.
- (207) Dilworth, J. R.; Zheng, Y.; Lu, S.; Wu, Q. *Inorg. Chim. Acta* **1992**, *194*, 99-103.
- (208) Singewald, E. T.; Mirkin, C. A.; Levy, A. D.; Stern, C. L. *Angew. Chem., Int. Ed. Engl.* **1994**, *33*, 2473-2475.
- (209) Singewald, E. T.; Shi, X.; Mirkin, C. A.; Schofer, S. J.; Stern, C. L. *Organometallics* **1996**, *15*, 3062-3069.
- (210) Singewald, E. T.; Slone, C. S.; Stern, C. L.; Mirkin, C. A.; Yap, G. P. A.; Liable-Sands, L. M.; Rheingold, A. L. *J. Am. Chem. Soc.* **1997**, *119*, 3048-3056.
- (211) Halpern, J.; Riley, D. P.; Chan, A. S. C.; Pluth, J. J. *J. Am. Chem. Soc.* **1977**, *99*, 8055-8057.
- (212) Singewald, E. T.; Mirkin, C. A.; Stern, C. L. *Angew. Chem., Int. Ed. Engl.* **1995**, *34*, 1624-1627.
- (213) Slone, C. S.; Mirkin, C. A.; Yap, G. P. A.; Guzei, I. A.; Rheingold, A. L. *J. Am. Chem. Soc.* **1997**, *119*, 10743-10753.
- (214) Werner, H.; Canepa, G.; Ilg, K.; Wolf, J. *Organometallics* **2000**, *19*, 4756-4766.
- (215) Canepa, G.; Sola, E.; Martín, M.; Lahoz, F. J.; Oro, L. A.; Werner, H. *Organometallics* **2003**, *22*, 2151-2160.

- (216) Çetinkaya, B.; Demir, S.; Özdemir, I.; Toupet, L.; Sémeril, D.; Bruneau, C.; Dixneuf, P. H. *New J. Chem.* **2001**, *25*, 519-521.
- (217) Crocker, M.; Green, M.; Nagle, K. J.; Williams, D. J. *J. Chem. Soc., Dalton Trans.* **1990**, 2571-2580.
- (218) Feiken, N.; Pregosin, P. S.; Trabesinger, G. *Organometallics* **1997**, *16*, 3735-3736.
- (219) den Reijer, C. J.; Rügger, H.; Pregosin, P. S. *Organometallics* **1998**, *17*, 5213-5215.
- (220) den Reijer, C. J.; Wörle, M.; Pregosin, P. S. *Organometallics* **2000**, *19*, 309-316.
- (221) Geldbach, T. J.; Pregosin, P. S. *Eur. J. Inorg. Chem.* **2002**, 1907-1918.
- (222) Geldbach, T. J.; Drago, D.; Pregosin, P. S. *Chem. Commun.* **2000**, 1629-1630.
- (223) Geldbach, T. J.; Pregosin, P. S.; Albinati, A.; Rominger, F. *Organometallics* **2001**, *20*, 1932-1938.
- (224) Geldbach, T. J.; Pregosin, P. S.; Albinati, A. *Organometallics* **2003**, *22*, 1443-1451.
- (225) Faller, J. W.; D'Alliessi, D. G. *Organometallics* **2003**, *22*, 2749-2757.
- (226) Kerschener, J. L.; Torres, E. M.; Fanwick, P. E.; Rothwell, I. P. *Organometallics* **1989**, *8*, 1424-1431.
- (227) Lockwood, M. A.; Fanwick, P. E.; Rothwell, I. P. *Polyhedron* **1995**, *14*, 3363-3366.
- (228) Lockwood, M. A.; Fanwick, P. E.; Rothwell, I. P. *Organometallics* **1997**, *16*, 3574-3575.
- (229) Lentz, M. R.; Fanwick, P. E.; Rothwell, I. P. *Organometallics* **2003**, *22*, 2259-2266.
- (230) Bellabarba, R. M.; Saunders, G. C.; Scott, S. *Inorg. Chem. Commun.* **2002**, *5*, 15-18.
- (231) Bennett, M. A.; Goh, L. Y.; Willis, A. C. *J. Chem. Soc., Chem. Commun.* **1992**, 1180-1182.
- (232) Bennett, M. A.; Goh, L. Y.; Willis, A. C. *J. Am. Chem. Soc.* **1996**, *118*, 4984-4992.

- (233) Ghebreyessus, K. Y.; Nelson, J. H. *Organometallics* **2000**, *19*, 3387-3392.
- (234) Nelson, J. H.; Ghebreyessus, K. Y.; Cook, V. C.; Edwards, A. J.; Wielandt, W.; Wild, S. B.; Willis, A. C. *Organometallics* **2002**, *21*, 1727-1733.
- (235) Winter, W. *Angew. Chem. Int. Ed. Engl.* **1976**, *15*, 241-242.
- (236) Tamm, M.; Bannenberg, T.; Dressel, B.; Fröhlich, R.; Holst, C. *Inorg. Chem.* **2002**, *41*, 47-59.
- (237) Tamm, M.; Baum, K.; Lügger, T.; Fröhlich, R.; Bergander, K. *Eur. J. Inorg. Chem.* **2002**, 918-928.
- (238) Tamm, M.; Dreßel, B.; Lügger, T.; Fröhlich, R.; Grimme, S. *Eur. J. Inorg. Chem.* **2003**, 1088-1098.
- (239) le Bozec, H.; Touchard, D.; Dixneuf, P. H. *Advances in Organometallic Chemistry*; Stone, F. G. A.; West, R. Ed., Academic Press: New York, 1981; Vol. 11, pp. 163-247.
- (240) Seddon, E. A.; Seddon, K. R. *The Chemistry of Ruthenium*; Elsevier Science B. V.: Amsterdam, 1984, pp. 821-832.
- (241) Bennett, M. A. *Comprehensive Organometallic Chemistry II*; Abel, E. W.; Stone, F. G. A.; Wilkinson, G.; Shriver, D. F.; Bruce, M. I. Ed., Pergamon: Oxford, 1995; Vol. 7, pp. 556-591.

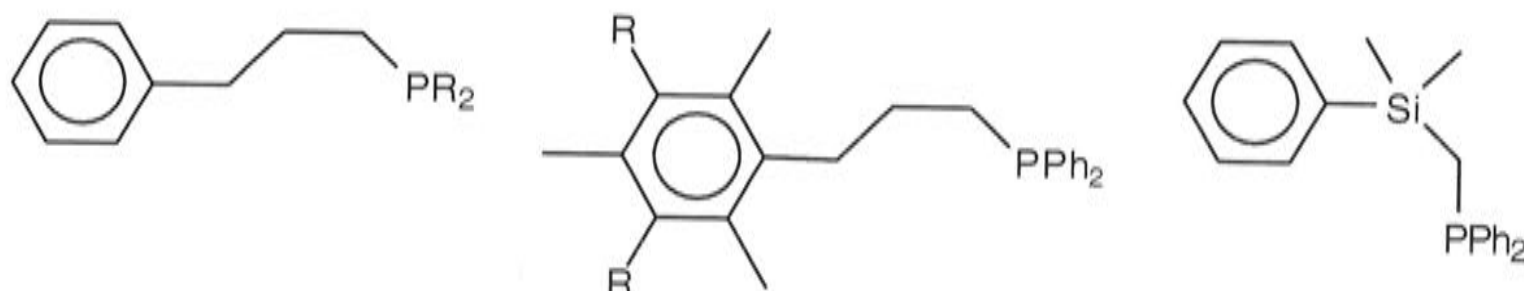
Chapter 2: Preparation of Ligands

The tethered complexes to be prepared can be regarded as containing a special class of bidentate ligands (see Chapter 1, Section 1.2) consisting of an aromatic moiety connected to a donor atom *via* a chain of atoms. In principle it is possible to vary the nature of the donor atom, the degree of substitution of the aromatic moiety, and the type and number of atoms which constitute the chain. In the course of this study, a number of novel tertiary phosphine ligands of this type have been prepared. Phosphorus was chosen as the donor atom as it stabilises metal atoms in a wide range of oxidation states, by a combination of its soft-base character and its ability to act as an electron acceptor, *via* $d(\pi)-\sigma^*$ bonding.¹ As described in Chapter 1, it was envisaged that the chelate effect of such ligands would enhance the stability of normally labile η^6 -arene complexes.

It seems likely that the most stable tethered complexes would contain either two or three methylene units in the strap, since these would give rise to five- and six-membered rings in conventional coordination chemistry. Shortly after my work commenced, a number of reports appeared in the literature concerning tethered arene-ruthenium complexes containing two-atom strapped phosphine ligands (see Chapter 7). For this reason, most effort has been concentrated on three-atom strapped phosphine ligands.

The first group of ligands to be synthesised, $C_6H_5(CH_2)_3PR_2$, was based on the 3-phenylpropyl skeleton, and contains either methyl (Me) **195**, phenyl (Ph) **118**, isopropyl (*i*-Pr) **196**, cyclohexyl (Cy) **197** or *tert*-butyl (*t*-Bu) **198** substituents on the phosphorus atom. The effect of the substituent on the formation and stability of the tethered complexes could therefore be examined. The chelating phosphine ligands **199** and **200** containing methyl substituents on the aromatic moiety were also synthesised. It was thought that these substituents might also influence the formation and stability of the derived tethered complexes. Further, the phosphine **201**,

which contains a dimethylsilyl moiety in the chain, was prepared to provide a comparison between chelating ligands of different chain length. The presence of the dimethylsilyl moiety may also be expected to influence the formation of the respective tethered complex due to the increased steric bulk.



195 R = Me
118 R = Ph
196 R = *i*-Pr
197 R = Cy
198 R = *t*-Bu

199 R = H
200 R = Me

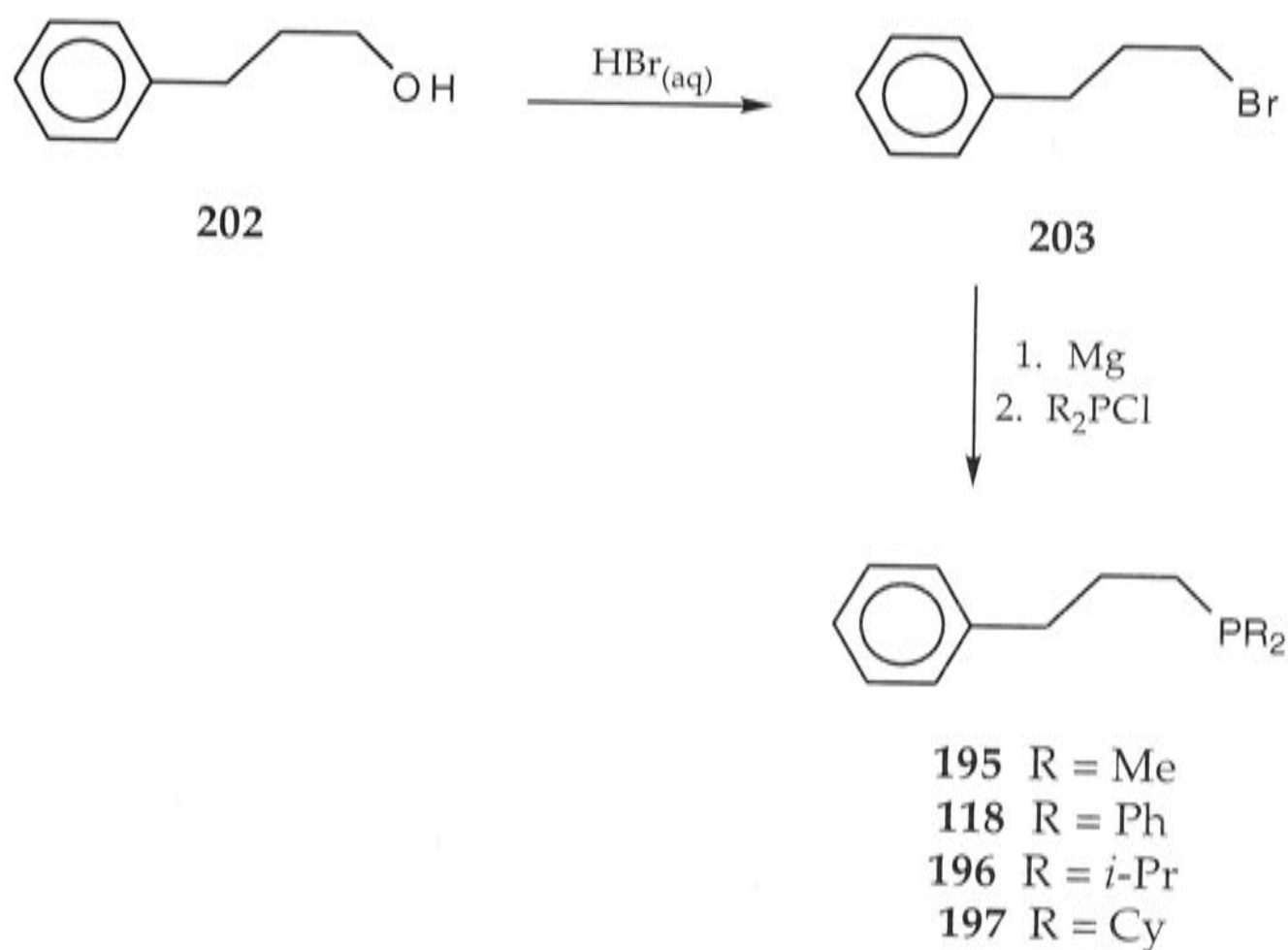
201

2.1 Preparation of Ligands

The ligands **118** and **195-197**, containing the 1-phenylpropane skeleton were synthesised as outlined in Scheme 36, starting from 3-phenylpropan-1-ol (**202**). In the first step, bromination of the alcohol **202** gave 1-bromo-3-phenylpropane (**203**).^{2,3} The corresponding Grignard reagent⁴ was treated with the appropriate chlorophosphine to afford the phosphines **118** and **195-197** in yields ranging between 48-96%, the properties and ³¹P{¹H}-NMR spectroscopic data of which are summarised in Table 4 (entries 1-4), respectively. The phosphines **118** and **197** were crystalline colourless solids that were purified by recrystallisation from ethanol, and **118** was structurally characterised⁵ by X-ray crystallography (see Chapter 3, pp. 171-174 and Appendix, Section A.1) [the structure was determined by Dr A. D. Bond (Cambridge)]. Ligands **195** and **196** were viscous oils that were purified by vacuum distillation.

Unfortunately the procedure outlined in Scheme 36 was not applicable to the synthesis of (3-phenylpropyl)di-*t*-butylphosphine (**198**), only starting materials and decomposition products being isolated. This may be due to

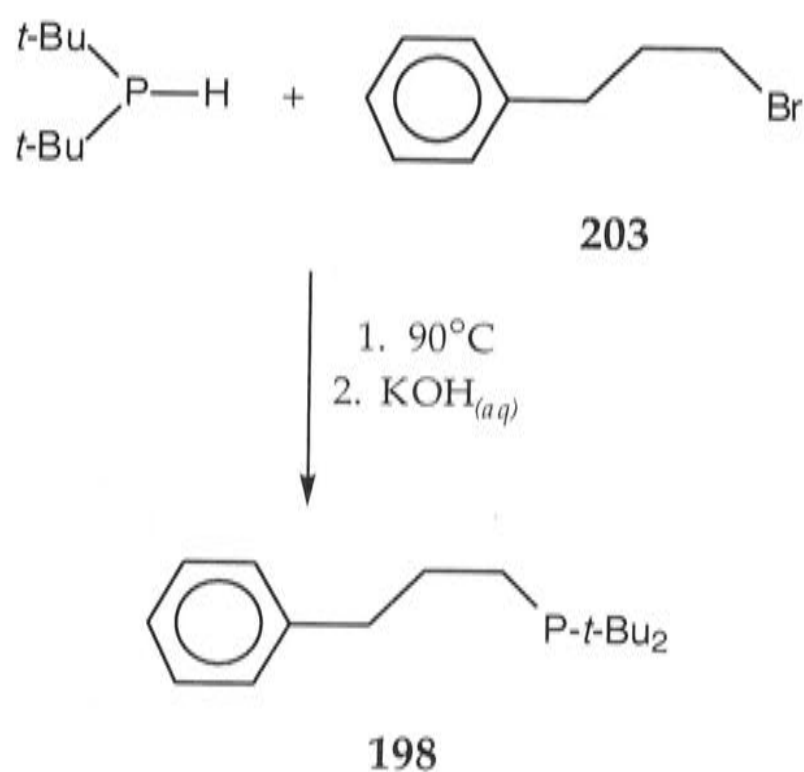
the bulky *t*-butyl groups of the di-*t*-butylchlorophosphine, which inhibited coupling to the (3-phenylpropyl)magnesium bromide. The preparation of phosphine **198** was achieved by a similar method to that employed by other workers for the preparation of $t\text{-Bu}_2\text{P}(\text{CH}_2)_3\text{Ph}$ ⁶ through the route depicted in Scheme 37. The di-*t*-butylphosphine, prepared from di-*t*-butylchlorophosphine,⁷ was heated with the bromide **203** in the absence of a solvent. The phosphonium bromide formed was converted into the desired phosphine **198** through treatment with potassium hydroxide solution, and was purified by vacuum distillation. The properties and $^{31}\text{P}\{^1\text{H}\}$ -NMR spectroscopic data are summarised in Table 4 (entry 5).



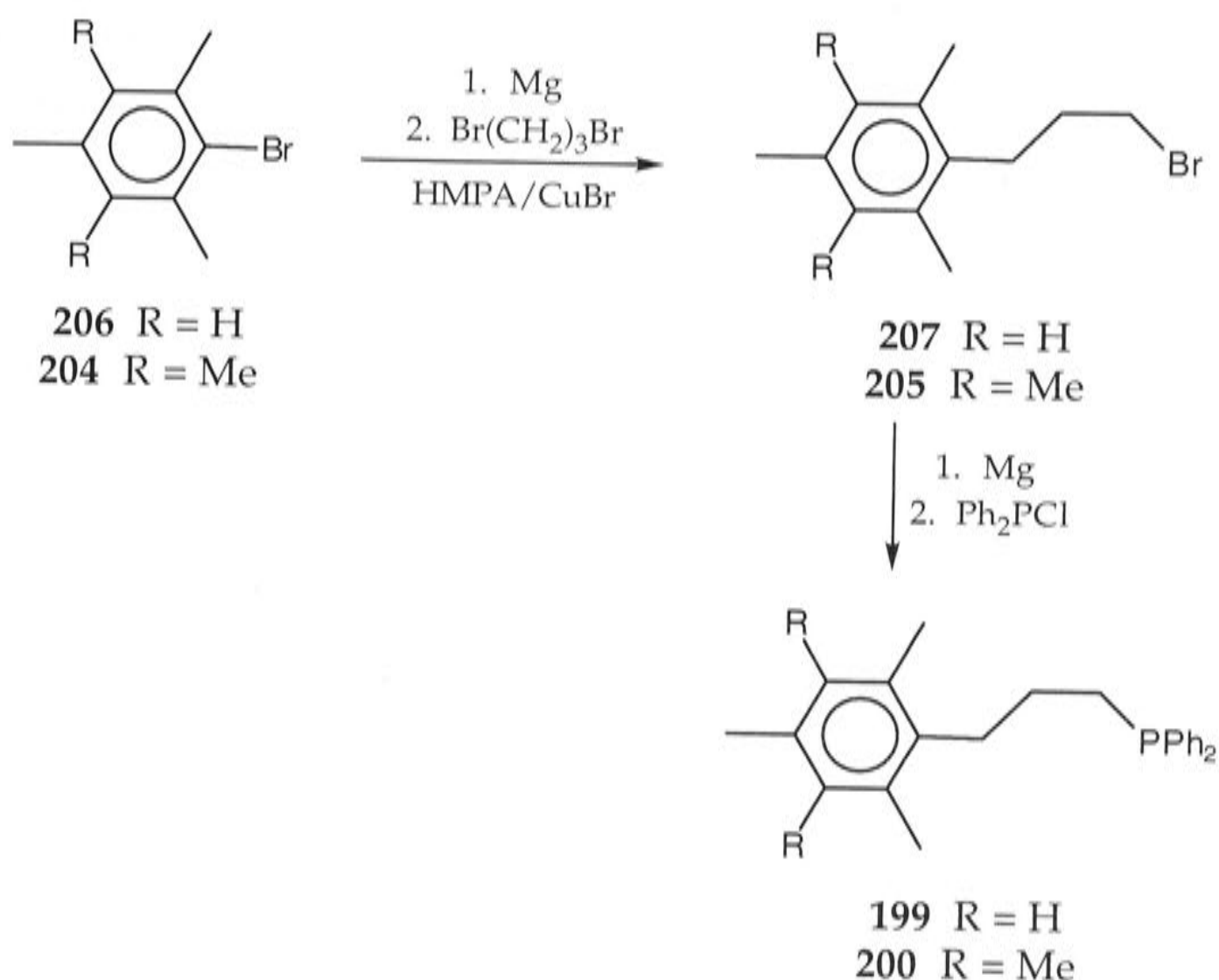
Scheme 36. Preparation of the chelating ligands **118** and **195-197**.

In order to prepare the chelating phosphines **199** and **200** that contain alkyl substituents on the aromatic moiety it was necessary to find a way to connect the methyl-substituted arene moiety to a tether. It was decided to introduce the phosphine donor atom after assembling the carbon skeleton, to eliminate any interference that the presence of the phosphorus atom may have on the coupling. A procedure that employed cuprous bromide to catalyse the coupling of arylmagnesium bromides

with α,ω -dibromoalkanes⁸ was investigated. The Grignard reagent derived from bromopentamethylbenzene (**204**)⁹ was treated with a slight excess of 1,3-dibromopropane in the presence of cuprous bromide and hexamethylphosphoric triamide (HMPA), and gave 1-bromo-3-(pentamethylphenyl)propane (**205**) (Scheme 38). Introduction of the PPh_2 group was achieved by treating the bromide **205** with magnesium and reacting the Grignard reagent formed with chlorodiphenylphosphine to afford 3-(pentamethylphenylpropyl)diphenylphosphine (**200**) as a crystalline colourless solid that was isolated in 49% overall yield. The $^{31}\text{P}\{^1\text{H}\}$ -NMR chemical shift of **200** was very similar to that of the unsubstituted analogue **118** (see Table 4).



Scheme 37. Preparation of the chelating ligand **198**.

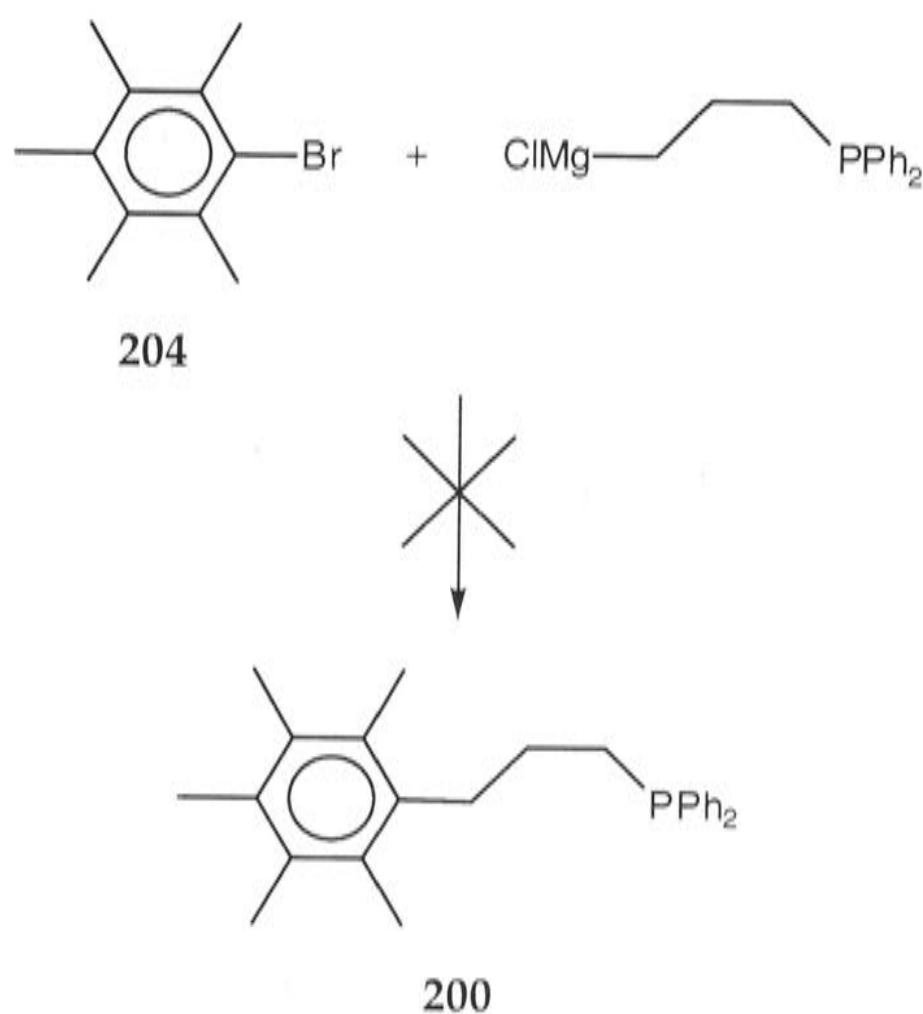


Scheme 38. Preparation of the chelating ligands **199** and **200**.

The mesityl analogue of **200**, namely 3-(mesitylpropyl)diphenylphosphine (**199**), was prepared using a similar procedure from **206** (Scheme 38). The precursor bromide, Br(CH₂)₃-2,4,6-C₆H₂Me₃, (**207**) was isolated in good yield and characterised by ¹H NMR spectroscopy and high resolution mass spectrometry. Previous reports of the preparation of **207** by alternative routes¹⁰⁻¹³ included no spectroscopic data and minimal physical data, thus making comparison of the properties of the compound obtained in the course of this work with those in the literature difficult. The ligand **199** was prepared by treating the Grignard reagent of the bromide **207** with chlorodiphenylphosphine. The crude product was purified using column chromatography to afford the desired phosphine **199** as a crystalline colourless solid in 57% overall yield; its ³¹P{¹H}-NMR resonance was identical to that of the phosphine **200**, and similar to that of the phosphine **118** (see Table 4). The properties **199** and **200** are summarised in Table 4 (entries 6 and 7).

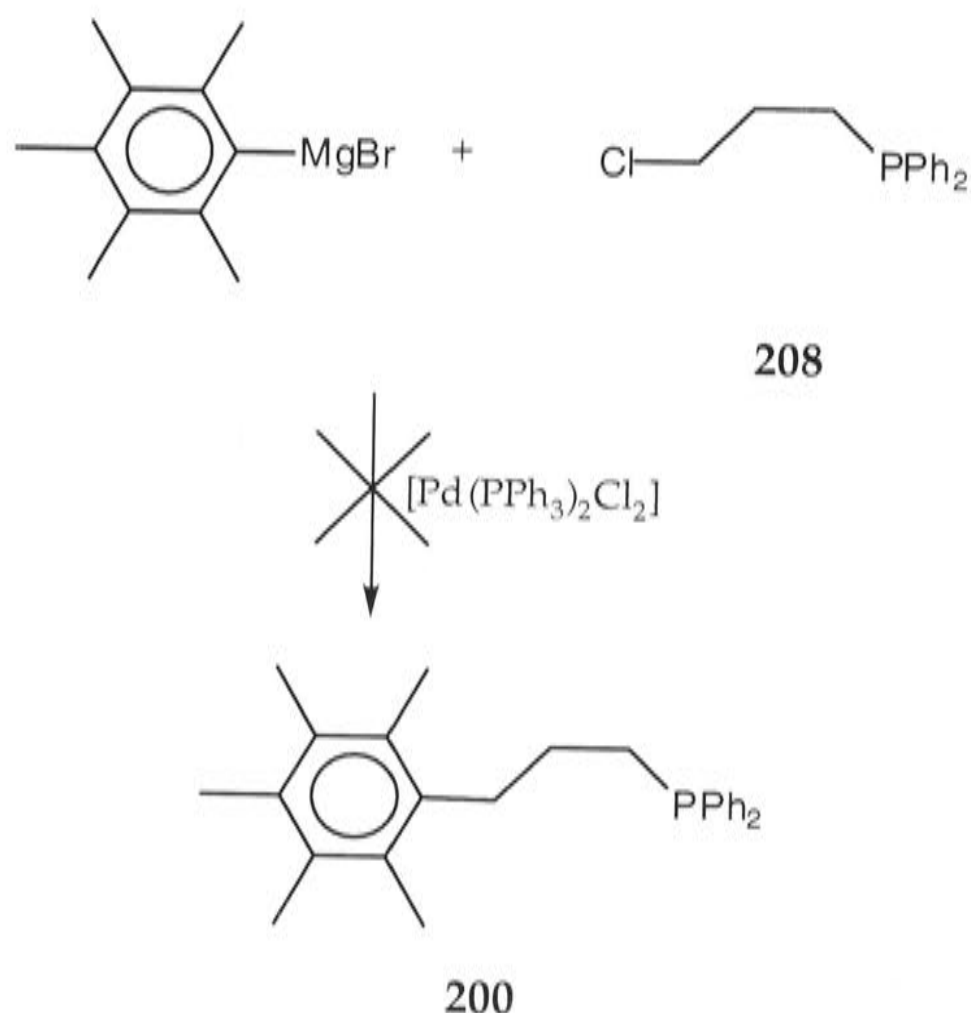
Initial attempts to prepare **200** involved the reaction of bromopentamethylbenzene (**204**)¹⁴ with the Grignard reagent¹⁵ derived from the reaction of the 1-chloro-3-propyldiphenylphosphine (**208**)¹⁶ with magnesium (Scheme 39). No product was obtained and only starting materials and decomposition products were isolated.

The coupling of aryl Grignard reagents to halides has been reported to be catalysed by metal-phosphine complexes of the type $[MCl_2L_2]$ ($M = Ni$,^{17,18} Pd ¹⁹; $L =$ monodentate phosphine, $L_2 =$ bidentate phosphine). Hence preparation of the phosphine **200** was attempted by treatment of the Grignard reagent C_6Me_5MgBr ⁹ with the phosphine **208** in the presence of the palladium catalyst $[PdCl_2(PPh_3)_2]$,²⁰ but this was unsuccessful, and only starting materials and decomposition products were isolated (Scheme 40). Possibly, the palladium(II) species reacts with some of compound **208**, causing a change in the coordination sphere of the palladium, thus rendering the catalyst inactive.



Scheme 39. Reaction of **203** with (3-propyldiphenylphosphine)magnesium chloride does not yield the ligand **200**.

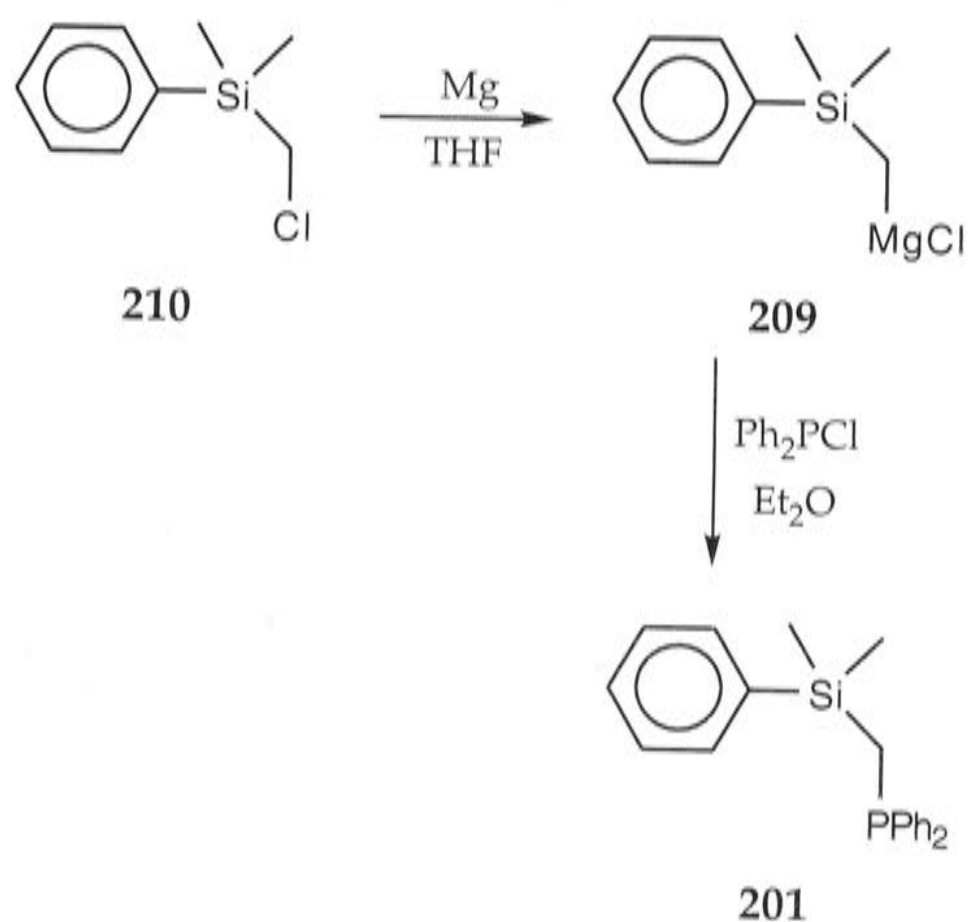
It appears that it is necessary in these syntheses to connect the aryl moiety to the chain before introducing the donor atom.



Scheme 40. Reaction of the pentamethylmagnesiumbromide with **208** does not yield the ligand **200**.

A ligand containing a dimethylsilyl moiety, in place of CH_2 , in the connecting unit adjacent to the arene, was also prepared. The preparation of [(phenyldimethylsilyl)methyl]magnesium chloride, $\text{C}_6\text{H}_5\text{SiMe}_2\text{CH}_2\text{MgCl}$, (**209**) through the reaction of (chloromethyl)dimethylphenylsilane, $\text{C}_6\text{H}_5\text{SiMe}_2\text{CH}_2\text{Cl}$, (**210**) and magnesium has been reported.²¹⁻²³ This reaction was carried out in ether²¹⁻²³ and it was stated that THF cannot be used.²³ Nevertheless, in contrast to the literature, the preparation of **74** was achieved in THF, and gave the product **201** as a crystalline colourless solid in 44% yield upon treatment with chlorodiphenylphosphine (Scheme 41). The low yield of **201** is attributed to the formation of a major by-product, methyldiphenylphosphine (**211**), which formed as a result of Si- CH_2 bond cleavage. It was removed from the product **201** by vacuum sublimation.

Compound **201** was purified by recrystallisation from ethanol and the properties as well as the $^{31}\text{P}\{^1\text{H}\}$ -NMR spectroscopic data are summarised in Table 4 (entry 8). The synthesis of closely related compounds, (dimethylsilyl)methyldiphenylphosphine, $\text{Ph}_2\text{PCH}_2\text{SiMe}_2\text{H}$, (**212**) (b.p. $105^\circ\text{C}/\sim 10^{-2}$ mm) and (methylphenylsilyl)methyldiphenylphosphine, $\text{Ph}_2\text{PCH}_2\text{SiPhMeH}$, ($150\text{-}155^\circ\text{C}/\sim 10^{-2}$ mm) has been reported.²⁴ They also show a singlet in their $^{31}\text{P}\{^1\text{H}\}$ -NMR spectra at $\delta -21.6$, similar to that of **201** ($\delta -22.3$). Compound **201** also showed a doublet in the $^{29}\text{Si}\{^1\text{H}\}$ -NMR spectrum at $\delta -3.90$ with a ^{29}Si - ^{31}P coupling of 16 Hz. Although the use of an alternative solvent for the preparation of the Grignard reagent **209**, such as ether, was not investigated, it seems unlikely that this would have prevented the Si-C bond cleavage, which presumably occurred during the work-up with aqueous ammonium chloride solution.



Scheme 41. Preparation of the chelating ligand **201**.

Cleavage of the Si- CH_2 bond in **201** was observed when a sample was dissolved in d_2 -dichloromethane, presumably induced by traces of water or hydrochloric acid. The amount of methyldiphenylphosphine (**211**) present increased with time, as shown by ^1H and $^{31}\text{P}\{^1\text{H}\}$ -NMR

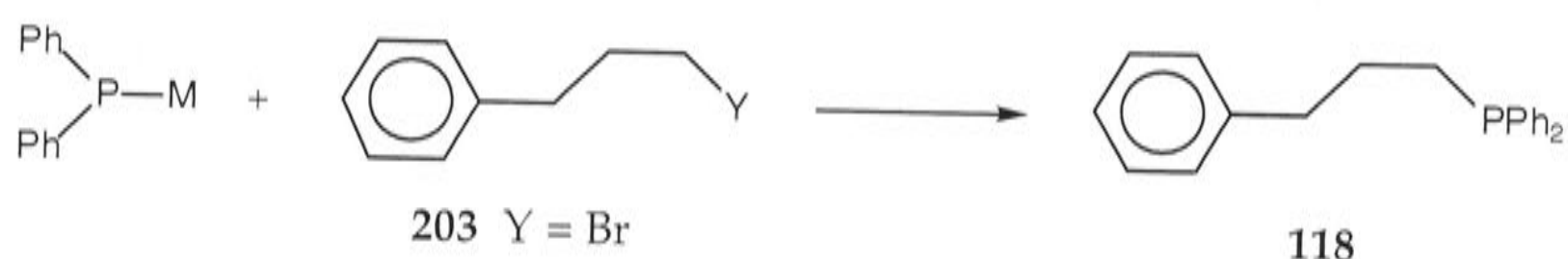
spectroscopy. The cleavage of a Si-CH₂ bond when the methylene unit is adjacent to a phosphorus atom has been reported previously.²⁵ The cleavage of Ph₂PCH₂SiMe₂H (**212**) was reported to be facilitated by protic reagents such as water, methanol and hydrochloric acid.²⁴ Addition of sodium hydroxide solution to an NMR sample of **201** in *d*₂-dichloromethane did not result in cleavage of the Si-CH₂ bond. However, addition of one drop of concentrated hydrochloric acid caused instant decomposition. The ¹H, ²⁹Si{¹H} and ³¹P{¹H}-NMR spectra of the resulting solution did not show any resonances corresponding to either starting material or Ph₂PMe (**211**). A new resonance at δ 3.8 was observed in the ³¹P{¹H}-NMR spectrum, but the species responsible was not characterised. It is clearly neither methyldiphenylphosphine (**211**) (δ -26.5) nor methyldiphenylphosphine oxide (δ 32.5). The ¹H NMR spectra also did not show any signals corresponding to the presence of these two compounds. The cleavage of the Si-CH₂ bond in **201** was confirmed by ²⁹Si{¹H}-NMR spectroscopy, which showed a new singlet at δ -3.07, indicating that the coupling with phosphorus was no longer present. The exact composition of either the silicon or phosphorus-containing fragments has not been determined.

During the course of this work, the syntheses of phosphines **118**, **196** and **197** were reported by other groups, as discussed below. The reported spectroscopic (³¹P{¹H}-NMR chemical shifts) and physical data, summarised in Table 4 are in good agreement with those obtained in the course of this work.

The phosphine **118** has been prepared through the reaction of triphenylphosphine with an alkali metal to generate the diphenylphosphide anion, MPPh₂ (M = K, Li), (Scheme 42) which was subsequently treated with the appropriate halide (Scheme 43).²⁶⁻²⁸

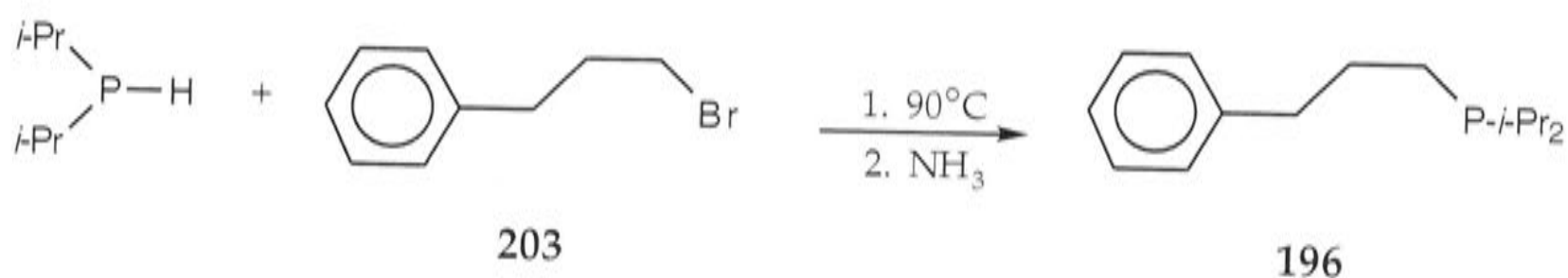


Scheme 42. Preparation of the diphenylphosphide anion MPPh_2 ($\text{M} = \text{K}$, Li).



Scheme 43. Preparation of the chelating ligand **118** ($\text{M} = \text{K}$, $\text{Y} = \text{Cl}$ ^{26,27} or $\text{M} = \text{Li}$, $\text{Y} = \text{Br}$ (**203**)²⁸).

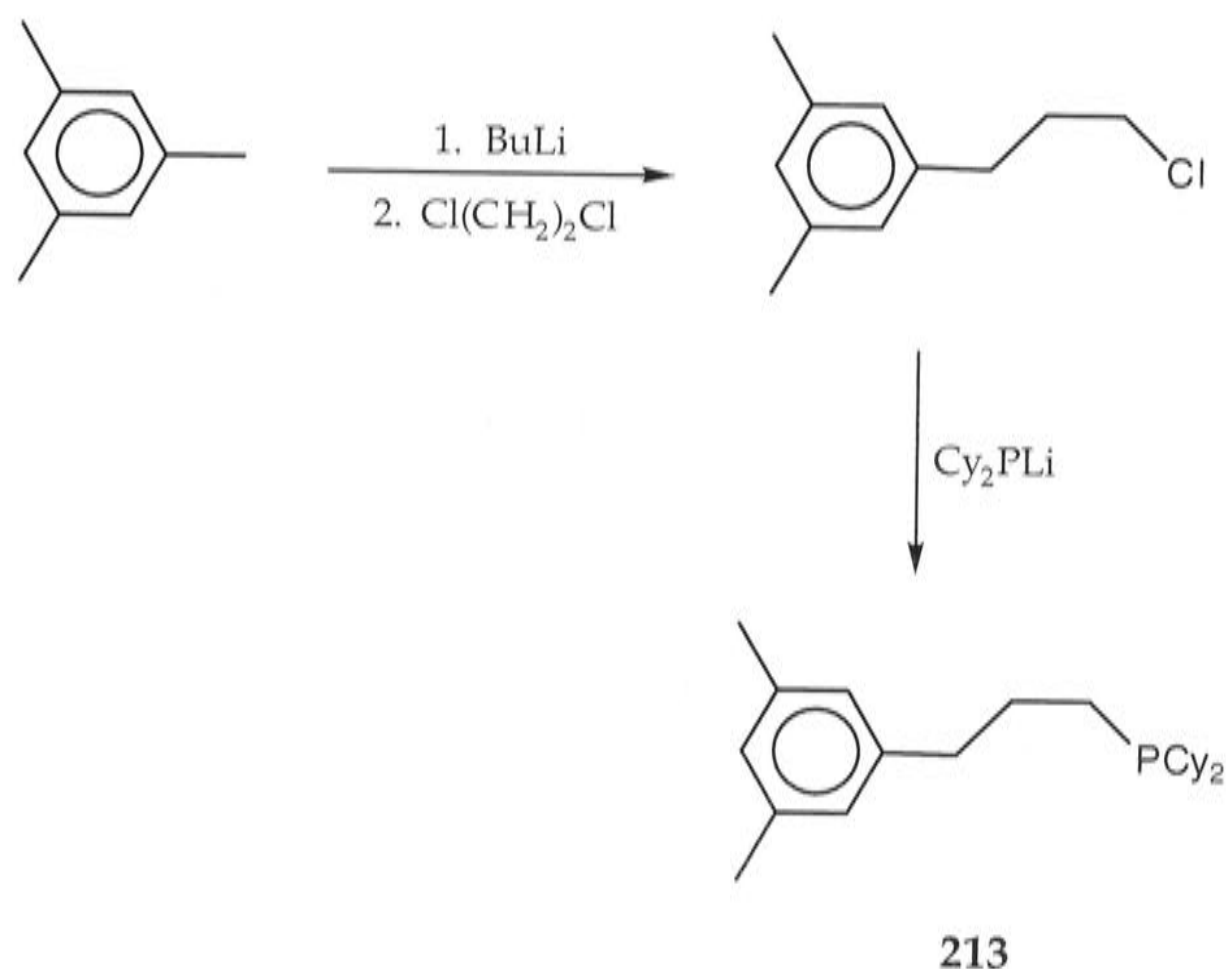
Compound **196** was prepared by heating 1-bromo-3-phenylpropane (**203**) with diisopropylphosphine in the absence of a solvent. The resulting phosphonium bromide was converted to **196** through treatment with a concentrated aqueous solution of ammonia (Scheme 44).⁶



Scheme 44. Preparation of the phosphine **196**.⁶

Closely related ligands containing bulky cyclohexyl substituents on the phosphorus atom have been prepared.²⁹⁻³² The phosphine **197** has been prepared independently by the route used in this work, as depicted in Scheme 36.³¹ An alternative preparative procedure for a similar phosphine, namely 3-(1,5-dimethylphenylpropyl)dicyclohexylphosphine, $\text{Cy}_2\text{P}(\text{CH}_2)_3\text{-3,5-C}_6\text{H}_3\text{Me}_2$, (**213**) was employed (Scheme 45).³² The compound 3-(1,5-dimethylphenylpropyl)chloride, $\text{Cl}(\text{CH}_2)_3\text{-3,5-C}_6\text{H}_3\text{Me}_2$, was formed through the reaction of 1,2-dichloroethane with the carbanion derived from the treatment of 1,3,5-trimethylbenzene with *n*-butyllithium. Subsequent treatment with the dicyclohexylphosphide

anion, obtained from the reaction of dicyclohexylphosphine with *n*-butyllithium, gave the **213** in 24% overall yield. A similar approach to the synthesis of either **199** or **200** was not investigated in this work. Dicyclohexyl(2-(4-phenyl)butyl)phosphine, $\text{Cy}_2\text{PCHMe}(\text{CH}_2)_2\text{C}_6\text{H}_5$, was also prepared from the reaction of the anion LiPCy_2 with 2-bromo-4-phenylbutane.³²



Scheme 45. Preparation of the phosphine **213**.³²

2.2 Summary

In this Chapter, the preparation of a group of potentially chelating tertiary phosphines has been described, which differ in the nature of the substituent on the phosphorus atom, the degree of substitution of the aromatic moiety, as well as the length and type of atoms that constitute the chain. The following Chapter will discuss the complexing behaviour of these ligands towards ruthenium.

Table 4. Properties of the chelating ligands **118** and **195-201**. $^{31}\text{P}\{^1\text{H}\}$ -NMR chemical shifts recorded in d_2 -dichloromethane unless otherwise stated.

Entry Number	Compound	Melting/Boiling Point ($^{\circ}\text{C}$) ^c	Overall Yield (%)	Reported Yield	Observed $^{31}\text{P}\{^1\text{H}\}$ -NMR shift (ppm)	Reported $^{31}\text{P}\{^1\text{H}\}$ -NMR shift (ppm)
1	195 ^a	86-88/1.5 mm	48	N/A	-51.6	N/A
2	118 ^b	56-58	76	76 ^d , 80 ^e	-16.2	-15.2 (in CDCl_3) ^d - 16.7 (in CDCl_3) ^e
3	196 ^a	90-92/0.2 mm	96	78 ^f	3.6	2.1 (in C_6D_6) ^f
4	197 ^b	not determined	64	87 ^g	-4.6	-4.7 ^g
5	198 ^a	107-109/0.1 mm	53	N/A	28.4	N/A
6	199 ^b	74-76	57	N/A	-16.5	N/A
7	200 ^b	90-92	49	N/A	-16.5	N/A
8	201 ^b	62-64	44	N/A	-22.3	N/A

^aColourless liquid; ^bcolourless solid; ^cno melting/boiling points were reported;^{6,26,28,31} ^dreported in references(26,27); ^ereported in reference(28); ^freported in reference(6); ^greported in reference(31).

N/A = Not Applicable

References

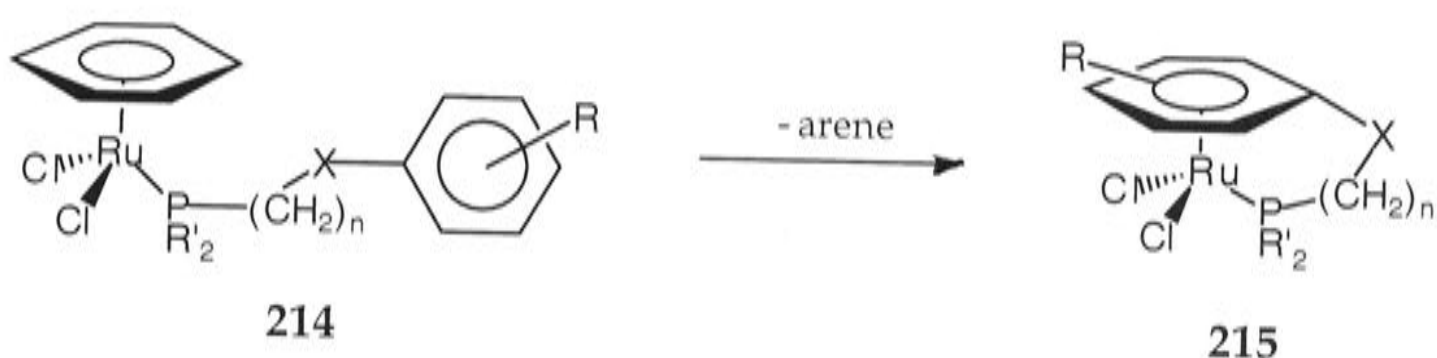
- (1) Cotton, F. A.; Wilkinson, G.; Murillo, C. A.; Bochmann, M. *Advanced Inorganic Chemistry*; 6th ed.; John Wiley & Sons, Inc.: New York, 1999, p. 642.
- (2) Norris, J. F.; Watt, M.; Thomas, R. *J. Am. Chem. Soc.* **1916**, *38*, 1071-1079.
- (3) Aspinall, G. O.; Baker, W. *J. Chem. Soc.* **1950**, 743-753.
- (4) Rupe, H.; Proske, H. *Chem. Ber.* **1910**, *43*, 1231-1243.
- (5) Bond, A. D.; Brown, D. B.; Harper, J. R.; Johnson, B. F. G. *Acta. Cryst.* **2001**, *E57*, o615-o616.
- (6) Werner, H.; Canepa, G.; Ilg, K.; Wolf, J. *Organometallics* **2000**, *19*, 4756-4766.
- (7) Timmer, K.; Thewissen, D. H. M. W.; Marsman, J. W. *Recl. Trav. Chim. Pays-Bas* **1988**, *107*, 248-255.
- (8) Nishimura, J.; Yamada, N.; Horiuchi, Y.; Ueda, E.; Ohbayashi, A.; Oku, A. *Bull. Chem. Soc. Jpn.* **1986**, *59*, 2035-2037.
- (9) Rathore, R.; Weigand, U.; Kochi, J. K. *J. Org. Chem.* **1996**, *61*, 5246-5256.
- (10) Ramart-Lucas, Mme.; Hoch, M. *J. Bull. Chim. Soc. Fr.* **1932**, *51*, 824-838.
- (11) Sordes, M. J.; Delépine, M. *C. R. Hebd Seances Acad. Sci.* **1932**, *195*, 247-249.
- (12) Marei, A.; Sammour, A.; Kassem, T. *J. Chem. U.A.R.* **1969**, *12*, 323-333.
- (13) Abramovitch, R. A.; Kress, A. O.; McManus, S. P.; Smith, M. *J. Org. Chem.* **1984**, *49*, 3114-3121.
- (14) Smith, L. I.; Nichols, J. *J. Org. Chem.* **1941**, *6*, 489-506.
- (15) Grim, S. O.; Barth, R. C. *J. Organomet. Chem.* **1975**, *94*, 327-332.
- (16) Uriarte, R.; Mazanec, T. J.; Tau, K. D.; Meek, D. W. *Inorg. Chem.* **1980**, *19*, 79-85.

- (17) Tamao, K.; Kiso, Y.; Sumitani, K.; Kumada, M. *J. Am. Chem. Soc.* **1972**, *94*, 9268-9269.
- (18) Tamao, K.; Sumitani, K.; Kiso, Y.; Zembayashi, M.; Fujioka, A.; Kodama, S.; Nakajima, I.; Minato, A.; Kumada, M. *Bull. Chem. Soc. Jpn.* **1976**, *49*, 1958-1969.
- (19) Kumada, M. *Pure Appl. Chem.* **1980**, *52*, 669-679.
- (20) Hartley, F. R. *Organometal. Chem. Rev. A* **1970**, *6*, 119-137.
- (21) Collier, M. R.; Lappert, M. F.; Pearce, R. *J. Chem. Soc., Dalton Trans.* **1973**, 445-451.
- (22) Shimizu, N.; Watanabe, S.; Hayakawa, F.; Yasuhara, S.; Tsauno, Y.; Inazu, T. *Bull. Chem. Soc. Jpn.* **1994**, *67*, 500-504.
- (23) Organ, M. G.; Murray, A. P. *J. Org. Chem.* **1997**, *62*, 1523-1526.
- (24) Holmes-Smith, R. D.; Osei, R. D.; Stobart, S. R. *J. Chem. Soc., Perkin Trans. I* **1983**, 861-866.
- (25) Brost, R. D.; Bruce, G. C.; Stobart, S. R. *J. Chem. Soc., Chem. Commun.* **1986**, 1580-1581.
- (26) Singewald, E. T.; Mirkin, C. A.; Levy, A. D.; Stern, C. L. *Angew. Chem., Int. Ed. Engl.* **1994**, *33*, 2473-2475.
- (27) Singewald, E. T.; Shi, X.; Mirkin, C. A.; Schofer, S. J.; Stern, C. L. *Organometallics* **1996**, *15*, 3062-3069.
- (28) Smith, P. D.; Wright, A. H. *J. Organomet. Chem.* **1998**, *559*, 141-147.
- (29) Abele, A.; Wursche, R.; Klinga, M.; Rieger, B. *J. Mol. Cat. A* **2000**, *160*, 23-33.
- (30) Simal, F.; Jan, D.; Demonceau, A.; Noels, A. F. *Tetrahedron Lett.* **1999**, *40*, 1653-1656.
- (31) Fürstner, A.; Liebl, M.; Lehmann, C. W.; Picquet, M.; Kunz, R.; Bruneau, C.; Touchard, D.; Dixneuf, P. H. *Chem. Eur. J.* **2000**, *6*, 1847-1857.
- (32) Jan, D.; Delaude, L.; Simal, F.; Demonceau, A.; Noels, A. F. *J. Organomet. Chem.* **2000**, *606*, 55-64.

Chapter 3: Preparation of Tethered Arene Complexes and their Precursors

3.1 Strategies to be Adopted

For the purpose of this work, I selected the two general approaches outlined in Schemes 16b and 16c (see Chapter 1). The first involves coordination of the phosphine to the Ru(II) centre to form the precursor non-tethered adducts of the type **214**. It was envisaged that the η^6 -arene might be displaced, allowing the free arene at the end of the chain to coordinate to the Ru(II), forming tethered complexes of the general form **215** (Scheme 46).



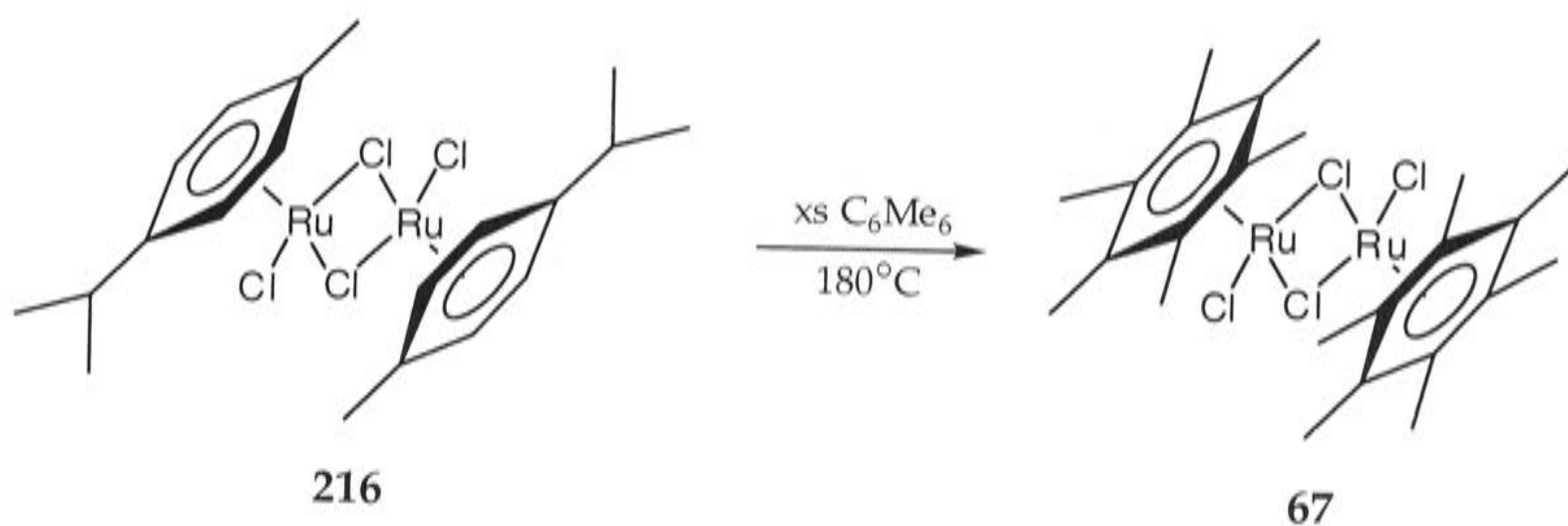
Scheme 46. One general approach to the preparation of tethered arene-ruthenium complexes.

The second approach involves the intramolecular construction of the tether, and will be discussed in Section 3.3.

As mentioned in Chapter 1 (Section 1.2.2), intermolecular exchange of a free arene with an η^6 -arene of various metal complexes is well established.¹⁻³ This tends to imply that the intramolecular method outlined in Scheme 46 might be successful.

It was necessary to decide which arene would be displaced most easily. The stability series for the arene ligand in a specific set of η^6 -arene metal complexes usually follows the order: $C_6Me_6 > C_6H_3Me_3 > C_6H_4Me_2 > C_6H_5Me > C_6H_6$, that is, η^6 -benzene is more readily displaced than η^6 -hexamethylbenzene.² This behaviour is illustrated in the preparation of $[RuCl_2(\eta^6-C_6Me_6)]_2$ (**67**), achieved by displacement of *p*-cymene from

$[\text{RuCl}_2(\eta^6\text{-}1,4\text{-MeC}_6\text{H}_4\text{CHMe}_2)]_2$ (**216**) by fusion with an excess of hexamethylbenzene (Scheme 47).⁴ This methodology has been extended to other permethylated arenes, such as mesitylene and 1,2,3,4-tetramethylbenzene; the respective products were prepared by heating **216** with an excess of the arene at reflux.⁵



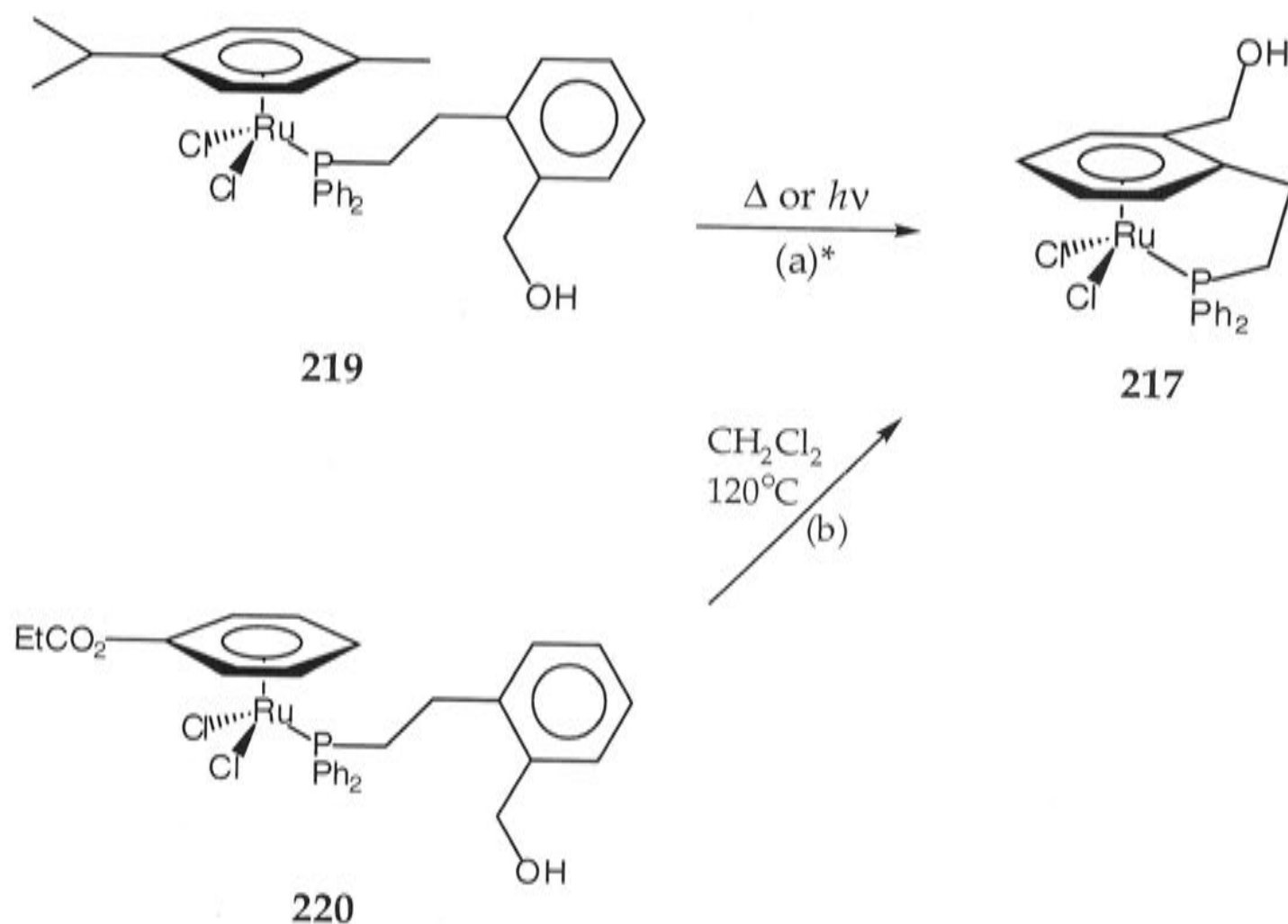
Scheme 47. Preparation of the di- μ -chloro dimer **67**.⁴

3.2 Strategy One; Initial Coordination of Donor Atom (Scheme 46)

During preliminary investigations, publications by Ward and co-workers and by Smith and Wright on the preparation of tethered arene-ruthenium(II) complexes appeared.^{6,7}

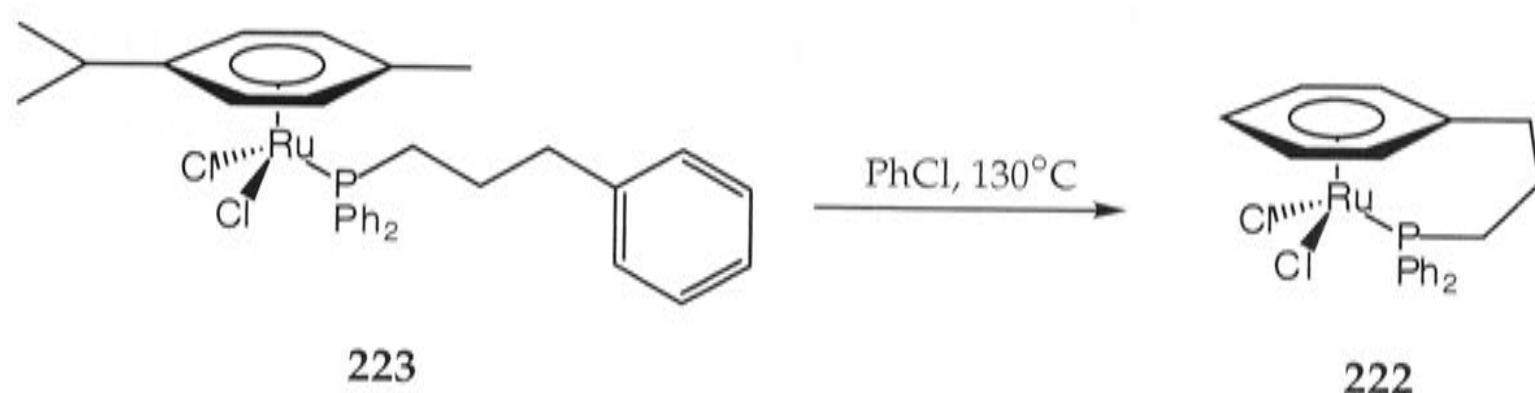
Ward *et al.*⁶ reported the synthesis of $[\text{RuCl}_2(\eta^1:\eta^6\text{-Ph}_2\text{P}(\text{CH}_2)_2\text{-}2\text{-C}_6\text{H}_4\text{CH}_2\text{OH})]$ (**217**), containing a substituted η^6 -coordinated arene. The phosphino-alcohol, *o*- $\text{C}_6\text{H}_4(\text{CH}_2\text{OH})(\text{CH}_2\text{CH}_2\text{PPh}_2)$ (**218**) reacted with the *p*-cymene ruthenium dimer **216** to afford the complex $[\text{RuCl}_2(\eta^6\text{-}1,4\text{-MeC}_6\text{H}_4\text{CHMe}_2)(\eta^1\text{-Ph}_2\text{P}(\text{CH}_2)_2\text{-C}_6\text{H}_4\text{-}1,2\text{-CH}_2\text{OH})]$ (**219**). Though the *p*-cymene could be displaced by either thermal or photochemical methods, **217** was formed in less than 5% yield (Scheme 48a). This was greatly improved by starting from the ethyl benzoate complex $[\text{RuCl}_2(\eta^6\text{-C}_6\text{H}_5\text{CO}_2\text{Et})(\eta^1\text{-Ph}_2\text{P}(\text{CH}_2)_2\text{-}1,2\text{-C}_6\text{H}_5\text{CH}_2\text{OH})]$ (**220**) (Scheme 48b), prepared from the electron-poor arene-ruthenium dimer $[\text{RuCl}_2(\eta^6\text{-C}_6\text{H}_5\text{CO}_2\text{Et})]_2$ (**221**). The yield of **217** was increased to 97% using

the *in situ* preparation, that is, the direct reaction of the ligand **218** and the dimer **221**. Ward *et al.*⁶ were the first to employ a η^6 -arene containing an electron withdrawing substituent, such as an ester, as a good leaving group in ruthenium(II) chemistry.



Scheme 48. Two synthetic routes to the tethered complex **217**.⁶ *Solvent was not specified.⁶

Smith and Wright reported that $[\text{RuCl}_2(\eta^1:\eta^6\text{-Ph}_2\text{P}(\text{CH}_2)_3\text{Ph})]$ (**222**) can be prepared in 50% yield by the thermal displacement of η^6 -coordinated *p*-cymene from the adduct $[\text{RuCl}_2(\eta^6\text{-1,4-MeC}_6\text{H}_4\text{CHMe}_2)(\eta^1\text{-Ph}_2\text{P}(\text{CH}_2)_3\text{Ph})]$ (**223**) in chlorobenzene at 130°C (Scheme 49), and in 75% yield by exhaustive bulk anodic oxidation of the starting material **223** in dichloromethane.⁷ As will become evident, there are several discrepancies between the results reported in this thesis and those reported by Smith and Wright.⁷ A further complication, which has caused problems during the course of my work, is that Smith and Wright's⁷ publication differs in important details from the original source of the work, the Ph.D. dissertation by P. D. Smith.⁸



Scheme 49. Smith and Wright's claimed preparation of the tethered arene complex **222**.⁷

Since these reports suggested that the general approach outlined in Scheme 46 was feasible, it was decided to prepare a number of different precursor complexes. As little was known about which arene is more easily displaced, it was decided to make potential precursor complexes of the type $[\text{RuCl}_2(\eta^6\text{-arene})\text{L}]$, where $\text{L} =$ a potentially strapping aryl-phosphine, and arene = C_6H_6 , $p\text{-MeC}_6\text{H}_4\text{CHMe}_2$ or $o\text{-MeC}_6\text{H}_4\text{CO}_2\text{Me}$. Methyl *o*-toluate was selected as the electron-poor arene, instead of ethyl benzoate, since the synthetic procedure to prepare $[\text{RuCl}_2(\eta^6\text{-1,2-MeC}_6\text{H}_4\text{CO}_2\text{Me})]_2$ (**224**) had already been established in Prof. Bennett's group.⁹ Hexamethylbenzene was not selected because it tends to form more stable $\eta^6\text{-arene}$ complexes² and is less easily displaced,⁴ as discussed above.

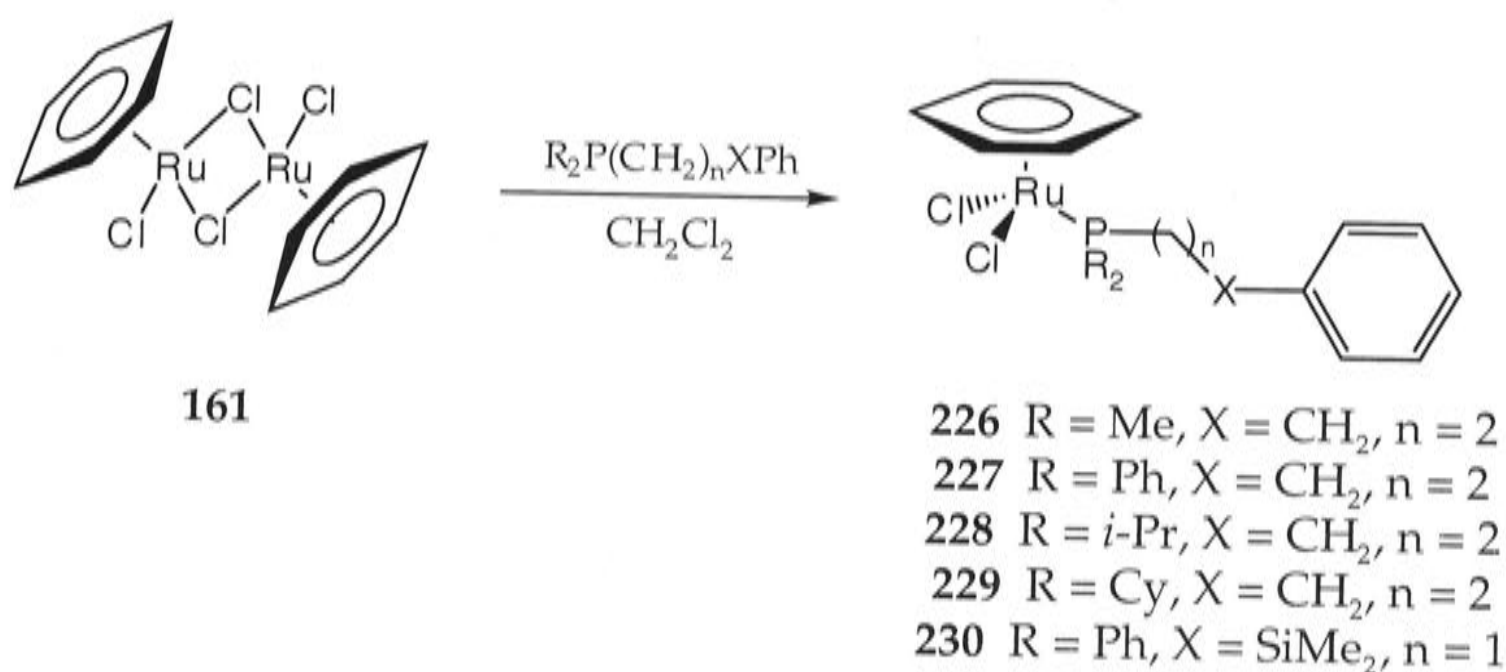
During the course of this work the preparations, essentially by the methods discussed so far, of a number of various tethered arene-ruthenium complexes were reported. Compounds $[\text{RuCl}_2(\eta^1:\eta^6\text{-R}_2\text{PCH}_2\text{CH(R')C}_6\text{H}_5)]$ ($\text{R} = \text{Ph}$, $\text{R}' = \text{H}$; $\text{R} = \text{Cy}$, $\text{R}' = \text{H}$; $\text{R} = \text{R}' = \text{Ph}$; $\text{R} = \text{Cy}$, $\text{R}' = \text{Ph}$) have been prepared by heating $[\text{RuCl}_2(\eta^6\text{-C}_6\text{H}_5\text{CO}_2\text{Et})]_2$ with the appropriate chelating phosphine in chloroform,¹⁰ complexes $[\text{RuCl}_2(\eta^1:\eta^6\text{-Cy}_2\text{P}(\text{CH}_2)_3\text{Ph})]$ (**225**),¹¹⁻¹³ $[\text{RuCl}_2(\eta^1:\eta^6\text{-Cy}_2\text{P}(\text{CH}_2)_3\text{-3,5-C}_6\text{Me}_2\text{H}_3)]$ ^{11,12} and $[\text{RuCl}_2(\eta^1:\eta^6\text{-Cy}_2\text{PCH}(\text{Me})(\text{CH}_2)_2\text{-3,5-C}_6\text{Me}_2\text{H}_3)]$,¹² were prepared from their corresponding *p*-cymene precursor complexes and compounds $[\text{RuCl}_2(\eta^1:\eta^6\text{-}t\text{-Bu}_2\text{PCH}_2\text{XPh})]$ ($\text{X} = \text{O}$, CH_2) were also prepared from the *p*-cymene analogues $[\text{RuCl}_2(\eta^6\text{-1,4-MeC}_6\text{H}_4\text{CHMe}_2)(\eta^1\text{-}t\text{-Bu}_2\text{PCH}_2\text{XPh})]$

(X = O, CH₂).¹⁴ Ward and co-workers⁶ also prepared multi-strapped arene-ruthenium complexes.¹⁵⁻¹⁷ These will all be discussed in Chapter 7 (Section 7.2).

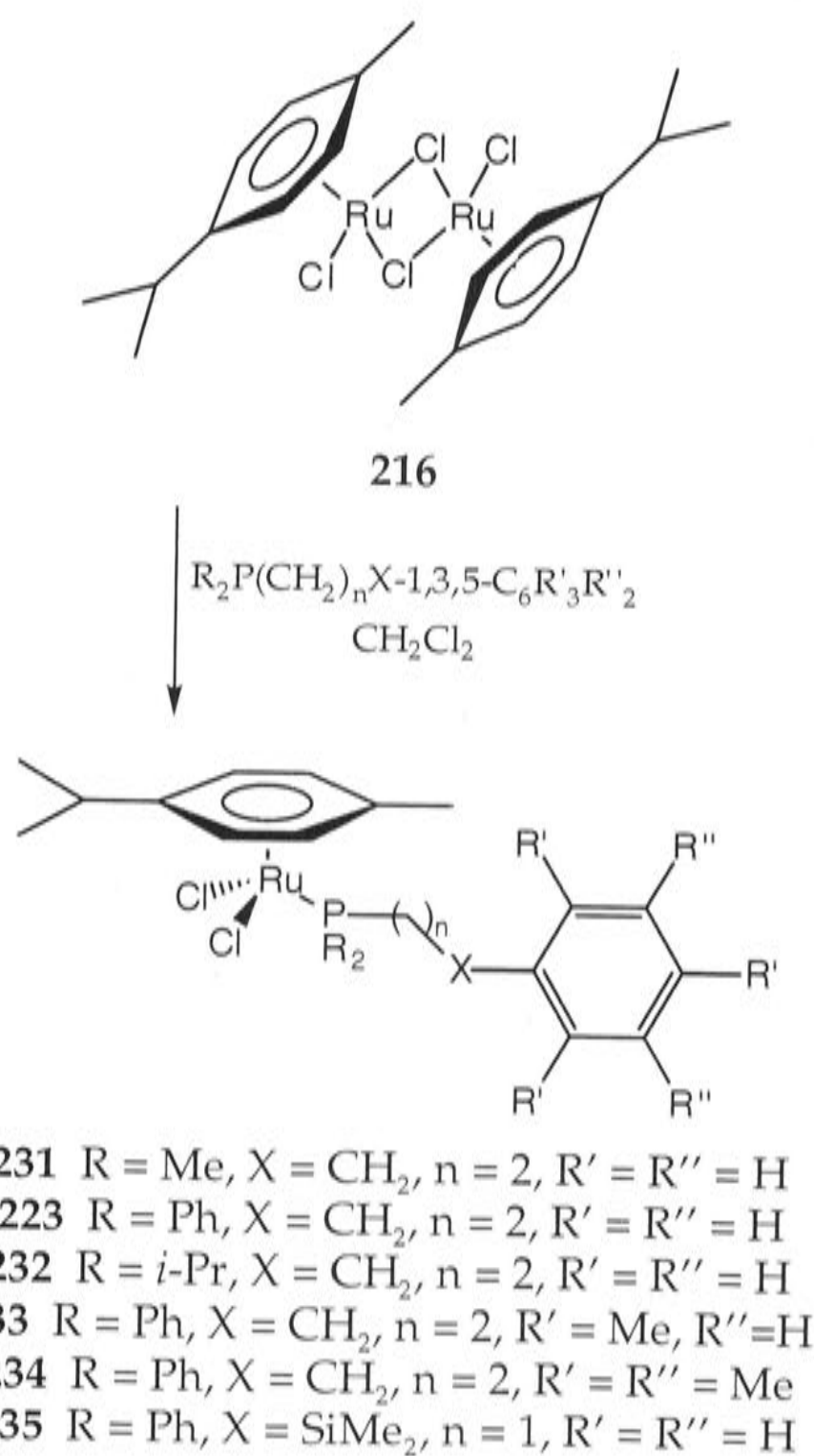
3.2.1 Preparation of the Non-Tethered Complexes

The derivatives of these arene complexes **223** and **226-242** were prepared as outlined in Schemes 50-52, by the reaction of two equivalents of the appropriate phosphine with the dimers [RuCl₂(η⁶-C₆H₆)]₂ (**161**), [RuCl₂(η⁶-1,4-MeC₆H₄CHMe₂)]₂ (**216**) or [RuCl₂(η⁶-1,2-MeC₆H₄CO₂Me)]₂ (**224**), respectively, following standard procedures,¹⁸⁻²⁰ at room temperature. The complexes were isolated in quantitative yields as generally air-stable, orange, microcrystalline solids by addition of *n*-hexane to a dichloromethane solution and removal of the solvents *in vacuo*. The non-tethered complexes were fully characterised, including elemental analyses. In some cases it was necessary to purify the products by column chromatography. Complex [RuCl₂(η⁶-1,2-MeC₆H₄CO₂Me)(η¹-*i*-Pr₂P(CH₂)₃Ph)] (**238**) was obtained only as a gummy semi-solid, despite attempted recrystallisation at -78°C.

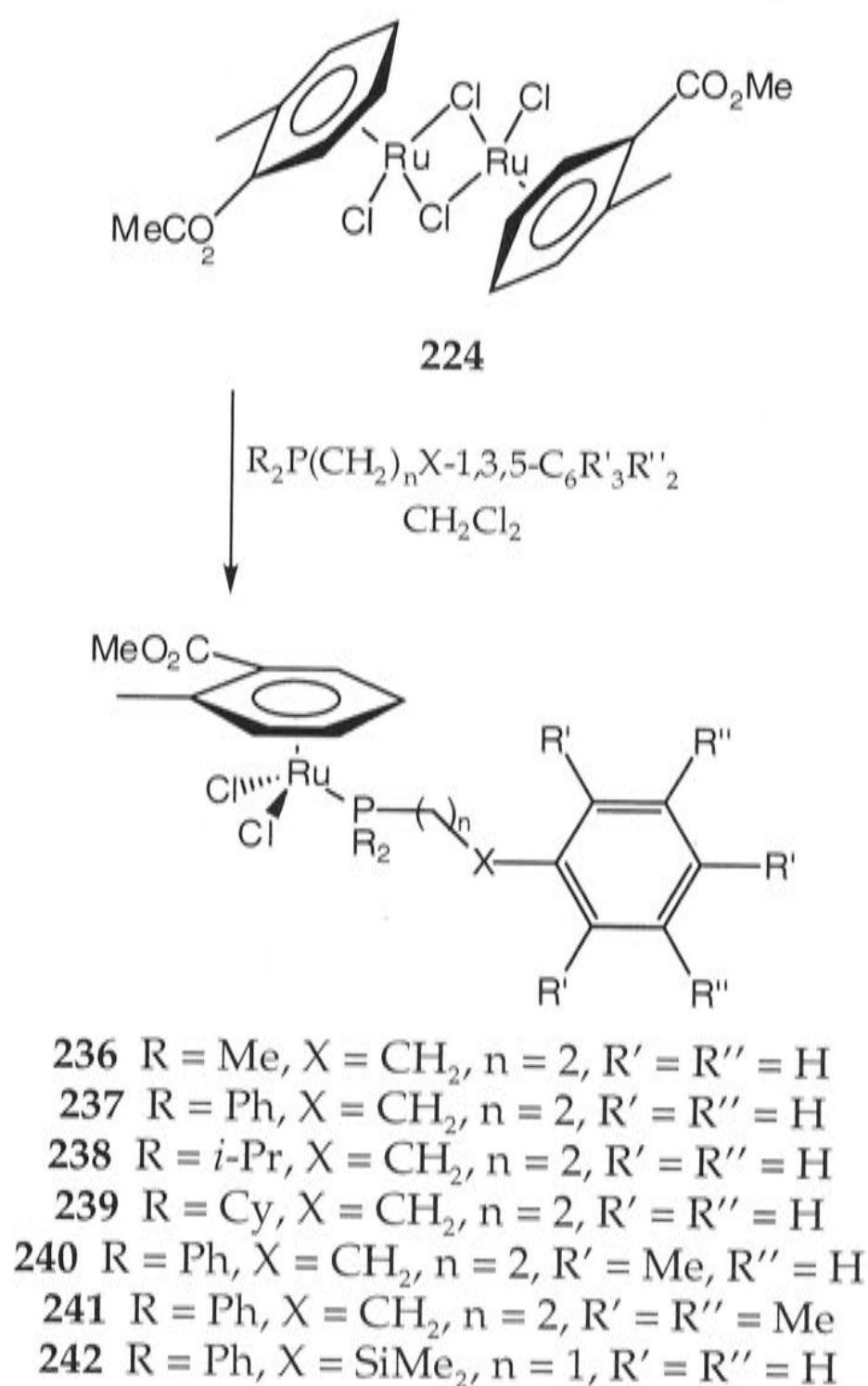
Although the reaction of the phosphine *t*-Bu₂P(CH₂)₃Ph (**198**) with the benzene, *p*-cymene and methyl *o*-toluate dimers, **161**, **216** and **224**, respectively, gave rise to the desired products [RuCl₂(η⁶-arene)(η¹-*t*-Bu₂P(CH₂)₃Ph)] (arene = C₆H₆ (**243**), 1,4-MeC₆H₄CHMe₂ (**244**), 1,2-MeC₆H₄CO₂Me (**245**)), these could not be separated from an unidentifiable impurity and could not be crystallised. The identity of the products was confirmed by ³¹P{¹H}-NMR spectroscopy. These complexes decomposed in the solid state on exposure to the atmosphere, by loss of η⁶-arene, as shown by ¹H and ³¹P{¹H}-NMR spectroscopy.



Scheme 50. Formation of the non-tethered complexes 226-230.



Scheme 51. Preparation of the non-tethered complexes 223 and 231-235.



Scheme 52. Formation of the non-tethered complexes **236-242**.

3.2.2 Characterisation Data

The spectroscopic data for each non-tethered complex are listed in Chapter 8, Section 8.2; the general features are discussed here. The 1H and $^{13}C\{^1H\}$ -NMR spectra all show resonances due to the η^6 -arene which lie upfield of those due to the free arene. The η^6 -benzene complexes generally show a singlet, due to the six chemically equivalent protons of the η^6 -benzene, in the region δ 5.2-5.6 in the 1H NMR spectra, whilst the $^{13}C\{^1H\}$ -NMR spectra show a doublet due to C_6H_6 ($J_{PC} = 2$ Hz) in the region δ 86.9-88.1. The signal due to C_6H_6 of complex $[RuCl_2(\eta^6-C_6H_6)(\eta^1-Me_2P(CH_2)_3Ph)]$ (**226**) displays a larger coupling, $J_{PC} = 13$ Hz, whilst $[RuCl_2(\eta^6-C_6H_6)((\eta^1-Ph_2PCH_2SiMe_2Ph))]$ (**230**)

shows only a singlet. The *p*-cymene and methyl *o*-toluate compounds show, in addition to resonances characteristic of the substituents on the η^6 -arene, ^1H NMR signals in the range δ 4.2-6.4 and the $^{13}\text{C}\{^1\text{H}\}$ -NMR spectra contain resonances due to the η^6 -arene in the region δ 74.9-115.0. The ^1H NMR spectra of complexes **233**, **234**, **240** and **241** containing the phosphines $\text{Ph}_2\text{P}(\text{CH}_2)_3$ -2,4,6- $\text{C}_6\text{H}_2\text{Me}_3$ (**199**) and $\text{Ph}_2\text{P}(\text{CH}_2)_3\text{C}_6\text{Me}_5$ (**200**) show resonances due to the methyl substituents in the range δ 1.9-2.2; the signal due to the chemically equivalent hydrogen atoms of the η^6 -arene compounds incorporating **199** is observed at *ca* δ 6.7. The P-methyl groups in $[\text{RuCl}_2(\eta^6\text{-1,2-MeC}_6\text{H}_4\text{CO}_2\text{Me})(\eta^1\text{-Me}_2\text{P}(\text{CH}_2)_3\text{Ph})]$ (**236**) are inequivalent, due to the planar chirality of the η^6 -methyl *o*-toluate,⁹ and appear as two doublets in the ^1H and $^{13}\text{C}\{^1\text{H}\}$ -NMR spectra. Similarly, the methyl protons of the P-isopropyl groups of $[\text{RuCl}_2(\eta^6\text{-1,2-MeC}_6\text{H}_4\text{CO}_2\text{Me})(\eta^1\text{-}i\text{-Pr}_2\text{P}(\text{CH}_2)_3\text{Ph})]$ (**238**) are inequivalent and appear as a multiplet in the ^1H NMR spectrum and as two doublets in the $^{13}\text{C}\{^1\text{H}\}$ -NMR spectrum.

Other diagnostic features of both the ^1H and $^{13}\text{C}\{^1\text{H}\}$ -NMR spectra of complexes incorporating phosphines of the type $\text{R}_2\text{P}(\text{CH}_2)_3$ -aryl are the signals due to the three methylene units which will eventually form the tether. The ^1H NMR spectra generally consist of three individual multiplets in the region δ 1.5-2.7 for each of the CH_2 groups, which appear in the order (from upfield to downfield); $\text{CH}_2\text{CH}_2\text{CH}_2$, CH_2P , CH_2Ph . Generally, the $^{13}\text{C}\{^1\text{H}\}$ -NMR spectra display three distinct doublets ($J_{\text{PC}} = 4\text{-}30$ Hz) in the region δ 19.7-37.7, in the same order as observed in the ^1H NMR spectra.

All of the non-tethered complexes prepared show a singlet in their $^{31}\text{P}\{^1\text{H}\}$ -NMR spectra. Although the complexes containing *t*- $\text{Bu}_2\text{P}(\text{CH}_2)_3\text{Ph}$ (**198**) could not be purified (see Section 3.2.1), their $^{31}\text{P}\{^1\text{H}\}$ -NMR singlets were located in the range δ 48.1-55.5.

The IR spectra of the methyl *o*-toluate compounds contain typical $\nu(\text{CO}_2)$ ester absorptions at approximately 1720 and 1260 cm^{-1} . The far IR spectra of the non-tethered complexes generally show two strong bands assigned to $\nu(\text{Ru-Cl})$ in the region 270-300 cm^{-1} , but in some cases just one broad peak is observed in this range, presumably because the bands overlap.

All of the benzene and *p*-cymene complexes show parent ions in their mass spectra (EI or FAB) and appear to be monomeric, as expected. In contrast, in the mass spectra of the methyl *o*-toluate complexes $[\text{RuCl}_2(\eta^6\text{-1,2-MeC}_6\text{H}_4\text{CO}_2\text{Me})(\eta^1\text{-R}_2\text{P}(\text{CH}_2)_3\text{Ph})]$ ($\text{R} = \text{Me}$ (236), Ph (237), *i*-Pr (238), Cy (239)) and $[\text{RuCl}_2(\eta^6\text{-1,2-MeC}_6\text{H}_4\text{CO}_2\text{Me})(\eta^1\text{-Ph}_2\text{P}(\text{CH}_2)_3\text{-2,4,6-C}_6\text{R}_2\text{Me}_3)]$ ($\text{R} = \text{H}$ (240) and $\text{R} = \text{Me}$ (241)), the highest mass ion is $[\text{M-Cl}]^+$ and $[\text{RuCl}_2(\eta^6\text{-MeC}_6\text{H}_4\text{CO}_2\text{Me})(\eta^1\text{-Ph}_2\text{PCH}_2\text{SiMe}_2\text{Ph})]$ (242) shows $[\text{M-arene}]^+$.

The molecular structures of $[\text{RuCl}_2(\eta^6\text{-1,4-MeC}_6\text{H}_4\text{CHMe}_2)(\eta^1\text{-Me}_2\text{P}(\text{CH}_2)_3\text{Ph})]$ (231), $[\text{RuCl}_2(\eta^6\text{-C}_6\text{H}_6)(\eta^1\text{-Ph}_2\text{P}(\text{CH}_2)_3\text{Ph})]$ (227), $[\text{RuCl}_2(\eta^6\text{-1,4-MeC}_6\text{H}_4\text{CHMe}_2)(\eta^1\text{-i-Pr}_2\text{P}(\text{CH}_2)_3\text{Ph})]$ (232), $[\text{RuCl}_2(\eta^6\text{-1,2-MeC}_6\text{H}_4\text{CO}_2\text{Me})(\eta^1\text{-Cy}_2\text{P}(\text{CH}_2)_3\text{Ph})]$ (239), $[\text{RuCl}_2(\eta^6\text{-1,4-MeC}_6\text{H}_4\text{CHMe}_2)(\eta^1\text{-Ph}_2\text{P}(\text{CH}_2)_3\text{-2,4,6-C}_6\text{H}_2\text{Me}_3)]$ (233), $[\text{RuCl}_2(\eta^6\text{-1,4-MeC}_6\text{H}_4\text{CHMe}_2)(\eta^1\text{-Ph}_2\text{P}(\text{CH}_2)_3\text{C}_6\text{Me}_5)]$ (234) and $[\text{RuCl}_2(\eta^6\text{-1,4-MeC}_6\text{H}_4\text{CHMe}_2)(\eta^1\text{-Ph}_2\text{PCH}_2\text{SiMe}_2\text{Ph})]$ (235) have been determined by X-ray crystallography [Drs A. D. Bond and T. Khimyak for 239 and 233, Dr J. E. Davies for 232, Drs J. E. Davies and T. Khimyak for 234 and Dr. T. Khimyak for 235 (Cambridge); Dr A. C. Willis for 231 and 227 (ANU)]. The CS Chem3D Pro (Chem3D) representations of 227, 239 and 233 are shown in Figures 5, 6 and 7, respectively. These structures will be discussed in Section 3.5.

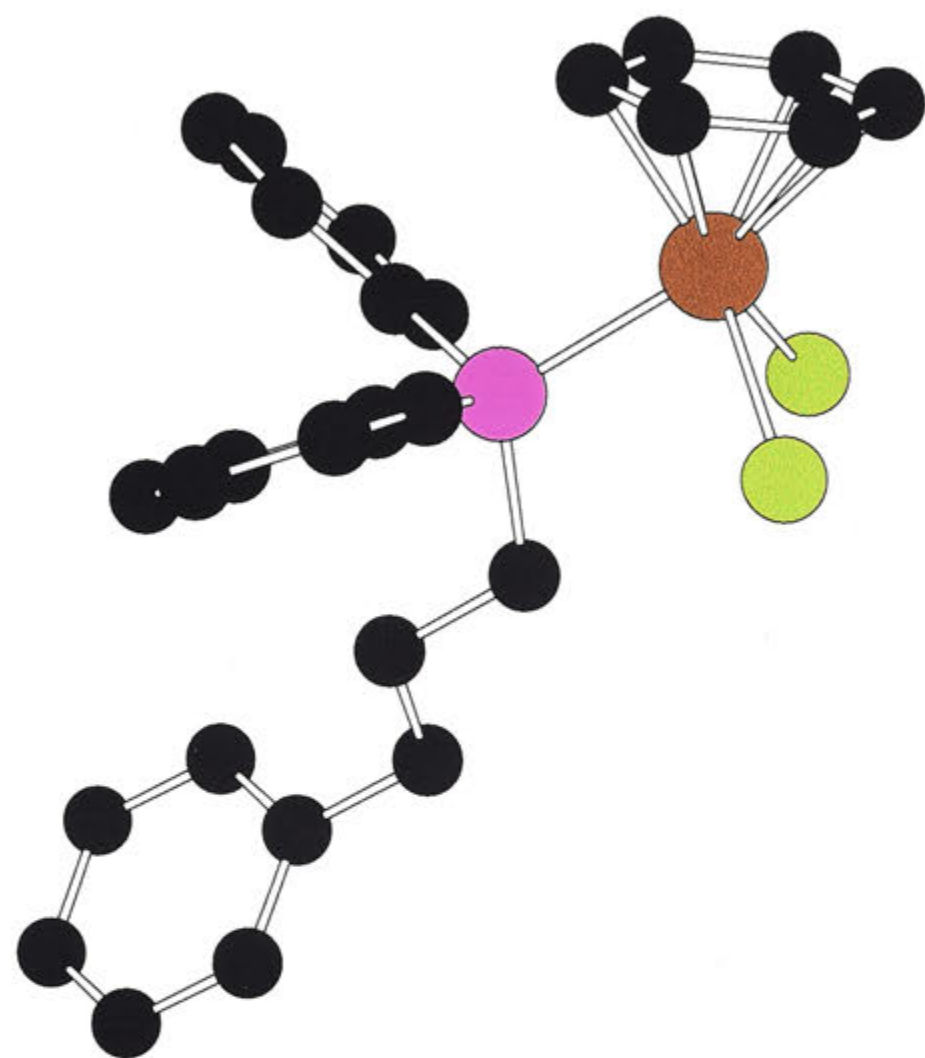


Figure 5. CS Chem3D Pro (Chem3D) representation of the molecular structure of $[\text{RuCl}_2(\eta^6\text{-C}_6\text{H}_6)(\eta^1\text{-Ph}_2\text{P}(\text{CH}_2)_3\text{Ph})]$ (**227**). Hydrogen atoms have been omitted for clarity.

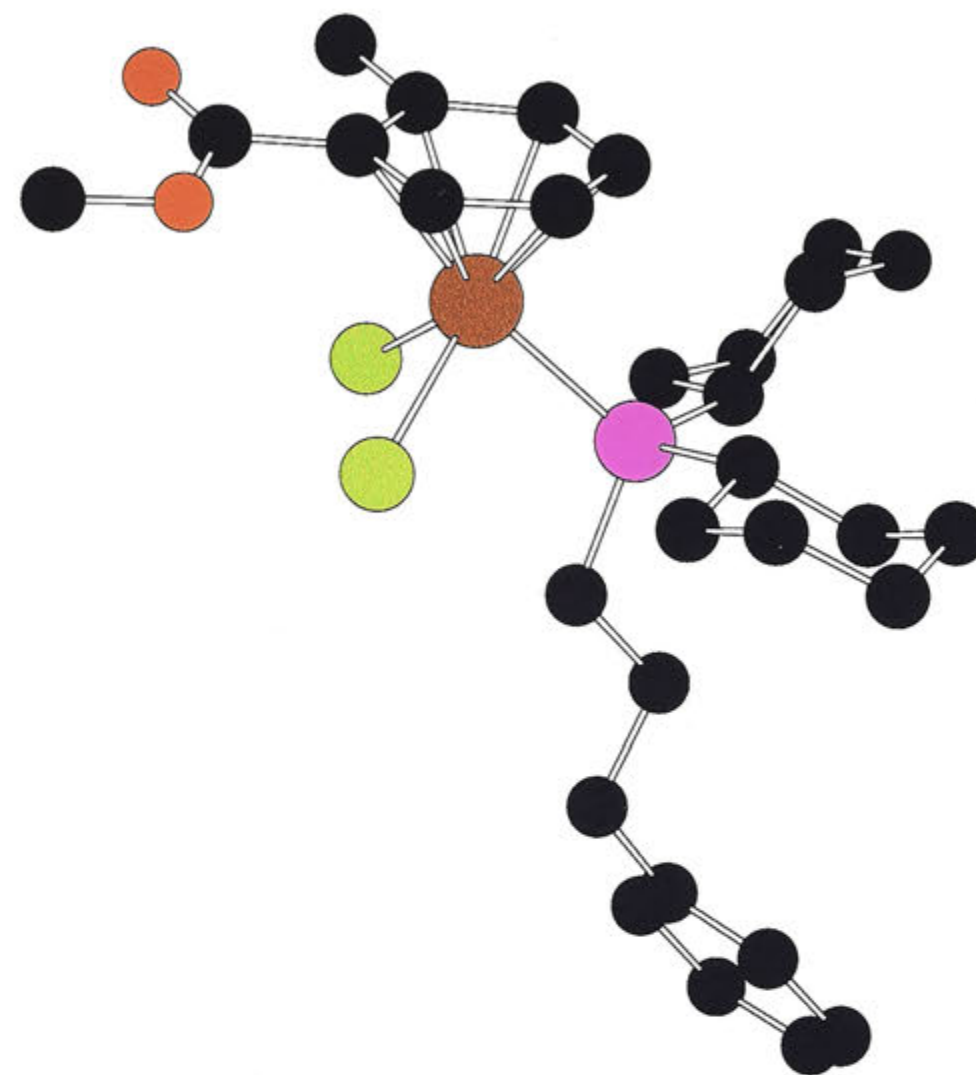


Figure 6. Chem3D representation of the molecular structure of $[\text{RuCl}_2(\eta^6\text{-1,2-MeC}_6\text{H}_4\text{CO}_2\text{Me})(\eta^1\text{-Cy}_2\text{P}(\text{CH}_2)_3\text{Ph})]$ (**239**), showing one of the independent molecules in the unit cell.[†] Hydrogen atoms have been omitted for clarity.

[†]Refer to Appendix (pp. 423-425) for details of the other conformer.

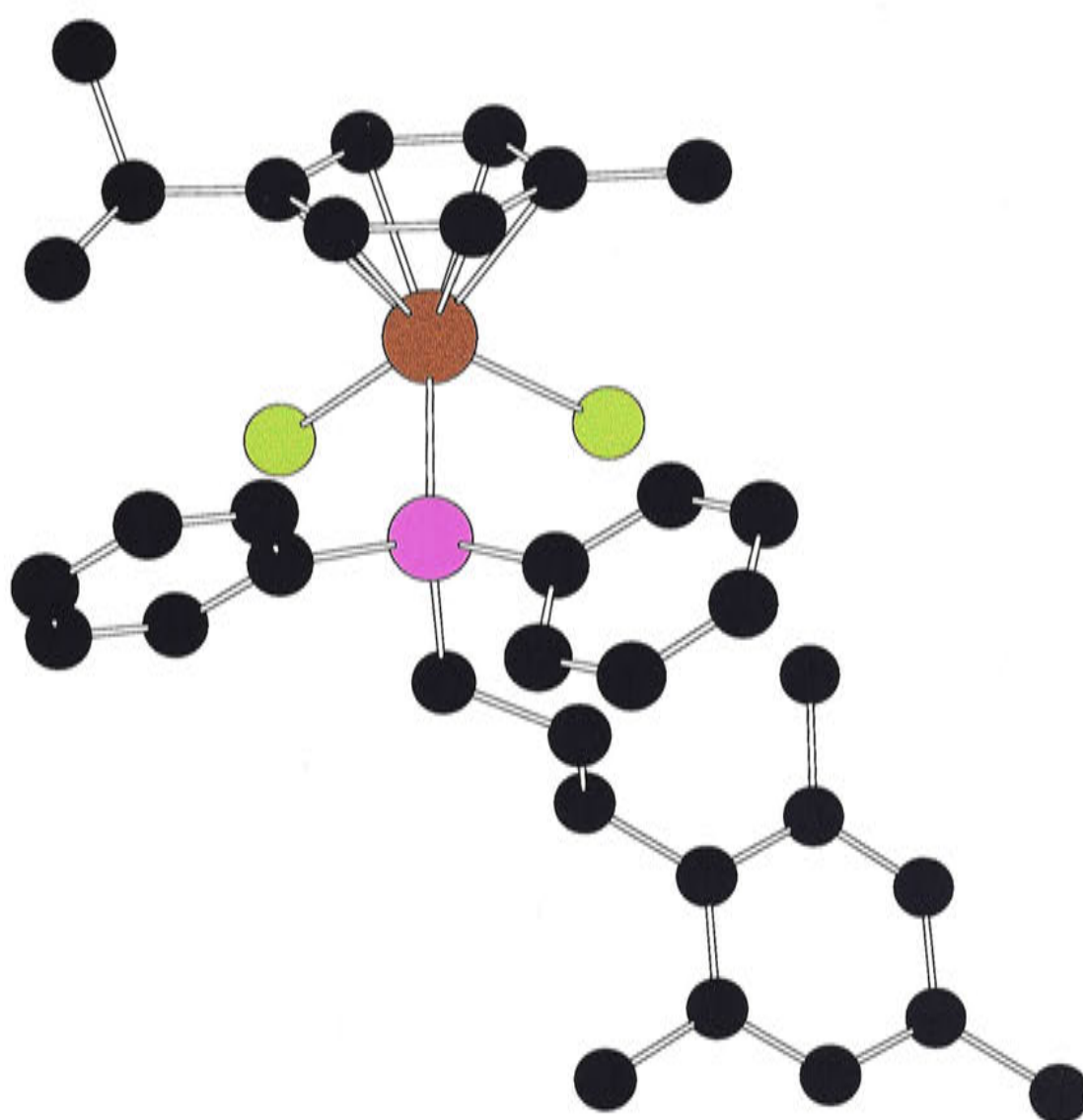
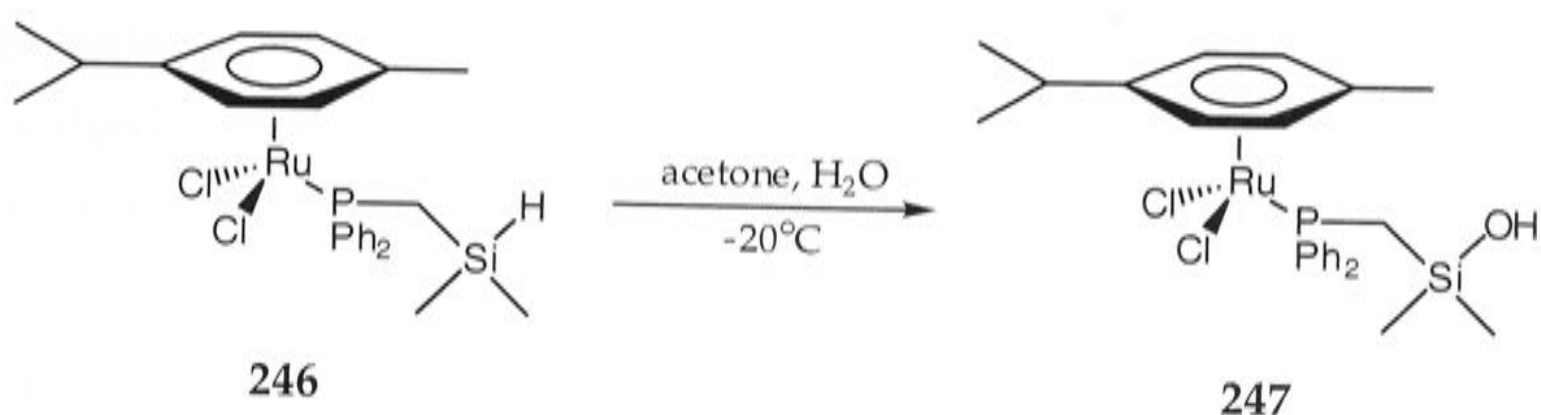


Figure 7. Chem3D representation of the molecular structure of $[\text{RuCl}_2(\eta^6\text{-1,4-MeC}_6\text{H}_4\text{CHMe}_2)(\eta^1\text{-Ph}_2\text{P}(\text{CH}_2)_3\text{-2,4,6-C}_6\text{H}_2\text{Me}_3)]$ (233). Hydrogen atoms have been omitted for clarity.

The cleavage of the Si-CH₂ bond observed in free Ph₂PCH₂SiMe₂Ph (201) (see Chapter 2, p. 82) did not occur in the non-tethered complexes $[\text{RuCl}_2(\eta^6\text{-arene})(\eta^1\text{-Ph}_2\text{PCH}_2\text{SiMe}_2\text{Ph})]$ (arene = C₆H₆ (230), 1,4-MeC₆H₄CHMe₂ (235) and 1,2-MeC₆H₄CO₂Me (242)). It is known that cleavage of the Si-CH₂ bond in Ph₂PCH₂SiR₃ compounds can be inhibited by complexation of the phosphine to a ruthenium(II) centre.²¹ For example, an acetone solution of the ruthenium complex $[\text{RuCl}_2(\eta^6\text{-1,4-MeC}_6\text{H}_4\text{CHMe}_2)(\eta^1\text{-Ph}_2\text{PCH}_2\text{SiMe}_2\text{H})]$ (246) reacted with water, over 120 days, to form the silanol complex $[\text{RuCl}_2(\eta^6\text{-1,4-MeC}_6\text{H}_4\text{CHMe}_2)(\eta^1\text{-Ph}_2\text{PCH}_2\text{SiMe}_2\text{OH})]$ (247), without cleavage of the Si-CH₂ bond (Scheme 53).



Scheme 53. Formation of the complex **247** containing the silanol moiety.²¹

3.2.3 Preparation of the Tethered Complexes

The general approach outlined in Scheme 46 was successful for all the desired tethered complexes, containing the tertiary phosphines $\text{R}_2\text{P}(\text{CH}_2)_3\text{Ph}$ ($\text{R} = \text{Me}$ (**195**)), Ph (**118**), *i*-Pr (**196**), Cy (**197**), *t*-Bu (**198**)), $\text{Ph}_2\text{P}(\text{CH}_2)_3\text{-2,4,6-C}_6\text{R}_2\text{Me}_3$ ($\text{R} = \text{H}$ (**199**), Me (**200**)) and $\text{Ph}_2\text{PCH}_2\text{SiMe}_2\text{Ph}$ (**201**), prepared in the course of this work (see Chapter 2). In agreement with Ward and co-workers,⁶ (see Section 3.2) the RuCl_2 complex of the aromatic ester methyl *o*-toluate, $[\text{RuCl}_2(\eta^6\text{-1,2-MeC}_6\text{H}_4\text{CO}_2\text{Me})]_2$ (**224**),⁹ was found to be the most suitable precursor. Each of the methyl *o*-toluate non-tethered complexes $[\text{RuCl}_2(\eta^6\text{-1,2-MeC}_6\text{H}_4\text{CO}_2\text{Me})(\eta^1\text{-R}_2\text{P}(\text{CH}_2)_3\text{Ph})]$ ($\text{R} = \text{Me}$ (**236**), Ph (**237**), *i*-Pr (**238**), Cy (**239**)), $[\text{RuCl}_2(\eta^6\text{-1,2-MeC}_6\text{H}_4\text{CO}_2\text{Me})(\eta^1\text{-Ph}_2\text{P}(\text{CH}_2)_3\text{-2,4,6-C}_6\text{R}_2\text{Me}_3)]$ ($\text{R} = \text{H}$ (**240**), Me (**241**)) and $[\text{RuCl}_2(\eta^6\text{-1,2-MeC}_6\text{H}_4\text{CO}_2\text{Me})(\eta^1\text{-Ph}_2\text{PCH}_2\text{SiMe}_2\text{Ph})]$ (**242**) was heated in dichloromethane or a mixture of dichloromethane and THF to 120°C for periods ranging from 6 to 72 hours. Methyl *o*-toluate was displaced and the tethered complexes $[\text{RuCl}_2(\eta^1:\eta^6\text{-R}_2\text{P}(\text{CH}_2)_3\text{Ph})]$ ($\text{R} = \text{Me}$ (**248**), Ph (**222**), *i*-Pr (**249**), Cy (**225**)) (Scheme 54), $[\text{RuCl}_2(\eta^1:\eta^6\text{-Ph}_2\text{P}(\text{CH}_2)_3\text{-2,4,6-C}_6\text{R}_2\text{Me}_3)]$ ($\text{R} = \text{H}$ (**250**), Me (**251**)) (Scheme 55) and $[\text{RuCl}_2(\eta^1:\eta^6\text{-Ph}_2\text{PCH}_2\text{SiMe}_2\text{Ph})]$ (**252**) (Scheme 56), respectively, were formed. Longer reaction times were generally required for those complexes containing smaller substituents on the phosphorus atom. For example, compound **222** with PPh_2 was formed in 48 hours, whereas only 16 hours was required to form **225** with the bulkier PCy_2 group.

The tethered complexes required purification since some decomposition occurred. Complexes **222**, **248** and **250-252** were purified by column chromatography, though it was necessary to re-chromatograph the crude product $[\text{RuCl}_2(\eta^1:\eta^6\text{-Ph}_2\text{P}(\text{CH}_2)\text{-2,4,6-C}_6\text{H}_2\text{Me}_3)]$ (**250**). Complexes **249** and **225** incorporating the bulky phosphines $\text{R}_2\text{P}(\text{CH}_2)_3\text{Ph}$ ($\text{R} = i\text{-Pr}$ (**196**), Cy (**197**)), were precipitated in a pure state by slow addition of *n*-hexane to a concentrated dichloromethane solution. The tethered complexes were isolated as orange, microcrystalline, air-stable solids, and have been fully characterised, including elemental analyses (see Chapter 8, Section 8.2); the diagnostic features of the spectral data will be discussed in Section 3.2.4. The ^1H and $^{13}\text{C}\{^1\text{H}\}$ -NMR spectroscopic data of the η^6 -arene terminus of the tether are summarised in Tables 5 and 6, respectively. The $^{31}\text{P}\{^1\text{H}\}$ -NMR spectroscopic data of the tethered complexes prepared are listed in Table 7. The far IR and mass spectrometry data are listed in Table 8. Reaction conditions and yields of isolated products are collected in Table 9.

The yields of complexes **248**, **222**, **249**, **225**, **253** and $[\text{RuCl}_2(\eta^1:\eta^6\text{-Ph}_2\text{PCH}_2\text{SiMe}_2\text{Ph})]$ (**252**), containing $\eta^6\text{-C}_6\text{H}_5$, are reasonable (61-91%). However, yields decreased for complexes $[\text{RuCl}_2(\eta^1:\eta^6\text{-Ph}_2\text{P}(\text{CH}_2)_3\text{-2,4,6-C}_6\text{H}_2\text{Me}_3)]$ (**250**) and $[\text{RuCl}_2(\eta^1:\eta^6\text{-Ph}_2\text{P}(\text{CH}_2)_3\text{C}_6\text{Me}_5)]$ (**251**) incorporating alkyl-substituted coordinated arenes. Variations in the reaction conditions were explored in an effort to improve the yields of both **250** and **251**. The reactions were monitored by ^1H and $^{31}\text{P}\{^1\text{H}\}$ -NMR spectroscopy, and the conditions employed are shown in Table 10. The yield of *ca* 18% for **250** could not be improved by use of di-*n*-butyl ether alone (entry 20), or a combination of dichloromethane with di-*n*-butyl ether (entry 21), which gave rise to **250** in yields below 10%. Complex **251** was prepared in *ca* 7% yield in a mixture of dichloromethane/THF, but the yield increased to 35% in neat di-*n*-butyl ether. This, however, could not be improved by using either neat dichloromethane (entry 24), di-*n*-butyl ether with dichloromethane (entry 27) or di-*n*-butyl ether with THF (entry 28). The use of a high boiling chlorinated solvent, *sym*-tetrachloroethane, with *d*₂-dichloromethane (entry 26) resulted

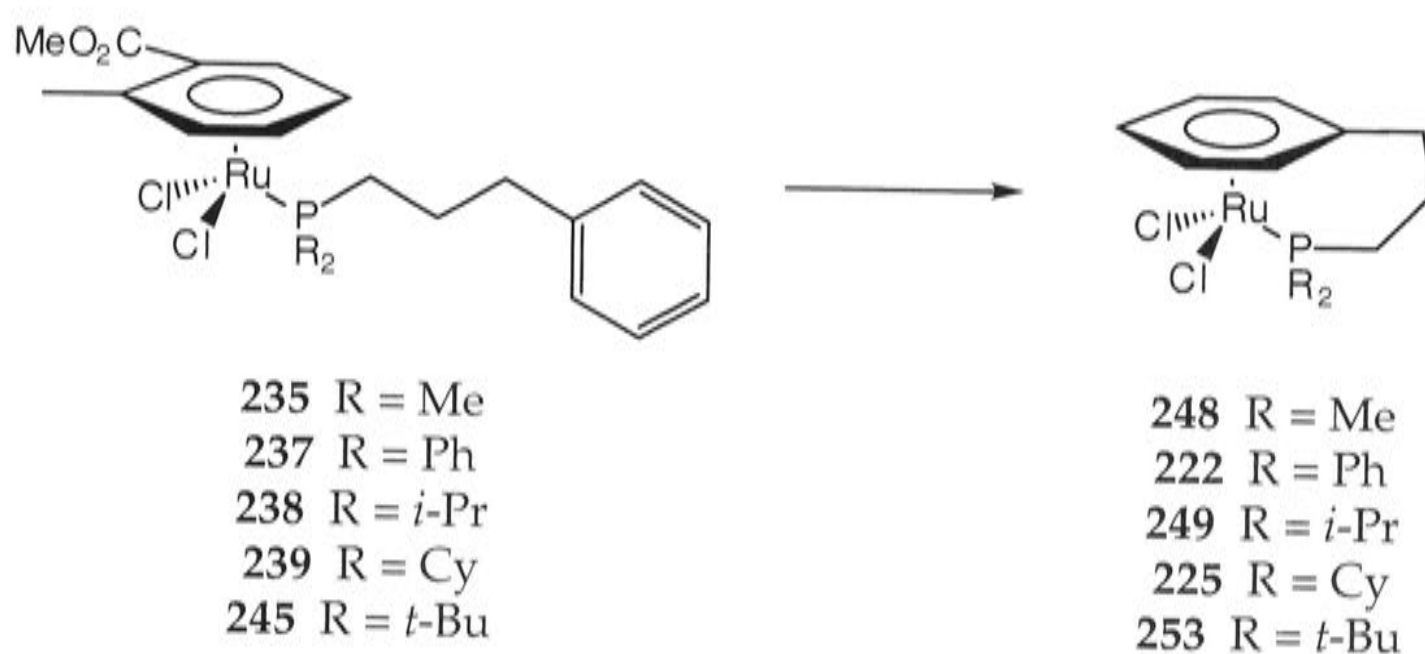
in decomposition. Although displacement of the η^6 -methyl *o*-toluate occurred when **241** was heated to 110°C *in vacuo* (2×10^{-5} Torr) in the absence of solvent (entry 23), complex decomposition resulted. Putting the reaction under pressure was similarly unsuccessful (entry 25); no reaction occurred. The formation of $[\text{RuCl}_2(\eta^1:\eta^6\text{-Ph}_2\text{P}(\text{CH}_2)_3\text{Ph})]$ (**222**) seems to be favoured by the presence of a small amount of THF, which both slightly increases the yield and reduces the reaction time. This behaviour is reminiscent of the effect of ether solvents in the synthesis of complexes of the type $[\text{Cr}(\text{CO})_3(\eta^6\text{-arene})]$.^{22,23}

In the cases of $[\text{RuCl}_2(\eta^1:\eta^6\text{-R}_2\text{P}(\text{CH}_2)_3\text{Ph})]$ (R = Me (**248**), Ph (**222**), *i*-Pr (**249**), Cy (**225**)) and **252**, containing $\text{Ph}_2\text{PCH}_2\text{SiMe}_2\text{Ph}$ (**201**), it is not necessary to isolate the initially formed non-tethered adducts, namely **236-239** and **242**, respectively; they can be formed *in situ* from the dimer $[\text{RuCl}_2(\eta^6\text{-1,2-MeC}_6\text{H}_4\text{CO}_2\text{Me})]_2$ (**224**) and the appropriate ligand at room temperature. As the preparation of both **250** and **251** was achieved in relatively low yields, the *in situ* preparation was not investigated.

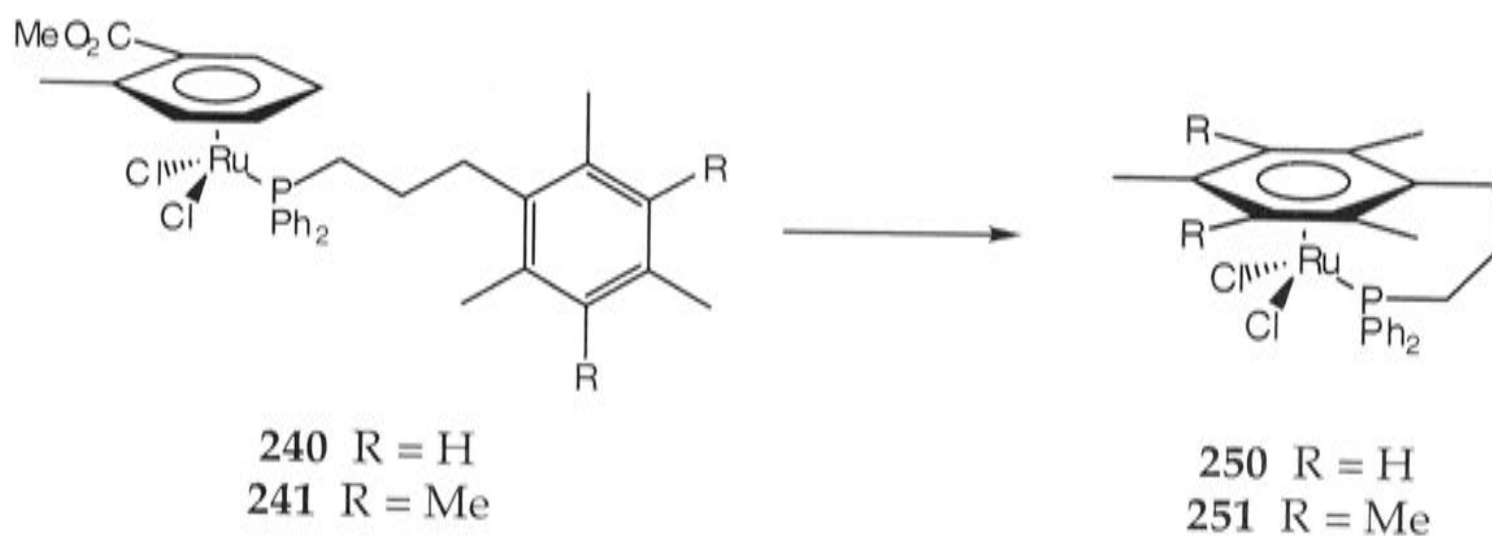
A crude sample of $[\text{RuCl}_2(\eta^6\text{-1,2-MeC}_6\text{H}_4\text{CO}_2\text{Me})(\eta^1\text{-}t\text{-Bu}_2\text{P}(\text{CH}_2)_3\text{Ph})]$ (**245**) was heated in dichloromethane at 120°C for 24 hours to afford the tethered complex $[\text{RuCl}_2(\eta^1:\eta^6\text{-}t\text{-Bu}_2\text{P}(\text{CH}_2)_3\text{Ph})]$ (**253**), though the reaction conditions were not optimised. Unlike most of the tethered complexes, which are stable indefinitely in solution, **253** was slowly converted into an unidentified product in dichloromethane. Like its precursor $[\text{RuCl}_2(\eta^6\text{-1,2-MeC}_6\text{H}_4\text{CO}_2\text{Me})(\eta^1\text{-Ph}_2\text{PCH}_2\text{SiMe}_2\text{Ph})]$ (**242**), the complex $[\text{RuCl}_2(\eta^1:\eta^6\text{-Ph}_2\text{PCH}_2\text{SiMe}_2\text{Ph})]$ (**252**) is stable with respect to Si-CH₂ bond cleavage in solution.

Complex $[\text{RuCl}_2(\eta^1:\eta^6\text{-Cy}_2\text{P}(\text{CH}_2)_3\text{Ph})]$ (**225**) could also be prepared from the η^6 -methyl *o*-toluate compound **239** at 80°C, in comparable yield to that

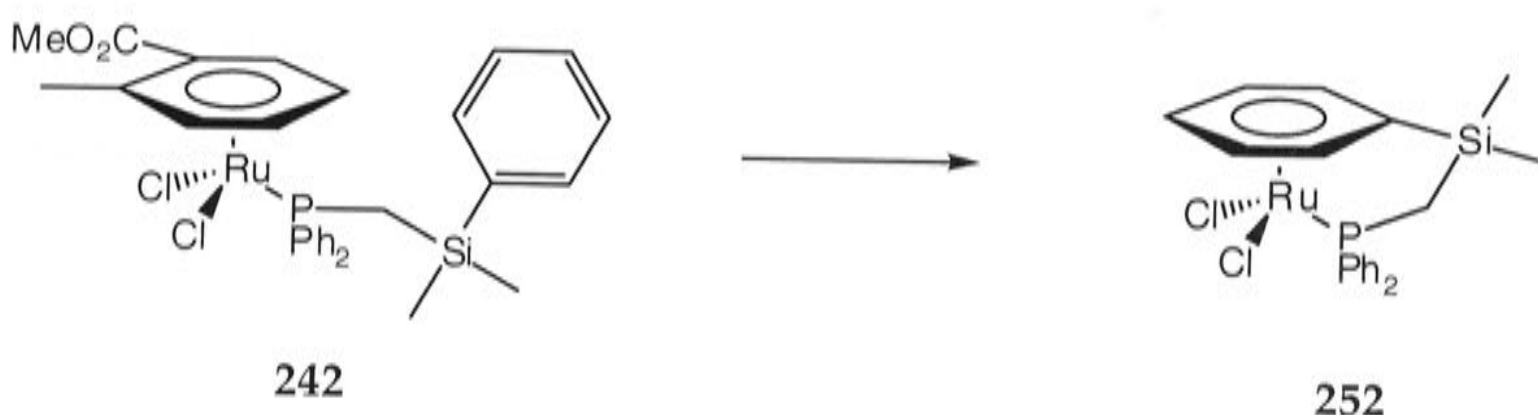
obtained at 120°C, although the reaction was considerably slower, requiring 192 hours (*cf.* 16 h at 120°C). There was no displacement of methyl *o*-toluate when a d_2 -dichloromethane solution of **239** was heated to 40°C (see Table 10, entry 17). Attempts to prepare $[\text{RuCl}_2(\eta^1:\eta^6\text{-R}_2\text{P}(\text{CH}_2)_3\text{Ph})]$ ($\text{R} = \text{Me}$ (**248**), Ph (**222**)) by UV-irradiation of the η^6 -methyl *o*-toluate species **236** and **237** at room temperature were unsuccessful (see Table 10, entries 2 and 16, respectively). Decomposition by loss of the aromatic ester and formation of phosphine oxide occurred.



Scheme 54. Preparation of the tethered complexes **248**, **222**, **249**, **225** and **253** from the methyl *o*-toluate precursors.



Scheme 55. Synthesis of the tethered complexes **250** and **251** from the methyl *o*-toluate precursors.



Scheme 56. Preparation of the tethered complex **252** from the methyl *o*-toluate precursor.

3.2.4 Characterisation Data

The ^1H and $^{13}\text{C}\{^1\text{H}\}$ -NMR spectra of all of the tethered complexes provide clear evidence for the coordination of the arene group at the end of the strap. Thus, the ^1H NMR spectra of complexes $[\text{RuCl}_2(\eta^1:\eta^6\text{-R}_2\text{P}(\text{CH}_2)_3\text{Ph})]$ ($\text{R} = \text{Me}$ (**248**), Ph (**222**), *i*-Pr (**249**), Cy (**225**), *t*-Bu (**253**)) and $[\text{RuCl}_2(\eta^1:\eta^6\text{-Ph}_2\text{PCH}_2\text{SiMe}_2\text{Ph})]$ (**252**) contain three resonances in a 2:2:1 intensity ratio due to C_6H_5 in the region δ 5.0-6.4, shifted upfield of those expected for free arenes (Table 5). They show the expected multiplicity (doublets and triplets) for η^6 -arenes, which, combined with their intensity, is used to assign each of them as *ortho*-, *meta*- or *para*- C_6H_5 . The ^1H NMR spectrum of $[\text{RuCl}_2(\eta^1:\eta^6\text{-}i\text{-Pr}_2\text{P}(\text{CH}_2)_3\text{Ph})]$ (**249**) in the region δ 4.9-6.6, shown in Figure 8b, clearly differs from that of the precursor $[\text{RuCl}_2(\eta^6\text{-1,2-MeC}_6\text{H}_4\text{CO}_2\text{Me})(\eta^1\text{-}i\text{-Pr}_2\text{P}(\text{CH}_2)_3\text{Ph})]$ (**238**) (Figure 8a). The low frequency chemical shifts are mirrored in the $^{13}\text{C}\{^1\text{H}\}$ -NMR spectra, which show the expected four η^6 -arene resonances in the region δ 80.0-101.1. Complex $[\text{RuCl}_2(\eta^1:\eta^6\text{-Ph}_2\text{P}(\text{CH}_2)_3\text{-2,4,6-C}_6\text{H}_2\text{Me}_3)]$ (**250**) shows ^1H NMR signals due to the methyl groups in the range δ 1.4-1.8, and a singlet due to the equivalent protons of the η^6 -arene at approximately δ 5.3 (Table 5). The ^1H NMR spectrum of $[\text{RuCl}_2(\eta^1:\eta^6\text{-Ph}_2\text{P}(\text{CH}_2)_3\text{C}_6\text{Me}_5)]$ (**251**) shows signals due to the methyl groups in the region δ 1.7-2.2 (Table 5). The resonances

due to the η^6 -arene in the $^{13}\text{C}\{^1\text{H}\}$ -NMR spectra of **250** and **251** lie in the range δ 84.8-106.3; the signal due to the *ipso*-carbon of **250** was not observed.

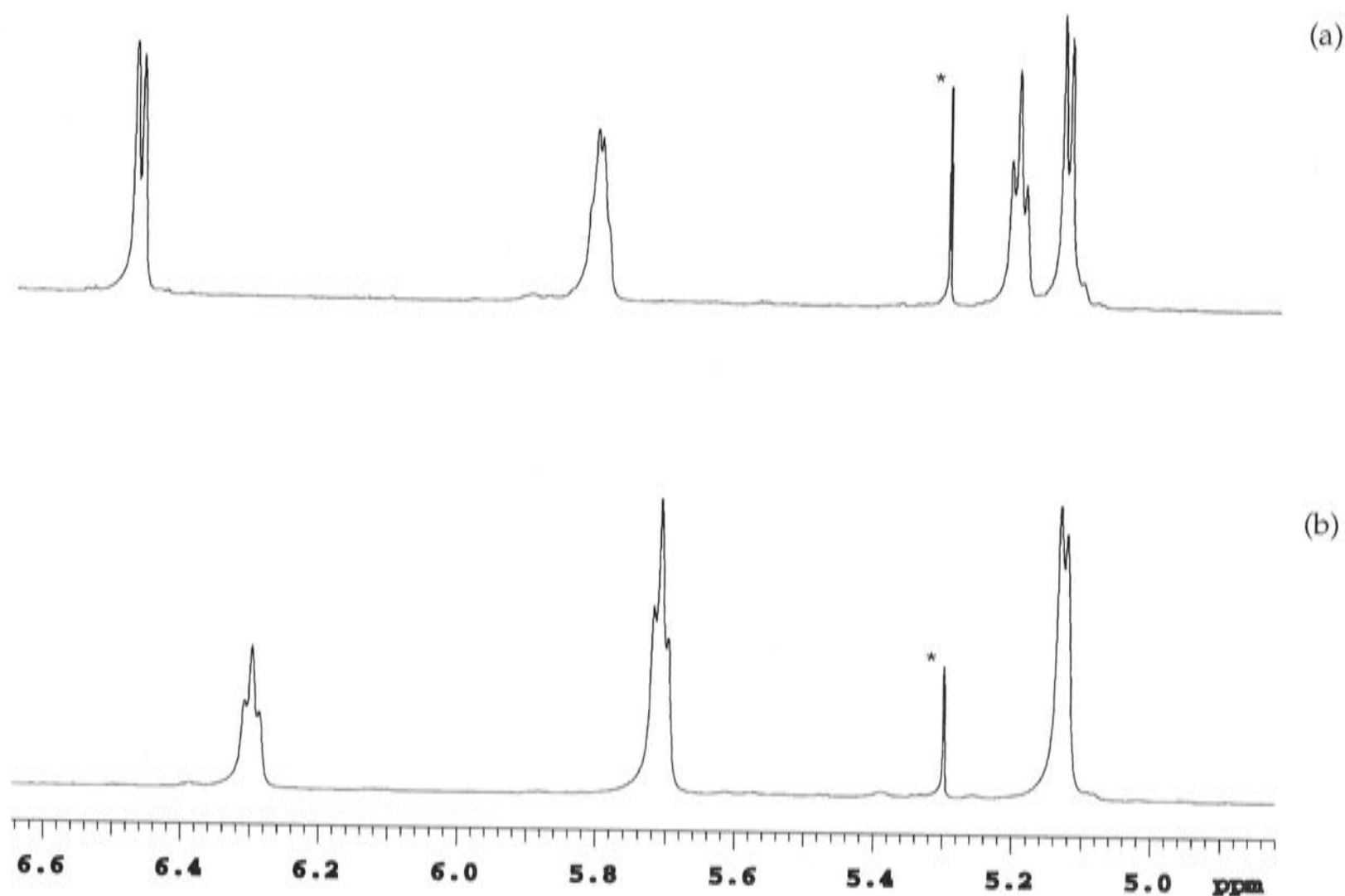


Figure 8. ^1H NMR spectra (500 MHz) of the coordinated aromatic protons of $[\text{RuCl}_2(\eta^6\text{-1,2-MeC}_6\text{H}_4\text{CO}_2\text{Me})(\eta^1\text{-}i\text{-Pr}_2\text{P}(\text{CH}_2)_3\text{Ph})]$ (**238**) (a) and $[\text{RuCl}_2(\eta^1:\eta^6\text{-}i\text{-Pr}_2\text{P}(\text{CH}_2)_3\text{Ph})]$ (**249**) (b) in d_1 -chloroform. *Residual CH_2Cl_2 .

The regions δ 1.8-2.7 and 20.5-34.6 in the ^1H and $^{13}\text{C}\{^1\text{H}\}$ -NMR spectra due, respectively, to the three methylene units of the tethered complexes are also diagnostic. The order (see Figure 9b) differs from that of the non-tethered complexes (see Figure 9a), being generally (from upfield to downfield); $\text{CH}_2\text{CH}_2\text{CH}_2$, CH_2Ph , CH_2P , though in some cases, such as for $[\text{RuCl}_2(\eta^1:\eta^6\text{-Ph}_2\text{P}(\text{CH}_2)_3\text{Ph})]$ (**222**) and $[\text{RuCl}_2(\eta^1:\eta^6\text{-Ph}_2\text{P}(\text{CH}_2)_3\text{-2,4,6-C}_6\text{H}_2\text{Me}_3)]$ (**250**) the CH_2P and CH_2Ph resonances overlap to give one multiplet. Generally, the $^{13}\text{C}\{^1\text{H}\}$ -NMR spectra display three distinct signals, of which two appear as singlets and CH_2P appears as a doublet ($J_{\text{PC}} = 11\text{-}31$ Hz). Thus, less ^{31}P -coupling is observed than in the non-tethered

complexes, presumably because of the different dihedral angles in the tether. Further, there is usually a characteristic upfield shift of the CH_2Ph signal compared with the spectra of the tethered complexes. For example, the CH_2Ph resonance of $[\text{RuCl}_2(\eta^6\text{-1,2-MeC}_6\text{H}_4\text{CO}_2\text{Me})(\eta^1\text{-}i\text{-Pr}_2\text{P}(\text{CH}_2)_3\text{Ph})]$ (238) is *ca* 10 ppm downfield of that observed in $[\text{RuCl}_2(\eta^1:\eta^6\text{-}i\text{-Pr}_2\text{P}(\text{CH}_2)_3\text{Ph})]$ (249). The resonances generally appear in the same order as in the ^1H NMR spectra.

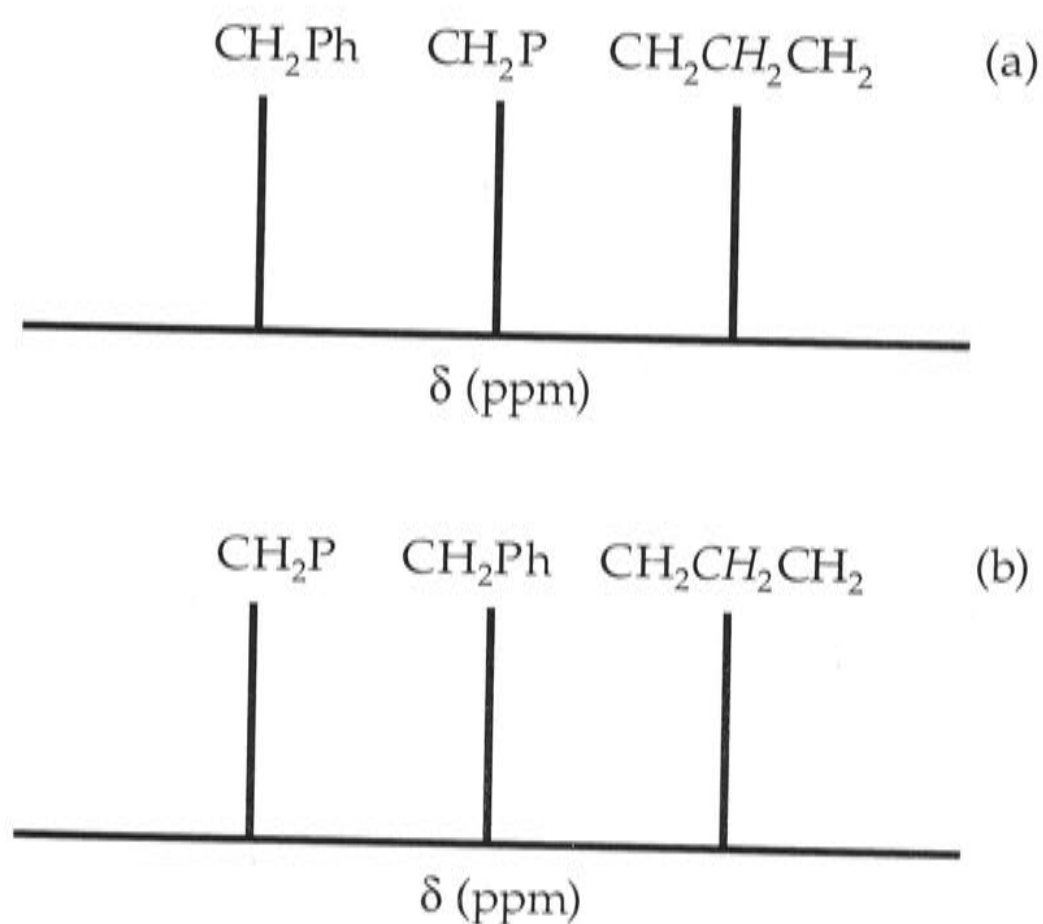


Figure 9. Diagrammatic representation of the general order observed of signals due to the methylene chain in both the ^1H and $^{13}\text{C}\{^1\text{H}\}$ -NMR spectra of the relevant non-tethered (a) and tethered complexes (b).

The X-ray structure of $[\text{RuCl}_2(\eta^1:\eta^6\text{-Ph}_2\text{PCH}_2\text{SiMe}_2\text{Ph})]$ (252) (see Section 3.2.5) shows that the methyl groups on the silicon atom are in different chemical environments. If the η^6 -arene is considered as a single atom, the non-planar chelate five-membered ring arene-Si-C-P-Ru can be compared to cyclopentane, which can exist in either the envelope or half-chair (also known as twist-envelope²⁴) conformations.^{25,26} Since the Si-C-Ru atoms, and the centre of the η^6 -arene, are all within the same plane, whereas the phosphorus is not, this pseudo five-membered ring is in the envelope conformation (Figure 10). The two methyl groups are in isoclinal positions,

where each is approximately equally disposed above and below the plane.²⁶ The ^1H NMR spectrum of **252** in CD_2Cl_2 at -10°C is shown in Figure 11 (the spectrum at room temperature is similar). It contains just a singlet due to the SiMe_2 protons at δ 0.37, indicating an apparent plane of symmetry through the SiMe_2 unit on the NMR timescale. This signal broadens as the sample is cooled, disappears at -100°C , and reappears as two broad signals at -110°C which are separated by 174 Hz at 300 MHz (see Figure 12), assigned to the chemically inequivalent methyl protons. The observed changes are presumably caused by conformational changes within the tether, which become slow on the NMR timescale at -110°C . The free energy of activation for this process, ΔG^\ddagger , at the coalescence point (*ca* $-105^\circ\text{C} \pm 5^\circ\text{C}$) can be estimated as $8.0 \pm 0.5 \text{ kcal mol}^{-1}$ from the equation:²⁷

$$\Delta G^\ddagger = RT[\ln(k_B/h) + \ln(T/k)] \quad (2)$$

R = the Gas Constant

T = coalescence temperature

k_B = Boltzmann Constant

h = Planck's Constant

$k = \pi\delta\nu/\sqrt{2}$

$\delta\nu$ = separation between peaks

Other regions of the spectrum also change when the solution is cooled. The multiplet at δ 5.18, assigned to the *meta*-protons of the η^6 -arene, broadens and finally disappears into the base-line at -100°C , while the *ortho*- and *para*-multiplets remain essentially unchanged. The PPh_2 groups give rise to a pair of sharp, well-resolved multiplets at -10°C in a ratio of 4:6, corresponding to the *ortho*- and *meta*-/*para*-protons, respectively. At -80°C the former broadens, at -100°C only one broad resonance is observed for all aromatic protons, and at -110°C four broad resonances are present, indicating two chemically inequivalent Ph groups. The methylene

resonance, which is observed as a well-resolved doublet at δ 2.80 ($J_{\text{PH}} = 15$ Hz) at -10°C appears as one broad signal at δ 2.75 at -100°C but does not separate into two resonances.

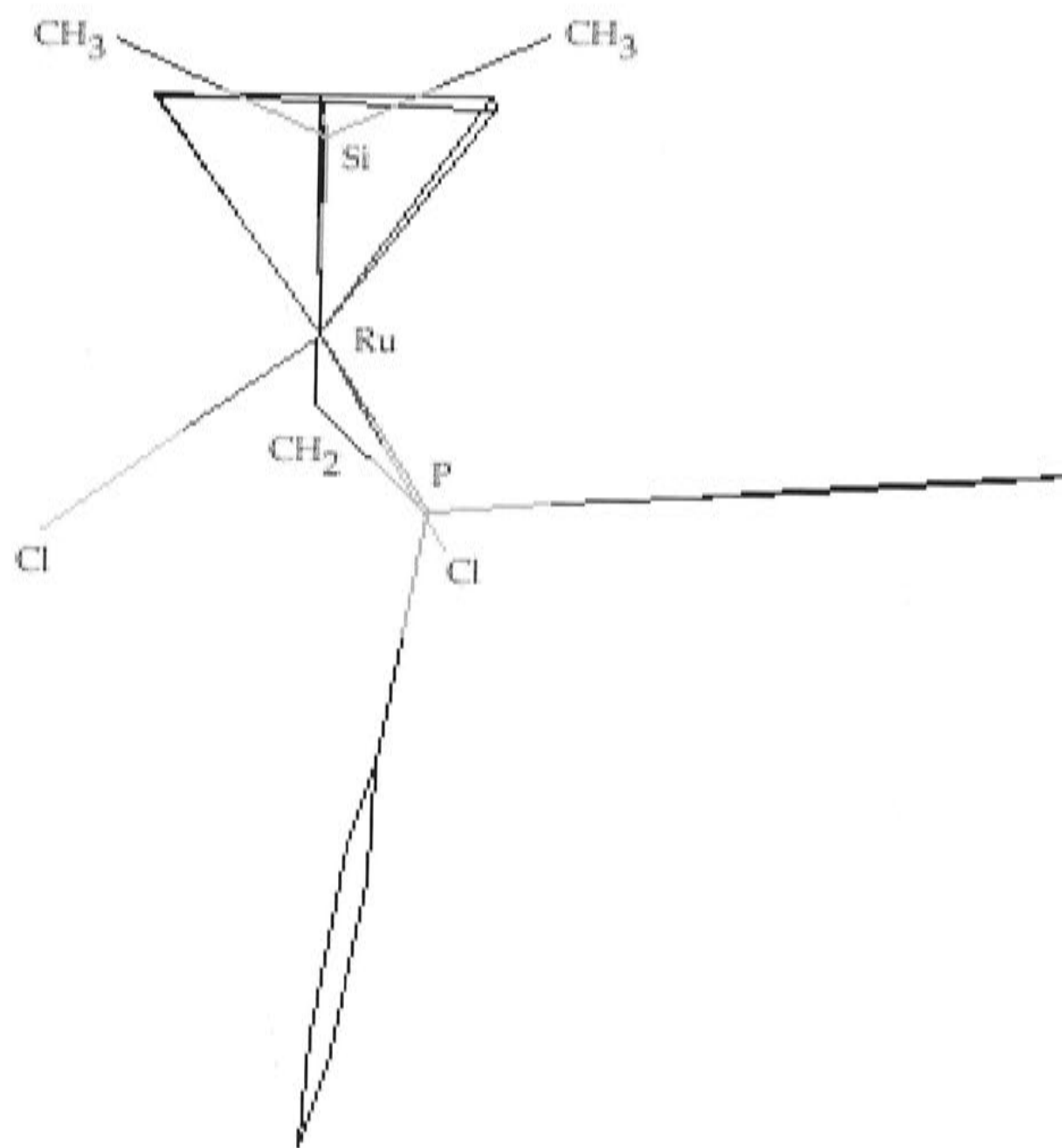


Figure 10. Chem3D representation of the molecular structure of $[\text{RuCl}_2(\eta^1:\eta^6\text{-Ph}_2\text{PCH}_2\text{SiMe}_2\text{Ph})]$ (252), from the perspective of the Si-CH₂ bond. Hydrogen atoms have been omitted for clarity.

These results indicate that the non-planar chelate ring (composed of arene-Si-C-P-Ru) is rapidly inverting between two different envelope conformations at temperatures above -100°C . The phosphorus atom either lies above (Figure 13a) or below (Figure 13b) the plane containing the arene-Si-C-Ru chain. This process is slow enough to be detected on the NMR timescale at *ca* -110°C . Thus, the conformation of the tether is somewhat flexible, since the chelate ring is able to convert between two different conformations.

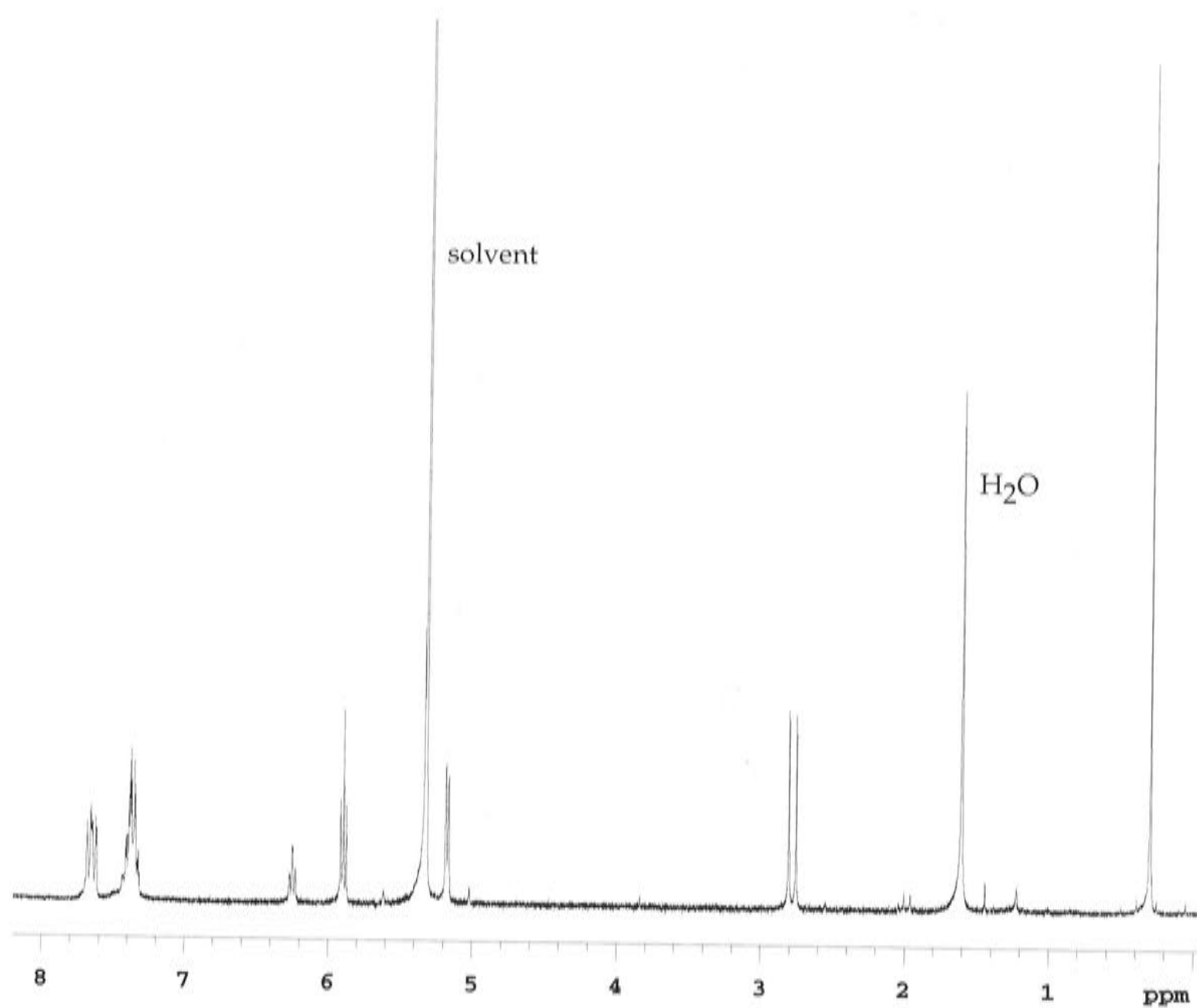


Figure 11. ¹H NMR spectrum (300 MHz) of $[\text{RuCl}_2(\eta^1:\eta^6\text{-Ph}_2\text{PCH}_2\text{SiMe}_2\text{Ph})]$ (252) at -10°C in d_2 -dichloromethane.

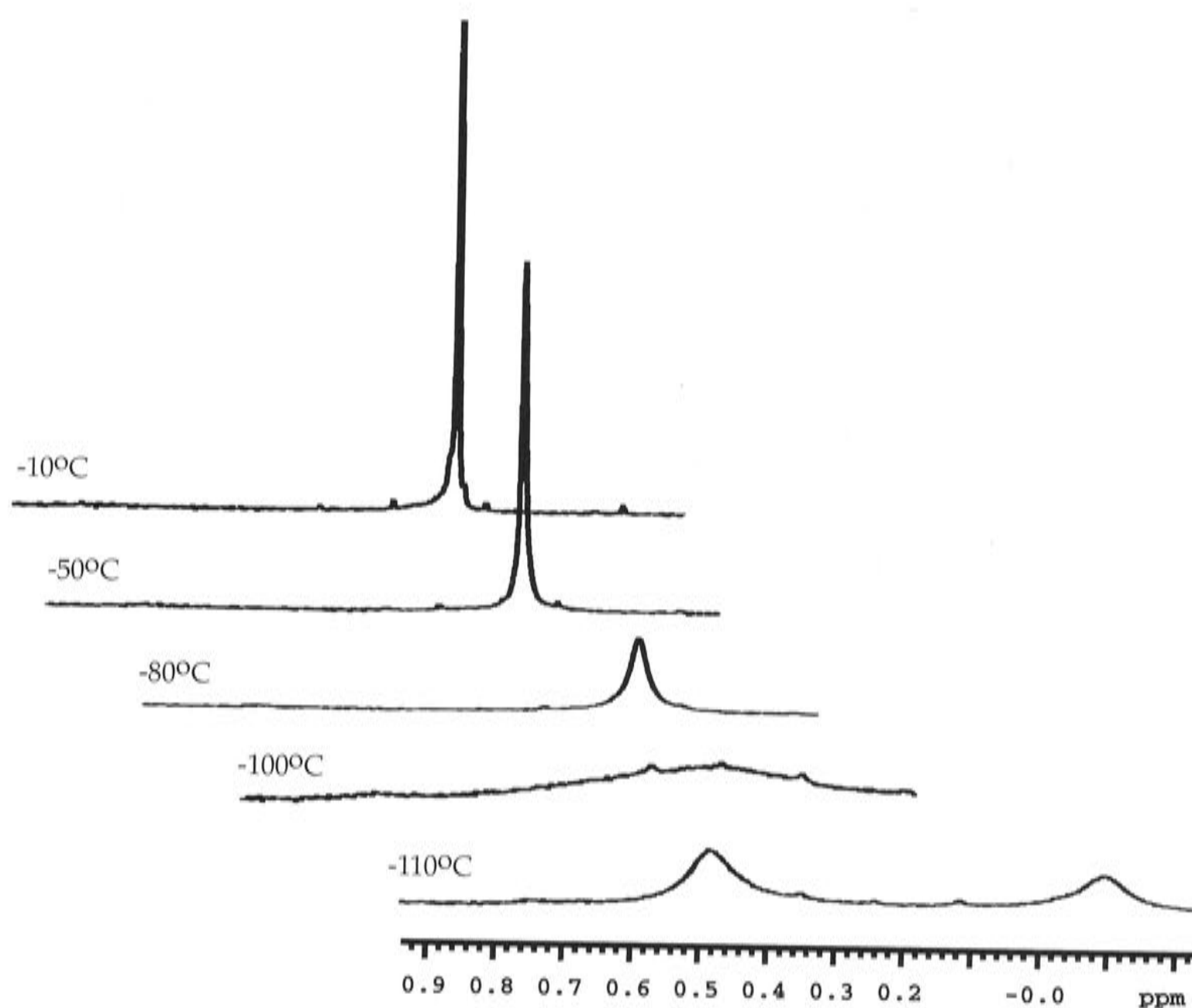


Figure 12. Variable temperature ^1H NMR spectra (300 MHz) of the SiMe_2 group of $[\text{RuCl}_2(\eta^1:\eta^6\text{-Ph}_2\text{PCH}_2\text{SiMe}_2\text{Ph})]$ (**252**) in d_2 -dichloromethane. Spectra at -100°C and -110°C show an arbitrary four-fold increase in intensity.



Figure 13. Diagrammatic representation of the two proposed conformations of the non-planar chelate ring arene-Si-C-P-Ru (C_6H_5 represented as X for simplicity).

Table 5. ^1H NMR chemical shifts for the aromatic protons of the η^6 -arene of the tethered Ru(II) complexes in d_1 -chloroform.

Entry Number	Complex	δ_{ortho}^a (ppm)	δ_{meta}^b (ppm)	δ_{para}^b (ppm)
1	[RuCl ₂ (η^1 : η^6 -Me ₂ P~Ph)] (248)	4.96	5.62	6.33
2	[RuCl ₂ (η^1 : η^6 -Ph ₂ P~Ph)] (222)	5.13	5.77	6.36
3	[RuCl ₂ (η^1 : η^6 - <i>i</i> -Pr ₂ P~Ph)] (249)	5.12	5.69	6.29
4	[RuCl ₂ (η^1 : η^6 -Cy ₂ P~Ph)] (225)	5.08	5.65	6.25
5	[RuCl ₂ (η^1 : η^6 - <i>t</i> -Bu ₂ P~Ph)] (253)	5.25	5.72	6.24
6	[RuCl ₂ (η^1 : η^6 -Ph ₂ P~-2,4,6-C ₆ H ₂ Me ₃)] (250)	1.36 ^c	5.25	1.79 ^c
7	[RuCl ₂ (η^1 : η^6 -Ph ₂ P~C ₆ Me ₅)] (251)	1.73 ^c	2.06 ^d	2.16 ^c
8	[RuCl ₂ (η^1 : η^6 -Ph ₂ PCH ₂ SiMe ₂ Ph)] (252)	5.18	5.88	6.26

^aDoublet ($J = 6$ Hz); ^btriplet ($J = 6$ Hz); ^cmethyl group attached to the phenyl moiety.

~ = (CH₂)₃

Table 6. $^{13}\text{C}\{^1\text{H}\}$ -NMR chemical shifts for the η^6 -arene in tethered Ru(II) complexes in d_1 -chloroform; multiplicity of the signals is not specified.

Entry Number	Complex	δ_{ipso} (ppm)	δ_{ortho} (ppm)	δ_{meta} (ppm)	δ_{para} (ppm)
1	[RuCl ₂ (η^1 : η^6 -Me ₂ P~Ph)] (248)	89.92	80.27	92.35	98.39
2	[RuCl ₂ (η^1 : η^6 -Ph ₂ P~Ph)] (222)	89.15	84.68	90.24	101.14
3	[RuCl ₂ (η^1 : η^6 - <i>i</i> -Pr ₂ P~Ph)] (249)	95.90	80.00	93.76	97.11
4	[RuCl ₂ (η^1 : η^6 -Cy ₂ P~Ph)] (225)	93.30	80.15	96.00	97.14
5	[RuCl ₂ (η^1 : η^6 - <i>t</i> -Bu ₂ P~Ph)] (253)	98.10	82.01	93.38	96.63
6	[RuCl ₂ (η^1 : η^6 -Ph ₂ P~-2,4,6-C ₆ H ₂ Me ₃)] (250)	*	84.81	92.34	96.30
7	[RuCl ₂ (η^1 : η^6 -Ph ₂ P~C ₆ Me ₅)] (251)	106.29	85.50	91.59	101.23
8	[RuCl ₂ (η^1 : η^6 -Me ₂ PCH ₂ SiMe ₂ Ph)] (252)	92.13	86.30	92.68	95.80

*Peak was not detected.

~ = (CH₂)₃

The tethered complexes all show a singlet in their $^{31}\text{P}\{^1\text{H}\}$ -NMR spectra. These chemical shifts are similar to, though distinguishable from, those of the non-tethered compounds, and are in the expected range for tertiary phosphines incorporating either Me, Ph, *i*-Pr, Cy or *t*-Bu substituents.

Table 7. $^{31}\text{P}\{^1\text{H}\}$ -NMR chemical shifts of the tethered complexes in d_1 -chloroform.

Entry Number	Complex	Chemical Shift (ppm)
1	$[\text{RuCl}_2(\eta^1:\eta^6\text{-Me}_2\text{P}\sim\text{Ph})]$ (248)	13.7
2	$[\text{RuCl}_2(\eta^1:\eta^6\text{-Ph}_2\text{P}\sim\text{Ph})]$ (222)	22.2
3	$[\text{RuCl}_2(\eta^1:\eta^6\text{-}i\text{-Pr}_2\text{P}\sim\text{Ph})]$ (249)	34.9
4	$[\text{RuCl}_2(\eta^1:\eta^6\text{-Cy}_2\text{P}\sim\text{Ph})]$ (225)	29.5
5	$[\text{RuCl}_2(\eta^1:\eta^6\text{-}t\text{-Bu}_2\text{P}\sim\text{Ph})]$ (253)	41.8
6	$[\text{RuCl}_2(\eta^1:\eta^6\text{-Ph}_2\text{P}\sim\text{-2,4,6-C}_6\text{H}_2\text{Me}_3)]$ (250)	28.8
7	$[\text{RuCl}_2(\eta^1:\eta^6\text{-Ph}_2\text{P}\sim\text{C}_6\text{Me}_5)]$ (251)	26.2
8	$[\text{RuCl}_2(\eta^1:\eta^6\text{-Ph}_2\text{PCH}_2\text{SiMe}_2\text{Ph})]$ (252)	24.0

$\sim = (\text{CH}_2)_3$

The far IR spectra of the tethered Ru(II) complexes show the two expected strong $\nu(\text{Ru-Cl})$ bands in the range 260-290 and 290-310 cm^{-1} . An indication of the stability of the tethered compounds is that they all show parent ions in their mass spectra (FAB or EI).

Table 8. Ru-Cl stretching frequencies (cm^{-1}) and highest mass peaks in the mass spectra results for various tethered complexes.

Entry Number	Complex	$\nu(\text{Ru-Cl})$ (cm^{-1})	Highest Mass Ion	m/z
1	$[\text{RuCl}_2(\eta^1:\eta^6\text{-Me}_2\text{P}\sim\text{Ph})]$ (248)	297, 278	$[\text{M}^+]^{\text{a}}$	352
2	$[\text{RuCl}_2(\eta^1:\eta^6\text{-Ph}_2\text{P}\sim\text{Ph})]$ (222)	303, 277	$[\text{M}^+]^{\text{b}}$	476
3	$[\text{RuCl}_2(\eta^1:\eta^6\text{-}i\text{-Pr}_2\text{P}\sim\text{Ph})]$ (249)	292, 272	$[\text{M}^+]^{\text{b}}$	409
4	$[\text{RuCl}_2(\eta^1:\eta^6\text{-Cy}_2\text{P}\sim\text{Ph})]$ (225)	292, 271	$[\text{M}^+]^{\text{b}}$	488
5	$[\text{RuCl}_2(\eta^1:\eta^6\text{-}t\text{-Bu}_2\text{P}\sim\text{Ph})]$ (253)	293, 266	$[\text{M}^+]^{\text{a}}$	436
6	$[\text{RuCl}_2(\eta^1:\eta^6\text{-Ph}_2\text{P}\sim\text{-}2,4,6\text{-C}_6\text{H}_2\text{Me}_3)]$ (250)	304, 288	$[\text{M}^+]^{\text{b}}$	518
7	$[\text{RuCl}_2(\eta^1:\eta^6\text{-Ph}_2\text{P}\sim\text{C}_6\text{Me}_5)]$ (251)	307, 286	$[\text{M}^+]^{\text{b}}$	546
8	$[\text{RuCl}_2(\eta^1:\eta^6\text{-Ph}_2\text{PCH}_2\text{SiMe}_2\text{Ph})]$ (252)	303, 270	$[\text{M}^+]^{\text{a}}$	508

^aFAB; ^bEI. $\sim = (\text{CH}_2)_3$

3.2.5 Structural Data

The molecular structures of the tethered compounds $[\text{RuCl}_2(\eta^1:\eta^6\text{-Me}_2\text{P}(\text{CH}_2)_3\text{Ph})]$ (**248**), $[\text{RuCl}_2(\eta^1:\eta^6\text{-}i\text{-Pr}_2\text{P}(\text{CH}_2)_3\text{Ph})]$ (**249**), $[\text{RuCl}_2(\eta^1:\eta^6\text{-}t\text{-Bu}_2\text{P}(\text{CH}_2)_3\text{Ph})]$ (**253**), $[\text{RuCl}_2(\eta^1:\eta^6\text{-Ph}_2\text{P}(\text{CH}_2)_3\text{-}2,4,6\text{-C}_6\text{H}_2\text{Me}_3)]$ (**250**), $[\text{RuCl}_2(\eta^1:\eta^6\text{-Ph}_2\text{P}(\text{CH}_2)_3\text{C}_6\text{Me}_5)]$ (**251**) and $[\text{RuCl}_2(\eta^1:\eta^6\text{-Ph}_2\text{PCH}_2\text{SiMe}_2\text{Ph})]$ (**252**) have been determined by single crystal X-ray analysis [Drs A. D. Bond and T. Khimyak for **249**, Dr J. E. Davies for **253** and Dr. T. Khimyak for **250** (Cambridge); Dr A. J. Edwards for **251**[†] and Dr A. C. Willis for **248** and **252** (ANU)]. Chem3D representations of **249**, **251** and **252** are shown in Figures 14, 15 and 16, respectively. A comparative discussion of the non-tethered and tethered complexes will be given in Section 3.5.

[†]Data were collected by Dr M. J. Hardie at Monash University.

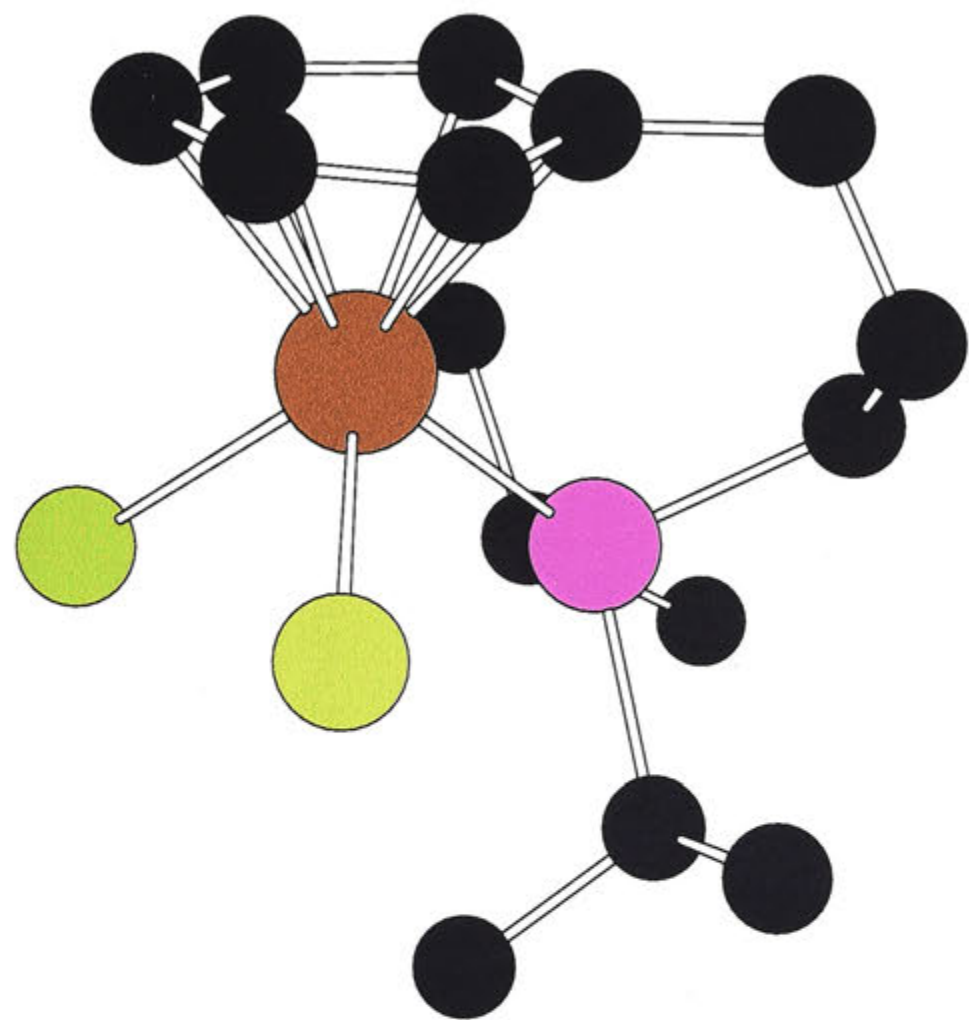


Figure 14. Chem3D representation of the molecular structure of $[\text{RuCl}_2(\eta^1:\eta^6\text{-}i\text{-Pr}_2\text{P}(\text{CH}_2)_3\text{Ph})]$ (**249**). Hydrogen atoms have been omitted for clarity.

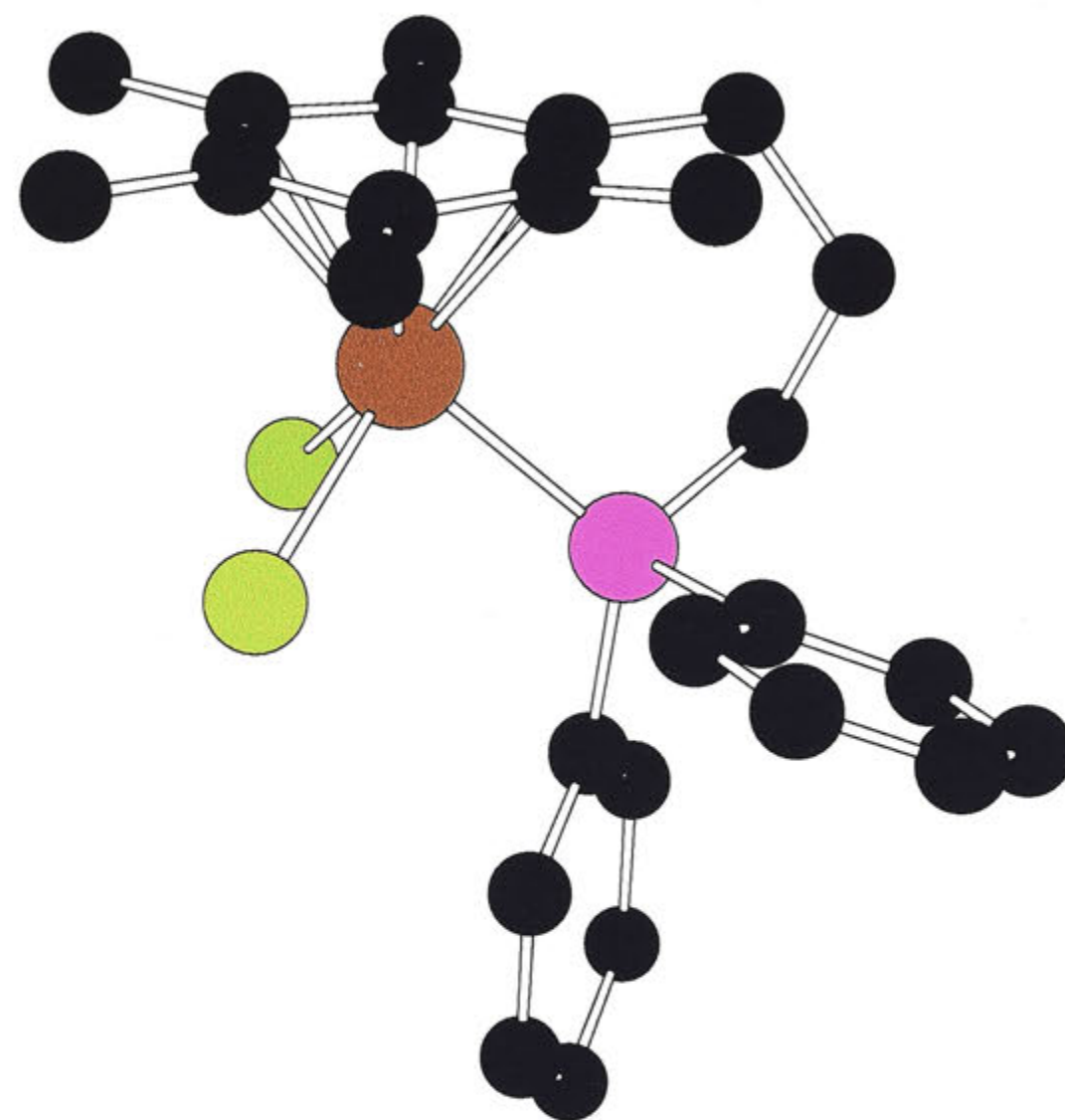


Figure 15. Chem3D representation of the molecular structure of $[\text{RuCl}_2(\eta^1:\eta^6\text{-Ph}_2\text{P}(\text{CH}_2)_3\text{C}_6\text{Me}_5)]$ (**251**). Hydrogen atoms have been omitted for clarity.

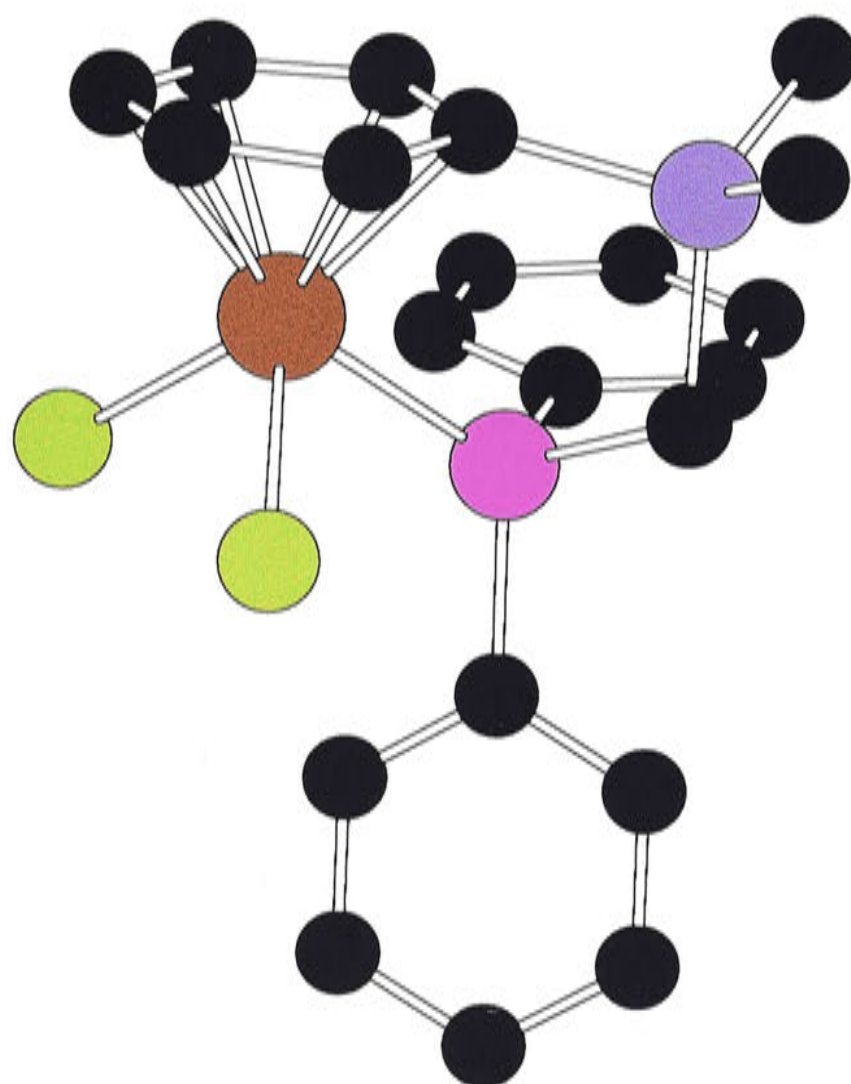


Figure 16. Chem3D representation of the molecular structure of $[\text{RuCl}_2(\eta^1:\eta^6\text{-Ph}_2\text{PCH}_2\text{SiMe}_2\text{Ph})]$ (**252**). Hydrogen atoms have been omitted for clarity.

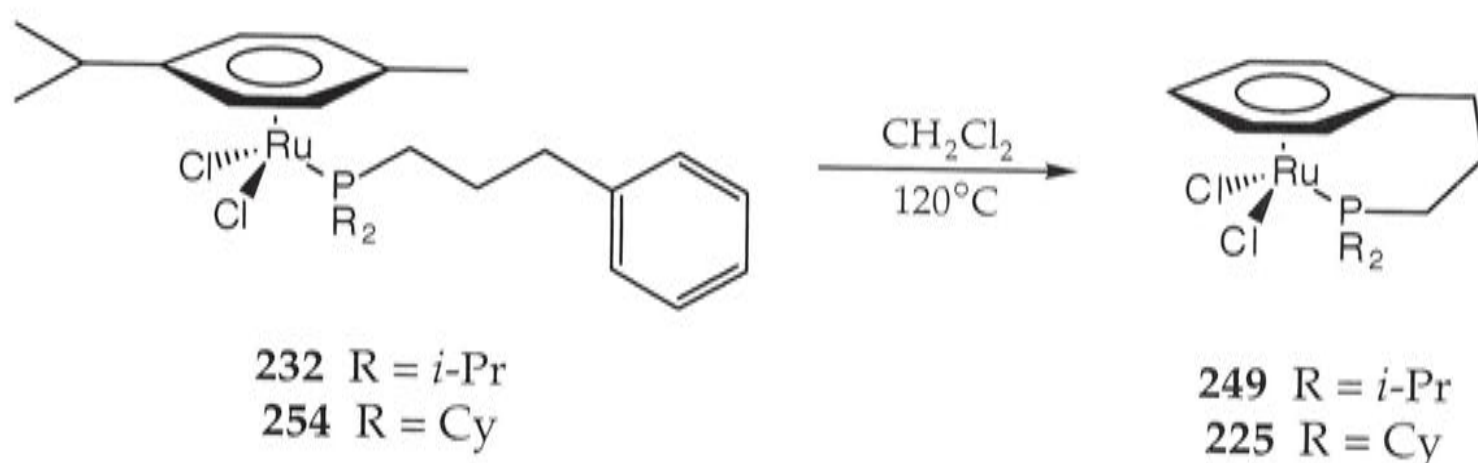
3.2.6 Formation of Tethered Complexes from η^6 -Benzene and η^6 -*p*-Cymene Precursor Complexes

In general, the η^6 -benzene and η^6 -*p*-cymene complexes were not as suitable as the η^6 -methyl *o*-toluate compounds as precursors to the tethered complexes, mainly because they could only be employed for some of the tertiary phosphines prepared in Chapter 2.

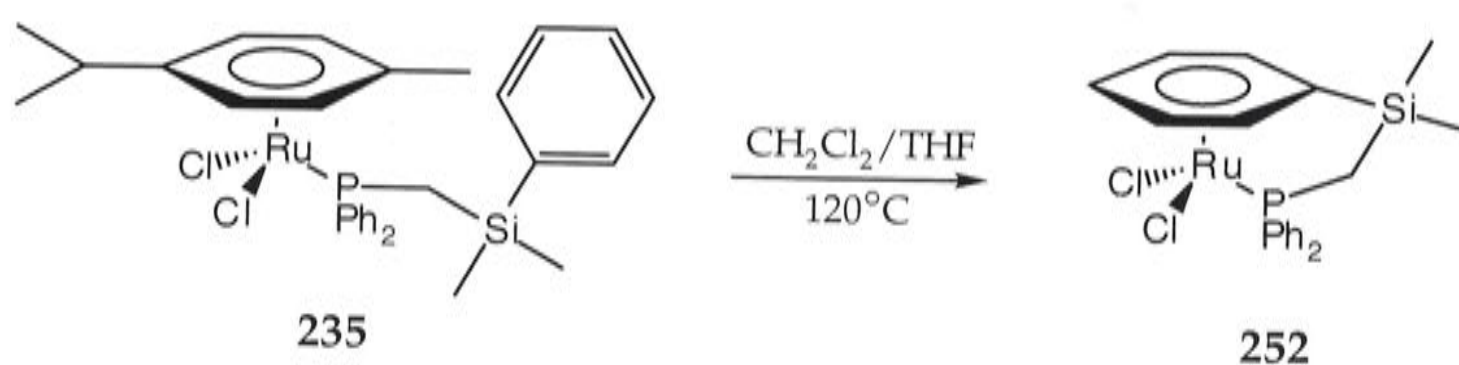
The η^6 -*p*-cymene of $[\text{RuCl}_2(\eta^6\text{-1,4-MeC}_6\text{H}_4\text{CHMe}_2)(\eta^1\text{-R}_2\text{P}(\text{CH}_2)_3\text{Ph})]$ ($\text{R} = i\text{-Pr}$ (**232**), Cy (**254**)) and $[\text{RuCl}_2(\eta^6\text{-1,4-MeC}_6\text{H}_4\text{CHMe}_2)(\text{Ph}_2\text{PCH}_2\text{SiMe}_2\text{Ph})]$ (**235**) was displaced at 120°C in CH_2Cl_2 to give rise to the tethered species $[\text{RuCl}_2(\eta^1:\eta^6\text{-R}_2\text{P}(\text{CH}_2)_3\text{Ph})]$ ($\text{R} = i\text{-Pr}$ (**249**), Cy (**225**)) (Scheme 57) and $[\text{RuCl}_2(\eta^1:\eta^6\text{-Ph}_2\text{PCH}_2\text{SiMe}_2\text{Ph})]$ (**252**) (Scheme 58), respectively, reaction times ranging from 42-168 hours. Though the yields of complexes **249** and **225** formed from the *p*-cymene precursors are comparable to those formed from the methyl *o*-toluate analogues, the reactions are

considerably slower. For example, conversion of the methyl *o*-toluate precursor $[\text{RuCl}_2(\eta^6\text{-1,2-MeC}_6\text{H}_4\text{CO}_2\text{Me})(\eta^1\text{-}i\text{-Pr}_2\text{P}(\text{CH}_2)_3\text{Ph})]$ (**238**) into the tethered species **249** required 6 hours (*cf.* 42 hours from **232**). The reaction of **254** to give the tethered species $[\text{RuCl}_2(\eta^1:\eta^6\text{-Cy}_2\text{P}(\text{CH}_2)_3\text{Ph})]$ (**225**) was also successful at 80°C in CH_2Cl_2 , though the reaction was much slower than that at 120°C. It was also possible to prepare complexes **249** and **225** directly from the *p*-cymene dimer $[\text{RuCl}_2(\eta^6\text{-1,4-MeC}_6\text{H}_4\text{CHMe}_2)]_2$ (**216**) and the phosphines $\text{R}_2\text{P}(\text{CH}_2)_3\text{Ph}$ ($\text{R} = i\text{-Pr}$ (**196**), Cy (**197**)), respectively, allowing the non-tethered complexes **232** and **254** to form *in situ*. The reaction of the *p*-cymene dimer **216** and $\text{Ph}_2\text{PCH}_2\text{SiMe}_2\text{Ph}$ (**201**) *in situ* to give $[\text{RuCl}_2(\eta^1:\eta^6\text{-Ph}_2\text{PCH}_2\text{SiMe}_2\text{Ph})]$ (**252**) was not investigated.

Under the same conditions it was not possible to displace the η^6 -*p*-cymene of either $[\text{RuCl}_2(\eta^6\text{-1,4-MeC}_6\text{H}_4\text{CHMe}_2)(\eta^1\text{-Ph}_2\text{P}(\text{CH}_2)_3\text{Ph})]$ (**223**), $[\text{RuCl}_2(\eta^6\text{-1,4-MeC}_6\text{H}_4\text{CHMe}_2)(\eta^1\text{-Ph}_2\text{P}(\text{CH}_2)_3\text{-2,4,6-C}_6\text{H}_2\text{Me}_3)]$ (**233**) or $[\text{RuCl}_2(\eta^6\text{-1,4-MeC}_6\text{H}_4\text{CHMe}_2)(\eta^1\text{-Ph}_2\text{P}(\text{CH}_2)_3\text{C}_6\text{Me}_5)]$ (**234**). No tethered complexes were formed and the precursors remained unchanged, as shown by ^1H NMR and $^{31}\text{P}\{^1\text{H}\}$ -NMR spectroscopy. The conditions used in these attempts are summarised in Table 10, entries 15, 19 and 22, respectively. The reaction of $[\text{RuCl}_2(\eta^6\text{-1,4-MeC}_6\text{H}_4\text{CHMe}_2)(\eta^1\text{-Me}_2\text{P}(\text{CH}_2)_3\text{Ph})]$ (**231**) under analogous conditions was not investigated.



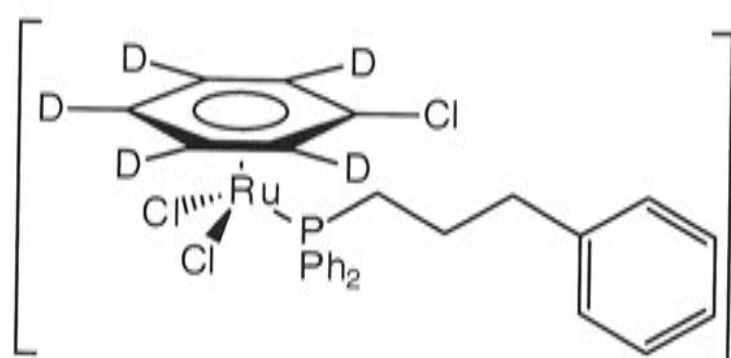
Scheme 57. Alternative preparation of the tethered complexes **249** and **225**.



Scheme 58. Alternative preparation of the tethered complex **252**.

Smith and Wright's claim⁷ that $[\text{RuCl}_2(\eta^1:\eta^6\text{-Ph}_2\text{P}(\text{CH}_2)_3\text{Ph})]$ (**222**) was formed in 50% yield by heating the *p*-cymene complex $[\text{RuCl}_2(\eta^6\text{-1,4-MeC}_6\text{H}_4\text{CHMe}_2)(\eta^1\text{-Ph}_2\text{P}(\text{CH}_2)_3\text{Ph})]$ (**223**) in chlorobenzene could not be confirmed, (see Table 10, entry 12) despite many attempts. An NMR experiment in *d*₅-chlorobenzene (Table 10, entry 13) showed that all of the *p*-cymene was displaced from **223** after 144 hours at 120°C, as shown by ¹H NMR spectroscopy, but the tethered species **222** was not formed. Instead, a new species, which showed a broad signal in the ³¹P{¹H}-NMR spectrum at δ 29.6, was observed. Its ²H NMR spectrum showed a triplet at δ 4.61 ($J = 7$ Hz), a doublet at δ 5.33 ($J = 6.5$ Hz) and a triplet at δ 6.46 ($J = 7$ Hz), which suggests the presence of $\eta^6\text{-d}_5\text{-chlorobenzene}$. The chemical shifts of the PPh₂ and CH₂ groups in the ¹H NMR spectrum were different from those observed for the parent complex **223**. Hence, it is postulated that the intermediate species $[\text{RuCl}_2(\eta^6\text{-C}_6\text{D}_5\text{Cl})(\eta^1\text{-Ph}_2\text{P}(\text{CH}_2)_3\text{Ph})]$ (**255**) formed in solution. The NMR scale reaction was also carried out in chlorobenzene containing *d*₅-chlorobenzene (*ca* 20%), to provide a lock to enable the reaction to be monitored by ³¹P{¹H}-NMR spectroscopy (Table 10, entry 14). The ³¹P{¹H}-NMR spectra showed a new broad signal at δ 29.6 that formed as the starting material was consumed. Again, the ²H NMR spectrum showed signals characteristic of $\eta^6\text{-d}_5\text{-chlorobenzene}$. Presumably both C₆H₅Cl and C₆D₅Cl are coordinated to the Ru(II), but the presence of the $\eta^6\text{-C}_6\text{H}_5\text{Cl}$ complex could not be confirmed by ¹H NMR spectroscopy, owing to the large excess of chlorobenzene. Attempts to isolate the intermediate species **255** were unsuccessful; decomposition occurred, and signals assignable to

free phosphine oxide, $\text{Ph}_2\text{P}(\text{O})(\text{CH}_2)_3\text{Ph}$, were observed in the ^1H and $^{31}\text{P}\{^1\text{H}\}$ -NMR spectra. A small amount of the tethered complex $[\text{RuCl}_2(\eta^1:\eta^6\text{-Ph}_2\text{P}(\text{CH}_2)_3\text{Ph})]$ (**222**) was observed in the $^{31}\text{P}\{^1\text{H}\}$ -NMR spectra during the course of both reactions, but was not present at the conclusion of the experiments. Likewise, the tethered compound $[\text{RuCl}_2(\eta^1:\eta^6\text{-Me}_2\text{P}(\text{CH}_2)_3\text{Ph})]$ (**248**) could not be prepared by heating $[\text{RuCl}_2(\eta^6\text{-1,4-MeC}_6\text{H}_4\text{CHMe}_2)(\eta^1\text{-Me}_2\text{P}(\text{CH}_2)_3\text{Ph})]$ (**231**) in chlorobenzene (Table 10, entry 1).

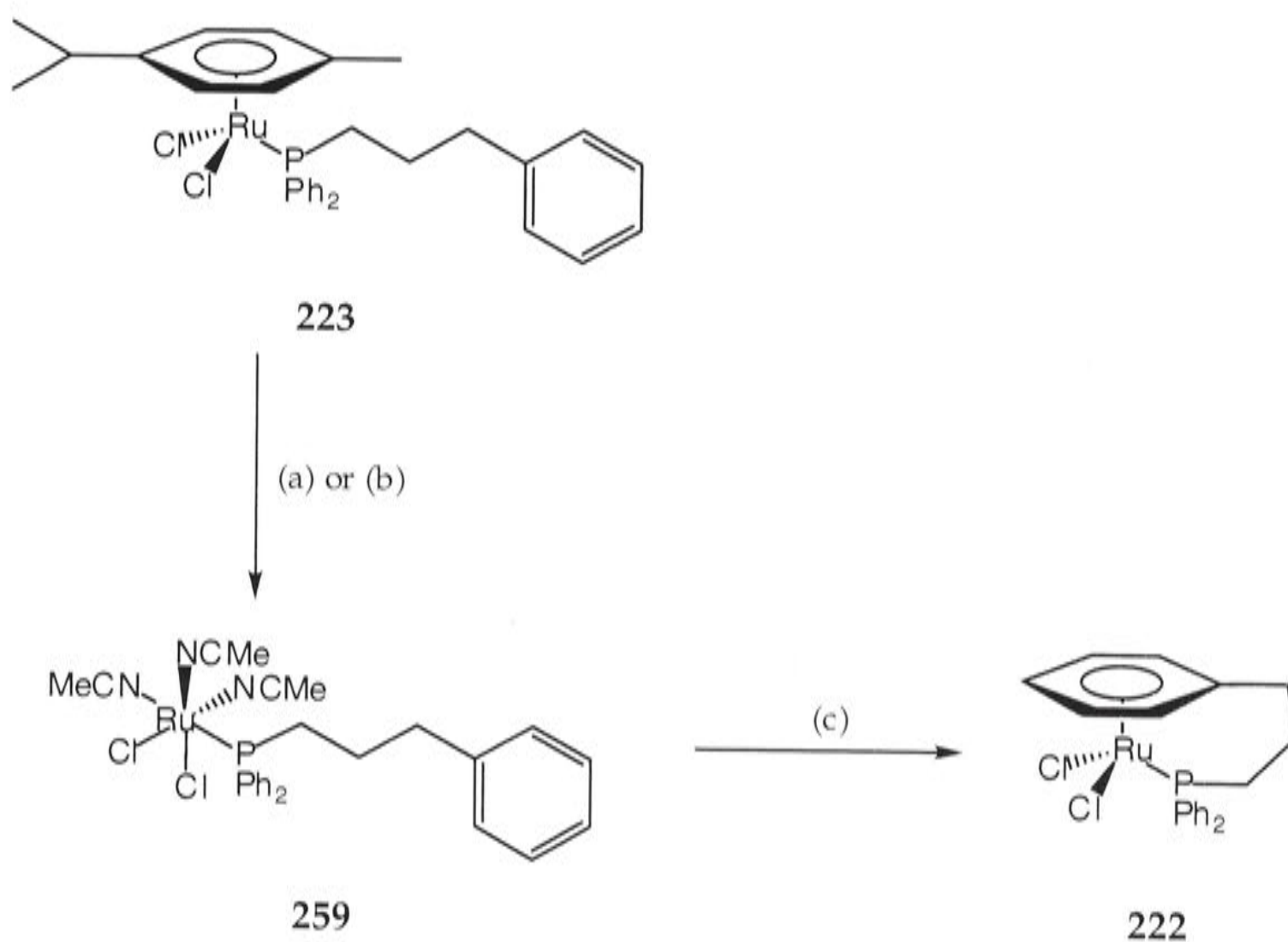


255

These failures are surprising in the light of the recent report by Lee *et al.*²⁸ of the preparation of complexes $[\text{RuCl}_2(\eta^1:\eta^6\text{-R}_2\text{P}(\text{CH}_2)_2\text{Ph})]$ ($\text{R} = \text{Et}$ (**256**), Ph (**257**) and Cy (**258**)) by similar methods (see Chapter 7, Section 7.2), where the chain consists of only two methylene units.

Although reported in reference(7), the formation of $[\text{RuCl}_2(\eta^1:\eta^6\text{-Ph}_2\text{P}(\text{CH}_2)_3\text{Ph})]$ (**222**) from $[\text{RuCl}_2(\eta^6\text{-1,4-MeC}_6\text{H}_4\text{CHMe}_2)(\eta^1\text{-Ph}_2\text{P}(\text{CH}_2)_3\text{Ph})]$ (**223**) in refluxing chlorobenzene is not mentioned in the Ph.D. dissertation of P. D. Smith.⁸ It is not clear what is the cause of this discrepancy. The thesis states that the tethered complex **222** was prepared from the intermediate tris(acetonitrile) species $[\text{RuCl}_2(\text{NCMe})_3(\eta^1\text{-Ph}_2\text{P}(\text{CH}_2)_3\text{Ph})]$ (**259**), and not from **223** itself, (**259** was obtained from the *p*-cymene species $[\text{RuCl}_2(\eta^6\text{-1,4-MeC}_6\text{H}_4\text{CHMe}_2)(\eta^1\text{-Ph}_2\text{P}(\text{CH}_2)_3\text{Ph})]$ (**223**)), in contrast with the statement in the publication.⁷ Controlled exhaustive anodic oxidation of **223** in acetonitrile was claimed, in both the publication⁷ and the thesis,⁸ to give to the tris(acetonitrile) complex

259 (the yield could not be determined due to residual electrolyte) (Scheme 59a), which, according to the thesis only, was then treated with trifluoroacetic acid and heated at reflux in chlorobenzene for 16 hours to afford the tethered species **222** (Scheme 59c). Although the description of the preparation of the tethered species **222** in the experimental section is highly ambiguous, the best interpretation appears to be that two separate experiments gave yields of 78 and 18%. The adduct **259** was also prepared by irradiation of **223** in acetonitrile (Scheme 59b), and was converted into the tethered species **222** by the method described above. The preparation of the tris(acetonitrile) adduct by anodic oxidation was the preferred procedure, in spite of both the time involved and the problem of removing the residual electrolyte, since photolysis did not exclusively give rise to **259**. The ligand disposition of complex **259** is that shown in references(7,8).



Scheme 59. Preparation of the tethered complex **222** according to the text in reference(8). Reaction conditions: (a) platinum gauze working electrode, 0.1M [Bu₄N]PF₆, CPE at + 1.22 V (*vs* Fc^{0/1}) to form an intermediate, followed by CPE at - 0.28 V (*vs* Fc^{0/1}) to afford complex **259**; (b) *hν*, MeCN; (c) CF₃CO₂H, C₆H₅Cl, 130°C.

In view of the observed lability of methyl *o*-toluate coordinated to Ru(II), an attempt was made to use $[\text{RuCl}_2(\eta^6\text{-1,2-MeC}_6\text{H}_4\text{CO}_2\text{Me})]_2$ (**224**) as a precursor to the peralkylated di- μ -chloro dimers $[\text{RuCl}_2(\eta^6\text{-C}_6\text{Me}_6)]_2$ (**67**), and $[\text{RuCl}_2(\eta^6\text{-C}_6\text{Et}_6)]_2$ (**260**). Whilst fusion of **224** with an excess of C_6Me_6 gave rise to **67**, under the conditions reported for the *p*-cymene dimer **216**,⁴ this could not be extended to **260**. The methyl *o*-toluate was displaced when **224** and C_6Et_6 were fused under the same conditions. The ^1H NMR spectrum of the isolated brown solid was consistent with the presence of $[\text{RuCl}_2(\eta^6\text{-C}_6\text{Et}_6)]_2$ (**260**), and the mass spectrum (EI) showed a peak corresponding to $[\text{M-Cl}]^+$. However, elemental analysis did not agree with the formulation, and the nature of the product is not known.

Attempts to prepare $[\text{RuCl}_2(\eta^1:\eta^6\text{-Ph}_2\text{P}(\text{CH}_2)_3\text{Ph})]$ (**222**) from the benzene precursor $[\text{RuCl}_2(\eta^6\text{-C}_6\text{H}_6)(\eta^1\text{-Ph}_2\text{P}(\text{CH}_2)_3\text{Ph})]$ (**227**) by heating or irradiation were unsuccessful (see Table 10, entries 3-11). The nature of the product obtained by heating **227** in acetonitrile will be discussed in Chapter 4 (see Section 4.2).

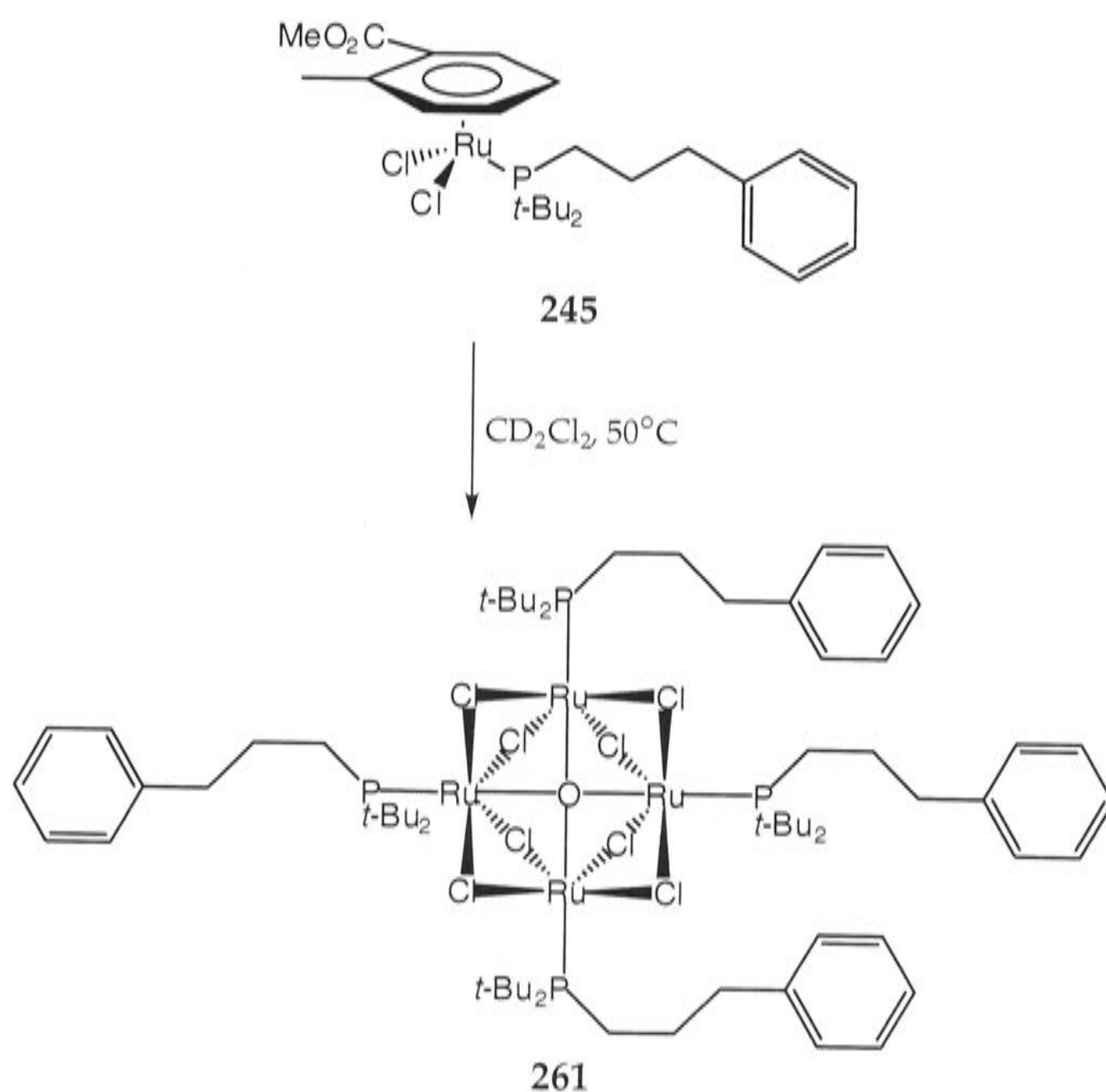
3.2.7 Reactions of Complexes Incorporating *t*-Bu₂P(CH₂)₃Ph (**198**)

As mentioned in Section 3.2.1, the non-tethered complexes $[\text{RuCl}_2(\eta^6\text{-C}_6\text{H}_6)(\eta^1\text{-}t\text{-Bu}_2\text{P}(\text{CH}_2)_3\text{Ph})]$ (**243**), $[\text{RuCl}_2(\eta^6\text{-1,4-MeC}_6\text{H}_4\text{CHMe}_2)(\eta^1\text{-}t\text{-Bu}_2\text{P}(\text{CH}_2)_3\text{Ph})]$ (**244**) and $[\text{RuCl}_2(\eta^6\text{-1,2-MeC}_6\text{H}_4\text{CO}_2\text{Me})(\eta^1\text{-}t\text{-Bu}_2\text{P}(\text{CH}_2)_3\text{Ph})]$ (**245**) lost their η^6 -arene at room temperature when the solutions were allowed to stand. Further, the ^1H NMR spectrum of the crude product obtained from reaction of $[\text{RuCl}_2(\eta^6\text{-1,2-MeC}_6\text{H}_4\text{CO}_2\text{Me})]_2$ (**224**) with *t*-Bu₂P(CH₂)₃Ph (**198**) at room temperature displayed signals due to both free and η^6 -coordinated methyl *o*-toluate. A brief investigation into the lability of the η^6 -methyl *o*-toluate of **245** was therefore carried out. A solution of crude **245** in *d*₂-dichloromethane darkened when heated at 50°C in a sealed NMR

tube for 28 hours (Table 10, entry 18). The $^{31}\text{P}\{^1\text{H}\}$ -NMR spectrum indicated that a mixture of products had been formed, including a small amount of the tethered species $[\text{RuCl}_2(\eta^1:\eta^6\text{-}t\text{-Bu}_2\text{P}(\text{CH}_2)_3\text{Ph})]$ (**253**), as well as a species that displayed a $^{31}\text{P}\{^1\text{H}\}$ -NMR resonance at *ca* δ 60.6; these other species were not characterised.

In one experiment, black crystals were deposited from the solution mentioned above, which were identified as the tetranuclear complex $[\text{Ru}_4(\mu_4\text{-O})(\mu_2\text{-Cl})_8(\eta^1\text{-}t\text{-Bu}_2\text{P}(\text{CH}_2)_3\text{Ph})_4]$ (**261**) (Scheme 60) by X-ray crystallography and mass spectrometry. Although the nature of the central atom (C, N or O) could not be determined unambiguously by X-ray crystallography, the mass spectrum (FAB) confirmed that the central atom was oxygen; the highest mass peak observed was m/z 1762, which corresponds to that expected for the parent ion. The oxygen atom is most probably derived from adventitious water present in the solution. The Chem3D representation of $[\text{Ru}_4(\mu_4\text{-O})(\mu_2\text{-Cl})_8(\eta^1\text{-}t\text{-Bu}_2\text{P}(\text{CH}_2)_3\text{Ph})_4]$ (**261**) is shown in Figure 17 [Dr A. C. Willis (ANU)]. The oxygen atom is equally disordered over two sites. There are four ruthenium atoms, each in an octahedral environment, coordinated in a pseudo-square planar arrangement around the disordered oxygen atoms. Each ruthenium atom is coordinated to two bridging chlorine atoms, and a phosphine, $t\text{-Bu}_2\text{P}(\text{CH}_2)_3\text{Ph}$ (**198**), coordinated only through the phosphorus atom, completes the coordination sphere. There is virtually no difference between the various Ru-P bond lengths (average = 2.32 Å), whilst the Ru-O bonds lie in the range 2.19-2.27 Å. The Ru-Cl bond lengths lie in the range 2.39-2.43 Å, which is similar to those observed for the various non-tethered and tethered arene complexes (see Section 3.5). The ruthenium atoms are separated by distances ranging between 3.08-3.12 Å. The tetranuclear species **261** is uncharged, hence the average oxidation state of each metal atom is +2.5. The complex shows an ESR spectrum in frozen CH_2Cl_2 at *ca* 5K with three g -values ($g_1 = 2.57$, $g_2 = 2.48$, $g_3 = 2.41$), which is similar to those of the mononuclear arene-ruthenium(III) complexes (see Chapter 5, Section 5.1), and to those of the

dinuclear complexes of the type $[\text{Ru}_2(\mu\text{-Cl})_3\text{L}_3]^{1+}$,^{28a} but at this stage, more detail comments cannot be made. Thus complex **261** appears to be paramagnetic, although the possibility that the ESR spectrum is due to an impurity cannot be discounted. The ESR spectrum does not directly provide any information about the oxidation state of the metal atoms in **261**. The d_2 -dichloromethane solution shows a highly deshielded singlet in the $^{31}\text{P}\{^1\text{H}\}$ -NMR spectrum at δ 267.0, which is well out of the range of diamagnetic Ru(II) complexes, and may well be a consequence of the paramagnetism. The elemental analysis was not in good agreement (*ca* 1.7% low in C, 1.2% in P) with that expected for $[\text{Ru}_4(\mu_4\text{-O})(\mu_2\text{-Cl})_8(\eta^1\text{-}t\text{-Bu}_2\text{P}(\text{CH}_2)_3\text{Ph})_4]$ (**261**).



Scheme 60. Formation of the tetranuclear species **261**.

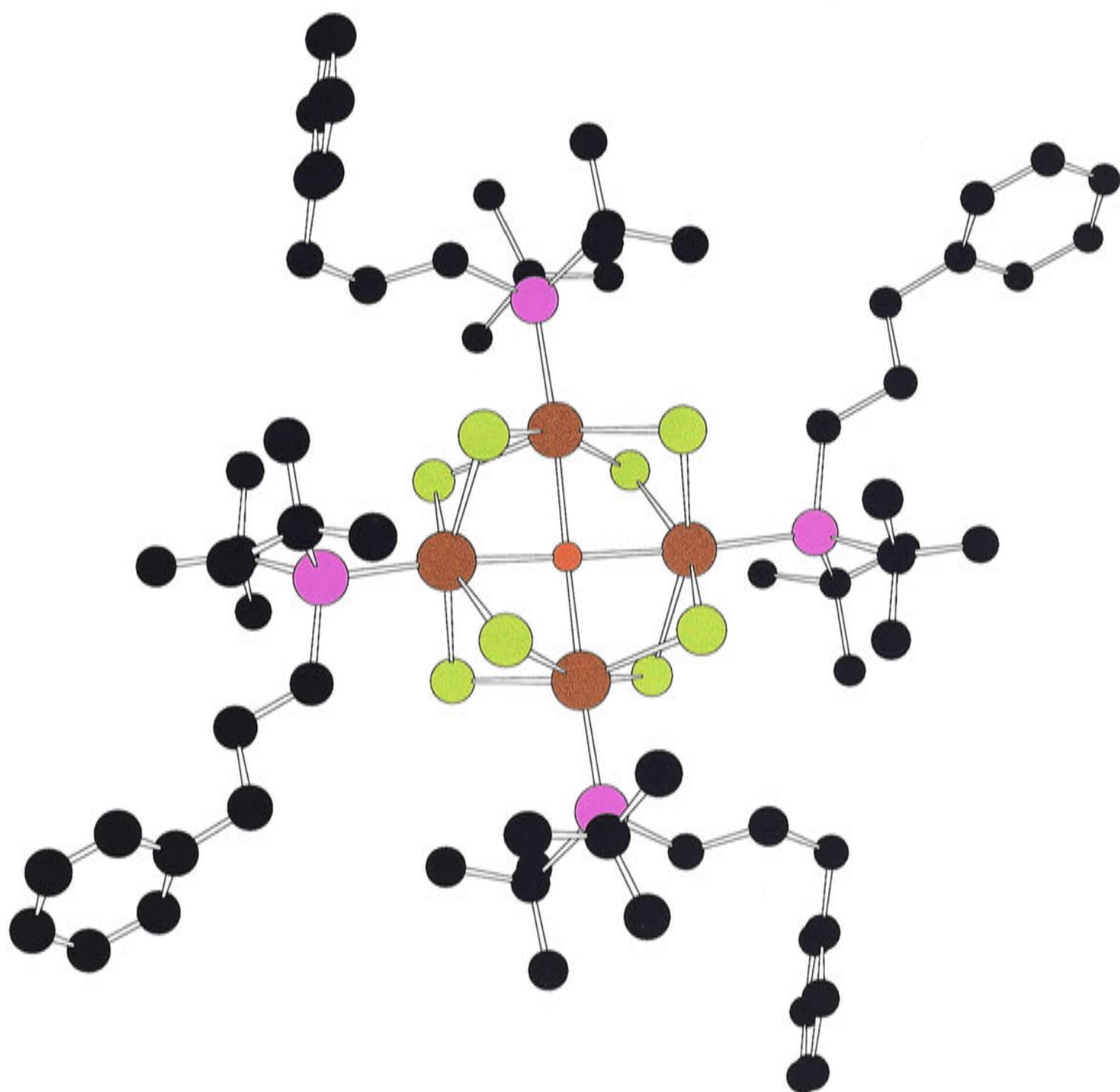


Figure 17. Chem3D representation of the molecular structure of $[\text{Ru}_4(\mu_4\text{-O})(\mu_2\text{-Cl})_8(\eta^1\text{-}t\text{-Bu}_2\text{P}(\text{CH}_2)_3\text{Ph})_4]$ (**261**). Hydrogen atoms have been omitted for clarity (average position for the oxygen atom is shown).

The Ru-O-Ru bonds in the Ru_4O unit of $[\text{Ru}_4(\mu_4\text{-O})(\mu_2\text{-Cl})_8(\eta^1\text{-}t\text{-Bu}_2\text{P}(\text{CH}_2)_3\text{Ph})_4]$ (**261**) can be compared to the Ru-O-Ru bond in $\text{K}_4[\text{Ru}_2(\mu_2\text{-O})\text{Cl}_{10}]$ ($\text{K}_4[\mathbf{262}]$), the anion of which was shown by Mellor *et al.* to be linear by X-ray crystallography.²⁹ The anion $[\mathbf{262}]^{4-}$ was also shown to be diamagnetic,²⁹ even though each Ru(IV) centre would be expected to have two unpaired electrons, although this feature was not accounted for until the following year by Dunitz and Orgel.³⁰ They suggest that the unpaired electrons were antiparallel but uncoupled, and, due to the long Ru \cdots Ru distance of 3.6 Å,²⁹ the possibility of electron pairing was discounted. The diamagnetism was explained by qualitative molecular-orbital theory, which showed that, in the ground state, all the electrons are in closed shells. The

two E_u orbitals, one from the ruthenium pair and one from O^{2-} , combine to give a bonding E_u^b orbital, which can be considered as a degenerate p -bonding orbital (Figure 18). The degree of π -bonding would be influenced by linearity of the anion $[262]^{4-}$, thus any departure from linearity would result in destabilisation of the complex $K_4[262]$.



Figure 18. One of the two perpendicular components of the bonding E_u^b π -orbital involving the Ru-O-Ru bonds in $[Ru_2(\mu_2-O)Cl_{10}]^{4-}$ ($[262]^{4-}$).³⁰

A more recent report has described the X-ray structure of $[262]^{4-}$ as a salt of the diprotonated form of histamine (4-(2-aminoethyl)-imidazole) $[C_5H_{11}N_3]_2[Ru_2(\mu_2-O)Cl_{10}]$.³¹ The Ru-O bond distance in $[262]^{4-}$ (*ca* 1.80 Å)³¹ is much shorter than that in $[Ru_4(\mu_4-O)(\mu_2-Cl)_8(\eta^1-t-Bu_2P(CH_2)_3Ph)_4]$ (**261**) (*ca* 2.22 Å), resulting in greater Ru-O-Ru separation in the latter (4.38 Å *vs* 3.6057 Å).³¹ However, the Ru-Cl distances in the two species are very similar (2.39-2.43 Å in **261** *vs* 2.35-2.38 Å in $[262]^{4-}$).³¹ A pentamethylcyclopentadienyl ruthenium(IV) complex containing a linear oxo-bridge and incorporating π -bonded ligands has been reported, namely $[Ru_2(\mu_2-O)Cl_4(\eta^5-C_5Me_5)_2]$.³² The Ru-O and Ru-Cl bond lengths are very similar to those observed in $[263]^{2-}$.^{31,32}

The Ru_4O unit of the molecular structure of $[Ru_4(\mu_4-O)(\mu_2-Cl)_8(\eta^1-t-Bu_2P(CH_2)_3Ph)_4]$ (**261**) is similar to the Ru_4O dianionic unit of the oxo cluster $[Ru_4(\mu_4-O)(\mu_2-Cl)_4(CO)_{10}]^{2-}$ ($[263]^{2-}$) ($[(Ph_3P)_2N]^+$ salt;^{33,34} $[NEt_4]^+$ salt³⁵) (see Figure 19). This, however, is where the similarities end; the bond lengths are very different in the two species since the oxidation state of the metal atoms in $[263]^{2-}$ is Ru(I). Further, the two sides of the tetranuclear unit in $[263]^{2-}$ are unbridged. The Ru-Cl bonds in $[263]^{2-}$ are of unequal lengths because the bridging chloride ligands do not lie directly over one another, in contrast to **261** (see Figure 20).

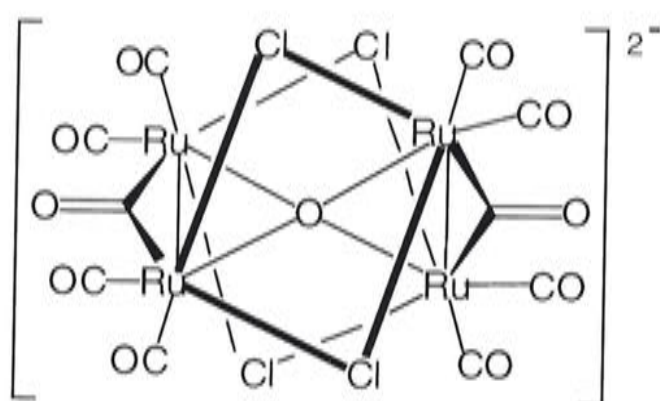


Figure 19. The oxo anion $[\text{Ru}_4(\mu_4\text{-O})(\mu_2\text{-Cl})_4(\text{CO})_{10}]^{2-}$ (**[263]**²⁻).³³⁻³⁵

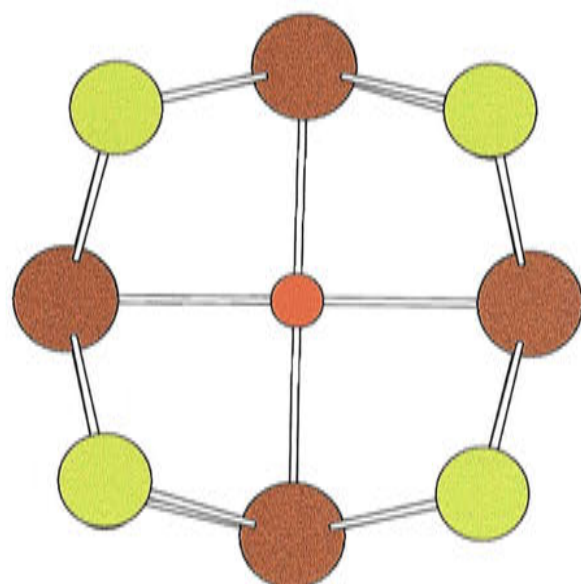
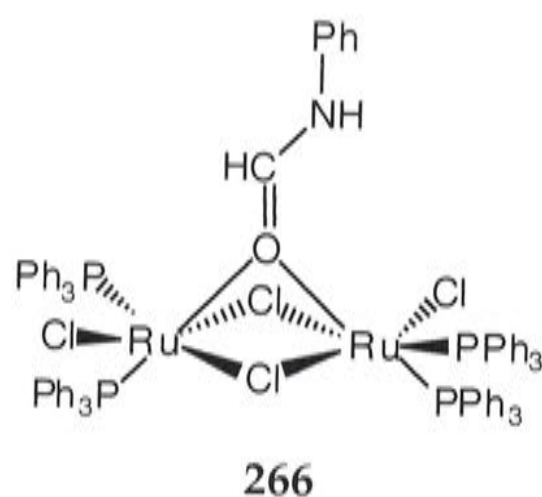


Figure 20. The $\text{Ru}_4(\mu_4\text{-O})(\mu_2\text{-Cl})_8$ unit of $[\text{Ru}_4(\mu_4\text{-O})(\mu_2\text{-Cl})_8(\eta^1\text{-}t\text{-Bu}_2\text{P}(\text{CH}_2)_3\text{Ph})_4]$ (**261**), showing the superposition of the μ-chloro ligands. The four phosphine ligands ($t\text{-Bu}_2\text{P}(\text{CH}_2)_3\text{Ph}$) have been omitted for clarity, and the average position of the oxygen atom is shown.

Other tetranuclear species containing planar M_4O units with a variety of transition metals have also been reported.³⁶⁻³⁸ These include vanadium, niobium and copper, in complexes $[\text{NBu}^n_4]_2[\text{V}_4(\mu_4\text{-O})(\mu_2\text{-Cl})_4\text{Cl}_4(\mu_2\text{-edt})_2]$ (edt = ethane-1,2-dithiolate),³⁶ $[\text{Nb}_4(\mu_4\text{-O})(\mu_2\text{-Cl})_8\{(\text{PhC})_4\}_2]^{2-}$ as $[\text{Mg}_2\text{Cl}_3(\text{THF})_6]^+$, Na^+ and $[\text{HPeEt}_3]^+$ salts,³⁷ and $[\text{Cu}_4(\mu_4\text{-O})\{\text{Zr}_2(\mu_4\text{-O})\}_2(\mu_2\text{-O-}i\text{-Pr})_8(\eta^1\text{-O-}i\text{-Pr})_{10}]$.³⁸ The only other planar M_4O unit to incorporate a Group 8 atom is the iron(III) species $[\text{Fe}_8(\mu_4\text{-O})(\mu_3\text{-O})_4(\eta^2\text{-OAc})_8(\text{tren})_4][\text{CF}_3\text{SO}_3]_6$ (tren = tris(2-aminoethyl)amine), which contains a central Fe_4O unit with four additional iron atoms (each of these are coordinated to a tren and acetate ligand) bound to the Fe_4O core *via* the μ₃-oxo groups.³⁹

If two of the Ru-Cl bonds in $[\text{Ru}_4(\mu_4\text{-O})(\mu_2\text{-Cl})_8(\eta^1\text{-}t\text{-Bu}_2\text{P}(\text{CH}_2)_3\text{Ph})_4]$ (**261**) were broken, then each of the octahedral ruthenium atoms would have three bridging and three terminal ligands. This arrangement is very similar to that in the series of confacial bioctahedra of the type $[\text{Ru}_2(\mu_2\text{-X})_3\text{Y}_6]^n$, where n can be a range of negative or positive integers depending on the ligands X and Y. Typical ligands are X = halide (F, Cl, Br, I), Y = halide, monodentate tertiary phosphines, tertiary arsines, ammonia, water and even η^6 -arenes, amongst others. The metal atoms can exist in a variety of different oxidation states, and many of these tris(μ_2 -halo) complexes are mixed-valence systems. Some examples include the $\text{Ru}^{\text{II/II}}$ complexes $[\text{Ru}_2(\mu_2\text{-I})_3(\text{PMe}_2\text{Ph})_6]^+$,⁴⁰ $[\text{Ru}_2(\mu_2\text{-F})_3(\text{PEt}_3)_6]^+$,⁴¹ $[\text{Ru}_2(\mu_2\text{-Cl})_3(\eta^6\text{-C}_6\text{H}_6)_2]^+$,⁴² and a more recent example of a complex containing a η^6 -arene, namely $[\text{Ru}_2(\mu_2\text{-Cl})_3\text{Cl}(\eta^6\text{-1,4-MeC}_6\text{H}_4\text{CHMe}_2)(\eta^4\text{-1,5-COD})]$,⁴³ and the $\text{Ru}^{\text{III/III}}$ complex $[\text{Ru}_2(\mu_2\text{-Br})_3\text{Br}_6]^{3-}$.⁴⁴ Some examples of mixed-valence tris(μ_2 -halo) complexes include the $\text{Ru}^{\text{II/III}}$ complexes $[\text{Ru}_2(\mu_2\text{-Cl})_3(\text{NH}_3)_6]^{2+}$ (**[264]**²⁺),⁴⁵ the neutral complex $[\text{Ru}_2(\mu_2\text{-Cl})_3\text{Cl}_2(\text{CO})_2(\text{P-}t\text{-Bu}_2\text{Me})_2]$ (**265**) incorporating *tert*-butyl groups on the terminally bound phosphine ligands,⁴⁶ and the stable mixed-valence $\text{Ru}^{\text{III/IV}}$ system $[\text{Ru}_2(\mu_2\text{-Cl})_3\text{Cl}_5\text{py}]^-$ (py = pyridine).⁴⁷ In the mixed-valence $\text{Ru}^{\text{II/III}}$ systems such as **[264]**²⁺ and **265** the average oxidation state is 2.5, identical to the average oxidation state observed in **261**.

There are some recent examples of dinuclear ruthenium species containing μ_2 -O bridges: the $\text{Ru}^{\text{II/II}}$ complexes $[\text{Ru}_2(\mu_2\text{-Cl})_2(\mu_2\text{-OH})(\eta^6\text{-arene})_2]^+$ (arene = benzene, *p*-cymene, 1,2,4,5-tetramethylbenzene and hexamethylbenzene)⁴⁸ and $[\text{Ru}_2(\mu_2\text{-Cl})_2(\mu_2\text{-O=CHNHPh})\text{Cl}_2(\text{PPh}_3)_4]$ (**266**).⁴⁹ The environment of the Ru(II) atom in **266** is very closely related to that in **261**, where a terminal phosphine is present instead of a chloride ligand.



Preliminary calculations using Density Functional Theory (DFT) performed by Dr John McGrady at the University of York⁵⁰ on the simplified tetranuclear species $[\text{Ru}_4(\mu_4\text{-O})(\mu_2\text{-Cl})_8(\text{PH}_3)_4]$ (**267**) have predicted that it would be paramagnetic with two unpaired electrons per tetranuclear unit, consistent with the observed paramagnetism. It does, however, have an unusual electronic structure. If **267** is considered, to a first approximation, as belonging to point group C_{4v} , then the oxygen p_z atomic orbital interacts with the totally symmetric combination of the Ru orbitals $d_{xz}/d_{yz}(a_1)$ and the p_x and p_y oxygen atomic orbitals interact with the appropriate combination of d_{xy} on the metal orbitals (e) (see the schematic energy orbital diagram in Figure 21). The schematic of the energy orbitals of **267** is very similar to the qualitative molecular-orbital assessment of $[\text{Ru}_2(\mu_2\text{-O})\text{Cl}_{10}]^{4+}$ (**[262]**⁴⁺) shown in Figure 18.³⁰ Since the oxygen ligand is a π -donor, this causes the three metal orbitals to be destabilised, and the most stable C_4 -symmetric state is the triplet ground state corresponding to the $(a_1)^1(e)^3$ configuration (see Figure 21). The orbital degeneracy gives rise to Jahn-Teller instability, so a small distortion occurs to the C_{2v} -symmetric structure, as illustrated in Figure 21. This results in unsymmetrical Ru-O bonds, calculated to be 2.10 and 2.19 Å (one long bond and one short). Although these are in the approximate range for the observed Ru-O distances (2.19-2.27 Å), the presence of the disorder in the crystals makes it impossible to determine whether there are two significantly different Ru-O separations. There is, however, a difference in the two distances Ru-O-Ru; Ru(1)-Ru(1*) (4.41 Å) is slightly longer than Ru(2)-Ru(2*) (4.37 Å), indicating that the shape containing the four ruthenium atoms is not a perfect square (atom labelling as shown in Figure 22). Therefore, if the oxygen atom were located in the centre of the metal

atoms, and were not disordered, two shorter and two longer Ru-O separations would be expected.

The models employed in the crystallography were based on a square (four ruthenium atoms at the corners) where the oxygen atom lay either above or below the plane containing the four ruthenium atoms. The model employed in the theoretical calculations was based on C_{4v} symmetry and the oxygen atom was located in the centre, whilst being free to move out of the plane of the metal atoms, but the Ru_4O unit was almost planar in the most stable structure. Thus it would appear that the oxygen would be predicted to lie within the plane of the ruthenium atoms if the disorder were not present in the crystal. The ranges of calculated Ru-P and Ru-Cl bond lengths, 2.28-2.33 Å and 2.46-2.47 Å, respectively, are also in good agreement with the experimental results (Ru-P: 2.3168(9)-2.3191(9) Å and Ru-Cl: 2.3867(9)-2.4250(9) Å). Whilst the theoretical calculations did not show any Ru-Ru bonding in the e orbitals, the a_1 orbital is formally Ru-Ru π -bonding. This implies that there is a net Ru-Ru bond order of 1/8; however, the Ru-Ru-overlap is weak, and the Ru-O bonding has more influence over the Ru-Ru bond distances. These were calculated to be 3.03 Å, again in good agreement with the experimental results (3.08-3.12 Å).

The information obtained from the theoretical calculations⁵⁰ raises many questions, but there are insufficient experimental data to answer them. Unfortunately further characterisation of **261** was prevented by the small amount isolated. Further studies should include electrochemical measurements, which may provide information about the possibility of communication between the metal centres, as well as the potential to add or subtract electrons from the energy levels indicated in Figure 21. The study could then be extended to other *t*-butyl substituted phosphines, which may allow isolation of a similar tetranuclear species without disorder at the central oxygen atom. Other tetranuclear species, containing only one phosphine per ruthenium, could potentially be prepared by the use of the

labile η^6 -methyl *o*-toluate precursors of the type $[\text{RuCl}_2(\eta^6\text{-1,2-MeC}_6\text{H}_4\text{CO}_2\text{Me})(t\text{-Bu}_2\text{PR})]$ (R = alkyl or alkoxy group).

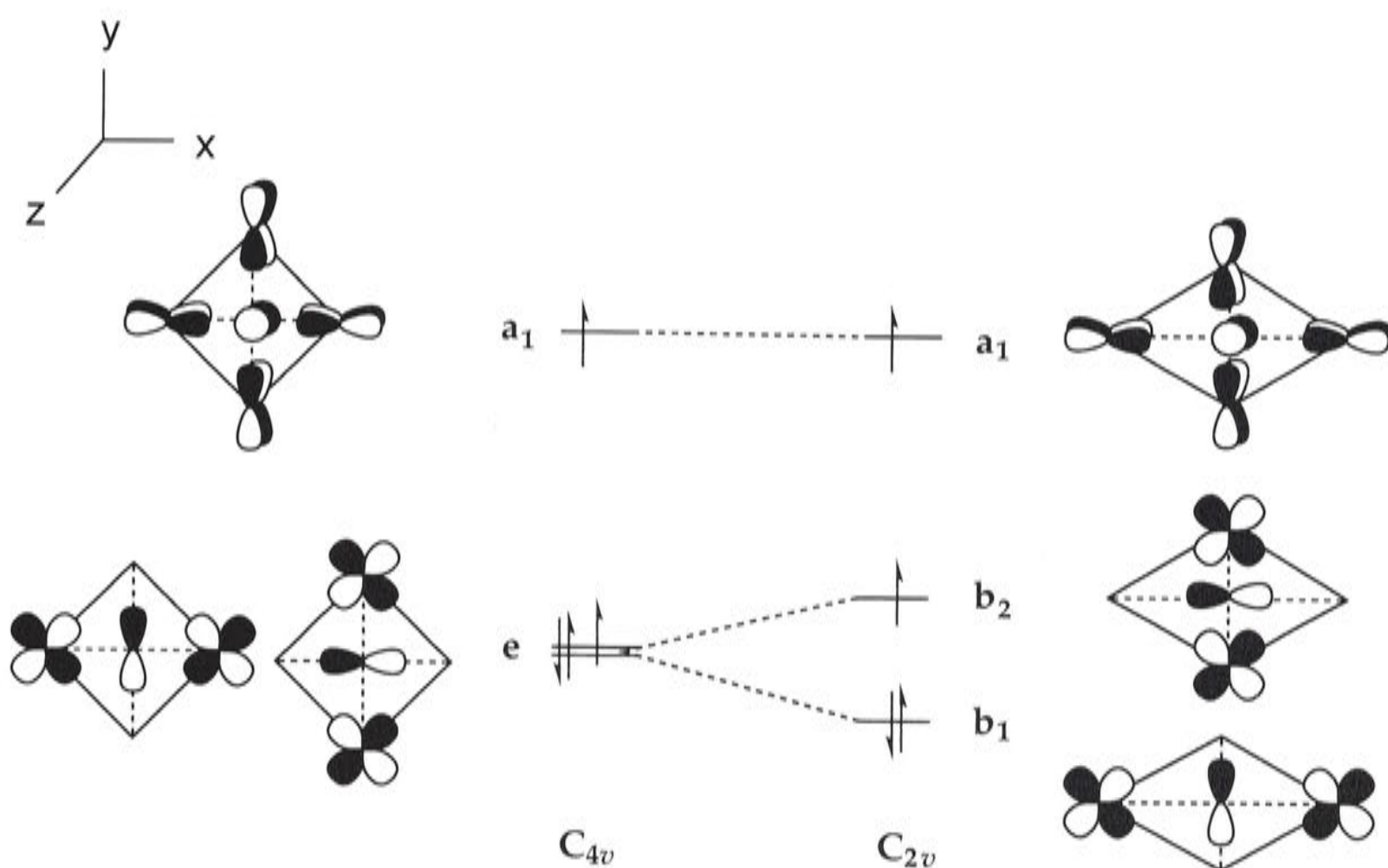


Figure 21. Schematic orbital energy diagram of the tetranuclear system $[\text{Ru}_4(\mu_4\text{-O}(\mu_2\text{-Cl})_8(\text{PH}_3)_4)]$ (267) in C_{4v} and C_{2v} symmetry, obtained from theoretical calculations.⁵⁰ For simplicity, the orbitals are represented with the atoms located as shown in Figure 22.

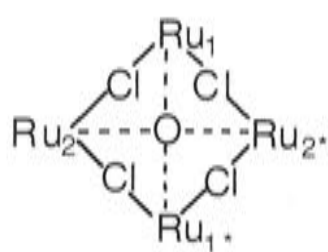


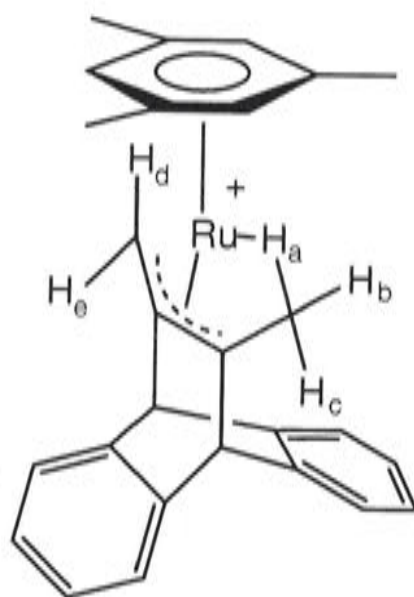
Figure 22. Diagrammatic representation of the tetranuclear species $[\text{Ru}_4(\mu_4\text{-O})(\mu_2\text{-Cl})_8(\text{PH}_3)_4]$ (267) used in the schematic orbital energy diagram (Figure 21), with the ruthenium atoms numbered as in the X-ray structure. The four remaining chloride ligands lie directly below those shown.

As mentioned in Section 3.2.3, the tethered complex $[\text{RuCl}_2(\eta^1:\eta^6\text{-}t\text{-Bu}_2\text{P}(\text{CH}_2)_3\text{Ph})]$ (253) is also unstable in solution. The $^{31}\text{P}\{^1\text{H}\}$ -NMR spectrum of a solution of the complex in d_2 -dichloromethane that had been left for several days displayed a resonance at *ca* δ 60.6. This

signal was also observed during the preparation of the non-tethered compounds $[\text{RuCl}_2(\eta^6\text{-C}_6\text{H}_6)(\eta^1\text{-}t\text{-Bu}_2\text{P}(\text{CH}_2)_3\text{Ph})]$ (**243**), $[\text{RuCl}_2(\eta^6\text{-1,4-MeC}_6\text{H}_4\text{CHMe}_2)(\eta^1\text{-}t\text{-Bu}_2\text{P}(\text{CH}_2)_3\text{Ph})]$ (**244**) and $[\text{RuCl}_2(\eta^6\text{-1,2-MeC}_6\text{H}_4\text{CO}_2\text{Me})(\eta^1\text{-}t\text{-Bu}_2\text{P}(\text{CH}_2)_3\text{Ph})]$ (**245**), and in the preparation of $[\{\text{RuCl}_2(t\text{-Bu}_2\text{P}(\text{CH}_2)_3\text{Ph})\}_4\text{O}]$ (**261**). It is also observed in the $^{31}\text{P}\{^1\text{H}\}$ -NMR spectrum of the crude reaction mixture from the preparation of the tethered species $[\text{RuCl}_2(\eta^1:\eta^6\text{-}t\text{-Bu}_2\text{P}(\text{CH}_2)_3\text{Ph})]$ (**253**), as well as in the formation of $[\{\text{RuCl}_2(\eta^1\text{-}t\text{-Bu}_2\text{P}(\text{CH}_2)_3\text{Ph})\}_4\text{O}]$ (**261**). The species responsible for this signal is therefore formed both at room temperature and upon heating in dichloromethane. This signal is not due to free phosphine oxide, $t\text{-Bu}_2\text{P}(\text{O})(\text{CH}_2)_3\text{Ph}$, which occurs at δ 63.0. There are also additional signals in the ^1H NMR spectra observed under the same conditions, including a doublet at approximately δ 1.18 ($J = 13$ Hz), presumably due to *t*-butyl methyl groups, which lies upfield of the analogous resonances due to the desired product. There is also a broad signal at δ -0.5, which may belong to a species containing an agostic interaction between a hydrogen of one of the *t*-butyl methyl groups and a vacant site on the ruthenium. Agostic interactions of this type between remote $\text{M} \leftarrow \text{H-C}$ atoms have been observed for many metals, including ruthenium.⁵¹ For example, the ruthenium complex $[\text{Ru}(\eta^6\text{-C}_6\text{H}_3\text{Me}_3)(\text{C}_{18}\text{H}_{15})]^+$ (**268**) shows a broad multiplet in the ^1H NMR spectrum at δ -1.13, due to H_a , H_b , H_c , H_d and H_e .⁵² The species responsible for the resonance at δ 60.6 was not isolated.

Preliminary investigations showed that the tethered complex **253** was formed by heating a dichloromethane solution of $[\text{RuCl}_2(\eta^6\text{-1,4-MeC}_6\text{H}_4\text{CHMe}_2)(\eta^1\text{-}t\text{-Bu}_2\text{P}(\text{CH}_2)_3\text{Ph})]$ (**244**) at 120°C, though the reaction proceeds more slowly than from the corresponding ester complex **245**. Because of the complications discussed above, the possible formation of the tethered complex **253** in the *in situ* reaction of the parent dimers $[\text{RuCl}_2(\eta^6\text{-1,4-}$

$\text{MeC}_6\text{H}_4\text{CHMe}_2)_2$ (**216**) or $[\text{RuCl}_2(\eta^6\text{-1,2-MeC}_6\text{H}_4\text{CO}_2\text{Me})]_2$ (**224**) and the free ligand $t\text{-Bu}_2\text{P}(\text{CH}_2)_3\text{Ph}$ (**198**) was not investigated.



268

Table 9. Summary of the reaction conditions employed in the preparation of the tethered complexes by η^6 -arene displacement.

Tethered Complex	Parent Complex(es)	Reaction Conditions ^a	Reaction Time (h)	Yield (%)
[RuCl ₂ (η^1 : η^6 -Me ₂ P~Ph)] (248)	236 \equiv [(<i>o</i> -mt)(η^1 -195)]	A	48	61
[RuCl ₂ (η^1 : η^6 -Me ₂ P~Ph)] (248)	236 \equiv [(<i>o</i> -mt)(η^1 -195)]	B	36	71
[RuCl ₂ (η^1 : η^6 -Me ₂ P~Ph)] (248)	dimer[(<i>o</i> -mt)] (224) + 195	A	48	72
[RuCl ₂ (η^1 : η^6 -Me ₂ P~Ph)] (248)	dimer[(<i>o</i> -mt)] (224) + 195	B	36	64
[RuCl ₂ (η^1 : η^6 -Ph ₂ P~Ph)] (222)	237 \equiv [(<i>o</i> -mt)(η^1 -118)]	A	72	66
[RuCl ₂ (η^1 : η^6 -Ph ₂ P~Ph)] (222)	237 \equiv [(<i>o</i> -mt)(η^1 -118)]	B	48	80
[RuCl ₂ (η^1 : η^6 -Ph ₂ P~Ph)] (222)	dimer[(<i>o</i> -mt)] (224) + 118	A	72	78
[RuCl ₂ (η^1 : η^6 -Ph ₂ P~Ph)] (222)	dimer[(<i>o</i> -mt)] (224) + 118	B	72	82
[RuCl ₂ (η^1 : η^6 - <i>i</i> -Pr ₂ P~Ph)] (249)	238 \equiv [(<i>o</i> -mt)(η^1 -196)]	A	6	91
[RuCl ₂ (η^1 : η^6 - <i>i</i> -Pr ₂ P~Ph)] (249)	dimer [(<i>o</i> -mt)] (224) + 196	A	10	96
[RuCl ₂ (η^1 : η^6 - <i>i</i> -Pr ₂ P~Ph)] (249)	232 \equiv [(<i>p</i> -cym)(η^1 -196)]	A	42	90
[RuCl ₂ (η^1 : η^6 - <i>i</i> -Pr ₂ P~Ph)] (249)	dimer[(<i>p</i> -cym)] (216) + 196	A	48	94
[RuCl ₂ (η^1 : η^6 -Cy ₂ P~Ph)] (225)	239 \equiv [(<i>o</i> -mt)(η^1 -197)]	A	192	90
[RuCl ₂ (η^1 : η^6 -Cy ₂ P~Ph)] (225)	239 \equiv [(<i>o</i> -mt)(η^1 -197)]	A	16	89
[RuCl ₂ (η^1 : η^6 -Cy ₂ P~Ph)] (225)	dimer[(<i>o</i> -mt)] (224) + 197	A	24	90
[RuCl ₂ (η^1 : η^6 -Cy ₂ P~Ph)] (225)	254 \equiv [(<i>p</i> -cym)(η^1 -197)]	A ^b	480	80
[RuCl ₂ (η^1 : η^6 -Cy ₂ P~Ph)] (225)	254 \equiv [(<i>p</i> -cym)(η^1 -197)]	A	48	82
[RuCl ₂ (η^1 : η^6 -Cy ₂ P~Ph)] (225)	Dimer[(<i>p</i> -cym)] (216) + 197	A	48	77
[RuCl ₂ (η^1 : η^6 - <i>t</i> -Bu ₂ P~Ph)] (253)	245 \equiv [(<i>o</i> -mt)(198)] ^c	A	24	90

Tethered Complex	Parent Complex(es)	Reaction Conditions ^a	Reaction Time (h)	Yield (%)
[RuCl ₂ (η ¹ :η ⁶ -Ph ₂ P~-2,4,6-C ₆ H ₂ Me ₃)] (250)	240 ≡ [(<i>o</i> -mt)(η ¹ -199)]	A	24	18
[RuCl ₂ (η ¹ :η ⁶ -Ph ₂ P~C ₆ Me ₅)] (251)	241 ≡ [(<i>o</i> -mt)(η ¹ -200)]	B	24	7
[RuCl ₂ (η ¹ :η ⁶ -Ph ₂ P~C ₆ Me ₅)] (251)	241 ≡ [(<i>o</i> -mt)(η ¹ -200)]	C ^d	16	35 ^e
[RuCl ₂ (η ¹ :η ⁶ -Ph ₂ PCH ₂ SiMe ₂ Ph)] (252)	235 ≡ [(<i>p</i> -cym)(η ¹ -201)]	B	168	51
[RuCl ₂ (η ¹ :η ⁶ -Ph ₂ PCH ₂ SiMe ₂ Ph)] (252)	242 ≡ [(<i>o</i> -mt)(η ¹ -201)]	B	72	71
[RuCl ₂ (η ¹ :η ⁶ -Ph ₂ PCH ₂ SiMe ₂ Ph)] (252)	dimer[(<i>o</i> -mt)] (224) + 201	B	72	75

^aReactions carried out at 120°C unless otherwise specified, ^btemperature of 80°C; ^ccomplex was not pure; ^dtemperature of 140°C; ^eincreased reaction time reduces yield of product.

~ = (CH₂)₃; A = CH₂Cl₂; B = CH₂Cl₂/THF; C = *n*-Bu₂O.

p-cym = *p*-cymene, 1,4-MeC₆H₄CHMe₂; *o*-mt = methyl *o*-toluate, 1,2-MeC₆H₄CO₂Me.

195 = Me₂P(CH₂)₃Ph

118 = Ph₂P(CH₂)₃Ph

196 = *i*-Pr₂P(CH₂)₃Ph

197 = Cy₂P(CH₂)₃Ph

198 = *t*-Bu₂P(CH₂)₃Ph

199 = Ph₂P(CH₂)₃=2,4,6-C₆H₂Me₃

200 = Ph₂P(CH₂)₃C₆Me₅

201 = Ph₂PCH₂SiMe₂Ph

216 = [RuCl₂(η⁶-1,4-MeC₆H₄CHMe₂)]₂

224 = [RuCl₂(η⁶-1,2-MeC₆H₄CO₂Me)]₂

Table 10. Summary of the reaction conditions employed in the various unsuccessful or low-yielding attempts to form the tethered complexes by η^6 -arene displacement; no reaction unless otherwise indicated.

Entry Number	Tethered Complex	Precursor RuCl ₂ Complex	Solvent	Reaction Conditions: Temperature (°C) or hv	Reaction Time (h)
1	[RuCl ₂ (η^1 : η^6 -Me ₂ P~Ph)] (248)	231 \equiv [(<i>p</i> -cym)(η^1 -195)]	C ₆ H ₅ Cl	130	18
2	[RuCl ₂ (η^1 : η^6 -Me ₂ P~Ph)] (248)	236 \equiv [(<i>o</i> -mt)(η^1 -195)]	CD ₂ Cl ₂	hv	1
3	[RuCl ₂ (η^1 : η^6 -Ph ₂ P~Ph)] (222)	227 \equiv [(ben)(η^1 -118)]	CD ₂ Cl ₂	hv	0.75
4	[RuCl ₂ (η^1 : η^6 -Ph ₂ P~Ph)] (222)	227 \equiv [(ben)(η^1 -118)]	(CD ₃) ₂ CO	hv	0.5
5	[RuCl ₂ (η^1 : η^6 -Ph ₂ P~Ph)] (222)	227 \equiv [(ben)(η^1 -118)]	CD ₃ CN	hv	0.75
6	[RuCl ₂ (η^1 : η^6 -Ph ₂ P~Ph)] (222)	227 \equiv [(ben)(η^1 -118)]	THF/(CD ₃) ₂ CO	hv	0.75
7	[RuCl ₂ (η^1 : η^6 -Ph ₂ P~Ph)] (222)	227 \equiv [(ben)(η^1 -118)]	CH ₃ CN	80	48 ^a
8	[RuCl ₂ (η^1 : η^6 -Ph ₂ P~Ph)] (222)	227 \equiv [(ben)(η^1 -118)]	Me ₂ CHCN	110	24
9	[RuCl ₂ (η^1 : η^6 -Ph ₂ P~Ph)] (222)	227 \equiv [(ben)(η^1 -118)]	THF	65	24
10	[RuCl ₂ (η^1 : η^6 -Ph ₂ P~Ph)] (222)	227 \equiv [(ben)(η^1 -118)]	none	215	^b
11	[RuCl ₂ (η^1 : η^6 -Ph ₂ P~Ph)] (222)	227 \equiv [(ben)(η^1 -118)]	none	210, <i>in vacuo</i>	^b
12	[RuCl ₂ (η^1 : η^6 -Ph ₂ P~Ph)] (222)	223 \equiv [(<i>p</i> -cym)(η^1 -118)]	C ₆ H ₅ Cl	130	18
13	[RuCl ₂ (η^1 : η^6 -Ph ₂ P~Ph)] (222)	223 \equiv [(<i>p</i> -cym)(η^1 -118)]	C ₆ D ₅ Cl	60-120 ^c	144 ^d
14	[RuCl ₂ (η^1 : η^6 -Ph ₂ P~Ph)] (222)	223 \equiv [(<i>p</i> -cym)(η^1 -118)]	C ₆ H ₅ Cl/C ₆ D ₅ Cl	120	32 ^d
15	[RuCl ₂ (η^1 : η^6 -Ph ₂ P~Ph)] (222)	223 \equiv [(<i>p</i> -cym)(η^1 -118)]	CH ₂ Cl ₂ /THF	120	48 ^e
16	[RuCl ₂ (η^1 : η^6 -Ph ₂ P~Ph)] (222)	237 \equiv [(<i>o</i> -mt)(η^1 -118)]	CD ₂ Cl ₂	hv	1

Entry Number	Tethered Complex	Precursor RuCl ₂ Complex	Solvent	Reaction Conditions: Temperature (°C) or hv	Reaction Time (h)
17	[RuCl ₂ (η ¹ :η ⁶ -Cy ₂ P~Ph)] (225)	239 ≡ [(<i>o</i> -mt)(η ¹ -197)]	CD ₂ Cl ₂	40	48
18	[RuCl ₂ (η ¹ :η ⁶ - <i>t</i> -Bu ₂ P~Ph)] (253) ^f	245 ≡ [(<i>o</i> -mt)(η ¹ -198)]	CD ₂ Cl ₂	50	28 ^g
19	[RuCl ₂ (η ¹ :η ⁶ -Ph ₂ P~-2,4,6-C ₆ H ₂ Me ₃)] (250)	233 ≡ [(<i>p</i> -cym)(η ¹ -199)]	CH ₂ Cl ₂	120	48 ^e
20	[RuCl ₂ (η ¹ :η ⁶ -Ph ₂ P~-2,4,6-C ₆ H ₂ Me ₃)] (250)	240 ≡ [(<i>o</i> -mt)(η ¹ -199)]	<i>n</i> -Bu ₂ O	140	16-24 ^h
21	[RuCl ₂ (η ¹ :η ⁶ -Ph ₂ P~-2,4,6-C ₆ H ₂ Me ₃)] (250)	240 [(<i>o</i> -mt)(η ¹ -199)]	<i>n</i> -Bu ₂ O / CH ₂ Cl ₂	140	22 ^h
22	[RuCl ₂ (η ¹ :η ⁶ -Ph ₂ P~C ₆ Me ₅)] (251)	234 ≡ [(<i>p</i> -cym)(η ¹ -200)]	CH ₂ Cl ₂	120	48 ^e
23	[RuCl ₂ (η ¹ :η ⁶ -Ph ₂ P~C ₆ Me ₅)] (251)	241 ≡ [(<i>o</i> -mt)(η ¹ -200)]	none	110, <i>in vacuo</i>	4
24	[RuCl ₂ (η ¹ :η ⁶ -Ph ₂ P~C ₆ Me ₅)] (251)	241 ≡ [(<i>o</i> -mt)(η ¹ -200)]	CH ₂ Cl ₂	120	24 ⁱ
25	[RuCl ₂ (η ¹ :η ⁶ -Ph ₂ P~C ₆ Me ₅)] (251)	241 ≡ [(<i>o</i> -mt)(η ¹ -200)]	CH ₂ Cl ₂	RT, 19,000 bar	24
26	[RuCl ₂ (η ¹ :η ⁶ -Ph ₂ P~C ₆ Me ₅)] (251)	241 ≡ [(<i>o</i> -mt)(η ¹ -200)]	<i>sym</i> - Cl ₂ CHCHCl ₂ /CD Cl ₂	120	17
27	[RuCl ₂ (η ¹ :η ⁶ -Ph ₂ P~C ₆ Me ₅)] (251)	241 ≡ [(<i>o</i> -mt)(η ¹ -200)]	<i>n</i> -Bu ₂ O / CH ₂ Cl ₂	140	23 ⁱ
28	[RuCl ₂ (η ¹ :η ⁶ -Ph ₂ P~C ₆ Me ₅)] (251)	241 ≡ [(<i>o</i> -mt)(η ¹ -200)]	<i>n</i> -Bu ₂ O / THF	140	16 ⁱ

^aA different product was formed in this reaction (see Chapter 4, p. 192); ^bexact reaction time is not known; ^ctemperature was gradually increased during the course of the reaction; ^da different product was formed in this reaction (see Section 3.2.6); ^eno reaction occurred; ^fcomplex was not pure; ^ga different product was formed in this reaction (see Section 3.2.7); ^hcomplex $[\text{RuCl}_2(\eta^1:\eta^6\text{-Ph}_2\text{P}(\text{CH}_2)_3\text{-2,4,6-C}_6\text{H}_2\text{Me}_3)]$ (**250**) was formed in yields below 10%; ⁱcomplex $[\text{RuCl}_2(\eta^1:\eta^6\text{-Ph}_2\text{P}(\text{CH}_2)_3\text{C}_6\text{Me}_5)]$ (**251**) was formed in yields below 18%.

$\sim = (\text{CH}_2)_3$

ben = benzene, C_6H_6

p-cym = *p*-cymene, $1,4\text{-MeC}_6\text{H}_4\text{CHMe}_2$

o-mt = methyl *o*-toluate, $1,2\text{-MeC}_6\text{H}_4\text{CO}_2\text{Me}$

195 = $\text{Me}_2\text{P}(\text{CH}_2)_3\text{Ph}$

118 = $\text{Ph}_2\text{P}(\text{CH}_2)_3\text{Ph}$

197 = $\text{Cy}_2\text{P}(\text{CH}_2)_3\text{Ph}$

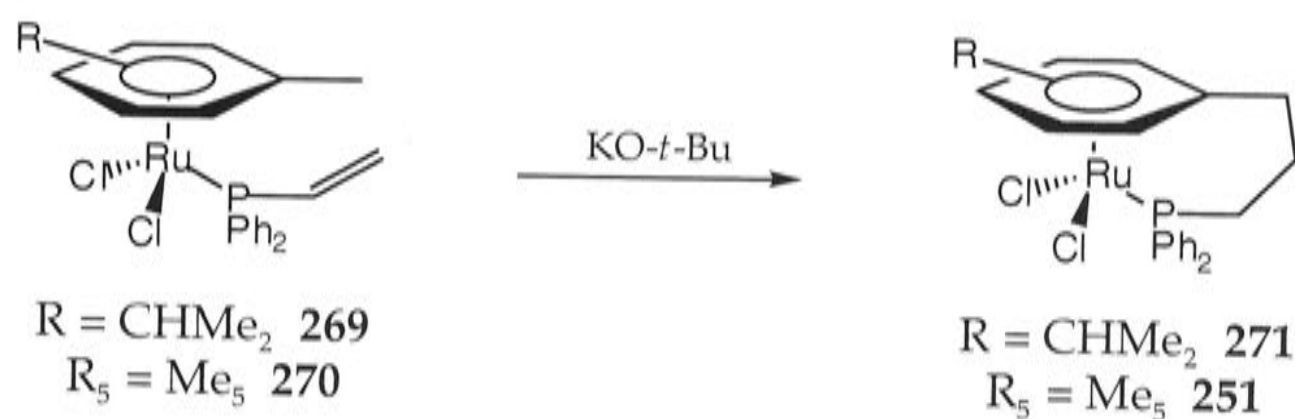
198 = $t\text{-Bu}_2\text{P}(\text{CH}_2)_3\text{Ph}$

199 = $\text{Ph}_2\text{P}(\text{CH}_2)_3\text{-2,4,6-C}_6\text{H}_2\text{Me}_3$

200 = $\text{Ph}_2\text{P}(\text{CH}_2)_3\text{C}_6\text{Me}_5$

3.3 Strategy Two; Intramolecular Construction of the Tether (Scheme 61).

It was envisaged that the procedure developed by Bennett and co-workers^{53,54} to prepare the vinyl thioether complex $[\text{Ru}(\text{SCH}=\text{CH}_2)(\eta^6\text{-C}_6\text{Me}_5(\text{CH}_2)_3\text{S}(\text{CH}_2)_2\text{S})]$ (**191**) (see Scheme 34, Chapter 1, Section 1.2.3) could be extended to ruthenium(II) complexes incorporating a phosphorus donor atom. The proposed methodology involves the reaction of complexes of the type $[\text{RuCl}_2(\eta^6\text{-C}_6\text{H}_{5-n}\text{R}_n\text{Me})(\eta^1\text{-Ph}_2\text{PCH}=\text{CH}_2)]$ incorporating both a methyl-substituted η^6 -arene and a vinyl phosphine. Treatment with a base may cause deprotonation of the methyl group, which might then undergo a Michael addition with the vinyl moiety, thus completing the tether and forming complexes of the type $[\text{RuCl}_2(\eta^1:\eta^6\text{-Ph}_2\text{P}(\text{CH}_2)_3\text{C}_6\text{H}_{5-n})]$. These possibilities are illustrated for the complexes $[\text{RuCl}_2(\eta^6\text{-arene})(\eta^1\text{-Ph}_2\text{PCH}=\text{CH}_2)]$ (arene = *p*-cymene (**269**) and hexamethylbenzene (**270**)) in Scheme 61.



Scheme 61. Proposed synthesis of the tethered complexes **271** ($\text{R} = \text{CHMe}_2$) and **251** ($\text{R} = \text{Me}_5$).

3.3.1 Preparation of Non-Tethered Compounds

The half-sandwich vinylphosphine ruthenium(II) complex $[\text{RuCl}_2(\eta^6\text{-1,4-MeC}_6\text{H}_4\text{CHMe}_2)(\text{Ph}_2\text{PCH}=\text{CH}_2)]$ (**269**) was prepared by treating $\text{Ph}_2\text{PCH}=\text{CH}_2$ (**272**) with $[\text{RuCl}_2(\eta^6\text{-1,4-MeC}_6\text{H}_4\text{CHMe}_2)]_2$ (**216**) in dichloromethane at room temperature. It was isolated as a microcrystalline, air-stable, orange solid in quantitative yield.

The formation of $[\text{RuCl}_2(\eta^6\text{-C}_6\text{Me}_6)(\text{Ph}_2\text{PCH=CH}_2)]$ (**270**) from the reaction of $[\text{RuCl}_2(\eta^6\text{-C}_6\text{Me}_6)]_2$ (**67**) and **272** under various conditions, dichloromethane at room temperature or at reflux, or propan-2-ol at reflux, proved to be surprisingly irreproducible. Complex **270** could only be reproducibly made by heating the triphenylstibine complex $[\text{RuCl}_2(\eta^6\text{-C}_6\text{Me}_6)(\text{SbPh}_3)]$ (**273**) with **272** in toluene. This reaction was based on the preparation of complexes of the type $[\text{RuClH}(\eta^6\text{-C}_6\text{Me}_6)\text{L}]$ (L = tertiary phosphine) achieved by Bennett and Latten, by the displacement of SbPh_3 from $[\text{RuClH}(\eta^6\text{-C}_6\text{Me}_6)(\text{SbPh}_3)]$.⁵⁵ It was isolated as a microcrystalline, air-stable, orange solid in quantitative yield.

The ^1H NMR spectra of the vinyldiphenylphosphine compounds **269** and **270** show multiplets in the region δ 5.2-6.8 due to the three vinyl protons. The ^1H and $^{13}\text{C}\{^1\text{H}\}$ -NMR spectra of the aromatic fragments of complexes **269** and **270** are unexceptional. The $^{31}\text{P}\{^1\text{H}\}$ -NMR spectra exhibit singlets at δ 22.8 and 22.7 for the *p*-cymene and hexamethylbenzene species, respectively, though the resonance of **270** was unexpectedly broad ($\nu_{1/2} = 63$ Hz). The IR spectra show C-H and C=H bands indicative of the vinyl group, and the far IR spectra of **269** and **270** each display a broad band due to $\nu(\text{Ru-Cl})$ at 288 and 298 cm^{-1} , respectively. Complexes **269** and **270** also show parent ions in their mass spectra (EI or FAB) with m/z 518 and 546, respectively.

3.3.2 Attempted Preparation of the Tethered Complexes

The *p*-cymene species $[\text{RuCl}_2(\eta^6\text{-1,4-MeC}_6\text{H}_4\text{CHMe}_2)(\text{Ph}_2\text{PCH=CH}_2)]$ (**269**) should react with KO-*t*-Bu at the $\text{C}_6\text{H}_4\text{Me}$ position to give rise to the tethered complex $[\text{RuCl}_2(\eta^1:\eta^6\text{-Ph}_2\text{P}(\text{CH}_2)_3\text{-4-C}_6\text{H}_4\text{CHMe}_2)]$ (**271**) (Scheme 61); deprotonation at the methine position is very unlikely. Deprotonation at one the methyl groups of $[\text{RuCl}_2(\eta^6\text{-C}_6\text{Me}_6)(\text{Ph}_2\text{PCH=CH}_2)]$ (**270**) and subsequent

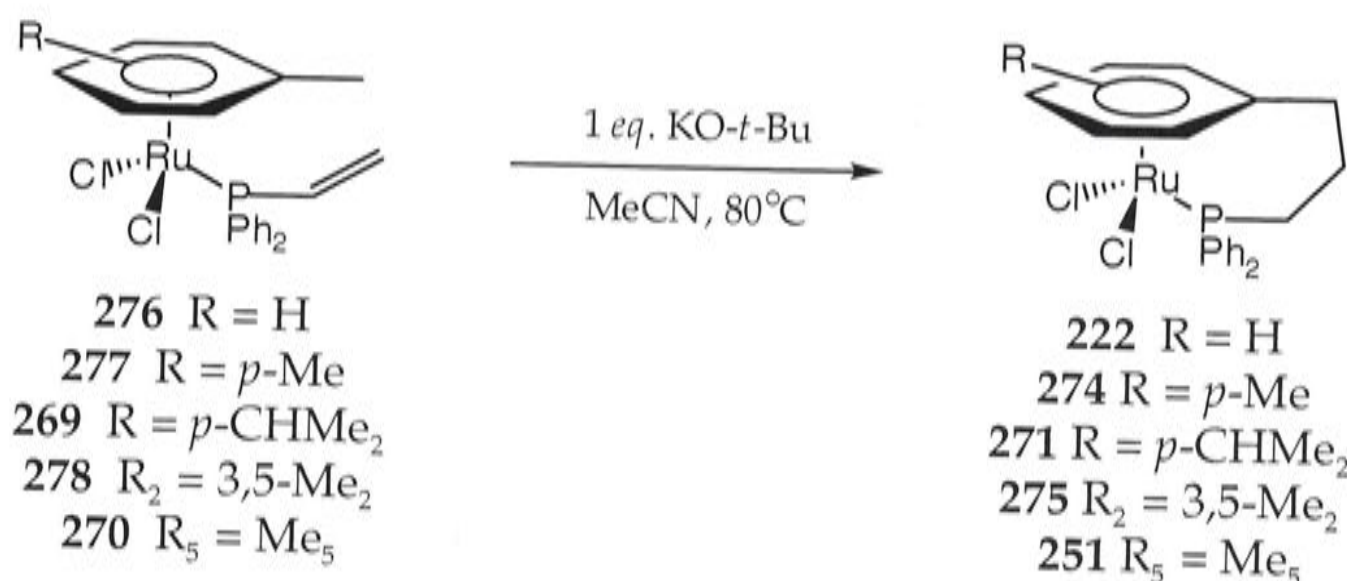
intramolecular condensation may give rise to $[\text{RuCl}_2(\eta^1:\eta^6\text{-Ph}_2\text{P}(\text{CH}_2)_3\text{C}_6\text{Me}_5)]$ (**251**) (Scheme 61).

Several attempts were made to prepare tethered complexes from the *p*-cymene and hexamethylbenzene complexes **269** and **270**, and the results are summarised in Table 11. The reactions were monitored by ^1H and $^{31}\text{P}\{^1\text{H}\}$ -NMR spectroscopy.

Treatment of either of the vinyl-diphenylphosphine complexes **269** or **270** with various molar ratios of KO-*t*-Bu in THF resulted in decomposition under all of the conditions employed, even at low temperature. Complex **269** also decomposed when treated with LiTMP (TMP = tetramethylpiperidide) and there was also no reaction when **269** was treated with the radical initiator, 2,2'-azobis(isobutyronitrile) (AIBN) in benzene.

While preliminary research into these reactions was being carried out, the preparations of the tethered complexes $[\text{RuCl}_2(\eta^1:\eta^6\text{-Ph}_2\text{P}(\text{CH}_2)_3\text{Ph})]$ (**222**), $[\text{RuCl}_2(\eta^1:\eta^6\text{-Ph}_2\text{P}(\text{CH}_2)_3\text{-4-C}_6\text{H}_4\text{Me})]$ (**274**), $[\text{RuCl}_2(\eta^1:\eta^6\text{-Ph}_2\text{P}(\text{CH}_2)_3\text{-4-C}_6\text{H}_4\text{CHMe}_2)]$ (**271**), $[\text{RuCl}_2(\eta^1:\eta^6\text{-Ph}_2\text{P}(\text{CH}_2)_3\text{-3,5-C}_6\text{H}_3\text{Me}_2)]$ (**275**) and $[\text{RuCl}_2(\eta^1:\eta^6\text{-Ph}_2\text{P}(\text{CH}_2)_3\text{C}_6\text{Me}_5)]$ (**251**) were described by Nelson and Ghebreyessus.^{5 6} The reactions of the compounds $[\text{RuCl}_2(\eta^6\text{-arene})(\text{Ph}_2\text{PCH}=\text{CH}_2)]$ (arene = toluene (**276**), *p*-xylene (**277**), *p*-cymene (**269**), mesitylene (**278**) and hexamethylbenzene (**270**)),⁵⁷ with one equivalent (eq.) of KO-*t*-Bu in refluxing acetonitrile (Scheme 62) were reported to give the required products in yields ranging from 48% for **251** up to 70% for **275**, with the least substituted complex $[\text{RuCl}_2(\eta^1:\eta^6\text{-Ph}_2\text{P}(\text{CH}_2)_3\text{Ph})]$ (**222**) being formed in 52% yield. The tethered complexes were also prepared without isolating the precursor vinyl-diphenylphosphine complexes, which were formed *in situ* from the appropriate $[\text{RuCl}_2(\eta^6\text{-arene})]_2$ dimer and treated with the base. Nelson and Ghebreyessus noted that use of greater than one equivalent of base caused

complex decomposition, which may account for the difficulties encountered in these preliminary experiments.



Scheme 62. Formation of the tethered complexes **222** (R = H), **274** (R = *p*-Me), **271** (R = *p*-CHMe₂), **275** (R₂ = 3,5-Me₂), **251** (R₅ = Me₅).⁵⁶

This methodology has also been extended to ruthenium-arsine complexes,⁵⁸ though it is apparently less general in its application and yields are lower.

Because the route to tethered complexes incorporating alkyl-substituted η⁶-arenes employed by Nelson and Ghebreyessus⁵⁶ appeared to be much simpler than the methodology outlined in Section 3.2.3, particularly for [RuCl₂(η¹:η⁶-Ph₂P(CH₂)₃C₆Me₅)] (**251**), some of these reported studies were repeated. The reactions were monitored by ¹H and ³¹P{¹H}-NMR spectroscopy and the results are listed in Table 11.

Both the mesitylene and hexamethylbenzene complexes [RuCl₂(η⁶-1,3,5-C₆H₃Me₃)(Ph₂PCH=CH₂)] (**278**) and [RuCl₂(η⁶-C₆Me₆)(Ph₂PCH=CH₂)] (**270**) were treated with one equivalent of KO-*t*-Bu in acetonitrile under the conditions specified by Nelson and Ghebreyessus.⁵⁶ The results, however, were irreproducible; sometimes the tethered complexes [RuCl₂(η¹:η⁶-Ph₂P(CH₂)₃-3,5-C₆H₃Me₂)] (**275**) or [RuCl₂(η¹:η⁶-Ph₂P(CH₂)₃C₆Me₅)] (**251**), respectively, were formed, though in poor yield, or frequently decomposition by loss of η⁶-arene occurred. For example, on one occasion complex **275** was isolated in only 23% yield (*cf.* 70% reported⁵⁶) in an amount

sufficient only for electrochemical studies (see Chapter 5, Section 5.2.2). There was also limited success with the *in situ* preparation, that is, the reaction of either $[\text{RuCl}_2(\eta^6\text{-1,3,5-C}_6\text{H}_3\text{Me}_3)]_2$ (**188**) or $[\text{RuCl}_2(\eta^6\text{-C}_6\text{Me}_6)]_2$ (**67**) with **272** and subsequent treatment with KO-*t*-Bu. In the attempts to form **275**, a mixture of both the vinylidiphosphine complex **278** and tethered species **275** formed, which could not be separated, even by chromatography. Since the vinylidiphosphine adduct **270** did not actually form when the dimer **67** and phosphine **272** were mixed in acetonitrile at room temperature, it is not surprising that there was no reaction upon addition of KO-*t*-Bu. This, however, is not unexpected, due to the problems encountered with the preparation of **270** discussed earlier. Thus the formation of complexes **275** and **251** was only successful starting from the isolated vinylidiphosphine adducts **278** and **270**, respectively.

I have no explanation for the failure to reproduce the preparations reported by Ghebreyessus and Nelson,⁵⁶ although in some cases the desired products could be detected. It should be noted that I used freshly sublimed KO-*t*-Bu⁵⁹ in my investigations, whereas Nelson and Ghebreyessus did not specify if the base was purified before use.⁵⁶

The identity of $[\text{RuCl}_2(\eta^6\text{-1,4-MeC}_6\text{H}_4\text{CHMe}_2)(\text{Ph}_2\text{PCH=CH}_2)]$ (**269**) prepared in the course of this work has been confirmed by structural analysis [Dr A. J. Edwards (ANU)], and the structure does not differ greatly from that reported by Nelson and co-workers.⁵⁷ The minor differences are discussed in the Appendix (see Section A.9).

Table 11. Summary of the reaction conditions employed in the attempted preparation of various tethered complexes by intramolecular condensation. Reactions carried out at 80°C with KO-*t*-Bu unless otherwise stated.

Entry Number	Tethered Complex	Precursor RuCl ₂ Complex [‡]	Solvent	Equivalents of Base Added	Reaction Time (h)	Result
1	[RuCl ₂ (η ¹ :η ⁶ -Ph ₂ P~-4-C ₆ H ₄ CHMe ₂)] (271)	269	THF	1.5 ^a	0.33	Decomposition
2	[RuCl ₂ (η ¹ :η ⁶ -Ph ₂ P~-4-C ₆ H ₄ CHMe ₂)] (271)	269	THF ^b	- ^a	2	Decomposition
3	[RuCl ₂ (η ¹ :η ⁶ -Ph ₂ P~-4-C ₆ H ₄ CHMe ₂)] (271)	269	C ₆ H ₆ ^c	-	5	No reaction
4	[RuCl ₂ (η ¹ :η ⁶ -Ph ₂ P~-3,5-C ₆ H ₃ Me ₂)] (275)	278	CH ₃ CN	1	48	Irreproducible ^d
5	[RuCl ₂ (η ¹ :η ⁶ -Ph ₂ P~-3,5-C ₆ H ₃ Me ₂)] (275)]	188*	CH ₃ CN	1 ^e	48	Mixture of 278 and 275
6	[RuCl ₂ (η ¹ :η ⁶ -Ph ₂ P~C ₆ Me ₅)] (251)	270	THF	1.4 ^f	24	Decomposition
7	[RuCl ₂ (η ¹ :η ⁶ -Ph ₂ P~C ₆ Me ₅)] (251)	270	CH ₃ CN	1	48	Irreproducible ^d
8	[RuCl ₂ (η ¹ :η ⁶ -Ph ₂ P~C ₆ Me ₅)] (251)	67*	CH ₃ CN	1 ^e	48	No reaction

^aReaction carried out at room temperature; ^bLiTMP as reagent; ^cAIBN as reagent; ^dconditions are those specified by Nelson and Ghebreyessus,⁵⁶; ^estoichiometry based on the monomeric species formed in solution; ^freaction carried out at -78°C.

[‡][RuCl₂(η⁶-arene)(Ph₂PCH=CH₂)] [arene = *p*-cym (269), mes (278), hmb (270)]; * [RuCl₂(η⁶-arene)]₂ [arene = mes (188), hmb (67)] plus Ph₂PCH=CH₂ (272).

~ = (CH₂)₃; *p*-cym = *p*-cymene, 1,4-MeC₆H₄CHMe₂; mes = mesitylene, 1,3,5-C₆H₃Me₃; hmb = hexamethylbenzene, C₆Me₆
 272 = Ph₂PCH=CH₂; 216 = [RuCl₂(η⁶-1,4-MeC₆H₄CHMe₂)]₂; 67 = [RuCl₂(η⁶-C₆Me₆)]₂

3.4 Preparation of Derivatives of Tethered Arene Complexes

In order to investigate the electrochemical behaviour of a range of tethered complexes, attempts were made to prepare derivatives. Due to the poor solubility of the tethered compounds, such as $[\text{RuCl}_2(\eta^1:\eta^6\text{-R}_2\text{P}(\text{CH}_2)_3\text{Ph})]$ ($\text{R} = \text{Me}$ (**248**), Ph (**222**)) in common organic solvents, it was also envisaged that the chloride ligands could be exchanged for groups that would enhance the solubility of the resulting complexes.

3.4.1 Preparation of Complexes of the Type $[\text{Ru}(\text{X})(\text{Y})(\eta^1:\eta^6\text{-R}_2\text{P}(\text{CH}_2)_3\text{Ph})]$

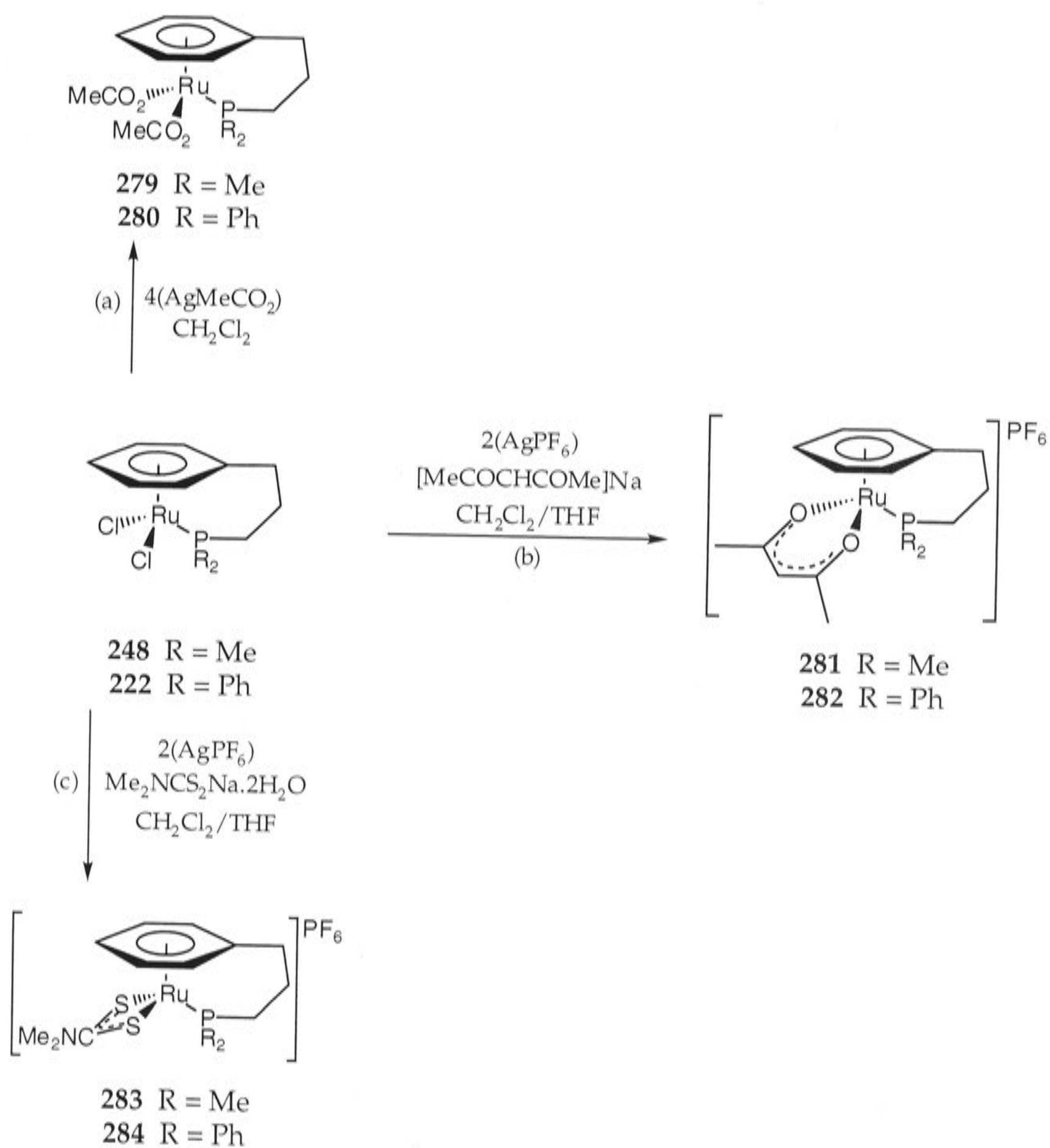
Treatment of $[\text{RuCl}_2(\eta^1:\eta^6\text{-R}_2\text{P}(\text{CH}_2)_3\text{Ph})]$ ($\text{R} = \text{Me}$ (**248**) and Ph (**222**)) with four equivalents of silver acetate, with the exclusion of light, in dichloromethane at room temperature afforded the monodentate bis(acetato) complexes $[\text{Ru}(\eta^1\text{-O}_2\text{CMe})_2(\eta^1:\eta^6\text{-R}_2\text{P}(\text{CH}_2)_3\text{Ph})]$ ($\text{R} = \text{Me}$ (**279**) and Ph (**280**)) (Scheme 63a). The products were isolated in nearly quantitative yield as microcrystalline, air-sensitive, green and yellow solids, respectively. This procedure was based on that employed to obtain complexes such as $[\text{Ru}(\eta^1\text{-O}_2\text{CMe})_2(\eta^6\text{-C}_6\text{Me}_6)(\text{PMe}_3)]$ from $[\text{RuCl}_2(\eta^6\text{-C}_6\text{Me}_6)(\text{PMe}_3)]$.⁶⁰ It was not possible to obtain satisfactory elemental analyses for the products, probably due to the presence of residual silver salts, but spectroscopic data are in agreement with the formulations.

The ^1H NMR spectra of **279** and **280** each show a singlet due to the methyl group of the acetate ligands at δ 1.91 and 1.58, respectively, as well as multiplets due to $\eta^6\text{-C}_6\text{H}_5$ (see Table 12). The $^{13}\text{C}\{^1\text{H}\}$ -NMR spectra show a singlet for the methyl groups at approximately δ 23.8, and a singlet due to the carbonyl carbon at *ca* δ 178.3 (see Table 13 for signals due to $\eta^6\text{-C}_6\text{H}_5$). A singlet at δ 19.4 and 28.1 for complexes **279** and **280**, respectively, is observed in the $^{31}\text{P}\{^1\text{H}\}$ -NMR spectra (see Table 14). The IR spectra show two bands due to C-O stretching in the

regions 1580-1620 and 1360-1380 cm^{-1} , separated by *ca* 220-260 cm^{-1} , a feature which is characteristic of monodentate acetate ligands.⁶¹ The highest mass ion of the observed in the FAB mass spectra is $[M-\text{O}_2\text{CMe}]^+$ (see Table 15).

The replacement of the two chloride ligands with the bidentate ligands acetylacetonate and dithiocarbamate was also investigated. Treatment of **248** and **222** with two equivalents of AgPF_6 followed by either sodium acetylacetonate⁶² or sodium dimethyldithiocarbamate gave $[\text{Ru}(\eta^2\text{-MeC(O)CHC(O)Me})(\eta^1:\eta^6\text{-R}_2\text{P}(\text{CH}_2)_3\text{Ph})]\text{PF}_6$ (R = Me (**281**) and Ph (**282**)) (Scheme 63b) and $[\text{Ru}(\eta^2\text{-S}_2\text{CNMe}_2)(\eta^1:\eta^6\text{-R}_2\text{P}(\text{CH}_2)_3\text{Ph})]\text{PF}_6$ (R = Me (**283**) and Ph (**284**)) (Scheme 63c). They were isolated as microcrystalline, air-stable, brown and yellow solids, respectively, generally in good yields, and were fully characterised, including elemental analyses.

Complexes **281-284** show the expected signals in their ^1H NMR and $^{13}\text{C}\{^1\text{H}\}$ -NMR spectra for the acac and dithiocarbamate ligands, respectively, as well as resonances characteristic of the η^6 -arene (see Tables 12 and 13). The cationic complexes **281-284** show, in addition to the characteristic signal due to the PF_6 anion, a singlet for the phosphorus atom in the tether in the region δ 12.3-36.5 (see Table 14). The IR spectra of **281-284** show bands indicative of the PF_6 anion, and all the mass spectra (FAB) show parent ions (see Table 15).



Scheme 63. Preparation of the derivatives of tethered complexes, 279-284.

Table 12. ^1H NMR signals in d_2 -dichloromethane for the aromatic protons of the η^6 -arene of the derivatives of the tethered complexes.

Complex	δ_{ortho}^a (ppm)	δ_{meta}^b (ppm)	δ_{para}^b (ppm)
$[\text{Ru}(\eta^1\text{-O}_2\text{CMe})_2(\eta^1:\eta^6\text{-Me}_2\text{P}\sim\text{Ph})]$ (279)	4.96	5.84	6.50
$[\text{Ru}(\eta^1\text{-O}_2\text{CMe})_2(\eta^1:\eta^6\text{-Ph}_2\text{P}\sim\text{Ph})]$ (280)	5.17	6.05	6.91
$[\text{Ru}(\eta^2\text{-MeC(O)CHC(O)Me})(\eta^1:\eta^6\text{-Me}_2\text{P}\sim\text{Ph})]\text{PF}_6$ (281)	5.02	5.75	6.24
$[\text{Ru}(\eta^2\text{-MeC(O)CHC(O)Me})(\eta^1:\eta^6\text{-Ph}_2\text{P}\sim\text{Ph})]\text{PF}_6$ (282)	5.20	5.86	6.36
$[\text{Ru}(\eta^2\text{-S}_2\text{CNMe}_2)(\eta^1:\eta^6\text{-Me}_2\text{P}\sim\text{Ph})]\text{PF}_6$ (283)	5.43	5.90	6.06
$[\text{Ru}(\eta^2\text{-S}_2\text{CNMe}_2)(\eta^1:\eta^6\text{-Ph}_2\text{P}\sim\text{Ph})]\text{PF}_6$ (284)	5.51	6.09	6.27

^aDoublet ($J = 6$ Hz); ^btriplet ($J = 6$ Hz).

$\sim = (\text{CH}_2)_3$

Table 13. $^{13}\text{C}\{^1\text{H}\}$ -NMR signals in d_2 -dichloromethane for the aromatic protons of the η^6 -arene of the derivatives of the tethered complexes; the multiplicity of the signals is not specified.

Complex	δ_{ipso} (ppm)	δ_{ortho} (ppm)	δ_{meta} (ppm)	δ_{para} (ppm)
$[\text{Ru}(\eta^1\text{-O}_2\text{CMe})_2(\eta^1:\eta^6\text{-Me}_2\text{P}\sim\text{Ph})]$ (279)	95.39	90.54 ^a	91.42 ^a	77.27
$[\text{Ru}(\eta^1\text{-O}_2\text{CMe})_2(\eta^1:\eta^6\text{-Ph}_2\text{P}\sim\text{Ph})]$ (280)	94.89	90.49 ^a	90.90 ^a	79.57
$[\text{Ru}(\eta^2\text{-MeC(O)CHC(O)Me})(\eta^1:\eta^6\text{-Me}_2\text{P}\sim\text{Ph})]\text{PF}_6$ (281)	101.72	96.67 ^a	99.50 ^a	93.79
$[\text{Ru}(\eta^2\text{-MeC(O)CHC(O)Me})(\eta^1:\eta^6\text{-Ph}_2\text{P}\sim\text{Ph})]\text{PF}_6$ (282)	101.37	94.52 ^a	97.95 ^a	92.96
$[\text{Ru}(\eta^2\text{-S}_2\text{CNMe}_2)(\eta^1:\eta^6\text{-Me}_2\text{P}\sim\text{Ph})]\text{PF}_6$ (283)	100.30	94.18 ^a	94.77 ^a	84.88
$[\text{Ru}(\eta^2\text{-S}_2\text{CNMe}_2)(\eta^1:\eta^6\text{-Ph}_2\text{P}\sim\text{Ph})]\text{PF}_6$ (284)	95.86	92.95 ^a	95.84 ^a	86.91

^aAssignments are interchangeable.

$\sim = (\text{CH}_2)_3$

Table 14. $^{31}\text{P}\{^1\text{H}\}$ -NMR shifts in d_2 -dichloromethane of the phosphorus atom of the tether of the derivatives of the tethered complexes.

Complex	Chemical Shift (ppm)
$[\text{Ru}(\eta^1\text{-O}_2\text{CMe})_2(\eta^1:\eta^6\text{-Me}_2\text{P}\sim\text{Ph})]$ (279)	19.4
$[\text{Ru}(\eta^1\text{-O}_2\text{CMe})_2(\eta^1:\eta^6\text{-Ph}_2\text{P}\sim\text{Ph})]$ (280)	28.1
$[\text{Ru}(\eta^2\text{-MeC(O)CHC(O)Me})(\eta^1:\eta^6\text{-Me}_2\text{P}\sim\text{Ph})]\text{PF}_6$ (281)	20.8
$[\text{Ru}(\eta^2\text{-MeC(O)CHC(O)Me})(\eta^1:\eta^6\text{-Ph}_2\text{P}\sim\text{Ph})]\text{PF}_6$ (282)	27.2
$[\text{Ru}(\eta^2\text{-S}_2\text{CNMe}_2)(\eta^1:\eta^6\text{-Me}_2\text{P}\sim\text{Ph})]\text{PF}_6$ (283)	12.3
$[\text{Ru}(\eta^2\text{-S}_2\text{CNMe}_2)(\eta^1:\eta^6\text{-Ph}_2\text{P}\sim\text{Ph})]\text{PF}_6$ (284)	36.5

$\sim = (\text{CH}_2)_3$

Table 15. Mass spectrometry (FAB) results for various tethered complexes.

Complex	Highest Mass Ion	m/z
$[\text{Ru}(\eta^1\text{-O}_2\text{CMe})_2(\eta^1:\eta^6\text{-Me}_2\text{P}\sim\text{Ph})]$ (279)	$[\text{M-OCOMe}]^+$	341
$[\text{Ru}(\eta^1\text{-O}_2\text{CMe})_2(\eta^1:\eta^6\text{-Ph}_2\text{P}\sim\text{Ph})]$ (280)	$[\text{M-OCOMe}]^+$	465
$[\text{Ru}(\eta^2\text{-MeC(O)CHC(O)Me})(\eta^1:\eta^6\text{-Me}_2\text{P}\sim\text{Ph})]\text{PF}_6$ (281)	$[\text{M}^+]$	381
$[\text{Ru}(\eta^2\text{-MeC(O)CHC(O)Me})(\eta^1:\eta^6\text{-Ph}_2\text{P}\sim\text{Ph})]\text{PF}_6$ (282)	$[\text{M}^+]$	505
$[\text{Ru}(\eta^2\text{-S}_2\text{CNMe}_2)(\eta^1:\eta^6\text{-Me}_2\text{P}\sim\text{Ph})]\text{PF}_6$ (283)	$[\text{M}^+]$	402
$[\text{Ru}(\eta^2\text{-S}_2\text{CNMe}_2)(\eta^1:\eta^6\text{-Ph}_2\text{P}\sim\text{Ph})]\text{PF}_6$ (284)	$[\text{M}^+]$	526

$\sim = (\text{CH}_2)_3$

The preparation of the complex $[\text{RuCl}(\eta^1\text{-O}_2\text{CMe})(\eta^1:\eta^6\text{-Me}_2\text{P}(\text{CH}_2)_3\text{Ph})]$ (**285**) was attempted by treating $[\text{RuCl}_2(\eta^1:\eta^6\text{-Me}_2\text{P}(\text{CH}_2)_3\text{Ph})]$ (**248**) with one equivalent of AgO_2CMe . The synthesis of $[\text{Ru}(\eta^2\text{-O}_2\text{CMe})(\eta^1:\eta^6\text{-Me}_2\text{P}(\text{CH}_2)_3\text{Ph})]\text{PF}_6$ was also attempted by reacting $[\text{Ru}(\eta^1\text{-O}_2\text{CMe})_2(\eta^1:\eta^6\text{-Me}_2\text{P}(\text{CH}_2)_3\text{Ph})]$ (**279**) with one equivalent of NH_4PF_6 . The ^1H and $^{31}\text{P}\{^1\text{H}\}$ -NMR spectra (see Chapter 8, pp. 383-385) indicated that a mixture of products had formed in both cases, which were not separated.

A number of efforts were made to prepare dimethyl derivatives of the type $[\text{Ru}(\text{Me})_2(\eta^1:\eta^6\text{-R}_2\text{P}\sim\text{arene})]$ ($\sim = (\text{CH}_2)_3$ or CH_2SiMe_2) by treating the RuCl_2 tethered complexes with either methyl lithium or dimethylzinc. Although spectroscopic evidence indicated that methyl-ruthenium compounds may have been formed, all attempts to isolate the products were unsuccessful. The spectral data obtained in these attempts are given in the Experimental Section (pp. 389-392).

The reactions of $[\text{RuCl}_2(\eta^1:\eta^6\text{-R}_2\text{P}(\text{CH}_2)_3\text{Ph})]$ ($\text{R} = \text{Me}$ (**248**) and Ph (**222**)) with methyl lithium gave insoluble, uncharacterisable solids.

Removal of the solvents from the reaction of $[\text{RuCl}_2(\eta^1:\eta^6\text{-Ph}_2\text{PCH}_2\text{SiMe}_2\text{Ph})]$ (**252**) and one equivalent of dimethylzinc at -78°C gave an uncrystallisable oil. It showed a singlet at $\delta -0.32$ in the ^1H NMR spectrum and a doublet at $\delta -4.75$ ($J_{\text{PC}} = 17$ Hz) in the $^{13}\text{C}\{^1\text{H}\}$ -NMR spectrum, which can be assigned to a Ru-CH_3 group. The spectra also showed that the tether was still intact, since multiplets due to coordinated aromatic protons were present. The $^{31}\text{P}\{^1\text{H}\}$ -NMR spectrum displayed just a single resonance at $\delta 36.4$. The FAB mass spectrum of the oil showed a highest mass peak at m/z 471 corresponding to $[\text{RuCl}(\eta^1:\eta^6\text{-Ph}_2\text{PCH}_2\text{SiMe}_2\text{C}_6\text{H}_5)]^+$. These features are consistent with the presence of $[\text{RuCl}(\text{Me})(\eta^1:\eta^6\text{-Ph}_2\text{PCH}_2\text{SiMe}_2\text{Ph})]$ (**286**); it seems unlikely that dimethylation would have occurred under such mild

conditions. However, there is only one singlet at $\delta -0.04$ due to SiMe_2 in the ^1H NMR spectrum, whereas the above formulation would require the Si-Me groups to be inequivalent. The nature of this product is therefore uncertain.

The reaction of dimethylzinc with either $[\text{RuCl}_2(\eta^1:\eta^6\text{-R}_2\text{P}(\text{CH}_2)_3\text{Ph})]$ ($\text{R} = \text{Ph}$ (**222**), Cy (**225**)) or $[\text{RuCl}_2(\eta^1:\eta^6\text{-R}_2\text{P}(\text{CH}_2)_3\text{C}_6\text{Me}_5)]$ (**251**) gave solids that could not be purified by crystallisation. The presence of Ru-CH_3 groups was detected in the ^1H NMR spectra, and the ^1H NMR spectrum of the reaction from **222** indicated that partial η^6 -arene displacement had occurred. There were several peaks in each of the $^{31}\text{P}\{^1\text{H}\}$ -NMR spectra of the products obtained from either **222** or **251**, although there was a single resonance at $\delta 62.6$ for the product from **225**.

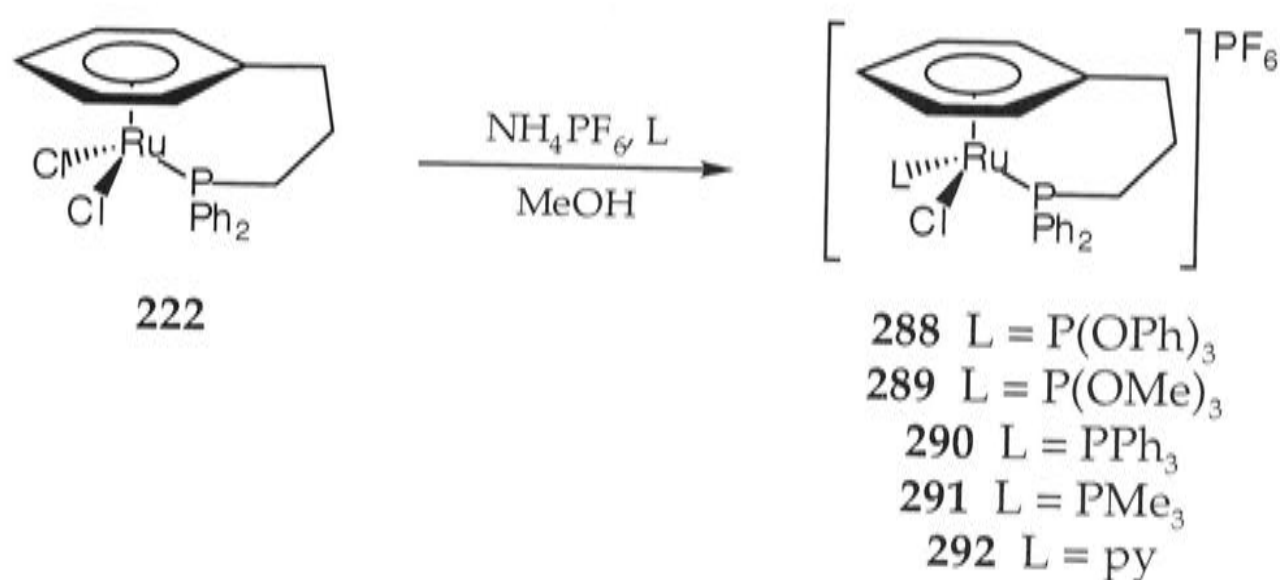
Several attempts were also made to prepare salts of the type $[\text{RuCl}(\text{L})(\eta^1:\eta^6\text{-R}_2\text{P}\sim\text{arene})]^+$ ($\sim = (\text{CH}_2)_3$ or CH_2SiMe_2), containing neutral donor ligands L , because it was anticipated that these could serve as precursors to tethered arene-ruthenium(0) complexes of the type $[\text{Ru}(\text{L})(\eta^1:\eta^6\text{-R}_2\text{P}(\text{CH}_2)_3\text{Ph})]$.^{63,64} The spectroscopic data obtained in these attempts are summarised in Chapter 8, (pp. 392-394).

Treatment of $[\text{RuCl}_2(\eta^1:\eta^6\text{-Ph}_2\text{PCH}_2\text{SiMe}_2\text{Ph})]$ (**252**) with AgPF_6 in acetone under CO caused some displacement of arene, as suggested by the appearance of several CO stretching bands in the IR spectrum. Some arene displacement also occurred when **252** was treated with $t\text{-BuNC}$. The reaction of $[\text{RuCl}_2(\eta^1:\eta^6\text{-Me}_2\text{P}(\text{CH}_2)_3\text{Ph})]$ (**248**) with $t\text{-BuNC}$ in the presence of NH_4PF_6 gave $[\text{RuCl}(t\text{-BuNC})(\eta^1:\eta^6\text{-Me}_2\text{P}(\text{CH}_2)_3\text{Ph})]\text{PF}_6$ (**[287]PF₆**), but the conversion was not complete.

Attempts to directly prepare $\text{Ru}(0)$ derivatives by reducing either $[\text{RuCl}_2(\eta^1:\eta^6\text{-R}_2\text{P}(\text{CH}_2)_3\text{Ph})]$ ($\text{R} = \text{Me}$ (**248**) or Ph (**222**)) or

$[\text{RuCl}_2(\eta^1:\eta^6\text{-Ph}_2\text{PCH}_2\text{SiMe}_2\text{Ph})]$ (**252**) with sodium naphthalide in the presence of *t*-BuNC at -78°C gave decomposition by loss of η^6 -arene.

The preparation of some cationic Group 15-donor derivatives of $[\text{RuCl}_2(\eta^1:\eta^6\text{-Ph}_2\text{P}(\text{CH}_2)_3\text{Ph})]$ (**222**) has recently been reported.⁶⁵ Compounds $[\text{RuCl}(\text{L})(\eta^1:\eta^6\text{-Ph}_2\text{P}(\text{CH}_2)_3\text{Ph})]$ ($\text{L} = \text{P}(\text{OPh})_3$ (**288**), $\text{P}(\text{OMe})_3$ (**289**), PPh_3 (**290**), PMe_3 (**291**), py (**292**)) were prepared by treating **222** with NH_4PF_6 and the appropriate ligand in methanol (Scheme 64).

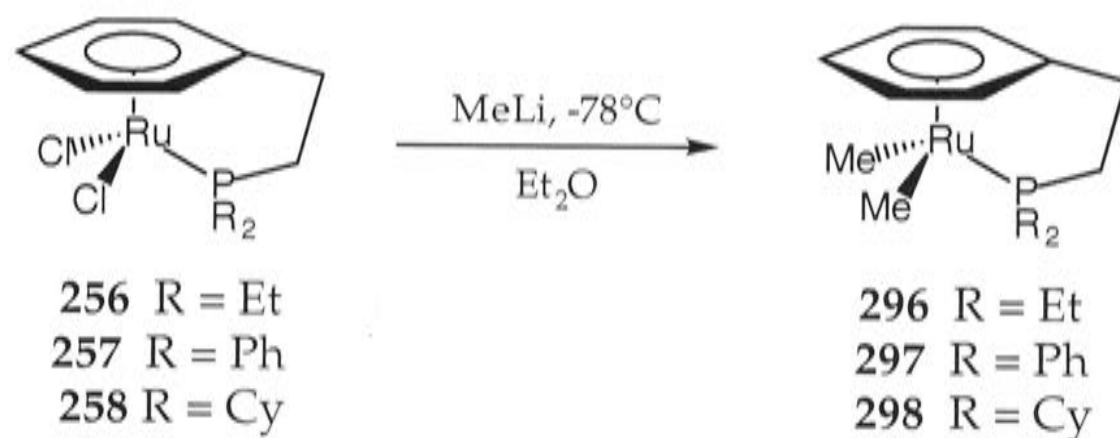


Scheme 64. Preparation of the derivatives **288** ($\text{L} = \text{P}(\text{OPh})_3$), **289** ($\text{L} = \text{P}(\text{OMe})_3$), **290** ($\text{L} = \text{PPh}_3$), **291** ($\text{L} = \text{PMe}_3$) and **292** ($\text{L} = \text{py}$).

The reaction of complexes $[\text{RuCl}_2(\eta^1:\eta^6\text{-Ph}_2\text{PCH}_2\text{CHRPh})]$ ($\text{R} = \text{H}$ (**257**) and $\text{R} = \text{Ph}$ (**293**)) [their preparation is summarised in Table 40, Chapter 7, Section 7.2] with NaI in acetone afforded the di-iodo derivatives $[\text{RuI}_2(\eta^1:\eta^6\text{-Ph}_2\text{PCH}_2\text{CHRPh})]$ ($\text{R} = \text{H}$ (**294**) and $\text{R} = \text{Ph}$ (**295**)).¹⁰

The synthesis of some tethered arene-ruthenium complexes containing σ -methyl groups has been reported recently.²⁸ Compounds $[\text{Ru}(\text{Me})_2(\eta^1:\eta^6\text{-R}_2\text{P}(\text{CH}_2)_2\text{Ph})]$ ($\text{R} = \text{Et}$ (**296**), Ph (**297**) and Cy (**298**)) were prepared by treating the dichloride parent species $[\text{RuCl}_2(\eta^1:\eta^6\text{-R}_2\text{P}(\text{CH}_2)_2\text{Ph})]$ ($\text{R} = \text{Et}$ (**256**), Ph (**257**) and Cy (**258**)) (their preparation is described in Chapter 7, Section 7.2) with an excess of methyl lithium at -78°C (Scheme 65).²⁸ A number of derivatives of compound **297** have been prepared;⁶⁶ in

particular, one of the methyl groups can be selectively cleaved by the acid of $[\text{H}(\text{Et}_2\text{O})_2]^+[\text{B}(3,5\text{-C}_6\text{H}_3(\text{CF}_3)_2)_4]^-$ ($\text{B}(3,5\text{-C}_6\text{H}_3(\text{CF}_3)_2)_4^- = [\text{BAr}^{\text{F}}_4]^-$) in the presence of CO or ethylene to give $[\text{RuMe}(\text{CO})(\eta^1:\eta^6\text{-R}_2\text{P}(\text{CH}_2)_2\text{Ph})][\text{BAr}^{\text{F}}_4]$ or $[\text{RuMe}(\text{CH}_2=\text{CH}_2)(\eta^1:\eta^6\text{-R}_2\text{P}(\text{CH}_2)_2\text{Ph})][\text{BAr}^{\text{F}}_4]$, respectively.



Scheme 65. Preparation of the σ -alkyl tethered complexes **296**, **297** and **298**.²⁸

It should be possible to prepare a range of derivatives of the RuCl_2 tethered complexes. The complex $[\text{RuCl}_2(\eta^1:\eta^6\text{-Ph}_2\text{P}(\text{CH}_2)_3\text{C}_6\text{Me}_5)]$ (**251**) would probably be the most suitable because the permethylated arene appears to be less easily displaced.

3.5 Discussion of Structural Data

As mentioned in Sections 3.2.2 and 3.2.5, the non-tethered compounds $[\text{RuCl}_2(\eta^6\text{-1,4-MeC}_6\text{H}_4\text{CHMe}_2)(\eta^1\text{-Me}_2\text{P}(\text{CH}_2)_3\text{Ph})]$ (**231**), $[\text{RuCl}_2(\eta^6\text{-C}_6\text{H}_6)(\eta^1\text{-Ph}_2\text{P}(\text{CH}_2)_3\text{Ph})]$ (**227**), $[\text{RuCl}_2(\eta^6\text{-1,4-MeC}_6\text{H}_4\text{CHMe}_2)(\eta^1\text{-}i\text{-Pr}_2\text{P}(\text{CH}_2)_3\text{Ph})]$ (**232**), $[\text{RuCl}_2(\eta^6\text{-1,2-MeC}_6\text{H}_4\text{CO}_2\text{Me})(\eta^1\text{-Cy}_2\text{P}(\text{CH}_2)_3\text{Ph})]$ (**239**), $[\text{RuCl}_2(\eta^6\text{-1,4-MeC}_6\text{H}_4\text{CHMe}_2)(\eta^1\text{-Ph}_2\text{P}(\text{CH}_2)_3\text{-2,4,6-C}_6\text{H}_2\text{Me}_3)]$ (**233**), $[\text{RuCl}_2(\eta^6\text{-1,4-MeC}_6\text{H}_4\text{CHMe}_2)(\eta^1\text{-Ph}_2\text{P}(\text{CH}_2)_3\text{C}_6\text{Me}_5)]$ (**234**) and $[\text{RuCl}_2(\eta^6\text{-1,4-MeC}_6\text{H}_4\text{CHMe}_2)(\eta^1\text{-Ph}_2\text{PCH}_2\text{SiMe}_2\text{Ph})]$ (**235**) and the tethered arene complexes $[\text{RuCl}_2(\eta^1:\eta^6\text{-Me}_2\text{P}(\text{CH}_2)_3\text{Ph})]$ (**248**), $[\text{RuCl}_2(\eta^1:\eta^6\text{-}i\text{-Pr}_2\text{P}(\text{CH}_2)_3\text{Ph})]$ (**249**), $[\text{RuCl}_2(\eta^1:\eta^6\text{-}t\text{-Bu}_2\text{P}(\text{CH}_2)_3\text{Ph})]$ (**253**), $[\text{RuCl}_2(\eta^1:\eta^6\text{-Ph}_2\text{P}(\text{CH}_2)_3\text{-2,4,6-C}_6\text{H}_2\text{Me}_3)]$ (**250**), $[\text{RuCl}_2(\eta^1:\eta^6\text{-Ph}_2\text{P}(\text{CH}_2)_3\text{C}_6\text{Me}_5)]$ (**251**) and

[RuCl₂(η¹:η⁶-Ph₂PCH₂SiMe₂Ph)] (252) have been characterised by X-ray crystallography. Selected bond distances are shown in Table 16; the Ru-centroid distances are listed in Table 17. The X-ray structural data confirm the conclusions about the molecular structure of the complexes drawn from the spectroscopic data. The chemically significant bond lengths and angles are listed in the Appendix. The crystal structures of the non-tethered and tethered complexes obtained in the course of this work show the expected half-sandwich geometry. The interbond angles of the tripod are approximately 90° (see Appendix), and are in good agreement with those obtained for the non-tethered complexes [RuCl₂(η⁶-arene)(PMePh₂)] (arene = C₆H₆ (299) and *p*-MeC₆H₄CHMe₂ (300))⁶⁷ and tethered compounds [RuCl₂(η¹:η⁶-R₂P(CH₂)₃Ph)] (R = Ph (222)^{7,56} and Cy (225)¹³).

Since the methyl *o*-toluate is more easily displaced than *p*-cymene (see Section 3.2.6), it seemed possible that it might be more weakly bound, and that this might be indicated by longer Ru-C bonds to the arene. However, there is no significant difference in either the Ru-C(arene) (see Table 16) or the Ru-centroid distances (see Table 17) for these two arenes, the averages (av.) being *ca* 2.21 Å and 1.707(9) Å, respectively. Similar values are also observed in the tethered complexes. There are many reported crystal structures of half-sandwich arene-ruthenium complexes containing either η⁶-benzene or η⁶-*p*-cymene, but there is only one reported example for an aromatic ester. The structure of one of the diastereoisomers of complex [RuCl₂(η⁶-1,2-MeC₄H₄CO₂Me)(NMDPP)] (NMDPP = (+)-neomenthylidiphenylphosphine) (301) has been determined.⁶⁸ The relevant bond lengths of [RuCl₂(η⁶-MeC₆H₄CO₂Me)(η¹-Cy₂P(CH₂)₃Ph)] (239) are in good agreement with those reported for 301.⁶⁸ There is virtually no difference between the Ru-centroid distances of reported complexes incorporating either η⁶-benzene, η⁶-*p*-cymene or η⁶-methyl *o*-toluate, namely [RuCl₂(η⁶-C₆H₆)(PPh₃)] (302)⁶⁹, [RuCl₂(η⁶-1,4-MeC₆H₄CHMe₂)(PPh₂-*n*-Bu)]⁷⁰ and 301,⁶⁸ 1.703, 1.704 and 1.694 Å, respectively. The Ru-centroid distance is

essentially unaffected by the degree of methyl substitution in tethered or non-tethered complexes.

There is also no significant difference between the average C-C(arene) distances, which are 1.38, 1.41 and 1.42 Å, for benzene, *p*-cymene and methyl *o*-toluate, respectively. The average C-C(ring) bond lengths of the aryl group of the ligands R₂P~aryl (~ = (CH₂)₃ or CH₂SiMe₂) for the non-tethered and tethered complexes are listed in Table 18. The average of the C-C bond lengths of the free aryl group in the non-tethered complexes lies in the usual range 1.36-1.40 Å, whereas the average bond lengths of the corresponding η⁶-arene in the tethered complexes are in the range 1.40-1.43 Å, indicating that there is a small increase (*ca* 0.04 Å) as a result of coordination, as expected. This is true for complexes containing either substituted or non-substituted aromatic groups.

Ring-slippage, defined as the distance between the perpendicular projection of the ruthenium on to the ring and the centre of the ring⁷¹ (*i.e.*, the distance between the Ru-centroid and Ru-least square-plane distances, *x* in Figure 23) of less than 0.08 Å was observed in both the non-tethered and tethered complexes, indicating that the η⁶-arene does not lie directly above the Ru(II) centre. Less ring-slippage, 0.014 Å, was observed in [RuCl₂(η¹:η⁶-*t*-Bu₂P(CH₂)₃Ph)] (253), indicating that the centre of the η⁶-arene lies almost directly above the metal. Slight ring-slippage was also observed for [RuCl₂(η¹:η⁶-Cy₂P(CH₂)₃Ph)] (225).¹³

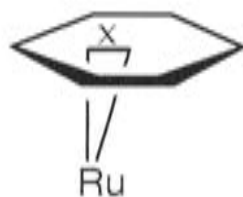


Figure 23. Diagrammatic representation of the ring-slippage distance *x* observed in the non-tethered and tethered complexes.

The Ru-P bond lengths in the tethered compounds, which are in the range 2.30-2.35 Å (see Table 16) are generally significantly shorter, by as much as 0.07 Å, than those of the non-tethered complexes, which lie between 2.33-2.39 Å. For example, the difference between the Ru-P bond lengths in non-tethered and tethered complexes containing *i*-Pr₂P(CH₂)₃Ph (**196**) is *ca* 0.055 Å. The exception to this trend is [RuCl₂(η¹:η⁶-Ph₂PCH₂SiMe₂Ph)] (**252**) whose Ru-P distance is longer by 0.037 Å than that in the η⁶-*p*-cymene complex [RuCl₂(η⁶-1,4-MeC₆H₄CHMe₂)(η¹-Ph₂PCH₂SiMe₂Ph)] (**235**). A possible reason for this difference will be discussed later.

The Ru-P bond lengths of the non-tethered and tethered complexes (see Table 16) reported here show good agreement with those reported in the literature; Table 19 shows reported non-tethered complexes with tertiary phosphines containing methyl and phenyl substituents and Table 20 gives Ru-P bond lengths of reported tethered complexes containing a variety of substituents on the phosphorus donor atom. The Ru-P bond lengths are generally greater when there are bulky substituents on phosphorus. For example, the non-tethered complex [RuCl₂(η⁶-1,4-MeC₆H₄CHMe₂)(η¹-Me₂P(CH₂)₃Ph)] (**231**) has a shorter Ru-P bond length (2.3290(7) Å) than [RuCl₂(η⁶-1,4-MeC₆H₄CHMe₂)(η¹-*i*-Pr₂P(CH₂)₃Ph)] (**232**) (2.393(3) Å), and the longest bonds are observed in the *t*-butyl substituted complexes [RuCl₂(η¹:η⁶-*t*-Bu₂P(CH₂)₂Ph)] (**303**)¹⁴ and [RuCl₂(η¹:η⁶-*t*-Bu₂P(CH₂)₃Ph)] (**253**). This behaviour is observed in both the non-tethered and tethered complexes, where the general trend of increasing Ru-P bond lengths is R = Me < Ph < *i*-Pr < Cy < *t*-Bu. The correlation between Ru-P bond length and the size of the substituents on the tertiary phosphine has been observed in complexes of the type [RuCl(η⁵-C₅Me₅)(PR₃)₂]; bulkier substituents give rise to longer Ru-P bonds, which were, in increasing order, R = Me₃ < Me₂Ph < MePh₂ < Ph₃.⁷²

The aromatic rings in the non-tethered and tethered complexes are almost planar, though the Ru-C(arene) distances are influenced by the phosphine ligand (see Table 16). Those *trans* to the P-donor for the non-tethered

(2.22-2.27 Å) and tethered (2.22-2.29 Å) complexes are significantly greater than those *trans* to the Ru-Cl bonds, 2.14-2.23 Å and 2.15-2.25 Å, for the non-tethered and tethered complexes, respectively, reflecting the relative *trans*-influences of Cl and PR₃. The Ru-Cl bond lengths do not differ greatly (see Table 16), and are in the range 2.40-2.45 Å for the non-tethered and tethered complexes, though a longer Ru-Cl bond (2.52 Å) was observed in [RuCl₂(η¹:η⁶-*i*-Pr₂P(CH₂)₃Ph)] (249). The Ru-P and Ru-Cl bond lengths are in good agreement with those observed in [RuCl₂(η⁶-arene)(PMePh₂)] (arene = C₆H₆ (299) and *p*-MeC₆H₄CHMe₂ (300))⁶⁷ and [RuCl₂(η¹:η⁶-R₂P(CH₂)₃Ph)] (R = Ph (222))^{7,56} and Cy (225)¹³.

The trigonal RuCl₂P fragment could, in principle, adopt either an eclipsed or staggered conformation with respect to the carbon atoms of the η⁶-arene. Of both the non-tethered and tethered complexes, [RuCl₂(η⁶-1,2-MeC₆H₄CO₂Me)(η¹-Cy₂P(CH₂)₃Ph)] (239) is the only one to adopt an eclipsed arrangement (see Figure 25); [RuCl₂(η⁶-1,4-MeC₆H₄CHMe₂)(η¹-*i*-Pr₂P(CH₂)₃Ph)] (232), (see Figure 26) [RuCl₂(η⁶-1,4-MeC₆H₄CHMe₂)(η¹-Ph₂P(CH₂)₃-aryl)] (aryl = 2,4,6-C₆H₂Me₃ (233) and C₆Me₅ (234)), [RuCl₂(η¹:η⁶-R₂P(CH₂)₃Ph)] (R = Me (248), *i*-Pr (249), *t*-Bu (253)), [RuCl₂(η¹:η⁶-Ph₂P(CH₂)₃C₆Me₅)] (251) and [RuCl₂(η¹:η⁶-Ph₂PCH₂SiMe₂Ph)] (252) adopt staggered conformations. In complexes [RuCl₂(η⁶-1,4-MeC₆H₄CHMe₂)(η¹-Me₂P(CH₂)₃Ph)] (231) (see Figure 27), [RuCl₂(η⁶-C₆H₆)(η¹-Ph₂P(CH₂)₃Ph)] (227), [RuCl₂(η⁶-1,4-MeC₆H₄CHMe₂)(η¹-Ph₂CH₂SiMe₂Ph)] (235) and [RuCl₂(η¹:η⁶-Ph₂P(CH₂)₃-2,4,6-C₆H₂Me₃)] (250) the conformation lies about half-way between eclipsed and staggered.

Table 16. Summary of the chemically significant bond lengths for the various non-tethered and tethered complexes.

RuCl ₂ Complex	Ru-P (Å)	Ru-Cl(1) (Å)	Ru-Cl(2) (Å)	Ru-C(arene) (Å) <i>trans-</i> to Phosphorus (two atoms)	Ru-C(arene) (Å) <i>trans-</i> to Chloride ligands (four atoms)
[(<i>p</i> -cym)(η ¹ -Me ₂ P~Ph)] (231)	2.3290(7)	2.4357(7)	2.4073(8)	2.221(3)-2.260(2)	2.160(2)-2.218(3)
[(ben)(η ¹ -Ph ₂ P~Ph)] (227)	2.3500(7)	2.4059(7)	2.3976(7)	2.219(3)-2.228(3)	2.1420(3)-2.182(3)
[(<i>p</i> -cym)(η ¹ - <i>i</i> -Pr ₂ P~Ph)] (232) ^a	2.393(3)	2.428(2)	2.421(3)	2.241(9)-2.262(9)	2.208(9)-2.227(10)
[(<i>o</i> -mt)(η ¹ -Cy ₂ P~Ph)] (239) ^b	2.3631(13)	2.4051(15)	2.4039(14)	2.262(5)-2.271(6)	2.181(5)-2.228(6)
[(<i>p</i> -cym)(η ¹ -Ph ₂ P~-2,4,6-C ₆ H ₂ Me ₃)] (233)	2.3253(7)	2.4136(7)	2.4397(7)	2.220(3)-2.226(3)	2.178(3)-2.232(3)
[(<i>p</i> -cym)(η ¹ -Ph ₂ P~C ₆ Me ₅)] (234) ^b	2.3406(10)	2.4130(11)	2.4160(11)	2.248(4)-2.252(4)	2.188(4)-2.226(4)
[(<i>p</i> -cym)(η ¹ -Ph ₂ PCH ₂ SiMe ₂ Ph)] (235)	2.3159(12)	2.4160(12)	2.4077(12)	2.218(5)-2.246(6)	2.162(5)-2.219(5)
[η ¹ :η ⁶ -Me ₂ P~Ph] (248) ^b	2.322(3)	2.405(2)	2.421(2)	2.257(9)	2.170(9)-2.193(8)
[η ¹ :η ⁶ -Ph ₂ P~Ph] (222) ^c	2.3187(13)	2.4271(14)	2.4039(14)	2.241(4)-2.246(5) [‡]	2.171(4)-2.199(4) [‡]
[η ¹ :η ⁶ -Ph ₂ P~Ph] (222) ^d	2.3243(11)	2.4183(12)	2.4002(11)	2.252-2.267 [‡]	2.177-2.202 [‡]
[η ¹ :η ⁶ - <i>i</i> -Pr ₂ P~Ph] (249)	2.338(2)	2.5247(18)	2.4185(19)	2.254(8)	2.163(8)-2.211(7)
[η ¹ :η ⁶ -Cy ₂ P~Ph] (225) ^e	2.347(3)	2.417(3)	2.420(3)	2.196-2.258 [‡]	2.159-2.206 [‡]
[η ¹ :η ⁶ - <i>t</i> -Bu ₂ P~Ph] (253)	2.413(9)	2.4464(9)	2.4141(9)	2.223(3)-2.230(4)	2.166(3)-2.238(3)
[η ¹ :η ⁶ -Ph ₂ P~-2,4,6-C ₆ H ₂ Me ₃] (250)	2.3230(10)	2.4159(10)	2.4425(10)	2.262(4)-2.282(4)	2.183(4)-2.212(4)
[η ¹ :η ⁶ -Ph ₂ P~C ₆ Me ₅] (251)	2.2995(14)	2.4016(12)	2.4163(12)	2.284(5)-2.285(5)	2.182(5)-2.249(5)
[η ¹ :η ⁶ -Ph ₂ PCH ₂ SiMe ₂ Ph] (252)	2.3526(7)	2.4050(7)	2.4159(7)	2.246(3)-2.250(3)	2.145(3)-2.193(3)

^aData for one of the four molecules in the unit cell are given; ^bdata for one of the two molecules in the unit cell are given; ^ccrystal structure reported in reference(7); ^dcrystal structure reported in reference(56); ^ecrystal structure reported in reference(13). [†]Estimated standard deviations (ESD's) are not stated since data was obtained from the Cambridge Structural Database (CSD).

ben = benzene, C₆H₆

p-cym = *p*-cymene, 1,4-MeC₆H₄CHMe₂

o-mt = methyl *o*-toluate, 1,2-MeC₆H₄CO₂Me

Table 17. Metal- η^6 -arene metrical data for the various non-tethered complexes.

RuCl ₂ Complex	Ru-centroid (Å)	Ru-least-squares plane of η^6 -arene (Å)	Ring-slippage (Å)
[(<i>p</i> -cym)(η^1 -Me ₂ P~Ph)] (231)	1.700(1)	1.6985(1)	0.073
[(ben)(η^1 -Ph ₂ P~Ph)] (227)	1.6894(16)	1.6881(2)	0.068
[(<i>p</i> -cym)(η^1 - <i>i</i> -Pr ₂ P~Ph)] (232) ^a	1.714(4)	1.7127(8)	0.067
[(<i>o</i> -mt)(η^1 -Cy ₂ P~Ph)] (239) ^b	1.713(2)	1.7114(4)	0.070
[(<i>p</i> -cym)(η^1 -Ph ₂ P~-2,4,6-C ₆ H ₂ Me ₃)] (233)	1.705(11)	1.7001(12)	0.039
[(<i>p</i> -cym)(η^1 -Ph ₂ P~C ₆ Me ₅)] (234) ^b	1.7127(18)	1.7122(3)	0.038
[(<i>p</i> -cym)(η^1 -Ph ₂ PCH ₂ SiMe ₂ Ph)] (235)	1.6995(19)	1.6986(3)	0.055
[η^1 : η^6 -Me ₂ P~Ph] (248) ^b	1.703(4)	1.7016(7)	0.074
[η^1 : η^6 -Ph ₂ P~Ph] (222) ^c	1.694 [†]	-	-
[η^1 : η^6 -Ph ₂ P~Ph] (222) ^d	1.701 [†]	-	-
[η^1 : η^6 - <i>i</i> -Pr ₂ P~Ph] (249)	1.701(4)	1.7003(7)	0.052

RuCl ₂ Complex	Ru-centroid (Å)	Ru-least-squares plane of η ⁶ -arene (Å)	Ring-slippage (Å)
[η ¹ :η ⁶ -Cy ₂ P~Ph] (225) ^e	1.701 [‡]	-	-
[η ¹ :η ⁶ - <i>t</i> -Bu ₂ P~Ph] (253)	1.6994(16)	1.6994(2)	0.014
[η ¹ :η ⁶ -Ph ₂ P~-2,4,6-C ₆ H ₂ Me ₃] (250)	1.7094(19)	1.7081(3)	0.065
[η ¹ :η ⁶ -Ph ₂ P~C ₆ Me ₅] (251)	1.717(2)	1.7160(4)	0.052
[η ¹ :η ⁶ -Ph ₂ PCH ₂ SiMe ₂ Ph] (252)	1.6880(13)	1.6873(2)	0.075

^aData for one of the four molecules in the unit cell are given; ^bdata for one of the two molecules in the unit cell are given; ^ccrystal structure reported in reference(7); ^dcrystal structure reported in reference(56); ^ecrystal structure reported in reference(13). [‡]ESD's are not stated since data was obtained from the CSD.

ben = benzene, C₆H₆

p-cym = *p*-cymene, 1,4-MeC₆H₄CHMe₂

o-mt = methyl *o*-toluate, 1,2-MeC₆H₄CO₂Me

Table 18. C-C(arene) distances (Å) for the arene (both free and coordinated) of the corresponding non-tethered and tethered RuCl₂ complexes.

Phosphine	Average C-C(arene) Bond Lengths (Å) of Free Arene in RuCl ₂ Non-Tethered Complexes	Average C-C(arene) Bond Lengths (Å) in η ⁶ -Arene of RuCl ₂ Tethered Complexes
Me ₂ P~Ph	1.36	1.41 ^a
Ph ₂ P~Ph	1.38	1.41 ^b
<i>i</i> -Pr ₂ P~Ph	1.39 ^c	1.41
Cy ₂ P~Ph	1.37	1.40 ^d
Ph ₂ P~2,4,6-C ₆ H ₂ Me ₃	1.39	1.42
Ph ₂ P~C ₆ Me ₅	1.40	1.43
Ph ₂ PCH ₂ SiMe ₂ Ph	1.37	1.41

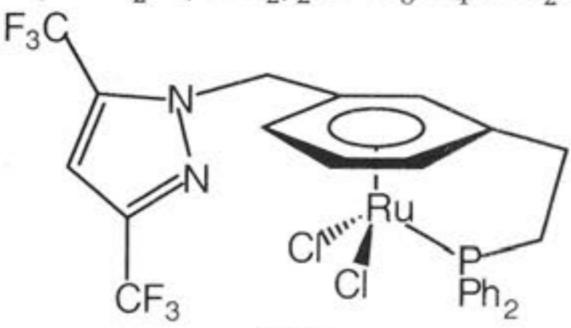
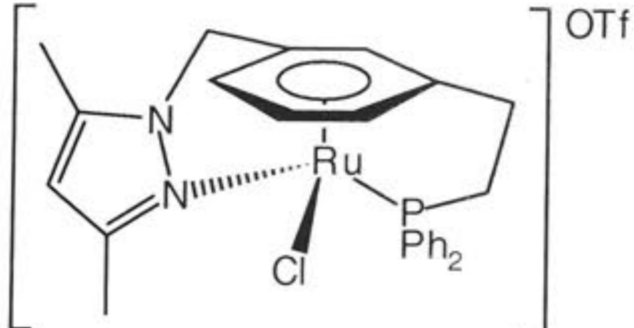
^aData from one of the two molecules in the unit cell are given; ^bcrystal structure reported in references(7,56); ^cdata from one of the four molecules in the unit cell are given; ^dcrystal structure reported in reference(13).

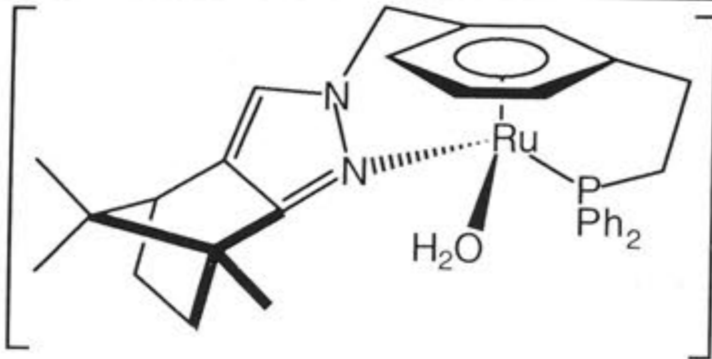
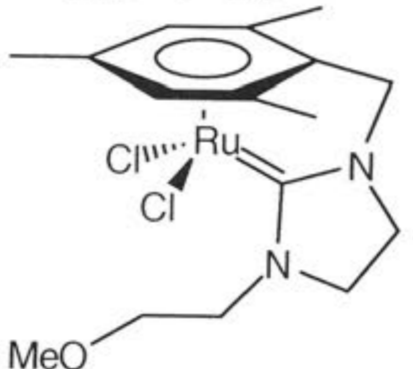
Table 19. Ru-P bond lengths in $[\text{RuCl}_2(\eta^6\text{-arene})(\text{PR}_3)]$ non-tethered complexes.

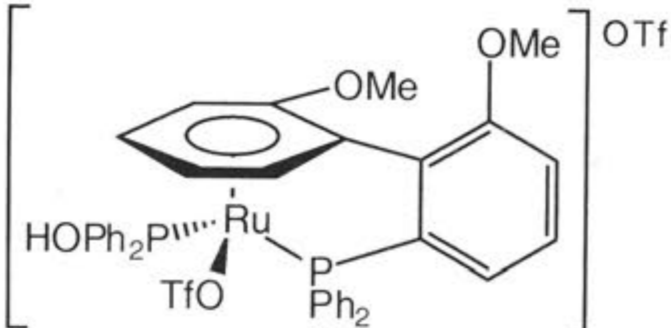
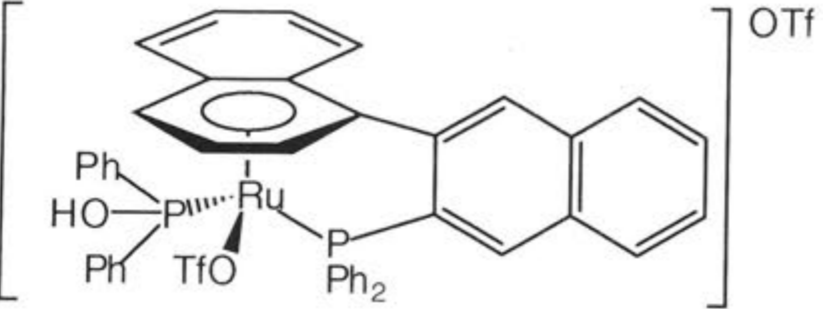
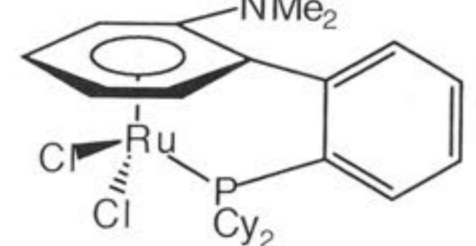
Complex	Ru-P Bond Length (Å)	Reference
$[\text{RuCl}_2(\eta^6\text{-C}_6\text{Me}_6)(\text{PMe}_3)]$ (304)	2.343(3)	73
$[\text{RuCl}_2(\eta^6\text{-C}_6\text{Et}_6)(\text{PMe}_3)]$ (305)	2.343(1)	74
$[\text{RuCl}_2(\eta^6\text{-C}_6\text{H}_6)(\text{PMePh}_2)]$ (299)	2.335 [‡]	67
$[\text{RuCl}_2(\eta^6\text{-1,4-MeC}_6\text{H}_4\text{CHMe}_2)(\text{PMePh}_2)]$ (300)	2.341 [‡]	67
$[\text{RuCl}_2(\eta^6\text{-1,2-MeC}_4\text{H}_4\text{CO}_2\text{Me})(\text{NMDPP})]$ (301)	2.357(6)	68
$[\text{RuCl}_2(\eta^6\text{-C}_6\text{H}_6)(\text{PPh}_3)]$ (302)	2.3641(1)	69
$[\text{RuCl}_2(\eta^6\text{-C}_6\text{Me}_6)(\text{PPh}_3)]$ (306)	2.3607(10)	73
$[\text{RuCl}_2(\eta^6\text{-C}_6\text{Et}_6)(\text{PPh}_3)]$ (307)	2.388(1)	74

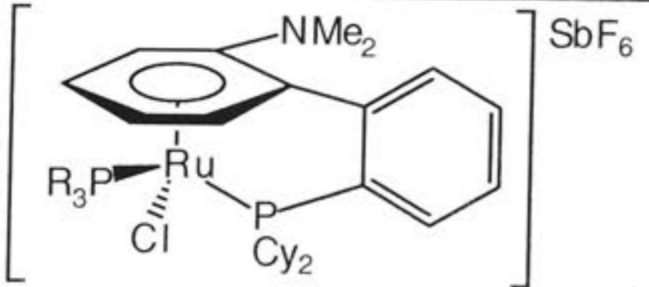
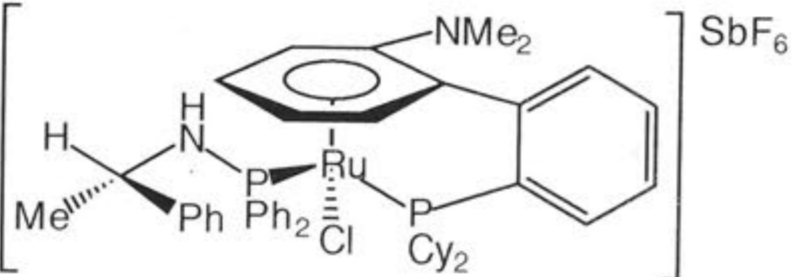
[‡]ESD not stated in reference(67).

Table 20. Ru-P bond lengths (Å) and dihedral angles (°), where applicable, of various tethered arene-ruthenium complexes.

Complex	Substituent	Ru-P Bond Length (Å)	Dihedral Angle (°)	Reference
[RuCl ₂ (η ¹ :η ⁶ -Ph ₂ P(CH ₂) ₂ -2-C ₆ H ₄ CH ₂ OH)] (217)	-	2.3261(7)	9	6
[RuCl ₂ (η ¹ :η ⁶ -Ph ₂ P(CH ₂) ₂ -3-C ₆ H ₄ CH ₂ OH)] (308)	-	2.3384(10)	6	6
	-	2.3222(1)	9	15 ^a
	-	2.479 ^b	7 (C ⁷) ^c 11.5 (C ⁹) ^c	17

Complex	Substituent	Ru-P Bond Length (Å)	Dihedral Angle (°)	Reference
 (R_{arene}, R_P, S_{Ru}) - 311 ^d	-	2.380(2)	7 (C ⁷) ^c 16.5 (C ⁹) ^c	16 ^a
 138	-	-	14	75
[RuI ₂ (η ¹ :η ⁶ -Ph ₂ P(CH ₂) ₂ Ph)] (294)	-	Molecule 1 2.320 ^b Molecule 2 2.324 ^b	9	10
[RuI ₂ (η ¹ :η ⁶ -Ph ₂ PCH ₂ CH(Ph)Ph)] (295)	-	2.305 ^b	6	10
[Ru(Me) ₂ (η ¹ :η ⁶ -Ph ₂ P(CH ₂) ₂)Ph] (297)	-	2.263(1)	8.5 ^{b,e}	28 ^a
[RuCl ₂ (η ¹ :η ⁶ -Ph ₂ P(CH ₂) ₂)Ph] ₂ [B(3,5-C ₆ H ₃ (CF ₃) ₂) ₄] ₂ (312)	-	2.3624(9) ^f	6.5 ^{b,e,f}	66
[RuCl(PPh ₃)(η ¹ :η ⁶ -Ph ₂ P~Ph)]PF ₆ (290)	-	2.3307(9)	-	65

Complex	Substituent	Ru-P Bond Length (Å)	Dihedral Angle (°)	Reference
[RuCl(NCMe)($\eta^1:\eta^6$ -Ph ₂ P~Ph)]PF ₆ (313)	-	2.3218(9)	-	65
[RuCl ₂ ($\eta^1:\eta^6$ -Ph ₂ P~-4-C ₆ H ₄ Me)] (274)	-	2.3127(9)	-	56
[RuCl ₂ ($\eta^1:\eta^6$ -Ph ₂ P~-4-C ₆ H ₄ CHMe ₂)] (271)	-	2.3226(11)	-	56
[RuCl ₂ ($\eta^1:\eta^6$ -Ph ₂ P~-3,5-C ₆ H ₃ Me ₂)] (275)	-	2.326(2)	-	56
 151	-	2.3529(16)	5.5 ^g	76
 155	-	Molecule 1 2.3389(14) ^h Molecule 2 2.345 ^{b,h,i}	4 ^g	76 ^a
 164	-	2.343(2)	j	77

Complex	Substituent	Ru-P Bond Length (Å)	Dihedral Angle (°)	Reference
 $\left[\text{Ru}(\text{NMe}_2)(\text{R}_3\text{P})(\text{Cl})(\text{Cy}_2) \right] \text{SbF}_6$	167 $\text{R}_3 = \text{Ph}_3$ 169 $\text{R}_3 = \text{PhMe}_2$ 170 $\text{R}_3 = \text{Me}_3$	2.398(2) 2.360(2) 2.348(3)	j	77
 (S)-171^d	-	2.390(2)	j	77
$[\text{Ru}(\text{Me})_2(\eta^1:\eta^6\text{-Cy}_2\text{P}(\text{CH}_2)_2\text{Ph})] \text{ (298)}$	-	2.3070(11)	14 ^{b,e}	28 ^a
$[\text{RuCl}(\text{=C=C=CPh}_2)(\eta^1:\eta^6\text{-Cy}_2\text{P}\sim\text{Ph})] \text{OTf (314)}$	-	2.3360(11)	-	13
$[\text{RuCl}(\text{NCMe})(\eta^1:\eta^6\text{-}t\text{-Bu}_2\text{P}(\text{CH}_2)_2\text{Ph})] \text{PF}_6 \text{ (315)}$	-	2.3976(13)	8	14

Note: dihedral angle values are approximate and are based on data obtained electronically, either from the CSD or by applying Crystals Issue 11.6⁷⁸ to data extracted from the CSD.

^aComplexes with similar ligands showed comparable Ru-P bond lengths and dihedral angles;^{15,16,66,79,80} ^bESD's are not stated since data were obtained from the CSD; ^catom labelling shown in Figure 24; ^dchirality assignments based on references(81,82); ^ethe atomic coordinates of these structures (electronic coordinates were not available) were entered into Crystals Issue 11.6 to obtain an approximate dihedral angle; ^hdata for only one half of the dimer is given; ^greading should be regarded with caution, since the carbon atom of the η^6 -arene attached to the tether does not lie within the mean plane of the arene; ^fthe bond length for the phosphorus atom of the tether is given; ⁱa search of the CSD revealed that there were two molecules in different crystallographic forms, which was not discussed in the literature;⁷⁶ ^jdihedral angle could not be determined since neither the atomic nor the electronic coordinates were available.

$\sim = (\text{CH}_2)_3$

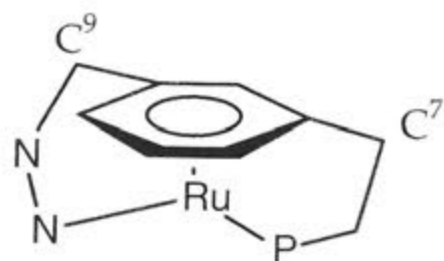


Figure 24. Atom labelling for the dihedral angles of complexes **310** and **311** listed in Table 20.

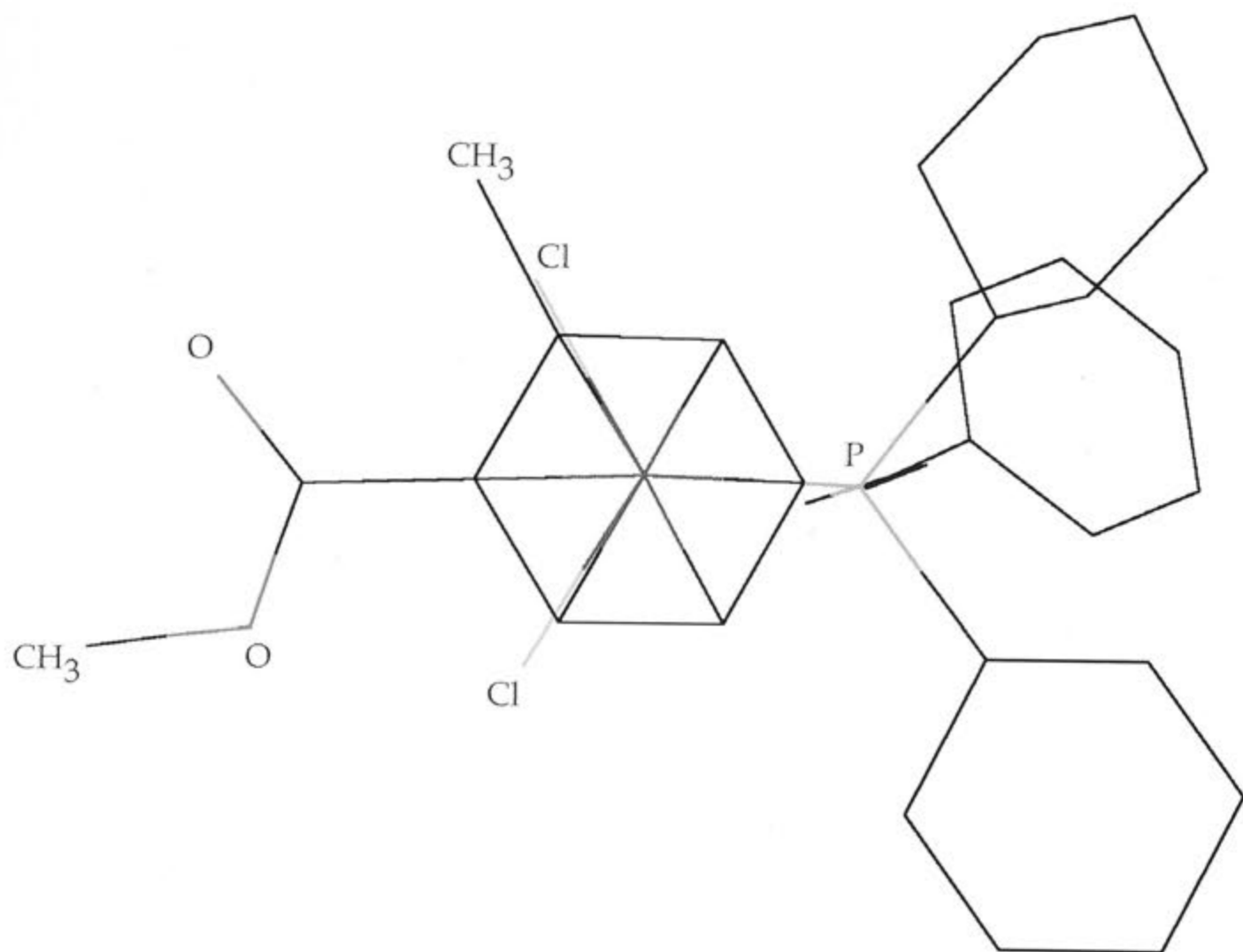


Figure 25. Chem3D representation of the molecular structure of compound $[\text{RuCl}_2(\eta^6\text{-1,2-MeC}_6\text{H}_4\text{CO}_2\text{Me})(\eta^1\text{-Cy}_2\text{P}(\text{CH}_2)_3\text{Ph})]$ (**239**), looking down on the η^6 -arene. Hydrogen atoms have been omitted for clarity.

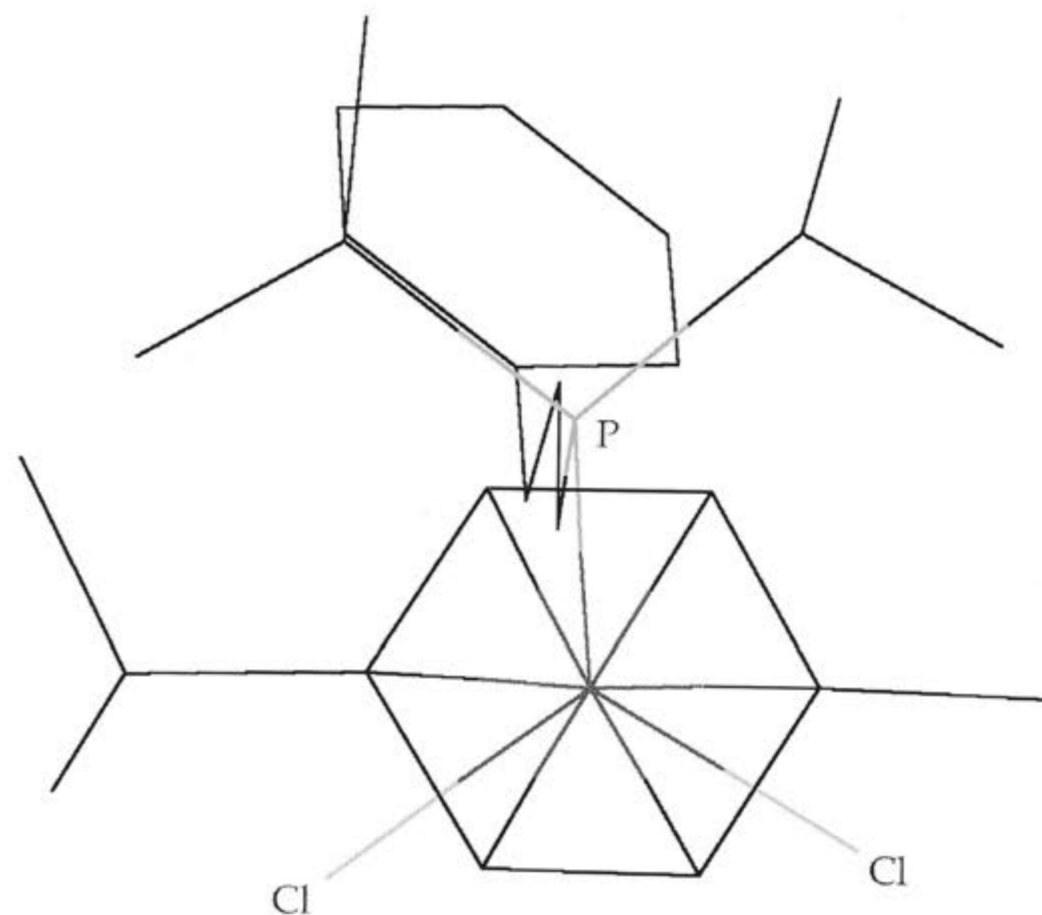


Figure 26. Chem3D representation of the molecular structure of compound $[\text{RuCl}_2(\eta^6\text{-1,4-MeC}_6\text{H}_4\text{CHMe}_2)(\eta^1\text{-}i\text{-Pr}_2\text{P}(\text{CH}_2)_3\text{Ph})]$ (**232**), looking down on the η^6 -arene. Hydrogen atoms and the solvent molecule (CH_2Cl_2) have been omitted for clarity.

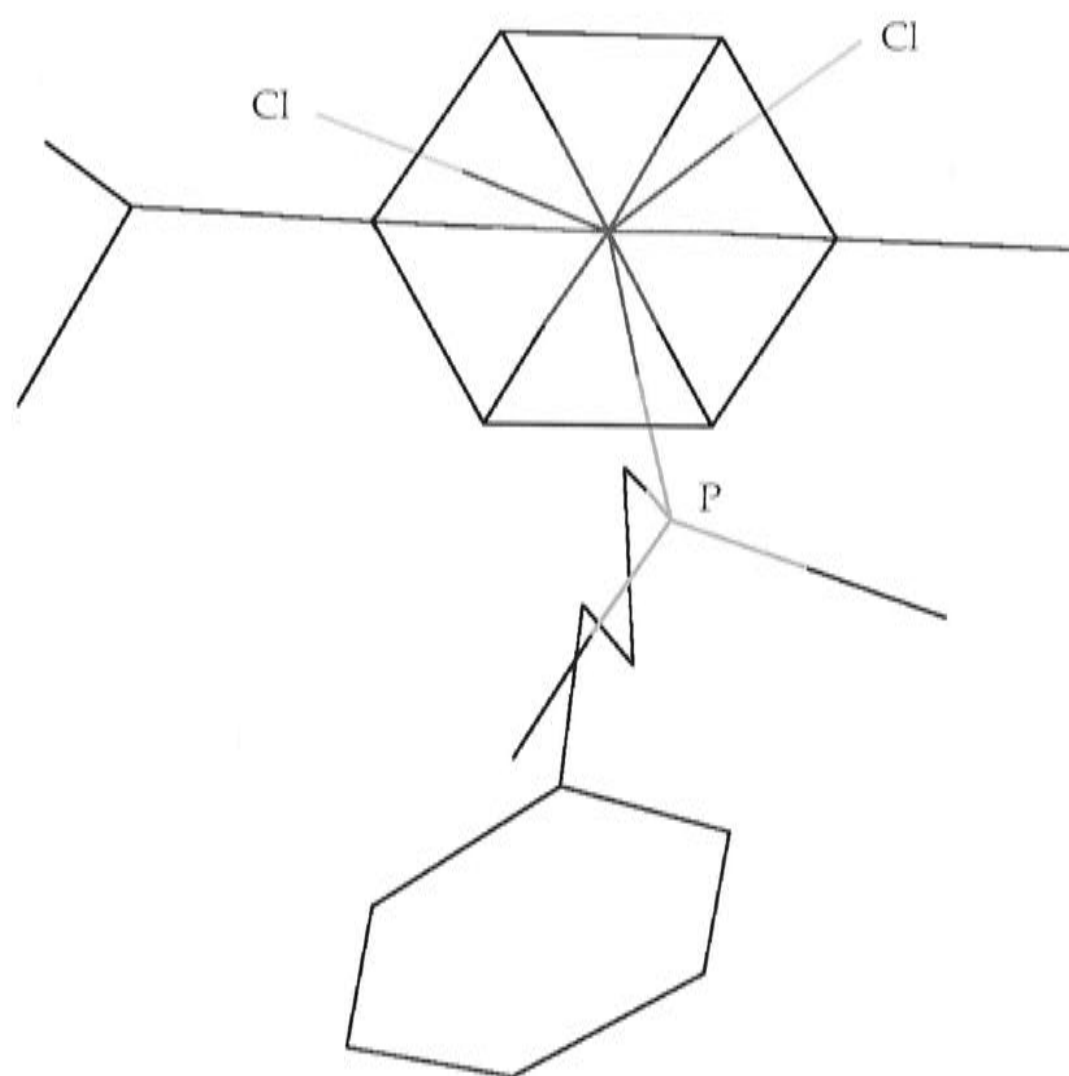


Figure 27. Chem3D representation of the molecular structure of compound $[\text{RuCl}_2(\eta^6\text{-1,4-MeC}_6\text{H}_4\text{CHMe}_2)(\eta^1\text{-Me}_2\text{P}(\text{CH}_2)_3\text{Ph})]$ (**231**), looking down on the η^6 -arene. Hydrogen atoms have been omitted for clarity.

The most significant difference between the non-tethered and tethered complexes is in the conformation of the tether itself. In complexes incorporating a three methylene unit strap, the five connected atoms $\text{P}-(\text{CH}_2)_3\text{-C}(\text{ring})$ can be compared to pentane, which can exist in three different principal conformations (see Figure 28) where adjacent atoms are in either *anti* (*a*) or *gauche* (*g*) positions.²⁴ The fourth conformer, g^-g^+ , can be excluded since it is extremely unstable due to severe steric interactions (see Figure 29).^{24,83} At room temperature, the enthalpy-preferred *aa* conformer and the entropy-preferred $a(g)^\pm$ conformer dominate the equilibrium. The *aa* conformer is favoured at lower temperatures, whereas higher temperatures favour the $a(g)^\pm$ conformer, while $(gg)^\pm$ is energetically disfavoured, since it is higher in enthalpy; the enthalpies of formation for the $a(g)^\pm$ and $(gg)^\pm$ conformers are 3.4 and 6.9 kJ mol^{-1} , respectively.

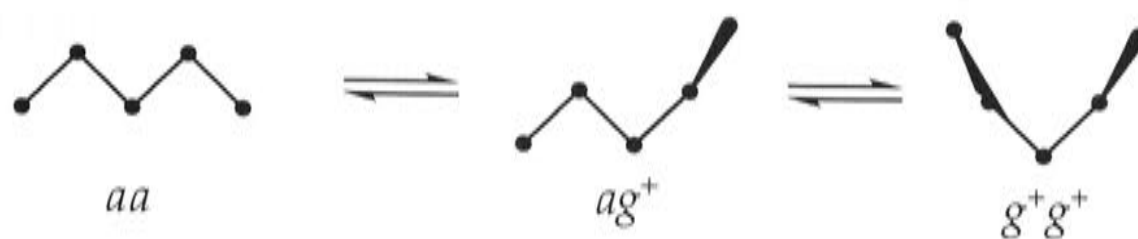


Figure 28. The three allowed conformers of pentanes.^{24,83}



Figure 29. The disfavoured g^-g^+ conformer of pentane (severe steric interaction indicated by dotted lines).^{24,83}

A related change in conformation is evident in the crystal structures of the non-tethered and tethered complexes. The *aa* conformation observed in the crystal structures of the non-tethered complexes is presumably the same as that present in the crystal structure of the free phosphine, $\text{Ph}_2\text{P}(\text{CH}_2)_3\text{Ph}$ (**118**) (see Figure 30). Figure 31 shows the *aa* conformation in the non-tethered complex $[\text{RuCl}_2(\eta^6\text{-1,4-MeC}_6\text{H}_4\text{CHMe}_2)(\eta^1\text{-Me}_2\text{P}(\text{CH}_2)_3\text{Ph})]$ (**231**). The torsion angles $\text{P}(1)\text{-C}(1)\text{-C}(2)\text{-C}(3)$ and $\text{C}(1)\text{-C}(2)\text{-C}(3)\text{-C}(4)$ lie in the range $165.1\text{-}176.9^\circ$, and are close to the "ideal" 180° ,²⁴ which minimises non-bonded hydrogen-hydrogen repulsions. However, the chain in the tethered complex $[\text{RuCl}_2(\eta^1:\eta^6\text{-Me}_2\text{P}(\text{CH}_2)_3\text{Ph})]$ (**248**) is present as one of the $(gg)^\pm$ conformers (Figure 32); it could be either g^+g^+ or g^-g^- , since **248** is not chiral. Thus rotation about both the $\text{C}(1)\text{-C}(2)$ and $\text{C}(2)\text{-C}(3)$ bonds has occurred, such that the torsion angles $\text{P}(1)\text{-C}(1)\text{-C}(2)\text{-C}(3)$ and $\text{C}(1)\text{-C}(2)\text{-C}(3)\text{-C}(4)$ are now $73(1)^\circ$ and $67(1)^\circ$, respectively. This is illustrated in Figures 33 and 34, which show that the phosphorus and $\text{C}(3)$ atoms lie on the same side of the $\text{C}(1)\text{-C}(2)$ bond (they are on opposite sides in both **118** and **231**) and the $\text{C}(1)$ and $\text{C}(4)$ atoms lie on the same side of the $\text{C}(2)\text{-C}(3)$ bond, respectively, confirming the $(gg)^\pm$ conformation of the tether.

The *aa* conformer is the most favoured, where the torsion angles C(1)-C(2)...C(3)-C(4) and C(2)-C(3)...C(4)-C(5) are $\pm 180^\circ$. Transition to the higher energy *a(g)*[±] conformers, where these torsion angles are $\pm 65^\circ$ and $\pm 180^\circ$ (or the reverse), respectively, involves requires activation energy (lowest is 15 kJ mol⁻¹).^{24,83} Further activation energy (the lowest is 19 kJ mol⁻¹) gives rise to the still higher-lying (*gg*)[±] conformers, where the torsion angles are $\pm 65^\circ$. Simultaneous rotation about both bonds C(2)-C(3) and C(3)-C(4) is a more difficult process than stepwise rotation about each bond individually,²⁴ and direct transition from the *aa* to (*gg*)[±] conformers is not favoured, due to the very high barriers that need to be overcome.⁸³ Therefore the conversion from *aa* to one of the (*gg*)[±] conformers must proceed *via* one of the *a(g)*[±] conformers. Further, since the *a(g)*[±] conformers are favoured at higher temperatures,²⁴ it is postulated that these conformers are present in the chain of the non-tethered complex in solution, during the formation of the tethered complex, which occurs at high temperatures. One of the (*gg*)[±] conformations is then adopted as the tethered complex is formed. Thus, the conversion of the *aa* conformer into one of the (*gg*)[±] conformers involves intermolecular interactions that are expected to be less favourable.

If the η^6 -arene is considered as a single atom, the formation of the tethered complexes containing three methylene units in the strap is analogous to the formation of a six-membered ring. According to the Thorpe-Ingold effect (also known as the *gem*-dialkyl effect^{84,85}), *gem* dimethyl groups promote ring-closure^{85,86} as a consequence of enthalpy, entropy and conformational effects. The Thorpe-Ingold effect can stabilise small (less than seven-membered) rings as well as increasing their rate of formation.⁸⁵ Transannular repulsion of the hydrogen atoms of adjacent CH₂ groups causes significant strain in the ring and this is reduced by replacing a CH₂ group by a heteroatom (in this case phosphorus), such that the presence of one or more heteroatoms facilitates ring-closure.⁸⁵ For these effects to occur with larger atoms, such as phosphorus, substituents larger than methyl, for example,

tert-butyl, are required.⁸⁴ There must also be a reduction in the bond angles involving the atoms of the ring to be formed in order for ring-closure to occur.⁸⁵ This is apparent in the crystal structures of non-tethered and tethered complexes containing phosphines $R_2P(CH_2)_3Ph$ ($R = Me$ (**195**), Ph (**118**), *i*-Pr (**196**) and Cy (**197**)). Compounds containing phosphines $Ph_2P(CH_2)_3$ -aryl (aryl = 2,4,6- $C_6H_2Me_3$ (**199**) and C_6Me_5 (**200**)) are not considered in this discussion since their formation is also influenced by steric factors, arising from the substituents on the aromatic groups. Comparison of angles of complexes containing *t*- $Bu_2P(CH_2)_3Ph$ (**198**) could not be carried out, since a crystal structure of a non-tethered complex containing **198** was not determined. The biggest difference in bond angles between the non-tethered and tethered complexes was observed for the bond angles P(1)-C(1)-C(2) (see Figure 35 for atom labelling) which are listed in Table 21. A reduction in the magnitude of the bond angles is observed in all cases, which increases with the size of the substituent on the phosphorus atom. Thus the tethered complexes $[RuCl_2(\eta^1:\eta^6-R_2P(CH_2)_3Ph)]$ ($R = i$ -Pr (**249**), Cy (**225**) and *t*-Bu (**253**)), where the donor atoms carry bulky substituents were formed more easily than those incorporating the smaller substituents $[RuCl_2(\eta^1:\eta^6-R_2P(CH_2)_3Ph)]$ ($R = Me$ (**248**) and Ph (**222**)). There is little difference observed in the angles C(1)-C(2)-C(3), which lie in the range 110.7-111.5° and 113.3-114.4° for the non-tethered and tethered complexes, respectively, nor is there any significant change in the C(2)-C(3)-C(4) angles, which are between 112.9-117.4° and 114.6-116.4° for the non-tethered and tethered complexes, respectively.

There is also a trend observed in the magnitude of the torsion angles in the tethered complexes containing phosphines of the type $R_2P(CH_2)_3Ph$ (listed in Table 22). The magnitude of the angle P(1)-C(1)-C(2)-C(3) increases with the size of the substituent on the donor atom. This results in a greater difference between the two torsion angles (P(1)-C(1)-C(2)-C(3) and C(1)-C(2)-C(3)-C(4)) when there are larger substituents on the phosphorus atom. For example, complex $[RuCl_2(\eta^1:\eta^6-i-Pr_2P(CH_2)_3Ph)]$ (**249**), with *iso*-propyl substituents, has

a difference of 17.8° , whereas the difference in **248**, with smaller methyl substituents, is 6° . Since there are no significant differences in the bond angles of the tether involving atoms P(1)-C(1)-C(2)-C(3)-C(4) in $[\text{RuCl}_2(\eta^1:\eta^6\text{-R}_2\text{P}(\text{CH}_2)_3\text{Ph})]$ (R = Me (**248**), Ph (**222**), *i*-Pr (**249**), Cy (**225**) and *t*-Bu (**253**)), the magnitude of the torsion angles in the tether might also be related to the ease of formation of the tethered complexes. Therefore it appears that the complexes with larger differences between their torsion angles in the strap are easier to form. The torsion angles of the respective non-tethered complexes are generally close to 180° .

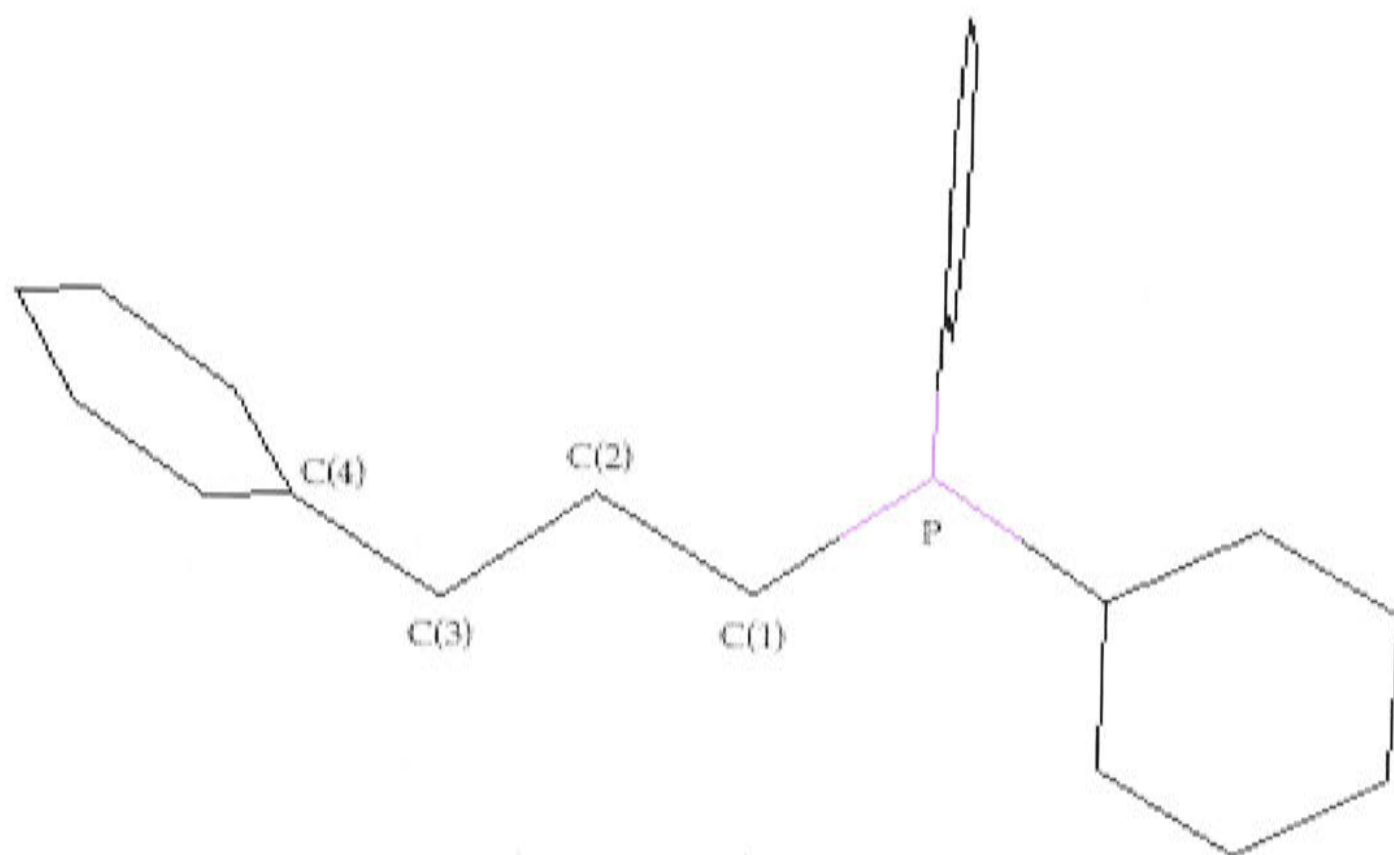


Figure 30. Chem3D representation of the molecular structure of compound $\text{Ph}_2\text{P}(\text{CH}_2)_3\text{Ph}$ (**118**) showing the *aa* conformation of the atoms P-C(1)-C(2)-C(3)-C(4). Hydrogen atoms have been omitted for clarity.

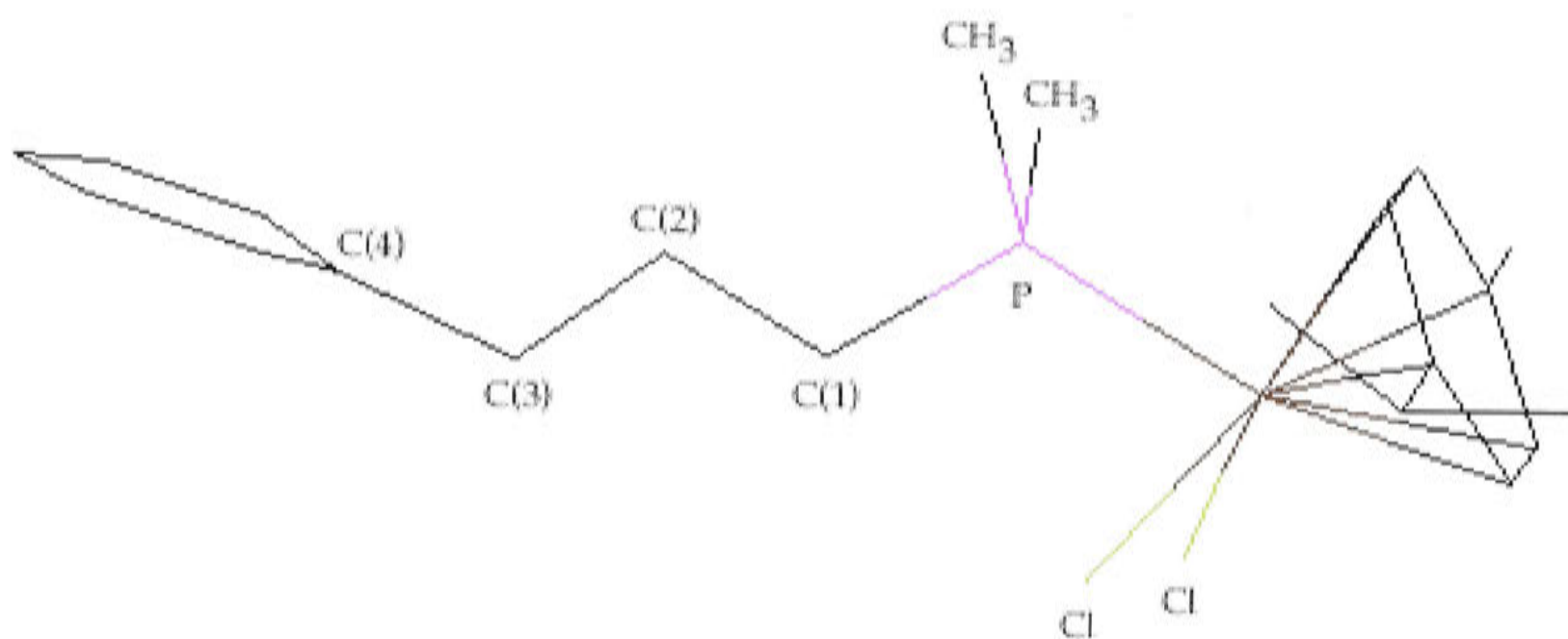


Figure 31. Chem3D representation of the molecular structure of $[\text{RuCl}_2(\eta^6\text{-1,4-MeC}_6\text{H}_4\text{CHMe}_2)(\eta^1\text{-Me}_2\text{P}(\text{CH}_2)_3\text{Ph})]$ (**231**) showing the *aa* conformation of the atoms P-C(1)-C(2)-C(3)-C(4). Hydrogen atoms have been omitted for clarity.

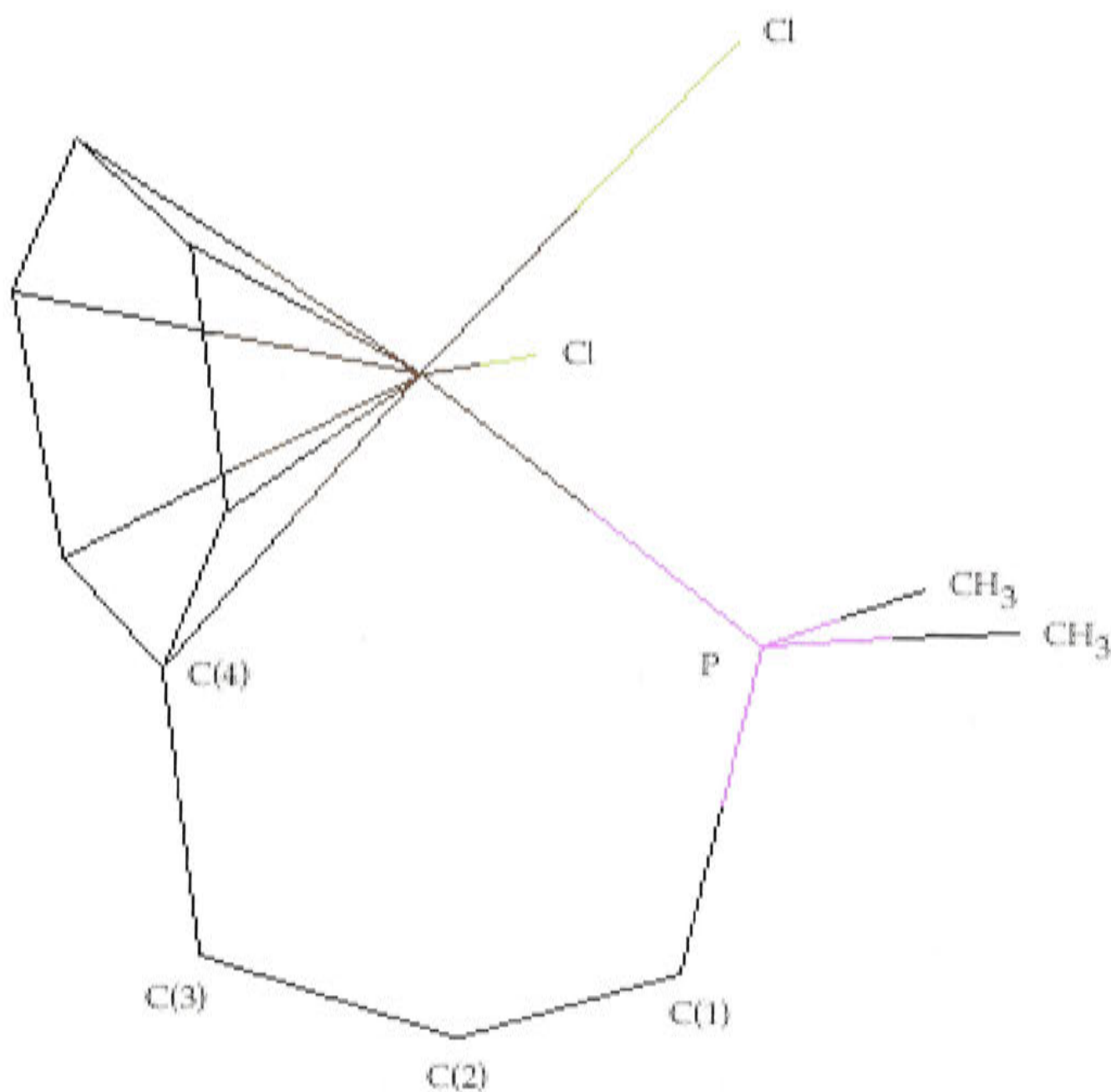


Figure 32. Chem3D representation of the molecular structure of $[\text{RuCl}_2(\eta^1:\eta^6\text{-Me}_2\text{P}(\text{CH}_2)_3\text{Ph})]$ (**248**), showing the *g⁺g⁺* conformation of the atoms P-C(1)-C(2)-C(3)-C(4). Hydrogen atoms have been omitted for clarity.

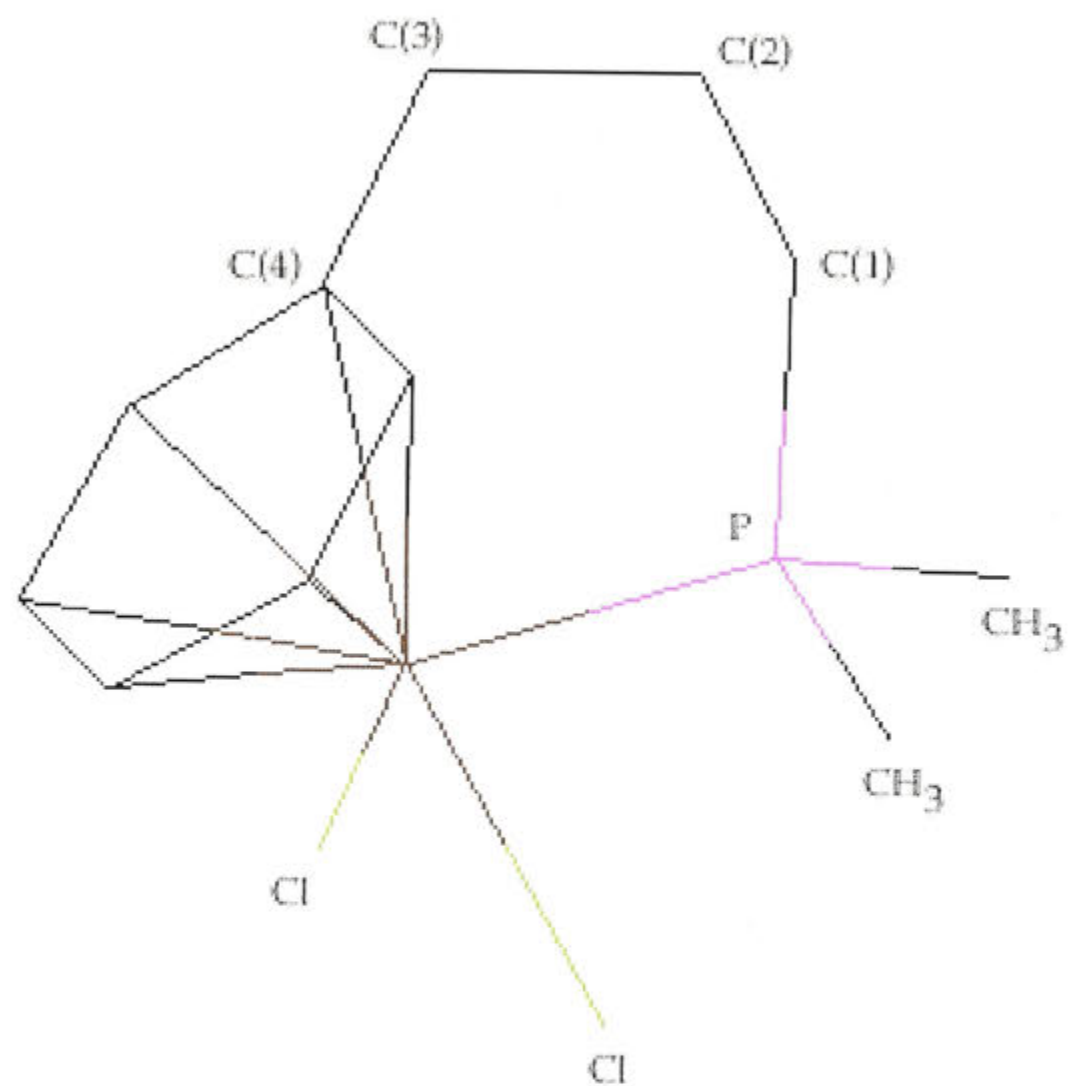


Figure 33. Chem3D representation of the molecular structure of compound [RuCl₂(η¹:η⁶-Me₂P(CH₂)₃Ph)] (248), with the C(1)-C(2) bond at the top of the molecule. Hydrogen atoms have been omitted for clarity.

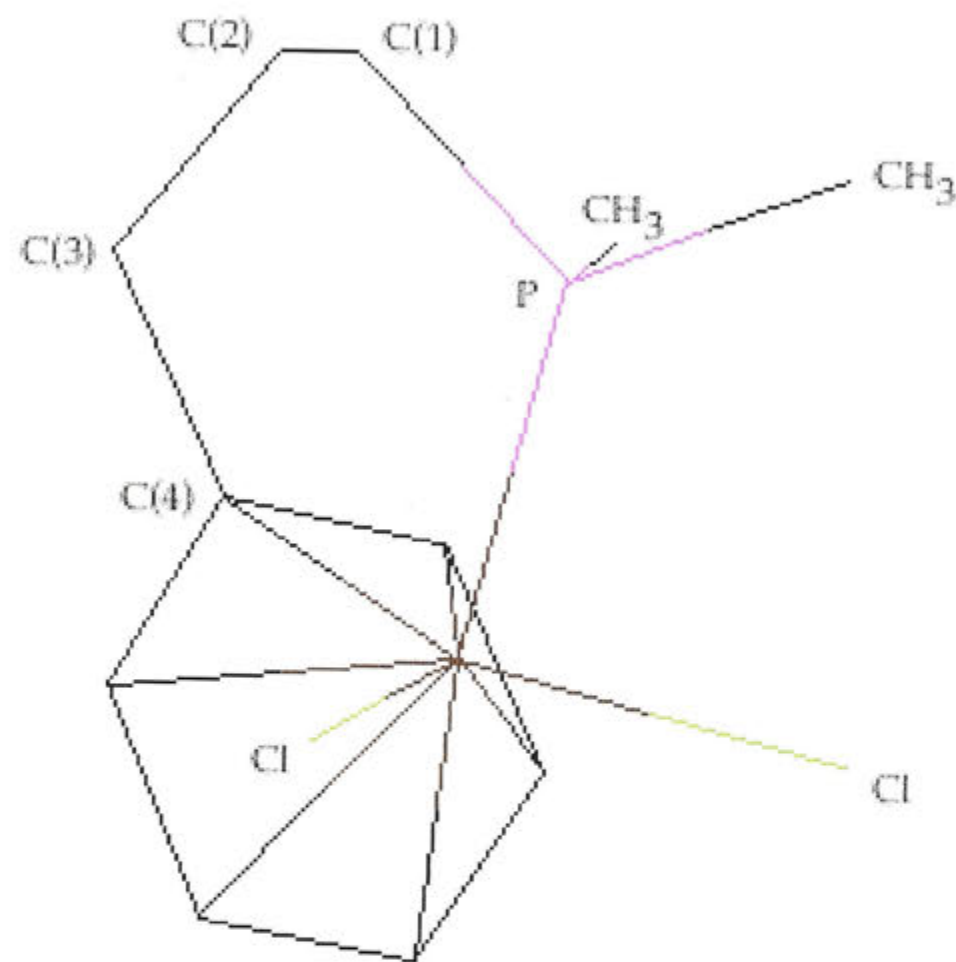


Figure 34. Chem3D representation of the molecular structure of compound [RuCl₂(η¹:η⁶-Me₂P(CH₂)₃Ph)] (248), with the C(2)-C(3) bond at the top of the molecule. Hydrogen atoms have been omitted for clarity.

Table 21. P(1)-C(1)-C(2) bond angles ($^{\circ}$) in the non-tethered and tethered complexes.

Phosphine	Bond Angle P(1)-C(1)-C(2) ($^{\circ}$) in Non-Tethered RuCl ₂ Complexes	Bond Angle P(1)-C(1)-C(2) ($^{\circ}$) in Tethered RuCl ₂ Complexes	Δ ($^{\circ}$)
Me ₂ P~Ph Ph ₂ P~Ph	116.7(2) 117.0(2)	114.1(7) 113.2 ^{†, 7} , 113.8 ^{†56}	2.6 3.2-3.8
<i>i</i> -Pr ₂ P~Ph Cy ₂ P~Ph	119.8(7) 119.5(4)	114.3(6) 113.5 ^{†13}	5.5 6.0

[†]ESDs are not stated since data was obtained from the CSD.

~ = (CH₂)₃

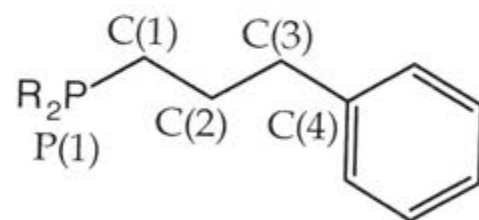


Figure 35. Atom labelling employed in Tables 21 and 22.

Table 22. Torsion angles of the strap of atoms P(1)-C(1)-C(2)-C(3)-C(4) in the tethered complexes of the type $[\text{RuCl}_2(\eta^1:\eta^6\text{-R}_2\text{P}(\text{CH}_2)_3\text{-aryl})]$.

Complex	Torsion Angle P(1)-C(1)-C(2)-C(3) (°)	Torsion Angle C(1)-C(2)-C(3)-C(4) (°)	Δ (°)
$[\eta^1:\eta^6\text{-Me}_2\text{P}\sim\text{Ph}]$ (248) ^a	73(1)	67(1)	6
$[\eta^1:\eta^6\text{-Ph}_2\text{P}\sim\text{Ph}]$ (222) ^b	76.8 [‡]	64.0 [‡]	12.8
$[\eta^1:\eta^6\text{-Ph}_2\text{P}\sim\text{Ph}]$ (222) ^c	76.7 [‡]	62.8 [‡]	13.9
$[\eta^1:\eta^6\text{-}i\text{-Pr}_2\text{P}\sim\text{Ph}]$ (249)	80.8(8)	63(1)	17.8
$[\eta^1:\eta^6\text{-Cy}_2\text{P}\sim\text{Ph}]$ (225) ^d	82.3 [‡]	61.6 [‡]	20.7
$[\eta^1:\eta^6\text{-}t\text{-Bu}_2\text{P}\sim\text{Ph}]$ (253)	83.1(3)	64.1(4)	19

^aData for one of the two molecules in the unit cell are given; ^bcrystal structure reported in reference(7); ^ccrystal structure reported in reference(56); ^dcrystal structure reported in reference(13). [‡]ESDs are not stated since data was obtained from the CSD. All angles are written as positive because the tethered complexes are not chiral.

$\sim = (\text{CH}_2)_3$

The formation of the tethered complex $[\text{RuCl}_2(\eta^1:\eta^6\text{-Ph}_2\text{PCH}_2\text{SiMe}_2\text{Ph})]$ (**252**) also results in conformational changes of the tether. The strap comprising atoms P-CH₂-Si-C(ring) can be compared to butane, which has two allowed conformations, *a* and *g*[±] (Figure 36a), differing in enthalpy by 3.4 kJ mol⁻¹.⁸³ Both conformers are expected to adopt a staggered conformation, where the two larger groups, C₆H₅ and PPh₂ are closer to one another in the *gauche* form than in the *anti* conformation (Figure 36b). The torsion angle for this chain is 160.1(3)° in the non tethered complex $[\text{RuCl}_2(\eta^6\text{-1,4-MeC}_6\text{H}_4\text{CHMe}_2)(\eta^1\text{-Ph}_2\text{P}(\text{CH}_2)_3\text{Ph})]$ (**235**), whereas rotation about the Si-CH₂ bond occurs as the tethered complex **252** is formed, and the torsion angle changes to 30.3(2)°. This is illustrated in Figure 37, which shows that the phosphorus and C(4) atoms lie on the same side of the Si-C(1) bond, indicating that the chain has adopted either one of the *g*[±] conformations; it could be either *ag*⁺ or *ag*⁻, since **252** is not chiral. The torsion angle in **252** is much lower than the 60° expected for perfectly staggered butanes,⁸³ indicating that the chain is somewhat strained. The formation of the pseudo five-membered ring causes a reduction in the bond angles involving the atoms P-CH₂-Si-C(ring). There is *ca* 11.1° difference between the P-CH₂-Si angles (123.3(3)° in $[\text{RuCl}_2(\eta^6\text{-1,4-MeC}_6\text{H}_4\text{CHMe}_2)(\eta^1\text{-Ph}_2\text{PCH}_2\text{SiMe}_2\text{Ph})]$ (**235**) *cf.* 112.2(1)° in **252**) and approximately 12.7° difference between the CH₂-Si-C(ring) (114.5(2)° in **235** *cf.* 101.8(1)° in **252**).

In complexes with the aryl(CH₂)₃PR₂ moieties, the benzylic carbon atom is coplanar with the carbon atoms of the attached arene, without distortion of the bond lengths or bond angles in the tether. In contrast, the presence of the two-atom strap in $[\text{RuCl}_2(\eta^1:\eta^6\text{-Ph}_2\text{PCH}_2\text{SiMe}_2\text{Ph})]$ (**252**) causes a bending of the Si-C(C₆H₅) bond out of the aromatic plane by approximately 14°. This may be the cause of both the lengthening of the Ru-P bond from $[\text{RuCl}_2(\eta^6\text{-MeC}_6\text{H}_4\text{CHMe}_2)(\eta^1\text{-Ph}_2\text{PCH}_2\text{SiMe}_2\text{Ph})]$ (**235**) to **252** (see Table 16), and the slightly shorter Ru-centroid distance (see Table 17). It is clear that

the complex **252** is somewhat strained, since the torsion angle P(1)-C(1)-Si(1)-C(4) is much smaller (30.3°) than the normal 60° for butanes,⁸³ but only the Ru-P bond length seems to be affected.

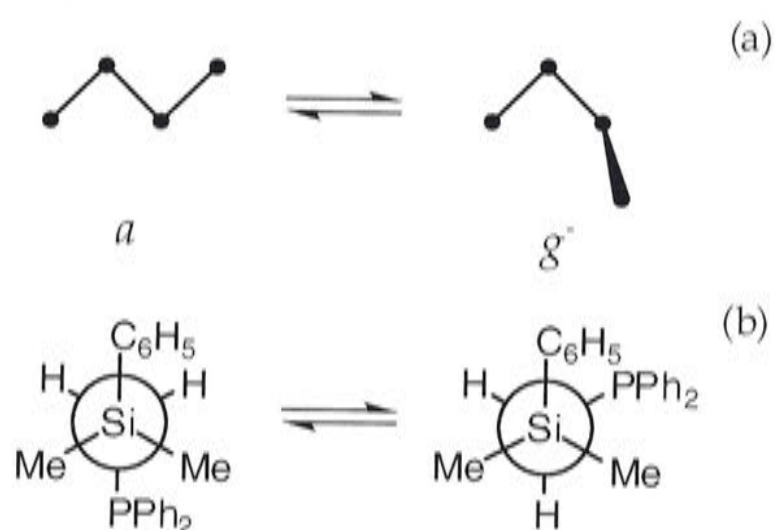


Figure 36. The two conformers of butanes (a), showing the expected staggered conformations (b).^{24,83}

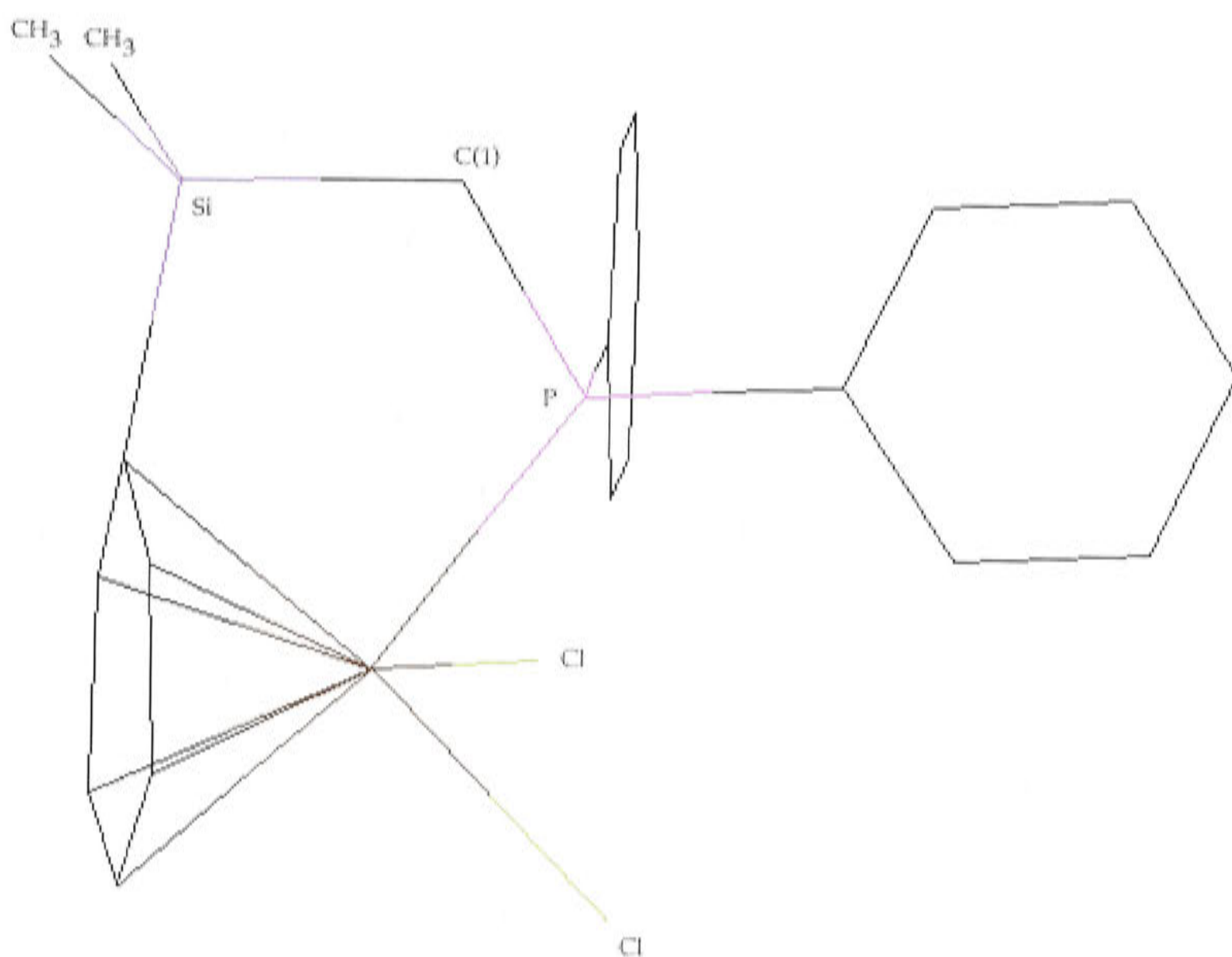


Figure 37. Chem3D representation of the molecular structure of compound $[\text{RuCl}_2(\eta^1:\eta^6\text{-Ph}_2\text{PCH}_2\text{SiMe}_2\text{Ph})]$ (**252**), with the C(1)-Si(1) bond at the top of the molecule. Hydrogen atoms have been omitted for clarity.

The corresponding dihedral angles for reported arene-ruthenium tethered complexes with a two-atom strap, which are listed in Table 20, are in the range 7-17° for complexes with both C, N and P-donor atoms (Figure 24 shows the atom labelling employed in multi-strapped complexes). There is only one pair for which the Ru-P bond lengths can be compared but, in contrast to the SiMe₂ system, there is a decrease in the Ru-P bond length (*ca* 0.03 Å) between [RuCl₂(η⁶-1,4-MeC₆H₄CHMe₂)(η¹-Ph₂P(CH₂)₂-2-C₆H₄CH₂OH)] (219) and the tethered complex [RuCl₂(η¹:η⁶-Ph₂P(CH₂)₂-2-C₆H₄CH₂OH)] (220).⁶

3.6 Summary

This Chapter has described the preparation of a variety of non-tethered η⁶-arene complexes containing *p*-cymene and methyl *o*-toluate as precursors to tethered arene-ruthenium(II) complexes. The most generally applicable precursors are the η⁶-methyl *o*-toluate complexes; the *p*-cymene precursor could only be used when the phosphorus atom carries bulky substituents. In agreement with Ward and co-workers,⁶ the aromatic ester, methyl *o*-toluate, was shown to be more labile than *p*-cymene. The preparation of tethered complexes *via* the intramolecular method described by Nelson and Ghebreyessus⁵⁶ was not satisfactory, despite its apparent convenience. These observations, as well as the mechanism of formation of the tethered complexes, will be discussed in Chapter 7 (Section 7.2). Some derivatives of the tethered complexes have also been described. A comparison of the reactivity of both non-tethered and tethered RuCl₂ complexes towards acetonitrile *via* η⁶-arene displacement will be made in Chapter 4.

References

- (1) Mahaffy, C. A.; Pauson, P. L. *J. Chem. Res., Synop.* **1979**, 126-127; *J. Chem. Res., Miniprint*, **1979**, 1752-1775.
- (2) Muetterties, E. L.; Bleeke, J. R.; Sievert, A. C. *J. Organomet. Chem.* **1979**, 178, 197-216.
- (3) Zimmerman, C. L.; Shaner, S. L.; Roth, S. A.; Willeford, B. R. *J. Chem. Res., Synop.* **1980**, 108; *J. Chem. Res., Miniprint*, **1980**, 197-216.
- (4) Bennett, M. A.; Huang, T.-N.; Matheson, T. W.; Smith, A. K. *Inorganic Syntheses*; Fackler, Jr, J. P. Ed., John Wiley & Sons, Inc.: New York, 1982; Vol. 21, pp. 74-78.
- (5) Hull, J. W.; Gladfelter, W. L. *Organometallics* **1984**, 3, 605-613.
- (6) Therrien, B.; Ward, T. R.; Pilkington, M.; Hoffmann, C.; Gilardoni, F.; Weber, J. *Organometallics* **1998**, 17, 330-337.
- (7) Smith, P. D.; Wright, A. H. *J. Organomet. Chem.* **1998**, 559, 141-147.
- (8) Smith, P. D. Ph.D. Dissertation; University of Nottingham: Nottingham, 1993.
- (9) Pertici, P.; Salvadori, P.; Biasci, A.; Vitulli, G.; Bennett, M. A.; Kane-Maguire, L. A. P. *J. Chem. Soc., Dalton Trans.* **1988**, 315-320.
- (10) Abele, A.; Wursche, R.; Klinga, M.; Rieger, B. *J. Mol. Cat. A* **2000**, 160, 23-33.
- (11) Simal, F.; Jan, D.; Demonceau, A.; Noels, A. F. *Tetrahedron Lett.* **1999**, 40, 1653-1656.
- (12) Jan, D.; Delaude, L.; Simal, F.; Demonceau, A.; Noels, A. F. *J. Organomet. Chem.* **2000**, 606, 55-64.
- (13) Fürstner, A.; Liebl, M.; Lehmann, C. W.; Picquet, M.; Kunz, R.; Bruneau, C.; Touchard, D.; Dixneuf, P. H. *Chem. Eur. J.* **2000**, 6, 1847-1857.
- (14) Jung, S.; Ilg, K.; Brandt, C. D.; Wolf, J.; Werner, H. *J. Chem. Soc., Dalton Trans.* **2002**, 318-327.
- (15) Therrien, B.; Ward, T. R. *Angew. Chem., Int. Ed. Engl.* **1999**, 38, 405-408.

- (16) Therrien, B.; König, A.; Ward, T. R. *Organometallics* **1999**, *18*, 1565-1568.
- (17) Therrien, B.; Ward, T. R. *Acta Cryst.* **2000**, *C56*, e561.
- (18) Zelonka, R. A.; Baird, M. C. *Can. J. Chem.* **1972**, *50*, 3063-3072.
- (19) Bennett, M. A.; Smith, A. K. *J. Chem. Soc., Dalton Trans.* **1974**, 233-241.
- (20) Werner, R.; Werner, H. *Chem. Ber.* **1982**, *115*, 3766-3780.
- (21) Brost, R. D.; Bruce, G. C.; Stobart, S. R. *J. Chem. Soc., Chem. Commun.* **1986**, 1580-1581.
- (22) Mahaffy, C. A. L.; Pauson, P. L. *Inorganic Syntheses*, Shriver, D. F. Ed., John Wiley & Sons, Inc.: New York, 1979; Vol. 19, pp. 154-158.
- (23) Davis, R.; Kane-Maguire, L. A. P. *Comprehensive Organometallic Chemistry*; Wilkinson, G.; Stone, F. G. A.; Abel, E. W. Ed., Pergamon: Oxford, 1982; Vol. 3, p. 1001.
- (24) Dale, J. *Stereochemistry and Conformational Analysis*; Universitetsforlaget: Oslo, 1978, pp. 95-98.
- (25) Eliel, E. L.; Wilen, S. H.; Mander, L. N. *Stereochemistry of Organic Compounds*; John Wiley & Sons, Inc.: New York, 1994, p. 758.
- (26) Bassindale, A. *The Third Dimension in Organic Chemistry*; John Wiley & Sons Ltd.: Chichester, 1984, pp. 92-93.
- (27) Sandström, J. *Dynamic NMR Spectroscopy*; Academic Press: London, 1982, p. 96.
- (28) Umezawa-Vizzini, K.; Guzman-Jimenez, I. Y.; Whitmire, K. H.; Lee, T. R. *Organometallics* **2003**, *22*, 3059-3065.
- (28a) Yeomans, B. D.; Humphrey, D. G.; Heath, G. A. *J. Chem. Soc., Dalton Trans.*, **1997**, 4153-4166.
- (29) Mathieson, A. McL.; Mellor, D. P.; Stephenson, N. C. *Acta Cryst.* **1952**, *5*, 185-186.
- (30) Dunitz, J. D.; Orgel, L. E. *J. Chem. Soc.* **1953**, 2594-2596.
- (31) Efimenko, I. A.; Balakaeva, T. A.; Kurbakova, A. P.; Gorbunova, Yu. E.; Mikhailov, Yu. N. *Russ. J. Coord. Chem.* **1994**, *20*, 277-281.
- (32) Rao, K. M.; Day, C. L.; Jacobsen, R. A.; Angelici, R. J. *Organometallics* **1992**, *11*, 2303-2304.

- (33) Lavigne, G.; Lugan, N.; Kalck, P.; Soulié, J. M.; Lerouge, O.; Saillard, J. Y.; Halet, J. F. *J. Am. Chem. Soc.* **1992**, *114*, 10669-10170.
- (34) Lugan, N.; Lavigne, G.; Soulié, J. M.; Fabre, S.; Kalck, P.; Saillard, J. Y.; Halet, J. F. *Organometallics* **1995**, *14*, 1712-1731.
- (35) Maurette, L.; Donnadiou, B.; Lavigne, G. *Angew. Chem. Int. Ed. Engl.* **1999**, *38*, 3707-3710.
- (36) Rambo, J. R.; Huffman, J. C.; Christou, G.; Eisenstein, O. *J. Am. Chem. Soc.* **1989**, *111*, 8027-8029.
- (37) Cotton, F. A.; Shang, M. *J. Am. Chem. Soc.* **1990**, *112*, 1584-1590.
- (38) Samuels, J. A.; Vaartstra, B. A.; Huffman, J. C.; Trojan, K. L.; Hatfield, W. E.; Caulton, K. G. *J. Am. Chem. Soc.* **1990**, *112*, 9623-9624.
- (39) Nair, V. S.; Hagen, K. S. *Inorg. Chem.* **1994**, *33*, 185-186.
- (40) Holmes, N. J.; Levason, W.; Webster, M. *J. Chem. Soc., Dalton Trans.* **1997**, 4223-4229.
- (41) Jasim, N. A.; Perutz, R. N.; Archibald, S. J. *J. Chem. Soc., Dalton Trans.* **2003**, 2184-2187.
- (42) Robertson, D. R.; Stephenson, T. A.; Arthur, T. *J. Organomet. Chem.* **1978**, *162*, 121-136.
- (43) da Silva, A. C.; Piotrowski, H.; Mayer, P.; Polborn, K.; Severin, K. *Eur. J. Inorg. Chem.* **2001**, 685-691.
- (44) Fergusson, J. E.; Greenaway, A. M. *Aust. J. Chem.* **1978**, *31*, 497-509.
- (45) Bottomley, F.; Tong, S. B. *Can. J. Chem.* **1971**, *49*, 3739-3743.
- (46) Huang, D.; Folting, K.; Caulton, K. G. *Inorg. Chem.* **1996**, *35*, 7035-7040.
- (47) Christie, R. M.; Heath, G. A.; MacGregor, S. A.; Schröder, M.; Yellowlees, L. J. *J. Chem. Soc., Chem. Commun.* **1990**, 1445-1446.
- (48) Fidalgo, E. G.; Plasseraud, L.; Stoeckli-Evans, H.; Süss-Fink, G. *Inorg. Chem. Commun.* **2001**, *4*, 308-310.
- (49) Kondo, T.; Kotachi, S.; Tsuji, Y.; Wantanabe, Y.; Mitsudo, T. *Organometallics* **1997**, *16*, 2562-2570.
- (50) McGrady, J. E., 2003, personal communication.

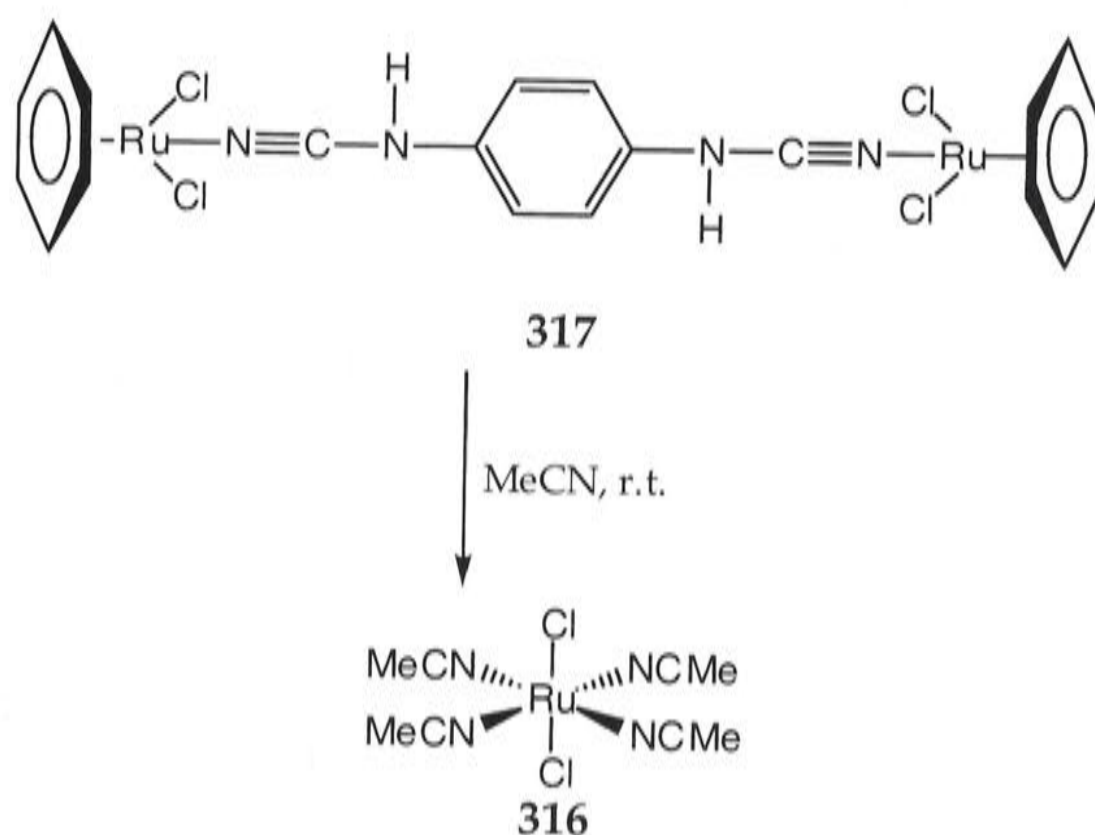
- (51) Brookhart, M.; Green, M. L. H.; Wong, L.-L. *Progress in Inorganic Chemistry*; Lippard, S. J. Ed., John Wiley & Sons, Inc.: New York, 1988; Vol. 36, pp. 1-124.
- (52) Bennett, M. A.; Pelling, S.; Robertson, G. B.; Wickramasinghe, W. A. *Organometallics* **1991**, *10*, 2166-2172.
- (53) Bennett, M. A.; Goh, L. Y.; Willis, A. C. *J. Chem. Soc., Chem. Commun.* **1992**, 1180-1182.
- (54) Bennett, M. A.; Goh, L. Y.; Willis, A. C. *J. Am. Chem. Soc.* **1996**, *118*, 4984-4992.
- (55) Bennett, M. A.; Latten, J. *Aust. J. Chem.* **1987**, *40*, 841-849.
- (56) Ghebreyessus, K. Y.; Nelson, J. H. *Organometallics* **2000**, *19*, 3387-3392.
- (57) Redwine, K. D.; Hansen, H. D.; Bowley, S.; Isbell, J.; Sanchez, M.; Vodak, D.; Nelson, J. H. *Synth. React. Inorg. Met.-Org. Chem.* **2000**, *30*, 379-407.
- (58) Nelson, J. H.; Ghebreyessus, K. Y.; Cook, V. C.; Edwards, A. J.; Wielandt, W.; Wild, S. B.; Willis, A. C. *Organometallics* **2002**, *21*, 1727-1733.
- (59) Fieser, L. F.; Fieser, M. *Reagents for Organic Synthesis*; John Wiley and Sons, Inc.: New York, 1967; Vol. 1, p. 911.
- (60) Isobe, K.; Bailey, P. M.; Maitlis, P. M. *J. Chem. Soc., Dalton Trans.* **1981**, 2003-2008.
- (61) Deacon, G. B.; Phillips, R. J. *Coord. Chem. Rev.* **1980**, *33*, 227-250.
- (62) West, R.; Riley, R. J. *Inorg. Nucl. Chem.* **1958**, *5*, 295-303.
- (63) Werner, H.; Werner, R. *Chem. Ber.* **1982**, *115*, 3781-3795.
- (64) Werner, H.; Weinand, R. *Z. Naturforsch.* **1983**, *38B*, 1518-1524.
- (65) Smith, P. D.; Gelbrich, T.; Hursthouse, M. B. *J. Organomet. Chem.* **2002**, *659*, 1-9.
- (66) Umezawa-Vizzini, K.; Lee, T. R. *Organometallics* **2003**, *22*, 3066-3076.
- (67) Bennett, M. A.; Robertson, G. B.; Smith, A. K. *J. Organomet. Chem.* **1972**, *43*, C41-C43.
- (68) Salvadori, P.; Pertici, P.; Marchetti, F.; Lazzaroni, R.; Vitulli, G.; Bennett, M. A. *J. Organomet. Chem.* **1989**, *370*, 155-171.

- (69) Elsegood, M. R. J.; Tocher, D. A. *Polyhedron* **1995**, *14*, 3147-3156.
- (70) Bruno, G.; Panzalorto, M.; Nicoló, F.; Arena, C. G.; Cardiano, P. *Acta Cryst.* **2000**, *C56*, e429.
- (71) Spek, A. L. *PLATON, An Integrated Tool for the Analysis of the Results of a Single Crystal Structure Determination*, University of Utrecht, Utrecht, The Netherlands, 2003.
- (72) Smith, D. C.; Haar, C. M.; Luo, L.; Li, C.; Cucullu, M. E.; Mahler, C. H.; Nolan, S. P.; Marshall, W. J.; Jones, N. L.; Fagan, P. J. *Organometallics* **1999**, *18*, 2357-2361.
- (73) Hansen, H. D.; Nelson, J. H. *Organometallics* **2000**, *19*, 4750-4755.
- (74) Baldwin, R.; Bennett, M. A.; Hockless, D. C. R.; Pertici, P.; Verrazzani, A.; Barretta, G. U.; Marchetti, F.; Salvadori, P. *J. Chem. Soc., Dalton Trans.* **2002**, 4488-4496.
- (75) Çetinkaya, B.; Demir, S.; Özdemir, I.; Toupet, L.; Sémeril, D.; Bruneau, C.; Dixneuf, P. H. *New J. Chem.* **2001**, *25*, 519-521.
- (76) den Reijer, C. J.; Wörle, M.; Pregosin, P. S. *Organometallics* **2000**, *19*, 309-316.
- (77) Faller, J. W.; D'Alliessi, D. G. *Organometallics* **2003**, *22*, 2749-2757.
- (78) Watkin, D. J.; Prout, C. K.; Carruthers, J. R.; Betteridge, P. W.; Cooper, R. I., *CRYSTALS Issue 11.6*, Oxford, U.K., 2001.
- (79) Geldbach, T. J.; Drago, D.; Pregosin, P. S. *Chem. Commun.* **2000**, 1629-1630.
- (80) Geldbach, T. J.; Pregosin, P. S.; Albinati, A.; Rominger, F. *Organometallics* **2001**, *20*, 1932-1938.
- (81) Cahn, R. S.; Ingold, C.; Prelog, V. *Angew. Chem. Int. Ed. Engl.* **1966**, *5*, 385-415.
- (82) ref. 25, p. 1122.
- (83) ref. 25, pp. 599-605.
- (84) Shaw, B. L. *J. Am. Chem. Soc.* **1975**, *97*, 3856-3857.
- (85) ref. 25, pp. 682-683.
- (86) Shaw, B. L. *J. Organomet. Chem.* **1980**, *200*, 307-318.

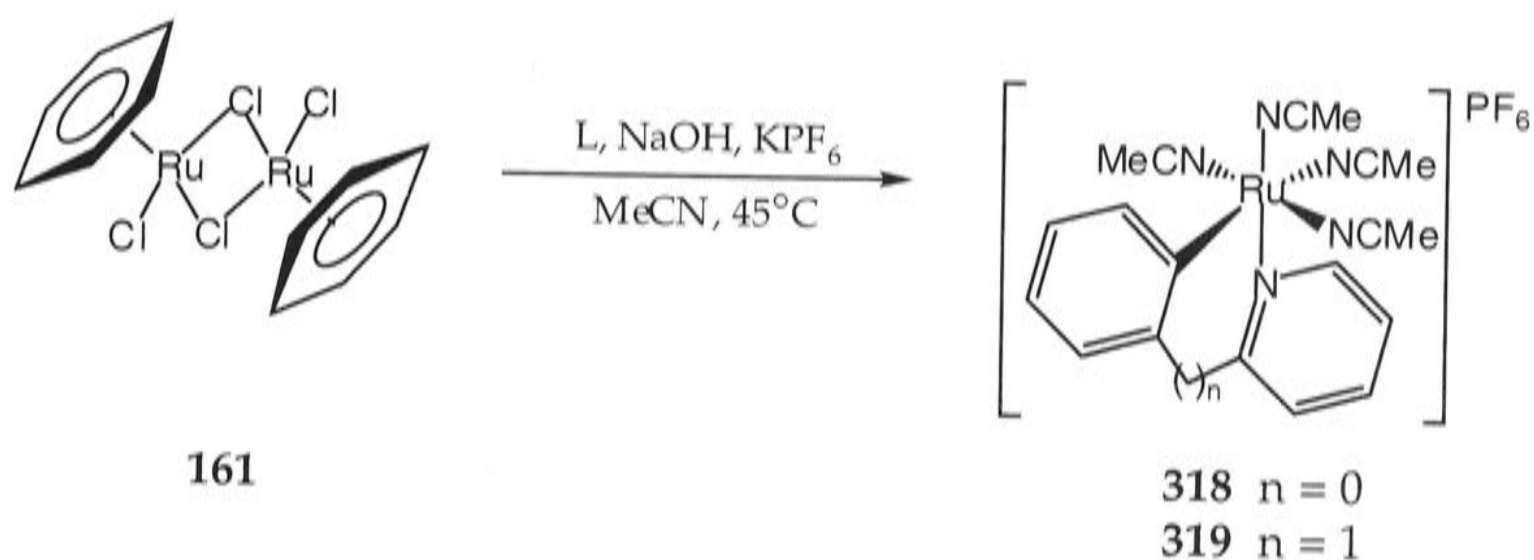
*Chapter 4: Arene Displacement Reactions of
Tethered Arene Complexes and their Precursors*

The reactions of the non-tethered and tethered arene complexes with a substrate that can displace the η^6 -arene have been compared in order to assess the extent to which forming the tether stabilises arene coordination at the ruthenium(II) level. Acetonitrile was selected as a substrate for two reasons. Firstly, it has a high affinity for Ru(II).¹⁻³ For example, the chloride ligands of $[\text{RuCl}_6]^{2-}$ are sequentially displaced by acetonitrile *via* complexes of the type $[\text{RuCl}_{6-n}(\text{NCMe})_n]^z$ to afford $[\text{Ru}(\text{NCMe})_6]^{2+}$.^{2,3} Acetonitrile is also known to replace the η^6 -arene of Ru(II) complexes under either photolytic, thermolytic or electrochemical conditions.⁴⁻¹⁰ For example, $[\text{RuCl}_2(\text{NCMe})_4]$ (**316**) has been synthesised, by among other methods, photolysis of $[\text{RuCl}_2(\eta^6\text{-}1,2\text{-C}_6\text{H}_4\text{-}n\text{-Bu}_2)]_2$ in acetonitrile.⁴ Compound **316** has also been indirectly prepared by the slow displacement of either η^6 -benzene or η^6 -*p*-cymene from dinuclear compounds of the type $[\{\text{RuCl}_2(\eta^6\text{-arene})\}_2(\mu\text{-L})]$ (L = 1,4-dicyanamidobenzene, *N,N'*-dicyano-4-4'-diaminobiphenyl, 2,5-dichloro-1,4-dicyanamidobenzene and 2,5-dimethyl-1,4-dicyanamidobenzene).⁵ For example, benzene was displaced from $[\{\text{RuCl}_2(\eta^6\text{-C}_6\text{H}_6)\}_2(\mu\text{-}1,4\text{-N}\equiv\text{C-NHC}_6\text{H}_4\text{NH-C}\equiv\text{N})]$ (**317**) by acetonitrile at room temperature to give **316** (Scheme 66).

Displacement of η^6 -benzene from $[\text{RuCl}_2(\eta^6\text{-C}_6\text{H}_6)]_2$ (**161**) by acetonitrile at 45°C in the presence of either 2-phenylpyridine or 2-benzylpyridine afforded the cationic complexes **318** ($n = 0$) and **319** ($n = 1$) (Scheme 67) *via* intermediates of the type $[\text{Ru}(\text{NCMe})(\eta^6\text{-C}_6\text{H}_6)(\text{L-H})]\text{PF}_6$ (L = 2-phenylpyridine or 2-benzylpyridine).⁶



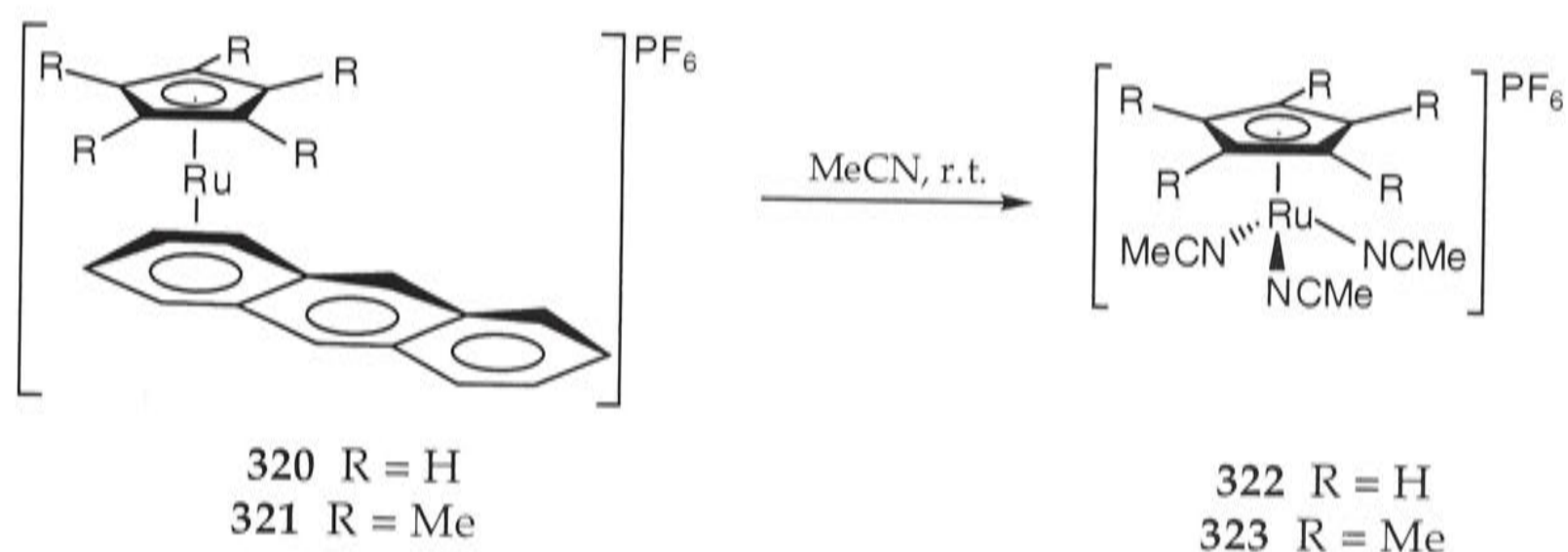
Scheme 66. Reaction of the dinuclear compound **317** with acetonitrile to give **316**.⁵



Scheme 67. Displacement of η^6 -benzene by acetonitrile to form complexes **318** ($n = 0$) and **319** ($n = 1$); L = 2-phenylpyridine or 2-benzylpyridine.⁶

The cation $[\text{Ru}(\eta^5\text{-C}_5\text{H}_5)(\eta^6\text{-C}_6\text{H}_6)]^+$ reacted when irradiated in acetonitrile to give $[\text{Ru}(\eta^5\text{-C}_5\text{H}_5)(\text{NCMe})_3]^+$.⁷ Polycyclic η^6 -arenes can also be displaced from Ru(II) complexes.^{8,9} For example, complexes of the type $[\text{Ru}(\eta^5\text{-C}_5\text{R}_5)(\eta^6\text{-arene})]\text{PF}_6$ (R = H, arene = naphthalene, anthracene (**320**), pyrene, chrysene; R = Me, arene = anthracene (**321**)) react with acetonitrile at room temperature, in the absence of light, to give the tris(acetonitrile) species $[\text{Ru}(\eta^5\text{-C}_5\text{R}_5)(\text{NCMe})_3]\text{PF}_6$ (R = H (**322**), Me (**323**)), as illustrated in

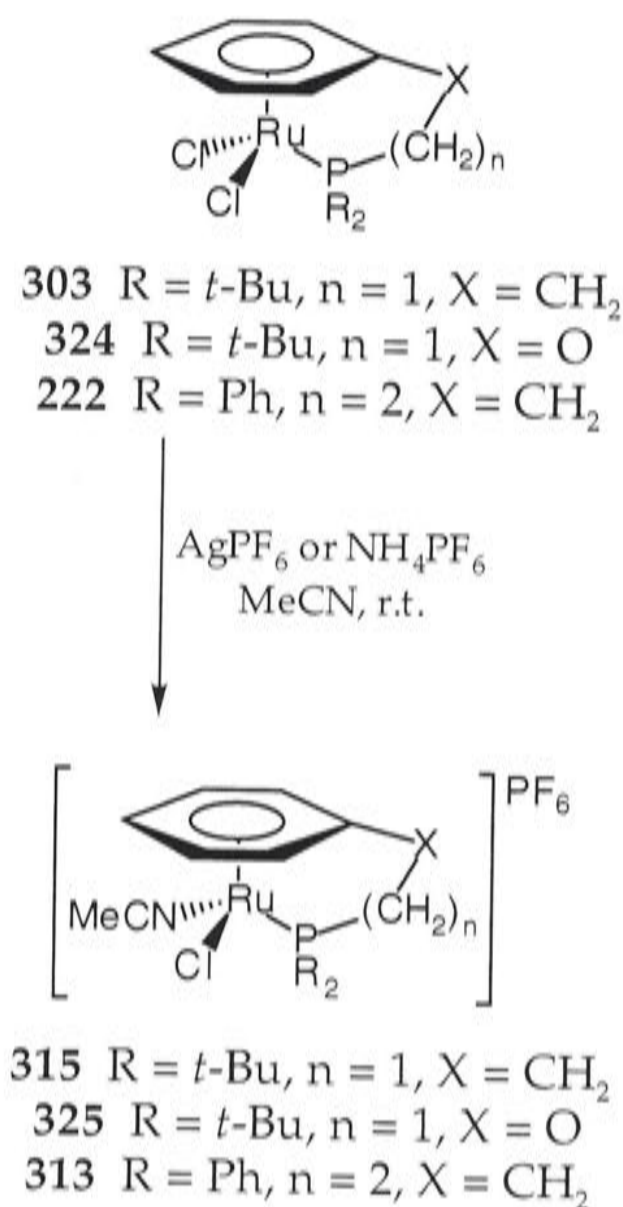
Scheme 68 for **320** and **321**.⁸ Coordinated anthracene has also been displaced from $[\text{Ru}(\eta^6\text{-C}_6\text{Me}_6)(\eta^6\text{-anthracene})][\text{PF}_6]_2$ by acetonitrile at room temperature to afford $[\text{Ru}(\eta^6\text{-C}_6\text{Me}_6)(\text{NCMe})_3][\text{PF}_6]_2$.⁹ The displacement of the polycyclic arene is in agreement with the observation that polycyclic η^6 -arenes are more labile than their monocyclic counterparts, presumably because the $\eta^4:\eta^2$ bonding modes are more easily accessible in polycyclic arenes.¹¹ For example, displacement of the η^6 -naphthalene from the Ru(0) complex $[\text{Ru}(\eta^6\text{-C}_{10}\text{H}_8)(\eta^4\text{-1,5-COD})]$ by various monocyclic arenes is catalysed by acetonitrile.^{11,12}



Scheme 68. Displacement of η^6 -anthracene by acetonitrile from complexes **320** and **321**.⁸

Cationic acetonitrile complexes of the type $[\text{RuCl}(\text{NCMe})(\eta^1:\eta^6\text{-R}_2\text{P}(\text{CH}_2)_n\text{XPh})]\text{PF}_6$ can be prepared by abstraction of one of the chloride ligands of tethered RuCl_2 complexes.^{13,14} Complexes $[\text{RuCl}_2(\eta^1:\eta^6\text{-}t\text{-Bu}_2\text{PCH}_2\text{XPh})]$ ($\text{X} = \text{CH}_2$ (**303**) and O (**324**)) or $[\text{RuCl}_2(\eta^1:\eta^6\text{-Ph}_2\text{P}(\text{CH}_2)_3\text{Ph})]$ (**222**) were treated with one equivalent of either AgPF_6 or NH_4PF_6 in acetonitrile at room temperature to give rise to $[\text{RuCl}(\text{NCMe})(\eta^1:\eta^6\text{-}t\text{-Bu}_2\text{PCH}_2\text{XPh})]$ ($\text{X} = \text{CH}_2$ (**315**) and O (**325**)) or

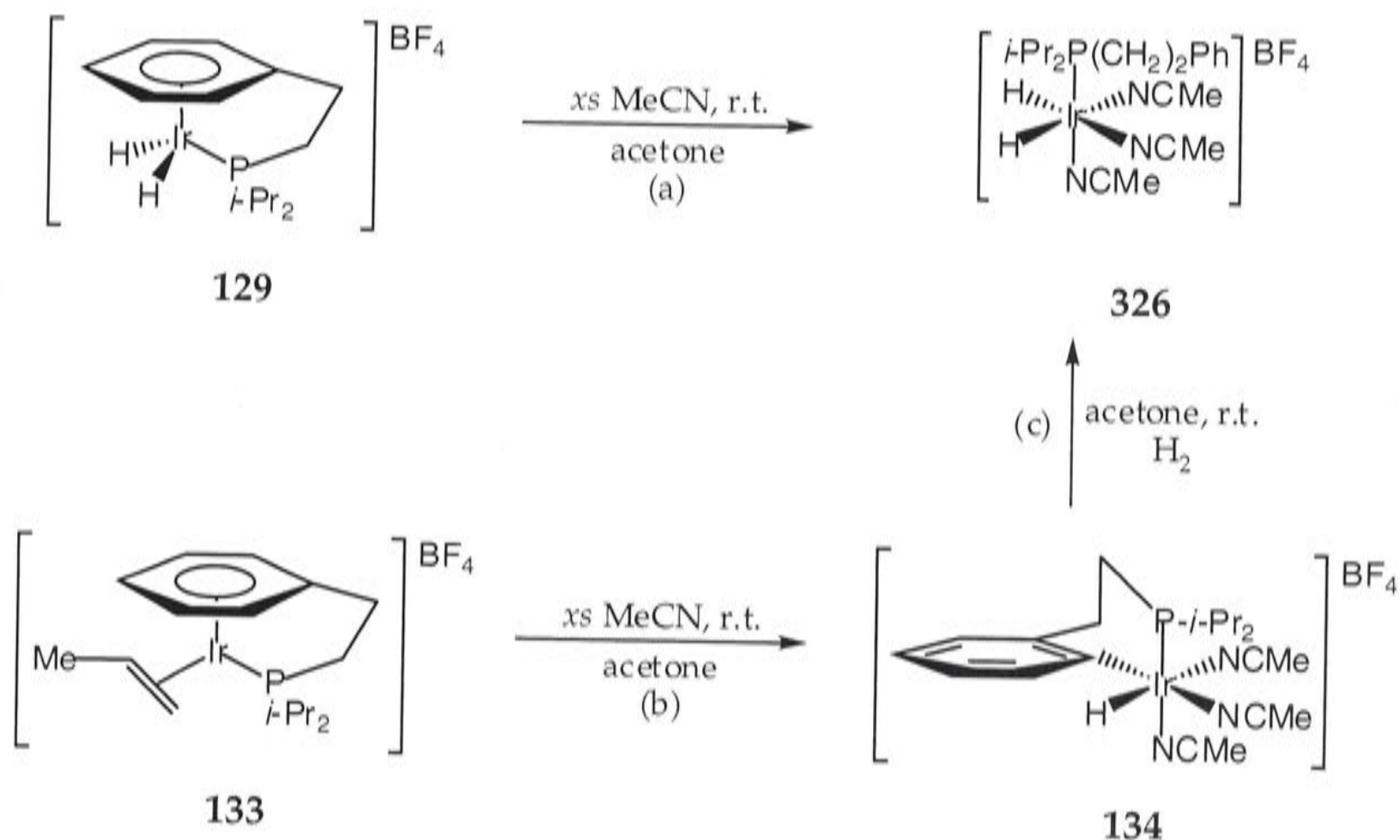
$[\text{RuCl}(\text{NCMe})(\eta^1:\eta^6\text{-Ph}_2\text{P}(\text{CH}_2)_3\text{Ph})]\text{PF}_6$ (**313**) in good yields (Scheme 69). Displacement of the η^6 -arene was not observed under these conditions.



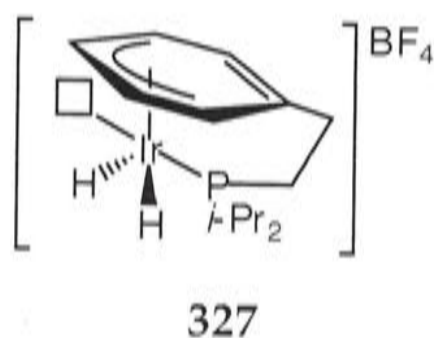
Scheme 69. Preparation of the derivatives **315**, **325** and **313**.^{13,14}

Oro and Werner *et al.*¹⁵ have recently reported the tethered η^6 -arene of the arene-hydrido-iridium(III) complex **129** was displaced by acetonitrile, at room temperature, to give the tris(acetonitrile) compound $[\text{Ir}(\text{H})_2(\eta^1\text{-}i\text{-Pr}_2\text{P}(\text{CH}_2)_2\text{Ph})(\text{NCMe})_3]\text{BF}_4$ (**326**) (Scheme 70a); no displacement of the hydride ligands occurred. Kinetic data suggested that this reaction may proceed *via* a coordinatively unsaturated intermediate of the type **327**. As mentioned in Chapter 1 (Section 1.2.2), the iridium(I) η^2 -alkene complex **133** reacted with an excess of acetonitrile to form the C-H bond activation product **134** (Scheme 70b), which was converted to the Ir(III)

tris-(acetonitrile) complex **326** upon treatment with hydrogen (Scheme 70c).



Scheme 70. Reaction of the tethered-arene Ir(I) and Ir(III) complexes, **133** and **129**, respectively, with acetonitrile.¹⁵

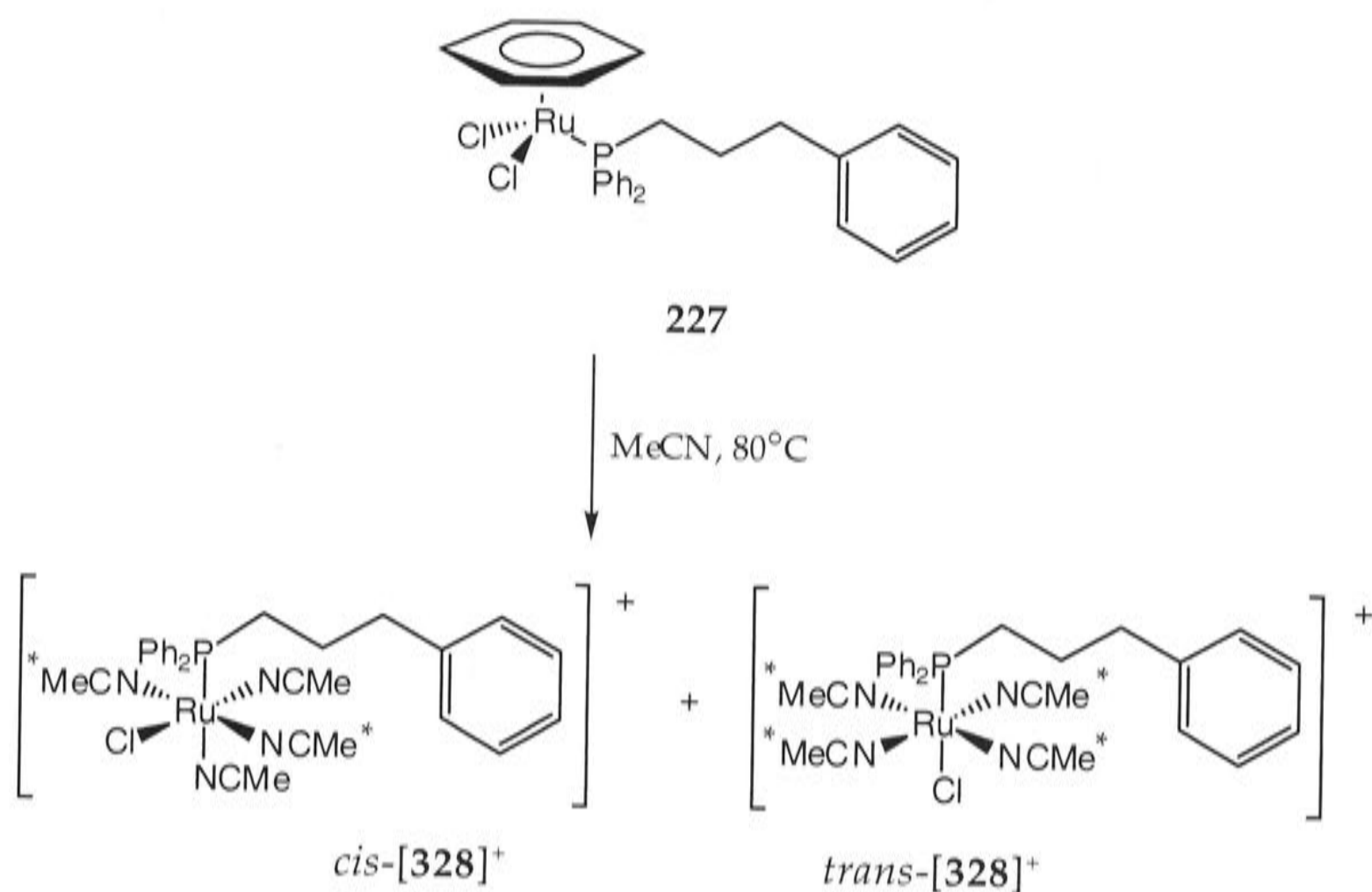


According to Smith and Wright,¹⁰ attempts to displace the η^6 -arene from $[\text{RuCl}_2(\eta^6\text{-1,4-MeC}_6\text{H}_4\text{CHMe}_2)(\text{Ph}_2\text{P}(\text{CH}_2)_3\text{Ph})]$ (**223**) by heating in acetonitrile failed, and the tris(acetonitrile) compound $[\text{RuCl}_2(\text{NCMe})_3(\text{Ph}_2\text{P}(\text{CH}_2)_3\text{Ph})]$ (**259**) could only be made by anodic oxidation of **223** in acetonitrile (see Scheme 59a, Chapter 3, Section 3.2.6), though no yield was stated. The Ph.D. thesis of P. D. Smith,¹⁶ in contrast, states that **259** was made either by anodic oxidation or photolysis of **223** in

acetonitrile (see Schemes 59a and 59b). Anodic oxidation was the method of choice, despite the presence of residual electrolyte, since photolysis experiments also gave rise to other unidentified products. However, the thesis fails to mention any attempts to prepare **259** by thermolysis of **223** in acetonitrile.

4.1 Reaction of Non-Tethered and Tethered Complexes with Acetonitrile

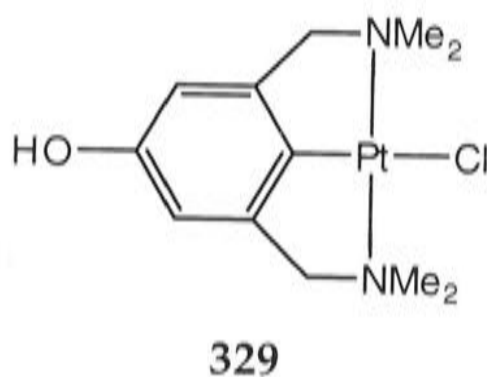
When complex $[\text{RuCl}_2(\eta^6\text{-C}_6\text{H}_6)(\eta^1\text{-Ph}_2\text{P}(\text{CH}_2)_3\text{Ph})]$ (**227**) was heated in boiling acetonitrile (82°C) for 48 hours, benzene was displaced, and a yellow oil was isolated which showed two singlets in the $^{31}\text{P}\{^1\text{H}\}$ -NMR spectrum (in CD_3CN) at δ 48.7 and 52.1 in a ratio of 5:1. The ^1H NMR spectrum showed no peaks assignable to either $\eta^6\text{-C}_6\text{H}_6$ or to the coordinated arene of the $\text{Ph}_2\text{P}(\text{CH}_2)_3\text{C}_6\text{H}_5$ unit, though there were peaks in the region δ 7.0-7.8 assignable to free aromatic groups. There was a large peak at δ 2.30, accompanied by two smaller peaks at δ 2.27 and 2.38, indicative of coordinated acetonitrile. A dichloromethane solution layered with ether deposited, over several days, moisture-sensitive yellow crystals, and their FAB-mass spectrum showed the highest mass peak at m/z 605, corresponding to $[\text{RuCl}(\text{NCMe})_4(\eta^1\text{-Ph}_2\text{P}(\text{CH}_2)_3\text{Ph})]^+$ (**[328]**⁺). The IR spectrum showed a $\nu(\text{CN})$ band at 2285 cm^{-1} and a $\nu(\text{Ru-Cl})$ band at 303 cm^{-1} . The X-ray structure of one of the yellow crystals showed that it was a salt, *trans*- $[\text{RuCl}(\text{NCMe})_4(\eta^1\text{-Ph}_2\text{P}(\text{CH}_2)_3\text{Ph})]\text{Cl}\cdot\text{H}_2\text{O}$ (*trans*-**[328]**Cl) (see Scheme 71).



Scheme 71. Reaction of the complex **227** to give the salt **[328]Cl**. *Represents acetonitrile ligands in either identical or very similar chemical environments.

The Chem3D representation of *trans*-[**328**]Cl [Dr D. C. R. Hockless (ANU)] is shown in Figure 38 (see page 195), and the chemically significant bond lengths and angles are summarised in Table 23. The metal is coordinated octahedrally by four acetonitrile ligands, chloride and the phosphorus atom of the ligand $\text{Ph}_2\text{P}(\text{CH}_2)_3\text{Ph}$ (**118**). The water molecule appears to be hydrogen-bonded to both the coordinated (Cl(1)) and outer-sphere (Cl(2)) chlorine atoms, though it was not possible to locate the hydrogen atoms of the H_2O . The interatomic distances for Cl(1)-O and Cl(2)-O of 3.34(1) and 3.10(1) Å, respectively, are characteristic of hydrogen bond interactions, where the hydrogen bond acceptor strength of Cl is in the order $\text{Cl}^- > \text{Cl-M}$.¹⁷ For example, an intermolecular hydrogen bond $\text{Cl}\cdots\text{H-O}$ (3.13 Å) occurs in the crystal structure of **329** between atoms the hydrogen of the hydroxyl group and chloride ligand bound to platinum.¹⁸ The X-ray crystal structure of a salt incorporating a cation similar to $[\mathbf{328}]^+$, $[\text{RuCl}(\text{NCMe})_4(\text{PPh}_3)][\text{Ru}_2\text{Cl}_2(\text{O}_2\text{CC}_6\text{H}_4\text{-}p\text{-Me})_4]$ has been reported.¹⁹ It

showed Ru-N bond lengths in the range 2.004(8)-2.018(9) Å, a Ru-P bond distance of 2.286(3) Å and a Ru-Cl bond length of 2.475 Å (ESD not available for data extracted from the CSD), which are in good agreement with those observed in [328]⁺. Similar Ru-N distances have been observed in other acetonitrile complexes.^{13,14,19,20}



The ¹H NMR spectrum in *d*₂-dichloromethane of the single crystals showed just a singlet at δ 2.28 due to the methyl groups of the equivalent CH₃CN ligands and only the singlet at δ 48.7 in the ³¹P{¹H}-NMR spectrum. Presumably the singlet at δ 52.1 is due to the minor isomer, *cis*-[328]Cl, in which there are three meridional CH₃CN ligands, the fourth one being *trans* to phosphorus. It is worth noting that the chemical shift of δ 48.7 is close to the value of δ 46.8 (calculated using the conversion factor δ 140.4²¹ for the reference, not cited¹⁰ but assumed to be P(OMe)₃, for the value δ -93.68) reported by Smith and Wright¹⁰ for the compound they formulated as the tris(nitrile) compound [RuCl₂(NCMe)₃(η¹:Ph₂P(CH₂)₃Ph)] (259).¹⁰

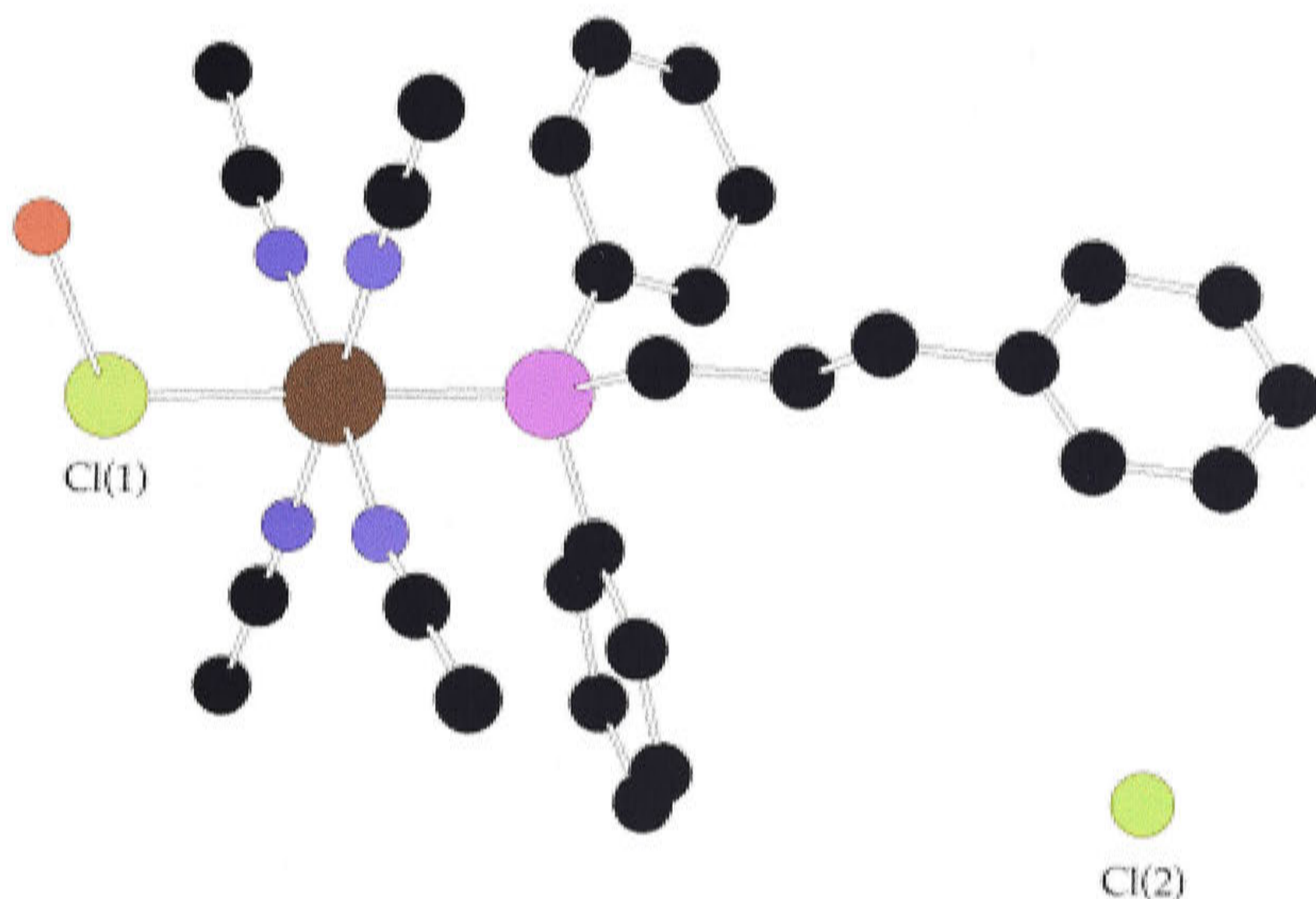


Figure 38. Chem3D representation of the molecular structure of $[\text{RuCl}(\text{NCMe})_4(\eta^1\text{-Ph}_2\text{P}(\text{CH}_2)_3\text{Ph})]\text{Cl}$ (**[328]Cl**), showing the hydrogen-bonding interaction between the inner-sphere chloride and the oxygen atom of the water molecule. Hydrogen atoms and the solvent molecule (CH_2Cl_2) have been omitted for clarity.

Table 23. Selected bond lengths (\AA) and angles ($^\circ$) for $[\text{RuCl}(\text{NCMe})_4(\eta^1\text{-Ph}_2\text{P}(\text{CH}_2)_3\text{Ph})]\text{Cl}$ (**[328]Cl**).

Ru(1)-Cl(1)	2.471(3)	Ru(1)-P(1)	2.296(4)
Ru-N	1.99(1)-2.03(1)	P-C	1.81(1)-1.83(1)
Cl(1)-Ru(1)-P(1)	177.3(1)	Cl(1)-Ru(1)-N	87.2(3)-90.6(3)
P(1)-Ru(1)-N	87.0(3)-95.2(3)		

Addition of NH_4PF_6 or NaPF_6 to a dichloromethane solution of the yellow oil **[328]Cl** at room temperature gave immediately the corresponding PF_6^- salt, **[328]PF₆**, which was isolated as a microcrystalline, pale yellow solid in 82% yield. The conductivity measurements (Λ_m values) of both the

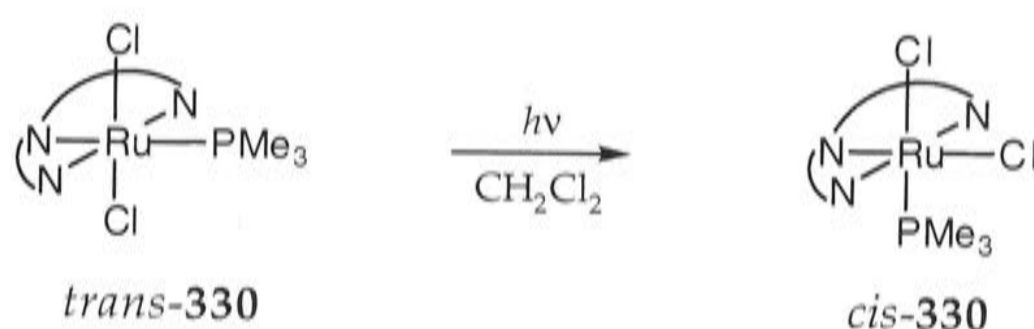
chloride salt $[\text{RuCl}(\text{NCMe})_4(\eta^1\text{-Ph}_2\text{P}(\text{CH}_2)_3\text{Ph})]\text{Cl}$ (**[328]Cl**) and the PF_6 salt $[\text{RuCl}(\text{NCMe})_4(\eta^1\text{-Ph}_2\text{P}(\text{CH}_2)_3\text{Ph})]\text{PF}_6$ (**[328]PF₆**) in nitromethane at *ca* 21°C were found to be 51.5 and 55.5 $\text{S cm}^2 \text{mol}^{-1}$, respectively, which fall just below the generally accepted range of 60-115 $\text{S cm}^2 \text{mol}^{-1}$ (for concentrations of *ca* 10^{-3}M) in this solvent.²² These values confirm that the tetrakis-cation $[\text{RuCl}(\text{NCMe})_4(\eta^1\text{-Ph}_2\text{P}(\text{CH}_2)_3\text{Ph})]^+$ (**[328]⁺**) had been formed. The slightly lower value for the chloride salt **[328]Cl** may be due to ion-pairing of the cation **[328]⁺** with chloride ion. It appears that the conductivities of only two analogous tetrakis-complexes have been recorded. For comparison, the Λ_m values for the salts $[\text{RuCl}(\text{Im})_4(\text{PPh}_3)]\text{Cl}$ (Im = imidazole) and $[\text{RuCl}(\text{MeIm})_4(\text{PPh}_3)]\text{Cl}$ (MeIm = *N*-methylimidazole) are 63 and 84 $\text{S cm}^2 \text{mol}^{-1}$, respectively.²³

The ^1H NMR spectrum of **[328]PF₆** in d_3 -acetonitrile showed peaks due to coordinated acetonitrile at δ 2.11, 2.15 and 2.19 in an intensity ratio 1:22:1. This is consistent with the presence of *trans*- and *cis*-**[328]PF₆** in a 5:1 ratio; of the eight acetonitrile ligands of the two different isomers, there are six groups that are in almost identical chemical environments, as indicated in Scheme 71; two of the meridional ligands of the *cis*-isomer and all four ligands of the *trans*-isomer. Since there is a five-fold excess of the *trans*-isomer present, and there are four different ligands, these integrate as 20 protons, and combined with the two in the *cis*-isomer, give an intensity of 22. Each of the signals due to the remaining chemically inequivalent ligands in the *cis*-isomer integrate only as one proton, thus giving three peaks of intensity 1:22:1. The ^1H and $^{13}\text{C}\{^1\text{H}\}$ -NMR data for the acetonitrile ligands of **[328]PF₆** are summarised in Table 24. The $^{31}\text{P}\{^1\text{H}\}$ -NMR spectrum shows two peaks at δ 46.4 and 48.7 in a ratio of 1:5, *i.e.* the ratio is apparently the reverse of that in **[328]Cl**. Hence it appears that the relative positions of the peaks due to the two isomers have changed, *i.e.* that replacing chloride for PF_6 has affected the $^{31}\text{P}\{^1\text{H}\}$ -NMR chemical shifts of

the two isomers differently. On this basis, the peaks at δ 46.4 and 48.7 in $[328]PF_6$ can be assigned to the *cis*- and *trans*-isomers, respectively.

The 5:1 ratio (*trans*:*cis*) of the isomers of $[328]Cl$ obtained after 48 hours' heating appears not to be the thermodynamic ratio. After 264 hours, the ratio was 7:1 and after 312 hours it was 10:1, indicating that the *trans*-isomer is more stable and that the conversion of the *cis*- to the *trans*-isomer is slow.

The conversion of *trans*-complexes of the type $[RuClN_3(PR_3)]$ (where N_3 is a tridentate nitrogen donor ligand) into the respective *cis*-isomer has been observed.²⁴ A dichloromethane solution of *trans*- $[RuCl_2(trpy)(PMe_3)]$ (**330**) (*trpy* = 2,2':6',2''-terpyridine) rearranges to the *cis*-isomer when irradiated (Scheme 72), and, in this system, the *cis*-isomer appears to be thermodynamically favoured product.



Scheme 72. Conversion of *trans*-**330** to *cis*-**330**. ($\text{N} \text{---} \text{N} \text{---} \text{N}$ = 2,2':6',2''-terpyridine).²⁴

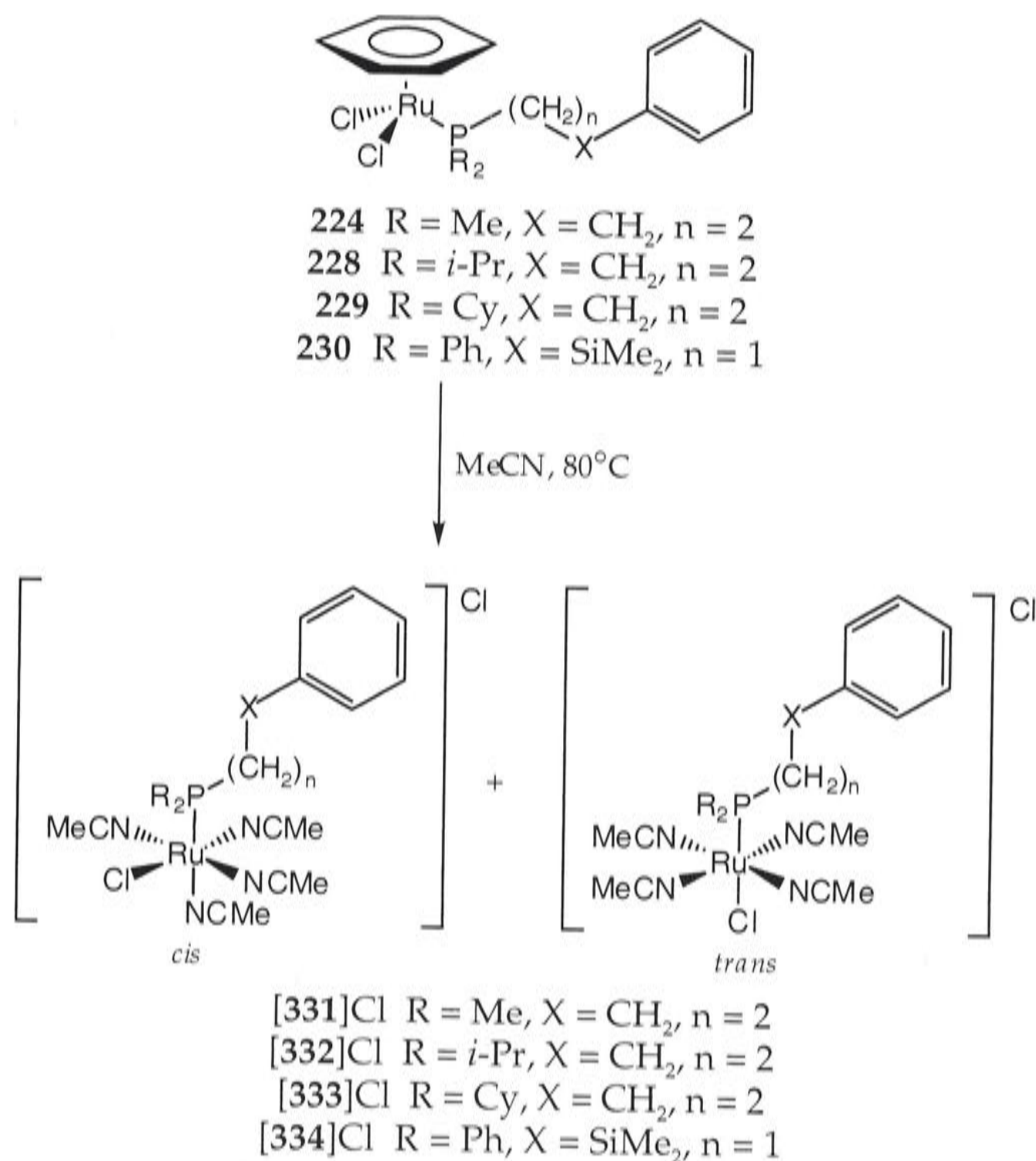
The reactions of the η^6 -benzene complexes $[RuCl_2(\eta^6-C_6H_6)(\eta^1-R_2P(CH_2)_3Ph)]$ ($R = \text{Me}$ (**226**), *i*-Pr (**228**), Cy (**229**)) and $[RuCl_2(\eta^6-C_6H_6)(\eta^1-Ph_2PCH_2SiMe_2Ph)]$ (**230**) with refluxing acetonitrile gave similarly a mixture of *cis*- and *trans*-isomers of the cationic complexes $[RuCl(NCMe)_4(\eta^1-R_2P(CH_2)_3Ph)]Cl$ ($R = \text{Me}$ (**[331]Cl**), *i*-Pr (**[332]Cl**), Cy (**[333]Cl**)) and $[RuCl(NCMe)_4(\eta^1-Ph_2PCH_2SiMe_2Ph)]Cl$ (**[334]Cl**), respectively

(Scheme 73), which were obtained as yellow oils and were converted into PF_6 salts by addition of NH_4PF_6 (NaPF_6 in the case of [334]Cl). These were generally solids, but [331] PF_6 and [334] PF_6 were obtained as uncrystallisable oils. No attempts were made to separate the isomers by fractional crystallisation.

The reactions from 228 and 229, which contain bulky substituents on the phosphorus atom, were complete within 24 hours, whereas 48 hours was required for 226 and 227 which have methyl and phenyl groups, respectively, on the phosphorus atom. The ^1H and $^{13}\text{C}\{^1\text{H}\}$ -NMR chemical shifts of the coordinated acetonitrile ligands are summarised in Table 24. The complexes all show two peaks, of generally unequal intensity, in their $^{31}\text{P}\{^1\text{H}\}$ -NMR spectra, differing in chemical shift by *ca* 2-5 ppm, due to *cis*- and *trans*-isomers. The ratio of isomers obtained and the $^{31}\text{P}\{^1\text{H}\}$ -NMR chemical shifts for both chloride and PF_6 salts are summarised in Table 25. The peaks could not be assigned to particular isomers, for reasons explained above. The FAB-mass spectra, where recorded (see Table 26), showed highest mass peaks corresponding to the cations [332] $^+$ and [333] $^+$. The mass spectra of the cations [331] $^+$ and [334] $^+$ were not recorded. The formulation as tetrakis-complexes is supported by the elemental analyses of the PF_6 salts, most notably for nitrogen. The results do not concur with those expected for tris-species.

Displacement of methyl *o*-toluate from $[\text{RuCl}_2(\eta^6\text{-1,2-MeC}_6\text{H}_4\text{CO}_2\text{Me})(\eta^1\text{-}i\text{-Pr}_2\text{P}(\text{CH}_2)_3\text{Ph})]$ (238) by acetonitrile occurred much more rapidly than from the corresponding η^6 -benzene complex $[\text{RuCl}_2(\eta^6\text{-C}_6\text{H}_6)(\eta^1\text{-}i\text{-Pr}_2\text{P}(\text{CH}_2)_3\text{Ph})]$ (228). The reaction was complete within one hour at reflux (*cf.* 24 hours from 228), and even occurred at room temperature in 96 hours. The approximate ratio of *cis*- and *trans*-isomers formed in the reaction at room temperature and at reflux were 2:1 and 1:1 (upfield:downfield), respectively. The latter value differs appreciably from

that obtained from the η^6 -benzene complex **228**, (2:1), under the same conditions.



Scheme 73. Preparation of the *cis* and *trans*-isomers of the chloride salts **[331]Cl**, **[332]Cl**, **[333]Cl** and **[334]Cl** from the η^6 -benzene compounds **226**, **228**, **229** and **230**, respectively.

The ¹H NMR spectra of [RuCl(NCMe)₄(η^1 -R₂P(CH₂)₃Ph)]Cl (R = Me (**[331]Cl**), [RuCl(NCMe)₄(η^1 -R₂P(CH₂)₃Ph)]PF₆ (R = *i*-Pr (**[332]PF₆**), Cy (**[333]PF₆**)), [RuCl(NCMe)₄(η^1 -Ph₂PCH₂SiMe₂Ph)]Cl (**[334]Cl**) all showed peaks in the region δ 2.1-2.4, characteristic of coordinated acetonitrile, indicating that a mixture of both *cis*- and *trans*-isomers was present. The

peaks are, however, very close together, preventing determination of the ratio of isomers; $^{31}\text{P}\{^1\text{H}\}$ -NMR spectroscopy is more useful, but the peaks could not be assigned to a particular isomer in these spectra.

Compound $[\text{RuCl}(\text{NCMe})_4(\eta^1\text{-Ph}_2\text{PCH}_2\text{SiMe}_2\text{Ph})]\text{Cl}$ ([334]Cl) shows all of the expected peaks in the ^1H NMR spectrum for both the *cis*- and *trans*-isomers, the most prominent at δ 2.29, due to the *trans*-isomer, is accompanied by others at δ 2.27, 2.32 and 2.37. These are present in approximate intensities 1:15 for peaks at δ 2.37:2.29, 2.32 and 2.37 combined. It is interesting to note that the ^1H NMR spectra of both [334]Cl and [334]PF₆ show two peaks due to the SiMe₂ protons, presumably one for each of the *cis*- and *trans*-isomers, at δ -0.066 and 0.012 and at δ -0.091 and -0.038, respectively.

The ^1H NMR spectrum of $[\text{RuCl}(\text{NCMe})_4(\eta^1\text{-Me}_2\text{P}(\text{CH}_2)_3\text{Ph})]\text{Cl}$ ([331]Cl) displayed three resonances, the largest at δ 2.41 due to *trans*-[331]Cl, as well as resonances at δ 2.28 and 2.29. The relative intensities are approximately 8:17 for peaks δ 2.28 and 2.29. Two doublets are observed for the PMe₂ groups, one for each isomer, at δ 1.36 and 1.44, each with J_{PH} of 10 Hz.

Only two CH₃CN peaks were present in the ^1H NMR spectrum of $[\text{RuCl}(\text{NCMe})_4(\eta^1\text{-}i\text{-Pr}_2\text{P}(\text{CH}_2)_3\text{Ph})]\text{Cl}$ ([332]Cl): the larger at δ 2.36, most probably due to the *trans*-isomer, is accompanied by one signal at δ 2.40, so presumably the signals due to the remaining acetonitrile ligands of the *cis*-isomer are masked by these signals. A similar observation was made for [332]PF₆, the signals now being present at δ 2.34 and 2.38, in an approximate intensity ratio 17:5. Two overlapping multiplets present in the region δ 1.04-1.18 are presumably due to the methyl protons of the

P-*i*-Pr₂ groups of each isomer. The region δ 1.78-1.91 showed a multiplet due to the CHMe₂ resonance, as well as two of the methylene signals.

There was only one dominant peak, due to coordinated acetonitrile, present in the ¹H NMR spectrum of [RuCl(NCMe)₄(η^1 -Cy₂P(CH₂)₃Ph)]Cl ([333]Cl) at δ 2.34, which presumably contains signals due to both isomers. The ¹H NMR spectrum of the PF₆ salt showed two resonances, one large one at δ 2.33, upfield of a signal at δ 2.39, present in an approximate ratio 11:7. The regions δ 1.70-1.80 and 2.02-2.10, due to the PCy₂ groups, contained complicated multiplets due to both the *cis*- and *trans*-isomers.

The ¹³C{¹H}-NMR spectra of all of the compounds [331]Cl, [328]Cl, [332]PF₆ and [333]PF₆ show resonances due to CH₃CN in the region δ 3.9-4.5, as well as signals due to CH₃CN that lie in the range δ 124.4-127.4. Assignment of peaks due to either the *cis*- or *trans*-isomers was not possible. Compound [332]PF₆ showed only one peak in its ¹³C{¹H}-NMR spectrum at δ 4.28 due to CH₃CN, which presumably contained the resonances due to both isomers.

The ³¹P{¹H} NMR spectra of each salt usually show two distinct resonances, due to the *cis*- and *trans*-isomers. Exceptionally, [RuCl(NCMe)₄(η^1 -Cy₂P(CH₂)₃Ph)]Cl ([333]Cl), shows only one signal (δ 44.5), presumably because the signals due to each isomer are coincident (see Table 25). Two signals, at δ 42.8 and 44.4, are observed for [333]PF₆. Complexes [RuCl(NCMe)₄(η^1 -*i*-Pr₂P(CH₂)₃Ph)]Cl ([332]Cl) and [332]PF₆ display nearly identical chemical shifts (δ 53.7 and 55.8 compared with δ 52.8 and 54.2, respectively). The intensity ratio of the peaks for [332]PF₆ was determined to be 1:2; that for [332]Cl was not determined precisely but appeared to be almost 2:1. This may be another instance in which

replacement of chloride ion by PF_6 causes reversal of the $^{31}\text{P}\{^1\text{H}\}$ -NMR chemical shifts of the isomers. The $^{31}\text{P}\{^1\text{H}\}$ -NMR spectrum of $[\text{RuCl}(\text{NCMe})_4(\eta^1\text{-Me}_2\text{P}(\text{CH}_2)_3\text{Ph})]\text{PF}_6$ (**[331]** PF_6) was not recorded, but the chloride salt **[331]**Cl showed two signals at δ 29.4 and 32.4 in a 5:3 ratio. The chemical shifts of $[\text{RuCl}(\text{NCMe})_4(\eta^1\text{-Ph}_2\text{PCH}_2\text{SiMe}_2\text{Ph})]$ (**[334]**Cl) and **[334]** PF_6 were very similar, δ 44.7 and 49.9 compared with δ 44.0 and 47.3, respectively, as were the ratio of isomers present, which was approximately 3:2.

An indication of the stability of the cations $[\text{RuCl}(\text{NCMe})_4(\eta^1\text{-R}_2\text{P}(\text{CH}_2)_3\text{Ph})]^+$ ($\text{R} = \text{Ph}, i\text{-Pr}, \text{Cy}$) and $[\text{RuCl}(\text{NC}(\text{CH}_2)_2\text{Me})_4(\eta^1\text{-R}_2\text{P}(\text{CH}_2)_3\text{Ph})]^+$ is that they all show parent ions in their FAB-mass spectra. These cations fragment through sequential loss of the nitrile and/or chloride ligands, and usually form cations of the type $[\text{Ru}(\text{Ph}_2\text{P}(\text{CH}_2)_3\text{Ph})]^+$. These fragmentation patterns are summarised in Tables 27-29. The peaks due to the matrix masked some of the fragment peaks that may have been present for $[\text{RuCl}(\text{NCMe})_4(\eta^1\text{-Cy}_2\text{P}(\text{CH}_2)_3\text{Ph})]^+$ (**[333]** $^+$). This was also the case for $[\text{RuCl}(\text{NCMe})_4(\eta^1\text{-}i\text{-Pr}_2\text{P}(\text{CH}_2)_3\text{Ph})]^+$ (**[332]** $^+$), which displayed only one fragment peak with m/z 455, corresponding to $[\text{RuCl}(\text{NCMe})_2(\eta^1\text{-}i\text{-Pr}_2\text{P}(\text{CH}_2)_3\text{Ph})]^+$.

Table 24. ^1H and $^{13}\text{C}\{^1\text{H}\}$ -NMR chemical shifts (ppm) in d_3 -acetonitrile of the acetonitrile ligands of the tetrakis acetonitrile complexes [331]Cl, [328]PF₆, [332]PF₆, [333]PF₆ and [334]Cl.

Complex	^1H Chemical Shift (ppm) for the CH ₃ CN Ligands	^{13}C Chemical Shift (ppm) for the CH ₃ CN Ligands
[RuCl(NCMe) ₄ (η^1 -Me ₂ P~Ph)]Cl ([331]Cl) ^a	2.28, 2.29, 2.41	4.39, 4.52, 124.45, 124.73
[RuCl(NCMe) ₄ (η^1 -Ph ₂ P~Ph)]Cl ([328]PF ₆)	2.11, 2.15, 2.19	3.93, 3.96, 4.06, 4.13, 125.12, 125.48
[RuCl(NCMe) ₄ (η^1 - <i>i</i> -Pr ₂ P~Ph)]PF ₆ ([332]PF ₆)	2.34, 2.38	4.28, 125.80, 127.44
[RuCl(NCMe) ₄ (η^1 -Cy ₂ P~Ph)]PF ₆ ([333]PF ₆)	2.33, 2.39	4.14, 4.33, 125.66, 127.32
[RuCl(NCMe) ₄ (η^1 - <i>i</i> -Pr ₂ PCH ₂ SiMe ₂ Ph)]Cl ([334]Cl) ^a	2.27, 2.29, 2.32, 2.37	not measured

^aRecorded in d_2 -dichloromethane.

~ = (CH₂)₃

Table 25. Ratio of isomers (upfield:downfield) of the tetrakis species obtained from η^6 -benzene precursor complexes and the $^{31}\text{P}\{^1\text{H}\}$ -NMR chemical shifts (ppm) in d_3 -acetonitrile.

Cation	Cl^-			PF_6^-		
	^{31}P Chemical Shifts (ppm)		Ratio	^{31}P Chemical Shifts (ppm)		Ratio
$[\text{RuCl}(\text{NCMe})_4(\eta^1\text{-Me}_2\text{P}\sim\text{Ph})]^+$	29.4	32.4	5:3	a	a	a
$[\text{RuCl}(\text{NCMe})_4(\eta^1\text{-Ph}_2\text{P}\sim\text{Ph})]^+$	48.7 ^b	52.1 ^b	5:1	46.4	48.7	1:5
$[\text{RuCl}(\text{NCMe})_4(\eta^1\text{-}i\text{-Pr}_2\text{P}\sim\text{Ph})]^+$	53.7	55.8	2:1 ^c	52.8	54.2	1:2
$[\text{RuCl}(\text{NCMe})_4(\eta^1\text{-Cy}_2\text{P}\sim\text{Ph})]^+$	44.5 ^d	-	one signal	42.8	44.4	5:6
$[\text{RuCl}(\text{NCMe})_4(\eta^1\text{-Ph}_2\text{PCH}_2\text{SiMe}_2\text{Ph})]^+$	44.7 ^e	49.9 ^e	3:2	44.0	47.3	3:2

^a $^{31}\text{P}\{^1\text{H}\}$ -NMR spectrum was not recorded; ^bassignment of isomers known (δ 48.7 and 52.1 are due to *trans*- and *cis*- $[\text{RuCl}(\text{NCMe})_4(\eta^1\text{-Ph}_2\text{P}(\text{CH}_2)_3\text{Ph})]\text{Cl}$ (**[328]**Cl), respectively); ^cratio was obtained by approximate integration of the peaks without delay time and is therefore approximate; ^donly one signal was observed, shown to be *trans*-isomer by ^1H -NMR spectroscopy; ^ein d_2 -dichloromethane.

$\sim = (\text{CH}_2)_3$

Table 26. Mass spectrometry (FAB) data for the tetrakis-cations [328]⁺, [335]⁺, [332]⁺ and [333]⁺.

Complex	Highest Mass Ion	<i>m/z</i>
[RuCl(NCMe) ₄ (η ¹ -Ph ₂ P~Ph)] ⁺	[M] ⁺	605
[RuCl(NC(CH ₂) ₂ CH ₃) ₄ (η ¹ -Ph ₂ P~Ph)] ⁺	[M] ⁺	717
[RuCl(NCMe) ₄ (η ¹ - <i>i</i> -Pr ₂ P~Ph)] ⁺	[M] ⁺	537
[RuCl(NCMe) ₄ (η ¹ -Cy ₂ P~Ph)] ⁺	[M] ⁺	576

~ = (CH₂)₃Table 27. Fragmentation pattern in the mass spectrum (FAB) of [RuCl(NCMe)₄(η¹-Ph₂P(CH₂)₃Ph)]⁺ ([328]⁺).

Fragment	Loss	Ion	<i>m/z</i>
[RuCl(NCMe) ₄ (η ¹ -Ph ₂ P~Ph)] ⁺	-	[M] ⁺	605
[RuCl(NCMe) ₂ (Ph ₂ P~Ph)] ⁺	2(MeCN)	[M-2xacetonitrile] ⁺	523
[RuCl(NCMe)(Ph ₂ P~Ph)] ⁺	3(MeCN)	[M-3xacetonitrile] ⁺	482
[RuCl(Ph ₂ P~Ph)] ⁺	4(MeCN)	[M-4xacetonitrile] ⁺	443
[Ru(Ph ₂ P~Ph)] ⁺	4(MeCN) and Cl	[M-Cl-4xacetonitrile] ⁺	405

~ = (CH₂)₃

Table 28. Fragmentation pattern in the mass spectrum (FAB) of $[\text{RuCl}(\text{NC}(\text{CH}_2)_2\text{Me})_4(\eta^1\text{-Ph}_2\text{P}(\text{CH}_2)_3\text{Ph})]^+$ ($[\text{335}]^+$).

Fragment	Loss	Ion	<i>m/z</i>
$[\text{RuCl}(\text{NC}(\text{CH}_2)_2\text{Me})_4(\eta^1\text{-Ph}_2\text{P}\sim\text{Ph})]^+$	-	$[\text{M}]^+$	717
$[\text{RuCl}(\text{NC}(\text{CH}_2)_2\text{Me})_3(\text{Ph}_2\text{P}\sim\text{Ph})]^+$	$\text{Me}(\text{CH}_2)_2\text{CN}$	$[\text{M}\text{-butyronitrile}]^+$	648
$[\text{Ru}(\text{NC}(\text{CH}_2)_2\text{Me})_3(\text{Ph}_2\text{P}\sim\text{Ph})]^+$	$\text{Me}(\text{CH}_2)_2\text{CN}$ and Cl	$[\text{M}\text{-Cl}\text{-butyronitrile}]^+$	614
$[\text{RuCl}(\text{NC}(\text{CH}_2)_2\text{Me})_2(\text{Ph}_2\text{P}\sim\text{Ph})]^+$	$2(\text{Me}(\text{CH}_2)_2\text{CN})$	$[\text{M}\text{-2xbutyronitrile}]^+$	579
$[\text{RuCl}(\text{NC}(\text{CH}_2)_2\text{Me})(\text{Ph}_2\text{P}\sim\text{Ph})]^+$	$3(\text{Me}(\text{CH}_2)_2\text{CN})$	$[\text{M}\text{-3xbutyronitrile}]^+$	510
$[\text{Ru}(\text{NC}(\text{CH}_2)_2\text{Me})(\text{Ph}_2\text{P}\sim\text{Ph})]^+$	$3(\text{Me}(\text{CH}_2)_2\text{CN})$ and Cl	$[\text{M}\text{-Cl}\text{-3xbutyronitrile}]^+$	476
$[\text{RuCl}(\text{Ph}_2\text{P}\sim\text{Ph})]^+$	$4(\text{Me}(\text{CH}_2)_2\text{CN})$	$[\text{M}\text{-4xbutyronitrile}]^+$	441
$[\text{Ru}(\text{Ph}_2\text{P}\sim\text{Ph})]^+$	$4(\text{Me}(\text{CH}_2)_2\text{CN})$ and Cl	$[\text{M}\text{-Cl}\text{-4xbutyronitrile}]^+$	405

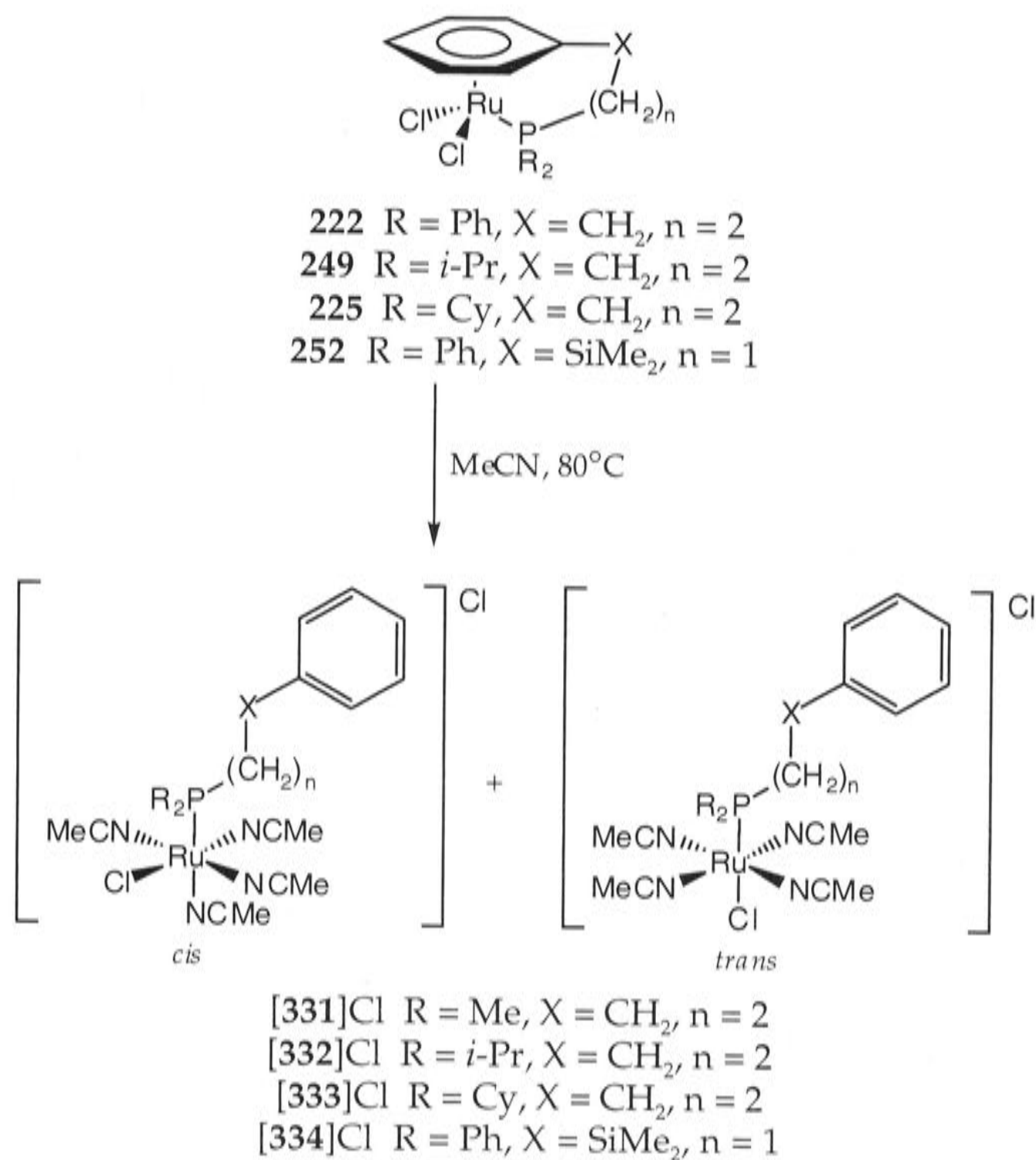
 $\sim = (\text{CH}_2)_3$ Table 29. Fragmentation pattern in the mass spectrum (FAB) of $[\text{RuCl}(\text{NCMe})_4(\eta^1\text{-Cy}_2\text{P}(\text{CH}_2)_3\text{Ph})]^+$ ($[\text{333}]^+$).

Fragment	Loss	Ion	<i>m/z</i>
$[\text{RuCl}(\text{NCMe})_4(\eta^1\text{-Cy}_2\text{P}\sim\text{Ph})]^+$	-	$[\text{M}]^+$	617
$[\text{RuCl}(\text{NCMe})_3(\text{Cy}_2\text{P}\sim\text{Ph})]^+$	MeCN	$[\text{M}\text{-acetonitrile}]^+$	576
$[\text{Ru}(\text{NCMe})_2(\text{Cy}_2\text{P}\sim\text{Ph})]^+$	$2(\text{MeCN})$ and Cl	$[\text{M}\text{-2xacetonitrile}]^+$	535
$[\text{RuCl}(\text{Cy}_2\text{P}\sim\text{Ph})]^+$	$4(\text{MeCN})$	$[\text{M}\text{-4xacetonitrile}]^+$	453

 $\sim = (\text{CH}_2)_3$

The tethered complexes $[\text{RuCl}_2(\eta^1:\eta^6\text{-R}_2\text{P}(\text{CH}_2)_3\text{Ph})]$ ($\text{R} = \text{Ph}$ (222), *i*-Pr (249), Cy (225)) and $[\text{RuCl}_2(\eta^1:\eta^6\text{-Ph}_2\text{PCH}_2\text{SiMe}_2\text{Ph})]$ (252) all react with boiling acetonitrile to give the same tetrakis-salts as those obtained from the benzene complexes (see Scheme 74), but the reaction is usually much slower. Its progress in each case was monitored by NMR spectroscopy. For example, the reaction of 225 with acetonitrile requires 384 hours for completion, whereas that of $[\text{RuCl}_2(\eta^6\text{-C}_6\text{H}_6)(\eta^1\text{-Cy}_2\text{P}(\text{CH}_2)_3\text{Ph})]$ (229) is complete within 24 hours. Similarly, complex 222 requires 264 hours for complete displacement of the η^6 -arene, compared with 48 hours for of $[\text{RuCl}_2(\eta^6\text{-C}_6\text{H}_6)(\eta^1\text{-Ph}_2\text{P}(\text{CH}_2)_3\text{Ph})]$ (227) (see page 192). The rate of reaction of the tethered complexes is also influenced by the nature of the substituent on phosphorus. Complex $[\text{RuCl}_2(\eta^1:\eta^6\text{-Ph}_2\text{P}(\text{CH}_2)_3\text{Ph})]$ (222), with less bulky phenyl substituents, reacts much faster than *iso*-propyl-substituted 249 (264 *vs* 456 hours). In contrast, the reaction of 252, in which there are two atoms in the strap, is complete within the same time as that required for $[\text{RuCl}_2(\eta^6\text{-C}_6\text{H}_6)(\eta^1\text{-Ph}_2\text{PCH}_2\text{SiMe}_2\text{Ph})]$ (230). The reaction of 252 on an NMR scale in d_3 -acetonitrile was also monitored by ^1H and $^{31}\text{P}\{^1\text{H}\}$ -NMR spectroscopy. The displacement of the η^6 -arene only started at 40°C; no reaction occurred at room temperature. The ratio of *cis*- and *trans*-isomers formed changed with time; it was approximately 1:1 up to 48 hours, and changed to 2:1 after 72 hours. The chloride salts were all converted into the more stable PF_6 derivatives, with the exception of $[\text{RuCl}_2(\eta^1:\eta^6\text{-Ph}_2\text{PCH}_2\text{SiMe}_2\text{Ph})]^+$, which decomposed upon treatment with NH_4PF_6 (complex $[\mathbf{334}]\text{PF}_6$), obtained from the corresponding benzene complex $[\text{RuCl}_2(\eta^6\text{-C}_6\text{H}_6)(\eta^1\text{-Ph}_2\text{PCH}_2\text{SiMe}_2\text{Ph})]$ (230), was prepared from NaPF_6 .

Unexpectedly, the ratio of *cis*- and *trans*-isomers formed from the tethered complexes was not the same as observed from the η^6 -benzene complexes; this is discussed in more detail below (see Table 30). Table 31 summarises the reaction conditions to form the *cis*- and *trans*-isomers of the tetrakis(acetonitrile) complexes from both non-tethered and tethered precursors.



Scheme 74. Preparation of the *cis*- and *trans*-isomers of the chloride salts [328]Cl, [332]Cl, [333]Cl and [334]Cl from the tethered compounds 222, 249, 225 and 252, respectively.

The $^{31}\text{P}\{^1\text{H}\}$ -NMR spectra of *cis*- and *trans*-[328]Cl formed from $[\text{RuCl}_2(\eta^1:\eta^6\text{-Ph}_2\text{P}(\text{CH}_2)_3\text{Ph})]$ (222) after 264 hours showed the two expected

peaks at δ 48.7 and 52.1, but the ratio was approximately 2:1 in favour of the *trans*-isomer. In contrast, the ratio starting from the η^6 -benzene complex $[\text{RuCl}_2(\eta^6\text{-C}_6\text{H}_6)(\eta^1\text{-Ph}_2\text{P}(\text{CH}_2)_3\text{Ph})]$ (**227**) after 264 hours was 7:1 (see page 197). Surprisingly, the PF_6 salt isolated as a microcrystalline solid from the sample of **[328]Cl**, obtained from the tethered complex **222**, though it contained the two expected resonances at δ 46.4 and 48.7, the observed *cis/trans* ratios in independent experiments were very different: 2:1 and 3:1, *cf.* 1:5 in the case of **[328]PF₆** obtained from the η^6 -benzene complex **227**. This irreproducibility suggests that there may have been selective recrystallisation or precipitation of one isomer during the process of isolation. In retrospect, it would have clearly been better to check the $^{31}\text{P}\{^1\text{H}\}$ -NMR spectra of the PF_6 salts *in situ* in CH_2Cl_2 solutions before attempting to isolate the PF_6 salts.

Similar behaviour was observed in two other systems. The approximate ratio of isomers of $[\text{RuCl}(\text{NCMe})_4(\eta^1\text{-}i\text{-Pr}_2\text{P}(\text{CH}_2)_3\text{Ph})]\text{Cl}$ (**[332]Cl**) was 3:1, which changed to 2:1 in the isolated PF_6 salt. Both ratios differ from those obtained for the salts derived from the reaction of acetonitrile with the $[\text{RuCl}_2(\eta^6\text{-C}_6\text{H}_6)(\eta^1\text{-}i\text{-Pr}_2\text{P}(\text{CH}_2)_3\text{Ph})]$ (**228**): 2:1 and 1:2, respectively. Likewise, the ratio of isomers of $[\text{RuCl}(\text{NCMe})_4(\eta^1\text{-Cy}_2\text{P}(\text{CH}_2)_3\text{Ph})]\text{PF}_6$ (**[333]PF₆**) was different from that observed for the same species derived from $[\text{RuCl}_2(\eta^6\text{-C}_6\text{H}_6)(\eta^1\text{-Cy}_2\text{P}(\text{CH}_2)_3\text{Ph})]$ (**229**). One isomer is favoured from **225**, whereas the opposite isomer appears to be favoured from **229**.

The only system that behaved as expected was that containing $\text{Ph}_2\text{PCH}_2\text{SiMe}_2\text{Ph}$ (**201**), where the ratio of *cis*- and *trans*-isomers of $[\text{RuCl}(\text{NCMe})_4(\eta^1\text{-Ph}_2\text{PCH}_2\text{SiMe}_2\text{Ph})]$ (**[334]Cl**) was approximately equal, from either the tethered complex $[\text{RuCl}_2(\eta^1:\eta^6\text{-Ph}_2\text{PCH}_2\text{SiMe}_2\text{Ph})]$ (**252**) or

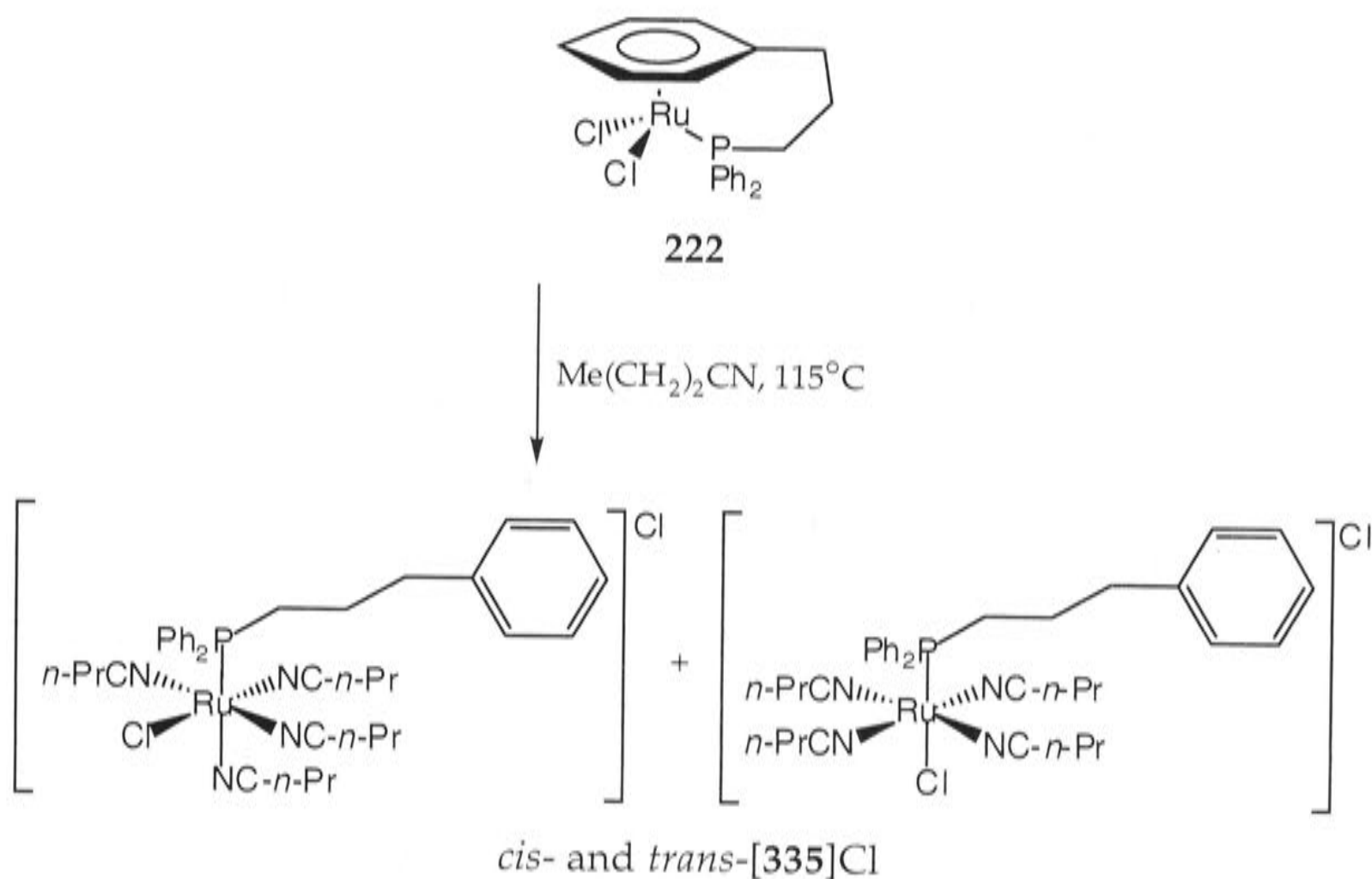
the non-tethered compound $[\text{RuCl}_2(\eta^6\text{-C}_6\text{H}_6)(\eta^1\text{-Ph}_2\text{PCH}_2\text{SiMe}_2\text{Ph})]$ (230). In these cases, the times required for complete displacement of the η^6 -arene in the non-tethered and tethered systems are approximately equal, and, when obtained, the PF_6 salt could not be crystallised.

The reaction of $[\text{RuCl}_2(\eta^1:\eta^6\text{-Ph}_2\text{P}(\text{CH}_2)_3\text{Ph})]$ (222) in refluxing butyronitrile for 14 hours caused displacement of the η^6 -arene, but the product could only be obtained as an oil. Because there were many signals in the ^1H NMR spectrum in the region δ 0.5–3, the number of butyronitrile ligands in the product could not be determined. However, the FAB-mass spectrum showed a molecular ion at m/z 717, corresponding to the formula $[\text{RuCl}(\text{NCCH}_2\text{CH}_2\text{CH}_3)_4(\eta^1\text{-Ph}_2\text{P}(\text{CH}_2)_3\text{Ph})]^+$ ($[\text{335}]^+$) (see Table 26 and Scheme 75). The $^{31}\text{P}\{^1\text{H}\}$ -NMR spectrum (in CD_2Cl_2) showed two resonances in a 1:2 ratio at δ 47.6 and 52.0, presumably due to the *trans* and *cis*-isomers, though it was not possible to assign them individually.

Attempts were made to convert $[\text{RuCl}(\text{CH}_3\text{CN})_4(\eta^1\text{-Ph}_2\text{P}(\text{CH}_2)_3\text{Ph})]\text{Cl}$ ($[\text{328}]\text{Cl}$) into the tethered complex $[\text{RuCl}_2(\eta^1:\eta^6\text{-Ph}_2\text{P}(\text{CH}_2)_3\text{Ph})]$ (222), for example, by treatment with zinc dust in methanol or with lithium chloride in acetone. The ^1H and $^{31}\text{P}\{^1\text{H}\}$ -NMR spectra indicated that a mixture of products were obtained in both cases.

In view of Smith and Wright's report¹⁰ of the formation of $[\text{RuCl}_2(\text{NCMe})_3(\eta^1\text{-Ph}_2\text{P}(\text{CH}_2)_3\text{Ph})]$ (259), various unsuccessful attempts were made to induce loss of one acetonitrile ligand from $[\text{RuCl}(\text{NCMe})_4(\eta^1\text{-Ph}_2\text{P}(\text{CH}_2)_3\text{Ph})]\text{Cl}$ ($[\text{328}]\text{Cl}$). These included heating *in vacuo* and treatment with phosphoric acid (60% in H_2O) or triflic acid, which either caused decomposition, or, in the case of the acids, gave rise to

unidentifiable complexes, respectively. In the case of triflic acid, two new peaks were detected in the $^{31}\text{P}\{^1\text{H}\}$ -NMR spectra (no peaks indicative of the parent complex $[\mathbf{328}]\text{Cl}$ were present), which formed after the solution was maintained at room temperature and then heated to 40°C ; these species were not isolated since their ^1H NMR spectra showed peaks assignable to coordinated aromatic protons. This result, in line with Smith and Wright's¹⁰ successful attempt to prepare $[\text{RuCl}_2(\eta^1:\eta^6\text{-Ph}_2\text{P}(\text{CH}_2)_3\text{Ph})]$ ($\mathbf{222}$) by heating $\mathbf{259}$ in chlorobenzene with trifluoroacetic acid, tends to suggest that triflic acid was not the most suitable reagent. The conversion of the tetrakis-species $[\text{RuCl}(\text{NC}(\text{CH}_2)_2\text{Me})_4(\eta^1\text{-Ph}_2\text{P}(\text{CH}_2)_3\text{Ph})]\text{Cl}$ ($[\mathbf{335}]\text{Cl}$) into the tris-complex $[\text{RuCl}_2(\text{NC}(\text{CH}_2)_2\text{Me})_3(\eta^1\text{-Ph}_2\text{P}(\text{CH}_2)_3\text{Ph})]$ ($\mathbf{336}$) was also attempted using hydrochloric acid, but this also gave rise to unidentifiable products. The conversion of the tetrakis-isomers to the respective tris-complexes was not investigated further.



Scheme 75. Preparation of the *cis*- and *trans*-isomers $[\mathbf{335}]\text{Cl}$ from the reaction of $\mathbf{222}$ with butyronitrile.

Table 30. Ratio[§] of isomers (upfield:downfield) of the tetrakis species, obtained from either the η^6 -benzene or respective tethered complexes, observed in their $^{31}\text{P}\{^1\text{H}\}$ -NMR spectra.

Cation	From η^6 -Benzene Complex		From Tethered Complex	
	Cl^-	PF_6^-	Cl^-	PF_6^-
$[\text{RuCl}(\text{NCMe})_4(\text{Ph}_2\text{P}\sim\text{Ph})]^+$	5:1	1:5	2:1 [†]	2:1 [‡]
$[\text{RuCl}(\text{NCMe})_4(i\text{-Pr}_2\text{P}\sim\text{Ph})]^+$	2:1 [†]	1:2	3:1 [†]	2:1
$[\text{RuCl}(\text{NCMe})_4(\text{Cy}_2\text{P}\sim\text{Ph})]^+$	one signal	5:6	one signal	7:4
$[\text{RuCl}(\text{NCMe})_4(\text{Ph}_2\text{PCH}_2\text{SiMe}_2\text{Ph})]^+$	3:2	3:2	2:1 [†]	not measured

[§]The reaction times were different for the respective non-tethered and tethered complexes.

[†]Ratio was obtained by approximate integration of the peaks without delay time and is therefore approximate;

[‡]irreproducible since ratio of 1:3 was obtained from an independent experiment.

$\sim = (\text{CH}_2)_3$

Table 31. Relative reaction times for the formation of the various tetrakis nitrile complexes.

Parent Complex	Product	Reaction Time (h)	Temperature (°C)	Yield
[RuCl ₂ (η ⁶ -C ₆ H ₆)(η ¹ -Me ₂ P~Ph)] (226)	[RuCl(NCMe) ₄ (Me ₂ P~Ph)]Cl ([331]Cl)	48	80	a
[RuCl ₂ (η ⁶ -C ₆ H ₆)(η ¹ -Ph ₂ P~Ph)] (227)	[RuCl(NCMe) ₄ (Ph ₂ P~Ph)]PF ₆ ([328]PF ₆)	48	80	82
[RuCl ₂ (η ¹ :η ⁶ -Ph ₂ P~Ph)] (222)	[RuCl(NCMe) ₄ (Ph ₂ P~Ph)]PF ₆ ([328]PF ₆)	264	80	67 ^b
[RuCl ₂ (η ¹ :η ⁶ -Ph ₂ P~Ph)] (222)	[RuCl(NC(CH ₂) ₂ Me) ₄ (Ph ₂ P~Ph)]Cl ([335]Cl)	14	115	90
[RuCl ₂ (η ⁶ -1,2-MeC ₆ H ₄ CO ₂ Me)(η ¹ - <i>i</i> -Pr ₂ P~Ph)] (238)	[RuCl(NCMe) ₄ (<i>i</i> -Pr ₂ P~Ph)]Cl ([332]Cl)	96	r.t.	a,d
[RuCl ₂ (η ⁶ -1,2-MeC ₆ H ₄ CO ₂ Me)(η ¹ - <i>i</i> -Pr ₂ P~Ph)] (238)	[RuCl(NCMe) ₄ (<i>i</i> -Pr ₂ P~Ph)]Cl ([332]Cl)	1	80	a,d
[RuCl ₂ (η ⁶ -C ₆ H ₆)(η ¹ - <i>i</i> -Pr ₂ P~Ph)] (228)	[RuCl(NCMe) ₄ (<i>i</i> -Pr ₂ P~Ph)]PF ₆ ([332]PF ₆)	24	80	87
[RuCl ₂ (η ¹ :η ⁶ - <i>i</i> -Pr ₂ P~Ph)] (249)	[RuCl(NCMe) ₄ (<i>i</i> -Pr ₂ P~Ph)]PF ₆ ([332]PF ₆)	456	80	85 ^c
[RuCl ₂ (η ⁶ -C ₆ H ₆)(η ¹ -Cy ₂ P~Ph)] (229)	[RuCl(NCMe) ₄ (Cy ₂ P~Ph)]Cl ([333]Cl)	24	80	93
[RuCl ₂ (η ¹ :η ⁶ -Cy ₂ P~Ph)] (225)	[RuCl(NCMe) ₄ (Cy ₂ P~Ph)]Cl ([333]Cl)	384	80	82 ^d
[RuCl ₂ (η ⁶ -C ₆ H ₆)(η ¹ -Ph ₂ PCH ₂ SiMe ₂ Ph)] (230)	[RuCl(NCMe) ₄ (Ph ₂ PCH ₂ SiMe ₂ Ph)]PF ₆ ([334]PF ₆)	48	80	a

Parent Complex	Product	Reaction Time (h)	Temperature (°C)	Yield
[RuCl ₂ (η ¹ :η ⁶ -Ph ₂ PCH ₂ SiMe ₂ Ph)] (252)	-	16	r.t. ^e	no reaction
[RuCl ₂ (η ¹ :η ⁶ -Ph ₂ PCH ₂ SiMe ₂ Ph)] (252)	[RuCl(NCMe) ₄ (Ph ₂ PCH ₂ SiMe ₂ Ph)]Cl ([334]Cl)	72	40 ^e	a,d
[RuCl ₂ (η ¹ :η ⁶ -Ph ₂ PCH ₂ SiMe ₂ Ph)] (252)	[RuCl(NCMe) ₄ (Ph ₂ PCH ₂ SiMe ₂ Ph)]Cl ([334]Cl)	48	80	a

^aYield was not determined; ^breaction had not proceeded to completion; ^csome decomposition occurred due to extensive reaction time required; ^dproduct was not converted to the PF₆ salt; ^ereaction conducted in *d*₃-acetonitrile.

~ = (CH₂)₃

4.2 Summary

The reactions of various non-tethered and tethered η^6 -arene complexes with acetonitrile, which gave rise to tetrakis-complexes of the type $[\text{RuCl}(\text{NCMe})_4(\eta^1\text{-R}_2\text{P}(\text{CH}_2)_n\text{XPh})]\text{Cl}$, have been described. The η^6 -methyl *o*-toluate complex reacted faster than the η^6 -benzene derivatives, which, in turn, reacted faster than the tethered species. Thus, tethering the η^6 -arene clearly hinders its displacement by acetonitrile. The reaction times of the non-tethered and tethered complexes are also influenced by the nature of the substituent on phosphorus. Non-tethered complexes with bulkier substituents reacted faster than those with less sterically demanding substituents. In contrast, tethered complexes containing bulky substituents reacted more slowly than those with methyl or phenyl substituents. Attempts to convert the tetrakis-isomer $[\text{RuCl}(\text{NCMe})_4(\eta^1\text{-Ph}_2\text{P}(\text{CH}_2)_3\text{Ph})]$ (**[328]**Cl) to the tris-adduct $[\text{RuCl}_2(\text{NCMe})_3(\eta^1\text{-Ph}_2\text{P}(\text{CH}_2)_3\text{Ph})]\text{Cl}$ (**259**) were not successful. This tends to suggest that the tetrakis-complexes formed during thermolysis of various η^6 -arene RuCl_2 compounds in acetonitrile are the thermodynamic products. The ratio of *cis*- and *trans*-isomers formed also appears to be dependent upon the nature of the parent complex, though there are unresolved problems in this area. This information may have mechanistic implications, and these observations will be discussed in Chapter 7 (Section 7.2).

References

- (1) Seddon, E. A.; Seddon, K. R. *The Chemistry of Ruthenium*; Elsevier Science B. V.: Amsterdam, 1984, p. 392.
- (2) Duff, C. M.; Heath, G. A. *Inorg. Chem.* **1991**, *30*, 2528-2535.
- (3) Duff, C. M.; Heath, G. A. *J. Chem. Soc., Dalton Trans.* **1991**, 2401-2411.
- (4) Bown, M.; Hockless, D. C. R. *Acta. Cryst.* **1996**, *C52*, 1105-1106.
- (5) Valerga, P.; Puerta, M. C.; Pandey, D. S. *J. Organomet. Chem.* **2002**, *648*, 27-32.
- (6) Fernandez, S.; Pfeffer, M.; Ritleng, V.; Sirlin, C. *Organometallics* **1999**, *18*, 2390-2394.
- (7) Gill, T. P.; Mann, K. R. *Organometallics* **1982**, *1*, 485-488.
- (8) McNair, A. M.; Mann, K. R. *Inorg. Chem.* **1986**, *25*, 2519-2527.
- (9) Freedman, D. A.; Mann, K. R. *Inorg. Chem.* **1989**, *28*, 3926-3929.
- (10) Smith, P. D.; Wright, A. H. *J. Organomet. Chem.* **1998**, *559*, 141-147.
- (11) Vitulli, G.; Pertici, P.; Salvadori, P. *J. Chem. Soc., Dalton Trans.* **1984**, 2255-2257.
- (12) Bennett, M. A.; Neumann, H.; Thomas, M.; Wang, X.; Pertici, P.; Salvadori, P.; Vitulli, G. *Organometallics* **1991**, *10*, 3237-3245.
- (13) Jung, S.; Ilg, K.; Brandt, C. D.; Wolf, J.; Werner, H. *J. Chem. Soc., Dalton Trans.* **2002**, 318-327.
- (14) Smith, P. D.; Gelbrich, T.; Hursthouse, M. B. *J. Organomet. Chem.* **2002**, *659*, 1-9.
- (15) Canepa, G.; Sola, E.; Martín, M.; Lahoz, F. J.; Oro, L. A.; Werner, H. *Organometallics* **2003**, *22*, 2151-2160.
- (16) Smith, P. D. Ph.D. Dissertation; University of Nottingham: Nottingham, 1993.

- (17) Desiraju, G. R.; Steiner, T. *The Weak Hydrogen Bond in Structural Chemistry and Biology*; Oxford University Press: Oxford, 1999, pp. 215-220.
- (18) Davies, P. J.; Veldman, N.; Grove, D. M.; Spek, A. L.; Lutz, B. T. G.; van Koten, G. *Angew. Chem. Int. Ed. Engl.* **1996**, *35*, 1959-1961.
- (19) Das, B. K.; Chakravarty, A. R. *Inorg. Chem.* **1992**, *31*, 1395-1400.
- (20) Abbenhuis, R. A. T. M.; del Río, I.; Bergshoef, M. M.; Boersma, J.; Veldman, N.; Spek, A. L.; van Koten, G. *Inorg. Chem.* **1998**, *37*, 1749-1758.
- (21) Verkade, J. D.; Quin, L. D. *Phosphorus-31 NMR Spectroscopy in Stereochemical Analysis: Organic Compounds and Metal Complexes*; VCH Publishers, Inc.: Deerfield Beach, 1987; Vol. 8, p. 11
- (22) Geary, W. J. *Coord. Chem. Rev.* **1971**, *7*, 81-122.
- (23) Batista, A. A.; Polato, E. A.; Queiroz, S. L.; Nascimento, O. R.; James, B. R.; Rettig, S. J. *Inorg. Chim. Acta* **1995**, *230*, 111-117.
- (24) Leising, R. A.; Kubow, S. A.; Churchill, M. R.; Buttrey, L. A.; Ziller, J. W.; Takeuchi, K. J. *Inorg. Chem.* **1990**, *29*, 1306-1312.

**Chapter 5: Redox Properties of Tethered and
Non-Tethered Arene Ruthenium(II) Complexes**

*5.1 Cyclic Voltammetry, Spectroelectrochemistry and ESR Spectroscopy of
Non-Tethered and Tethered Complexes*

This Chapter deals with the redox properties of the tethered complexes described in Chapter 3 and comparable non-tethered complexes of the type $[\text{RuCl}_2(\eta^6\text{-arene})(\text{PR}_3)]$ ($\text{R} = \text{Me}, \text{Ph}$). Several different electrochemical methods, including cyclic voltammetry (CV), spectroelectrochemistry, ESR spectroscopy and controlled potential electrolysis (CPE), have been employed to assess the stability of the one-electron oxidation products.

The non-tethered complexes $[\text{RuCl}_2(\eta^6\text{-C}_6\text{R}_6)(\text{PMe}_3)]$ ($\text{R} = \text{H}$ (337), Me (304)) and $[\text{RuCl}_2(\eta^6\text{-arene})(\text{PPh}_3)]$ (arene = C_6H_6 (302), 1,4- $\text{MeC}_6\text{H}_4\text{CHMe}_2$ (338), 1,3,5- $\text{C}_6\text{H}_3\text{Me}_3$ (339), C_6Me_6 (306)), and the tethered complexes $[\text{RuCl}_2(\eta^1:\eta^6\text{-R}_2\text{P}(\text{CH}_2)_3\text{Ph})]$ ($\text{R} = \text{Me}$ (248), Ph (222), *i*-Pr (249), Cy (225)), $[\text{RuCl}_2(\eta^1:\eta^6\text{-Ph}_2\text{P}(\text{CH}_2)_3\text{-2,4,6-C}_6\text{H}_2\text{Me}_3)]$ (250), $[\text{RuCl}_2(\eta^1:\eta^6\text{-Ph}_2\text{P}(\text{CH}_2)_3\text{C}_6\text{Me}_5)]$ (251) and $[\text{RuCl}_2(\eta^1:\eta^6\text{-Ph}_2\text{PCH}_2\text{SiMe}_2\text{Ph})]$ (252), each can be oxidized by one-electron oxidation at room temperature in dichloromethane to form species that are stable on CV timescales. The electrode potentials ($E_{1/2}$) of the non-tethered complexes lie in the range + 0.50-0.87 V (*vs* $\text{Fc}^{0/1}$); similarly, the tethered complexes exhibit $E_{1/2}$ -values in the region + 0.55-0.79 V (*vs* $\text{Fc}^{0/1}$) (Table 32). The difference between the anodic peak potential (E_{pa}) and the cathodic peak potential (E_{pc}), expressed as ΔE_{p} , is consistent with a one-electron process ($\text{Ru}^{\text{II/III}}$) since ΔE_{p} is always close (in the absence of resistance effects) to $2.3\text{RT}/n\text{F}$ (59/ n mV at 25°C, where n = number of electrons¹). Uncompensated solution resistance, in a solvent with a low dielectric constant (especially dichloromethane), will increase the peak-to-peak separation.^{1a} The

peak-to-peak separations are similar to those of ferrocene under identical conditions.

The cyclic voltammograms (CVs) of complexes **306** and **251** are shown in Figures 39 and 40, respectively, and represent typical examples for both the non-tethered and tethered complexes alike. The cyclic voltammetry and alternating current voltammetry (ACV) of $[\text{RuCl}_2(\eta^1:\eta^6\text{-Ph}_2\text{P}(\text{CH}_2)_3\text{Ph})]$ (**222**) in CH_2Cl_2 were compared with those of ferrocene (Figure 41). The ACV traces of **222** and ferrocene at 293K show two symmetric peaks with a peak width at half height of 130 mV and *ca* 100 mV, respectively ($90/n$ mV is to be expected for a one-electron process at 25°C^2). The ACV traces of ferrocene do not superimpose as well as those for **222**, which implies that the reversibility of the $\text{Ru}^{\text{II/III}}$ couple for **222** is at least equal to that of $\text{Fc}^{0/\text{I}}$. For the *t*-butyl substituted compound $[\text{RuCl}_2(\eta^1:\eta^6\text{-}t\text{-Bu}_2\text{P}(\text{CH}_2)_3\text{Ph})]$ (**253**), the ratio of the anodic peak current (i_{pa}) to the cathodic peak current (i_{pc}) was > 1 , which indicates that the oxidized form was not stable at a scan rate of 100 mV s^{-1} (Figure 42). This behaviour has been described loosely in the literature as "quasi-reversible". Strictly speaking, the terms "reversible", "irreversible" and "quasi-reversible" should only be used when describing CV if they are applied to rates of heterogeneous transfer. Chemical stability was determined from CV by measuring the $i_{\text{pa}}/i_{\text{pc}}$ ratio. The cyclic voltammetric behaviour of the non-tethered and tethered complexes is virtually identical; thus this technique does not distinguish between the two types of complexes. Devanne and Dixneuf³ have also shown by CV that non-tethered complexes of the type $[\text{RuCl}_2(\eta^6\text{-arene})\text{L}]$ (L = tertiary phosphine) are stable or "quasi-reversible" one-electron oxidation.

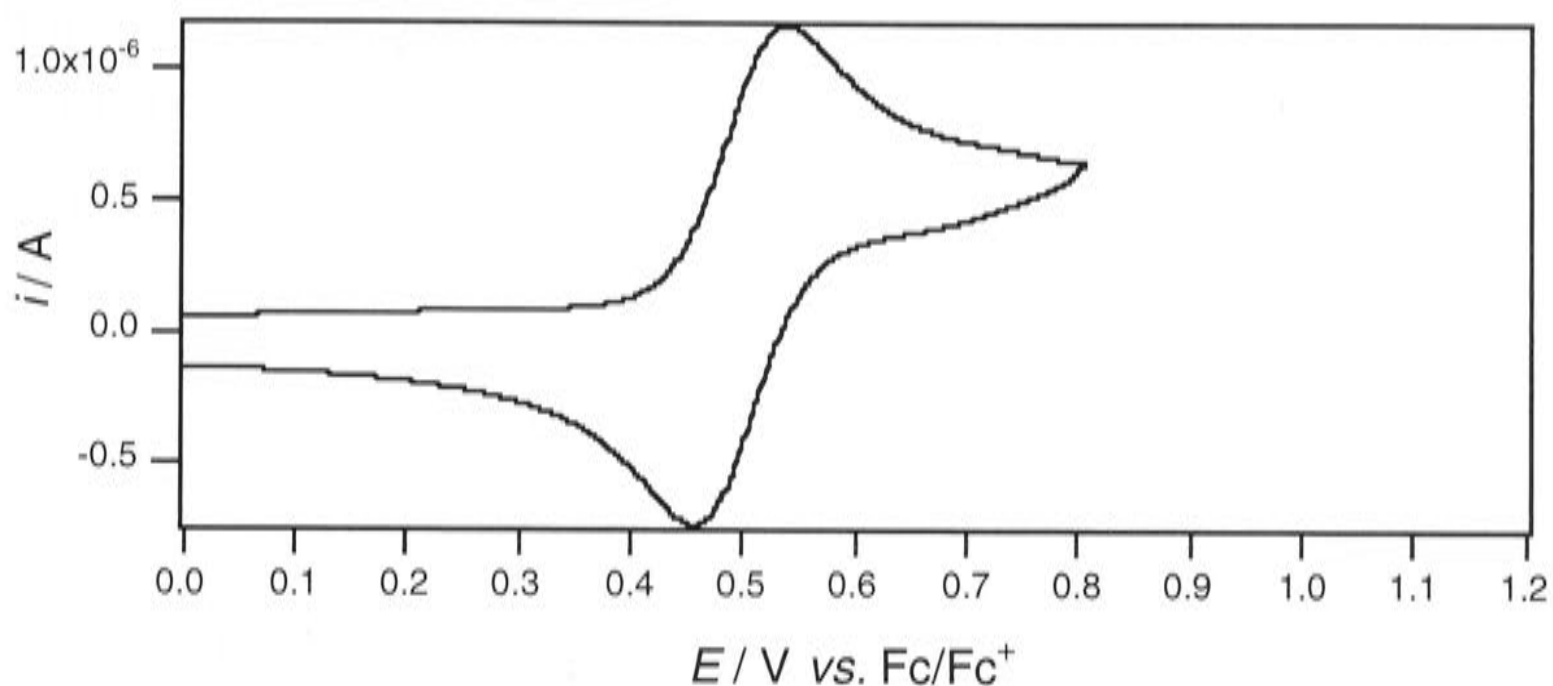


Figure 39. Cyclic voltammogram of $[RuCl_2(\eta^6-C_6Me_6)(PPh_3)]$ (**306**) recorded at a scan rate of 100 mVs^{-1} in $0.5M [Bu^n_4N]PF_6/CH_2Cl_2$ at $293K$.

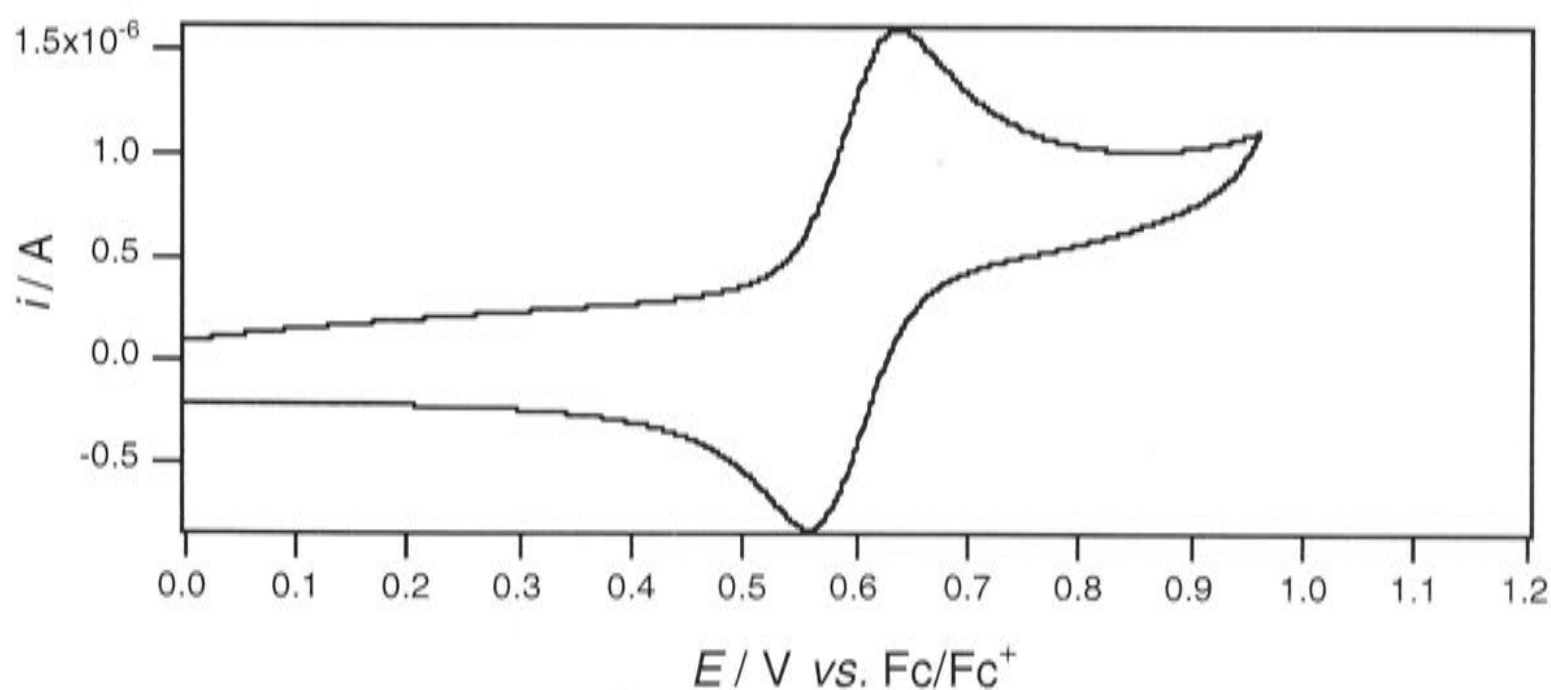


Figure 40. Cyclic voltammogram of $[RuCl_2(\eta^1:\eta^6-Ph_2P(CH_2)_3C_6Me_5)]$ (**251**) recorded at a scan rate of 100 mVs^{-1} in $0.2M [Bu^n_4N]PF_6/CH_2Cl_2$ at $253K$.

In general, the electrode potential ($E_{1/2}$ for any redox couple) is proportional to the energy difference between the oxidised and reduced species, allowing for resistance effects. The electron removed during the oxidation process comes from the highest occupied molecular orbital (HOMO), therefore higher oxidation potentials are observed for metal complexes with more stable HOMOs.⁴⁻⁶ In the present series, higher oxidation potentials correspond to stabilisation of the arene-Ru(II) species

compared with its one-electron oxidation product. For example, $[\text{RuCl}_2(\eta^6\text{-1,2,4,5-C}_6\text{H}_2\text{Me}_4)(\text{PPh}_3)]$ has a higher electrode potential [$E_{1/2} = +0.71$ V (*vs* $\text{Fc}^{0/1}$ in MeCN)] and is more stable at the Ru(II) level than $[\text{RuCl}_2(\eta^6\text{-1,4-C}_6\text{H}_4\text{CHMe}_2)(\text{PPh}_3)]$ (**338**) [$E_{1/2} = +0.78$ V (*vs* $\text{Fc}^{0/1}$ in MeCN)] (see Table 33 for conversion factor⁷).³ The magnitude of the electrode potential is related to the nature of the ligands, and decreases as electron donation towards the metal is increased. The $E_{1/2}$ value is also decreased by replacement of PPh_3 by the more electron donating PMe_3 . For example, $[\text{RuCl}_2(\eta^6\text{-C}_6\text{Me}_6)(\text{PPh}_3)]$ (**306**) has a lower electrode potential than the η^6 -benzene analogue $[\text{RuCl}_2(\eta^6\text{-C}_6\text{H}_6)(\text{PPh}_3)]$ (**302**), which has a higher potential than its PMe_3 derivative $[\text{RuCl}_2(\eta^6\text{-C}_6\text{H}_6)(\text{PMe}_3)]$ (**337**). This correlation is also apparent in the tethered complexes; $[\text{RuCl}_2(\eta^1:\eta^6\text{-Me}_2\text{P}(\text{CH}_2)_3\text{Ph})]$ (**248**) has a lower electrode potential than the PPh_2 analogue $[\text{RuCl}_2(\eta^1:\eta^6\text{-Ph}_2\text{P}(\text{CH}_2)_3\text{Ph})]$ (**222**), but **222** has a higher $E_{1/2}$ than the alkyl-substituted derivative $[\text{RuCl}_2(\eta^1:\eta^6\text{-Ph}_2\text{P}(\text{CH}_2)_3\text{C}_6\text{Me}_5)]$ (**251**).

This correlation between $E_{1/2}$ and the nature of the ligands of metal complexes has been observed previously for reported non-tethered and tethered RuCl_2 complexes; some examples are listed in Table 33. A similar reduction in the electrode potential with stepwise incorporation of alkyl substitution on the ring is observed, for example, in the $[\text{Cr}(\eta^6\text{-arene})_2]^{n+}$ ($n = 0, 1$) couples,⁸⁻¹⁰ and between $[\text{Fe}(\eta^5\text{-C}_5\text{H}_5)_2]^{n+}$ ($n = 0, 1$) and $[\text{Fe}(\eta^5\text{-C}_5\text{Me}_5)_2]^{n+}$ ($n = 0, 1$).¹¹⁻¹⁴ The electrode potentials are referenced to $\text{Fc}^{0/1}$, where applicable, using conversion factors stated in Table 33. The ferrocene/ferrocenium couple was chosen as the reference since it has been adopted by the Commission on Electrochemistry of the IUPAC (International Union of Pure and Applied Chemistry).^{15,16} Further, it is readily used as an internal standard, which avoids errors due to the effects of junction potentials,¹⁷ giving more reliable electrode potentials. Comparison of electrode potentials, which have not been determined by use of an internal standard (such as ferrocene) is likely to lead to error.

Further, the electrode potentials are solvent dependent. Thus the converted electrode potentials listed in Table 33 should be considered with some caution.

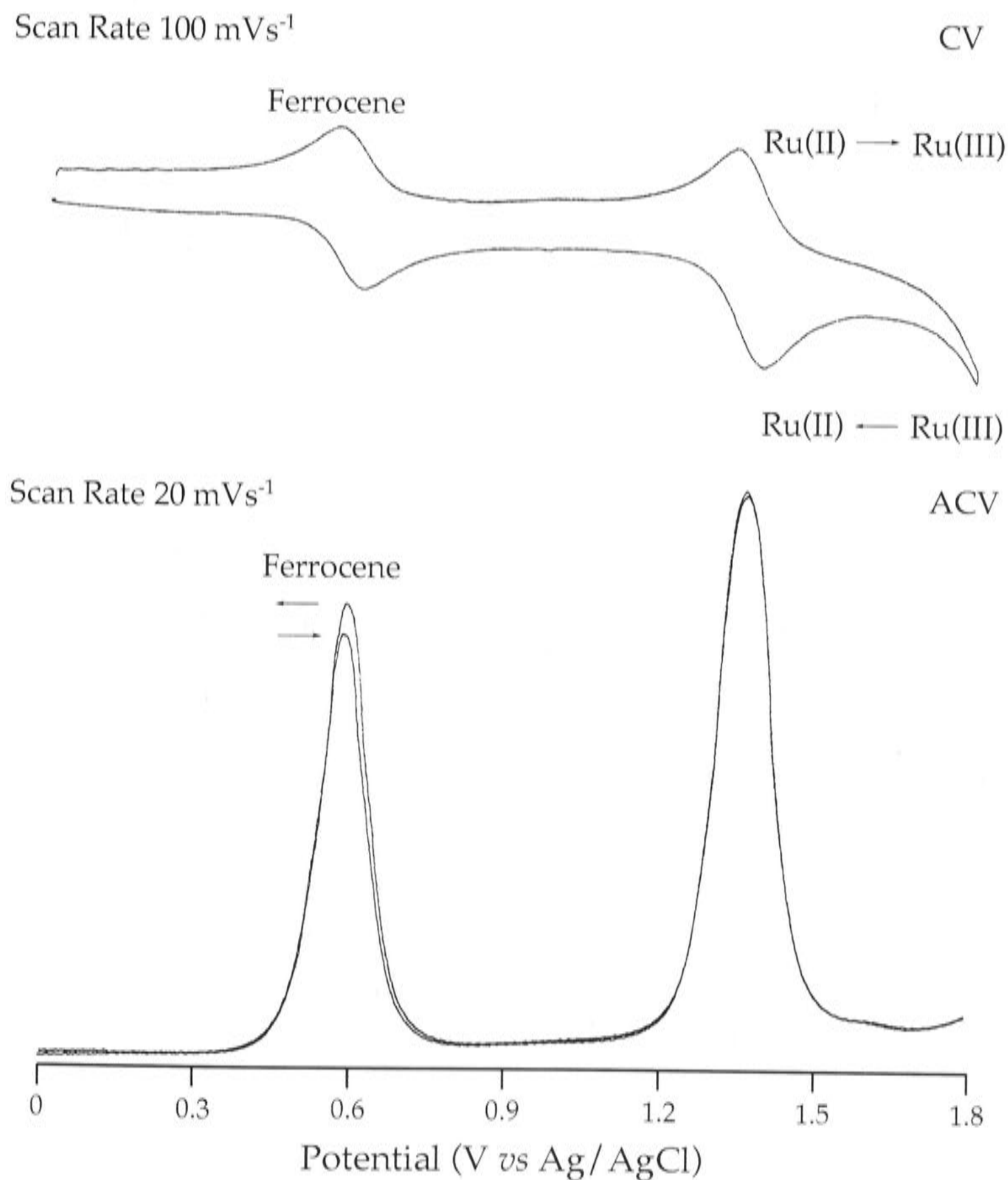


Figure 41. CV and ACV traces of $[\text{RuCl}_2(\eta^1:\eta^6\text{-Ph}_2\text{P}(\text{CH}_2)_3\text{Ph})]$ (**222**) at 293K in 0.5M $[\text{Bu}_4\text{N}]\text{PF}_6/\text{CH}_2\text{Cl}_2$.

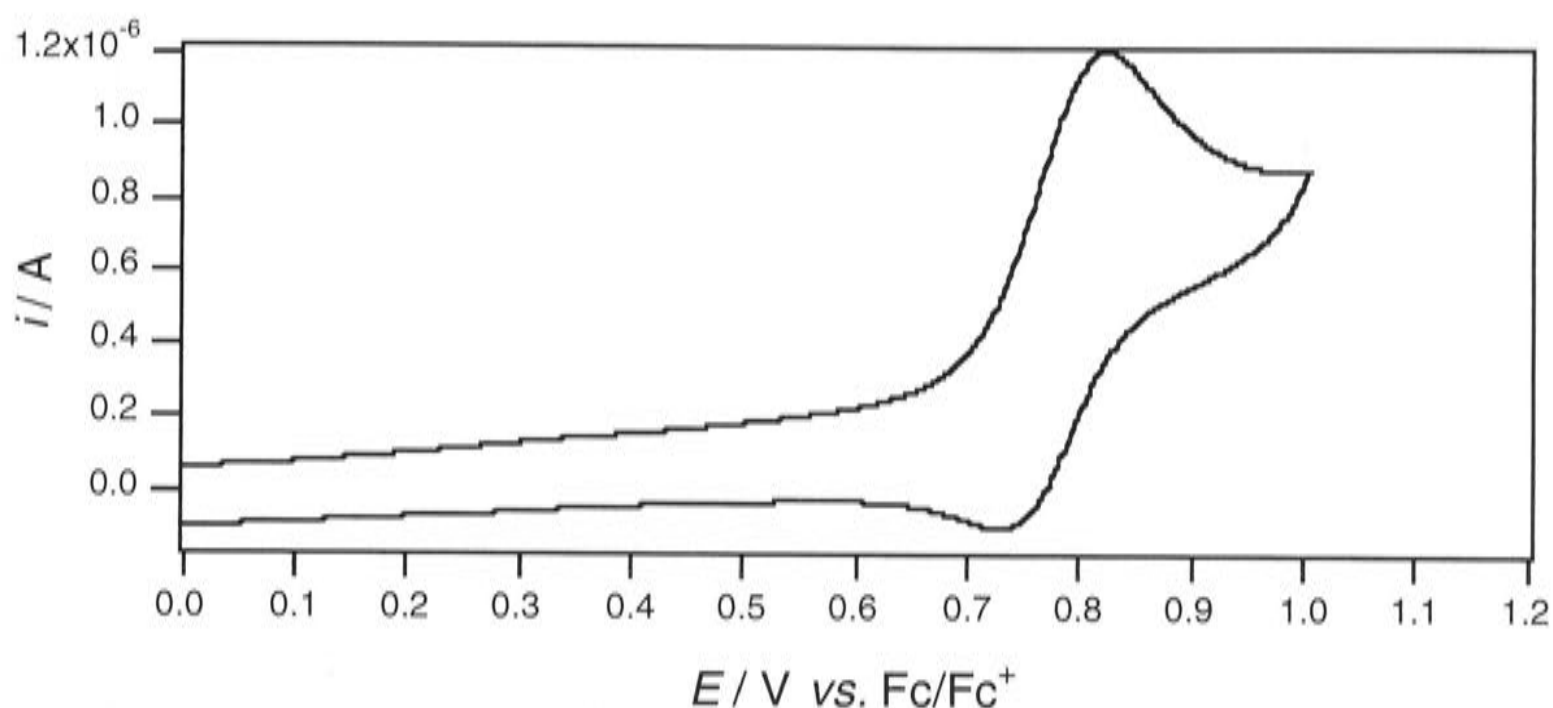


Figure 42. Cyclic voltammogram of $[\text{RuCl}_2(\eta^1:\eta^6\text{-}t\text{-Bu}_2\text{P}(\text{CH}_2)_3\text{Ph})]$ (253) recorded at a scan rate of 100 mVs^{-1} in $0.5\text{M } [\text{Bu}^n_4\text{N}]\text{PF}_6/\text{CH}_2\text{Cl}_2$ at 293K .

The tetramethylbenzene complex $[\text{RuCl}_2(1,2,4,5\text{-C}_6\text{H}_2\text{Me}_4)(\text{PMe}_3)]$ has a lower $E_{1/2}$ value ($+ 0.58 \text{ V vs Fc}^{0/1}$ in MeCN) than the mesitylene derivative $[\text{RuCl}_2(1,3,5\text{-C}_6\text{H}_3\text{Me}_3)(\text{PMe}_3)]$ ($E_{1/2} = + 0.63 \text{ V vs Fc}^{0/1}$ in MeCN).³ Replacement of the chloride ligands by σ -alkyl groups causes significant reduction in the $E_{1/2}$ value, which are $- 0.44$ and $- 0.32 \text{ V}$ (*vs Fc*^{0/1} in CH_2Cl_2) for complexes $[\text{RuMe}_2(\eta^6\text{-C}_6\text{Me}_6)(\text{PR}_3)]$ ($\text{R} = \text{Me}$ (57), Ph (5)), respectively.¹⁸ These values are significantly lower than those observed in this work for the chloride analogues, $[\text{RuCl}_2(\eta^6\text{-C}_6\text{Me}_6)(\text{PR}_3)]$ ($\text{R} = \text{Me}$ (304), Ph (306)), with $E_{1/2}$ of $+ 0.50$ and $+ 0.54 \text{ V}$ (*vs Fc*^{0/1} in CH_2Cl_2), respectively. Similarly, Nelson and Ghebreyessus¹⁹ have shown that $E_{1/2}$ decreases with increasing substitution on the η^6 -arene of the tether; complexes $[\text{RuCl}_2(\eta^1:\eta^6\text{-Ph}_2\text{P}(\text{CH}_2)_3\text{-aryl})]$ (aryl = C_6Me_5 (251), $3,5\text{-C}_6\text{H}_3\text{Me}_2$ (275), $4\text{-C}_6\text{H}_4\text{CHMe}_2$ (271), $4\text{-C}_6\text{H}_4\text{Me}$ (274) and Ph (222)) show $E_{1/2}$ values in the range $+ 0.47\text{-}0.74 \text{ V}$ (*vs Fc*^{0/1} in CH_2Cl_2).¹⁹

Where the CV of either non-tethered or tethered compounds have been studied in the literature, the $E_{1/2}$ values are generally in good agreement with those observed in this study. For example, $[\text{RuCl}_2(\eta^6\text{-C}_6\text{H}_6)(\text{PPh}_3)]$ (302) was found in this work to have $E_{1/2} = + 0.87 \text{ V}$ (*vs Fc*^{0/1} in CH_2Cl_2), compared with the reported value $+ 0.81 \text{ V}$ (*vs Fc*^{0/1} in CH_2Cl_2)²⁰, though

the behaviour was stated to be "quasi-reversible", as was reported also for $[\text{RuCl}_2(\eta^6\text{-}1,4\text{-MeC}_6\text{H}_4\text{CHMe}_2)(\text{PPh}_3)]$ (**338**).³ The reported $E_{1/2}$ values for $[\text{RuCl}_2(\eta^1:\eta^6\text{-Ph}_2\text{P}(\text{CH}_2)_3\text{C}_6\text{Me}_5)]$ (**251**) and $[\text{RuCl}_2(\eta^1:\eta^6\text{-Ph}_2\text{P}(\text{CH}_2)_3\text{Ph})]$ (**222**), + 0.47 V and + 0.74 V (*vs* $\text{Fc}^{0/1}$ in CH_2Cl_2) are in reasonable agreement with those observed in this work, + 0.55 and + 0.77 V (*vs* $\text{Fc}^{0/1}$ in CH_2Cl_2), respectively. Smith and Wright also investigated the cyclic voltammetry of **222**, $E_{1/2} = ca + 1.01$ V (*vs* $\text{Fc}^{0/1}$ in CH_2Cl_2)²¹ (the quoted electrode potential has been converted to ferrocene/ferrocenium using the conversion factor - 0.31 V for the estimated standard potential of $\text{Fc}^{0/1}$ of + 0.31 V *vs* SCE⁷), which is in poor agreement with the observations from both this work and those reported by Nelson and Ghebreyessus,¹⁹ presumably due to the errors involved with the effects of the junction potentials.¹⁷ The behaviour of **222** was reported to be "quasi-reversible",²¹ which is in contrast to the results reported here and to those reported by Nelson and Ghebreyessus.¹⁹

The derivatives $[\text{Ru}(\eta^2\text{-MeC}(\text{O})\text{CHC}(\text{O})\text{Me})(\eta^1:\eta^6\text{-R}_2\text{P}(\text{CH}_2)_3\text{Ph})]\text{PF}_6$ (R = Me (**281**), Ph (**282**)), and $[\text{Ru}(\eta^2\text{-S}_2\text{CNMe}_2)(\eta^1:\eta^6\text{-R}_2\text{P}(\text{CH}_2)_3\text{Ph})]\text{PF}_6$ (R = Me (**283**), Ph (**284**)), displayed higher electrode potentials than the parent species, and were in the range + 0.88 - 1.10 V (*vs* $\text{Fc}^{0/1}$) (see Table 32). Whilst the dithiocarbamate compounds **283** and **284** could be oxidized by CV to stable species ($i_{\text{pa}}/i_{\text{pc}} = 1$). The $i_{\text{pa}}/i_{\text{pc}}$ ratios indicate that the acac derivatives **281** and **282** were chemically very unstable and semi-stable, respectively.

In order to assess the lifetime and thermal stability of the one-electron oxidation products, spectroelectrochemistry was carried out at *ca* 228K in dichloromethane in the presence of 0.3M $[\text{Bu}''_4\text{N}]\text{BF}_4$. During spectroelectrochemical experiments, the electronic (UV/Vis) spectra were recorded every five minutes as the parent Ru(II) compound was oxidised, with an applied potential (E_{appl}) usually about 300 mV greater than the $E_{1/2}$ -value of the complex. In most cases, characteristic, reproducible changes were observed. Once oxidation was complete, the potential was switched to zero (*vs* Ag/AgCl; - 0.55 V *vs* $\text{Fc}^{0/1}$). If the redox process were

reversible, the spectrum of the starting material would be regenerated. Evidence will be presented that the one-electron oxidation of product does indeed contain arene-ruthenium(III) species.

Table 32. Electrode potentials of non-tethered, tethered complexes and derivatives of tethered complexes (*vs* $\text{Fc}^{0/1}$). All complexes show chemically stable electrochemical waves unless otherwise indicated.

Complex	$E_{1/2}$ (Volts)	ΔE_p (mVs^{-1})
$[\text{RuCl}_2(\eta^6\text{-C}_6\text{H}_6)(\text{PMe}_3)]$ (337)	+ 0.76 ^a	75
$[\text{RuCl}_2(\eta^6\text{-C}_6\text{H}_6)(\text{PPh}_3)]$ (302)	+ 0.87 ^b	75
$[\text{RuCl}_2(\eta^6\text{-1,4-MeC}_6\text{H}_4\text{CHMe}_2)(\text{PPh}_3)]$ (338)	+ 0.70 ^a	75
$[\text{RuCl}_2(\eta^6\text{-1,3,5-C}_6\text{H}_3\text{Me}_3)(\text{PPh}_3)]$ (339)	+ 0.66 ^a	85
$[\text{RuCl}_2(\eta^6\text{-C}_6\text{Me}_6)(\text{PMe}_3)]$ (304)	+ 0.50 ^a	90
$[\text{RuCl}_2(\eta^6\text{-C}_6\text{Me}_6)(\text{PPh}_3)]$ (306)	+ 0.54 ^a	75
$[\text{RuCl}_2(\eta^1:\eta^6\text{-Me}_2\text{P}\sim\text{Ph})]$ (248)	+ 0.71 ^a	70
$[\text{RuCl}_2(\eta^1:\eta^6\text{-Ph}_2\text{P}\sim\text{Ph})]$ (222)	+ 0.77 ^a	60
$[\text{RuCl}_2(\eta^1:\eta^6\text{-}i\text{-Pr}_2\text{P}\sim\text{Ph})]$ (249)	+ 0.78 ^a	75
$[\text{RuCl}_2(\eta^1:\eta^6\text{-Cy}_2\text{P}\sim\text{Ph})]$ (225)	+ 0.76 ^a	75
$[\text{RuCl}_2(\eta^1:\eta^6\text{-}t\text{-Bu}_2\text{P}\sim\text{Ph})]$ (253)	+ 0.82 ^{a,t}	75
$[\text{RuCl}_2(\eta^1:\eta^6\text{-Ph}_2\text{P}\sim\text{-2,4,6-C}_6\text{H}_2\text{Me}_3)]$ (250)	+ 0.65 ^b	80
$[\text{RuCl}_2(\eta^1:\eta^6\text{-Ph}_2\text{P}\sim\text{C}_6\text{Me}_5)]$ (251)	+ 0.55 ^b	80
$[\text{RuCl}_2(\eta^1:\eta^6\text{-Ph}_2\text{PCH}_2\text{SiMe}_2\text{Ph})]$ (252)	+ 0.79 ^a	60

Complex	$E_{1/2}$ (Volts)	ΔE_p (mVs ⁻¹)
[Ru(η^2 -MeC(O)CHC(O)Me)(η^1 : η^6 -Ph ₂ P(CH ₂) ₃ Ph)]PF ₆ (281)	+ 1.10 ^{a,‡}	-
[Ru(η^2 -MeC(O)CHC(O)Me)(η^1 : η^6 -Ph ₂ P(CH ₂) ₃ Ph)]PF ₆ (282)	+ 1.10 ^a	100
[Ru(η^2 -S ₂ CNMe ₂)(η^1 : η^6 -Me ₂ P(CH ₂) ₃ Ph)]PF ₆ (283)	+ 0.88 ^a	80
[Ru(η^2 -S ₂ CNMe ₂)(η^1 : η^6 -Ph ₂ P(CH ₂) ₃ Ph)]PF ₆ (284)	+ 0.94 ^a	70

^aExperiments were recorded at a scan rate of 100 mVs⁻¹ in 0.5M [Buⁿ₄N]PF₆/CH₂Cl₂ solution at 293K. ^bExperiments were recorded at a scan rate of 100 mVs⁻¹ in 0.2M [Buⁿ₄N]PF₆/CH₂Cl₂ solution at 253K. [†]Semi-stable; [‡]chemically unstable (E_{pa} only).

~ = (CH₂)₃

Table 33. Electrode potentials of various reported non-tethered and tethered arene-ruthenium complexes. The oxidised species were chemically stable on the voltammetric timescale, with the data recorded in dichloromethane and quoted *vs* Fc^{0/1}, unless indicated otherwise.

Complex	Electrode Potential, $E_{1/2}$ (Volts)	Conversion Factor (Volts)	Reference
[RuCl ₂ (η^6 -C ₆ H ₆)(PPh ₃)] (302)	+ 0.81	- 0.55 ^a	20
[RuCl ₂ (η^6 -1,4-MeC ₆ H ₄ CHMe ₂)(PPh ₃)] (338)	+ 0.78 ^{b,c}	- 0.31 ^d	3
[RuCl ₂ (η^6 -1,3,5-C ₆ H ₃ Me ₃)(PMe ₃)]	+ 0.63 ^{b,c}	- 0.31 ^d	3

Complex	Electrode Potential, $E_{1/2}$ (Volts)	Conversion Factor (Volts)	Reference
[RuCl ₂ (η ⁶ -1,2,4,5-C ₆ H ₂ Me ₄)(PPh ₃)]	+ 0.71 ^{b,c}	- 0.31 ^d	3
[RuMe ₂ (η ⁶ -C ₆ Me ₆)(PMe ₃)] (57)	- 0.44	- 0.31 ^d	18
[RuMe ₂ (η ⁶ -C ₆ Me ₆)(PPh ₃)] (5)	- 0.32	- 0.31 ^d	18
[RuCl ₂ (η ¹ :η ⁶ -Ph ₂ P~Ph)] (222)	+ 1.01 ^b	- 0.31 ^d	21
[RuCl ₂ (η ¹ :η ⁶ -Ph ₂ P~Ph)] (222)	+ 0.74	-	19
[RuCl ₂ (η ¹ :η ⁶ -Ph ₂ P~-4-C ₆ H ₄ Me)] (274)	+ 0.67	-	19
[RuCl ₂ (η ¹ :η ⁶ -Ph ₂ P~-4-C ₆ H ₄ CHMe ₂)] (271)	+ 0.66	-	19
[RuCl ₂ (η ¹ :η ⁶ -Ph ₂ P~-3,5-C ₆ H ₃ Me ₂)] (275)	+ 0.61	-	19
[RuCl ₂ (η ¹ :η ⁶ -Ph ₂ P~C ₆ Me ₅)] (251)	+ 0.47	-	19
[Ru(η ¹ :η ⁶ -SC ₆ H ₃ -2-Ph-6-C ₆ H ₅)-(2,6-Ph ₂ C ₆ H ₃ S)(PPh ₃)] (116)	+ 0.53 ^e	-	22

^aFc^{0/1} was measured as + 0.55 V (*vs* Ag/AgCl in CH₂Cl₂) in reference(20); ^boxidised species was semi-stable; ^cin acetonitrile; ^destimated standard potential of Fc^{0/1} of + 0.31 V *vs* SCE (in MeCN) in reference(7); ^eelectrode potential *vs* Ag wire as a pseudo reference electrode; ~ = (CH₂)₃.

The UV/Vis spectra of a variety of non-tethered species $[\text{RuCl}_2(\eta^6\text{-C}_6\text{R}_6)(\text{PMe}_3)]$ ($\text{R} = \text{H}$ (337), Me (302)), $[\text{RuCl}_2(\eta^6\text{-C}_6\text{R}_6)(\text{PPh}_3)]$ ($\text{R} = \text{H}$ (304), Me (306)) and the tethered complexes $[\text{RuCl}_2(\eta^1:\eta^6\text{-R}_2\text{P}(\text{CH}_2)_3\text{Ph})]$ ($\text{R} = \text{Me}$ (248), Ph (222), *i*-Pr (249), Cy (225), *t*-Bu (253), $[\text{RuCl}_2(\eta^1:\eta^6\text{-Ph}_2\text{P}(\text{CH}_2)_3\text{-2,4,6-C}_6\text{H}_2\text{Me}_3)]$ (250), $[\text{RuCl}_2(\eta^1:\eta^6\text{-Ph}_2\text{P}(\text{CH}_2)_3\text{C}_6\text{Me}_5)]$ (251) and $[\text{RuCl}_2(\eta^1:\eta^6\text{-Ph}_2\text{PCH}_2\text{SiMe}_2\text{Ph})]$ (252) show similar absorptions, which undergo characteristic changes on formation of the corresponding one-electron oxidation products. The band maxima and molar absorptivities are summarised in Table 34. The differences between the spectra characteristic of the two oxidation states are not as great as those observed in complexes of the type $[\text{Ru}(\text{acac})_2(\text{LL}')]$ ($\text{LL}' = \text{heterobidentate ligand}$)^{23,24} and $[\text{Ru}(\text{acac})_2(\eta^2\text{-C}_2\text{H}_4)(\text{L})]$ ($\text{L} = \eta^2\text{-C}_2\text{H}_4, \text{SbPh}_3, \text{NH}_3$).²⁵ It was not possible to assign the bands due to particular transitions, although the bands are presumed to arise from charge transfer within the Ru-arene, Ru-P and Ru-Cl moieties, in addition to the ligands themselves; in the case of Ru(III), ligand-to-metal charge transfer bands also would be expected.²⁶ Isosbestic points were observed in some cases, indicating that only two species were present at equal concentrations.²⁷ However, this will only occur when the two species have absorption bands that overlap,²⁷ which is not the case for most of the arene-ruthenium complexes considered in this study. Thus, even though isosbestic points, or near to isosbestic points, are not observed in all cases, it is assumed that only two species, *i.e.* Ru(II) and Ru(III), were present during either the oxidation or reduction steps.

I shall now discuss the results of the experiments for a series of non-tethered and tethered complexes. The behaviour is best understood for the complex $[\text{RuCl}_2(\eta^1:\eta^6\text{-Ph}_2\text{P}(\text{CH}_2)_3\text{C}_6\text{Me}_5)]$ (251), which will therefore be discussed in most detail. The electronic (UV/Vis) spectrum of 251 exhibits a broad band at 27400 cm^{-1} ($\epsilon = 4300 \text{ L mol}^{-1} \text{ cm}^{-1}$). Applying a potential of $+0.65 \text{ V}$ (*vs* $\text{Fc}^{0/1}$) to the solution at *ca* 228K caused the gradual

loss of this band and the formation of new bands at 29100 cm^{-1} ($\epsilon = 5100\text{ L mol}^{-1}\text{ cm}^{-1}$), 24600 cm^{-1} ($\epsilon = 4500\text{ L mol}^{-1}\text{ cm}^{-1}$) and 19500 cm^{-1} ($\epsilon = 2200\text{ L mol}^{-1}\text{ cm}^{-1}$) (Figure 43). When the exhaustive oxidation was complete, the original Ru(II) spectrum was regenerated after applying a potential of -0.55 V (*vs* $\text{Fc}^{0/1}$). It is reasonable to assume that the product responsible for the new spectrum contains Ru(III), since a one-electron oxidation occurred in the cyclic voltammetry of **251** at *ca* 300 mV below the E_{appl} . During both oxidation and reduction, two close to isosbestic points were observed at *ca* 27500 and 26800 cm^{-1} . The Ru(III) species was regenerated and allowed to warm slowly to room temperature; the electronic (UV/Vis) spectra are shown in Figure 44. No change in the spectrum was observed until a temperature of 263K was reached. Even though there was some distortion, at 263K and 283K (green and red spectra, respectively), the absorption maxima were still closer to that of the Ru(III) compound than of its Ru(II) precursor. Over a period of about one hour at 283K , however, the UV//Vis spectra reverted towards those of the Ru(II) compound **251**, although some arene-Ru(III) species $[\mathbf{251}]^+$, was still present.

The ESR spectrum of the anodic oxidation product of **251** as a frozen glass in CH_2Cl_2 at 5K showed three individual g -values; $g_1 = 2.32$, $g_2 = 2.19$, $g_3 = 2.00$ (Figure 45). The sample was removed from the spectrometer, and the ESR spectrum was recorded after it had been maintained at ambient temperature for *ca* 30 min . When the solution was again cooled to 5K , the same ESR signal was still observed, although the intensity had decreased, as shown in Figure 46. It does, however, confirm that some of the cation $[\mathbf{251}]^+$ is still present. The ESR spectrum of $[\mathbf{251}]^+$ is similar to that of the pseudo octahedral complexes *mer*- $[\text{RuCl}_3(\text{PBU}''_2\text{Ph})_3]^{28}$ and the presumed $[\text{Ru}(\text{Me})(\text{Ph})(\eta^6\text{-C}_6\text{Me}_6)(\text{PMePh}_2)]^+$ ($[\mathbf{6}]^+$),¹⁸ shown in Figures 2 and 4 (see Chapter 1, pages 10 and 28, respectively).

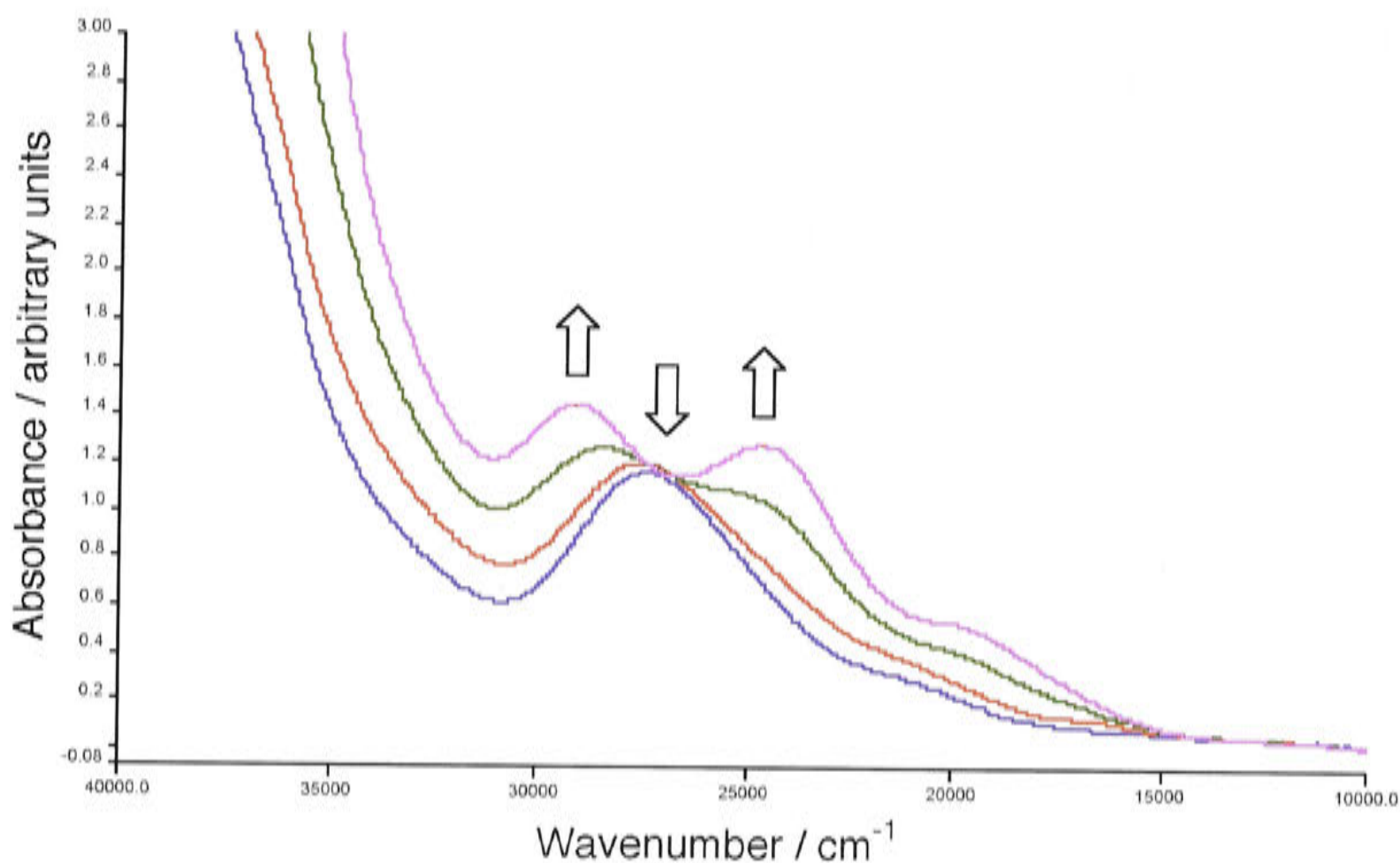


Figure 43. Electronic spectra recorded during one-electron oxidation of $[\text{RuCl}_2(\eta^1:\eta^6\text{-Ph}_2\text{P}(\text{CH}_2)_3\text{C}_6\text{Me}_5)]$ (**251**) in 0.3M $[\text{Bu}^n_4\text{N}]\text{BF}_4/\text{CH}_2\text{Cl}_2$ at *ca* 228K [$E_{\text{appl}} = +0.65$ V *vs* $\text{Fc}^{0/1}$].

Thus the electrochemical one-electron oxidation of complex $[\text{RuCl}_2(\eta^1:\eta^6\text{-Ph}_2\text{P}(\text{CH}_2)_3\text{C}_6\text{Me}_5)]$ (**251**) was shown to be fully chemically stable by cyclic voltammetry and spectroelectrochemistry. Further, the spectroelectrochemical and ESR spectra show that the electrogenerated Ru(III) species was stable, for *ca* one hour, under ambient conditions. This evidence strongly suggests that the electrogenerated species is indeed the arene-ruthenium(III) complex $[\text{RuCl}_2(\eta^1:\eta^6\text{-Ph}_2\text{P}(\text{CH}_2)_3\text{C}_6\text{Me}_5)]^+$ (**[251]⁺**).

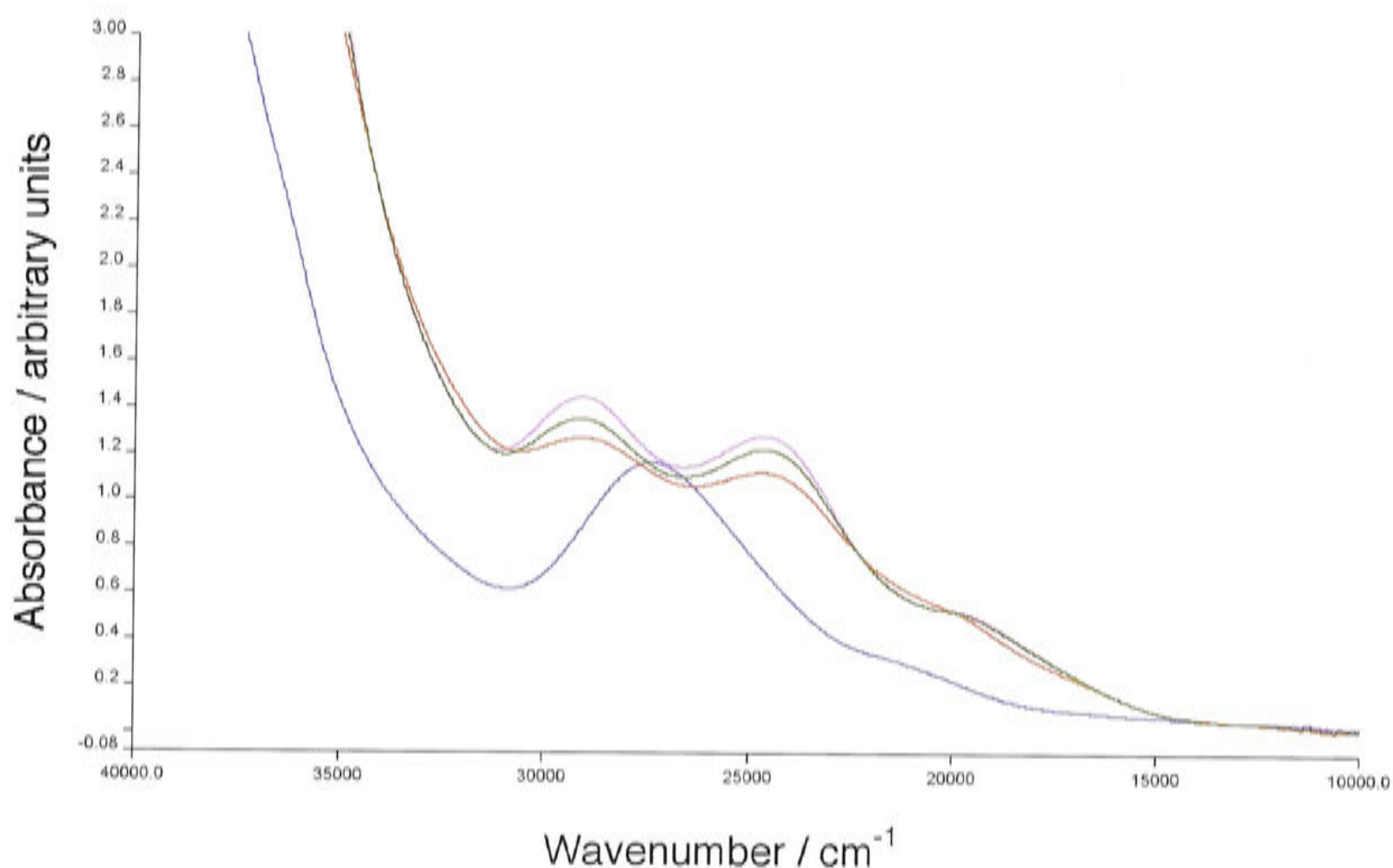


Figure 44. Electronic spectra recorded during one-electron oxidation of $[\text{RuCl}_2(\eta^1:\eta^6\text{-Ph}_2\text{P}(\text{CH}_2)_3\text{C}_6\text{Me}_5)]$ (**251**) in 0.3M $[\text{Bu}^n_4\text{N}]\text{BF}_4/\text{CH}_2\text{Cl}_2$ at *ca* 228K [$E_{\text{appl}} = + 0.65 \text{ V vs Fe}^{0/1}$]. The blue line represents the spectrum of the parent Ru(II) complex, and the pink line represents that of the electrogenerated Ru(III) cation, both at *ca* 228K. The green line represents that at *ca* 263K and the red line that at approx. 283K.

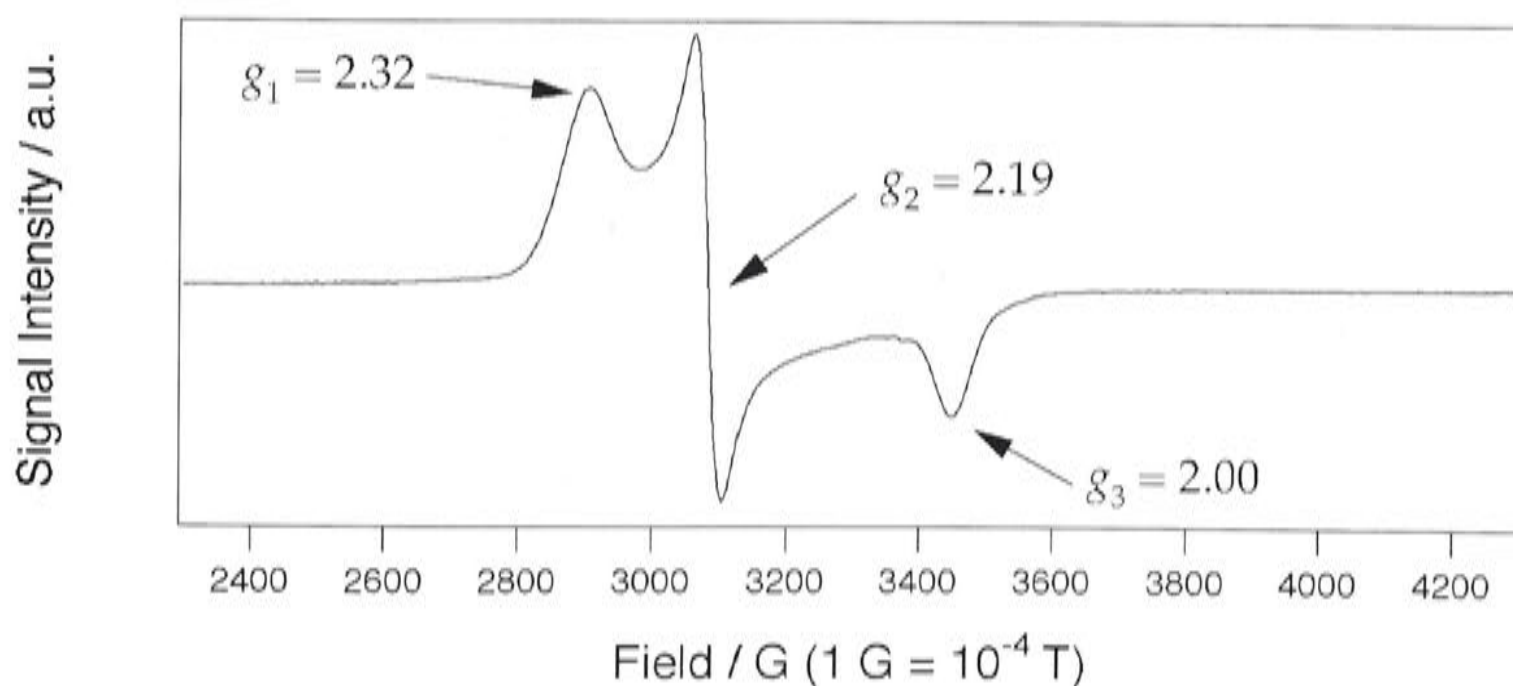


Figure 45. The ESR spectrum at *ca* 5K of the species prepared from the anodic oxidation of $[\text{RuCl}_2(\eta^1:\eta^6\text{-Ph}_2\text{P}(\text{CH}_2)_3\text{C}_6\text{Me}_5)]$ (**251**) in 0.4M $[\text{Bu}^n_4\text{N}]\text{PF}_6/\text{CH}_2\text{Cl}_2$ at *ca* 228K [$E_{\text{appl}} = + 0.65 \text{ V vs Fe}^{0/1}$].

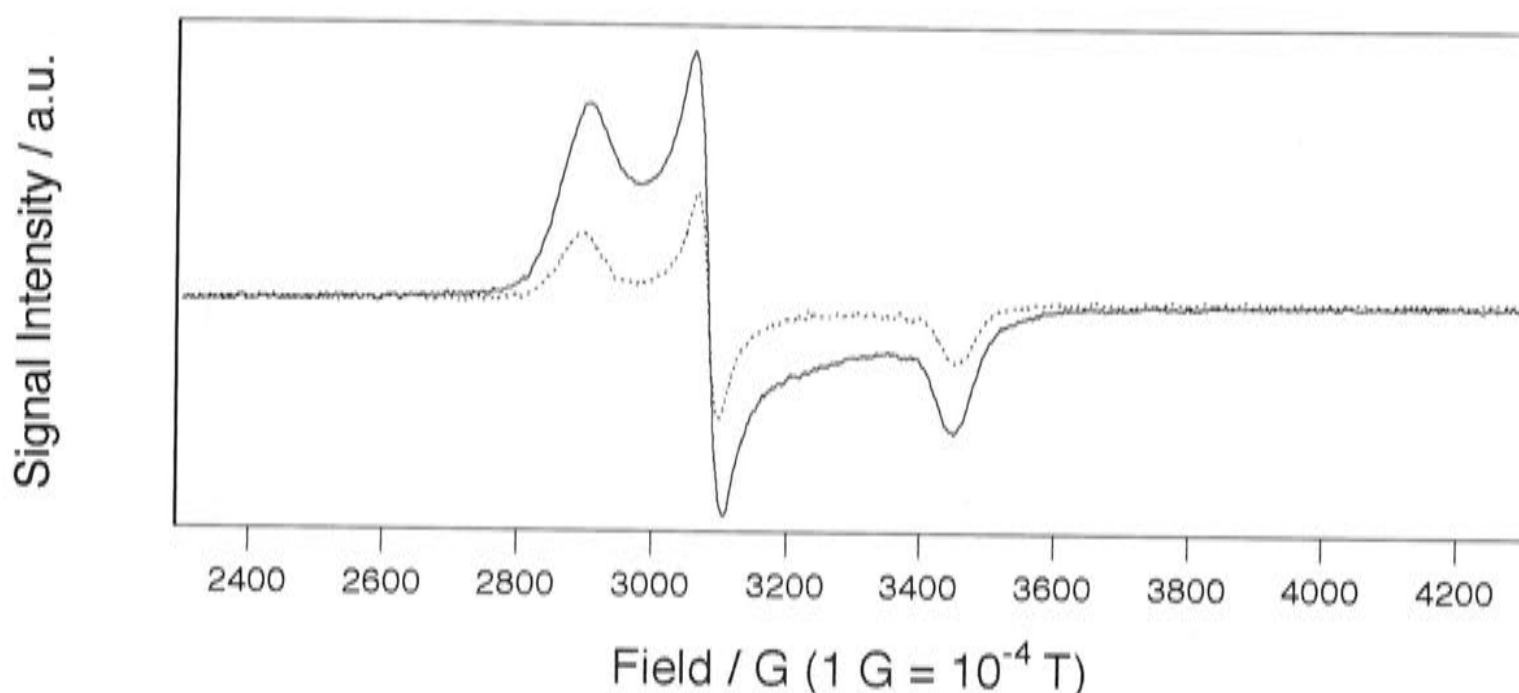


Figure 46. The ESR spectrum, (solid line) at *ca* 5K of the species prepared from the anodic oxidation of $[\text{RuCl}_2(\eta^1:\eta^6\text{-Ph}_2\text{P}(\text{CH}_2)_3\text{C}_6\text{Me}_5)]$ (**251**) in 0.4M $[\text{Bu}^n_4\text{N}]\text{PF}_6/\text{CH}_2\text{Cl}_2$ at *ca* 228K [$E_{\text{appl}} = +0.65$ V (*vs* $\text{Fc}^{0/1}$)]. The dotted line shows the ESR spectrum after the sample had been maintained at ambient temperature for *ca* 30 min.

The general behaviour and features of the UV/Vis spectra of the tethered compounds $[\text{RuCl}_2(\eta^1:\eta^6\text{-Ph}_2\text{P}(\text{CH}_2)_3\text{-3,5-C}_6\text{H}_3\text{Me}_2)]$ (**275**)¹⁹ and $[\text{RuCl}_2(\eta^1:\eta^6\text{-Ph}_2\text{P}(\text{CH}_2)_3\text{-2,4,6-C}_6\text{H}_2\text{Me}_3)]$ (**250**) at *ca* 228K were very similar to those of $[\text{RuCl}_2(\eta^1:\eta^6\text{-Ph}_2\text{P}(\text{CH}_2)_3\text{C}_6\text{Me}_5)]$ (**251**), which suggests that similar processes were occurring. In these cases, isosbestic points were observed at *ca* 27200 and 27800 cm^{-1} for **275**, and at *ca* 26400 and 27500 cm^{-1} for **250**. When the electrogenerated arene-Ru(III) species were allowed to warm slowly to room temperature, the spectra reverted towards those of the parent Ru(II) compounds, although some arene-Ru(III) species were still present. Clearly, the arene-Ru(III) cations containing alkyl substituents on the η^6 -arene exhibit some thermal stability. Due to the low yielding syntheses of both **275** and **250** (see Chapter 3), there was not enough sample isolated to record the ESR spectra.

The spectroelectrochemical behaviour of $[\text{RuCl}_2(\eta^1:\eta^6\text{-}i\text{-Pr}_2\text{P}(\text{CH}_2)_3\text{Ph})]$ (**249**) is very similar to that of the complexes $[\text{RuCl}_2(\eta^1:\eta^6\text{-Ph}_2\text{P}(\text{CH}_2)_3\text{-aryl})]$ (aryl = C_6Me_5 (**251**), 2,4,6- $\text{C}_6\text{H}_2\text{Me}_3$ (**250**) and 3,5- $\text{C}_6\text{H}_3\text{Me}_2$ (**275**)) described above. The electronic (UV/Vis) spectrum of **249** exhibits a broad band at

28700 cm^{-1} ($\epsilon = 2500 \text{ L mol}^{-1} \text{ cm}^{-1}$). Applying a potential of + 0.79 V (*vs* $\text{Fc}^{0/1}$) to the solution at *ca* 228K caused the gradual loss of this band and the formation of new bands at 34400 cm^{-1} ($\epsilon = 3900 \text{ L mol}^{-1} \text{ cm}^{-1}$) and 28000 cm^{-1} ($\epsilon = 3100 \text{ L mol}^{-1} \text{ cm}^{-1}$) (Figure 47). The original Ru(II) spectrum was regenerated by applying a potential of - 0.55 V (*vs* $\text{Fc}^{0/1}$) after the exhaustive oxidation was complete. During both oxidation and reduction, an isosbestic point (35000 cm^{-1}), and two close to isosbestic points at *ca* 31400 and 30700 cm^{-1} were observed. Thus, the one-electron oxidation of **249** results in the formation of a Ru(III) species at low temperatures. The UV/Vis spectra of the Ru(III) species, when warmed slowly to room temperature, over approximately one hour, showed virtually no change in the absorption maxima until *ca* 268K (see Figure 48), where the spectrum lay between those indicative of each oxidation state. At 283K, however, the spectrum was virtually identical to that of the parent Ru(II) complex **249**, with some loss of definition. Thus, in this case also, the Ru(III) species does not decompose by irreversible loss of η^6 -arene.

The ESR spectrum of a dichloromethane solution of $[\text{RuCl}_2(\eta^1:\eta^6\text{-}i\text{-Pr}_2\text{P}(\text{CH}_2)_3\text{Ph})]$ (**249**) that had been electro-oxidised in an ESR cavity at *ca* 228K showed one very broad signal at $g = 2.16$ (Figure 49). When a similar electrogenerated solution was transferred to an ESR tube and cooled to *ca* 5K, the frozen glass showed three distinct g -values ($g_1 = 2.30$, $g_2 = 2.22$, $g_3 = 1.93$) (see Figure 50), very similar to those observed for $[\text{RuCl}_2(\eta^1:\eta^6\text{-Ph}_2\text{P}(\text{CH}_2)_3\text{C}_6\text{Me}_5)]$ (**251**). The ESR signal had disappeared when the sample was maintained at ambient temperature for approximately 30 min, showing that the one-electron oxidation product had not survived at room temperature.

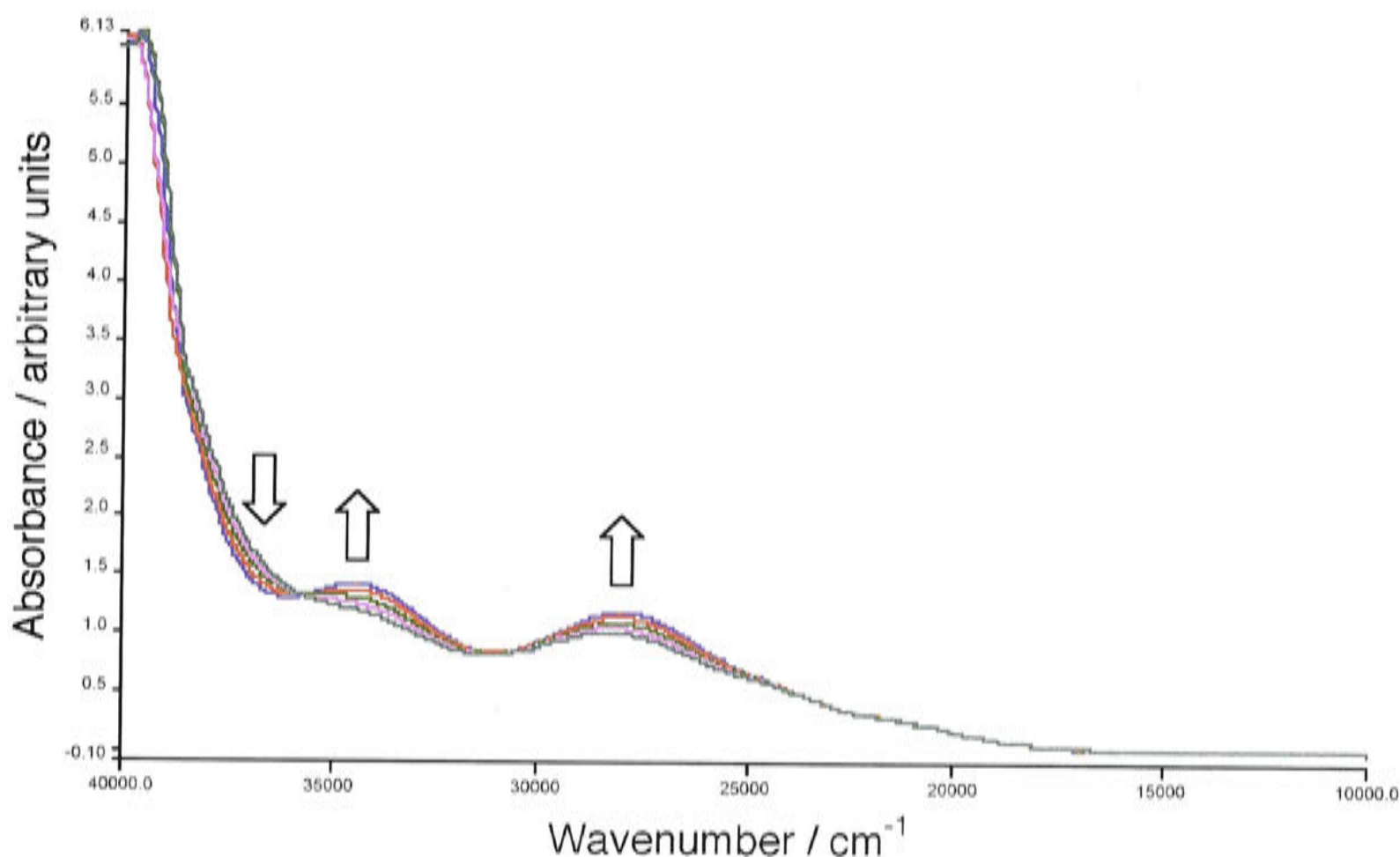


Figure 47. Electronic spectra recorded during one-electron oxidation of $[\text{RuCl}_2(\eta^1:\eta^6\text{-}i\text{-Pr}_2\text{P}(\text{CH}_2)_3\text{Ph})]$ (**249**) in 0.3M $[\text{Bu}^n_4\text{N}]\text{BF}_4/\text{CH}_2\text{Cl}_2$ at *ca* 228K [$E_{\text{appl}} = + 0.79 \text{ V}$ (*vs* $\text{Fc}^{0/1}$)].

The two ESR spectra obtained under the conditions described differ because in solution one relies on diffusion rates to ensure complete oxidation of the Ru(II) complex. Transition metal complexes usually have short spin-lattice relaxation times, which, by the Uncertainty Principle, give rise to wide resonance lines.²⁹ Relaxation times generally increase with decreasing temperature, and ESR spectra of T. M. complexes cannot normally be observed at room temperature.³⁰ The samples therefore need to be cooled to liquid nitrogen temperature, and in the case of low spin d^5 metal ions, liquid helium temperature (*ca* 5K),³¹ in order to observe well resolved ESR spectra.^{29,30} In general, the best frozen solution results are obtained when the solvent freezes to form a glass.³² Further, it must form a uniform glass, otherwise paramagnetic aggregates form, which cause the resonance to broaden.³³ Removal of oxygen is also essential to prevent broadening of the spectrum.

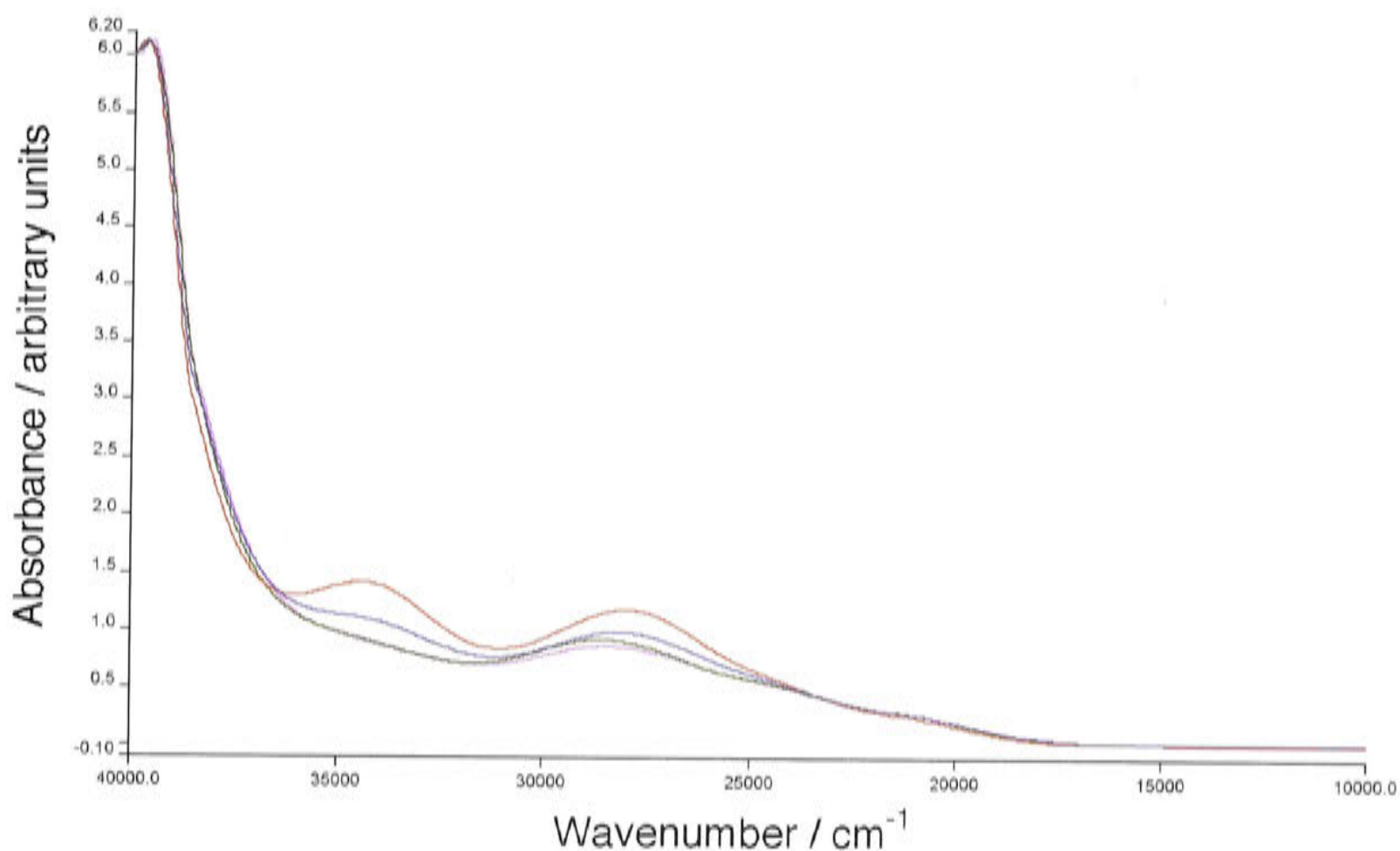


Figure 48. Electronic spectra recorded during one-electron oxidation of $[\text{RuCl}_2(\eta^1:\eta^6\text{-}i\text{-Pr}_2\text{P}(\text{CH}_2)_3\text{Ph})]$ (**249**) in 0.3M $[\text{Bu}^n_4\text{N}]\text{BF}_4/\text{CH}_2\text{Cl}_2$ at *ca* 228K [$E_{\text{appl}} = + 0.79$ V (*vs* $\text{Fc}^{0/1}$)]. The pink line represents the spectrum of the parent Ru(II) complex, and the red line represents that of the electrogenerated Ru(III) cation, both at *ca* 228K. The blue line represents that at *ca* 268K and the green line that at approx. 283K.

The tethered complexes $[\text{RuCl}_2(\eta^1:\eta^6\text{-R}_2\text{P}(\text{CH}_2)_3\text{Ph})]$ (R = Cy (**225**), *t*-Bu (**253**)) displayed similar spectroelectrochemical behaviour at *ca* 228K to **249**, although in these cases no isosbestic points were observed during the oxidation and reduction processes. The Ru(III) species reverted to the parent Ru(II) complexes when they were allowed to warm slowly to room temperature, with some loss of definition in the electronic (UV/Vis) spectra.

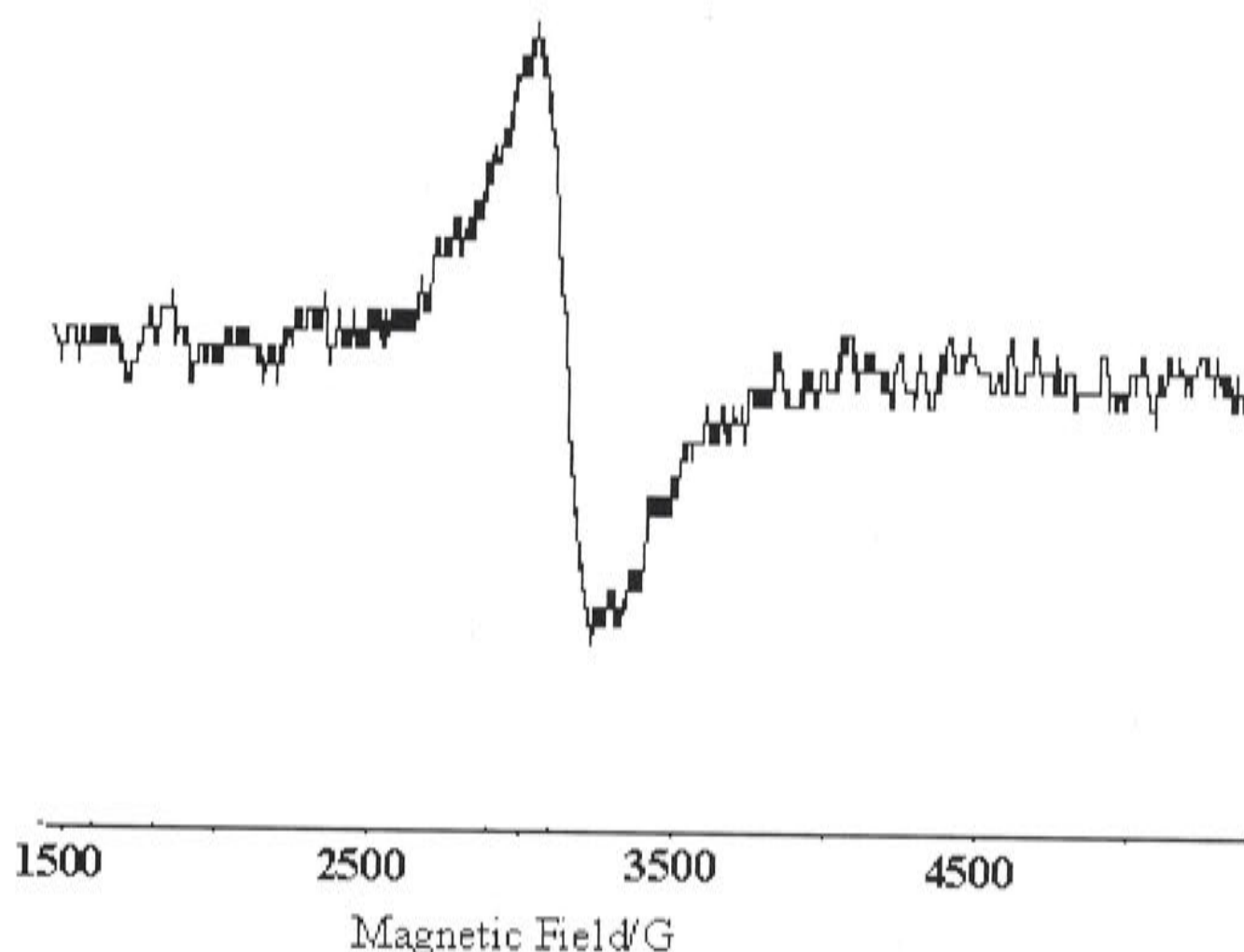


Figure 49. The ESR spectrum at *ca* 228K of the species prepared from the anodic oxidation of $[\text{RuCl}_2(\eta^1:\eta^6\text{-}i\text{-Pr}_2\text{P}(\text{CH}_2)_3\text{Ph})]$ (**249**) in 0.3M $[\text{Bu}^n_4\text{N}]\text{PF}_6/\text{CH}_2\text{Cl}_2$ at *ca* 228K [$E_{\text{appl}} = +0.88$ V (*vs* $\text{Fc}^{0/1}$)].

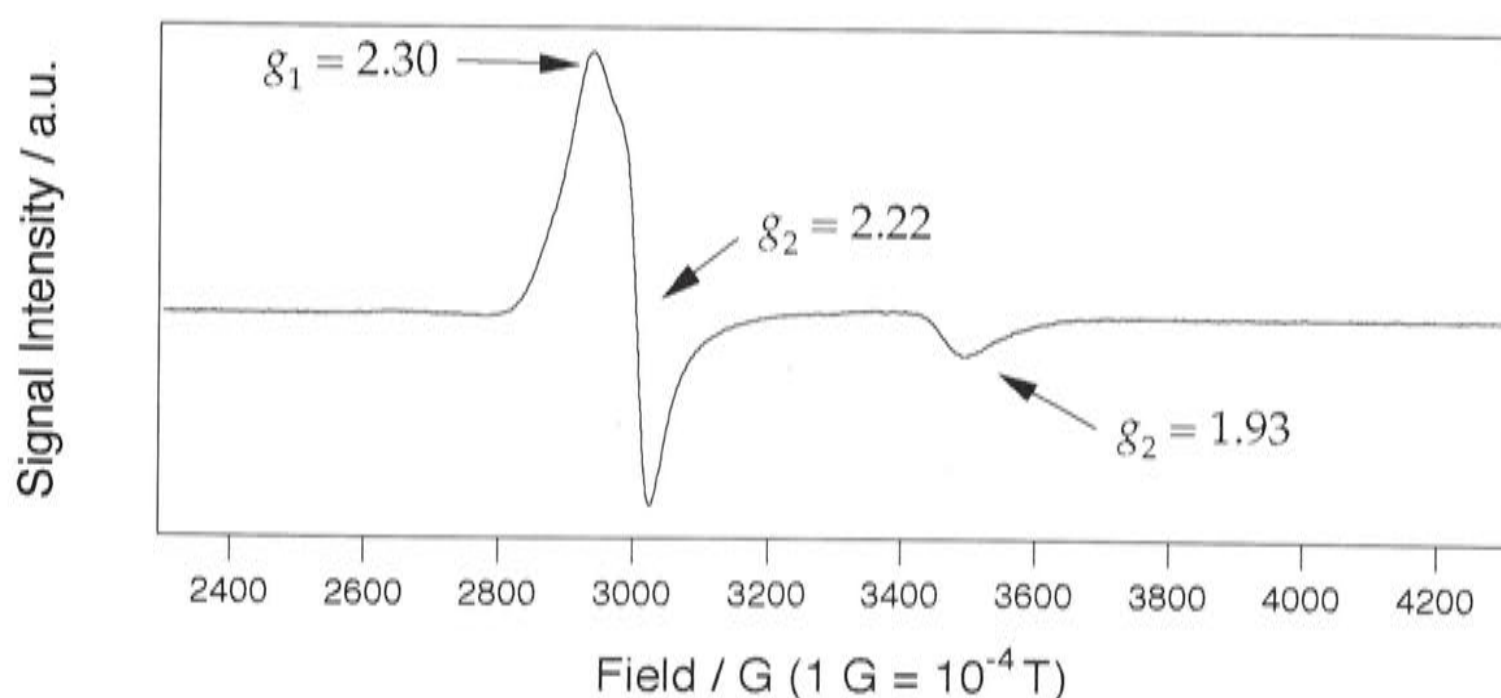


Figure 50. The ESR spectrum at *ca* 5K of the species prepared from the anodic oxidation of $[\text{RuCl}_2(\eta^1:\eta^6\text{-}i\text{-Pr}_2\text{P}(\text{CH}_2)_3\text{Ph})]$ (**249**) in 0.4M $[\text{Bu}^n_4\text{N}]\text{PF}_6/\text{CH}_2\text{Cl}_2$ at *ca* 228K [$E_{\text{appl}} = +0.88$ V (*vs* $\text{Fc}^{0/1}$)].

In the cases discussed so far, the electronic spectra of the electrogenerated tethered arene-ruthenium(III) compounds showed considerable thermal stability, but in other cases, complications arose due to decomposition,

presumably *via* loss of η^6 -arene. Whilst complexes $[\text{RuCl}_2(\eta^1:\eta^6\text{-Me}_2\text{P}(\text{CH}_2)_3\text{Ph})]$ (**248**) and $[\text{RuCl}_2(\eta^1:\eta^6\text{-Ph}_2\text{PCH}_2\text{SiMe}_2\text{Ph})]$ (**252**) showed fully reversible spectroelectrochemical properties at *ca* 228K, the electrogenerated-Ru(III) species decomposed at temperatures above *ca* 273 and 263K, respectively, presumably *via* loss of the η^6 -arene, when the solutions were allowed to warm to room temperature. The UV/Vis spectra at temperatures above *ca* 263K showed the presence of new maxima in the region *ca* 37000 to 17000 cm^{-1} . The species responsible for these bands were not characterised, but presumably arise from replacement of the η^6 -arene by solvent molecules or other potential ligands.

In contrast to the previous cases, the spectroelectrochemical behaviour of the chelate compound $[\text{RuCl}_2(\eta^1:\eta^6\text{-Ph}_2\text{P}(\text{CH}_2)_3\text{Ph})]$ (**222**) was not reversible, even at *ca* 228K. Although two close to isosbestic points were observed in the region 28000 to 27000 cm^{-1} on electrochemical oxidation, the resulting arene-ruthenium(III) species could not be reduced back to the parent Ru(II) complex **222**, despite the application of a potential as high as -1.03 V (*vs* $\text{Fc}^{0/1}$). Instead, a new Ru(II) species formed, which was slowly allowed to warm to room temperature. The presence of a new species was confirmed by the observation of bands in the region 38000 to 25000 cm^{-1} , whose absorptions were different, but the maxima were identical, to those of the original Ru(II) complex **222**. The new Ru(II) complex was not characterised.

The spectroelectrochemical behaviour of the non-tethered complexes $[\text{RuCl}_2(\eta^6\text{-C}_6\text{R}_6)(\text{PR}'_3)]$ ($\text{R} = \text{H}$, $\text{R}' = \text{Me}$ (**337**); $\text{R}' = \text{Ph}$ (**302**), $\text{R} = \text{R}' = \text{Me}$ (**304**), $\text{R}' = \text{Ph}$ (**306**)) was generally similar to that of the tethered complexes, but the one-electron oxidation products were much less stable. The behaviour of the non-tethered complexes was influenced by the nature of the tertiary phosphine; complexes containing triphenylphosphine

displayed reversible behaviour, whereas those incorporating trimethylphosphine did not.

The electronic (UV/Vis) spectrum of $[\text{RuCl}_2(\eta^6\text{-C}_6\text{Me}_6)(\text{PPh}_3)]$ (306) exhibits a broad band at 26700 cm^{-1} ($\epsilon = 1700\text{ L mol}^{-1}\text{ cm}^{-1}$). Applying a potential of $+0.86\text{ V}$ (*vs* $\text{Fc}^{0/1}$) to the solution at *ca* 228K caused gradual loss of this band and the formation of new bands at 29500 cm^{-1} ($\epsilon = 2500\text{ L mol}^{-1}\text{ cm}^{-1}$), 23400 cm^{-1} ($\epsilon = 2400\text{ L mol}^{-1}\text{ cm}^{-1}$) and 19600 cm^{-1} ($\epsilon = 1300\text{ L mol}^{-1}\text{ cm}^{-1}$), (Figure 51). The original Ru(II) spectrum was regenerated by applying a potential of -0.55 V (*vs* $\text{Fc}^{0/1}$). During both oxidation and reduction, two close to isosbestic points were observed at *ca* 26800 and 26300 cm^{-1} . When the arene-Ru(III) species was allowed to warm slowly to room temperature, over approximately one hour, the band maxima in the electronic (UV/Vis) spectra did not change significantly, but there was an increase in the absorption maxima from *ca* 273K (see Figure 52). The nature of the new species is not known, though it is assumed that the Ru(III) species decomposed *via* loss of the η^6 -arene. This behaviour is in contrast to that of the analogous tethered complex $[\text{RuCl}_2(\eta^1:\eta^6\text{-Ph}_2\text{P}(\text{CH}_2)_3\text{C}_6\text{Me}_5)]$ (251) (see pp. 230-232).

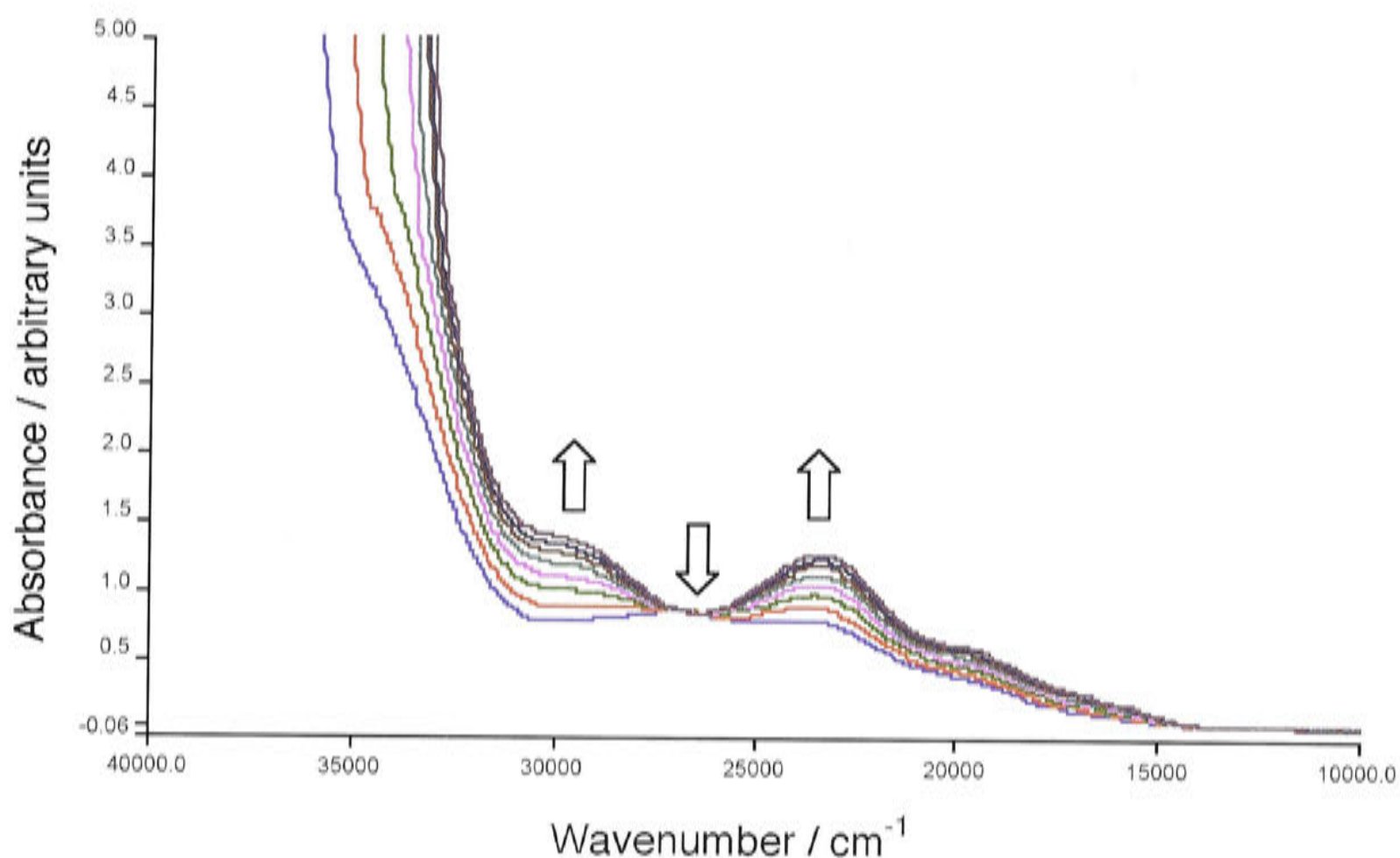


Figure 51. Electronic spectra recorded during one-electron oxidation of $[\text{RuCl}_2(\eta^6\text{-C}_6\text{Me}_6)(\text{PPh}_3)]$ (**306**) in 0.3M $[\text{Bu}^n_4\text{N}]\text{BF}_4/\text{CH}_2\text{Cl}_2$ at *ca* 228K [$E_{\text{appl}} = +0.86$ V (*vs* $\text{Fc}^{0/1}$)].

The ESR spectrum of the anodic oxidation product of $[\text{RuCl}_2(\eta^6\text{-C}_6\text{Me}_6)(\text{PPh}_3)]$ (**306**) as a frozen glass at 5K in CH_2Cl_2 showed three individual g values ($g_1 = 2.37$, $g_2 = 2.15$, $g_3 = 1.94$) (Figure 53), very similar to those observed for both $[\text{RuCl}_2(\eta^1:\eta^6\text{-Ph}_2\text{P}(\text{CH}_2)_3\text{C}_6\text{Me}_5)]^+$ (**[251]**⁺) and $[\text{RuCl}_2(\eta^1:\eta^6\text{-}i\text{-Pr}_2\text{P}(\text{CH}_2)_3\text{Ph})]^+$ (**[249]**⁺). However, this ESR signal did not survive at room temperature.

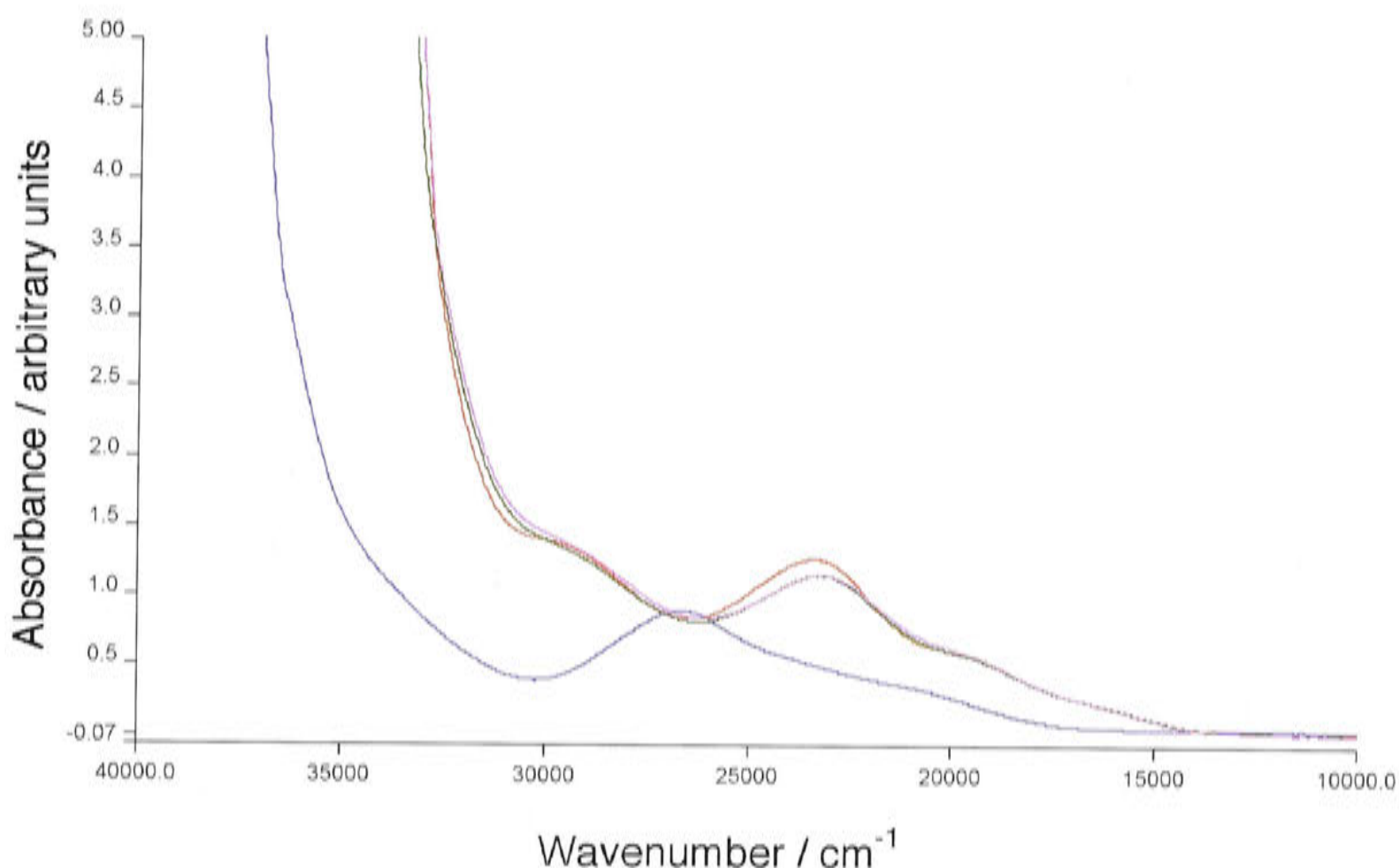


Figure 52. Electronic spectra recorded during one-electron oxidation of $[\text{RuCl}_2(\eta^6\text{-C}_6\text{Me}_6)(\text{PPh}_3)]$ (**306**) in 0.3M $[\text{Bu}^n_4\text{N}]\text{BF}_4/\text{CH}_2\text{Cl}_2$ at *ca* 233K [$E_{\text{appl}} = +0.86$ V (*vs* $\text{Fc}^{0/1}$)]. The blue line represents the spectrum of the parent Ru(II) complex, and the red line represents that of the electrogenerated Ru(III) cation, $[\mathbf{306}]^+$, both at *ca* 228K. The green line represents that at *ca* 273K and the pink line that at approx. 283K.

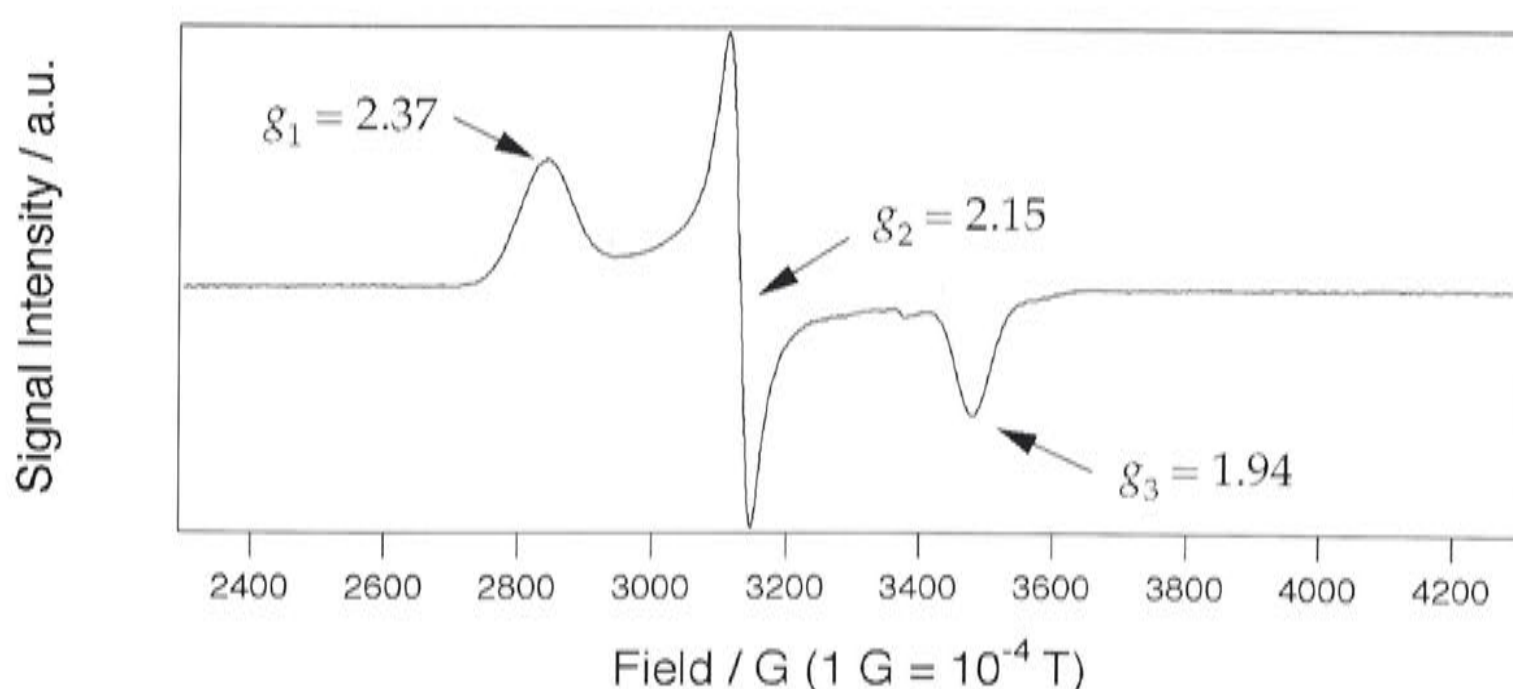


Figure 53. The ESR spectrum at *ca* 5K of the species prepared from the anodic oxidation of $[\text{RuCl}_2(\eta^6\text{-C}_6\text{Me}_6)(\text{PPh}_3)]$ (**306**) in 0.4M $[\text{Bu}^n_4\text{N}]\text{PF}_6/\text{CH}_2\text{Cl}_2$ at *ca* 228K [$E_{\text{appl}} = +0.64$ V (*vs* $\text{Fc}^{0/1}$)].

Complex $[\text{RuCl}_2(\eta^6\text{-C}_6\text{H}_6)(\text{PPh}_3)]$ (**302**) displays similar spectroelectrochemical behaviour at *ca* 228K to that of **306**, with two

isosbestic points at *ca* 26300 and 26800 cm^{-1} . The electrogenerated Ru(III) species was also unstable above *ca* 233K, as new bands with absorption maxima above those of the parent Ru(III) species were present at *ca* 30300 cm^{-1} . The species responsible for these bands was not characterised. It is presumed that the Ru(III) species decomposed *via* loss of the η^6 -arene.

The one-electron oxidation products of the corresponding trimethylphosphine complexes $[\text{RuCl}_2(\eta^6\text{-C}_6\text{R}_6)(\text{PMe}_3)]$ ($\text{R} = \text{H}$ (**337**), Me (**304**)) could be generated at *ca* 228K, but in contrast to the triphenylphosphine complexes **302** and **306**, they could not be reduced back to the parent arene-Ru(II) compounds, even at applied potentials of -0.55 and -1.56 V (*vs* $\text{Fc}^{0/1}$), respectively. The new Ru(II) species, in each case, showed a similar, though not identical, UV/Vis spectrum to those of their parent complexes, though there were differences in the absorption maxima. The new Ru(II) species generated from **337** showed a UV/Vis spectrum, with absorption maxima greater than that of **337** in the regions *ca* 37000 to 32300 cm^{-1} and 27500 to 21700 cm^{-1} , but the remainder of the spectrum had a absorption maxima lower than that of **337**. The UV/Vis spectrum of the new Ru(II) compound prepared from **337** displayed a higher absorption than the parent Ru(II) complex throughout almost the entire spectrum, in the regions *ca* 40000 to 25800 cm^{-1} and 22500 to 10000 cm^{-1} . Each of the new Ru(II) species could be oxidised to generate a new Ru(III) compound; these were not stable above *ca* 238K. Nothing further is known about the nature of the new species formed in these experiments.

Thus the non-tethered and tethered complexes exhibit different spectroelectrochemical behaviour. The tethered complexes generally showed reversible behaviour at *ca* 228K, and most of the oxidation products displayed some thermal stability; complexes with alkyl-substituted η^6 -arenes were the most stable. In contrast, only the non-tethered complexes containing triphenylphosphine displayed reversible spectroelectrochemical behaviour at *ca* 228K; those

incorporating trimethylphosphine did not. The non-tethered arene-Ru(III) species were thermally unstable above *ca* 228K.

5.2 Controlled Potential Electrolysis of $[\text{RuCl}_2(\eta^1:\eta^6\text{-Ph}_2\text{P}(\text{CH}_2)_3\text{Ph})]$ (222) in Nitriles

Smith and Wright²¹ reported the preparation of $[\text{RuCl}_2(\text{NCMe})_3(\eta^1\text{-Ph}_2\text{P}(\text{CH}_2)_3\text{Ph})]$ (259) *via* CPE of $[\text{RuCl}_2(\eta^6\text{-1,4-MeC}_6\text{H}_4\text{CHMe}_2)(\eta^1\text{-Ph}_2\text{P}(\text{CH}_2)_3\text{Ph})]$ (223) in acetonitrile at room temperature (see Scheme 59a, Chapter 3, Section 3.2.6).^{21,34} Since the tetrakis-complex $[\text{RuCl}(\text{NCMe})_4(\eta^1\text{-Ph}_2\text{P}(\text{CH}_2)_3\text{Ph})]\text{Cl}$ ([328]Cl) is the thermodynamic product obtained by heating either $[\text{RuCl}_2(\eta^6\text{-C}_6\text{H}_6)(\eta^1\text{-Ph}_2\text{P}(\text{CH}_2)_3\text{Ph})]$ (227) or $[\text{RuCl}_2(\eta^1:\eta^6\text{-Ph}_2\text{P}(\text{CH}_2)_3\text{Ph})]$ (222) in refluxing acetonitrile (see Chapter 4, Section 4.1), Smith and Wright's claim was re-examined. The electrode potentials of the products formed are quoted *vs* both Ag/AgCl and $\text{Fc}^{0/1}$, for ease of comparison with the electrochemical results described earlier (see Section 5.1). Ferrocene was employed as the internal standard and was oxidised at + 0.55 V (in CH_2Cl_2) or at + 0.47 V (in MeCN) *vs* Ag/AgCl. All CV traces shown were recorded at 100 mVs^{-1} .

Table 34. Principal electronic band maxima (in cm^{-1}) at *ca* 228K for the isolated non-tethered and tethered arene-Ru(II) complexes [values in brackets are the molar absorptivities (ϵ) in $\text{L mol}^{-1} \text{cm}^{-1}$]. All potentials are quoted *vs* $\text{Fc}^{0/1}$.

Complex	λ (cm^{-1}) [ϵ ($\text{L mol}^{-1} \text{cm}^{-1}$)]	Complex	λ (cm^{-1}) [ϵ ($\text{L mol}^{-1} \text{cm}^{-1}$)]	$E_{1/2}$ ($\text{Ru}^{\text{II}}/\text{Ru}^{\text{III}}$) (<i>vs</i> $\text{Fc}^{0/1}$)
[RuCl ₂ (η^6 -C ₆ H ₆)(PMe ₃)] (337)	21300 [460] 29500 [1600]	[337] ⁺	17800 [800] 23700 [2300] 30000 [2800]	+ 0.76
[RuCl ₂ (η^6 -C ₆ Me ₆)(PMe ₃)] (304)	^a	[304] ⁺	^a	+ 0.50
[RuCl ₂ (η^6 -C ₆ H ₆)(PPh ₃)] (302)	27200 [3600]	[302] ⁺	16600 [1700] 23300 [4500]	+ 0.87
[RuCl ₂ (η^6 -C ₆ Me ₆)(PPh ₃)] (306)	26700 [1700]	[306] ⁺	19600 [1300] 23400 [2400] 29500 [2500]	+ 0.54
[RuCl ₂ ($\eta^1:\eta^6$ -Me ₂ P~Ph)] (248)	21600 [440] 30100 [1500]	[248] ⁺	17800 [600] 30000 [2500]	+ 0.71
[RuCl ₂ ($\eta^1:\eta^6$ -Ph ₂ P~Ph)] (222)	27900 [2000]	[222] ⁺	19500 [900]	+ 0.77
[RuCl ₂ ($\eta^1:\eta^6$ - <i>i</i> -Pr ₂ P~Ph)] (249)	28700 [2500]	[249] ⁺	28000 [3100] 34400 [3900]	+ 0.78
[RuCl ₂ ($\eta^1:\eta^6$ -Cy ₂ P~Ph)] (225)	28700 [1400]	[225] ⁺	19500 [1100]	+ 0.76
RuCl ₂ ($\eta^1:\eta^6$ - <i>t</i> -Bu ₂ P~Ph)] (253)	27800 [1800]	[253] ⁺	18800 [1100] 27500 [2600]	+ 0.82

Complex	λ (cm ⁻¹) [ϵ (L mol ⁻¹ cm ⁻¹)]	Complex	λ (cm ⁻¹) [ϵ (L mol ⁻¹ cm ⁻¹)]	$E_{1/2}$ (Ru ^{II} /Ru ^{III}) (vs Fc ^{0/I})
[RuCl ₂ (η^1 : η^6 -Ph ₂ P~-3,5-C ₆ H ₂ Me ₃)] ^b (275)	27800 [2100]	[275] ⁺	19800 [1500] 25400 [2400]	+ 0.61 ^c
[RuCl ₂ (η^1 : η^6 -Ph ₂ P~-2,4,6-C ₆ H ₂ Me ₃)] (250)	27800 [2300]	[250] ⁺	29900 [3100] 25000 [2200]	+ 0.65
[RuCl ₂ (η^1 : η^6 -Ph ₂ P~-C ₆ Me ₅)] (251)	27400 [4300]	[251] ⁺	29800 [3100] 19500 [2200] 24600 [4500]	+ 0.55
[RuCl ₂ (η^1 : η^6 -Ph ₂ PCH ₂ SiMe ₂ Ph)] (252)	27200 [2700]	[252] ⁺	29100 [5100] 28200 [3300]	+ 0.79

^aContinuous absorption between 10000 and 40000 cm⁻¹, ^bprepared by literature methods¹⁹; ^creported $E_{1/2}$ value.¹⁹

~ = (CH₂)₃

A cyclic voltammogram (CV) of $[\text{RuCl}_2(\eta^1:\eta^6\text{-Ph}_2\text{P}(\text{CH}_2)_3\text{Ph})]$ (**222**) in acetonitrile showed a process with $i_{\text{pa}}/i_{\text{pc}}$ ratio of slightly less than one, with $E_{1/2} = +1.27$ V (*vs* Ag/AgCl), $+0.80$ V (*vs* $\text{Fc}^{0/1}$) at room temperature (Figure 54). The oxidation is likely to be a one-electron process since $\Delta E_p = 80$ mV, which is the same as ferrocene recorded under the same conditions. An additional reduction peak is present in the region $+0.50$ to $+0.69$ V (*vs* Ag/AgCl; $+0.03$ to $+0.22$ V *vs* $\text{Fc}^{0/1}$) only if the scan is first extended past the oxidation process, indicating that it is associated with the reduction of a secondary product of the oxidation. The peak grew in size after several minutes of scanning. This behaviour was not observed during the cyclic voltammetry of **222** in dichloromethane, where the electrode potentials are slightly different from those observed in acetonitrile; $E_{1/2} = +1.32$ V (*vs* Ag/AgCl), $+0.77$ V (*vs* $\text{Fc}^{0/1}$) (see Table 32). Steady state voltammetry (performed by stirring the solution) gave the position of zero current and indicated that the solution contains only the starting material **222**, since no reduction process was observed (see Figure 55). Exhaustive oxidation at $+1.50$ V (*vs* Ag/AgCl; $+1.03$ V (*vs* $\text{Fc}^{0/1}$)) in acetonitrile yielded a deep orange solution, and the CV displayed the presence of a new compound with $i_{\text{pa}}/i_{\text{pc}}$ equal to one, and $E_{1/2} = +0.72$ V (*vs* Ag/AgCl), $+0.25$ V (*vs* $\text{Fc}^{0/1}$) (Figure 54). Coulometry experiments according to equation three (see Chapter 8, Section 8.1.1, p. 336) gave the number of electrons as one. The species that formed is the same as that detected during a normal CV experiment of $[\text{RuCl}_2(\eta^1:\eta^6\text{-Ph}_2\text{P}(\text{CH}_2)_3\text{Ph})]$ (**222**) in acetonitrile, which displayed an additional reduction wave at in the region $+0.50$ to $+0.69$ V. Similarly, steady state voltammetry indicated that the solution contained only the Ru(III) species, since no oxidation process was observed (see Figure 56).

Since η^6 -arene displacement at the Ru(II) level occurs slowly (Chapter 4) the new Ru(III) species must form as a result of displacement of the η^6 -arene at the Ru(III) level. A wave due to free chloride ion (see below) was not visible in the cyclic voltammogram of the Ru(III) species (see

Figure 54), indicating that both chloride ligands were still present. Thus, the most likely hypothesis is that the η^6 -arene is displaced by three acetonitrile ligands at the Ru(III) level to form the cation $[\text{RuCl}_2(\text{NCMe})_3(\eta^1\text{-Ph}_2\text{P}(\text{CH}_2)_3\text{Ph})]^+$ (**[259]⁺**) (see Scheme 76a).

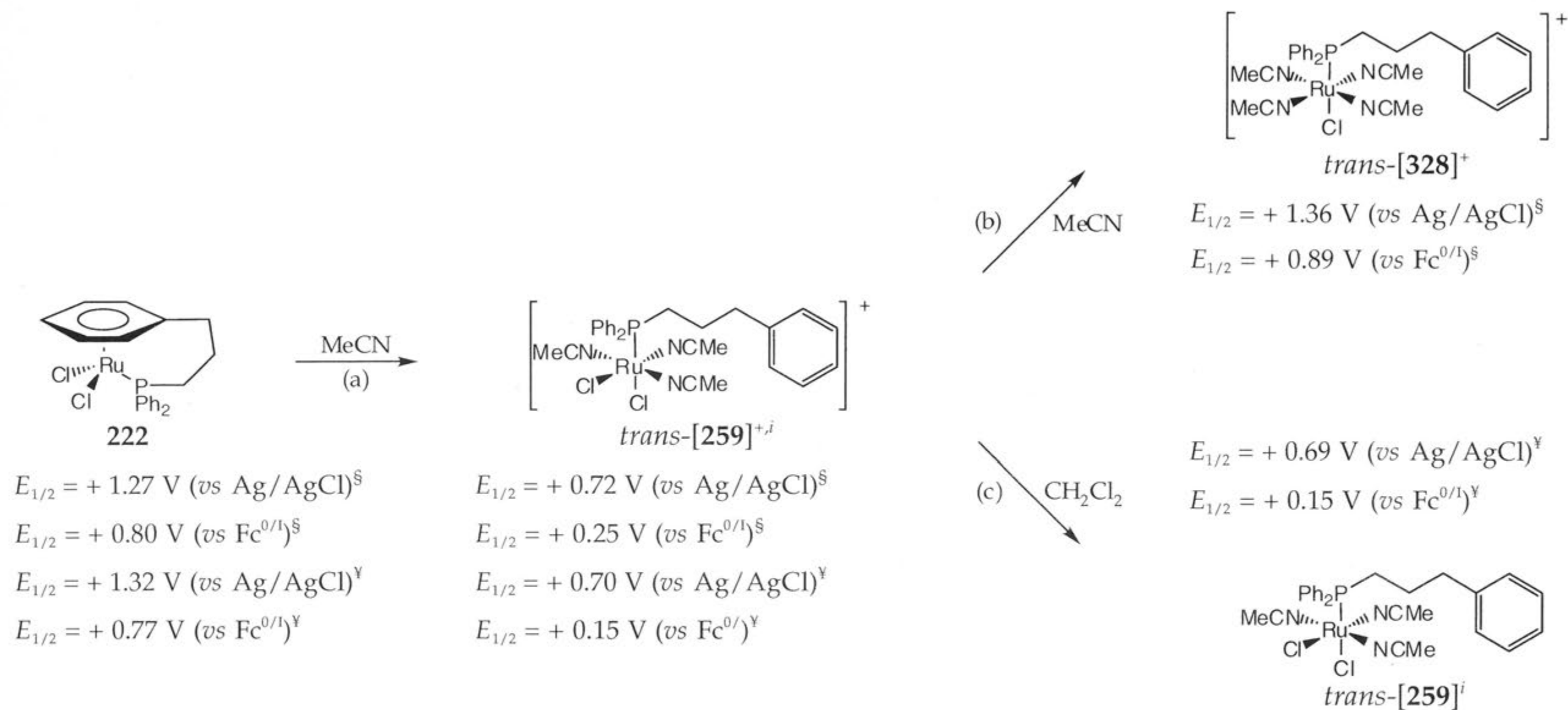
Reduction of **[259]⁺** *via* exhaustive electrolysis at 0.0 V (*vs* Ag/AgCl; -0.47 V (*vs* $\text{Fc}^{0/1}$)) in acetonitrile gave a yellow solution, which showed two waves, of approximately equal height (Figure 57), one with $i_{\text{pa}}/i_{\text{pc}}$ slightly below one, with $E_{1/2} = +1.36$ V (*vs* Ag/AgCl), +0.89 V (*vs* $\text{Fc}^{0/1}$), the other showed no reverse peak (on the timescale of the CV) with $E_{\text{pa}} = +1.15$ V (*vs* Ag/AgCl), +0.68 V (*vs* $\text{Fc}^{0/1}$). The reduction process was confirmed is likely to be one-electron since $\Delta E_p = 80$ mV. Due to instrumental difficulties, it was not possible to accurately determine the number of electrons involved. However, given that the peak current for the final Ru(II) product were approximately 70% of the Ru(III) intermediate species, the primary species formed was the Ru(II) product. The possibility of the formation of other minor species, which were not isolated, cannot be discounted. The chemically unstable wave can be assigned as being due to free chloride ion (discussed below; see Figure 58). This Ru(II) species is clearly not the original tethered complex $[\text{RuCl}_2(\eta^1:\eta^6\text{-Ph}_2\text{P}(\text{CH}_2)_3\text{Ph})]$ (**(222)**) ($E_{1/2} = +1.27$ V (*vs* Ag/AgCl), +0.80 V (*vs* $\text{Fc}^{0/1}$)) (see Figure 59), nor is it simply the Ru(II) compound $[\text{RuCl}_2(\text{NCMe})_3(\eta^1\text{-Ph}_2\text{P}(\text{CH}_2)_3\text{Ph})]$ (**(259)**), derived by reduction of **[259]⁺** ($E_{1/2} = +0.72$ V (*vs* Ag/AgCl), +0.25 V (*vs* $\text{Fc}^{0/1}$)) (compare CVs in Figure 57). Therefore, this species is believed to be $[\text{RuCl}(\text{NCMe})_4(\eta^1\text{-Ph}_2\text{P}(\text{CH}_2)_3\text{Ph})]^+$, (**[328]⁺**), formed by replacement of one chloride of $[\text{RuCl}_2(\text{NCMe})_3(\eta^1\text{-Ph}_2\text{P}(\text{CH}_2)_3\text{Ph})]$ (**(259)**) by an additional acetonitrile ligand, at the Ru(II) level (see Scheme 76b).

Thus the sequence of events is believed to be as follows: initial anodic oxidation of the tethered compound $[\text{RuCl}_2(\eta^1:\eta^6\text{-Ph}_2\text{P}(\text{CH}_2)_3\text{Ph})]$ (**(222)**) in

acetonitrile gives the tris(acetonitrile) cation $[\text{RuCl}_2(\text{NCMe})_3(\eta^1\text{-Ph}_2\text{P}(\text{CH}_2)_3\text{Ph})]^+$ (**[259]**⁺), presumably *via* the intermediate arene-ruthenium(III) cation $[\text{RuCl}_2(\eta^1:\eta^6\text{-Ph}_2\text{P}(\text{CH}_2)_3\text{Ph})]^+$ (**[222]**⁺). On cathodic reduction of **[259]**⁺ in acetonitrile, **259** loses chloride ion and generates the tetrakis(acetonitrile) complex $[\text{RuCl}(\text{NCMe})_4(\eta^1\text{-Ph}_2\text{P}(\text{CH}_2)_3\text{Ph})]^+$ (**[328]**⁺).

In an attempt to confirm the formation of **[328]**⁺, the CV of a pure, authentic sample of *cis*- and *trans*- $[\text{RuCl}(\text{NCMe})_4(\eta^1\text{-Ph}_2\text{P}(\text{CH}_2)_3\text{Ph})]\text{Cl}$ (**[328]**Cl), prepared by heating the complex $[\text{RuCl}_2(\eta^6\text{-C}_6\text{H}_6)(\eta^1\text{-Ph}_2\text{P}(\text{CH}_2)_3\text{Ph})]$ (**328**) in acetonitrile (Chapter 4, Section 4.1), was recorded (see Figure 58). The wave of the authentic compound was similar, but not identical, to that of the electrogenerated sample of **[328]**Cl; the authentic sample showed two chemically unstable waves (on the CV timescale), one with $E_{\text{pa}} = +1.48 \text{ V}$ (*vs* Ag/AgCl), $+1.01 \text{ V}$ (*vs* $\text{Fc}^{0/1}$) and the other with $E_{\text{pa}} = +1.12 \text{ V}$ (*vs* Ag/AgCl), $+0.65 \text{ V}$ (*vs* $\text{Fc}^{0/1}$). The latter peak is similar in E_{pa} to that observed for free chloride ion ($E_{\text{pa}} = +1.15 \text{ V}$ (*vs* Ag/AgCl), $+0.68 \text{ V}$ (*vs* $\text{Fc}^{0/1}$)), formed during the reduction of $[\text{RuCl}_2(\text{NCMe})_3(\eta^1\text{-Ph}_2\text{P}(\text{CH}_2)_3\text{Ph})]^+$ (**[259]**⁺) in acetonitrile, and is due to the chemically unstable oxidation of free chloride (on the CV timescale). This assignment was confirmed by addition of $[\text{Bu}^n_4\text{N}]\text{Cl}$ (Figure 58). The first wave is due to the *cis*- and *trans*-isomers of **[328]**Cl, and is similar to that of the electrogenerated sample of **[328]**⁺ ($E_{1/2} = +1.36 \text{ V}$ (*vs* Ag/AgCl), $+0.89 \text{ V}$ (*vs* $\text{Fc}^{0/1}$)). Since the CV of the *cis*- and *trans*-isomers of **[328]**Cl does not have a reverse peak (E_{pc}) following oxidation, the electrode potential cannot be determined by measuring the difference between the E_{pa} and E_{pc} values. However, the $E_{1/2}$ is likely to be approximately 35 mV less than the E_{pa} potential, thus accounting for the disparity between the $E_{1/2}$ and E_{pa} values. The difference in the electrochemical behaviour of the two samples of **[328]**Cl may be attributed to the fact that the authentic sample is a mixture of both the *cis*- and *trans*-isomers, whereas the CV of only the *trans*-isomer was recorded in the electrogenerated sample.

Convincing evidence for the formation of the tetrakis-complex $[\text{RuCl}(\text{NCMe})_4(\eta^1\text{-Ph}_2\text{P}(\text{CH}_2)_3\text{Ph})]^+$ (**[328]**⁺) by reduction of $[\text{RuCl}_2(\text{NCMe})_3(\eta^1\text{-Ph}_2\text{P}(\text{CH}_2)_3\text{Ph})]^+$ (**[259]**⁺) in acetonitrile was obtained from the NMR spectra (in CD_3CN) of the crude oil, obtained after removal of the solvent from the electrogenerated solution. The ^1H NMR spectrum showed a multiplet in the region δ 7.05-7.65, corresponding to free aromatic signals; there were no signals in the range δ 4-6, showing the absence of η^6 -arene. The ^1H NMR spectrum also showed a singlet at δ 2.11, confirming the presence of coordinated acetonitrile ligands. The $^{31}\text{P}\{^1\text{H}\}$ -NMR spectrum showed just a singlet resonance at δ 48.5 (*cf.* δ 48.7 for an authentic sample of *trans*- $[\text{RuCl}(\text{NCMe})_4(\eta^1\text{-Ph}_2\text{P}(\text{CH}_2)_3\text{Ph})]\text{Cl}$ (**[328]**Cl)), in addition to a singlet at δ 31.0 assigned to phosphine oxide, $\text{Ph}_2\text{P}(\text{O})(\text{CH}_2)_3\text{Ph}$, arising from some decomposition. The IR spectrum displayed a weak band at 2252 cm^{-1} , indicative of coordinated acetonitrile. Unfortunately it was not possible to obtain a mass spectrum.



Scheme 76. Formation of the tetrakis-complex $[\text{RuCl}(\text{NCMe})_4(\eta^1\text{-Ph}_2\text{P}(\text{CH}_2)_3\text{Ph})]^+$ ($[\mathbf{328}]^+$) and tris-species $[\text{RuCl}_2(\text{NCMe})_3(\eta^1\text{-Ph}_2\text{P}(\text{CH}_2)_3\text{Ph})]$ ($\mathbf{259}$) during exhaustive anodic oxidation experiments. ⁱFormation of *trans*-isomer only shown; *cis*-isomer was also formed. [§]Recorded in acetonitrile; ^Υrecorded in dichloromethane. Reaction conditions: (a) platinum gauze working electrode, 0.1M $[\text{Bu}^n_4\text{N}]\text{BF}_4$, +1.50V (vs Ag/AgCl), +1.03 V (vs $\text{Fc}^{0/1}$); (b) platinum gauze working electrode, 0.1M $[\text{Bu}^n_4\text{N}]\text{BF}_4$, 0.0 V (vs Ag/AgCl), -0.47 V (vs $\text{Fc}^{0/1}$); (c) platinum gauze working electrode, 0.3M $[\text{Bu}^n_4\text{N}]\text{BF}_4$, 0.0 V (vs Ag/AgCl), -0.55 V (vs $\text{Fc}^{0/1}$).

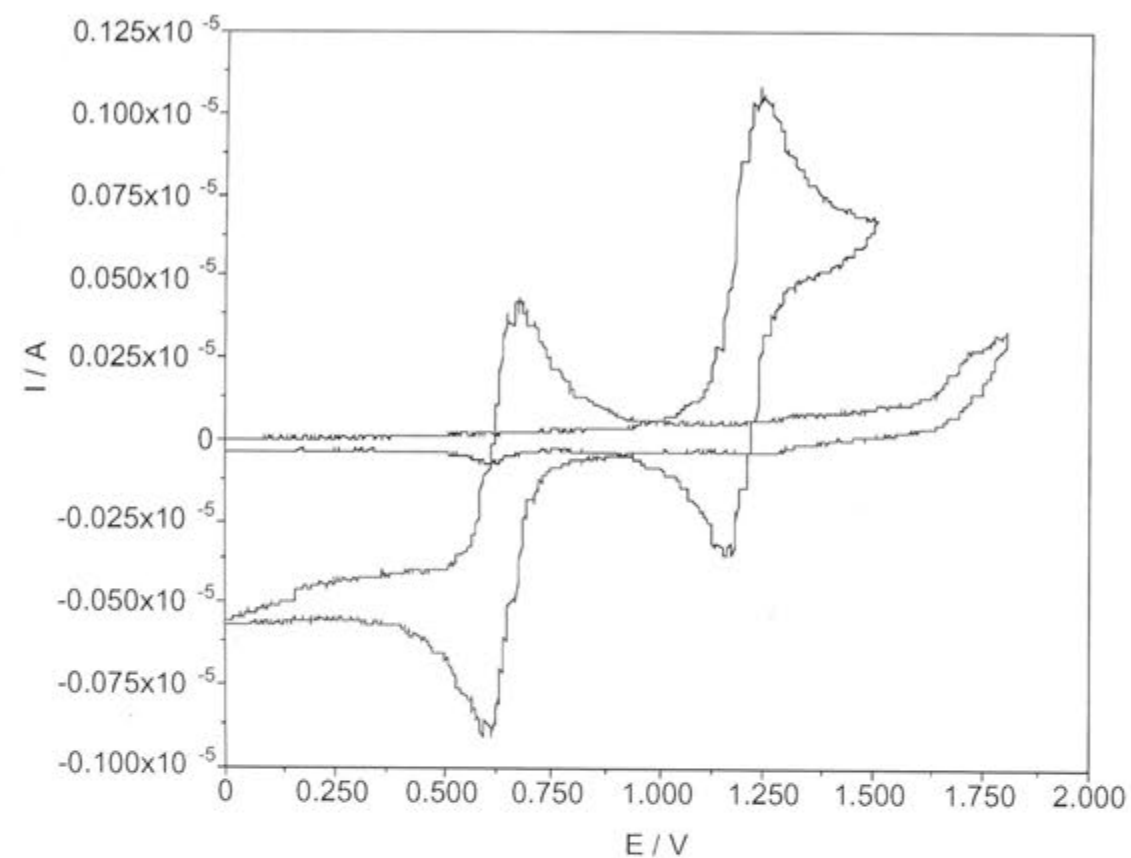


Figure 54. Cyclic voltammogram (black) of $[\text{RuCl}_2(\eta^1:\eta^6\text{-Ph}_2\text{P}(\text{CH}_2)_3\text{Ph})]$ (**222**) in 0.1M $[\text{Bu}^n_4\text{N}]\text{BF}_4/\text{CH}_3\text{CN}$ at 293K (*vs* Ag/AgCl); cyclic voltammogram (blue) of $[\text{RuCl}_2(\text{NCMe})_3(\eta^1\text{-Ph}_2\text{P}(\text{CH}_2)_3\text{Ph})]^+$ (**[259]⁺**) in 0.1M $[\text{Bu}^n_4\text{N}]\text{BF}_4/\text{CH}_3\text{CN}$ at 293K (*vs* Ag/AgCl).

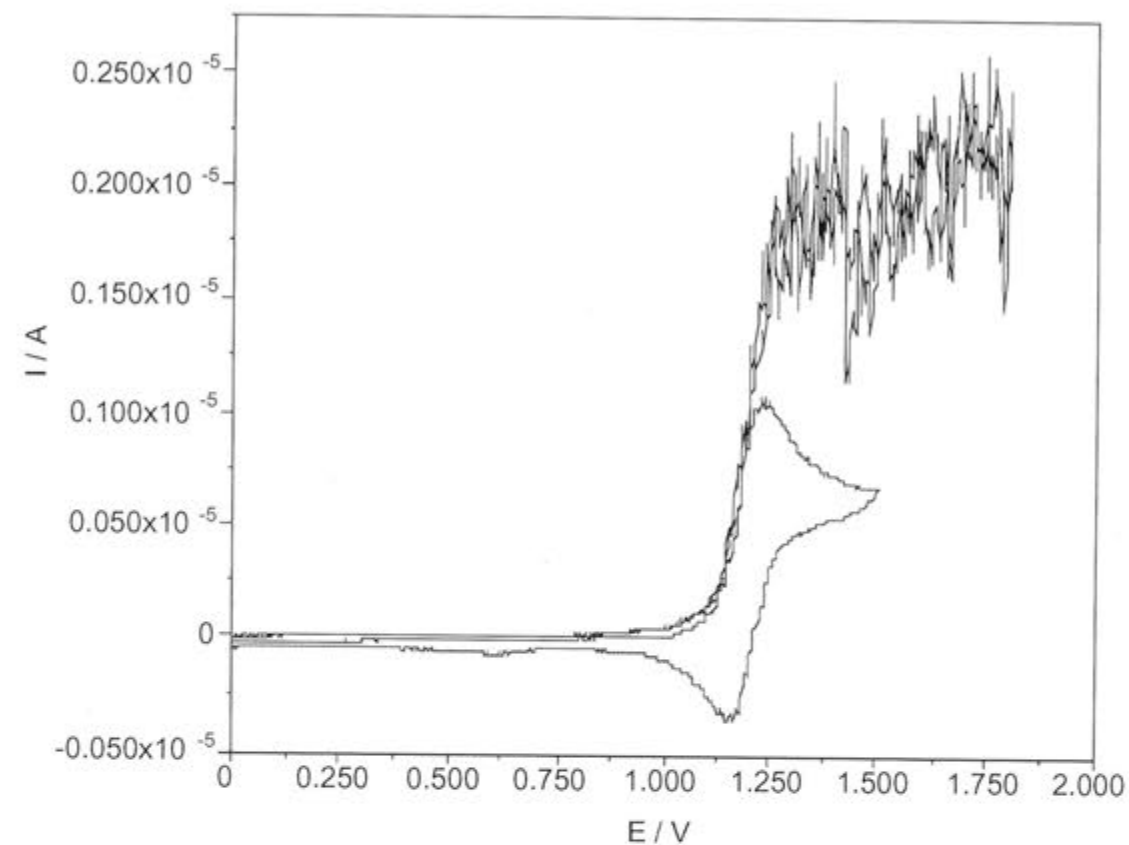


Figure 55. Cyclic voltammogram (blue) of $[\text{RuCl}_2(\eta^1:\eta^6\text{-Ph}_2\text{P}(\text{CH}_2)_3\text{Ph})]$ (**222**) in 0.1M $[\text{Bu}^n_4\text{N}]\text{BF}_4/\text{CH}_3\text{CN}$ at 293K (*vs* Ag/AgCl); as a stirred solution (black).

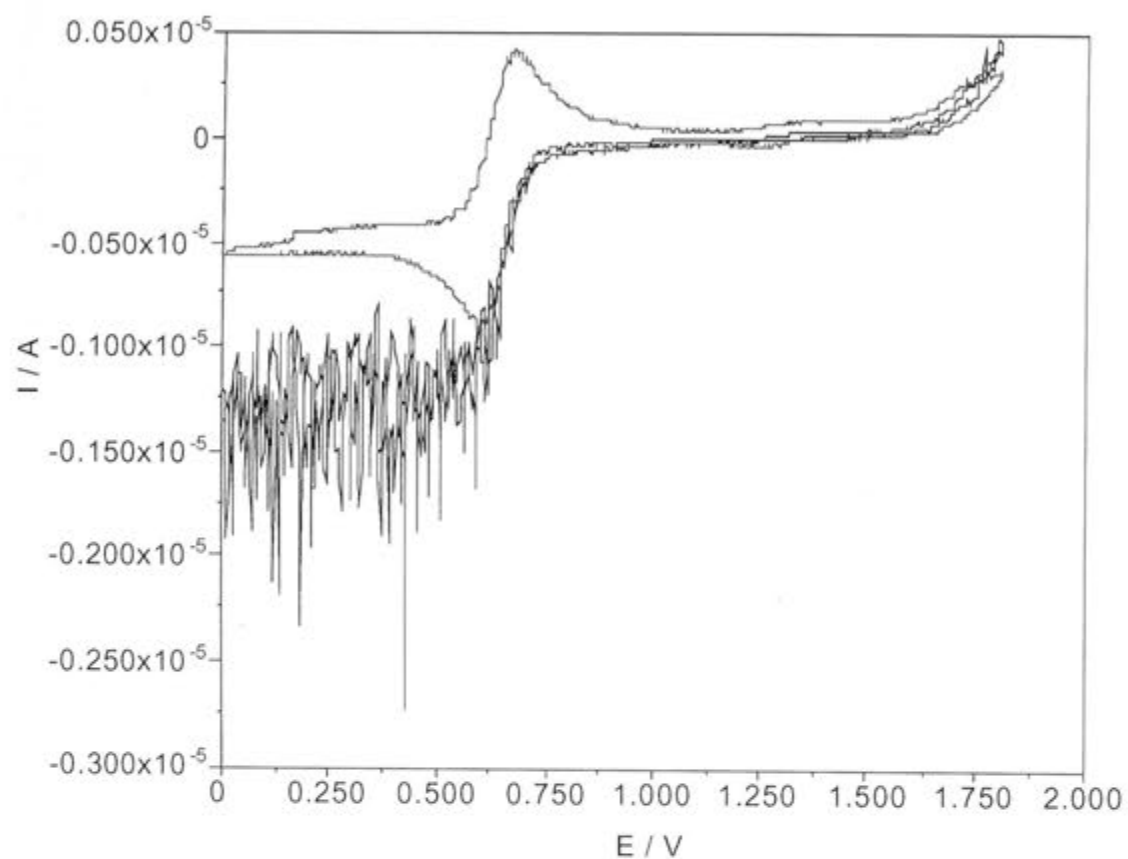


Figure 56. Cyclic voltammogram (blue) of $[\text{RuCl}_2(\text{NCMe})_3(\eta^1\text{-Ph}_2\text{P}(\text{CH}_2)_3\text{Ph})]^+$ (**[259]⁺**) in 0.1M $[\text{Bu}^n_4\text{N}]\text{BF}_4/\text{CH}_3\text{CN}$ at 293K (*vs* Ag/AgCl); as a stirred solution (black).

Note the contrast with $[\text{RuCl}_2(\eta^1:\eta^6\text{-Ph}_2\text{P}(\text{CH}_2)_3\text{Ph})]$ (**(222)**) in Figure 55.

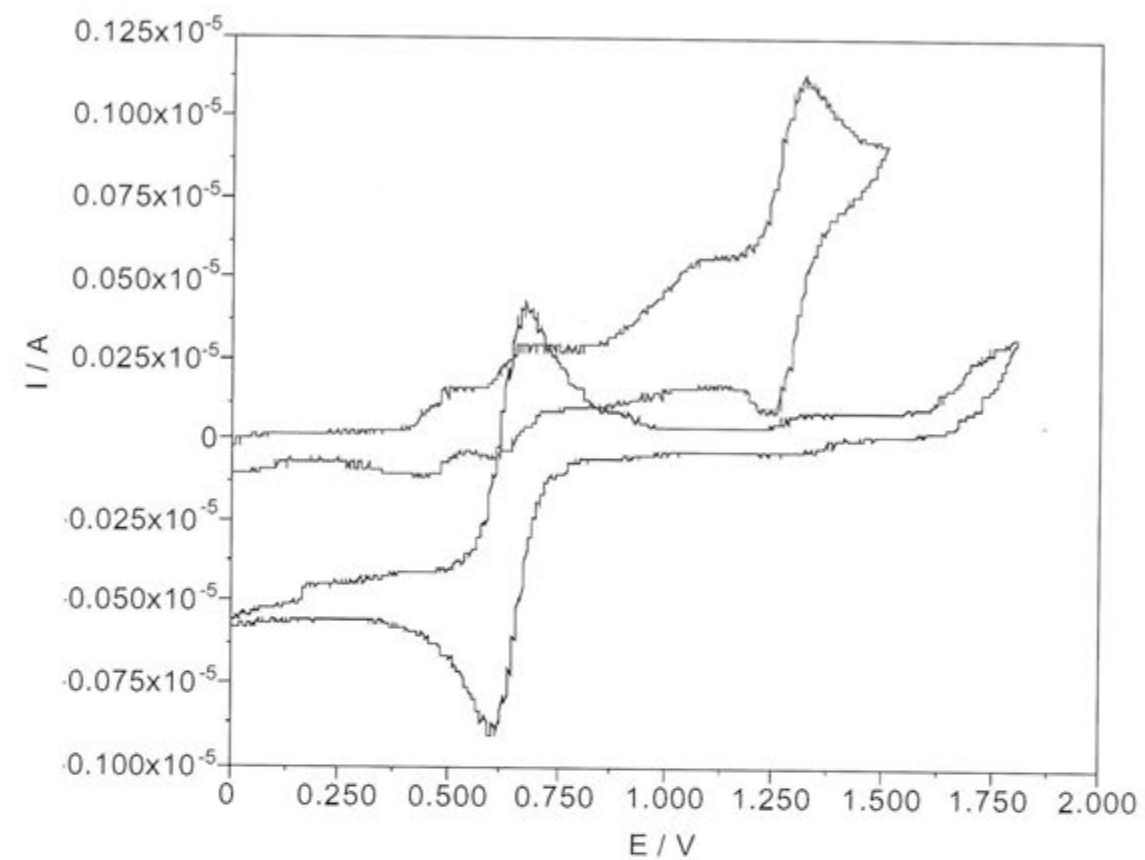


Figure 57. Cyclic voltammogram (black) of $[\text{RuCl}_2(\text{NCMe})_3(\eta^1\text{-Ph}_2\text{P}(\text{CH}_2)_3\text{Ph})]^+$ (**[259]⁺**) in 0.1M $[\text{Bu}^n_4\text{N}]\text{BF}_4/\text{CH}_3\text{CN}$ at 293K (*vs* Ag/AgCl); cyclic voltammogram (blue) of $[\text{RuCl}(\text{NCMe})_4(\eta^1\text{-Ph}_2\text{P}(\text{CH}_2)_3\text{Ph})]^+$ (**[328]⁺**) in 0.1M $[\text{Bu}^n_4\text{N}]\text{BF}_4/\text{CH}_3\text{CN}$ at 293K (*vs* Ag/AgCl).

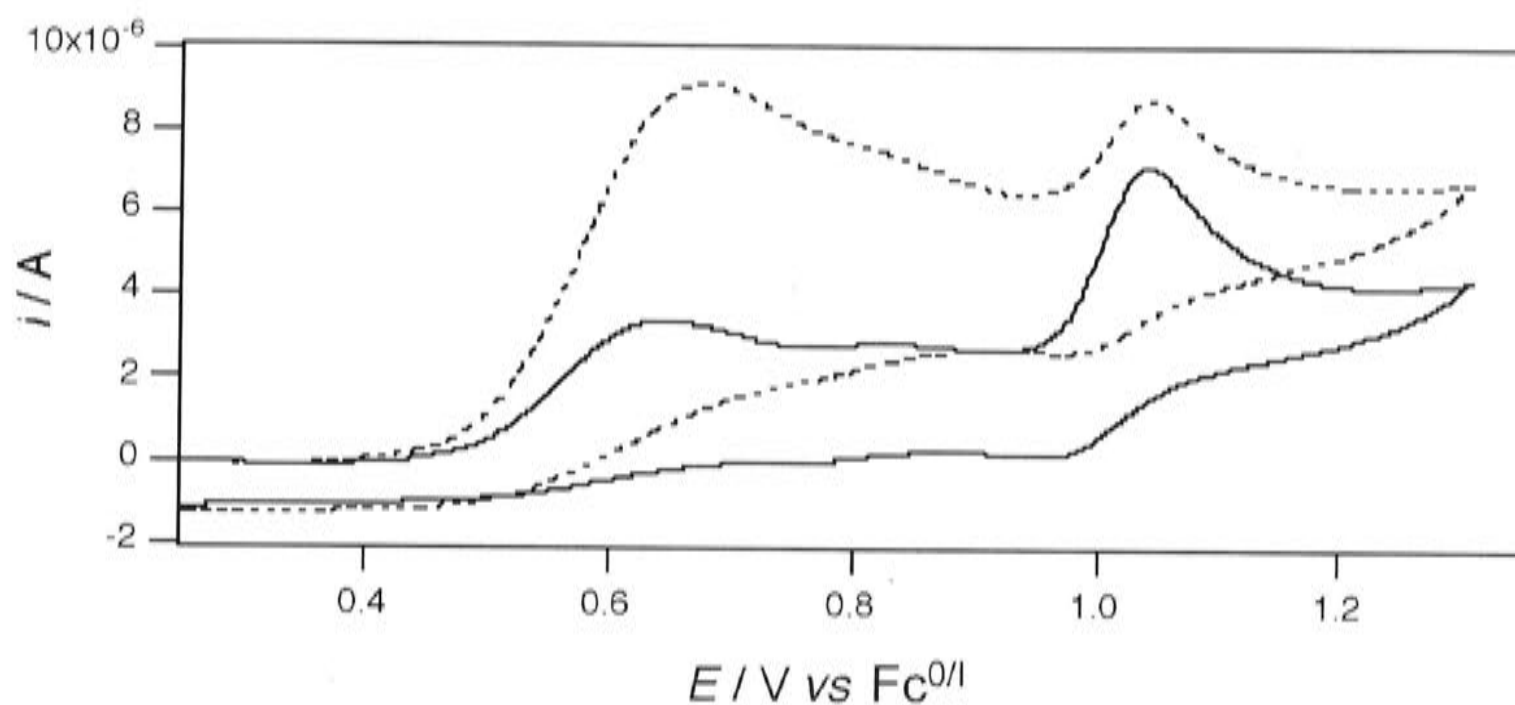


Figure 58. Cyclic voltammogram (solid line) of $[\text{RuCl}(\text{NCMe})_4(\eta^1\text{-Ph}_2\text{P}(\text{CH}_2)_3\text{Ph})]\text{Cl}$ (**[328]**Cl) (prepared from $[\text{RuCl}_2(\eta^1:\eta^6\text{-Ph}_2\text{P}(\text{CH}_2)_3\text{Ph})]$ (**222**) and CH_3CN) in 0.1M $[\text{Bu}^n_4\text{N}]\text{PF}_6/\text{CH}_3\text{CN}$ at 298K; cyclic voltammogram (dashed line) of $[\text{RuCl}(\text{NCMe})_4(\eta^1\text{-Ph}_2\text{P}(\text{CH}_2)_3\text{Ph})]\text{Cl}$ (**[328]**Cl) with $[\text{Bu}^n_4\text{N}]\text{Cl}$ in 0.1M $[\text{Bu}^n_4\text{N}]\text{PF}_6/\text{CH}_3\text{CN}$ at 298K.

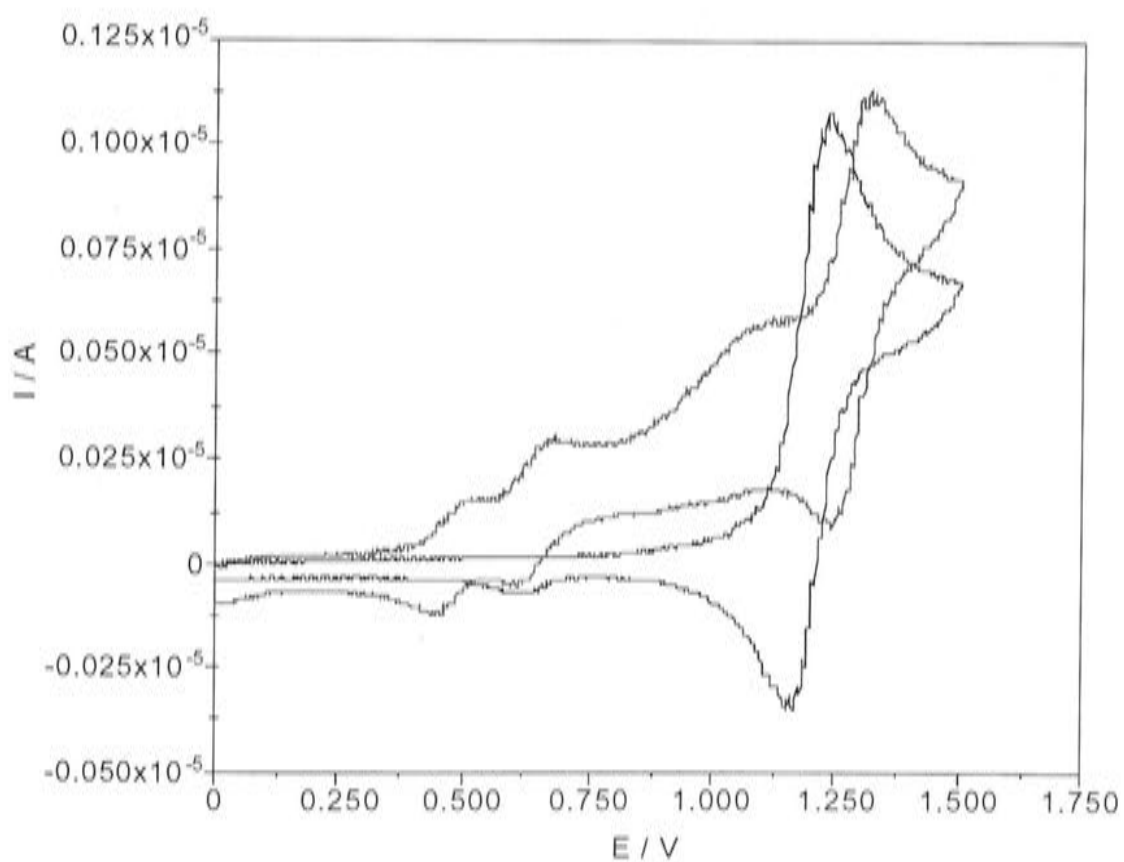


Figure 59. Cyclic voltammogram (blue) of $[\text{RuCl}(\text{NCMe})_4(\eta^1\text{-Ph}_2\text{P}(\text{CH}_2)_3\text{Ph})]^+$ (**[328]**⁺) in CH_3CN at 293K (*vs* Ag/AgCl); cyclic voltammogram (black) of $[\text{RuCl}_2(\eta^1:\eta^6\text{-Ph}_2\text{P}(\text{CH}_2)_3\text{Ph})]$ (**222**) in 0.1M $[\text{Bu}^n_4\text{N}]\text{BF}_4/\text{CH}_3\text{CN}$ at 293K (*vs* Ag/AgCl).

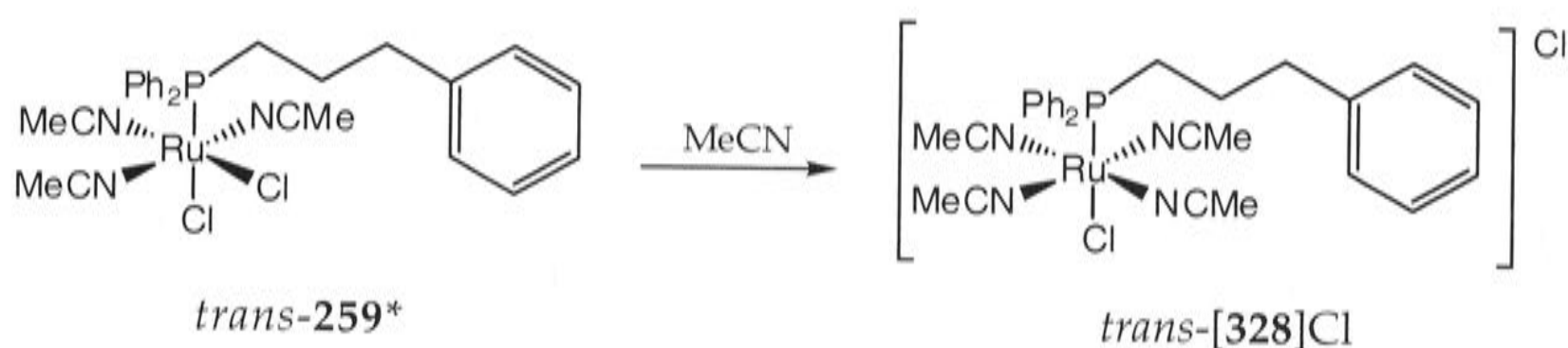
Since it is clear that chloride is very easily replaced by acetonitrile at the Ru(II) level, attempts to generate the tris-complex **259** must therefore be

carried out in the absence of an excess of acetonitrile. The crude oil, obtained by removal of the solvent from $[\text{RuCl}_2(\text{NCMe})_3(\eta^1\text{-Ph}_2\text{P}(\text{CH}_2)_3\text{Ph})]^+$ (**[259]**⁺) generated as described above, was dissolved in dichloromethane and 0.3M $[\text{Bu}^n_4\text{N}]\text{BF}_4$ was added. The CV showed a wave with $i_{\text{pa}}/i_{\text{pc}}$ equal to one, and $E_{1/2} = + 0.70 \text{ V}$ (*vs* Ag/AgCl), $+ 0.15 \text{ V}$ (*vs* $\text{Fc}^{0/1}$), (*cf.* $+ 0.72$ (*vs* Ag/AgCl), $+ 0.25 \text{ V}$ (*vs* $\text{Fc}^{0/1}$) in MeCN) with $\Delta E_p = 70 \text{ mV}$ (Figure 60). Again, steady state voltammetry gave the position of zero current and implied that the solution contained only **[259]**⁺, since there was no reduction process observed. Reduction of **[259]**⁺ *via* exhaustive electrolysis at 0.0 V (*vs* Ag/AgCl), $- 0.55 \text{ V}$ (*vs* $\text{Fc}^{0/1}$) in dichloromethane gave rise to an orange solution, which showed two different oxidation and reduction processes in its CV; the major product with a $i_{\text{pa}}/i_{\text{pc}}$ ratio of slightly less than one, and $E_{1/2} = + 0.69 \text{ V}$ (*vs* Ag/AgCl), $+ 0.14 \text{ V}$ (*vs* $\text{Fc}^{0/1}$), $\Delta E_p = 60 \text{ mV}$, and a minor product with a $i_{\text{pa}}/i_{\text{pc}}$ ratio just below one, and $E_{1/2} = + 1.32 \text{ V}$ (*vs* Ag/AgCl), $+ 0.77 \text{ V}$ (*vs* $\text{Fc}^{0/1}$), $\Delta E_p = 90 \text{ mV}$. The $E_{1/2}$ of the major product was identical to that of the Ru(III) species **[259]**⁺ (Figure 60). The fact that less than one electron was transferred during the reduction suggests that the intermediate Ru(III) species may undergo some decomposition. Steady state voltammetry gave the position of zero current and suggested that the solution only contains Ru(II) species, since no oxidation processes were observed (Figure 62), in contrast to the steady state behaviour of **[259]**⁺ (see Figure 61). Since the CV (Figure 60) does not show a peak due to free chloride ion (see above), and is identical to that of the Ru(III) species **[259]**⁺, the new Ru(II) product can only be $[\text{RuCl}_2(\text{NCMe})_3(\eta^1\text{-Ph}_2\text{P}(\text{CH}_2)_3\text{Ph})]$ (**259**) (see Scheme 76c). Its CV is distinctly different from that of the parent compound $[\text{RuCl}_2(\eta^1:\eta^6\text{-Ph}_2\text{P}(\text{CH}_2)_3\text{Ph})]$ (**222**) (see Figure 63). The minor product $E_{1/2} = + 1.32 \text{ V}$ (*vs* Ag/AgCl), $+ 0.77 \text{ V}$ (*vs* $\text{Fc}^{0/1}$) (see Figure 60) is attributed to the presence of starting material **222** ($E_{1/2} = + 0.77 \text{ V}$ (*vs* $\text{Fc}^{0/1}$) in CH_2Cl_2 , as described earlier in this Chapter). The formation of **222** during reduction of **[259]**⁺ was confirmed since it was not present in the CV of $[\text{RuCl}_2(\text{NCMe})_3(\eta^1\text{-Ph}_2\text{P}(\text{CH}_2)_3\text{Ph})]^+$ (**[259]**⁺) (Figure 60).

Owing to the large excess of electrolyte, the ^1H NMR spectra (in CD_2Cl_2) of the crude oils, either obtained after removal of solvent from the deep orange solution of the Ru(III) complex $[\text{RuCl}_2(\text{NCMe})_3(\eta^1\text{-Ph}_2\text{P}(\text{CH}_2)_3\text{Ph})]^+$ (**[259]**⁺), or from its reduced Ru(II) analogue **259**, were identical, but owing to the large excess of electrolyte, were uninformative. The $^{31}\text{P}\{^1\text{H}\}$ -NMR spectrum of **259**, however, showed two resonances at δ 66.7 and 67.3, the latter being the more intense (the spectrum was only measured in this region and it is not known whether any $[\text{RuCl}_2(\eta^1:\eta^6\text{-Ph}_2\text{P}(\text{CH}_2)_3\text{Ph})]$ (**222**) was present at this stage). The resonance at δ 67.3 was also observed in the $^{31}\text{P}\{^1\text{H}\}$ -NMR spectrum of the Ru(III) species **[259]**⁺, presumably due to spontaneous reduction during removal of the solvent, though it was not possible to assign this signal to an individual isomer. The $^{31}\text{P}\{^1\text{H}\}$ -NMR spectrum of **259** must, however, be acquired immediately; if the solution was allowed to stand for several days, quantitative conversion to the *trans*- and *cis*-isomers of the tetrakis-complex $[\text{RuCl}(\text{NCMe})_4(\eta^1\text{-Ph}_2\text{P}(\text{CH}_2)_3\text{Ph})]\text{Cl}$ (**[328]**Cl) occurred, presumably resulting from reaction with small amounts of acetonitrile present in the oil. This was indicated by the appearance of the two expected signals in the $^{31}\text{P}\{^1\text{H}\}$ -NMR spectrum, along with two, less intense signals at δ 23.0 and 31.6; approximate intensities of the four signals, in order of decreasing field, were 2:3:36:5, respectively. The signal at δ 23.0 confirmed the presence of a small amount (*ca* 4%) of **222**, *cf.* 22.2 for an authentic sample, and the peak at δ 31.6 can be attributed to phosphine oxide, arising from decomposition. The IR spectrum of $[\text{RuCl}_2(\text{NCMe})_3(\eta^1\text{-Ph}_2\text{P}(\text{CH}_2)_3\text{Ph})]$ (**259**) showed a weak band at 2253 cm^{-1} characteristic of the coordinated acetonitrile. It was, however, not possible to obtain a mass spectrum.

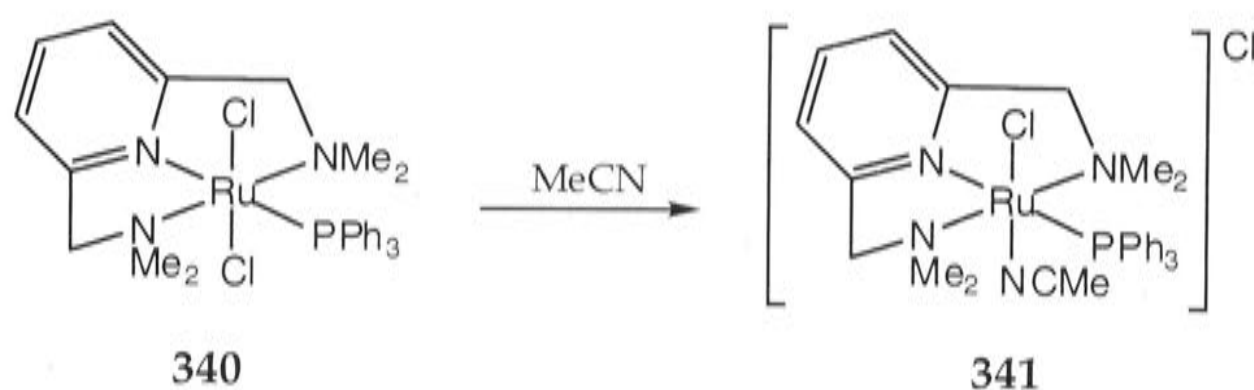
As expected, addition of excess acetonitrile to the tris-complex **259**, either at room temperature or more rapidly upon heating, caused disappearance of the resonance at δ 67.3 and appearance of a singlet at δ 47.9 (in CD_2Cl_2 ; *cf.* 48.1 from an authentic sample of **[328]**Cl, see Chapter 4, Section 4.1)

(Scheme 77). In this case, the minor peak at δ 51.5 was not observed. It should be noted that the δ_p values in the range of 67 for the tris-complex **259** are very different from the report of δ 46.8 reported by Smith and Wright for this compound.²¹



Scheme 77. Reaction of *trans*-**259** with acetonitrile to give tetrakis-[**328**]Cl.
*The *cis*-isomer of **259** may also be present.

The displacement of a chloride ligand by acetonitrile of a tris-complex to form a tetrakis-nitrile species, where the chloride changes from inner- to outer-sphere, has been reported.³⁵ The tris-complex [RuCl₂(NN′N)(PPh₃)] (**340**) (NN′N = 2,6-bis[(dimethylamino)methyl]pyridine) reacted rapidly with acetonitrile at 55°C to form the cationic species [RuCl(NCMe)(NN′N)(PPh₃)]Cl **341** (Scheme 78).



Scheme 78. Reaction of tris-complex **340** with acetonitrile to afford the cationic compound **341**.³⁵

Although a number of compounds of the type [RuCl₂L₃(PR₃)] (L = N-donor) have been reported, compounds of this type which incorporate acetonitrile are rare. Some additional examples of complexes of the type [RuCl₂L₃(PR₃)] are listed in Table 35. There are few examples of electrode potentials of such complexes reported in the literature, making

comparison with the results obtained in this work difficult. The $E_{1/2}$ of *trans*- and *cis*-isomers of $[\text{RuCl}_2(\eta^3\text{-trpy})(\text{PMe}_3)]$ (trpy = 2,2':6,2''-terpyridine) are *ca* + 0.33 and + 0.50 V (*vs* $\text{Fc}^{0/1}$ in CH_2Cl_2 [conversion factors of + 0.24 V (estimated standard potential of SSCE {Saturated Sodium Chloride Electrode} *vs* SCE)³⁶ and - 0.31 V⁷]), respectively.³⁷ Complex $[\text{RuCl}_2(\text{NCMe})_3(\eta^1\text{-Ph}_2\text{P}(\text{CH}_2)_3\text{Ph})]$ (**259**) has $E_{1/2} = \text{ca} + 0.03$ V (*vs* $\text{Fc}^{0/1}$ in MeCN [conversion factor - 0.31 V for the estimated standard potential of $\text{Fc}^{0/1}$ of + 0.31 V *vs* SCE]³⁶);²¹ which is in poor agreement with the results obtained in this work. It should be noted that the $E_{1/2}$ for $[\text{RuCl}_2(\eta^1:\eta^6\text{-Ph}_2\text{P}(\text{CH}_2)_3\text{Ph})]$ (**222**) reported by Smith and Wright²¹ was also in poor agreement with the results reported in this work and with those of Nelson and Ghebreyessus¹⁹ (see Section 5.1).

Table 35. Ruthenium(II) complexes of the type $[\text{RuCl}_2\text{L}_3(\text{PR}_3)]$ (L = N-donor).

Complex	Substituent	Reference
$[\text{RuCl}_2(\text{L})_3(\text{PPh}_3)]$ $[\text{RuCl}_2(\eta^3\text{-L})(\text{PR}_3)]$	$\text{L}_3 = 3\text{NH}_3, 3\text{py}, 3\text{ArNH}_2$ $\text{NN}'\text{N}, \text{trpy}; 2,6\text{-py}(\text{NPh})_2;$ $2,6\text{-py}(\text{NCy})_2, 2,6\text{-}$ $\text{py}(\text{NCHMePh})_2, 2,6\text{-}$ $\text{py}(\text{NCHMeNaph})_2; \text{R}_3 =$ $\text{Me}_3, \text{Et}_3, n\text{-Pr}_3, n\text{-Bu}_3, \text{Ph}_3,$ $\text{Ph}_2\text{H}, \text{Bz}_3$	38-40 35,37,41,42 43
$[\text{RuCl}_2(\eta^3\text{-}2,6\text{-bis}[1\text{-(4-methoxyphenylimino)ethyl]pyridine})(\text{PPh}_3)]$	-	44

Naph = naphthyl

NN'N = 2,6-bis[(dimethylamino)methyl]pyridine

py = Pyridine

trpy = 2,2':6,2''-terpyridine

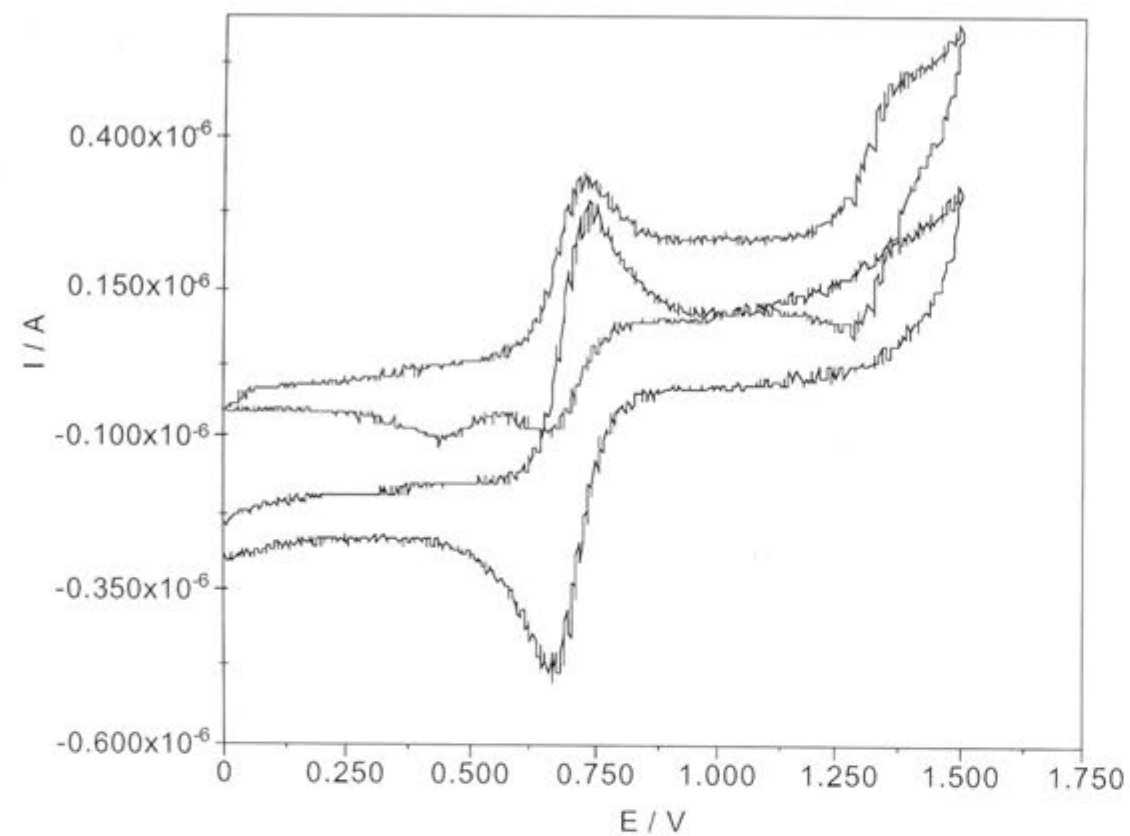


Figure 60. Cyclic voltammogram (black) of $[\text{RuCl}_2(\text{NCMe})_3(\eta^1\text{-Ph}_2\text{P}(\text{CH}_2)_3\text{Ph})]^+$ ($[\mathbf{259}]^+$) in 0.3M $[\text{Bu}_4\text{N}]\text{BF}_4/\text{CH}_2\text{Cl}_2$ at 293K (*vs* Ag/AgCl); cyclic voltammogram (blue) of $[\text{RuCl}_2(\text{NCMe})_3(\eta^1\text{-Ph}_2\text{P}(\text{CH}_2)_3\text{Ph})]$ ($\mathbf{259}$) in 0.3M $[\text{Bu}_4\text{N}]\text{BF}_4/\text{CH}_2\text{Cl}_2$ at 293K (*vs* Ag/AgCl).

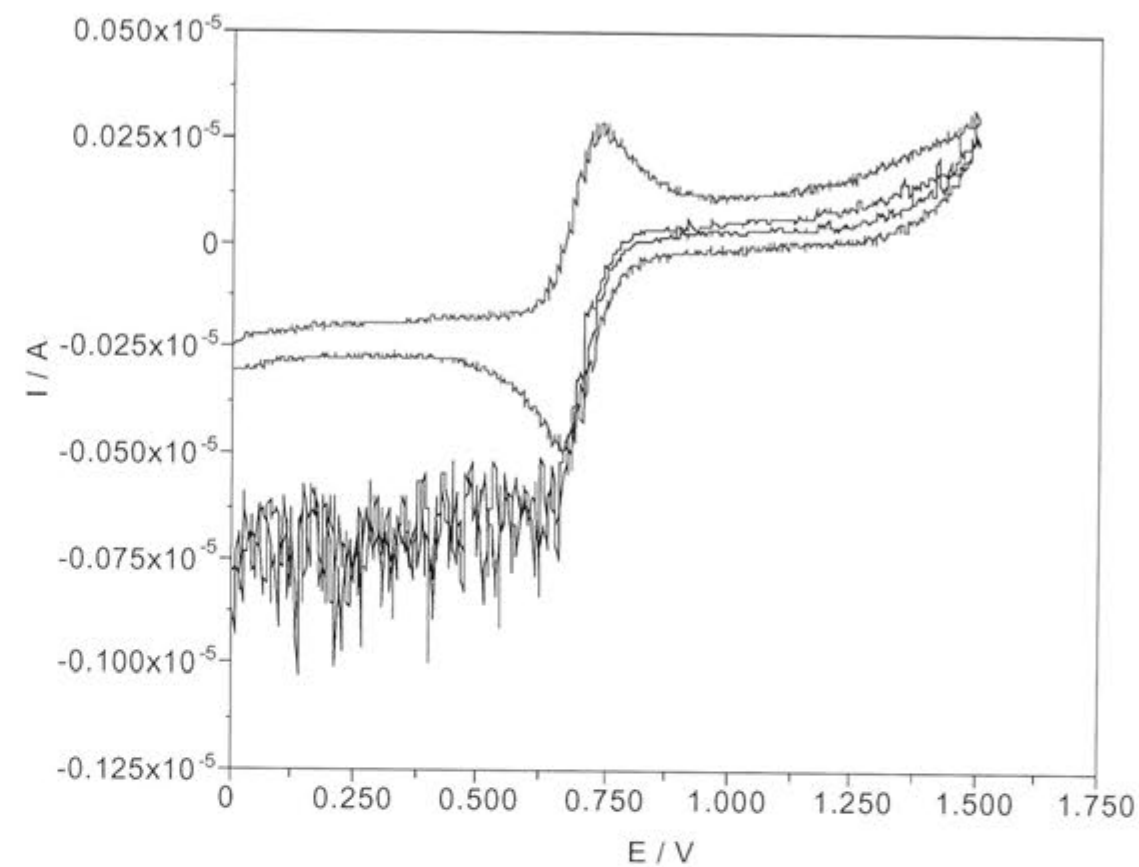


Figure 61. Cyclic voltammogram of $[\text{RuCl}_2(\text{NCMe})_3(\eta^1\text{-Ph}_2\text{P}(\text{CH}_2)_3\text{Ph})]^+$ ($[\mathbf{259}]^+$) in 0.3M $[\text{Bu}_4\text{N}]\text{BF}_4/\text{CH}_2\text{Cl}_2$ at 293K (*vs* Ag/AgCl) (blue); as a stirred solution (black).

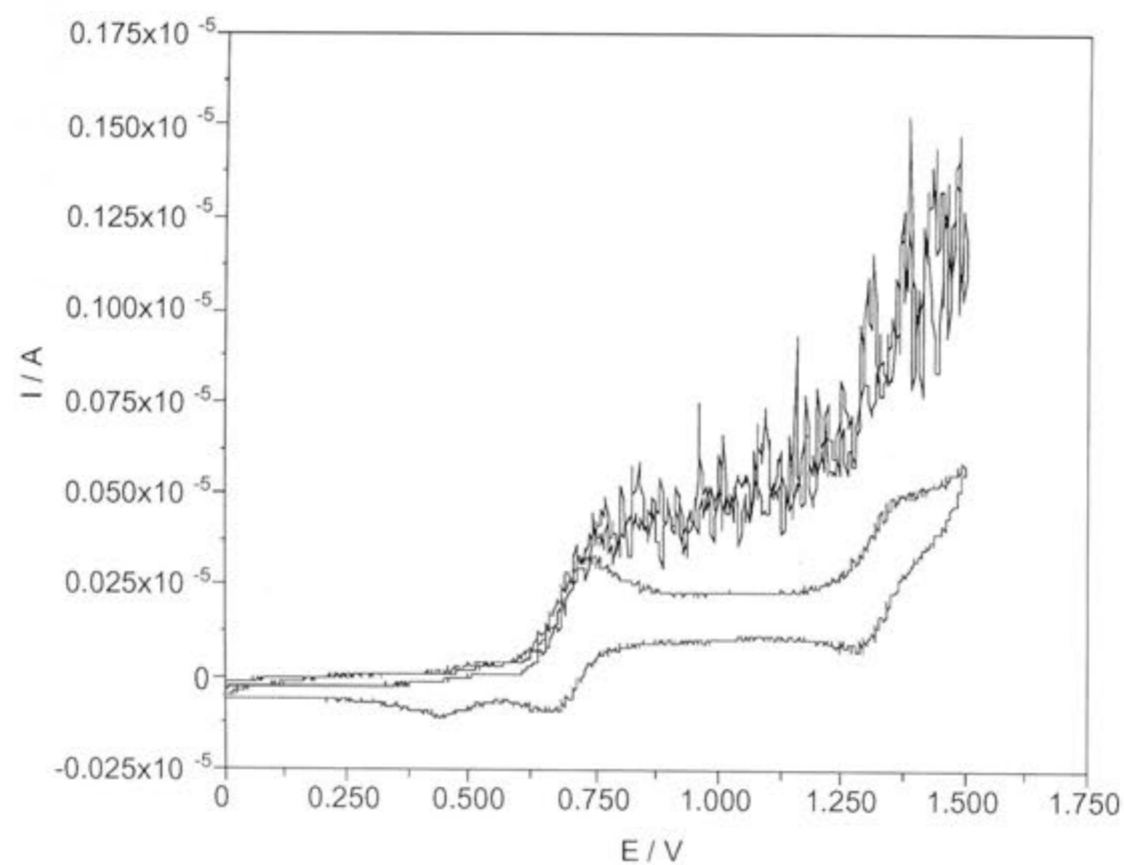


Figure 62. Cyclic voltammogram of $[\text{RuCl}_2(\text{NCMe})_3(\eta^1\text{-Ph}_2\text{P}(\text{CH}_2)_3\text{Ph})]$ (**259**) in 0.3M $[\text{Bu}_4\text{N}]\text{BF}_4/\text{CH}_2\text{Cl}_2$ at 293K (*vs* Ag/AgCl) (blue); as a stirred solution (black).

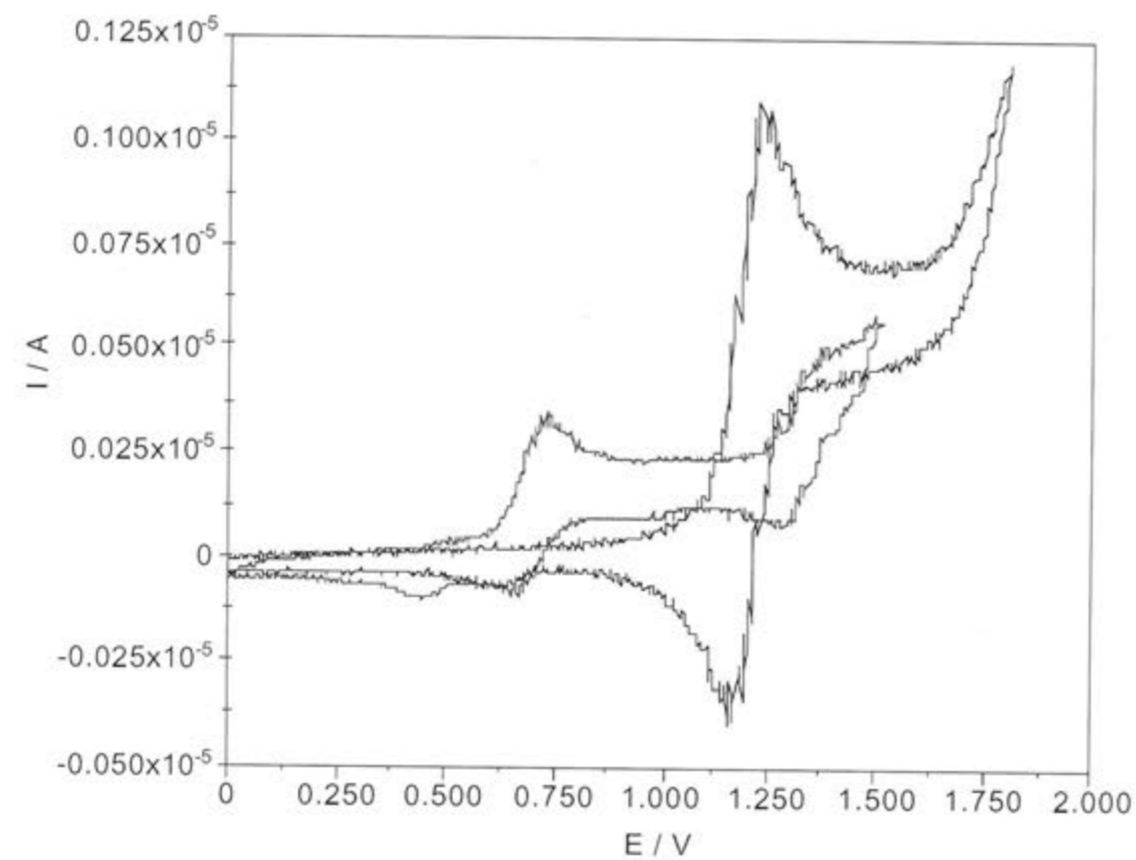


Figure 63. Cyclic voltammogram (blue) of $[\text{RuCl}_2(\text{NCMe})_3(\eta^1\text{-Ph}_2\text{P}(\text{CH}_2)_3\text{Ph})]$ (**259**) in 0.3M $[\text{Bu}_4\text{N}]\text{BF}_4/\text{CH}_2\text{Cl}_2$ at 293K (*vs* Ag/AgCl); cyclic voltammogram (black) of $[\text{RuCl}_2(\eta^1:\eta^6\text{-Ph}_2\text{P}(\text{CH}_2)_3\text{Ph})]$ (**222**) in 0.1M $[\text{Bu}_4\text{N}]\text{BF}_4/\text{CH}_3\text{CN}$ at 293K (*vs* Ag/AgCl).

For comparison with these results, the electrochemical behaviour of $[\text{RuCl}_2(\eta^1:\eta^6\text{-Ph}_2\text{P}(\text{CH}_2)_3\text{Ph})]$ (**222**) was also investigated in butyronitrile. The CV showed a main oxidation process with $E_{\text{pa}} = + 1.26 \text{ V}$ (*vs* Ag/AgCl), $+ 0.73 \text{ V}$ (*vs* $\text{Fc}^{0/1}$), and no reverse peak was detected when the potential was switched (Figure 64). This indicates that the species formed upon oxidation is more stable in butyronitrile than in acetonitrile, thus it would therefore appear that butyronitrile displaces the η^6 -arene of **222** at the Ru(III) level more rapidly than does acetonitrile (see Figure 54). In order to determine the $E_{1/2}$ value, differential pulse voltammetry was performed, which gave $E_{1/2} = + 1.20 \text{ V}$ (*vs* Ag/AgCl), $+ 0.67 \text{ V}$ (*vs* $\text{Fc}^{0/1}$), $\Delta E_{\text{p}} = 40 \text{ mV}$ (*cf.* $E_{1/2} = + 1.27 \text{ V}$ (*vs* Ag/AgCl), $+ 0.80 \text{ V}$ (*vs* $\text{Fc}^{0/1}$) in MeCN). A second process was evident in the CV of **222** in butryonitrile, with $E_{1/2} = + 0.50$ to $+0.78 \text{ V}$ (*vs* Ag/AgCl; $- 0.03$ to $+ 0.25 \text{ V}$ *vs* $\text{Fc}^{0/1}$), which was attributed to a secondary product [i.e. formed as a result of the main oxidation process] (see Figure 64).

Experiments similar to those conducted in acetonitrile showed that a Ru(III) species $[\text{RuCl}_2(\text{NC}(\text{CH}_2)_2\text{Me})_3(\eta^1\text{-Ph}_2\text{P}(\text{CH}_2)_3\text{Ph})]^+$ (**[336]⁺**) formed upon exhaustive oxidation of **222** at $+ 1.50 \text{ V}$ (*vs* Ag/AgCl), $+ 0.98 \text{ V}$ (*vs* $\text{Fc}^{0/1}$) in butyronitrile (Scheme 79a). The CV trace of **[336]⁺** gave a $i_{\text{pa}}/i_{\text{pc}}$ ratio of one, with $E_{1/2} = + 0.68 \text{ V}$ (*vs* Ag/AgCl), $+ 0.15 \text{ V}$ (*vs* $\text{Fc}^{0/1}$), $\Delta E_{\text{p}} = 120 \text{ mV}$ (*cf.* $E_{1/2} = + 0.72 \text{ V}$ (*vs* Ag/AgCl), $+ 0.25 \text{ V}$ (*vs* $\text{Fc}^{0/1}$) for $[\text{RuCl}_2(\text{NCMe})_3(\eta^1\text{-Ph}_2\text{P}(\text{CH}_2)_3\text{Ph})]^+$ (**[259]⁺**) in MeCN) (Figure 64). Coulometry experiments gave the number of electrons as 0.8, which indicates that most of the tethered species **222** had been converted into the cation **[336]⁺**. Steady state voltammetry gave the position of zero current and suggested that the solution contained only the Ru(III) species **[336]⁺**, because no oxidation process was observed. Reduction of **[336]⁺** *via* exhaustive electrolysis at 0.0 V (*vs* Ag/AgCl; $- 0.53 \text{ V}$ (*vs* $\text{Fc}^{0/1}$)) in butyronitrile gave rise to an orange solution, which displayed a two waves, of unequal height; the major one with $i_{\text{pa}}/i_{\text{pc}}$ slightly less than one, with $E_{1/2} = + 0.64 \text{ V}$ (*vs* Ag/AgCl), $+ 0.12 \text{ V}$ (*vs* $\text{Fc}^{0/1}$), $\Delta E_{\text{p}} = 80 \text{ mV}$ (*cf.* $E_{1/2} =$

+ 1.36 V (*vs* Ag/AgCl), + 0.89 V (*vs* Fc^{0/1}) for [RuCl₂(NCMe)₃(η¹-Ph₂P(CH₂)₃Ph)] (259) in MeCN), the other chemically unstable with $E_{pa} = + 1.29$ V (*vs* Ag/AgCl), + 0.77 V (*vs* Fc^{0/1}), (Figure 65). The fact that less than one electron was transferred during the reduction implies that the intermediate Ru(III) species [336]⁺ may undergo some decomposition. Again, steady state voltammetry showed the position of zero current and suggests that solution contained only Ru(II) species, since there were no oxidation processes observed. Since no wave due to free chloride ion (see above) was observed and given that the $E_{1/2}$ of this new Ru(II) species is virtually identical to the CV of the Ru(III) species [336]⁺ (see Figure 65), the new Ru(II) complex formed can only be [RuCl₂(NC(CH₂)₂Me)₃(η¹-Ph₂P(CH₂)₃Ph)] (336) ($E_{1/2} = + 0.68$ V (*vs* Ag/AgCl), + 0.15 V (*vs* Fc^{0/1})) (see Scheme 79b). The smaller chemically unstable wave was due to the starting complex ($E_{pa} = + 1.26$ V (*vs* Ag/AgCl), + 0.74 V (*vs* Fc^{0/1})) (see Figure 66), which had been re-formed during the reduction; it was not observed in the CV of [RuCl₂(NC(CH₂)₂Me)₃(η¹-Ph₂P(CH₂)₃Ph)]⁺ ([336]⁺) (Figure 66).

The formation of tris-[RuCl₂(NC(CH₂)₂Me)₃(η¹-Ph₂P(CH₂)₃Ph)]⁺ ([336]⁺) is analogous to the generation of tris-[RuCl₂(NCMe)₃(η¹-Ph₂P(CH₂)₃Ph)]⁺ ([259]⁺). The formation of tris-[RuCl₂(NC(CH₂)₂Me)₃(η¹-Ph₂P(CH₂)₃Ph)] (336), is however, in contrast to the reduction of the tris-[259]⁺ in acetonitrile, which lost chloride ion to form the tetrakis-species [RuCl₂(NCMe)₄(η¹-Ph₂P(CH₂)₃Ph)]⁺ ([328]⁺). Thus butyronitrile does not displace chloride ion as easily as acetonitrile does.

As in the previous instance, the ¹H NMR spectrum (in CD₂Cl₂) of the crude oil, obtained after removal of the solvent from 336, was largely uninformative. The ³¹P{¹H}-NMR spectrum, however, showed two resonances, at δ 67.3 and 67.7, the former being the more intense (since the spectrum was only recorded in this region it was not established if any

[RuCl₂(η¹:η⁶-Ph₂P(CH₂)₃Ph)] (**222**) was present at this stage). The chemical shifts in the region δ 67 are very similar to those of [RuCl₂(NCMe)₃(η¹-Ph₂P(CH₂)₃Ph)] (**259**), (δ 66.7 and 67.3), and are clearly not due to the tetrakis-species [RuCl₂(NC(CH₂)₂Me)₄(η¹-Ph₂P(CH₂)₃Ph)]Cl ([**335**]Cl) [δ 47.6 and 52.0] (see Chapter 4, Section 4.1). If the sample was allowed to stand for several days, quantitative conversion to the *trans*- and *cis*-isomers of the tetrakis-complex [RuCl(NC(CH₂)₂Me)₄(η¹-Ph₂P(CH₂)₃Ph)]Cl ([**335**]Cl) occurred, presumably resulting from reaction with small amounts of butyronitrile present in the oil. The conversion, however, was slower than that observed for the analogous acetonitrile complexes. The formation of *cis*- and *trans*-isomers of [**335**]Cl was indicated by the appearance of the two expected signals in the ³¹P{¹H}-NMR spectrum (see Chapter 4, Section 4.1), accompanied by two other single resonances at δ 22.4 and 31.4. The four signals were present in approximate intensities, in order of decreasing field, of 2:3:9:3, respectively. The peak at δ 22.4 confirmed the additional presence (*ca* 12%) of regenerated **222**. The IR spectrum of **336** showed a ν(CN) band at 2251 cm⁻¹ indicative of the coordinated nitrile ligands. The mass spectrum could not, however, be obtained.

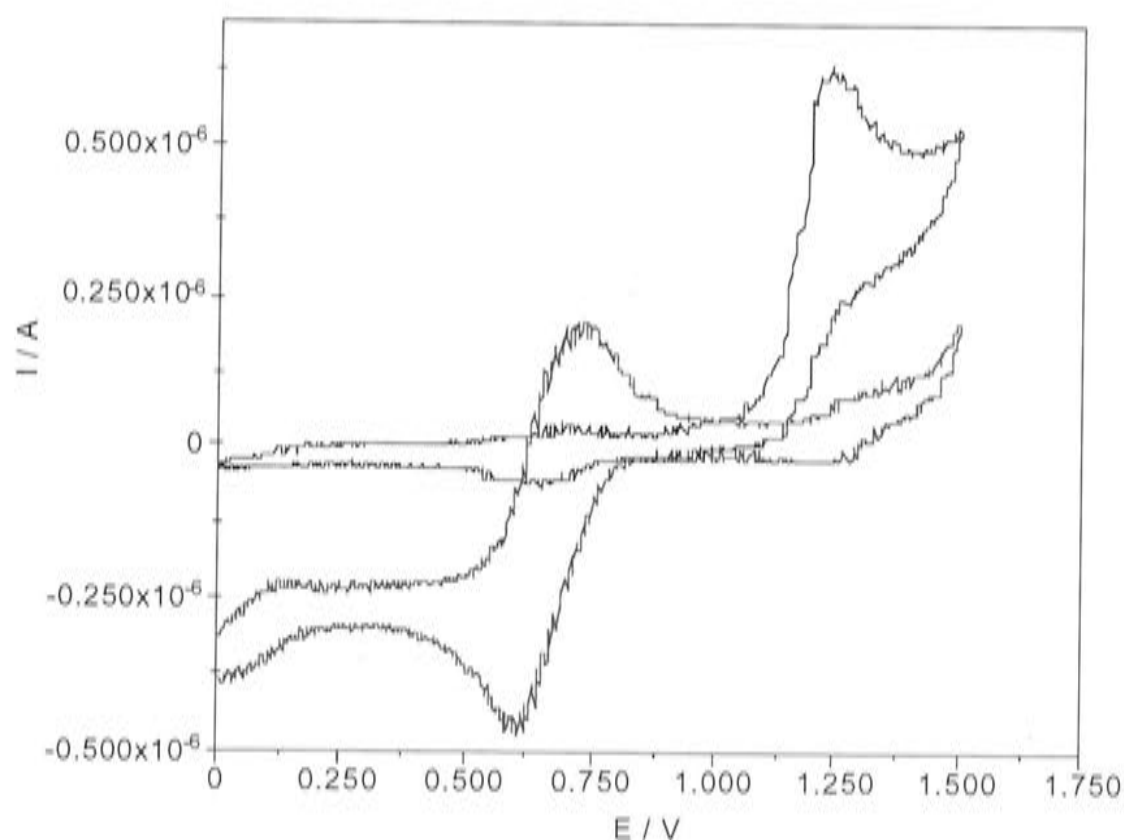


Figure 64. Cyclic voltammogram (black) of $[\text{RuCl}_2(\eta^1:\eta^6\text{-Ph}_2\text{P}(\text{CH}_2)_3\text{Ph})]$ (**222**) in 0.1M $[\text{Bu}^n_4\text{N}]\text{BF}_4/\text{CH}_3(\text{CH}_2)_2\text{CN}$ at 293K (*vs* Ag/AgCl); cyclic voltammogram (blue) of $[\text{RuCl}_2(\text{NC}(\text{CH}_2)_2\text{Me})_3(\eta^1\text{-Ph}_2\text{P}(\text{CH}_2)_3\text{Ph})]^+$ (**[336]⁺**) in 0.1M $[\text{Bu}^n_4\text{N}]\text{BF}_4/\text{CH}_3(\text{CH}_2)_2\text{CN}$ at 293K (*vs* Ag/AgCl).

The results of the CPE experiments cast doubt on the conclusions reported by Smith and Wright,²¹ who stated that the tris-complex $[\text{RuCl}_2(\text{NCMe})_3(\eta^1\text{-Ph}_2\text{P}(\text{CH}_2)_3\text{Ph})]$ (**259**) was prepared *via* exhaustive electrolysis of the non-tethered complex $[\text{RuCl}_2(\eta^6\text{-1,4-MeC}_6\text{H}_4\text{CHMe}_2)(\eta^1\text{-Ph}_2\text{P}(\text{CH}_2)_3\text{Ph})]$ (**223**) in acetonitrile at room temperature (see Scheme 59a, Chapter 3, Section 3.2.6). Whilst anodic oxidation of **223** in acetonitrile probably gave rise to **[259]⁺**, it is clear that exhaustive reduction in acetonitrile at room temperature gives the tetrakis-complex $[\text{RuCl}(\text{NCMe})_4(\eta^1\text{-Ph}_2\text{P}(\text{CH}_2)_3\text{Ph})]^+$ (**[328]⁺**), rather than the tris-compound **259**. Therefore, it seems likely that Smith and Wright actually formed the tetrakis-complex **[328]⁺** during reduction of **[259]⁺** in acetonitrile at room temperature. Further, since acetonitrile rapidly replaces a chloride ligand of the tris-species **259** to give the tetrakis-complex **[328]⁺**, the formation of **259** is unlikely under the conditions employed by Smith and Wright.²¹ This will be discussed in more detail in Chapter 7 (Section 7.2), in relation to the observations in Chapter 4.

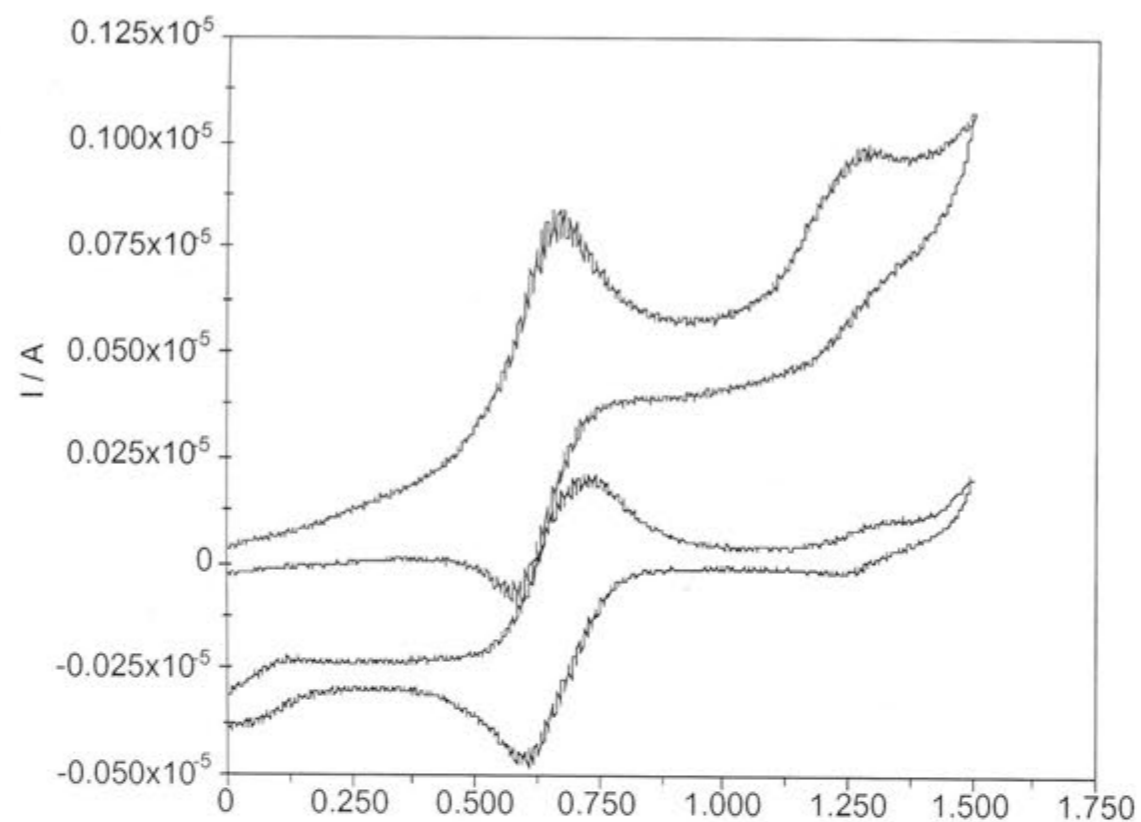


Figure 65. Cyclic voltammogram (black) of $[\text{RuCl}_2(\text{NC}(\text{CH}_2)_2\text{Me})_3(\eta^1\text{-Ph}_2\text{P}(\text{CH}_2)_3\text{Ph})]^+$ (**[336]⁺**) in 0.1M $[\text{Bu}_4\text{N}]\text{BF}_4/\text{CH}_3(\text{CH}_2)_2\text{CN}$ at 293K (*vs* Ag/AgCl); cyclic voltammogram (blue) of $[\text{RuCl}_2(\text{NC}(\text{CH}_2)_2\text{Me})_3(\eta^1\text{-Ph}_2\text{P}(\text{CH}_2)_3\text{Ph})]$ (**336**) in 0.1M $[\text{Bu}_4\text{N}]\text{BF}_4/\text{CH}_3(\text{CH}_2)_2\text{CN}$ at 293K (*vs* Ag/AgCl).

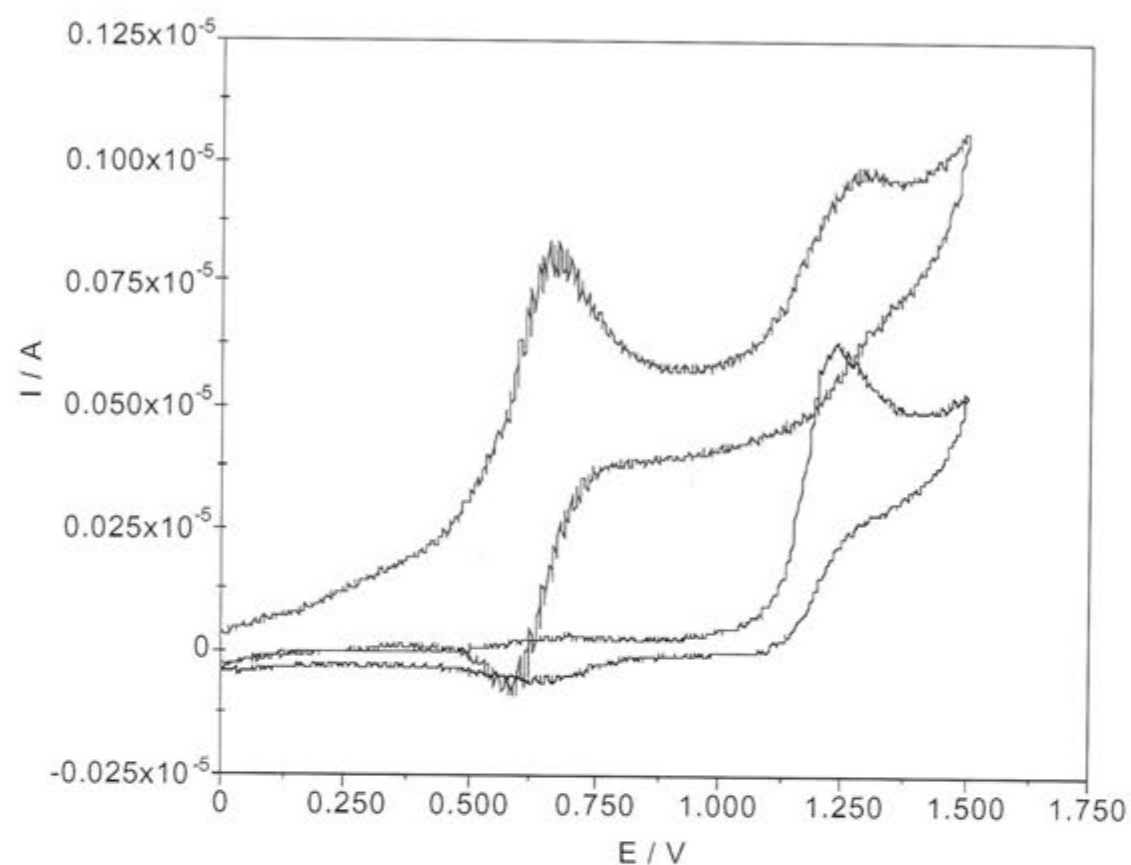
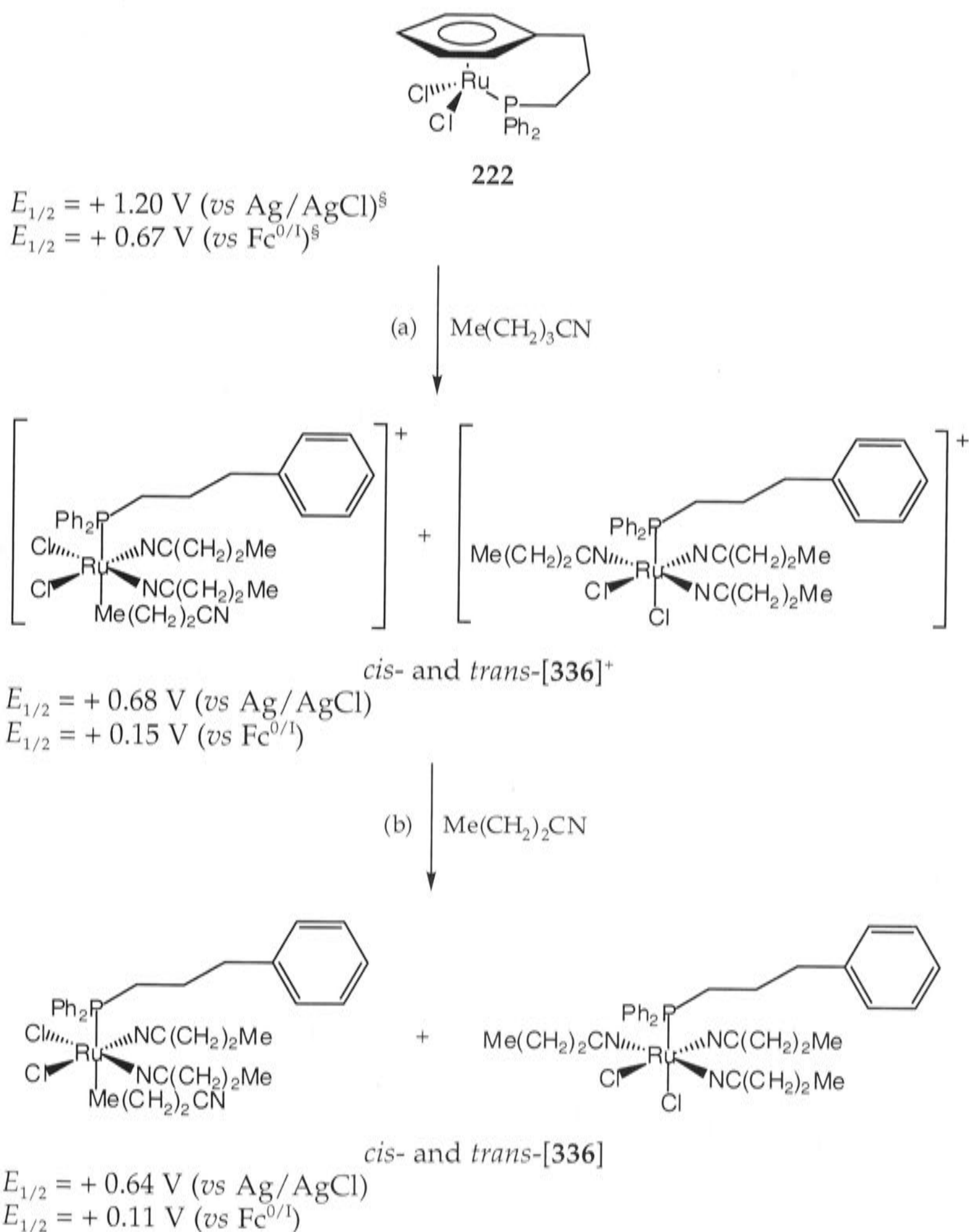


Figure 66. Cyclic voltammogram (blue) of $[\text{RuCl}_2(\text{NC}(\text{CH}_2)_2\text{Me})_3(\eta^1\text{-Ph}_2\text{P}(\text{CH}_2)_3\text{Ph})]$ (**336**) in 0.1M $[\text{Bu}_4\text{N}]\text{BF}_4/\text{CH}_3(\text{CH}_2)_2\text{CN}$ at 293K (*vs* Ag/AgCl); cyclic voltammogram (black) of $[\text{RuCl}_2(\eta^1:\eta^6\text{-Ph}_2\text{P}(\text{CH}_2)_3\text{Ph})]$ (**222**) in 0.1M $[\text{Bu}_4\text{N}]\text{BF}_4/\text{CH}_3(\text{CH}_2)_2\text{CN}$ at 293K (*vs* Ag/AgCl).



Scheme 79. Formation of the tris-complex $[\text{RuCl}_2(\text{NC}(\text{CH}_2)_3\text{Me})_3(\eta^1\text{-Ph}_2\text{P}(\text{CH}_2)_3\text{Ph})]$ (**336**) during exhaustive anodic oxidation experiments in butyronitrile. [§]Electrode potential obtained from differential pulse voltammetry (CV showed chemically unstable electrochemical behaviour). Reaction conditions: (a) platinum gauze working electrode, 0.1M $[\text{Bu}_4\text{N}]\text{BF}_4$, + 0.97 V (vs $\text{Fc}^{0/1}$); (b) platinum gauze working electrode, 0.1M $[\text{Bu}_4\text{N}]\text{BF}_4$, - 0.53 V (vs $\text{Fc}^{0/1}$).

Both CV and $^{31}\text{P}\{^1\text{H}\}$ -NMR spectroscopy show that the parent complex $[\text{RuCl}_2(\eta^1:\eta^6\text{-Ph}_2\text{P}(\text{CH}_2)_3\text{Ph})]$ (**222**) was formed as a by-product in the CPE of $[\mathbf{259}]^+$ in dichloromethane, although the amount (*ca* 4% by $^{31}\text{P}\{^1\text{H}\}$ -NMR spectroscopy) is not consistent with the 78% yields obtained in the Ph.D. dissertation of P. D. Smith³⁴ (see Scheme 59c, Chapter 3, Section 3.2.6).

5.3 Summary

The non-tethered and tethered complexes generally show virtually identical cyclic voltammetric behaviour, that is, chemically stable one-electron oxidation with $E_{1/2}$ -values in the range +0.50 to +0.87 V (*vs* $\text{Fc}^{0/1}$). The spectroelectrochemical behaviour of these complexes was generally the same below *ca* 228K, though there were differences above this temperature. The electrogenerated arene-Ru(III) complexes could be detected by means of their UV/Vis spectra; the non-tethered compounds were not stable above *ca* 238K, whereas many of the electrogenerated tethered-Ru(III) species displayed some thermal stability under ambient conditions. Typical ESR spectra for Ru(III) were detected at 5K, with the g -values ranging between 1.93 and 2.37. The stability of $[\text{RuCl}_2(\eta^1:\eta^6\text{-Ph}_2\text{P}(\text{CH}_2)_3\text{Ph})]$ (**222**), in a variety of solvents was investigated using CPE experiments. Displacement of the η^6 -arene and coordination of several solvent molecules occurred readily at the ruthenium(III) level giving complexes of the type $[\text{RuCl}_2(\text{NCR})_3(\eta^1\text{-Ph}_2\text{P}(\text{CH}_2)_3\text{Ph})]^+$ ($\text{R} = \text{Me}$ ($[\mathbf{259}]^+$), $(\text{CH}_2)_2\text{Me}$ ($[\mathbf{336}]^+$)); reduction of $[\mathbf{259}]^+$ in acetonitrile caused replacement of one chloride ligand by acetonitrile giving the tetrakis-complex $[\text{RuCl}(\text{NCMe})_4(\eta^1\text{-Ph}_2\text{P}(\text{CH}_2)_3\text{Ph})]^+$ ($[\mathbf{328}]^+$). These observations will be discussed in Chapter 7, Section 7.2. The spectroelectrochemistry and ESR data suggest that the pentamethyl-substituted tethered arene complex $[\text{RuCl}_2(\eta^1:\eta^6\text{-Ph}_2\text{P}(\text{CH}_2)_3\text{C}_6\text{Me}_5)]$ (**251**) is an obvious candidate for attempting the isolation of salts of the arene-ruthenium(III) cation $[\mathbf{251}]^+$ because of the greater stability of $[\mathbf{251}]^+$ at room temperature. Investigation

into the preparation of arene-ruthenium(III) complexes *via* chemical oxidation reactions will be discussed in Chapter 6.

References

- (1) Bard, A. J.; Faulkner, L. R. *Electrochemical Methods: Fundamentals and Applications*; 2nd ed.; John Wiley & Sons, Inc.: New York, 2001, p. 241.
 - (1a) ref. 1, p. 233.
 - (2) ref. 1, p. 399.
- (3) Devanne, D.; Dixneuf, P. H. *J. Organomet. Chem.* **1990**, *390*, 371-378.
- (4) Treichel, P. M. *Advances in Organometallic Chemistry*; Stone, F. G. A.; West, R. Ed., Academic Press: New York, 1973; Vol. 11, pp. 21-86.
- (5) Sarapu, A. C.; Fenske, R. F. *Inorg. Chem.* **1975**, *14*, 247-253.
- (6) Bursten, B. E.; Green, M. R. *Progress in Inorganic Chemistry*, Lippard, S. J. Ed., John Wiley & Sons, Inc.: New York, 1988; Vol. 36, pp. 393-485.
 - (7) ref. 1, p. 899.
 - (8) Suskina, I. A.; Gribov, B. G.; Idrisova, R. A.; Denisovich, L. I.; Gubin, S. P. *Dokl. Akad. Nauk SSSR* **1971**, 425-427.
 - (9) Yur'eva, L. P.; Peregudova, S. M.; Nekrasov, L. N.; Korotkov, A. P.; Zaitseva, N. N.; Zakurin, N. V.; Vasil'kov, A. Yu. *J. Organomet. Chem.* **1981**, *219*, 43-51.
 - (10) Yur'eva, L. P.; Peregudova, S. M.; Kravtsov, D. N.; Vasil'kov, A. Yu.; Nekrasov, L. N.; Asfandiarov, N. L.; Timoshenko, M. M.; Chizhov, Yu. V. *J. Organomet. Chem.* **1987**, *336*, 371-376.
 - (11) Deeming, A. J. *Comprehensive Organometallic Chemistry*; Wilkinson, G.; Stone, F. G. A.; Abel, E. W. Ed., Pergamon: Oxford, 1982; Vol. 4, p. 481.
 - (12) Koepp, H. M.; Wendt, H.; Strehlow, H. Z. *Elektrochem.* **1960**, *64*, 483-491.

- (13) Hoh, G. L. K.; McEwen, W. E.; Kleinberg, J. *J. Am. Chem. Soc.* **1961**, *83*, 3949-3953.
- (14) Gale, R. J.; Singh, P. *J. Organomet. Chem.* **1980**, *199*, C44-C46.
- (15) Gritzner, G.; Kuta, J. *Pure Appl. Chem.* **1982**, *54*, 1527-1532.
- (16) Gritzner, G.; Kuta, J. *Pure Appl. Chem.* **1984**, *56*, 461-466.
- (17) Boéré, R. T.; Roemmele, T. L. *Coord. Chem. Rev.* **2000**, *210*, 369-445.
- (18) Ceccanti, A.; Diversi, P.; Ingrosso, G.; Laschi, F.; Lucherini, A.; Magagna, S.; Zanello, P. *J. Organomet. Chem.* **1996**, *526*, 251-262.
- (19) Ghebreyessus, K. Y.; Nelson, J. H. *Organometallics* **2000**, *19*, 3387-3392.
- (20) Bhalla, R.; Boxwell, C. J.; Duckett, S. B.; Dyson, P. J.; Humphrey, D. G.; Steed, J. W.; Suman, P. *Organometallics* **2002**, *21*, 924-928.
- (21) Smith, P. D.; Wright, A. H. *J. Organomet. Chem.* **1998**, *559*, 141-147.
- (22) Dilworth, J. R.; Zheng, Y.; Lu, S.; Wu, Q. *Inorg. Chim. Acta* **1992**, *194*, 99-103.
- (23) Bennett, M. A.; Heath, G. A.; Hockless, D. C. R.; Kovácik, I.; Willis, A. C. *J. Am. Chem. Soc.* **1998**, *120*, 932-941.
- (24) Bennett, M. A.; Heath, G. A.; Hockless, D. C. R.; Kovácik, I.; Willis, A. C. *Organometallics* **1998**, *17*, 5867-5873.
- (25) Bennett, M. A.; Byrnes, M. J.; Willis, A. C. *Organometallics* **2003**, *22*, 1018-1028.
- (26) Lever, A. B. P. *Inorganic Electronic Spectroscopy*; Elsevier Publishing Company, Inc.: Amsterdam, 1984, p. 334.
- (27) Drago, R. S. *Physical Methods in Chemistry*; Saunders College Publishing: Philadelphia, 1977, p. 92.
- (28) Hudson, A.; Kennedy, M. J. *J. Chem. Soc. A* **1969**, 1116-1120.
- (29) Ebsworth, E. A. V.; Rankin, D. W. H.; Craddock, S. *Structural Methods in Inorganic Chemistry*; Blackwell Scientific Publications: Oxford, 1987, pp. 105-106.
- (30) ref. 27, p. 486.

- (31) ref. 27, p. 492
- (32) ref. 27, pp. 317-318.
- (33) ref. 27, p. 649.
- (34) Smith, P. D. Ph.D. Dissertation; University of Nottingham: Nottingham, 1993.
- (35) Abbenhuis, R. A. T. M.; del Río, I.; Bergshoef, M. M.; Boersma, J.; Veldman, N.; Spek, A. L.; van Koten, G. *Inorg. Chem.* **1998**, *37*, 1749-1758.
- (36) ref. 1.
- (37) Leising, R. A.; Kubow, S. A.; Churchill, M. R.; Buttrey, L. A.; Ziller, J. W.; Takeuchi, K. J. *Inorg. Chem.* **1990**, *29*, 1306-1312.
- (38) Poddar, R. K.; Agarwala, U. J. *Inorg. Nucl. Chem.* **1973**, *35*, 567-575.
- (39) Poddar, R. K.; Agarwala, U. J. *Inorg. Nucl. Chem.* **1973**, *35*, 3769-3779.
- (40) Hundekar, A. M.; Gopinathan, C. *Ind. J. Chem.* **1986**, *25A*, 376.
- (41) Leising, R. A.; Kubow, S. A.; Takeuchi, K. J. *Inorg. Chem.* **1990**, *29*, 4569-4574.
- (42) del Río, I.; Gossage, R. A.; Lutz, M.; Spek, A. L.; van Koten, G. *J. Organomet. Chem.* **1999**, *583*, 69-79.
- (43) Bianchini, C.; Lee, H. M. *Organometallics* **2000**, *19*, 1833-1840.
- (44) Çetinkaya, B.; Çetinkaya, E.; Brookhart, M.; White, P. S. *J. Mol. Cat. A* **1999**, *142*, 101-112.

*Chapter 6: Chemical Oxidation Reactions of
Tethered and Non-Tethered Arene Complexes*

The spectroelectrochemistry and ESR results of Chapter 5 show that, of the tethered complexes, the peralkylated systems might be sufficiently stable to allow isolation of the arene-Ru(III) species, despite the high electrode potentials. The tethered complex $[\text{RuCl}_2(\eta^1:\eta^6\text{-Ph}_2\text{P}(\text{CH}_2)_3\text{C}_6\text{Me}_5)]$ (**251**) displayed the lowest electrode potential ($E_{1/2} = + 0.55 \text{ V vs Fc}^{0/1}$), indicating that the arene-Ru(III) species is more accessible than the other similar arene-Ru(III) systems. Further, the one-electron oxidation product of **251** was the most thermally stable.

As noted in Chapter 5 (Section 5.1), the potentials for the $\text{Ru}^{\text{II/III}}$ couple of the arene-ruthenium(II) complexes lie in the range $+ 0.50\text{-}0.87 \text{ V vs Fc}^{0/1}$ in CH_2Cl_2 . The lower values correspond to complexes containing alkyl-substituted η^6 -arenes, which were selected as precursors in attempts to generate the corresponding arene-ruthenium(III) species *via* chemical oxidation reactions. The chemical oxidant chosen must have a greater potential (generally at least *ca* 50 mV) than that of the Ru(II) complex to be oxidised, and, for three reasons, the triarylamminium salt $[\text{N}(\text{C}_6\text{H}_4\text{Br-4})_3]\text{SbCl}_6$ (**[48]SbCl₆**) ($E^{\circ'} = + 0.70 \text{ V vs Fc}^{0/1}$ in CH_2Cl_2 , based on the conversion factor stated in Table 3, Chapter 1, Section 1.1.3),^{1,2} was selected. First, as noted in Chapter 1, it is relatively chemically inert, unlike other oxidants of comparable potential, such as $[\text{NO}]^+$, even though $[\text{NO}]^+$ would be a strong enough oxidant ($E^{\circ'} = + 1.00 \text{ V vs Fc}^{0/1}$).³ Secondly, the redox potential is considerably greater than several of the arene-ruthenium(II) complexes to be studied. Chlorine is not a strong enough oxidant ($E^{\circ'} = + 0.18 \text{ V vs Fc}^{0/1}$ in MeCN, based on the conversion factor stated in Table 3),^{2,4} and it also acts as a two-electron oxidant.

The formal electrode potential of silver ion in dichloromethane is reported to be $+ 0.41 \text{ V vs SCE}$.⁵ In Table 2 of reference(2), the conversion factor to $\text{Fc}^{0/1}$ is given as $- 0.46 \text{ V}$, but this does not lead to the listed potential of Ag^+ of $+$

0.65 V (*vs* $\text{Fc}^{0/1}$). If it is assumed that the latter value is correct, it is clear that the Ag^+ would oxidise some of the arene-ruthenium(II) complexes, thus allowing anions other than $[\text{SbCl}_6]^-$ to be used. However, the finely divided silver produced can be difficult to remove.

The most compelling advantage of the oxidant $[\mathbf{48}]^+$ is that it is commercially available as the $[\text{SbCl}_6]^-$ salt, and does not need to be generated *in situ*. Its PF_6 salt, which was prepared *in situ*⁶ by reacting $\text{N}(\text{C}_6\text{H}_4\text{Br-4})_3$ with $[\text{NO}]\text{PF}_6$, has been used to oxidise manganese(I) complexes such as *cis,cis*- $[\text{Mn}(\text{CN})(\text{CO})_2\{\text{P}(\text{OPh})_3\}(\eta^2\text{-dppm})]$.⁷

6.1 Chemical Oxidation Reactions of Arene-Ruthenium(II) Complexes

In initial experiments, the arene-Ru(II) compounds were treated with a slight deficiency of oxidant $[\text{N}(\text{C}_6\text{H}_4\text{Br-4})_3]\text{SbCl}_6$ ($[\mathbf{48}]\text{SbCl}_6$), since it was envisaged that excess oxidant would be difficult to remove due to its limited solubility ($[\mathbf{48}]\text{SbCl}_6$ is less soluble in CH_2Cl_2 than $[\mathbf{48}]\text{ClO}_4$).⁸

Complex $[\text{RuCl}_2(\eta^1:\eta^6\text{-Ph}_2\text{P}(\text{CH}_2)_3\text{C}_6\text{Me}_5)]$ (**251**) was treated with either 0.9 or one equivalent of $[\mathbf{48}]\text{SbCl}_6$ at *ca* -40°C in dichloromethane in the absence of light. The product was precipitated by addition of *n*-hexane and isolated as a microcrystalline pink solid in good yield (Scheme 80). Its colour is recognisably different from that of the Ru(II) precursor **251**, which is orange. It was soluble in both dichloromethane and THF, but not in *n*-hexane. In order to prevent reversion to the Ru(II) precursor, the product was routinely handled in the absence of light and moisture, whilst being maintained at low temperature (*ca* -40°C). In addition, in view of the expected lability of the η^6 -arene, the sample was handled under an inert atmosphere, although there is no specific evidence regarding its sensitivity to air, light, temperature or moisture. Elemental analyses of two independent samples were in only moderate agreement (an example is given on page 410, Chapter 8, Section 8.2) with the values expected for the formulation $[\mathbf{251}][\text{SbCl}_6].0.5\text{CH}_2\text{Cl}_2$, established by X-ray crystallography (see later) and showed that the samples

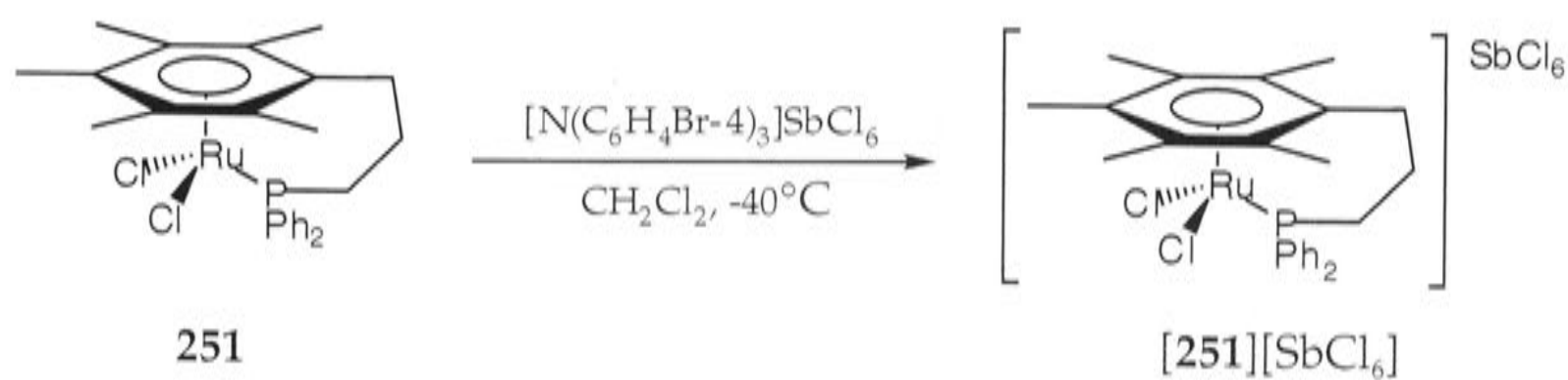
contained no nitrogen that could have arisen from the presence of either unchanged oxidant [48]SbCl₆ or its reduction product N(C₆H₄Br-4)₃ (49) in the solid product [251][SbCl₆]. Despite this, both the UV/Vis and ESR spectra of two similarly prepared, independent samples show the presence of unchanged [48]SbCl₆.

The UV/Vis spectrum in CH₂Cl₂ shows a broad, ill-resolved maximum at 492 nm (20300 cm⁻¹) [$\epsilon = 2300 \text{ L mol}^{-1}\text{cm}^{-1}$] in a range of broad, otherwise featureless absorption between *ca* 28500 and 20500 cm⁻¹ (Figure 67) *cf.* 365 nm (27400 cm⁻¹) [$\epsilon = 4300 \text{ L mol}^{-1}\text{cm}^{-1}$] for the parent complex 251. In addition, there are two broad maxima at *ca* 346 nm (28900 cm⁻¹) [$\epsilon = 2300 \text{ L mol}^{-1}\text{cm}^{-1}$] and 798 nm (12500 cm⁻¹) [$\epsilon = 2200 \text{ L mol}^{-1}\text{cm}^{-1}$], whose profiles are is similar to that of the oxidant [48]SbCl₆, which showed two maxima at *ca* 360 nm (27800 cm⁻¹) and 700 nm (14300 cm⁻¹) [ϵ was not determined] in CH₃CN.⁹ There was also a maximum at *ca* 270 nm (37000 cm⁻¹), but this was not observed in the electronic spectrum of 251[SbCl₆] since it was masked by the absorption due to the ruthenium(III) species. Schmidt and Steckhan¹⁰ also report the UV/Vis spectrum of [48]SbCl₆ in CHCl₃, but have only quoted $\lambda_{\text{max}} = 700 \text{ nm}$ (14300 cm⁻¹), without the extinction coefficient. The λ_{max} at *ca* 270 nm is probably due to the SbCl₆ anion, since the UV/Vis spectra of either the BF₄ or PF₆ salts in CH₃CN do not show any significant absorption below *ca* 320 nm (31300 cm⁻¹).^{6,9} Thus the maxima at *ca* 346 and 798 nm in the electronic spectrum of [251][SbCl₆] may be due to a small amount of unchanged oxidant (this sample was not the same as that used in the elemental analyses). In agreement with this assignment, the electronic spectrum of a dichloromethane solution of 251 treated with 0.7 equivalents of 48 did not show the absorptions at *ca* 350 or 800 nm. This problem of sampling arose because of the small scale on which the experiments had to be carried out and the limited amount and sensitivity of the samples available.

The UV/Vis spectrum of the electrogenerated sample of [251]⁺ (Figure 68) showed three maxima at *ca* 344 nm (29100 cm⁻¹) [$\epsilon = 5100 \text{ L mol}^{-1}\text{cm}^{-1}$], 407 nm

(24600 cm^{-1}) [$\epsilon = 4500 \text{ L mol}^{-1}\text{cm}^{-1}$] and 512 nm (19500 cm^{-1}) [$\epsilon = 2200 \text{ L mol}^{-1}\text{cm}^{-1}$]. Comparison of the two electronic spectra is difficult because of the very poor resolution of the spectrum of the isolated solid **251**[SbCl₆] (Figure 67) in solution, although the ranges of absorption are the same; *ca* 29000 to 20000 cm^{-1} . It is not clear why the electronic spectrum of the isolated solid is so poorly resolved. I have not investigated further the cause of the discrepancy between the observed maxima of the two UV/Vis spectra.

The ¹H NMR spectrum (in CD₂Cl₂) of [**251**][SbCl₆] showed only three signals, a multiplet at δ 1.81, and two doublets at δ 2.23 ($J = 1 \text{ Hz}$) and 2.30 ($J = 2 \text{ Hz}$), presumably corresponding to the CH₂ groups. The magnitude of these chemical shifts was similar to, but distinct from, those observed for [RuCl₂($\eta^1:\eta^6$ -Ph₂P(CH₂)₃C₆Me₅)] (**251**), namely, multiplets at δ 2.16 and 2.40, and a doublet at δ 2.22 ($J = 2.5 \text{ Hz}$) in CDCl₃ (see Chapter 8, p. 410). No signal was detected in the ³¹P{¹H}-NMR spectrum of [**251**][SbCl₆]. A dichloromethane solution of [**251**][SbCl₆] displayed an ESR signal at *ca* 5K in frozen CH₂Cl₂, which was similar to that observed for an electrogenerated sample of [**251**]⁺, (see Figure 69). However, a signal due to unchanged [**48**]SbCl₆ was also evident. The ESR spectrum was recorded on a different sample from that used for the elemental analyses. A few crystals of [**251**][SbCl₆] suitable for X-ray crystallography were obtained from CH₂Cl₂/*n*-hexane at *ca* -11°C; the results will be described later.



Scheme 80. Synthesis of the arene-Ru(III) complex [**251**][SbCl₆] *via* chemical oxidation of **251** by [N(C₆H₄Br-4)₃]SbCl₆ ([**48**]SbCl₆).

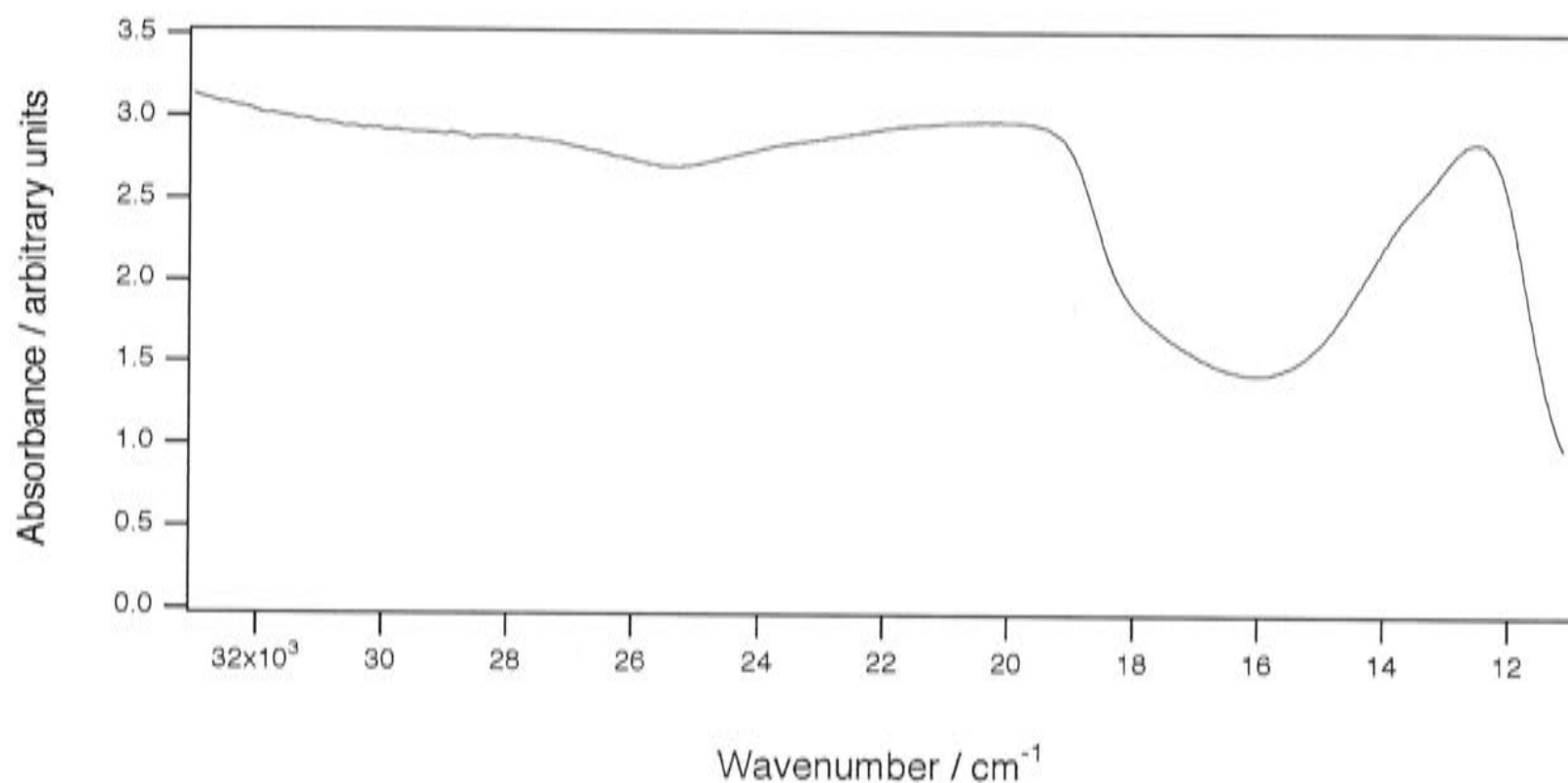


Figure 67. Electronic spectrum of isolated $[\text{RuCl}_2(\eta^1:\eta^6\text{-Ph}_2\text{P}(\text{CH}_2)_3\text{C}_6\text{Me}_5)][\text{SbCl}_6]$ (**[251]** $[\text{SbCl}_6]$) in CH_2Cl_2 at ambient temperature.

Treatment of $[\text{RuCl}_2(\eta^1:\eta^6\text{-}i\text{-Pr}_2\text{P}(\text{CH}_2)_3\text{Ph})]$ (**249**) with one equivalent of the oxidant $[\text{N}(\text{C}_6\text{H}_4\text{Br-4})_3]\text{SbCl}_6$ (**[48]** SbCl_6) did not yield any isolable product, and it is not clear whether **[249]** $[\text{SbCl}_6]$ was actually formed. Since the electrode potential of **249** ($E_{1/2} = +0.78$ V *vs* $\text{Fc}^{0/1}$ in CH_2Cl_2) is greater than that of **[48]** SbCl_6 ($E_{1/2} = +0.70$ V *vs* $\text{Fc}^{0/1}$ in CH_2Cl_2), complete oxidation is expected only when a large excess of oxidant is used. However, treatment of **249** with a tenfold excess of oxidant also failed to yield any isolable product.

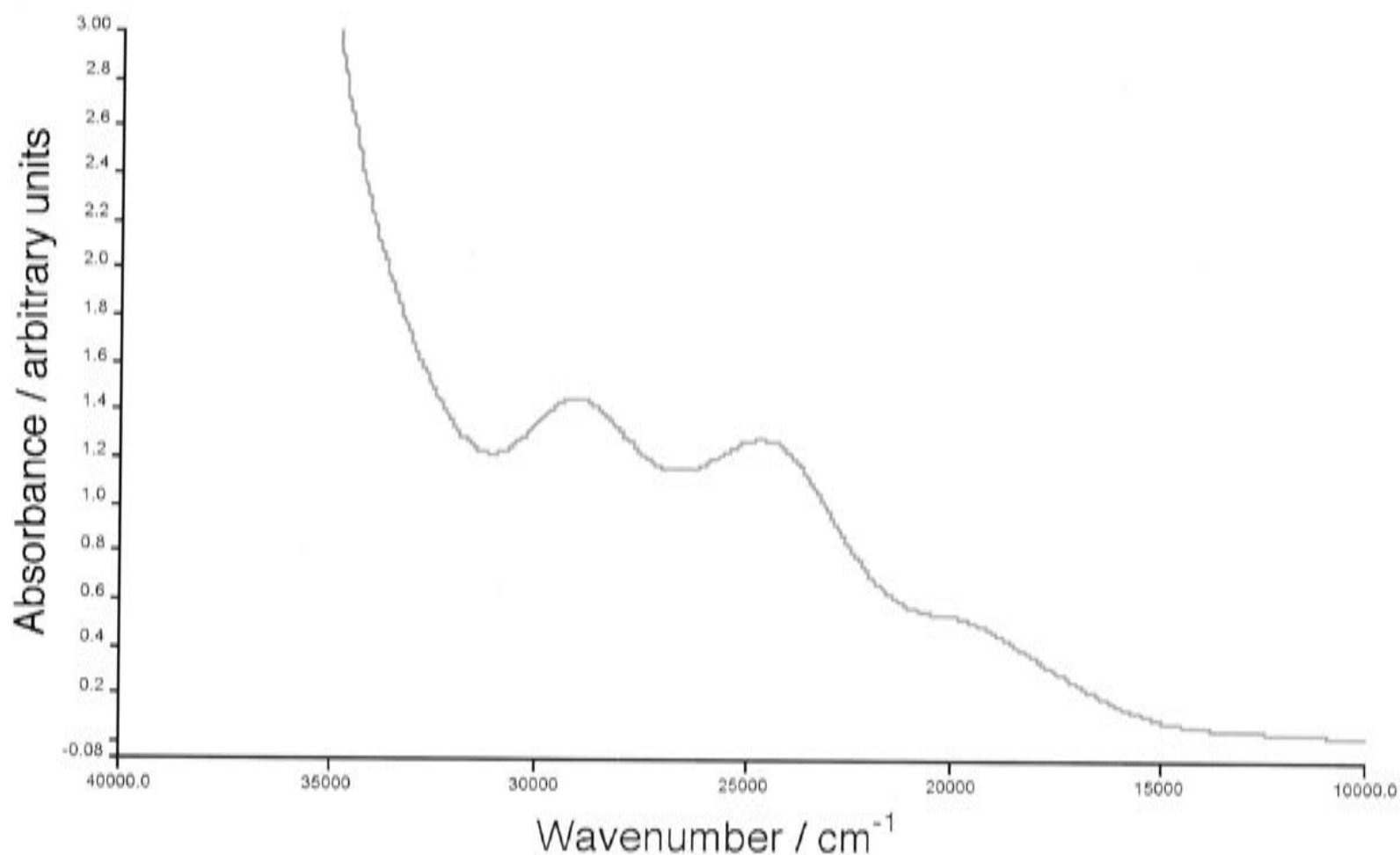


Figure 68. Electronic spectrum of the electrogenerated cation $[\text{RuCl}_2(\eta^1:\eta^6\text{-Ph}_2\text{P}(\text{CH}_2)_3\text{C}_6\text{Me}_5)]^+$ ($[[251]^+$) in CH_2Cl_2 at *ca* 228K.[†]

Whilst the reaction of $[\text{RuCl}_2(\eta^6\text{-C}_6\text{Me}_6)(\text{PPh}_3)]$ (**306**) with 0.9 equivalents of $[\text{48}]\text{SbCl}_6$ led to the formation of an arene-Ru(III) product, the product that crystallised was a 1:1 molecular adduct of SbCl_3 with the Ru(II) precursor (see page 277). The use of 1.1 equivalents gave $[\text{306}][\text{SbCl}_6]$ as a microcrystalline pink solid in good yield (Scheme 81a). It is also noticeably different in colour from the orange parent complex **306**, and it is soluble in both dichloromethane and THF, but not in *n*-hexane. As before, the arene-Ru(III) complex was handled as if it were sensitive to light, air, moisture and temperature in order to prevent reversion to the parent Ru(II) complex. Elemental analysis was in excellent (C, H, P) or moderate (Cl) agreement for the formulation $[\text{306}][\text{SbCl}_6]$, confirming that the sample did not contain

[†]The electronic spectra in Figures 67 and 68 cannot be superimposed, since they were recorded on different instruments, at different times, in different countries.

nitrogen due to the presence of either oxidant [48]SbCl₆ or the amine N(C₆H₄Br-4)₃ (49) reduction product. Although the X-ray structure showed the presence of CH₂Cl₂, this was not evident in the elemental analysis.

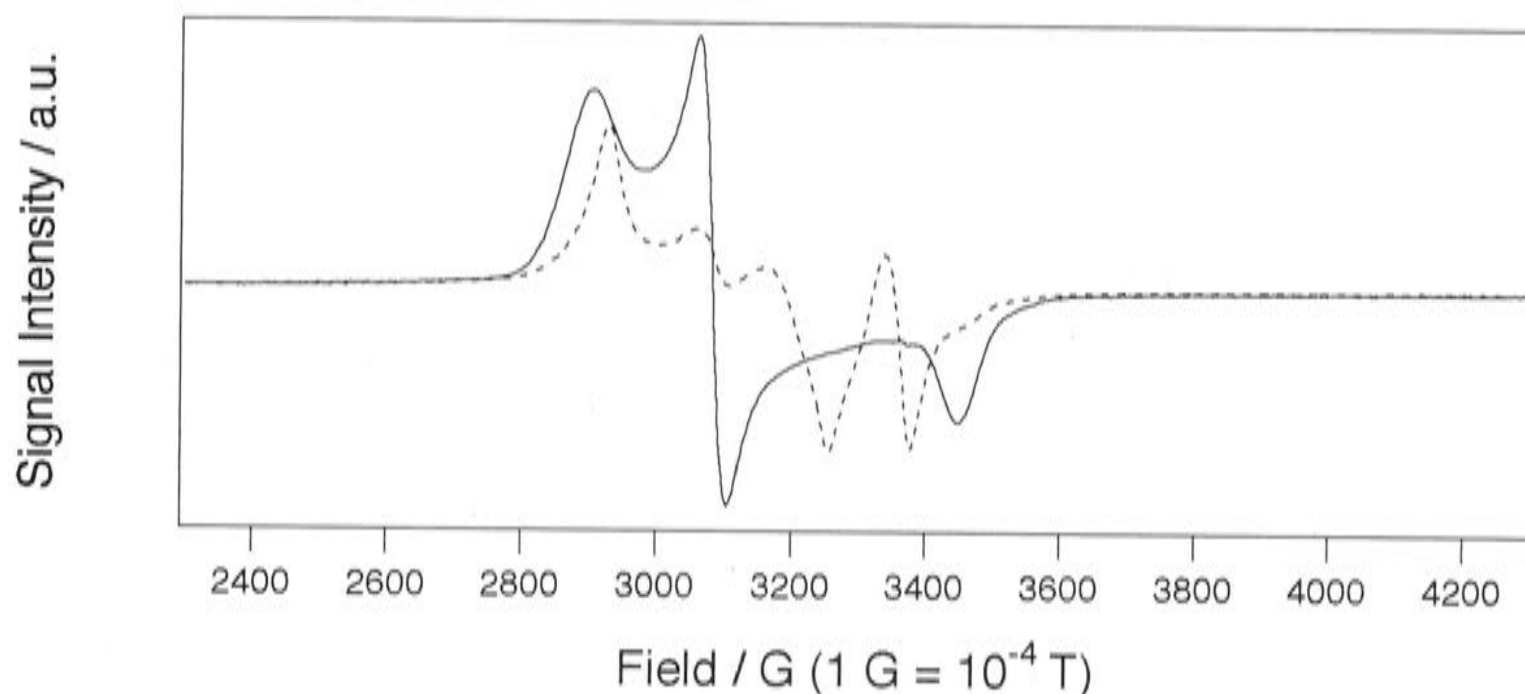


Figure 69. The ESR spectrum (solid line) at *ca* 5K of the species prepared from the anodic oxidation of [RuCl₂(η¹:η⁶-Ph₂P(CH₂)₃C₆Me₅)] (251) in 0.4M [Buⁿ₄N]PF₆/CH₂Cl₂ at *ca* 228K [*E*_{appl} = + 0.65 V (*vs* Fc^{0/1})]. The dotted line shows the spectrum at *ca* 5K of isolated [RuCl₂(η¹:η⁶-Ph₂P(CH₂)₃C₆Me₅)] [SbCl₆] ([251][SbCl₆]) in CH₂Cl₂.

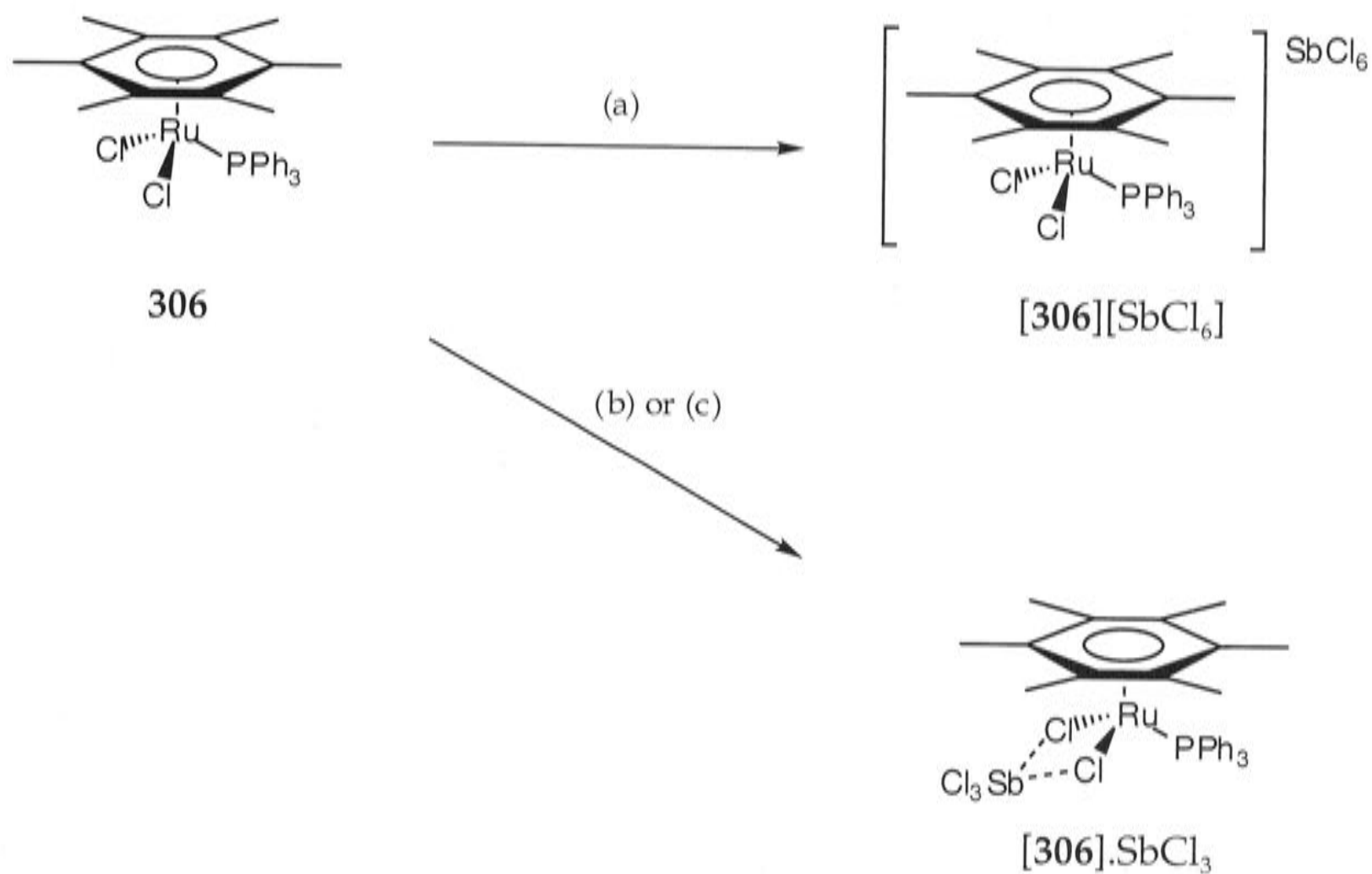
The UV/Vis spectrum in CH₂Cl₂ is somewhat better resolved than that of [RuCl₂(η¹:η⁶-Ph₂P(CH₂)₃C₆Me₅)] [SbCl₆] ([251][SbCl₆]). There is a broad absorption at *ca* 483 nm (20700 cm⁻¹) [*ε* = 2100 L mol⁻¹ cm⁻¹], and a sharper one at *ca* 355 nm (28200 cm⁻¹) [*ε* = 1900 L mol⁻¹ cm⁻¹] with no trace of the band at *ca* 800 nm (12500 cm⁻¹) (Figure 70). This indicates that the oxidant [48]SbCl₆ was not present, and that the λ_{max} values at *ca* 355 nm could be due only to the product. The electronic spectrum of the parent Ru(II) complex in CH₂Cl₂ shows a sharp absorption at 375 nm (26700 cm⁻¹) [*ε* = 1700 L mol⁻¹ cm⁻¹]. The UV/Vis spectra of the electrogenerated sample of [306]⁺, (Figure 71) showed three maxima at *ca* 339 nm (29500 cm⁻¹) [*ε* = 2500 L mol⁻¹ cm⁻¹], 427 nm (23400 cm⁻¹) [*ε* = 2400 L mol⁻¹ cm⁻¹] and 510 nm (19600 cm⁻¹) [*ε* = 1300 L mol⁻¹ cm⁻¹]. Again, the agreement between the observed λ_{max} values is poor, but the spans of the peaks giving rise to the maxima lie within the same range; *ca* 28000 to

21000 cm^{-1} for [251][SbCl₆] and approximately 30000 to 20000 cm^{-1} for the electrogenerated [251]⁺.

The ESR spectrum of one sample in frozen dichloromethane recorded at *ca* 5K showed the presence of some residual oxidant 48⁺ (see comments on p. 272), but was otherwise in good agreement with that observed for the electrogenerated [RuCl₂(η^6 -C₆Me₆)(PPh₃)]⁺ (306⁺) (see Figure 72). Neither the ¹H or ³¹P{¹H}-NMR spectra were recorded. Crystals suitable for X-ray analysis were obtained from a dichloromethane solution layered with *n*-hexane at *ca* -11°C. It should be noted that, despite numerous attempts, it was only possible to grow extremely small crystals of [306][SbCl₆] which were suitable for X-ray crystallography, and that which proved suitable for single crystal diffraction analysis was actually twinned. The structure will be discussed later.

The structure of the 1:1 molecular adduct [RuCl₂(η^6 -C₆Me₆)(PPh₃)]₂SbCl₃ ([306]₂SbCl₃), presumably formed *via* reduction of the initially formed arene-Ru(III) species [306][SbCl₆] (Scheme 81b), will be discussed below. The other products of this reaction are not known. Complex [306]₂SbCl₃ could also be formed independently by reaction of 306 with SbCl₃ in dichloromethane at room temperature (Scheme 81c). The unit cell dimensions of the crystals obtained of the product from this reaction (Scheme 81c) are identical to those obtained in the chemical oxidation reaction (Scheme 81b). The ¹H NMR spectrum (in CDCl₃) of [306]₂SbCl₃ shows two signals at δ 1.75 and a multiplet at 7.2-7.9 ppm, attributable to C₆(CH₃)₆ and C₆H₅, respectively. The ³¹P{¹H}-NMR spectrum shows a single resonance at δ 36.8. The chemical shifts differ appreciably from those of the parent complex 306, which shows signals in the ¹H NMR spectrum (in CD₂Cl₂) at δ 1.70 and a multiplet at 7.2-7.9 ppm, and a singlet at δ 30.4 in the ³¹P{¹H}-NMR spectrum.¹¹ During the course of these studies it has become apparent that the nature of the product formed is influenced by the amount of oxidant used. Thus a slight excess of [48]SbCl₆ ensures complete

conversion of the arene-Ru(II) complex **306** into the one-electron oxidation product $[\mathbf{306}][\text{SbCl}_6]$.



Scheme 81. Reaction of the arene-Ru(II) complex **306** with $[\mathbf{48}]\text{SbCl}_6$ to give either the one-electron oxidation product $[\mathbf{306}][\text{SbCl}_6]$ or the 1:1 molecular adduct $[\mathbf{306}].\text{SbCl}_3$. (a) 1.1 eq. $[\text{N}(\text{C}_6\text{H}_4\text{Br-4})_3]\text{SbCl}_6$ ($[\mathbf{48}]\text{SbCl}_6$), CH_2Cl_2 , -40°C ; (b) 0.9 eq. $[\text{N}(\text{C}_6\text{H}_4\text{Br-4})_3]\text{SbCl}_6$ ($[\mathbf{48}]\text{SbCl}_6$), CH_2Cl_2 , -40°C ; (c) SbCl_3 , CH_2Cl_2 , r.t.

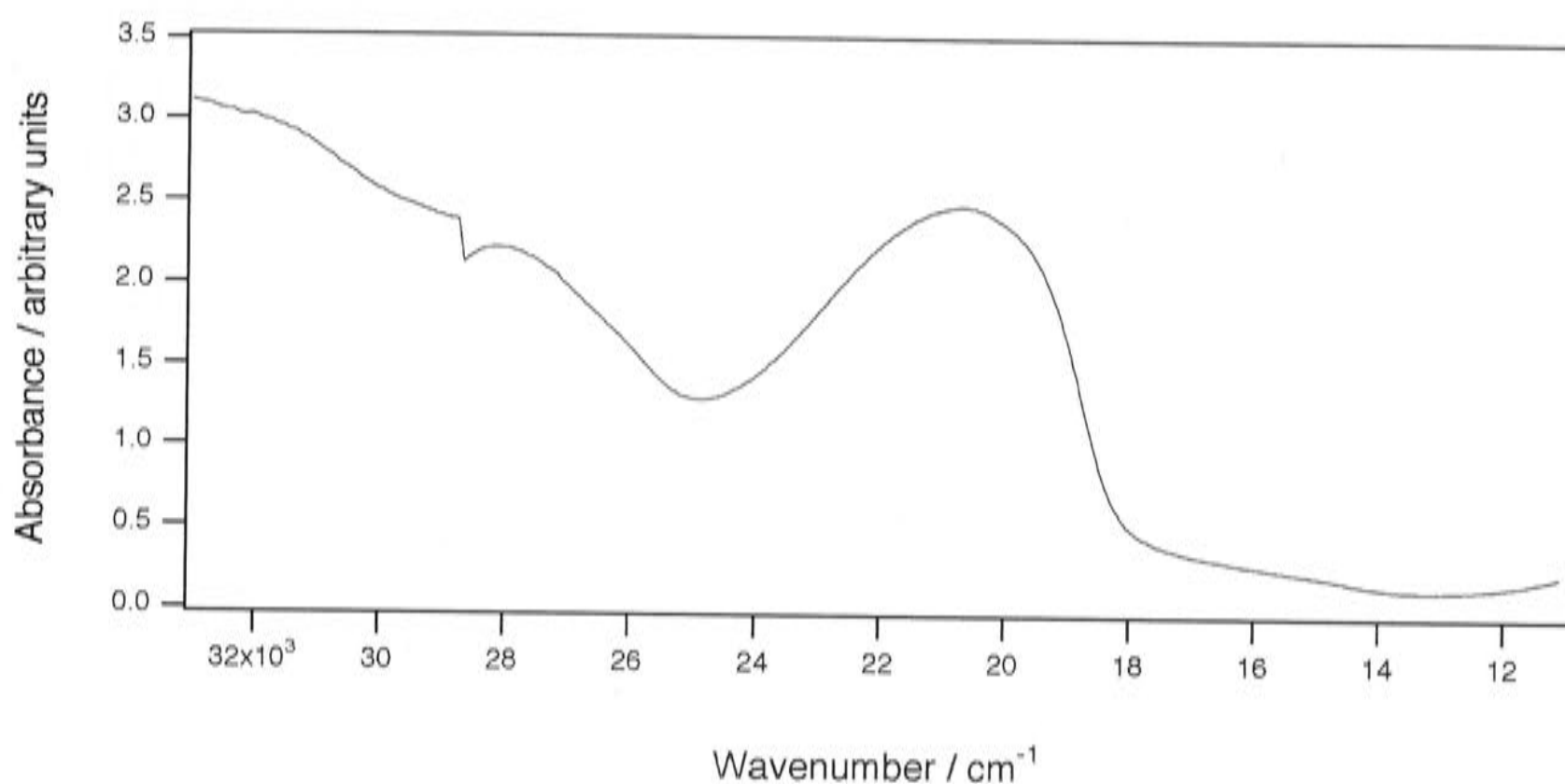


Figure 70. Electronic spectrum of isolated $[\text{RuCl}_2(\eta^6\text{-C}_6\text{Me}_6)(\text{PPh}_3)][\text{SbCl}_6]$ (**[306]** $[\text{SbCl}_6]$) in CH_2Cl_2 at ambient temperature.

The reaction of complexes $[\text{RuCl}_2(\eta^6\text{-arene})(\text{PPh}_3)]$ (arene = *p*-cymene (**338**) and mesitylene (**339**)) with a slight deficit of the oxidant **[48]** SbCl_6 did not yield any isolable arene-Ru(III) products. The reaction of **338** did not show any characteristic colour changes to indicate consumption of the oxidant (*i.e.* the solution was still deep blue). The UV/Vis spectrum of the crude solid obtained from the reaction of **338** showed a maximum at 390 nm; 25600 cm^{-1} , which was virtually identical to that of the parent complex itself; 375 nm; 26000 cm^{-1} . The ESR spectrum in frozen CH_2Cl_2 recorded at 5K showed only organic radical species, most probably residual oxidant. Presumably, the electrode potential of **[48]** SbCl_6 ($E_{1/2} = 0.70\text{ V vs Fc}^{0/1}$ in CH_2Cl_2) is not sufficiently greater than that of **338**, which has approximately the same $E_{1/2}$ value (see p. 225, Chapter 5). In the case of **339**, the orange solution became brown on addition of a slight deficit of the oxidant and on evaporation of the solvent, a brown solid was obtained. Its electronic spectrum, however, showed only the presence of **[48]** SbCl_6 , with sharp maxima at 275 nm (36400 cm^{-1}), 368 nm (27200 cm^{-1}) and 729 nm (13700 cm^{-1}), virtually identical to that of **[48]** SbCl_6 in CH_3CN , which showed three maxima at *ca* 270 nm (37000 cm^{-1}), 360 nm (27800 cm^{-1}) and 700 nm (14300 cm^{-1}).⁹

Again, the ESR spectrum of the solid in frozen CH_2Cl_2 recorded at 5K was characteristic of an organic radical species, confirming the presence of $[\mathbf{48}]\text{SbCl}_6$. Since the electrode potential of $[\mathbf{48}]\text{SbCl}_6$ is sufficiently greater than that of $\mathbf{339}$ ($E_{1/2} = 0.66 \text{ V vs Fc}^{0/1}$ in CH_2Cl_2), the arene-Ru(III) species $[\mathbf{339}][\text{SbCl}_6]$ should have formed, but perhaps it was too unstable to be isolated. The isolation of the Ru(III) complexes $[\mathbf{338}][\text{SbCl}_6]$ and $[\mathbf{339}][\text{SbCl}_6]$, based on *p*-cymene and mesitylene, probably requires the use of stronger triarylammonium ions, i.e. those with larger electrode potentials, such as $[\text{N}(\text{C}_6\text{H}_3\text{Br}_2\text{-2,4})_3]^+$.²

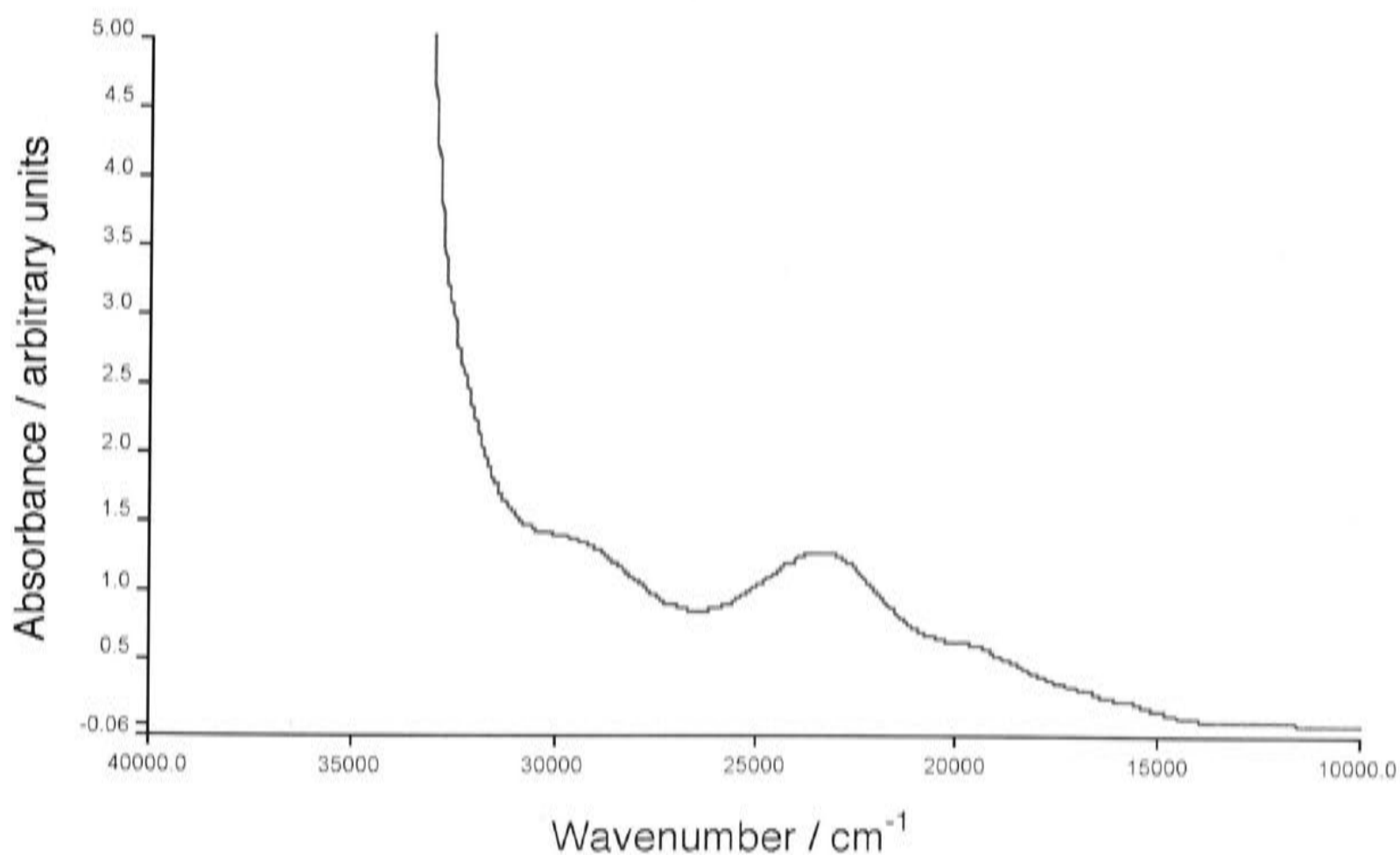


Figure 71. Electronic spectrum of the electrogenerated cation $[\text{RuCl}_2(\eta^6\text{-C}_6\text{Me}_6)(\text{PPh}_3)]^+$ ($[\mathbf{306}]^+$) in CH_2Cl_2 at *ca* 228K.[†]

[†]The electronic spectra in Figures 70 and 71 cannot be superimposed, since they were recorded on different instruments, at different times in different countries.

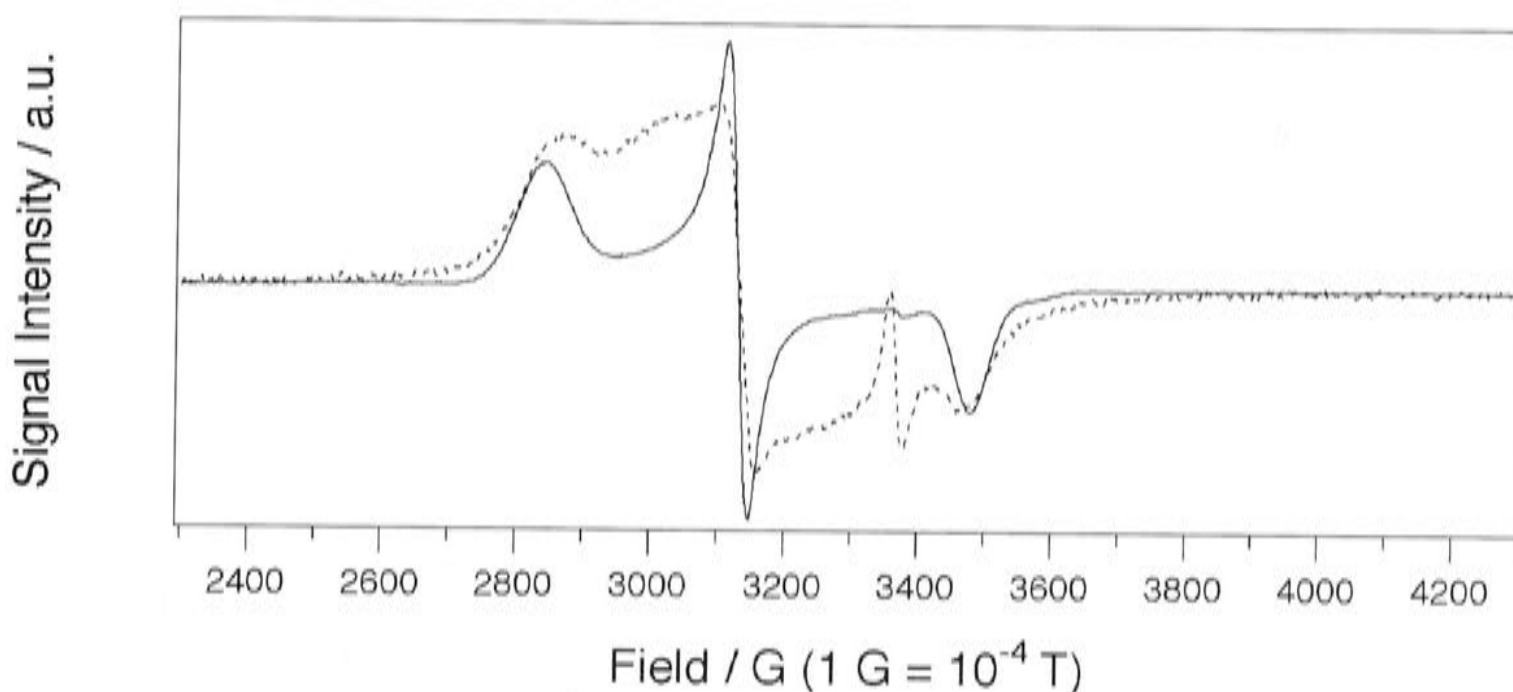


Figure 72. The ESR spectrum (solid line) at *ca* 5K of the species prepared from the anodic oxidation of $[\text{RuCl}_2(\eta^6\text{-C}_6\text{Me}_6)(\text{PPh}_3)]$ (**306**) in 0.4M $[\text{Bu}^n_4\text{N}]\text{PF}_6/\text{CH}_2\text{Cl}_2$ at *ca* 228K [$E_{\text{appl}} = + 0.64$ V (*vs* $\text{Fc}^{0/1}$)]. The dotted line shows the spectrum at *ca* 5K of isolated $[\text{RuCl}_2(\eta^6\text{-C}_6\text{Me}_6)(\text{PPh}_3)][\text{SbCl}_6]$ (**[306][SbCl₆]**) in CH_2Cl_2 .

The crystal structures of the arene-Ru(III) complexes **[306][SbCl₆]** [Dr A. C. Willies (ANU)] and **[251][SbCl₆]** (Drs A. D. Rae and A. C. Willis (ANU)), Figures 73 and 74, respectively. They confirm the presence of the intact cations **[306]⁺** and **[251]⁺** and of the SbCl_6^- anion, thus confirming the Ru(III) oxidation state for the metal atom in each complex. Selected bond distances are listed in Table 36, and the Ru-centroid data are summarised in Table 37. Hence the structural data confirm the conclusion drawn primarily from the ESR spectra and supplemented by the UV/Vis spectroscopic data of **[306][SbCl₆]** and **[251][SbCl₆]**, that the desired one-electron oxidation products were formed by oxidising the parent arene-Ru(II) complexes. The cations **[306]⁺** and **[251]⁺** show the expected half-sandwich geometry, the essential features of which are similar in both arene-Ru(II) and Ru(III) complexes. There are, however, some significant changes in metal-ligand bond lengths that occur upon oxidation; these will be discussed below. The interbond angles of the tripod are approximately 90° (see Appendix), as observed for the non-tethered and tethered complexes previously described (see Chapter 3). The antimony atom of the SbCl_6^- ion is in an octahedral environment, with an average Sb-Cl bond length of 2.36 Å and 2.37 Å observed for the anion in

each of the cations $[306]^+$ and $[251]^+$, respectively. This is in excellent agreement with previously reported values; for example, the average Sb-Cl bond length in the SbCl_6^- component of $[\text{WCl}_4(\eta^2\text{-dmpe})][\text{SbCl}_6]$ (dmpe = 1,2-bis(dimethylphosphino)ethane) is 2.36 Å.¹² No significant cation-anion interactions were observed in either $[306][\text{SbCl}_6]$ and $[251][\text{SbCl}_6]$.

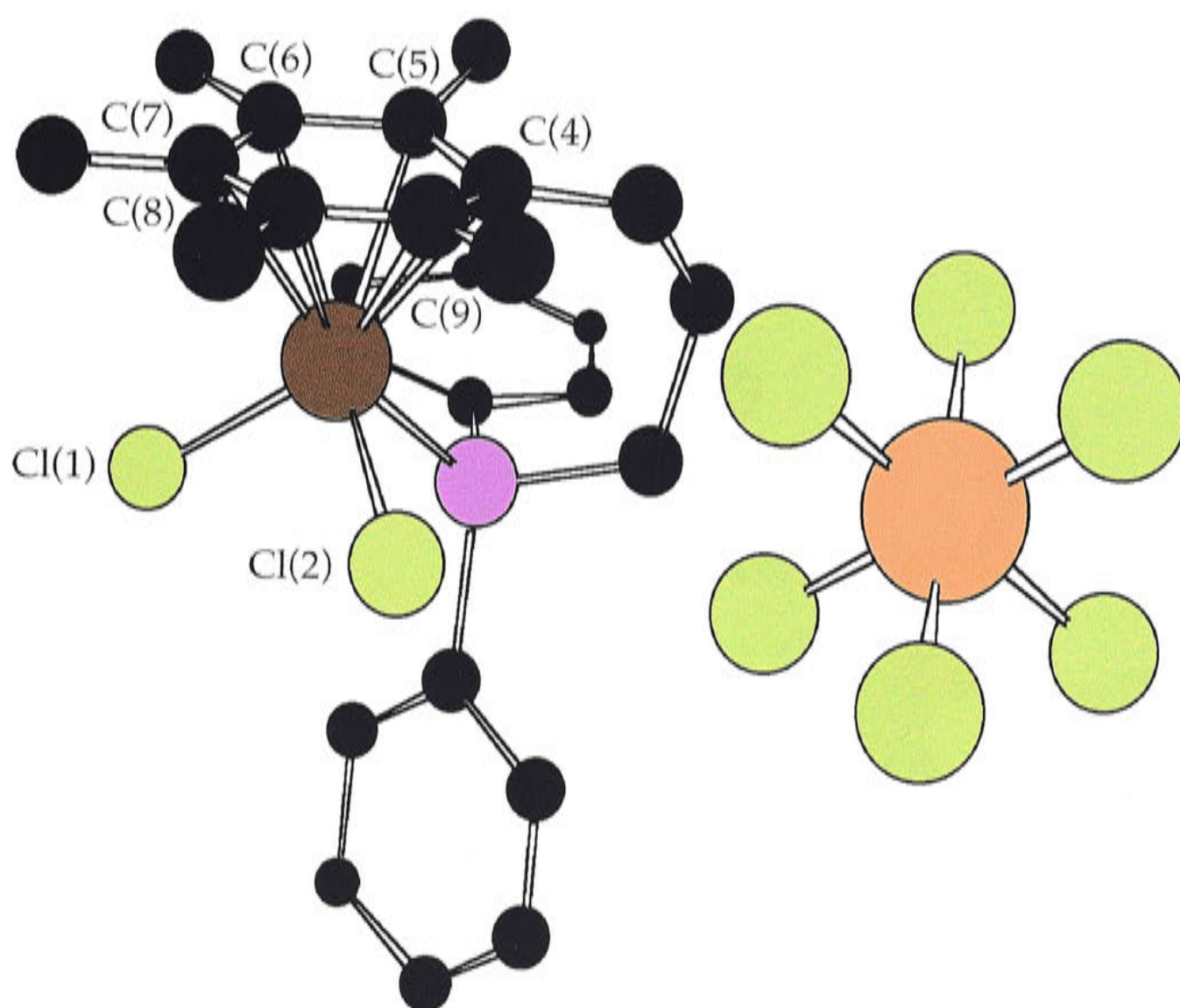


Figure 73. Chem3D representation of the molecular structure of $[\text{RuCl}_2(\eta^1:\eta^6\text{-Ph}_2\text{P}(\text{CH}_2)_3\text{C}_6\text{Me}_5)][\text{SbCl}_6]$ ($[251][\text{SbCl}_6]$). Hydrogen atoms and the solvent molecule (CH_2Cl_2) have been omitted for clarity.

The Ru-C(arene) bond distances in the arene-Ru(III) compounds $[306][\text{SbCl}_6]$ (2.312(7)-2.346(7) Å) and $[251][\text{SbCl}_6]$ (2.228(5)-2.336(5) Å) are approximately 0.1 Å longer than those in the corresponding Ru(II) species **306** (2.208-2.282 Å)¹³ and **251** (2.182(5)-2.285(5) Å). In contrast to both tethered and non-tethered arene-Ru(II) complexes (see Chapter 3, Section 3.5), there are no apparent *trans*-influences observed in the Ru-C(arene) bond distances, that is, the distances *trans* to phosphorus are not significantly longer than

those *trans* to the chloride ligands. The Ru-centroid bond distances also increase from Ru(II) to Ru(III) complexes; **[306][SbCl₆]** (1.84 Å) and **[251][SbCl₆]** (1.81 Å) are *ca* 0.1 Å longer than those of their arene-Ru(II) counterparts **306** (1.74 Å)¹³ and **251** (1.72 Å) (Table 37), consistent with a weakening of the metal-arene interaction on oxidation of the metal atom. Slight ring-slippage (defined in Chapter 3, Section 3.5) was observed in the arene-Ru(III) species **[306][SbCl₆]** (0.042 Å) and **[251][SbCl₆]** (0.064 Å), which was similar to that observed in both the parent Ru(II) compounds **251** (0.052 Å) and **306** (0.047 Å)¹³ (see Table 37).

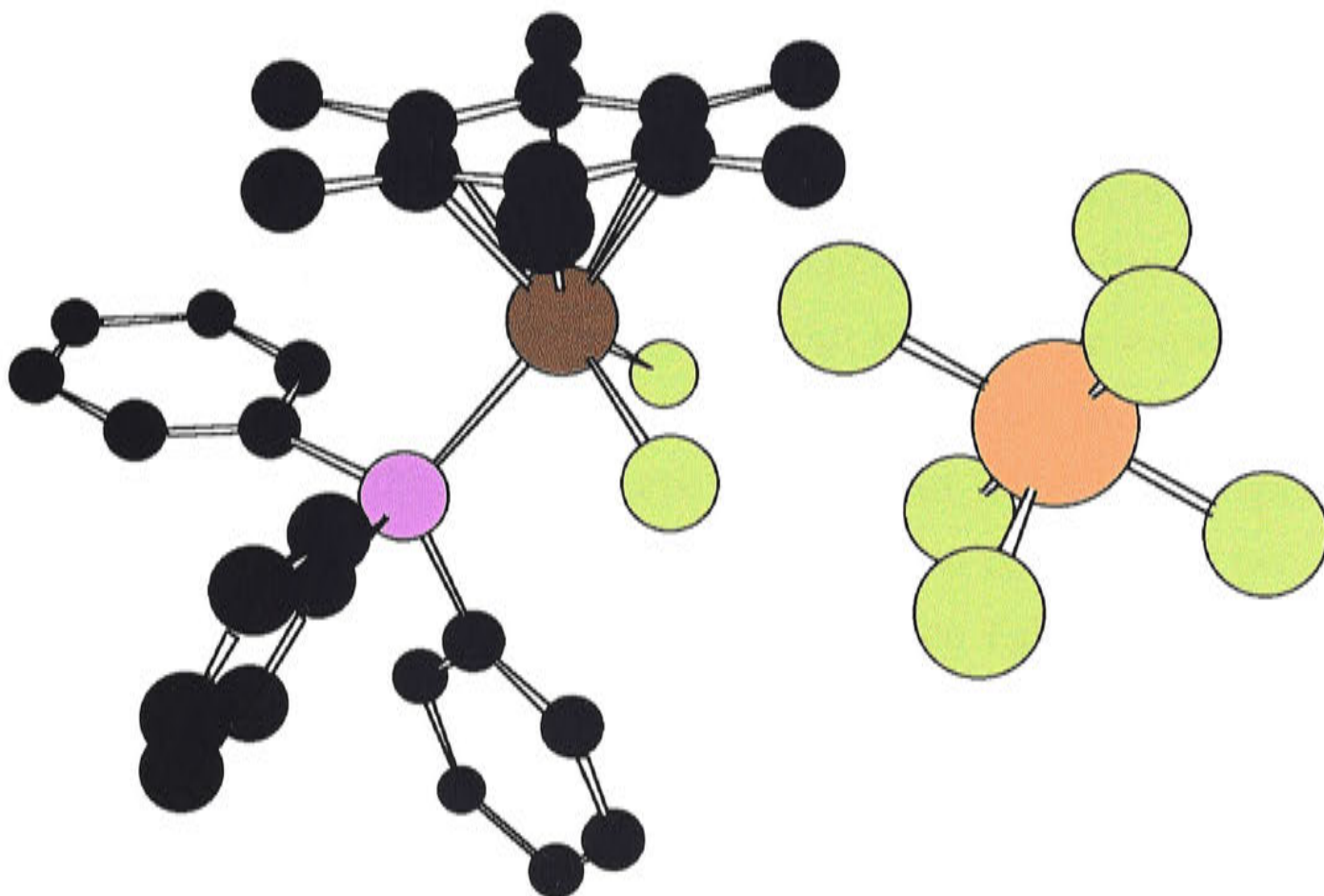


Figure 74. Chem3D representation of the molecular structure of **[RuCl₂(η⁶-C₆Me₆)(PPh₃)]****[SbCl₆]** (**[306][SbCl₆]**). Hydrogen atoms and the solvent molecule (CH₂Cl₂) have been omitted for clarity.

The Ru-Cl bond lengths, in contrast, decrease on oxidation of the Ru(II) complexes; the Ru-Cl bond lengths are *ca* 0.1 Å shorter in the arene-Ru(III) species **[306][SbCl₆]** (av. 2.31 Å) and **[251][SbCl₆]** (av. 2.32 Å) than those of their arene-Ru(II) counterparts **306** (av. 2.41 Å)¹³ and **251** (av. 2.41 Å) (Table 36). The Ru-P bond lengths of the Ru(II) species **[306][SbCl₆]** (2.38 Å) and **[251][SbCl₆]** (2.32 Å) are similar to those observed in the Ru(II) analogues **306** (2.36 Å)¹³ and **251** (2.30 Å) (see Table 36). The average C-C(arene) bond

lengths in the arene-Ru(III) species [306][SbCl₆] (1.42 Å) and [251][SbCl₆] (1.43 Å) are not significantly different (1.43 Å) from those in the corresponding arene-Ru(II) precursors 306¹³ and 251, respectively.

Although the η^6 -arene of [306][SbCl₆] is almost planar, there is a slight deviation from planarity in the tethered complex [251][SbCl₆]. Atom C(4) lies *ca* 0.12 Å below the plane comprising atoms C(5), C(6), C(8) and C(9), and atom C(7) also lies slightly below the plane, but to a much lesser extent (*ca* 0.03 Å) (see Figure 75). Thus, in contrast to the η^6 -arene of 251, which is essentially planar, the η^6 -arene of [251][SbCl₆] has appears to adopt an arrangement towards that of a boat conformation (see Figure 76a). There are no significant changes within the conformation of the tether in the Ru(II) and Ru(III) systems, except for the angle Ru(1)-C(4)-C(3), which is greater in the Ru(II) complex (130.4(4)°) than for Ru(III) (125.9(4)°) (Table 38; the atom labelling employed is shown in Figure 77), but this is to be expected due to the decrease in the Ru-C(4) bond length between the Ru(II) and Ru(III) species. The bond lengths P(1)-C(1) are 1.827(5) and 1.818(5) Å, respectively, and the C-C bond distances within the chain are also comparable (av. 1.53 Å in both cases), with C(2)-C(3) being the longest (see Table 38). There is no significant difference between the Ru(1)-P(1)-C(1) bond angles, both being *ca* 107°. There is very little difference between the angles subtended by the atoms comprising the tether, with the exception of Ru(1)-C(4)-C(3) as discussed above. The angles between the P(1), C(1), C(2), C(3) and C(4) atoms lie between 112.9(4)-117.4(4)° for Ru(II) and are in the range 115.0(4)-119.1(5)° for Ru(III); the smaller value corresponds to the bond angle P(1)-C(1)-C(2) with the angle C(2)-C(3)-C(4) being the greatest in magnitude. Since there are no significant changes between the tethers in the Ru(II) and Ru(III) structures, but the Ru-C(arene) bond lengths have increased in the Ru(III) structure, it is postulated that the slight distortion of the η^6 -arene towards an inverted boat conformation is due to the presence of the tether. Therefore it appears that the η^6 -arene undergoes minor conformational changes in order to maintain coordination, since the C(4) atom is unable to move any further from the Ru(III) centre, its movement being restricted by

the presence of the adjacent chain of atoms C(3)-C(2)-C(1)-P(1). Since the boat conformer of cyclohexane is less stable than the alternative chair conformer¹⁴ by 4.7-6.2 kcal mol⁻¹,¹⁵ it would not be unreasonable to postulate that the η^6 -arene of [251][SbCl₆] would prefer to adopt an arrangement towards that of the chair conformation. This, however, is not possible, since it would result loss of η^6 -arene coordination, as depicted in Figure 76b.

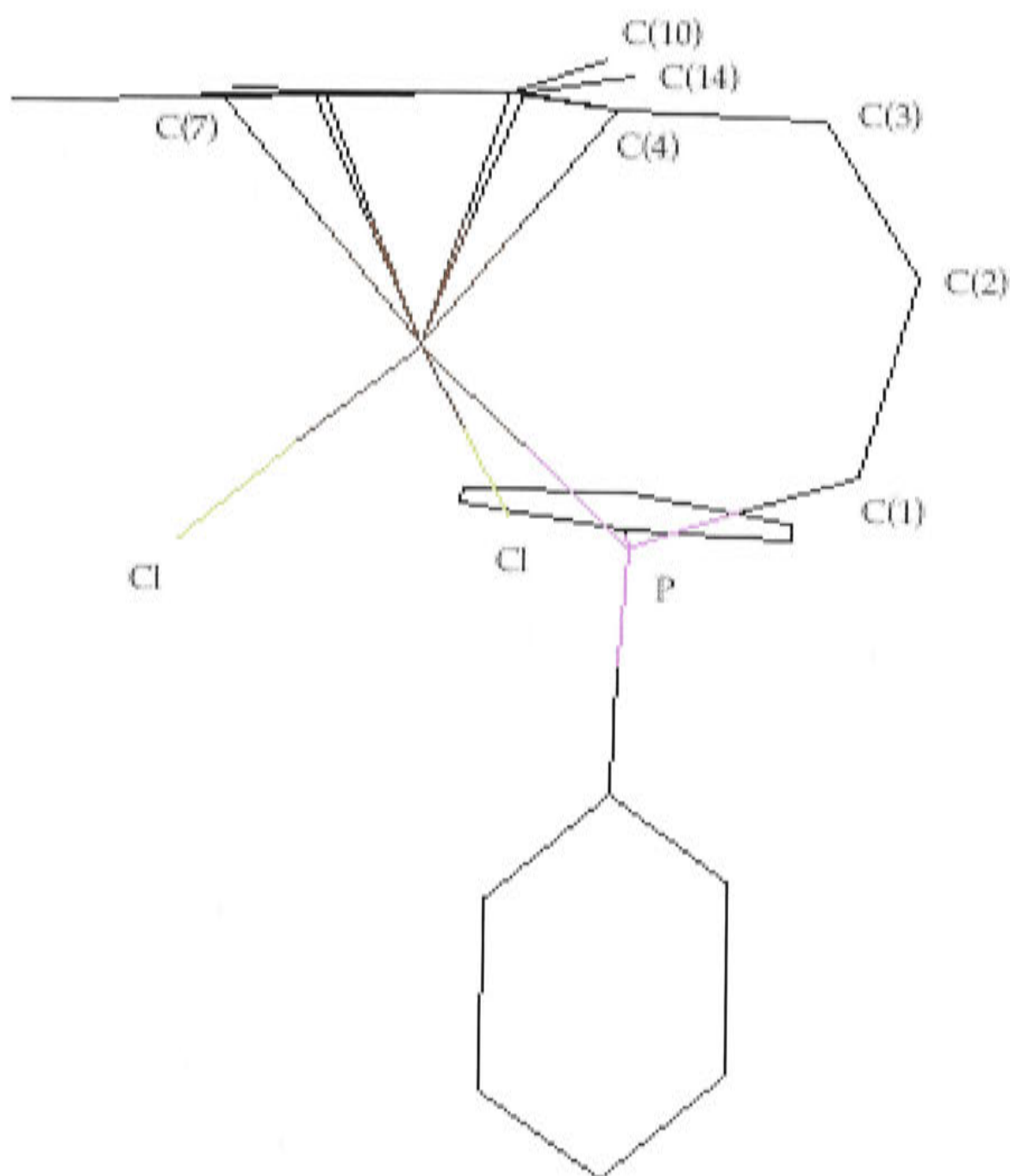


Figure 75. Chem3D representation of the molecular structure of compound [RuCl₂(η^1 : η^6 -Ph₂P(CH₂)₃C₆Me₅)] [SbCl₆] ([251][SbCl₆]). Hydrogen atoms, the anion (SbCl₆⁻) and the solvent molecule (CH₂Cl₂) have been omitted for clarity.

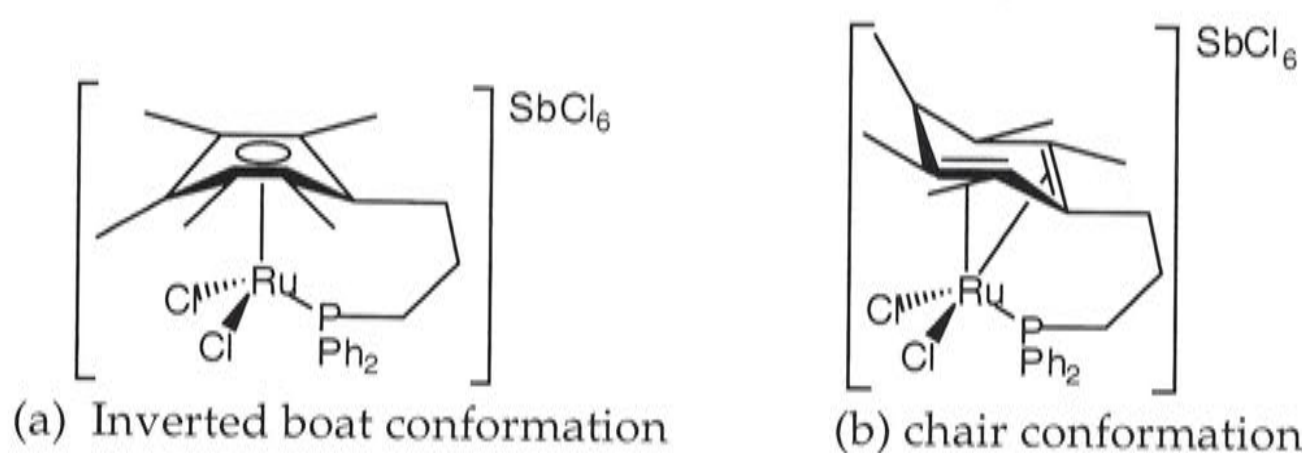


Figure 76. Extreme representation (not to scale) of the inverted boat conformation of the η^6 -arene in complex $[\text{RuCl}_2(\eta^1:\eta^6\text{-Ph}_2\text{P}(\text{CH}_2)_3\text{C}_6\text{Me}_5)][\text{SbCl}_6]$ (**[251]**)[SbCl_6], (a); possible chair conformation leading to $\eta^2:\eta^2$ -coordination, (b).

There is also a change in position of one of the methyl groups of the η^6 -arene upon oxidation. In complex **251**, most of the angles $\text{Ru}(1)\text{-C}(\text{arene})\text{-C}(\text{Me})$ are in the range $129.9(4)\text{-}129.9(3)^\circ$ (see Table 38), the exception being $\text{Ru}(1)\text{-C}(5)\text{-C}(10)$ (atom labelling is as shown in Figure 77), with an angle of $136.9(4)^\circ$, indicating that this methyl group lies above the plane comprising the η^6 -arene and the other alkyl substituents. This is also the case in the arene-Ru(III) complex **[251]**[SbCl_6], where $\text{Ru}(1)\text{-C}(5)\text{-C}(10)$ is now slightly greater than in **251** ($138.1(3)^\circ$), but the angle $\text{Ru}(1)\text{-C}(9)\text{-C}(14)$ has also increased to $131.2(4)^\circ$. The other methyl groups essentially all lie in the same plane, with angles $\text{Ru}(1)\text{-C}(\text{arene})\text{-C}(\text{Me})$ being approximately 128° . Thus both atoms C(10) and C(14) lie above the plane containing the other methyl-substituents, as illustrated in Figure 75.

The trigonal RuCl_2P fragment of complex **[306]**[SbCl_6] adopts a staggered arrangement relative to the carbon atoms of the aromatic ring, as observed in the Ru(II) analogue **306**.¹³ In the tethered complex **[251]**[SbCl_6], the RuCl_2P fragment lies about half-way between eclipsed and staggered conformations (Figure 78), in contrast to the Ru(II) counterpart **251** which adopts a staggered conformation (Figure 79). Thus there is a slight rotation of the η^6 -arene between the Ru(II) complex and the one-electron oxidation product.

The molecular geometry of the ruthenium(II) component of the 1:1 molecular adduct $[\text{RuCl}_2(\eta^6\text{-C}_6\text{Me}_6)(\text{PPh}_3)]\cdot\text{SbCl}_3$ ($[\mathbf{306}]\cdot\text{SbCl}_3$) [Dr A. C. Willis (ANU)] (the Chem3D representation is shown in Figure 80) is very similar to that of complex **306**.¹³ Selected bond lengths are summarised in Table 36; Table 37 lists the Ru-centroid data. The interbond angles of the tripod (*ca* 90°) are similar to those observed for the non-tethered and tethered complexes previously described in Chapter 3 (see Appendix).

With one exception, the metal-ligand bond distances in the 1:1 molecular adduct $[\mathbf{306}]\cdot\text{SbCl}_3$ are very similar to those of **306**.¹³ In particular, there is no difference in Ru-C(arene) bond distances; complex $[\mathbf{306}]\cdot\text{SbCl}_3$ (av. 2.24 Å) and compound **306** (av. 2.25 Å).¹³ Those distances in $[\mathbf{306}]\cdot\text{SbCl}_3$ *trans* to the P-donor (2.25-2.26 Å) are significantly greater than those *trans* to the Ru-Cl bonds (2.21-2.25 Å), reflecting the relative *trans*-influences of Cl and PR₃; this behaviour was also observed in **306**.¹³ There is no significant difference between the Ru-centroid distances in both complexes $[\mathbf{306}]\cdot\text{SbCl}_3$ and **306**, 1.718(5) and 1.739(2) Å,¹³ respectively (Table 37). The ring-slippage observed for $[\mathbf{306}]\cdot\text{SbCl}_3$ (0.033 Å) was less significant than observed in **306** (0.047 Å),¹³ which indicates that the center of η^6 -arene of **306** is further away from the metal centre than in complex $[\mathbf{306}]\cdot\text{SbCl}_3$.

There is very little difference between the Ru-P bond lengths; 2.381(3) Å in compound $[\mathbf{306}]\cdot\text{SbCl}_3$ and 2.3607(10) observed in complex **306**.¹³ The C-C(arene) distances in $[\mathbf{306}]\cdot\text{SbCl}_3$ (1.43 Å) are identical to those observed in that reported for **306**.¹³ The RuCl₂P fragment adopts a staggered arrangement with respect to the η^6 -arene, as was observed for both **306** and $[\text{RuCl}_2(\eta^6\text{-C}_6\text{Me}_6)(\text{PPh}_3)]\cdot\text{SbCl}_3$ ($[\mathbf{306}]\cdot\text{SbCl}_3$).

There is a close association between the antimony atom of the SbCl₃ group and the chloride ligands of the Ru(II) component of $[\mathbf{306}]\cdot\text{SbCl}_3$, as indicated by the appropriate bond distances: Cl(1)-Sb = 2.949(3) Å and Cl(2)-Sb = 2.995(3) Å. Not only does this result in a slight lengthening of the Ru-Cl bonds (av. Ru-Cl = 2.44 Å, *cf.* 2.41 Å for **306**¹³), but it also influences the bond

lengths of the SbCl_3 unit. The $\text{Sb-Cl}(3)$ and $\text{Sb-Cl}(4)$ bonds for the chlorine atoms *trans* to the Ru-Cl groups are longer, 2.433(4) and 2.403(3) Å, respectively, compared to the remaining $\text{Sb-Cl}(5)$ bond length of 2.88(3) Å. These bond lengths, however, are significantly greater than those observed in the free molecule (av. 2.36 Å) by X-ray diffraction.¹⁶ Antimony trichloride has a trigonal pyramidal geometry, the angles about the Cl-Sb-Cl atoms are 95.2° ,¹⁶ the corresponding angles in $[\mathbf{306}].\text{SbCl}_3$ are very similar and range between 92.3 and 95.2° .

There are some other examples of both mononuclear and binuclear complexes in which SbCl_3 molecules interact with the chlorine atoms of Ru-Cl bonds.^{17,18} The antimony atom of the SbCl_3 unit adopts an octahedral arrangement by interacting with each of the chloride ligands of the $[\text{RuCl}_3(\text{CO})_3]$ unit of $[\text{H}_5\text{O}_2][\text{RuCl}_3(\text{CO})_3].\text{SbCl}_3$ (**342**).¹⁷ The Sb-Cl bond distances of the SbCl_3 entity lie in the range 2.364(2)-2.387(2) Å, and the antimony atom is approximately 3.186(2)-3.419(2) Å away from the chloride atoms of the metal complex. The SbCl_3 component of the molecular adduct $[\text{RuCl}_2(\text{CO})_3]_2.\text{SbCl}_3$ (**343**) also interacts with either one (to give a four coordinate Sb atom) or two (Sb atom becomes five coordinate) of the chloride ligands of the metal component.¹⁸ The Sb-Cl bond lengths SbCl_3 unit lie between 2.344(5)-2.351(5) Å, with the Sb atom being situated 3.347(5)-3.604(5) Å away from the chloride atoms of the metal complex. These distances, however, are quite different from those observed in $[\mathbf{306}].\text{SbCl}_3$, which has longer Sb-Cl bond lengths (up to 2.43 Å) and much shorter separations (*ca* 3 Å) between the antimony atom and the chloride ligands of $[\text{RuCl}_2(\eta^6\text{-C}_6\text{Me}_6)(\text{PPh}_3)].\text{SbCl}_3$ ($[\mathbf{306}].\text{SbCl}_3$). Thus the greater distances between the Sb atom and the chloride ligands of the metal complexes **342** and **343** are indicative of a weaker interaction between the SbCl_3 and metal complex units. It would therefore appear that the SbCl_3 of $[\mathbf{306}].\text{SbCl}_3$ is acting as a Lewis acid, causing charge transfer from the Ru-Cl bonds to antimony, *via* the chloride atoms, which causes the Ru-Cl bonds to increase in length.

Table 36. Summary of the chemically significant bond lengths of the arene-ruthenium(II) complexes $[\text{RuCl}_2(\eta^6\text{-C}_6\text{Me}_6)(\text{PPh}_3)]$ (**306**),¹³ $[\text{RuCl}_2(\eta^6\text{-C}_6\text{Me}_6)(\text{PPh}_3)]\cdot\text{SbCl}_3$ (**[306].SbCl₃**) and $[\text{RuCl}_2(\eta^1:\eta^6\text{-Ph}_2\text{P}(\text{CH}_2)_3\text{C}_6\text{Me}_5)]$ (**251**) and the arene-ruthenium(III) complexes $[\text{RuCl}_2(\eta^6\text{-C}_6\text{Me}_6)(\text{PPh}_3)][\text{SbCl}_6]$ (**[306][SbCl₆]**) and $[\text{RuCl}_2(\eta^1:\eta^6\text{-Ph}_2\text{P}(\text{CH}_2)_3\text{C}_6\text{Me}_5)][\text{SbCl}_6]$ (**[251][SbCl₆]**).

Complex	Ru-P (Å)	Ru-Cl(1) (Å)	Ru-Cl(2) (Å)	Ru-C (arene) (Å)
$[\text{RuCl}_2(\eta^6\text{-C}_6\text{Me}_6)(\text{PPh}_3)]\cdot\text{SbCl}_3$ ([306].SbCl₃)	2.381(3)	2.452(3)	2.433(3)	2.208(11)-2.261(12)
$[\text{RuCl}_2(\eta^6\text{-C}_6\text{Me}_6)(\text{PPh}_3)]$ (306) ^a	2.3607(10)	2.4117(10)	2.4118(10)	2.208-2.282 ^b
$[\text{RuCl}_2(\eta^6\text{-C}_6\text{Me}_6)(\text{PPh}_3)][\text{SbCl}_6]$ ([306][SbCl₆])	2.375(3)	2.308(3)	2.312(3)	2.312(7)-2.346(7)
$[\text{RuCl}_2(\eta^1:\eta^6\text{-Ph}_2\text{P}\sim\text{C}_6\text{Me}_5)]$ (251)	2.2995(14)	2.4016(12)	2.4163(12)	2.182(5)-2.285(5)
$[\text{RuCl}_2(\eta^1:\eta^6\text{-Ph}_2\text{P}\sim\text{C}_6\text{Me}_5)][\text{SbCl}_6]$ ([251][SbCl₆])	2.3235(13)	2.3228(13)	2.3106(13)	2.228(5)-2.336(5)

^aCrystal structure reported in reference(13); ^bESDs not given since data were obtained from Cambridge Structural Database. Information not available, which was required for comparison, in the reported structure of $[\text{RuCl}_2(\eta^6\text{-C}_6\text{Me}_6)(\text{PPh}_3)]$ (**306**)¹³ was obtained either from the CSD or by applying PLATON¹⁹ to data extracted from the CSD.

$\sim = (\text{CH}_2)_3$

Table 37. Metal- η^6 -arene data of [306].SbCl₃, [306][SbCl₆] and [251][SbCl₆].

Complex	Ru-centroid (Å)	Ru-least-squares plane of η^6 -arene (Å)	Ring-slippage (Å)
[RuCl ₂ (η^6 -C ₆ Me ₆)(PPh ₃)]·SbCl ₃ ([306].SbCl ₃)	1.718(5)	1.7178(7)	0.033
[RuCl ₂ (η^6 -C ₆ Me ₆)(PPh ₃)] (306) ^a	1.739(2) ^b	1.7380(13) ^b	0.047 ^b
[RuCl ₂ (η^6 -C ₆ Me ₆)(PPh ₃)] [SbCl ₆] ([306][SbCl ₆])	1.844(5)	1.843(4)	0.042
[RuCl ₂ (η^1 : η^6 -Ph ₂ P~C ₆ Me ₅)] (251)	1.717(2)	1.716(4)	0.052
[RuCl ₂ (η^1 : η^6 -Ph ₂ P~C ₆ Me ₅)] [SbCl ₆] ([251][SbCl ₆])	1.8092(2)	1.8082(3)	0.064

^aCrystal structure reported in reference(13); ^bdistances calculated using PLATON.¹⁹

~ = (CH₂)₃

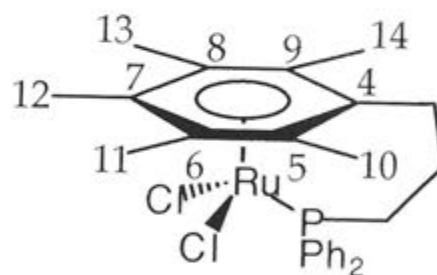


Figure 77. Atom labelling for the carbon atoms of the η^6 -arene of complexes [RuCl₂(η^1 : η^6 -Ph₂P(CH₂)₃Ph)] (251) and [RuCl₂(η^1 : η^6 -Ph₂P(CH₂)₃Ph)][SbCl₆] ([251][SbCl₆]) listed in Table 38.

Table 38. Selected bond lengths (Å) and bond angles (°) for the arene-Ru(II) complex $[\text{RuCl}_2(\eta^1:\eta^6\text{-Ph}_2\text{P}(\text{CH}_2)_3\text{Ph})]$ (**251**) and the arene-Ru(III) analogue $[\text{RuCl}_2(\eta^1:\eta^6\text{-Ph}_2\text{P}(\text{CH}_2)_3\text{Ph})][\text{SbCl}_6]$ (**[251][SbCl₆]**). Atom labelling used on the η^6 -arene is shown in Figure 77.

Bond Length (Å), Bond Angle (°)	$[\text{RuCl}_2(\eta^1:\eta^6\text{-Ph}_2\text{P}(\text{CH}_2)_3\text{Ph})]$ (251)	$[\text{RuCl}_2(\eta^1:\eta^6\text{-Ph}_2\text{P}(\text{CH}_2)_3\text{Ph})][\text{SbCl}_6]$ ([251][SbCl₆])
P(1)-C(1)	1.827(5)	1.818(5)
C(1)-C(2)	1.530(7)	1.527(7)
C(2)-C(3)	1.535(8)	1.546(7)
C(3)-C(4)	1.511(7)	1.508(7)
Ru(1)-P(1)-C(1)	106.7(2)	106.96(17)
P(1)-C(1)-C(2)	112.9(4)	115.0(4)
C(1)-C(2)-C(3)	117.3(4)	116.0(4)
C(2)-C(3)-C(4)	117.4(4)	119.1(5)
Ru(1)-C(4)-C(3)	130.4(4)	125.9(4)
Ru(1)-C(5)-C(10)	136.9(4)	138.1(3)
Ru(1)-C(6)-C(11)	128.7(3)	128.6(4)
Ru(1)-C(7)-C(12)	129.3(3)	128.0(4)
Ru(1)-C(6)-C(13)	129.9(3)	128.3(4)
Ru(1)-C(9)-C(14)	126.9(4)	131.2(4)

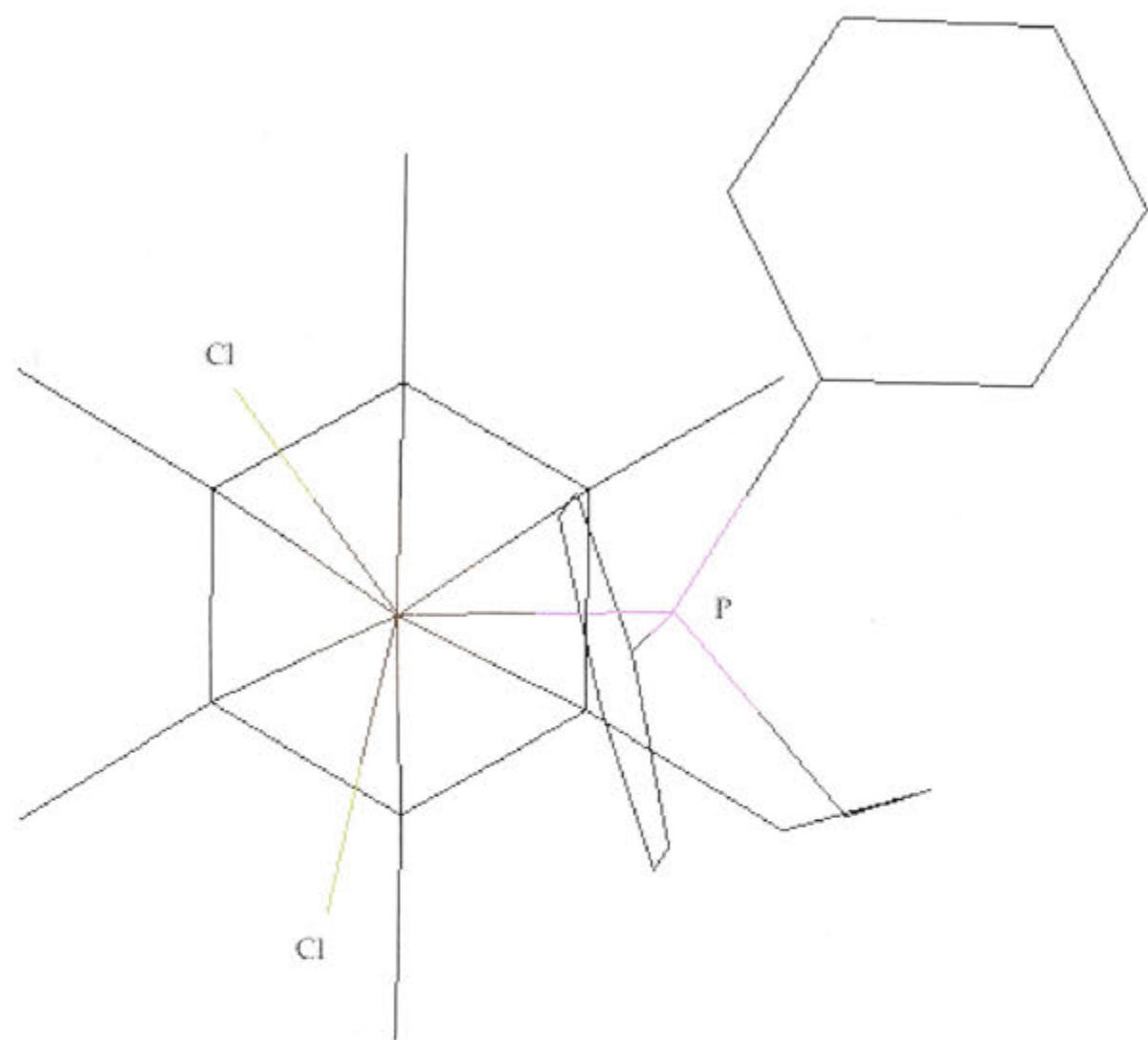


Figure 78. Chem3D representation of the molecular structure of compound $[\text{RuCl}_2(\eta^1:\eta^6\text{-Ph}_2\text{P}(\text{CH}_2)_3\text{C}_6\text{Me}_5)][\text{SbCl}_6]$ (**251**) looking down on the η^6 -arene. Hydrogen atoms, the anion (SbCl_6^-) and the solvent molecule (CH_2Cl_2) have been omitted for clarity.

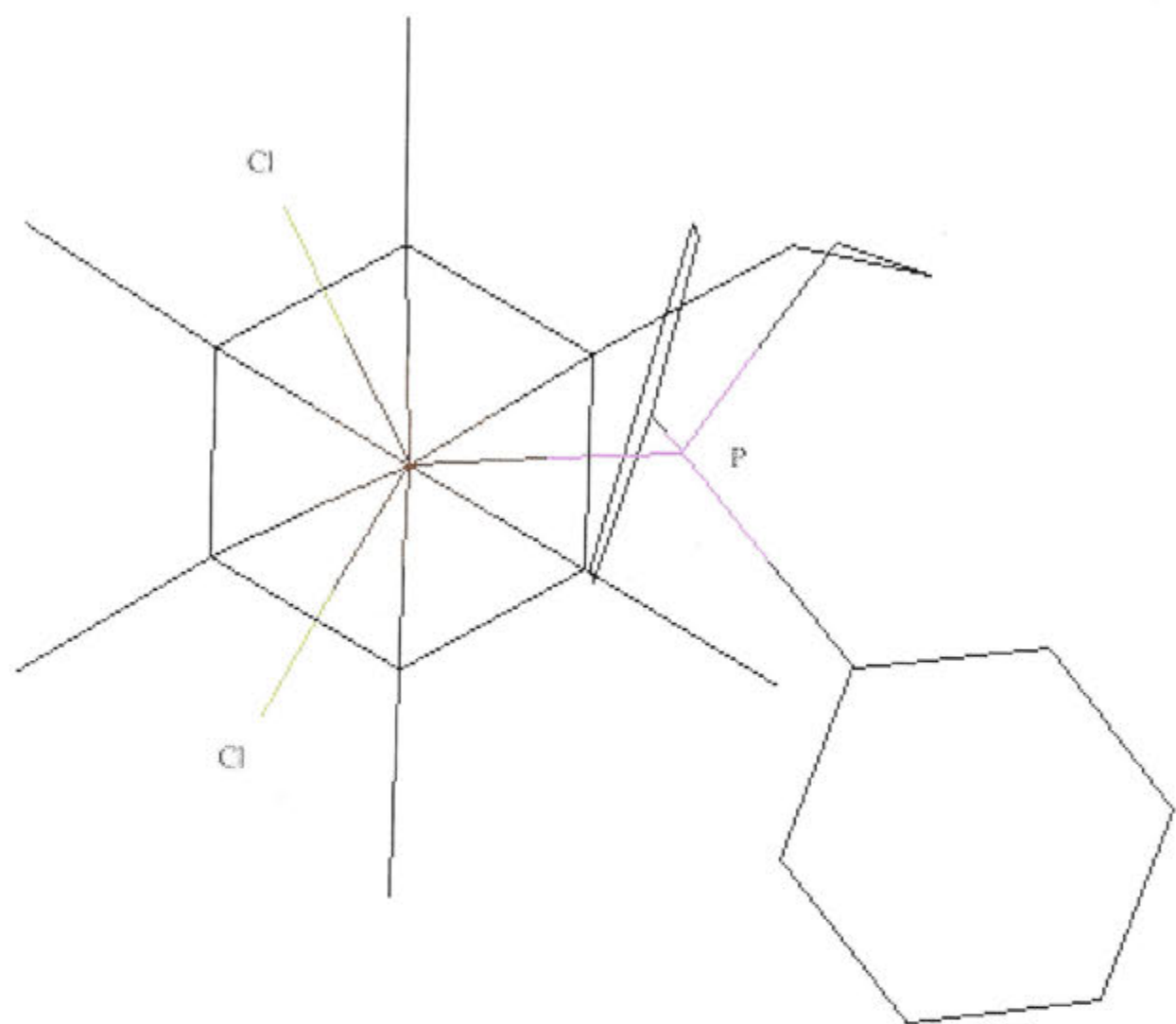


Figure 79. Chem3D representation of the molecular structure of compound $[\text{RuCl}_2(\eta^1:\eta^6\text{-Ph}_2\text{P}(\text{CH}_2)_3\text{C}_6\text{Me}_5)]$ (**251**) looking down on the η^6 -arene. Hydrogen atoms have been omitted for clarity.

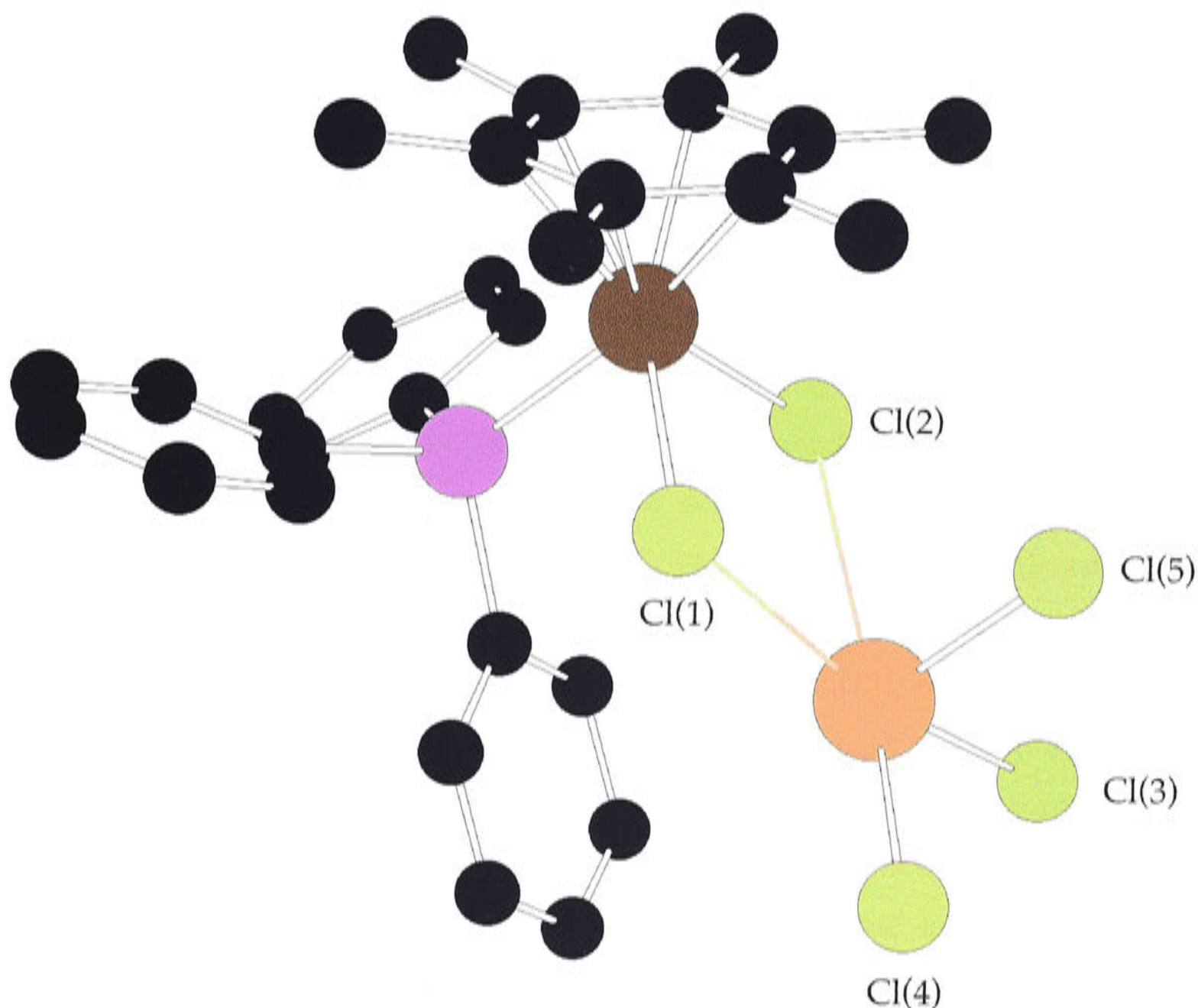


Figure 80. Chem3D representation of the molecular structure of $[\text{RuCl}_2(\eta^6\text{-C}_6\text{Me}_6)(\text{PPh}_3)]\cdot\text{SbCl}_3$ (**[306]** $\cdot\text{SbCl}_3$). Hydrogen atoms have been omitted for clarity.

It has not been possible to investigate the lability of the η^6 -arene of complexes $[\text{RuCl}_2(\eta^1:\eta^6\text{-Ph}_2\text{P}(\text{CH}_2)_3\text{C}_6\text{Me}_5)][\text{SbCl}_6]$ (**[251]** $[\text{SbCl}_6]$) and $[\text{RuCl}_2(\eta^6\text{-C}_6\text{Me}_6)(\text{PPh}_3)][\text{SbCl}_6]$ (**[306]** $[\text{SbCl}_6]$) in detail, due to the small amount of material available. Both arene-Ru(III) species react rapidly with acetonitrile, as expected from the results described in the previous Chapter (Section 5.2) presumably *via* displacement of the η^6 -arene, to give yellow solids, the nature of which is not known. The pink solids **[251]** $[\text{SbCl}_6]$ and **[306]** $[\text{SbCl}_6]$ dissolved in acetonitrile immediately gave a bright green solution, which over *ca* 1 min turned yellow. Evaporation of the solvents gave yellow solids, but their nature is unknown. In the case of **[251]** $[\text{SbCl}_6]$ the ^1H NMR

spectrum showed an intense singlet at δ 2.14, presumably due to coordinated acetonitrile (see Chapter 4, Section 4.1). There were no signals characteristic of the η^6 -arene, nor were there any attributable to the methyl groups of η^1 - $\text{Ph}_2\text{P}(\text{CH}_2)_3\text{C}_6\text{Me}_5$ (**200**). The latter were most probably masked by the presence of the large peaks due to both coordinated acetonitrile and d_3 -acetonitrile (quintet at 1.96 ppm) which span the region 1.8-2.2 ppm; signals due to η^1 - $\text{Ph}_2\text{P}(\text{CH}_2)_3\text{C}_6\text{Me}_5$ of $[\text{RuCl}_2(\eta^6\text{-1,2-MeC}_6\text{H}_4\text{CO}_2\text{Me})(\eta^1\text{-Ph}_2\text{P}(\text{CH}_2)_3\text{C}_6\text{Me}_5)]$ (**241**) lie in the region 2.0-2.1 in CDCl_3 (see Chapter 8, Section 8.2). There were three multiplets which are possibly attributable to the three methylene groups, each centred around 1.32, 1.58 and 3.06 ppm, *cf.* 2.21, 2.52 and 2.76 ppm in CDCl_3 for **241**. The $^{31}\text{P}\{^1\text{H}\}$ -NMR spectrum (CD_3CN) showed a singlet at δ 104.3 (*cf.* δ 26.2 for **251** in CDCl_3 ; see page 113, Chapter 3, Section 3.2.4). The ^1H NMR spectrum (CD_3CN) of the yellow solid isolated from the reaction of $[\text{306}][\text{SbCl}_6]$ and acetonitrile showed an intense signal at δ 2.23, presumably due to coordinated acetonitrile. Surprisingly there was no resonance attributable to free C_6Me_6 , which occurs at δ 2.17. The peak at δ 2.23 was not due to $\eta^6\text{-C}_6\text{Me}_6$, since this signal appears at higher frequency than that for free hexamethylbenzene.²⁰ The $^{31}\text{P}\{^1\text{H}\}$ -NMR spectrum (CD_3CN) showed a singlet at δ 23.6 (*cf.* δ 29.0 in CD_2Cl_2 for $[\text{RuCl}_2(\eta^6\text{-C}_6\text{Me}_6)(\text{PPh}_3)]$ (**306**)).

The crude sample of $[\text{RuCl}_2(\eta^6\text{-1,3,5-C}_6\text{H}_3\text{Me}_3)(\text{PPh}_3)][\text{SbCl}_6]$ ($[\text{339}][\text{SbCl}_6]$) also reacted with acetonitrile; the observations were the same as for complexes $[\text{251}][\text{SbCl}_6]$ and $[\text{306}][\text{SbCl}_6]$. The ^1H NMR spectrum (CD_3CN) of the isolated yellow solid showed only a large signal at δ 2.27, characteristic of coordinated acetonitrile; there were no signals indicative of either free or η^6 -mesitylene. No signal was detected in the $^{31}\text{P}\{^1\text{H}\}$ -NMR spectrum.

Unfortunately these preliminary investigations of the NMR spectra of the products of these reactions do not allow any conclusions to be drawn about the nature of the products. It is, however, clear that the reaction of arene-ruthenium complexes occurs more rapidly at the Ru(III) level than it does with Ru(II) complexes.

6.2 Theoretical Calculations

Calculations using DFT have been performed by Dr John McGrady at the University of York²¹ on the simplified arene-Ru(II) species $[\text{RuCl}_2(\eta^6\text{-C}_6\text{H}_6)(\text{PH}_3)]$ (**344**) and its arene-Ru(III) counterpart $[\text{RuCl}_2(\eta^6\text{-C}_6\text{H}_6)(\text{PH}_3)]^+$ (**[344]**⁺). Idealised C_s symmetry was imposed in each case. A calculated orbital energy diagram for **344** is shown in Figure 81. The HOMO of the neutral species is strongly destabilised by a Ru-Cl antibonding interaction. The other two orbitals are also Ru-Cl π antibonding, but to a lesser extent than the HOMO. As a result of the Ru-Cl antibonding character in the HOMO, oxidation causes a decrease (*ca* 0.1 Å) in the Ru-Cl bond lengths from 2.43 Å in **344** to 2.33 Å **[344]**⁺. This reflects nicely the observed trends (see page 283).

A comparison of calculated and observed bond lengths for the arene-Ru(II) and arene-Ru(III) species are listed in Table 39. In addition to the contraction in Ru-Cl bond lengths, oxidation also causes a significant increase (*ca* 0.1 Å) in the calculated Ru-C(arene) bond lengths (2.29 Å in **344**, 2.41 Å in **[344]**⁺). Again, this trend was also observed in the X-ray structures of the non-tethered systems **306** (2.25 Å)¹³ and its Ru(III) counterpart **[306][SbCl₆]** (2.33 Å), and in the case of tethered systems **251** (2.23 Å) and the respective Ru(III) species **[251][SbCl₆]** (2.31 Å). The magnitude of the Ru-C bond contraction is somewhat underestimated by the calculations, probably because the calculations are based on η^6 -benzene rather than its methyl-substituted analogue.²¹ Calculated Ru-P bond lengths, in contrast, are almost identical in the neutral and oxidised forms (2.32 Å), which is identical to those observed in the X-ray structures of the Ru(II) species **306**¹³ and **251**, as well as in the Ru(III) analogues **[306][SbCl₆]** and **[251][SbCl₆]**.

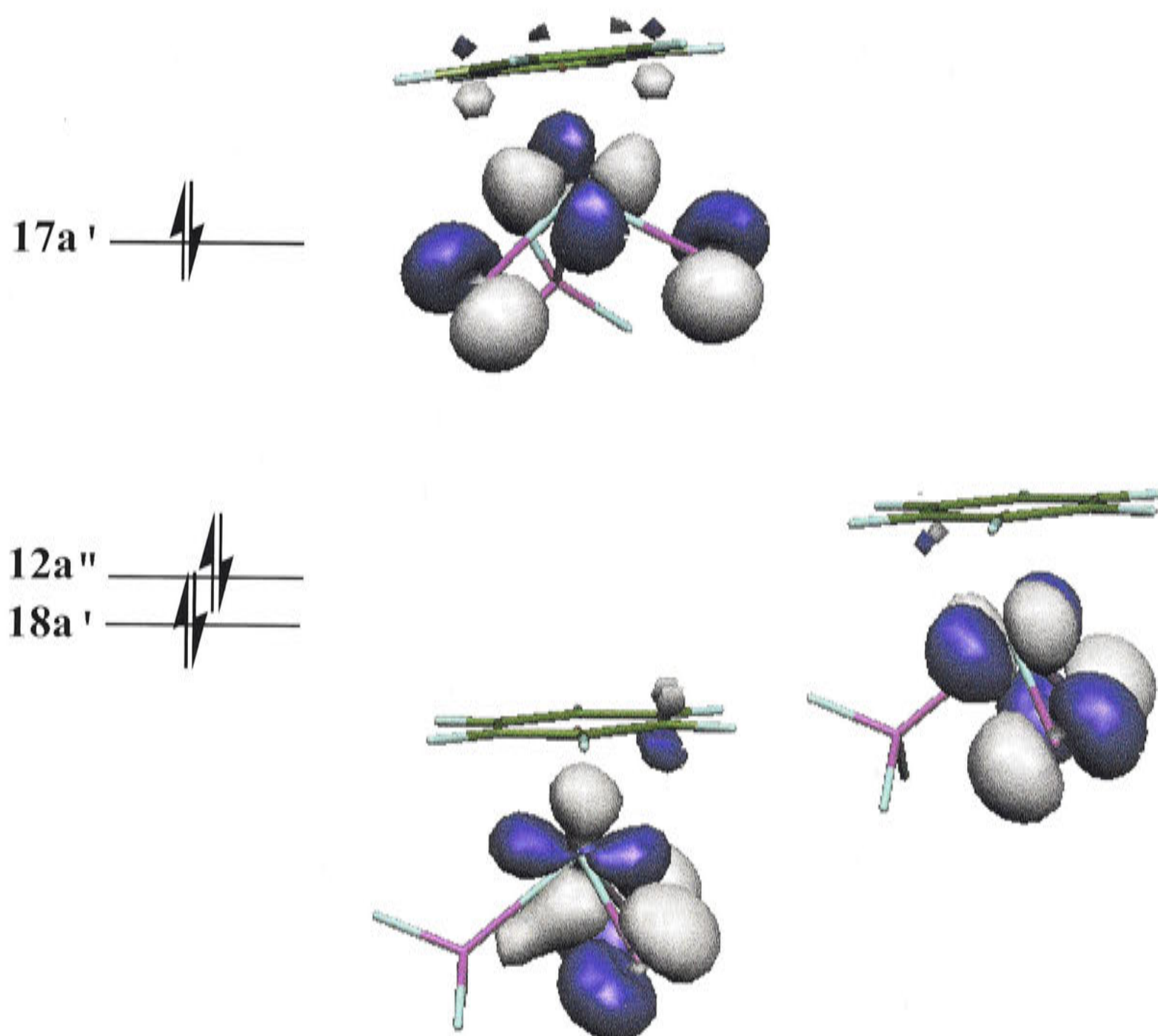


Figure 81. Calculated orbital energy diagram of the three occupied d symmetry orbitals of the Ru(II) species $[\text{RuCl}_2(\eta^6\text{-C}_6\text{H}_6)(\text{PH}_3)]$ (344).

Table 39. Calculated²¹ and observed bond lengths for arene-Ru(II) and arene-Ru(III) complexes.

Compound	Bond Length		
	Average Ru-C (Å)	Ru-Cl (Å)	Ru-P (Å)
[RuCl ₂ (η ⁶ -C ₆ H ₆)(PH ₃)] (344) ^a	2.29	2.43	2.33
[RuCl ₂ (η ⁶ -C ₆ Me ₆)(PPh ₃)] (306) ^{b,c}	2.25	2.41	2.32
[RuCl ₂ (η ¹ :η ⁶ -Ph ₂ P(CH ₂) ₃ C ₆ Me ₅)] (251) ^b	2.23	2.41	2.30
[RuCl ₂ (η ⁶ -C ₆ H ₆)(PH ₃)] ⁺ ([344] ⁺) ^a	2.41	2.33	2.32
[RuCl ₂ (η ⁶ -C ₆ Me ₆)(PPh ₃)] ⁺ ([306] ⁺) ^b	2.33	2.31	2.34
[RuCl ₂ (η ¹ :η ⁶ -Ph ₂ P(CH ₂) ₃ C ₆ Me ₅)] ⁺ ([251] ⁺) ^b	2.31	2.32	2.32

^aCalculated²¹; ^bobserved; ^ccrystal structure reported in reference(13).

6.3 Summary

These results clearly illustrate that, with the use of the triarylammonium oxidant $[\text{N}(\text{C}_6\text{H}_4\text{Br-4})_3][\text{SbCl}_6]$ (**[48][SbCl₆]**), it is possible to isolate arene-Ru(III) compounds containing permethylated η^6 -arenes, whose existence was strongly suggested by electrochemical studies (Chapter 5, Section 5.1). There are distinct differences in the Ru-C(arene) and Ru-Cl distances between the precursor Ru(II) complexes $[\text{RuCl}_2(\eta^1:\eta^6\text{-Ph}_2\text{P}(\text{CH}_2)_3\text{C}_6\text{Me}_5)]$ (**(251)**) and $[\text{RuCl}_2(\eta^6\text{-C}_6\text{Me}_6)(\text{PPh}_3)]$ (**(306)**) and their respective oxidation products $[\text{RuCl}_2(\eta^1:\eta^6\text{-Ph}_2\text{P}(\text{CH}_2)_3\text{C}_6\text{Me}_5)][\text{SbCl}_6]$ (**[(251)][SbCl₆]**) and $[\text{RuCl}_2(\eta^6\text{-C}_6\text{Me}_6)(\text{PPh}_3)][\text{SbCl}_6]$ (**[(306)][SbCl₆]**). The longer Ru-C(arene) and shorter Ru-Cl bond lengths in the arene-Ru(III) systems, compared with their parent Ru(II) compounds, have been reproduced in theoretical calculations.²¹ The fact that the arene-Ru(III) species **[(306)][SbCl₆]** has been isolated, when electrochemical studies suggested that it was highly unstable, together with other observations that arise from the work described here, will be discussed in the next Chapter.

References

- (1) Reynolds, R.; Line, L. L.; Nelson, R. F. *J. Am. Chem. Soc.* **1974**, *96*, 1087-1092.
- (2) Connelly, N. G.; Geiger, W. G. *Chem. Rev.* **1996**, *96*, 877-910.
- (3) Kochi, J. K. *Acc. Chem. Res.* **1992**, *25*, 39-47.
- (4) Parsons, R. *Handbook of Electrochemical Constants*; Butterworths Publications Limited: London, 1959, p. 73.
- (5) Song, L.; Trogler, W. C. *Angew. Chem. Int. Ed. Engl.* **1992**, *31*, 770-772.
- (6) Ebersson, L.; Larsson, B. *Acta. Chem. Scand.* **1986**, *B40*, 210-225.
- (7) Connelly, N. G.; Hassard, K. A.; Dunne, B. J.; Orpen, A. G.; Raven, S. J.; Carriedo, G. A.; Riera, V. J. *Chem. Soc., Dalton Trans.* **1988**, 1623-1629.

- (8) Bell, F. A.; Ledwith, A.; Sherrington, D. C. *J. Chem. Soc. C* **1969**, 2719-2720.
- (9) Ebersson, L.; Larsson, B. *Acta Chem. Scand.* **1987**, B41, 367-378.
- (10) Schmidt, W.; Steckhan, E. *Chem. Ber.* **1980**, 113, 577-585.
- (11) Bennett, M. A.; Huang, T.-N.; Latten, J. L. *J. Organomet. Chem.* **1984**, 272, 189-205.
- (12) Saboonchian, V.; Wilkinson, G.; Hussain-Bates, B.; Hursthouse, M. B. *Polyhedron* **1991**, 10, 595-603.
- (13) Hansen, H. D.; Nelson, J. H. *Organometallics* **2000**, 19, 4750-4755.
- (14) Eliel, E. L.; Wilen, S. H.; Mander, L. N. *Stereochemistry of Organic Compounds*; John Wiley & Sons, Inc: New York, 1994, p. 686.
- (15) ref. 14, p. 689.
- (16) Lindqvist, I.; Niggli, A. *J. Inorg. Nucl. Chem.* **1956**, 2, 345-347.
- (17) Teulon, P.; Roziere, J. Z. *Anorg. Allgem. Chem.* **1981**, 483, 219-224.
- (18) Teulon, P.; Roziere, J. *J. Organomet. Chem.* **1981**, 214, 391-397.
- (19) Spek, A. L. *PLATON, An Integrated Tool for the Analysis of the Results of a Single Crystal Structure Determination*, University of Utrecht, Utrecht, The Netherlands, 2003.
- (20) Bennett, M. A.; Huang, T.-N.; Matheson, T. W.; Smith, A. K. *Inorganic Syntheses*; Fackler, Jr, J. P. Ed., John Wiley & Sons, Inc.: New York, 1982; Vol. 21, pp. 74-78.
- (21) McGrady, J. E., 2003, personal communication.

Chapter 7: Discussion of the Results of the Work Described in this Thesis

The aims of this Thesis, as set out in Chapter 1, pp. 60-61, have been achieved to a large extent. In summary, it has been shown that one-electron oxidation products of the half-sandwich ruthenium(II) complexes $[\text{RuCl}_2(\eta^6\text{-arene})(\text{PR}_3)]$ can be generated as long-lived species at *ca* -45°C and characterised by their electronic and ESR spectra. Two examples of these arene-ruthenium(III) complexes have been isolated and characterised structurally for the first time, namely, $[\text{RuCl}_2(\eta^1:\eta^6\text{-Ph}_2\text{P}(\text{CH}_2)_3\text{C}_6\text{Me}_5)][\text{SbCl}_6]$ (**[251]** $[\text{SbCl}_6]$) and $[\text{RuCl}_2(\eta^6\text{-C}_6\text{Me}_6)(\text{PPh}_3)][\text{SbCl}_6]$ (**[306]** $[\text{SbCl}_6]$), thus illustrating the effect of removal of one electron on the metal-arene bond in complexes of this type. The effect of the presence of a flexible two- or three-atom tether between the η^6 -arene and the P-donor on the stability of the arene-Ru(II) and arene-Ru(III) species has been investigated. In this Chapter I attempt a general discussion of the observations.

7.1 Arene-Ruthenium(III)

As noted in Chapter 1, previous evidence for the transient existence of arene-ruthenium(III) species of the type $[\text{RuX}_2(\eta^6\text{-arene})(\text{PR}_3)]^+$ ($\text{X} = \text{halide}$) rests mainly on the observation of generally reversible cyclic voltammetry of the corresponding ruthenium(II) complexes (see Chapter 5, p. 225).¹⁻⁴ In the non-tethered series, I have shown that the one-electron oxidation products $[\text{RuCl}_2(\eta^6\text{-C}_6\text{R}_6)(\text{PR}'_3)]^+$ ($\text{R} = \text{H}$; $\text{R}' = \text{Me}$ (**337**), Ph (**302**) and $\text{R} = \text{Me}$; $\text{R}' = \text{Me}$ (**304**), Ph (**306**)) can be electrogenerated at *ca* 228K, but only the PPh_3 derivatives display reversible spectroelectrochemical behaviour at this temperature. The decomposition process is likely to involve loss of η^6 -arene from the labile Ru(III) centre, but since nothing is known about the nature of the products, the reasons for this difference in stability between the PPh_3 and PMe_3 complexes remain unknown. Although spectroelectrochemistry is a very useful technique for monitoring changes in oxidation state, and for assessing both the reversibility of the process and the thermal stability of the electrogenerated species, in this case, it provides no detailed structural

information on the nature of the product(s) formed. Moreover, although spectroelectrochemistry indicated that $[306]^+$ is unstable at room temperature in solution, this cation can be isolated as its $[\text{SbCl}_6]^-$ salt at low temperature, indicating that the stability of the salt depends on the nature and the relative sizes of the cation and anion.

The spectroelectrochemical results show that the tethered complexes of the $[\text{RuCl}_2(\eta^6\text{-arene})(\text{PR}_3)]^+$ class, in which there is a tris(methylene) tether between the arene and the P-donor, generally retain their reversible electrochemical behaviour at least up to *ca* 270K, especially when there are isopropyl substituents on phosphorus or methyl substituents on the arene. In contrast to the non-tethered systems, they tend to decompose by spontaneous reduction to their Ru(II) precursor, presumably at the expense of water in the solvent. Evidently the tether slows down the irreversible loss of coordinated arene at the Ru(III) level, as was envisaged in the original research outline (p. 1). As in the non-tethered series, however, the arene-ruthenium(III) complex $[337]^+$, having no methyl groups on the arene and methyl groups on phosphorus, does not survive above *ca* 238K, and the same is true for the system $[302]^+$ having phenyl groups on phosphorus. In contrast, the *i*-Pr₂P tethered derivative $[\text{RuCl}_2(\eta^1:\eta^6\text{-}i\text{-Pr}_2\text{P}(\text{CH}_2)_3\text{Ph})]^+$ ($[249]^+$) is considerably more stable and survives to *ca* 268K. Comparison of $E_{1/2}$ values for compounds $[\text{RuCl}_2(\eta^6\text{-C}_6\text{H}_6)(\text{PMe}_3)]$ (337) and $[\text{RuCl}_2(\eta^1:\eta^6\text{-Me}_2\text{P}(\text{CH}_2)_3\text{Ph})]$ (248) (see Table 32, p. 225) suggests that the presence of the tether has no marked thermodynamic stabilising effect on arene-ruthenium(III) relative to arene-ruthenium(II).

The most important factor contributing to the stability of the arene-ruthenium(III) complexes studied in this Thesis appears to be the presence of the methyl groups on the η^6 -arene. Thus, the electrogenerated tethered cation $[251]^+$ survives for a limited period in solution, even at room temperature. Several effects probably contribute to this enhanced stability. First, the electron donating methyl groups shift the redox potentials, as expected, in favour of Ru(III) relative to Ru(II) (see Chapter 5, p. 220 and Table 32, p. 225).

The methyl groups probably exert a thermodynamic strengthening effect on the ruthenium(III)-arene bond and their bulk also serves to inhibit loss of arene from the coordination sphere, *i.e.* a kinetic effect. This behaviour is well established in metal-arene chemistry. For example, displacement of the arene from $[\text{Fe}(\eta^6\text{-arene})_2][\text{PF}_6]_2$ by potassium thiocyanate, to form $\text{Fe}(\text{NCS})_3$, requires 24 h at room temperature for arene = C_6Me_6 (**[345]** $[\text{PF}_6]_2$), but only 15 min under the same conditions for arene = C_6H_6 (**[346]** $[\text{PF}_6]_2$).⁵ Likewise, **[346]** $[\text{PF}_6]_2$ decomposes immediately in acetonitrile, whereas its C_6Me_6 analogue **[345]** $[\text{PF}_6]_2$ is stable for several days.⁶ Similar observations have been made for Ru(II) complexes of the type $[\text{RuMe}_2(\eta^6\text{-arene})(\text{PMe}_2\text{Ph})]$; the C_6Me_6 complex **56** is stable at room temperature,⁷ whereas the C_6H_6 complex **79** decomposes above -40°C in the solid state.⁸ Further, the displacement of η^6 -hexamethylbenzene by benzene from its $\text{Cr}(\text{CO})_3$ complex is not favoured enthalpically.⁹

At this stage one cannot say whether the number of atoms in the tether plays a significant role in the stabilisation of arene-ruthenium(III) species. Both the electrogenerated two-atom tethered cation $[\text{RuCl}_2(\eta^1:\eta^6\text{-Ph}_2\text{PCH}_2\text{SiMe}_2\text{Ph})]^+$ (**[252]**⁺) and the three-atom cation $[\text{RuCl}_2(\eta^1:\eta^6\text{-Me}_2\text{P}(\text{CH}_2)_3\text{Ph})]^+$ (**[248]**⁺) decompose above *ca* 228K; its phenyl analogue **[222]**⁺ could not be generated reversibly. More work with a wider range of two-atom tethered complexes containing a methyl-substituted arene would be necessary to answer this question.

The crucial role played by the methyl substituents on the η^6 -arene is most evident in the fact that only the fully methylated arene-Ru(III) species $[\text{RuCl}_2(\eta^1:\eta^6\text{-Ph}_2\text{P}(\text{CH}_2)_3\text{C}_6\text{Me}_5)][\text{SbCl}_6]$ (**[251]** $[\text{SbCl}_6]$) and its non-tethered analogue $[\text{RuCl}_2(\eta^6\text{-C}_6\text{Me}_6)(\text{PPh}_3)][\text{SbCl}_6]$ (**[306]** $[\text{SbCl}_6]$) could be isolated in this work. They were obtained by treatment of the Ru(II) precursors **251** and **306**, respectively, with $[\text{N}(\text{C}_6\text{H}_4\text{Br-4})_3]\text{SbCl}_6$ (**[48]** $[\text{SbCl}_6]$). Attempts to extend the procedure to other members of the tethered or non-tethered series failed. Clearly, the arene-ruthenium(III) complexes themselves are strong oxidants and only with the permethylated arenes are the reduction potentials of the

Ru(II) complexes sufficiently below that of $[48]^+$ [$E_{1/2} = + 0.55$ V for **251**; + 0.54 V for **306**; + 0.70 V for $[48]^+$,^{10,11} all potentials are quoted *vs* $Fe^{0/I}$ in CH_2Cl_2] to allow stoichiometric oxidation of the Ru(II)-arene complexes. Although the formation of both $[251][SbCl_6]$ and $[306][SbCl_6]$ shows that the presence of the tether is not absolutely necessary for the isolation of arene-Ru(III) complexes, the ready formation of the charge transfer complex $[306].SbCl_3$ in the reaction between **306** and $[48][SbCl_6]$ suggests that the tether may impart kinetic stabilisation. The tethered complex $[251][SbCl_6]$ does not appear to decompose in the same way as the non-tethered compound $[306][SbCl_6]$ under the same conditions. Evidently the nature of the anion influences the mode of decomposition of $[[306]]^+$; the isolated $SbCl_6$ salt reverts back to a Ru(II) complex, namely the 1:1 molecular adduct $[306].SbCl_3$. In contrast, the electrogenerated BF_4 salt presumably decomposed *via* loss of η^6 -arene. This is another example of the effect that the anion has on paramagnetic cations. Geiger *et al.*¹² have stabilised the 17-electron species $[Cr(\eta^6-C_6H_6)(CO)_3]^+$ ($[1]^+$) with the large anion $[B(C_6F_5)_4]^-$ to the extent that one of the CO ligands, and not the η^6 -benzene, was displaced by triphenylphosphine.

As noted in Chapter 6, the main advantage of the oxidant $[N(C_6H_4Br-4)_3]SbCl_6$ ($[48][SbCl_6]$) is its commercial availability; an obvious disadvantage is that the anion is not chemically inert. It would be desirable in future work to employ bulky, poorly nucleophilic anions in place of $[SbCl_6]^-$, best would be $[B(C_6F_5)_4]^-$ or $[B(3,5-C_6H_3(CF_3)_2)_4]^-$ ($[BAr^F_4]^-$). In particular, $[B(C_6F_5)_4]^-$ has been used to isolate arene-chromium(I) cations $[Cr(\eta^6-C_6H_6)(CO)_3]^+$ ($[1]^+$) and $[Cr(\eta^5-C_5H_5)(CO)_2]^+$,¹² which are otherwise detectable only by cyclic voltammetry.¹³⁻¹⁵ The anion present in the supporting electrolyte influences the electrochemical behaviour of complexes of the type $[Cr(\eta^6\text{-arene})(CO)_3]$.^{16,17} For example, in the presence of $[Bu^*_4N]PF_6$, the decomposition of the oxidized species $[1]^+$ was slowed down so that the electrochemical process became chemically reversible, in contrast to the behaviour using $[Bu^*_4N]Y$ ($Y = ClO_4^-, BF_4^-, CF_3SO_3^-$).¹⁶

The main changes that accompany one-electron oxidation of **251** and **306** are contractions (and, presumably, strengthening) of the Ru-Cl bonds and a lengthening of the metal-arene carbon bonds, presumably reflecting a weakening of the metal-arene interaction. In contrast, the Ru-P bond lengths do not differ significantly between the Ru(II) and Ru(III) complexes. A weak metal-arene interaction at the Ru(III) level is also implied by the rapid displacement of the arene by acetonitrile, the corresponding process at the Ru(II) level being much slower. Despite the weakening of the metal-arene bond on oxidation, the hapticity of the ring and the overall geometry of the complexes do not change. The behaviour contrasts with the reversible η^6 - to η^4 -change in arene coordination which occurs on successive one-electron reduction in the Ru(II) complexes $[\text{Ru}(\eta^6\text{-arene})(\eta^4\text{-arene}')]^{2+}$ to $[\text{Ru}(\eta^4\text{-arene})(\eta^6\text{-arene}')]$,¹⁸ and in the mixed valence ions of ruthenium $[2_n]$ cyclophanes.¹⁹ Reversible η^6 - to η^4 -changes also occur in the isoelectronic complexes $[\text{M}(\eta^5\text{-C}_5\text{Me}_5)(\eta^6\text{-arene})]^{2+}$ ($\text{M} = \text{Rh}, \text{Ir}$) to $[\text{M}(\eta^5\text{-C}_5\text{Me}_5)(\eta^4\text{-arene})]$.²⁰

The trends in bond-lengths are reproduced by calculations using DFT performed by Dr John McGrady at the University of York²¹ on the model system $[\text{RuCl}_2(\eta^6\text{-C}_6\text{H}_6)(\text{PH}_3)]^{n+}$ ($[\mathbf{344}]^{n+}$) [$n = 0, 1$], which show that the shortening of the Ru-Cl bond lengths on oxidation is caused by removal of the electron from a HOMO which is strongly Ru-Cl antibonding. The cause of the weaker metal-arene interaction on oxidation is not so evident from the calculations but, qualitatively, it can be attributed to a weakening of the Ru(d)-arene(π^*) back-bonding interaction and possibly also competition for a vacant metal orbital between the arene π -orbitals and chlorine p -orbitals. The theoretical calculations show that the unpaired electron is located in a Ru-Cl-based orbital and this conclusion is supported by the ESR spectra of $[\mathbf{251}]^+$ and $[\mathbf{306}]^+$, which are typical of low-spin d^5 -metal complexes.²²

A similar contraction (*ca* 0.1 Å) in the metal-chlorine bond length is observed on one-electron oxidation of $[\text{FeCl}(\eta^5\text{-C}_5\text{Me}_5)(\eta^2\text{-dppe})]$,^{23,24} and the theoretical calculations show, as in the case for $[\text{RuCl}_2(\eta^6\text{-C}_6\text{H}_6)(\text{PH}_3)]^{n+}$ ($[\mathbf{344}]^{n+}$) [$n = 0, 1$] described above, that the electron is removed from the HOMO which is

antibonding with respect to chloride.²⁴ However, the changes in the other metal-ligand bond lengths are different to those observed in the arene-Ru complexes described in this thesis; there is a small, barely significant lengthening (*ca* 0.03 Å) in metal-C(cyclopentadienyl) bonds, and a significant lengthening of the Fe-P bond lengths (0.09 Å) upon oxidation.^{23,24} Although the complexes of the type $[\text{RuCl}_2(\eta^6\text{-arene})(\text{PR}_3)]^{n+}$ ($n = 0, 1$) are isoelectronic with $[\text{FeCl}(\eta^5\text{-C}_5\text{Me}_5)(\eta^2\text{-dppe})]^{n+}$ ($n = 0, 1$), and show the same effects in the M-Cl bond lengths, clearly the change in other M-ligand bond distances are not the same, and other effects need to be considered.

Oxidatively induced contraction of metal-chloride bonds has also been observed in some Group 6 complexes; *ca* 0.1 Å in $[\text{Mo}(\eta^5\text{-C}_5\text{H}_5)\text{Cl}_2(\text{PMe}_3)_2]^{n+}$ ($n = 0, 1$), as well as a lengthening of both the Mo-P and M-cyclopentadienyl carbon bonds (*ca* 0.05 Å),²⁵ despite the negative charge on the η^5 -cyclopentadienyl ligand.²⁵ The W-Cl bond in $[\text{WTp}^*\text{Cl}(\text{CO})(\text{MeC}\equiv\text{CMe})]^{n+}$ ($\text{Tp}^* = \text{hydro-tris}(3,5\text{-dimethylpyrazolyl})\text{borate}$; ²⁶ $n = 0, 1$) also contracts by *ca* 0.1 Å upon oxidation, and there is also a slight shortening of the W-N bond lengths (*ca* 0.4 Å), as well as a notable lengthening of the W-C(O) bond (*ca* 0.15 Å); there is no significant difference in the W-C(alkyne) bonds.²⁷ There is also a marked contraction of the Re-Cl bond in $[\text{ReCl}(\text{CN-}t\text{-Bu})_3(\text{PCy}_3)_2]^{n+}$ [$n = 0, 1$] (*ca* 0.18 Å) and a lengthening of both the Re-C (*ca* 0.1 Å) and Re-P (*ca* 0.04 Å) bonds on oxidation.²⁸

Also, in the chelate octahedral ruthenium complexes $[\text{Ru}(\text{acac})_2(\eta^2:\eta^1\text{-CH}_2=\text{CHC}_6\text{H}_4\text{NMe}_2)]^{n+}$ ($n = 0, 1$), the bond lengths to the side-bonded alkene increase (*ca* 0.09 Å) on oxidation, those to the oxygen atoms of the anionic ligands decrease (*ca* 0.06 Å), while those to the nitrogen atom remain almost unchanged.²⁹

For comparison, it is noteworthy that metal-arene bond lengths in the bis(arene) Group 6 complexes $[\text{M}(\eta^6\text{-arene})_2]^{n+}$ ($\text{M} = \text{Cr, Mo}$; $n = 0, 1$) are almost invariant on oxidation. For example, the most recent reports of the molecular structure of $[\text{Cr}(\eta^6\text{-C}_6\text{H}_6)_2]$ (**347**),³⁰⁻³² determined by X-ray

crystallography, give an average Cr-C bond length of 2.132 Å, which is virtually identical to that of the one-electron oxidation product [347]⁺; the Cr-C bond lengths in the bromide,³³ iodide³⁴ and hydroxide^{35,36} salts lie in the range 2.13-2.14 Å. It is not possible to make a direct comparison for [Mo(η⁶-C₆H₆)₂]ⁿ⁺ (348) [n = 0, 1]; there are no bond lengths reported in the publication describing the determination of its X-ray structure.³⁷ The average Mo-C distance in the one-electron oxidation product [347]⁺ is 2.27 Å,³⁸ which is identical to that reported for [Mo(η⁶-C₆H₅Me)₂].³⁹ This behaviour is in agreement with DFT calculations on [M(η⁶-C₆H₆)₂]ⁿ⁺ (M = Cr (347), Mo (348)) [n = 0, 1].²¹ Further, semi-empirical and *ab initio* calculations have indicated that the electron of 347 is removed from a Cr-C(arene) non-bonding orbital on oxidation, thus accounting for the invariance on the Cr-C(arene) bond lengths.⁴⁰

The arene-ruthenium(III) cations characterised in this work expand the limited organometallic chemistry of trivalent ruthenium with π-donor ligands. Evidence for the existence of [RuCl₃(η⁶-C₆Me₆)] (66) as an isolable species,⁴¹ and of complexes [Ru(Me)₂(η⁶-C₆Me₆)(PR₃)]⁺ (R = Ph₃ (5), MePh₂ (55), Me₂Ph (56), Me₃ (57) and Et₃ (58)) as intermediates in C-H bond activation processes,⁷ is noted in Chapter 1. The anionic ligand [C₅Me₅]⁻, which is isoelectronic with C₆Me₆, affords a few isolable complexes both of Ru(III) and Ru(IV).^{42,43} Examples of the former are the di-μ-chloro dimer [Ru(η⁵-C₅Me₅)Cl₂]₂,^{44,45} which was shown by X-ray crystallography to exist in two isomeric forms,^{46,47} and half-sandwich complexes of the type [RuCl₂(η⁵-C₅Me₅)(PR₃)] (R = Me, Ph, *i*-Pr, Cy).⁴⁸ There are also examples of half-sandwich Ru(IV) complexes, such as [RuH₃(η⁵-C₅Me₅)(PR₃)] (R = *i*-Pr, Cy, *t*-Bu)⁴⁸ and the recently reported complexes containing η³-allyl ligands, [RuCl₂(η⁵-C₅Me₅)(η³-MeC(R)CHC(R)O)] (R = Me, *t*-Bu) and [RuCl₂(η⁵-C₅Me₅)(η³-CH₂C(Me)CHC(Me)CH₂)].⁴⁹ Even these Ru(III) and Ru(IV) compounds are readily reduced back to Ru(II).

7.2 Formation and Stability of the Arene-Ruthenium(II) Tethered Complexes

The most generally applicable precursors to the tris(methylene)-tethered complexes $[\text{RuCl}_2(\eta^1:\eta^6\text{-R}_2\text{P}(\text{CH}_2)_3\text{-aryl})]$ are the methyl *o*-toluate derivatives $[\text{RuCl}_2(\eta^6\text{-1,2-MeC}_6\text{H}_4\text{CO}_2\text{Me})(\eta^1\text{-R}_2\text{P}(\text{CH}_2)_3\text{-aryl})]$. Several reports suggest that the ethyl benzoate derivatives would serve as well.⁵⁰⁻⁵⁴ The report of Smith and Wright³ that the *p*-cymene derivative $[\text{RuCl}_2(\eta^6\text{-1,4-MeC}_6\text{H}_4\text{CHMe}_2)(\eta^1\text{-Ph}_2\text{P}(\text{CH}_2)_3\text{Ph})]$ (**223**) affords the $\eta^1:\eta^6$ -chelate complex **222** on heating in chlorobenzene (see Chapter 3, pp. 91-92) could not be confirmed, although this report is often cited as a precedent for this preparative method,^{55,56} and the methodology has also been employed by Demonceau *et al.*,⁵⁷ Noels *et al.*,⁵⁸ as well as Dixneuf and Fürstner.⁵⁹ In the tris(methylene)-tethered series, the *p*-cymene complexes can only be employed as precursors when the phosphorus atom carries bulky substituents such as *iso*-propyl, cyclohexyl or *tert*-butyl, and these reactions are slower than those starting from the aromatic ester precursors. However, this conclusion may only hold in the tris(methylene) series: the two atom-tethered complex $[\text{RuCl}_2(\eta^1:\eta^6\text{-Ph}_2\text{PCH}_2\text{SiMe}_2\text{Ph})]$ (**252**) can be made from the *p*-cymene precursor $[\text{RuCl}_2(\eta^6\text{-1,4-MeC}_6\text{H}_4\text{CHMe}_2)(\eta^1\text{-Ph}_2\text{PCH}_2\text{SiMe}_2\text{Ph})]$ (**235**) and, according to a recent report, the complexes $[\text{RuCl}_2(\eta^1:\eta^6\text{-R}_2\text{P}(\text{CH}_2)_2\text{Ph})]$ can be made by heating $[\text{RuCl}_2(\eta^6\text{-1,4-MeC}_6\text{H}_4\text{CHMe}_2)(\eta^1:\eta^6\text{-R}_2\text{P}(\text{CH}_2)_2\text{Ph})]$ in chlorobenzene for R = Et and Ph, as well as for Cy.⁵⁶

In general, the tethered arene complexes would be expected to be more stable than their non-tethered counterparts on the basis of the chelate effect;⁶⁰ the free energy of formation of the tethered complexes should be largely controlled by the positive entropy change associated with complex formation. For example, complex $[\text{Ni}(\text{H}_2\text{N}(\text{CH}_2)_2\text{NH}_2)_3]^{2+}$, which contains three chelate rings, from $[\text{Ni}(\text{H}_2\text{O})_6]^{2+}$, has a formation constant nearly twice that of the ammine $[\text{Ni}(\text{NH}_3)_6]^{2+}$.⁶¹ In the precursor complexes containing the potentially chelating ligands, the dangling arene cannot travel very far from the metal centre, thus the probability that it can coordinate to the metal atom is larger

than if this end were a free arene, analogous to the chelation model described by Schwarzenbach.⁶²

The formation of the three-atom strapped complexes is analogous to the formation of a six-membered ring (the η^6 -arene is considered as a single atom in this case). In organic chemistry, the ease of ring-closure is enhanced by replacement of the hydrogen atoms by alkyl substituents; this is known as the Thorpe-Ingold effect.^{63,64} In organometallic chemistry, the presence of bulky-substituents, such as *tert*-butyl, on a phosphorus atom favours the formation of cyclometallated complexes.⁶⁵ In order for ring-closure to occur, there must be a reduction in the bond angles of the atoms that constitute the ring;⁶⁴ this was observed X-ray structures of the non-tethered and tethered complexes, and is discussed in more detail in Chapter 3 (see pp. 170-180).

It is well known that cyclometallation of tertiary phosphines is strongly favoured by the presence of bulky substituents on phosphorus. Since this process involves the formation of a chelate ring, there is a clear analogy with the formation of tethered arene complexes. The factors controlling this process have been described by Shaw,^{63,65} and, by analogy, it can be argued in the present case that the bulky substituents favour a conformation of the aliphatic chain which brings the dangling aromatic ring into proximity with the metal centre. Further, the bulky substituents can give rise to restricted rotation about M-P and P-C bonds, hence the loss of internal rotational entropy on formation of the tethered complexes will be relatively small. The observed fluxional behaviour of the two-atom tether described in Chapter 3, pp. 106-110, in complex $[\text{RuCl}_2(\eta^1:\eta^6\text{-Ph}_2\text{PCH}_2\text{SiMe}_2\text{Ph})]$ (252) shows that the aliphatic chains are not rigid and that different conformations are readily interconvertible.

Recent measurements have been performed on the relative enthalpies of formation of a series of tertiary phosphine complexes.^{66,67} For example, such measurements on the reaction shown in Scheme 82, establish the order for $-\Delta\text{H}$ as $\text{PPh}_3 > \text{P-}i\text{-Pr}_3 > \text{PCy}_3$.⁶⁶ Similarly for the reaction shown in Scheme

83, the order for $-\Delta H$ is $P(\text{OMe})_3 > P\text{Me}_3 > P\text{Me}_2\text{Ph} > P(\text{OPh})_3 > P\text{MePh}_2 > P\text{Et}_3 > P\text{Bu}^n_3 > P\text{Ph}_3$.⁶⁷ These trends are largely dependent on electronic factors and indicate that formation of sterically bulky phosphine complexes is not favoured enthalpically. As noted in Chapter 3, p. 157, the Ru-P bond lengths in the tethered complexes are generally greater when there are bulky substituents on phosphorus. In the series of complexes $[\text{RuCl}(\eta^5\text{-C}_5\text{Me}_5)(\text{PR}_3)_2]$ ($\text{R}_3 = \text{Me}_3, \text{Me}_2\text{Ph}, \text{MePh}_2, \text{Ph}_3$ and Et_3), similar to those mentioned in Scheme 83, there is a good correlation between the Ru-P bond lengths and the enthalpy of reaction.⁶⁸



Scheme 82. The reaction of $[\text{RuCl}_2(=\text{CH}-\text{CH}=\text{CPh}_2)(\text{PPh}_3)_2]$ with two equivalents of various phosphines.⁶⁶

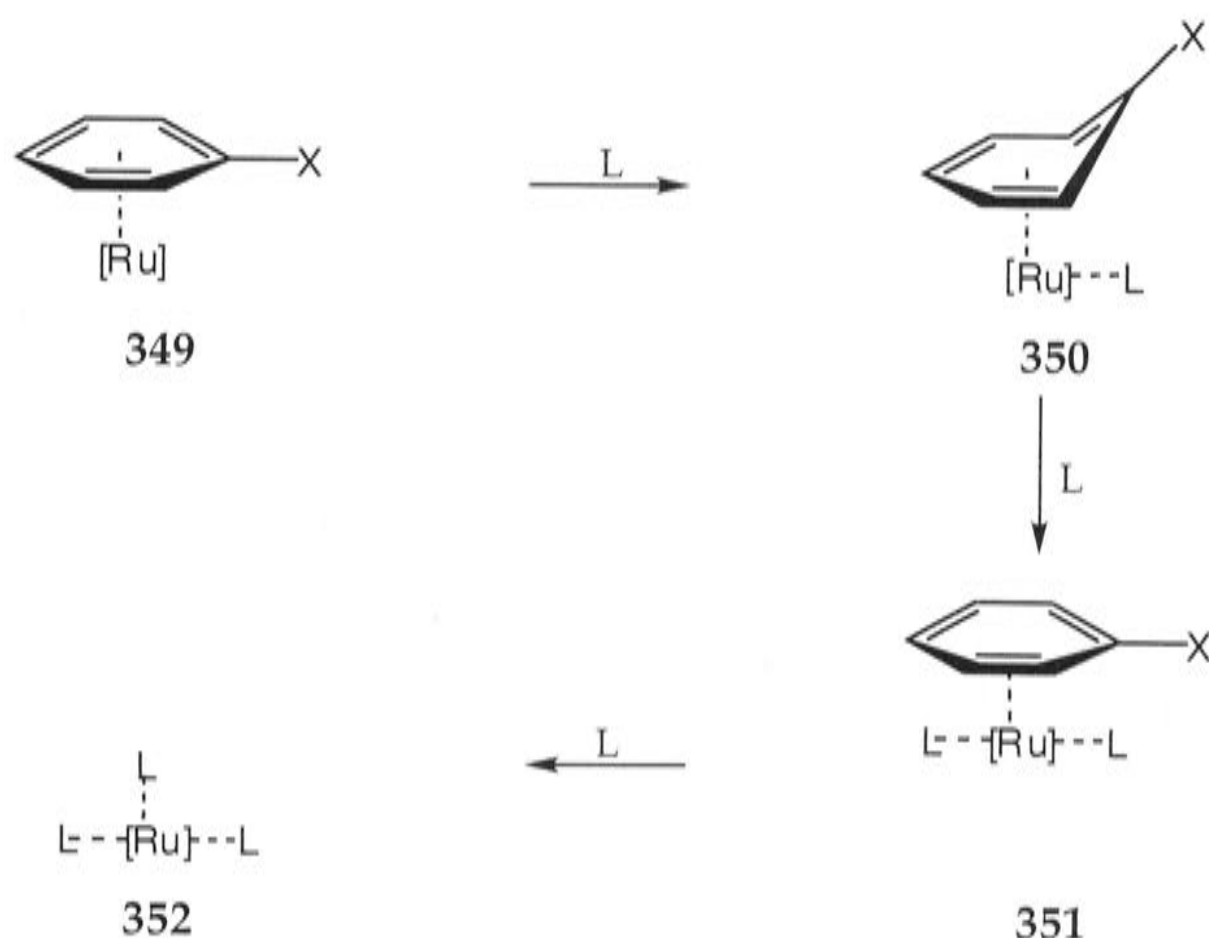


Scheme 83. The reaction of $[\text{RuCl}(\eta^5\text{-C}_5\text{Me}_5)(\eta^4\text{-1,5-COD})]$ with two equivalents of various phosphines.⁶⁷

The synthesis of the tethered complexes described in Chapter 3 establishes that the methyl *o*-toluate is more easily replaced by the tethered ligands than *p*-cymene. Moreover, methyl *o*-toluate is displaced by acetonitrile more rapidly than is benzene from complexes $[\text{RuCl}_2(\eta^6\text{-arene})(\eta^1\text{-}i\text{-Pr}_2\text{P}(\text{CH}_2)_3\text{Ph})]$ (arene = C_6H_6 (228), 1,2- $\text{MeC}_6\text{H}_4\text{CO}_2\text{Me}$ (238)) (Chapter 4, pp. 198-199). The ease of displacement of methyl *o*-toluate is also illustrated in the facile formation of $[\text{Ru}_4(\mu_4\text{-O})(\mu_2\text{-Cl})_8(\eta^1\text{-}t\text{-Bu}_2\text{P}(\text{CH}_2)_3\text{Ph})_4]$ (261) from a crude sample of $[\text{RuCl}_2(\eta^6\text{-1,2-MeC}_6\text{H}_4\text{CO}_2\text{Me})(\eta^1\text{-}t\text{-Bu}_2\text{P}(\text{CH}_2)_3\text{Ph})]$ (245) (Chapter 3, pp. 122-125). Although the Ru-C(arene) bond lengths (av. 2.22 Å) in the methyl *o*-toluate complex $[\text{RuCl}_2(\eta^6\text{-1,2-MeC}_6\text{H}_4\text{CO}_2\text{Me})(\eta^1\text{-Cy}_2\text{P}(\text{CH}_2)_3\text{Ph})]$ (239) do not differ significantly from those in their benzene or *p*-cymene analogues, it may well be that the aromatic ester is more weakly bound than benzene or *p*-cymene. In agreement with this supposition, the displacement

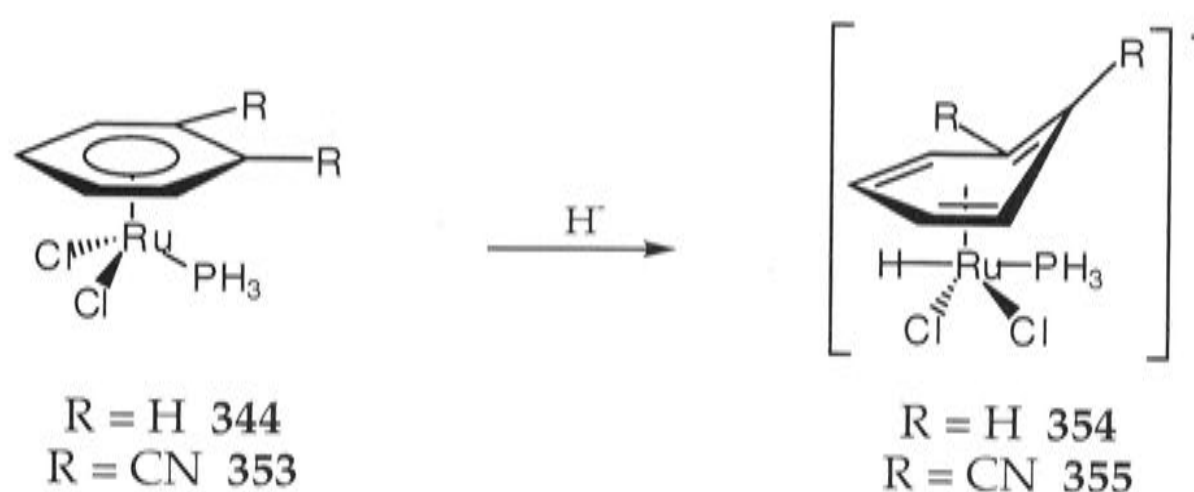
of η^6 -methyl benzoate by benzene from its $\text{Cr}(\text{CO})_3$ complex is enthalpically strongly favoured,⁹ although in the $[\text{Cr}(\eta^6\text{-arene})(\text{CO})_3]$ series also there is no significant lengthening of the Cr-C(arene) distances as a consequence of the ester substituent on the aromatic ring (see for example, the structures of $[\text{Cr}(\eta^6\text{-C}_6\text{H}_5\text{Me})(\text{CO})_3]$ ⁶⁹ and $[\text{Cr}(\eta^6\text{-C}_6\text{H}_5\text{CO}_2\text{Me})(\text{CO})_3]$ ^{70,71}).

In $[\text{ML}_3(\eta^6\text{-arene})]$ complexes, arene replacement, by another arene or other ligands, is thought to occur *via* an intramolecular associative process in which the original arene slides off the metal *via* a series of η^4 - and η^2 -intermediates or transition states.⁷² Complexes of the type $[\text{RuCl}_2(\eta^6\text{-arene})(\text{PR}_3)]$ (349), [represented as $[\text{Ru}](\eta^6\text{-arene})$ for simplicity] can be assumed to react initially with a ligand L to form species of the type $[\text{Ru}](\eta^4\text{-arene})\text{L}$ (350) (Scheme 84). Reaction with another ligand gives the η^2 -compound $[\text{Ru}](\eta^2\text{-arene})\text{L}_2$ (351) and complete arene displacement occurs upon reaction with a final ligand to give $[\text{Ru}]\text{L}_3$ (352).



Scheme 84. Postulated intramolecular associative mechanism of η^6 -arene replacement by L (L = another arene or other ligands) in $[\text{RuCl}_2(\eta^6\text{-arene})(\text{PR}_3)]$ (349) complexes; $\text{RuCl}_2(\text{PR}_3)$ fragment represented as [Ru] for simplicity.

Calculations using DFT have been performed by John McGrady at the University of York²¹ on the reaction of $[\text{RuCl}_2(\eta^6\text{-C}_6\text{H}_6)(\text{PH}_3)]$ (**344**) and $[\text{RuCl}_2(\eta^6\text{-1,2-C}_6\text{H}_4(\text{CN})_2)]$ (**353**) with the two electron donor H^- to give the η^4 -species $[\text{RuCl}_2(\text{H})(\eta^4\text{-C}_6\text{H}_6)(\text{PH}_3)]^-$ (**[354]**⁻) and $[\text{RuCl}_2(\text{H})(\eta^4\text{-1,2-C}_6\text{H}_4(\text{CN})_2)(\text{PH}_3)]^-$ (**[355]**⁻) (Scheme 85). The addition of H^- was used to model the hapticity change in the η^6 -arene, and was designed to represent the η^2 -coordination of the arene at the end of the strap, and is illustrated for modelling purposes only. The isomer of species **[354]**⁻ and **[355]**⁻ depicted in Scheme 85 show that the hydride ligand is *trans* to the phosphine, which is the conformation that is the easiest to model, but may not necessarily be the most stable. The cyano substituents were chosen as the simplest conjugating system to model, in place of the ester substituent in methyl *o*-toluate, 1,2-MeC₆H₄CO₂Me. The reaction of the η^6 -cyano complex **353** is exothermic ($\Delta\text{H} = -112 \text{ kcal mol}^{-1}$), and the reaction of the η^6 -benzene complex **344** was also exothermic, but to a smaller extent ($\Delta\text{H} = -86 \text{ kcal mol}^{-1}$). Thus formation of the η^4 -intermediate **[355]**⁻, incorporating the arene with electron-withdrawing substituents, is *ca* 30 kcal mol⁻¹ more favoured than the unsubstituted η^6 -benzene analogue **[354]**⁻. At this stage there is no information about the geometry of the η^4 -intermediate.



Scheme 85. Calculated reaction of the η^6 -species **344** and **353** with H^- to give the η^4 -analogues **[354]**⁻ and **[355]**⁻.

The tethered complexes that contain methyl substituents on the arene are more difficult to prepare than their unsubstituted counterparts by the methyl

o-toluate displacement method, and, unfortunately, the apparently convenient procedure described by Nelson and Ghebreyessus,⁴ based on the intramolecular base-promoted cyclisation, proved to be low-yielding and irreproducible (see Chapter 3, pp. 142-143). In the case of the pentamethyl-substituted complex $[\text{RuCl}_2(\eta^1:\eta^6\text{-Ph}_2\text{P}(\text{CH}_2)_3\text{C}_6\text{Me}_5)]$ (**251**), some improvement of yield in the methyl *o*-toluate displacement was achieved by use of di-*n*-butyl ether in place of CH_2Cl_2 . This effect appears similar to the well-known promoting effect of ethers,⁷³ such as THF,⁷⁴ in the formation of $[\text{Cr}(\eta^6\text{-arene})(\text{CO})_3]$ complexes from $\text{Cr}(\text{CO})_6$ (**110**)⁷⁵ and, in this case, labile intermediates may be formed. Further, the arene exchange process in d^6 complexes of the type $[\text{ML}_3(\eta^6\text{-arene})]$ does not occur readily in the absence of a donor solvent, such as an ether, but this process can also occur *via* intermediates of the type $[\text{ML}_3\text{L}'_2(\eta^2\text{-arene})]$ ($\text{L}' = \text{ligand or donor solvent}$).⁷⁶ Unfortunately, however, this procedure could not be extended to the mesityl analogue $[\text{RuCl}_2(\eta^1:\eta^6\text{-Ph}_2\text{P}(\text{CH}_2)_3\text{-2,4,6-C}_6\text{H}_2\text{Me}_3)]$ (**250**), for which the yield remained poor (Chapter 3, p. 101).

In the early days of metal-arene chemistry, it was suggested that the three-fold symmetry of mesitylene was an important factor in stabilising mesitylene complexes.^{5,77,78} Although this suggestion is now discounted,⁷⁹ there is some evidence that 1,3,5-substituted arenes, such as mesitylene and hexamethylbenzene, do not react as rapidly as either benzene or unsymmetrically substituted arenes such as 1,2,4-trimethylbenzene and 1,2,3,4-tetramethylbenzene. For example, the acetonitrile-catalysed displacement of naphthalene by arenes from the zerovalent ruthenium complex $[\text{Ru}(\eta^6\text{-C}_{10}\text{H}_8)(\eta^4\text{-1,5-COD})]$ (**356**) occurs quantitatively at room temperature over two days in the case of both 1,2,4-trimethylbenzene and 1,2,3,4-tetramethylbenzene, but requires 70-80°C for five days in the case of mesitylene (with considerable decomposition).⁸⁰ This procedure was not extendable to the hexamethylbenzene analogue, $[\text{Ru}(\eta^6\text{-C}_6\text{Me}_6)(\eta^4\text{-1,5-COD})]$, which was prepared *via* cyclotrimerisation of 2-butyne on **356**.⁸¹ Thus there may be a kinetic barrier to the coordination of arenes having three-fold symmetry.

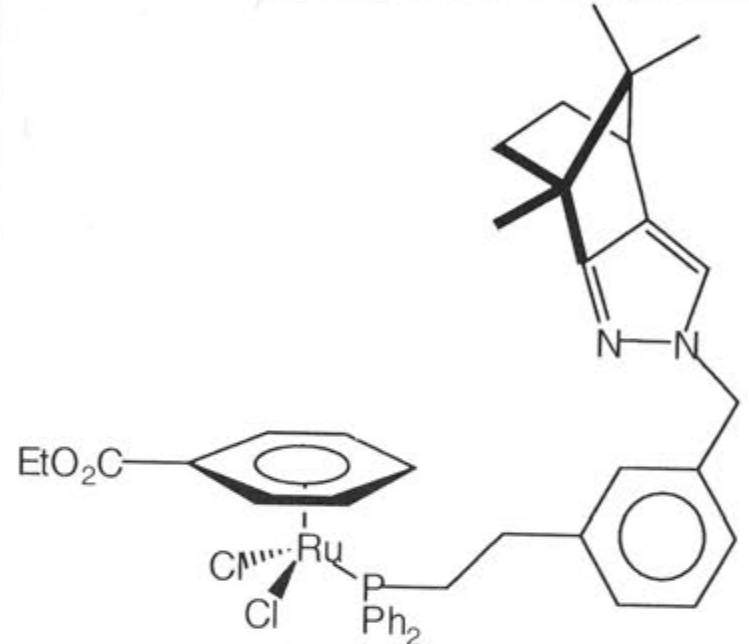
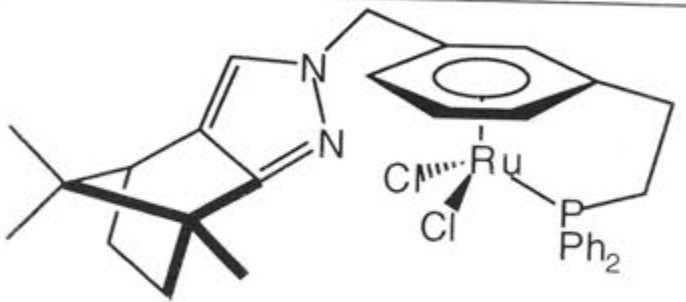
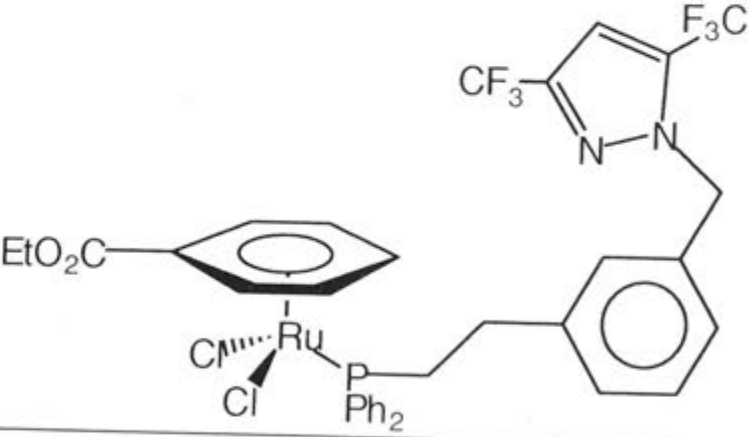
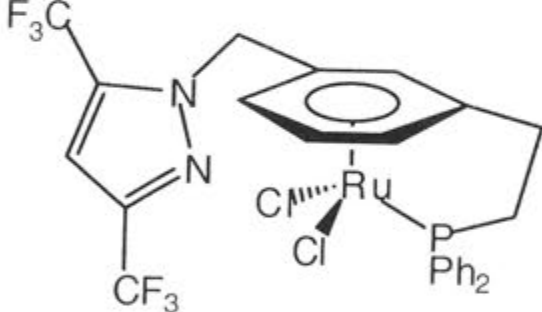
As noted in Chapter 1, since I began my work, several other workers have reported the synthesis of tethered arene-ruthenium(II) complexes by displacement of ethyl benzoate⁵⁰⁻⁵⁴ or *p*-cymene^{3,55-59} as discussed in this Thesis. Their results, with literature citations, are summarised in Table 40. The synthetic procedure based on the methyl *o*-toluate compound has also been published.^{82,83}

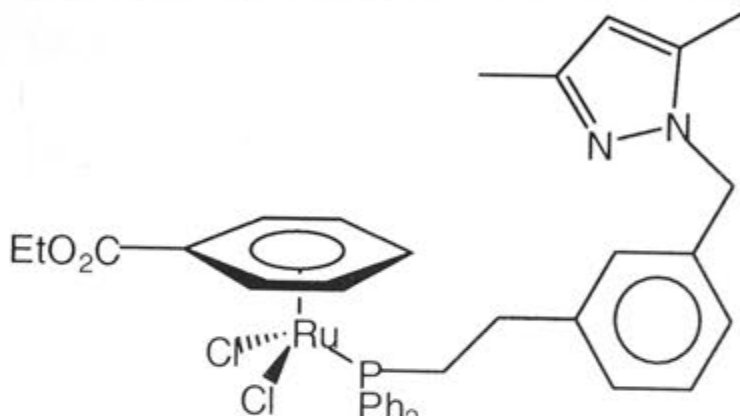
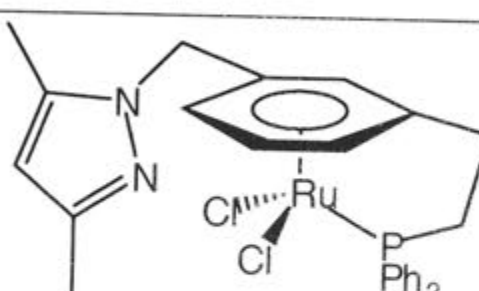
Wright *et al.*³ were the first to report the use of chlorobenzene as a solvent for the preparation of tethered arene complexes *via* the general approach depicted Scheme 16b (Chapter 1, p. 36). Since chlorobenzene is known to form η^6 -arene complexes of ruthenium(II), such as $[\text{Ru}(\eta^5\text{-C}_5\text{H}_5)(\eta^6\text{-C}_6\text{H}_5\text{Cl})]\text{PF}_6$,⁸⁶ and $[\text{Ru}(\eta^6\text{-C}_6\text{H}_5\text{Cl})(\eta^6\text{-C}_6\text{H}_6)]^{2+}$,⁸⁷ its selection as a solvent is somewhat unusual. Further, during attempts to reproduce the preparation of the chelate complex $[\text{RuCl}_2(\eta^1:\eta^6\text{-Ph}_2\text{P}(\text{CH}_2)_3\text{Ph})]$ (**222**) reported by Smith and Wright,³ I have detected a η^6 -*d*₅-chlorobenzene intermediate (Chapter 3, pp. 119-120).

Various possible alternative routes to tethered-arene ruthenium complexes containing permethylated ligands of the type $\text{R}_2\text{P}(\text{CH}_2)_2\text{XC}_6\text{Me}_5$ ($\text{X} = \text{CH}_2, \text{O}$) have been considered. There was insufficient time to investigate the possibility of heating the bis(acetato) derivative $[\text{Ru}(\text{OCOMe})_2(\eta^1\text{-Ph}_2\text{P}(\text{CH}_2)_3\text{C}_6\text{Me}_5)]$, in the hope that the lability of the acetate groups might assist formation of the tethered $\eta^1:\eta^6$ -coordination mode. A completely different approach, which attempts to make use of the ability of $[\text{Ru}(\eta^6\text{-C}_{10}\text{H}_8)(\eta^4\text{-1,5-COD})]$ (**356**) to cyclotrimerise alkynes,⁸¹ is shown in Scheme 86. The reaction of **356** with $\text{Ph}_2\text{P}(\text{CH}_2)_3\text{C}\equiv\text{CMe}$ could give the intermediate species **367**, which might then afford the tethered species $[\text{Ru}(\eta^1:\eta^6\text{-Ph}_2\text{P}(\text{CH}_2)_3\text{C}_6\text{Me}_5)(\eta^4\text{-1,5-COD})]$ (**368**) upon treatment with 2-butyne. The η^4 -1,5-COD might then be removed through the reaction with aqueous hydrochloric acid to give rise to the desired tethered complex **251**, based on the analogous procedure employed for other complexes.⁸⁸

Table 40. Summary of the tethered-arene ruthenium(II) complexes incorporating phosphorus donor atoms which have been reported.

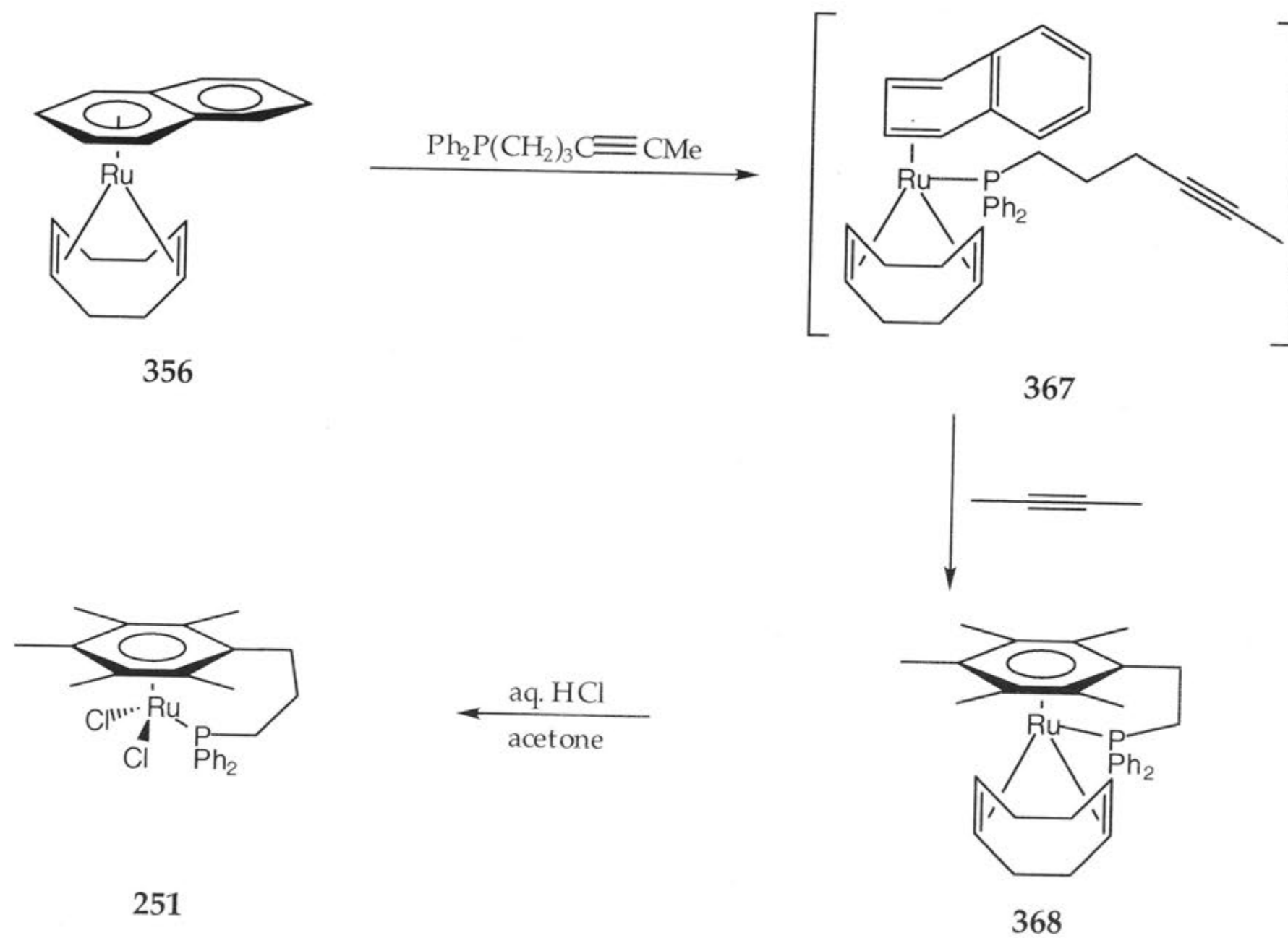
Precursor(s)	Solvent	Temperature (°C)	Product	Yield (%)	Reference
[RuCl ₂ (η ⁶ -C ₆ H ₅ CO ₂ Et)(η ¹ -Ph ₂ P(CH ₂) ₂ -1,2-C ₆ H ₅ CH ₂ OH)] (220)	CH ₂ Cl ₂	120	[RuCl ₂ (η ¹ :η ⁶ -Ph ₂ P(CH ₂) ₂ -2-C ₆ H ₄ CH ₂ OH)] (217)	quantitative ^a	50
[RuCl ₂ (η ⁶ -C ₆ H ₅ CO ₂ Et)(η ¹ -Ph ₂ P(CH ₂) ₂ -1,3-C ₆ H ₅ CH ₂ OH)]	CH ₂ Cl ₂	120	[RuCl ₂ (η ¹ :η ⁶ -Ph ₂ P(CH ₂) ₂ -3-C ₆ H ₄ CH ₂ OH)] (308)	65	50
[RuCl ₂ (η ⁶ -C ₆ H ₅ CO ₂ Et)] ₂ (221) + <i>o</i> -C ₆ H ₄ (CH ₂ OH)(CH ₂ CH ₂ PPh ₂) (218)	CH ₂ Cl ₂	120	[RuCl ₂ (η ¹ :η ⁶ -Ph ₂ P(CH ₂) ₂ -2-C ₆ H ₄ CH ₂ OH)] (217)	97	50
[RuCl ₂ (η ⁶ -C ₆ H ₅ CO ₂ Et)] ₂ (221) + <i>m</i> -C ₆ H ₄ (CH ₂ OH)(CH ₂ CH ₂ PPh ₂)	CH ₂ Cl ₂	120	[RuCl ₂ (η ¹ :η ⁶ -Ph ₂ P(CH ₂) ₂ -3-C ₆ H ₄ CH ₂ OH)] (308)	quantitative ^a	50

Precursor(s)	Solvent	Temperature (°C)	Product	Yield (%)	Reference
	CH ₂ Cl ₂	110	 $(R_{arene}R_P)^c$ and $(R_{arene}S_P)^c$	quantitative ^{a,b}	51
	CH ₂ Cl ₂	120		29 ^{b,d} ; 34 ^{b,d}	52

Precursor(s)	Solvent	Temperature (°C)	Product	Yield (%)	Reference
 [RuCl ₂ (η ⁶ -C ₆ H ₅ CO ₂ Et)] ₂ (221) + Ph ₂ P(CH ₂) ₂ Ph [RuCl ₂ (η ⁶ -C ₆ H ₅ CO ₂ Et)] ₂ (221) + Ph ₂ PCH ₂ CH(Ph)C ₆ H ₅ [RuCl ₂ (η ⁶ -C ₆ H ₅ CO ₂ Et)] ₂ (221) + Cy ₂ P(CH ₂) ₂ Ph [RuCl ₂ (η ⁶ -C ₆ H ₅ CO ₂ Et)] ₂ (221) + Cy ₂ PCH ₂ CH(Ph)C ₆ H ₅	CH ₂ Cl ₂	120		27 ^b	53
[RuCl ₂ (η ⁶ -1,4-MeC ₆ H ₄ CHMe ₂)(η ¹ -Ph ₂ P(CH ₂) ₃ Ph)] (223)	CHCl ₃	60	[RuCl ₂ (η ¹ :η ⁶ -Ph ₂ P(CH ₂) ₂ Ph)] (257)	quantitative ^a	54
[RuCl ₂ (η ⁶ -1,4-MeC ₆ H ₄ CHMe ₂)(η ¹ -Et ₂ P(CH ₂) ₂ Ph)] (358)	CHCl ₃	69	[RuCl ₂ (η ¹ :η ⁶ -Ph ₂ PCH ₂ CH(Ph)C ₆ H ₅)] (293)	quantitative ^a	54
[RuCl ₂ (η ⁶ -1,4-MeC ₆ H ₄ CHMe ₂)(η ¹ -Ph ₂ P(CH ₂) ₂ Ph)] (359)	CHCl ₃	60	[RuCl ₂ (η ¹ :η ⁶ -Cy ₂ P(CH ₂) ₂ Ph)] (258)	quantitative ^a	54
[RuCl ₂ (η ⁶ -1,4-MeC ₆ H ₄ CHMe ₂)(η ¹ -Cy ₂ PCH ₂ CH(Ph)C ₆ H ₅)] (360)	CHCl ₃	60	[RuCl ₂ (η ¹ :η ⁶ -Cy ₂ PCH ₂ CH(Ph)C ₆ H ₅)] (357)	quantitative ^a	54
	C ₆ H ₅ Cl	130	[RuCl ₂ (η ¹ :η ⁶ -Ph ₂ P(CH ₂) ₃ Ph)] (222)	50	3
	C ₆ H ₅ Cl	130	[RuCl ₂ (η ¹ :η ⁶ -Et ₂ P(CH ₂) ₂ Ph)] (256)	80	56
	C ₆ H ₅ Cl	130	[RuCl ₂ (η ¹ :η ⁶ -Ph ₂ P(CH ₂) ₂ Ph)] (257)	62	56
	C ₆ H ₅ Cl	130	[RuCl ₂ (η ¹ :η ⁶ -Cy ₂ P(CH ₂) ₂ Ph)] (258)	94	56

Precursor(s)	Solvent	Temperature (°C)	Product	Yield (%)	Reference
[RuCl ₂ (η ⁶ -1,4-MeC ₆ H ₄ CHMe ₂)(η ¹ -Cy ₂ P(CH ₂) ₃ Ph)] (254)	C ₆ H ₅ Cl	120 ^e ; 140 ^f	[RuCl ₂ (η ¹ :η ⁶ -Cy ₂ P(CH ₂) ₃ Ph)] (225)	82 ^e ; 91 ^f	57-59
[RuCl ₂ (η ⁶ -1,4-MeC ₆ H ₄ CHMe ₂)(η ¹ -Cy ₂ PCH(Me)(CH ₂) ₂ Ph)] (361)	C ₆ H ₅ Cl	120	[RuCl ₂ (η ¹ -Cy ₂ PCH(Me)(CH ₂) ₂ Ph)] (362)	63	58
[RuCl ₂ (η ⁶ -1,4-MeC ₆ H ₄ CHMe ₂)(η ¹ -Cy ₂ P(CH ₂) ₃ -3,5-C ₆ H ₃ Me ₂)] (363)	C ₆ H ₅ Cl	120	[RuCl ₂ (η ¹ :η ⁶ -Cy ₂ P(CH ₂) ₃ -3,5-C ₆ H ₃ Me ₂)] (364)	95	57,58
[RuCl ₂ (η ⁶ -1,4-MeC ₆ H ₄ CHMe ₂)(η ¹ - <i>t</i> -Bu ₂ PCH ₂ OPh)] (365)	C ₆ H ₅ Cl	130	[RuCl ₂ (η ¹ :η ⁶ - <i>t</i> -Bu ₂ PCH ₂ OPh)] (324)	88	55
[RuCl ₂ (η ⁶ -1,4-MeC ₆ H ₄ CHMe ₂)(η ¹ - <i>t</i> -Bu ₂ P(CH ₂) ₂ Ph)] (366)	C ₆ H ₅ Cl	130	[RuCl ₂ (η ¹ :η ⁶ - <i>t</i> -Bu ₂ P(CH ₂) ₂ Ph)] (303)	98	55

^bExact yield was not specified; ^athese complexes were then converted into multi-strapped compounds *via* the nitrogen donor atom; ^cchirality assignments based on references(84,85); ^dtwo diastereomers were formed; ^ereported in reference(57); ^freported in reference(59).



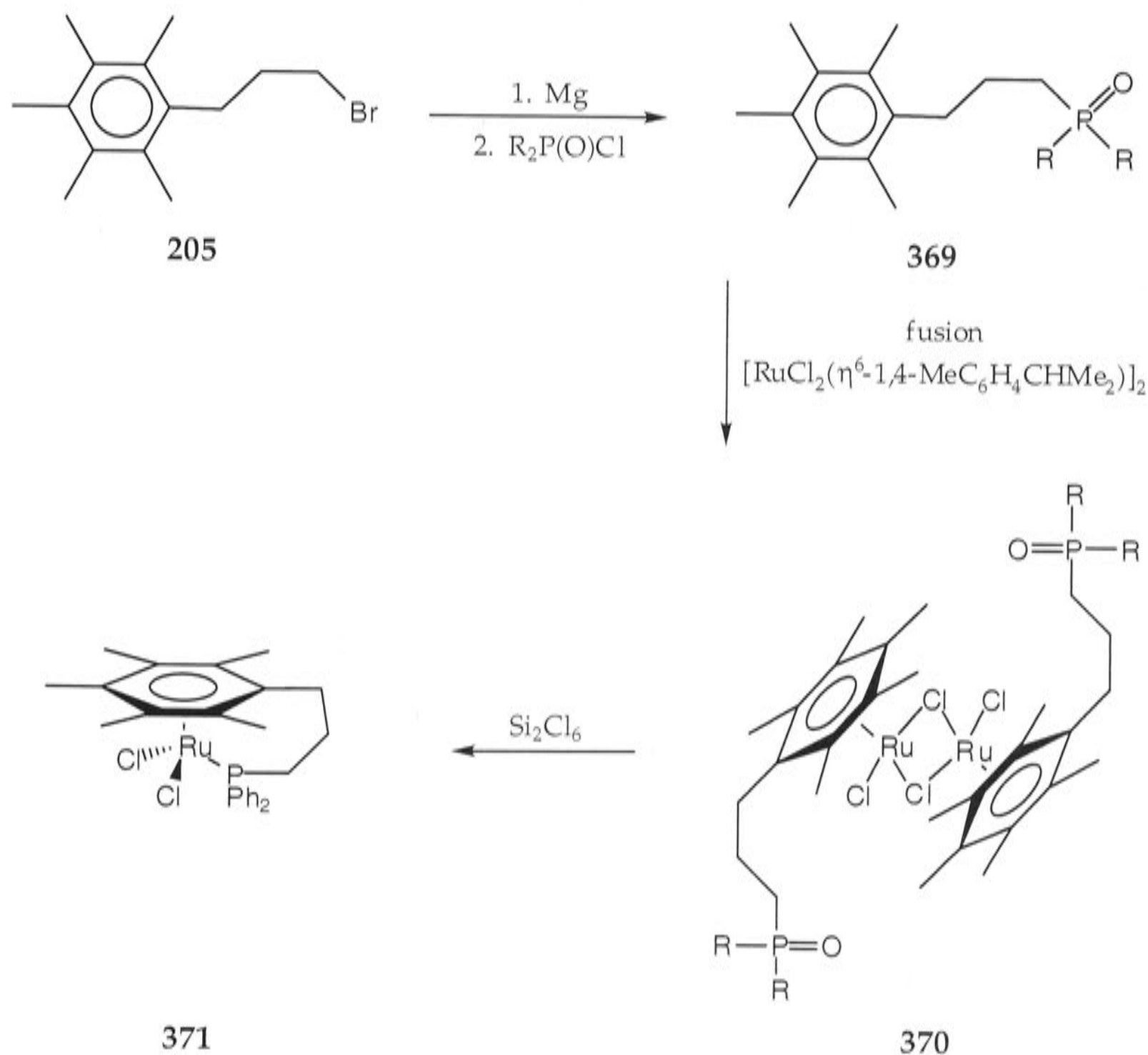
Scheme 86. Potential route towards the tethered complex 251.

There are also two possible approaches outlined in Schemes 87 and 88, in which the arene is attached to ruthenium(II) before the P-donor (see Scheme 16a, Chapter 1). In Scheme 87, the P-donor is masked as its oxide $R_2P(O)(CH_2)_3C_6Me_5$ (**369**), which could be made by treating $BrMg(CH_2)_3C_6Me_5$ (**205**) with the desired phosphinic chloride. The $\eta^6-C_6Me_5$ group is attached to the Ru(II) centre by the standard method⁸⁹ (alternatively, the dimer $[RuCl_2(\eta^6-1,2-MeC_6H_4CO_2Me)_2]_2$ (**224**), see Chapter 3, p. 122) could also be employed to afford **370**, and the P-donor is finally generated by Si_2Cl_6 reduction of the P=O group, giving rise to tethered complexes of the type $[RuCl_2(\eta^1:\eta^6-R_2P(CH_2)_3C_6Me_5)]$ (**371**). Alternatively, as shown in Scheme 88, the starting point is the alcohol $C_6Me_5(CH_2)_2OH$ (**372**) and, after attachment of the C_6Me_5 group to ruthenium(II) to give rise to the dimer $[RuCl_2(\eta^6-C_6Me_5(CH_2)_2OH)]_2$ (**373**), the dangling hydroxyl is converted into the appropriate phosphorus ester, based on the methodology reported by Kurosawa and co-workers to give complex **374**.⁹⁰

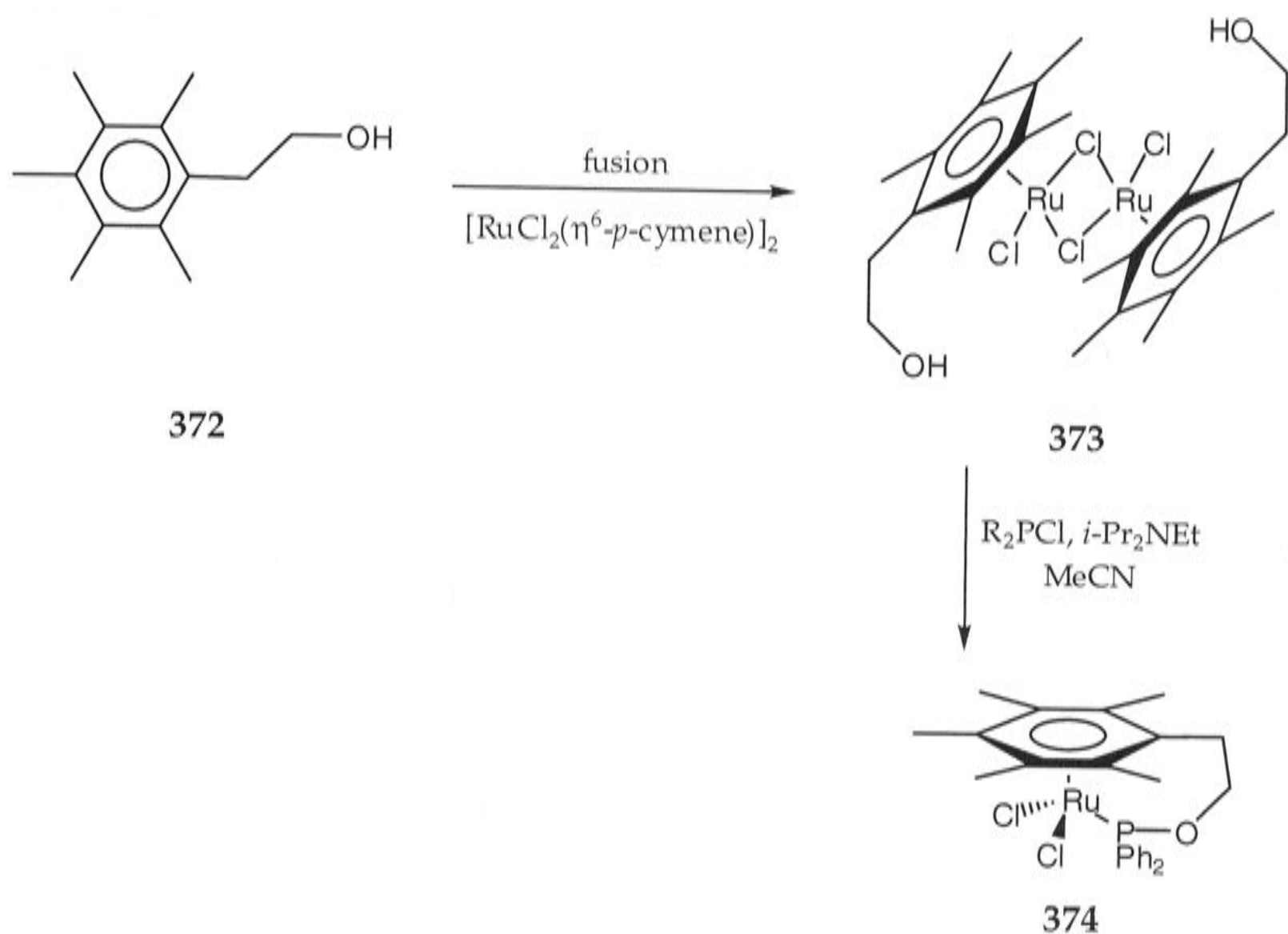
The product of displacement of either the non-tethered or tethered arene from $[RuCl_2(\eta^6-C_6H_6)(\eta^1-R_2P(CH_2)_3Ph)]$ (R = Me (**226**), Ph (**227**), *i*-Pr (**228**) and Cy (**229**)), $[RuCl_2(\eta^6-C_6H_6)(Ph_2PCH_2SiMe_2Ph)]$ (**230**), $[RuCl_2(\eta^1:\eta^6-R_2P(CH_2)_3Ph)]$ (R = Me (**248**), Ph (**222**), *i*-Pr (**249**) and Cy (**225**)) and $[RuCl_2(\eta^1:\eta^6-Ph_2PCH_2SiMe_2Ph)]$ (**252**) by acetonitrile is the appropriate P-donor salt $[RuCl(NCMe)_4(\eta^1-P-donor)]Cl$ formed as a *cis-trans* isomeric mixture. The *cis*-compound is slowly converted into the *trans*-isomer on heating, though the conversion is never complete.

The complex formulated by Smith and Wright³ as $[RuCl_2(NCMe)_3(\eta^1-Ph_2P(CH_2)_3Ph)]$ (**259**), resulting from reaction of the *p*-cymene complex $[RuCl_2(\eta^6-1,4-MeC_6H_4CHMe_2)(\eta^1-Ph_2P(CH_2)_3Ph)]$ (**223**) with acetonitrile (Chapter 3, p. 121), is in fact the tetrakis-complex $[RuCl(NCMe)_4(\eta^1-Ph_2P(CH_2)_3Ph)]Cl$ (**[328]Cl**). Clearly, in addition to the arene, one chloride is readily replaced by acetonitrile under the reaction conditions. An indication of the high affinity of acetonitrile for Ru(II) is that the chloride salt **[328]Cl** cannot be converted into the neutral tris(nitrile) complex **259**, even under

vigorous conditions (Chapter 4, p. 211). Future attempts to generate the tris-complex **259** from the tetrakis-compound might focus on a redox process. The electrode potential of the cation $[328]^+$ is + 0.89 V (*vs* $\text{Fc}^{0/1}$ in CH_2Cl_2), which is sufficiently lower than that of the triarylamimium cations $[\text{N}(\text{C}_6\text{H}_4\text{CN-4})_3]^+$ or $[\text{N}(\text{C}_6\text{H}_3\text{Br}_2\text{-4})_3]^+$ ($E_{1/2} = + 1.08$ and + 1.14 V *vs* $\text{Fc}^{0/1}$ in CH_2Cl_2 , respectively^{11,91}). Since Ru(III) has a much lower affinity for acetonitrile than does Ru(II),⁹²⁻⁹⁴ the outer-sphere chloride of tetrakis-[**328**]Cl may coordinate to the Ru(III) at the expense of NCMe, and reduction to Ru(II) in the absence of acetonitrile may give rise to tris-[$\text{RuCl}_2(\text{NCMe})_3(\eta^1\text{-Ph}_2\text{P}(\text{CH}_2)_3\text{Ph})$] (**259**).



Scheme 87. Suggested alternative route to the tethered complexes of the type **371**.

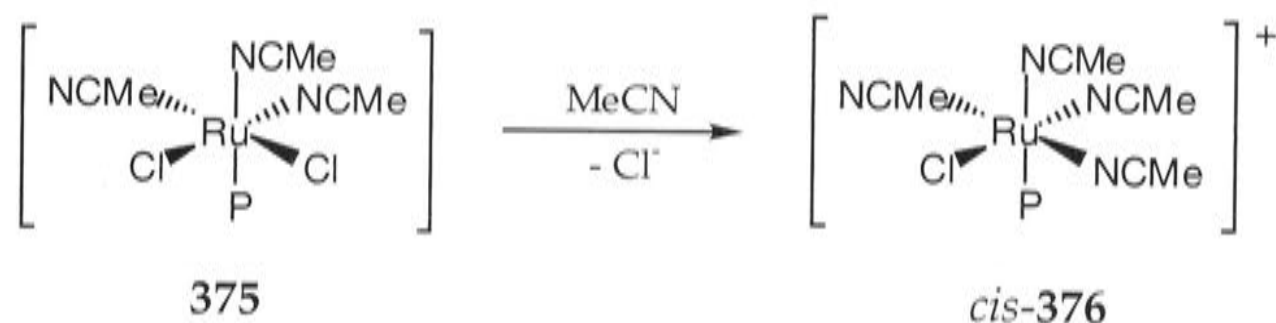


Scheme 88. Potential route to the tethered complexes of the type 374.

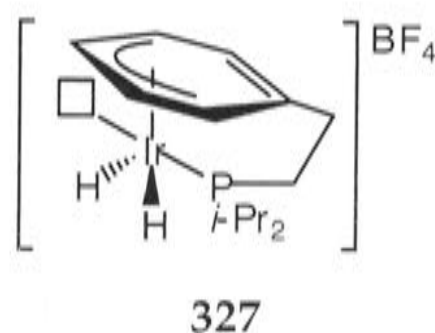
However, the tris(nitrile) complex **328** can be isolated (though not in a pure state) from an electrochemical procedure in which $[\text{RuCl}_2(\eta^1:\eta^6\text{-Ph}_2\text{P}(\text{CH}_2)_3\text{Ph})]$ (**222**) is first electro-oxidised in acetonitrile, presumably generating $[\text{RuCl}_2(\text{NCMe})_3(\eta^1\text{-Ph}_2\text{P}(\text{CH}_2)_3\text{Ph})]^+$ (**[259]⁺**), and subsequently electro-reduced in the absence of acetonitrile. The affinity of butyronitrile for Ru(II) is evidently less than that of acetonitrile: reaction of $[\text{RuCl}_2(\text{NC}(\text{CH}_2)_2\text{Me})_3(\eta^1\text{-Ph}_2\text{P}(\text{CH}_2)_3\text{Ph})]^+$ (**[336]⁺**), which is electrogenerated in the same way as its acetonitrile analogue, gives the tris-complex **336**, even when it is electro-reduced in butyronitrile.

The tethered arene of $[\text{RuCl}_2(\eta^1:\eta^6\text{-R}_2\text{P}(\text{CH}_2)_3\text{Ph})]$ (R = Me (**248**), Ph (**222**), *i*-Pr (**249**) and Cy (**225**)) is displaced more slowly by acetonitrile than is benzene from the respective non-tethered complexes of the type $[\text{RuCl}_2(\eta^6\text{-C}_6\text{H}_6)(\eta^1\text{-R}_2\text{P}(\text{CH}_2)_3\text{Ph})]$, indicating the kinetic stabilisation of arene coordination by the three-atom strap. In addition, after a given reaction time, the proportion of

the thermodynamically less stable *cis*-isomer is higher in the product from the tethered complexes, suggesting that it may be the kinetic product of arene displacement. Since no kinetic studies have been performed on these two-step reactions (replacement of arene and of chloride), any postulated mechanistic sequence must be regarded with caution. One can assume that the arene slides off the metal centre *via* η^4 - and η^2 -intermediates (see Scheme 84).⁷² If the trigonal arrangement of the remaining groups is retained, the entering ligands should arrange themselves in a facial (OC-6-21)⁹⁵ array to give intermediates of the type **375** (Scheme 89). Subsequent replacement of one of the chloride ligands then gives the *cis*-tetrakis(nitrile) cations of the type **376**. Isomerisation of either of these species could lead to the thermodynamically more stable *trans*-isomer. In support of this proposal, Oro, Werner *et al.*⁹⁶ have reported kinetic studies of the reaction of $[\text{IrH}_2(\eta^1:\eta^6\text{-}i\text{-Pr}_2\text{P}(\text{CH}_2)_2\text{Ph})]\text{BF}_4$ (**129**) with acetonitrile at room temperature, to afford $[\text{IrH}_2(\text{NCMe})_3(\eta^1\text{-}i\text{-Pr}_2\text{P}(\text{CH}_2)_2\text{Ph})]\text{BF}_4$ (**326**), and they suggest that the reaction proceeds *via* coordinatively unsaturated intermediates of the type **327**.



Scheme 89. Postulated mechanistic sequence for the formation of *trans*-tetrakis(nitrile) cations of the type **376** (tertiary phosphines represented as P for simplicity).



The presence of the two-atom strap does not appear to exert the same kinetic stabilisation of arene coordination. Thus the η^6 -arene of complexes $[\text{RuCl}_2(\eta^6\text{-C}_6\text{H}_6)(\text{Ph}_2\text{PCH}_2\text{SiMe}_2\text{Ph})]$ (230) and $[\text{RuCl}_2(\eta^1:\eta^6\text{-Ph}_2\text{PCH}_2\text{SiMe}_2\text{Ph})]$ (252) is replaced by acetonitrile to the same extent after 48 h (Chapter 4, p. 207). This effect may be a consequence of the strain induced by the deviation (*ca* 14°) of the arene-SiMe₂ bond from planarity (Chapter 3, p. 179 and Figure 37). On the other hand, the recent report that two-atom tethered arene-Ru(II) dimethyl complexes $[\text{RuMe}_2(\eta^1:\eta^6\text{-Ph}_2\text{P}(\text{CH}_2)_2\text{Ph})]$ (297) are stable at room temperature,⁵⁶ whereas the non-tethered complex $[\text{RuMe}_2(\eta^6\text{-C}_6\text{H}_6)(\text{PMe}_2\text{Ph})]$ (79) decomposes at -40°C ,⁸ suggests that in this case even the two-atom strap affords kinetic stabilisation. As noted on pp. 151-152 (Chapter 3), there is evidence for the formation of a similar methyl-ruthenium(II) complex with the $\text{Ph}_2\text{PCH}_2\text{SiMe}_2\text{Ph}$ (201) system. At this stage it is not clear why similar compounds could not be obtained by analogous methods in the three-atom tethered system containing $\text{Ph}_2\text{P}(\text{CH}_2)_3\text{Ph}$ (118).

The limited studies performed so far, as well as those reported by Smith *et al.*⁹⁷ (see Scheme 64, Chapter 3, p. 153), indicate that the tethered complex $[\text{RuCl}_2(\eta^1:\eta^6\text{-Ph}_2\text{P}(\text{CH}_2)_3\text{Ph})]$ (222) forms an even more extensive range of derivatives than the non-tethered analogues. In particular, one can synthesise dithiocarbamato complexes from the tethered systems $[\text{RuCl}_2(\eta^1:\eta^6\text{-R}_2\text{P}(\text{CH}_2)_3\text{Ph})]$ (R = Me (248), Ph (222)) (Chapter 3, p. 146), whereas attempts to make the corresponding η^6 -benzene bis(dithiocarbamato) complexes were frustrated by the ready loss of benzene.⁹⁸

References

- (1) Devanne, D.; Dixneuf, P. H. *J. Organomet. Chem.* **1990**, *390*, 371-378.
- (2) Bhalla, R.; Boxwell, C. J.; Duckett, S. B.; Dyson, P. J.; Humphrey, D. G.; Steed, J. W.; Suman, P. *Organometallics* **2002**, *21*, 924-928.
- (3) Smith, P. D.; Wright, A. H. *J. Organomet. Chem.* **1998**, *559*, 141-147.
- (4) Ghebreyessus, K. Y.; Nelson, J. H. *Organometallics* **2000**, *19*, 3387-3392.
- (5) Tsutsui, M.; Zeiss, H. H. *Naturwissenschaften* **1957**, *44*, 420.
- (6) Abdul-Rahman, S.; Houlton, A.; Roberts, R. M. G.; Silver, J. J. *Organomet. Chem.* **1989**, *359*, 331-341.
- (7) Ceccanti, A.; Diversi, P.; Ingrosso, G.; Laschi, F.; Lucherini, A.; Magagna, S.; Zanello, P. *J. Organomet. Chem.* **1996**, *526*, 251-262.
- (8) Bennett, M. A.; Smith, A. K. *J. Chem. Soc., Dalton Trans.* **1974**, 233-241.
- (9) Al-Takhin, G.; Connor, J. A.; Skinner, H. A.; Zafarani-Moattar, M. T. *J. Organomet. Chem.* **1984**, *260*, 189-197.
- (10) Reynolds, R.; Line, L. L.; Nelson, R. F. *J. Am. Chem. Soc.* **1974**, *96*, 1087-1092.
- (11) Connelly, N. G.; Geiger, W. G. *Chem. Rev.* **1996**, *96*, 877-910.
- (12) Camire, N.; Nafady, A.; Geiger, W. E. *J. Am. Chem. Soc.* **2002**, *124*, 7260-7261.
- (13) Howell, J. O.; Goncalves, J. M.; Amatore, C.; Klasinc, L.; Whightman, R. M.; Kochi, J. K. *J. Am. Chem. Soc.* **1984**, *106*, 3968-3976.
- (14) Zoski, C. G.; Sweigart, D. A.; Stone, N. J.; Rieger, P. H.; Mocellin, E.; Mann, T. F.; Mann, D. R.; Gosser, D. K.; Doeff, M. M.; Bond, A. M. *J. Am. Chem. Soc.* **1988**, *110*, 2109-2116.
- (15) Hunter, A. D.; Mozol, V.; Tsai, S. D. *Organometallics* **1992**, *11*, 2251-2262.

- (16) Stone, N. J.; Sweigart, D. A.; Bond, A. M. *Organometallics* **1986**, *5*, 2553-2555.
- (17) Gassman, P. G.; Deck, P. A. *Organometallics* **1994**, *13*, 1934-1939.
- (18) Denisovich, L. I.; Zol'nikova, G. P.; Kritskaya, I. I.; Kravtsov, D. N. *Organometallic Chemistry in the USSR* **1989**, *2*, 330-332.
- (19) Boekelheide, V. *Pure Appl. Chem.* **1986**, *58*, 1-6.
- (20) Bowyer, W. J.; Geiger, W. E. *J. Am. Chem. Soc.* **1985**, *107*, 5657-5663.
- (21) McGrady, J. E., 2003, personal communication.
- (22) Hudson, A.; Kennedy, M. J. *J. Chem. Soc. A* **1969**, 1116-1120.
- (23) Roger, C.; Hamon, P.; Toupet, L.; Rabaâ, H.; Saillard, J.-Y.; Hamon, J.-R.; Lapinte, C. *Organometallics* **1991**, *10*, 1045-1054.
- (24) Tilset, M.; Fjeldahl, I.; Hamon, J.-R.; Hamon, P.; Toupet, L.; Saillard, J.-Y.; Costuas, K.; Haynes, A. *J. Am. Chem. Soc.* **2001**, *123*, 9984-10000.
- (25) Krueger, S. T.; Poli, R.; Rheingold, A. L.; Staley, D. L. *Inorg. Chem.* **1989**, *28*, 4599-4607.
- (26) Trofimenko, S. *Scorpionates: The Coordination Chemistry of Polypyrazolylborate Ligands*; Imperial College Press: London, 1999, p. 20.
- (27) Bartlett, I. M.; Carlton, S.; Connelly, N. G.; Harding, D. J.; Hayward, O. D.; Orpen, A. G.; Ray, C. D.; Reiger, P. H. *Chem. Commun.* **1999**, 2403-2404.
- (28) Heinekey, D. M.; Voges, M. H.; Barnhart, D. M. *J. Am. Chem. Soc.* **1996**, *118*, 10792-10802.
- (29) Bennett, M. A.; Heath, G. A.; Hockless, D. C. R.; Kováčik, I.; Willis, A. C. *J. Am. Chem. Soc.* **1998**, *120*, 932-941.
- (30) Cotton, F. A.; Dollase, W. A.; Wood, J. S. *J. Am. Chem. Soc.* **1963**, *85*, 1543-1544.
- (31) Keulen, E.; Jellinek, F. *J. Organomet. Chem.* **1966**, *5*, 490-492.
- (32) Förster, E.; Albrecht, G.; Dürselen, W.; Kurras, E. *J. Organomet. Chem.* **1969**, *19*, 215-217.
- (33) Spek, A. L.; Duisenberg, A. J. M. *Cryst. Struct. Comm.* **1981**, *10*, 1531-1534.
- (34) Morosin, B. *Acta Cryst.* **1974**, *B30*, 838-839.

- (35) Braga, D.; Costa, A. L.; Grepioni, F.; Scaccianoce, L.; Tagliavini, E. *Organometallics* **1996**, *15*, 1084-1086.
- (36) Braga, D.; Costa, A. L.; F. Grepioni; Scaccianoce, L.; Tagliavini, E. *Organometallics* **1997**, *16*, 2070-2079.
- (37) Schneider, R.; Fischer, E. O. *Naturwissenschaften* **1961**, *48*, 452-453.
- (38) O'Hare, D.; Kurmoo, M.; Lewis, R.; Powell, H. *J. Chem. Soc., Dalton Trans.* **1992**, 1351-1355.
- (39) Miao, F. M. *Cryst. Struct. Comm.* **1982**, *11*, 153-156.
- (40) Mingos, D. M. P. *Comprehensive Organometallic Chemistry*; Wilkinson, G.; Stone, F. G. A.; Abel, E. W. Ed., Pergamon: Oxford, 1982; Vol. 3, p. 28, and references cited therein.
- (41) Kölle, U.; Görissen, R.; Hörnig, A. *Inorg. Chim. Acta* **1994**, *218*, 33-39.
- (42) Bennett, M. A.; Bruce, M. I.; Matheson, T. W. *Comprehensive Organometallic Chemistry*; Pergamon: Oxford, 1982; Vol. 4, pp. 775-796.
- (43) Bennett, M. A.; Khan, K.; Wenger, E. *Comprehensive Organometallic Chemistry II*; Abel, E. W.; Stone, F. G. A.; Wilkinson, G.; Shriver, D. F.; Bruce, M. I. Ed., Pergamon: Oxford, 1995; Vol. 7, pp. 476-530.
- (44) Tilley, T. D.; Grubbs, R. H.; Bercaw, J. E. *Organometallics* **1984**, *3*, 274-278.
- (45) Oshima, N.; Suzuki, H.; Moro-Oka, Y. *Chem. Lett.* **1984**, 1161-1164.
- (46) Kölle, U.; Kossakowski, J.; Klaff, N.; Wesemann, L.; Englert, U.; Heberich, G. E. *Angew. Chem. Int. Ed. Engl.* **1991**, *30*, 690-691.
- (47) Koelle, U.; Lueken, H.; Handrick, K.; Schilder, H.; Burdett, J. K.; Balleza, S. *Inorg. Chem.* **1995**, *34*, 6273-6278.
- (48) Arliguie, T.; Chaudret, B. *J. Chem. Soc., Chem. Commun.* **1986**, 985-986.
- (49) Clemente, M. E. N.; Saavedra, P. J.; Vásquez, M. C.; Paz-Sandoval, M. A.; Arif, A. M.; Ernst, R. D. *Organometallics* **2002**, *21*, 592-605.

- (50) Therrien, B.; Ward, T. R.; Pilkington, M.; Hoffmann, C.; Gilardoni, F.; Weber, J. *Organometallics* **1998**, *17*, 330-337.
- (51) Therrien, B.; Ward, T. R. *Angew. Chem., Int. Ed. Engl.* **1999**, *38*, 405-408.
- (52) Therrien, B.; König, A.; Ward, T. R. *Organometallics* **1999**, *18*, 1565-1568.
- (53) Therrien, B.; Ward, T. R. *Acta Cryst.* **2000**, C56, e561.
- (54) Abele, A.; Wursche, R.; Klinga, M.; Rieger, B. *J. Mol. Cat. A* **2000**, *160*, 23-33.
- (55) Jung, S.; Ilg, K.; Brandt, C. D.; Wolf, J.; Werner, H. *J. Chem. Soc., Dalton Trans.* **2002**, 318-327.
- (56) Umezawa-Vizzini, K.; Guzman-Jimenez, I. Y.; Whitmire, K. H.; Lee, T. R. *Organometallics* **2003**, *22*, 3059-3065.
- (57) Simal, F.; Jan, D.; Demonceau, A.; Noels, A. F. *Tetrahedron Lett.* **1999**, *40*, 1653-1656.
- (58) Jan, D.; Delaude, L.; Simal, F.; Demonceau, A.; Noels, A. F. *J. Organomet. Chem.* **2000**, *606*, 55-64.
- (59) Fürstner, A.; Liebl, M.; Lehmann, C. W.; Picquet, M.; Kunz, R.; Bruneau, C.; Touchard, D.; Dixneuf, P. H. *Chem. Eur. J.* **2000**, *6*, 1847-1857.
- (60) Fraústo da Silva, J. J. R. *J. Chem. Ed.* **1983**, *60*, 390-392.
- (61) Cotton, F. A.; Wilkinson, G.; Murillo, C. A.; Bochmann, M. *Advanced Inorganic Chemistry*; 6th ed.; John Wiley & Sons, Inc.: New York, 1999, p. 45.
- (62) Schwarzenbach, G. *Helv. Chim. Acta* **1952**, *35*, 2344-2359.
- (63) Shaw, B. L. *J. Organomet. Chem.* **1980**, *200*, 307-318.
- (64) Eliel, E. L.; Wilen, S. H.; Mander, L. N. *Stereochemistry of Organic Compounds*; John Wiley & Sons, Inc.: New York, 1994, pp. 682-683.
- (65) Shaw, B. L. *J. Am. Chem. Soc.* **1975**, *97*, 3856-3857.
- (66) Cucullu, M. E.; Li, C.; Nolan, S. P.; Nguyen, S. T.; Grubbs, R. H. *Organometallics* **1998**, *17*, 5565-5568.
- (67) Luo, L.; Nolan, S. P.; Fagan, P. J. *Organometallics* **1993**, *12*, 4305-4311.

- (68) Smith, D. C.; Haar, C. M.; Luo, L.; Li, C.; Cucullu, M. E.; Mahler, C. H.; Nolan, S. P.; Marshall, W. J.; Jones, N. L.; Fagan, P. J. *Organometallics* **1999**, *18*, 2357-2361.
- (69) van Meurs, F.; van Koningsveld, H. *J. Organomet. Chem.* **1977**, *131*, 423-428.
- (70) Carter, O. L.; McPhail, A. T.; Sim, G. A. *J. Chem. Soc. A* **1967**, 1619-1626.
- (71) Saillard, P. J.-Y.; Grandjean, D. *Acta Cryst.* **1976**, *B32*, 2285-2289.
- (72) Muetterties, E. L.; Bleeke, J. R.; Sievert, A. C. *J. Organomet. Chem.* **1979**, *178*, 197-216.
- (73) Zybilla, C. E. *Synthetic Methods of Organometallic and Inorganic Chemistry*; Herrmann, W. A. Ed., Georg Thieme Verlag: Stuttgart, 1997; Vol. 8, p. 55.
- (74) Anderson, W. P.; Hsu, N.; Stanger, Jr, C. W.; Munson, B. J. *Organomet. Chem.* **1974**, *69*, 249-257.
- (75) Slawisch, A. *Gmelins Handbuch der Anorganischen Chemie*; Supplement to 8th ed.; Verlag Chemie: Weinheim, 1971; Vol. 3, pp. 181-289.
- (76) Muetterties, E. L.; Bleeke, J. R.; Wucherer, E. J.; Albright, T. A. *Chem. Rev.* **1982**, *82*, 499-525.
- (77) Fischer, E. O.; Böttcher, R. *Chem. Ber.* **1956**, *89*, 2397-2400.
- (78) Fischer, E. O.; Schreiner, S.; Reckziegel, A. *Chem. Ber.* **1961**, *94*, 258-262.
- (79) Bennett, M. A. In *Rodd's Chemistry of Carbon Compounds*; 2nd ed.; Coffey, S. Ed., Elsevier Scientific Publishing Company: Amsterdam, 1974, p. 382.
- (80) Bennett, M. A.; Neumann, H.; Thomas, M.; Wang, X.; Pertici, P.; Salvadori, P.; Vitulli, G. *Organometallics* **1991**, *10*, 3237-3245.
- (81) Pertici, P.; Verrazzani, A.; Vitulli, G.; Baldwin, R.; Bennett, M. A. *J. Organomet. Chem.* **1998**, *551*, 37-47.
- (82) Bennett, M. A.; Edwards, A. J.; Harper, J. R.; Khimyak, T.; Willis, A. C. *J. Organomet. Chem.* **2001**, *629*, 7-18.

- (83) Bennett, M. A.; Harper, J. R. In *Modern Coordination Chemistry: The Legacy of Joseph Chatt*; Leigh, G. J.; Winterton, N. Ed.; The Royal Society of Chemistry: Cambridge, 2002, pp. 163-168.
- (84) Cahn, R. S.; Ingold, C.; Prelog, V. *Angew. Chem. Int. Ed. Engl.* **1966**, *5*, 385-415.
- (85) ref. 64, p. 1122.
- (86) Cambie, R. C.; Coulson, S. A.; Mackay, L. G.; Janssen, S. J.; Rutledge, P. S.; Woodgate, P. D. *J. Organomet. Chem.* **1991**, *409*, 385-409.
- (87) Bennett, M. A.; Matheson, T. W. *J. Organomet. Chem.* **1979**, *175*, 87-93.
- (88) Bennett, M. A. *Comprehensive Organometallic Chemistry II*; Abel, E. W.; Stone, F. G. A.; Wilkinson, G.; Shriver, D. F.; Bruce, M. I. Ed., Pergamon: Oxford, 1995; Vol. 7, p. 557.
- (89) Bennett, M. A.; Huang, T.-N.; Matheson, T. W.; Smith, A. K. *Inorganic Syntheses*; Fackler, Jr, J. P. Ed., John Wiley & Sons, Inc.: New York, 1982; Vol. 21, pp. 74-78.
- (90) Miyaki, Y.; Onishi, T.; Kurosawa, H. *Inorg. Chim. Acta* **2000**, *300-302*, 369-377.
- (91) Steckhan, E. *Top. Curr. Chem.* **1987**, *142*, 1-69.
- (92) Seddon, E. A.; Seddon, K. R. *The Chemistry of Ruthenium*; Elsevier Science B. V.: Amsterdam, 1984, p. 392.
- (93) Duff, C. M.; Heath, G. A. *Inorg. Chem.* **1991**, *30*, 2528-2535.
- (94) Duff, C. M.; Heath, G. A. *J. Chem. Soc., Dalton Trans.* **1991**, 2401-2411.
- (95) Huheey, J. E.; Keiter, E. A.; Keiter, R. L. *Inorganic Chemistry: Principles of Structure and Reactivity*; 4th ed.; HarperCollins College Publishers: New York, 1993, p. A-75.
- (96) Canepa, G.; Sola, E.; Martín, M.; Lahoz, F. J.; Oro, L. A.; Werner, H. *Organometallics* **2003**, *22*, 2151-2160.
- (97) Smith, P. D.; Gelbrich, T.; Hursthouse, M. B. *J. Organomet. Chem.* **2002**, *659*, 1-9.
- (98) Robertson, D. R.; Stephenson, T. A. *J. Chem. Soc., Dalton Trans.* **1978**, 486-495.

Chapter 8: Experimental Section

8.1 General Information

The compounds ammonium hexafluorophosphate, 1-bromo-3-phenylpropanol, bromomesitylene (206), chlorodicyclohexylphosphine, chlorodi-*iso*-propylphosphine, (chloromethyl)dimethylphenylsilane (210), 1,3-dibromopropane, anhydrous di-*n*-butyl ether, sodium dimethyldithiocarbamate dihydrate, dimethylzinc (2.0 M solution in toluene), di-*t*-butylchlorophosphine, hexaethylbenzene, hexamethylbenzene, methyllithium (0.05 M solution in ether), α -phellandrene, pentamethylbenzene, hydrated ruthenium chloride, silver acetate, silver hexafluorophosphate, sodium hexafluorophosphate, γ -terpinene, *t*-butylisocyanide, *o*-toluic acid, triphenylantimony, trimethylphosphine, triphenylphosphine, $[\text{N}(\text{C}_6\text{H}_4\text{Br}-4)_3]\text{SbCl}_6$ ([48] SbCl_6) and vinyl-diphenylphosphine were obtained from commercial suppliers and used as supplied. Chlorodiphenylphosphine was distilled under reduced pressure prior to use. Bromopentamethylbenzene (204) was obtained by bromination of pentamethylbenzene.¹ The salt $[\text{Bu}^n_4\text{N}]\text{PF}_6$ was obtained by neutralising commercial aqueous $[\text{Bu}^n_4\text{N}]\text{OH}$ with HPF_6 ; it was recrystallised three times from methanol/water (4:1) and dried *in vacuo* for 8 h. The salt $[\text{Bu}^n_4\text{N}]\text{BF}_4$ was obtained by neutralising commercial aqueous $[\text{Bu}^n_4\text{N}]\text{OH}$ with HBF_4 ; it was recrystallised three times from methanol/micropore water (4:1) and dried *in vacuo*.² Chlorodimethylphosphine was prepared in three steps from PSCl_3 .³⁻⁶ Cuprous bromide⁷ and sodium naphthalide were freshly prepared before use. Potassium-*t*-butoxide was purified by sublimation before use.⁸ Sodium acetylacetonate,⁹ 1-bromo-3-phenylpropane (203),¹⁰ di-*t*-butylphosphine,¹¹ $\text{Ph}_2\text{P}(\text{CH}_2)_3\text{Cl}$ (208),¹² and the complexes $[\text{PdCl}_2(\text{PPh}_3)_2]$,¹³ $[\text{RuCl}_2(\eta^6-1,4-\text{MeC}_6\text{H}_4\text{CHMe}_2)(\eta^1-\text{Cy}_2\text{P}(\text{CH}_2)_3\text{C}_6\text{H}_5)]$ (254),¹⁴ $[\text{RuCl}_2(\eta^6-1,3,5-\text{C}_6\text{H}_3\text{Me}_3)]_2$ (188),¹⁵ $[\text{RuCl}_2(\eta^6-1,4-\text{MeC}_6\text{H}_4\text{CHMe}_2)]_2$ (216),¹⁶ $[\text{RuCl}_2(\eta^6-\text{C}_6\text{Me}_6)]_2$ (67),¹⁶

$[\text{RuCl}_2(\eta^6\text{-C}_6\text{H}_6)]_2$ (161),^{15,17} $[\text{RuCl}_2(\eta^6\text{-C}_6\text{H}_6)(\text{PPh}_3)]$ (302),^{15,17} $[\text{RuCl}_2(\eta^6\text{-C}_6\text{Me}_6)(\text{PPh}_3)]$ (306),¹⁸ $[\text{RuCl}_2(\eta^6\text{-C}_6\text{Me}_6)(\text{SbPh}_3)]$,¹⁸ $[\text{RuCl}_2(\eta^6\text{-1,3,5-C}_6\text{H}_3\text{Me}_3)(\text{Ph}_2\text{PCH=CH}_2)]$ (278),¹⁹ and $[\text{RuCl}_2(\eta^6\text{-1,2-MeC}_6\text{H}_4\text{CO}_2\text{Me})]_2$ (224)²⁰ were prepared as described previously. The complexes $[\text{RuCl}_2(\eta^6\text{-C}_6\text{H}_6)(\text{PMe}_3)]$ (337),²¹ $[\text{RuCl}_2(\eta^6\text{-C}_6\text{Me}_6)(\text{PMe}_3)]$ (304)²² and $[\text{RuCl}_2(\eta^6\text{-1,4-MeC}_6\text{H}_4\text{CHMe}_2)(\text{PPh}_3)]$ (338)¹⁵ were prepared by procedures similar to those reported. The complex $[\text{RuCl}_2(\eta^6\text{-C}_6\text{Me}_6)(\text{Ph}_2\text{PCH=CH}_2)]$ (270) was prepared either through heating the adduct $[\text{RuCl}_2(\eta^6\text{-C}_6\text{Me}_6)(\text{SbPh}_3)]$ (273) with vinylidiphenylphosphine (272) in toluene, by the general procedure reported,²³ or by the method of Nelson and co-workers.¹⁹

The preparation of complexes $[\text{RuCl}_2(\eta^1:\eta^6\text{-Ph}_2\text{P}(\text{CH}_2)_3\text{-3,5-C}_6\text{R}_3\text{Me}_2)]$ (R = H (275) and Me (251)) by the methodology reported by Nelson and co-workers¹⁹ gave irreproducible results, despite the fact that equimolar amounts of the ruthenium complex and KO-*t*-Bu were used, as stipulated by the authors. The tethered complexes 275 and 251 were formed in some cases, but the yields were poor (< 23%) and decomposition by loss of η^6 -arene occurred frequently (see Chapter 3, Section 3.3.2 for more details). Thus the preparation of 251 was carried out by the methodology described in this Thesis.

All reactions were carried out under purified nitrogen or argon with the use of standard Schlenk techniques, most solvents being purified and deoxygenated before use.²⁴ Pentane and benzene were dried over sodium wire and distilled from sodium/benzophenone under an atmosphere of nitrogen. *n*-Hexane and toluene were either dried over sodium wire and distilled from sodium/benzophenone under an atmosphere of nitrogen or distilled from calcium hydride under an atmosphere of argon. THF and ether were either dried over sodium wire and distilled from sodium/benzophenone under an atmosphere of nitrogen or dried over

calcium hydride and distilled from lithium aluminium hydride under an atmosphere of argon. Methanol and ethanol were distilled from magnesium turnings under an atmosphere of nitrogen. Acetonitrile was distilled from calcium hydride under an atmosphere of nitrogen or argon. Dichloromethane was either distilled from calcium hydride under an atmosphere of nitrogen or argon, or was pre-dried over potassium hydroxide and distilled over phosphorus pentoxide under nitrogen. Hexamethylphosphoric triamide was distilled from calcium hydride under reduced pressure. Chlorobenzene was distilled from phosphorus pentoxide under an atmosphere of nitrogen. Acetone was distilled from potassium carbonate under an atmosphere of nitrogen. Propan-2-ol was distilled from magnesium turnings activated with iodine under an atmosphere of nitrogen. *sym*-Tetrachloroethane was distilled from potassium carbonate under an atmosphere of nitrogen and then distilled from calcium hydride under reduced pressure. Di-*n*-butyl ether was distilled from sodium under nitrogen. Propan-2-ol was distilled over magnesium activated with iodine under nitrogen. Butyronitrile was distilled from calcium hydride under nitrogen. Nitromethane was distilled from calcium chloride under nitrogen. The HPLC grade solvents for the CPE experiments were dried over CaH_2 and stored under nitrogen; acetonitrile and pyridine were purchased from Fisher and butyronitrile was purchased from Aldrich.

Nuclear magnetic resonance spectra were recorded either on Varian XL-200E, Varian Gemini 300 BB, Varian VXR 300 or Inova VXR 500 spectrometers in Canberra, on Bruker DPX-400, Bruker DRX-400 or Bruker DRX-500 spectrometers in Cambridge, or on a Bruker ARX 250 spectrometer in Edinburgh. All NMR spectra were recorded at ambient temperature, except where stated otherwise. All coupling constants are given in Hertz. The chemical shifts (δ) for ^1H and $^{13}\text{C}\{^1\text{H}\}$ -NMR were measured relative to residual signals of the solvents and $^{29}\text{Si}\{^1\text{H}\}$ and $^{31}\text{P}\{^1\text{H}\}$ -NMR were reported relative to external TMS (tetramethylsilane) and 85% H_3PO_4 , respectively. A delay time of five seconds was employed

for the $^{31}\text{P}\{^1\text{H}\}$ -NMR spectra in cases where the ratio of peaks was determined accurately.

Fast Atom Bombardment (FAB) mass spectra were measured either on a VG ZAB2-SEQ spectrometer in Canberra or on a MSI Concept IH spectrometer in Cambridge, using either 3-nitrobenzyl alcohol or (3-nitrophenyl)octylether as a matrix. Liquid Secondary Ion (LSI) mass spectra were measured on a Kratos Concept IH spectrometer in Cambridge using 3-nitrobenzyl alcohol as a matrix. Electron Impact (EI) mass spectra were measured either on a VG Micromass 7070 spectrometer in Canberra or on a Kratos Concept IH spectrometer in Cambridge. Electrospray Ionisation (ESI) mass spectra were recorded on a Micromass Quattro-LC spectrometer in Cambridge using acetonitrile to generate the positive ion. Matrix-Assisted Laser Desorption/Ionisation (MALDI) mass spectra were measured on a Kratos MALDI 4 spectrometer in Cambridge. Gas Chromatograph/Mass Spectra were obtained on a 5970 MSD Hewlett Packard BP1 Detector, using a 12.5 m long column.

Infrared spectra in the range $4000\text{-}400\text{ cm}^{-1}$ were measured either on neat liquids, or for solids, as KBr discs or Nujol mulls (on NaCl windows), or, for solutions in calcium fluoride cells on a Perkin Elmer Spectrum One spectrometer in Canberra or on Perkin Elmer FT-IR Paragon 1000 spectrometers in Cambridge and in Edinburgh. Spectra in the range $500\text{-}150\text{ cm}^{-1}$ were measured as polythene discs on a Perkin Elmer FTIR-1800 instrument in Canberra.

UV/Vis spectra were measured using either a λ -9 spectrometer (Perkin Elmer) controlled by a Datalink PC running UV Winlab software (version 2.70.01) in Edinburgh or on a Cary 1E UV-Visible Spectrophotometer controlled by a AcerView 56e PC, or on a Cary 5 UV-Vis-NIR Spectrophotometer controlled by a Gateway PC, both running UV Winlab software (version 2.00), in Canberra.

Chromatography was performed using either activity III neutral aluminium oxide, 90 active or activity I acidic aluminium oxide, 90 active.

Microanalyses were carried out at the Analytical Services Unit, ANU, Canberra or at the University of Cambridge Chemical Laboratory.

Melting points were determined using a Gallenkamp apparatus and are uncorrected.

Conductance measurements were determined on solutions of highly purified nitromethane using a Radiometer CDC344 immersion electrode at *ca* 21°C.

8.1.1 Cyclic Voltammetry and Controlled Potential Electrolysis: General Conditions

Cyclic voltammetry (CV) experiments were carried out using either PAR-273 or 170 potentiostats controlled through a PC with standard PAR software (Canberra). Alternating current voltammetry (ACV) was performed on the PAR-170 potentiostat (Canberra). A standard three-electrode configuration was used, as shown in Figure 82. The working electrode was a platinum disc and the auxiliary electrode was a platinum mesh. The reference electrode was Ag/AgCl.²⁵ The internal compartment of the reference electrode was filled with 0.05M [Buⁿ₄N]Cl/0.45M [Buⁿ₄N]PF₆ in acetonitrile. The electrochemical cell was a jacketed glass cell (*ca* 5 mL). The electrolyte solutions were purged with N₂ and maintained under an inert atmosphere. Under these conditions ferrocene and decamethylferrocene were oxidised at + 0.55 V and - 0.05 V, respectively. The ferrocene or decamethylferrocene were added as internal standards to obtain the reliable electrode potentials, relative to

either of these metallocenes.^{26,27} Typical scan rates for CV were 50 to 500 mVs^{-1} and 20 mVs^{-1} for ACV.

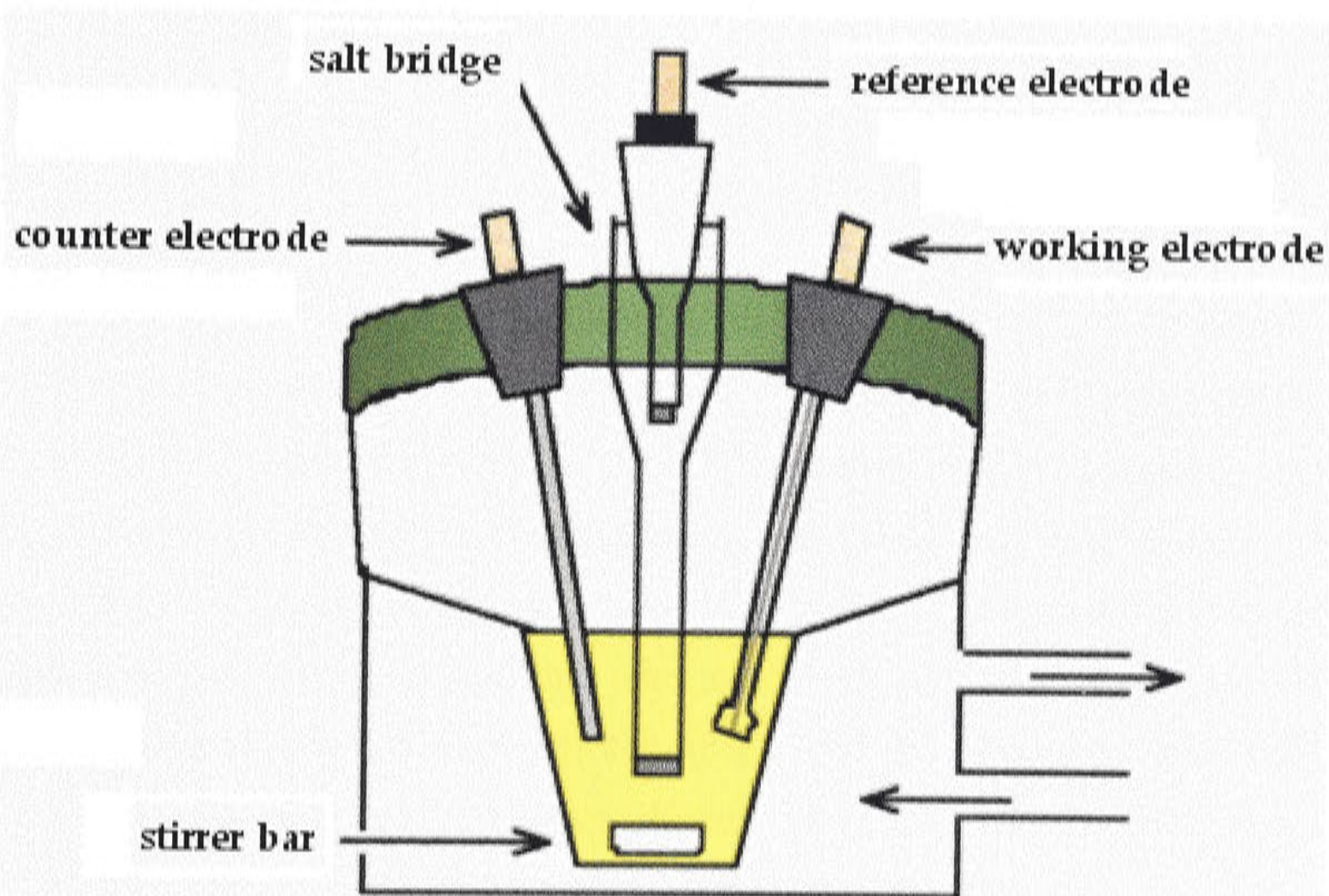


Figure 82. Schematic of the jacketed three-electrode cell for cyclic voltammetry and alternating current voltammetry experiments.

Controlled potential electrolysis (CPE) experiments were performed on an EcoChemie Autolab potentiostat/galvanostat controlled by a PC running GPES software (version 4.8) in Edinburgh. The experiments were conducted in an H-cell, illustrated in Figure 83. The working electrode was a large basket of platinum gauze. The Ag/AgCl reference electrode (0.45M $[\text{Bu}^n_4\text{N}]\text{BF}_4$ and 0.05M $[\text{Bu}^n_4\text{N}]\text{Cl}$ in CH_2Cl_2) and platinum microdisc electrodes were placed in the centre of the basket. The platinum microdisc electrode allows conventional cyclic voltammetric experiments to be conducted such that the progress of the electrolysis can be monitored. The platinum gauze counter electrode was separated by sintered glass frits from the test solution, which allowed a current to flow but restricted movement of the test species to the working electrode compartment. The potential applied was at least 60 mV beyond the $E_{1/2}$ for an oxidation process in order to achieve exhaustive electrolysis. The

solution was purged with nitrogen prior to the experiments and kept under an atmosphere of nitrogen throughout the experiment. The number of electrons involved in a reduction or oxidation process can be calculated from the relationship:

$$Q = neF \quad (3)$$

where Q is the charge in Coulombs, n is the number of moles of the electroactive species, e is the number of electrons in the redox process and F is Faraday's constant (96485 C mol^{-1}). This experiment is usually termed coulometry. During such experiments the solution was continuously stirred in order to improve mass transfer to the working electrode. Following complete reduction or oxidation the product was then investigated using CV experiments at a platinum microdisc electrode (as outlined above). Under these conditions ferrocene was oxidised at $+ 0.55 \text{ V}$ (CH_2Cl_2) and $+ 0.47 \text{ V}$ (CH_3CN).

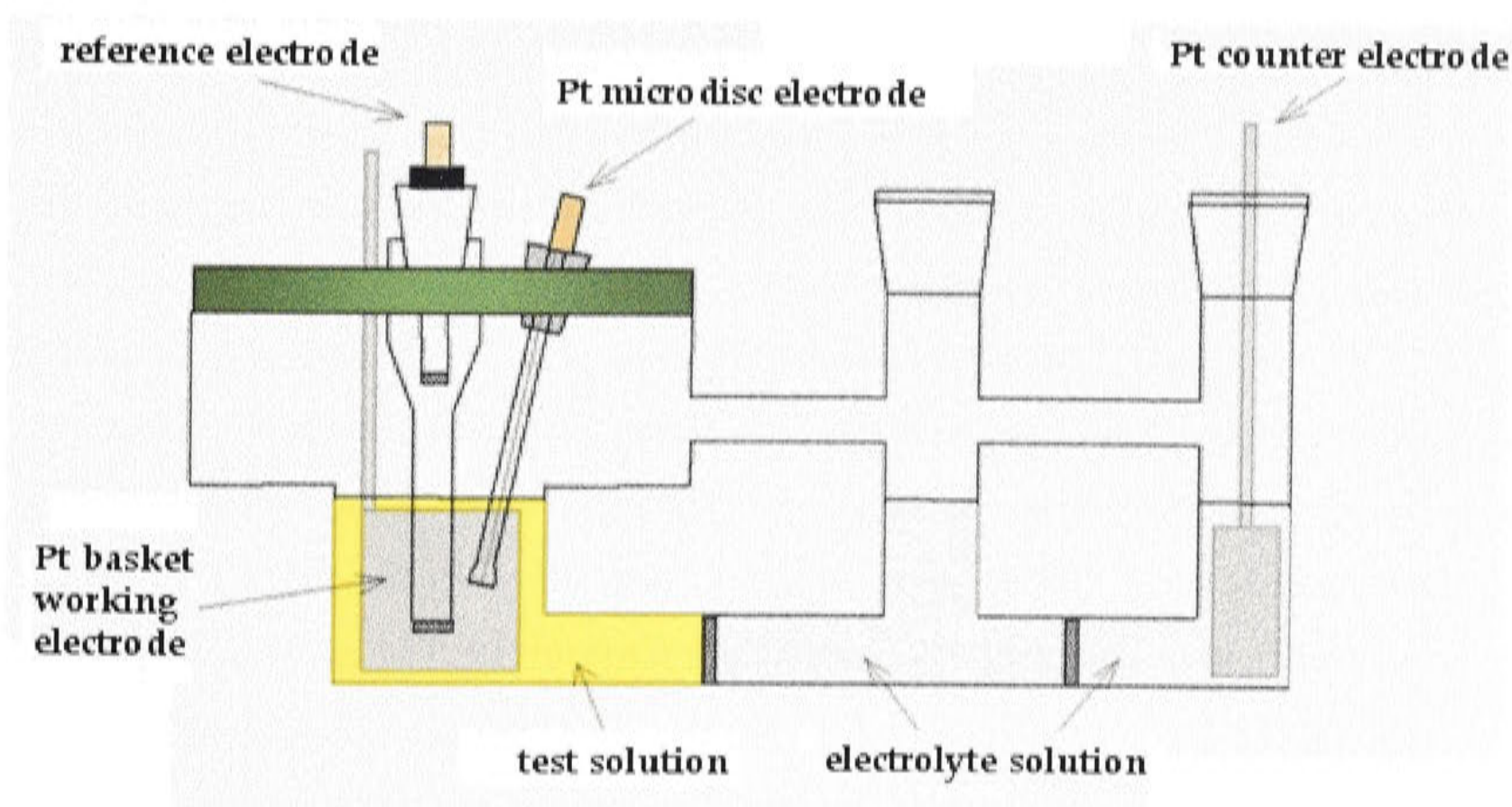


Figure 83. H-type cell used for bulk electrolysis experiments.

8.1.2 Spectroelectrochemistry: General Conditions

UV/Vis spectroelectrochemistry was carried out in Edinburgh on the λ -9 spectrometer (Perkin Elmer) (see p. 333). Using the cell shown in Figure 84, the products of a bulk electrolysis experiment could be monitored by electronic UV/Vis absorption spectroscopy.²⁸ The optically transparent thin layer electrode (OTTLE) cell consisted of a rhodium/platinum gauze working electrode with a transparency of *ca* 40% fitted into a quartz cell with a path length of 0.5 mm. A quartz extension was fitted into the cell which acts as a reservoir for the sample solution. To complete the conventional three-electrode system, a platinum wire counter electrode and a Ag/AgCl reference electrode were placed to this reservoir, both electrodes being separated from the sample solution by porous frits. The cell assembly was then placed in a PTFE block which was placed in the spectrometer. Control of the temperature was achieved by passing dry, pre-cooled nitrogen between the inner pair of quartz windows of the cell. The temperature was monitored using a thermocouple connected to a digital thermometer. To prevent the inner pair of quartz windows from fogging, dry nitrogen, at room temperature, was passed between the inner and outer quartz windows, and the sample chamber of the spectrometer was flushed with nitrogen. The reference electrode consisted of either a solution of 0.45M [Buⁿ₄N]BF₄ and 0.05M [Buⁿ₄N]Cl in CH₂Cl₂; or an ESR Ag/AgCl reference electrode, from CH Instruments, Inc., part number CHI111. This consisted of a Teflon cap with a coated Ag wire, a glass tubing and a porous glass tip sealed to the glass tubing with Teflon heat shrinkable tubing. The reference electrode compartment was filled with an aqueous 3M KCl solution.

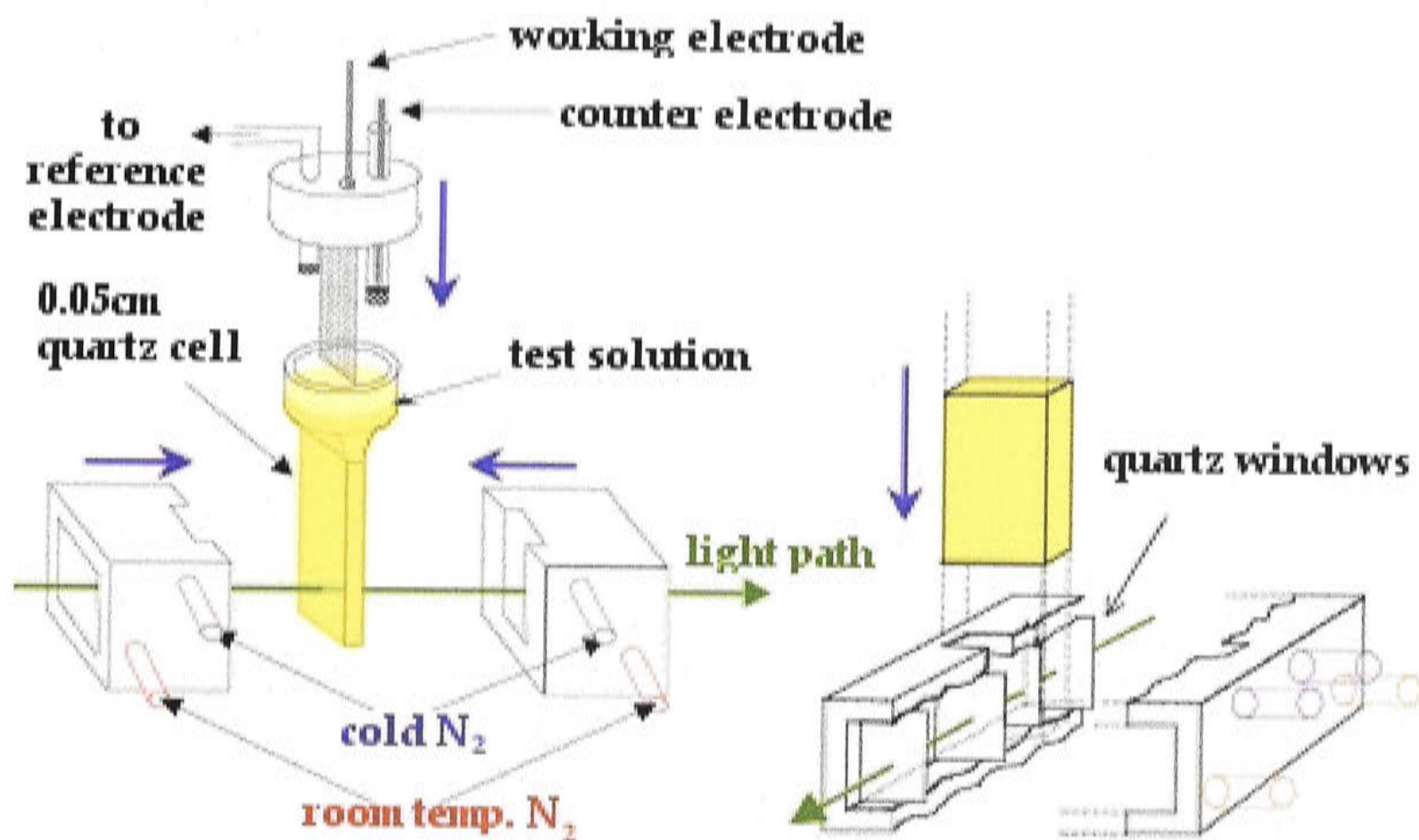


Figure 84. Schematic of the experimental setup for *in situ* UV/VIS/NIR experiments.

8.1.3 Electron Spin Resonance: General Conditions

In situ electrochemical X-band ESR spectra were recorded on a Bruker X-band ER200D-SRC Electron Spin Resonance Spectrometer in Edinburgh. The cell shown in Figure 85 was used, consisting of a rhodium/platinum working electrode fitted into a quartz flat body with a volume of 2 mL and a width of 0.1 mm. Two quickfit joints were fitted to the top of the cell to provide access to a three electrode system. This was completed using a platinum counter electrode and a Ag/AgCl reference electrode, both electrodes being separated from the sample solution by porous frits. The Ag/AgCl reference electrode, from CH Instruments, Inc., part number CHI111, was described on p. 337. The reference electrode compartment was filled with an aqueous 3M KCl solution. Samples for ESR study were generated *in situ* using a BAS CV-27 potentiostat. The temperature was controlled using a Bruker ER4111Vt variable temperature unit.

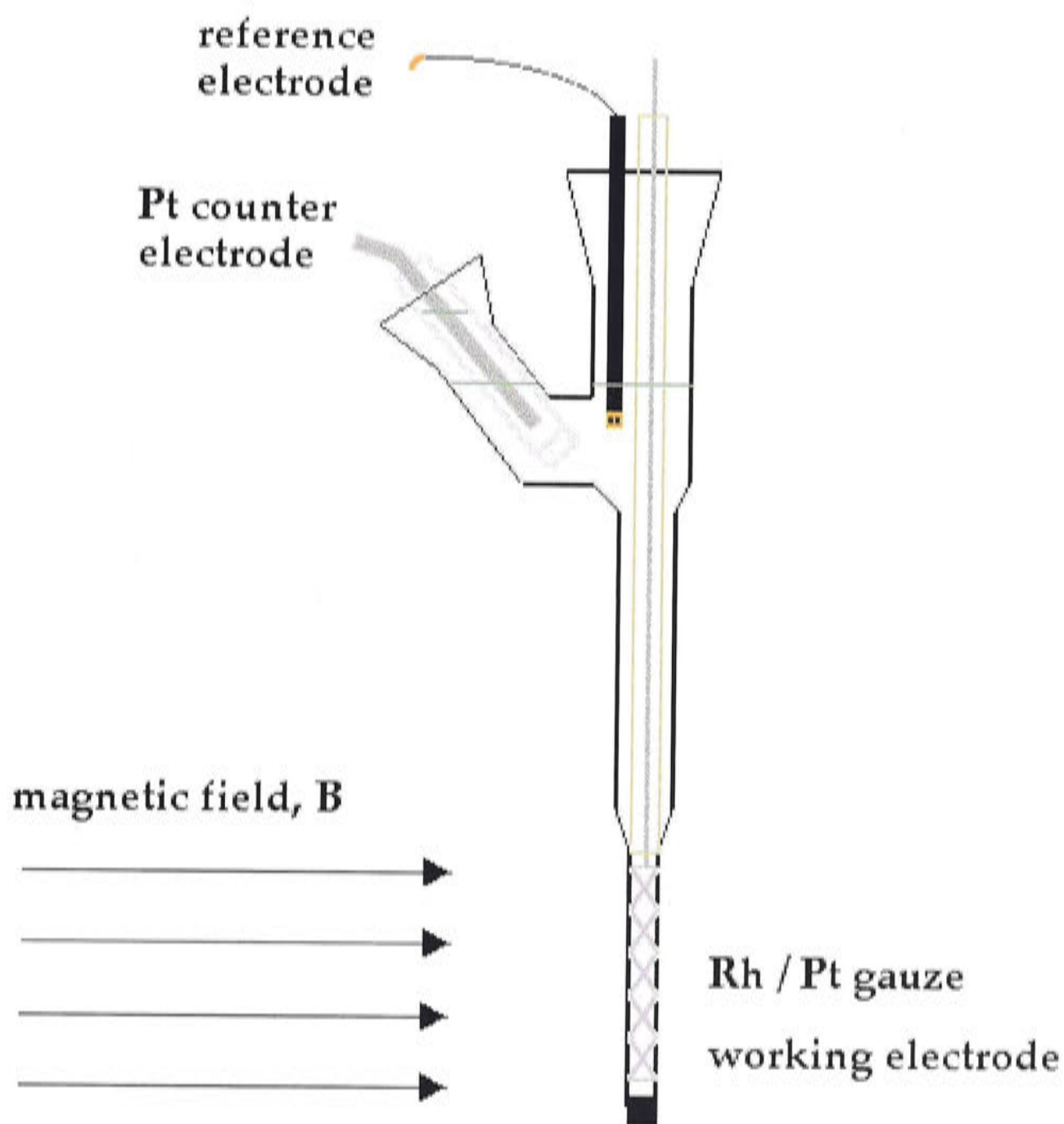


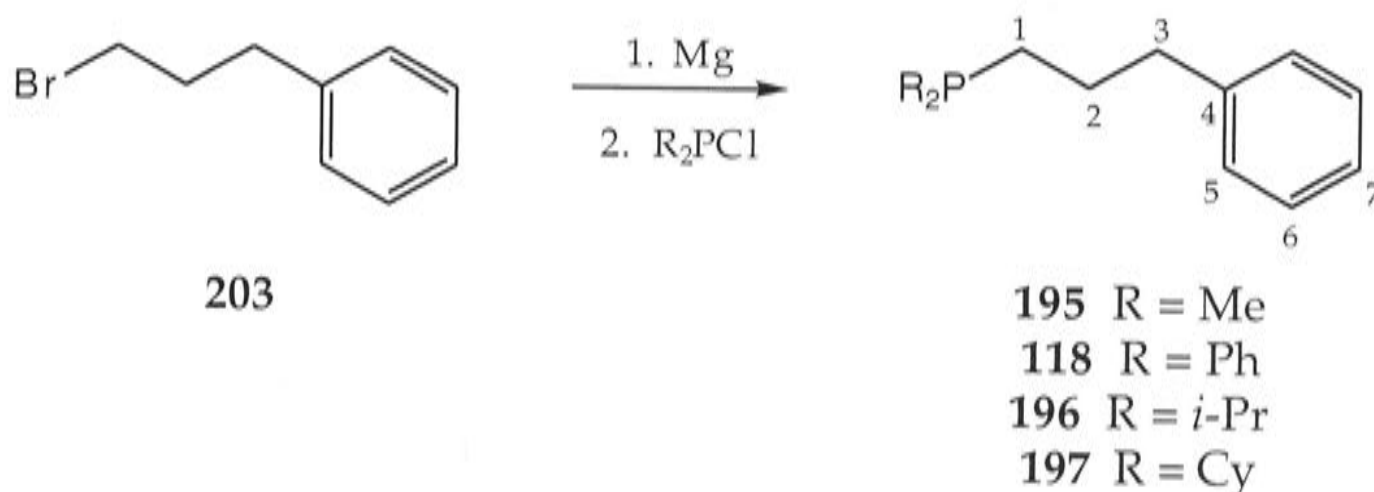
Figure 85. Schematic of the experimental set-up for ESR measurements.

For low temperature ESR experiments in Canberra, solutions of oxidised Ru(III) compounds were prepared in a divided controlled potential electrolysis cell separated with a porosity no. 5 (1.0 - 1.7 μm) sintered glass frit. The working and auxiliary electrodes were identically sized Pt mesh plates symmetrically arranged with respect to each other with a Ag wire reference electrode (isolated by a salt bridge) positioned to within 1 mm of the surface working electrode. The electrolysis cell was jacketed in a glass sleeve and cooled to 233K using a Lauda variable temperature methanol circulating bath. The working and auxiliary electrode compartments were each approximately of 20 mL volume, were continually purged with argon during the electrolysis. The number of electrons transferred during the bulk-oxidation process was calculated from Equation 3. In order to

ensure that oxygen was not introduced and to minimise temperature fluctuations during the transfer process, the bottom of the working electrode compartment was connected *via* glass tubing to an evacuated 2 mm diameter cylindrical ESR tube suspended in a dry ice/ethanol bath. Opening the tap on the bottom of the electrolysis cell at the completion of electrolysis allowed the solution to flow rapidly into a cylindrical ESR tube which was sealed with a Young's tap before being further cooled in liquid nitrogen. The ESR cell was then transferred to a Bruker ESP 300e spectrometer employing a rectangular TE_{102} cavity and with the modulation frequency set at 100 kHz.

The conditions used by Dr John McGrady (University of York), who performed the calculations²⁹ using the Amsterdam Density Functional (ADF) program, ADF2003.01,^{30,31} were as follows. A double- ζ Slater-type basis set, extended with a single polarisation function, was used to describe the hydrogen, carbon, phosphorus and chlorine atoms, while ruthenium was modelled with a triple- ζ basis set extended with a single polarisation function. Electrons in orbitals up to and including 1s {C}, 2p{P, Cl}, and 4p{Ru} were considered part of the core and treated in accordance with the frozen core approximation. The local density approximation was employed in all cases,³² along with the local exchange-correlation potential of Vosko, Wilk and Nusair³³ and gradient corrections to exchange and correlation proposed by Becke³⁴ and Perdew.³⁵ All structures were optimised using the gradient algorithm of Versluis and Ziegler.³⁶

8.2 Successful and Attempted Preparation of Compounds

8.2.1 Preparation of (3-phenylpropyl)dimethylphosphine (**195**)

1-Bromo-3-phenylpropane, (**203**), (15.3 mL, 0.10 mol) was added dropwise to a stirred suspension of magnesium (2.57 g, 0.11 mol) in dry THF (30 mL). Dry THF (20 mL) was added and the mixture was heated at reflux for 30 min. The solution was allowed to cool, transferred to a separate flask with dry ether (30 mL), stirred, and treated dropwise with chlorodimethylphosphine (7.5 mL, 0.095 mol) in dry ether (40 mL) at 0°C. The mixture was heated at reflux for 30 min, cooled to 0°C, and treated dropwise with degassed 10% aqueous NH₄Cl (30 mL). The mixture was allowed to come to room temperature, the organic phase was removed, and the aqueous phase extracted with dry ether (3 × 50 mL). The combined organic layers were dried (Na₂SO₄), solvents were removed *in vacuo*, and the residue was distilled under reduced pressure to afford the title compound **195** as a colourless liquid, b.p. 86-88°C/1.5 mm (8.60 g, 48%).

For the ligands R₂P(CH₂)₃aryl, the carbon atoms and the attached hydrogen atoms are numbered as shown above. This numbering system will also apply to the ruthenium complexes.

¹H-NMR (300 MHz, CD₂Cl₂): δ 1.07 (dd, 6H, ¹J_{HP} = 2 Hz, ²J_{HP} = 0.5 Hz, Me₂P), 1.46 (m, 2H, H²), 1.83 (m, 2H, H¹), 2.78 (t, 2H, J = 8 Hz, H³), 7.25-7.30 (m, 3H, H⁶, H⁷), 7.35-7.40 (m, 2H, H⁵). ¹³C{¹H}-NMR (75.4 MHz, CD₂Cl₂): δ 14.25 (d, ¹J_{PC} = 13 Hz, Me₂P), 28.14 (d, ²J_{PC} = 13 Hz, C²), 32.08 (d, ¹J_{PC} = 10 Hz, C¹), 37.84 (d, ³J_{PC} = 11 Hz, C³), 126.12 (C⁷), 128.66 (C⁵ or C⁶), 128.77 (C⁶ or C⁵), 142.73 (C⁴).

$^{31}\text{P}\{^1\text{H}\}$ -NMR (121.5 MHz, CD_2Cl_2): δ -51.6. IR (cm^{-1} , KBr): 3061 w, 3025 m [$\nu(\text{C-H})$], 1603 m, 1496 m [$\nu(\text{C=C})$]. EIMS; m/z : 179 [M^+]. High resolution MS; m/z : 180.106818. $\text{C}_{11}\text{H}_{17}\text{P}$ requires: 180.106789. Anal. found C, 73.11; H, 9.27%. $\text{C}_{11}\text{H}_{17}\text{P}$ requires: C, 73.31; H, 9.51%.

8.2.2 Preparation of (3-phenylpropyl)diphenylphosphine (118)

Compound **118** was prepared in 76% yield as a white solid, m.p. 56-58°C, from 1-bromo-3-phenylpropane (**203**) and chlorodiphenylphosphine in a similar way. Crystals suitable for X-ray crystallography were obtained from a CH_2Cl_2 -toluene solution.

^1H -NMR (300 MHz, CD_2Cl_2): δ 1.76 (m, 2H, H^2), 2.08 (m, 2H, H^1), 2.75 (t, 2H, $J = 8$ Hz, H^3), 7.15-7.45 (m, 15H, H^5 , H^6 , H^7 , PPh_2). $^{13}\text{C}\{^1\text{H}\}$ -NMR (75.4 MHz, CD_2Cl_2): δ 27.59 (d, $^2J_{\text{PC}} = 12$ Hz, C^2), 28.10 (d, $^1J_{\text{PC}} = 17$ Hz, C^1), 37.43 (d, $^3J_{\text{PC}} = 13$ Hz, C^3), 126.13 (C^7), 128.34 (d, $J_{\text{PC}} = 5$ Hz), (PPh_2), 128.79 (d, $J_{\text{PC}} = 3$ Hz, PPh_2), 132.98 (d, $J_{\text{PC}} = 19$ Hz, PPh_2), 139.36 (d, $J_{\text{PC}} = 14$ Hz, PPh_2), 142.29 (C^4). $^{31}\text{P}\{^1\text{H}\}$ -NMR (121.5 MHz, CD_2Cl_2): δ -16.2 (lit.^{37,38} δ -15.2; lit.³⁹ δ -16.7[†] in CDCl_3). IR (cm^{-1} , KBr): 3065 w, 3026 w, [$\nu(\text{C-H})$], 1599 w, 1494 m [$\nu(\text{C=C})$]. GCMS; m/z : 303 [M^+]. Anal. found C, 82.68; H, 6.66; P, 10.34%. $\text{C}_{21}\text{H}_{21}\text{P}$ requires: C, 82.87; H, 6.95; P, 10.18%.

8.2.3 Preparation of (3-phenylpropyl)diisopropylphosphine (196)

Compound **196** was prepared in 96% yield as a colourless liquid, b.p. 90-92°C/0.2 mm, from 1-bromo-3-phenylpropane (**203**) and chlorodi-*iso*-propylphosphine in a similar way.

[†]Calculated using the conversion factor δ 140.4⁴⁰ for the reference, not cited³⁹ but assumed to be $\text{P}(\text{OMe})_3$, for the value δ -157.1.

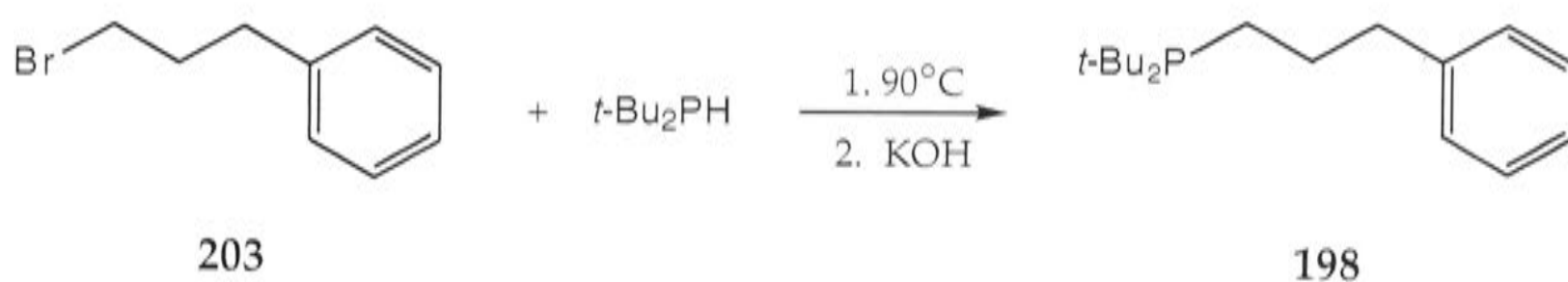
$^1\text{H-NMR}$ (400 MHz, CD_2Cl_2): δ 1.03 (dd, 6H, $J = 10.9, 7.0$ Hz, PCHMe_2), 1.07 (dd, 6H, $J = 13.8, 7.1$ Hz, PCHMe_2), 1.40 (m, 2H, H^1), 1.70 (m, 2H, PCHMe_2), 1.79 (m, 2H, H^2), 2.71 (t, $J = 8$ Hz, H, H^3), 7.15-7.20 (m, 3H, Ph), 7.25-7.30 (m, 2H, Ph). $^{13}\text{C}\{^1\text{H}\}\text{-NMR}$ (100.6 MHz, CD_2Cl_2): δ 18.88 (d, $^2J_{\text{PC}} = 9.5$ Hz, PCHMe_2), 20.22 (d, $^2J_{\text{PC}} = 15.9$ Hz, $\text{PCH}=\text{CH}_3$), 21.60 (d, $^2J_{\text{PC}} = 18$ Hz, C^2), 23.62 (d, $^1J_{\text{PC}} = 13$ Hz, PCHMe_2), 30.38 (d, $^1J_{\text{PC}} = 19$ Hz, C^1), 37.84 (d, $^3J_{\text{PC}} = 12$ Hz, C^3), 125.92 (C^7), 128.48 (C^5 or C^6), 128.63 (C^6 or C^5), 141.74 (C^4). $^{31}\text{P}\{^1\text{H}\}\text{-NMR}$ (161.97 MHz, CD_2Cl_2): δ 3.6 (lit.⁴¹ δ 2.1 in C_6D_6). IR (cm^{-1} , neat): 3062 m, 3026 m [$\nu(\text{C-H})$], 1603 m, 1496 s [$\nu(\text{C=C})$], 1454 s, 1383 m, 1365 m [$\nu((\text{CH}_3)_2\text{CH})$]. High resolution MS; m/z : 236.16843. $\text{C}_{15}\text{H}_{25}\text{P}$ requires: 236.16939.

8.2.4 Preparation of (3-phenylpropyl)dicyclohexylphosphine (197)

This compound **197** was prepared in 64% yield as a white solid, from 1-bromo-3-phenylpropane (**203**) and chlorodicyclohexylphosphine, according to the procedure described in reference(14).

$^{31}\text{P}\{^1\text{H}\}\text{-NMR}$ (161.97 MHz, CD_2Cl_2): δ -4.6. (lit.¹⁴ δ -4.65).

8.2.5 Preparation of (3-phenylpropyl)di-*t*-butylphosphine (198)

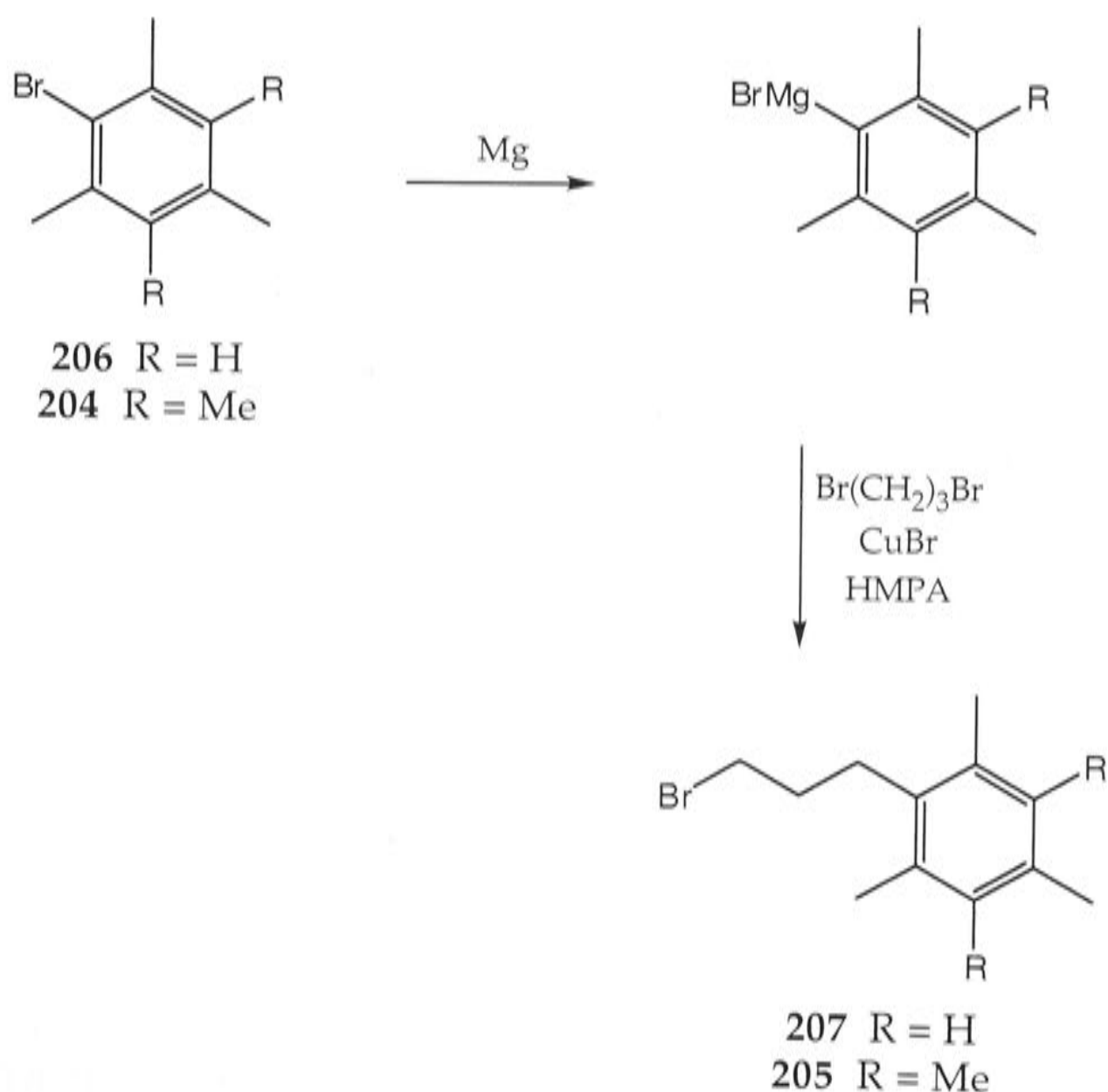


This procedure is based on that described in reference(41). A mixture of di-*t*-butylphosphine (6.49 g, 44.4 mmol) and 1-bromo-3-phenylpropane, (**203**), (6.1 mL, 39.8 mmol) was heated for 4 days at 90°C. The reaction mixture was cooled and a colourless viscous liquid was obtained. The liquid was dissolved in degassed water (40 mL) and the solution was washed with ether (5 × 20 mL). The aqueous phase was then layered with ether (80 mL) and treated with KOH until the aqueous phase became basic (pH ~ 9). The organic phase was removed and the aqueous phase was

washed with ether (2 x 20 mL). The combined organic layers were washed with water (3 x 20 mL) and then dried (Na_2SO_4), and the solvent was removed *in vacuo*. The residue was distilled to afford the title compound **198** as a colourless liquid b.p. 107-109°C/0.1 mm (5.56 g, 53%).

$^1\text{H-NMR}$ (400 MHz, CD_2Cl_2): δ 1.21 (d, 18H, $J = 11$ Hz, PCMe_3), 1.44 (m, 2H, H^2), 1.86 (m, 2H, H^1), 2.74 (t, 2H, $J = 8$ Hz, H^3), 7.15-7.24 (m, 3H, PPh_2), 7.27-7.30 (m, 2H, PPh_2). $^{13}\text{C}\{^1\text{H}\}$ -NMR (100.6 MHz, CD_2Cl_2): δ 20.84 (d, $^2J_{\text{PC}} = 21$ Hz, C^2), 29.41 (d, $^2J_{\text{PC}} = 13.5$ Hz, PCMe_3), 31.02 (d, $^1J_{\text{PC}} = 21$ Hz, PCMe_3), 32.29 (d, $^1J_{\text{PC}} = 26$ Hz, C^1), 37.52 (d, $^3J_{\text{PC}} = 13$ Hz, C^3), 125.56 (C^7), 128.15 (C^5 or C^6), 128.42 (C^6 or C^5), 142.50 (C^4). $^{31}\text{P}\{^1\text{H}\}$ -NMR (161.97 MHz, CD_2Cl_2): δ 28.4. IR (cm^{-1} , neat): 3062 m, 3026 m [$\nu(\text{C-H})$], 1603 m, 1496 s [$\nu(\text{C=C})$], 1470 s, 1387 m, 1365 s [$\nu((\text{CH}_3)_3\text{C})$]. EIMS; m/z : 264 [M^+]. High resolution MS; m/z : 264.20189. $\text{C}_{17}\text{H}_{29}\text{P}$ requires: 264.20068.

8.2.6 Preparation of 1-bromo-3-(mesityl)propane (**207**)



This procedure is based on that described in reference(42). A solution of bromomesitylbenzene, (**206**), (11.5 mL, 75 mmol) in dry THF (10 mL) was added dropwise to a stirred suspension of magnesium (2.93 g, 121 mmol) in dry THF (10 mL). The reaction was initiated with a small amount of reacting Mg/BrCH₂CH₂Br and the mixture was heated at reflux for 1 h. The solution was allowed to cool, transferred to a separate dropping funnel with dry THF (20 mL), and added dropwise to a mixture of 1,3-dibromopropane (9.2 mL, 91 mmol), dry HMPA (6.8 mL), freshly prepared copper(I) bromide (551 mg, 5 mol% to the Grignard reagent) in dry THF (20 mL) at reflux. Dry THF (20 mL) was then added and the reaction mixture was heated at reflux for 20 h. The reaction mixture was allowed to cool to room temperature, poured onto a slurry of ice/conc. HCl (500 mL), and the aqueous phase extracted with ether (4 × 100 mL). The organic phase was washed with water (3 × 100 mL), 1M KOH (3 × 100 mL) and then again with water (3 × 100 mL). The organic phase was then dried (Na₂SO₄). The solvent was removed by evaporation and the mesitylene and excess 1,3-dibromopropane were removed *in vacuo* (0.3 mm) to afford the title compound **207** as a colourless solid (12.95 g, 71%).

¹H-NMR (300 MHz, CDCl₃): δ 1.99 (m, 2H, H²), 2.24 (s, 3H, C⁷-Me), 2.29 (s, 6H, C⁵-Me), 2.73 (m, 2H, H³), 3.50 (t, 2H, *J* = 6.5 Hz, H¹), 6.83 (s, 2H, H⁶). High resolution MS; *m/z*: 240.04972, 242.04785. C₁₂H₁₇⁷⁹Br and C₁₂H₁₇⁸¹Br require: 240.05136, 242.04945, respectively.

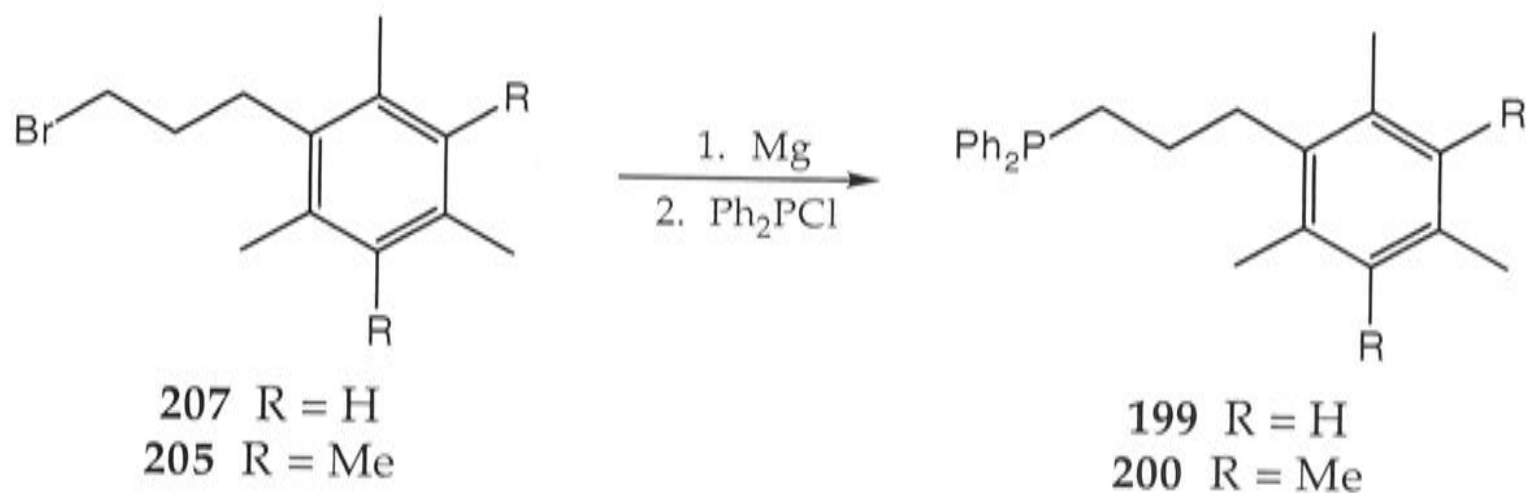
8.2.7 Preparation of 1-bromo-3-(pentamethylphenyl)propane (**205**)

This compound **205** was prepared as a colourless solid in 63% yield, m.p. 34-38°C, from bromopentamethylbenzene (**204**), magnesium and 1,3-dibromopropane in a similar way.

¹H-NMR (400 MHz, CDCl₃): δ 2.00 (m, 2H, H²), 2.21 (s, 6H, H⁵), 2.22 (s, 3H, H⁷), 2.25 (s, 6H, H⁶), 2.83 (m, 2H, H³), 3.51 (t, 2H, *J* = 6.5 Hz, H¹). ¹³C{¹H}-NMR (75.4 MHz, CDCl₃): δ 16.41 (C⁵-Me), 16.80 (C⁷-Me), 16.85 (C⁶-Me), 29.30 (C²), 32.74 (C³), 34.10 (C¹), 131.71 (C⁷), 132.62 (C⁵ or C⁶), 132.87 (C⁶

or C⁵), 134.61 (C⁴). IR (cm⁻¹, KBr): 553 m [ν(C-Br)]. EIMS; *m/z*: 270 [*M*⁺]. High resolution MS; *m/z*: 268.083032, 270.080666. C₁₄H₂₁⁷⁹Br and C₁₄H₂₁⁸¹Br require: 268.082662, 270.080616, respectively. Anal. found C, 62.13; H, 7.91%. C₁₄H₂₁Br require: C, 62.46; H, 7.86%.

8.2.8 Preparation of (3-mesitylpropyl)diphenylphosphine (199)



A solution of 1-bromo-3-(mesityl)phenylpropane, (**207**), (5.97 g, 24.7 mmol) in dry THF (20 mL) was added dropwise to a stirred suspension of magnesium (0.66 g, 27.1 mmol) in dry THF (10 mL). The reaction was initiated with a small amount of reacting Mg/BrCH₂CH₂Br. The reaction mixture was heated at reflux for 30 min, allowed to cool and transferred to a separate flask with dry ether (20 mL). Chlorodiphenylphosphine (4.2 mL, 23.4 mmol) in dry ether (10 mL) was added dropwise to the stirred Grignard reagent at 0°C. After addition of dry ether (20 mL), the reaction mixture was allowed to warm to room temperature, heated at reflux for 1 h, cooled to 0°C, stirred and treated dropwise with degassed 10% aqueous NH₄Cl (30 mL). The organic phase was removed and the aqueous layer was extracted with dry ether (4 × 50 mL). The combined organic phases were dried (Na₂SO₄) and the solvents were removed *in vacuo*. The residue was purified by column chromatography (activity I acidic alumina, dichloromethane). The solvent was removed *in vacuo* to afford the title compound **199** as a colourless solid, m.p. 74-76°C (7.41 g, 80%).

¹H-NMR (300 MHz, CD₂Cl₂): δ 1.54 (m, 2H, H²), 2.19 (s, 6H, C⁵-Me), 2.20 (s, 3H, C⁷-Me), 2.27-2.33 (m, 2H, H¹), 2.70 (t, 2H, *J* = 8 Hz, H³), 6.77 (s, 2H, H⁶),

7.30-7.35 (m, 6H, PPh₂), 7.40-7.45 (m, 4H, PPh₂). ¹³C{¹H}-NMR (100.6 MHz, CD₂Cl₂): δ 19.71 (C⁵-Me), 20.73 (C⁷-Me), 25.78 (d, ¹J_{PC} = 16 Hz, C²), 28.42 (d, ¹J_{PC} = 12 Hz, C¹), 30.99 (d, ³J_{PC} = 13 Hz, C³), 128.59, 128.65, 128.72 (C⁵-C⁷), 128.94 (PPh₂), 132.88 (d, ¹J_{PC} = 19 Hz, PPh₂), 135.95 (PPh₂), 136.00 (C⁴), 139.36 (d, ¹J_{PC} = 14 Hz, PPh₂). ³¹P{¹H}-NMR (121.5 MHz, CD₂Cl₂): δ -16.5. IR (cm⁻¹, nujol): 3052 m, 3000 m [ν(C-H)], 1613 w, 1583 w, 1480 s [ν(C=C)]. EIMS; *m/z*: 346 [M⁺]. High resolution MS; *m/z*: 346.18562. C₂₄H₂₇P requires: 346.18504.

8.2.9 Preparation of (3-pentamethylphenylpropyl)diphenylphosphine (200)

Compound **200** was prepared in 77% yield, as a colourless solid m.p. 90-92°C from 1-bromo-3-(pentamethyl)phenylpropane (**205**) and chlorodiphenylphosphine in a similar way.

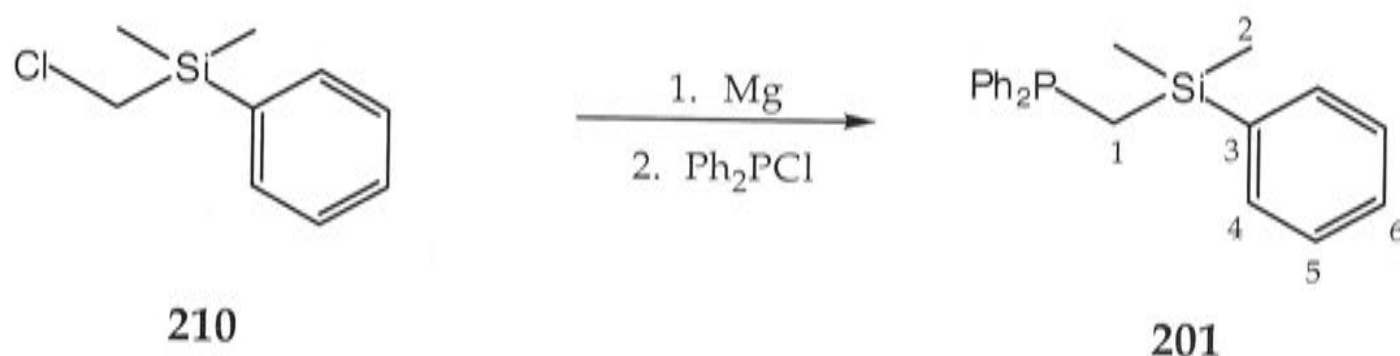
¹H-NMR (300 MHz, CD₂Cl₂): δ 1.54 (m, 2H, H²), 2.15 (s, 6H, C⁵-Me), 2.17 (s, 6H, C⁶-Me), 2.19 (s, 3H, C⁷-Me), 2.22-2.25 (m, 2H, H¹), 2.80 (t, 2H, *J* = 8 Hz, H₃), 7.30-7.35 (m, 6H, PPh₂), 7.40-7.45 (m, 4H, PPh₂). ¹³C{¹H}-NMR (75.4 MHz, CD₂Cl₂): δ 16.48 (C⁵-Me), 16.86 (C⁶-Me, C⁷-Me), 26.49 (d, ²J_{PC} = 16 Hz, C²), 28.47 (d, ¹J_{PC} = 12 Hz, C¹), 32.34 (d, ³J_{PC} = 13 Hz, C³), 128.64 (C⁷), 128.75 (d, *J*_{PC} = 3 Hz, PPh₂), 131.61 (C⁵, C⁶), 132.53 (d, *J*_{PC} = 3 Hz, PPh₂), 132.97 (d, *J*_{PC} = 18 Hz, PPh₂), 135.98 (C⁴), 139.50 (d, *J*_{PC} = 14 Hz, PPh₂). ³¹P{¹H}-NMR (121.5 MHz, CD₂Cl₂): δ -16.5. IR (cm⁻¹, KBr): 3065 w [ν(C-H)], 1583 w, 1479 m [ν(C=C)]. EIMS; *m/z*: 374 [M⁺]. High resolution MS; *m/z*: 374.217049. C₂₆H₃₁P requires: 374.216340.

Attempts to prepare Ph₂P(CH₂)₃C₆Me₅ (**200**) by the reaction of the Grignard reagent,⁴³ derived from 1-chloro-3-propyldiphenylphosphine (**208**) and magnesium, with bromopentamethylbenzene (**204**) did not yield the desired product.

Similarly, reaction of the Grignard reagent,⁴⁴ derived from bromopentamethylbenzene (**204**) and magnesium, with

1-chloro-3-propyldiphenylphosphine (**208**) in the presence of a catalytic quantity of $[\text{PdCl}_2(\text{PPh}_3)_2]$ failed to afford the phosphine **200**.

8.2.10 Preparation of (phenyldimethylsilyl)methyldiphenylphosphine (**201**)

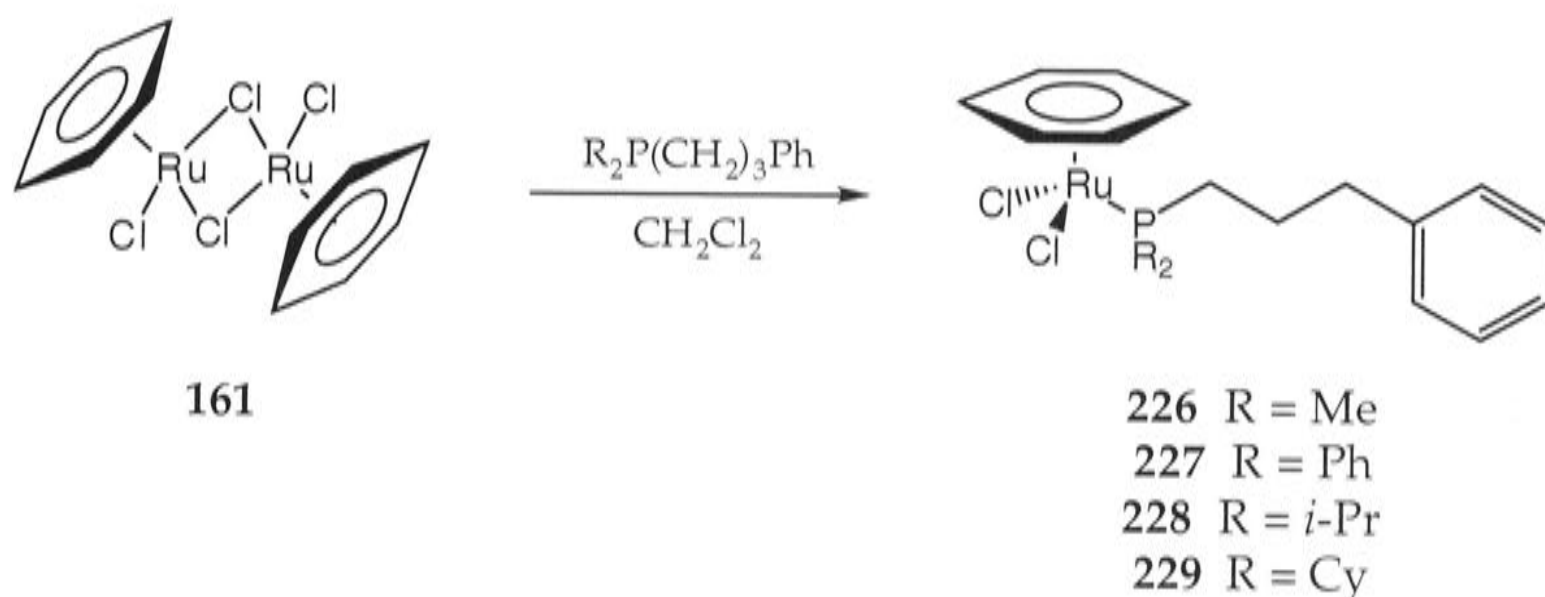


(Chloromethyl)dimethylphenylsilane, (**210**), (3.9 mL, 22 mmol) was added dropwise to a stirred suspension of magnesium (0.56 g, 23 mmol) in dry THF (10 mL). After addition of dry THF (10 mL), the reaction mixture was heated at reflux for 30 min, allowed to cool, transferred to a separate flask with dry ether (20 mL), stirred and treated dropwise at 0°C with a solution of chlorodiphenylphosphine (3.7 mL, 21 mmol) in dry ether (15 mL). After addition of more dry ether (10 mL), the solution was heated at reflux for 30 min, cooled to 0°C, stirred, and treated dropwise with degassed 10% aqueous NH_4Cl (15 mL). The organic phase was removed and the aqueous layer was extracted with dry ether (4 × 40 mL). The combined organic layers were dried (Na_2SO_4) and the solvents were removed *in vacuo* to give a sticky solid that contained $\text{Ph}_2\text{PCH}_2\text{SiMe}_2\text{C}_6\text{H}_5$ (**201**) and Ph_2MeP (**211**) in *ca* 7:1 ratio, as shown by $^{31}\text{P}\{^1\text{H}\}$ -NMR spectroscopy. The minor product was removed by sublimation (50°C, $7 \cdot 10^{-6}$ mm) on to a liquid nitrogen-cooled probe and the residue was recrystallised from hot dry ethanol (5 mL) to give the title compound **201** as a colourless solid, m.p. 62-64°C (3.18 g, 44%).

For the ligand $\text{Ph}_2\text{PCH}_2\text{SiMe}_2\text{Ph}$ (**201**), the carbon atoms and the attached hydrogen atoms are numbered as shown above. This numbering system will also apply to the ruthenium complexes.

$^1\text{H-NMR}$ (300 MHz, CD_2Cl_2): δ 0.17 (s, 6H, H^2), 1.62 (d, 2H, $J = 1$ Hz, H^1), 7.30-7.35 (m, 9H, H^6 , H^7 , PPh_2), 7.40-7.50 (m, 6H, H^5 , PPh_2). $^{13}\text{C}\{^1\text{H}\}\text{-NMR}$ (75.4 MHz, CD_2Cl_2): δ -1.76 (d, $^4J_{\text{PC}} = 4$ Hz, C^2), 14.02 (d, $^1J_{\text{PC}} = 30$ Hz, C^1), 128.01 (C^6), 128.52 (C^4 or C^5), 128.65 (d, $J_{\text{PC}} = 6$ Hz, PPh_2), 129.28 (C^5 or C^4), 132.77 (d, $J_{\text{PC}} = 20$ Hz, PPh_2), 133.85 (C^3), 141.53 (d, $J_{\text{PC}} = 15$ Hz, PPh_2). $^{29}\text{Si}\{^1\text{H}\}\text{-NMR}$ (74.49 MHz, CD_2Cl_2): δ -3.90 (d, $^2J_{\text{PSi}} = 16$ Hz). $^{31}\text{P}\{^1\text{H}\}\text{-NMR}$ (121.5 MHz, CD_2Cl_2): δ -22.3. IR (cm^{-1} , KBr): 3063 w, 3048 w, 3003 w [$\nu(\text{C-H})$], 1582 w, 1476 m [$\nu(\text{C=C})$]. EIMS; m/z : 333 [M^+]. High resolution MS; m/z : 333.123093. $\text{C}_{21}\text{H}_{23}\text{P}$ requires: 333.133843.

8.2.11 Preparation of $[\text{RuCl}_2(\eta^6\text{-C}_6\text{H}_6)(\eta^1\text{-Me}_2\text{P}(\text{CH}_2)_3\text{Ph})]$ (**226**)



A solution containing the ruthenium complex $[\text{RuCl}_2(\eta^6\text{-C}_6\text{H}_6)]_2$, (**161**), (310 mg, 0.62 mmol) and (3-phenylpropyl)dimethylphosphine, (**195**), (0.24 mg, 1.31 mmol) in dry dichloromethane (20 mL) was stirred for 4 h and filtered through Celite, which was washed then with dichloromethane (2 x 20 mL). Addition of *n*-hexane (40 mL) to the filtrate and removal of the solvents *in vacuo* gave a residue which was triturated with ether to afford the title compound **226** as an orange-brown solid (465 mg, 87%).

$^1\text{H-NMR}$ (300 MHz, CDCl_3): δ 1.57 (d, 6H, $^1J_{\text{PH}} = 12$ Hz, PMe_2), 1.91 (m, 2H, H^2), 2.09 (m, 2H, H^1), 2.73 (t, 2H, $J = 7$ Hz, H^3), 5.44 (s, 6H, C_6H_6), 7.15-7.25 (m, 3H, H^6 , H^7), 7.30-7.35 (m, 2H, H^5). $^{13}\text{C}\{^1\text{H}\}\text{-NMR}$ (75.4 MHz, CDCl_3): δ 12.94 (d, $^1J_{\text{PC}} = 35$ Hz, PMe_2), 25.58 (d, $^2J_{\text{PC}} = 4$ Hz, C^2), 30.57 (d, $^1J_{\text{PC}} = 30$ Hz,

C^1), 36.64 (d, $^3J_{PC} = 13$ Hz, C^3), 87.01 (d, $J_{PC} = 13$ Hz, C_6H_6), 126.09 (C^7), 128.19 (C^5 or C^6), 128.38 (C^6 or C^5), 140.97 (C^4). $^{31}P\{^1H\}$ -NMR (121.5 MHz, $CDCl_3$): δ 13.8. IR (cm^{-1} , polythene): 290 s, 273 s [$\nu(Ru-Cl)$]. FABMS; m/z : 430 [M^+]. Anal. found: C, 47.71; H, 5.42; P, 6.91%. $C_{17}H_{23}Cl_2PRu$ requires: C, 47.45; H, 5.39; P, 7.20%.

8.2.12 Preparation of $[RuCl_2(\eta^6-C_6H_6)(\eta^1-Ph_2P(CH_2)_3Ph)]$ (227)

Complex **227** was prepared in 98% yield, as an orange solid, from **161** and (3-phenylpropyl)diphenylphosphine (**118**) in a similar way. Red crystals suitable for X-ray crystallography were obtained from dichloromethane/ether by vapour diffusion.

1H -NMR (300 MHz, $CDCl_3$): δ 1.48 (m, 2H, H^2), 2.47 (t, 2H, $J = 6$ Hz, H^1), 2.64 (m, 2H, H^3), 5.34 (s, 6H, C_6H_6), 6.90-7.80 (m, 15H, PPh_2 , C_6H_5). $^{13}C\{^1H\}$ -NMR (75.4 MHz, $CDCl_3$): δ 23.04 (d, $^2J_{PC} = 29$ Hz, C^2), 25.19 (d, $^1J_{PC} = 7$ Hz, C^1), 36.84 (d, $^3J_{PC} = 13$ Hz, C^3), 88.32 (d, $J_{PC} = 3$ Hz, C_6H_6), 125.70 (C^7), 128.13, 128.30, 128.38, 128.50 (C^5 , C^6 , PPh_2), 130.66 (d, $J_{PC} = 3$ Hz, PPh_2), 132.87 (d, $J_{PC} = 9$ Hz, PPh_2), 141.43 (C^4). $^{31}P\{^1H\}$ -NMR (121.5 MHz, $CDCl_3$): δ 23.7. IR (cm^{-1} , polythene): 295 s, 278 s [$\nu(Ru-Cl)$]. FAB-MS; m/z : 554 [M^+]. Anal. found: C, 58.32; H, 4.67; P, 5.84%. $C_{27}H_{27}Cl_2PRu$ requires: C, 58.49; H, 4.91; P, 5.59%.

8.2.13 Preparation of $[RuCl_2(\eta^6-C_6H_6)(\eta^1-i-Pr_2P(CH_2)_3Ph)]$ (228)

Complex **228** was prepared in 95% yield, as an orange solid from **161** and (3-phenylpropyl)di-*iso*-propylphosphine (**196**) in a similar way.

1H -NMR (400 MHz, $CDCl_3$): δ 1.02-1.09 (m, 12H, $PCHMe_2$), 1.74 (m, 2H, H^2), 1.87 (m, 2H, $PCHMe_2$), 1.96 (m, 2H, H^3), 2.53 (t, 2H, $J = 6$ Hz, H^1), 5.59 (s, 6H, C_6H_6), 7.05-7.10 (m, 3H, H^6 , H^7), 7.15-7.20 (m, 2H, H^5). $^{13}C\{^1H\}$ -NMR (121.5 MHz, $CDCl_3$): δ 19.54 (d, $^2J_{PC} = 20$ Hz, $PCHMe_2$), 19.65 (d, $^1J_{PC} = 25$ Hz, C^1), 26.36 (d, $^2J_{PC} = 5$ Hz, C^2), 27.48 (d, $^1J_{PC} = 23$ Hz, $PCHMe_2$), 37.66 (d, $^3J_{PC} = 12$ Hz, C^3), 87.48 (d, $J_{PC} = 2$ Hz, C_6H_6), 126.07 (C^7), 128.17 (C^5 or C^6), 128.47 (C^6 or C^5),

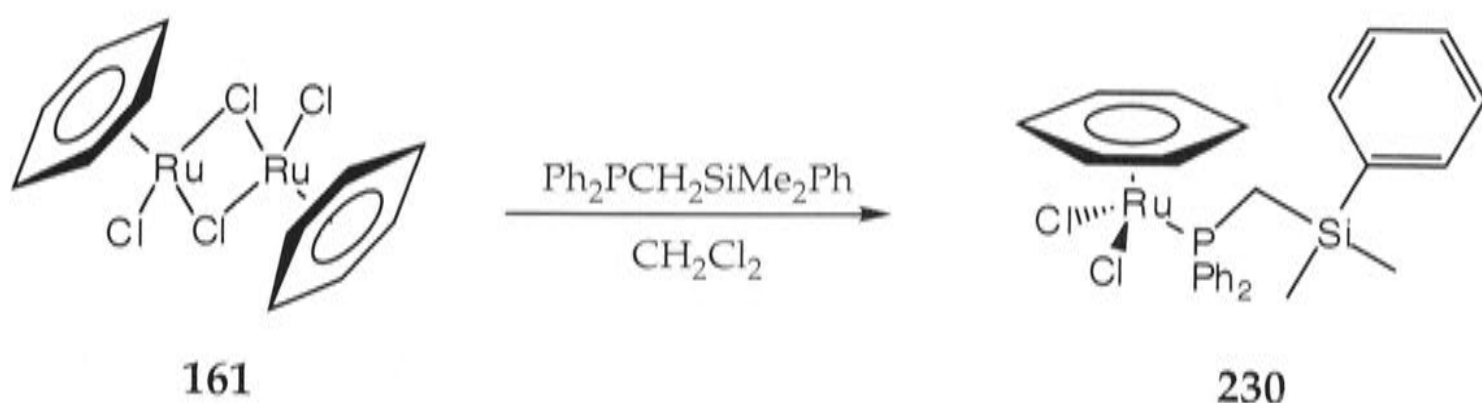
141.68 (C⁴). ³¹P{¹H}-NMR (161.97 MHz, CDCl₃): δ 37.3. IR (cm⁻¹, KBr and polythene): 1453 s, 1385 m, 1365 m [ν((CH₃)₂CH)], 279 s, 261 s [ν(Ru-Cl)]. EIMS; *m/z*: 451 [M-Cl]⁺. Anal. found: C, 51.16; H, 6.36; P, 6.58%. C₂₁H₃₁Cl₂PRu.0.1CH₂Cl₂ requires: C, 51.21; H, 6.35; P, 6.26%. The presence of dichloromethane was evident in the ¹H NMR spectrum.

8.2.14 Preparation of [RuCl₂(η⁶-C₆H₆)(η¹-Cy₂P(CH₂)₃Ph)] (229)

Complex **229** was prepared in 95% yield, as an orange-brown solid from **161** and (3-phenylpropyl)dicyclohexylphosphine (**197**) in a similar way.

¹H-NMR (400 MHz, CDCl₃): δ 1.23-1.35 (m, 6H, Cy), 1.55 (m, 2H, H²), 1.70-1.89 (m, 12H, Cy), 2.06-2.23 (m, 4H, Cy), 2.25 (m, 2H, H³), 2.59 (t, 2H, *J* = 7.5 Hz, H¹), 5.64 (s, 6H, C₆H₆), 7.15-7.20 (m, 3H, H⁶, H⁷), 7.25-7.30 (m, 2H, H⁵). ¹³C{¹H}-NMR (100.6 MHz, CDCl₃): δ 15.38 (d, *J*_{PC} = 24 Hz, Cy), 26.36 (Cy), 26.83 (d, ²*J*_{PC} = 7 Hz, C²), 27.46 (d, ¹*J*_{PC} = 19 Hz, C¹), 27.46 (Cy), 29.04 (Cy), 29.46 (Cy), 37.63 (d, ³*J*_{PC} = 12 Hz, C³), 29.95 (Cy), 37.93 (d, ¹*J*_{PC} = 22 Hz, Cy), 86.93 (d, *J*_{PC} = 2 Hz, C₆H₆), 125.90 (C⁷), 128.35 (C⁵ or C⁶), 128.53 (C⁶ or C⁵), 141.83 (C⁴). ³¹P{¹H}-NMR (161.97 MHz, CDCl₃): δ 29.6. IR (cm⁻¹, polythene): 284 s, 263 s [ν(Ru-Cl)]. EIMS; *m/z*: 532 [M⁺]. Anal. found: C, 56.48; H, 6.78; P, 5.45%. C₂₇H₃₉Cl₂PRu.0.1CH₂Cl₂ requires: C, 56.64; H, 6.99; P, 5.52%. The presence of dichloromethane was evident in the ¹H NMR spectrum.

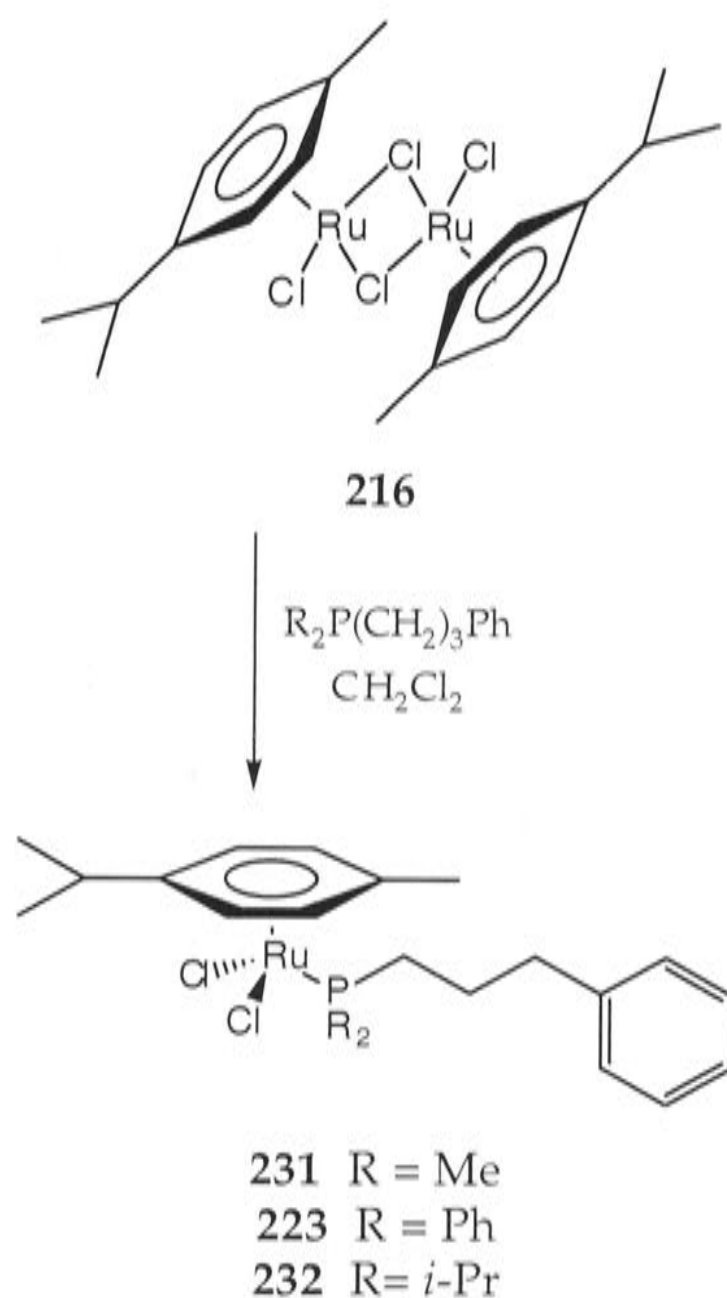
8.2.15 Preparation of [RuCl₂(η⁶-C₆H₆)(η¹-Ph₂PCH₂SiMe₂Ph)] (230)



Complex **230** was prepared in 84% yield, as an orange solid from **161** and (phenyldimethylsilyl)methyldiphenylphosphine (**201**) in a similar way.

$^1\text{H-NMR}$ (300 MHz, CDCl_3): δ -0.18 (s, 6H, H^2), 2.21 (d, 2H, $J = 15$ Hz, H^1), 5.23 (s, 6H, C_6H_6), 7.05-7.90 (m, 15H, PPh_2 , C_6H_5). $^{13}\text{C}\{^1\text{H}\}$ -NMR (75.4 MHz, CDCl_3): δ -1.27 (C^2), 10.01 (d, $^1J_{\text{PC}} = 24$ Hz, C^1), 88.13 (C_6H_6), 127.40 (C^6), 128.15 (d, $J_{\text{PC}} = 10$ Hz, PPh_2), 128.58 (C^4 or C^5), 130.57 (C^5 or C^4), 132.47 (d, $J_{\text{PC}} = 9$ Hz, PPh_2), 133.13 (C^3), 134.39 (d, $J_{\text{PC}} = 45$ Hz, PPh_2), 138.64 (d, $J_{\text{PC}} = 3$ Hz, PPh_2). $^{31}\text{P}\{^1\text{H}\}$ -NMR (121.5 MHz, CDCl_3): δ 24.5. IR (cm^{-1} , polythene): 292 s, 275 s [$\nu(\text{Ru-Cl})$]. FABMS; m/z : 584 [M^+]. Anal. found: C, 55.47; H, 5.08; P, 5.21%. $\text{C}_{27}\text{H}_{29}\text{Cl}_2\text{PRuSi}$ requires: C, 55.48; H, 5.00; P, 5.30%.

8.2.16 Preparation of $[\text{RuCl}_2(\eta^6\text{-1,4-MeC}_6\text{H}_4\text{CHMe}_2)(\eta^1\text{-Me}_2\text{P}(\text{CH}_2)_3\text{Ph})]$
(231)



A solution containing the ruthenium complex $[\text{RuCl}_2(\eta^6\text{-1,4-MeC}_6\text{H}_4\text{CHMe}_2)]_2$ (216), (325 mg, 0.53 mmol) and (3-phenylpropyl)dimethylphosphine, (195), (191 mg, 1.06 mmol) in dry

dichloromethane (20 mL) was stirred for 3 h and filtered through Celite, which was then washed with dichloromethane (2 × 20 mL). Addition of *n*-hexane (40 mL) to the filtrate and removal of the solvents *in vacuo* gave the title compound **231** as an orange solid (512 mg, 99%). Red crystals suitable for X-ray crystallography were obtained by layering a CH₂Cl₂ solution with *n*-hexane.

¹H-NMR (300 MHz, CDCl₃): δ 1.19 (d, 6H, *J* = 7 Hz, PMe₂), 1.51 (d, 6H, *J* = 13 Hz, MeC₆H₄CHMe₂), 1.84 (m, 2H, H²), 2.01 (s, 3H, MeC₆H₄CHMe₂), 2.06 (m, 2H, H¹), 2.71 (t, 2H, *J* = 7 Hz, H³), 2.79 (m, 1H, MeC₆H₄CHMe₂), 5.32 (m, 4H, MeC₆H₄CHMe₂), 7.15-7.23 (m, 3H, H⁶, H⁷), 7.25-7.35 (m, 2H, H⁵).
¹³C{¹H}-NMR (75.4 MHz, CDCl₃): δ 12.23 (d, ¹*J*_{PC} = 32 Hz, PMe₂), 17.76 (MeC₆H₄CHMe₂), 21.63 (MeC₆H₄CHMe₂), 25.23 (d, ²*J*_{PC} = 5 Hz, C²), 29.65 (MeC₆H₄CHMe₂), 30.14 (C¹), 36.78 (d, ³*J*_{PC} = 12 Hz, C³), 84.18 (d, *J*_{PC} = 5 Hz), 88.83 (d, *J*_{PC} = 5 Hz), 93.04, 106.09 (MeC₆H₄CHMe₂), 125.78 (C⁷), 128.11 (C⁵, C⁶), 140.81 (C⁴). ³¹P{¹H}-NMR (121.5 MHz, CDCl₃): δ 11.3. IR (cm⁻¹, polythene): 294 s, 278 s[v(Ru-Cl)]. FABMS; *m/z*: 486 [*M*⁺]. Anal. found: C, 51.91; H, 6.70; P, 6.17%. C₂₁H₃₁Cl₂PRu requires: C, 51.85; H, 6.42; P, 6.37%.

8.2.17 Preparation of [RuCl₂(η⁶-1,4-MeC₆H₄CHMe₂)(η¹-Ph₂P(CH₂)₃Ph)] (**223**)

Complex **223** was prepared in 96% yield, as an orange solid from **216** and (3-phenylpropyl)diphenylphosphine (**118**) in a similar way.

¹H-NMR (300 MHz, CDCl₃): δ 0.79 (d, 6H, *J* = 8 Hz, MeC₆H₄CHMe₂), 1.34 (m, 2H, H²), 1.90 (s, 3H, MeC₆H₄CHMe₂), 2.42 (t, 2H, *J* = 8 Hz, H¹), 2.53 (m, 1H, MeC₆H₄CHMe₂), 2.64 (m, 2H, H³), 5.09 (d, 2H, *J* = 6 Hz, MeC₆H₄CHMe₂), 5.29 (d, 2H, *J* = 6 Hz, MeC₆H₄CHMe₂), 6.90-7.85 (m, 15H, PPh₂, C₆H₅).
¹³C{¹H}-NMR (75.4 MHz, CDCl₃): δ 17.15 (MeC₆H₄CHMe₂), 21.04 (MeC₆H₄CHMe₂), 22.19 (d, ²*J*_{PC} = 29 Hz, C²), 25.00 (d, ¹*J*_{PC} = 9 Hz, C¹), 29.71 (MeC₆H₄CHMe₂), 36.71 (d, ³*J*_{PC} = 12 Hz, C³), 85.42 (d, *J*_{PC} = 6 Hz), 90.35 (d, *J*_{PC} = 4 Hz), 93.28, 107.56 (MeC₆H₄CHMe₂), 125.52 (C⁷), 128.00 (d, *J*_{PC} = 4 Hz, PPh₂), 128.13 (d, *J*_{PC} = 4 Hz, PPh₂), 130.35 (C⁵, C⁶), 132.31 (d, *J*_{PC} = 42 Hz, PPh₂), 132.95 (d, *J*_{PC} = 9 Hz, PPh₂), 141.41 (C⁴). ³¹P{¹H}-NMR (121.5 MHz, CDCl₃): δ 24.7

(lit.³⁹ δ 23.3⁺). IR (cm⁻¹, polythene): 288 s [v(Ru-Cl)]. EIMS; m/z : 610 [M^+]. Anal. found: C, 61.36; H, 5.89; P, 5.36%. C₃₁H₃₅Cl₂PRu requires: C, 60.98; H, 5.78; P, 5.07%.

8.2.18 Preparation of [RuCl₂(η^6 -1,4-MeC₆H₄CHMe₂)(η^1 -*i*-Pr₂P(CH₂)₃Ph)]
(232)

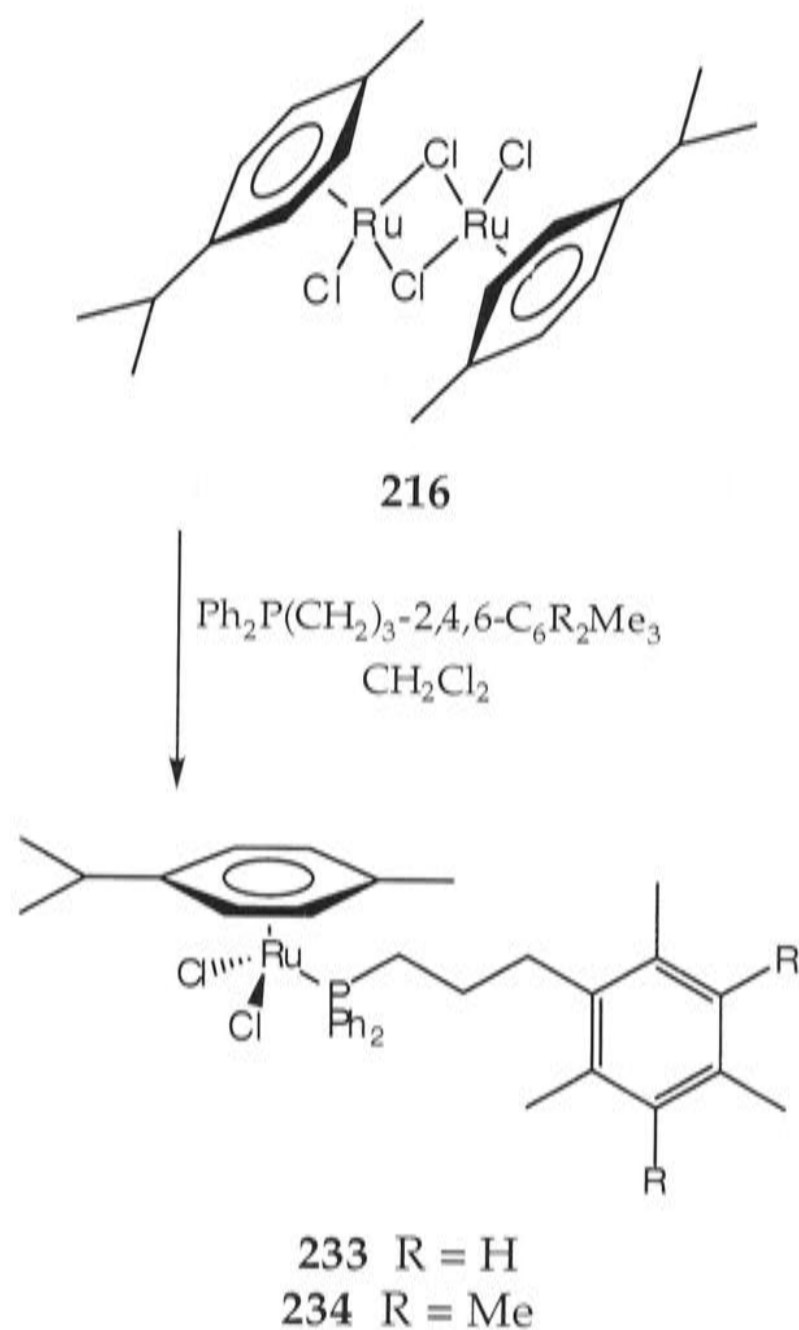
Complex **232** was prepared in 97% yield, as an orange solid from **216** and (3-phenylpropyl)di-*iso*-propylphosphine (**196**) in a similar way. Crystals suitable for X-ray crystallography were obtained from the slow evaporation of a CH₂Cl₂ solution layered with *n*-hexane.

¹H-NMR (400 MHz, CDCl₃): δ 1.24-1.35 (m, 12H, PCHMe₂), 1.28 (d, 6H, $J = 7$ Hz, MeC₆H₄CHMe₂), 1.82 (m, 2H, H²), 2.10 (s, 3H, MeC₆H₄CHMe₂), 2.12-2.18 (m, 2H, PCHMe₂), 2.54-2.64 (m, 3H, H¹, MeC₆H₄CHMe₂), 2.85 (m, 2H, H³), 5.56 (s, 4H, MeC₆H₄CHMe₂), 7.15-7.20 (m, 3H, H⁶, H⁷), 7.25-7.30 (m, 2H, H⁵).

¹³C{¹H}-NMR (100.6 MHz, CDCl₃): δ 18.03 (MeC₆H₄CHMe₂), 19.18 (d, ²J_{PC} = 48 Hz, PCHMe₂), 19.41 (d, ¹J_{PC} = 23 Hz, C¹), 22.28 (MeC₆H₄CHMe₂), 26.78 (C²), 26.97 (d, ¹J_{PC} = 22 Hz, PCHMe₂), 30.61 (MeC₆H₄CHMe₂), 37.82 (d, ³J_{PC} = 11 Hz, C³), 83.42 (d, $J_{PC} = 5$ Hz), 88.66, 93.87, 108.00 (MeC₆H₄CHMe₂), 125.86 (C⁷), 128.32 (C⁵ or C⁶), 128.47 (C⁶ or C⁵), 141.83 (C⁴). ³¹P{¹H}-NMR (161.97 MHz, CDCl₃): δ 32.6. IR (cm⁻¹, polythene): 288 s, [v(Ru-Cl)]. EIMS; m/z : 543 [M^+]. Anal. found: C, 54.78; H, 7.23; P, 5.77%. C₂₅H₃₉Cl₂PRu.0.1CH₂Cl₂ requires: C, 54.71; H, 7.17; P, 5.62%. The presence of dichloromethane was evident in the ¹H NMR spectrum.

⁺Calculated using the conversion factor δ 140.4⁴⁰ for the reference, not cited³⁹ but assumed to be P(OMe)₃, for the value δ -117.08.

Preparation of $[\text{RuCl}_2(\eta^6\text{-1,4-MeC}_6\text{H}_4\text{CHMe}_2)(\eta^1\text{-Ph}_2\text{P}(\text{CH}_2)_3\text{-2,4,6-C}_6\text{H}_2\text{Me}_3)]$
(233)



Complex **233** was prepared from **216** and (3-mesitylpropyl)diphenylphosphine (**199**) in a similar way. The residue was extracted with CH_2Cl_2 , transferred to a column of neutral alumina (activity III), and the product was eluted with dichloromethane followed by THF. The eluate was evaporated to dryness *in vacuo* and the title compound **233** was isolated in 84% yield as an orange solid by addition of *n*-hexane to a solution in CH_2Cl_2 . Crystals suitable for X-ray crystallography were obtained by layering a CH_2Cl_2 solution with *n*-hexane.

$^1\text{H-NMR}$ (400 MHz, CDCl_3): δ 0.786 (d, 6H, $J = 7$ Hz, $\text{MeC}_6\text{H}_4\text{CHMe}_2$), 1.16 (m, 2H, H^2), 1.88 (s, 3H, $\text{MeC}_6\text{H}_4\text{CHMe}_2$), 1.97 (s, $\text{C}^5\text{-Me}$), 2.14 (s, $\text{C}^7\text{-Me}$), 2.41 (m, 2H, H^1), 2.51 (m, 1H, $\text{MeC}_6\text{H}_4\text{CHMe}_2$), 2.68 (m, 2H, H^3), 5.10 (d, 2H, $J = 6$ Hz, $\text{MeC}_6\text{H}_4\text{CHMe}_2$), 5.18 (d, 2H, $J = 6$ Hz, $\text{MeC}_6\text{H}_4\text{CHMe}_2$), 6.68 (s, 1H, H^6),

7.40-7.45 (m, 6H, PPh₂), 7.85-7.90 (m, 4H, PPh₂). ¹³C{¹H}-NMR (100.6 MHz, CDCl₃): δ 17.27 (MeC₆H₄CHMe₂), 19.45 (C⁵-Me), 20.70 (C⁷-Me), 21.24 (MeC₆H₄CHMe₂), 22.40 (d, ²J_{PC} = 9 Hz, C²), 23.00 (d, ¹J_{PC} = 28 Hz, C¹), 29.95 (MeC₆H₄CHMe₂), 30.80 (d, ³J_{PC} = 13 Hz, C³), 85.60 (d, J_{PC} = 5.5 Hz), 90.56 (d, J_{PC} = 4 Hz), 93.58, 107.72 (MeC₆H₄CHMe₂), 128.24 (d, J_{PC} = 9 Hz, PPh₂), 128.66 (C⁷), 130.50 (PPh₂), 132.44 (d, J_{PC} = 42 Hz, PPh₂), 133.19 (d, J_{PC} = 8 Hz, PPh₂), 134.93 (C⁵ or C⁶), 135.58 (C⁶ or C⁵), 135.81 (C⁴). ³¹P{¹H}-NMR (161.97 MHz, CDCl₃): δ 24.8. IR (cm⁻¹, polythene): 300 s, 282 s [ν(Ru-Cl)]. EIMS; *m/z*: 653 [*M*⁺]. Anal. found: C, 62.62; H, 6.15; P, 4.94%. C₃₄H₄₂Cl₂PRu. requires: C, 62.57; H, 6.33 P, 4.75%.

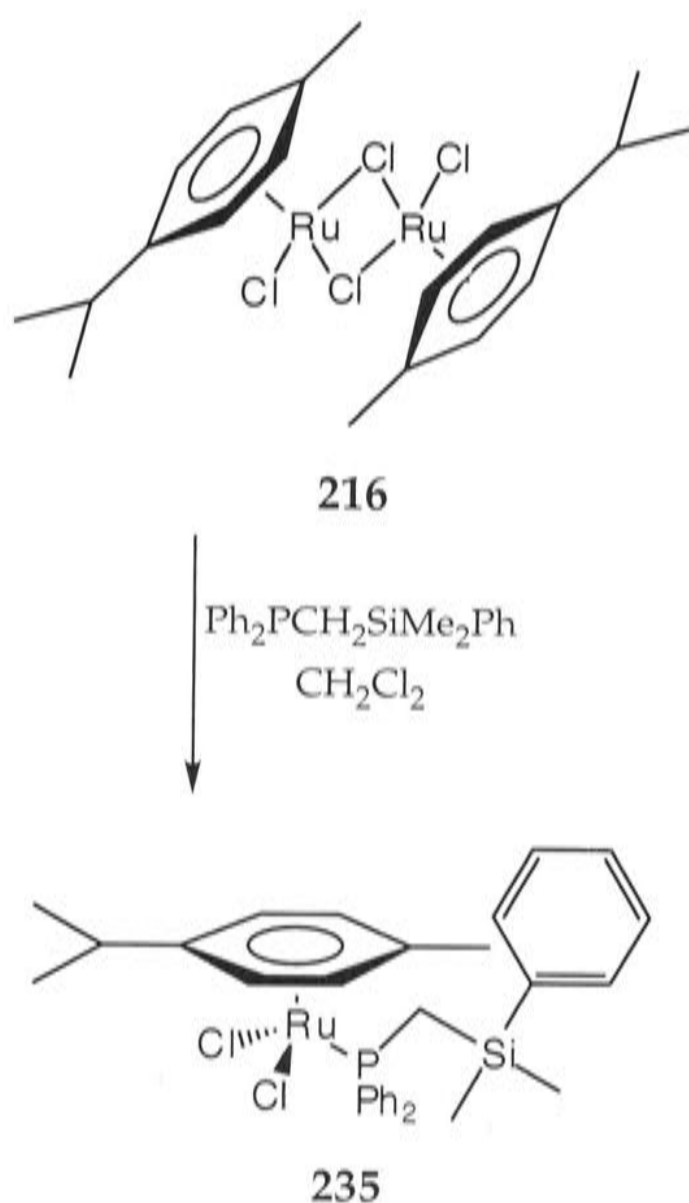
8.2.19 Preparation of [RuCl₂(η⁶-1,4-MeC₆H₄CHMe₂)(η¹-Ph₂P(CH₂)₃C₆Me₅)]
(234)

Complex **234** was prepared from **216** and (3-pentamethylphenylpropyl)diphenylphosphine (**200**) in a similar way. The residue was extracted with CH₂Cl₂, transferred to a column of neutral alumina (activity III), and the product was eluted with dichloromethane followed by THF. The eluate was evaporated to dryness *in vacuo* and the title compound **234** was isolated in 85% yield as an orange solid by addition of *n*-hexane to a solution in CH₂Cl₂. Crystals suitable for X-ray crystallography were obtained by the slow evaporation of a CH₂Cl₂ solution layered with *n*-hexane.

¹H-NMR (400 MHz, CDCl₃): δ 0.794 (d, 6H, *J* = 7 Hz, MeC₆H₄CHMe₂), 1.20 (m, 2H, H²), 1.88 (s, 3H, MeC₆H₄CHMe₂), 1.94 (s, C⁵-Me), 2.10 (s, C⁶-Me), 2.14 (s, C⁷-Me), 2.46-2.57 (m, 3H, H¹, MeC₆H₄CHMe₂), 2.70 (q, 2H, *J* = 16.5 Hz, H³), 5.11 (d, 2H, *J* = 6 Hz, MeC₆H₄CHMe₂), 5.29 (dd, 2H, ¹*J* = 6 Hz, ²*J* = 1.2 Hz, MeC₆H₄CHMe₂), 7.40-7.50 (m, 6H, PPh₂), 7.85-7.90 (m, 4H, PPh₂). ¹³C{¹H}-NMR (100.6 MHz, CDCl₃): δ 16.11 (C⁵-Me), 16.67 (C⁶-Me), 16.77 (C⁷-Me), 17.26 (MeC₆H₄CHMe₂), 21.24 (MeC₆H₄CHMe₂), 22.83 (d, ²J_{PC} = 8 Hz, C²), 23.02 (d, ¹J_{PC} = 10 Hz, C¹), 29.94 (MeC₆H₄CHMe₂), 32.09 (d, ³J_{PC} = 12 Hz, C³), 85.59 (d, J_{PC} = 5.5 Hz), 90.54 (d, J_{PC} = 4 Hz), 93.58, 107.72 (MeC₆H₄CHMe₂),

128.20 (d, $J_{PC} = 9$ Hz, PPh_2), 130.46 (PPh_2), 131.56 (C^7), 132.24 (C^5 or C^6), 132.45 (C^6 or C^5), 132.59 (d, $J_{PC} = 13$ Hz, PPh_2), 133.24 (d, $J_{PC} = 8$ Hz, PPh_2), 135.71 (C^4). $^{31}P\{^1H\}$ -NMR (161.97 MHz, $CDCl_3$): δ 24.8. IR (cm^{-1} , polythene): 287 s [$\nu(Ru-Cl)$]. EIMS; m/z : 680 [M^+]. Anal. found: C, 63.61; H, 6.72; P, 4.65%. $C_{36}H_{45}Cl_2PRu$ requires: C, 63.52; H, 6.66; P, 4.55%.

8.2.20 Preparation of $[RuCl_2(\eta^6-1,4-MeC_6H_4CHMe_2)(\eta^1-Ph_2PCH_2SiMe_2Ph)]$
(235)



Complex **235** was prepared from **216** and (phenyldimethylsilyl)methyldiphenylphosphine (**201**) in a similar way. The residue was extracted with CH_2Cl_2 , transferred to a column of neutral alumina (activity III), and the product was eluted with dichloromethane followed by THF. The eluate was evaporated to dryness *in vacuo* and the title compound **235** was isolated in 84% yield as an orange solid by addition of *n*-hexane to a solution in CH_2Cl_2 . Crystals suitable for X-ray

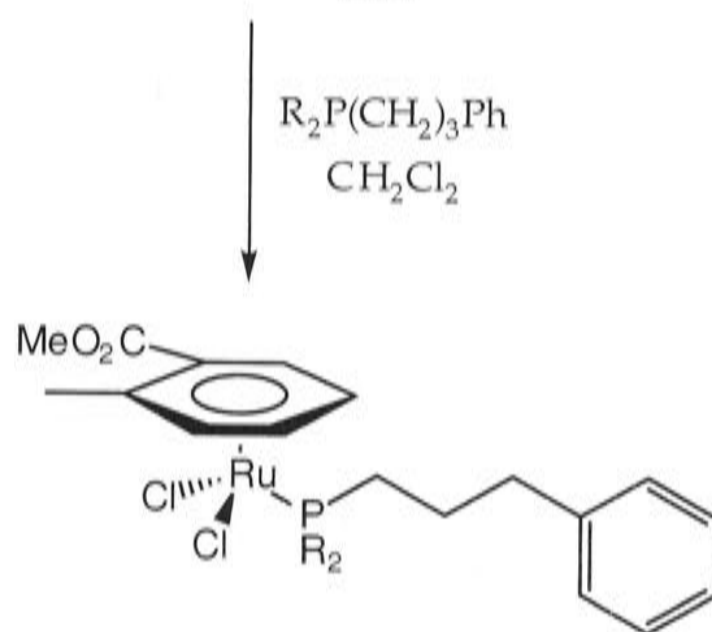
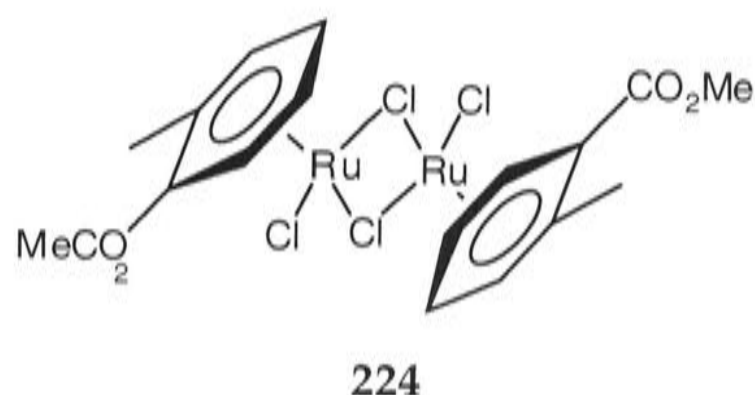
crystallography were obtained from dichloromethane/*n*-hexane by vapour diffusion.

$^1\text{H-NMR}$ (400 MHz, CDCl_3): δ -0.24 (s, 6H, H^2), 0.74 (d, 6H, $J = 7$ Hz, $\text{MeC}_6\text{H}_4\text{CHMe}_2$), 1.79 (s, 3H, $\text{MeC}_6\text{H}_4\text{CHMe}_2$), 2.24 (d, 2H, $J = 7$ Hz, H^1), 2.49 (m, 1H, $\text{MeC}_6\text{H}_4\text{CHMe}_2$), 4.49 (d, 2H, $J = 6$ Hz, $\text{MeC}_6\text{H}_4\text{CHMe}_2$), 5.18 (dd, 2H, $^1J = 6$ Hz, $^2J = 1.5$ Hz, $\text{MeC}_6\text{H}_4\text{CHMe}_2$), 7.10-7.95 (m, 15H, PPh_2 , C_6H_5).

$^{13}\text{C}\{^1\text{H}\}$ -NMR (100.6 MHz, CDCl_3): δ -1.58 (C^2), 9.15 (d, $^1J_{\text{PC}} = 25$ Hz, C^1), 17.19 ($\text{MeC}_6\text{H}_4\text{CHMe}_2$), 21.18 ($\text{MeC}_6\text{H}_4\text{CHMe}_2$), 29.94 ($\text{MeC}_6\text{H}_4\text{CHMe}_2$), 85.15 (d, $J_{\text{PC}} = 25$ Hz), 86.33, 90.75 (d, $J_{\text{PC}} = 25$ Hz), 92.58, 107.79 ($\text{MeC}_6\text{H}_4\text{CHMe}_2$), 127.46 (C^6), 128.08 (d, $J_{\text{PC}} = 10$ Hz, PPh_2), 128.64 (PPh_2), 130.46 (C^4 or C^5), 132.74 (d, $J_{\text{PC}} = 9$ Hz, PPh_2), 133.30 (C^5 or C^4), 134.34 (d, $J_{\text{PC}} = 43$ Hz, PPh_2), 138.67 (C^3).

$^{31}\text{P}\{^1\text{H}\}$ -NMR (161.97 MHz, CDCl_3): δ 22.2. IR (cm^{-1} , polythene): 291 s, 276 s [$\nu(\text{Ru-Cl})$]. EIMS; m/z : 640 [M^+]. Anal. found: C, 53.22; H, 5.34; P, 4.16%. $\text{C}_{31}\text{H}_{35}\text{Cl}_2\text{PRu}\cdot\text{CH}_2\text{Cl}_2$ requires: C, 52.97; H, 5.42; P, 4.27%.

8.2.21 Preparation of $[\text{RuCl}_2(\eta^6\text{-1,2-MeC}_6\text{H}_4\text{CO}_2\text{Me})(\eta^1\text{-Me}_2\text{P}(\text{CH}_2)_3\text{Ph})]$
(236)



- 236** R = Me
237 R = Ph
238 R = *i*-Pr
239 R = Cy

A solution containing the ruthenium complex $[\text{RuCl}_2(\eta^6\text{-1,2-MeC}_6\text{H}_4\text{CO}_2\text{Me})]_2$, (**224**), (46 mg, 0.071 mmol) and (3-phenylpropyl)dimethylphosphine (30 mg, 0.17 mmol) in dry dichloromethane (10 mL) was stirred for 1 h and filtered through Celite, which was washed with dichloromethane (2 × 20 mL). Addition of *n*-hexane (40 mL) to the filtrate and removal of the solvents *in vacuo* gave the title compound **236** as an orange-pink solid (61 mg, 85%).

$^1\text{H-NMR}$ (300 MHz, CDCl_3): δ 1.53 (overlapping d, 6H, sep = 10 Hz, Me_2P), 1.85 (m, 2H, H^2), 2.04 (m, 2H, H^1), 2.49 (s, 3H, MeC_6H_4), 2.70 (m, 2H, H^3), 3.83 (s, 3H, CO_2Me), 4.79 (t, 1H, $J = 5.5$ Hz), 5.38 (d, 1H, $J = 5$ Hz), 5.54 (m, 1H), 6.21 (dd, 1H, $^1J = 5.5$ Hz, $^2J = 3.5$ Hz, $\text{MeC}_6\text{H}_4\text{CO}_2\text{Me}$), 7.15-7.20 (m, 3H, H^6, H^7), 7.25-7.30 (m, 2H, H^5). $^{13}\text{C}\{^1\text{H}\}\text{-NMR}$ (75.4 MHz, CDCl_3): δ 12.33 (d, $^1J_{\text{PC}} = 35$ Hz, MeMeP), 13.25 (d, $^1J_{\text{PC}} = 34$ Hz, MeMeP), 19.84 (MeC_6H_4), 25.61

(d, $^2J_{PC} = 4$ Hz, C²), 30.38 (d, $^1J_{PC} = 30$ Hz, C¹), 36.83 (d, $^3J_{PC} = 13$ Hz, C³), 52.77 (CO₂Me), 76.06, 87.74 (d, $J_{PC} = 8$ Hz), 90.57, 91.37, 102.83, 114.84 (d, $J_{PC} = 5$ Hz, MeC₆H₄CO₂Me), 126.25 (C⁷), 128.54 (C⁵, C⁶), 141.09 (C⁴), 165.78 (C₆H₄CO₂Me). ³¹P{¹H}-NMR (121.5 MHz, CDCl₃): δ 15.7. IR (cm⁻¹, KBr and polythene): 1722 m, 1259 m [ν(C=O)], 279 s [ν(Ru-Cl)]. FABMS; *m/z*: 467 [M-Cl]⁺. Anal. found: C, 47.43; H, 5.62; P, 6.29%. C₂₀H₂₇Cl₂O₂PRu requires: C, 47.81; H, 5.42; P, 6.16%.

8.2.22 Preparation of [RuCl₂(η⁶-1,2-MeC₆H₄CO₂Me)(η¹-Ph₂P(CH₂)₃Ph)] (237)

Complex **237** was prepared in 96% yield, as a brown solid from **224** and (3-phenylpropyl)diphenylphosphine (**118**) in a similar way.

¹H-NMR (300 MHz, CDCl₃): δ 1.46 (m, 2H, H²), 2.41 (m, 2H, H¹), 2.45 (s, 3H, MeC₆H₄), 2.70 (m, 2H, H³), 3.77 (s, 3H, CO₂Me), 4.41 (t, 1H, *J* = 5 Hz), 4.77 (d, 1H, *J* = 6 Hz), 5.38 (q, 1H, *J* = 6 Hz), 6.17 (d, 1H, *J* = 5 Hz, MeC₆H₄CO₂Me), 6.90-7.80 (m, 15H, C₆H₅). ¹³C{¹H}-NMR (75.4 MHz, CDCl₃): δ 19.25 (MeC₆H₄CO₂Me), 23.72 (d, $^2J_{PC} = 30$ Hz, C²), 24.95 (d, $^1J_{PC} = 7$ Hz, C¹), 36.46 (d, $^3J_{PC} = 13$ Hz, C³), 52.54 (CO₂Me), 79.17, 85.44, 89.16, 94.44, 113.56 (d, $J_{PC} = 4$ Hz, MeC₆H₄CO₂Me), 125.45 (C⁷), 127.87, 128.06, 128.21 (C⁵, C⁶, PPh₂), 130.46 (d, $J_{PC} = 15$ Hz, PPh₂), 132.44 (d, $J_{PC} = 9$ Hz, PPh₂), 132.84 (d, $J_{PC} = 9$ Hz, PPh₂), 141.01 (C⁷), 164.69 (CO₂Me). ³¹P{¹H}-NMR (121.5 MHz, CDCl₃): δ 27.8. IR (cm⁻¹, KBr and polythene): 1727 m, 1261 m [ν(C=O)], 290 [ν(Ru-Cl)]. FABMS; *m/z*: 591 [M-Cl]⁺. Anal. found: C, 57.59; H, 5.35; P, 4.79%. C₃₀H₃₁Cl₂O₂PRu requires: C, 57.51; H, 4.99; P, 4.94%

8.2.23 Preparation of [RuCl₂(η⁶-1,2-MeC₆H₄CO₂Me)(η¹-*i*-Pr₂P(CH₂)₃Ph)]

(238)

Complex **238** was prepared in 95% yield, as a brown, gummy, semi-solid from **224** and (3-phenylpropyl)di-*iso*-propylphosphine (**196**) in a similar way.

$^1\text{H-NMR}$ (500 MHz, CDCl_3): δ 1.19-1.28 (m, 12H, PCHMe_2), 2.11 (m, 2H, H^2), 2.49 (s, 3H, MeC_6H_4), 2.57 (m, 2H, H^1), 2.70 (t, 1H, $J = 7$ Hz, H^3), 3.88 (s, 3H, CO_2Me), 5.08 (d, 1H, $J = 4$ Hz), 5.19 (m), 5.80 (m), 6.43 (d, 1H, $J = 5$ Hz, $\text{MeC}_6\text{H}_4\text{CO}_2\text{Me}$), 7.10-7.18 (m, 3H, Ph), 7.20-7.30 (m, 2H, Ph). $^{13}\text{C}\{^1\text{H}\}\text{-NMR}$ (100.6 MHz, CDCl_3): δ 19.48 (d, $^2J_{\text{PC}} = 21$ Hz, PCHMe_2), 19.55 (d, $^2J_{\text{PC}} = 20$ Hz, PCHMe_2), 19.77 ($\text{MeC}_6\text{H}_4\text{CO}_2\text{Me}$), 20.07 (d, $^1J_{\text{PC}} = 25$ Hz, C^1), 26.52 (d, $^2J_{\text{PC}} = 8.5$ Hz, C^2), 27.74 (d, $^1J_{\text{PC}} = 29$ Hz, PCHMe_2), 27.98 (d, $^1J_{\text{PC}} = 25$ Hz, PCHMe_2), 37.65 (d, $^3J_{\text{PC}} = 12$ Hz, C^3), 52.87 (CO_2Me), 75.93, 83.89, 86.60 (d, $J_{\text{PC}} = 10$ Hz), 88.17, 94.03, 114.90 (d, $J_{\text{PC}} = 3.5$ Hz, $\text{MeC}_6\text{H}_4\text{CO}_2\text{Me}$), 125.89 (C^7), 128.32 (C^5 or C^6), 128.51 (C^6 or C^5), 141.59 (C^4), 165.21 (CO_2Me). $^{31}\text{P}\{^1\text{H}\}\text{-NMR}$ (161.97 MHz, CDCl_3): δ 40.1. IR (cm^{-1} , KBr and polythene): 1723 m [$\nu(\text{C}=\text{O})$], 1452 s, 1387 m, 1369 m [$\nu((\text{CH}_3)_2\text{CH})$], 1257 m [$\nu(\text{C}=\text{O})$], 328 s, 291 s [$\nu(\text{Ru-Cl})$]. FABMS; m/z : 523 [M-Cl] $^+$.

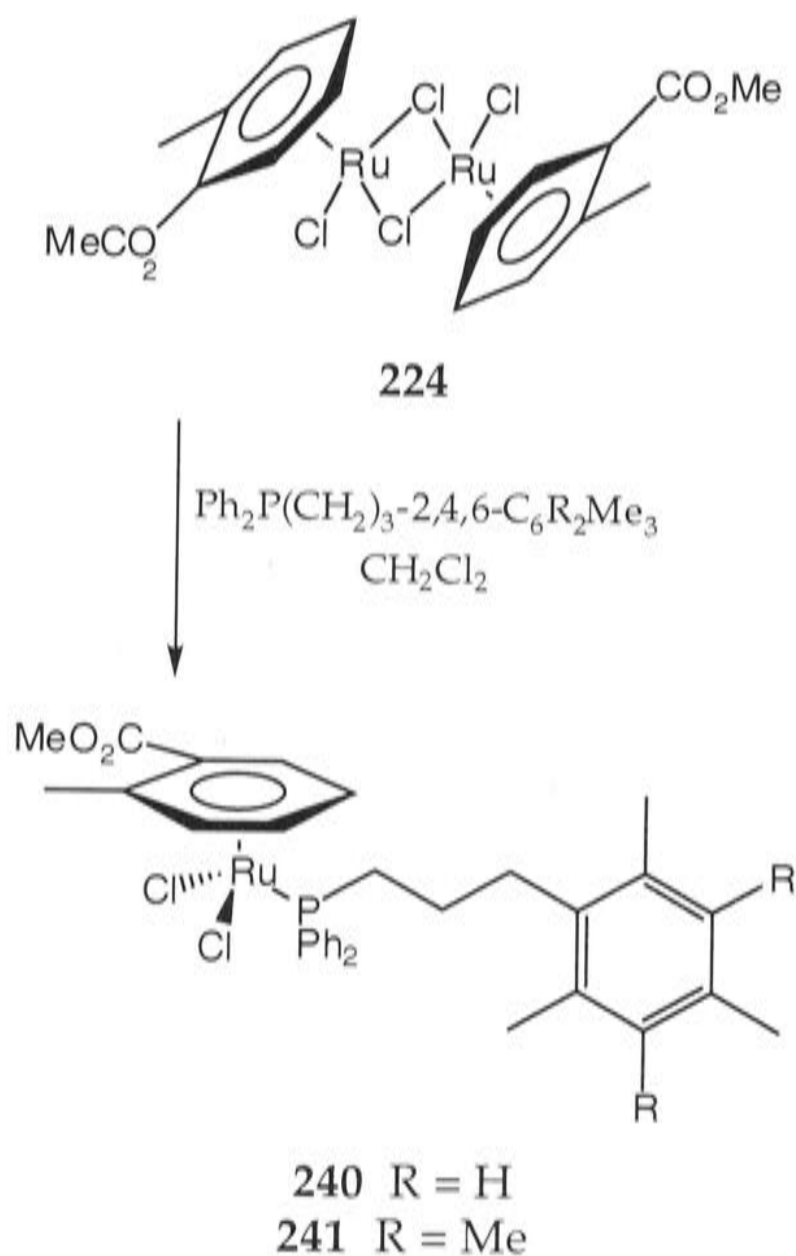
8.2.24 Preparation of $[\text{RuCl}_2(\eta^6\text{-1,2-MeC}_6\text{H}_4\text{CO}_2\text{Me})(\eta^1\text{-Cy}_2\text{P}(\text{CH}_2)_3\text{Ph})]$ (**239**)

Complex **239** was prepared from **224** and (3-phenylpropyl)dicyclohexylphosphine (**197**) in a similar way. The residue was extracted with CH_2Cl_2 , transferred to a column of neutral alumina (activity III), and the product was eluted with dichloromethane followed by THF. The eluate was evaporated to dryness *in vacuo* and the title compound **239** was isolated in 90% yield as an orange-brown solid by addition of *n*-hexane to a solution in CH_2Cl_2 . Crystals suitable for X-ray crystallography were obtained by the slow evaporation of a CH_2Cl_2 solution layered with *n*-hexane.

$^1\text{H-NMR}$ (400 MHz, CDCl_3): δ 1.20-1.30 (m, 6H, Cy), 1.55-1.60 (m, 2H, H^2), 1.70-1.85 (m, 12H, Cy), 2.04 (m, 2H, H^1), 2.10-2.20 (m, 4H, Cy), 2.48 (s, 3H, MeC_6H_4), 2.56 (m, 2H, H^3), 3.89 (s, 3H, CO_2Me), 5.00 (d, 1H, $J = 5.5$ Hz), 5.13 (t, 1H, $J = 5.5$ Hz), 5.81 (q, 1H, $J = 9$ Hz), 6.44 (d, 1H, $J = 5.5$ Hz, $\text{MeC}_6\text{H}_4\text{CO}_2\text{Me}$), 7.10-7.15 (m, 3H, Ph), 7.20-7.25 (m, 2H, Ph). $^{13}\text{C}\{^1\text{H}\}\text{-NMR}$ (100.6 MHz, CDCl_3): δ 19.74 (d, $^2J_{\text{PC}} = 25$ Hz, C^2), 19.80 (MeC_6H_4), 26.34 (Cy),

26.88 (Cy), 27.41 (d, $J_{PC} = 10$ Hz, Cy), 28.41 (d, $^1J_{PC} = 24$ Hz, C^1), 29.40 (d, $J_{PC} = 10$ Hz, Cy), 37.53 (d, $^3J_{PC} = 12$ Hz, C^3), 37.84 (d, $^1J_{PC} = 40$ Hz, Cy), 38.06 (d, $^1J_{PC} = 40$ Hz, Cy), 52.86 (CO_2Me), 74.89, 82.84, 86.62, 89.79 (d, $J_{PC} = 10$ Hz), 94.32, 114.98 (d, $J_{PC} = 4$ Hz, $MeC_6H_4CO_2Me$), 125.90 (C^7), 128.33 (C^5 or C^6), 128.56 (C^6 or C^5), 141.65 (C^4), 165.25 (CO_2Me). $^{31}P\{^1H\}$ -NMR (161.97 MHz, $CDCl_3$): δ 32.8. IR (cm^{-1} , KBr and polythene): 1724 m, 1262 m [$\nu(C=O)$], 292 s, 273 s [$\nu(Ru-Cl)$]. EIMS; m/z : 603 $[M-Cl]^+$. Anal. found: C, 56.83; H, 6.80; P, 4.51%. $C_{30}H_{43}Cl_2O_2PRu$ requires: C, 56.42; H, 6.79; P, 4.85%.

8.2.25 Preparation of $[RuCl_2(\eta^6-1,2-MeC_6H_4CO_2Me)(\eta^1-Ph_2P(CH_2)_3-2,4,6-C_6R_2Me_3)]$ (**240**)



Complex **240** was prepared in 95% yield, as a red solid from **224** and (3-mesitylpropyl)diphenylphosphine (**199**) in a similar way.

$^1\text{H-NMR}$ (300 MHz, CDCl_3): δ 2.00 (s, 6H, $\text{C}^5\text{-Me}$), 2.15 (s, 3H, $\text{H}^7\text{-Me}$), 2.22 (m, 2H, H^2), 2.41-2.46, (m 2H, H^1), 2.45 (s, 3H, MeC_6H_4), 2.74 (m, 2H, H^3), 3.75 (s, 3H, CO_2Me), 4.44 (t, 1H, $J = 5$ Hz), 4.82 (d, 1H, $J = 6$ Hz), 5.42 (q, 1H, $J = 5$ Hz), 6.14 (d, 1H, $J = 6$ Hz, $\text{MeC}_6\text{H}_4\text{CO}_2\text{Me}$), 6.69 (s, 2H, H^6), 7.40-7.45 (m, 6H, PPh_2), 7.75-7.85 (m, 4H, PPh_2). $^{13}\text{C}\{^1\text{H}\}\text{-NMR}$ (121.5 MHz, CD_2Cl_2): δ 19.52 ($\text{C}^5\text{-Me}$, MeC_6H_4), 20.66 ($\text{C}^7\text{-Me}$), 22.67 (d, $^2J_{\text{PC}} = 9$ Hz, C^2), 24.33 (d, $^1J_{\text{PC}} = 30$ Hz, C^1), 30.62 (d, $^3J_{\text{PC}} = 13$ Hz, C^3), 52.82 (CO_2Me), 79.40, 85.75 (d, $J_{\text{PC}} = 9$ Hz), 86.02 (d, $J_{\text{PC}} = 4$ Hz), 89.61, 94.44, 113.78 ($\text{MeC}_6\text{H}_4\text{CO}_2\text{Me}$), 128.35 (d, $J_{\text{PC}} = 10$ Hz, PPh_2), 128.66 (C^7), 130.59 (C^5 or C^6), 130.77 (C^6 or C^5), 132.85 (d, $J_{\text{PC}} = 8$ Hz, PPh_2), 133.19 (d, $J_{\text{PC}} = 8$ Hz, PPh_2), 135.16 (d, $J_{\text{PC}} = 43$ Hz, PPh_2), 135.91 (C^4), 165.04 (CO_2Me). $^{31}\text{P}\{^1\text{H}\}\text{-NMR}$ (161.97 MHz, CDCl_3): δ 27.9. IR (cm^{-1} , KBr and polythene): 1727 m, 1259 m [$\nu(\text{C}=\text{O})$], 291 s [$\nu(\text{Ru-Cl})$]. FABMS; m/z : 633 [M-Cl] $^+$. Anal. found: C, 59.47; H, 5.97; P, 4.44%. $\text{C}_{33}\text{H}_{37}\text{Cl}_2\text{O}_2\text{PRu}$ requires: C, 59.28; H, 5.58; P, 4.63%.

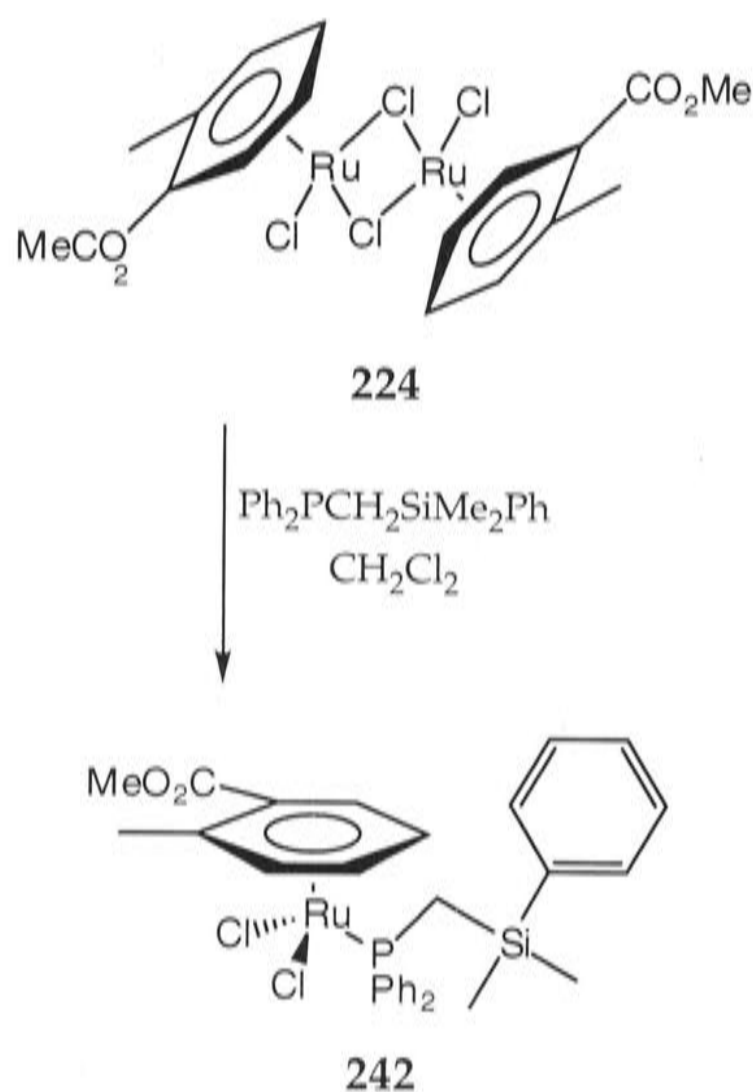
8.2.26 Preparation of $[\text{RuCl}_2(\eta^6\text{-1,2-MeC}_6\text{H}_4\text{CO}_2\text{Me})(\eta^1\text{-Ph}_2\text{P}(\text{CH}_2)_3\text{C}_6\text{Me}_5)]$
(241)

Complex **241** was prepared in 98% yield, as an orange solid from **224** and (3-pentamethylphenylpropyl)diphenylphosphine (**200**) in a similar way.

$^1\text{H-NMR}$ (300MHz, CDCl_3): δ 1.95 (s, 6H, $\text{C}^5\text{-Me}$), 2.09 (s, 6H, $\text{C}^6\text{-Me}$), 2.13 (s, 3H, $\text{C}^7\text{-Me}$), 2.21 (m, 2H, H^2), 2.44 (s, 3H, MeC_6H_4), 2.52 (m, 2H, H^1), 2.76 (m, 2H, H^3), 3.75 (s, 3H, CO_2Me), 4.44 (t, 1H, $J = 5.5$ Hz), 4.83 (d, 1H, $J = 5$ Hz), 5.42 (q, 1H, $J = 5$ Hz), 6.14 (d, 1H, $J = 6$ Hz, $\text{MeC}_6\text{H}_4\text{CO}_2\text{Me}$), 7.40-7.45 (m, 6H, PPh_2), 7.75-7.85 (m, 4H, PPh_2). $^{13}\text{C}\{^1\text{H}\}\text{-NMR}$ (75.4 MHz, CDCl_3): δ 16.23 ($\text{C}^5\text{-Me}$), 16.71 ($\text{C}^6\text{-Me}$), 16.81 ($\text{C}^7\text{-Me}$), 19.63 (MeC_6H_4), 23.19 (d, $^2J_{\text{PC}} = 9$ Hz, C^2), 24.13 (d, $^1J_{\text{PC}} = 30$ Hz, C^1), 31.95 (d, $^3J_{\text{PC}} = 13$ Hz, C^3), 52.89 (CO_2Me), 79.41, 85.64 (d, $J_{\text{PC}} = 9$ Hz), 86.01 (d, $J_{\text{PC}} = 4$ Hz), 89.64, 94.45, 113.85 (d, $J_{\text{PC}} = 4$ Hz, $\text{MeC}_6\text{H}_4\text{CO}_2\text{Me}$), 128.34 (d, $J_{\text{PC}} = 10$ Hz, PPh_2), 130.69 (dd, $J_{\text{PC}} = 14$ Hz, PPh_2), 131.64 (C^7), 132.40 (C^5 or C^6), 132.62 (C^6 or C^5), 132.87 (d, $J_{\text{PC}} = 8$ Hz, PPh_2), 133.28 (d, $J_{\text{PC}} = 9$ Hz, PPh_2), 135.50 (C^4), 165.09 (CO_2Me). $^{31}\text{P}\{^1\text{H}\}\text{-NMR}$ (80.96 MHz, CDCl_3): δ 27.9. IR (cm^{-1} , KBr and polythene): [$\nu(\text{C}=\text{O})$] 1721 m, 1262

m [$\nu(\text{C}=\text{O})$], 289 s [$\nu(\text{Ru}-\text{Cl})$]. FABMS; m/z : 661 [$M-\text{Cl}$] $^+$. Anal. found: C, 59.24; H, 6.00; P, 4.12%. $\text{C}_{35}\text{H}_{41}\text{Cl}_2\text{O}_2\text{PRu}\cdot 0.2\text{CH}_2\text{Cl}_2$ requires: C, 59.24; H, 5.85; P, 4.34%. The presence of CH_2Cl_2 was evident in the ^1H NMR spectrum.

8.2.27 Preparation of $[\text{RuCl}_2(\eta^6\text{-1,2-MeC}_6\text{H}_4\text{CO}_2\text{Me})(\eta^1\text{-Ph}_2\text{PCH}_2\text{SiMe}_2\text{Ph})]$
(242)



Complex **242** was prepared in 96% yield, as an orange solid from **224** and (phenyldimethylsilyl)methyldiphenylphosphine (**201**) in a similar way.

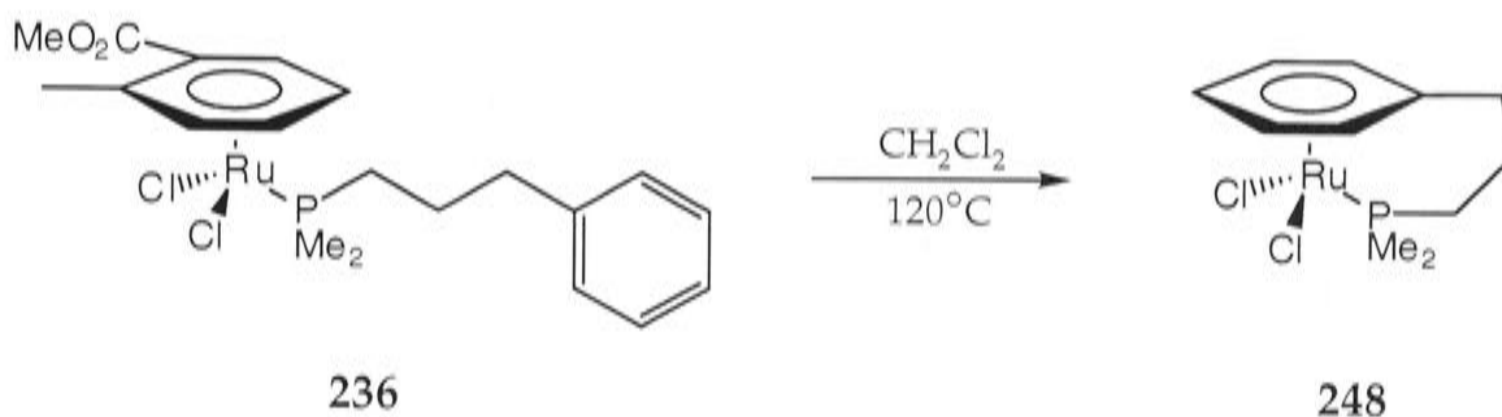
^1H -NMR (300 MHz, CDCl_3): δ -0.19 (s, 6H, H^2), 2.33 (d, 2H, $J = 8$ Hz, H^1), 2.41 (s, 3H, MeC_6H_4), 3.75 (s, 3H, CO_2Me), 4.23 (t, 1H, $J = 5$ Hz), 4.69 (d, 1H, $J = 5$ Hz), 5.31 (q, 1H, $J = 5$ Hz), 6.13 (d, 1H, $J = 5$ Hz, $\text{C}_6\text{H}_4\text{CO}_2\text{Me}$), 7.10-7.85 (m, 15H, PPh_2). $^{13}\text{C}\{^1\text{H}\}$ -NMR (75.4 MHz, CDCl_3): δ -1.35 (d, $^4J_{\text{PC}} = 6$ Hz, C^2), 11.30 (d, $^1J_{\text{PC}} = 25$ Hz, C^1), 19.59 (MeC_6H_4), 52.73 ($\text{CH}_3\text{C}_6\text{H}_4\text{CO}_2\text{CH}_3$), 79.31, 85.08 (d, $J_{\text{PC}} = 4$ Hz), 89.75, 94.67, 113.74 (d, $J_{\text{PC}} = 4$ Hz, $\text{MeC}_6\text{H}_4\text{CO}_2\text{Me}$), 127.43 (C^6), 128.12 (d, $J_{\text{PC}} = 10$ Hz, PPh_2), 128.63 (C^4 or C^5), 130.61 (d, $J_{\text{PC}} = 11$ Hz, PPh_2), 132.35 (d, $J_{\text{PC}} = 9$ Hz, PPh_2), 132.77 (d, $J_{\text{PC}} = 9$ Hz, PPh_2), 133.13 (C^5 or

C⁴), 138.64 (d, $J_{PC} = 3$ Hz, C³), 165.06 (CO₂Me). ³¹P{¹H}-NMR (121.5 MHz, CDCl₃): δ 26.3. IR (cm⁻¹, KBr and polythene): 1722, 1258 [ν (C=O)], 288 [ν (Ru-Cl)]. FABMS; m/z : 506 [M -arene]⁺. Anal. found: C, 54.54; H, 5.04; P, 4.52%. C₃₀H₃₃Cl₂O₂PRuSi requires: C, 54.88; H, 5.07; P, 4.72%.

8.2.28 Attempted preparation of [RuCl₂(η^6 -arene)(η^1 -*t*-Bu₂P(CH₂)₃Ph)] (arene = C₆H₆ (**243**), 1,4-MeC₆H₄CHMe₂ (**244**), 1,2-MeC₆H₄CO₂Me (**245**))

Preparation of the complexes **243-245** was attempted by reacting the dimers [RuCl₂(η^6 -C₆H₆)]₂ (**161**), [RuCl₂(η^6 -1,4-MeC₆H₄CHMe₂)]₂ (**216**) and [RuCl₂(η^6 -1,2-MeC₆H₄CO₂Me)]₂ (**224**), respectively, with (3-phenylpropyl)di-*tert*-butylphosphine (**198**) in a similar way to those methods described above. Compounds **243** (δ_p 54.4), **244** (δ_p 48.1) and **245** (δ_p 55.5) were obtained as brown, gummy, semi-solids that could not be separated from unidentifiable impurities.

8.2.29 Preparation of [RuCl₂(η^1 : η^6 -Me₂P(CH₂)₃Ph)] (**248**) (a)



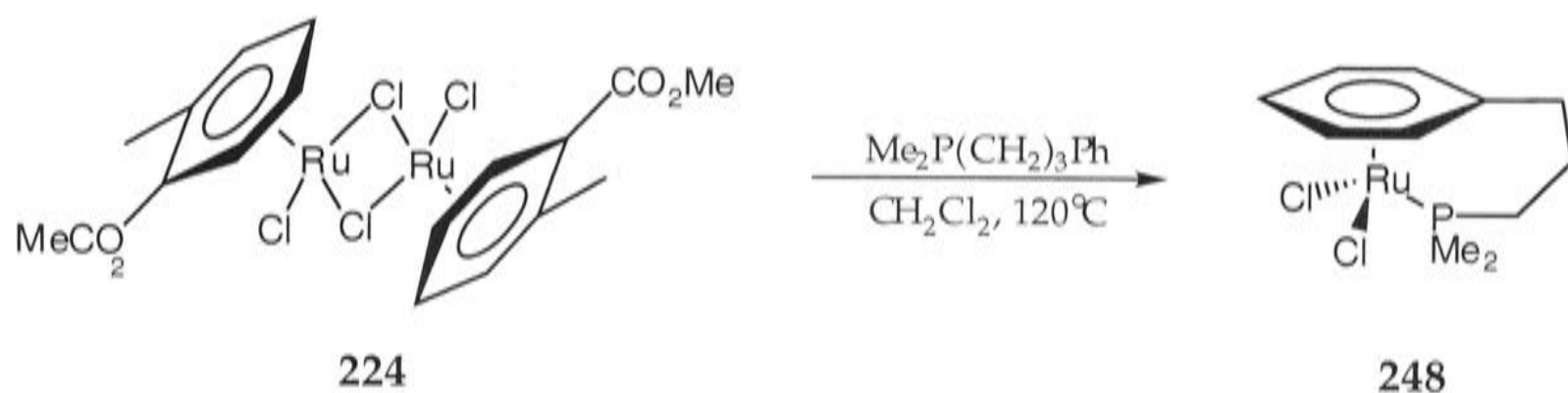
A solution of the ruthenium complex [RuCl₂(η^6 -1,2-MeC₆H₄CO₂Me)(η^1 -Me₂P(CH₂)₃Ph)], (**236**), (99 mg, 0.20 mmol) in dry dichloromethane (2.5 mL) in a 10 mL pressure Schlenk tube fitted with a Rotaflo tap was subjected to three freeze-pump-thaw cycles, and then heated at 120°C for 48 h. The solution was cooled to 0°C and the solvent was removed *in vacuo*. The residue was extracted with dichloromethane, transferred to a

column of neutral alumina (activity III), and the product was eluted with dichloromethane followed by THF. The eluate was evaporated to dryness *in vacuo* and the title compound **248** was isolated as an orange solid (42 mg, 61%) by addition of *n*-hexane to a solution in dichloromethane. Red crystals suitable for X-ray crystallography were obtained from dichloromethane/ether by vapour diffusion.

$^1\text{H-NMR}$ (300 MHz, CDCl_3): δ 1.54 (d, 6H, $^2J_{\text{PH}} = 12$ Hz, PMe_2), 1.79 (m, 2H, H^2), 2.26 (m, 2H, H^3), 2.54 (m, 2H, H^1), 4.96 (d, 2H, $J = 5$ Hz, H^5), 5.62 (t, 2H, $J = 6$ Hz, H^6), 6.33 (t, 1H, $J = 6$ Hz, H^7). $^{13}\text{C}\{^1\text{H}\}\text{-NMR}$ (75.4 MHz, CDCl_3): δ 13.22 (d, $^1J_{\text{PC}} = 36$ Hz, PMe_2), 21.20 (C^2), 24.72 (d, $^1J_{\text{PC}} = 30$ Hz, C^1), 30.08 (C^3), 80.27 (C^5), 89.92 (C^4), 92.35 (d, $J_{\text{PC}} = 4$ Hz, C^6), 98.39 (d, $J_{\text{PC}} = 12$ Hz, C^7). $^{31}\text{P}\{^1\text{H}\}\text{-NMR}$ (121.5 MHz, CDCl_3): δ 13.7. IR (cm^{-1} , polythene): 297 s, 278 s [$\nu(\text{Ru-Cl})$]. FABMS; m/z : 352 [M^+]. Anal. found: C, 37.25; H, 4.92; P, 8.50%. $\text{C}_{11}\text{H}_{17}\text{Cl}_2\text{PRu}$ requires: C, 37.51; H, 4.87; P, 8.79%.

A similar experiment employing CH_2Cl_2 (2.5 mL) containing a drop of THF heated at 120°C for 36 h gave the complex **248** in 71% yield.

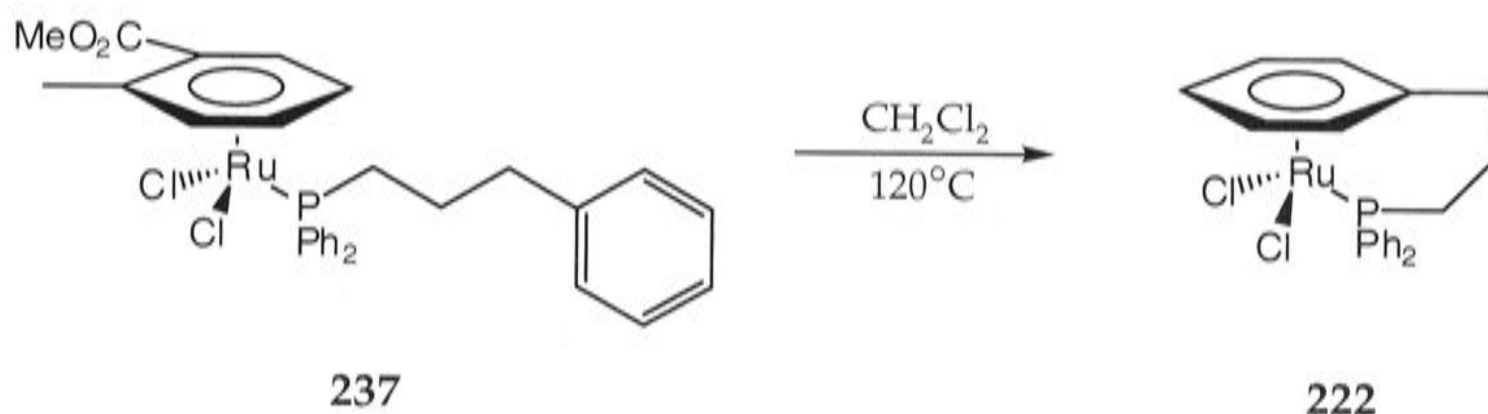
8.2.30 Preparation of $[\text{RuCl}_2(\eta^1:\eta^6\text{-Me}_2\text{P}(\text{CH}_2)_3\text{Ph})]$ (**248**) (b)



A solution of the ruthenium complex $[\text{RuCl}_2(\eta^6\text{-1,2-MeC}_6\text{H}_4\text{CO}_2\text{Me})]_2$, (**224**), (200 mg, 0.31 mmol) in dry dichloromethane (10 mL) was treated with (3-phenylpropyl)dimethylphosphine, (**195**), (119 mg, 0.66 mmol) and stirred for 1 h at room temperature. The mixture was then heated at 120°C for 48 h in a 35 mL pressure Schlenk tube and worked up as described above. The yield of the title compound **248** was 157 mg (72%).

The reaction time could be reduced to 36 h by the addition of a few drops of THF to the dichloromethane solution.

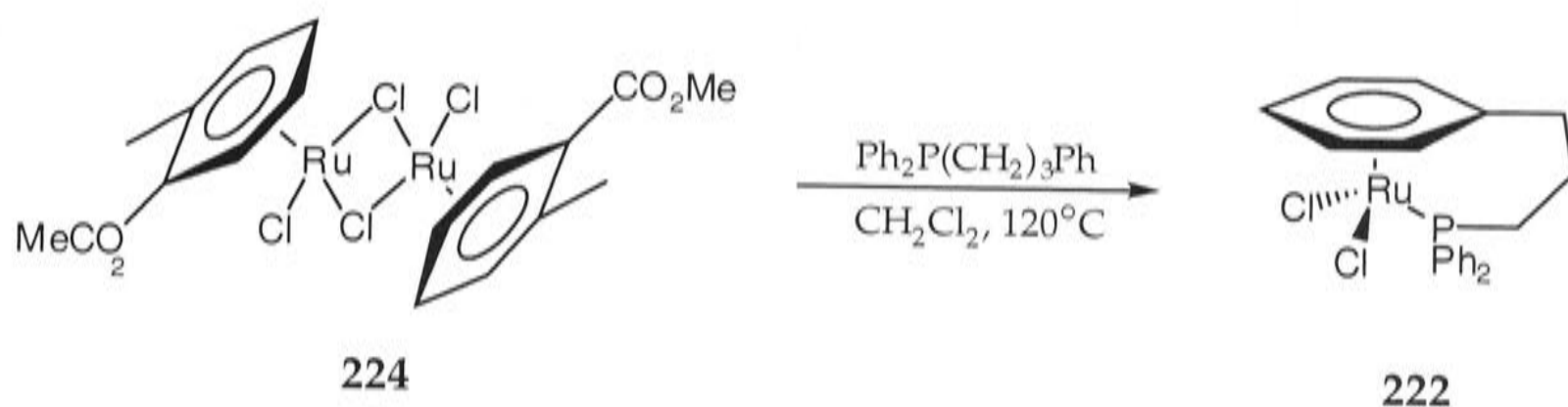
8.2.31 Preparation of $[\text{RuCl}_2(\eta^1:\eta^6\text{-Ph}_2\text{P}(\text{CH}_2)_3\text{Ph})]$ (**222**) (a)



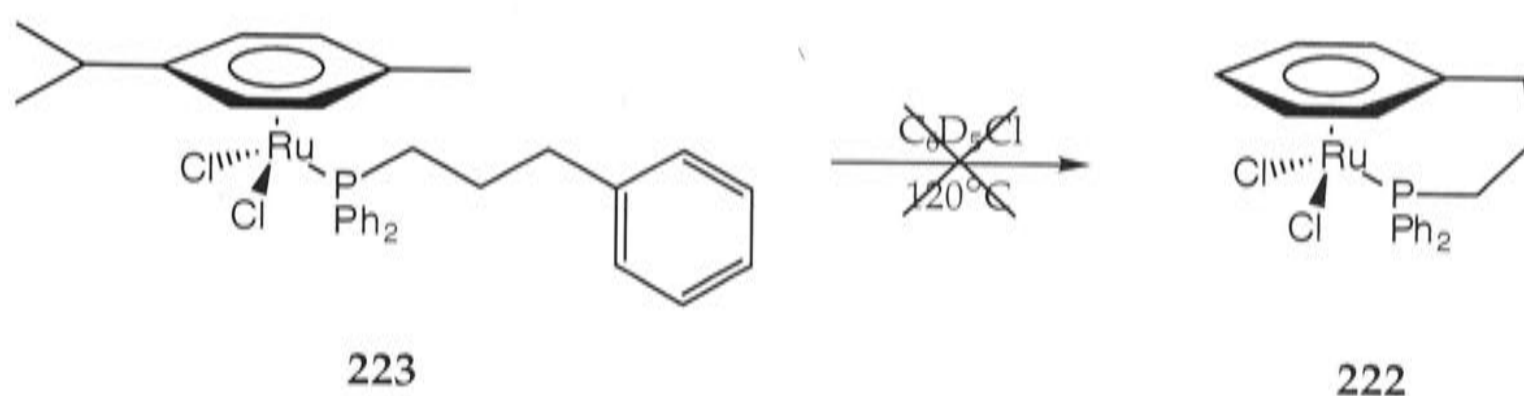
Complex **222** was obtained by heating complex $[\text{RuCl}_2(\eta^6\text{-1,2-MeC}_6\text{H}_4\text{CO}_2\text{Me})(\eta^1\text{-Ph}_2\text{P}(\text{CH}_2)_3\text{Ph})]$, (**237**), (840 mg, 1.34 mmol) in dry dichloromethane (20 mL) at 120°C for 72 h. The reaction was worked up as described above for complex **248**. The yield of orange solid was 420 mg (66%). Yields of 70-80% could be achieved using dichloromethane containing a few drops of THF and heating for 48 h.

$^1\text{H-NMR}$ (300 MHz, CDCl_3): δ 2.15 (m, 2H, H^2), 2.56 (m, 4H, H^1 , H^3), 5.13 (d, 2H, $J = 6$ Hz, H^5), 5.77 (t, 2H, $J = 6$ Hz, H^6), 6.36 (t, 1H, $J = 6$ Hz, H^7), 7.35-7.45 (m, 6H, PPh_2) 7.50-7.60 (m, 4H, PPh_2). $^{13}\text{C}\{^1\text{H}\}\text{-NMR}$ (75.4 MHz, CDCl_3): δ 20.45 (C^2), 22.91 (d, $J_{\text{PC}} = 31$ Hz, C^1), 30.80 (C^3), 84.68 (C^5), 89.15 (C^4), 90.24 (d, $J_{\text{PC}} = 4$ Hz, C^6), 101.14 (d, $J_{\text{PC}} = 10$ Hz, C^7), 128.11 (d, $J_{\text{PC}} = 10$ Hz, PPh_2), 130.62 (d, $J_{\text{PC}} = 3$ Hz, PPh_2), 132.60 (d, $J_{\text{PC}} = 50$ Hz, PPh_2), 134.35 (d, $J_{\text{PC}} = 8$ Hz, PPh_2). $^{31}\text{P}\{^1\text{H}\}\text{-NMR}$ (121.5 MHz, CDCl_3): δ 22.2 (lit.³⁹ δ 23.0[†]; lit.¹⁹ δ 20.1). IR (cm^{-1} , polythene): 303 m, 277 m [$\nu(\text{Ru-Cl})$]. EIMS; m/z : 476 [M^+]. Anal. found: C, 52.88; H, 4.43; P, 6.14%. $\text{C}_{21}\text{H}_{21}\text{Cl}_2\text{PRu}$ requires: C, 52.95; H, 4.44; P, 6.50%.

[†]Calculated using the conversion factor δ 140.4⁴⁰ for the reference, not cited³⁹ but assumed to be $\text{P}(\text{OMe})_3$, for the value δ -117.45.

8.2.32 Preparation of $[\text{RuCl}_2(\eta^1:\eta^6\text{-Ph}_2\text{P}(\text{CH}_2)_3\text{Ph})]$ (**222**) (*b*)

A solution of the ruthenium complex $[\text{RuCl}_2(\eta^6\text{-1,2-MeC}_6\text{H}_4\text{CO}_2\text{Me})]_2$ (**224**), (214 mg, 0.33 mmol) in dry dichloromethane (10 mL) was treated with (3-phenylpropyl)diphenylphosphine, (**118**), (212 mg, 0.70 mmol) and stirred for 1 h at room temperature. The mixture was then heated at 120°C for 72 h in a 35 mL pressure Schlenk tube and worked up as described above for complex **248**. The yield of the title compound **222** was 248 mg (78%). Addition of a few drops of THF to the dichloromethane solution failed to reduce the reaction time.

8.2.33 Attempted preparation of $[\text{RuCl}_2(\eta^1:\eta^6\text{-Ph}_2\text{P}(\text{CH}_2)_3\text{Ph})]$ (**222**) following Smith and Wright³⁹

A solution of the ruthenium complex $[\text{RuCl}_2(\eta^6\text{-1,4-MeC}_6\text{H}_4\text{CHMe}_2)(\eta^1\text{-Ph}_2\text{P}(\text{CH}_2)_3\text{Ph})]$ (**223**) in d_5 -chlorobenzene (0.5 mL) was heated to 120°C for 144 h and the NMR spectra were measured. There was no evidence for the presence of **222**, but **223** had disappeared. The observed resonances can be assigned to free *p*-cymene and a second species whose ^2H and

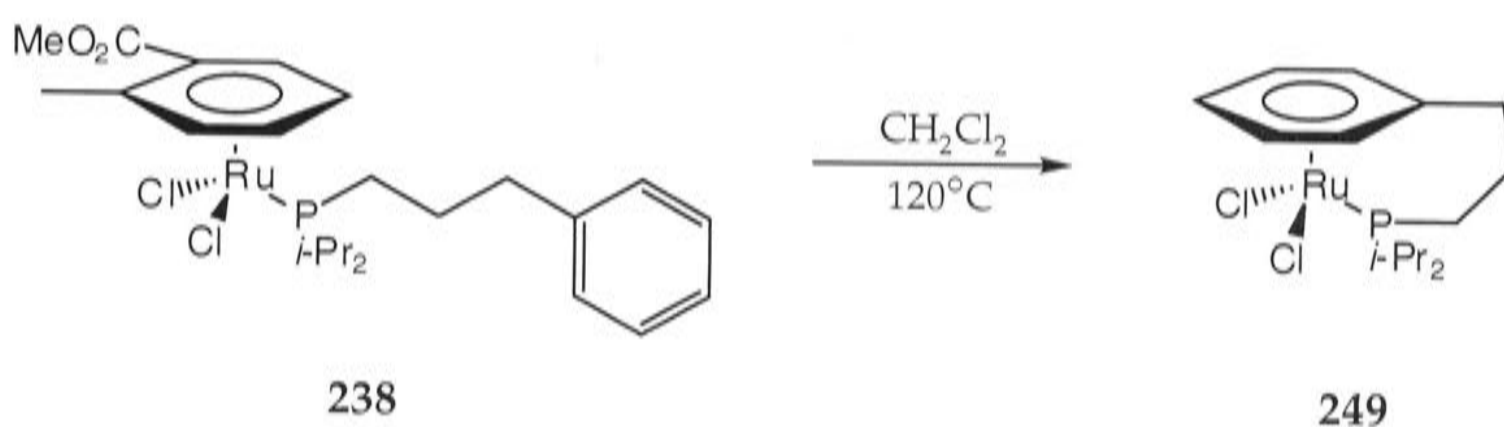
$^{31}\text{P}\{^1\text{H}\}$ -NMR spectra are consistent with a species $[\text{RuCl}_2(\eta^6\text{-C}_6\text{D}_5\text{Cl})(\eta^1\text{-Ph}_2\text{P}(\text{CH}_2)_3\text{Ph})]$ (**255**).

^1H -NMR (300 MHz, $\text{C}_6\text{D}_5\text{Cl}$): δ 1.94 (m, 2H, H^2), 2.09 (m, 2H, H^3), 2.56 (t, 2H, $^1J_{\text{PH}} = 7$ Hz, H^1), 6.95-7.20 (m, 15H, PPh_2 , C_6H_5). ^2H -NMR (300 MHz, $\text{C}_6\text{D}_5\text{Cl}$): δ 4.61 (t, $J = 7$ Hz), 5.33 (d, $J = 6.5$ Hz), 6.46 (t, $J = 7$ Hz).

$^{31}\text{P}\{^1\text{H}\}$ -NMR (121.5 MHz, $\text{C}_6\text{D}_5\text{Cl}$): δ 29.6 (br.) [br. = broad].

The presence of **255** could also be detected in a similar reaction mixture obtained from complex **223** in d_5 -chlorobenzene (0.1 mL) and chlorobenzene (0.4 mL). Attempts to isolate **255** failed.

8.2.34 Preparation of $[\text{RuCl}_2(\eta^1:\eta^6\text{-}i\text{-Pr}_2\text{P}(\text{CH}_2)_3\text{Ph})]$ (**249**) (a)

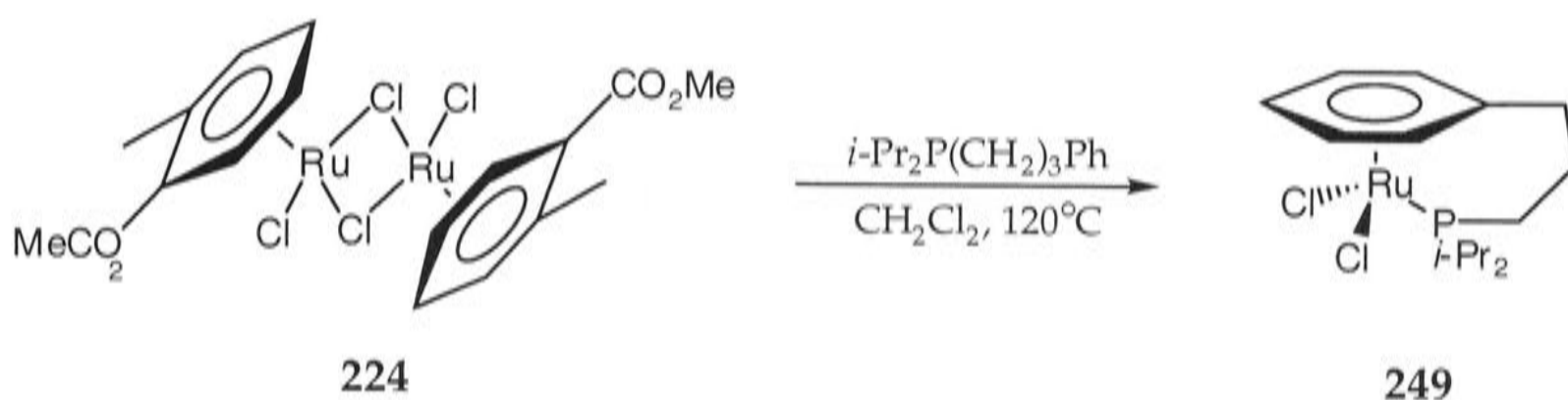


Complex **249** was obtained by heating $[\text{RuCl}_2(\eta^6\text{-1,2-MeC}_6\text{H}_4\text{CO}_2\text{Me})(\eta^1\text{-}i\text{-Pr}_2\text{P}(\text{CH}_2)_3\text{Ph})]$, (**238**), (107 mg, 0.19 mmol) in dry dichloromethane (2 mL) at 120°C for 6 h. The solvent was removed *in vacuo* and the residue was dissolved in dichloromethane (2 mL) and the product was precipitated upon slow addition of *n*-hexane. The solid was collected by filtration and was washed with *n*-hexane to afford the title compound **249** as an orange solid was 71 mg (91%). Crystals suitable for X-ray crystallography were obtained by layering a CH_2Cl_2 solution with *n*-hexane.

^1H -NMR (300 MHz, CDCl_3): δ 1.17 (dd, 6H, $J = 15.5, 7$ Hz, PCHMe_2), 1.22 (dd, 6H, $^1J = 14$ Hz, $^2J = 7$ Hz, PCHMe_2), 1.84 (m, 2H, PCHMe_2), 2.09 (m, 2H, H^2), 2.39 (m, 2H, H^1), 2.71 (m, 2H, H^3), 5.10 (d, 2H, $J = 5.5$ Hz, H^5), 5.69 (t, 2H, $J = 6$ Hz, H^6), 6.28 (t, 1H, $J = 5.5$ Hz, H^7). $^{13}\text{C}\{^1\text{H}\}$ -NMR (125.7 MHz, CDCl_3): δ 15.89 (d, $^2J_{\text{PC}} = 25$ Hz, PCHMe_2), 19.46 (PCHMe_2), 24.26 (d, $^1J_{\text{PC}} = 24$ Hz, C^1),

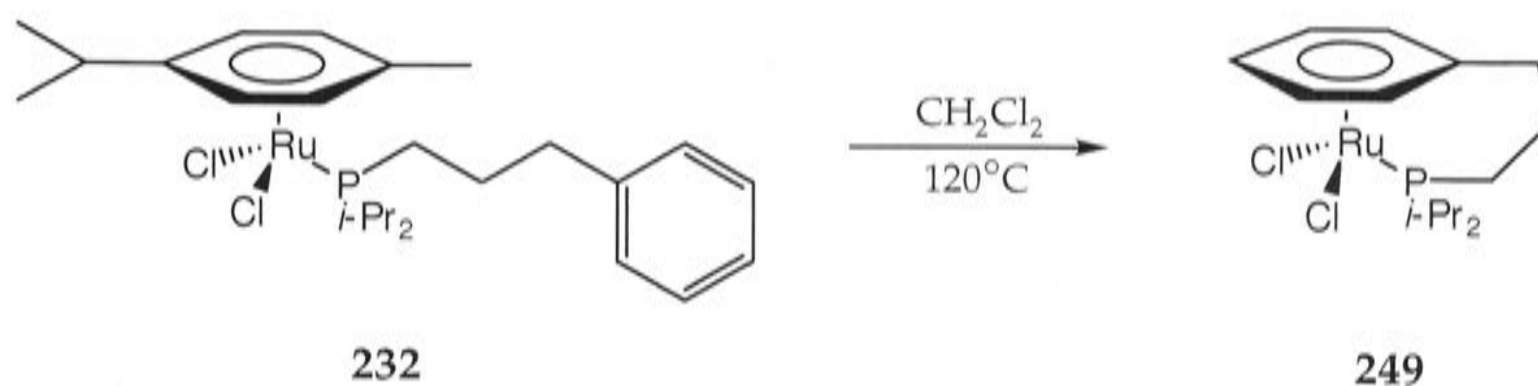
24.90 (C²), 30.04 (C³), 80.00 (C⁵), 93.76 (d, $J_{PC} = 3$ Hz, C⁶), 95.90 (C⁴), 97.11 (d, $J_{PC} = 11$ Hz, C⁷). ³¹P{¹H}-NMR (121.5 MHz, CDCl₃): δ 34.5. IR (cm⁻¹, KBr and polythene): 1450 s, 1384 m, 1363 m [$\nu((\text{CH}_3)_2\text{CH})$], 292 s, 272 s [$\nu(\text{Ru}-\text{Cl})$]. EIMS; m/z : 409 [M^+]. Anal. found: C, 41.43; H, 5.76; P, 7.16%. C₁₅H₂₅Cl₂PRu.0.5CH₂Cl₂ requires: C, 41.30; H, 5.81; P, 7.16%. The presence of dichloromethane was evident in the ¹H NMR spectrum.

8.2.35 Preparation of [RuCl₂(η¹:η⁶-*i*-Pr₂P(CH₂)₃Ph)] (249) (b)



A solution of the ruthenium complex [RuCl₂(η⁶-1,2-MeC₆H₄CO₂Me)]₂, (**224**), (202 mg, 0.32 mmol) in dry dichloromethane (10 mL) was treated with (3-phenylpropyl)di-*iso*-propylphosphine, (**196**), (253 mg, 0.64 mmol) and stirred for 1 h at room temperature. The mixture was then heated at 120°C for 10 h in a 35 mL pressure Schlenk tube and worked up as described above. The yield of the title compound **249** was 247 mg (96%).

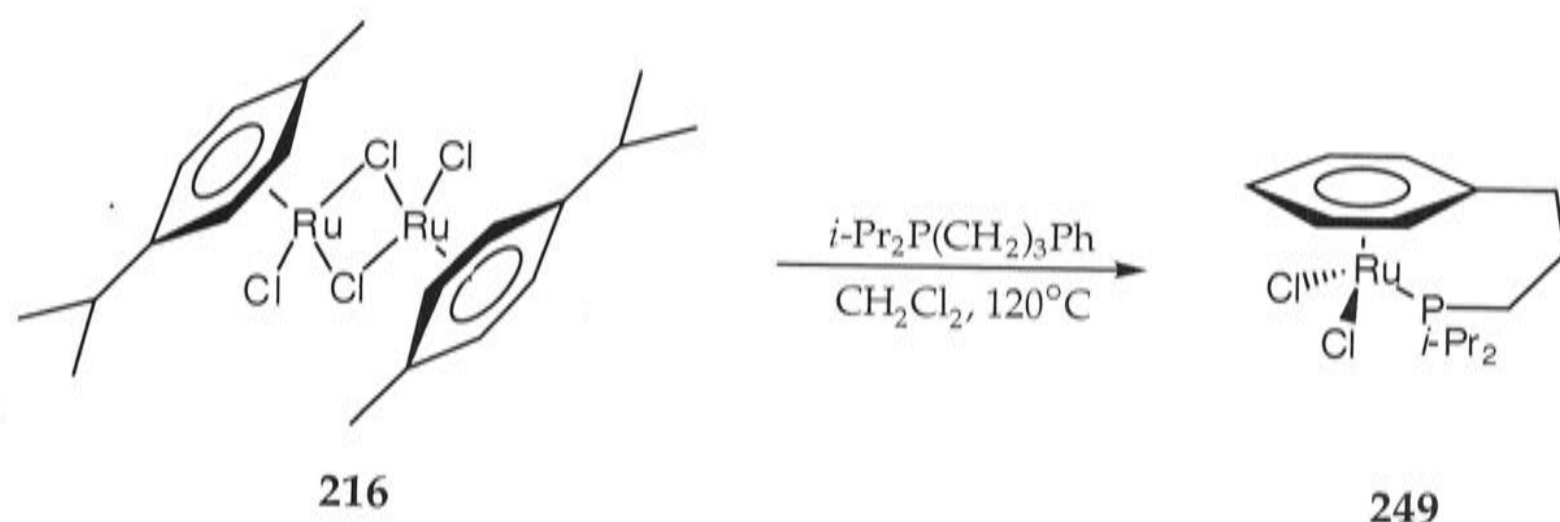
8.2.36 Preparation of [RuCl₂(η¹:η⁶-*i*-Pr₂P(CH₂)₃Ph)] (249) (c)



Complex **249** was obtained by heating [RuCl₂(η⁶-1,4-MeC₆H₄CHMe₂)(η¹-*i*-Pr₂P(CH₂)₃Ph)], (**232**), (100 mg, 0.19 mmol) in dry dichloromethane

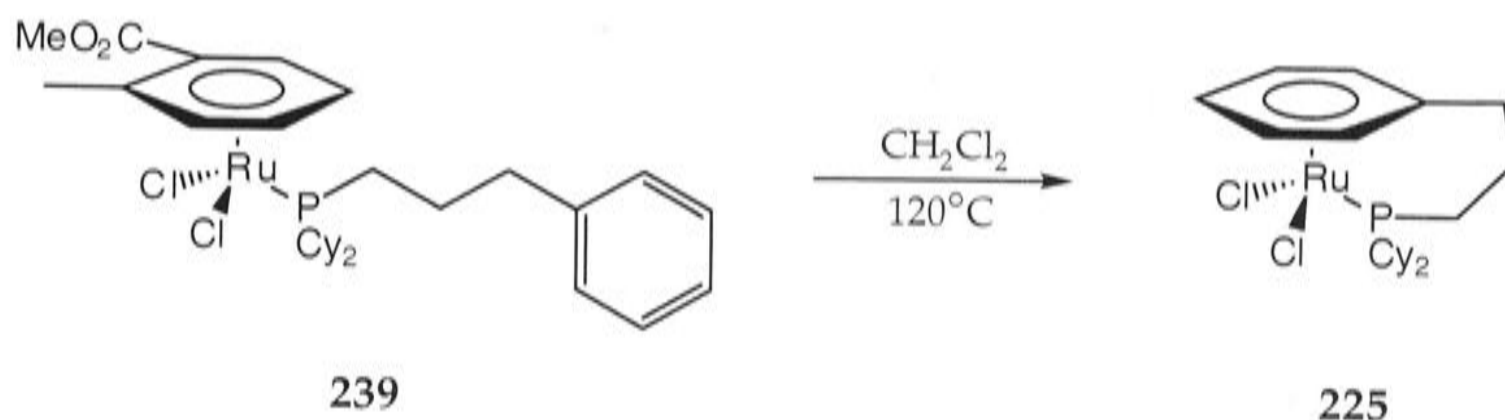
(2 mL) at 120°C for 42 h and worked up as described above. The yield of orange solid was 68 mg (90%).

8.2.37 Preparation of $[\text{RuCl}_2(\eta^1:\eta^6\text{-}i\text{-Pr}_2\text{P}(\text{CH}_2)_3\text{Ph})]$ (**249**) (*d*)



A solution of the ruthenium complex $[\text{RuCl}_2(\eta^6\text{-}1,4\text{-MeC}_6\text{H}_4\text{CHMe}_2)]_2$ (**224**), (191 mg, 0.31 mmol) in dry dichloromethane (10 mL) was treated with (3-phenylpropyl)di-*iso*-propylphosphine, (**196**), (152 mg, 0.64 mmol) and stirred for 1 h at room temperature. The mixture was then heated at 120°C for 48 h in a 35 mL pressure Schlenk tube and worked up as described above. The yield of the title compound **249** was 239 mg (94%).

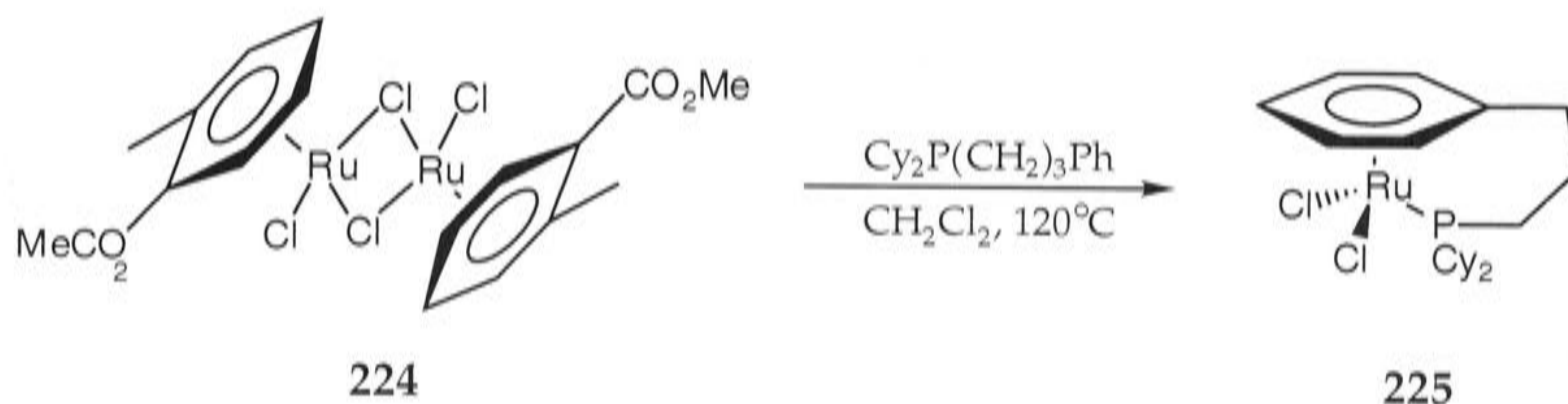
8.2.38 Preparation of $[\text{RuCl}_2(\eta^1:\eta^6\text{-Cy}_2\text{P}(\text{CH}_2)_3\text{Ph})]$ (**225**) (*a*)



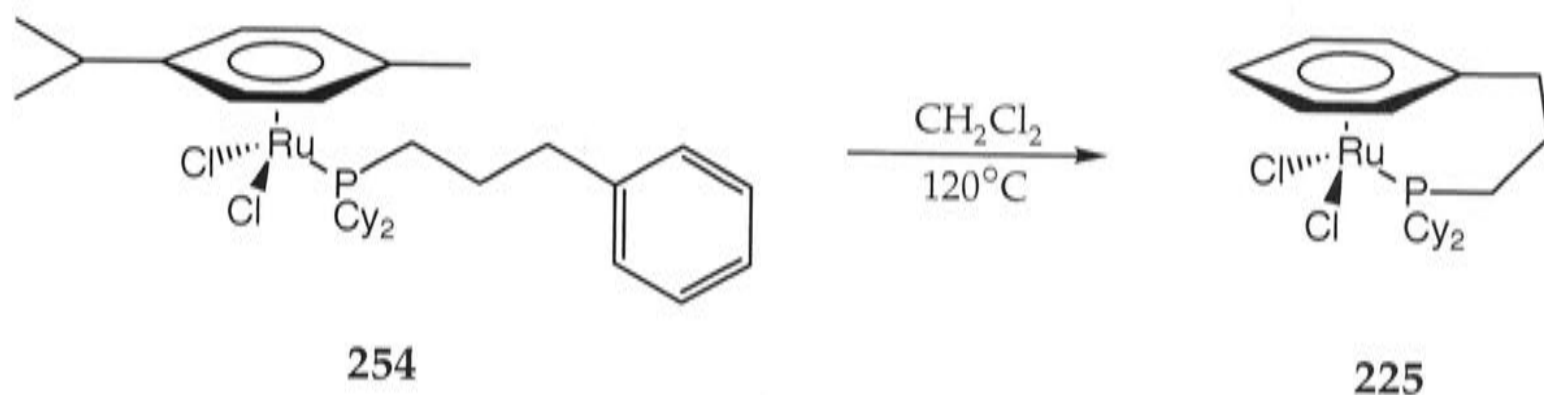
Complex **225** was obtained by heating $[\text{RuCl}_2(\eta^6\text{-}1,2\text{-MeC}_6\text{H}_4\text{CO}_2\text{Me})(\eta^1\text{-Cy}_2\text{P}(\text{CH}_2)_3\text{Ph})]$, (**239**), (212 mg, 0.33 mmol) in dry dichloromethane (2 mL) at 120°C for 16 h and worked up as described above for complex **249**. The yield of orange solid was 144 mg (89%). A similar experiment that was heated at 80°C for 192 h gave 148 mg (90%) of the complex **225**.

$^1\text{H-NMR}$ (300 MHz, CDCl_3): δ 1.10-1.40 (m, 10H, Cy), 1.60-2.05 (m, 14H, H^2 , Cy), 2.36 (t, 2H, $J = 6$ Hz, H^3), 2.49 (m, 2H, H^1), 5.08 (d, 2H, $J = 5$ Hz, H^5), 5.65 (t, 2H, $J = 6$ Hz, H^6), 6.25 (t, 1H, $J = 6$ Hz, H^7). $^{13}\text{C}\{^1\text{H}\}\text{-NMR}$ (100.6 MHz, CDCl_3): δ 15.38 (d, $J_{\text{PC}} = 24$ Hz, Cy), 25.06 (Cy), 26.12 (Cy), 26.82 (d, $^2J_{\text{PC}} = 10$ Hz, C^2), 27.51 (d, $^1J_{\text{PC}} = 11$ Hz, C^1), 27.73 (d, $^3J_{\text{PC}} = 3$ Hz, C^3), 29.09 (Cy), 29.95 (Cy), 33.13 (d, $^1J_{\text{PC}} = 31$ Hz, Cy), 80.15 (C^5), 93.30 (d, $J_{\text{PC}} = 4$ Hz, C^4), 96.00 (C^6), 97.14 (d, $J_{\text{PC}} = 11$ Hz, C^7). $^{31}\text{P}\{^1\text{H}\}\text{-NMR}$ (121.5 MHz, CDCl_3): δ 29.5 (lit.¹⁴ δ 29.3 in CD_2Cl_2). IR (cm^{-1} , polythene): 292 s, 271 s [$\nu(\text{Ru-Cl})$]. EIMS; m/z : 488 (lit.¹⁴ 488) [M^+]. Anal. found: C, 51.53; H, 6.77; P, 6.49%. $\text{C}_{21}\text{H}_{33}\text{Cl}_2\text{PRu}$ requires: C, 51.64; H, 6.81; P, 6.34%.

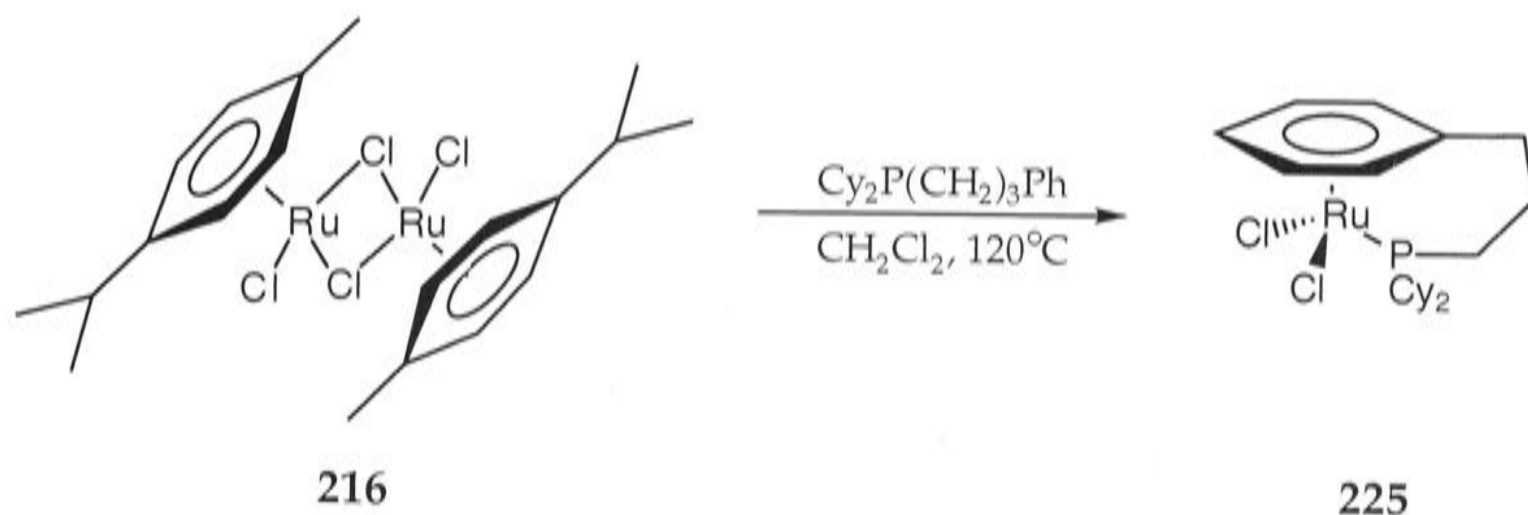
8.2.39 Preparation of $[\text{RuCl}_2(\eta^1:\eta^6\text{-Cy}_2\text{P}(\text{CH}_2)_3\text{Ph})]$ (**225**) (b)



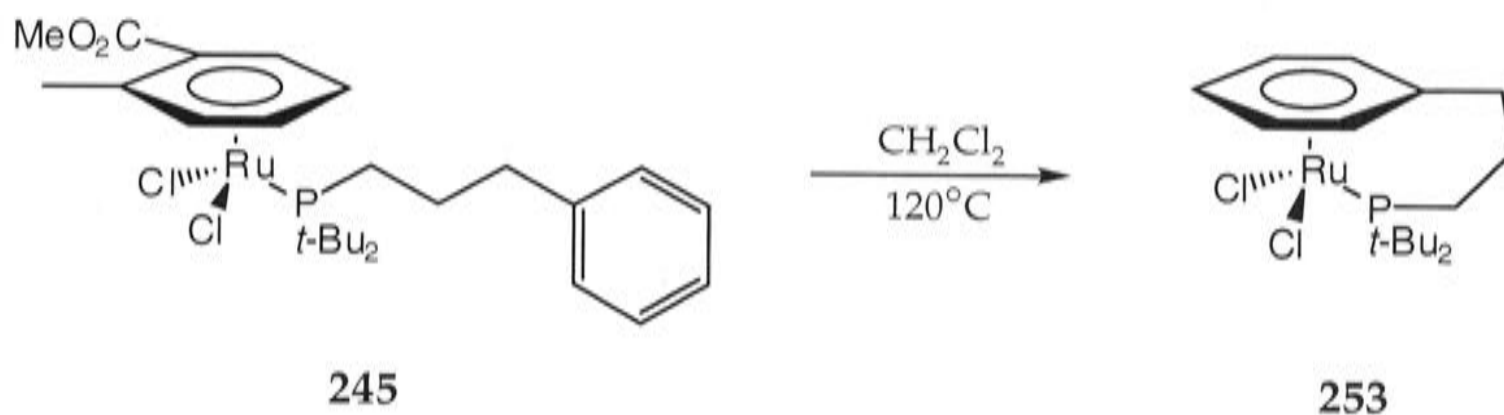
A solution of the ruthenium complex $[\text{RuCl}_2(\eta^6\text{-1,2-MeC}_6\text{H}_4\text{CO}_2\text{Me})]_2$, (**224**), (203 mg, 0.31 mmol) in dry dichloromethane (10 mL) was treated with (3-phenylpropyl)dicyclohexylphosphine, (**197**), (204 mg, 0.64 mmol) and stirred for 1 h at room temperature. The mixture was then heated at 120°C for 24 h in a 35 mL pressure Schlenk tube and worked up as described above for complex **249**. The yield of the title compound **225** was 275 mg (90%).

8.2.40 Preparation of $[\text{RuCl}_2(\eta^1:\eta^6\text{-Cy}_2\text{P}(\text{CH}_2)_3\text{Ph})]$ (**225**) (c)

Complex **225** was obtained by heating $[\text{RuCl}_2(\eta^6\text{-1,4-MeC}_6\text{H}_4\text{CHMe}_2)(\eta^1\text{-Cy}_2\text{P}(\text{CH}_2)_3\text{Ph})]$, (**254**), (150 mg, 0.24 mmol) in dry dichloromethane (3 mL) at 120°C for 48 h and worked up as described above for complex **249**. The yield of orange solid was 97 mg (82%). A similar experiment at 80°C for 480 h gave 44 mg (80%) of the complex **225**.

8.2.41 Preparation of $[\text{RuCl}_2(\eta^1:\eta^6\text{-Cy}_2\text{P}(\text{CH}_2)_3\text{Ph})]$ (**225**) (d)

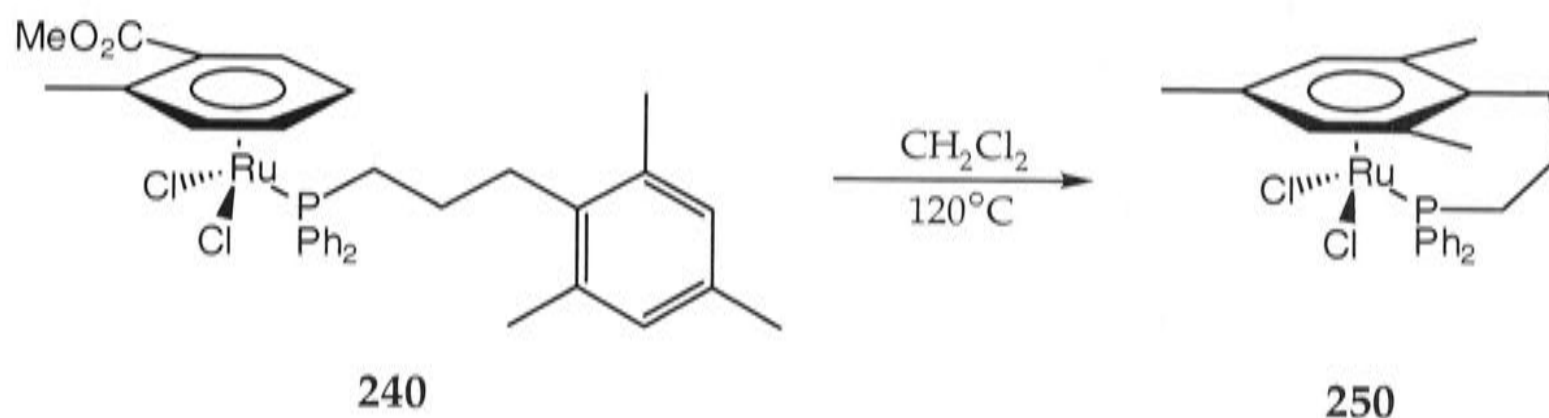
A solution of the ruthenium complex $[\text{RuCl}_2(\eta^6\text{-1,4-MeC}_6\text{H}_4\text{CHMe}_2)]_2$, (**224**), (201 mg, 0.33 mmol) in dry dichloromethane (10 mL) was treated with (3-phenylpropyl)dicyclohexylphosphine, (**197**), (207 mg, 0.66 mmol) and stirred for 1 h at room temperature. The mixture was then heated at 120°C for 48 h in a 35 mL pressure Schlenk tube and worked up as described above for complex **249**. The yield of the title compound **225** was 247 mg (77%).

8.2.42 Preparation of $[\text{RuCl}_2(\eta^1:\eta^6\text{-}t\text{-Bu}_2\text{P}(\text{CH}_2)_3\text{Ph})]$ (**253**)

Complex **253** was obtained by heating $[\text{RuCl}_2(\eta^6\text{-}1,2\text{-MeC}_6\text{H}_4\text{CO}_2\text{Me})(\eta^1\text{-}t\text{-Bu}_2\text{P}(\text{CH}_2)_3\text{Ph})]$, (**245**), (210 mg, 0.36 mmol) in dry dichloromethane (2 mL) at 120°C for 24 h and worked up as described above for complex **249**. The yield of brown solid was 141 mg (90%). Crystals suitable for X-ray crystallography were obtained from dichloromethane/*n*-hexane by vapour diffusion at 4°C .

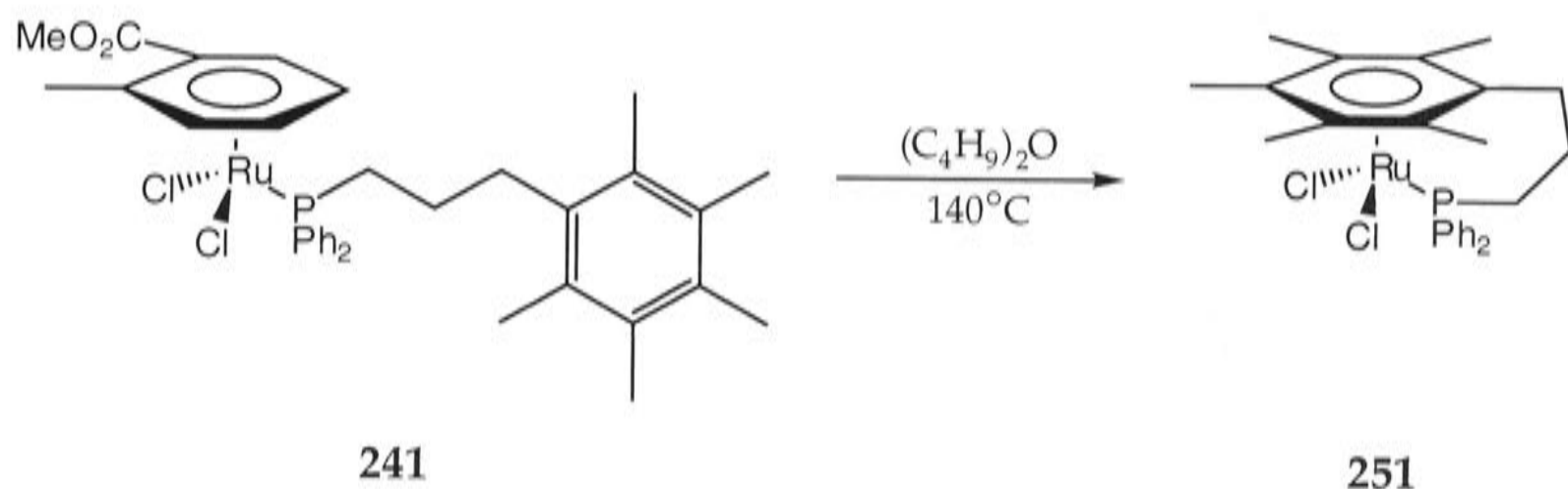
$^1\text{H-NMR}$ (400 MHz, CDCl_3): δ 1.39 (d, 18H, PCMe_3), 1.92 (m, 2H, H^2), 2.15 (m, 2H, H^3), 2.34 (m, 2H, H^1), 5.25 (d, 2H, $J = 5.5$ Hz, H^5), 5.72 (t, 2H, $J = 6$ Hz, H^6), 6.24 (t, 1H, $J = 6$ Hz, H^7). $^{13}\text{C}\{^1\text{H}\}\text{-NMR}$ (100.6 MHz, CDCl_3): δ 18.86 (d, $^2J_{\text{PC}} = 17$ Hz, C^2), 27.71 (d, $^1J_{\text{PC}} = 64$ Hz, C^1), 29.67 (PCMe_3), 30.74 (PCMe_3), 39.01 (d, $^3J_{\text{PC}} = 15$ Hz, C^3), 82.01 (C^5), 93.38 (C^6), 96.63 (C^7), 98.10 (C^4). $^{31}\text{P}\{^1\text{H}\}\text{-NMR}$ (161.97 MHz, CDCl_3): δ 41.8. IR (cm^{-1} , KBr and polythene): 1452 s, 1391 m, 1367 s [$\nu((\text{CH}_3)_3\text{C})$], 293 m, 266 s [$\nu(\text{Ru-Cl})$]. FABMS; m/z : 436 $[\text{M}]^+$. Anal. found: C, 46.41; H, 6.43; P, 7.00%. $\text{C}_{17}\text{H}_{29}\text{Cl}_2\text{PRu}$ requires: C, 46.79; H, 6.70; P, 7.10%.

[†]Complex **245** was not pure.

8.2.43 Preparation of $[\text{RuCl}_2(\eta^1:\eta^6\text{-Ph}_2\text{P}(\text{CH}_2)_3\text{-2,4,6-C}_6\text{H}_2\text{Me}_3)]$ (**250**)

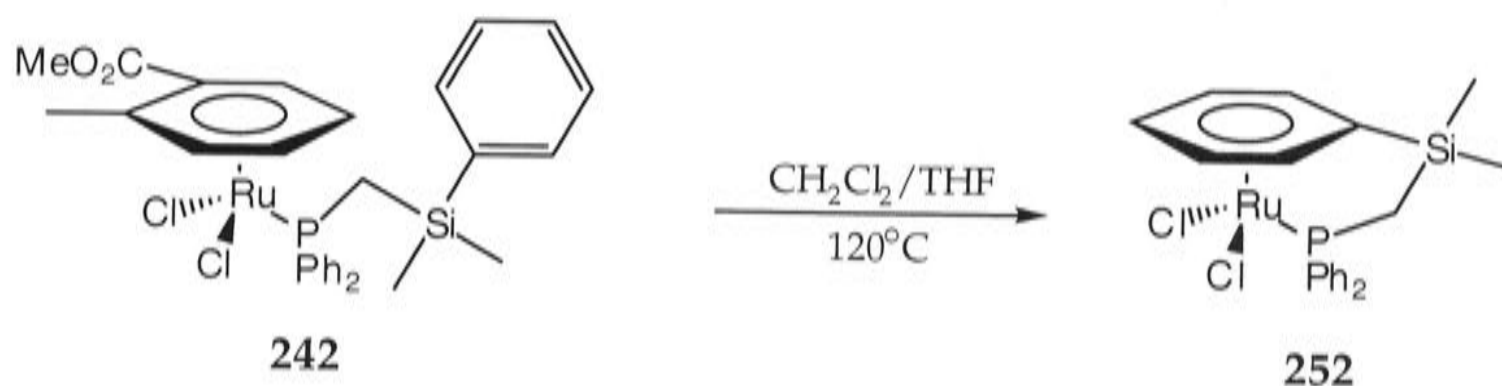
Complex **250** was obtained by heating $[\text{RuCl}_2(\eta^6\text{-1,2-MeC}_6\text{H}_4\text{CO}_2\text{Me})(\eta^1\text{-Ph}_2\text{P}(\text{CH}_2)_3\text{-2,4,6-C}_6\text{H}_2\text{Me}_3)]$, (**240**), (170 mg, 0.23 mmol) in dry dichloromethane (3 mL) at 120°C for 24 h. The solution was cooled to 0°C and the solvent was removed *in vacuo*. The residue was extracted with CH_2Cl_2 , transferred to a column of neutral alumina (activity III), and the product was eluted with CH_2Cl_2 followed by THF. The eluate was evaporated to dryness and re-chromatographed. The eluate was evaporated to dryness, redissolved in CH_2Cl_2 and treated with *n*-hexane. Evaporation to dryness gave a gummy residue that, on trituration with *n*-hexane, afforded the title compound **250** which was isolated as an orange solid (24 mg, 18%). Orange crystals suitable for X-ray crystallography were obtained by layering a CH_2Cl_2 solution with *n*-hexane.

$^1\text{H-NMR}$ (400 MHz, CDCl_3): δ 1.36 (s, 6H, $\text{C}^5\text{-Me}$), 1.79 (s, 6H, $\text{C}^7\text{-Me}$), 2.16 (m, 2H, H^2), 2.39 (m 4H, H^1, H^3), 5.25 (s, 1H, H^6), 7.20-7.25 (m, 6H, PPh_2), 7.50-7.55 (m, 4H, PPh_2). $^{13}\text{C}\{^1\text{H}\}\text{-NMR}$ (100.6 MHz, CDCl_3): δ 11.39 ($\text{C}^7\text{-Me}$), 18.73 ($\text{C}^5\text{-Me}$), 20.54 (d, $^1J_{\text{PC}} = 26$ Hz, C^1), 25.36 (C^2), 34.64 (C^3), 84.81 (C^5), 92.34 (C^6), 96.30 (C^7), 127.65 (d, $J_{\text{PC}} = 10$ Hz, PPh_2), 129.90 (PPh_2), 132.73 (d, $J_{\text{PC}} = 48$ Hz, PPh_2), 133.78 (d, $J_{\text{PC}} = 9$ Hz, PPh_2). $^{31}\text{P}\{^1\text{H}\}\text{-NMR}$ (161.97 MHz, CDCl_3): δ 28.8. IR (cm^{-1} , polythene): 304 s, 288 s [$\nu(\text{Ru-Cl})$]. EIMS; m/z : 518 [M^+]. Anal. found: C, 57.21; H, 5.83%. $\text{C}_{24}\text{H}_{27}\text{Cl}_2\text{PRu}\cdot 0.4\text{C}_6\text{H}_{14}$ requires: C, 57.35; H, 5.94%. The presence of *n*-hexane was evident in the ^1H NMR spectrum.

8.2.44 Preparation of $[\text{RuCl}_2(\eta^1:\eta^6\text{-Ph}_2\text{P}(\text{CH}_2)_3\text{C}_6\text{Me}_5)]$ (**251**)

Complex **251** was obtained by heating $[\text{RuCl}_2(\eta^6\text{-1,2-MeC}_6\text{H}_4\text{CO}_2\text{Me})(\eta^1\text{-Ph}_2\text{P}(\text{CH}_2)_3\text{C}_6\text{Me}_5)]$, (**241**), (104 mg, 0.15 mmol) in dry di-*n*-butyl ether (10 mL) at 140°C for 16 h. The compound was worked up as described on p. 365 for complex **248**. The yield of orange solid was 29 mg (35%). Use of dichloromethane containing a few drops of THF instead of di-*n*-butyl ether at 120°C for 24 h gave a yield of only 7%. Orange crystals suitable for X-ray analysis were obtained from dichloromethane/ether by vapour diffusion.

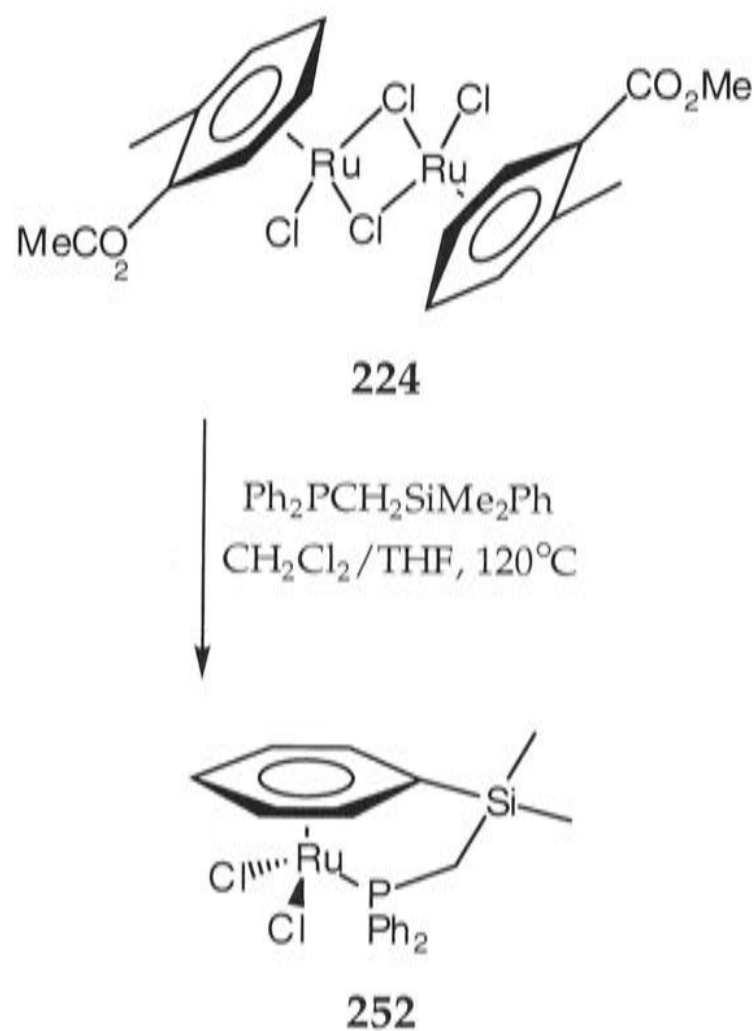
$^1\text{H-NMR}$ (400 MHz, CDCl_3): δ 1.73 (s, 6H, $\text{C}^5\text{-Me}$), 2.06 (d, 6H, $J = 0.5$ Hz, $\text{C}^6\text{-Me}$), 2.16 (m, 2H, H^2), 2.22 (d, 3H, $J = 2.5$ Hz, $\text{C}^7\text{-Me}$), 2.40 (m, 2H, H^1), 2.56 (t, 2H, $J = 6$ Hz, H^3), 7.25-7.30 (m, 6H, PPh_2), 7.60-7.65 (m, 4H, PPh_2). $^{13}\text{C}\{^1\text{H}\}\text{-NMR}$ (100.6 MHz, CDCl_3): δ 14.94 ($\text{C}^7\text{-Me}$), 15.58 ($\text{C}^6\text{-Me}$), 16.08 ($\text{C}^5\text{-Me}$), 21.73 (d, $^1J_{\text{PC}} = 31$ Hz, C^1), 22.67 (C^2), 25.01 (C^3), 85.50 (C^5), 91.59 (C^6), 101.23 (d, $J_{\text{PC}} = 4$ Hz, C^7), 106.29 (d, $J_{\text{PC}} = 11$ Hz, C^4), 127.63 (d, $J_{\text{PC}} = 10$ Hz, PPh_2), 129.67 (PPh_2), 132.81 (d, $J_{\text{PC}} = 46$ Hz, PPh_2), 133.39 (d, $J_{\text{PC}} = 8.5$ Hz, PPh_2). $^{31}\text{P}\{^1\text{H}\}\text{-NMR}$ (121.5 MHz, CDCl_3): δ 26.2 (lit.¹⁹ δ 25.2). IR (cm^{-1} , polythene): 307 s, 286 s [$\nu(\text{Ru-Cl})$]. FABMS; m/z : 546 [M^+]. Anal. found: C, 57.41; H, 5.96; P, 5.66%. $\text{C}_{26}\text{H}_{31}\text{Cl}_2\text{PRu}$ requires: C, 57.14; H, 5.72; P, 5.67%.

8.2.45 Preparation of $[\text{RuCl}_2(\eta^1:\eta^6\text{-Ph}_2\text{PCH}_2\text{SiMe}_2\text{Ph})]$ (**252**) (a)

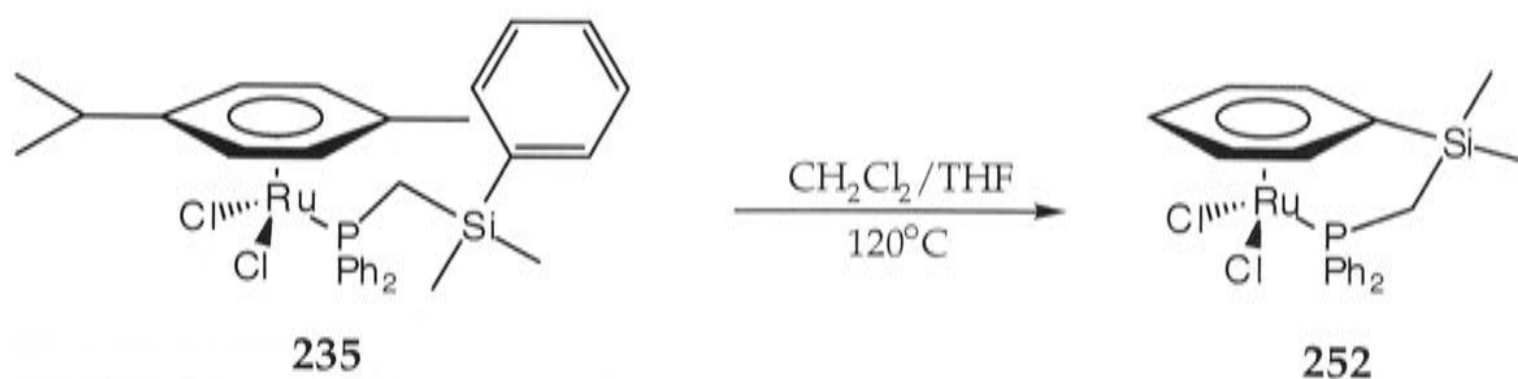
Complex **252** was obtained by heating $[\text{RuCl}_2(\eta^6\text{-1,2-MeC}_6\text{H}_4\text{CO}_2\text{Me})(\eta^1\text{-Ph}_2\text{PCH}_2\text{SiMe}_2\text{Ph})]$, (**242**), (675 mg, 1.03 mmol) in dry dichloromethane (17 mL) with dry THF (14 drops) at 120°C for 72 h. The compound was worked up as described above for complex **248**. The yield of orange solid was 371 mg (71%). Orange crystals suitable for X-ray crystallography were obtained by layering a CH_2Cl_2 solution with *n*-hexane.

$^1\text{H-NMR}$ (300 MHz, CDCl_3): δ 0.33 (s, 6H, H^2), 2.80 (d, 2H, $J = 15$ Hz, H^1), 5.18 (d, 2H, $J = 6$ Hz, H^4), 5.88 (t, 2H, $J = 6$ Hz, H^5), 6.26 (t, 1H, $J = 6$ Hz, H^6), 7.25-7.40 (m, 6H, PPh_2), 7.70-7.75 (m, 4H, PPh_2). $^{13}\text{C}\{^1\text{H}\}\text{-NMR}$ (75.4 MHz, CDCl_3): δ -2.77 (d, $^4J_{\text{PC}} = 5$ Hz, C^2), 29.71 (d, $^1J_{\text{PC}} = 17$ Hz, C^1), 86.30 (C^4), 92.13 (d, $J_{\text{PC}} = 2$ Hz, C^3), 92.68 (d, $J_{\text{PC}} = 6$ Hz, C^5), 95.80 (d, $J_{\text{PC}} = 12$ Hz, C^6), 128.02 (d, $J_{\text{PC}} = 10$ Hz), 130.40 (d, $J_{\text{PC}} = 3$ Hz, PPh_2), 132.97 (d, $J_{\text{PC}} = 10$ Hz, PPh_2), 133.91 (d, $J_{\text{PC}} = 45$ Hz, PPh_2). $^{31}\text{P}\{^1\text{H}\}\text{-NMR}$ (121.5 MHz, CDCl_3): δ 24.0. IR (cm^{-1} , polythene): 303 s, 270 s [$\nu(\text{Ru-Cl})$]. FABMS; m/z : 508 [M^+]. Anal. found: C, 50.09; H, 4.55; P, 6.20%. $\text{C}_{21}\text{H}_{23}\text{Cl}_2\text{PRuSi}$ requires: C, 48.90; H, 4.58; P, 6.12%.

Variable temperature NMR spectra of compound **252** are described in Section 3.2.4 (pp. 106-110).

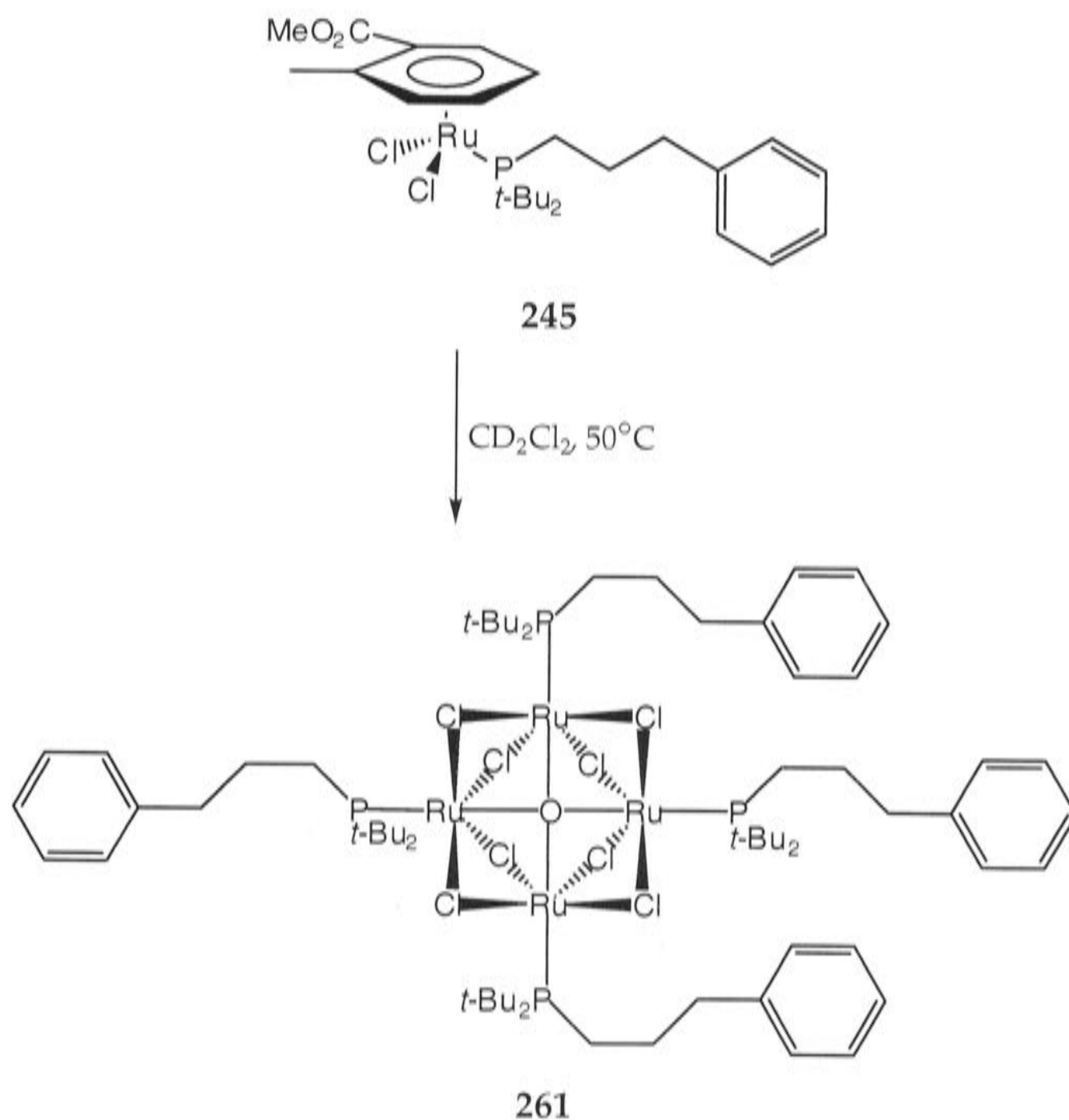
8.2.46 Preparation of $[\text{RuCl}_2(\eta^1:\eta^6\text{-Ph}_2\text{PCH}_2\text{SiMe}_2\text{Ph})]$ (**252**) (b)

A solution of the ruthenium complex $[\text{RuCl}_2(\eta^6\text{-1,2-MeC}_6\text{H}_4\text{CO}_2\text{Me})]_2$, (**224**), (200 mg, 0.31 mmol) in dry dichloromethane (10 mL) with dry THF (8 drops) was treated with (3-phenyldimethylsilyl)methyldiphenylphosphine, (**201**), (207 mg, 0.62 mmol) and stirred for 1 h at room temperature. The mixture was then heated at 120°C for 72 h in a 35 mL pressure Schlenk tube and worked up as described on p. 365 for complex **248**. The yield of the title compound **252** was 235 mg (75%).

8.2.47 Preparation of $[\text{RuCl}_2(\eta^1:\eta^6\text{-Ph}_2\text{PCH}_2\text{SiMe}_2\text{Ph})]$ (**252**) (c)

Complex **252** was obtained by heating $[\text{RuCl}_2(\eta^6\text{-1,4-MeC}_6\text{H}_4\text{CHMe}_2)(\eta^1\text{-Ph}_2\text{PCH}_2\text{SiMe}_2\text{Ph})]$, (**235**), (5 mg, 7.8×10^{-3} mmol) in dry dichloromethane (1 mL) with dry THF (1 drop) at 120°C for 168 h. The solvents were removed *in vacuo* and the residue was triturated with *n*-hexane to afford 2 mg (57%) of the orange solid.

8.2.48 Preparation of $[\text{Ru}_4(\mu_4\text{-O})(\mu_2\text{-Cl})_8(\eta^1\text{-}t\text{-Bu}_2\text{P}(\text{CH}_2)_3\text{Ph})_4]$ (**261**)



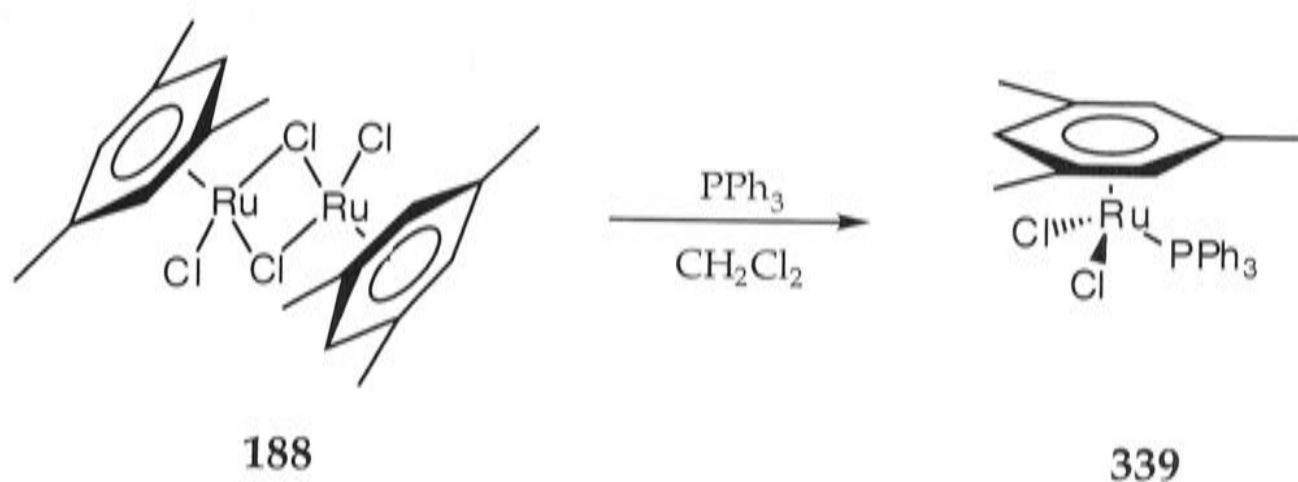
A solution of the ruthenium complex $[\text{RuCl}_2(\eta^6\text{-1,2-MeC}_6\text{H}_4\text{CO}_2\text{Me})(\eta^1\text{-}t\text{-Bu}_2\text{P}(\text{CH}_2)_3\text{Ph})]$, (**245**), in dry d_2 -dichloromethane (0.5 mL) was heated to 50°C for 48 h to give a dark brown solution. In one experiment, black crystals of complex **261** suitable for X-ray crystallography were obtained by

[†]Complex **245** was not pure.

layering a CD_2Cl_2 solution with *n*-hexane. The yield has not been estimated, but is likely to be very low.

$^{31}\text{P}\{^1\text{H}\}$ -NMR (121.5 MHz, CD_2Cl_2): δ 267.0. FABMS; m/z : 1762 $[\text{M}]^+$. Anal. found: C, 44.67; H, 6.35; P, 5.82%. $\text{C}_{68}\text{H}_{116}\text{Cl}_8\text{OP}_4\text{Ru}_4$ requires: C, 46.37; H, 6.64; P, 7.03%. ESR (5K, CH_2Cl_2): $g_1 = 2.57$, $g_2 = 2.48$, $g_3 = 2.41$.

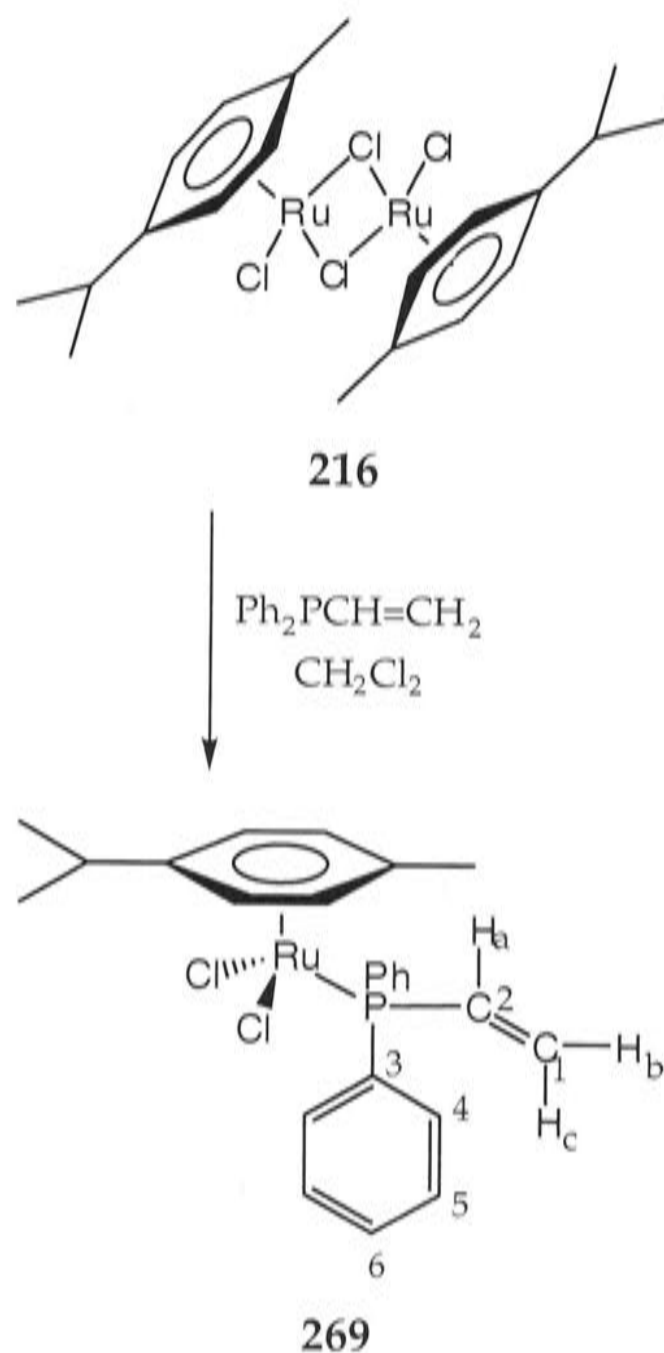
8.2.49 Preparation of $[\text{RuCl}_2(\eta^6\text{-1,3,5-C}_6\text{Me}_3\text{H}_3)(\text{PPh}_3)]$ (339)



Davies *et al.*⁴⁵ report that they prepared complex $[\text{RuCl}_2(\eta^6\text{-1,3,5-C}_6\text{H}_3\text{Me}_3)(\text{PPh}_3)]$ (339) according to the report by Bennett *et al.*,¹⁵ however, this paper does not report the preparation of 339.

A solution of the ruthenium complex $[\text{RuCl}_2(\eta^6\text{-1,3,5-C}_6\text{H}_3\text{Me}_3)]_2$, (188), (106 mg, 0.18 mmol) and triphenylphosphine (96 mg, 0.36 mmol) in dry dichloromethane (30 mL) was stirred for 4 h and filtered through Celite, which was then washed with dichloromethane (2 x 20 mL). Addition of *n*-hexane (40 mL) to the filtrate and removal of the solvents *in vacuo* gave a residue which was triturated with ether to afford the title compound as an orange solid (193 mg, 96%).

^1H -NMR (300 MHz, CDCl_3): δ 1.99 (s, 9H, $\text{C}_6\text{H}_3\text{Me}_3$), 4.63 (s, 3H, $\text{C}_6\text{H}_3\text{Me}_3$), 7.30-7.35 (m, 9H, Ph), 7.70-7.75 (m, 6H, Ph). $^{31}\text{P}\{^1\text{H}\}$ -NMR (121.5 MHz, CDCl_3): δ 32.2.

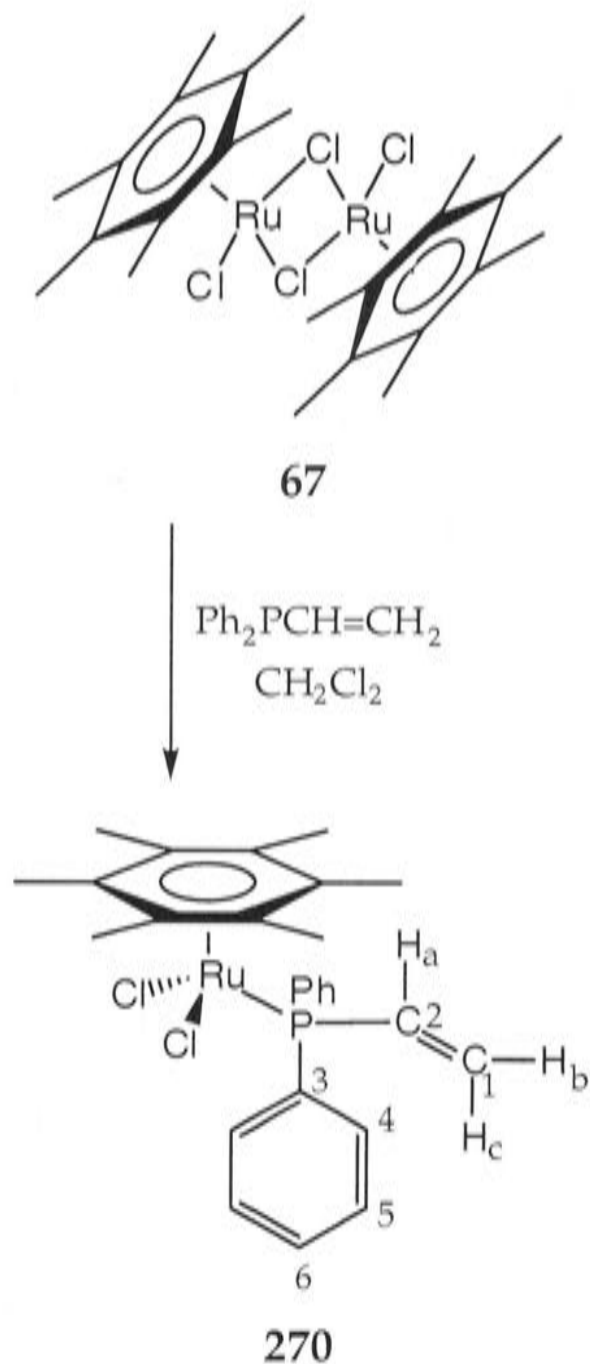
8.2.50 Preparation of $[\text{RuCl}_2(\eta^6\text{-1,4-MeC}_6\text{H}_4\text{CHMe}_2)(\text{Ph}_2\text{PCH}=\text{CH}_2)]$ (**269**)

A solution of the ruthenium complex $[\text{RuCl}_2(\eta^6\text{-1,4-MeC}_6\text{H}_4\text{CHMe}_2)]_2$, (**216**), (200 mg, 0.33 mmol) and diphenylvinylphosphine, (**272**), (0.14 mL, 0.66 mmol) in dry dichloromethane (20 mL) was stirred for 2.5 h and filtered through Celite, which was then washed with dichloromethane (2 × 20 mL). Addition of *n*-hexane (40 mL) to the filtrate and removal of the solvents *in vacuo* gave the title compound **269** as a red solid (312 mg, 92%). Red crystals suitable for X-ray crystallography were obtained from THF/*n*-hexane by vapour diffusion.

$^1\text{H-NMR}$ (300 MHz, CDCl_3): δ 0.94 (d, 6H, $J = 8$ Hz, $\text{MeC}_6\text{H}_4\text{CHMe}_2$), 1.90 (s, 3H, $\text{MeC}_6\text{H}_4\text{CHMe}_2$), 2.57 (m, 1H, $\text{MeC}_6\text{H}_4\text{CHMe}_2$), 5.18 (app. t, 1H, $^3J_{\text{PH}} = ^3J_{\text{HaHc}} = 19$ Hz, H^c), 5.30 (dd, 4H, $^1J = 16$ Hz, $^2J = 6$ Hz, $\text{MeC}_6\text{H}_4\text{CHMe}_2$), 5.90

(dd, 1H, $^3J_{\text{PH}} = 38$ Hz, $^3J_{\text{HaHb}} = 12$ Hz, H^b), 6.98 (ddd, 1H, $^2J_{\text{PH}} = 30$ Hz, $^3J_{\text{HaHc}} = 18$ Hz, $^3J_{\text{HaHb}} = 12$ Hz, H^a), 7.45-7.50 (m, 6H, H⁵, H⁶), 7.80-7.85 (m, 4H, H⁴). $^{13}\text{C}\{^1\text{H}\}$ -NMR (75.4 MHz, CDCl_3): δ 17.45 ($\text{MeC}_6\text{H}_4\text{CHMe}_2$), 21.04 ($\text{MeC}_6\text{H}_4\text{CHMe}_2$), 30.09 ($\text{MeC}_6\text{H}_4\text{CHMe}_2$), 85.91 (d, $J_{\text{PC}} = 6$ Hz), 89.32 (d, $J_{\text{PC}} = 4$ Hz), 94.88, 108.83 ($\text{MeC}_6\text{H}_4\text{CHMe}_2$), 129.06 (d, $^1J_{\text{PC}} = 10$ Hz, C³), 130.90 (d, $^3J_{\text{PC}} = 4$ Hz, C⁵), 131.44 (d, $^4J_{\text{PC}} = 2$ Hz, C⁶), 132.15 (C¹), 133.74 (d, $^1J_{\text{PC}} = 47$ Hz, C²), 134.64 (d, $^2J_{\text{PC}} = 9$ Hz, C⁴). $^{31}\text{P}\{^1\text{H}\}$ -NMR (80.96 MHz, CDCl_3): δ 22.8 (lit.⁴⁶ δ 21.6; lit.¹⁹ δ 21.8]. IR (cm^{-1} , KBr and polythene): 3045 w [$\nu(\text{C-H})_{\text{str.}}$], 1625 w [$\nu(\text{C=C})$], 1435 s, 985 m, 942 m [$\nu(\text{C-H})_{\text{def.}}$], 288 s [$\nu(\text{Ru-Cl})$] (lit.⁴⁶ (nujol mull on CsI windows) 292 (br.) [$\nu(\text{Ru-Cl})$]) EIMS; m/z : 518 [M^+]. Anal. found: C, 55.20; H, 5.04; P, 6.13%. $\text{C}_{24}\text{H}_{27}\text{Cl}_2\text{PRu}$ requires: C, 55.60; H, 5.25; P, 5.97%.

8.2.51 Preparation of $[\text{RuCl}_2(\eta^6\text{-C}_6\text{Me}_6)(\text{Ph}_2\text{PCH=CH}_2)]$ (270)

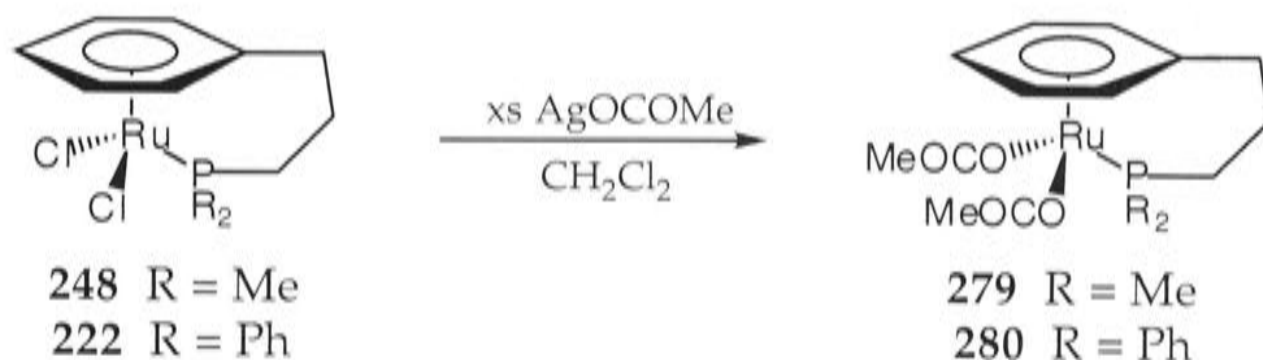


The complex **270** was prepared in 97% yield, as an orange solid, from $[\text{RuCl}_2(\eta^6\text{-C}_6\text{Me}_6)]_2$ (**67**) and diphenylvinylphosphine (**272**) in a similar way.

$^1\text{H-NMR}$ (300 MHz, CDCl_3): δ 1.75 (s, 18H, C_6Me_6), 5.26 (app. t, 1H, $^3J_{\text{PH}} = ^3J_{\text{HaHc}} = 18$ Hz, H^c), 5.75 (dd, 1H, $^3J_{\text{PH}} = 37$ Hz, $^3J_{\text{HaHb}} = 12$ Hz, H^b), 6.76 (ddd, 1H, $^2J_{\text{PH}} = 30$ Hz, $^3J_{\text{HaHc}} = 18$ Hz, $^3J_{\text{HaHb}} = 12$ Hz, H^a), 7.35-7.40 (m, 6H, H^5 , H^6), 7.70-7.75 (m, 4H, H^4). $^{13}\text{C}\{^1\text{H}\}\text{-NMR}$ (75.4 MHz, CDCl_3): δ 15.16 (C_6Me_6), 96.14 (C_6Me_6), 127.90 (d, $^1J_{\text{PC}} = 9$ Hz, C^3), 130.12 (C^5), 130.28 (d, $^4J_{\text{PC}} = 2$ Hz, C^6), 130.69 (C^1), 134.17 (C^2), 134.79 (d, $^2J_{\text{PC}} = 9$ Hz, C^4). $^{31}\text{P}\{^1\text{H}\}\text{-NMR}$ (80.96 MHz, CDCl_3): δ 28.7 (br., $\nu_{1/2} = 63$ Hz) [lit.⁴⁶ δ 27.7; lit.¹⁹ δ 29.3]. IR (cm^{-1} , KBr and polythene): 3046 w [$\nu(\text{C-H})_{\text{str.}}$], 1621 w [$\nu(\text{C=C})$], 1436 s, 987 m, 950 m [$\nu(\text{C-H})_{\text{def.}}$], 298 s [$\nu(\text{Ru-Cl})$] (lit.⁴⁶ (nujol mull on CsI windows) 295, 274 [$\nu(\text{Ru-Cl})$]). FABMS; m/z : 546 [M^+]. Anal. found: C, 56.88; H, 5.94; P, 5.45%. $\text{C}_{26}\text{H}_{31}\text{Cl}_2\text{PRu}$ requires: C, 57.14; H, 5.72; P, 5.67%.

Inexplicably, this reaction failed in Cambridge, and it was necessary to prepare the triphenylstibine complex $[\text{RuCl}_2(\eta^6\text{-C}_6\text{Me}_6)(\text{SbPh}_3)]$ (**273**), which was heated at 110°C with diphenylvinylphosphine (**272**) for 16 h (95%).

8.2.52 Preparation of $[\text{Ru}(\text{OCOMe})_2(\eta^1:\eta^6\text{-Me}_2\text{P}(\text{CH}_2)_3\text{Ph})]$ (**279**)



A solution of the ruthenium complex $[\text{RuCl}_2(\eta^1:\eta^6\text{-Me}_2\text{P}(\text{CH}_2)_3\text{Ph})]$, (**248**), (48 mg, 0.14 mmol) in dry dichloromethane (10 mL) was treated silver acetate (95 mg, 0.57 mmol) in the absence of light and stirred for 2.5 h, filtered through Celite, which was then washed with dry

dichloromethane (2 x 20 mL). Addition of dry *n*-hexane (30 mL) to the filtrate and removal of the solvents *in vacuo* gave the title compound **279** as an air-sensitive green solid (57 mg, 97%).

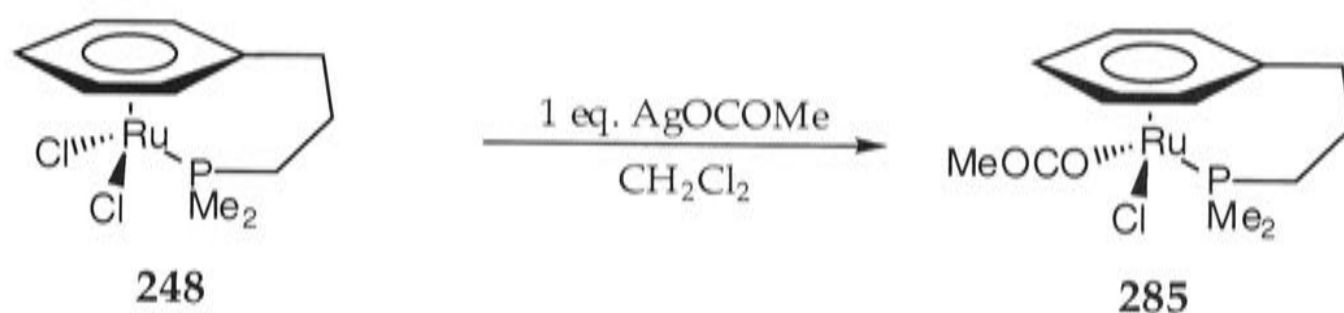
$^1\text{H-NMR}$ (300 MHz, CD_2Cl_2): δ 1.17 (d, 6H, $J = 11$ Hz, PMe_2), 1.91 (s, 6H, MeOCO), 1.98 (m, 2H, H^2), 2.27 (m, 2H, H^3), 2.62 (m, 2H, H^1), 4.96 (d, 2H, $J = 6$ Hz, H^5), 5.84 (t, 2H, $J = 6$ Hz, H^6), 6.50 (t, 1H, $J = 6$ Hz, H^7). $^{13}\text{C}\{^1\text{H}\}\text{-NMR}$ (75.4 MHz, CD_2Cl_2): δ 12.43 (d, $^1J_{\text{PC}} = 30$ Hz, PMe_2), 21.54 (C^2), 23.76 (MeOCO), 25.18 (d, $^1J_{\text{PC}} = 32$ Hz, C^1), 29.78 (d, $^3J_{\text{PC}} = 3$ Hz, C^3), 77.27 (C^7), 90.54 (C^6 or C^5), 91.42 (d, $J_{\text{PC}} = 4$ Hz, C^5 or C^6), 95.39 (d, $J_{\text{PC}} = 11$ Hz, C^4), 178.31 (MeOCO). $^{31}\text{P}\{^1\text{H}\}\text{-NMR}$ (121.5 MHz, CD_2Cl_2): δ 19.4. IR (cm^{-1} , KBr): 1598 s, 1578 s [$\nu_{\text{as}}(\text{OCO})$], 1376 s [$\nu_{\text{s}}(\text{OCO})$]. FABMS; m/z : 341 [M-OCOMe] $^+$.

8.2.53 Preparation of $[\text{Ru}(\text{OCOMe})_2(\eta^1:\eta^6\text{-Ph}_2\text{P}(\text{CH}_2)_3\text{Ph})]$ (**280**)

Complex **280** was prepared similarly to **279** in 93% yield, as an air-sensitive dark yellow solid, from $[\text{RuCl}_2(\eta^1:\eta^6\text{-Ph}_2\text{P}(\text{CH}_2)_3\text{Ph})]$ (**222**) and silver acetate.

$^1\text{H-NMR}$ (300 MHz, CD_2Cl_2): δ 1.58 (s, 6H, MeOCO), 2.11 (m, 2H, H^2), 2.61 (m, 2H, H^3), 2.80 (m, 2H, H^1), 5.17 (d, 2H, $J = 5.5$ Hz, H^5), 6.05 (t, 2H, $J = 6$ Hz, H^6), 6.91 (t, 1H, $J = 6$ Hz, H^7), 7.25-7.40 (m, 6H, PPh_2), 7.45-7.50 (m, 4H, PPh_2). $^{13}\text{C}\{^1\text{H}\}\text{-NMR}$ (75.4 MHz, CD_2Cl_2): δ 20.74 (C^2), 23.32 (C^1), 23.78 (MeOCO), 30.13 (C^3), 79.57 (C^7), 90.49 (d, $J_{\text{PC}} = 4$ Hz, C^5 or C^6), 90.90 (C^6 or C^5), 94.89 (d, $J_{\text{PC}} = 11$ Hz, C^4), 128.19 (d, $J_{\text{PC}} = 10$ Hz, PPh_2), 130.35 (d, $J_{\text{PC}} = 3$ Hz, PPh_2), 132.92 (PPh_2), 133.66 (d, $J_{\text{PC}} = 9$ Hz, PPh_2), 178.27 (MeOCO). $^{31}\text{P}\{^1\text{H}\}\text{-NMR}$ (121.5 MHz, CD_2Cl_2): δ 28.1. IR (cm^{-1} , KBr): 1619 s [$\nu_{\text{as}}(\text{OCO})$], 1358 s [$\nu_{\text{s}}(\text{OCO})$]. FABMS; m/z : 465 [M-OCOMe] $^+$.

8.2.54 Attempted preparation of $[\text{RuCl}(\eta^1\text{-OCOMe})(\eta^1:\eta^6\text{-Me}_2\text{P}(\text{CH}_2)_3\text{Ph})]$
(285)

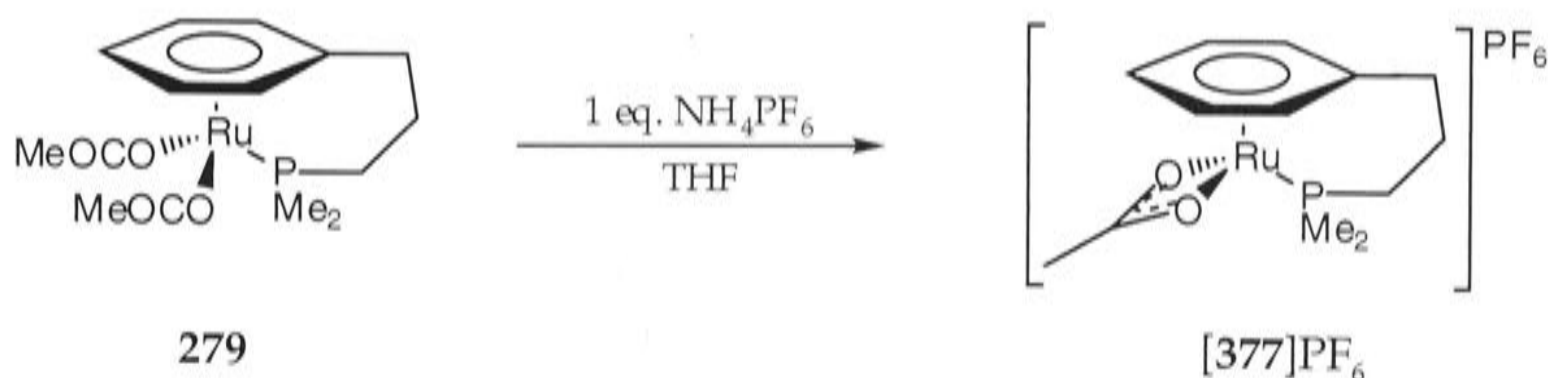


A solution of the ruthenium complex $[\text{RuCl}_2(\eta^1:\eta^6\text{-Me}_2\text{P}(\text{CH}_2)_3\text{Ph})]$, (248), (50 mg, 0.14 mmol) in dry dichloromethane (10 mL) was treated with silver acetate (24 mg, 0.14 mmol) in the absence of light and stirred at room temperature for 3.5 h, filtered through Celite, which was then washed with dry dichloromethane (3×5 mL). Addition of dry *n*-hexane (30 mL) to the filtrate and removal of the solvents *in vacuo* gave a mixture of compounds 285 (δ_p 15.6), $[\text{Ru}(\eta^1\text{-OCOMe})_2(\eta^1:\eta^6\text{-Me}_2\text{P}(\text{CH}_2)_3\text{Ph})]$ (279)

$[\delta_p$ 19.4] and unreacted 248 (δ_p 13.6).

The ^1H NMR (300 MHz, CD_2Cl_2) spectrum showed three sets of the characteristic signals for the PMe_2 , $\eta^6\text{-C}_6\text{H}_5$ and CH_2 protons.

8.2.55 Attempted preparation of $[\text{Ru}(\eta^2\text{-OCOMe})(\eta^1:\eta^6\text{-Me}_2\text{P}(\text{CH}_2)_3\text{Ph})]\text{PF}_6$
([377] PF_6)



A solution of the ruthenium complex $[\text{Ru}(\eta^1\text{-OCOMe})_2(\eta^1:\eta^6\text{-Me}_2\text{P}(\text{CH}_2)_3\text{Ph})]$, (279), (57 mg, 0.14 mmol) in dry THF (10 mL) was treated with NH_4PF_6 (23 mg, 0.14 mmol) and stirred at room temperature for 2.5

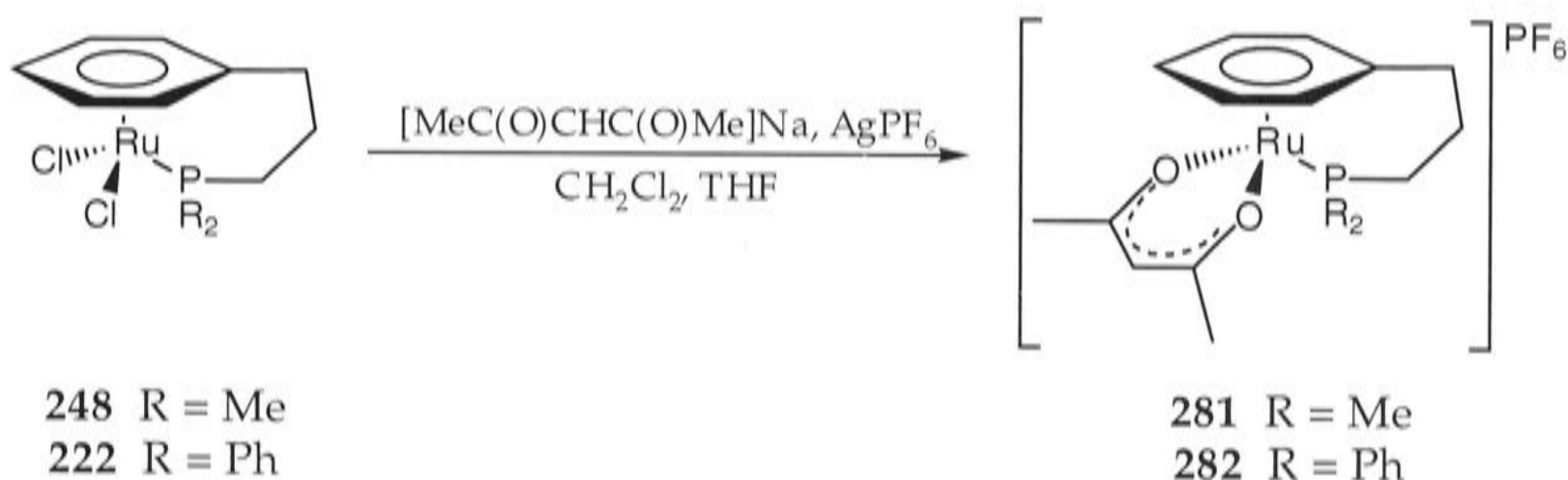
h, filtered through Celite, which was then washed with dry dichloromethane (2 x 20 mL). The solvents were removed *in vacuo* to give a dark green solid, but the nature of the products is unknown.

The ^1H NMR (300 MHz, CD_2Cl_2) in the region δ 1-3 was very complicated, and also showed many multiplets in the region δ 4.9-6.5 attributable to $\eta^6\text{-C}_6\text{H}_5$.

$^{31}\text{P}\{^1\text{H}\}$ -NMR (121.5 MHz, CD_2Cl_2): δ 13.3, 16.0, -143.8 (sept, $J_{\text{PF}} = 713$ Hz, PF_6).

8.2.56 Preparation of $[\text{Ru}(\eta^2\text{-MeC(O)CHC(O)Me})(\eta^1:\eta^6\text{-Me}_2\text{P}(\text{CH}_2)_3\text{Ph})]\text{PF}_6$

(281)



A solution of the ruthenium complex $[\text{RuCl}_2(\eta^1:\eta^6\text{-Me}_2\text{P}(\text{CH}_2)_3\text{Ph})]$, (**248**), (77 mg, 0.22 mmol) and sodium acetylacetonate (25 mg, 0.20 mmol) in dry dichloromethane (20 mL) and dry THF (20 mL) was treated with AgPF_6 (113 mg, 0.45 mmol) and stirred at room temperature for 6.5 h, filtered through Celite, which was then washed with dry dichloromethane (3 x 10 mL). The solvents were removed *in vacuo* and the residue was extracted with dry dichloromethane (10 mL) and filtered. Addition of dry *n*-hexane (20 mL) to the filtrate and removal of the solvents *in vacuo* gave the title compound **281** as a brown solid (103 mg, 90%).

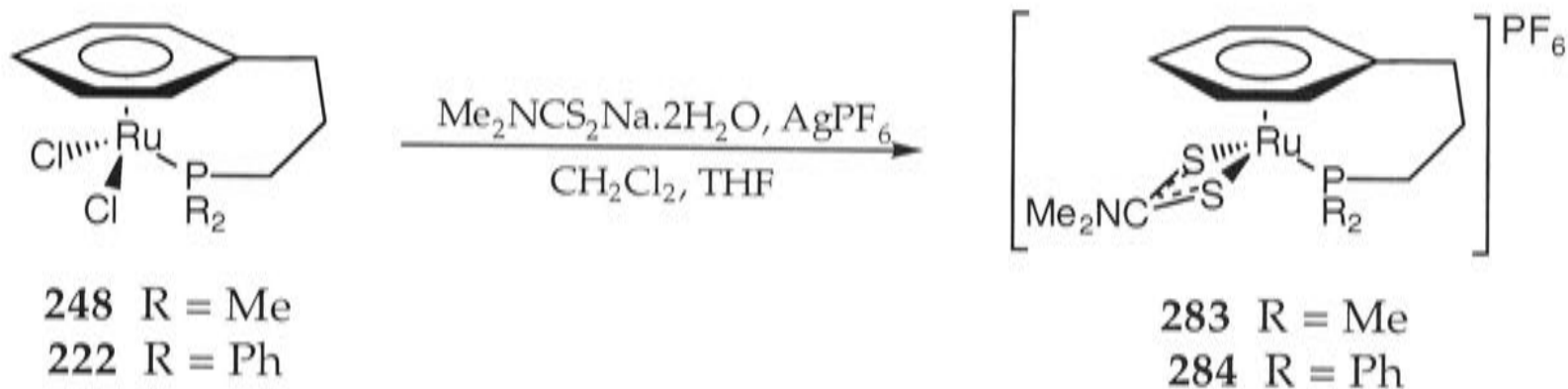
^1H -NMR (300 MHz, CD_2Cl_2): δ 1.17 (d, $J = 11$ Hz, 6H, PMe_2), 1.93 (s, 6H, $\text{CH}(\text{COMe})_2$), 1.20 (m, 2H, H^2), 2.31 (m, 2H, H^3), 2.61 (m, 2H, H^1), 5.02 (d, 2H, $J = 6$ Hz, H^5), 5.41 (s, 1H, $\text{CH}(\text{COMe})_2$), 5.75 (t, 2H, $J = 6$ Hz, H^6), 6.24 (t, 1H, $J = 6$ Hz, H^7). $^{13}\text{C}\{^1\text{H}\}$ -NMR (75.4 MHz, CD_2Cl_2): δ 11.15 (d, $^1J_{\text{PC}} = 30$ Hz,

PMe₂), 22.34 (C²), 25.09 (d, ¹J_{PC} = 33 Hz, C¹), 26.78 (CH(COMe)₂), 30.21 (d, ³J_{PC} = 3 Hz, C³), 78.72 (CH(COMe)₂), 93.79 (d, J_{PC} = 12 Hz, C⁷), 96.67 (d, J_{PC} = 3 Hz, C⁵ or C⁶), 99.50 (C⁶ or C⁵), 101.72 (C⁴), 189.20 (CH(COMe)₂). ³¹P{¹H}-NMR (121.5 MHz, CD₂Cl₂): δ 20.8 (PMe₂), -143.8 (sept, J_{PF} = 712 Hz, PF₆). IR (cm⁻¹, KBr): 1578 m [ν_s(CO)], 1513 m [ν_{as}(CC)], 1271w [ν_s(CC)], 839 s, 558 m [ν(PF₆)]. FABMS; *m/z*: 381 [M⁺]. Anal. found: C, 37.23; H, 4.66; P, 11.78%. C₁₆H₂₄F₆O₂P₂Ru requires: C, 36.58; H, 4.60; P, 11.79%.

8.2.57 Preparation of [Ru(η²-MeC(O)CHC(O)Me)(η¹:η⁶-Ph₂P(CH₂)₃Ph)]PF₆
(282)

Complex **282** was prepared in 96% yield, as a yellow-brown solid, from [RuCl₂(η¹:η⁶-Ph₂P(CH₂)₃Ph)] (**222**), sodium acetylacetonate and AgPF₆ in a similar way and worked up as described above for complex **281**.

¹H-NMR (300 MHz, CD₂Cl₂): δ 1.61 (s, 6H, CH(COMe)₂), 2.26 (m, 2H, H²), 2.61 (m, 2H, H³), 2.73 (m, 2H, H¹), 4.66 (s, 1H, CH(COMe)₂), 5.20 (d, 2H, J = 5.5 Hz, H⁵), 5.86 (t, 2H, J = 6 Hz, H⁶), 6.36 (t, 1H, J = 6 Hz, H⁷), 7.25-7.55 (m, 10H, PPh₂). ¹³C{¹H}-NMR (75.4 MHz, CD₂Cl₂): δ 20.67 (C²), 22.52 (d, ¹J_{PC} = 32 Hz, C¹), 26.68 (CH(COMe)₂), 30.50 (C³), 81.89 (CH(COMe)₂), 92.96 (d, J_{PC} = 4 Hz, C⁷), 94.52 (C⁵ or C⁶), 97.95 (d, J_{PC} = 11 Hz, C⁶ or C⁵), 101.37 (C⁴), 129.06 (d, J_{PC} = 10 Hz, PPh₂), 129.97 (d, J_{PC} = 47 Hz, PPh₂), 131.67 (d, J_{PC} = 3 Hz, PPh₂), 133.35 (d, J_{PC} = 10 Hz, PPh₂), 188.30 (CH(COMe)₂). ³¹P{¹H}-NMR (121.5 MHz, CD₂Cl₂): δ 27.2 (PPh₂), -143.8 (sept, J_{PF} = 712 Hz, PF₆). IR (cm⁻¹, KBr): 1577 m [ν_s(CO)], 1523 s [ν_{as}(CC)], 1276 w [ν_s(CC)] 838 s, 557 m [ν(PF₆)]. FABMS; *m/z*: 505 [M⁺]. Anal. found: C, 48.75; H, 4.66; P, 9.57%. C₂₆H₂₈F₆O₂P₂Ru requires: C, 48.08; H, 4.34; P, 9.54%.

8.2.58 Preparation of $[Ru(\eta^2-S_2CNMe_2)(\eta^1:\eta^6-Me_2P(CH_2)_3Ph)]PF_6$ (283)

Complex **283** was prepared from $[RuCl_2(\eta^1:\eta^6-Me_2P(CH_2)_3Ph)]$ (**248**), sodium dimethyldithiocarbamate dihydrate and $AgPF_6$ in a similar way. The reaction mixture was filtered through Celite and the solvents were removed *in vacuo*. The residue was extracted with CH_2Cl_2 , transferred to a column of neutral alumina (activity III), and the product was eluted with dichloromethane. The eluate was evaporated to dryness *in vacuo* and the title compound was isolated as a yellow solid (53%) by addition of *n*-hexane to a solution in CH_2Cl_2 .

1H -NMR (300 MHz, CD_2Cl_2): δ 1.41 (d, 6H, $J = 10$ Hz, PMe_2), 1.78 (m, 2H, H^2), 2.21 (m, 2H, H^3), 2.65 (m, 2H, H^1), 3.17 (s, 6H, S_2CNMe_2), 5.43 (d, 2H, $J = 6$ Hz, H^5), 5.90 (t, 2H, $J = 6$ Hz, H^6), 6.06 (t, 1H, $J = 6$ Hz, H^7). $^{13}C\{^1H\}$ -NMR (75.4 MHz, CD_2Cl_2): δ 13.57 (d, $^1J_{PC} = 36$ Hz, PMe_2), 21.33 (C^2), 26.07 (d, $^1J_{PC} = 32$ Hz, C^1), 30.68 (d, $^3J_{PC} = 2$ Hz, C^3), 38.74 (S_2CNMe_2), 84.48 (C^7), 94.18 (d, $J_{PC} = 4$ Hz, C^5 or C^6), 94.77 (d, $J_{PC} = 11$ Hz, C^6 or C^5), 100.30 (C^4), 212.23 (d, $J_{PC} = 3$ Hz, S_2CNMe_2). $^{31}P\{^1H\}$ -NMR (121.5 MHz, CD_2Cl_2): δ 12.3 (PMe_2), -143.9 (sept, $J_{PF} = 710$ Hz, PF_6). IR (cm^{-1} , KBr): 1543 m [$\nu(C=N)$], 1258 w [$\nu(CS_2)$], 836 s, 557 m [$\nu(PF_6)$]. FABMS; m/z : 402 [M^+]. Anal. found: C, 31.56; H, 4.40; N, 2.58%. $C_{14}H_{23}F_6NPRuS_2$ requires: C, 30.77; H, 4.24; N, 2.56%.

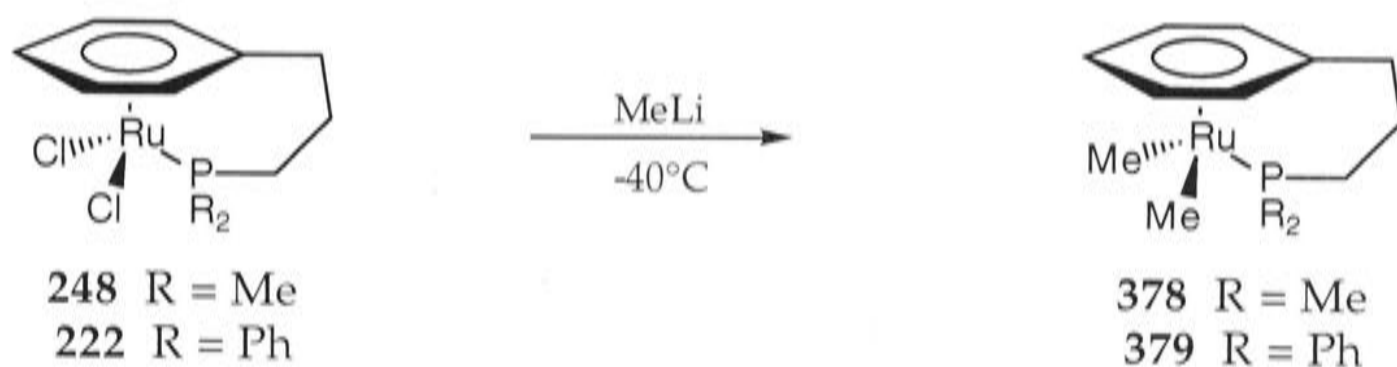
8.2.59 Preparation of $[Ru(\eta^2-S_2CNMe_2)(\eta^1:\eta^6-Ph_2P(CH_2)_3Ph)]PF_6$ (284)

Complex **284** was prepared in 60% yield, as a yellow solid, from $[RuCl_2(\eta^1:\eta^6-Ph_2P(CH_2)_3Ph)]$ (**222**), sodium dimethyldithiocarbamate

dihydrate and AgPF_6 in a similar way and worked up as described above for complex **283**.

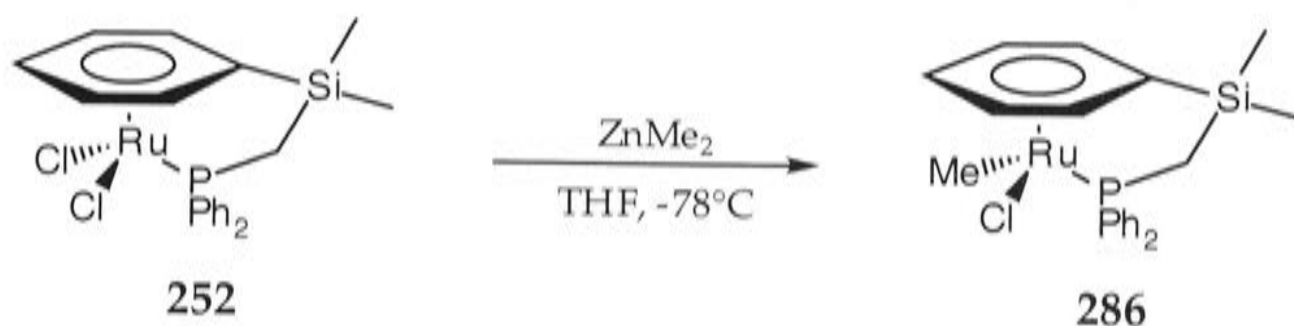
^1H -NMR (300 MHz, CD_2Cl_2): δ 2.02 (m, 2H, H^2), 2.51 (m, 2H, H^3), 2.56 (s, 6H, S_2CNMe_2), 2.74 (m, 2H, H^1), 5.51 (d, 2H, $J = 6$ Hz, H^5), 6.09 (t, 2H, $J = 6$ Hz, H^6), 6.27 (t, 1H, $J = 6$ Hz, H^7) 7.30-7.50 (m, 10H, PPh_2). $^{13}\text{C}\{^1\text{H}\}$ -NMR (75.4 MHz, CD_2Cl_2): δ 20.22 (C^2), 24.28 (d, $^1J_{\text{PC}} = 31$ Hz, C^1), 31.07 (C^3), 38.10 (S_2CNMe_2), 86.91 (C^7), 92.95 (d, $J_{\text{PC}} = 3$ Hz, C^5 or C^6), 95.84 (d, $J_{\text{PC}} = 10$ Hz, C^6 or C^5), 98.56 (C^4), 128.01 (d, $J_{\text{PC}} = 10$ Hz, PPh_2), 130.23 (d, $J_{\text{PC}} = 51$ Hz, PPh_2), 131.25 (d, $J_{\text{PC}} = 2$ Hz, PPh_2), 134.26 (d, $J_{\text{PC}} = 9$ Hz, PPh_2), 209.83 (d, $J_{\text{PC}} = 2$ Hz, S_2CNMe_2). $^{31}\text{P}\{^1\text{H}\}$ -NMR (121.5 MHz, CD_2Cl_2): δ 36.5 (PPh_2), -143.9 (sept, $J_{\text{PF}} = 712$ Hz, PF_6). IR (cm^{-1} , KBr): 1541 m [$\nu(\text{C}=\text{N})$], 1256 w [$\nu(\text{CS}_2)$], 835 s, 557 m [$\nu(\text{PF}_6)$]. FABMS; m/z : 526 [M^+]. Anal. found: C, 43.27; H, 4.41; N, 2.34%. $\text{C}_{24}\text{H}_{27}\text{F}_6\text{NPRuS}_2$ requires: C, 42.99; H, 4.06; N, 2.09%.

8.2.60 Attempted preparations of $[\text{RuMe}_2(\eta^1:\eta^6\text{-R}_2\text{P}(\text{CH}_2)_3\text{Ph})]$ ($\text{R} = \text{Me}$ (378), Ph (379))



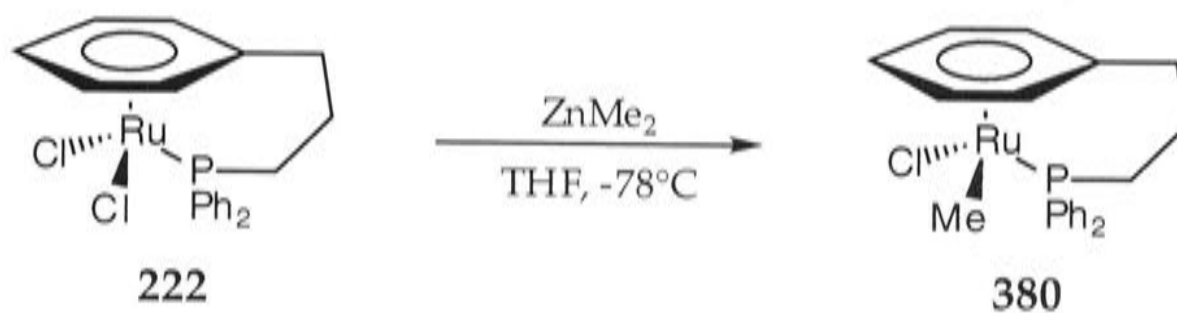
Reaction of the ruthenium complexes **248** and **222** with an excess of methyllithium in THF at -40°C and subsequent warming to room temperature gave insoluble brown solids that showed no identifiable signals in the ^1H or $^{31}\text{P}\{^1\text{H}\}$ -NMR spectra.

Various attempts, with dimethylzinc as the alkylating agent, using different reactant ratios, toluene in place of THF, and hydrolysing the reaction mixture, failed to give tractable products.

8.2.61 Attempted preparation of $[\text{RuCl}(\text{Me})(\eta^1:\eta^6\text{-Ph}_2\text{PCH}_2\text{SiMe}_2\text{Ph})]$ (**286**)

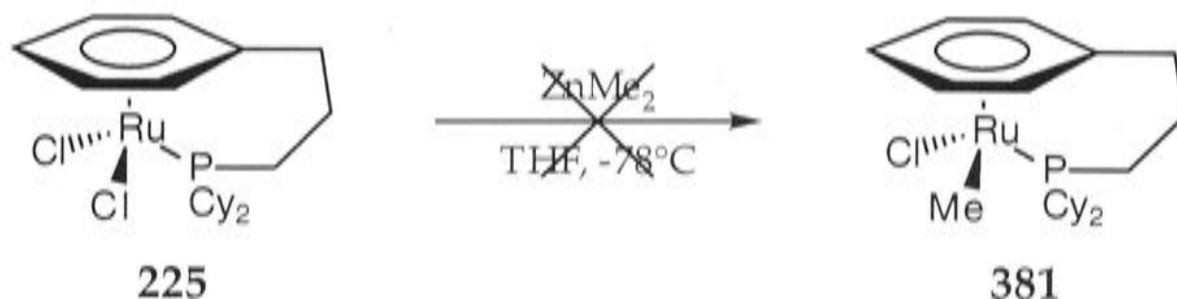
A solution of the ruthenium complex $[\text{RuCl}_2(\eta^1:\eta^6\text{-Ph}_2\text{PCH}_2\text{SiMe}_2\text{Ph})]$ (49 mg, 0.098 mmol) in dry THF (15 mL) at -78°C was treated dropwise with a solution of dimethylzinc in toluene (2.0 M, 49 μl , 0.1 mmol) and the reaction mixture was allowed to warm to room temperature. The solvent was removed *in vacuo* and the residue was washed with dry *n*-hexane (5 mL). The residue was dissolved in dry toluene (15 mL), filtered and the solvents were removed *in vacuo*. The residue was dissolved in dry THF (1 mL) and dry *n*-hexane (3 mL) was added. The solvents were removed *in vacuo* to afford a yellow solid, which may be **286**.

$^1\text{H-NMR}$ (400 MHz, C_6D_6): δ -0.32 (s, RuMe), -0.04 (s, 6H, C^2), 1.19 (d, 2H, $J = 9$ Hz, C^1), 5.55 (t, 2H, $J = 5.5$ Hz, H^5), 5.94 (d, 2H, $J = 6$ Hz, H^4), 6.02 (t, 1H, $J = 6$ Hz, H^6), 7.30-7.40 (m, 6H, PPh_2), 7.45-7.55 (m, 4H, PPh_2). $^{13}\text{C}\{-^1\text{H}\}$ -NMR (100.6 MHz, C_6D_6): δ -4.75 (d, $^1J_{\text{PC}} = 17$ Hz, RuMe), -3.04 (d, $^2J_{\text{PC}} = 9$ Hz, C^2), 29.45 (d, $^1J_{\text{PC}} = 17$ Hz, C^1), 87.24 (C^6), 89.54 (d, $^3J_{\text{PC}} = 13$ Hz, C^3), 98.30 (d, $J_{\text{PC}} = 6.5$ Hz, C^4 or C^5), 98.70 (d, $J_{\text{PC}} = 7.5$ Hz, C^5 or C^4), 130.26 (PPh_2), 132.33 (d, $J_{\text{PC}} = 9$ Hz, PPh_2), 133.93 (PPh_2), 135.17 (d, $J_{\text{PC}} = 11$ Hz, PPh_2). $^{31}\text{P}\{^1\text{H}\}$ -NMR (161.97 MHz, C_6D_6): δ 34.4. LSIMS; m/z : 471 $[\text{RuCl}(\eta^1:\eta^6\text{-Ph}_2\text{PCH}_2\text{SiMe}_2\text{Ph})]^+$.

8.2.62 Attempted preparation of $[\text{RuCl}(\text{Me})(\eta^1:\eta^6\text{-Ph}_2\text{P}(\text{CH}_2)_3\text{Ph})]$ (380)

The reaction of complex $[\text{RuCl}_2(\eta^1:\eta^6\text{-Ph}_2\text{P}(\text{CH}_2)_3\text{Ph})]$ (222) with dimethylzinc was carried out under similar conditions to those described for complex $[\text{RuCl}_2(\eta^1:\eta^6\text{-Ph}_2\text{PCH}_2\text{SiMe}_2\text{Ph})]$ (252) to afford an orange-brown oil that could not be purified, even by column chromatography. The ^1H NMR spectrum suggested that a Ru-Me bond might be present.

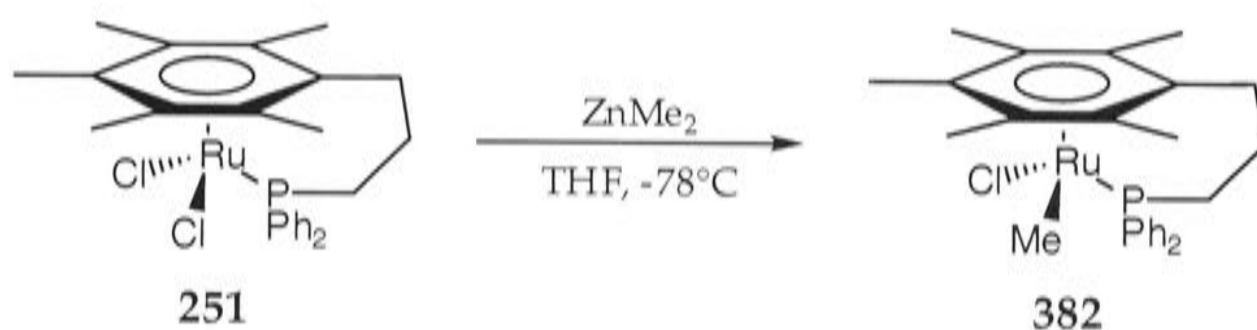
^1H -NMR (400 MHz, d_8 -toluene): δ 0.27 (s, RuMe), 4.33 (d, 2H, $J = 6$ Hz, H^5), 7.45-7.50 (m, 6H, PPh_2), 7.55-7.65 (m, 4H, PPh_2). $^{31}\text{P}\{^1\text{H}\}$ -NMR (161.97 MHz, d_8 -toluene): δ 19.6, 27.0, 28.5, 32.1, 47.5. LSIMS; m/z : 438 $[\text{Ru}(\eta^1:\eta^6\text{-Ph}_2\text{P}(\text{CH}_2)_3\text{Ph})]^+$.

8.2.63 Attempted preparation of $[\text{RuCl}(\text{Me})(\eta^1:\eta^6\text{-Cy}_2\text{P}(\text{CH}_2)_3\text{Ph})]$ (381)

The reaction of complex $[\text{RuCl}_2(\eta^1:\eta^6\text{-Cy}_2\text{P}(\text{CH}_2)_3\text{Ph})]$ (225) with dimethylzinc was carried out under similar conditions to those described for complex $[\text{RuCl}_2(\eta^1:\eta^6\text{-Ph}_2\text{PCH}_2\text{SiMe}_2\text{Ph})]$ (252) to give a brown solid that could not be crystallised. The ^1H NMR spectrum did not show any signals indicative of a Ru-Me bond.

^1H -NMR (400 MHz, d_8 -toluene): δ 1.3-1.9 (m), 3.2-4.1 (m). $^{31}\text{P}\{^1\text{H}\}$ -NMR (161.97 MHz, d_8 -toluene): δ 62.6. LSIMS; m/z : 455 $[\text{RuCl}(\eta^1:\eta^6\text{-Cy}_2\text{P}(\text{CH}_2)_3\text{Ph})]^+$, 420 $[\text{Ru}(\eta^1:\eta^6\text{-Cy}_2\text{P}(\text{CH}_2)_3\text{Ph})]^+$. Multi-nuclear NMR techniques failed to provide sufficient information about the nature of the product.

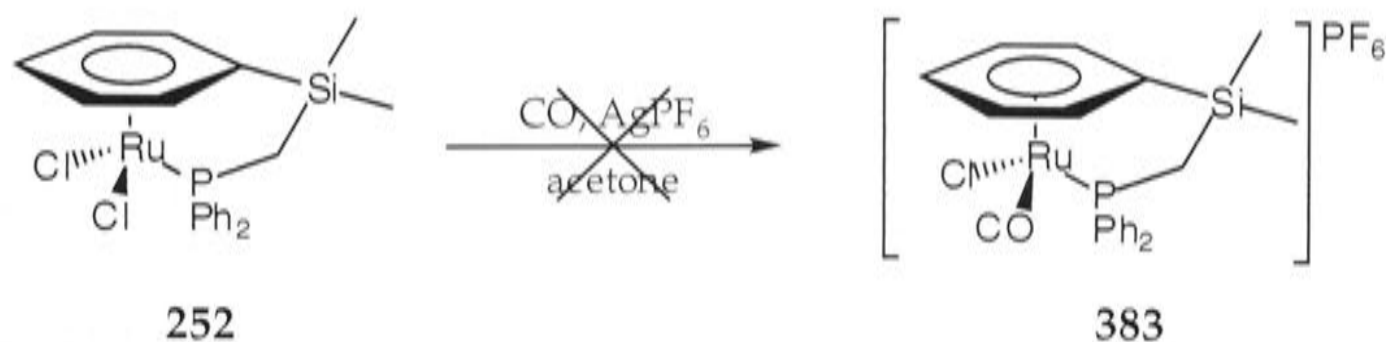
8.2.64 Attempted preparation of $[\text{RuCl}(\text{Me})(\eta^1:\eta^6\text{-Ph}_2\text{P}(\text{CH}_2)_3\text{C}_6\text{Me}_5)]$ (382)



The reaction of complex $[\text{RuCl}_2(\eta^1:\eta^6\text{-Ph}_2\text{P}(\text{CH}_2)_3\text{C}_6\text{Me}_5)]$ (251) with dimethylzinc was carried out under similar conditions to those described for complex $[\text{RuCl}_2(\eta^1:\eta^6\text{-Ph}_2\text{PCH}_2\text{SiMe}_2\text{Ph})]$ (252) to afford a brown oil that could not be crystallised. The ^1H NMR spectrum suggested that a Ru-Me bond might be present.

^1H -NMR (400 MHz, d_8 -toluene): δ 0.30 (s, RuMe). $^{31}\text{P}\{^1\text{H}\}$ -NMR (161.97 MHz, d_8 -toluene): δ 20.2, 25.4, 27.5, 29.2, 38.4. LSIMS; m/z : 511 $[\text{RuCl}(\eta^1:\eta^6\text{-Ph}_2\text{P}(\text{CH}_2)_3\text{C}_6\text{Me}_5)]^+$, 475 $[\text{Ru}(\eta^1:\eta^6\text{-Ph}_2\text{P}(\text{CH}_2)_3\text{C}_6\text{Me}_5)]^+$.

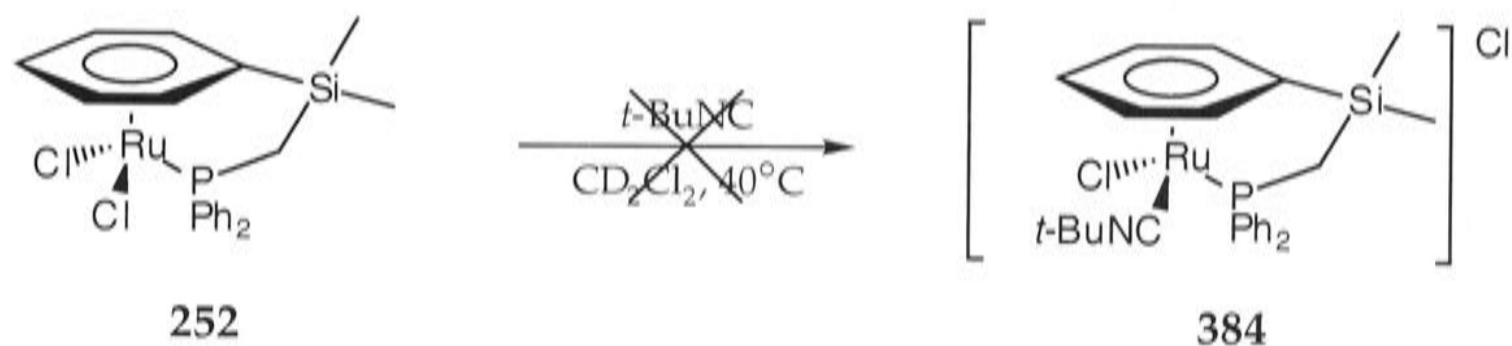
8.2.65 Attempted preparation of $[\text{RuCl}(\eta^1:\eta^6\text{-Ph}_2\text{PCH}_2\text{SiMe}_2)(\text{CO})]\text{PF}_6$ (383)



A solution of AgPF_6 (24 mg, 0.095 mmol) in dry acetone (5 mL) was added to a suspension of the ruthenium complex $[\text{RuCl}_2(\eta^1:\eta^6\text{-Ph}_2\text{CH}_2\text{SiMe}_2\text{Ph})]$, (252), (47 mg, 0.093 mmol) in dry acetone (10 mL) under an atmosphere of CO with the exclusion of light. The reaction mixture was stirred at room temperature for 1.5 h, filtered through Celite which was then washed with dry acetone (3×5 mL) whilst maintaining a CO atmosphere. The solvent was removed *in vacuo* to afford a yellow-brown oil. The appearance of several $\text{C}\equiv\text{O}$ stretching bands indicated that some η^6 -arene displacement had occurred.

IR (cm^{-1} , nujol): 2077, 1997 and 1963 [$\nu(\text{C}\equiv\text{O})$].

8.2.66 Attempted preparation of $[\text{RuCl}(\text{CN-}t\text{-Bu})(\eta^1:\eta^6\text{-Ph}_2\text{PCH}_2\text{SiMe}_2\text{Ph})]\text{Cl}$ (384)

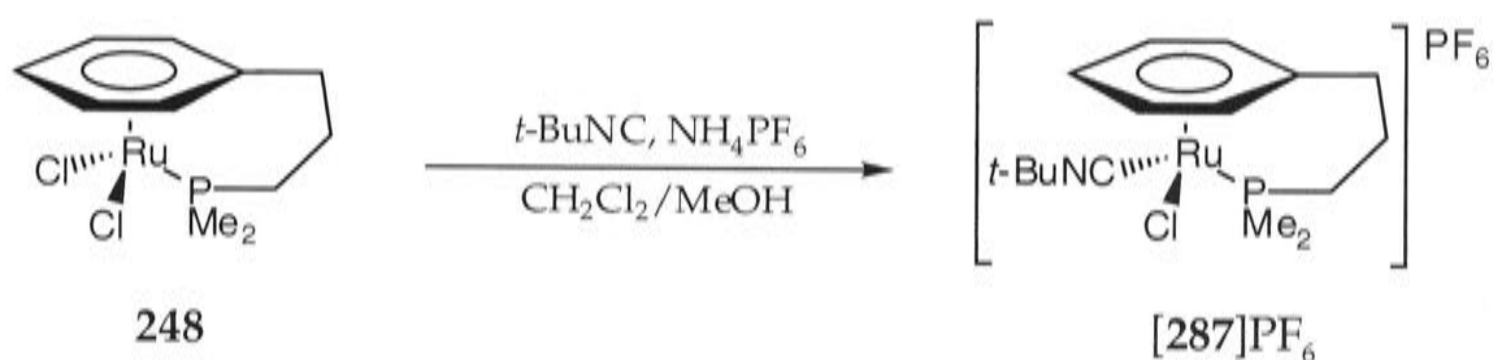


A solution of the ruthenium complex $[\text{RuCl}_2(\eta^1:\eta^6\text{-Ph}_2\text{PCH}_2\text{SiMe}_2\text{Ph})]$, (252), (14 mg, 0.028 mmol) and $t\text{-BuNC}$ (6 μl , 0.052 mmol) in d_2 -dichloromethane was heated to 40°C for 64 h. The NMR spectra showed partial formation of a new species derived from displacement of the η^6 -arene.

$^1\text{H-NMR}$ (300 MHz, CD_2Cl_2): δ 0.10 (s, H^2), 1.58 (CMe_3), 2.18 (d, $J = 15$ Hz, H^1), 7.25-7.40 (m, 3H, $\text{CH}_2\text{C}_6\text{H}_5$), 7.65-7.70 (m, 2H, $\text{CH}_2\text{C}_6\text{H}_5$). $^{31}\text{P}\{^1\text{H}\}\text{-NMR}$ (121.5 MHz, CD_2Cl_2): δ 20.0.

8.2.67 Attempted preparation of $[\text{RuCl}(\text{CN-}t\text{-Bu})(\eta^1:\eta^6\text{-Me}_2\text{P}(\text{CH}_2)_3\text{Ph})]\text{PF}_6$

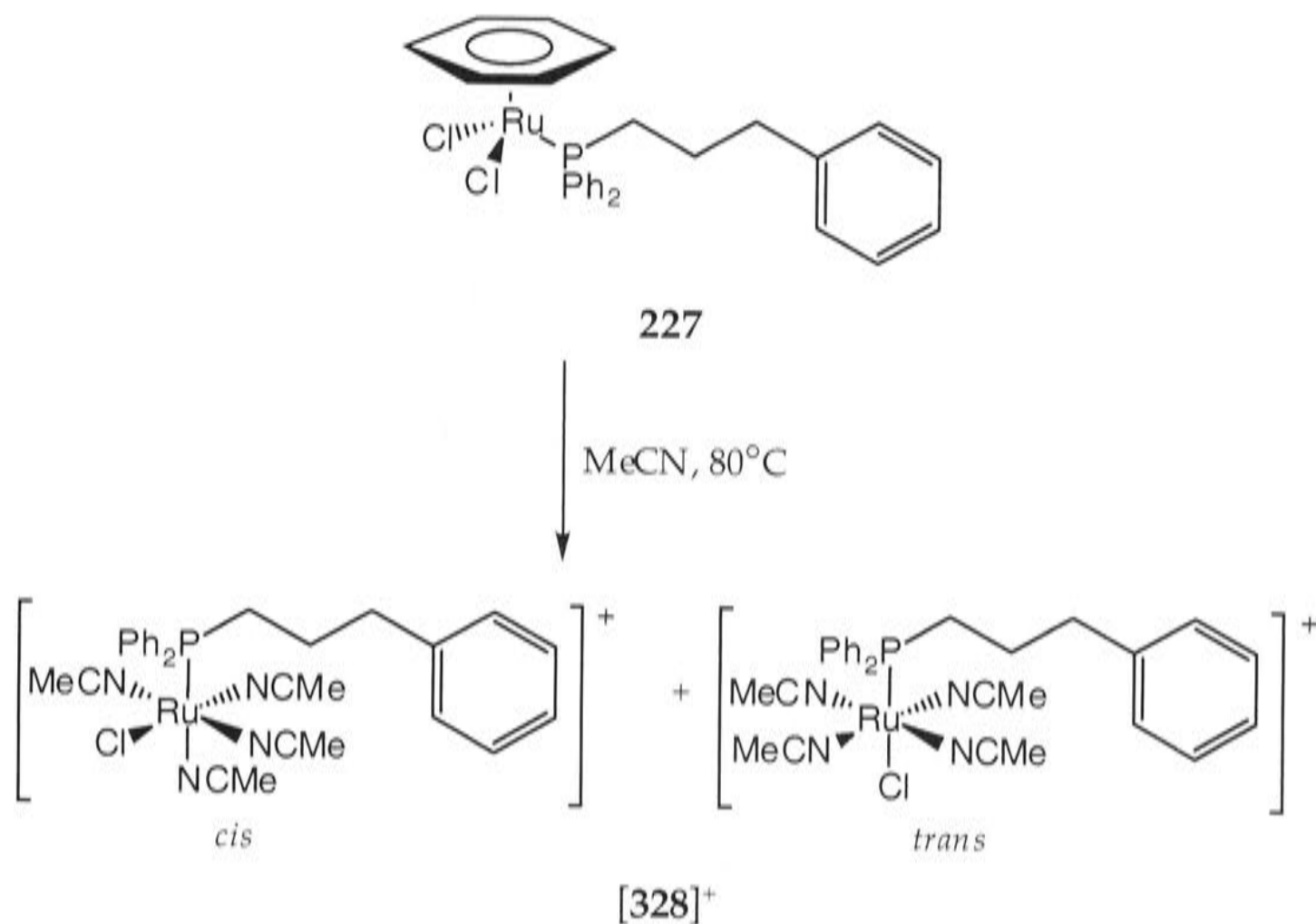
(287)



A solution of the ruthenium complex $[\text{RuCl}_2(\eta^1:\eta^6\text{-Me}_2\text{P}(\text{CH}_2)_3\text{Ph})]$, (**248**), (107 mg, 0.30 mmol), *t*-BuNC (34 μl , 0.30 mmol) and NH_4PF_6 (67 mg, 0.41 mmol) in dry dichloromethane (4 mL) and dry methanol (20 mL) was stirred at room temperature for 1.5 h. The NH_4Cl was precipitated from solution by addition of dry ether (20 mL) and the solution was filtered and the solvent was removed *in vacuo*. The solid was then dissolved in dry acetone (70 mL) and the solution was filtered through Celite. The solvent was removed *in vacuo* and the orange solid was washed with ether (3 \times 5 mL). The ^1H NMR spectrum was consistent with the presence of a mixture of $[\mathbf{287}]\text{PF}_6$ and unchanged **248**, in *ca* 1:3 ratio.

^1H -NMR (300 MHz, d_6 -acetone): δ 1.57 (s, CMe_3), 1.68 (d, $^1J_{\text{PH}} = 12$ Hz, PMe_2), 1.76-1.84 (m, H^2), 1.79 (d, $^1J_{\text{PH}} = 12$ Hz, PMe_2), 2.35 (m, H^3), 2.57 (m, H^1), 6.19 (t, $J = 6$ Hz), 6.51 (d, $J = 7$ Hz), 6.63 (t, $J = 5$ Hz).

8.2.68 Preparation of *cis*- and *trans*- $[\text{RuCl}(\text{NCMe})_4(\eta^1\text{-Ph}_2\text{P}(\text{CH}_2)_3\text{Ph})]^+$
 ($[\mathbf{328}]^+$) from the η^6 -Benzene Precursor $\mathbf{227}$ (a)



A solution of the ruthenium complex $[\text{RuCl}_2(\eta^6\text{-C}_6\text{H}_6)(\eta^1\text{-Ph}_2\text{P}(\text{CH}_2)_3\text{Ph})]$, ($\mathbf{227}$), (116 mg, 0.21 mmol) in dry acetonitrile (20 mL) was heated under reflux for 48 h. The solvent was then removed *in vacuo* to give quantitatively an oil containing *trans*- and *cis*- $[\mathbf{328}]\text{Cl}$ (δ_{p} 48.7 and 52.1, respectively, *ca* 5:1). X-ray quality crystals of *trans*- $[\mathbf{328}]\text{Cl}$ were obtained in 22% yield by layering a CH_2Cl_2 solution with ether.

$^1\text{H-NMR}$ (300 MHz, CD_2Cl_2): δ 1.59 (m, 2H, H^2), 2.28 (s, 12H, MeCN), 2.47 (m, 2H, H^1), 2.68 (t, 2H, $J = 7$ Hz, H^3), 7.10-7.50 (m, 15H, PPh_2 , Ph).

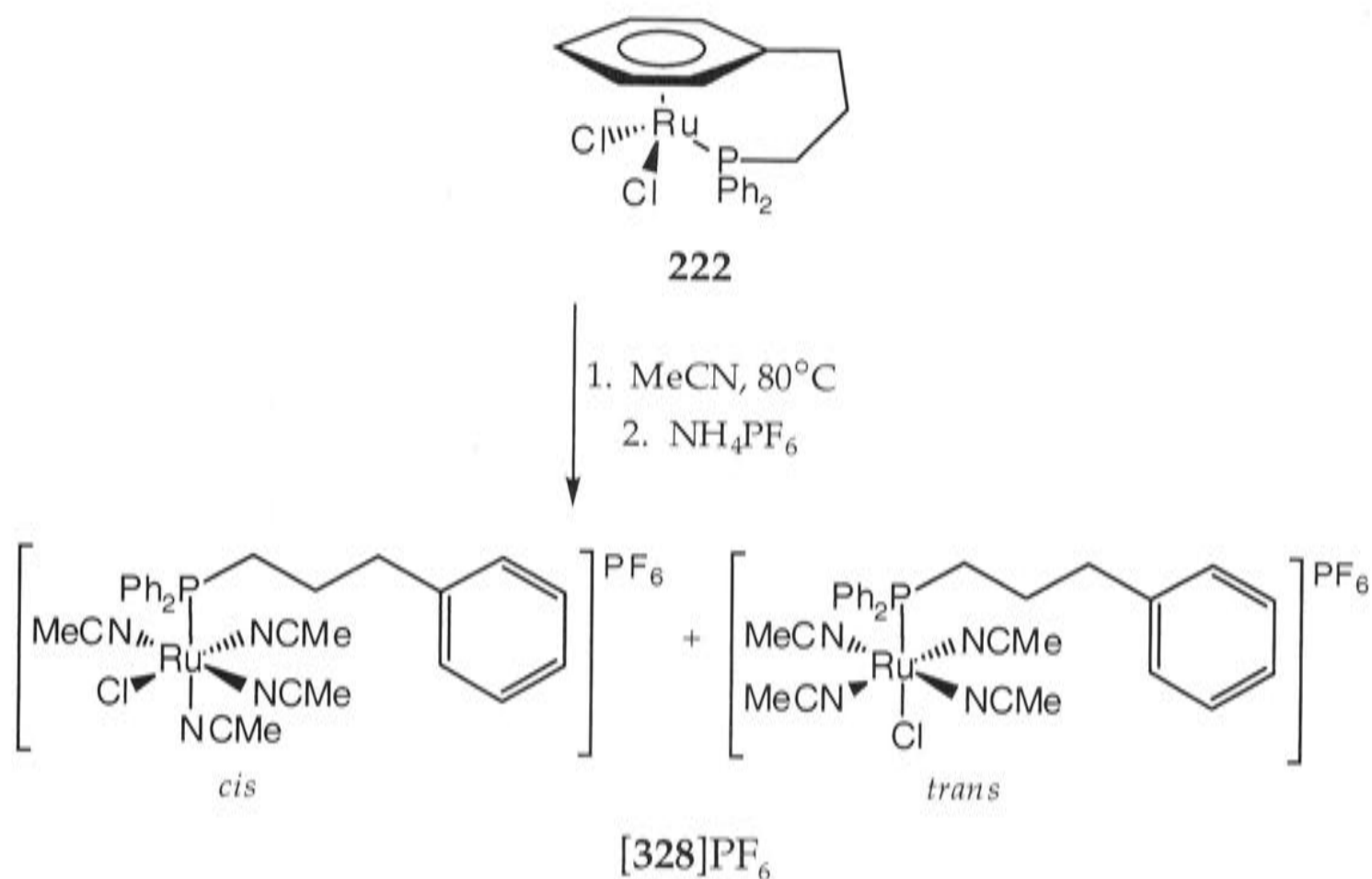
$^{13}\text{C}\{^1\text{H}\}\text{-NMR}$ (75.4 MHz, CD_2Cl_2): δ 4.87 (MeCN), 25.61 (d, $^2J_{\text{PC}} = 7$ Hz, C^2), 27.17 (d, $^1J_{\text{PC}} = 29$ Hz, C^1), 36.88 (d, $^3J_{\text{PC}} = 14$ Hz, C^3), 124.68 (MeCN), 126.47 (C^7), 128.77, 128.87, 129.00, 129.13 (C^5 , C^6 , PPh_2), 130.79 (d, $J_{\text{PC}} = 3$ Hz, PPh_2), 132.74 (d, $J_{\text{PC}} = 9$ Hz, PPh_2), 141.59 (C^4). $^{31}\text{P}\{^1\text{H}\}\text{-NMR}$ (121.5 MHz, CD_2Cl_2): δ 48.1. IR (cm^{-1} , KBr and polythene): 2285 w [$\nu(\text{CN})$], 303 m [$\nu(\text{Ru-Cl})$].

FABMS; m/z : 605 [M^+]. Λ_{m} (MeNO_2): 51.5 $\text{S cm}^2 \text{mol}^{-1}$.

The *cis*- and *trans*-isomers of compound [328]PF₆ were obtained by heating [RuCl₂(η⁶-C₆H₆)(η¹-Ph₂P(CH₂)₃Ph)] (227) in dry acetonitrile (40 mL) at 80°C for 48 h. The solvent was removed *in vacuo*, the residue was dissolved in dichloromethane and NH₄PF₆ (60 mg, 0.37 mmol) was then added. The solution was filtered and the volume of solvent was reduced *in vacuo*. The title compound *cis*- and *trans*-[328]PF₆ was obtained as a pale yellow solid (215 mg, 82%) by addition of ether to a solution in CH₂Cl₂. Analysis of resonances in the ³¹P{¹H}-NMR spectrum showed the compound to be a mixture of *cis*- and *trans*- isomers in the ratio of 1:5.

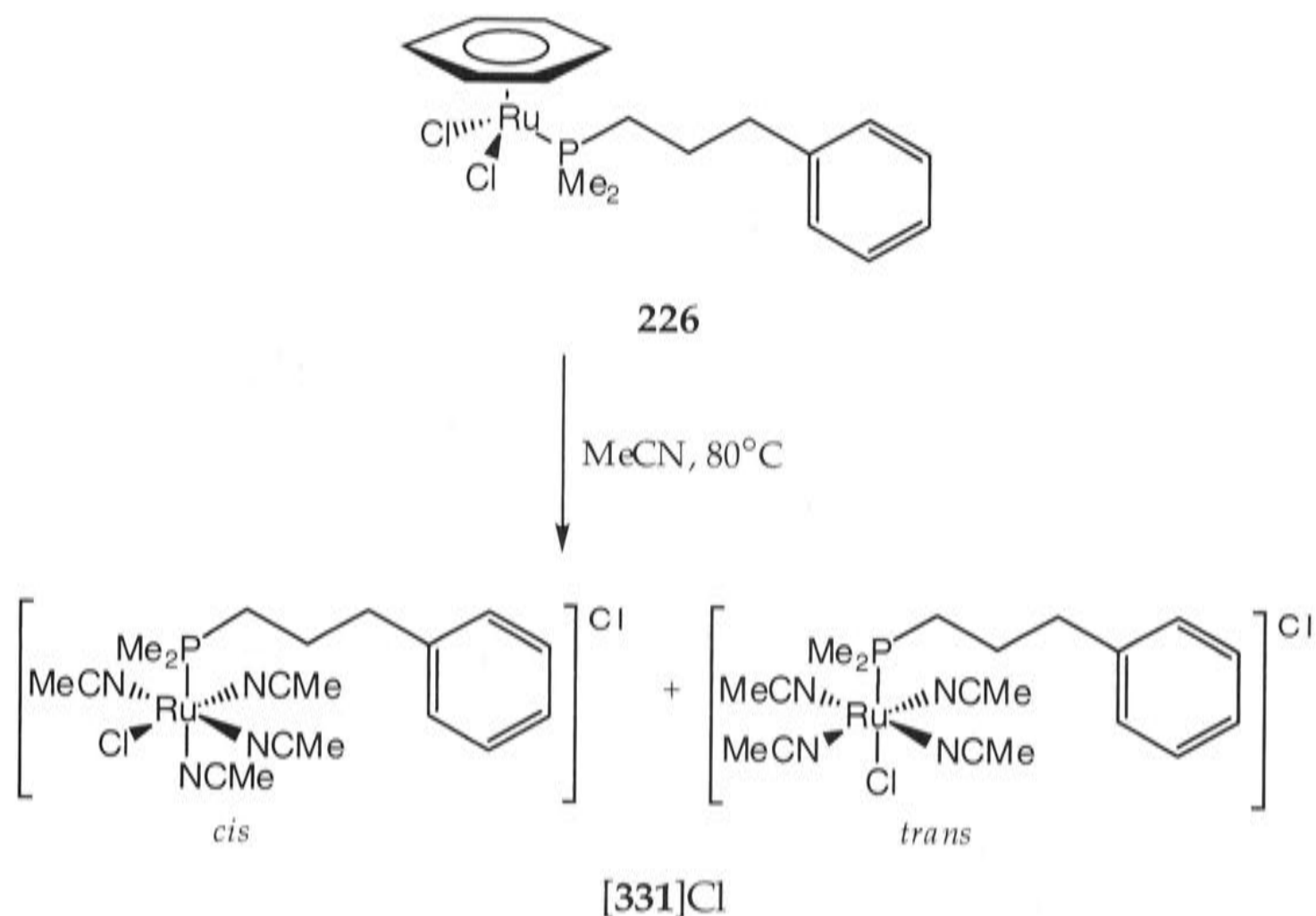
¹H-NMR (300 MHz, CD₃CN): δ 1.46-1.57 (m, 12H, H²), 2.11 (s, 3H, *cis*-MeCN), 2.15 (s, 66H, *trans*-, *cis*-MeCN), 2.19 (s, 3H, *cis*-MeCN), 2.41-2.65 (m, 24H, H¹, H³), 7.05-7.60 (m, 90H, PPh₂, Ph). ¹³C{¹H}-NMR (75.4 MHz, CD₃CN): δ 3.93 (*cis*-MeCN), 3.96 (*cis*-MeCN), 4.06 (*trans*-MeCN), 4.13 (*cis*-MeCN), 26.00 (d, ²J_{PC} = 7 Hz, C²), 26.27 (d, ²J_{PC} = 14 Hz, C²), 27.35 (d, ¹J_{PC} = 30 Hz, C¹), 27.39 (d, ¹J_{PC} = 27 Hz, C¹), 37.18 (d, ³J_{PC} = 13 Hz, C³), 37.28 (d, ³J_{PC} = 13 Hz, C³), 125.04 (*cis*-MeCN), 125.07 (*cis*-MeCN), 125.12 (*cis*-MeCN), 125.48 (*trans*-MeCN), 126.86 (C⁷ or PPh₂), 127.08 (C⁷ or PPh₂), 127.10 (C⁷ or PPh₂), 129.08 (d, J_{PC} = 10 Hz, PPh₂), 129.34 (C⁵ or C⁶), 129.41 (PPh₂), 129.54 (C⁵ or C⁶), 130.93 (C⁶ or C⁵), 131.24 (C⁵ or C⁶), 132.55 (d, J_{PC} = 46 Hz, PPh₂), 132.69 (d, J_{PC} = 46 Hz, PPh₂), 133.44 (d, J_{PC} = 9 Hz, PPh₂), 133.85 (d, J_{PC} = 9 Hz, PPh₂), 142.40 (C⁴), 142.69 (C⁴). ³¹P{¹H}-NMR (121.5 MHz, CD₃CN): δ 46.4 (*cis*-, PPh₂), 48.7 (*trans*-, PPh₂), -143.1 (sept, J_{PF} = 707 Hz, PF₆). IR (cm⁻¹, KBr and polythene): 2285 w [ν(CN)] 840 s, 557 m [ν(PF₆)], 303 s [ν(Ru-Cl)]. Anal. found: C, 44.68; H, 4.56; N, 6.96%. C₂₉H₃₃ClF₆N₄P₂Ru.0.5CH₂Cl₂: requires C, 44.71; H, 4.32; N, 7.07%. The presence of dichloromethane was evident in the ¹H NMR spectrum. Λ_m (MeNO₂): 55.5 S cm² mol⁻¹.

8.2.69 Preparation of *cis*- and *trans*-[RuCl(Ph₂P(CH₂)₃Ph)(η¹-NCMe)₄]PF₆ ([328]PF₆) from the Tethered Precursor 222 (b)



The *cis*- and *trans*-isomers of compound [328]PF₆ were prepared in 67% yield, as a pale yellow solid, by heating complex [RuCl₂(η¹:η⁶-Ph₂P(CH₂)₃Ph)] (222) in dry acetonitrile at 80°C for 264 h. Addition of NH₄PF₆ afforded the salt [328]PF₆. Analysis of resonances in the ³¹P{¹H}-NMR spectrum showed the compound to be a mixture of *cis*- and *trans*- isomers in the ratio of *ca* 2:1.

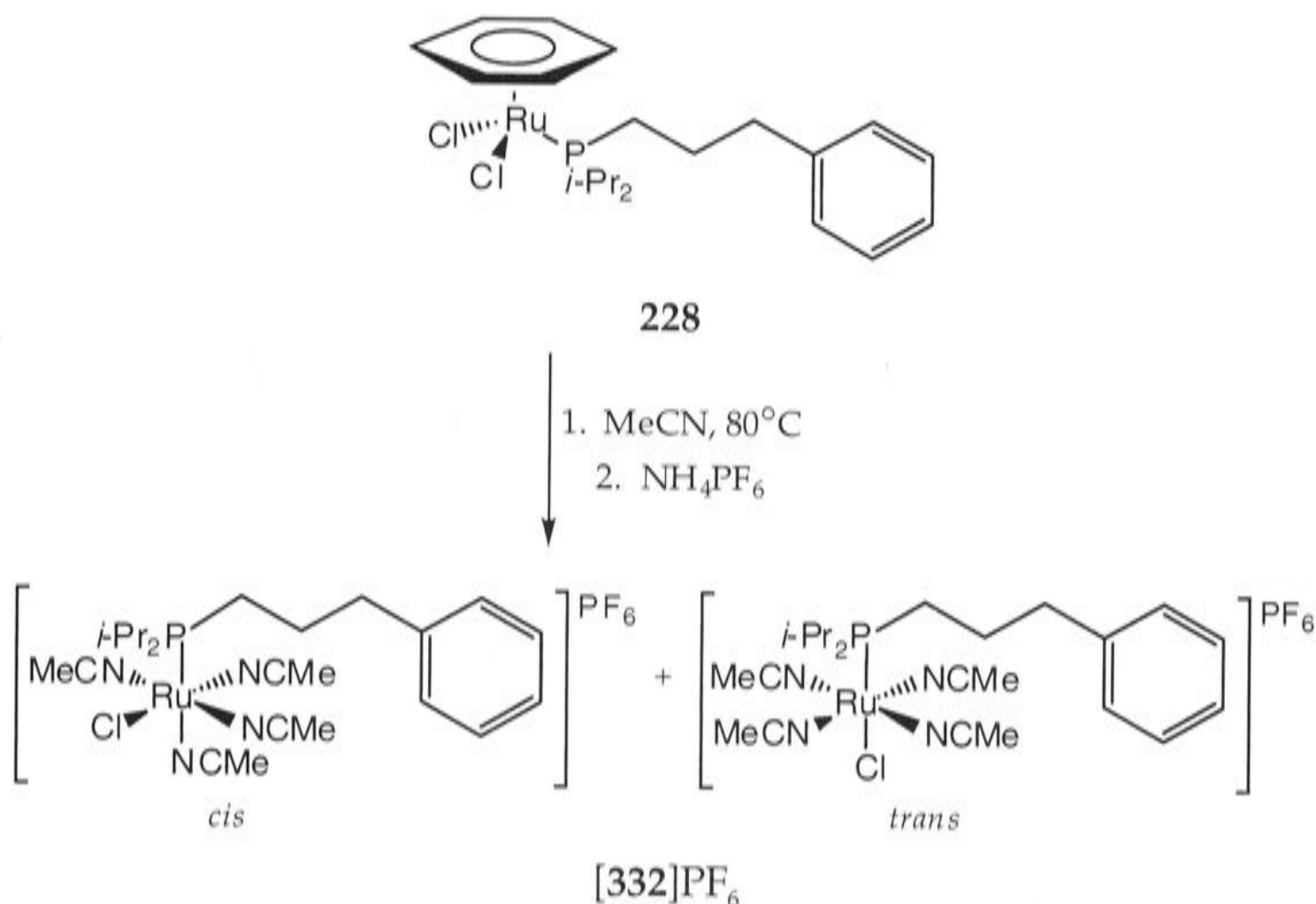
8.2.70 Preparation of *cis*- and *trans*-[RuCl(NCMe)₄(η¹-Me₂P(CH₂)₃Ph)]PF₆
 ([331]Cl) from the η⁶-Benzene Precursor 226



A solution of the ruthenium complex [RuCl₂(η⁶-C₆H₆)(η¹-Me₂P(CH₂)₃Ph)] (226) in dry acetonitrile was heated at reflux for 48 h. The solvent was removed *in vacuo*, to afford the title compound as an uncrystallisable yellow oil. Analysis of resonances in the ³¹P{¹H}-NMR spectrum showed the compound to be a mixture of isomers.

¹H-NMR (300 MHz, CD₃CN): δ 1.36 (d, 6H, ¹J_{PH} = 10 Hz, PMe₂), 1.44 (d, 6H, ¹J_{PH} = 10 Hz, PMe₂), 1.81 (m, 2H, H²), 2.28 (s, MeCN), 2.29 (s, MeCN), 2.41 (s, MeCN) (12H, *ca* 6:4:5), 2.47 (m, 2H, H¹), 2.66 (m, 2H, H³), 7.10-7.20 (m, 5H, PPh₂). ¹³C{¹H}-NMR (75.4 MHz, CD₃CN): δ 4.39 (MeCN), 4.52 (MeCN), 12.14 (d, ¹J_{PC} = 5.5 Hz, PMe₂), 12.54 (d, ¹J_{PC} = 5.5 Hz, PMe₂), 25.72 (C₂), 28.56 (d, ¹J_{PC} = 30 Hz, C¹), 37.59 (d, ³J_{PC} = 30 Hz, C³), 124.45 (MeCN), 124.73 (MeCN), 126.72 (C⁷), 127.84 (C⁷), 129.29 (C⁵ or C⁶), (129.43 (C⁶ or C⁵), 142.62 (C⁴), 142.78 (C⁴). ³¹P{¹H}-NMR (121.5 MHz, CD₃CN): δ 29.4, 32.4 *ca* 5:3.

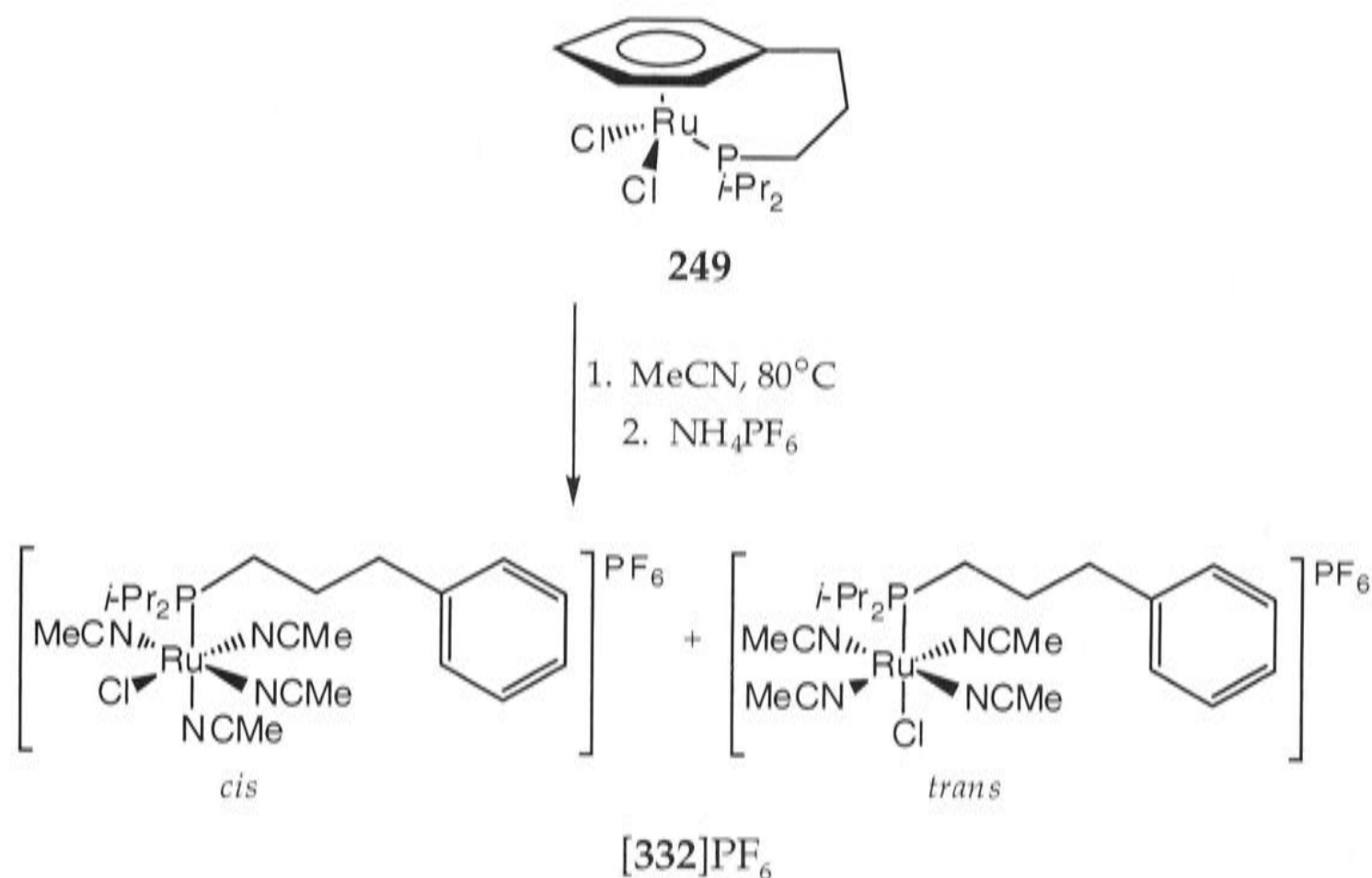
8.2.71 Preparation of *cis*- and *trans*-[RuCl(NCMe)₄(η¹-*i*-Pr₂P(CH₂)₃Ph)]PF₆ ([332]PF₆) from the η⁶-Benzene Precursor 228 (a)



The *cis*- and *trans*-isomers of compound [332]PF₆ were prepared in 87% yield, as a pale yellow solid, by heating complex [RuCl₂(η⁶-C₆H₆)(η¹-*i*-Pr₂P(CH₂)₃Ph)] (228) in dry acetonitrile at 80°C for 24 h. Addition of NH₄PF₆ afforded the salt [332]PF₆. Analysis of resonances in the ³¹P{¹H}-NMR spectrum showed the compound to be a mixture of isomers. ¹H-NMR (300 MHz, CD₃CN): δ 1.04-1.18 (m, 12H, PCHMe₂), 1.78-1.91 (m, 6H, H¹, H², PCHMe₂), 2.34 (s, MeCN), 2.38 (s, MeCN) (12H, *ca* 3:1), 2.71 (m, 2H, H³), 7.15-7.20 (m, 6H, PPh₂), 7.25-7.30 (m, 5H, PPh₂). ¹³C{¹H}-NMR (75.4 MHz, CD₃CN): δ 4.28 (MeCN), 15.84 (d, ²J_{PC} = 17 Hz, PCHMe₂), 18.07 (d, ²J_{PC} = 26 Hz, PCHMe₂), 21.67 (d, ¹J_{PC} = 25 Hz, C¹), 22.38 (d, ²J_{PC} = 23 Hz, C¹), 24.47 (d, ¹J_{PC} = 27 Hz, PCHMe₂), 25.06 (d, ¹J_{PC} = 25 Hz, PCHMe₂), 27.10 (d, ²J_{PC} = 6 Hz, C²), 27.33 (d, ²J_{PC} = 5 Hz, C²), 37.55 (d, ³J_{PC} = 11 Hz, C³), 37.78 (d, ³J_{PC} = 11 Hz, C³), 125.80 (*trans*-MeCN), 126.83 (C⁷), 126.95 (C⁷), 127.43 (*cis*-MeCN), 129.37 (C⁵ or C⁶), 129.44 (C⁶ or C⁵), 129.52 (C⁵ or C⁶), 129.65 (C⁶ or C⁵), 142.47 (C⁴), 142.62 (C⁴). ³¹P{¹H}-NMR (121.5 MHz, CD₃CN): δ 52.8 (P-*i*-Pr₂), 54.2

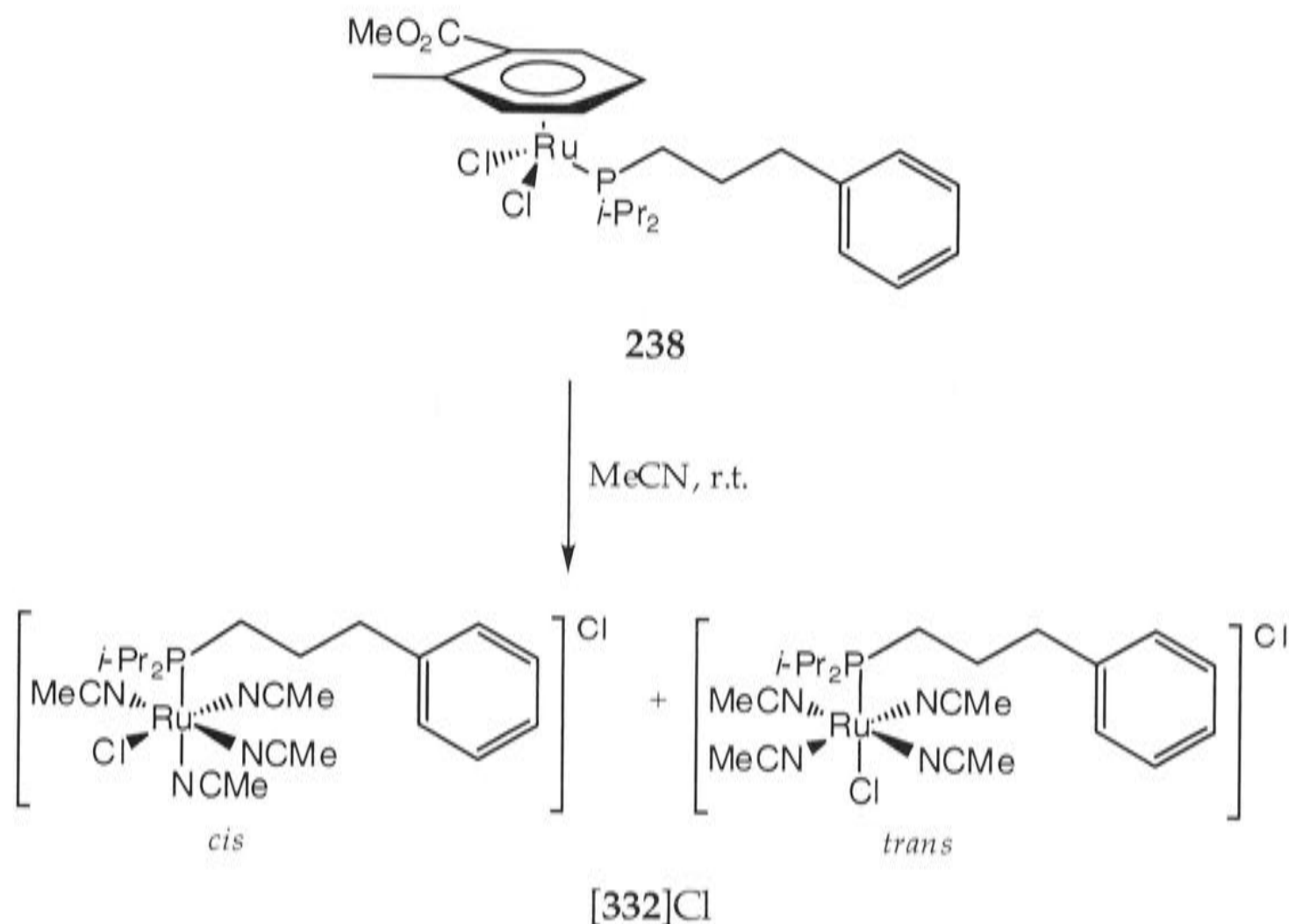
(P-*i*-Pr₂) [*ca* 1:2], -143.1 (sept, $J_{\text{PF}} = 707$ Hz, PF₆). FABMS; m/z : 537 [M]⁺. Anal. found: C, 40.06; H, 5.54; N, 7.13%. C₂₃H₃₇ClF₆N₄P₂Ru: requires C, 40.50; H, 5.57; N, 8.21%.

8.2.72 Preparation of *cis*- and *trans*-[RuCl(NCMe)₄(η¹-*i*-Pr₂P(CH₂)₃Ph)]PF₆ ([332]PF₆) from the Tethered Precursor 249 (b)



The *cis*- and *trans*-isomers of compound [332]PF₆ were prepared in 85% yield by heating complex [RuCl₂(η¹:η⁶-*i*-Pr₂P(CH₂)₃Ph)] (222) in dry acetonitrile at 80°C for 465 h. Addition of NH₄PF₆ afforded the salt [332]PF₆. The isomer ratio (*ca* 2:1) differed from that in (a).

8.2.73 Preparation of *cis*- and *trans*-[RuCl(NCMe)₄(η¹-*i*-Pr₂P(CH₂)₃Ph)]Cl ([332]Cl) from the η⁶-Methyl *o*-toluate Precursor 238

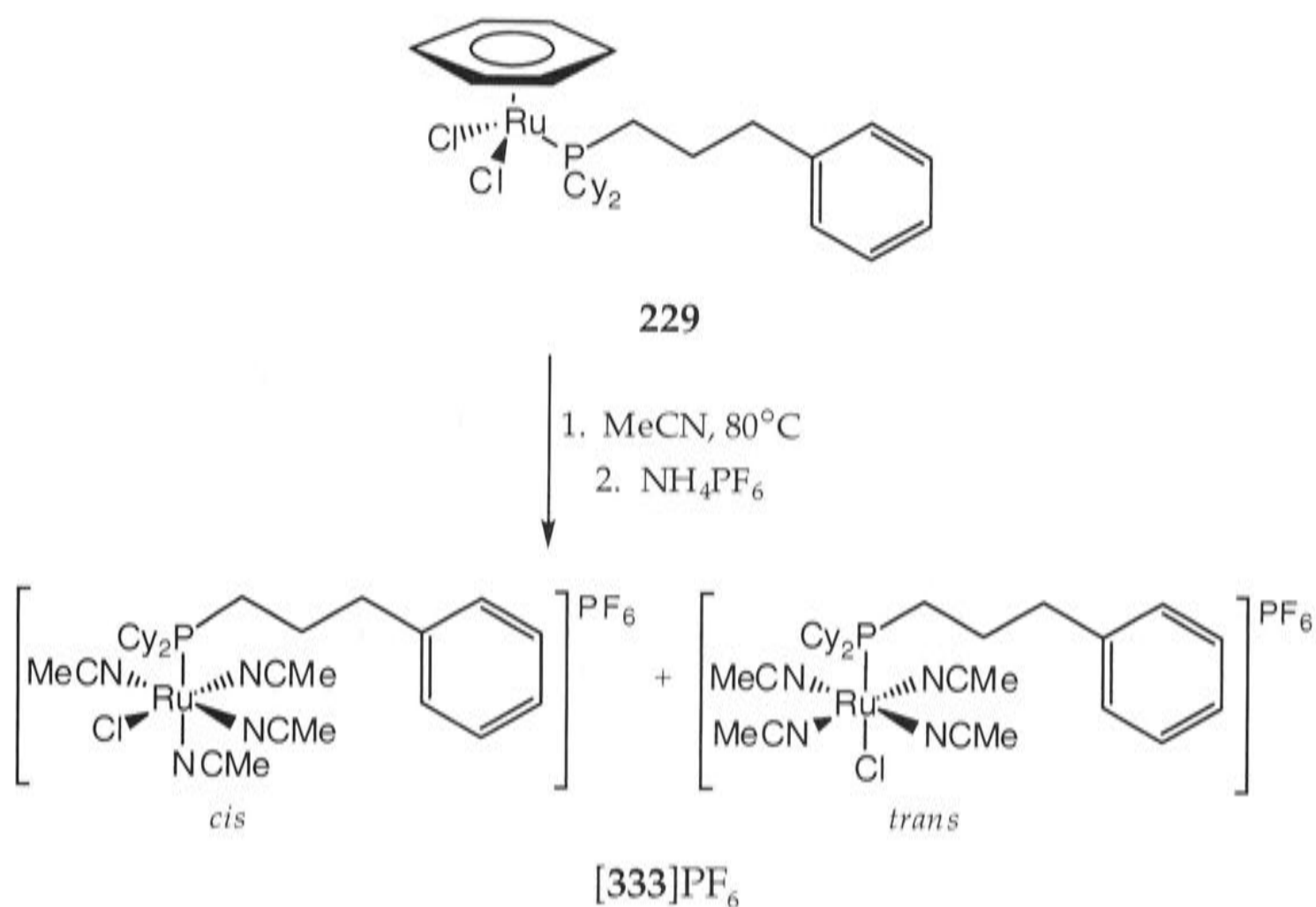


A solution of the ruthenium complex [RuCl₂(η⁶-1,2-MeC₆H₄CO₂Me)(η¹-*i*-Pr₂P(CH₂)₃Ph)] in dry acetonitrile was stirred for 96 h. The solvent was removed *in vacuo* and the title compound was isolated as an uncrystallisable yellow oil. Analysis of resonances in the ³¹P{¹H}-NMR spectrum showed the compound to be a mixture of isomers.

³¹P{¹H}-NMR (121.5 MHz, CD₃CN): δ 54.3 (P-*i*-Pr₂), 56.3 (P-*i*-Pr₂), *ca* 2:1.

A separate reaction mixture was heated at 80°C for 1 h, giving a different isomer ratio (*ca* 1:1).

8.2.74 Preparation of *cis*- and *trans*-[RuCl(NCMe)₄(η¹-Cy₂P(CH₂)₃Ph)]PF₆ ([333]PF₆) from the η⁶-Benzene Precursor **229** (a)

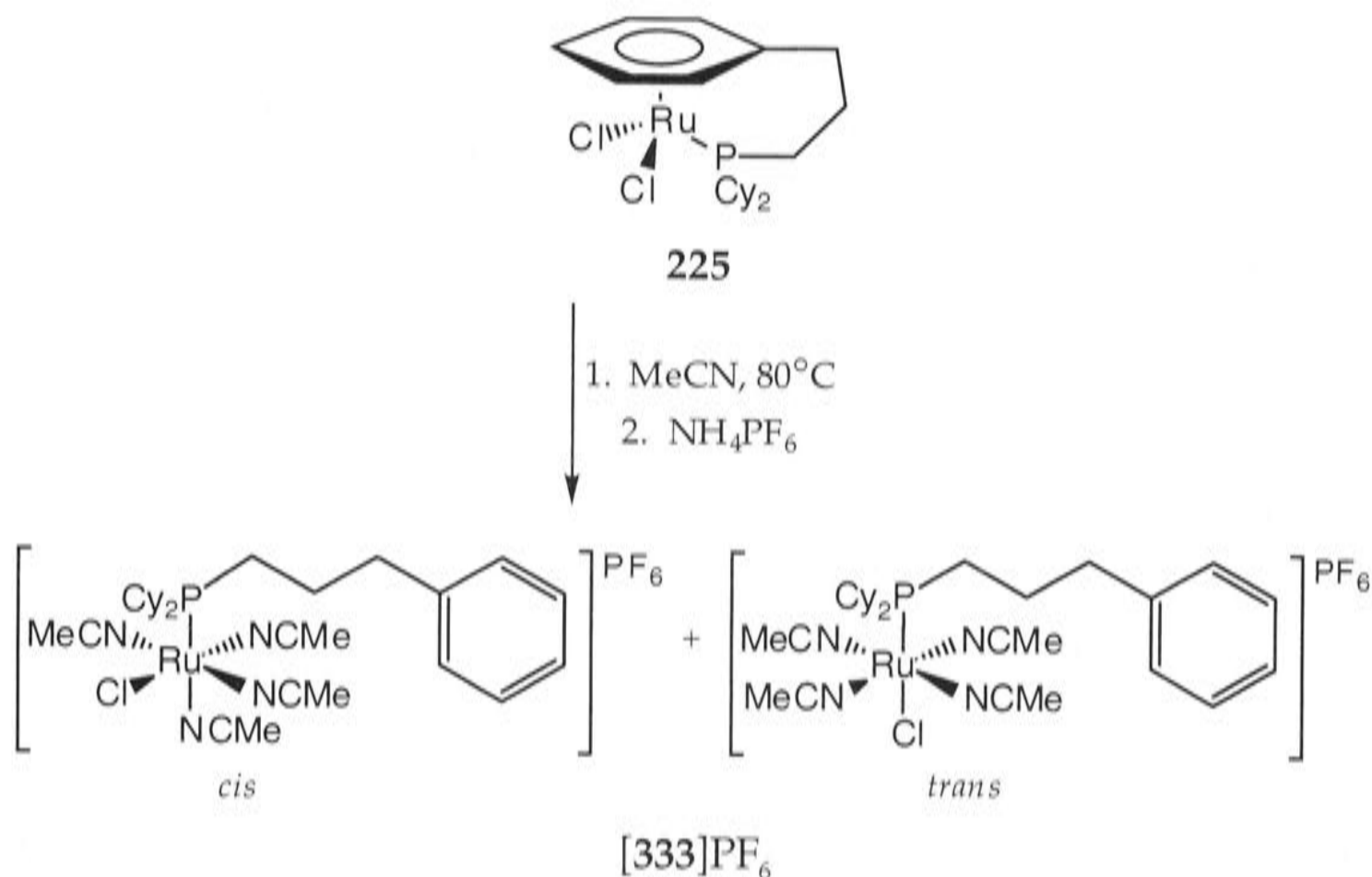


The *cis*- and *trans*-isomers of [333]PF₆ were prepared in 93% yield, as a pale yellow solid, by heating complex [RuCl₂(η⁶-C₆H₆)(η¹-Cy₂P(CH₂)₃Ph)] (**229**) in dry acetonitrile at 80°C for 24 h. Addition of NH₄PF₆ afforded the salt [333]PF₆. Analysis of resonances in the ³¹P{¹H}-NMR spectrum showed the compound to be a mixture of isomers.

¹H-NMR (300 MHz, CD₃CN): δ 1.24-1.40 (m, 10H, Cy), 1.70-1.80 (m, 14H, Cy), 1.87-1.90 (m, 2H, H²), 2.02-2.10 (m, 2H, H¹), 2.33 (s, MeCN), 2.39 (s, MeCN) (12H, *ca* 9:8) 2.69-2.74 (m, 2H, H³), 7.20-7.25 (m, 6H, Ph), 7.30-7.35 (m, 4H, Ph). ¹³C{¹H}-NMR (75.4 MHz, CD₃CN): δ 4.14 (MeCN), 4.33 (MeCN), 21.29 (d, ²J_{PC} = 25 Hz, C²), 22.00 (d, ²J_{PC} = 23 Hz, C²), 27.09, 27.22, 27.45, (d, J_{PC} = 5 Hz), 27.68, 27.81, 27.90, 27.96, 28.02, 28.43 (Cy, C¹), 34.49 (d, ¹J_{PC} = 24 Hz, Cy), 35.22 (d, ¹J_{PC} = 24 Hz, Cy), 37.42 (d, ³J_{PC} = 11 Hz, C³), 37.65 (d, ³J_{PC} = 11 Hz, C³), 125.66 (MeCN), 126.97 (C⁷), 127.03 (C⁷), 127.32 (MeCN), 129.34 (C⁵ or C⁶), 129.72 (C⁶ or C⁵), 142.47 (C⁴), 142.62 (C⁴). ³¹P{¹H}-NMR (121.5 MHz, CD₃CN): δ 42.8 (PCy₂), 44.4 (PCy₂) [*ca* 5:6], -143.9 (sept, J_{PF} = 708

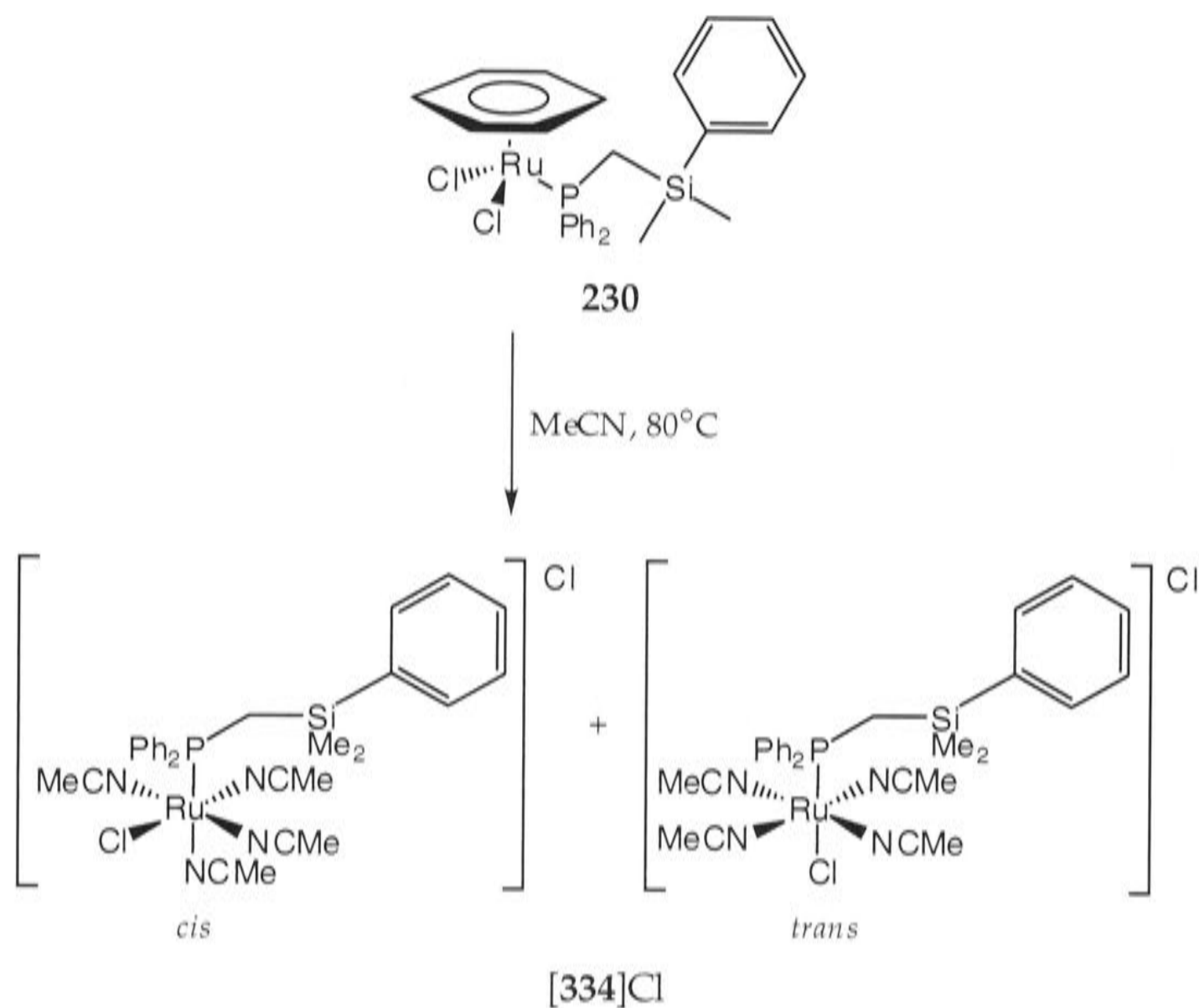
Hz, PF₆). FABMS; *m/z*: 576 [M⁺]. Anal. found: C, 43.66; H, 5.66; N, 6.99%. C₂₉H₄₅ClF₆N₄P₂Ru.0.5CH₂Cl₂: requires C, 43.72; H, 5.73; N, 6.89%. The presence of dichloromethane was evident in the ¹H NMR spectrum.

8.2.75 Preparation of *cis*- and *trans*-[RuCl(NCMe)₄(η¹-Cy₂P(CH₂)₃Ph)]PF₆ ([333]PF₆) from the Tethered Precursor 225 (b)



The *cis*- and *trans*-isomers of [333]PF₆ were prepared in 82% yield by heating complex [RuCl₂(η¹:η⁶-Cy₂P(CH₂)₃Ph)] (225) in dry acetonitrile at 80°C for 384 h. Addition of NH₄PF₆ afforded the salt [333]PF₆. The isomer ratio (*ca* 7:4) differed from that in (a).

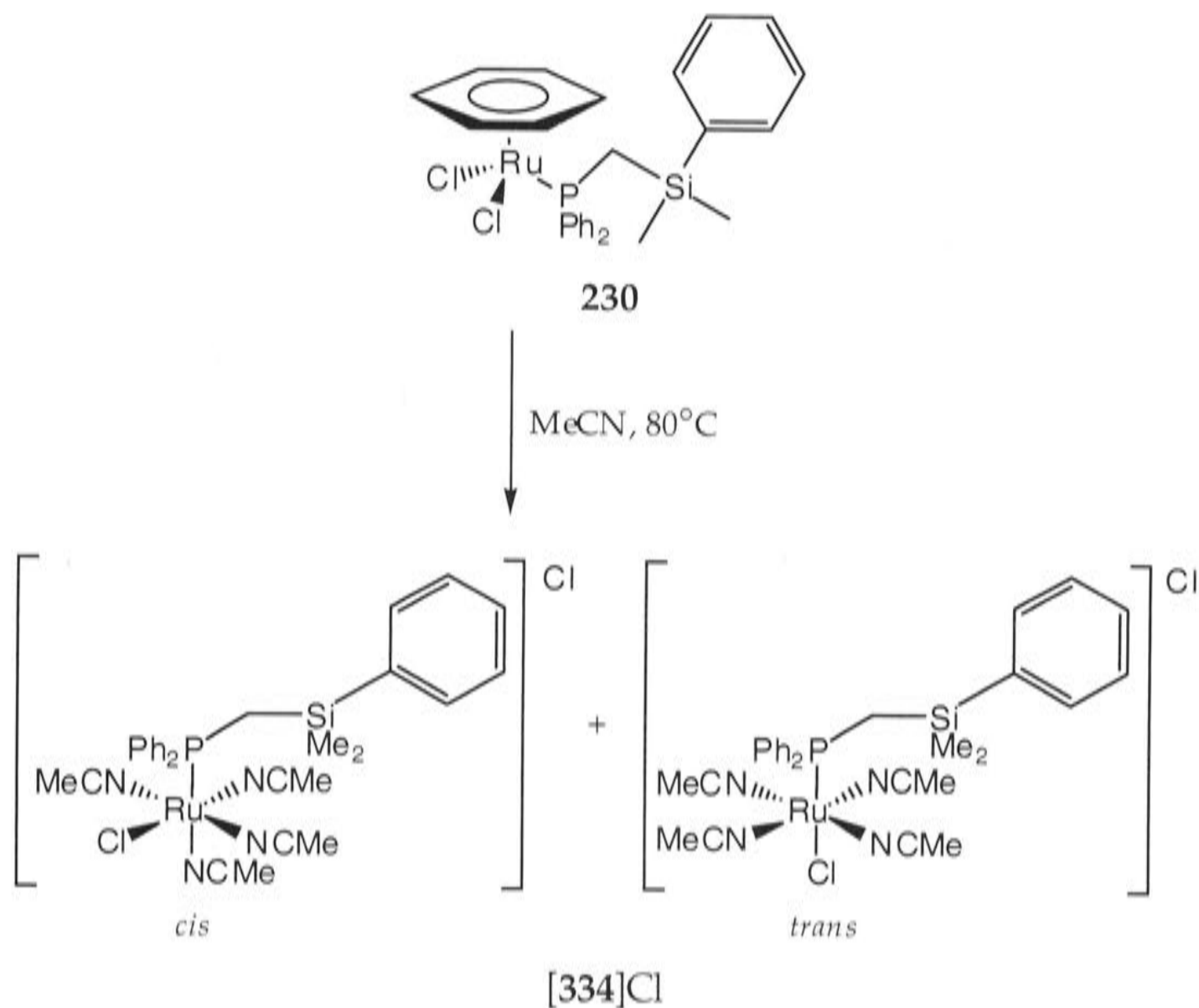
8.2.76 Preparation of *cis*- and *trans*-[RuCl(NCMe)₄(η¹-Ph₂PCH₂SiMe₂Ph)]Cl ([334]Cl) from the η⁶-Benzene Precursor 230 (a)



A solution of the ruthenium complex [RuCl₂(η⁶-C₆H₆)(η¹-Ph₂PCH₂SiMe₂Ph)] (230) in dry acetonitrile was heated at reflux for 48 h. The solvent was removed *in vacuo* to afford the title compound as an uncrystallisable yellow oil. Addition of NaPF₆ afforded [334]PF₆ as an uncrystallisable yellow oil. Analysis of resonances in the ³¹P{¹H}-NMR spectrum showed the compound to be a mixture of isomers.

¹H-NMR (300 MHz, CD₂Cl₂): δ -0.066 (s, 3H, C²), 0.012 (s, 3H, C²), 2.27 (s, MeCN), 2.29 (s, MeCN), 2.32 (s, MeCN), 2.37 (s, MeCN) (12H, *ca* 3:40:2:3), 7.25-7.50 (m, 15H, PPh₂). ³¹P{¹H}-NMR (121.5 MHz, CD₂Cl₂): δ 44.0 (PPh₂), 47.3 (PPh₂) [*ca* 3:2], -143.1 (sept, *J*_{PF} = 708 Hz, PF₆).

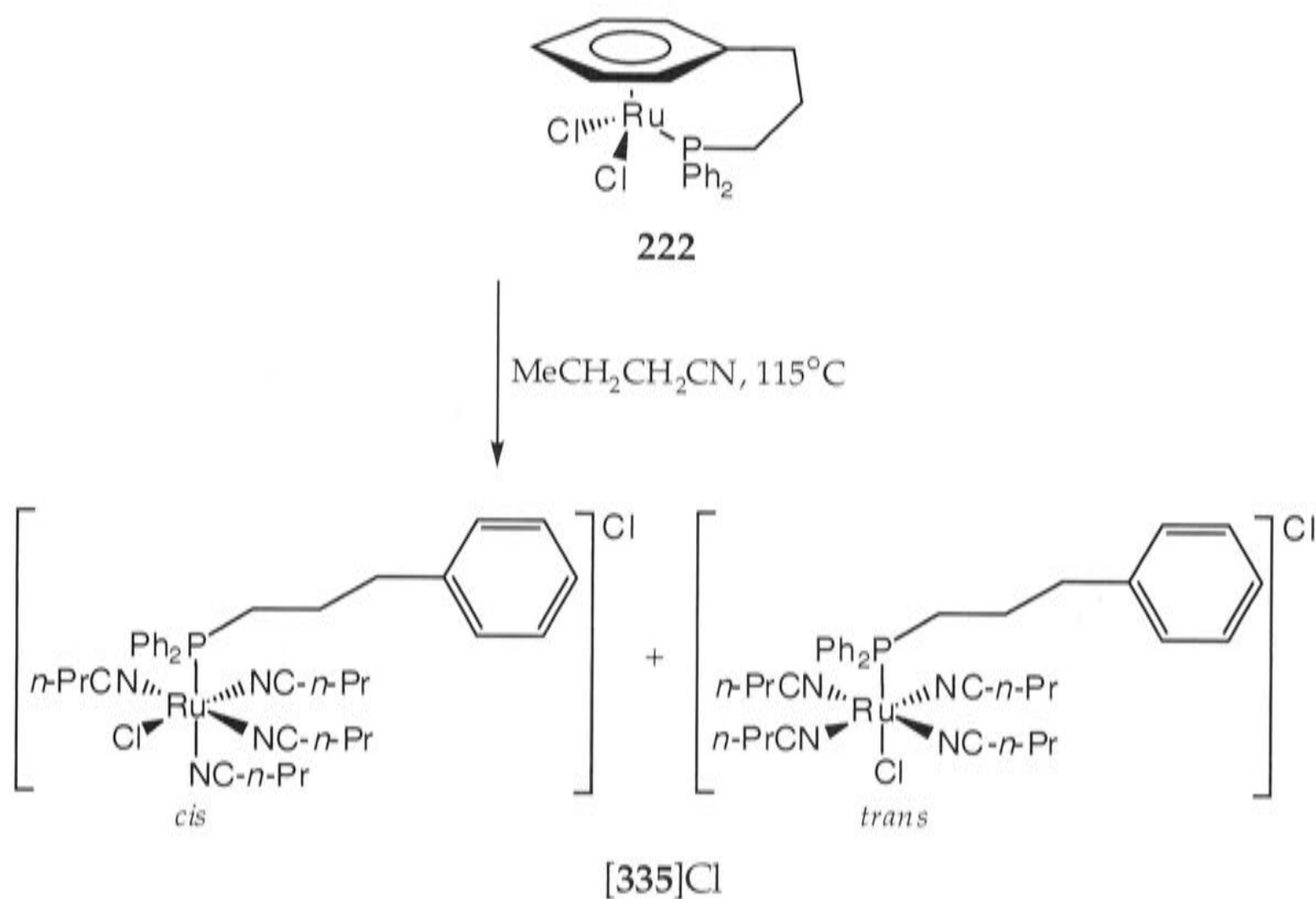
8.2.77 Preparation of *cis*- and *trans*-[RuCl(NCMe)₄(η¹-Ph₂PCH₂SiMe₂Ph)]Cl ([334]Cl) from the Tethered Precursor 230 (b)



The *cis*- and *trans*-isomers of compound [334]Cl were prepared by heating complex [RuCl₂(η¹:η⁶-Ph₂PCH₂SiMe₂Ph)] (252) in dry *d*₃-acetonitrile at 80°C for 48 h. Analysis of resonances in the ³¹P{¹H}-NMR spectrum showed the compound to be a mixture of isomers.

³¹P{¹H}-NMR (121.5 MHz, CD₂Cl₂): δ 44.7, 50.0, *ca* 2.1.

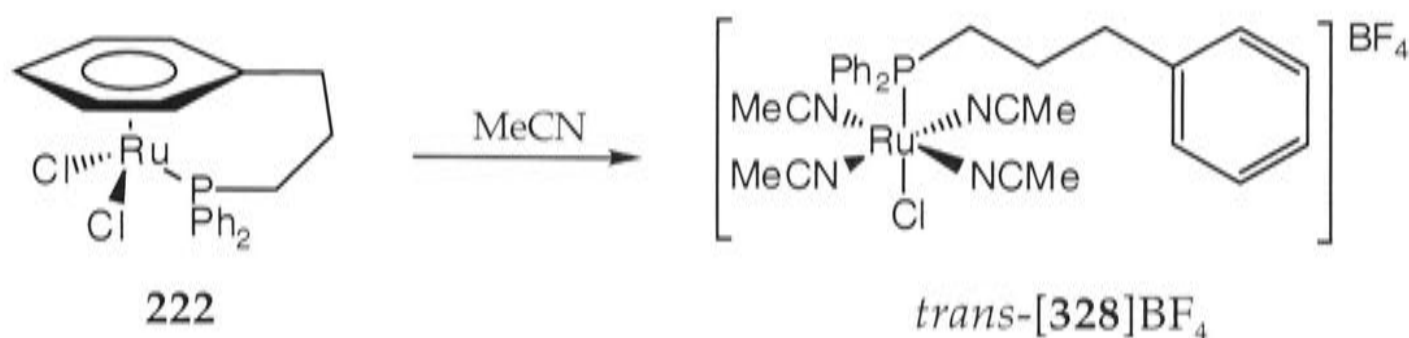
8.2.78 Preparation of *cis*- and *trans*-[RuCl(NC(CH₂)₂Me)₄(η¹-Ph₂P(CH₂)₃Ph)]Cl ([335]Cl) from the Tethered Precursor 222



The *cis*- and *trans*-isomers of compound [335]PF₆ were prepared in 90% yield, as a yellow solid, by heating complex [RuCl₂(η¹:η⁶-Ph₂P(CH₂)₃Ph)] (222) in dry butyronitrile at 115°C for 19 h. Analysis of resonances in the ³¹P{¹H}-NMR spectrum showed the compound to be a mixture of *cis*- and *trans*- isomers in the ratio of 1:2.

¹H-NMR (300 MHz, CD₂Cl₂): δ 0.70-2.65 (m, 34H, H¹, H², H³, butyronitrile), 7.00-7.70 (m, 15H, PPh₂, Ph). ³¹P{¹H}-NMR (121.5 MHz, CD₂Cl₂): δ 47.6 (*trans*), 52.0 (*cis*). FABMS; *m/z*: 717 [M⁺].

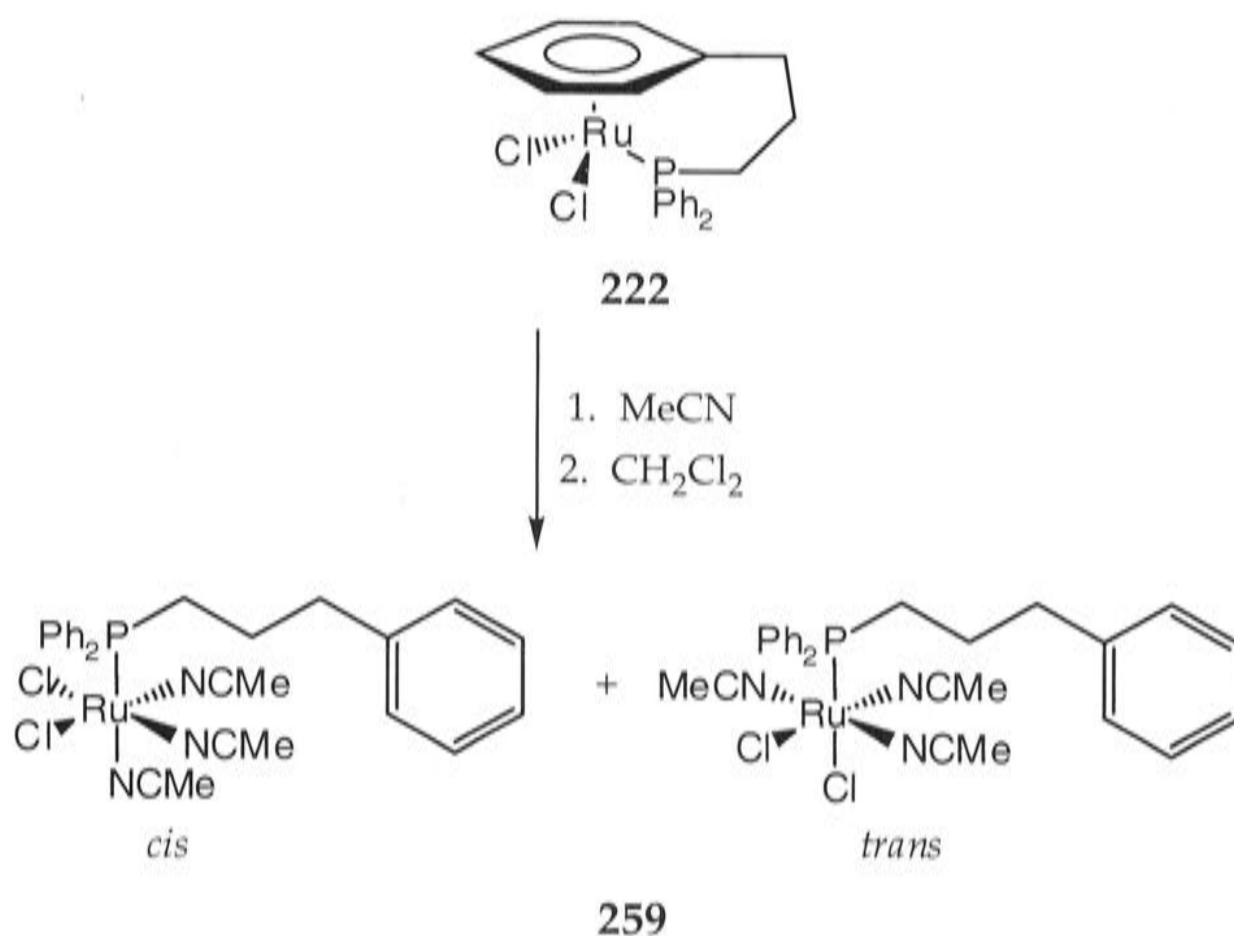
8.2.79 Electrolytic formation of $trans\text{-}[\text{RuCl}(\text{NCMe})_4(\eta^1\text{-Ph}_2\text{P}(\text{CH}_2)_3\text{Ph})]\text{BF}_4$ ($[\mathbf{328}]\text{BF}_4$) from the Tethered Precursor $\mathbf{222}$



A solution of the ruthenium complex $[\text{RuCl}_2(\eta^1:\eta^6\text{-Ph}_2\text{P}(\text{CH}_2)_3\text{Ph})]$, ($\mathbf{222}$), (10 mg, 0.02 mmol) in acetonitrile (15 mL) containing $[\text{Bu}^n_4\text{N}]\text{BF}_4$ (0.1M) was electrolysed at + 1.5 V (*vs* Ag/AgCl), using a H-cell under a dinitrogen atmosphere at 293K. The current fell exponentially during exhaustive electrolysis producing a dark orange solution. The potential was switched to 0.0 V (*vs* Ag/AgCl) and the solution was electrolysed forming a yellow solution. This solution was removed from the cell and the solvent was removed *in vacuo* to afford the title compound $trans\text{-}[\mathbf{328}]\text{BF}_4$ as an oil containing the excess of electrolyte. The presence of $trans\text{-}[\mathbf{328}]\text{BF}_4$ was detected by NMR spectroscopy. Yields were not determined.

$^1\text{H-NMR}$ (250 MHz, CD_3CN): δ 2.11 (s, 12H, MeCN), 7.05-7.65 (m, 15H, PPh_2 , Ph). $^{31}\text{P}\{^1\text{H}\}\text{-NMR}$ (101 MHz, CD_3CN): δ 48.5. IR (cm^{-1} , CH_3CN): 2252 w [$\nu(\text{CN})$].

8.2.80 Electrolytic formation of *cis*- and *trans*-[RuCl(NCMe)₃(η¹-Ph₂P(CH₂)₃Ph)] (**259**) from the Tethered Precursor **222**

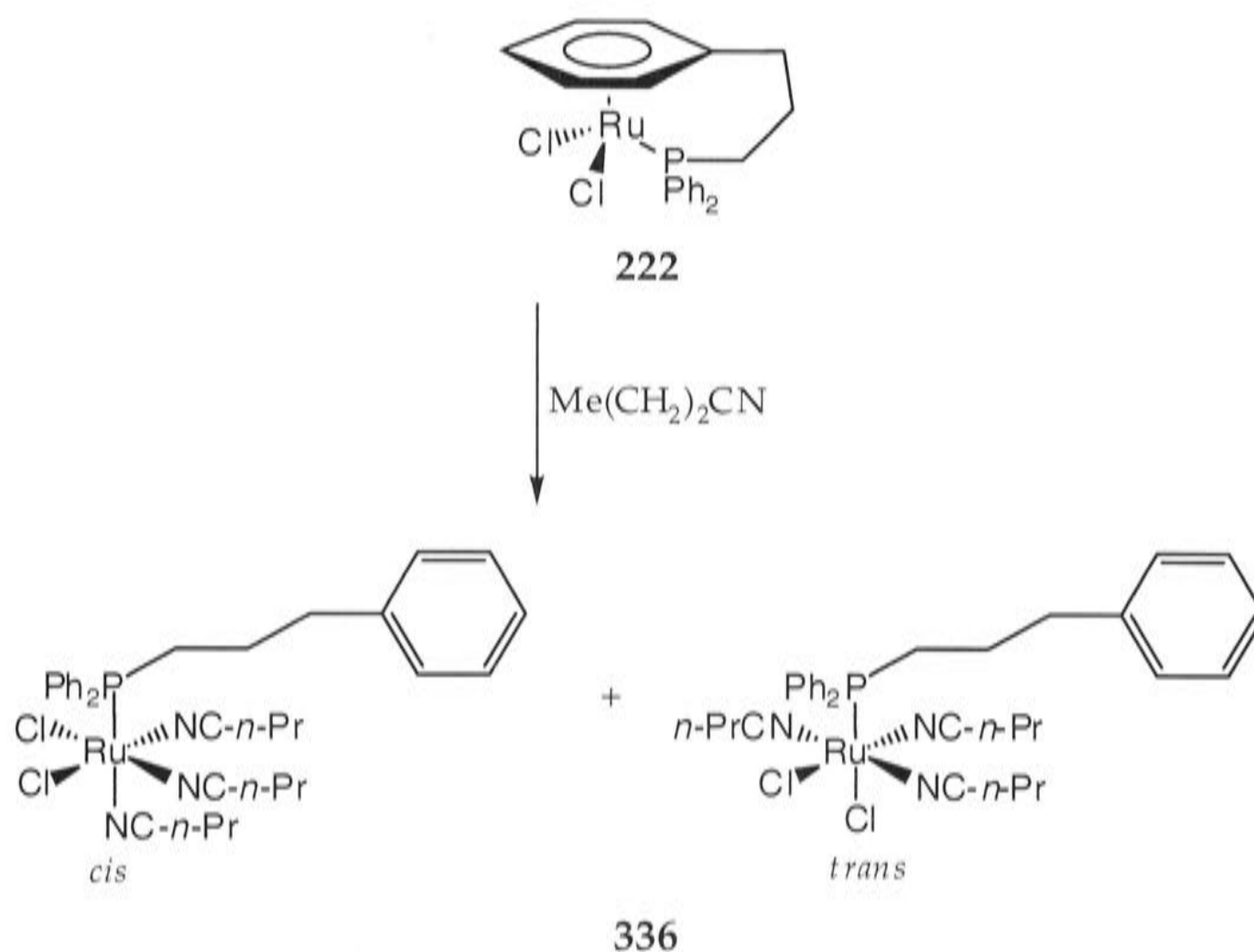


A solution of the ruthenium complex [RuCl₂(η¹:η⁶-Ph₂P(CH₂)₃Ph)], (**222**), (9 mg, 0.019 mmol) in acetonitrile (15 mL) containing [Buⁿ₄N]BF₄ (0.1M) was electrolysed at + 1.5 V (*vs* Ag/AgCl), using a H-cell under a dinitrogen atmosphere at 293K. The current fell exponentially during exhaustive electrolysis producing a dark orange solution. The solution was removed from the cell and the solvent was removed *in vacuo*. The residue was dissolved in dry dichloromethane (10 mL) containing [Buⁿ₄N]BF₄ (0.3M) and placed back into the appropriate compartment of the H-cell. The potential was switched to 0.0 V (*vs* Ag/AgCl) and the solution was electrolysed forming a yellow solution. This solution was removed from the cell and the solvent was removed *in vacuo* to afford the title compound **259** as an oil containing the excess of electrolyte. Analysis of the resonances in the ³¹P{¹H}-NMR spectrum showed the compound to be a mixture of isomers. Yields were not determined.

³¹P{¹H}-NMR (121.5 MHz, CD₂Cl₂): δ 66.7, 67.3, *ca* 1:2. IR (cm⁻¹, CH₂Cl₂): 2253 w [ν(CN)].

A dichloromethane solution of *cis*- and *trans*-**259**[†] was treated with acetonitrile (1 mL) and the mixture heated at 40°C for 68 h to yield *trans*-[**328**]Cl (δ_p 46.7) as a yellow oil; the *cis*-isomer (δ_p 51.5) was not observed.

8.2.81 Electrolytic formation of *cis*- and *trans*-[RuCl(NC(CH₂)₂Me)₃(η^1 -Ph₂P(CH₂)₃Ph)] (**336**) from the Tethered Precursor **222**



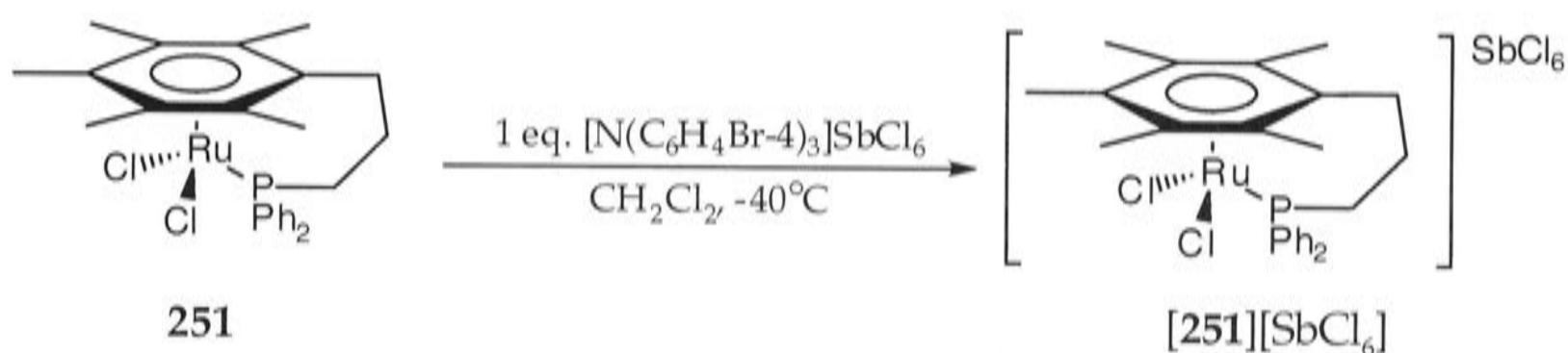
A solution of the ruthenium complex [RuCl₂(η^1 : η^6 -Ph₂P(CH₂)₃Ph)], (**222**), (9 mg, 0.019 mmol) in butyronitrile (15 mL) containing [Buⁿ₄N]BF₄ (0.1M) was electrolysed at + 1.5 V (*vs* Ag/AgCl), using a H-cell under a dinitrogen atmosphere at 293K. The current fell exponentially during exhaustive electrolysis producing a dark orange solution. The potential was switched to 0.0 V (*vs* Ag/AgCl) and the solution was electrolysed forming a orange-yellow solution. This solution was removed from the cell and the solvent was removed *in vacuo* to afford the title compound

[†]Complex **259** was not pure; it contained excess electrolyte.

336 as an oil containing the excess of electrolyte. Analysis of the resonances in the $^{31}\text{P}\{^1\text{H}\}$ -NMR spectrum showed the compound to be a mixture of isomers. Yields were not determined.

^1H -NMR (121.5 MHz, CD_2Cl_2): δ 7.00-7.80 (m, 15H, PPh_2 , Ph). $^{31}\text{P}\{^1\text{H}\}$ -NMR (121.5 MHz, CD_2Cl_2): δ 67.3, 67.7, *ca* 1:10. IR (cm^{-1} , $\text{CH}_3\text{CH}_2\text{CH}_2\text{CN}$): 2251 w [$\nu(\text{CN})$].

8.2.82 Preparation of $[\text{RuCl}_2(\eta^1:\eta^6\text{-Ph}_2\text{P}(\text{CH}_2)_3\text{C}_6\text{Me}_5)][\text{SbCl}_6]$ (**[251][SbCl₆]**)

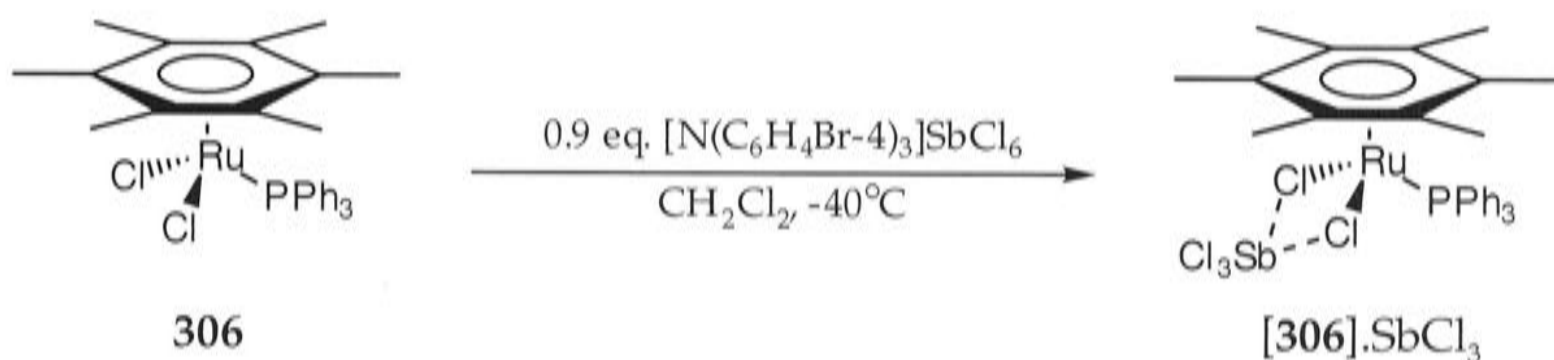


A solution of $[\text{N}(\text{C}_6\text{H}_4\text{Br-4})_3]\text{SbCl}_6$, **[48]** SbCl_6 (133 mg, 0.16 mmol) in dichloromethane (40 mL) was added dropwise to a solution of $[\text{RuCl}_2(\eta^1:\eta^6\text{-Ph}_2\text{P}(\text{CH}_2)_3\text{C}_6\text{Me}_5)]$, (**251**), (101 mg, 0.18 mmol) in dichloromethane (10 mL) at -40°C with the exclusion of light. After all the oxidant had been consumed the colour had changed from orange to brown-pink. The reaction mixture was then stirred for a further 15 min. *n*-Hexane (30 mL) was then added and the dichloromethane was removed *in vacuo*. The solvent was removed by filtration and the solid was washed with dichloromethane (2 mL), followed by *n*-hexane (2×5 mL) and then dried *in vacuo* to afford the title compound **[251][SbCl₆]** as a pink solid (137 mg, 84%). Orange crystals suitable for X-ray diffraction were obtained by layering a CH_2Cl_2 solution with *n*-hexane at -11°C .

^1H -NMR (300 MHz, CD_2Cl_2): δ 1.81 (m, H^2), 2.23 (d, $J = 1$ Hz, H^1 or H^3), 2.30 (d, $J = 2$ Hz, H^3 or H^1). UV/Vis (CH_2Cl_2): 492 nm (20300 cm^{-1}) [$\epsilon = 2300 \text{ L mol}^{-1} \text{ cm}^{-1}$]. Anal. found: C, 32.75; H, 2.81; P, 2.32; Cl, 34.55%. $\text{C}_{26}\text{H}_{31}\text{Cl}_8\text{PRuSb} \cdot 0.5\text{CH}_2\text{Cl}_2$: requires C, 34.47; H, 3.49; P, 3.35; Cl, 34.55%. The presence of dichloromethane was evident in the crystal structure.

$^1\text{H-NMR}$ (300 MHz, CDCl_3): δ 1.75 (s, 18H, C_6Me_6), 7.20-7.90 (m, 15H, Ph).
 $^{31}\text{P}\{^1\text{H}\}\text{-NMR}$ (121.5 MHz, CDCl_3): δ 36.8. Anal. found: C, 45.66; H, 4.20; P, 3.66; Cl, 18.63%. $\text{C}_{30}\text{H}_{33}\text{Cl}_5\text{P}_2\text{RuSb}$: requires C, 43.69; H, 4.03; P, 3.76; Cl, 21.50%.

8.2.85 Preparation of $[\text{RuCl}_2(\eta^6\text{-C}_6\text{Me}_6)(\text{PPh}_3)]\cdot\text{SbCl}_3$ (**[306]** $\cdot\text{SbCl}_3$) (**b**)



Compound $[\mathbf{306}]\cdot\text{SbCl}_3$ was also obtained by treating $[\text{RuCl}_2(\eta^6\text{-C}_6\text{Me}_6)(\text{PPh}_3)]$ (**306**) with 0.9 eq. of **[48]** SbCl_6 in CH_2Cl_2 at -40°C in the absence of light. Orange crystals of the title compound suitable for X-ray diffraction were obtained by layering a CH_2Cl_2 solution with *n*-hexane at -11°C .

Attempts to prepare similarly the one-electron oxidation products **[338]** $[\text{SbCl}_6]$, **[339]** $[\text{SbCl}_6]$ and **[249]** $[\text{SbCl}_6]$ failed; there was no evidence for the formation of SbCl_3 adducts of **338**, **339**, and **249** in these reactions.

Notes and References

- (1) Smith, L. I.; Nichols, J. *J. Org. Chem.* **1941**, *6*, 489-506.
- (2) Jack, L. A. , University of Edinburgh, 2001, generous donation.
- (3) Reinhardt, H.; Bianchi, D.; Mölle, D. *Chem. Ber.* **1957**, *90*, 1656-1660.
- (4) Niebergall, H.; Langenfeld, B. *Chem. Ber.* **1962**, *95*, 64-76.
- (5) Parshall, G. W. *Inorganic Syntheses*; Lippard, S. J. Ed., John Wiley & Sons, Inc.: New York, 1974; Vol. 15, pp. 191-193.
- (6) Neumann, H., The Australian National University, 1999, generous donation.
- (7) Brauer, G. *Handbook of Preparative Inorganic Chemistry*; 2nd ed.; Academic Press, Inc.: London, 1965; Vol. II, pp. 1006-1007.
- (8) Fieser, L. F.; Fieser, M. *Reagents for Organic Synthesis*; John Wiley and Sons, Inc.: New York, 1967; Vol. 1, p. 911.
- (9) West, R.; Riley, R. J. *Inorg. Nucl. Chem.* **1958**, *5*, 295-303.
- (10) Aspinall, G. O.; Baker, W. J. *Chem. Soc.* **1950**, 743-753.
- (11) Timmer, K.; Thewissen, D. H. M. W.; Marsman, J. W. *Recl. Trav. Chim. Pays-Bas* **1988**, *107*, 248-255.
- (12) Uriarte, R.; Mazanec, T. J.; Tau, K. D.; Meek, D. W. *Inorg. Chem.* **1980**, *19*, 79-85.
- (13) Hartley, F. R. *Organometal. Chem. Rev. A* **1970**, *6*, 119-137.
- (14) Fürstner, A.; Liebl, M.; Lehmann, C. W.; Picquet, M.; Kunz, R.; Bruneau, C.; Touchard, D.; Dixneuf, P. H. *Chem. Eur. J.* **2000**, *6*, 1847-1857.
- (15) Bennett, M. A.; Smith, A. K. *J. Chem. Soc., Dalton Trans.* **1974**, 233-241.
- (16) Bennett, M. A.; Huang, T.-N.; Matheson, T. W.; Smith, A. K. *Inorganic Syntheses*; Fackler, Jr, J. P. Ed., John Wiley & Sons, Inc.: New York, 1982; Vol. 21, pp. 74-78.
- (17) Zelonka, R. A.; Baird, M. C. *Can. J. Chem.* **1972**, *50*, 3063-3072.

- (18) Bennett, M. A.; Huang, T.-N.; Latten, J. L. *J. Organomet. Chem.* **1984**, 272, 189-205.
- (19) Ghebreyessus, K. Y.; Nelson, J. H. *Organometallics* **2000**, 19, 3387-3392.
- (20) Pertici, P.; Salvadori, P.; Biasci, A.; Vitulli, G.; Bennett, M. A.; Kane-Maguire, L. A. P. *J. Chem. Soc., Dalton Trans.* **1988**, 315-320.
- (21) Werner, H.; Werner, R. *Chem. Ber.* **1982**, 115, 3781-3795.
- (22) Werner, H.; Kletzin, H. *J. Organomet. Chem.* **1982**, 228, 289-300.
- (23) Bennett, M. A.; Latten, J. *Aust. J. Chem.* **1987**, 40, 841-849.
- (24) Amarego, W. L. F.; Perrin, D. D. *Purification of Laboratory Chemicals*; 4th ed.; Butterworth Heinemann: Oxford, 1996.
- (25) Duff, C. M.; Heath, G. A. *Inorg. Chem.* **1991**, 30, 2528-2535.
- (26) Gritzner, G.; Kuta, J. *Pure Appl. Chem.* **1982**, 54, 1527-1532.
- (27) Gritzner, G.; Kuta, J. *Pure Appl. Chem.* **1984**, 56, 461-466.
- (28) Heath, G. A.; Yellowlees, L. J.; Braterman, P. S. *J. Chem. Soc., Chem. Commun.* **1981**, 287-289.
- (29) McGrady, J. E., 2003, personal communication.
- (30) *ADF 2003.01, Theoretical Chemistry*, Vrije Universiteit, Amsterdam, The Netherlands, Baerends, E. J.; Ellis, D. E.; Ros, P. *Chem. Phys.* **1973**, 2, 41-51.
- (31) *ADF 2003.01, Theoretical Chemistry*, Vrije Universiteit, Amsterdam, The Netherlands, te Velde, G.; Baerends, E. J. *J. Comp. Phys.* **1992**, 99, 84-98.
- (32) Parr, R. G.; Yang, W. *Density Functional Theory of Atoms and Molecules*; Oxford University Press, Inc.: New York, 1989.
- (33) Vosko, S. H.; Wilk, L.; Nusair, M. *Can. J. Phys.* **1980**, 58, 1200-1211.
- (34) Becke, A. D. *Phys. Rev. A* **1988**, 38, 3098-3100.
- (35) Perdew, J. P. *Phys. Rev. B* **1986**, 33, 8822-8824.
- (36) Versluis, L.; Ziegler, T. *J. Chem. Phys.* **1988**, 88, 322-328.
- (37) Singewald, E. T.; Mirkin, C. A.; Levy, A. D.; Stern, C. L. *Angew. Chem., Int. Ed. Engl.* **1994**, 33, 2473-2475.

- (38) Singewald, E. T.; Shi, X.; Mirkin, C. A.; Schofer, S. J.; Stern, C. L. *Organometallics* **1996**, *15*, 3062-3069.
- (39) Smith, P. D.; Wright, A. H. *J. Organomet. Chem.* **1998**, *559*, 141-147.
- (40) Verkade, J. D.; Quin, L. D. *Phosphorus-31 NMR Spectroscopy in Stereochemical Analysis: Organic Compounds and Metal Complexes*; VCH Publishers, Inc.: Deerfield Beach, 1987; Vol. 8, p. 11.
- (41) Werner, H.; Canepa, G.; Ilg, K.; Wolf, J. *Organometallics* **2000**, *19*, 4756-4766.
- (42) Nishimura, J.; Yamada, N.; Horiuchi, Y.; Ueda, E.; Ohbayashi, A.; Oku, A. *Bull. Chem. Soc. Jpn.* **1986**, *59*, 2035-2037.
- (43) Grim, S. O.; Barth, R. C. *J. Organomet. Chem.* **1975**, *94*, 327-332.
- (44) Rathore, R.; Weigand, U.; Kochi, J. K. *J. Org. Chem.* **1996**, *61*, 5246-5256.
- (45) Davies, D. L.; Fawcett, J.; Krafczyk, R.; Russell, D. R.; Singh, K. *J. Chem. Soc., Dalton Trans.* **1998**, 2349-2352.
- (46) Redwine, K. D.; Hansen, H. D.; Bowley, S.; Isbell, J.; Sanchez, M.; Vodak, D.; Nelson, J. H. *Synth. React. Inorg. Met.-Org. Chem.* **2000**, *30*, 379-407.

Appendix of Structural Data

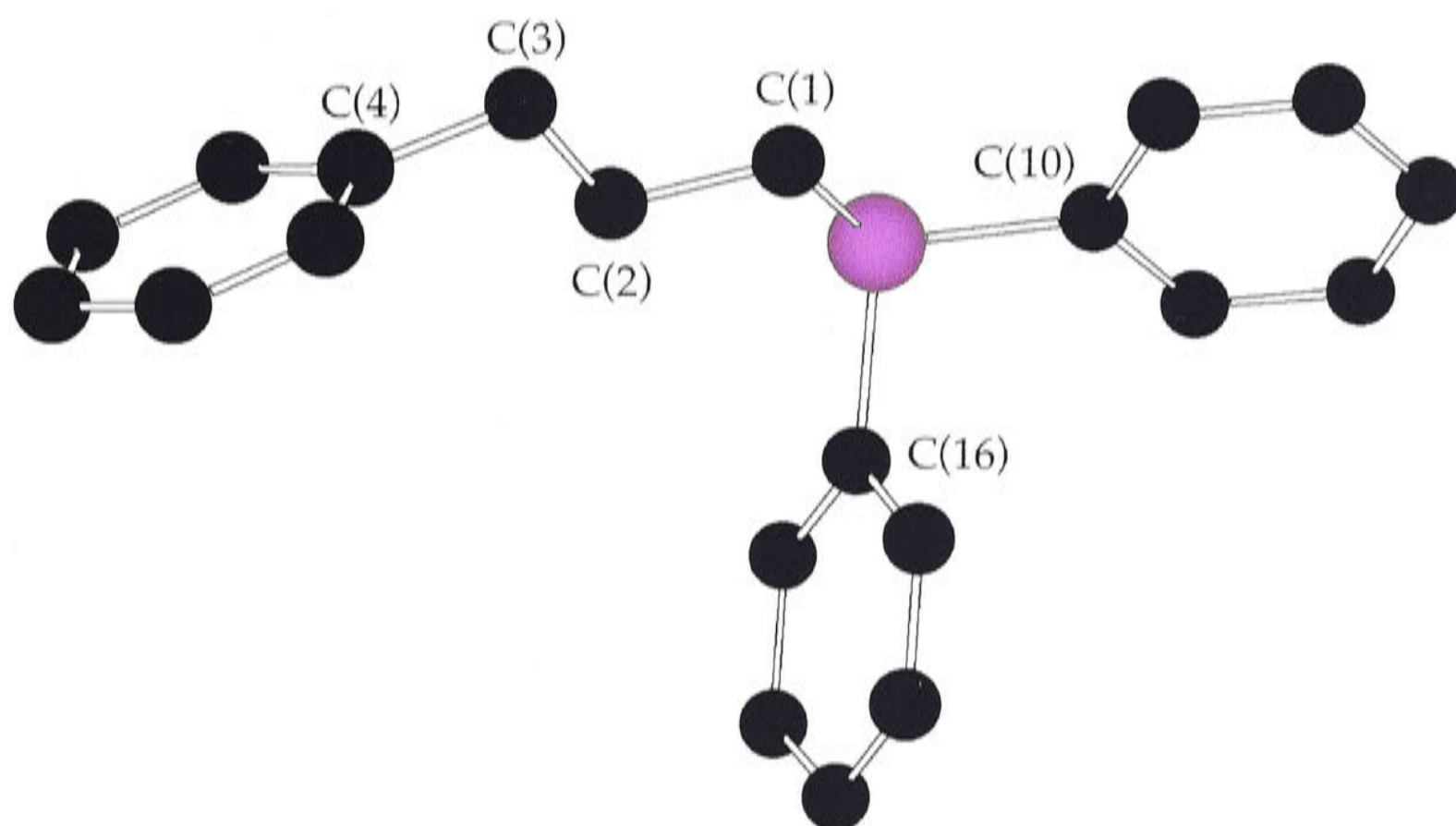
A.1 $\text{Ph}_2\text{P}(\text{CH}_2)_3\text{Ph}$ (118)

Figure 86. Chem3D representation of the molecular structure of $\text{Ph}_2\text{P}(\text{CH}_2)_3\text{Ph}$ (118). Hydrogen atoms have been omitted for clarity. The structure was determined by Dr A. D. Bond (Cambridge).

Table 41. Selected bond lengths (\AA) for the phosphine $\text{Ph}_2\text{P}(\text{CH}_2)_3\text{Ph}$ (118).

P(1)-C(1)	1.841(2)	P(1)-C(10)	1.826(2)
P(1)-C(16)	1.842(2)	C(1)-C(2)	1.523(3)
C(2)-C(3)	1.535(3)	C(3)-C(4)	1.504(3)
C(10)-P(1)-C(1)	103.38(9)	C(1)-P(1)-C(16)	99.67(10)
C(10)-P(1)-C(16)	101.85(9)		

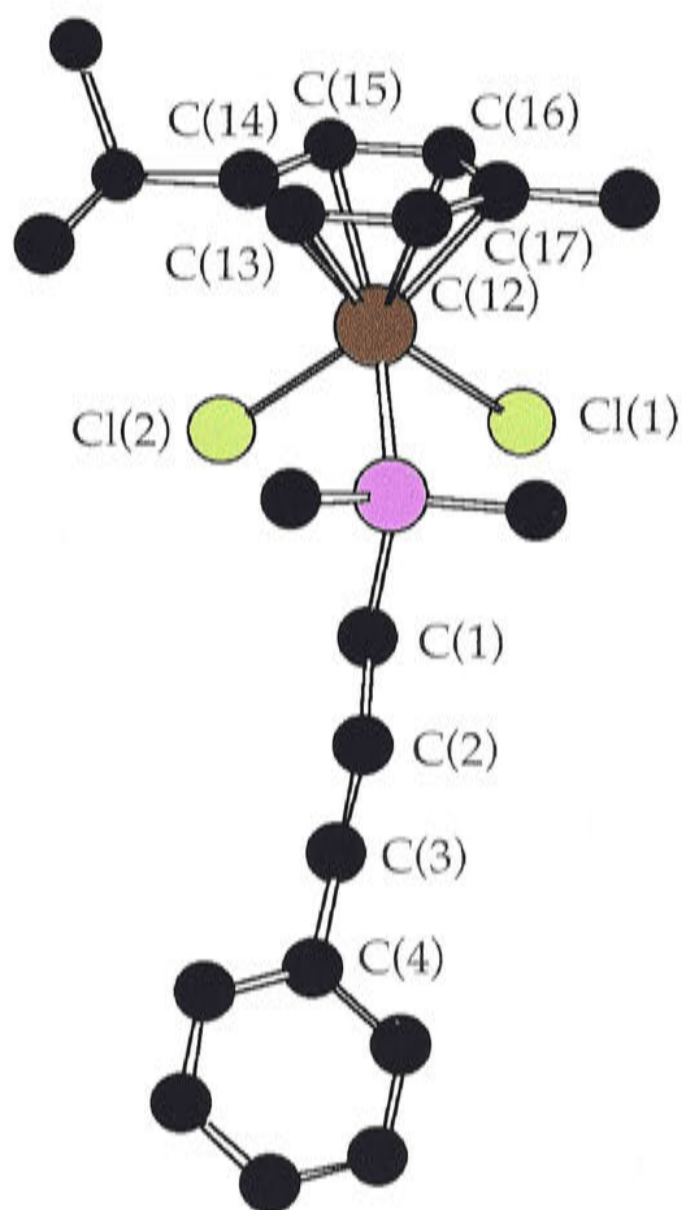
A.2 $[\text{RuCl}_2(\eta^6\text{-1,4-MeC}_6\text{H}_4\text{CHMe}_2)(\eta^1\text{-Me}_2\text{P}(\text{CH}_2)_3\text{Ph})]$ (**231**)

Figure 87. Chem3D representation of the molecular structure of $[\text{RuCl}_2(\eta^6\text{-1,4-MeC}_6\text{H}_4\text{CHMe}_2)(\eta^1\text{-Me}_2\text{P}(\text{CH}_2)_3\text{Ph})]$ (**231**). Hydrogen atoms have been omitted for clarity. The structure was determined by Dr A. C. Willis (ANU).

In the crystal structure of **231**, atoms C(2), C(3) and C(4) were disordered over two sites of approximately 90% and 10% occupancy, and the relative populations were refined while restraints were imposed upon angles and distances involving these sites.

Table 42. Selected bond lengths (Å) and angles (°) for the non-tethered complex $[\text{RuCl}_2(\eta^6\text{-1,4-MeC}_6\text{H}_4\text{CHMe}_2)(\eta^1\text{-Me}_2\text{P}(\text{CH}_2)_3\text{Ph})]$ (231).

Ru(1)-Cl(1)	2.4357(7)	Ru(1)-Cl(2)	2.4073(8)
Ru(1)-P(1)	2.3290(7)	Ru(1)-C(12)	2.160(2)
Ru(1)-C(13)	2.184(2)	Ru(1)-C(14)	2.218(3)
Ru(1)-C(15)	2.260(2)	Ru(1)-C(16)	2.231(3)
Ru(1)-C(17)	2.199(2)	P-C	1.804(3)–1.809(4)
C-C(arene)	1.382(4)–1.427(4)		
Cl(1)-Ru(1)-Cl(2)	88.55(3)	Cl(1)-Ru(1)-P(1)	88.44(3)
Cl(2)-Ru(1)-P(1)	83.75(3)		

A.3 $[\text{RuCl}_2(\eta^6\text{-C}_6\text{H}_6)(\eta^1\text{-Ph}_2\text{P}(\text{CH}_2)_3\text{Ph})]$ (227)

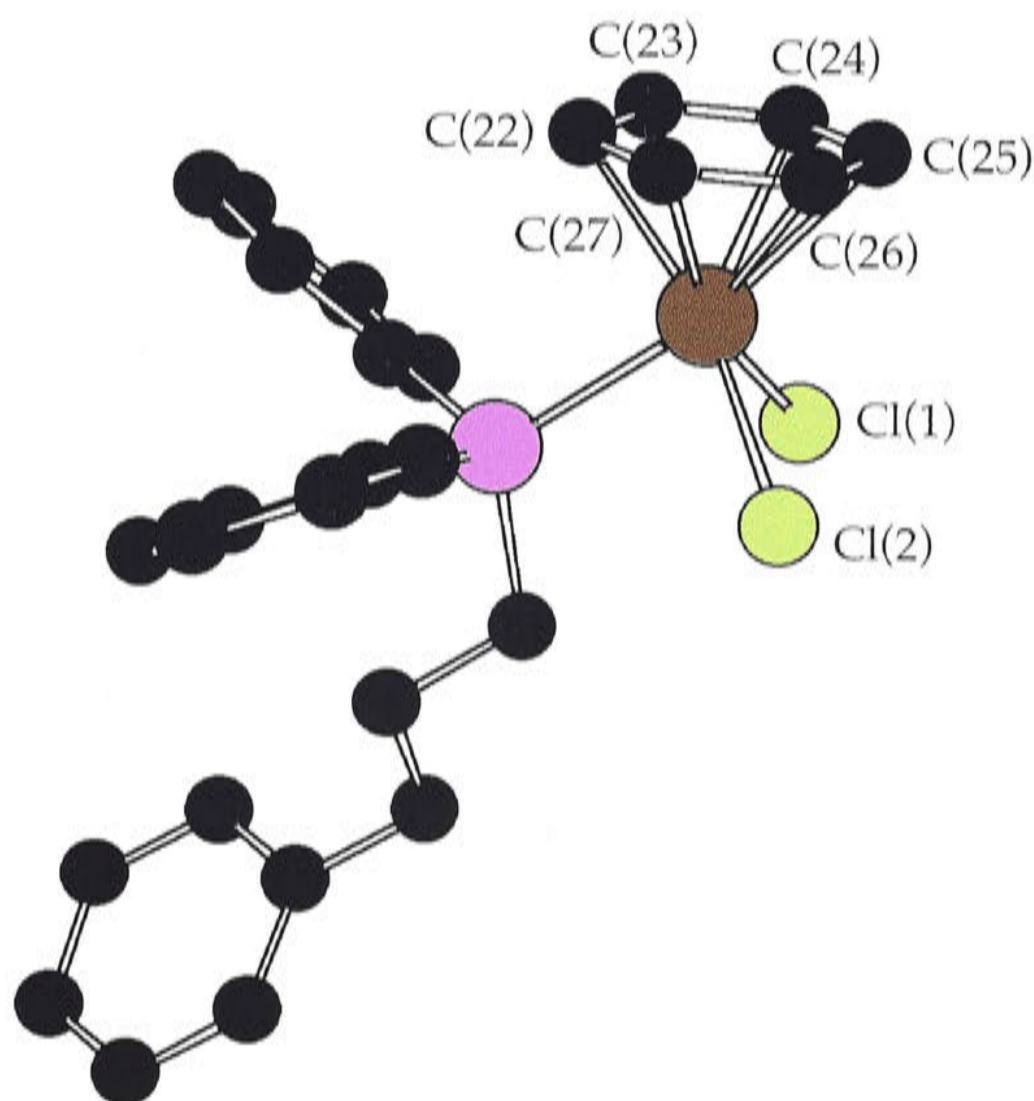


Figure 88. Chem3D representation of the molecular structure of $[\text{RuCl}_2(\eta^6\text{-C}_6\text{H}_6)(\eta^1\text{-Ph}_2\text{P}(\text{CH}_2)_3\text{Ph})]$ (227). Hydrogen atoms have been omitted for clarity. The structure was determined by Dr A. C. Willis (ANU).

Table 43. Selected bond lengths (Å) and angles (°) for the non-tethered complex $[\text{RuCl}_2(\eta^6\text{-C}_6\text{H}_6)(\eta^1\text{-Ph}_2\text{P}(\text{CH}_2)_3\text{Ph})]$ (**227**).

Ru(1)-Cl(1)	2.4059(7)	Ru(1)-Cl(2)	2.3976(7)
Ru(1)-P(1)	2.3500(7)	Ru(1)-C(22)	2.1420(3)
Ru(1)-C(23)	2.156(3)	Ru(1)-C(24)	2.163(3)
Ru(1)-C(25)	2.228(3)	Ru(1)-C(26)	2.219(3)
Ru(1)-C(27)	2.182(3)	P-C	1.822(3)–1.836(3)
C-C(arene)	1.361(6)–1.410(6)		
Cl(1)-Ru(1)-Cl(2)	88.75(3)	Cl(1)-Ru(1)-P(1)	85.98(3)
Cl(2)-Ru(1)-P(1)	85.29(2)		

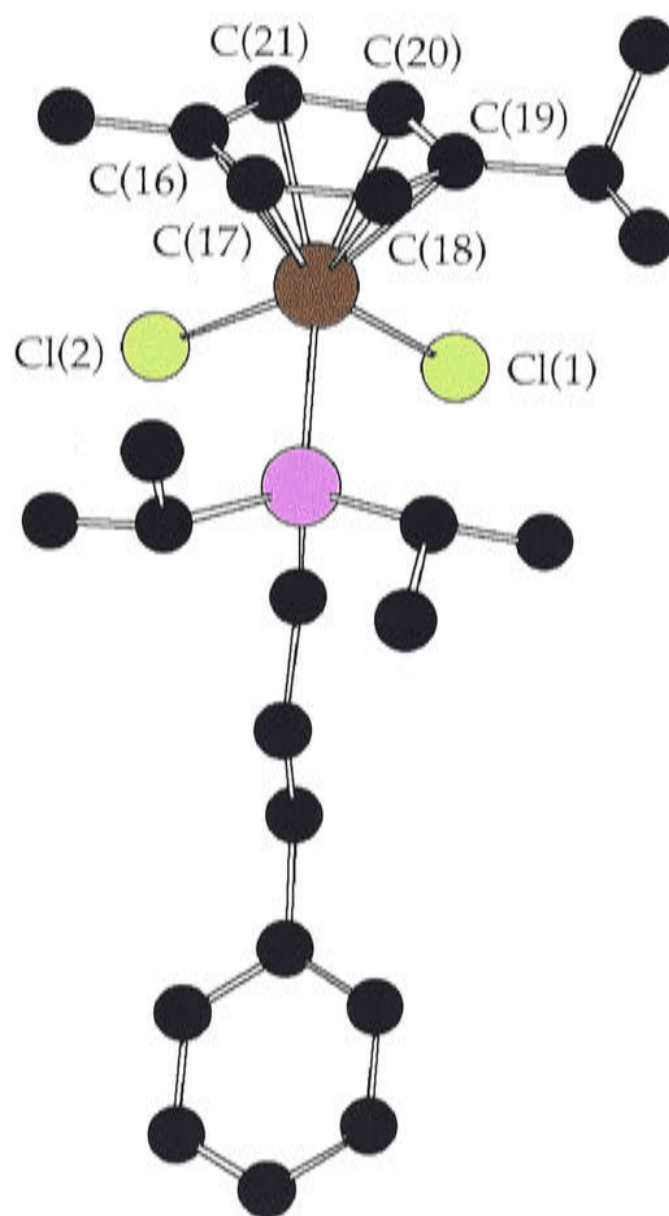
A.4 $[\text{RuCl}_2(\eta^6\text{-}1,4\text{-MeC}_6\text{H}_4\text{CHMe}_2)(\eta^1\text{-}i\text{-Pr}_2\text{P}(\text{CH}_2)_3\text{Ph})]$ (232)

Figure 89. Chem3D representation of the molecular structure of $[\text{RuCl}_2(\eta^6\text{-}1,4\text{-MeC}_6\text{H}_4\text{CHMe}_2)(\eta^1\text{-}i\text{-Pr}_2\text{P}(\text{CH}_2)_3\text{Ph})]$ (232), showing one of the independent molecules in the unit cell.¹ Hydrogen atoms and the solvent molecule (CH_2Cl_2) have been omitted for clarity. The structure was determined by Dr J. E. Davies (Cambridge).

¹The other molecules do not differ significantly.

Table 44. Selected bond lengths (Å) and angles (°) for the non-tethered complex $[\text{RuCl}_2(\eta^6\text{-1,4-MeC}_6\text{H}_4\text{CHMe}_2)(\eta^1\text{-}i\text{-Pr}_2\text{P}(\text{CH}_2)_3\text{Ph})]$ (232).

Molecule 1		Molecule 2	
Ru(1A)-Cl(1A)	2.428(2)	Ru(1B)-Cl(1B)	2.429(3)
Ru(1A)-Cl(2A)	2.421(3)	Ru(1B)-Cl(2B)	2.432(3)
Ru(1A)-P(1A)	2.393(3)	Ru(1B)-P(1B)	2.392(3)
Ru(1A)-C(16A)	2.208(9)	Ru(1B)-C(16B)	2.183(9)
Ru(1A)-C(17A)	2.209(9)	Ru(1B)-C(17B)	2.227(9)
Ru(1A)-C(18A)	2.241(9)	Ru(1B)-C(18B)	2.280(9)
Ru(1A)-C(19A)	2.262(10)	Ru(1B)-C(19B)	2.250(10)
Ru(1A)-C(20A)	2.227(10)	Ru(1B)-C(20B)	2.211(10)
Ru(1A)-C(21A)	2.158(10)	Ru(1B)-C(21B)	2.179(10)
P-C	1.834(9)–1.870(10)	P-C	1.830(10)–1.861(11)
C-C(arene)	1.405(13)–1.500(14)	C-C(arene)	1.394(14)–1.475(13)
Cl(1A)-Ru(1)-Cl(2A)	87.95(10)	Cl(1B)-Ru(1B)-Cl(2B)	87.37(9)
Cl(1A)-Ru(1A)-P(1A)	87.46(9)	Cl(1B)-Ru(1B)-P(1B)	87.23(9)
Cl(2A)-Ru(1A)-P(1A)	85.27(10)	Cl(2B)-Ru(1B)-P(1B)	86.56(9)

Molecule 3		Molecule 4	
Ru(1C)-Cl(1C)	2.425(3)	Ru(1D)-Cl(1D)	2.419(3)
Ru(1C)-Cl(2C)	2.415(3)	Ru(1D)-Cl(2D)	2.421(3)
Ru(1C)-P(1C)	2.390(3)	Ru(1D)-P(1D)	2.389(3)
Ru(1C)-C(16C)	2.237(11)	Ru(1D)-C(16D)	2.213(9)
Ru(1C)-C(17C)	2.234(10)	Ru(1D)-C(17D)	2.227(9)
Ru(1C)-C(18C)	2.191(10)	Ru(1D)-C(18D)	2.257(9)
Ru(1C)-C(19C)	2.227(10)	Ru(1D)-C(19D)	2.233(10)
Ru(1C)-C(20C)	2.205(11)	Ru(1D)-C(20D)	2.212(10)
Ru(1C)-C(21C)	2.222(10)	Ru(1D)-C(21D)	2.166(10)
P-C	1.806(11)-1.865(12)	P-C	1.820(10)-1.847(10)
C-C(arene)	1.373(15)-1.429(16)	C-C(arene)	1.389(13)-1.448(14)
Cl(1C)-Ru(1C)-Cl(2C)	87.63(10)	Cl(1D)-Ru(1D)-Cl(2D)	86.50(10)
Cl(1C)-Ru(1C)-P(1C)	86.93(10)	Cl(1D)-Ru(1D)-P(1D)	86.66(9)
Cl(2C)-Ru(1C)-P(1C)	86.18(10)	Cl(2D)-Ru(1D)-P(1D)	86.74(10)

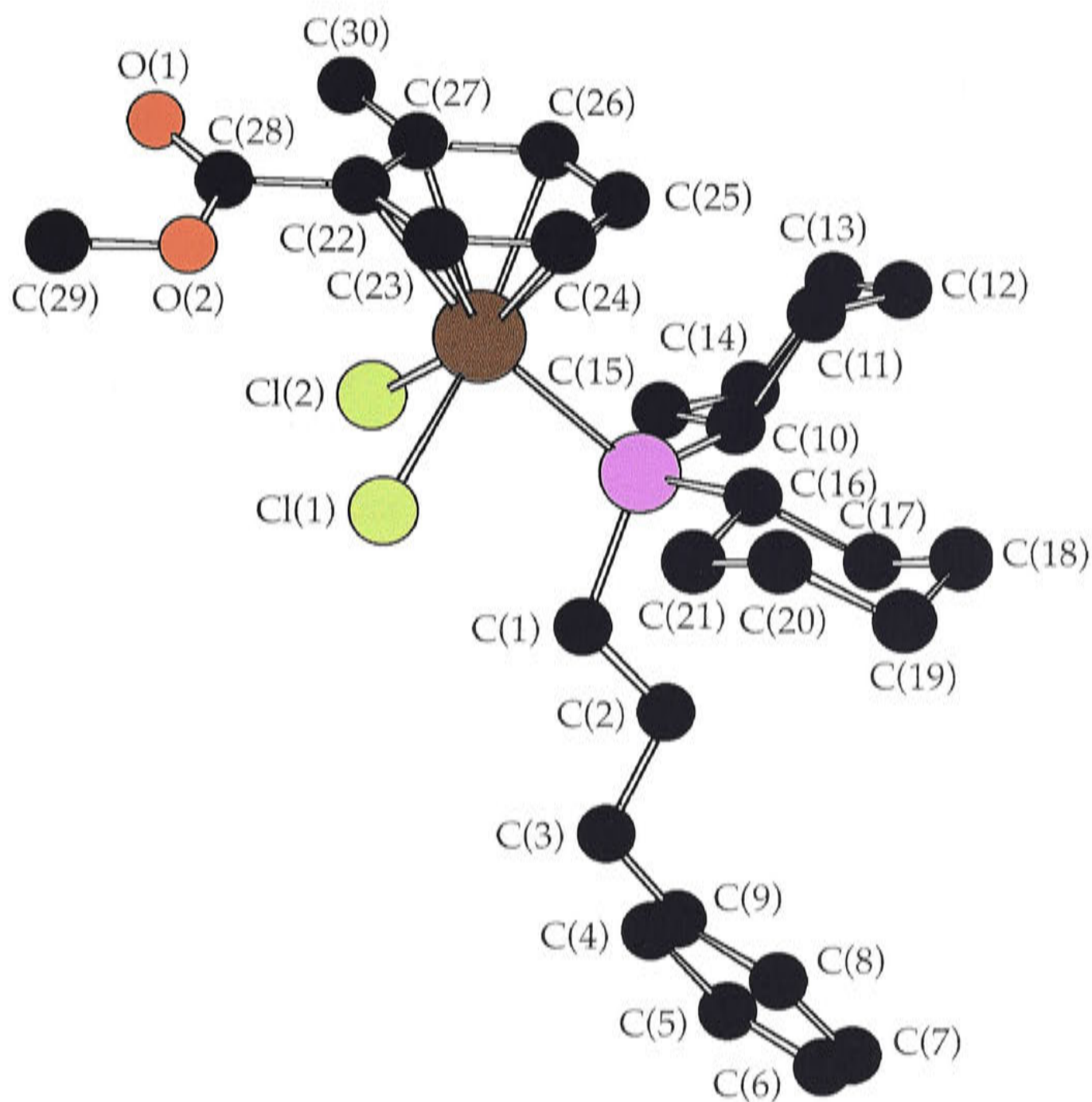
A.5 $[\text{RuCl}_2(\eta^6\text{-1,2-MeC}_6\text{H}_4\text{CO}_2\text{Me})(\eta^1\text{-Cy}_2\text{P}(\text{CH}_2)_3\text{Ph})]$ (239)

Figure 90. Chem3D representation of the molecular structure of $[\text{RuCl}_2(\eta^6\text{-1,2-MeC}_6\text{H}_4\text{CO}_2\text{Me})(\eta^1\text{-Cy}_2\text{P}(\text{CH}_2)_3\text{Ph})]$ (239), showing one of the independent molecules in the unit cell.[†] Hydrogen atoms have been omitted for clarity. The structure was determined by Drs A. D. Bond and T. Khimyak (Cambridge).

[†]The other molecule differs conformationally about the C(22)-C(28) bond.

The crystals obtained for $\text{RuCl}_2(\eta^6\text{-1,2-MeC}_6\text{H}_4\text{CO}_2\text{Me})(\eta^1\text{-Cy}_2\text{P}(\text{CH}_2)_3\text{Ph})$ (**239**) were thin plates. The compound crystallised in this instance with two molecules per crystallographic asymmetric unit. One of the molecules is well ordered and has the conformation illustrated in Figure 90. The second molecule possesses a dominant alternative conformation illustrated in Figure 91, with disorder of the cyclohexyl groups (each carbon atom in the rings has 72 and 28% occupancy) and a variation of the position of the methyl substituent on the tolyl ring, which is disordered across the tolyl ring. The crystal therefore contains at least three substantially different conformations. In view of the disorder involved in one of the molecules, the values used in Chapter 3 are those derived from the well ordered conformer.

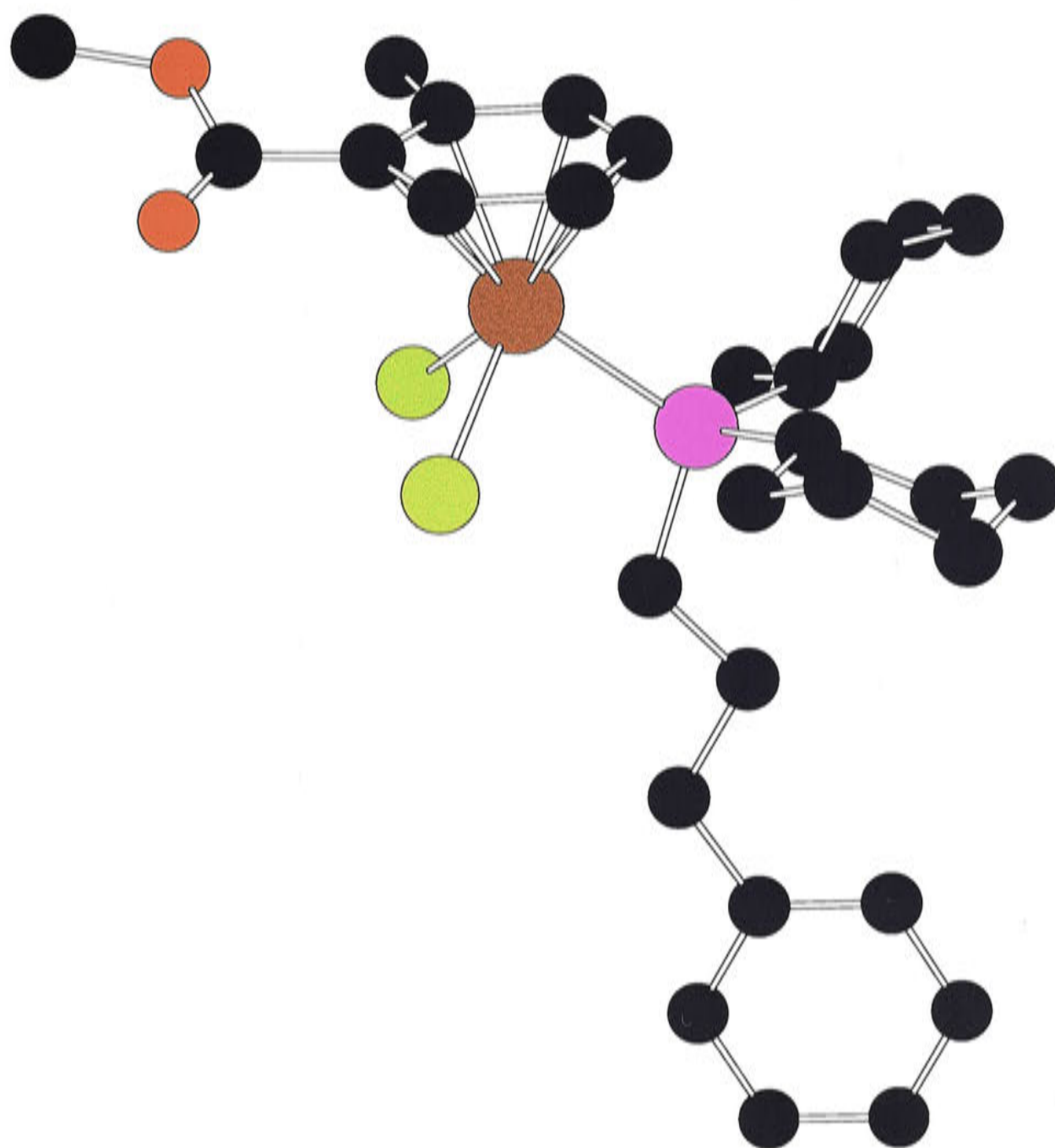


Figure 91. Chem3D representation of the molecular structure of $[\text{RuCl}_2(\eta^6\text{-1,2-MeC}_6\text{H}_4\text{CO}_2\text{Me})(\eta^1\text{-Cy}_2\text{P}(\text{CH}_2)_3\text{Ph})]$ (239), showing one of the independent molecules in the unit cell.[†] Hydrogen atoms have been omitted for clarity. The structure was determined by Drs A. D. Bond and T. Khimyak (Cambridge).

[†]The other conformer is well ordered.

Table 45. Selected bond lengths (Å) and angles (°) for the non-tethered complex [RuCl₂(η⁶-1,2-MeC₆H₄CO₂Me)(η¹-Cy₂P(CH₂)₃Ph)] (239).

Molecule 1		Molecule 2	
Ru(1A)-Cl(1A)	2.4051(15)	Ru(1B)-Cl(1B)	2.408(2)
Ru(1A)-Cl(2A)	2.4039(14)	Ru(1B)-Cl(2B)	2.397(2)
Ru(1A)-P(1A)	2.3631(13)	Ru(1B)-P(1B)	2.3652(18)
Ru(1A)-C(22A)	2.262(5)	Ru(1B)-C(22B)	2.245(7)
Ru(1A)-C(23A)	2.181(5)	Ru(1B)-C(23B)	2.163(8)
Ru(1A)-C(24A)	2.203(5)	Ru(1B)-C(24B)	2.186(7)
Ru(1A)-C(25A)	2.189(5)	Ru(1B)-C(25B)	2.182(7)
Ru(1A)-C(26A)	2.228(6)	Ru(1B)-C(26B)	2.247(8)
Ru(1A)-C(27A)	2.271(6)	Ru(1B)-C(27B)	2.237(7)
P-C	1.844(5)–1.857(5)	P-C	1.800(11)–1.835(8)
C-C(arene)	1.406(8)–1.434(8)	C-C(arene)	1.384(11)–1.459(12)
Cl(1A)-Ru(1)-Cl(2A)	87.03(5)	Cl(1B)-Ru(1B)-Cl(2B)	87.61(9)
Cl(1A)-Ru(1A)-P(1A)	87.02(5)	Cl(1B)-Ru(1B)-P(1B)	87.48(8)
Cl(2A)-Ru(1A)-P(1A)	88.23(5)	Cl(2B)-Ru(1B)-P(1B)	86.84(7)

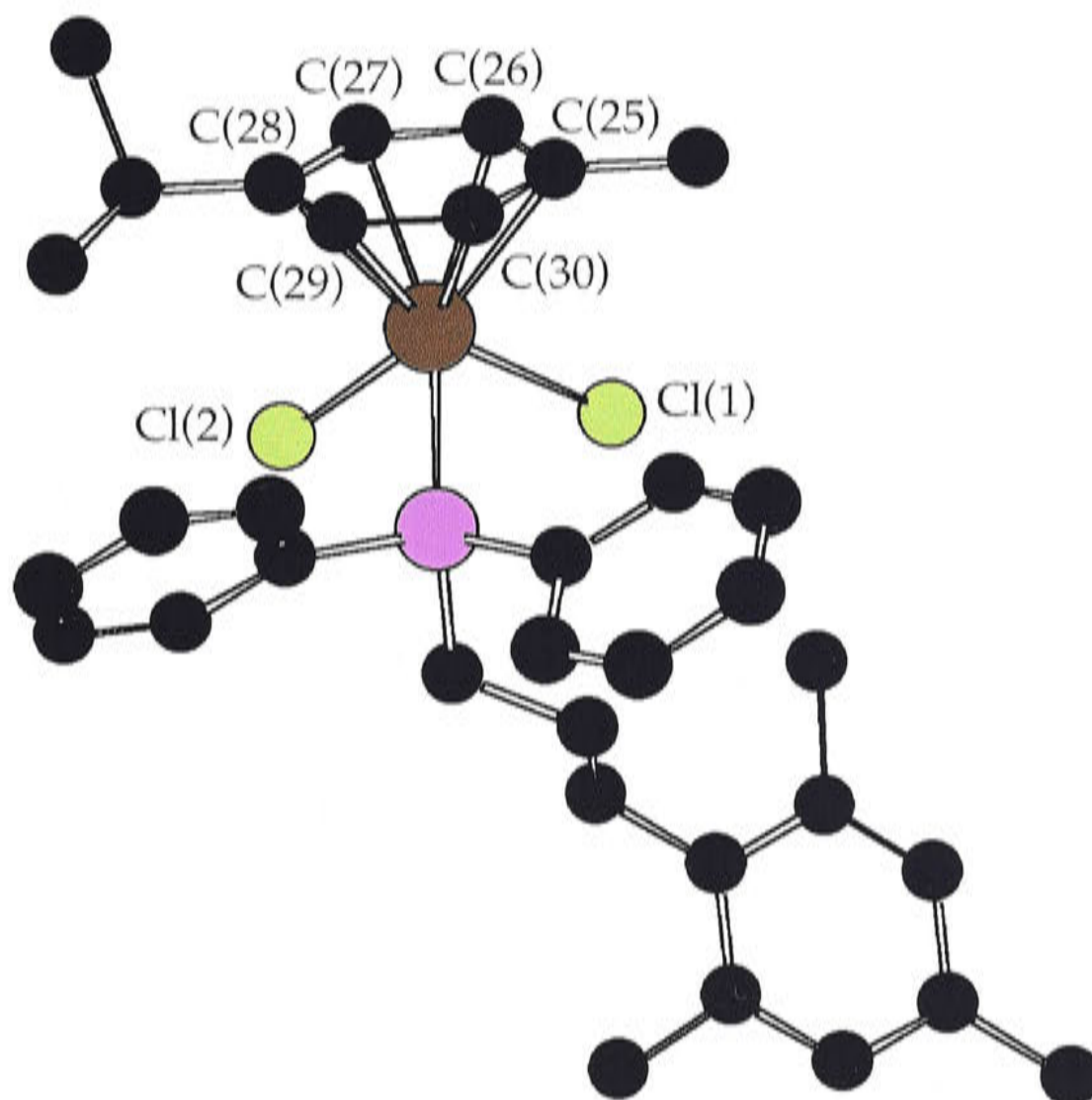
A.6 $[\text{RuCl}_2(\eta^6\text{-1,4-MeC}_6\text{H}_4\text{CHMe}_2)(\eta^1\text{-Ph}_2\text{P}(\text{CH}_2)_3\text{-2,4,6-C}_6\text{H}_2\text{Me}_3)]$ (233)

Figure 92. Chem3D representation of the molecular structure of $[\text{RuCl}_2(\eta^6\text{-1,4-MeC}_6\text{H}_4\text{CHMe}_2)(\eta^1\text{-Ph}_2\text{P}(\text{CH}_2)_3\text{-2,4,6-C}_6\text{H}_2\text{Me}_3)]$ (233). Hydrogen atoms have been omitted for clarity. The structure was determined by Drs A. D. Bond and T. Khimyak (Cambridge).

Table 46. Selected bond lengths (Å) and angles (°) for the non-tethered complex $[\text{RuCl}_2(\eta^6\text{-1,4-MeC}_6\text{H}_4\text{CHMe}_2)(\eta^1\text{-Ph}_2\text{P}(\text{CH}_2)_3\text{-2,4,6-C}_6\text{H}_2\text{Me}_3)]$ (233).

Ru(1)-Cl(1)	2.4136(7)	Ru(1)-Cl(2)	2.4397(7)
Ru(1)-P(1)	2.3523(7)	Ru(1)-C(25)	2.217(3)
Ru(1)-C(26)	2.226(3)	Ru(1)-C(27)	2.220(3)
Ru(1)-C(28)	2.232(3)	Ru(1)-C(29)	2.192(3)
Ru(1)-C(30)	2.178(3)	P-C	1.825(3)–1.841(3)
C-C(arene)	1.374(4)–1.438(4)		
Cl(1)-Ru(1)-Cl(2)	89.07(2)	Cl(1)-Ru(1)-P(1)	85.07(2)
Cl(2)-Ru(1)-P(1)	84.94(2)		

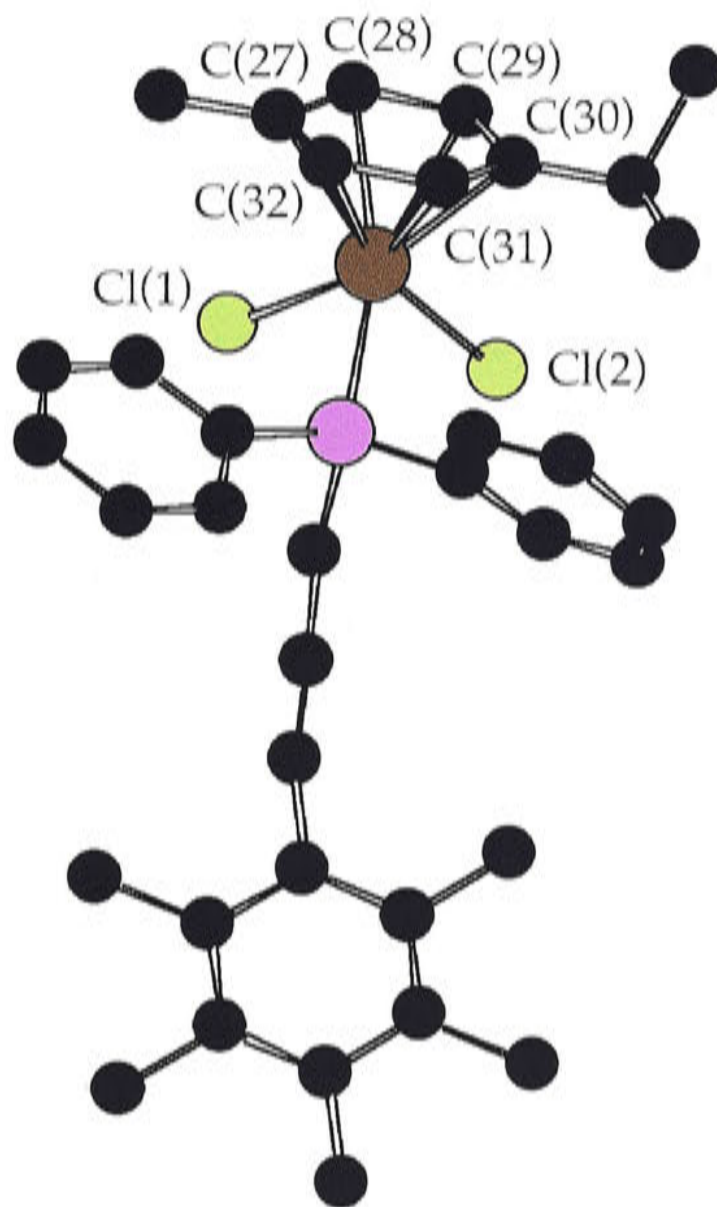
A.7 $[\text{RuCl}_2(\eta^6\text{-}1,4\text{-MeC}_6\text{H}_4\text{CHMe}_2)(\eta^1\text{-Ph}_2\text{P}(\text{CH}_2)_3\text{C}_6\text{Me}_5)]$ (234)

Figure 93. Chem3D representation of the molecular structure of $[\text{RuCl}_2(\eta^6\text{-}1,4\text{-MeC}_6\text{H}_4\text{CHMe}_2)(\eta^1\text{-Ph}_2\text{P}(\text{CH}_2)_3\text{C}_6\text{Me}_5)]$ (234), showing one of the independent molecules in the unit cell.¹ Hydrogen atoms have been omitted for clarity. The structure was determined by Drs J. E. Davies and T. Khimyak (Cambridge).

¹The other molecule does not differ significantly.

Table 47. Selected bond lengths (Å) and angles (°) for the non-tethered complex $[\text{RuCl}_2(\eta^6\text{-1,4-MeC}_6\text{H}_4\text{CHMe}_2)(\eta^1\text{-Ph}_2\text{P}(\text{CH}_2)_3\text{C}_6\text{Me}_5)]$ (234).

Molecule 1		Molecule 2	
Ru(1A)-Cl(1A)	2.4130(11)	Ru(1B)-Cl(1B)	2.4181(11)
Ru(1A)-Cl(2A)	2.4160(11)	Ru(1B)-Cl(2B)	2.4179(11)
Ru(1A)-P(1A)	2.3406(10)	Ru(1B)-P(1B)	2.3394(11)
Ru(1A)-C(27A)	2.226(4)	Ru(1B)-C(27B)	2.218(4)
Ru(1A)-C(28A)	2.188(4)	Ru(1B)-C(28B)	2.180(4)
Ru(1A)-C(29A)	2.205(4)	Ru(1B)-C(29B)	2.202(4)
Ru(1A)-C(30A)	2.248(4)	Ru(1B)-C(30B)	2.219(4)
Ru(1A)-C(31A)	2.252(4)	Ru(1B)-C(31B)	2.248(4)
Ru(1A)-C(32A)	2.213(4)	Ru(1B)-C(32B)	2.265(4)
P-C	1.817(4)–1.834(4)	P-C	1.828(4)–1.838(4)
C-C(arene)	1.397(7)–1.432(7)	C-C(arene)	1.397(7)–1.447(6)
Cl(1A)-Ru(1)-Cl(2A)	85.68(4)	Cl(1B)-Ru(1B)-Cl(2B)	87.61(9)
Cl(1A)-Ru(1A)-P(1A)	88.10(4)	Cl(1B)-Ru(1B)-P(1B)	86.19(4)
Cl(2A)-Ru(1A)-P(1A)	84.97(4)	Cl(2B)-Ru(1B)-P(1B)	85.90(4)

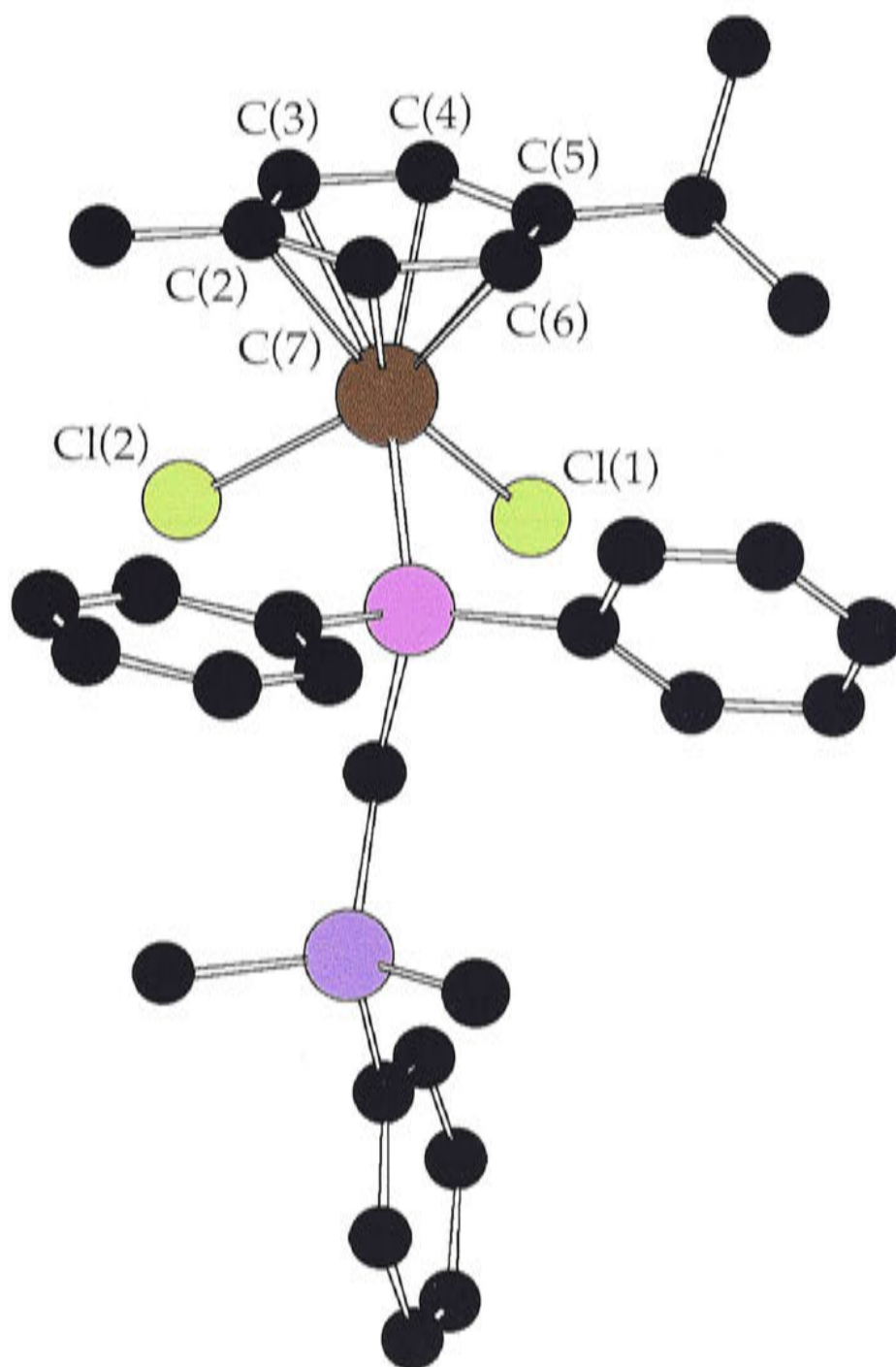
A.8 $[\text{RuCl}_2(\eta^6\text{-1,4-MeC}_6\text{H}_4\text{CHMe}_2)(\eta^1\text{-Ph}_2\text{PCH}_2\text{SiMe}_2\text{Ph})]$ (235)

Figure 94. Chem3D representation of the molecular structure of $[\text{RuCl}_2(\eta^6\text{-1,4-MeC}_6\text{H}_4\text{CHMe}_2)(\eta^1\text{-Ph}_2\text{PCH}_2\text{SiMe}_2\text{Ph})]$ (235). Hydrogen atoms and the solvent molecule (CH_2Cl_2) have been omitted for clarity. The structure was determined by Dr T. Khimyak (Cambridge).

There was some disorder observed in the crystal lattice of 235. The solvent molecule was disordered over three sites, and was refined to approximately 50%, 30% and 20% occupancy. All of the atoms in the solvent molecule were modelled with an isotropic displacement parameter.

Table 48. Selected bond lengths (Å) and angles (°) for the non-tethered complex $[\text{RuCl}_2(\eta^6\text{-1,4-MeC}_6\text{H}_4\text{CHMe}_2)(\eta^1\text{-Ph}_2\text{PCH}_2\text{SiMe}_2\text{Ph})]$ (235).

Ru(1)-Cl(1)	2.4160(12)	Ru(1)-Cl(2)	2.4077(12)
Ru(1)-P(1)	2.3519(12)	Ru(1)-C(2)	2.207(5)
Ru(1)-C(3)	2.218(5)	Ru(1)-C(4)	2.246(5)
Ru(1)-C(5)	2.219(5)	Ru(1)-C(6)	2.193(5)
Ru(1)-C(7)	2.162(5)	P-C	1.820(5)–1.839(5)
C-C(arene)	1.382(7)–1.429(7)		
Cl(1)-Ru(1)-Cl(2)	87.57(4)	Cl(1)-Ru(1)-P(1)	84.62(4)
Cl(2)-Ru(1)-P(1)	87.59(4)		

A.9 $[\text{RuCl}_2(\eta^6\text{-1,4-MeC}_6\text{H}_4\text{CHMe}_2)(\text{Ph}_2\text{PCH}=\text{CH}_2)]$ (269)

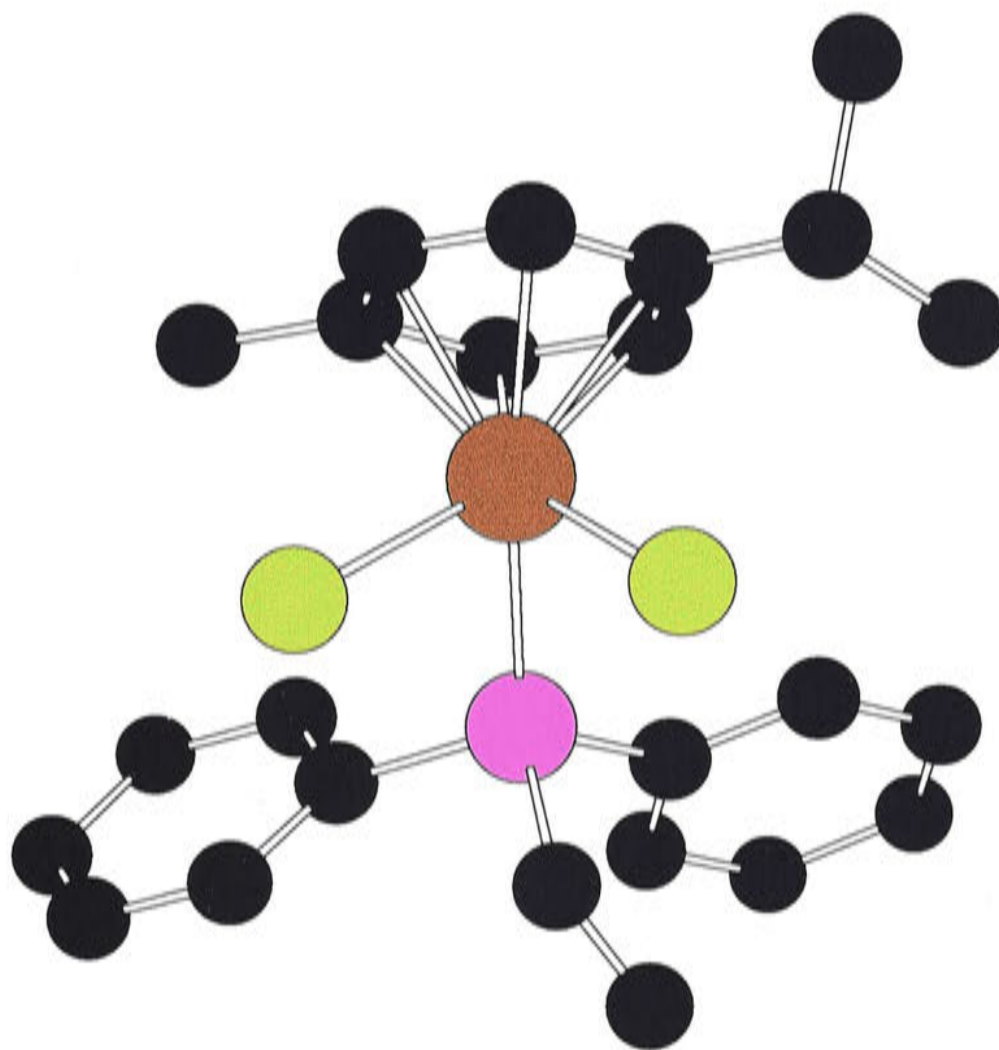


Figure 95. Chem3D representation of the molecular structure of $[\text{RuCl}_2(\eta^6\text{-1,4-MeC}_6\text{H}_4\text{CHMe}_2)(\text{Ph}_2\text{PCH}=\text{CH}_2)]$ (269). Hydrogen atoms have been omitted for clarity. The structure was determined by Dr A. J. Edwards (ANU).

Crystals of the complex **269** that were suitable for X-ray analysis were grown by vapour diffusion of *n*-hexane into a THF solution (Figure 95). The crystal structure of complex **269**, obtained from dichloromethane/ether, has been reported by Nelson and co-workers.¹ The significant bond lengths and angles for both data sets are shown in Table 49; the atom labelling employed for this Table is shown in Figure 96. Whilst there are no significant differences between the bond lengths of the two molecules, the Cl-Ru-P bond angles are somewhat different. Hence the two crystal structures are conformationally different, that is, two crystallographically distinct forms of the same molecule. Figure 92 shows the differences about the chloride and phosphine ligands. The packing of the molecules in the two distinct crystals is also different. The structure in this study shows some close interactions (*ca* 3 Å) between the chloride ligands and one of the phenyl groups on the phosphorus atom of an adjacent molecule, which are packed in a herringbone type arrangement. There are also some short distance (*ca* 3.5 Å) interactions [determined by applying PLATON² to data in reference(1), both intramolecular and intermolecular, in the packing arrangement of the structure reported by Nelson and co-workers.¹

Table 49. Selected observed and reported¹ bond lengths (Å) and angles (°) for the complex $[\text{RuCl}_2(\eta^6\text{-1,4-MeC}_6\text{H}_4\text{CHMe}_2)(\text{Ph}_2\text{PCH=CH}_2)]$ (**269**). Atom labelling employed is shown in Figure 96 for ease of comparison.

Bond Length (Å), Bond Angle (°)	Observed	Reported ^{a,b}
Ru(1)-Cl(1)	2.4172(7)	2.414(2)
Ru(1)-Cl(2)	2.4118(7)	2.412(2)
Ru(1)-P(1)	2.3485(7)	2.343(2)
Ru(1)-C(1)	2.224(3)	2.218
Ru(1)-C(2)	2.221(3)	2.205
Ru(1)-C(3)	2.238(3)	2.187
Ru(1)-C(4)	2.244(3)	2.217
Ru(1)-C(5)	2.210(3)	2.218
Ru(1)-C(6)	2.185(3)	2.240
P-C	1.815(3)–1.827(3)	1.810–1.836
C-C(arene)	1.388(4)–1.431(4)	1.391–1.424
Cl(1)-Ru(1)-Cl(2)	87.8(1)	88.98(6)
Cl(1)-Ru(1)-P(1)	86.7(1)	83.97(5)
Cl(2)-Ru(1)-P(1)	81.1(1)	83.29(5)

^aReported in reference(1); ^bESDs are not available for data extracted from the CSD.

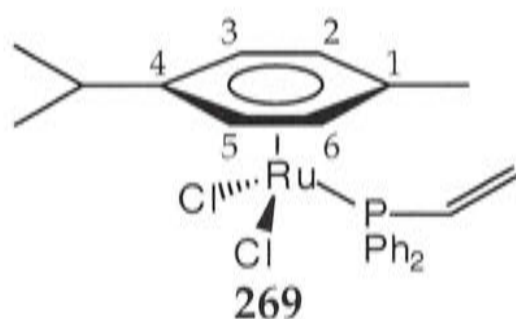


Figure 96. Numbering scheme for the complex $[\text{RuCl}_2(\eta^6\text{-1,4-MeC}_6\text{H}_4\text{CHMe}_2)(\text{Ph}_2\text{PCH=CH}_2)]$ (**269**) employed for ease of comparison of data in Table 49.

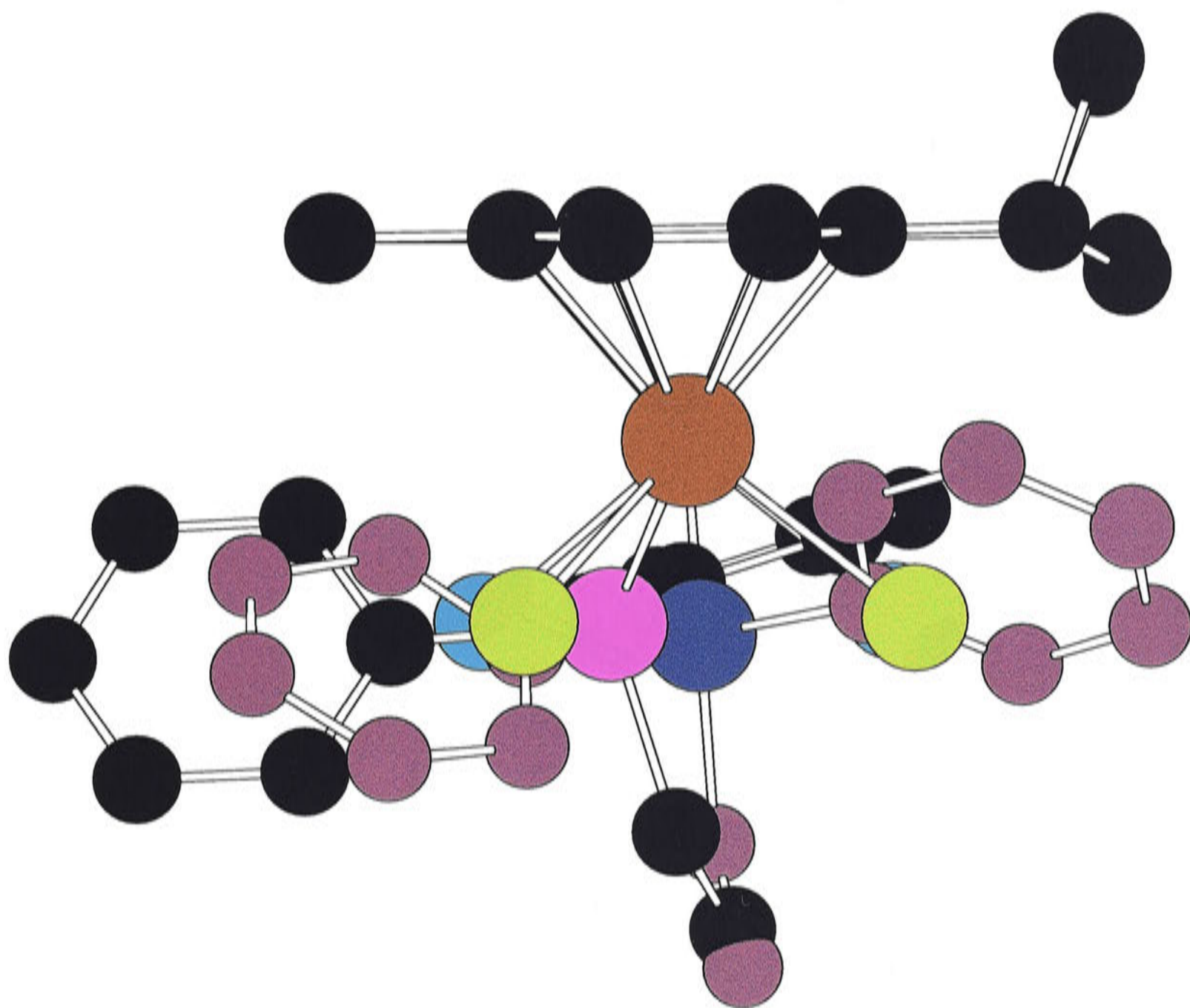


Figure 97. The Chem3D representation of the reported¹ X-ray structure of $[\text{RuCl}_2(\eta^6\text{-1,4-MeC}_6\text{H}_4\text{CHMe}_2)(\text{Ph}_2\text{PCH=CH}_2)]$ (**269**) superimposed over the Chem3D representation of the X-ray structure of **269** obtained in this study. The atom labelling for the structure obtained in this study is identical to that employed for other Chem3D representations (as indicated in the Abbreviations list); for ease of comparison the reported structure¹ has the ruthenium and carbon atoms of the η^6 -arene labelled as shown in the Abbreviations list, and atoms which are conformationally different are shown as indicated below:

- phosphorus
- chlorine
- carbon

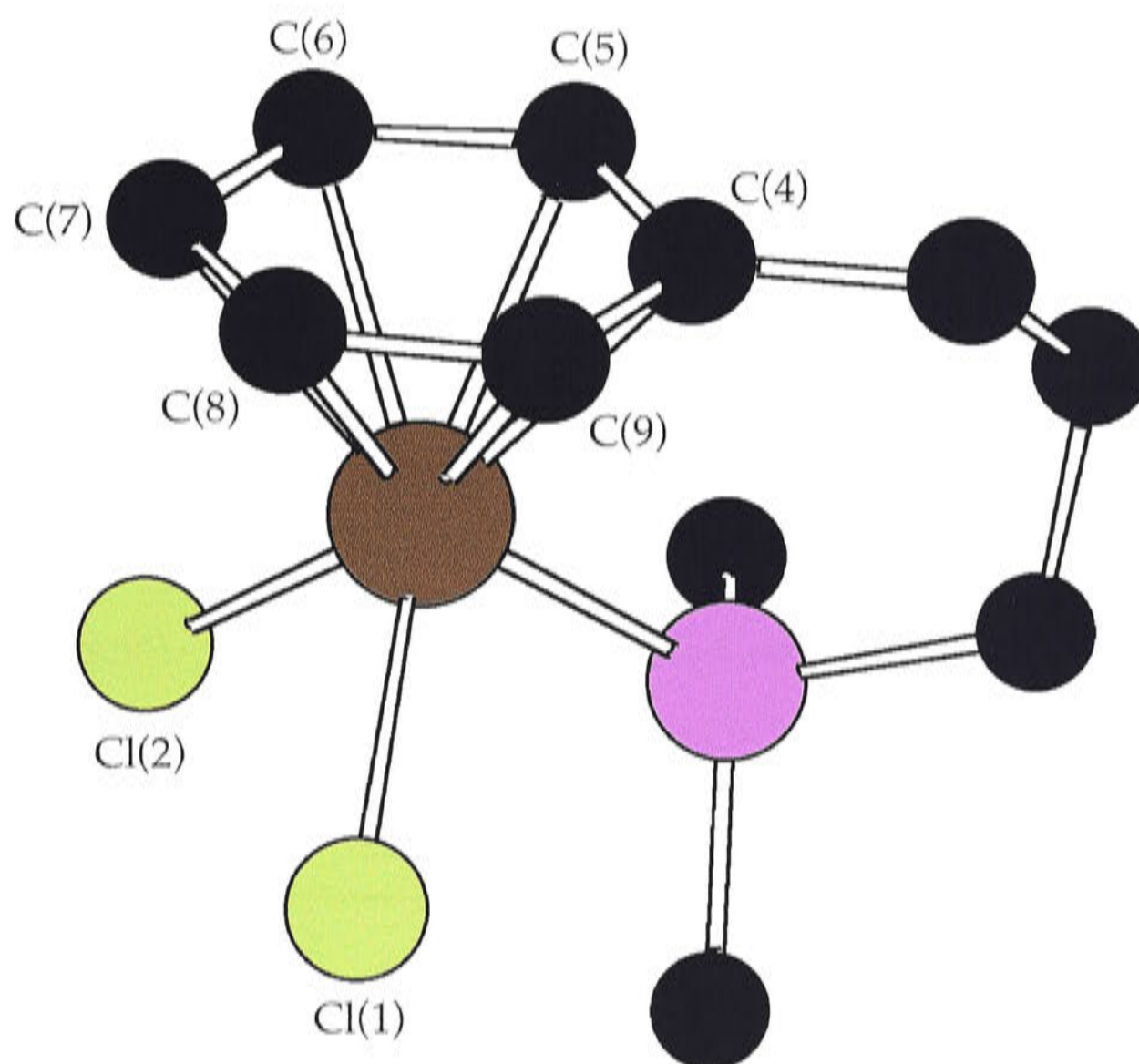
A.10 $[\text{RuCl}_2(\eta^1:\eta^6\text{-Me}_2\text{P}(\text{CH}_2)_3\text{Ph})]$ (248)

Figure 98. Chem3D representation of the molecular structure of $[\text{RuCl}_2(\eta^1:\eta^6\text{-Me}_2\text{P}(\text{CH}_2)_3\text{Ph})]$ (248), showing one of the independent molecules in the unit cell.¹ Hydrogen atoms have been omitted for clarity. The structure was determined by Dr A. C. Willis (ANU).

¹The other molecule does not differ significantly.

Table 50. Selected bond lengths (Å) and angles (°) for the tethered complex [RuCl₂(η¹:η⁶-Me₂P(CH₂)₃Ph)] (248).

Molecule 1		Molecule 2	
Ru(1)-Cl(1)	2.405(2)	Ru(2)-Cl(3)	2.415(2)
Ru(1)-Cl(2)	2.421(2)	Ru(2)-Cl(4)	2.421(3)
Ru(1)-P(1)	2.322(3)	Ru(2)-P(2)	2.303(2)
Ru(1)-C(4)	2.193(8)	Ru(2)-C(15)	2.194(9)
Ru(1)-C(5)	2.185(9)	Ru(2)-C(16)	2.189(9)
Ru(1)-C(6)	2.181(9)	Ru(2)-C(17)	2.158(9)
Ru(1)-C(7)	2.257(9)	Ru(2)-C(18)	2.253(9)
Ru(1)-C(8)	2.257(9)	Ru(2)-C(19)	2.24(1)
Ru(1)-C(9)	2.170(9)	Ru(2)-C(20)	2.182(9)
P-C	1.79(1)–1.82(1)	P-C	1.79(1)–1.82(1)
C-C(arene)	1.36(1)–1.42(1)	C-C(arene)	1.36(2)–1.43(1)
Cl(1)-Ru(1)-Cl(2)	87.68(9)	Cl(3)-Ru(2)-Cl(4)	87.8(1)
Cl(1)-Ru(1)-P(1)	89.34(9)	Cl(3)-Ru(2)-P(2)	89.17(8)
Cl(2)-Ru(1)-P(1)	83.83(9)	Cl(4)-Ru(2)-P(2)	84.72(9)

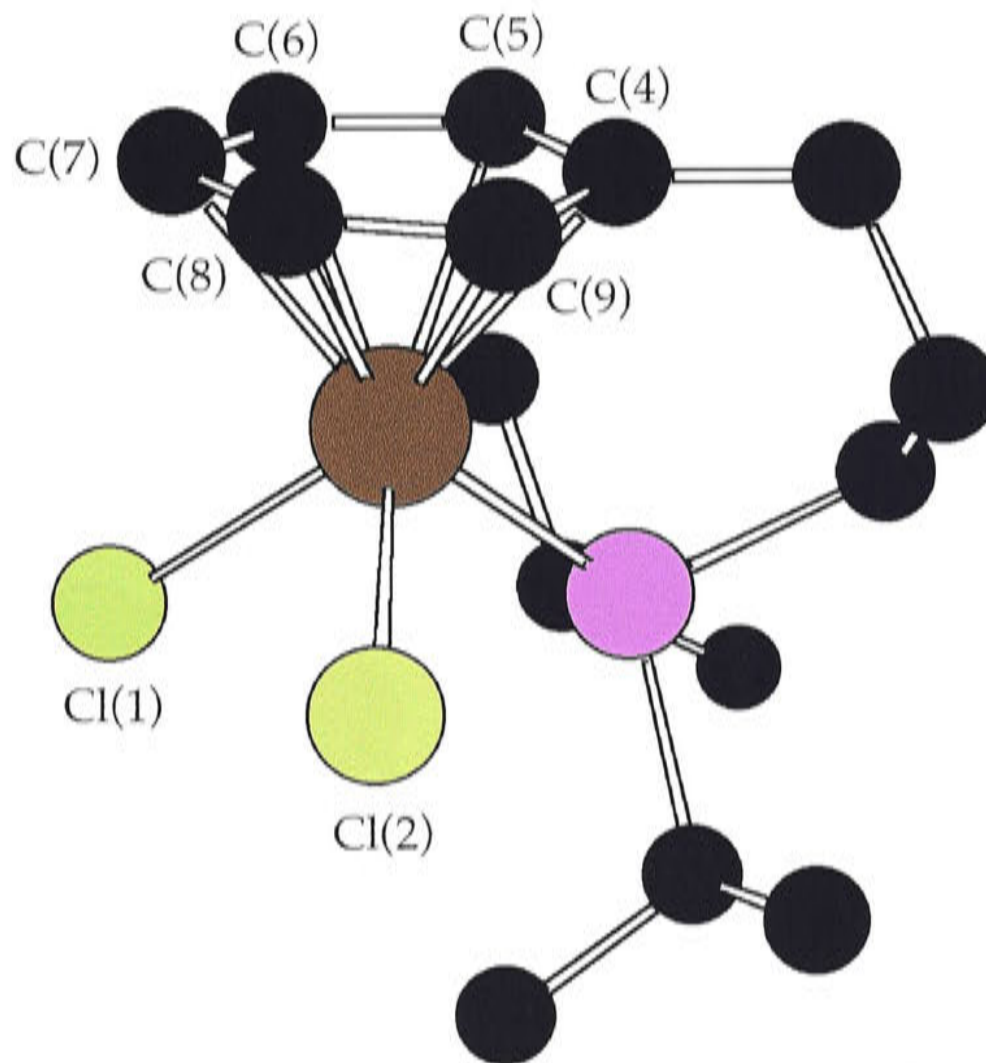
A.11 $[\text{RuCl}_2(\eta^1:\eta^6\text{-}i\text{-Pr}_2\text{P}(\text{CH}_2)_3\text{Ph})]$ (249)

Figure 99. Chem3D representation of the molecular structure of $[\text{RuCl}_2(\eta^1:\eta^6\text{-}i\text{-Pr}_2\text{P}(\text{CH}_2)_3\text{Ph})]$ (249). Hydrogen atoms have been omitted for clarity. The structure was determined by Drs A. D. Bond and T. Khimyak (Cambridge).

Table 51. Selected bond lengths (Å) and angles (°) for the tethered complex $[\text{RuCl}_2(\eta^1:\eta^6\text{-}i\text{-Pr}_2\text{P}(\text{CH}_2)_3\text{Ph})]$ (249).

Ru(1)-Cl(1)	2.5247(18)	Ru(1)-Cl(2)	2.4185(19)
Ru(1)-P(1)	2.338(2)	Ru(1)-C(4)	2.211(7)
Ru(1)-C(5)	2.194(7)	Ru(1)-C(6)	2.163(8)
Ru(1)-C(7)	2.254(8)	Ru(1)-C(8)	2.254(8)
Ru(1)-C(9)	2.171(8)	P-C	1.834(9)–1.861(8)
C-C(arene)	1.371(13)–1.435(13)		
Cl(1)-Ru(1)-Cl(2)	88.85(6)	Cl(1)-Ru(1)-P(1)	86.43(7)
Cl(2)-Ru(1)-P(1)	92.51(7)		

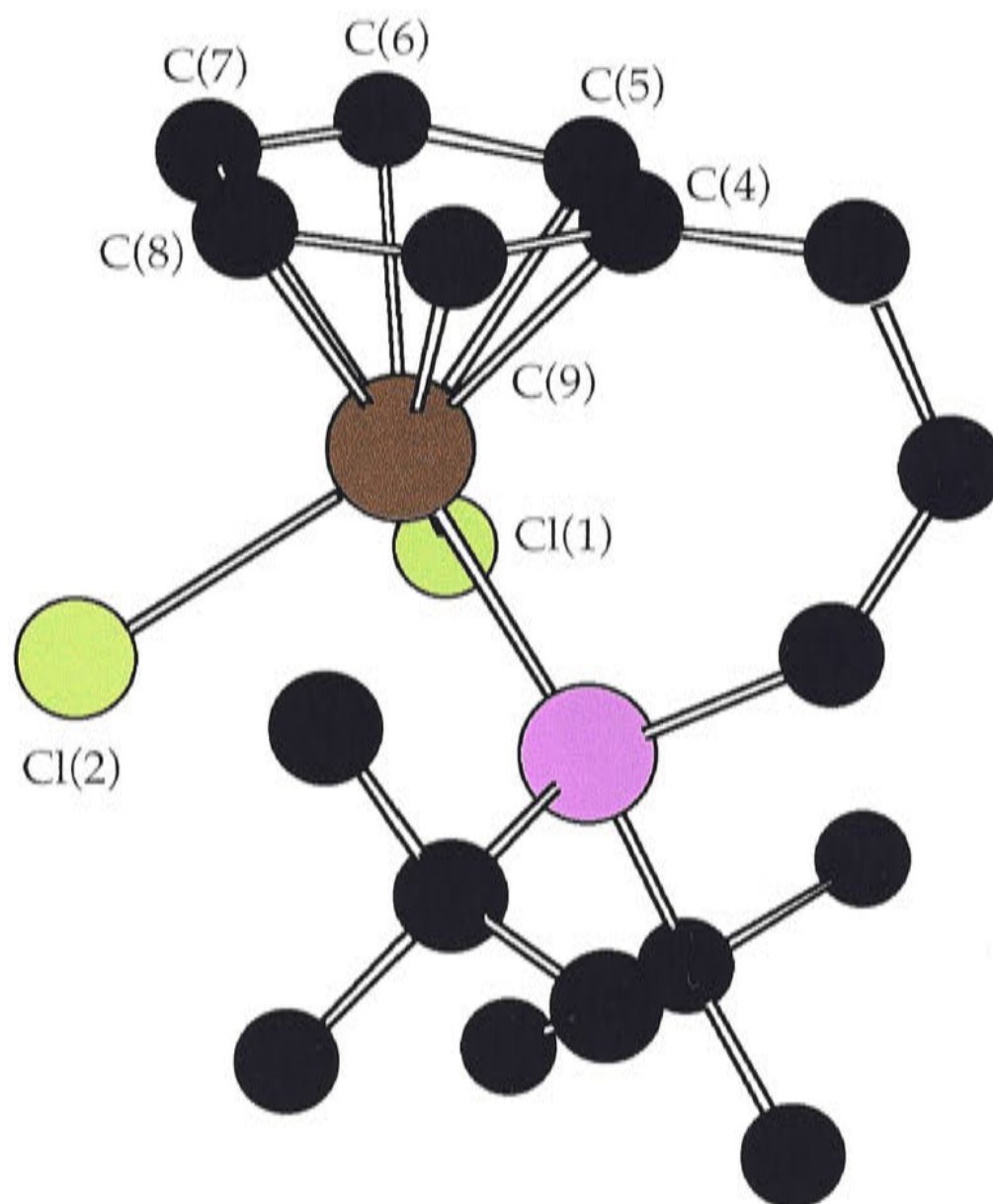
A.12 $[\text{RuCl}_2(\eta^1:\eta^6\text{-}t\text{-Bu}_2\text{P}(\text{CH}_2)_3\text{Ph})]$ (253)

Figure 100. Chem3D representation of the molecular structure of $[\text{RuCl}_2(\eta^1:\eta^6\text{-}t\text{-Bu}_2\text{P}(\text{CH}_2)_3\text{Ph})]$ (253). Hydrogen atoms have been omitted for clarity. The structure was determined by Dr J. E. Davies (Cambridge).

Table 52. Selected bond lengths (Å) and angles (°) for the tethered complex $[\text{RuCl}_2(\eta^1:\eta^6\text{-}t\text{-Bu}_2\text{P}(\text{CH}_2)_3\text{Ph})]$ (253).

Ru(1)-Cl(1)	2.4464(9)	Ru(1)-Cl(2)	2.4141(9)
Ru(1)-P(1)	2.413(9)	Ru(1)-C(4)	2.238(3)
Ru(1)-C(5)	2.181(3)	Ru(1)-C(6)	2.223(3)
Ru(1)-C(7)	2.230(4)	Ru(1)-C(8)	2.166(3)
Ru(1)-C(9)	2.204(3)	P-C	1.844(3)–1.902(4)
C-C(arene)	1.382(5)–1.433(5)		
Cl(1)-Ru(1)-Cl(2)	86.58(3)	Cl(1)-Ru(1)-P(1)	97.35(3)
Cl(2)-Ru(1)-P(1)	89.54(3)		

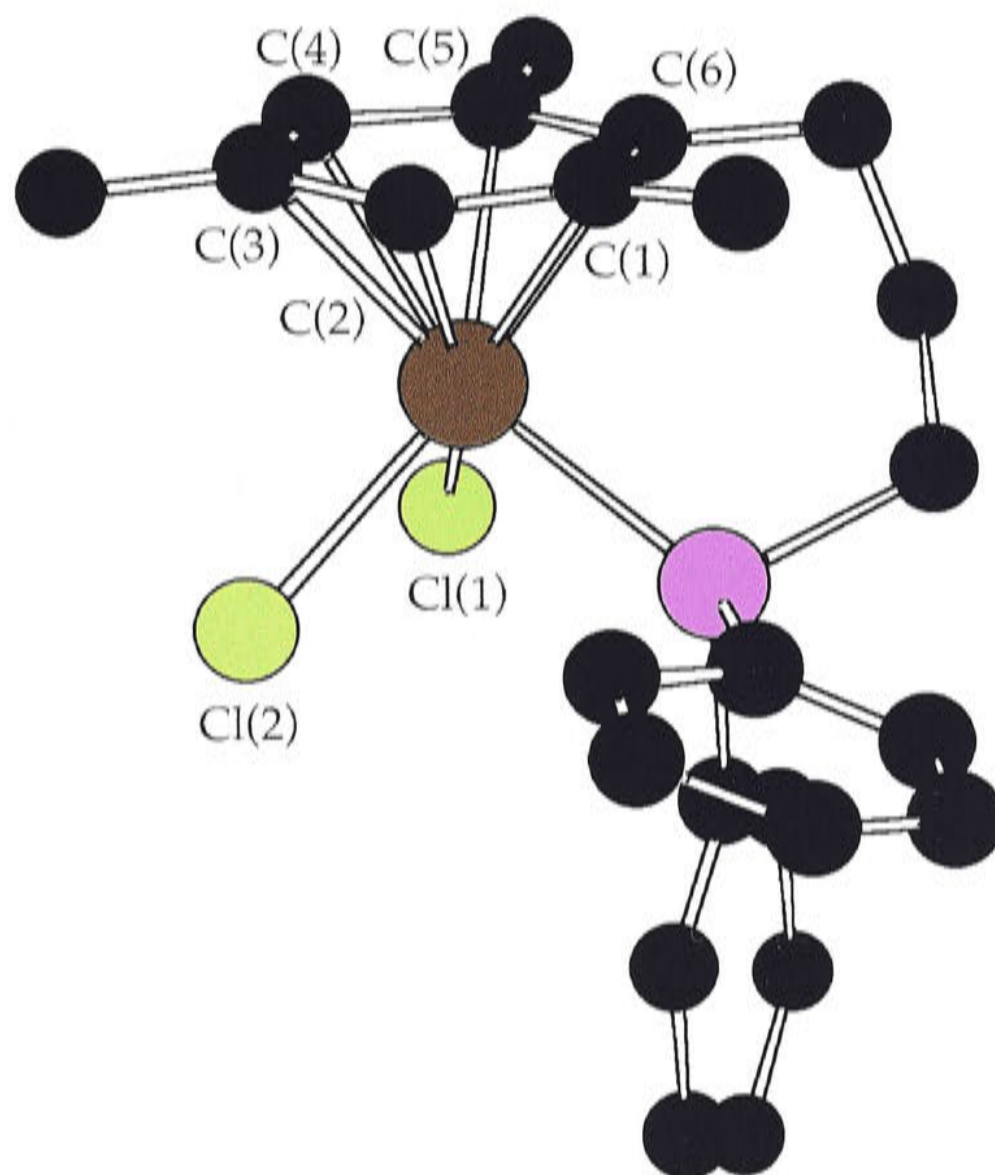
A.13 $[\text{RuCl}_2(\eta^1:\eta^6\text{-Ph}_2\text{P}(\text{CH}_2)_3\text{-2,4,6-C}_6\text{H}_2\text{Me}_3)]$ (250)

Figure 101. Chem3D representation of the molecular structure of $[\text{RuCl}_2(\eta^1:\eta^6\text{-Ph}_2\text{P}(\text{CH}_2)_3\text{-2,4,6-C}_6\text{H}_2\text{Me}_3)]$ (250). Hydrogen atoms and the solvent molecule (CH_2Cl_2) have been omitted for clarity. The structure was determined by Dr T. Khimyak (Cambridge).

Table 53. Selected bond lengths (Å) and angles (°) for the tethered complex [RuCl₂(η¹:η⁶-Ph₂P(CH₂)₃-2,4,6-C₆H₂Me₃)] (**250**).

Ru(1)-Cl(1)	2.4159(10)	Ru(1)-Cl(2)	2.4425(10)
Ru(1)-P(1)	2.3230(10)	Ru(1)-C(1)	2.212(4)
Ru(1)-C(2)	2.183(4)	Ru(1)-C(3)	2.282(4)
Ru(1)-C(4)	2.262(4)	Ru(1)-C(5)	2.203(4)
Ru(1)-C(6)	2.200(4)	P-C	1.828(4)–1.845(4)
C-C(arene)	1.393(6)–1.439(6)		
Cl(1)-Ru(1)-Cl(2)	87.52(4)	Cl(1)-Ru(1)-P(1)	86.35(4)
Cl(2)-Ru(1)-P(1)	90.34(4)		

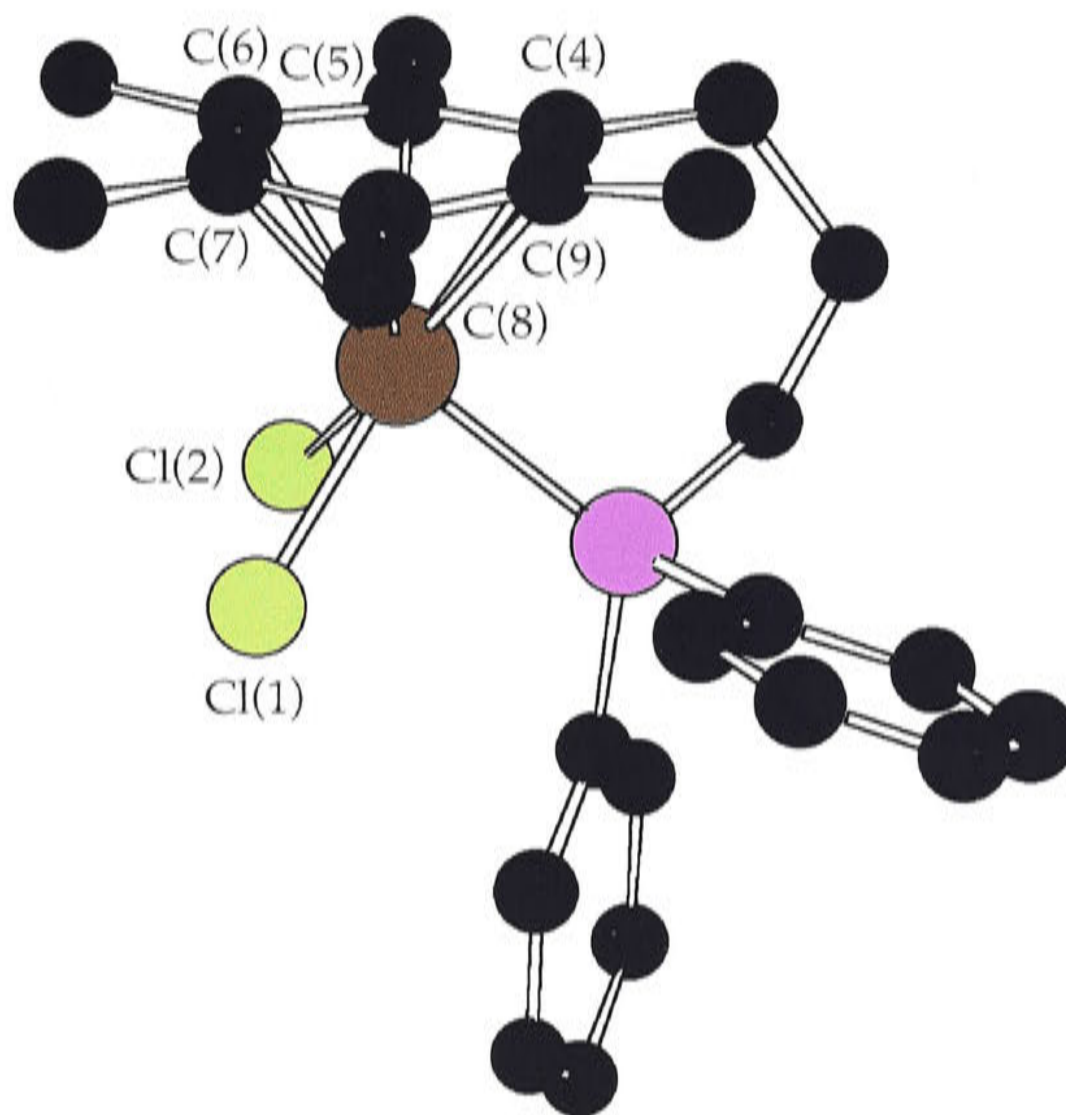
A.14 $[\text{RuCl}_2(\eta^1:\eta^6\text{-Ph}_2\text{P}(\text{CH}_2)_3\text{C}_6\text{Me}_5)]$ (251)

Figure 102. Chem3D representation of the molecular structure of $[\text{RuCl}_2(\eta^1:\eta^6\text{-Ph}_2\text{P}(\text{CH}_2)_3\text{C}_6\text{Me}_5)]$ (251). Hydrogen atoms have been omitted for clarity. The structure was determined by Dr A. J. Edwards (ANU).[†]

[†]Data were collected by Dr M. J. Hardie at Monash University.

Table 54. Selected bond lengths (Å) and angles (°) for the tethered complex $[\text{RuCl}_2(\eta^1:\eta^6\text{-Ph}_2\text{P}(\text{CH}_2)_3\text{C}_6\text{Me}_5)]$ (251).

Ru(1)-Cl(1)	2.4016(12)	Ru(1)-Cl(2)	2.4163(12)
Ru(1)-P(1)	2.2995(14)	Ru(1)-C(4)	2.203(5)
Ru(1)-C(5)	2.249(5)	Ru(1)-C(6)	2.201(5)
Ru(1)-C(7)	2.284(5)	Ru(1)-C(8)	2.285(5)
Ru(1)-C(9)	2.182(5)	P-C	1.822(5)–1.834(5)
C-C(arene)	1.394(7)–1.454(7)		
Cl(1)-Ru(1)-Cl(2)	88.58(4)	Cl(1)-Ru(1)-P(1)	88.83(5)
Cl(2)-Ru(1)-P(1)	82.29(4)		

A.15 $[\text{RuCl}_2(\eta^1:\eta^6\text{-Ph}_2\text{PCH}_2\text{SiMe}_2\text{Ph})]$ (252)

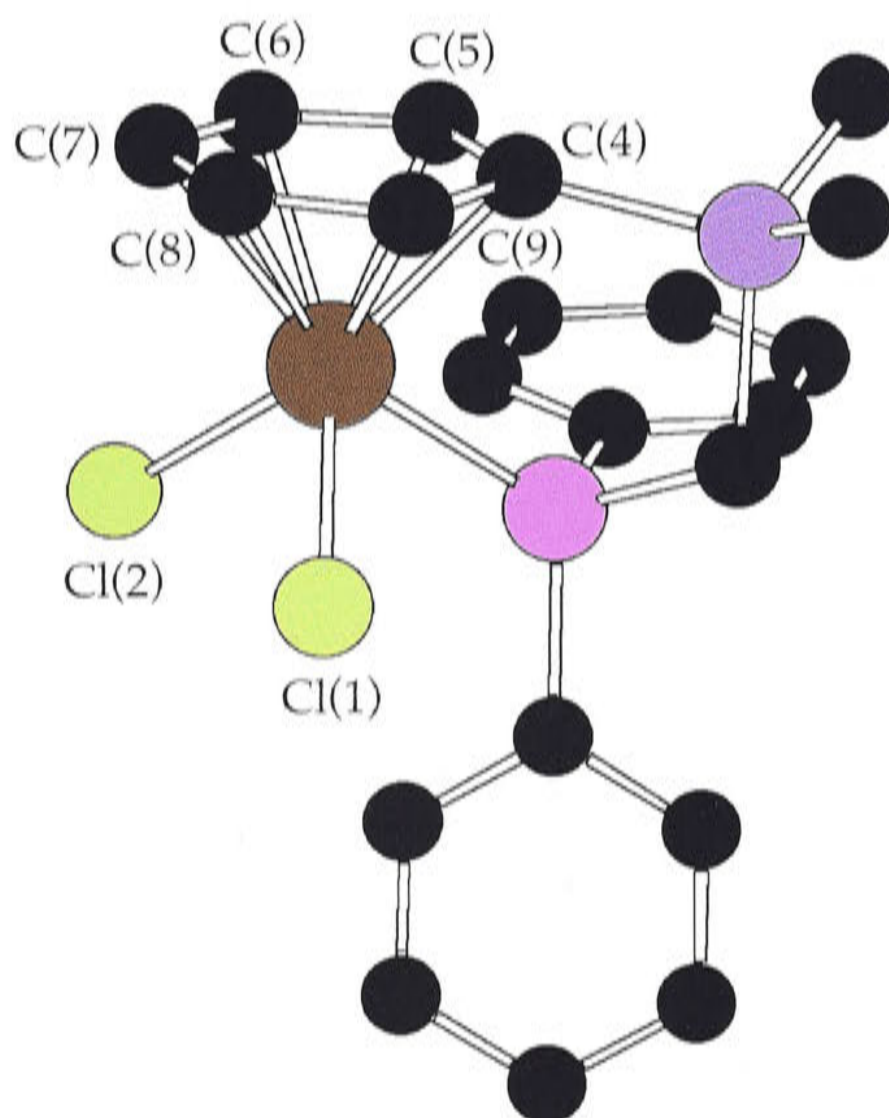


Figure 103. Chem3D representation of the molecular structure of $[\text{RuCl}_2(\eta^1:\eta^6\text{-Ph}_2\text{PCH}_2\text{SiMe}_2\text{Ph})]$ (252). Hydrogen atoms have been omitted for clarity. The structure was determined by Dr A. C. Willis (ANU).

Table 55. Selected bond lengths (Å) and angles (°) for the tethered complex [RuCl₂(η¹:η⁶-Ph₂PCH₂SiMe₂Ph)] (252).

Ru(1)-Cl(1)	2.4050(7)	Ru(1)-Cl(2)	2.4159(7)
Ru(1)-P(1)	2.3526(7)	Ru(1)-C(4)	2.180(2)
Ru(1)-C(5)	2.180(2)	Ru(1)-C(6)	2.193(3)
Ru(1)-C(7)	2.250(3)	Ru(1)-C(8)	2.246(3)
Ru(1)-C(9)	2.145(3)	P-C	1.818(2)–1.831(2)
Si-C	1.847(3)–1.902(3)	C-C(arene)	1.405(4)–1.436(4)
Cl(1)-Ru(1)-Cl(2)	89.90(3)	Cl(1)-Ru(1)-P(1)	84.26(2)
Cl(2)-Ru(1)-P(1)	94.29(3)		

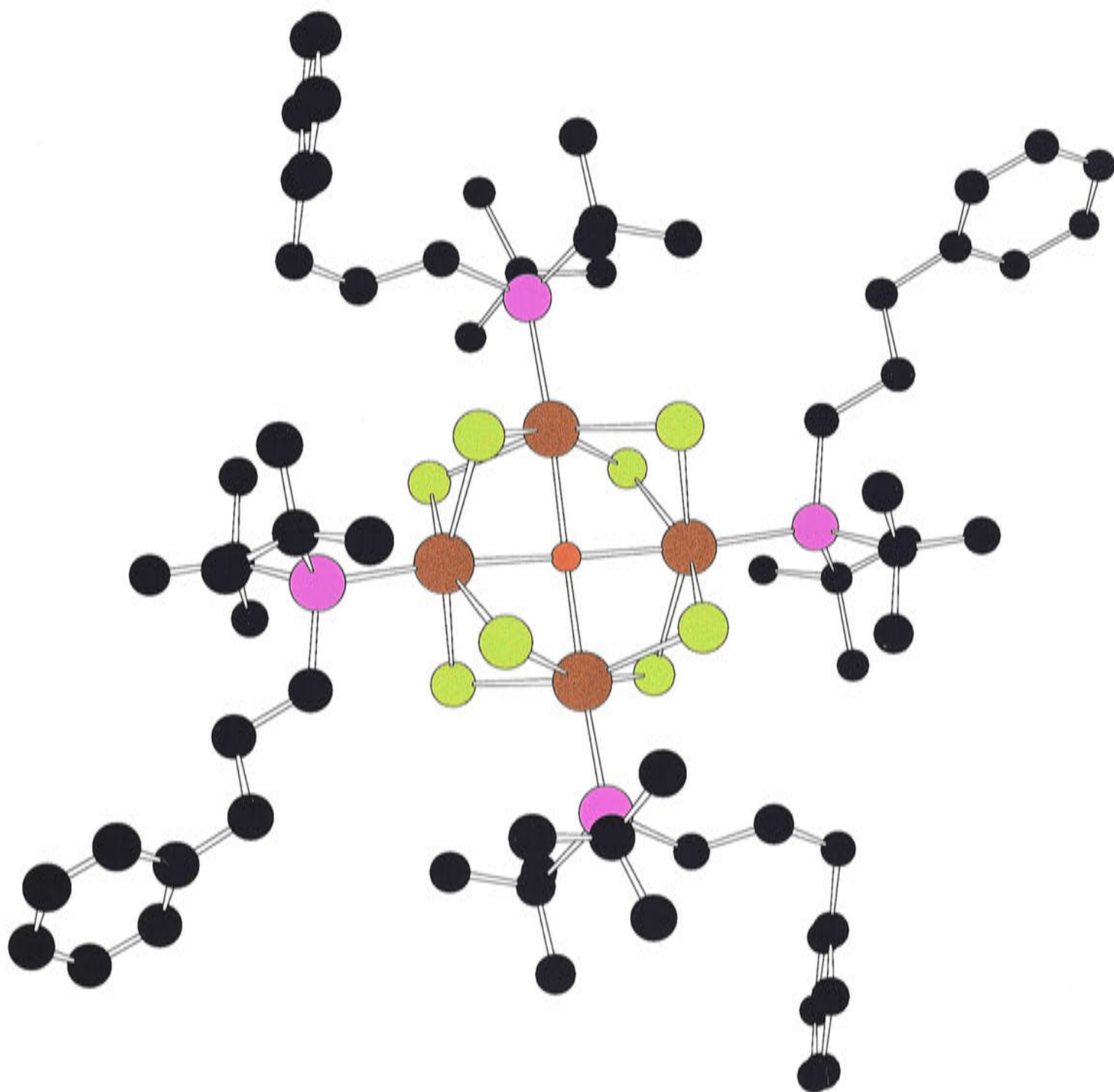
A.16 $[\text{Ru}_4(\mu_4\text{-O})(\mu_2\text{-Cl})_8(\eta^1\text{-}t\text{-Bu}_2\text{P}(\text{CH}_2)_3\text{Ph})_4]$ (**261**)

Figure 104. Chem3D representation of the molecular structure of $[\text{Ru}_4(\mu_4\text{-O})(\mu_2\text{-Cl})_8(\eta^1\text{-}t\text{-Bu}_2\text{P}(\text{CH}_2)_3\text{Ph})_4]$ (**261**). Hydrogen atoms have been omitted for clarity (average position for the oxygen atom is shown). The structure was determined by Dr A. C. Willis (ANU).

As mentioned previously (see Chapter 2, Section 3.2.7), in the crystal structure of **261**, the central oxygen atom was disordered over two sites, each with 50% occupancy. Restraints were initially used in the refinement to equalise the Ru-O bond lengths, but were totally removed in the final refinement cycles. Disorder is also observed in one of the phosphines. Atoms C(101) and C(102) (in the phenyl group) are each disordered over

two sites, each with *ca* 64% and 36% occupancy; the minor occupancy was refined anisotropically.

The chemically significant bonds lengths and angles of the tetranuclear species $[\text{Ru}_4(\mu_4\text{-O})(\mu_2\text{-Cl})_8(\eta^1\text{-}t\text{-Bu}_2\text{P}(\text{CH}_2)_3\text{Ph})_4]$ (**261**) are given in Chapter 3 (Section 3.2.7).

A.17 $[\text{RuCl}(\text{NCMe})_4(\eta^1\text{-Ph}_2\text{P}(\text{CH}_2)_3\text{Ph})]\text{Cl}$ (**[328]Cl**)

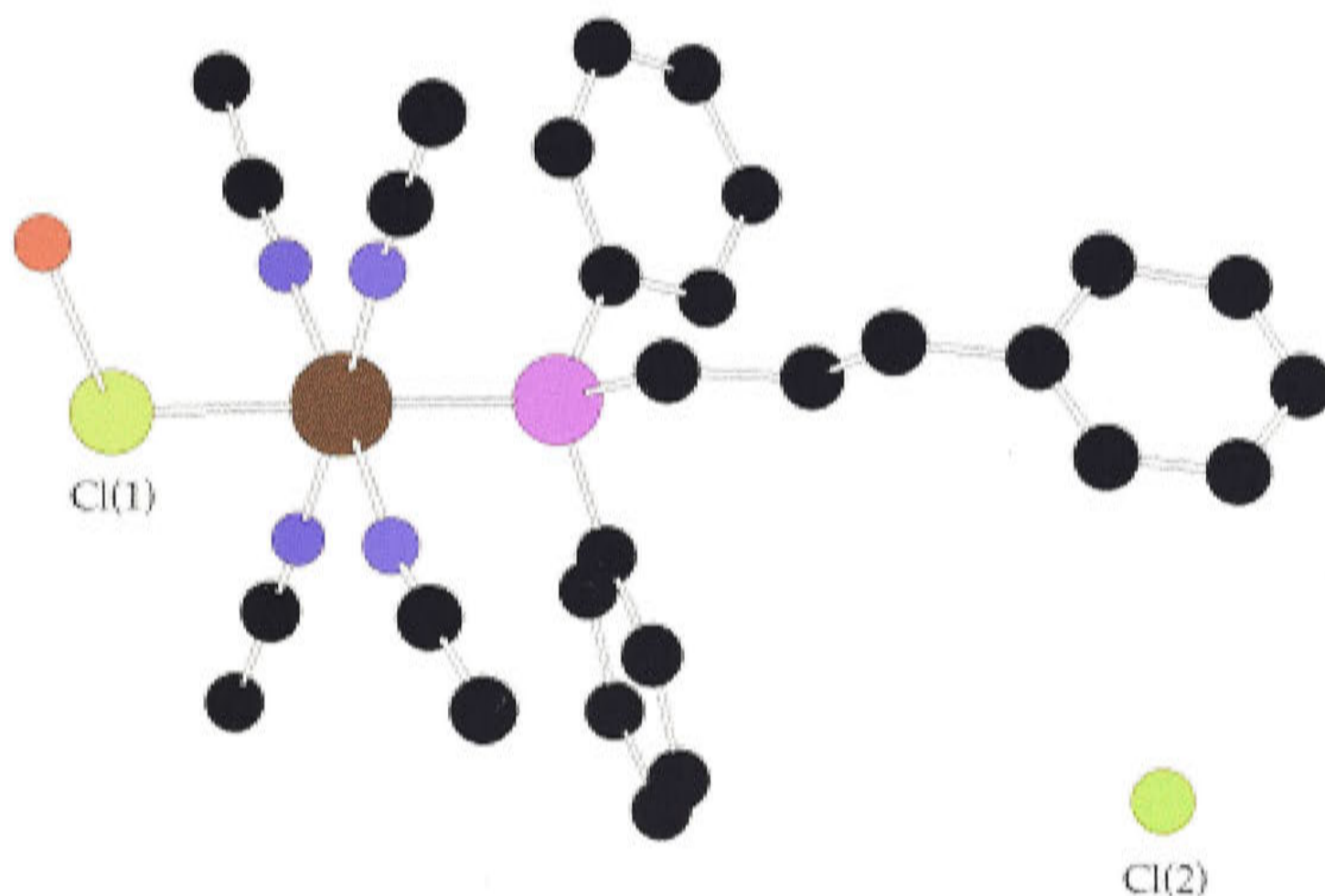


Figure 105. Chem3D representation of the molecular structure of $[\text{RuCl}(\text{NCMe})_4(\eta^1\text{-Ph}_2\text{P}(\text{CH}_2)_3\text{Ph})]\text{Cl}$ (**[328]Cl**), showing the hydrogen-bonding interaction between the inner-sphere chloride and the oxygen atom of the water molecule. Hydrogen atoms and the solvent molecule (CH_2Cl_2) have been omitted for clarity. The structure was determined by Dr D. C. R. Hockless (ANU).

Table 56. Selected bond lengths (Å) and angles (°) for the tethered arene-ruthenium(III) complex $[\text{RuCl}_2(\eta^1:\eta^6\text{-Ph}_2\text{P}(\text{CH}_2)_3\text{C}_6\text{Me}_5)][\text{SbCl}_6]$ (**[251]** $[\text{SbCl}_6]$).

Ru(1)-Cl(1)	2.3228(13)	Ru(1)-Cl(2)	2.3106(13)
Ru(1)-P(1)	2.3235(13)	Ru(1)-C(4)	2.228(5)
Ru(1)-C(5)	2.336(5)	Ru(1)-C(6)	2.334(5)
Ru(1)-C(7)	2.302(5)	Ru(1)-C(8)	2.323(5)
Ru(1)-C(9)	2.309(5)	P-C	1.808(5)–1.819(5)
C-C(arene)	1.413(7)–1.448(7)	Sb-Cl	2.3615(15)–2.3731(14)
Cl(1)-Ru(1)- Cl(2)	97.88(5)	Cl(1)-Ru(1)- P(1)	88.58(5)
Cl(2)-Ru(1)-P(1)	82.36(5)		

A.19 $[\text{RuCl}_2(\eta^6\text{-C}_6\text{Me}_6)(\text{PPh}_3)][\text{SbCl}_6]$ (**[306]** $[\text{SbCl}_6]$)

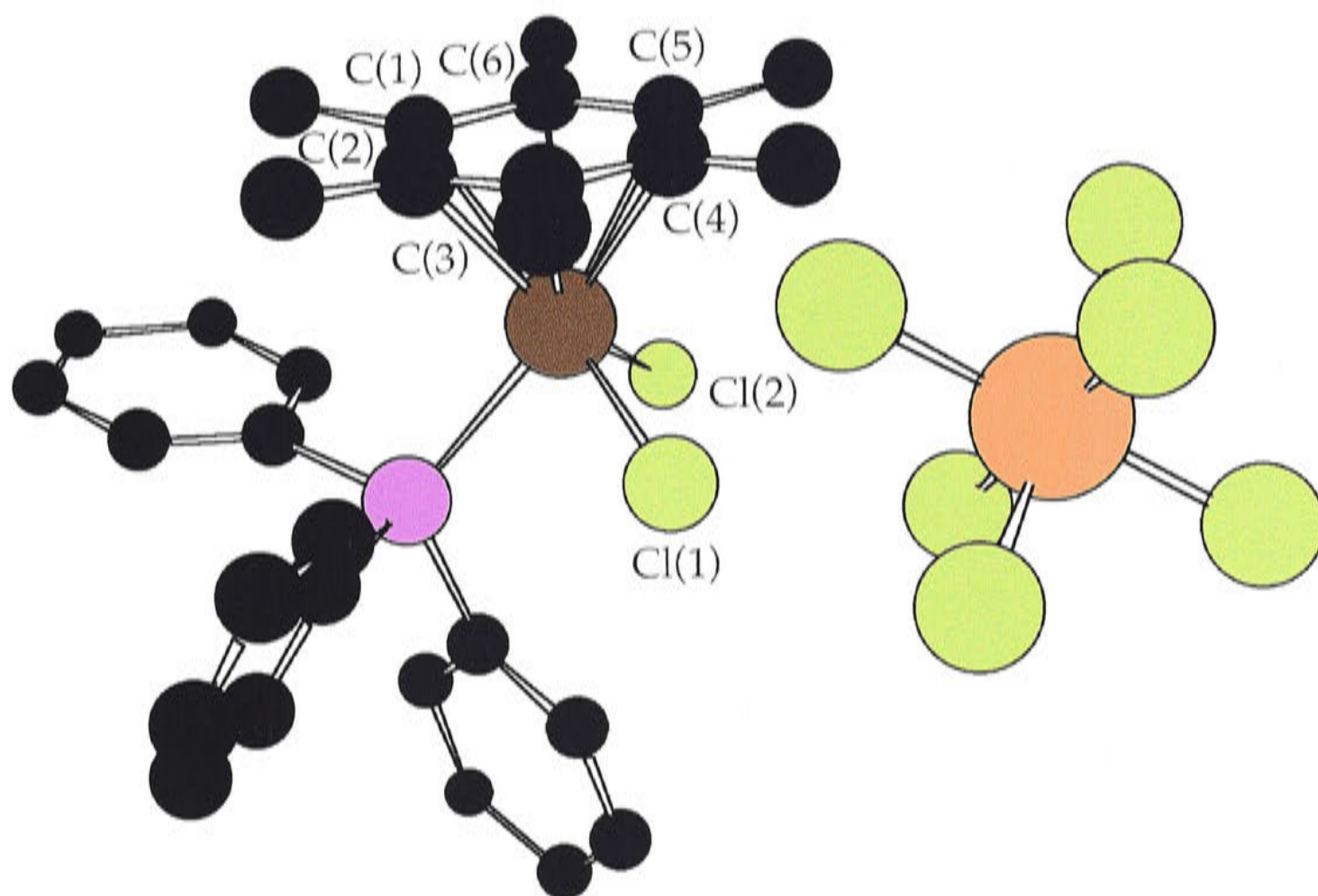


Figure 107. Chem3D representation of the molecular structure of $[\text{RuCl}_2(\eta^6\text{-C}_6\text{Me}_6)(\text{PPh}_3)][\text{SbCl}_6]$ (**[306]** $[\text{SbCl}_6]$). Hydrogen atoms and the solvent molecule (CH_2Cl_2) have been omitted for clarity. The structure was determined by Drs A. D. Rae and A. C. Willis (ANU).

Table 57. Selected bond lengths (Å) and angles (°) for the non-tethered ruthenium(III) complex $[\text{RuCl}_2(\eta^6\text{-C}_6\text{Me}_6)(\text{PPh}_3)][\text{SbCl}_6]$ (**[306]** $[\text{SbCl}_6]$).

Ru(1)-Cl(1)	2.308(3)	Ru(1)-Cl(2)	2.312(3)
Ru(1)-P(1)	2.375(3)	Ru(1)-C(1)	2.346(7)
Ru(1)-C(2)	2.330(7)	Ru(1)-C(3)	2.313(8)
Ru(1)-C(4)	2.312(7)	Ru(1)-C(5)	2.328(7)
Ru(1)-C(6)	2.345(7)	P-C	1.828(8)
C-C(arene)	1.423(4)	Sb-Cl	2.352(3)-2.372(3)
Cl(1)-Ru(1)- Cl(2)	96.7(1)	Cl(1)-Ru(1)- P(1)	85.2(1)
Cl(2)-Ru(1)-P(1)	83.9(1)		

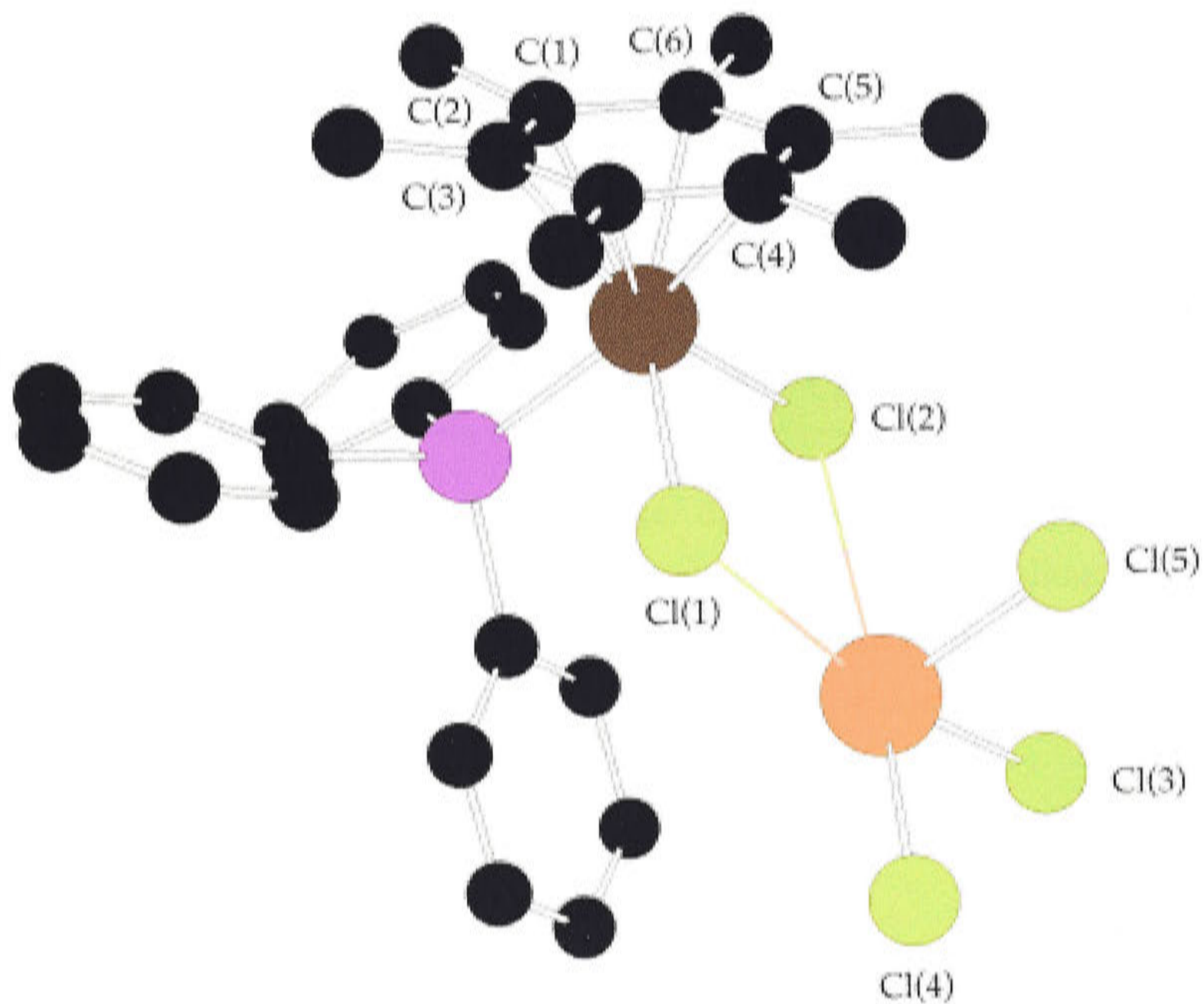
A.20 $[\text{RuCl}_2(\eta^6\text{-C}_6\text{Me}_6)(\text{PPh}_3)]\cdot\text{SbCl}_3$ ([306]SbCl₃)

Figure 108. Chem3D representation of the molecular structure of $[\text{RuCl}_2(\eta^6\text{-C}_6\text{Me}_6)(\text{PPh}_3)]\cdot\text{SbCl}_3$ ([306]SbCl₃). Hydrogen atoms have been omitted for clarity. The structure was determined by Dr A. C. Willis (ANU).

Table 58. Selected bond lengths (Å) and angles (°) for the non-tethered complex $[\text{RuCl}_2(\eta^6\text{-C}_6\text{Me}_6)(\text{PPh}_3)]\cdot\text{SbCl}_3$ ([306]SbCl₃).

Ru(1)-Cl(1)	2.452(3)	Ru(1)-Cl(2)	2.433(3)
Ru(1)-P(1)	2.381(3)	Ru(1)-C(1)	2.208(11)
Ru(1)-C(2)	2.25(1)	Ru(1)-C(3)	2.22(1)
Ru(1)-C(4)	2.261(12)	Ru(1)-C(5)	2.253(11)
Ru(1)-C(6)	2.218(12)	P-C	1.84(1)–1.844(12)
C-C(arene)	1.411(16)–1.446(16)	Sb-Cl	2.388(3)–2.433(4)
Cl(1)-Ru(1)- Cl(2)	88.34(9)	Cl(1)-Ru(1)-P(1)	86.34(11)
Cl(2)-Ru(1)-P(1)	86.9(1)	Cl(3)-Sb(1)-Cl(4)	95.21(14)
Cl(3)-Sb(1)-Cl(5)	92.40(13)	Cl(4)-Sb(1)-Cl(5)	92.30(12)

Structure reports presented in portable document format (pdf) files [generated using PRINTCIF (International Union of Crystallography's typesetting service)], are presented in the format used by *Acta Crystallographica* and are located on the accompanying compact disc.

A.21 Crystal Data and Details of Data Structure Collection and Refinement (Tables 59-65).

Table 59. Compounds $\text{Ph}_2\text{P}(\text{CH}_2)_3\text{Ph}$ (118), $[\text{RuCl}_2(\eta^6\text{-1,4-MeC}_6\text{H}_4\text{CHMe}_2)(\eta^1\text{-Me}_2\text{P}(\text{CH}_2)_3\text{Ph})]$ (231) and $[\text{RuCl}_2(\eta^6\text{-1,4-MeC}_6\text{H}_4\text{CHMe}_2)(\eta^1\text{-Ph}_2\text{P}(\text{CH}_2)_3\text{Ph})]$ (227).

	$\text{Ph}_2\text{P}(\text{CH}_2)_3\text{Ph}$ (118)	$[\text{RuCl}_2(\eta^6\text{-1,4-MeC}_6\text{H}_4\text{CHMe}_2)(\eta^1\text{-Me}_2\text{P}(\text{CH}_2)_3\text{Ph})]$ (231)	$[\text{RuCl}_2(\eta^6\text{-C}_6\text{H}_6)(\eta^1\text{-Ph}_2\text{P}(\text{CH}_2)_3\text{Ph})]$ (227)
Empirical Formula	$\text{C}_{21}\text{H}_{21}\text{P}$	$\text{C}_{21}\text{H}_{31}\text{Cl}_2\text{PRu}$	$\text{C}_{27}\text{H}_{27}\text{Cl}_2\text{PRu}$
Formula Weight	304.35	486.43	554.46
Temperature (K)	180(2)	296(1)	296(1)
Wavelength (Å)	0.71073	0.71069	0.71069
Crystal System	monoclinic	monoclinic	monoclinic
Space Group	$P2_1/c$ (No. 14)	$P2_1/c$ (No. 14)	$P2_1/c$ (No. 14)
Unit Cell Dimensions			
a (Å)	5.7499(2)	13.521(2)	13.780(2)
b (Å)	18.0970(11)	11.988(2)	10.058(2)
c (Å)	16.0028(8)	14.706(2)	18.435(3)
α (°)			
β (°)	91.421(3)	112.33(1)	109.02(1)
γ (°)			
V (Å ³)	1664.67(14)	2204.8(7)	2414.2(7)
Z	4	4	4
D_{calc} (g cm ⁻³)	1.214	1.465	1.521

	Ph ₂ P(CH ₂) ₃ Ph (118)	[RuCl ₂ (η ⁶ -1,4-MeC ₆ H ₄ CHMe ₂)(η ¹ -Me ₂ P(CH ₂) ₃ Ph)] (231)	[RuCl ₂ (η ⁶ -C ₆ H ₆)(η ¹ -Ph ₂ P(CH ₂) ₃ Ph)] (227)
μ(MKα) (cm ⁻¹)	1.60 (Mo)	10.16 (Mo)	9.47 (Mo)
F(000)	648	1000	1128
Crystal Size (mm)	0.21 x 0.18 x 0.14	0.44 x 0.31 x 0.08	0.45 x 0.19 x 0.10
Crystal Colour, Habit	Orange, block	Orange-red, plate	Orange-red, needle
θ Range for Data	4-27	2-28	2-30
Collection (°)			
Number of Reflections	13665	5568	7641
Unique Observed	3785 [R _{int} = 0.0684]	5352 [R _{int} = 0.015]	7433 [R _{int} = 0.016]
Absorption Correction	2390 [I > 2σ(I)]	4012 [I > 2σ(I)]	5341 [I > 2σ(I)]
Structure Solution	Multiscan	Analytical	Analytical
Refinement Program	Direct Methods (SHELXS97) ³	Direct Methods (SIR92) ⁴	Direct Methods (SIR92) ⁴
Refinement	<i>Direct Methods</i> (SHELXL97) ⁵	teXsan 1997 ⁶	teXsan 1997 ⁶
Transmission Factors	Full-matrix least squares on F ²	Full-matrix least squares on F	Full-matrix least squares on F
Number of Parameters	0.868-0.978	0.75-0.92	0.826-0.913
	199	236	280

	Ph ₂ P(CH ₂) ₃ Ph (118)	[RuCl ₂ (η ⁶ -1,4-MeC ₆ H ₄ CHMe ₂)(η ¹ -Me ₂ P(CH ₂) ₃ Ph)] (231)	[RuCl ₂ (η ⁶ -C ₆ H ₆)(η ¹ -Ph ₂ P(CH ₂) ₃ Ph)] (227)
Final <i>R</i> Indices	<i>R</i> ₁ = 0.0515,	<i>R</i> ₁ = 0.027,	<i>R</i> ₁ = 0.036,
Goodness of Fit	ω <i>R</i> ₂ = 0.1272 0.991	ω <i>R</i> ₂ = 0.031 1.48	ω <i>R</i> ₂ = 0.031 1.44
ρ _{min} and ρ _{max} (eÅ ⁻³)	0.669 and -0.542	0.45 and -0.34	0.45 and -0.47
Diffractometer	Nonius Kappa CCD	Rigaku AFC-6S	Phillips PW1100/20

Table 60. Complexes [RuCl₂(η⁶-1,4-MeC₆H₄CHMe₂)(η¹-*i*-Pr₂P(CH₂)₃Ph)] (232), [RuCl₂(η⁶-1,2-MeC₆H₄CO₂Me)(η¹-Cy₂P(CH₂)₃Ph)] (239) and [RuCl₂(η⁶-1,4-MeC₆H₄CHMe₂)(η¹-Ph₂P(CH₂)₃-2,4,6-C₆H₂Me₃)] (233).

	[RuCl ₂ (η ⁶ -1,4-MeC ₆ H ₄ CHMe ₂)(η ¹ - <i>i</i> -Pr ₂ P(CH ₂) ₃ Ph)] (232)	[RuCl ₂ (η ⁶ -1,2-MeC ₆ H ₄ CO ₂ Me)(η ¹ -Cy ₂ P(CH ₂) ₃ Ph)] (239)	[RuCl ₂ (η ⁶ -1,4-MeC ₆ H ₄ CHMe ₂)(η ¹ -Ph ₂ P(CH ₂) ₃ -2,4,6-C ₆ H ₂ Me ₃)] (233)
Empirical Formula	C ₂₅ H ₃₉ Cl ₂ PRu.C _{0.75} H _{1.50} Cl _{1.50}	C ₃₀ H ₄₃ Cl ₂ O ₂ PRu	C ₃₄ H ₄₁ Cl ₂ PRu
Formula Weight	606.20	638.58	652.61
Temperature (K)	180(2)	180(2)	180(2)
Wavelength (Å)	0.71069	0.71073	0.71069
Crystal System	triclinic	monoclinic	monoclinic
Space Group	<i>P</i> $\bar{1}$ (No. 2)	<i>P</i> 2 ₁ / <i>a</i> (No. 14)	<i>P</i> 2 ₁ / <i>n</i> (No. 14)

	[RuCl ₂ (η ⁶ -1,4-MeC ₆ H ₄ CHMe ₂)(η ¹ - <i>i</i> -Pr ₂ P(CH ₂) ₃ Ph)] (232)	[RuCl ₂ (η ⁶ -1,2-MeC ₆ H ₄ CO ₂ Me)(η ¹ -Cy ₂ P(CH ₂) ₃ Ph)] (239)	[RuCl ₂ (η ⁶ -1,4-MeC ₆ H ₄ CHMe ₂)(η ¹ -Ph ₂ P(CH ₂) ₃ -2,4,6-C ₆ H ₂ Me ₃)] (233)
Unit Cell Dimensions			
<i>a</i> (Å)	12.3319(7)	18.6170(5)	9.7536(3)
<i>b</i> (Å)	20.3616(9)	13.7565(3)	17.5094(6)
<i>c</i> (Å)	23.0825(1)	23.5110(6)	18.4834(5)
α (°)	101.183(3)		
β (°)	96.955(3)	100.0540(10)	98.956(2)
γ (°)	92.414(3)		
<i>V</i> (Å ³)	5631.2(5)	5928.8(3)	3118.17(17)
<i>Z</i>	8	8	4
<i>D</i> _{calc} (g cm ⁻³)	1.430	1.431	1.390
μ (MK α) (cm ⁻¹)	9.58 (Mo)	7.88 (Mo)	7.47 (Mo)
<i>F</i> (000)	2508	2656	1352
Crystal Size (mm)	0.12 × 0.09 × 0.09	0.30 × 0.18 × 0.15	0.23 × 0.18 × 0.16
Crystal Colour, Habit	Orange, block	Red, block	Red, block
θ Range for Data Collection (°)	4-22	3-27	4-27
Number of Reflections	28860	31382	20863
Unique Observed	14247 [<i>R</i> _{int} = 0.1073] 8685 [<i>I</i> > 2 σ (<i>I</i>)]	13500 [<i>R</i> _{int} = 0.0474] 10626 [<i>I</i> > 2 σ (<i>I</i>)]	7065 [<i>R</i> _{int} = 0.0572] 5113 [<i>I</i> > 2 σ (<i>I</i>)]

	[RuCl ₂ (η ⁶ -1,4-MeC ₆ H ₄ CHMe ₂)(η ¹ -i-Pr ₂ P(CH ₂) ₃ Ph)] (232)	[RuCl ₂ (η ⁶ -1,2-MeC ₆ H ₄ CO ₂ Me)(η ¹ -Cy ₂ P(CH ₂) ₃ Ph)] (239)	[RuCl ₂ (η ⁶ -1,4-MeC ₆ H ₄ CHMe ₂)(η ¹ -Ph ₂ P(CH ₂) ₃ -2,4,6-C ₆ H ₂ Me ₃)] (233)
Absorption Correction	Multiscan	Multiscan	Multiscan
Structure Solution	Direct Methods (SHELXS97) ³	Direct Methods (SHELXS97) ³	Direct Methods (SHELXS97) ⁷
Refinement Program	Direct Methods (SHELXL93) ⁸	Direct Methods (SHELXL97) ⁵	Direct Methods (SHELXL97) ⁵
Refinement	Full-matrix least squares on F ²	Full-matrix least squares on F ²	Full-matrix least squares on F ²
Transmission Factors	0.783-0.917	0.787-0.889	0.767-0.887
Number of Parameters	1134	569	349
Final R Indices	R ₁ = 0.0711, ωR ₂ = 0.1460	R ₁ = 0.0764, ωR ₂ = 0.1829	R ₁ = 0.0382 ωR ₂ = 0.794
Goodness of Fit	1.045	1.032	1.039
ρ _{min} and ρ _{max} (eÅ ⁻³)	0.583 and -0.752	1.580 and -2.396	0.515 and -0.593
Diffractometer	Nonius Kappa CCD	Nonius Kappa CCD	Nonius Kappa CCD

Table 61. Complexes $[\text{RuCl}_2(\eta^6\text{-1,4-MeC}_6\text{H}_4\text{CHMe}_2)(\eta^1\text{-Ph}_2\text{P}(\text{CH}_2)_3\text{C}_6\text{Me}_5)]$ (234), $[\text{RuCl}_2(\eta^6\text{-1,4-MeC}_6\text{H}_4\text{CHMe}_2)(\eta^1\text{-Ph}_2\text{PCH}_2\text{SiMe}_2\text{Ph})]$ (235) and $[\text{RuCl}_2(\eta^6\text{-1,4-MeC}_6\text{H}_4\text{CHMe}_2)(\text{Ph}_2\text{PCH}=\text{CH}_2)]$ (269).

	$[\text{RuCl}_2(\eta^6\text{-1,4-MeC}_6\text{H}_4\text{CHMe}_2)(\eta^1\text{-Ph}_2\text{P}(\text{CH}_2)_3\text{C}_6\text{Me}_5)]$ (234)	$[\text{RuCl}_2(\eta^6\text{-1,4-MeC}_6\text{H}_4\text{CHMe}_2)(\eta^1\text{-Ph}_2\text{PCH}_2\text{SiMe}_2\text{Ph})]$ (235)	$[\text{RuCl}_2(\eta^6\text{-1,4-MeC}_6\text{H}_4\text{CHMe}_2)(\text{Ph}_2\text{PCH}=\text{CH}_2)]$ (269)
Empirical Formula	$\text{C}_{36}\text{H}_{45}\text{Cl}_2\text{PRu}$	$\text{C}_{31}\text{H}_{37}\text{Cl}_2\text{PRuSi}\cdot\text{CH}_2\text{Cl}_2$	$\text{C}_{24}\text{H}_{27}\text{Cl}_2\text{PRu}$
Formula Weight	680.66	725.56	518.43
Temperature (K)	180(2)	180(2)	200(2)
Wavelength (Å)	0.71069	0.71070	0.71073
Crystal System	monoclinic	monoclinic	monoclinic
Space Group	$P2_1$ (No. 4)	$P2_1/n$ (No. 14)	$P2_1/c$ (No. 14)
Unit Cell Dimensions			
a (Å)	7.56240(10)	11.4810(4)	13.2119(3)
b (Å)	17.9312(5)	20.4170(8)	7.8283(2)
c (Å)	23.7705(7)	14.6920(4)	21.5823(4)
α (°)			
β (°)	97.980(2)	93.198(2)	90.992(1)
γ (°)			
V (Å ³)	3192.14(14)	3438.6(2)	2231.85(9)
Z	4	4	4
D_{calc} (g cm ⁻³)	1.416	1.402	1.543
$\mu(\text{MK}\alpha)$ (cm ⁻¹)	7.33 (Mo)	8.68 (Mo)	1.02 (Mo)
$F(000)$	1416	1488	1056

	[RuCl ₂ (η ⁶ -1,4-MeC ₆ H ₄ CHMe ₂)(η ¹ -Ph ₂ P(CH ₂) ₃ C ₆ Me ₅)] (234)	[RuCl ₂ (η ⁶ -1,4-MeC ₆ H ₄ CHMe ₂)(η ¹ -Ph ₂ PCH ₂ SiMe ₂ Ph)] (235)	[RuCl ₂ (η ⁶ -1,4-MeC ₆ H ₄ CHMe ₂)(Ph ₂ PCH=CH ₂)] (269)
Crystal Size (mm)	0.16 x 0.14 x 0.02	0.13 x 0.10 x 0.10	0.06 x 0.26 x 0.15
Crystal Colour, Habit	Red, block	Red, block	Red, tablet
θ Range for Data	4-27	4-25	3-30
Collection (°)			
Number of Reflections	23453	10089	30982
Unique Observed	12467 [<i>R</i> _{int} = 0.0679]	5969 [<i>R</i> _{int} = 0.0264]	6410 [<i>R</i> _{int} = 0.066]
Absorption Correction	10771 [<i>I</i> > 2σ(<i>I</i>)]	4763 [<i>I</i> > 2σ(<i>I</i>)]	4814 [<i>I</i> > 3σ(<i>I</i>)]
Structure Solution	Multiscan	None	Analytical
Refinement Program	Direct Methods (SHELXS97) ⁷ Direct Methods (SHELXL97) ⁵	Direct Methods (SIR92) ⁴ Direct Methods (SHELXL97) ⁵	Direct Methods (SIR92) ⁴ maxus 1999 ⁹
Refinement	Full-matrix least squares on F ²	Full-matrix least squares on F ²	Full-matrix least squares on F
Transmission Factors	0.855-0.985	0.896-0.918	0.819-0.945
Number of Parameters	737	359	253
Final <i>R</i> Indices	<i>R</i> ₁ = 0.01413 ω <i>R</i> ₂ = 0.0887	<i>R</i> ₁ = 0.0517 ω <i>R</i> ₂ = 0.1295	<i>R</i> ₁ = 0.040, ω <i>R</i> ₂ = 0.042
Goodness of Fit	1.033	1.018	1.883

	[RuCl ₂ (η ⁶ -1,4-MeC ₆ H ₄ CHMe ₂)(η ¹ -Ph ₂ P(CH ₂) ₃ C ₆ Me ₅)] (234)	[RuCl ₂ (η ⁶ -1,4-MeC ₆ H ₄ CHMe ₂)(η ¹ -Ph ₂ PCH ₂ SiMe ₂ Ph)] (235)	[RuCl ₂ (η ⁶ -1,4-MeC ₆ H ₄ CHMe ₂)(Ph ₂ PCH=CH ₂)] (269)
ρ _{min} and ρ _{max} (eÅ ⁻³)	0.553 and -0.889	1.464 and -1.081	1.13 and -1.29
Diffractometer	Nonius Kappa CCD	Nonius Kappa CCD	Nonius Kappa CCD

Table 62. Complexes [RuCl₂(η¹:η⁶-Me₂P(CH₂)₃Ph)] (248), [RuCl₂(η¹:η⁶-*i*-Pr₂P(CH₂)₃Ph)] (249) and [RuCl₂(η¹:η⁶-*t*-Bu₂P(CH₂)₃Ph)] (253).

	[RuCl ₂ (η ¹ :η ⁶ -Me ₂ P(CH ₂) ₃ Ph)] (248)	[RuCl ₂ (η ¹ :η ⁶ - <i>i</i> -Pr ₂ P(CH ₂) ₃ Ph)] (249)	[RuCl ₂ (η ¹ :η ⁶ - <i>t</i> -Bu ₂ P(CH ₂) ₃ Ph)] (253)
Empirical Formula	C ₁₁ H ₁₇ Cl ₂ PRu	C ₁₅ H ₂₅ Cl ₂ PRu	C ₁₇ H ₂₉ Cl ₂ PRu
Formula Weight	352.21	408.29	436.34
Temperature (K)	296(1)	180(2)	180(2)
Wavelength (Å)	1.54178	0.71073	0.71069
Crystal System	monoclinic	triclinic	monoclinic
Space Group	<i>P</i> 2 ₁ / <i>c</i> (No. 14)	<i>P</i> 1̄ (No. 2)	<i>P</i> 2 ₁ / <i>n</i> (No. 14)
Unit Cell Dimensions			
<i>a</i> (Å)	13.649(1)	8.1421(7)	11.0865(6)
<i>b</i> (Å)	13.453(1)	8.6186(6)	13.0809(9)
<i>c</i> (Å)	14.479(1)	13.5805(10)	12.7082(7)
α (°)		90.996(3)	

	[RuCl ₂ (η ¹ :η ⁶ - Me ₂ P(CH ₂) ₃ Ph)] (248)	[RuCl ₂ (η ¹ :η ⁶ - <i>i</i> - Pr ₂ P(CH ₂) ₃ Ph)] (249)	[RuCl ₂ (η ¹ :η ⁶ - <i>t</i> - Bu ₂ P(CH ₂) ₃ Ph)] (253)
β (°)	102.892(7)	95.536(3)	102.163(3)
γ (°)		117.212(4)	
V (Å ³)	2591.8(4)	841.52(11)	1801.59(19)
Z	8	2	4
D _{calc} (g cm ⁻³)	1.805	1.611	1.609
μ(MKα) (cm ⁻¹)	148.50 (Cu)	13.30 (Mo)	12.48 (Mo)
F(000)	1408	416	896
Crystal Size (mm)	0.14 x 0.14 x 0.07	0.30 x 0.12 x 0.05	0.19 x 0.16 x 0.02
Crystal Colour, Habit	Orange, block	Red, block	Orange, block
θ Range for Data	2-60	4-28	4-27
Collection (°)			
Number of Reflections	4226	7604	11435
Unique Observed	4049 [R _{int} = 0.049]	3387 [R _{int} = 0.0628]	4108 [R _{int} = 0.0708]
Absorption Correction	2589 [I > 2σ(I)]	2640 [I > 2σ(I)]	2718 [I > 2σ(I)]
Structure Solution	Analytical	Multiscan	Multiscan
Refinement Program	Direct Methods (SIR92) ⁴ teXsan 1997 ⁶	Direct Methods (SHELXS97) ³ Direct Methods (SHELXL97) ⁵	Direct Methods (SIR92) ⁴ Direct Methods (SHELXL93) ⁸
Refinement	Full-matrix least squares on F	Full-matrix least squares on F ²	Full-matrix least squares on F ²

	[RuCl ₂ (η ¹ :η ⁶ -Me ₂ P(CH ₂) ₃ Ph)] (248)	[RuCl ₂ (η ¹ :η ⁶ -i-Pr ₂ P(CH ₂) ₃ Ph)] (249)	[RuCl ₂ (η ¹ :η ⁶ -t-Bu ₂ P(CH ₂) ₃ Ph)] (253)
Transmission Factors	0.15-0.41	0.882-0.936	0.930-0.975
Number of Parameters	272	176	196
Final R Indices	R ₁ = 0.042	R ₁ = 0.0685	R ₁ = 0.0392
Goodness of Fit	ωR ₂ = 0.056	ωR ₂ = 0.1806	ωR ₂ = 0.0754
ρ _{min} and ρ _{max} (eÅ ⁻³)	1.81	1.045	0.995
Diffraction	1.35 and -1.14	2.492 and -1.222	0.637 and -0.770
Diffraction	Rigaku AFC-6R	Nonius Kappa CCD	Nonius Kappa CCD

Table 63. Complexes [RuCl₂(η¹:η⁶-Ph₂P(CH₂)₃-2,4,6-C₆H₂Me₃)] (250), [RuCl₂(η¹:η⁶-Ph₂P(CH₂)₃C₆Me₅)] (251) and [RuCl₂(η¹:η⁶-Ph₂PCH₂SiMe₂Ph)] (252).

	[RuCl ₂ (η ¹ :η ⁶ -Ph ₂ P(CH ₂) ₃ -2,4,6-C ₆ H ₂ Me ₃)] (250)	[RuCl ₂ (η ¹ :η ⁶ -Ph ₂ P(CH ₂) ₃ C ₆ Me ₅)] (251)	[RuCl ₂ (η ¹ :η ⁶ -Ph ₂ PCH ₂ SiMe ₂ Ph)] (252)
Empirical Formula	C ₂₄ H ₂₇ Cl ₂ PRu.CH ₂ Cl ₂	C ₂₆ H ₃₁ Cl ₂ PRu	C ₂₁ H ₂₃ Cl ₂ PRuSi
Formula Weight	603.32	546.48	506.45
Temperature (K)	180(2)	180(2)	296(1)
Wavelength (Å)	0.71070	0.71073	0.71069
Crystal System	triclinic	monoclinic	monoclinic
Space Group	P $\bar{1}$ (No. 2)	C2/c (No. 15)	P2 ₁ /n (No. 14)

	[RuCl ₂ (η ¹ :η ⁶ -Ph ₂ P(CH ₂) ₃ - 2,4,6-C ₆ H ₂ Me ₃)] (250)	[RuCl ₂ (η ¹ :η ⁶ - Ph ₂ P(CH ₂) ₃ C ₆ Me ₅)] (251)	[RuCl ₂ (η ¹ :η ⁶ - Ph ₂ PCH ₂ SiMe ₂ Ph)] (252)
Unit Cell Dimensions			
<i>a</i> (Å)	8.1450(5)	29.4890(4)	11.124(3)
<i>b</i> (Å)	9.0570(5)	8.4700(1)	13.114(2)
<i>c</i> (Å)	18.7720(6)	22.7143(4)	14.965(2)
<i>α</i> (°)	101.286(3)		
<i>β</i> (°)	91.615(3)	125.4491(6)	95.85(2)
<i>γ</i> (°)	113.800(11)		
<i>V</i> (Å ³)	1233.64(11)	4621.72(12)	2171.8(7)
<i>Z</i>	2	8	4
<i>D</i> _{calc} (g cm ⁻³)	1.624	1.571	1.549
<i>μ</i> (MoKα) (cm ⁻¹)	11.46 (Mo)	9.9 (Mo)	10.86 (Mo)
<i>F</i> (000)	612	2240	1024
Crystal Size (mm)	0.16 x 0.14 x 0.05	0.10 x 0.03 x 0.03	0.37 x 0.20 x 0.08
Crystal Colour, Habit	Orange, block	Orange, needle	Orange, plate
<i>θ</i> Range for Data Collection (°)	4-25	3-26	2-28
Number of Reflections	6616	16326	6541
Unique Observed	4248 [<i>R</i> _{int} = 0.0539] 3529 [<i>I</i> > 2σ(<i>I</i>)]	4879 [<i>R</i> _{int} = 0.065] 3487 [<i>I</i> > 3σ(<i>I</i>)]	5427 [<i>R</i> _{int} = 0.0515] 3892 [<i>I</i> > 2σ(<i>I</i>)]
Absorption Correction	None	Empirical	Analytical

	[RuCl ₂ (η ¹ :η ⁶ -Ph ₂ P(CH ₂) ₃ -2,4,6-C ₆ H ₂ Me ₃)] (250)	[RuCl ₂ (η ¹ :η ⁶ -Ph ₂ P(CH ₂) ₃ C ₆ Me ₅)] (251)	[RuCl ₂ (η ¹ :η ⁶ -Ph ₂ PCH ₂ SiMe ₂ Ph)] (252)
Structure Solution	Direct Methods (SIR92) ⁴	Heavy Atom (DIRDIF92)	Direct Methods (SIR92) ⁴
Refinement Program	Direct Methods (SHELXL97) ⁵	maXus 1999 ⁹	teXsan 1997 ⁶
Refinement	Full-matrix least squares on F ²	Full-matrix least squares on F	Full-matrix least squares on F
Transmission Factors	0.838-0.945	0.965-0.971	0.81-0.92
Number of Parameters	283	272	236
Final R Indices	R ₁ = 0.041 ωR ₂ = 0.093	R ₁ = 0.032 ωR ₂ = 0.072	R ₁ = 0.025 ωR ₂ = 0.023
Goodness of Fit	1.03	2.38	1.48
ρ _{min} and ρ _{max} (eÅ ⁻³)	0.594 and -0.855	0.54 and -0.64	0.45 and -0.45
Diffractometer	Nonius Kappa CCD	Nonius Kappa CCD	Rigaku AFC-6S

Table 64. Complexes $[\text{Ru}_4\text{Cl}_8\text{O}(\eta^1\text{-}t\text{-Bu}_2\text{P}(\text{CH}_2)_3\text{Ph})_4]$ (**261**), $[\text{RuCl}(\text{NCMe})_4(\text{Ph}_2\text{P}(\text{CH}_2)_3\text{Ph})]\text{Cl}$ (**[328]Cl**) and $[\text{RuCl}_2(\eta^1:\eta^6\text{-Ph}_2\text{P}(\text{CH}_2)_3\text{C}_6\text{Me}_5)][\text{SbCl}_6]$ (**[251][SbCl}_6]**).

	$[\text{Ru}_4\text{Cl}_8\text{O}(\eta^1\text{-}t\text{-Bu}_2\text{P}(\text{CH}_2)_3\text{Ph})_4]$ (261)	$[\text{RuCl}(\text{NCMe})_4(\text{Ph}_2\text{P}(\text{CH}_2)_3\text{Ph})]\text{Cl}$ (<i>trans</i> - [328]Cl)	$[\text{RuCl}_2(\eta^1:\eta^6\text{-Ph}_2\text{P}(\text{CH}_2)_3\text{C}_6\text{Me}_5)][\text{SbCl}_6]$ ([251][SbCl}_6])
Empirical Formula	$\text{C}_{68}\text{H}_{116}\text{Cl}_8\text{OP}_4\text{Ru}_4$	$\text{C}_{29}\text{H}_{30}\text{Cl}_2\text{N}_4\text{PRu.H}_2\text{O.CH}_2\text{Cl}_2$	$\text{C}_{26}\text{H}_{31}\text{Cl}_8\text{PRuSb.CH}_2\text{Cl}_2$
Formula Weight	1761.46	743.50	965.88
Temperature (K)	200(2)	183	200(2)
Wavelength (Å)	0.71073	1.54178	0.71073
Crystal System	monoclinic	monoclinic	monoclinic
Space Group	$P2_1/c$ (No. 14)	$P2_1/c$ (No. 14)	$P2_1/a$ (No. 14)
Unit Cell Dimensions			
a (Å)	17.0534(2)	17.542(3)	17.0763(3)
b (Å)	12.8564(1)	12.023(2)	12.2811(3)
c (Å)	18.2272(2)	17.995(2)	17.6716(4)
α (°)			
β (°)	105.7708(4)	113.615(8)	108.3562(9)
γ (°)			
V (Å ³)	3845.80(7)	3477.3(8)	3517.44(13)
Z	2	4	4
D_{calc} (g cm ⁻³)	1.521	1.420	1.824
$\mu(\text{MK}\alpha)$ (cm ⁻¹)	1.171 (Mo)	71.43 (Cu)	2.02 (Mo)
$F(000)$	1800	1520	1900
Crystal Size (mm)	0.32 × 0.08 × 0.02	0.24 × 0.20 × 0.12	0.35 × 0.25 × 0.03

	$[\text{Ru}_4\text{Cl}_8\text{O}(\eta^1\text{-}t\text{-Bu}_2\text{P}(\text{CH}_2)_3\text{Ph})_4]$ (261)	$[\text{RuCl}(\text{NCMe})_4(\text{Ph}_2\text{P}(\text{CH}_2)_3\text{-Ph})]\text{Cl}$ (<i>trans</i> - [328] Cl)	$[\text{RuCl}_2(\eta^1:\eta^6\text{-Ph}_2\text{P}(\text{CH}_2)_3\text{C}_6\text{Me}_5)][\text{SbCl}_6]$ ([251])[SbCl_6])
Crystal Colour, Habit θ Range for Data Collection ($^\circ$) Number of Reflections Unique Observed Absorption Correction Structure Solution Refinement Program Refinement Transmission Factors Number of Parameters Final R Indices Goodness of Fit ρ_{min} and ρ_{max} ($\text{e}\text{\AA}^{-3}$) Diffractometer	Black, plate 3-27 85909 8810 $R_{\text{int}} = 0.06$ 4856 [$I > 3\sigma(I)$] Analytical Direct Methods (SIR92) ⁴ CRYSTALS 2001 ¹⁰ Full-matrix least squares on F 0.802-0.977 397 $R_1 = 0.0246$ $\omega R_2 = 0.0283$ 0.9661 0.51 and -0.52 Nonius Kappa CCD	Yellow, prism 2-60 5671 5742 [$R_{\text{int}} = 0.114$] 2534 [$I > 2\sigma(I)$] Empirical Direct Methods (SIR92) ⁴ teXsan (1992-1997) ^{6,11,12} Full-matrix least squares on F 0.55-1.00 370 $R_1 = 0.054$ $\omega R_2 = 0.060$ 1.88 0.55 and -0.61 Rigaku AFC-6R	Orange, plate 3-25 48872 6171 [$R_{\text{int}} = 0.060$] 3334 [$I > 2\sigma(I)$] Analytical Direct Methods (SIR92) ⁴ CRYSTALS 2001 ¹⁰ Full-matrix least squares on F 0.685-0.943 364 $R_1 = 0.0284$ $\omega R_2 = 0.0148$ 1.0581 0.72 and -0.59 Nonius Kappa CCD

Table 65. Complexes $[\text{RuCl}_2(\eta^6\text{-C}_6\text{Me}_6)(\text{PPh}_3)][\text{SbCl}_6]$ (**[306]** $[\text{SbCl}_6]$) and $[\text{RuCl}_2(\eta^6\text{-C}_6\text{Me}_6)(\text{PPh}_3)].\text{SbCl}_3$ (**[306]** $.\text{SbCl}_3$).

	$[\text{RuCl}_2(\eta^6\text{-C}_6\text{Me}_6)(\text{PPh}_3)][\text{SbCl}_6]$ ([306] $[\text{SbCl}_6]$)	$[\text{RuCl}_2(\eta^6\text{-C}_6\text{Me}_6)(\text{PPh}_3)].\text{SbCl}_3$ ([306] $.\text{SbCl}_3$)
Empirical Formula	$\text{C}_{30}\text{H}_{33}\text{Cl}_8\text{PRuSb}.\text{CH}_2\text{Cl}_2$	$\text{C}_{30}\text{H}_{33}\text{Cl}_5\text{PRuSb}$
Formula Weight	1015.94	824.65
Temperature (K)	200	200
Wavelength (Å)	0.71073	0.71073
Crystal System	monoclinic	monoclinic
Space Group	$P2_1/c$ (No. 14)	$P2_1/n$ (No. 14)
Unit Cell Dimensions		
<i>a</i> (Å)	12.4261(3)	11.9142(5)
<i>b</i> (Å)	8.0591(2)	15.0473(7)
<i>c</i> (Å)	36.681(1)	17.7552(10)
α (°)		
β (°)	91.1345(9)	97.6502(3)
γ (°)		
<i>V</i> (Å ³)	3872.85(17)	3154.(3)
<i>Z</i>	4	4
<i>D</i> _{calc} (g cm ⁻³)	1.742	1.736
$\mu(\text{MK}\alpha)$ (cm ⁻¹)	1.839 (Mo)	1.829 (Mo)
<i>F</i> (000)	2004	1632
Crystal Size (mm)	0.20 × 0.14 × 0.02	0.08 × 0.03 × 0.02
Crystal Colour, Habit	Brown, plate	Orange, needle
θ Range for Data Collection (°)	2-23	3-23
Number of Reflections	26288	16547
Unique	4893 [<i>R</i> _{int} = 0.07]	4245 [<i>R</i> _{int} = 0.14]
Observed	3196 [<i>I</i> > 3 σ (<i>I</i>)]	2089 [<i>I</i> > 2 σ (<i>I</i>)]
Absorption Correction	Analytical	Analytical
Structure Solution	Direct methods (SIR92) ⁴	Direct methods (SIR92) ⁴
Refinement Program	RAELS2000 ¹³	CRYSTALS 2001 ¹⁰
Refinement	Full-matrix least squares on <i>F</i>	Full-matrix least squares on <i>F</i>
Transmission Factors	0.748-0.967	0.898-0.968
Number of Parameters	172	343
Final <i>R</i> Indices	<i>R</i> ₁ = 0.050	<i>R</i> ₁ = 0.0424
	ωR_2 = 0.062	ωR_2 = 0.0446

	[RuCl ₂ (η ⁶ -C ₆ Me ₆)(PPh ₃)] [SbCl ₆] ([306] [SbCl ₆])	[RuCl ₂ (η ⁶ -C ₆ Me ₆)(PPh ₃)] . SbCl ₃ ([306] . SbCl ₃)
Goodness of Fit	1.30	1.0571
ρ_{\min} and ρ_{\max} (eÅ ⁻³)	1.27 and -0.86	0.61 and -0.65
Diffractometer	Nonius Kappa CCD	Nonius Kappa CCD

References

- (1) Redwine, K. D.; Hansen, H. D.; Bowley, S.; Isbell, J.; Sanchez, M.; Vodak, D.; Nelson, J. H. *Synth. React. Inorg. Met.-Org. Chem.* **2000**, *30*, 379-407.
- (2) Spek, A. L. *PLATON, An Integrated Tool for the Analysis of the Results of a Single Crystal Structure Determination*, University of Utrecht, Utrecht, The Netherlands, 2003.
- (3) Sheldrick, G. M. *SHELXS97*, University of Göttingen, Germany, 1997.
- (4) Altomare, A.; Cascarano, G.; Giacovazzo, C.; Guagliardi, A.; Burla, M. C.; Polidori, G.; Camalli, M. *J. Appl. Cryst.* **1994**, *27*, 435.
- (5) Sheldrick, G. M. *SHELXL97*, University of Göttingen, Germany, 1997.
- (6) *teXsan, Single Crystal Structure Analysis Software*, Version 1.8, Research Forest Drive, The Woodlands, TX 77381, U.S.A., 1997.
- (7) Sheldrick, G. M. *SHELXS97*, University of Göttingen, Germany, 1990.
- (8) Sheldrick, G. M. *SHELXL93*, University of Göttingen, Germany, 1993.
- (9) Mackay, S.; Gilmore, C. J.; Edwards, C.; Stewart, N.; Shankland, K. *maXus Computer Program for the Solution and Refinement of Crystal Structures*, Nonius, The Netherlands; Macscience, Japan and the University of Glasgow, 1999.

- (10) Watkin, D. J.; Prout, C. K.; Carruthers, J. R.; Betteridge, P. W.; Cooper, R. I. *CRYSTALS Issue 11.6*, Oxford, U.K., 2001.
- (11) *teXsan, Single Crystal Structure Analysis Software*, Version 1.7, Research Forest Drive, The Woodlands, TX 77381, U.S.A., 1992.
- (12) *teXsan, Single Crystal Structure Analysis Software*, Version 1.7, Research Forest Drive, The Woodlands, TX 77381, U.S.A., 1995.
- (13) Rae, A. D. *RAELS2000*, The Australian National University, Canberra, Australia, 2000.

"I must say here, in passing, that those captains who have scientists must, upon departure, take a good supply of patience. I admit that although I have no lack of it, the scientists have frequently driven me to the end of my tether... .."

*Nicolas Baudin aboard Le Géographe
Taken from "The Navigators" by Klaus Toft*